Advances in Experimental Medicine and Biology 1124

Hikaru Hashitani
Richard J. Lang *Editors*

Smooth Muscle Spontaneous Activity

Physiological and Pathological Modulation

Springer

Advances in Experimental Medicine and Biology

Volume 1124

Advances in Experimental Medicine and Biology presents multidisciplinary and dynamic findings in the broad fields of experimental medicine and biology. The wide variety in topics it presents offers readers multiple perspectives on a variety of disciplines including neuroscience, microbiology, immunology, biochemistry, biomedical engineering and cancer research. *Advances in Experimental Medicine and Biology* has been publishing exceptional works in the field for over 30 years and is indexed in Medline, Scopus, EMBASE, BIOSIS, Biological Abstracts, CSA, Biological Sciences and Living Resources (ASFA-1), and Biological Sciences. The series also provides scientists with up to date information on emerging topics and techniques. 2017 Impact Factor: 1.760

More information about this series at http://www.springer.com/series/5584

Hikaru Hashitani • Richard J. Lang
Editors

Smooth Muscle Spontaneous Activity

Physiological and Pathological Modulation

Springer

Editors
Hikaru Hashitani
Nagoya City University
Nagoya
Aichi
Japan

Richard J. Lang
Monash University
Melbourne
VIC
Australia

ISSN 0065-2598 ISSN 2214-8019 (electronic)
Advances in Experimental Medicine and Biology
ISBN 978-981-13-5894-4 ISBN 978-981-13-5895-1 (eBook)
https://doi.org/10.1007/978-981-13-5895-1

This Springer imprint is published by the registered company Springer Nature Singapore Pte Ltd.
The registered company address is: 152 Beach Road, #21-01/04 Gateway East, Singapore 189721, Singapore

Preface

Over the last 50 years, there have been a series of books published on *Smooth Muscle* including *Smooth Muscle* (Bülbring et al. 1970); *The Physiology of Smooth Muscle* (Bülbring and Shuba 1976); *Smooth Muscle: An Assessment of Current Knowledge* (Bülbring et al. 1981); *Frontiers in Smooth Muscle Research* (Sperelakis and Wood 1989) and *Smooth Muscle Excitation* (Bolton and Tomita 1996). The early books were reviews written by research scientists that had an association with one of the pioneers of smooth muscle physiology, Professor Edith Bülbring, and the Department of Pharmacology, Oxford University, while the latter two books arose after international gatherings that recognised the distinguished contributions to smooth muscle physiology of Professor Emil Bolzer as well as the retirement of Professor Tadao Tomita.

Just as important, these books reflexed the application of the most up-to-date technology to smooth muscle research. *Smooth Muscle* (1970) and *The Physiology of Smooth Muscle* (1976) reviewed existing knowledge of the structure and innervation of smooth muscle, the acceptance of membrane potential recordings with 'sharp' microelectrodes, the ionic basis of the action potential, the interpretation of electrical waveforms using cable analysis of syncytia and their pharmacological modification upon drug application or nerve stimulation. *Smooth Muscle: An Assessment of Current Knowledge* (1981) expanded this ultrastructural and electrophysiological knowledge into investigations into the mechanisms of calcium control and agonist modulation of contraction. *Frontiers in Smooth Muscle Research* (1989) and *Smooth Muscle Excitation* (1996), arising from international meetings, tended to be more experimental rather than review in nature and somewhat broader in scope. *Frontiers in Smooth Muscle Research* (1989) focused more on the biochemistry of smooth muscle, including the mechanisms of excitation-contraction coupling, energetics, biochemistry of contractile proteins, ion pumping and IP_3 metabolism, while *Smooth Muscle Excitation* (1996) detailed the most recent findings upon the application of patch clamp technology and the fluorescent imaging of calcium to unravel the role of calcium stores, their mechanisms of release and influence on contraction and the membrane ion channels underlying the electrical activity, as well as the recognition that cells other than smooth muscle cells may be driving spontaneous contraction.

Our book was conceived to again present more extensive reviews of the major smooth muscles currently under study: airways, phasic and tonic

gastrointestinal muscles, upper and lower urinary tracts, various reproductive organs and vessels of the vasculature and lymphatics.

What is clear from the reviews herein is that there are very few smooth muscle syncytia that are in fact 'homocellular' and 'myogenic', as thought in the 1960s. Over the last 25 years, it has become evident that many smooth muscle organs contain syncytia that are 'heterocellular': smooth muscle and interstitial cells in the oviduct, prostate and urethra; the 'SIP' syncytium in the gastrointestinal tract; atypical/typical smooth muscle and interstitial cells in the renal pelvis; mucosa, interstitial and smooth muscle cells in the bladder and seminal vessels; endothelium and mural cells, i.e. vascular smooth muscle cells and pericytes, in arteries, veins and the microvasculature. In addition, the basic mechanisms of Ca^{2+} mobilisation, voltage-dependent and independent Ca^{2+} entry, internal store uptake and release of Ca^{2+} and Ca^{2+} extrusion/exchange pumps are coupled together in tissue-specific manners. It's the subtle variations in the combination of these mechanisms that are detailed in this book that establishes the unique functions of each smooth muscle organ.

This increase in complexity of cells present and their underlying mechanisms of rhythmicity reveals numerous new areas of investigation to accelerate our understanding of an individual smooth muscle's function and dysfunction, as well as to identify clinically relevant targets for pharmaceutical intervention. At present, there are numerous exciting gene-based techniques that are beginning to be applied to smooth muscle research, such as cell-specific expression of fluorescent marker proteins and the in situ visualisation and manipulation of cells, contraction or calcium using optogenetic techniques. Further transcriptome analyses of the molecular phenotype of the cells in particular smooth muscle organs will allow increasingly more cell-specific identification and mutation/knockin of channels or proteins using Cre-Lox genetic technology, even the time-determined in situ excitation/inhibition of particular cells with synthetic receptors that can be activated by unique ligands not found anywhere in the smooth muscle organ. All of these techniques will permit more sophisticated in situ investigations in animal models with engineered smooth muscle pathologies relevant to the human condition. This volume of reviews includes current knowledge obtained from the few early adopters of these genetic techniques based on their 'pre-genetic' investigations. It is hoped that the other reviews herein will also inform future research into the physiology and pathology of other spontaneously active smooth muscles.

Nagoya, Aichi, Japan — Hikaru Hashitani
Melbourne, VIC, Australia — Richard J. Lang
September 2018

Introduction

The gastrointestinal (GI) tract displays various motility patterns, in the form of wiggling, expansion or constriction, and thus their contractile behaviour is in marked contrast with the heart which develops highly-coordinated, rhythmic beating. Textbooks of physiology describe the contractile activity of the GI tract as peristalsis that can be further divided into several patterns such as pendulous, propulsive or segmenting movements. These GI tract movements have been considered myogenic in origin, i.e., arising from the smooth muscle wall. Pacemaker cells that drive the spontaneous contractile activity appear to be distributed within the musculature, either scattered or forming a network, since similar contractile activity can be seen in different segments of the GI tract. The complex movements in segments of the GI tract are really mysterious and have attracted the interest of many smooth muscle researchers. Such spontaneous movements can also be seen in other smooth muscle tissues, such as those in the urinary tract, genital or vascular systems. However, the origin and cellular mechanisms, and sometimes even their precise physiological function, have yet to be elucidated.

Professor Edith Bülbring at University Oxford, one of the pioneers of smooth muscle research, was fascinated by the spontaneous rhythmic activity in smooth muscle tissues. Her achievements in understanding the mechanisms underlying spontaneous activity in smooth muscle tissues were remembered, together with the summary of the physiological and pharmacological properties of smooth muscles, in a book titled "*Smooth Muscle*", which was written together with her students, A.F. Brading, A.W. Jones and T. Tomita nearly 50 years ago [1]. Initially, the generation of spontaneous activity in smooth muscle tissues was considered to be tightly linked with cellular metabolism, since the activity was highly sensitive to the temperature. As lowering the temperature slows or prevents spontaneous movements, the metabolic changes in the smooth muscle cells were thought to modulate ionic mechanisms such as action potentials or slow potential changes (slow waves) that underlie muscle contractions [2]. The 'metabolic theory' was more clearly interpreted by Golenhofen [3] as follows; 'the metabolic changes occurred within smooth muscle cells (basic activity) elicit mechanical activity termed "minute rhythm" in smooth muscle tissues, by generating membrane electrical activity, and in physiological conditions the "minute rhythm" is further modulated by neuronal and humoral factors such as autonomic nerves or hormones'.

The electrical events generated in the cell membrane, in association with the spontaneous movement of smooth muscle tissues, are either in the form of action potentials or slow waves. They were considered to be myogenic in origin, since the spontaneous activity could be modulated but not prevented, by chemicals which block the actions of any neural influences. Putative pacemaker cells were thought to distribute within the smooth muscle tissues rather heterogeneously, since spontaneously electrical activity varied in their form and properties in a region dependent manner [4, 5]. Many attempts had been made to identify the localization of pacemaker cells. One of the most remarkable experiments was carried out in the isolated dog intestine, in which the pacemaker cells were predominantly distributed in the myenteric layers [6]. Thus, in the obliquely cut edge of the intestinal wall, the largest electrical activity of smooth muscle cells was recorded in the region between the circular and longitudinal smooth muscle layers.

The notion that specialised smooth muscle cells, i.e. pacemaker cells, are distributed within the musculature and generate spontaneous electrical activity that passively propagates to neighbouring smooth muscle cells to depolarize their membranes, is not astounding. In the heart, it was clearly demonstrated that pacemaker cells within the sino-atrial node generate pacemaker potentials that spread along specialized conducting muscle bundles to drive cardiac muscle cells in the cardiac chambers [7]. Thus, prior to the book "*Smooth Muscle*", it appears that studies of pacemaker mechanisms in smooth muscle were interpreted using the existing knowledge of cardiac pacemaking mechanisms, presumably due to the difficulty in the precise analysis of the electrophysiological properties of smooth muscle cells [1].

An important turning point in the research of smooth muscle rhythmicity is the discovery of the intestinal motility disorders observed in *c-kit* signaling deficient mice or *W/Wv* mutant mice [8]. Dr. H. Maeda (Kumamoto University) and his colleagues originally aimed to develop animal models that were devoid of mast cells to facilitate the understandings of their role in immune protective mechanisms. They generated *c-kit* deficient mice using *c-kit* antibodies since mast cells require the expression of *c-kit* gene encoding tyrosine kinase at the cell membrane for their growth and maturation. Thus, the occurrence of intestinal motility disorders in these *c-kit* deficient or mutant mice was a rather accidental and fortuitous finding. Professor K. Nishi at the Pharmacology Department of Kumamoto University immediately recognized the importance of Maeda's finding, and started to investigate what was happening in these *c-kit* deficient or mutant mice (K. Nishi, personal communication). Professors K.M. Sanders (University of Nevada at Reno) and J.D. Huizinga (McMaster University) further advanced the research on the mutant mice, and found that the diseased intestine had a lack of a population of cells called interstitial cells of Cajal (ICC) within the GI tract wall. Eventually, it has been established that these cells might be the pacemaker cells driving the spontaneous GI motility [9].

Ten years before the discovery of the *c-kit* deficient or mutant mouse, the fundamental roles of ICC in generating spontaneous activity of the GI smooth muscle had already been proposed by L. Thuneberg in 1982 [10], based on the distribution and morphological characteristics of these cells. He found

that interstitial cells distributed at the myenteric layer of intestine were rich in mitochondria and were connected with each other as well as neighbouring smooth muscle cells via gap junctions. It has already been known that the spontaneous activity of excised GI smooth muscle tissues is maintained for several hours if they are placed in a balanced oxygenated physiological salt solution kept at an adequate temperature. It was therefore reasonable to assume the importance of mitochondria as a source of energy supply in maintaining the spontaneous activity, while gap junctional connections would allow propagation of electrical activity generated in ICC to the smooth muscles cells. This unique proposal by the anatomist, however, was not recognized for a decade by the majority of smooth muscle researchers. Using methylene blue staining, the distribution of these mitochondria-rich cells in the gut wall was originally described by the Spanish anatomist S.R. Cajal, as being unidentified cells, either primitive nerves or interstitial cells (Historic background of ICC is reviewed in detail by Komuro et al. [11]).

The symposium on smooth muscle, organized by Professors T.B. Bolton (University College London) and T. Tomita (Nagoya University) took place in April 1995 at Nagoya, Japan, shortly after the joint meeting between the 72nd Physiological Society of Japan and Physiological Societies of Great Britain and Eire held at Nagoya University. These two organizers were well-known researchers of smooth muscle, and the presentations were summarized in a book "*Smooth Muscle Excitation*" [12]. The symposium had two stages, the 1st stage held in Nagoya for a couple of days was formal in style, while the 2nd stage was held on the Izu peninsula, again for two days, in a rather informal style, after an enjoyable bus trip. An important aspect of the symposium, especially in the 2nd stage, was the invitation of young students to the meeting. The idea for having the symposium in such a unique style, mixing young students and established researchers together was proposed by Professor T. Tomita. Smooth muscle research is often tough, largely due to the technical difficulties involved, so that the collection of data is excruciatingly slow. Thus, smooth muscle research has not been particularly attractive to young students. Professor T. Tomita aimed to encourage young students to understand that smooth muscle is not just a "*headache muscle*", rather it is a very interesting frontier.

In this symposium, Professors K.M. Sanders and J.D. Huizinga introduced the role of ICC in the spontaneous activity of the GI smooth muscle tissues [13, 14]. Although the role of ICC as the pacemaker of spontaneous activity of gut had already been published [9, 15], their presentations and notions were novel to many of the smooth muscle researchers present. In the poster presentation at Nagoya, the interpretation of the structural characteristics of ICC was described by Professor L. Thuneberg. It was the first time that I met him, and I found immediately that he was a really serious scholar who quietly presented his fundamental findings.

Nevertheless, at that time, I had some doubts as to the idea that ICC are the pacemaker cells in intestinal smooth muscle tissues. To that point, electrical activity had only been recorded in the smooth muscle cells of the intestine and there had been no demonstrations of propagation of electrical signals between ICC and the muscle layer. My doubts were clearly dissolved by the

elegant experiments carried out by Professor G.D.S. Hirst (Melbourne University), who successfully identified electrical activity in both ICC and smooth muscle cells using dye-injection during their recordings. The 'driving potential' (also known as pacemaker potential) generated in ICC had very steep upstroke followed by long plateau component, a time course completely different from the slow wave recorded in smooth muscle cells. Simultaneous recordings of the spontaneous electrical activity in both ICC and neighbouring smooth muscle cells indicated that these two types of cells were electrically coupled, and that the driving potential invariably preceded slow wave [16]. These results clearly showed that slow waves recorded from smooth muscle cells were formed upon electrotonic spread of depolarizing potentials generated in ICC.

There are several subtypes of ICC distributed in the GI wall, and some of them are directly innervated by myenteric or autonomic nerves [11, 17]. These histological and ultrastructural characteristics of ICC and their neighbouring smooth muscle cells may facilitate further interpretation of their function and how they influence the electrical and mechanical properties of the various regions of the GI tract [1].

A group of researchers, who were interested in the properties of ICC held the 1st International Symposium on Interstitial Cells of Cajal (ICC) in Lorne, Australia, in December 2002 (organized by G.D.S. Hirst). Although spontaneous movements had been known in many types of smooth muscle tissues, the symposium mainly focused on the ICC in GI tract, since the pacemaking role of ICC was recognized only in GI muscles at that time. There were 11 speakers in the symposium, and all the topics were related on the properties of GI smooth muscles. Since then, similar symposia had been held every year. The initial 2 symposia included papers related exclusively to ICC in GI muscles. However, later symposia contained papers relating to a variety of smooth muscle tissues. At the 5th International Symposium on ICC, held in August 2007 at County Monaghan, Ireland (organizer: Professor Noel McHale at the Dundalk Institute of Technology), the papers presented included topics on the urinary tract (renal pelvis, urinary bladder, urethra), arteries, corpus cavernosum, biliary tract and uterus, in addition to ICC in GI tissues. The 6th International Symposium on ICC, held in February 2010 at Miyazaki, Japan (organizer H. Suzuki) covered even wider topics relating to ICC, such as their histological and histochemical characteristics, as well as pacemaker cells different from ICC, neural regulation of the activities of pacemaker cells, intracellular mechanisms for generating automatic activity in pacemaker cells, and ion channels contributing the generation of pacemaker activity.

Thus, spontaneous activity is observed in many types of smooth muscle tissues, and this book covers the properties of smooth muscle cells in the GI tract, urinary tract (bladder, urethra, renal pelvis, ureter), reproductive system (oviduct, uterus, prostate, seminal vesicle, cavernosal tissue), airways as well as blood and lymphatic vessels. Intrinsic activity is produced by ICC distributed in smooth muscles of the GI tract, while 'similar-looking' interstitial cells distributed in smooth muscles of the uro-genital organs may have other roles. In GI smooth muscle tissues, ICC are histochemically characterised by their expression of c-kit protein at the membrane [11]. However, similar

expression occurs in other types of cells such as mast cells, so that the tandem expression of other markers such as vimentin and anoctamin-1 (Ano1 or TMEM 16A) have been developed to more specifically identify ICC [11]. Thus, the presence of cells immuno-positive to these markers has been used to suggest that these cells are pacemakers in a number of smooth muscle organs. However, these suggestions appear somewhat premature. For example, in the upper urinary tract c-kit negative interstitial cells display rhythmic activity which modulates pacemaker activity generated by atypical smooth muscle cells [18] (Chap. 3). Uterine smooth muscle tissue is rather unique, although this tissue has a distribution of c-kit positive interstitial cells that are not rhythmically active. Their role has yet to be determined, but it has been suggested that they act as transducers of electrical signals between different regions of smooth muscle cells [19] and that some of the smooth muscles themselves act as the organ's pacemaker (Chap. 10). Interestingly, the involvement of ICC in the sphincter muscles of the GI tract, and their important role in maintaining the sustained contractions of these smooth muscles have been established (Chap. 2). Sustained contraction of smooth muscle cells is also known in the corpus cavernosum to maintain the penis in an flaccid condition, but in this case with there no involvement of ICC-like cells (Chap. 7). Thus, there seem to be a large divergence in the role of ICC or ICC-like cells in smooth muscle tissues, again highlighting that tissue-specificity is a significant feature of smooth muscle organs and that the results obtained in intestinal muscles are not always applicable to other smooth muscle tissues. These variations might be one of the characteristic features of smooth muscle tissue so that detailed analysis of individual tissues is required before a comprehensive understanding of their pacemaker mechanisms is obtained.

Associated with the confirmation of the histological properties of pacemaker cells in individual smooth muscle tissues, the cellular mechanism of the generation of pacemaker potential has also been given attention. Again, an understanding of the mechanisms in GI ICC is further advanced compared to pacemaker mechanisms in other types of smooth muscle tissue. Tokutomi et al. [20] first showed the possible involvement of Ca^{2+}-sensitive Cl^- current in the generation of pacemaker potentials in intestinal ICC. However, the contribution of Cl^--current was not initially accepted, because it was rather difficult to explain the data obtained in experiments using large tissue segments. The spontaneous electrical activity of smooth muscle in the guinea-pig stomach, for example, remained unaltered, or only slightly reduced, in solutions containing lowered Cl^- concentrations [4, 5]. In hindsight, it is now understood that the interpretation of experimental results using solutions with modified ionic compositions is difficult, due to the involvement of unexpected non-specific actions of the substitutions on the smooth muscle cells and/or ICC.

It is generally known that simplification of systems will facilitate the understanding of their mechanisms and experiments using single cells, or sometimes a piece of cell membrane, have been used extensively in the last 30 years, to study pacemaking mechanisms in smooth muscle and their pacemaker cells. Techniques developed also include the measurement of Ca^{2+}

dynamics in cells and their intracellular compartments such as sarcoplasmic reticulum or mitochondria, the activity of single ion channels distributed in the membranes of cell wall or cell organelles, structural modulation of ion channels by changing the sequence of amino acids of channel proteins, double staining of targeted cells with several protein specific antibodies, and more recently the transgenic modulation or identification of particular cell types. The analysis of the function of pacemaker cells using many of these "new" techniques will be found in chapters included in this book.

In isolated gastric muscle tissues of the guinea-pig, the co-ordination between an elevation of intracellular Ca^{2+} concentration in ICC and the generation of a pacemaker potential in ICC was clearly shown by Hirst et al. [21]. Possible involvement of inositol trisphosphate (IP_3) in the initial steps of the generation of pacemaker potential was also suggested in the stomach, where gastric muscles isolated from IP_3-receptor knock-out mice did not display slow waves [22]. It was speculated that the periodical production of IP_3 triggers the release of tiny packets of Ca^{2+} from the internal stores, and this local elevation of intracellular Ca^{2+} activates Cl^- channels to elicit a transient depolarization of the membrane, called unitary potentials [16], or spontaneous transient depolarizations (STDs) as observed in lymphatic tissues [23]. When the amplitude of summed STDs or unitary potentials exceeds the threshold level for the activation of T-type Ca^{2+} channels, a driving (or pacemaker) potential is generated in ICC. These processes were proposed over 15 years ago [24], and although additional data may be required for a fuller interpretation of the ICC pacemaker mechanisms of ICC, this initial observation still seems to be relevant in the understanding of spontaneous electrical activity in intestinal smooth muscle tissues. Of course, now the mechanisms of the spontaneous movements of smooth muscle tissues is being examined in more detail at sub-cellular levels which are also described in some chapters in this book. The authors of each chapter of this book are all well-established researchers in their field and leading experts in the function of the smooth muscle tissue/organs they study.

Our understandings on the cellular mechanism of spontaneous movements in smooth muscle tissues has thus greatly improved since the discovery of the pivotal role of ICC as the pacemaker cells in the GI tract. Readers of this book, however, will also find that ICC have multiple roles, such as pathways of low resistance conduction between ICC themselves and neighbouring smooth muscle cells, intermediaries of neural signals from myenteric or autonomic nerves to smooth muscle cells, or acting as mechanical sensors of stretch in the GI wall. In other smooth muscle tissues such as urogenital organs, lymphatic vessels or reproductive organs, it is less likely that groups of cells having histological or histochemical similarities to ICC are undertaking a pacemaker role driving spontaneous contractile activity. Moreover, it remains to be determined whether these cells have roles other than pacemaking, as do ICC in the GI tract. Many smooth muscle tissues distributed in urogenital organs are known to be sensitive to factors such as hormones, while their intrinsic activity also changes depending on their physiological conditions. One typical examples can be found in uterine smooth muscle, where the spontaneous irregular activity of the smooth muscle wall in

non-pregnant rats is changed to a periodical generation of burst of spikes during pregnancy [25]. Most smooth muscle tissues also change their spontaneous activity in response to the hormonal and humoral conditions, and it remains unclear whether these changes include their pacemaker cells directly or indirectly through the change in the properties of their smooth muscle cells. Thus, there are a lot of questions to be solved, and I presume many of them will be clarified soon. I am confident that the contents of this book will greatly advance the understanding of smooth muscle function and encourage further analysis of the remaining mysteries underlying smooth muscle rhythmicity.

References

1. Bürbling E, Brading AF, Jones AW, Tomita T. Smooth muscle. London: E. Arnold; 1970.
2. Bozler E. Conduction, automaticity and tonus of visceral muscles. Experientia. 1948;4:213–8.
3. Golenhofen K. Slow rhythms in smooth muscle (minute-rhythm). In: Bürbling E, Brading AF, Jones AW, Tomita T, editors. Smooth muscle. London: E. Arnold; 1970. p. 316–42.
4. Kuriyama H. Effects of ions and drugs on the electrical activity of smooth muscle. In: Bürbling E, Brading AF, Jones AW, Tomita T, editors. Smooth muscle. London: E. Arnold; 1970. p. 366–95.
5. Tomita T. Electrical properties of mammalian smooth muscle. In: Bürbling E, Brading AF, Jones AW, Tomita T, editors. Smooth muscle. London: E. Arnold; 1970. p. 197–243.
6. Hara Y, Kubota M, Szurszewski JH. Electrophysiology of smooth muscle of the small intestine of some mammals. J Physiol. 1986;372: 501–20.
7. Noble D. The initiation of the heartbeat. Oxford: Oxford University Press; 1975.
8. Maeda H, Yamagata A, Nishikawa S, Yoshinaga K, Kobayashi S, Nishi K, Nishikawa S. Requirement of c-kit for development of intestinal pacemaker system. Development. 1992;116:369–75.
9. Ward SM, Burns AJ, Torihashi S, Sanders KM. Mutation of the proto-oncogene *c-kit* blocks development of interstitial cells and electrical rhythmicity in murine intestine. J Physiol. 1994;480:91–7.
10. Thuneberg L. Interstitial cells of Cajal: intestinal pacemaker cells? Adv Embryol Cell Biol. 1982;71:1–130.
11. Komuro T, Tokui K, Zhou DS. Identification of the interstitial cells of Cajal. Histol Histopathol. 1996;11:769–86.
12. Bolton TB, Tomita T. Smooth muscle excitation. London: Academic Press; 1996.
13. Sanders KM, Ward SM. Electrical rhythmicity in gastrointestinal muscles. In: Bolton TB, Tomita T, editors. Smooth muscle excitation. London: Academic Press; 1996. p. 417–26.
14. Huizinga JD, Liu LW, Malysz J, Lee JCF, Das S, Farraway L. Interstitial cells of Cajal as pacemaker cells of the gut. In: Bolton TB, Tomita T, edi-

tors. Smooth muscle excitation. London: Academic Press; 1996. p. 417–26.
15. Huizinga JD, Thuneburg L, Kluppel M, Malysz J, Mikkelsen HB, Bernstein A. W/kit gene required for intestinal pacemaker activity. Nature. 1995;373:347–9.
16. Dickens EJ, Hirst GDS, Tomita T. Identification of rhythmically active cells in guinea-pig stomach. J Physiol. 1999;514:515–31.
17. Komuro T, Seki K, Horiguchi K. Ultrastructural characterization of the interstitial cells of Cajal. Arch Histol Cytol. 1999;62:295–316.
18. Hashitani H, Nguyen M, Noda N, Mitsui R, Higashi R, Ohta K, Nakamura K-I, Lang RJ. Interstitial cell modulation of pyeloureteric peristalsis in the mouse renal pelvis examined using FIBSEM tomography and calcium indicators. Pflugers Arch. 2017;469:797–813.
19. Parkington HC, Tonta MA, Iqbal J, Sheehan PM, Lang RJ, Coleman HA. Co-ordinating contraction in the pregnant uterus. In: Abstract of the 6th international symposium on ICC, Smooth muscle rhythms, Miyazaki.
20. Tokutomi N, Maeda H, Tokutomi Y, Sato D, Sugita M, Nishikawa S, Nakao J, Imamura T, Nishi K. Rhythmic Cl^- current and physiological roles of the intestinal *c-kit* positive cells. Pflügers Arch. 1995;431:169–77.
21. Hirst GDS, Bramich NJ, Teramoto N, Suzuki H, Edwards FR. Regenerative component of slow waves in the guinea-pig gastric antrum involves a delayed increase in $[Ca^{2+}]_i$ and Cl^- channels. J Physiol. 2002;540:907–19.
22. Suzuki H, Takano H, Yamamoto Y, Komuro T, Saito M, Kato K, Mikoshiba K. Properties of gastric smooth muscles obtained from mice which lack inositol trisphosphate receptors. J Physiol. 2000;525:105–11.
23. van Helden DF. Pacemaker potentials in lymphatic smooth muscle of the guinea-pig mesentery. J Physiol. 1993;471:465–97.
24. Kito Y, Suzuki H. Electrophysiological properties of gastric pacemaker potentials. J Smooth Muscle Res. 2003;39:163–73.
25. Kuriyama H, Suzuki H. Changes in electrical properties of rat myometrium during gestation and following hormonal treatments. J Physiol. 1976;260:315–33.

Nagoya, Japan Hikaru Suzuki

Contents

Contributors

Jane E. Bourke Department of Pharmacology, Biomedicine Discovery Institute, Monash University, Clayton, VIC, Australia

Andrew P. Braun Department of Physiology and Pharmacology, Libin Cardiovascular Institute, Cumming School of Medicine, University of Calgary, Calgary, AB, Canada

Theodor Burdyga Department of Cellular and Molecular Physiology, Institute of Translational Medicine, University of Liverpool, Liverpool, UK

Basu Chakrabarty Drug Discovery Biology, Monash Institute of Pharmaceutical Sciences, Melbourne, VIC, Australia

Caroline Cobine Department of Physiology and Cell Biology, University of Nevada, Reno School of Medicine, Reno, NV, USA

William C. Cole Department of Physiology and Pharmacology, Libin Cardiovascular Institute, Cumming School of Medicine, University of Calgary, Calgary, AB, Canada

Rose E. Dixon Department of Physiology and Membrane Biology, School of Medicine, Tupper Hall, University of California, Davis, Davis, CA, USA

Betty Exintaris Drug Discovery Biology, Monash Institute of Pharmaceutical Sciences, Melbourne, VIC, Australia

Christopher H. Fry School of Physiology, Pharmacology and Neuroscience, University of Bristol, Bristol, UK

Grant R. Gordon Department of Physiology and Pharmacology, Libin Cardiovascular Institute, Cumming School of Medicine, University of Calgary, Calgary, AB, Canada

Hikaru Hashitani Department of Cell Physiology, Graduate School of Medical Sciences, Nagoya City University, Nagoya, Japan

Tokumasa Hayashi Department of Urology, Kurume University School of Medicine, Kurume, Japan

Mark A. Hollywood Smooth Muscle Research Centre, Dundalk Institute of Technology, Dundalk, Co. Louth, Ireland

Sung Jin Hwang Department of Physiology and Cell Biology, University of Nevada, Reno School of Medicine, Reno, NV, USA

Mohammad S. Imtiaz Department of Electrical and Computer Engineering, Bradley University, Peoria, IL, USA

Kathleen Keef Department of Physiology and Cell Biology, University of Nevada, Reno School of Medicine, Reno, NV, USA

Bo Hyun Kim Department of Physiology and Cell Biology, University of Nevada, Reno School of Medicine, Reno, NV, USA

Maggie Lam Department of Pharmacology, Biomedicine Discovery Institute, Monash University, Clayton, VIC, Australia

Emma Lamanna Department of Pharmacology, Biomedicine Discovery Institute, Monash University, Clayton, VIC, Australia

Richard J. Lang School of Biomedical Sciences, Faculty of Medicine, Nursing and Health Sciences, Monash University, Clayton, VIC, Australia

Sophie Lee Drug Discovery Biology, Monash Institute of Pharmaceutical Sciences, Melbourne, VIC, Australia

Karen D. McCloskey School of Medicine, Dentistry and Biomedical Sciences, Queen's University Belfast, Belfast, UK

Retsu Mitsui Department of Cell Physiology, Graduate School of Medical Sciences, Nagoya City University, Nagoya, Japan

Clodagh Prendergast Department of Cellular and Molecular Physiology, Harris-Wellbeing Preterm Birth Centre, Institute of Translational Medicine, University of Liverpool, Liverpool, UK

Kenton M. Sanders Department of Physiology and Cell Biology, University of Nevada, Reno School of Medicine, Reno, NV, USA

Gerard P. Sergeant Smooth Muscle Research Centre, Dundalk Institute of Technology, Dundalk, Co. Louth, Ireland

Hikaru Suzuki Department of Cell Physiology, Graduate School of Medical Sciences, Nagoya City University, Nagoya, Japan

Makoto Takano Division of Integrated Autonomic Function, Department of Physiology, Kurume University School of Medicine, Kurume, Japan

Mitsue Takeya Division of Integrated Autonomic Function, Department of Physiology, Kurume University School of Medicine, Kurume, Japan

Keith D. Thornbury Smooth Muscle Research Centre, Dundalk Institute of Technology, Dundalk, Co. Louth, Ireland

Dirk F. van Helden Faculty of Health and Medicine, School of Biomedical Sciences and Pharmacy, University of Newcastle, Newcastle, NSW, Australia

Pierre-Yves von der Weid Department of Physiology and Pharmacology, Inflammation Research Network and Smooth Muscle Research Group, Snyder Institute for Chronic Diseases, Cumming School of Medicine, University of Calgary, Calgary, AB, Canada

Sean M. Ward Department of Physiology and Cell Biology, University of Nevada, Reno School of Medicine, Reno, NV, USA

Susan Wray Department of Cellular and Molecular Physiology, Harris-Wellbeing Preterm Birth Centre, Institute of Translational Medicine, University of Liverpool, Liverpool, UK

Part I

Gastrointestinal Tract

1 Spontaneous Electrical Activity and Rhythmicity in Gastrointestinal Smooth Muscles

Kenton M. Sanders

Abstract

The gastrointestinal (GI) tract has multifold tasks of ingesting, processing, and assimilating nutrients and disposing of wastes at appropriate times. These tasks are facilitated by several stereotypical motor patterns that build upon the intrinsic rhythmicity of the smooth muscles that generate phasic contractions in many regions of the gut. Phasic contractions result from a cyclical depolarization/repolarization cycle, known as electrical slow waves, which result from intrinsic pacemaker activity. Interstitial cells of Cajal (ICC) are electrically coupled to smooth muscle cells (SMCs) and generate and propagate pacemaker activity and slow waves. The mechanism of slow waves is dependent upon specialized conductances expressed by pacemaker ICC. The primary conductances responsible for slow waves in mice are Ano1, Ca^{2+}-activated Cl^- channels (CaCCs), and $Ca_V3.2$, T-type, voltage-dependent Ca^{2+} channels. Release of Ca^{2+} from intracellular stores in ICC appears to be the initiator of pacemaker depolarizations, activation of T-type current provides voltage-dependent Ca^{2+} entry into ICC, as slow waves propagate through ICC networks, and Ca^{2+}-induced Ca^{2+} release and activation of Ano1 in ICC amplifies slow wave depolarizations. Slow waves conduct to coupled SMCs, and depolarization elicited by these events enhances the open-probability of L-type voltage-dependent Ca^{2+} channels, promotes Ca^{2+} entry, and initiates contraction. Phasic contractions timed by the occurrence of slow waves provide the basis for motility patterns such as gastric peristalsis and segmentation. This chapter discusses the properties of ICC and proposed mechanism of electrical rhythmicity in GI muscles.

Keywords

Interstitial cells of Cajal · Pacemaker · Ca^{2+} transient · Slow wave · SIP syncytium · ANO1 channels · T-type Ca^{2+} channels · Electrophysiology · Gastrointestinal motility

1.1 Introduction

GI smooth muscles are complex tissues composed of multiple cell types. Smooth muscle cells (SMCs) provide the motor responsible for force development and movement of nutrients and waste products, but at least two additional types of cells, known as interstitial cells, are electrically coupled to SMCs and provide moment-to-moment modulation of SMC excitability.

K. M. Sanders (✉)
Department of Physiology and Cell Biology, University of Nevada, Reno School of Medicine, Reno, NV, USA
e-mail: ksanders@medicine.nevada.edu

H. Hashitani, R. J. Lang (eds.), *Smooth Muscle Spontaneous Activity*, Advances in Experimental Medicine and Biology 1124, https://doi.org/10.1007/978-981-13-5895-1_1

Together with SMCs, interstitial cells of Cajal (ICC) and platelet-derived growth factor receptor α positive (PDGFRα$^+$) cells form a multicellular syncytium known as the SMC, ICC, and PDGFRα$^+$ cell (SIP) syncytium [1]. SIP cells each express intrinsic electrophysiological mechanisms and a variety of receptors for neurotransmitters, hormones, paracrine substances, and inflammatory mediators. SIP cells are innervated by enteric motor neurons and receive and transduce neurotransmitter signals. The integrated output of the SIP syncytium sets the moment-to-moment excitability of SMCs [2]. The contractile behavior in most smooth muscle regions of the GI tract is phasic in nature, consisting of a rhythmic contraction-relaxation cycle. Phasic contractions are the basis for the major motility patterns of the GI tract, such as segmentation and peristalsis, and the phasic nature of contractions is intrinsic to the muscle tissues. Phasic contractions of smooth muscle cells (SMCs) are driven by electrical slow waves, which are generated by ICC [3–5]. There are several types of ICC present in the GI tracts of mammals and humans. Common nomenclature used to identify the different classes of ICC and categorize their functions is provided in Table 1.1.

ICC are organized into networks in the pacemaker regions of the GI tract. Once a slow wave is generated, it regenerates cell to cell, propagating actively through the ICC network. Slow waves conduct passively into SMCs, because SMCs do not express the unique conductances that contribute to slow waves and therefore have no means for their regeneration (i.e., depolarization of a SMC does not produce a slow wave-like event). Depolarization of SMCs by slow waves enhances the open-probability of L-type voltage-

Table 1.1 Nomenclature for ICC in the GI tract

Anatomical location	Common name	Organ distribution	Functions
Plane of the myenteric plexus between circular and longitudinal muscle layers	ICC-MY[a]	STM, SI, CLN	Pacemaker activity, innervated by motor neurons in CLN
Intramuscular localization, within muscle bundles and in close contact with varicose processes of enteric motor neurons	ICC-IM[b]	ESG (smooth muscle portion), STM, SI, CLN	Express receptors for and provide transduction for neurotransmitters released by enteric motor neurons; mediators of responses to stretch
Intramuscular-type ICC within plane of the deep muscular plexus in small intestine	ICC-DMP[c]	SI	Express receptors for and provide transduction for neurotransmitters released by enteric motor neurons
Submucosal border of circular muscle layer	ICC-SM	CLN, STM	Pacemaker activity in CLN; limited number of cells in STM and function of STM cells unknown
Serosal surface of longitudinal muscle layer	ICC-SS	CLN	Unknown function at present time
Septal spaces between muscle bundles in larger animals	ICC-SEP	STM, SI, CLN	Appear to be extensions of ICC-MY or ICC-SM networks and actively propagate slow waves in thicker GI muscles of large mammals and humans

Organ abbreviations: Esophagus (ESG); stomach (STM); small intestine (SI); colon (CLN)

[a]Also referred to as ICC-MP by some authors, but this is misleading because these cells do not penetrate and are not part of the myenteric plexus. They are distributed around the ganglia and tertiary plexus

[b]Some authors have broken this term down to specify in which muscle layer the cells are found (e.g., ICC-CM for cells in the circular muscle layer and ICC-LM for cells in the longitudinal muscle layer). Since no functional differences have been reported for the cells in these different locations, the term ICC-IM is used throughout this chapter

[c]ICC-DMP are most likely the ICC-IM of the small intestine. They show a distinctive localization in laboratory animals and have received considerable experimental attention, so they are designated separately. Larger animals tend to have ICC-IM distributed through the circular muscle layer, as observed in the stomach and colon of laboratory animals.

dependent Ca^{2+} channels that are ubiquitously expressed in GI SMCs. In some SMCs of the small bowel and colon activation of L-type Ca^{2+} channels results in generation of Ca^{2+} action potentials, which are superimposed upon the peaks of slow waves. In the stomach slow waves depolarize SMCs but action potentials are not typically generated. In either case Ca^{2+} entry into SMCs initiates contraction (excitation-contraction coupling), and in both cases the slow wave depolarization/repolarization cycle determines the period of enhanced open probability of L-type Ca^{2+} channels in SMCs (contraction) and the period of time in which Ca^{2+} channel open probability is low (relaxation). This chapter discusses the characteristics of slow waves in GI muscles, the apparatus required for slow waves, the mechanism of slow wave generation and propagation, and how nerves and other factors influence cells of the SIP syncytium to increase or decrease the gain for excitation-contraction coupling. It should also be noted that in some regions of the GI tract, such as the internal anal sphincter [6], slow waves occur at sufficient frequencies to cause summation of cytoplasmic Ca^{2+} and tonic contraction (similar to a partial tetanus), but this topic is covered in another chapter.

1.2 Nature of Electrical Rhythmicity in GI Smooth Muscles

Contractile rhythmicity in GI organs was likely recognized as soon as the abdomens of freshly killed animals were sliced open. Gut motility persists for various periods of time after the death of an animal because it is not driven by circulating factors in blood or by neural input from the central or enteric nervous systems. The basic motility patterns are intrinsic to the cells and tissues of the *tunica muscularis*, and cells of the SIP syncytium appear to be rather resistant to the hypoxia that rapidly kills the heart and brain. Placing metal electrodes on organs of the gut allowed electrical recording of gut activity nearly 100 years ago [7, 8], but it is likely that these recordings were heavily contaminated by movements. At the time of the initial recordings the electrophysiological basis for muscle contraction was unknown, and it was not possible to block movements independently of upstream mechanisms. Therefore, we have no way of knowing whether the first electrical recordings of GI muscle activity contained electrophysiological information (i.e., events based on changes in transmembrane potentials in cells within the muscles or organs) or were "biopotentials" resulting from muscle movements [9]. Better techniques developed with time, such as sucrose gap, which was a means of obtaining pseudo-transmembrane potential recording, provided valuable information about the waveforms of electrical slow waves in the gut [10, 11]. Voltage-clamping of GI muscle strips was attempted with sucrose gaps, and several ideas about the mechanism of slow waves were developed based on these experiments [12, 13]. However, true voltage-control (and space clamp) of the many electrically coupled cells in the SIP syncytium may have been difficult to accomplish with this approach.

Eventually cell impalement techniques were adopted to directly measure transmembrane potential in a dynamic manner [14–17]. Small SMCs are difficult to impale, and impalements of cells among moving muscle cells are difficult to maintain, but this technique provided, and still provides, the most accurate means of measuring resting membrane potentials, slow waves, and action potentials in intact muscles (Fig. 1.1). Microelectrode studies allowed investigators to better understand the ionic mechanisms that cause slow waves, the responses to neurotransmitters, and the effects of bioactive compounds. Information obtained from these recordings is dependent upon many voltage- and non-voltage-dependent and receptor-operated ion channels expressed in cells of the SIP syncytium [18]. It remains technically difficult to voltage-clamp intact GI muscles, except perhaps with small bundles of cells, as used by David Hirst and collaborators in many studies of smooth muscle tissues [19–21]. It should be reemphasized that GI muscles are syncytial in nature, and the complete syncytium (SIP syncytium) contains SMCs, ICC, and PDGFRα^{+} cells [1]. Thus, intracellular record-

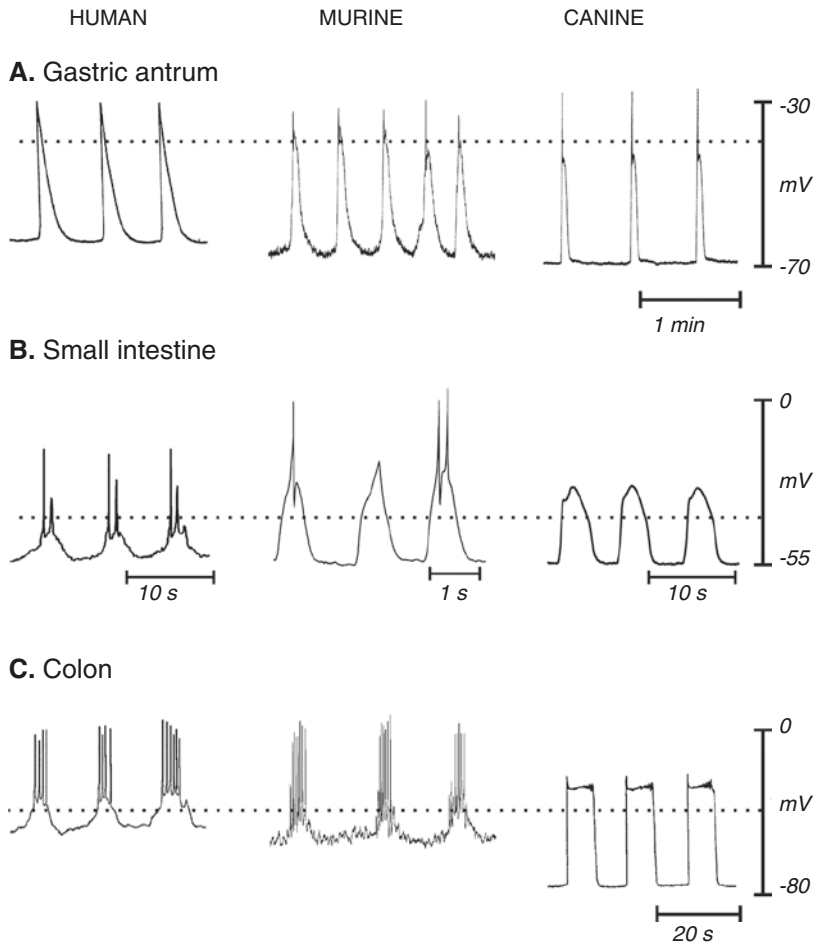

Fig. 1.1 Electrical activity recorded from stomach, small bowel, and colon of three species. Recordings were made with intracellular microelectrodes from the circular muscle layers of isolated strips of muscle from the antrum, ileum or jejunum and proximal colon. The major features of electrical activity that vary in waveform in different regions of the GI tract and in different species are displayed. From a relatively stable membrane potential between slow waves (resting membrane potential), a sharp upstroke depolarization occurs when a propagating slow wave reaches the point of recording. The upstroke typically repolarizes quickly to a pseudo-stable plateau potential that can last for several seconds before repolarization to the resting potential. Resting potentials vary, making it necessary for slow waves in different regions to depend upon different voltage-dependent Ca^{2+} channels to carry the main current during the upstroke (see text for details). The plateau potential depends upon sustained activation of Ano1 channels that are activated by Ca^{2+} release events in the ER of ICC. In some regions slow waves initiate Ca^{2+} action potentials in SMCs. These are initiated in the small bowel and colon when the depolarization reaches about −40 mV (dotted lines in each panel). Ca^{2+} action potentials are superimposed upon the slow wave plateau phase. Slow waves with or without superimposed action potentials generate phasic contractions. Copied with permission from [2]

ing from a single cell within the SIP syncytium is complex and contains membrane potential information not only from the impaled cell but also from electrically coupled cells. The complexity of the SIP syncytium was unknown to investigators during the early use of both sucrose gap and intracellular microelectrode recording, and several behaviors believed to be intrinsic to SMCs are now known to originate in cells other than SMCs (e.g., slow waves, fast (purinergic) inhibitory junction potentials, cholinergic excitatory junction potentials (EJPs); see [4, 5, 22, 23]).

1.2.1 Terminology Used for Rhythmic Electrical Potentials in GI Muscles

Electrical rhythmicity in GI muscles has been given many terms throughout the history of electrical recording, including pacesetter potentials [24], pacemaker potentials [25], electrical control activity [15, 26], basic electrical rhythm (BER) [27], slow waves [28], and action potentials [16, 29]. Recognizing the syncytial connectivity between SMCs and ICC, David Hirst and coworkers developed even more specific terminology, with different terms applied to slow waves recorded from different cell types [30–32]. For example, events recorded from SMCs of the circular muscle of the guinea pig antrum were called slow waves, events recorded from ICC in proximity to myenteric plexus (ICC-MY) were referred to as driving potentials, and those recorded from the longitudinal muscle were called follower potentials. Use of specific terms to distinguish events in different cells may be more precise, because depolarization of SMCs activates local voltage-dependent conductances that sculpt waveforms into voltage transients with unique profiles. However, since all of these events originate from a common source in a given tissue [2, 3, 5, 33–35], we prefer to use the term *slow waves* because this is the common term used in the modern literature.

1.2.2 Waveform Features of Electrical Slow Waves

Slow waves have two basic components that have been given various descriptive terms by different authors, and the two components have been attributed to a variety of mechanisms. This review will focus mainly on recent information and not address the many mechanisms proposed in older studies or in older reviews [12, 36, 37]. In Tadao Tomita's concept, the first component of the slow wave was the driving potential that propagates through the tissue. The second component was called the regenerative potential and was thought to be initiated locally by the depolarization caused by the driving potential. The second component was later thought to result from activation of conductances in intramuscular interstitial ICC (ICC-IM) [33, 38]. In Joseph Szurszewski's concept, the first and second components were termed the upstroke depolarization and plateau potential, respectively. These events have now been attributed to specific conductances expressed by ICC and will be described in greater detail later in this review.

Slow waves occur without inputs from nerves, hormones, or paracrine substances in GI muscles, and therefore these muscles are referred to as autonomous and slow waves as myogenic. Slow waves occur for many hours in vitro and persist in isolated muscles for many days in organotypic cultures [39]. The slow wave cycle typically contains a period of relatively stable resting potential (aka diastolic period or period of most negative membrane potential), although a gradual, inter-slow wave depolarization is observed in some intracellular electrical recordings. In most cases recordings from cells in intact muscle strips represent propagating slow waves, so there is only a brief exponential foot before development of the upstroke potential [16]. When recordings are made from impalements of SMCs the upstroke potential occurs at a maximum of about 1 V/s, but in many regions of muscle the upstroke velocity of slow waves in SMCs is only about 100 mV/s. The upstroke depolarization is transient, and after reaching a peak, partial repolarization occurs before a pseudo-stable state known as the plateau phase is reached [16]. The plateau phase can last from a second to many seconds depending upon the region of the GI tract and species [36]. Membrane potential eventually escapes from the plateau phase, and repolarization causes restoration of the resting potential, thus completing the cycle. Slow wave frequency varies from up to 80 cycles per minute, in phasic muscles that utilize summation of excitable events to generate tone [40], to just a few events per minute in muscles with well-defined phasic contractions. Slower frequencies allow complete relaxation between contractions and/or time for propulsive events to propagate for many cm. Frequency is an important parameter of slow

wave activity because regional sites of pacemaker dominance resides in cells that generate the highest frequency of pacemaker activity. The factors that set slow wave frequency and why and how frequencies change in disease states are poorly understood at the present time. However, this is an important area of investigation for future studies because abnormal frequencies, generation of ectopic pacemakers (emergence of atypical dominant pacemaker sites), breakdown in natural frequency gradients, and lack of ability of the normal dominant pacemaker region to drive slow waves downstream appear to be fundamental to GI motility disorders, such as gastroparesis [41–43].

The vast majority of intracellular electrical recordings reported in the literature have been made by impalement of SMCs, but a few skilled investigators have impaled ICC directly to obtain first-hand recordings of pacemaker activity. For example, cells were impaled in guinea pig gastric muscles, and the majority of cells were identified as SMCs by dye injection [34]. Occasionally, slow waves with much faster upstroke depolarizations and greater maximal levels of depolarization were observed in impaled cells and called driving potentials. Lucifer yellow or neurobiotin injection during recording showed that driving potentials originated in ICC. Recordings were also made by impalements of SMCs and ICC simultaneously [33, 34]. These recordings clearly showed that initiation of slow waves (aka driving potentials; with greater total amplitude and upstroke velocities) occurred in ICC, and lower amplitude events with reduced upstroke velocities occurred in SMCs (Fig. 1.2). Coupling between ICC-MY and SMCs in both the circular and longitudinal muscle layers was also investigated by simultaneous impalements, and these experiments showed strong coupling between cells of a given type, but far weaker coupling between ICC-MY and SMCs. A lower level of coupling between ICC-MY and SMCs is an important property, allowing conservation of current within an ICC-MY network to facilitate generation of slow waves and active propagation while still permitting enough current to pass to SMCs to depolarize these cells.

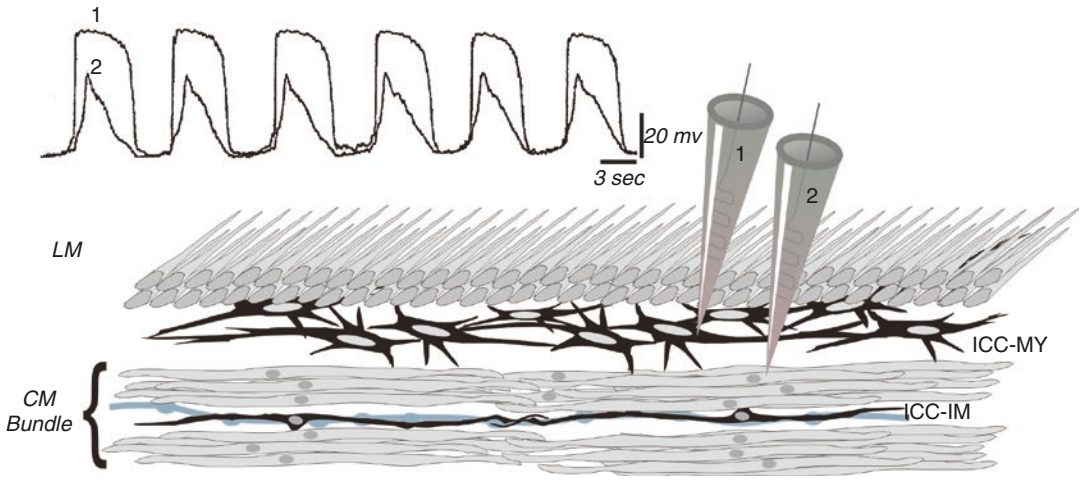

Fig. 1.2 Simultaneous recording from ICC-MY and SMC. Recording from ICC-MY and SMCs simultaneously shows that the upstroke of slow waves originates in ICC-MY and conducts with decrement to electrically coupled SMCs. The conductances present in SMCs cannot support active propagation of slow waves in these cells; however, the depolarization can activate other voltage-dependent conductances that support contractions (L-type Ca^{2+} channels and shape the slow wave; various voltage-dependent K^+ channels). The peak of the slow wave reaches about −10 mV (approximately the equilibrium potential for Cl^- ions) and is relatively constant for durations of a second or more. Anatomical drawing depicts circular (CM) and longitudinal (LM) muscle layers, ICC-MY in a network between CM and LM, and ICC-IM, lying in close apposition to an enteric motor neurons (gray varicose process). Redrawn from [2], and original data was provided by Professor David Hirst

Direct recordings from ICC-MY in the small intestine from two species have also been reported [44–47]. These studies investigated the ionic conductances responsible for the upstroke and plateau phases of slow waves. As in studies of gastric cells, impalements were validated by injection of Lucifer Yellow during recording. Slow waves in ICC-MY of the murine small intestine also were found to be more robust than in SMCs, having upstroke velocities (*dV/dt*) of approximately 2 V/s, amplitudes of more than 60 mV, and maximal depolarizations to about −10 mV at their apexes. Nifedipine did not affect the upstrokes or frequency of slow waves, but Ni^{2+} slowed the rate of the upstroke depolarization and reduced slow wave frequency. Mibefradil, a T-type Ca^{2+} channel antagonist, also reduced *dV/dt* of the upstroke depolarization and reduced slow wave frequency. In the presence of mibefradil, the period of the inter-slow wave interval increased and a greater depolarization level was required before the threshold for slow wave generation was reached. During the slow depolarization, small oscillations in membrane potential were noted. Pinacidil, an ATP-dependent K channel (K_{ATP}) agonist that elicits strong hyperpolarization of GI SMCs [48], also hyperpolarized ICC-MY, but failed to inhibit slow wave activity. In fact the maximum amplitude of slow waves in ICC-MY increased in the presence of pinacidil, and depolarization to approximately the same maximum point (about −10 mV) occurred. DIDS, a Cl^- conductance antagonist, and reduced extracellular [Cl^-] reduced the plateau phase. High enough concentrations of DIDS or T-type Ca^{2+} channel antagonists or membrane-permeable Ca^{2+} chelators (BAPTA-AM or MAPTA-AM) blocked slow wave activity [31, 45]. The actions of the Ca^{2+} chelators suggest that the Cl^- conductance may be due to Ca^{2+}-activated Cl^- channels (CaCCs). Taken together, these observations suggested that the upstroke potential depends upon a T- type Ca^{2+} conductance and the plateau potentials depend upon a Cl^- conductance.

As in mice, the upstroke depolarization of slow waves in ICC-MY of the rabbit small intestine were unaffected by nifedipine, but there were also interesting differences in the electrical events recorded from rabbit ICC-MY. The upstroke velocities of rabbit slow waves reached 10 V/s, and the events were reduced somewhat by Ni^{2+} and by leaving Ca^{2+} out of the extracellular solution [49]. These data suggest that the upstroke depolarization in rabbit slow waves is only partially mediated by Ca^{2+} influx, and the inward current is much less sensitive to block by Ni^{2+} than in mouse. Replacement of $[Ca^{2+}]_o$ with $[Sr^{2+}]_o$ in rabbits enhanced upstroke depolarization velocity but reduced the amplitude and duration of the plateau phase. Thus, Sr^{2+} appears to be an effective charge carrier for the upstroke conductance, but less effective in activating CaCCs. DIDS, cyclopiazonic acid and bumetanide, an inhibitor of the $Na^+K^+Cl^-$ co-transporter (NKCC1), also reduced the amplitude and duration of plateau potentials. In both rabbit and mouse Ca^{2+} free solution and replacement of Ca^{2+} with Sr^{2+} reduced the frequency of slow waves dramatically. These data generally supported the mechanism proposed for slow waves in the mouse small intestine, but the differences observed suggest that conductances involved in slow waves may vary from species to species.

1.2.3 Origination of Pacemaker Activity

Discussions about pacemaker sites in the GI tract often refer to the location of the dominant pacemaker in GI organs. For example, the dominant, organ-level pacemaker region in the stomach drives gastric peristalsis, resulting in propagation of slow waves and contractions from the proximal corpus to the pyloric sphincter [50]. A more specific question about pacemaker regions in GI muscles relates to the local source of pacemaker activity. Muscles removed from phasic regions of the GI track display intrinsic pacemaker activity. Within segments of muscle no specific pacemaker site appears to be dominant and the point of origin of slow waves shifts from cycle to cycle [51]. Dissection experiments, in which muscle strips are split in various ways, reveal dominant planes of activity through the thickness of the *tunica muscularis*. With this approach the

dominant pacemaker in canine gastric antral muscles was found to reside in the myenteric region. Even in small muscle strips containing the myenteric plexus region, pacemaker activity shifted from moment to moment along the length of the muscle strip [52]. In the stomach slow waves persisted in muscle tissues separated from the myenteric region, but these events occurred at reduced frequencies [53]. This observation suggests that cells within the thickness of the gastric *tunica muscularis*, such as the ICC that line septa (ICC-SEP) between muscle bundles or ICC-IM, are capable of generating pacemaker activity, albeit at a lower frequency.

Studies of animal models have shown that the organ-level dominant pacemaker in the stomach exists in the orad corpus where the frequency of slow waves is greatest [16, 54, 55]. The dominant pacemaker in the human stomach is also likely to reside in the proximal corpus; however, comparison of slow waves recorded from gastric antral and corpus muscles does not clearly resolve a dominant slow wave frequency gradient [56]. It should also be noted that an anatomical region was found in the guinea pig corpus where intramuscular ICC (ICC-IM) are plentiful, but ICC-MY are absent. Slow waves were generated from this region at a frequency matching the frequency of slow waves in the intact stomach [55]. Thus, dominant pacemaker activity may originate from ICC-IM or ICC-SEP in these animals.

Organ-level pacemaker dominance would be difficult in the small intestine because slow wave frequency is higher than in the stomach, and the propagation velocity of slow waves is relatively slow. Therefore, slow wave propagation is normally limited to rather small segments of tissue, because when an event is initiated at any point along the intestine it tends to soon collide with slow waves generated at more distal or more proximal pacemakers. Older studies suggested that slow waves originated in the longitudinal muscle layer in the small intestine [12], but that concept has been refuted by more recent work. Dissection experiments from several species and experiments on mutant animals in which ICC-MY fail to develop show that dominant pacemaker activity emerges from the myenteric region in the small bowel [5, 57]. The muscle wall of the mouse small bowel is devoid of slow waves in the absence of ICC-MY, suggesting that only these cells are pacemakers in this region of the murine GI tract. However, in dogs, isolated circular muscle strips from the region of muscle near the deep muscular plexus displayed rhythmic activity, suggesting that ICC-DMP may also be capable of pacemaker activity in this species [58].

The colon has two discrete regions of pacemaker activity, one lying along the submucosal border of the circular muscle layer that produces slow waves [59–62] and another pacemaker area, producing higher frequency activity known as myenteric potential oscillations (MPOs) is located in the myenteric region. The two colonic pacemakers occur at such different frequencies, that one cannot not drive or dominate the other. Therefore, these events summate in the circular muscle layer [60, 61].

When morphology and ultrastructure investigations were performed on the regions of tissue from which dominant frequency pacemaker activity was recorded, networks of ICC were identified (Fig. 1.3) [53, 63–66]. Early structural descriptions of ICC included the suggestion that ICC might serve as pacemakers in the GI tract because gap junctions between ICC and SMCs were observed [67–71]. ICC within pacemaker regions are electrically coupled to each other via numerous gap junctions, forming the basis of these syncytial networks. Gap junctions between ICC and SMCs are less abundant (e.g., [53]) but capable of conveying slow waves from ICC-MY to SMCs.

1.2.4 Propagation of Slow Waves

Slow waves propagate actively within GI muscles, and this is why long distance coordination and sequencing of contractions, such as in gastric peristalsis, is possible. Dissection experiments showed that continuous structural integrity of tissues determined to be pacemaker areas is necessary for active propagation. For example, experiments on dog colon showed

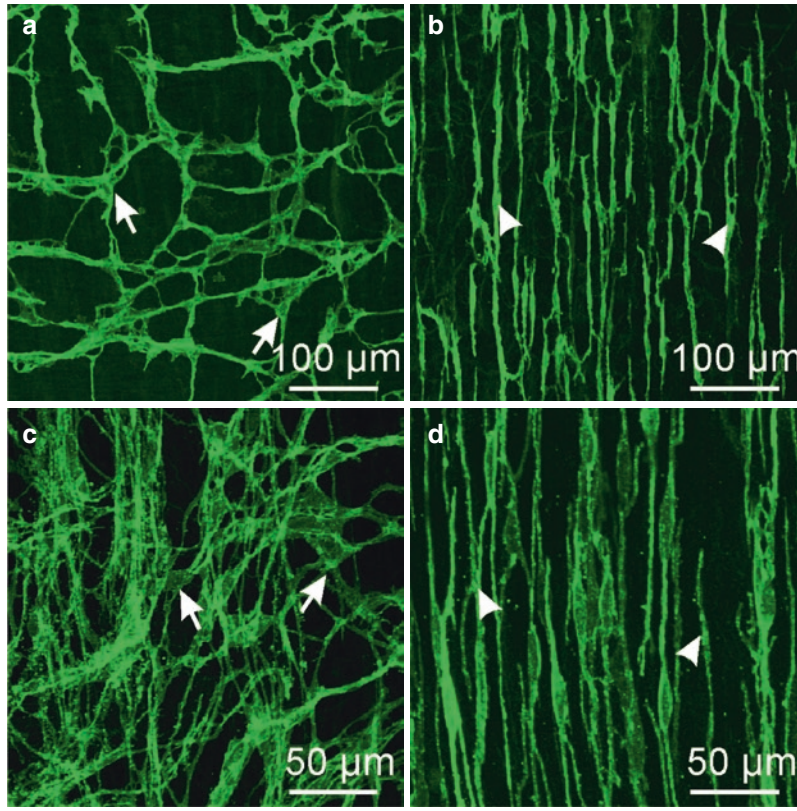

Fig. 1.3 ICC in murine and monkey small intestine. (**a**, **b**) are whole mounts imaged by confocal microscopy of ICC-MY (**a**) labeled with anti-c-Kit antibody (arrows) and ICC-DMP (**b**; arrowheads) in murine small intestine. ICC-MY have multiple processes and form an extensive interconnected network via gap junction coupling between ICC and with adjacent SMCs. ICC-DMP run in parallel with the circular muscle fibers and are concentrated very close to the submucosal edge of the circular muscle layer in the mouse. ICC-DMP are closely associated with the processes of enteric motor neurons (not shown) and PDGFRα^{+} cells (not shown). (**c**, **d**) are images from the small intestine of *Macaca fascicularis* (cynomolgus monkey). ICC-MY (**c**; arrows) in this species also display a network of cells between the circular and longitudinal muscle layers and ICC-DMP (**d**; arrowheads) are also present near the submucosal surface of the circular muscle layer. Redrawn from [206]

that slow waves propagate actively, as long as the ICC-SM network along the submucosal surface of the circular muscle layer remains intact. If a thin section of tissue at the submucosal surface (pacemaker area) is damaged or removed, slow waves decay in amplitude within a few mm from an active area [72]. In contrast, when the myenteric pacemaker region was separated from gastric muscles, active propagation occurred at approximately the same velocity [53]. Complete removal of the myenteric pacemaker region caused a decrease in the frequency of slow waves, but pacemaker activity persisted and slow waves propagated within isolated strips of circular muscle. These data indicate that cells capable of active propagation penetrate into the circular muscle layer in some regions. The cells capable of slow wave regeneration within the circular muscle in the stomach are not known but could be either ICC-SEP between muscle bundles or the ICC-IM within muscle bundles. ICC-SEP have not been isolated for study of their specific properties.

Active propagation of electrical events is a common property of excitable cells when the cells are longer in length than a few space constants or when the cells are

arranged into a syncytium connected by gap junctions. The SIP syncytium is an example of the latter case, and SMCs and ICC are electrically coupled to other cells of the same type and to each other. Many studies of propagation velocity were performed on whole organs and tissues in vitro with extracellular electrodes [50, 73, 74]. However, data from studies of this type are misleading because the recordings are likely to be contaminated by mechanical artifacts, making it impossible to know with precision when an electrical event passes a recording point [75, 76]. Measurements of slow wave propagation velocity in strips and sheets of muscle have also been made using intracellular microelectrodes. This approach provides more precise determination of the point in time when events pass a recording site [77]. With this approach, anisotropic propagation was observed in muscles of the canine antrum. The propagation velocity in the axis of the circular muscle was 23 mm/s but only 11 mm/s perpendicular to the circular muscle axis. The cause of the anisotropy in slow wave propagation is not fully understood but may be due to relatively lower cell-to-cell resistance in the circular axis than in the longitudinal axis.

The mechanism of slow wave propagation in tissues has been explored using muscle strips and partitioned recording chambers. Muscle strips pulled through latex partitions provide the opportunity to make intracellular recordings from parts of the tissue exposed to different external solutions (Fig. 1.4). One chamber serves as the site of unfettered slow wave generation, and the second chamber provides a site to record the effects of various test solutions on slow wave propagation. Slow waves recorded from two well-spaced cells in canine colonic muscles were of equal amplitude under control conditions, but drugs to block IP_3 receptors (IP_3 Rs), reduced $[Ca^{2+}]_o$ and antagonists of T-type voltage-dependent Ca^{2+} channels (Ni^{2+} and Mn^{2+}) inhibited slow wave propagation. The amplitudes of propagating slow waves decayed to the resting potential in less than 3 mm from the partition [78].

Other experiments tested the propagation in canine antral muscles and used a triple partitioned chamber [79]. In these experiments the central chamber served as the test chamber and simultaneous intracellular recordings were made in the chambers to the left and right (Chambers A&C) of the central chamber (Chamber B). Coupling of slow waves recorded in chambers A&C was 1:1 under control conditions and the propagation velocity of slow waves was 22 mm/min, confirming previous studies [77]. Propagation velocity decreased and coupling between chambers A&C broke down when temperature was decreased in Chamber B. For example, propagation velocity fell from 19 mm/s at 37 °C to 3.6 mm/s at 27 °C. Slow waves failed to propagate from chamber A to chamber C below 21 °C. The upstroke velocity of slow waves also decreased from 720 mV/s at 37 °C to 522 mV/s at 24 °C. Depolarization or hyperpolarization of the central test chamber also inhibited propagation and coupling of slow waves in chambers A&C. Finally, reduced extracellular Ca^{2+} or antagonists of T-type voltage-dependent Ca^{2+} channels (e.g., Ni^{2+} or mibefradil) inhibited slow wave upstroke depolarization velocity and propagation. These experiments suggested that voltage-dependent Ca^{2+} entry, possibly due to T-type Ca^{2+} channels, is required for active propagation of slow waves.

The slow wave upstroke depolarization is the leading edge of propagating slow waves, and the rate-of-rise (*dV/dt*) of the upstroke is an indication of the inward current density depolarizing the SIP syncytium. Various Ca^{2+} channel antagonists have been tested on *dV/dt* of canine antral slow waves. Nicardipine, an L-type Ca^{2+} channel antagonist, had no effect on upstroke velocity or propagation velocity [80]. However, Ni^{2+} and mibefradil, both T-type Ca^{2+} channel antagonists, reduced *dV/dt* and propagation velocity in a concentration-dependent manner. Reduction in extracellular Ca^{2+} also reduced upstroke and propagation velocities such that slow waves failed to propagate actively when $[Ca^{2+}]_o$ was reduced below 0.5 mM. These observations are consistent with the idea that dihydropyridine-insensitive, T-type voltage-dependent Ca^{2+} chan-

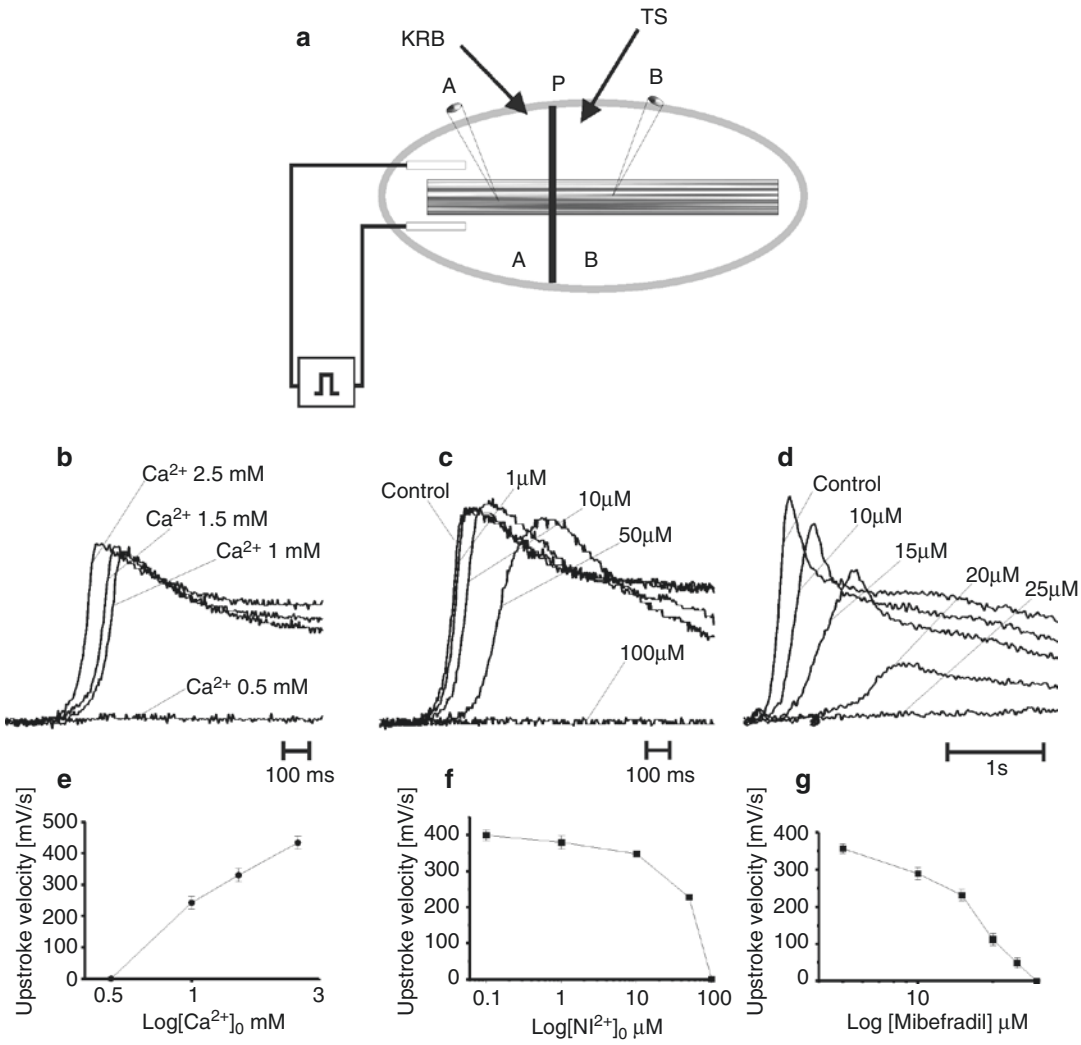

Fig. 1.4 Role of Ca^{2+} entry in slow wave propagation. (**a**) Shows a partitioned chamber apparatus used to study slow wave propagation. Slow waves can be reliably generated in Chamber A perfused with Krebs solution (KRB). Slow waves are initiated by passing a current pulse through electrodes placed on either side of the muscle strip. The muscle is pulled through a latex partition into Chamber B that can be independently perfused with Test Solutions (TS). Cells in Chambers A and B record control slow waves, and propagating slow waves, as modified by the Test Solution. (**b**–**d**) Show control slow waves (as recorded in Chamber A) and slow waves exposed to Test Solutions containing reduced $[Ca^{2+}]_o$ (**b**), extracellular Ni^{2+} (**c**), or mibefradil (**d**). Each Test Solution caused a concentration-dependent decrease in propagation velocity (not shown in this example) and decreased upstroke velocity, as shown by superimposed slow waves. $[Ca^{2+}]_o$ of 0.5 mM, Ni^{2+} at 100 μM, and mibefradil at 25 μM did not support active propagation, and slow waves decayed in amplitude before reaching the impaled cell in Chamber B. Graphs in (**e**–**g**) summarize this series of experiments. Redrawn from [80]

nels are required for slow wave propagation (Fig. 1.4). Another interesting observation from this study was that cyclopiazonic acid, which depletes Ca^{2+} stores in cells, significantly blocked the plateau phase of slow waves without affecting the upstroke or propagation velocity [80].

1.2.5 Electrical Pacing of GI Muscles

Gastrointestinal muscles can be paced electrically by applying current pulses, 1–2 s in duration [81]; however, the degree to which slow

wave frequency can be enhanced is limited by the duration and refractory properties of slow waves. Pacing has been suggested as a therapy for motility disorders, such as gastroparesis; however, the power required for direct pacing of slow waves has restricted the usefulness of this technique in patients [82]. The effects of pacing were investigated in muscles of the canine antrum [83]. At pacing frequencies of 3.5 cycles per minute nearly identical slow waves were elicited by each pulse, but as frequency increased, an alternating pattern developed, in which every other slow wave displayed a greatly attenuated plateau phase. Complete slow wave block occurred when the interval between repolarization and the next stimulus was less than about 2 s. The muscarinic agonist reduced the refractory period. Similar properties of slow wave refractoriness were observed in the guinea pig stomach, and about 6 s were required between slow waves for full restoration of amplitude [84]. As in other excitable cells, the refractory period was inversely related to the amplitude and duration of the depolarization. Acetylcholine also reduced the refractory period in guinea pig stomach, and this was attributed to the activation of protein kinase C (PKC), because the effects of acetylcholine were mimicked by phorbol-12-myristate-acetate and blocked by an inhibitor of protein kinase C.

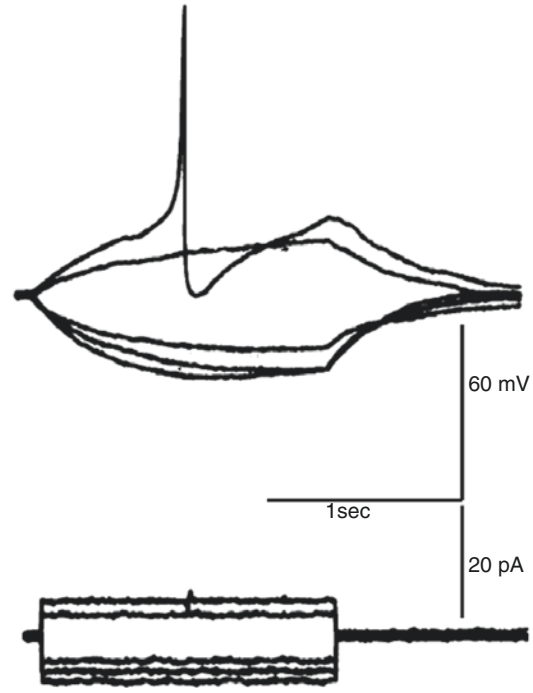

Fig. 1.5 Ca^{2+} action potential in an isolated smooth muscle cell from rabbit jejunum. Cell held under current clamp conditions and hyperpolarized or depolarized by passing constant current pulses. Depolarization activated Ca^{2+} action potential. Redrawn from [92]

1.3 Ca^{2+} Action Potentials

Depolarization of SMCs elicits action potentials that occur by activation of inward current carried by L-type voltage-dependent Ca^{2+} channels [85–88]. Ca^{2+} entry into SMCs through L-type (dihydropyridine-sensitive) Ca^{2+} channels during action potentials is substantial, as indicated by the rapid upstroke velocities of action potentials (up to approximately 20 V/s), [89]. Activation of L-type Ca^{2+} channels is a major mechanism through which GI SMCs achieve excitation-contraction coupling [90, 91]. We know that SMCs are the source of Ca^{2+} action potentials in the SIP syncytium, because isolated cells generate these events (Fig. 1.5) [92] and muscles devoid of slow waves through loss of ICC persist in generating action potentials [93, 94]. When action potentials occur in phasic GI muscles, they are superimposed upon the slow wave depolarizations [36]. This is an example of the integration achieved by contributions of different cells in the SIP syncytium: ICC generate slow waves, these events conduct into SMCs, and the depolarization of SMCs elicits action potentials. In taenia coli action potentials occur in the absence of slow waves [14]. Single action potentials couple to twitch-like contractions and trains of action potential firing creates tetanic-like contractions [95–97]. While action potentials are not a common behavior in most regions in the stomach, they do occur in the terminal antrum and pyloric sphincter [16, 98].

1.4 Relationship Between Electrical and Contractile Behaviors

Depolarization of smooth muscle cells increases the open-probability of L-type Ca^{2+} channels, initiating Ca^{2+} entry and contraction. As shown in Fig. 1.1, slow waves typically depolarize cells into the range of potentials in which L-type Ca^{2+} channels are activated in SMCs. In some muscles, such as the corpus and antrum of the stomach, slow wave depolarizations of SMCs are sufficient to activate enough Ca^{2+} entry to elicit contractions, but in other regions of the gut slow waves elicit only small amplitude contractions and major contraction requires generation of Ca^{2+} action potentials [99]. The relationship between slow waves and contractions was studied in detail in canine gastric muscles [100]. A one-to-one correlation between slow waves and phasic contractions occurs in gastric corpus and antrum. Two components of contraction are apparent, one appears to correlate with the upstroke depolarization and a second depends upon the amplitude and duration of the plateau phase of the slow wave. A mechanical threshold was observed in which the increase in the force of phasic contractions correlated with the amplitude of the plateau potential. The curve describing the increase in force as a function of voltage is similar to the activation curve for L-type Ca^{2+} channels. This relationship was revisited when it became possible to record slow waves, Ca^{2+} transients and contractions simultaneously in strips of canine gastric antral muscle [90]. These experiments utilized muscles loaded with the ratiometric Ca^{2+} sensor, indo-1. A sequence of activation occurred that was initiated by the upstroke depolarizations of slow wave, followed by a rise in the fluorescence ratio indicating an increase in $[Ca^{2+}]_i$ in SMCs and then development of contraction (Fig. 1.6). If the amplitude of the plateau phase of the slow wave was increased by an excitatory agonist, a secondary phase of the Ca^{2+} transient developed, and this was associated with a secondary phase of contraction. In the same manner, decreasing the plateau with a dihydropyridine to block L-type Ca^{2+} channels reduced the amplitude of Ca^{2+} transients and diminished contractile force.

Loss of slow waves and/or propagation of slow waves disrupts normal motility patterns in the small intestine. Observation of intestinal motility with radiological contrast fluid showed peristaltic waves that moved contents through the proximal small intestine [101]. Movements of this sort were not observed in the intestines of W/W^V mice. Loss of ICC-MY leads to aberrant motility initiated by sporadic Ca^{2+} action potentials in clusters of cells that do not propagate very far in tissues. The motor activity in W/W^V muscles was blocked by nifedipine, showing it was unrelated to slow wave activity. The ability of ICC-MY to coordinate contractions was further studied in sheets of intestinal muscle and intact loops of exteriorized small intestine [102]. Impalements of cells in circular and longitudinal muscle layers, validated by filling of cells with propidium iodide during recording, showed that both layers of muscle in the small intestine are paced by ICC-MY. Slow waves of equal amplitude and frequency were present in both layers in wild-type mice and absent in tissues from W/W^V mice that have only a few ICC-MY. Movements of the longitudinal muscles were tabulated by an imaging technique called motility mapping in which changes in the distances between points in surface marker arrays are used to describe motor patterns. Ileal contractions occurred in wild-type mice and propagated along segments of bowel at 5.6 mm/s with little variation in wave-to-wave period or velocity. W/W^V tissues displayed forceful contractions, but these were uncoordinated and unstable in terms of site of initiation or propagation pattern. The velocity of spread of contractile movements was difficult to determine because contractions were abrupt and spread for short distances. The major motility defect noted in animals with reduced ICC-MY was loss of organization and propagation of coherent phasic contractions. An interesting point illustrated by these studies

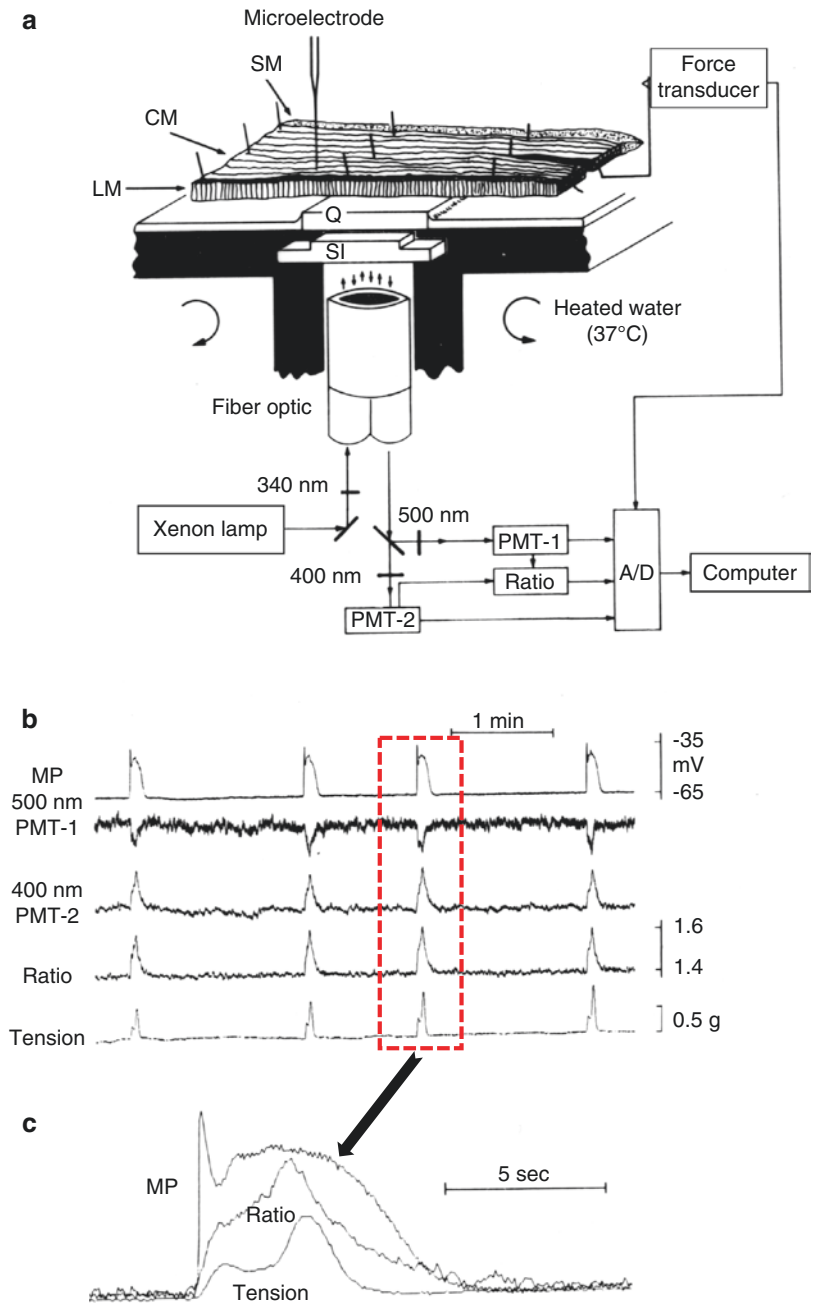

Fig. 1.6 Measurement of membrane potential, fluorescence of a Ca^{2+} indicator and contraction in muscles of canine antrum. (**a**) Apparatus to make simultaneous measurements that includes illumination of the muscle strip in selected areas with 340 nm light and collection of 400 and 500 nm signals and analogue determination of the F_{400}/F_{500} ratio. After determination of the continuous ratio, signals were digitized, along with tension and membrane potential (MP), and recorded on a computer. Antral muscles were cut in cross-section through the thickness of the *tunica muscularis* and pinned over a quartz window (Q). Measurements were made on longitudinal muscle (LM) or areas of muscle near the submucosal (SM) surface of the circular muscle (CM) or from CM close to the myenteric plexus. A microelectrode was used to impale SMCs near the field of view. (**b**) Recordings of MP, 500 nm signal, 400 nm signal, the F_{400}/F_{500} ratio, and tension. Note the correlation between these signals. (**c**) One slow wave cycle is shown at higher resolution from the events outlined by the dotted line box in **b**, and the traces are superimposed. Note the initiation of the signal complex by the upstroke depolarization of the slow wave, followed by initiation of a Ca^{2+} transient and then initiation of contraction. Figure is redrawn from [90]

is the integrated behavior of ICC and SMCs in intestinal muscles. Each type of cell has its own intrinsic ability to influence excitation-contraction coupling. SMCs have the ability to generate action potentials, and this can produce a form of phasic contractions in muscles lacking ICC. However, in small intestinal tissues with a normal ICC-MY network, slow waves override the intrinsic behavior of SMCs, organize excitation-contraction coupling into a contractile pattern driven by the frequency and duration of slow waves, and convey this information to large numbers of cells through slow wave propagation.

Studies to better understand the correlation between electrical activity and contractions have also been performed on colonic muscles. As described previously there are regional differences in the electrical activity of the colon [62], and the relationship between electrical and mechanical activities were evaluated in mouse colon [103]. Slow waves with plateau potentials were recorded from cells near the submucosal border of the CM, and some of these recordings were made from ICC-SM. These events generate smaller amplitude and higher frequency (12–21 cycles per minute) contractions. When recordings were made from the serosal surface in either LM or CM, clusters of membrane potential oscillations or action potentials were recorded at about 3.4 cycles per minute. These events coupled to phasic contraction of large amplitude. These contractions were superimposed when contractions in the CM axis were recorded, but only the low frequency contractions were apparent in the LM recordings. Similar types of patterns are displayed in recordings from human colon; however, the slow wave frequency is only 3 cycles per minute, and this frequency appears to be the dominant frequency of phasic contractions [104]. Thus, the dominant phasic contractile pattern appears to emanate from the pacemaker cells along the submucosal surface of the CM in human colon. How these basic patterns are integrated to form colonic motility is poorly understood.

1.5 The Pacemaker Cells

As above, the dominant pacemaker cells in stomach and small intestine are ICC-MY. These cells are stellate in shape with a prominent nuclear region and multiple processes (Fig. 1.3). Gap junctions are plentiful, connecting ICC-MY into a network running in the space between the circular and longitudinal muscle layers. ICC-MY are distributed on both the longitudinal and circular muscle sides of myenteric ganglia. Labeling of ICC was accomplished in early studies with methylene blue [70, 105]; however, this histological label is not specific. Antibodies against vimentin have also been used, but again this protein is not specific for ICC [106]. Antibodies to c-Kit were found to label cells in the gut wall [107], and these cells were later identified as ICC [3, 5, 108]. Labeling with c-Kit antibodies has been the standard for identifying ICC for the past 20 years, and it was also used to suggest that gastrointestinal stromal tumors arise from ICC [109]. Labeling with c-Kit antibodies in some species, such as primates or humans, can be hampered by issues of non-specificity, because mast cells also express *KIT* and these cells are present in the *tunica muscularis*. However, the shape and size of mast cells and ICC are different, making it possible to distinguish the two cell types. Better discrimination is possible in whole mounts than in cryosections, because of the better resolution of cell shape in the former. More recently additional immunolabels for ICC have emerged, such as antibodies for CaCCs, encoded by *Ano1* [110, 111], or Na^+K^+ Cl^- cotransporter 1 (NKCC1), encoded by *Slc12a2* [47, 112, 113]. Both of these genes are highly expressed in ICC and not resolved in other cells in GI muscles, making them useful for studies of the tissue distribution of ICC.

Unfortunately, enzymes utilized to disperse tissues often damage extracellular epitopes of c-Kit, making it difficult to label ICC with c-Kit antibodies after dispersing cells. Thus, it is difficult to identify ICC unequivocally in mixtures of cells resulting from enzymatic dispersion of GI muscles. This problem was solved, at least for mice, by development of a reporter strain in which a bright green

fluorescent protein (copGFP) was knocked-in to *Kit*, making use of endogenous, cell-specific promoters to accomplish constitutive labeling of ICC [114, 115]. These mice have been useful for molecular and functional studies of pacemaker activity in ICC because cells can be identified by their constitutive fluorescence. Fluorescence activated cell sorting (FACS) has also been used to purify ICC [116], and this made it possible to collect enough cells for gene array studies and deep sequencing of ICC transcriptomes [117, 118]. Genome-wide expression data has generated many new ideas about the nature and functions of ICC, such as expression of additional receptors that might regulate the functions of ICC and participate in regulation of motility, potential interactions of ICC with the extracellular matrix, connectivity with enteric motor neurons and mediation of neurotransmitter effects, additional ion channels that might have function, and a possible role for ICC in generating bioactive molecules (e.g., paracrine mediators).

1.5.1 Studies of Cultured ICC

Due to the difficulties in identifying ICC for physiological studies, investigators developed cell cultures from enzymatically dispersed cells, and identified cells as ICC by c-Kit labeling or by morphological criteria (e.g., multipolar cells with a prominent nucleus that may or may not be integrated into a network). Cell cultures were promising because electrical rhythmicity is preserved [25, 119], and many studies used these cultures to evaluate the expression and function of ion channels, the basis for electrical rhythmicity, and responses to drugs. However, several confounding factors hamper interpretations of the results from these studies: (i) ICC exhibit significant plasticity in culture, and the native phenotype changes rapidly; (ii) it is hard to know whether the ionic conductances found in these cells are native or develop as cells remodel. (iii) ICC, or the cells they become in culture, form gap junctions with other cells. Thus, it is difficult to know whether the electrical activity recorded from cells in networks is intrinsic to ICC or to another type of cell that is electrically coupled to ICC. A plethora of ion channels have been attributed to ICC and reported as functional from experiments on cultured cells, but studies on freshly dispersed cells have failed to resolve many of the conductances described. Expression of *Ano1*, a conductance of primary importance to the functions of ICC (see below), appears to be suppressed in cultured cells, as this conductance has not been described in studies of these cells. Other unrecognized conductances may also contribute to slow waves in some organs or species, so additional studies to analyze these conductances are still needed.

1.5.2 Specialized Conductances and Transporters in ICC that Contribute to Pacemaker Activity

The rapid decline in the native phenotype in cell culture underscores the importance of studying ICC in situ or developing techniques to investigate these cells soon after they are dispersed from tissues. A clever approach using partial dispersion of the myenteric region of the mouse small intestine was developed to record from cells soon after disruption of the extracellular matrix [120]. Slow wave-like activity was recorded from cells identified as ICC-MY. Slow wave-like events occurred at 16 cycles per minute with durations of 489 ms. The *dV/dt* of these events was 7 V/s. Under voltage clamp these cells produced unique currents that were not subject to the duration of the depolarizing stimulus and persisted for what appeared to be a fixed duration (~500 ms) even after repolarization. Because of this property, the currents were termed "autonomous currents," and reversal potential of the current was found to be +3 mV. Removal of $[Ca^{2+}]_o$ caused a gradual decline in the autonomous current, and this was judged to be due to depletion of internal Ca^{2+} stores. Acetylcholine increased the duration of the autonomous currents, consistent with the effects of muscarinic stimulation on slow waves. The authors concluded that the autonomous current in ICC-MY was likely due to a nonselective cation conductance.

Cells from the reporter strain of mice expressing copGFP in ICC can be voltage-clamped

shortly after enzymatic dispersion [115]. Molecular evaluation showed that these cells display robust expression of *Ano1* CaCCs, and voltage-clamp revealed a current with properties similar to the autonomous current discussed above. Depolarization activated an inward current with a duration that was independent of the duration of the depolarizing pulse. In contrast to the autonomous current, the inward current in ICC of copGFP mice reversed at the equilibrium potential for Cl^- ions (E_{Cl}). Another interesting property was that the latency for activation after depolarization varied significantly with the strength of the depolarization, which suggested a secondary process might be involved in activating the Cl^- conductance. It was reasoned, based on many experiments performed on whole muscles, that Ca^{2+} might be a factor in activating the Cl^- conductance in ICC. Ni^{2+}, reduced $[Ca^{2+}]_o$, and replacement of $[Ca^{2+}]_o$ with Ba^{2+} all blocked activation of the inward current. ICC also express CaCCs with a single channel conductance of 8 pS, consistent with the expression of Ano1. The inward currents in ICC, termed *slow wave currents* in this study, were blocked by niflumic acid, a well-known, however not highly specific, antagonist of CaCCs. Slow wave-like events in single ICC under current clamp were also blocked by niflumic acid.

Expression of *Ano1* (aka *Tmem16a*) in ICC was first revealed by a microarray study of gene expression in ICC isolated from the murine intestine [118]. After development of antibodies to Ano1 protein (aka Dog1) and discovery that *Tmem16a* encodes CaCCs [121–123], expression of Ano1 protein in ICC was found throughout the GI tracts of several species including humans [6, 110, 111, 124, 125] (Fig. 1.7). Several *Ano1* splice variants are expressed in ICC [111], and this diversity may convey different Ca^{2+} sensitivities or pharmacology [126, 127] and be of clinical interest since the complement of splice variants changes in diabetes [128]. Several CaCC antagonists inhibited slow waves in gastric and small intestinal muscles [111]. Probably of greatest importance was the concentration-dependent reduction in slow wave frequency caused by CaCC antagonists. This suggests that CaCC are a key conductance in the basic pacemaker mechanism. It is of interest to note that gastric slow waves are far more sensitive to niflumic acid (IC_{50} = 5.4 μM) and DIDS (IC_{50} = 150 μM) than small intestinal slow waves (IC_{50s} = 150 μM and 1368 μM for niflumic acid and DIDS, respectively). While these rather nonspecific CaCC antagonists were investigated in the original study, the potency of so-called third generation CaCC antagonists ($CaCC_{inh}$-A01, $T16A_{inh}$-A01, benzbromarone, hexachlorophene, and dichlorophene) were recently compared for their ability to block slow waves [129]. Sensitivities to these antagonists varied significantly, and again their potency for blocking gastric slow waves exceeded their potency in the small intestine. For example, one of the more potent antagonists, $CaCC_{inh}$-A01, blocked slow waves in the murine stomach at 5 μM, but more than 30 μM was needed to inhibit slow waves in the small intestine. The reasons for these differences are not entirely understood, but possibilities are: (i) channels in addition to Ano1 contribute to slow waves in small intestinal ICC; (ii) splice variants with different sensitivities to CaCC antagonists may be expressed in the two regions; (iii) local Ca^{2+} concentrations activating Ano1 channels differ in gastric and small intestinal ICC. The latter points arises from the observation that the inhibitory effects of Ano1 antagonists decrease as intracellular Ca^{2+} increases [127]. It is possible that Ca^{2+} reaches higher levels in the nanodomains created by junctions between endoplasmic reticulum (ER) and the plasma membranes in small intestinal ICC than in gastric ICC, and therefore Ano1 channels display reduced sensitivity to Ano1 antagonists in intestinal ICC.

The role of Ano1 channels in pacemaker activity was more clearly defined by studies on intact GI muscles from mice with genetically deactivated Ano1 channels [111]. Unfortunately, $Ano1^{-/-}$ mice have a short life span, and most animals die before 20 days of age [130]. Therefore, it was necessary to study animals shortly after birth. In one experiment, intracellular recordings were made from ten newborn siblings; slow waves were observed in all $Ano1^{+/+}$ and $Ano1^{+/-}$ muscles and were absent in three

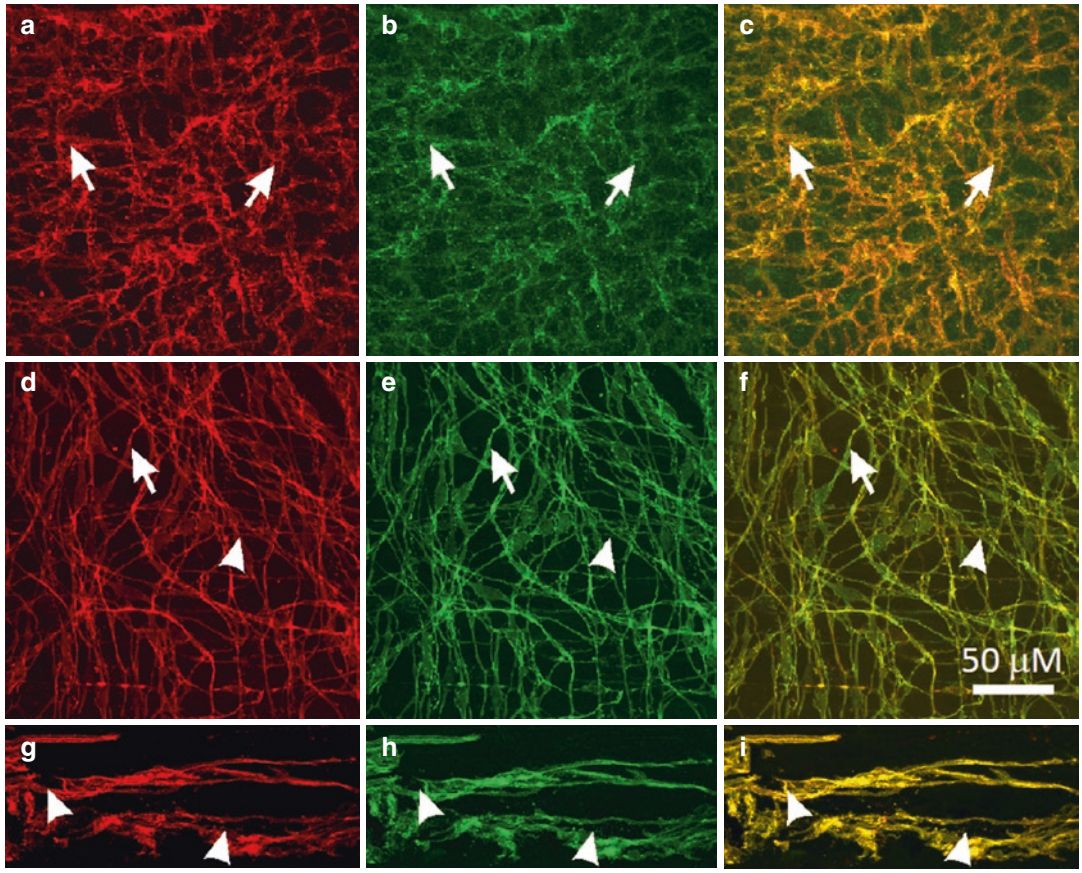

Fig. 1.7 Expression of Ano1 in ICC. (**a**–**c**) c-Kit-LI (**a**, red) and ANO1-LI (**b**, green) in ICC-MY (arrows) of the murine small intestine. (**c**) Shows merged file demonstrating co-localization of c-Kit-LI and ANO1-LI (yellow). (**d**–**f**) Co-localization of c-Kit-LI and ANO1-LI in ICC of the monkey small intestine. ICC-MY (**d**; arrowheads) and ICC-DMP (**d**; arrows) are labeled by c-Kit antibody (red) and the same cells display ANO1-LI (**e**; green) in the small intestine. (**f**) Co-localization of Kit-LI and ANO1-LI (yellow) in ICC-MY and ICC-DMP. (**g**–**i**) c-Kit-LI (arrowheads; **g**; red) and ANO1-LI (arrowheads; **h**; green) are expressed in ICC-MY in the human small intestine. Merged images demonstrate co-localization of these proteins in ICC-MY (**i**; yellow). Scale bar in *F* applies to all panels

Ano1$^{-/-}$ siblings [111]. After 6 days in organotypic culture, which avoids the changes in ICC phenotype observed in cell cultures, slow waves increased in amplitude in homozygotes and heterozygotes, but were still absent in the *Ano1*$^{-/-}$ muscles. Several mice in one litter survived and were studied 23 days after birth. Mice from *Ano1*$^{+/+}$ and *Ano1*$^{+/-}$ mice again displayed normal slow wave activity in the small intestine and stomach, but slow waves were absent in *Ano1*$^{-/-}$ muscles (Fig. 1.8).

Use of constitutive genetic knockouts provided strong evidence for the role of Ano1 in slow waves, but inducible deactivation of *Ano1*, which avoids some of the shortcomings of constitutive knockouts, has also been performed on adult mice using Cre-loxP technology [131]. Theoretically, combining cell-specific iCre mice with mice with a floxed gene should result in knockout of the gene after treatment with tamoxifen. However, this does not typically result in a 100% knockout [132, 133], and *Ano1* was knocked down by only 50% in intestinal muscles. *Ano1* knockout mice showed differences in relative expression with some having dramatic reduction in Ano1 protein and others displaying

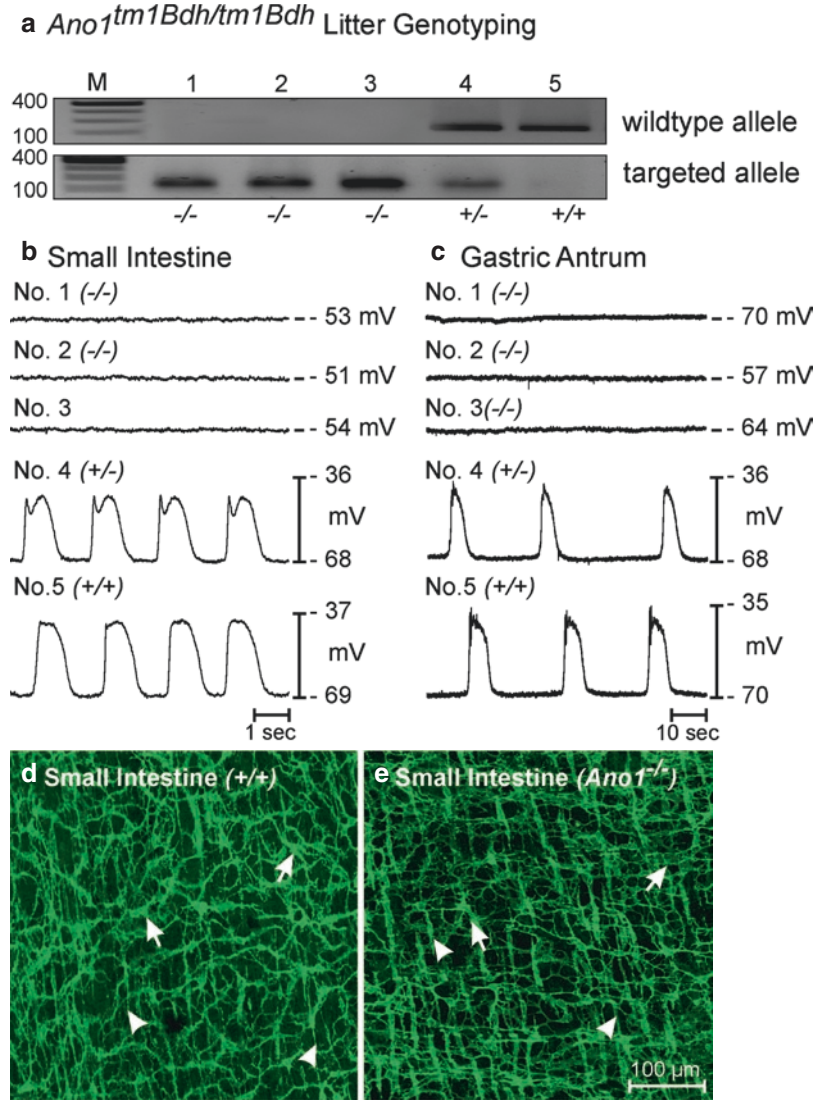

Fig. 1.8 Loss of slow waves in small intestinal and gastric muscles in *Ano1*$^{-/-}$ mice. (**a**) Genotypes of *Ano1*$^{-/-}$ mice. The wild-type allele was absent in *animals 1–3* in this litter, demonstrating that these animals were *Ano1*$^{-/-}$. *Animal 4* was a heterozygote and *animal 5* was a wild-type homozygote. (**b**, **c**) Electrical recording from jejunal and antral circular muscles from each animal with intracellular electrodes. Slow waves were absent in *Ano1*$^{-/-}$ mice, and normal in animals with wild-type alleles. (**d**, **e**) ICC-MY (arrows) and ICC-DMP (arrowheads), with an apparently normal distribution and density, were present in tissues of *Ano1*$^{-/-}$ mice (small intestine shown). Scale bar for **d** and **e** is shown in **e**. Figure is redrawn from [206] with permission

only moderate knockdown of Ano1. Consistent with the expression patterns, intracellular recordings from jejunal muscles displayed various slow wave behaviors, ranging from complete loss of slow waves to irregular amplitude slow waves to normal amplitude slow waves. The normal amplitude slow waves were of shorter duration, and the irregular amplitude slow waves often occurred at higher than normal frequencies. By comparing expression levels of Ano1 with slow wave behavior, the authors concluded that as the expression of Ano1 in small intestinal ICC-MY decreases the duration of slow waves and the regularity of the slow wave pattern also decreases. Reduced Ano1 in ICC decreases slow wave entrainment, and cells in different clusters of ICC establish independent firing behaviors (uncoordinated pacemaker activity). Similar slow wave patterns have been observed after treatment of intestinal and gastric muscles with the gap junction blockers, heptanol and 18-β glycyrrhetinic acid [134, 135].

The study by Malysz and colleagues [131] is an important contribution because it is likely to predict some of the behaviors manifest in human

motility disorders associated with ICC loss or ICC dysfunction. For example, a primary defect observed in the slow waves recorded from mice with partial reduction in Ano1 was reduction in the duration of the plateau phase. This phase is important for the induction of action potentials in small intestinal SMCs, so shortening of the plateau phase would tend to predispose the small intestine to weakened contractions and possibly cause conditions akin to pseudo-obstruction. It is unlikely that all ICC are lost in most human disease, but as the study by Malysz and colleagues suggests, abnormal slow wave patterns can develop far before ICC are lost or become totally dysfunctional. Abnormal slow wave patterns are likely to translate to abnormal and less effective motility patterns.

A fundamental need for the pacemaker class of ICC is a mechanism to facilitate active propagation and entrainment of slow waves. Such behavior is evident in the propagation studies discussed earlier and suggested that voltage-dependent Ca^{2+} entry may be a key property of pacemaker ICC. Lack of effects to dihydropyridines, significant reduction in the upstroke and propagation velocities in response to T-type Ca^{2+} channel antagonists [79, 80] and inhibition of slow wave currents in isolated ICC by these antagonists [115] strongly suggest a role for T-type Ca^{2+} channels, but, as discussed previously, experiments on rabbit small intestinal ICC suggest there may be some variability among species in the channels responsible for upstroke depolarization. *Cacna1h* (α1H isoform of T-type channels and primary subunit of $Ca_V3.2$) is expressed in ICC-MY of the small intestine, as determined by genome-wide gene array study [118]. ICC-DMP, the other class of ICC in the small intestine that do not generate slow waves [5], displayed relatively low expression of *Cacna1h* in the same screen [118]. Expression of *Cacna1h* was confirmed by quantitative PCR [136]. Isolated ICC also express *Cacna1h*, and lower levels of *Cacna1g* were also detected. ICC displayed two phases of voltage-dependent inward current in response to depolarization [137]. A small component of the inward current was blocked by nicardipine, and the second component was blocked by Ni^{2+} (30 μM) and mibefradil (1 μM). Replacement of Ca^{2+} with Ba^{2+} did not affect the current amplitude, suggesting either ion was a suitable charge carrier and equally permeable to the conductance present in ICC, a well-known property of T-type Ca^{2+} channels [138]. Consistent with the properties of channels encoded by *Cacna1h* [139], half-inactivation of the dihydropyridine-resistant conductance in ICC occurred at −59 mV and half activation occurred at −36 mV. The T-type conductance in ICC is also highly temperature sensitive, which is consistent with $Ca_V3.2$ channels [139]. Increasing temperature from 20 to 30 °C increased the amplitude of the current from −7 to −19 pA and decreased the activation time constant by more than half. Lowering temperature or addition of Ni^{2+} (30 μM) reduced *dV/dt* of the slow wave upstroke in intact muscles, but the effects of temperature were reduced after addition of Ni^{2+} or in *Cacna1h*$^{-/-}$ mice. The upstroke of slow waves recorded directly from ICC-MY in situ was also highly temperature sensitive [140]. Taken together, these observations suggest that a T-type Ca^{2+} current is present in murine ICC (from expression of *Cacna1h* and/or *Cacna1g*), such a conductance is functional and a key initiator of slow wave upstroke depolarization, and blocking this conductance interferes with propagation of slow waves.

T-type Ca^{2+}current density is not extraordinary in ICC, in murine small intestinal ICC it averaged 6.6 pA/pF at −20 mV in the presence of nicardipine [137]. Actually, the maximum current density for the dihydropyridine-sensitive component of the inward current in jejunal ICC is similar. Thus, why is T-current necessary for slow wave propagation and dihydropyridine-sensitive current minimally important? The answer is likely to lie in the resting potentials of ICC in situ. In the small intestine the resting potentials of ICC-MY are −69 mV [46], where T-current is available (in fact this potential is near the activation threshold for this conductance in ICC; [137]), but activation of L-type channels occurs nearly 20 mV positive to the resting potential. Therefore, T-type Ca^{2+} channel activation is likely to establish the threshold for activation of slow waves, and L-type Ca^{2+} currents may contrib-

ute more during the plateau phase, possibly due to the sustained activation of L-type current in the voltage-range near the peaks of slow waves (i.e., window current [91]). The resting potential of the SIP syncytium is very important for the generation of slow waves, potentially in determining the frequency of slow waves, and in predetermining the availability of the voltage-dependent channels responsible for slow wave propagation. T-type Ca^{2+} currents are clearly important for slow wave propagation in stomach and small intestine (where resting membarne potentials (RMPs) are typically in the range of −60 to −70 mV), but may not be as important in the colon (where RMP in most species is in the range of −50 mV).

Regulation of membrane potential results from integration of inputs from the three cell types in the SIP syncytium. Through generation of spontaneous transient inward currents (STICs) and slow wave currents, ICC provide depolarizing influences by activation of CaCCs [2]. However, between periods of inward current activation, ICC may aid in restoration of negative membrane potentials to insure periods of reduced Ca^{2+} channel open probability, reduced Ca^{2+} entry and relaxation. Such behavior may be necessary to maintain the phasic contractile nature of the muscles. ICC also express genes encoding several inward rectifier K^+ channels, including *Kcnj2* (Kir2.1), *Kcnj4* (Kir2.3), *Kcnj14* (Kir2.4) *and Kcnj5* (Kir3.4), *Kcnj8* (Kir 6.1) and *Kcnj11* (Kir6.2), that might contribute to regulation of the membrane potential [141]. Voltage clamp of mouse colonic ICC causes activation of an inward current when extracellular K^+ ($[K^+]_o$) is made equal to $[K^+]_i$. This current is blocked by Ba^{2+} (10 μM) or ML-133 (10 μM). Expression of *Kcnj8* (Kir 6.1) and *Kcnj11* (Kir6.2) suggests the presence of a K_{ATP} conduction. However, no evidence was obtained for functional K_{ATP}, and no responses were observed upon application of K_{ATP} agonists or antagonists. This is another significant difference in the phenotypes of freshly dispersed and cultured ICC, as pinacidil causes hyperpolarization of cultured murine colonic ICC and this response is blocked by glybenclamide [142]. Expression of *Kcnj5* (Kir3.4) also suggests the presence of G protein-regulated inward rectifiers; however, no current was elicited by dialysis of ICC with Gβγ and none of the current blocked by Ba^{2+} was sensitive to tertiapin Q [141]. ML-133 caused depolarization of isolated colonic ICC under current clamp and depolarization of cells in intact colonic muscle strips. These experiments suggest that Kir2 family channels participate in regulation of membrane potentials in murine ICC, and this influences the resting membrane potentials of intact muscles.

The effects of bumetanide on slow waves [47, 112] suggest an important role for NKCC1 in pacemaker activity. Cl^- channels provide inward current during slow waves, so a transmembrane gradient supporting efflux of Cl^- must be maintained in spite of ongoing slow wave activity. This appears to occur through active accumulation of Cl^- via NKCC1, a secondary active transporter, which utilizes the Na^+ gradient to transport Cl^- against its concentration gradient [143]. *Slc12a2* and the encoded protein, NKCC1, are expressed robustly in ICC-MY in the small intestine [47, 112, 113]. In contrast, NKCC1 immunoreactivity was not resolved in ICC-DMP, suggesting that antibodies against NKCC1 with extracellular epitopes might provide an effective means of labeling ICC-MY vs. ICC-DMP selectively, facilitating separation of these two classes of ICC from mouse small intestine. The gramicidin-permeabilized patch technique, which has been reported not to disturb $[Cl^-]_i$ [144], was used to measure the reversal potentials of STICs in ICC [113]. STICs reversed at −9 mV, and the reversal potential shifted as the Cl^- equilibrium potential (E_{Cl}) was adjusted to more negative or more positive values. Thus, E_{STICs} may approximate E_{Cl} in ICC-MY. Treatment of cells with bumetanide shifted E_{STICs} to −56 mV within 5 min, suggesting that when active accumulation of Cl^- is inhibited, $[Cl^-]_i$ is decreased, causing a negative shift in E_{Cl} and decreasing the driving force for STICs and slow wave currents that are carried by Cl^- ions. This was in fact the result, and both STICs and slow wave currents were inhibited by bumetanide [113].

Another consequence of cotransport of ions by NKCC1 is that the transporter brings half as much Na^+ into cells as Cl^-. Therefore, a means

must also be available to rid the cells of excess Na^+ and this is mostly likely accomplished by the Na^+K^+ ATPase (Na^+ pump). A role for the Na^+ pump in pacemaker activity was proposed many years ago by Ladd Prosser and colleagues [12]. In their model slow wave depolarization occurred by turning off the electrogenic Na^+ pump (depolarization) and repolarization was the result of activating the Na^+ pump. At the heart of this idea was the observation that ouabain caused depolarization to approximately the same level of depolarization as the peaks of slow waves. During the plateau of the slow wave recovery of Cl^- by NKCC1 may cause accumulation of Na^+ in a restricted volume that activates the Na^+ pump. Activation of the pump could possibly contribute to repolarization of slow waves, but the precise role of the Na^+ pump in the pacemaker mechanism is still awaiting clarification.

A schematic showing the stepwise integration of the conductances and transporters described above to accomplish the slow wave upstroke depolarization, cell-to-cell propagation, sustained depolarization during the plateau phase, and repolarization is shown in Fig. 1.9. The information incorporated into Fig. 1.9 has benefited from the experimental advantages provided by the use of transgenic mice. It is possible that such a fundamental mechanism is conserved among species, and there is evidence that c-Kit$^+$ ICC-like networks, Ano1 expression and a role for these cells in GI motility is present even in non-

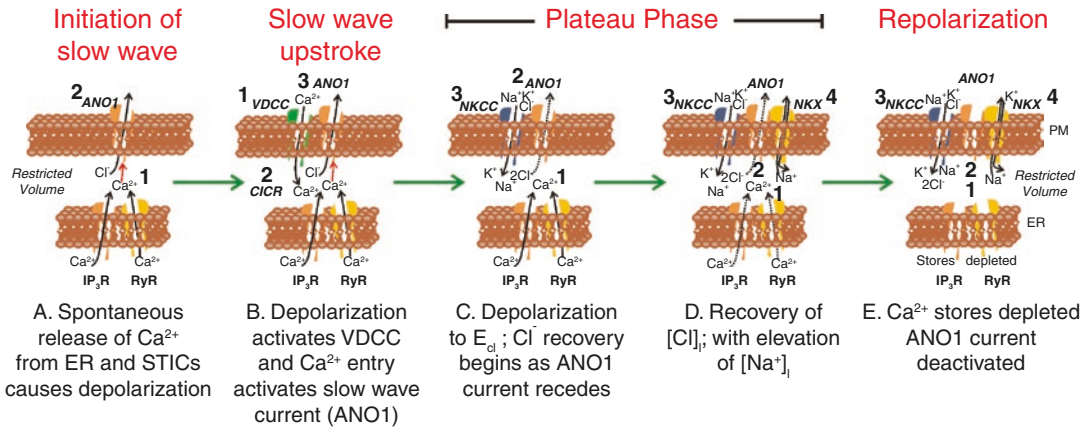

Fig. 1.9 Proposed contributions of ion channels and transporters during the slow wave cycle corresponding to experimental evidence from the murine small intestine. Each panel represents the restricted volumes of nanodomains formed by close contacts between the plasma membrane (PM) and the endoplasmic reticulum (ER). Images are idealized membrane regions with ion channels and transporters that appear to be functional depicted in each snapshot through the slow wave cycle. Numbers in each panel show sequence of events. (**A**) Ca^{2+} release occurs spontaneously from ER through Ca^{2+} release channels (IP_3R and RyR) (**1**). Due to the close apposition of the PM, Ca^{2+} transients activate Ano1 channels (**2**). Efflux of Cl^- ions causes STICs. (**B**) Depolarization from STICs activates voltage-dependent Ca^{2+}channels (T-Type) (**1**) initiating upstroke of the slow wave. Entry of Ca^{2+} into nanodomains initiates Ca^{2+}-induced Ca^{2+} release (CICR; **2**). Ca^{2+} release activates Ano1 channels in PM (**3**). (**C**) Asynchronous release of Ca^{2+} from stores (**1**) in different cellular locations (not shown) sustains activation of Ano1 channels causing membrane potential to linger near E_{Cl} and creating the plateau potential (**2**). Because membrane potential is near E_{Cl} there is little efflux of Cl^- during the plateau (dotted arrow through Ano1 channel). However, loss of Cl^- during the depolarization initiates recovery via NKCC1 (**3**). (**D**) As long as Ca^{2+} is sustained (**1**), Ano1 channels are activated (**2**) and membrane potential remains in the plateau phase. Recovery of Cl^- proceeds and this is associated with influx of Na^+, as NKCC1 uses the energy of the Na^+ gradient to cause accumulation of $[Cl^-]_i$ against its electrochemical gradient. Removal of excess Na^+ is accomplished by the Na^+K^+ ATPase (NKX) (**4**). (**E**) When available Ca^{2+} stores are depleted (**1**), Ca^{2+} recovery by SERCA or extrusion by the plasmalemmal Ca^{2+} ATPase (PMCA) (pumps not shown) causes reduction in Ca^{2+} in nanodomains and deactivation of Ano1 channels (**2**). Recovery of gradients may extend into the period between slow waves via the actions of NKCC1 (**3**) and NKX (**4**)

mammalian vertebrates, such as *Danio rerio* (zebra fish) [145, 146] and *Myoxocephalus scorpius* (shorthorn sculpin) [147]. However, it must also be recognized that the driver for electrical rhythmicity in GI muscles may vary among organs and species and may have developed different or extended attributes in humans. At the present time physiological studies on species other than mice have depended largely on a pharmacological approach, and there have been few experiments reported on freshly dispersed ICC from other species. As discussed above, the pharmacology of Ano1 channels, for example, can be difficult to interpret, as block of these channels depends upon $[Ca^{2+}]_i$ and expression and combination of splice variants [127]. Thus, inability of a CaCC antagonist to block slow waves in a given tissue may not be proof that Ano1 is not involved. While Ano1 is expressed by ICC in a variety of mammalian and non-mammalian species (mouse, monkey, fish, and human; [110, 111, 118, 125, 147]), its universal function in slow waves is yet to be determined. A caveat for universal acceptance of Ca^{2+} entry through T-type Ca^{2+} channels is also warranted because these channels are highly dependent upon the resting potentials upon which slow waves are superimposed. Even if isoforms of T-type channels are expressed, depolarized regions of the GI tract cannot rely on the availability of these channels due to their properties of voltage-dependent inactivation. In cells resting at more depolarized levels (e.g., ~−50 mV), it is likely that L-type Ca^{2+} channels, with nearly full availability in this potential range, provide the voltage-dependent Ca^{2+} entry mechanism that initiates Ca^{2+} release (see next section), activates Ano1, and coordinates activity in the SIP syncytium. Such a mechanism is apparent in the slow wave activity present in the internal anal sphincter [6], for example.

1.6 Ca^{2+} Signaling in ICC

As described in the previous section, major ionic conductances expressed in ICC are either Ca^{2+} dependent (CaCCs) or result in Ca^{2+} entry (voltage-dependent Ca^{2+} channels). Pharmacological and gene knockout studies suggest that these conductances play a prominent role in the generation and propagation of pacemaker activity in ICC. Thus, Ca^{2+} handling mechanisms are of central importance to GI rhythmicity. This realization and the development of sensitive techniques to monitor intracellular Ca^{2+} signals prompted investigators to characterize the mechanisms involved in Ca^{2+} waves and transients in ICC. Ca^{2+} waves occur in networks of ICC, as observed through the use of membrane-permeable Ca^{2+} indicators [148–155]. These studies, conducted mainly on gastric and small intestinal muscles, revealed many important features of Ca^{2+} handling in ICC networks. Newer studies have utilized optogenetic sensors and added to our understanding of Ca^{2+} dynamics [156, 157].

Loading of mouse ileum with Fluo3-AM allowed visualization of Ca^{2+} transients in ICC and SMCs simultaneously [155]. SMCs displayed whole-cell Ca^{2+} events that rapidly shoot through the lengths of cells, and between the whole-cell events, localized Ca^{2+} transients were observed. Cyclopiazonic acid (CPA, 3–5 μM) or thapsigargin (1 μM) blocked the local responses, and no effect was observed with ryanodine (30 μM). ICC were also loaded with Fluo-3, and these cells were identified with methylene blue or c-Kit antibodies. A strong temporal relationship between Ca^{2+} events in SMCs and ICC was observed in only one-third of muscle preparations. In another third of the muscles, Ca^{2+} waves in ICC and SMC were not synchronized. It was concluded from this study that all ICC-MY may not be pacemakers, and they may have additional roles in intestinal motor activity.

ICC network behavior was further investigated in whole mount preparations of guinea pig stomach [149] and mouse jejunum [153] loaded with Fluo-4. Visualization of Ca^{2+} waves was facilitated in these studies by careful removal of longitudinal muscle fibers. Ca^{2+} waves at an average frequency of 4.9 cycles per minute spread through ICC networks in gastric muscles (verified by c-Kit immunolabeling) with an average velocity of 3.2 mm/s. Thus, the frequency and velocity of spread of Ca^{2+} waves matched the frequency [34] and propagation velocities of slow

waves in the gastric antrum [77]. An interesting difference was that the anisotropic propagation of slow waves occurring in intact muscles was not observed in the propagation of Ca^{2+} waves in ICC networks. Thus, the order of magnitude greater slow wave propagation velocity in the circular vs. longitudinal axis in intact muscles must be a property of the interactions between ICC and SMCs. The Ca^{2+} waves exhibited either sharp upstrokes with somewhat slower return to baseline or events with more sustained, plateau-like maintenance of elevated fluorescence before return to baseline. The direction of propagation was variable, suggesting that the site from which primary pacemaker activity occurred shifted from event to event, as seen in electrical recording [51, 77]. Consistent with the idea that ICC are pacemaker cells, Ca^{2+} waves in ICC-MY preceded events in adjacent SMCs by about 50 ms. Tetrodotoxin (TTX) did not block Ca^{2+} waves in ICC-MY, but in some cases it reduced the frequency of Ca^{2+} waves, suggesting that nerves don't initiate the Ca^{2+} waves but basal neural inputs have chronotropic influences on the generation of pacemaker activity. Nicardipine blocked Ca^{2+} waves in SMCs, but did not affect events in ICC-MY.

In the mouse jejunum loaded with Fluo4-AM, regular Ca^{2+} waves were observed in ICC-MY at the slow wave frequency, and a 1:1 relationship between slow waves and Ca^{2+} waves was observed directly by intracellular electrical recording from cells near the field of view [153]. This study also showed a lag between Ca^{2+} waves in ICC-MY and SMCs, supporting the idea that ICC are pacemaker cells. While most cells fired along a linear wave-front (high level of coherence) with each slow wave cycle, there were also periods in which ectopic pacemaker activity emerged and small clusters of cells escaped from the dominant pattern of propagation. The sequence of activation of ICC-MY within networks showed significant variability from event to event, and the rates at which ICC-MY activated during propagated events also varied. Electrical coupling is obviously important for the cell-to-cell spread of Ca^{2+} waves, as propagation was disrupted by the gap junction uncoupler 18β-glycyrrhetinic acid (β-GA). After treatment with β-GA, single or small clusters of ICC-MY persisted in generating Ca^{2+} waves, albeit at disparate frequencies. These observations suggest that individual ICC-MY are intrinsically active as pacemaker cells, but active propagation entrains slow waves into coherent waves of activation. The Ca^{2+} waves were blocked by mibefradil and upon depletion of intracellular Ca^{2+} stores with inhibitors of the sarcoplasmic reticulum Ca^{2+}-ATPase (SERCA).

Loading of cells with Fluo-4 and imaging Ca^{2+} waves in ICC-MY were also performed on muscles of the human small intestine [151]. Biphasic Ca^{2+} waves (6 cycles per minute) were observed in jejunal ICC-MY, identified by c-Kit immunolabeling (Fig. 1.10). The Ca^{2+} waves corresponded to electrical slow waves, recorded simultaneously in some experiments, in both frequency and duration. The upstroke phase of Ca^{2+} waves was a discreet event, occurring at least 2 s before the peak of the plateau phase of the Ca^{2+} waves. The Ca^{2+} waves observed in human jejunum ICC-MY exhibited similar pharmacological responses as those observed in mice. The Ca^{2+} waves were blocked by CPA, disrupted by 2-APB and caffeine, and the frequencies and amplitudes were decreased or disrupted by Ni^{2+} or mibefradil. As in murine ICC-MY, treatment with β-GA also disrupted coherent propagation.

A contrasting view regarding the role of T-type Ca^{2+} current in Ca^{2+} waves in ICC-MY of the small intestine was reported in another study utilizing Fluo-4 AM loaded cells [158]. Mibefradil had no effect on these responses, but Ca^{2+} waves were reduced by the sodium-calcium exchange (NCX) inhibitor, KB-R7943. It was suggested that NCX might provide a mechanism for refilling Ca^{2+} stores. A significant decrease in Ca^{2+} waves was also observed with 2-APB or the phospholipase C inhibitor, U73122. Double immunolabeling showed that c-Kit^+ cells express IP_3 receptor 1 (IP_3R1). These authors concluded that IP_3 synthesis is ongoing in ICC-MY, and IP_3 has a stimulatory effect on Ca^{2+} release, providing the clock mechanism responsible for slow wave generation and setting pacemaker frequency. Although voltage-dependent Ca^{2+} entry was discounted in this study, no explanation was

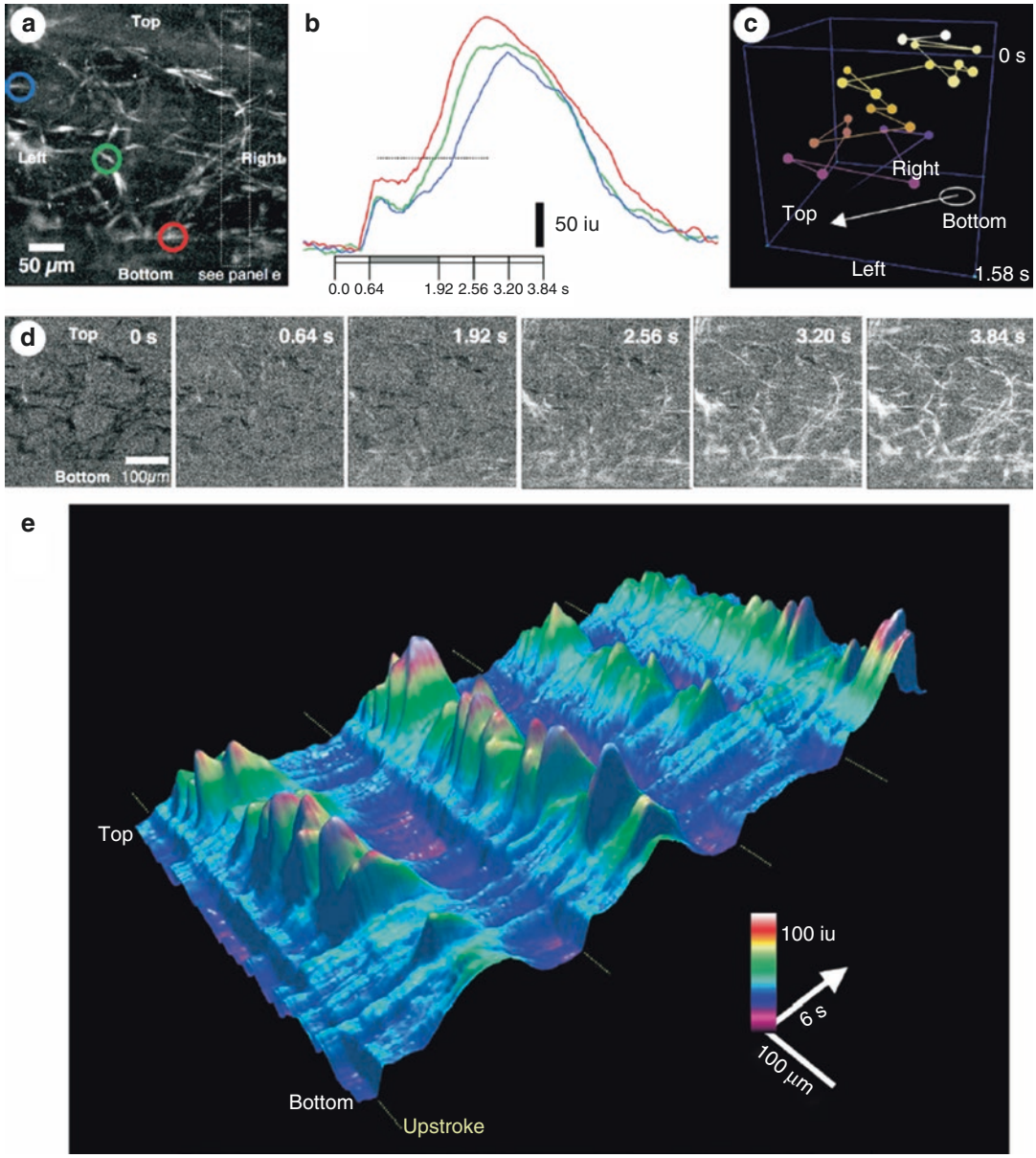

Fig. 1.10 Propagation of Ca^{2+} waves in ICC-MY network in human jejunum. (**a**) Averaged Ca^{2+} waves show active ICC-MY. Colored circles represent regions (ROIs) of interest that have temporal changes in fluorescence plotted as colored traces in (**b**). Note the two phases of the Ca^{2+} transients and delay in second phase from the red to the blue ROI. (**c**) Shows an ST cube depicting the propagation of waves (*white* to *mauve lines*) from the bottom to the top of the field of view (FOV) in **a** (*balls* represent individual ICC-MY observed in **a**). Note that the Ca^{2+} traverses the FOV in a zigzag pattern. (**d**) Image sequence propagation of Ca^{2+} at different times during one slow wave cycle. The frames correspond to changes in fluorescence as a function of time in (**b**). The upstroke phase occurs at 0.64 s, and the plateau phase occurred between 1.92 and 3.84 s. (**e**) Shows a 3-dimensional ST map of 4 slow wave cycles in ICC-MY within the FOV shown in (**a**). The upstroke phase and plateau phase were constructed from 1 or 2 adjacent ICC-MY. The upstroke phase (small initial hump in fluorescence) occurs before each plateau (major peaks in fluorescence in which highest amplitude of fluorescence occurs during each cycle). Plateau phase in cells varies in rate-of-rise and amplitude from cycle to cycle across the FOV. Copied with permission from [150]

provided to explain coordination and propagation of slow waves in ICC networks.

As described previously, the colon is more complex than small bowel and stomach in that there are two pacemaker zones with different frequencies. Slow waves are generated in ICC at the submucosal border of the circular muscle layer (ICC-SM) [61, 63, 134, 159]. Ca^{2+} waves were recorded from ICC-SM in the canine colon at the same frequency as slow waves [152]. These waves were highly coherent, propagating through the ICC network as seen in small bowel and stomach. Another pacemaker frequency was found in ICC-MY, that generated Ca^{2+} waves at the frequency of the electrical activity known as myenteric potential oscillations (MPOs) [60, 152]. In contrast to ICC-SM, the ICC-MY Ca^{2+} waves were unsynchronized, demonstrating characteristic differences in Ca^{2+} handling mechanisms or electrical coupling in these two populations of colonic ICC. ICC-MY in mouse colons were synchronized by neural inputs, and this response was blocked by atropine, suggesting innervation of these cells by cholinergic motor neurons [160]. Spontaneous or evoked colonic migrating motor complexes (CMMC) increased the frequency and amplitude of Ca^{2+} waves in ICC-MY. N(ω)-nitro-L-arginine and MRS2500, a P2Y1 antagonist, increased the Ca^{2+} transients ICC-MY and appeared to increase coupling between cells. Sodium nitroprusside inhibited Ca^{2+} waves in ICC-MY. These data show that ICC-MY are under tonic inhibition from inhibitory motor neurons. Inhibitory neural inputs inhibit release of Ca^{2+} and possibly reduce coupling between ICC-MY. Excitatory neural inputs activate Ca^{2+} waves and synchronization between cells and aid in coordination of contractions of circular and longitudinal muscles during the CMMC.

Human and dog GI muscles are far thicker than laboratory rodents, and therefore simple conduction of slow waves into SMCs is unlikely to activate the full thickness of the muscle layers because the amplitude of slow wave decays to nothing within a few mm without active propagation [72]. A mechanism of active electrical propagation into the thickness of the circular muscle layer was noted in canine colon, utilizing the ICC in septa between muscle bundles (ICC-SEP). ICC-SEP are active spontaneously when ICC-SM are removed [66]. The question of active propagation into the circular muscle was further investigated using imaging to monitor Ca^{2+} wave propagation into the thick circular muscle layer of canine jejunum, which also has a population of ICC-SEP [151]. ICC-MY and ICC-SEP form a three-dimensional network in which Ca^{2+} waves, and presumably slow waves, propagate from ICC-MY to ICC-SEP deep into the circular muscle layer. Thus, ICC-MY appear to be electrically coupled to ICC-SEP, based on the propagation of Ca^{2+} waves; however, gap junctions between ICC-MY and ICC-SEP have not been demonstrated definitively.

Fluo4-AM loading and whole tissue imaging was also used to evaluate the role of Ano1 channels in Ca^{2+} transients and waves [148]. *Ano1*$^{-/-}$ mice display an absence of slow waves in the small intestine and stomach [111]. These mice were utilized to evaluate whether Ca^{2+} transients could organize and propagate as coherent waves in the absence of Ano1 [148]. Potential developmental defects that might occur in constitutive knockout mice were controlled for by also testing the pharmacological blockade of Ano1 channels or acute deactivation via shRNA treatments of organotypic cultures. Synchronicity of Ca^{2+} transients was significantly depressed in *Ano1*$^{-/-}$ mice, and this behavior was also observed after treatment of wild-type muscles with Ano1 channel antagonists. Ano1 antagonists had no effect on Ca^{2+} transients in *Ano1*$^{-/-}$ tissues. Pretreatments with shRNA reduced *Ano1* by 75%, and the synchronicity of Ca^{2+} transients and presence of slow waves (i.e., slow waves were absent in 80% of cells impaled) were reduced to a similar extent. Morphological examination showed that ICC networks were intact and appeared normal in shRNA-treated and *Ano1*$^{-/-}$ muscles. The reductions in *Ano1* expression, coherent Ca^{2+} waves in ICC-MY networks, and slow wave activity were accompanied by weakened contractile activity with abnormal amplitudes and frequencies in *Ano1*$^{-/-}$ muscles.

Studies using membrane-permeable Ca^{2+} indicators have clearly demonstrated a link between Ca^{2+} release and Ca^{2+} entry events in ICC and pacemaker activity. These experiments, however, have limits and lack resolution due to only moderate signal-to-noise ratio, contaminating signals from other cells also loaded with dye, and relatively rapid photobleaching, especially with higher power imaging requiring stronger illumination. More recently, optogenetic sensors have been used, making it possible to selectively image Ca^{2+} transients in ICC by utilization of Cre-loxP technology. The bright, high signal-to-noise images produced with this technique allows dynamic resolution of subcellular Ca^{2+} transients and greater fluorophore longevity during sustained illumination. Cellular Ca^{2+} dynamics can also be resolved in ICC in situ at high magnification and at relatively high frame rates (e.g., 100 frames per second). Use of this technique, coupled with imaging by confocal microscopy, allows visualization of specific types of ICC because these cells are arranged in a fairly planar fashion within the *tunica muscularis* (e.g., ICC-MY of all organs, ICC-DMP in the small intestine, and ICC-SS and ICC-SM in the colon). GCaMPs are foreign proteins and Ca^{2+} buffers, but mice expressing GCaMP3 in ICC appeared to have normal slow waves and responses to neural inputs [156].

Optogenetic techniques have been used to study cellular mechanisms in the intramuscular class of ICC in the small intestine (ICC-DMP) which are located near the submucosal surface of the circular muscle layer [156]. ICC-DMP were investigated because they lack a voltage-dependent mechanism that allows development of slow waves but still manifest localized Ca^{2+} transients and activation of Ano1 channels to generate STICs. Under control conditions, ICC-DMP fire Ca^{2+} transients from multiple locations, and these events are independent and stochastic in nature. There was little correlation between events at different sites within single cells or within adjacent cells, suggesting the lack of a voltage-dependent mechanism insulates the activity of these cells from events occurring in adjacent cells. There are neural inputs to ICC-DMP, with tonic inhibition of Ca^{2+} transients resulting from nitrergic input [156]. Intracellular Ca^{2+} stores were judged to be the source of Ca^{2+} in the spontaneous Ca^{2+} transients in ICC-DMP because: (i) exposing muscles to Ca^{2+} free solution for many minutes did not significantly affect the amplitude, duration, or spatial spread of Ca^{2+} transients, and (ii) Ca^{2+} transients were reduced or blocked by CPA, thapsigargin, ryanodine, and xestospongin C [156].

Ca^{2+} handling in ICC-MY has also been investigated in muscles with cell-specific expression of GCaMP3. Instead of Ca^{2+} waves spreading smoothly through ICC networks, as reported in previous studies using membrane-permeable Ca^{2+} indicators, higher resolution allowed observation of temporal clusters of discrete and localized Ca^{2+} transients in each cell as Ca^{2+} waves traversed ICC-MY networks [157]. Simultaneous recording of slow waves within fields of view showed that Ca^{2+} transients are clustered temporally within each slow wave cycle, and the clusters of Ca^{2+} transients developed shortly (~175 ms) after each slow wave upstroke depolarization (Fig. 1.11). Firing of Ca^{2+} transients persisted during each cluster for approximately the duration of the plateau phase of the slow waves. Multiple unique Ca^{2+} release sites were detected in ICC-MY, and local events did not spread to become global increases in $[Ca^{2+}]_{cyt}$. Activity in cell soma and processes was distinguished and analyzed by use of masking techniques and found to be equivalent in both regions of ICC-MY. Although the basic organization of the Ca^{2+} transient clusters (CTCs) was rhythmic and persistent in all recordings, Ca^{2+} transients at each site of initiation appeared to be stochastic in nature and characterized by irregular firing from CTC-to-CTC, occasional multiple transients firing from what appeared to be the same site during a single CTC, and transients of varying durations and spatial spread. CTCs were dependent upon Ca^{2+} entry and were abolished when $[Ca^{2+}]_o$ was reduced below 0.5 mM or when cells were treated with T-type Ca^{2+} channel antagonists (NNC 55-0396 and TTA-A2; [161, 162]). CTCs were resistant to either 1 μM nicardipine or isradipine (antagonists

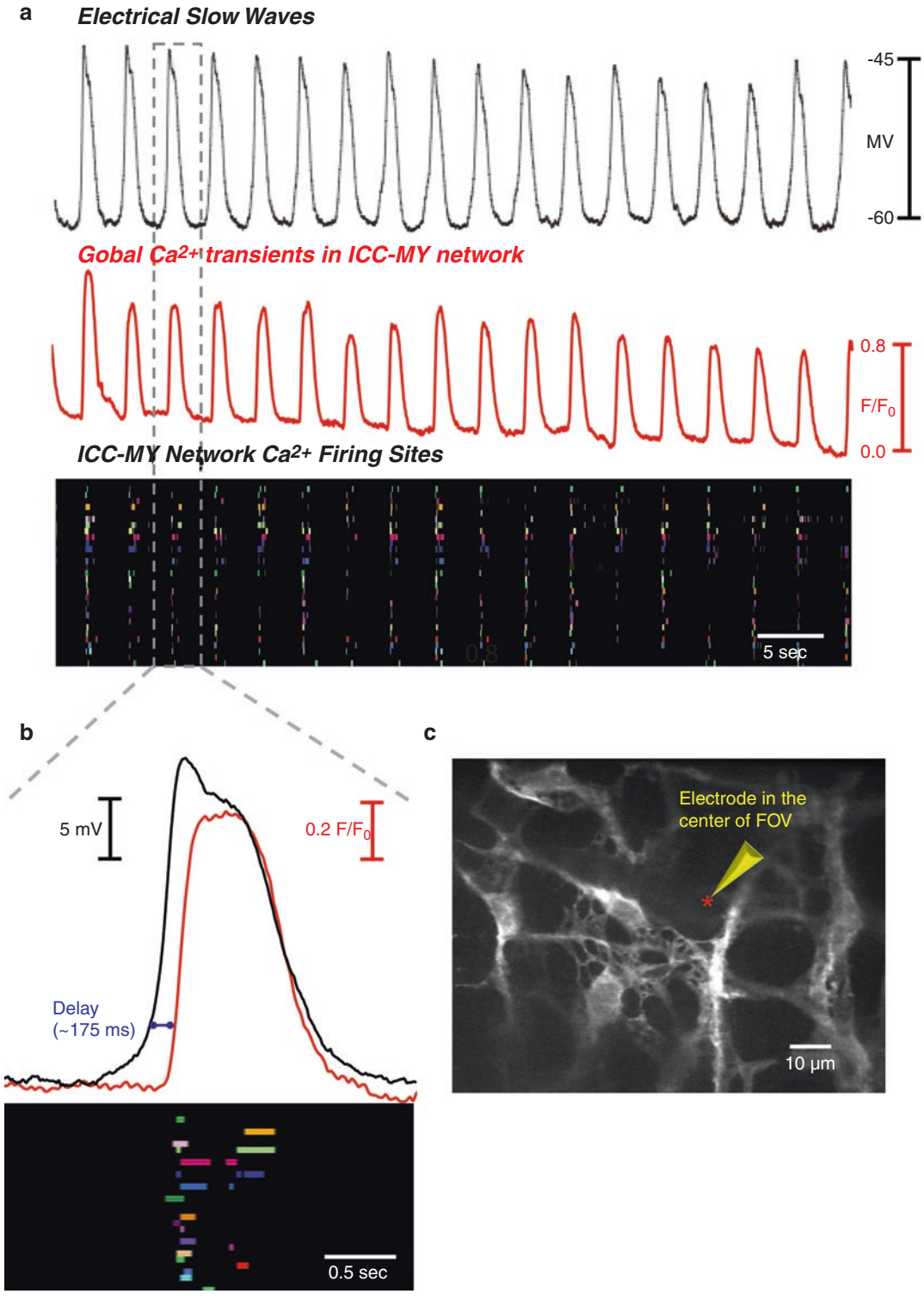
a
Electrical Slow Waves
-45
MV
-60
Gobal Ca2+i transients in ICC-MY network
0.8
F/F0
0.0
ICC-MY Network Ca2+ Firing Sites
5 sec
b
5 mV
0.2 F/F0
Delay
(~175 ms)
0.5 sec
c
Electrode in the
center of FOV
10 µm

of L-type channels encoded by *Cacna1c* and *Cacna1d*). This study led to the conclusion that CTCs are due to Ca^{2+} release from internal stores, and organization of Ca^{2+} release into CTCs is initiated by Ca^{2+} entry through T-type Ca^{2+} channels and initiation of Ca^{2+}-induced Ca^{2+} release (CICR). The specific mechanisms of CICR are discussed in the section below. It is still a question whether the longer durations of slow waves observed in other regions of the GI tract or in other species (see Fig. 1.1) are due to longer duration CTCs in pacemaker ICC in these muscles. This level of resolution of Ca^{2+} transients underlying GI pacemaker activity might become an assay for disease-dependent changes in ICC that develop and compromise the normal functions of these cells. Changes in basic Ca^{2+} signaling may affect motility behaviors long before disruption of ICC networks occur, but future studies will be required to test this hypothesis.

1.6.1 Role of Ca^{2+} Stores in Pacemaker Activity

The role of Ca^{2+} stores in pacemaker activity is presented in a separate section because it is of such fundamental importance in GI pacemaker activity and responses to enteric motor neurotransmitters. As described in the section above, electrical rhythmicity is linked mechanistically to the Ca^{2+} waves arising from and propagating through pacemaker cells, and the frequency of these events may be determined by the rates at which Ca^{2+} stores release and are refilled. Ca^{2+} release from stores is accomplished by two types of ER Ca^{2+} channels, IP_3 receptors (IP_3Rs) or ryanodine receptors (RyRs). Descriptions of a few representative studies on different types of preparations are provided to illustrate major features of Ca^{2+} release and the types of Ca^{2+} release channels expressed and utilized in ICC pacemaker activity. A seminal study, performed on murine gastric muscles investigated global knockouts of *Itpr1*, showed that slow waves are independent of L-type Ca^{2+} channels in wild-type mice, and slow waves are absent in *Itpr1*$^{-/-}$ mice (Fig. 1.12) [163]. Responses to nitrergic and cholinergic neural inputs were also compromised in these mice. These results demonstrate that IP_3 receptors play a fundamental role in the functions of ICC, and this conclusion has been supported by many studies of intact muscles. In pyloric smooth muscle, for example, slow waves were blocked by CPA, caffeine, and heparin loading [164]. However, no role for ryanodine-sensitive receptors was observed, as 10–20 μM ryanodine failed to inhibit slow waves. A combination of low Ca^{2+} and Cd^{2+} also failed to inhibit slow wave activity, and these authors concluded that Ca^{2+} entry was not involved in entrainment of slow waves or electrical

Fig. 1.11 Ca^{2+} clusters in ICC-MY during slow wave activity. (**a**) Slow waves and Ca^{2+} waves in ICC-MY networks recorded simultaneously from jejunum muscle from a mouse expressing GCaMP3 exclusively in ICC. Imaging performed with a confocal microscope to restrict view to ICC-MY. Note the one-to-one relationship between the slow waves and Ca^{2+} transients. If fact the waves were not smooth changes in global Ca^{2+} observed in lower resolution monitoring. When higher resolution was used, facilitated by the superior performance of GCaMP3 as a sensor and low background from restricting GCaMP3 expression to ICC, Ca^{2+} waves were seen to be composed of many localized Ca^{2+} transients occurring in different sites within cell soma and processes. Each firing site was assigned a color and these are plotted in the occurrence map (third panel in **a**). Mapping Ca^{2+} transients in this manner shows that the transients are temporally clustered together at the frequency of the slow waves. (**b**) Increased sweep speed of simultaneous Ca^{2+} transient and slow wave outlined by gray box in (**a**). The occurrence map from this slow wave cycle is shown beneath the traces. Each Ca^{2+} firing site in the FOV was assigned a different color, and this analysis shows that Ca^{2+} transients occurred with different delays after the initiation of the slow wave upstroke, the durations of Ca^{2+} transients was highly variable, and multiple events occurred from the same site on occasion. Note that the Ca^{2+} clusters begin with a slight delay after the upstroke of the slow wave, and all occur within the duration of the slow wave. These observations suggest that the duration of the slow wave plateau depolarization is determined by the spread in time of Ca^{2+} transients, as the open probability of Ano1 channels (causing depolarization) will continue to be elevated as long as Ca^{2+} release events persist. (**c**) Shows ICC-MY network and site of recording within the FOV and within a few μM from the cells being imaged. Copied with permission from [157]

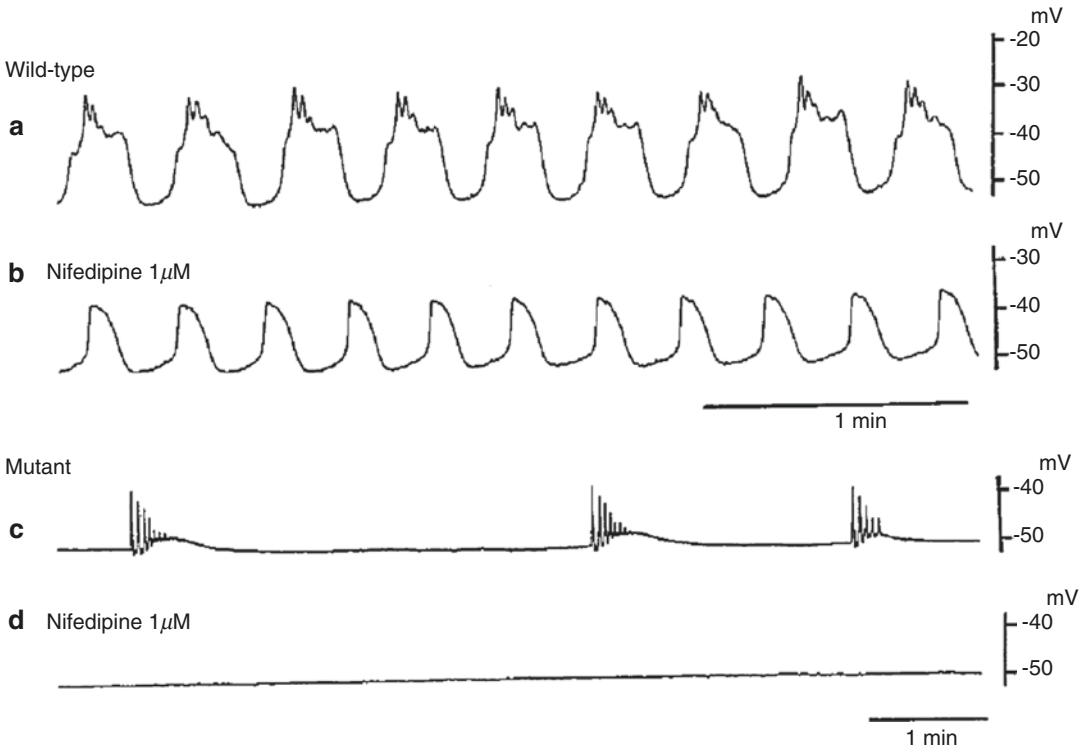

Fig. 1.12 Loss of slow waves in Itpr1$^{-/-}$ mice. (**a**) Slow wave activity recorded by intracellular microelectrode from murine antral smooth muscle from a mouse 20 days after birth. (**b**) Slow waves are decreased in duration and amplitude by nifedipine. (**c**) Electrical activity recorded from mouse antrum from a 19-day-old *Itpr1*$^{-/-}$ mouse. Slow waves are absent and activity is spike-like complexes occurring without a constant frequency. (**d**) Electrical activity is abolished by nifedipine. Redrawn with permission from [163]

rhythmicity. Slow waves can be initiated by depolarization, or in some cases by anode break (i.e., at termination of a hyperpolarization). Slow waves initiated in pyloric muscle in response to depolarization or anode break were also blocked by heparin loading but not by ryanodine. It was concluded that Ca^{2+} release from the ER via IP_3 receptors is fundamental to electrical rhythmicity and proposed that responses to depolarization are due to voltage-dependent enhancement in IP_3 synthesis or responsiveness of IP_3R, as observed in SMCs [165]. This idea has also been proposed by other authors [31, 166], but no verification of voltage-dependent IP_3 production or voltage-dependent sensitization of IP_3R in ICC has been provided to date.

Another study of intact muscles characterized the effects of several Ca^{2+} store-active drugs on electrical rhythmicity in the murine small intestine [167]. CPA (1–3 μM) depolarized muscles and decreased slow wave frequency by 46%, but when compared with elevated $[K^+]_o$, which also caused depolarization and decreased slow wave frequency, the effects of CPA were significantly greater and could not be explained by depolarization alone. Thapsigargin (1 μM), another SERCA pump inhibitor, blocked slow waves after relatively long periods of exposure. Similar effects were produced by xestospongin C, an inhibitor of IP_3R, caffeine and inhibitors of phospholipase C (U-73122, neomycin, and 2-nitro-4-carboxyphenyl-*N*,*N*-diphenylcarbamate).

In contrast ryanodine (50 μM) depolarized muscles and caused minor effects on slow waves that were judged to be the result of the depolarization. Ca^{2+} stores are also important in slow wave propagation, as investigated with partitioned chambers, where slow waves could be reliably

induced in a chamber perfused with normal Krebs solution and effects of Ca^{2+} store-active drugs could be evaluated in another chamber. Slow wave propagation was blocked by 2-APB in canine colonic muscles, and CPA greatly inhibited the plateau potentials of propagated slow waves in the canine gastric antrum [78, 80]. These studies all concluded that Ca^{2+} release from stores occurs via IP_3R, and ryanodine receptors are not a significant factor in slow wave generation and propagation.

IP_3Rs and RyRs are broadly expressed in cells of the SIP syncytium, making studies on intact GI muscles complicated because drugs blocking these receptors might have a multiplicity of effects. Attempts to avoid these problems have utilized cultured ICC, in which phenotypic changes might also be a confounding factor. Nevertheless, rhythmic inward currents were blocked by xestospongin C, thapsigargin, and heparin dialysis of cells [168]. Another study of this type needs to be discussed because of the uniqueness of its conclusion that ryanodine receptors are involved and fundamental to Ca^{2+} signaling in ICC. Cell cluster preparations were developed from partially digested murine gastric muscles containing circular and longitudinal muscles and myenteric plexus [169]. ICC were present in the cell clusters and identified by c-Kit labeling. After 2–4 days in culture, the clusters were loaded with Fluo-3 and Ca^{2+} oscillations were monitored. Nifedipine blocked Ca^{2+} transients in SMCs, and under these conditions remaining Ca^{2+} transients were viewed to be oscillations in pacemaker ICC. RyR subtype 3 was found to be expressed in c-Kit^+ cells, and FKBP12 and FKBP12.6 (modulators of the Ca^{2+} conductance of ryanodine receptors) were expressed in the cell clusters. Recent focused expression studies and transcriptome analysis show that RyR1-3 receptors are expressed in small intestinal ICC, and the predominant paralog is RyR2 [156]. *Fkbp1a* is expressed in all of the SIP cells, not just SMCs [117]. Both ryanodine and FK506, an immunosuppressant drug, inhibited Ca^{2+} oscillations in c-Kit^+ cells in cell clusters [169]. These were the first experiments identifying a potential role for RyRs in the generation of rhythmic activity. More recently, the role of Ca^{2+} stores in generating Ca^{2+} transients was investigated by imaging ICC of the murine small intestine in situ [156, 157]. These studies showed that Ca^{2+} transients in ICC-DMP were blocked by CPA and thapsigargin and by ryanodine (100 μM). Xestospongin C (10 μM) also blocked Ca^{2+} transients in ICC-DMP. Different effects were noted in pacemaker ICC-MY, where ryanodine (100 μM) blocked Ca^{2+} transients completely, but these events were far less sensitive to xestospongin C. In both types of ICC, interplay or amplification of Ca^{2+} release events appears to occur between IP_3Rs and RyRs. The sequence of activation (i.e., RyR releasing Ca^{2+} and being amplified by release from IP_3R or in reverse) is unknown at present, but in small intestinal ICC-MY the dominant release channels appear to be RyRs. Finding that Ca^{2+} release can be organized into CTCs (Fig. 1.11) and this depends upon Ca^{2+} entry via T-type Ca^{2+} channels suggests that CICR may be a fundamental factor in linking the voltage-dependent mechanism of propagation to regeneration of slow waves, as depicted in Fig. 1.9.

While not assaying Ca^{2+} release events directly, another study monitored activation of CaCCs and development of STICs and slow wave currents in isolated murine small intestinal ICC [170]. STICs and slow wave currents activated by depolarization were inhibited significantly by CPA and thapsigargin, showing the need for functional Ca^{2+} stores to generate these basic ICC behaviors. Tetracaine (also an inhibitor of RyRs) blocked STICs and reduced slow wave currents, and ryanodine at 50 μM had an initial small increase in STICs, but with a longer exposure inhibited these events. The same was true for slow wave currents when exposure time was increased to several minutes. Xestospongin C also had inhibitory effects on STICs and slow wave currents. The possibility that some of the store-active drugs might have nonselective effects and inhibit Ano1 was also tested. Ryanodine, CPA, and thapsigargin all had little or no effect on Ano1 directly.

The representative studies above suggest there is diversity in the Ca^{2+} release apparatus in the ICC found in different anatomical niches within a given GI muscle, and diversity between organs also occurs. More studies will be needed to verify

this idea more broadly and to better understand how this diversity facilitates specific functions, determines the frequency of Ca^{2+} release events, or shapes the waveforms of electrical responses. There are also important structural questions about the relationship between the plasma membrane and Ca^{2+} release sites and channels, and these will be addressed in the section below on nanodomains in ICC.

1.6.2 Role of Mitochondria in Pacemaker Activity

A typical observation in ultrastructural studies of ICC is that these cells display an abundance of mitochondria, particularly in the perinuclear spaces [64, 171, 172]. Studies of cultured ICC and intact GI muscles have suggested a role for mitochondria in the Ca^{2+} handling required for pacemaker activity and propagation of slow waves. Several drugs used commonly to block key mitochondrial ion channels and transporters and to deactivate the electron transport chain reduce electrical rhythmicity in cultured ICC and slow waves in intact GI muscles of several species [168]. Oligomycin, a compound that blocks synthesis of ATP, was not effective in blocking slow waves either in the cultured cells or in intact muscles. Thus, compromising the metabolic role of mitochondria did not seem to be responsible for the effects of mitochondrial drugs on pacemaker activity. Many of the same compounds have been shown to inhibit slow waves in strips of muscles from several species [62, 166, 173], propagation of slow waves [78, 79], spread of Ca^{2+} waves in ICC networks [151, 153], and spontaneous transient depolarizations (aka unitary potentials; [19, 174]). Mitochondrial involvement was thought to involve uptake or regulation of Ca^{2+} release during the slow wave cycle [168], and a biophysically based model was developed, incorporating mitochondrial Ca^{2+} uptake into a slow wave mechanism [175]. However, more recent experiments have suggested more direct Ca^{2+} regulation of the pacemaker mechanism in ICC (i.e., via activation of Ano1 CaCCs), so the role of mitochondria in the pacemaker mechanism and the effects of mitochondrial agents on slow waves were revisited. All of the mitochondrial agents used in prior studies of slow wave generation and propagation reduced or blocked Ca^{2+} transients in ICC-MY, but had far less effect on Ca^{2+} transients in ICC-DMP [176]. The effects of mitochondrial drugs share similarities with the effects of T-type channel and Ano1 antagonists on Ca^{2+} transients, and mitochondrial drugs were found to be effective blockers of $Ca_V3.2$ and/or Ano1 channels expressed in HEK293 cells. Thus, the role of mitochondria in the pacemaker activity of ICC is questionable at present, as most of the effects noted in past studies can be explained by the nonspecific effects on key ion channels involved in pacemaker activity.

1.6.3 Nanodomains as the Basis for Functional Pacemaker Units in ICC

We have proposed that signaling in microdomains (aka pacemaker units, but the current preferred terminology is nanodomains due to size and volume of these junctions) is important for the pacemaker mechanism because the concentrations of key ions involved in transmembrane currents and transport are far more likely to reach effective concentrations in these small volumes than in the cytoplasm. A striking finding is that Ano1 channels, which are activated tonically in HEK293 cells bearing homologous expression of Ano1 splice variants when cells are dialyzed with elevated internal Ca^{2+} (100–500 nM), depending upon splice variant [121–123, 126–128], are not activated by cytosolic $[Ca^{2+}]_i$ of 1 μM in ICC [170]. This observation suggests that Ano1 channels are clustered into areas of plasma membrane that are serviced by Ca^{2+} released from stores, but protected from changes in $[Ca^{2+}]_{cyt}$. Clustering of Ano1 channels also favors generation of STICs that occur through the opening of many channels in response to localized Ca^{2+} release. Clustered Ano1 channels are likely to occur in nanodomains, but questions remain whether other key proteins involved in pacemaker activity (e.g., $Ca_V3.2$, NKCC1, IP_3R1, RYR, the sodium pump

and possibly Na^+Ca^{2+} exchange proteins) are also co-localized in these nanodomains. The high probability for Ca^{2+} release events to occur repetitively from specific sites in the cell soma and processes [157] favors the idea that specialized ER domains, containing elevated numbers of Ca^{2+} release channels, are present. Depolarization of network ICC leads to activation of T-type Ca^{2+} channels in ICC which appears to be the voltage-dependent mechanism allowing active propagation of slow waves through the network [2]. As T-type Ca^{2+} channels are activated, Ca^{2+} entry occurs, but the relatively low current density due to T-type Ca^{2+} channels in ICC [137] suggests that Ca^{2+} entry is focused into nanodomains where a rise in $[Ca^{2+}]$ is effective in activating CICR and CaCCs. A schematic showing the key proteins and their arrangement within nanodomains to facilitate CICR in ICC is shown in Fig. 1.9.

1.7 Dynamic Modulation of Intrinsic Electrical Rhythmicity

Until now, we have concentrated on spontaneous slow wave generation in ICC and propagation in ICC networks in GI muscles, but these cells do not operate in isolation, and many factors, too numerous to describe comprehensively in this chapter, influence slow waves and thus motility patterns in the gut. Transcriptome data indicate that ICC express myriad receptors for neurotransmitters, hormones, paracrine substances, and inflammatory mediators, and they also express effector proteins that facilitate reactions to a variety of physical factors such as stretch, compression (as might occur in muscle contraction), temperature, and pH [117]. ICC may also be secretory cells, and, as an example of this idea, they express a reactome consistent with production of PGE_2 or PGI_2 (e.g., *Pla2g4a*, *Ptgs1*, *Ptges3*, *Ptgis*). It should also be understood that due to the electrical coupling between SMCs, ICC, and PDGFRα$^+$ cells (SIP syncytium), electrophysiological responses of any SIP cell can potentially affect the functions of ICC. For example, neurotransmitters or hormones linked to enhanced production of cAMP and activation of protein kinase A in SMCs tend to activate K_{ATP} channels and cause hyperpolarization of SMCs [46, 177–179]. Hyperpolarization of SMCs conducts to ICC and can influence voltage-dependent mechanisms in these cells (e.g., Ca^{2+} entry mechanisms and slow wave propagation). Similarly, P2Y1 receptor agonists (e.g., purine neurotransmitters) cause activation of small-conductance Ca^{2+}-activated K^+ channels in PDGFRα$^+$ cells, causing profound hyperpolarization of these cells and other SIP cells [22, 49, 180]. Integration of inputs to the SIP syncytium are illustrated in Fig. 1.13.

Neural inputs have chronotropic effects on gastric slow waves [54] and affect coupling between slow waves and generation of action potentials by SMCs in other regions of the GI tract [99, 181]. Studies of *W/W^V* mutants, in which ICC fail to develop in some regions of the GI tract [3, 5, 108], show that cholinergic and nitrergic neural inputs to gastric muscles are reduced in the absence of the intramuscular class of ICC [182, 183]. The extent and significance of ICC in enteric motor neurotransmission has been hotly debated in the literature [184–187], but it seems beyond debate at this point that ICC are innervated. Therefore, post-junctional responses that alter membrane conductances in ICC will influence the integrated motor output of the SIP syncytium.

The discussion above describes how Ca^{2+} transients are fundamental to ICC behavior. Recent studies have investigated how neural inputs influence Ca^{2+} transients in ICC-DMP in the murine small intestine. ICC-DMP represent the intramuscular class of ICC in the small intestine and varicosities of motor neurons are closely associated with these cells and form synaptic-like connections of less than 20 nM between nerves and ICC [106, 188, 189]. Receptors for major enteric motor neurotransmitters are expressed by ICC-DMP [118, 190, 191], and the cells bind neurotransmitters, undergo receptor internalization, and translocate signaling molecules in response to nerve stimulation [192, 193]. Muscles expressing optogenetic Ca^{2+} sensors in ICC showed that

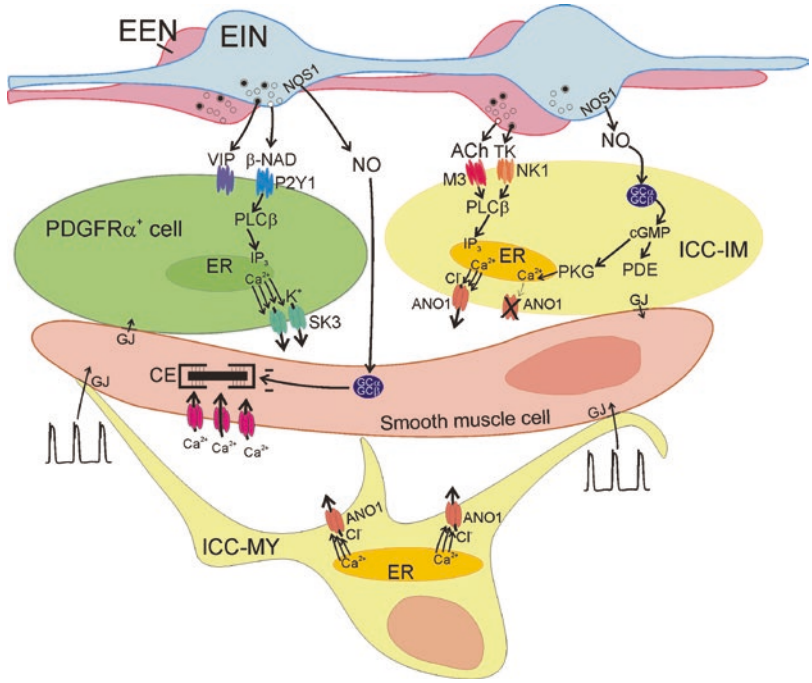

Fig. 1.13 Schematic showing integration of inputs in the SIP syncytium. Schematic is developed from experimental evidence obtained from murine small intestine. SIP syncytium consists of SMCs, PDGFRα+ cells, and ICC (in small intestine the ICC are ICC-MY and ICC-IM; see Table 1.1 for additional details). ICC-MY are pacemaker cells and generate electrical slow waves by processes described in detail in Fig. 1.8 and depicted here as Ca^{2+} release from ER and activation of Ano1 channels in plasma membrane. Slow wave conduct through gap junctions (GJ) and depolarize SMCs. Depolarization activates Ca^{2+} entry through L-type Ca^{2+} channels and initiates cross bridge cycling of contractile elements (CE). Slow waves are omnipresent, but their impact on SMC contraction is modulated by inputs from enteric excitatory (EEN) and inhibitory (EIN) neurons that are intermingled and closely associated with PDGFRα+ cells and ICC-IM. EENs release ACh and tachykinins (substance P and possibly neurokinin A). These neurotransmitters bind to muscarinic type 3 (M3) receptors and neurokinin 1 (NK1) receptors expressed by ICC-IM. Both receptors couple through $G_{q/11}$ and activate phospholipase Cβ (PLCβ) and production of IP_3 and diacylglycerol (not shown). IP_3 binds to IP_3Rs in the ER (not shown) and causes intense release of Ca^{2+} (depicted as multiple black arrows from ER) and activation of Ano1 channels in the plasma membrane. This is a depolarizing response that conducts to SMCs via GJs and summates with the slow waves that are ongoing in the syncytium. EINs release NO, purines (β-NAD), and peptides (depicted here as VIP but also likely to include PACAP). NO binds to soluble guanylyl cyclase (GCα/GCβ dimer) in ICC, SMCs, and possibly in PDGFRα+ cells (not shown) that also express these subunits but no response has been documented. GCα/GCβ dimers in ICC generate cGMP and activate protein kinase G (PKG) or inhibit phosphodiesterases (PDE). The mechanisms coupled to these effectors are not entirely understood. But PKG is linked to reduction in Ca^{2+} release from ER (dotted arrow), and this decreases or halts activation of Ano1 currents (X). This is a hyperpolarizing trend that can also conduct to SMCs via GJs. In SMCs GCα/GCβ dimers can also be activated by NO, causing reduced Ca^{2+} sensitization of the CE and reduction in the force of contraction. β-NAD (and possibly other purines) is/are released from EINs and bind to P2Y1 receptors on PDGFRα+ cells. This activates PLCβ, generates IP_3, and causes Ca^{2+} release from ER. Ca^{2+} release activates small-conductance Ca^{2+}-activated K^+ channels in PDGFRα+ cells. This pathway generates strong hyperpolarization that conducts to SMCs via GJ. Hyperpolarization of SMCs tends to reduce the open probability of L-type Ca^{2+} channels, restricting Ca^{2+} entry and reducing the force of contractions. Functions and responses of SIP cells to inhibitory peptides are not yet clarified

stimulation of enteric motor neurons by electrical field stimulation (EFS) causes initial inhibition of Ca^{2+} transients followed by intense activation that persists well after termination of the stimulus [194]. Atropine decreased the frequency of Ca^{2+} transients somewhat, but a larger decrease was caused by RP 67580 or SR 140333, both NK1 receptor antagonists. The brief inhibitory period

at the initiation of EFS was due to nitrergic neural regulation [195].

SMCs express nonselective cation channels that respond to muscarinic stimulation [196–198]. Ano1 channels, which are not expressed by GI SMCs, mediate muscarinic responses in ICC [23]. To address the controversy about the role of ICC in excitatory neurotransmission experiments were performed on *Ano1*$^{-/-}$ mice. When inhibitory responses are blocked, EFS of gastric muscles elicits EJPs in post-junctional cells. EJPs are absent in mice lacking Ano1, and contractile responses are also diminished. Pharmacological block of Ano1 channels also reduced EJPs and contractile responses. Inhibiting acetylcholinesterase caused development of a slow depolarization that followed the normal fast EJP. This event was retained in the Ano1$^{-/-}$ mice and was likely due to overflow of neurotransmitter to extrajunctional muscarinic receptors on SMCs. These experiments demonstrate primary innervation and transduction of cholinergic responses by ICC, and the results are consistent with previous evaluations of cholinergic innervation of ICC-IM using a variety of experimental tests and approaches [182, 199].

A study using a membrane-permeable Ca^{2+} indicator reported that the oscillatory activities of ICC-MY and ICC-DMP in the small intestine undergo phase-amplitude coupling [154], and the output of this coupling generates a slow wave pattern known as waxing and waning [200, 201]. ICC-MY and ICC-DMP are distinct populations of cells in the murine small intestine and separated by most of the thickness of the circular muscle layer. The only means of coupling between these cells seems to be via electrical coupling through SMCs. Thus, electrical events in one type of ICC might "couple" or interact with the electrical events in the other population of cells. Such an interaction seems unlikely, however, because the electrical events generated by ICC-DMP are STICs [202] due to activation of Ano1 CaCCs and generated by transient bursts of Ca^{2+} release from intracellular stores [156]. Neither the Ca^{2+} transients nor the STICs [170] are oscillatory in nature. These events occur in a stochastic manner with little or no correlation in the timing between events in the same cell or between the events in adjacent cells [156]. Recordings of Ca^{2+} transients for several minutes in adjacent ICC-DMP in full thickness small intestinal sheets of muscle (in which ICC-MY are present and slow waves are omnipresent) revealed no cyclical influences on Ca^{2+} transients in ICC-DMP. High resolution observations of ICC-DMP showed that Ca^{2+} transients in ICC-DMP are not regulated by membrane potential. Depolarizations of the SIP syncytium occurring through slow wave activity exert no apparent influence on the stochastic nature of Ca^{2+} release events in ICC-DMP [156]. Hyperpolarization of tissues upon the opening of K^+ channels in other SIP cells also has no influence on Ca^{2+} transients in ICC-DMP. Lack of voltage-dependent regulation is likely to result from the fact that ICC-DMP do not express functional voltage-dependent Ca^{2+} channels [118, 170].

As discussed previously in this chapter, Ca^{2+} entry facilitates coordinated release of Ca^{2+}, due to Ca^{2+}-induced Ca^{2+} release in ICC-MY, but lacking such a mechanism in ICC-DMP frees these cells to fire Ca^{2+} transients independently. This is an important characteristic of intramuscular ICC that are innervated by enteric motor neurons, express receptors and post-receptor effector mechanisms. As discussed previously, neurotransmitters released from excitatory or inhibitory motor neurons enhance or suppress Ca^{2+} transients, respectively. If Ca^{2+} transients were regulated by voltage, then their responses to neural inputs may be unpredictable due to net hyperpolarizing or depolarizing influences that might originate elsewhere in the SIP syncytium. For example, if depolarization enhanced Ca^{2+} transients, then periods of depolarization (peaks of slow waves or responses to paracrine stimuli, etc.) would tend to predetermine neural responses. If hyperpolarization shut down Ca^{2+} release, then such a trend could render inhibitory neurotransmission ineffective and perhaps limit excitatory responses. Being unaffected by membrane potential allows neural responses of ICC-DMP to be independent, and therefore neural influences can be superimposed upon (i.e., summate with) the

intrinsic activities of the SIP syncytium. In normal GI organs enteric motor neurons determine motility patterns, so it is important that their commands not be circumvented by the intrinsic behaviors of SIP cells.

Stretch is another factor that affects electrical rhythmicity; however, there is less known about this stimulus than regulation by nerves and hormones. Stretch of tissues making up the walls of hollow organs is inevitable as the organs are filled or as boluses of luminal contents are shifted from one segment to another. In one study murine gastric antral muscles were stretched by a computer-driven apparatus that allowed precise selection of ramp speed and maximum tension [203]. Stretch of muscles caused rate-dependent changes in membrane potential and slow wave frequency. Responses to stretch were mediated by ICC-IM, as the responses did not occur in W/W^{V} mice that have reduced numbers of ICC-IM in the stomach. Indomethacin treatment also blocked the responses to stretch, and the responses were absent in *Ptgs2*$^{-/-}$ mice. These findings suggest that stretch-dependent activation of prostaglandin synthesis may be a chronotropic mechanism affecting pacemaker activity in the gastric antrum.

1.8 Areas in Need of Future Investigation

There are currently many shortcomings in our understanding of electrical rhythmicity in GI muscles. A goal of biomedical research is to understand human physiology and pathophysiology such that pharmaceuticals appropriate for the treatment of human disorders can be designed. Few treatments for common GI motility disorders exist, and this may be because understanding of human disease is based on animal models that do not translate to human physiology and pathophysiology with fidelity. Comprehensive study of electrical rhythmicity in human GI muscles is lacking, and it was surprising, for example, to learn recently that the frequency of electrical slow waves in the stomach may be higher than the literature has reported confidently for several decades [56]. Studies of human gastric muscles in vitro revealed many discrepancies from textbook descriptions of human gastric electrophysiology, including the presence of slow wave activity in the gastric fundus, a slow wave frequency in antral muscles about twice that reported from surface electrode recording, and no clear gradient in slow wave frequency from proximal to distal stomach. A more definitive understanding of human electrical rhythmicity is needed to understand what actually drives changes in slow wave activity, gastric contractions, and gastric emptying in motility disorders, such as gastroparesis. As mentioned previously, most recent work investigating the mechanisms of pacemaker activity have been performed on mice, and it is unclear whether these mechanisms are common to other species and humans. Better means of identifying ICC in mixed cell populations after tissue dispersion are needed to facilitate comparative physiological and molecular studies of these cells in isolation of the other cells in whole muscles. Work toward understanding the molecular phenotypes of ICC has started [117, 118], and the data from these studies suggest a broader role for ICC than previously suspected, including responses to hormones and paracrine substances and possibility a role as secretory cells. Transcriptomic data may also provide insights on how to recover the phenotype of ICC when cells are lost or damaged in disease. It would be valuable to develop a cell culture or organoid model of ICC that could be used for high-throughput screening of inflammatory mediators and/or drugs. Some progress has been made in this regard [169, 204], but it will be necessary to optimize conditions to maximize retention of the native phenotype in these in vitro preparations. Of many challenges remaining in the study of ICC, the largest are to understand what happens to ICC in a variety of human motility disorders and develop the means, possibly through manipulation of tissue stem cells or reseeding of progenitor cells [205], to reestablish functional networks of cells. Motility disorders involving loss or damage to ICC networks will be very difficult to treat effectively until these challenges are met.

Acknowledgments The author is grateful for the editorial assistance of Dr. Bernard Drumm, whose careful reading of the manuscript and many suggestions improved the text and figures. I would also like to acknowledge my long-term collaborations with Profs. Sean Ward and Sang Don Koh for countless discussions, contributions, and data without which my knowledge and ability to write a chapter on GI rhythmicity would have been impossible. I would also like to acknowledge many astute contributions from Prof. David Hirst who, through yearly working trips to Reno, challenged many of the concepts we had developed from studies of cultured ICC and forced us to seek better techniques and preparations in which to investigate the mechanism of electrical slow waves in ICC. I am also extremely grateful to Nancy Horowitz, Yulia Bayguinov, Lauren O'Kane, Dr. Doug Redelman, and Byoung Koh for excellent and consistent technical support for investigations of ICC. As always, I am extremely grateful to the NIDDK for the support received through a Program Project Grant, P01 DK41315-29 and a MERIT Award, R37 DK40569.

References

1. Sanders KM, Koh SD, Ro S, Ward SM. Regulation of gastrointestinal motility-insights from smooth muscle biology. Nat Rev Gastroenterol Hepatol. 2012;9(11):633–45.
2. Sanders KM, Ward SM, Koh SD. Interstitial cells: regulators of smooth muscle function. Physiol Rev. 2014;94(3):859–907.
3. Huizinga JD, Thuneberg L, Kluppel M, Malysz J, Mikkelsen HB, Bernstein A. W/kit gene required for interstitial cells of Cajal and for intestinal pacemaker activity. Nature. 1995;373(6512):347–9.
4. Langton P, Ward SM, Carl A, Norell MA, Sanders KM. Spontaneous electrical activity of interstitial cells of Cajal isolated from canine proximal colon. Proc Natl Acad Sci U S A. 1989;86(18):7280–4.
5. Ward SM, Burns AJ, Torihashi S, Sanders KM. Mutation of the proto-oncogene c-kit blocks development of interstitial cells and electrical rhythmicity in murine intestine. J Physiol. 1994;480. (Pt 1:91–7.
6. Cobine CA, Hannah EE, Zhu MH, Lyle HE, Rock JR, Sanders KM, et al. ANO1 in intramuscular interstitial cells of Cajal plays a key role in the generation of slow waves and tone in the internal anal sphincter. J Physiol. 2017;595(6):2021–41.
7. Alvarez WCaM LJ. Action current in stomach and intestine. Am J Phys. 1922;58:476–93.
8. Richter CP. Action currents from the stomach. Am J Phys. 1924;67:612–33.
9. Sanders KM, Ward SM, Hennig GW. Extracellular gastrointestinal electrical recordings: movement not electrophysiology. Nat Rev Gastroenterol Hepatol. 2017;14(6):372.
10. Kuriyama H, Tomita T. The action potential in the smooth muscle of the guinea pig taenia coli and ureter studied by the double sucrose-gap method. J Gen Physiol. 1970;55(2):147–62.
11. Szurszewski JH. Mechanism of action of pentagastrin and acetylcholine on the longitudinal muscle of the canine antrum. J Physiol. 1975;252(2):335–61.
12. Connor JA, Prosser CL, Weems WA. A study of pacemaker activity in intestinal smooth muscle. J Physiol. 1974;240(3):671–701.
13. Ohba M, Sakamoto Y, Tomita T. The slow wave in the circular muscle of the guinea-pig stomach. J Physiol. 1975;253(2):505–16.
14. Bulbring E. Smooth muscle potentials recorded in the taenia coli of the guineapig. J Physiol. 1954;123(3):55P–6P.
15. El-Sharkaway TY, Daniel EE. Ionic mechanisms of intestinal electrical control activity. Am J Phys. 1975;229(5):1287–98.
16. el-Sharkawy TY, Morgan KG, Szurszewski JH. Intracellular electrical activity of canine and human gastric smooth muscle. J Physiol. 1978;279:291–307.
17. Daniel EE, Honour AJ, Bogoch A. Electrical activity of the longitudinal muscle of dog small intestine studied in vivo using microelectrodes. Am J Phys. 1960;198:113–8.
18. Koh SD, Ward SM, Ordog T, Sanders KM, Horowitz B. Conductances responsible for slow wave generation and propagation in interstitial cells of Cajal. Curr Opin Pharmacol. 2003;3(6):579–82.
19. Beckett EA, Bayguinov YR, Sanders KM, Ward SM, Hirst GD. Properties of unitary potentials generated by intramuscular interstitial cells of Cajal in the murine and guinea-pig gastric fundus. J Physiol. 2004;559.(Pt 1:259–69.
20. Hirst GD, Dickens EJ, Edwards FR. Pacemaker shift in the gastric antrum of guinea-pigs produced by excitatory vagal stimulation involves intramuscular interstitial cells. J Physiol. 2002;541.(Pt 3: 917–28.
21. Hirst GD, Silverberg GD, van Helden DF. The action potential and underlying ionic currents in proximal rat middle cerebral arterioles. J Physiol. 1986;371:289–304.
22. Kurahashi M, Zheng H, Dwyer L, Ward SM, Don Koh S, Sanders KM. A functional role for the 'fibroblast-like cells' in gastrointestinal smooth muscles. J Physiol. 2011;589.(Pt 3:697–710.
23. Sung TS, Hwang SJ, Koh SD, Bayguinov Y, Peri LE, Blair PJ, et al. The cells and conductance mediating cholinergic neurotransmission in the murine proximal stomach. J Physiol. 2018;596:1549–74.
24. Code CF, Szurszewski JH. The effect of duodenal and mid small bowel transection on the frequency gradient of the pacesetter potential in the canine small intestine. J Physiol. 1970;207(2):281–9.
25. Thomsen L, Robinson TL, Lee JC, Farraway LA, Hughes MJ, Andrews DW, et al. Interstitial cells of Cajal generate a rhythmic pacemaker current. Nat Med. 1998;4(7):848–51.

26. Daniel EE, Robinson K, Duchon G, Henderson RM. The possible role of close contacts (nexuses) in the propagation of control electrical activity in the stomach and small intestine. Am J Dig Dis. 1971;16(7):611–22.
27. Christensen J, Schedl HP, Clifton JA. The small intestinal basic electrical rhythm (slow wave) frequency gradient in normal men and in patients with variety of diseases. Gastroenterology. 1966;50(3):309–15.
28. Bortoff A. Electrical transmission of slow waves from longitudinal to circular intestinal muscle. Am J Phys. 1965;209(6):1254–60.
29. Bozler E. The relation of the action potentials to mechanical activity in intestinal muscle. Am J Phys. 1946;146:496–501.
30. Suzuki H, Hirst GD. Regenerative potentials evoked in circular smooth muscle of the antral region of guinea-pig stomach. J Physiol. 1999;517(Pt 2):563–73.
31. Hirst GD, Bramich NJ, Teramoto N, Suzuki H, Edwards FR. Regenerative component of slow waves in the guinea-pig gastric antrum involves a delayed increase in [Ca(2+)](i) and Cl(−) channels. J Physiol. 2002;540.(Pt 3:907–19.
32. Hirst GD, Edwards FR. Generation of slow waves in the antral region of guinea-pig stomach—a stochastic process. J Physiol. 2001;535.(Pt 1:165–80.
33. Cousins HM, Edwards FR, Hickey H, Hill CE, Hirst GD. Electrical coupling between the myenteric interstitial cells of Cajal and adjacent muscle layers in the guinea-pig gastric antrum. J Physiol. 2003;550.(Pt 3:829–44.
34. Dickens EJ, Hirst GD, Tomita T. Identification of rhythmically active cells in guinea-pig stomach. J Physiol. 1999;514(Pt 2):515–31.
35. Ordog T, Ward SM, Sanders KM. Interstitial cells of Cajal generate electrical slow waves in the murine stomach. J Physiol. 1999;518. (Pt 1:257–69.
36. Szurszewski JH. Electrical basis for gastrointestinal motility. In: Johnson LR, editor. Physiology of the gastrointestinal tract. 2nd ed. New York: Raven Press; 1981. p. 1435–66.
37. Tomita T. Electrical activity (spikes and slow waves) in gastrointestinal smooth muscles. In: Bulbring E, Brading AF, Tomita T, editors. Smooth muscle: An assessment of current knowledge. London: Edward Arnold; 1981. p. 127–56.
38. Dickens EJ, Edwards FR, Hirst GD. Selective knockout of intramuscular interstitial cells reveals their role in the generation of slow waves in mouse stomach. J Physiol. 2001;531.(Pt 3:827–33.
39. Horner MJ, Ward SM, Gerthoffer WT, Sanders KM, Horowitz B. Maintenance of morphology and function of canine proximal colon smooth muscle in organ culture. Am J Phys. 1997;272(3. Pt 1):G669–80.
40. Hall KA, Ward SM, Cobine CA, Keef KD. Spatial organization and coordination of slow waves in the mouse anorectum. J Physiol. 2014;592(17):3813–29.
41. Forster J, Damjanov I, Lin Z, Sarosiek I, Wetzel P, McCallum RW. Absence of the interstitial cells of Cajal in patients with gastroparesis and correlation with clinical findings. J Gastrointest Surg. 2005;9(1):102–8.
42. Grover M, Bernard CE, Pasricha PJ, Lurken MS, Faussone-Pellegrini MS, Smyrk TC, et al. Clinical-histological associations in gastroparesis: results from the Gastroparesis Clinical Research Consortium. Neurogastroenterol Motil. 2012;24(6):531–9. e249
43. Ordog T, Takayama I, Cheung WK, Ward SM, Sanders KM. Remodeling of networks of interstitial cells of Cajal in a murine model of diabetic gastroparesis. Diabetes. 2000;49(10):1731–9.
44. Kito Y, Sanders KM, Ward SM, Suzuki H. Interstitial cells of Cajal generate spontaneous transient depolarizations in the rat gastric fundus. Am J Physiol Gastrointest Liver Physiol. 2009;297(4):G814–24.
45. Kito Y, Suzuki H. Properties of pacemaker potentials recorded from myenteric interstitial cells of Cajal distributed in the mouse small intestine. J Physiol. 2003;553.(Pt 3:803–18.
46. Kito Y, Ward SM, Sanders KM. Pacemaker potentials generated by interstitial cells of Cajal in the murine intestine. Am J Phys Cell Phys. 2005;288(3): C710–20.
47. Kito Y, Mitsui R, Ward SM, Sanders KM. Characterization of slow waves generated by myenteric interstitial cells of Cajal of the rabbit small intestine. Am J Physiol Gastrointest Liver Physiol. 2015;308(5):G378–88.
48. Jun JY, Kong ID, Koh SD, Wang XY, Perrino BA, Ward SM, et al. Regulation of ATP-sensitive K(+) channels by protein kinase C in murine colonic myocytes. Am J Phys Cell Phys. 2001;281(3):C857–64.
49. Kito Y, Kurahashi M, Mitsui R, Ward SM, Sanders KM. Spontaneous transient hyperpolarizations in the rabbit small intestine. J Physiol. 2014;592.(Pt 21:4733–45.
50. Kelly KA, Code CF, Elveback LR. Patterns of canine gastric electrical activity. Am J Phys. 1969;217(2):461–70.
51. Publicover NG, Sanders KM. A technique to locate the pacemaker in smooth muscles. J Appl Physiol. 1984;57(5):1586–90.
52. Bauer AJ, Reed JB, Sanders KM. Slow wave heterogeneity within the circular muscle of the canine gastric antrum. J Physiol. 1985;366:221–32.
53. Horiguchi K, Semple GS, Sanders KM, Ward SM. Distribution of pacemaker function through the tunica muscularis of the canine gastric antrum. J Physiol. 2001;537.(Pt 1:237–50.
54. Forrest AS, Ordog T, Sanders KM. Neural regulation of slow-wave frequency in the murine gastric antrum. Am J Physiol Gastrointest Liver Physiol. 2006;290(3):G486–95.
55. Hashitani H, Garcia-Londono AP, Hirst GD, Edwards FR. Atypical slow waves generated in gastric corpus provide dominant pacemaker activity in guinea pig stomach. J Physiol. 2005;569(Pt 2):459–65.
56. Rhee PL, Lee JY, Son HJ, Kim JJ, Rhee JC, Kim S, et al. Analysis of pacemaker activity in the human stomach. J Physiol. 2011;589.(Pt 24:6105–18.

57. Hara Y, Kubota M, Szurszewski JH. Electrophysiology of smooth muscle of the small intestine of some mammals. J Physiol. 1986;372:501–20.
58. Jimenez M, Cayabyab FS, Vergara P, Daniel EE. Heterogeneity in electrical activity of the canine ileal circular muscle: interaction of two pacemakers. Neurogastroenterol Motil. 1996;8(4):339–49.
59. Durdle NG, Kingma YJ, Bowes KL, Chambers MM. Origin of slow waves in the canine colon. Gastroenterology. 1983;84(2):375–82.
60. Smith TK, Reed JB, Sanders KM. Interaction of two electrical pacemakers in muscularis of canine proximal colon. Am J Phys. 1987;252(3. Pt 1):C290–9.
61. Smith TK, Reed JB, Sanders KM. Origin and propagation of electrical slow waves in circular muscle of canine proximal colon. Am J Phys. 1987;252(2 Pt 1):C215–24.
62. Yoneda S, Takano H, Takaki M, Suzuki H. Properties of spontaneously active cells distributed in the submucosal layer of mouse proximal colon. J Physiol. 2002;542.(Pt 3:887–97.
63. Berezin I, Huizinga JD, Daniel EE. Interstitial cells of Cajal in the canine colon: a special communication network at the inner border of the circular muscle. J Comp Neurol. 1988;273(1):42–51.
64. Berezin I, Huizinga JD, Daniel EE. Structural characterization of interstitial cells of Cajal in myenteric plexus and muscle layers of canine colon. Can J Physiol Pharmacol. 1990;68(11):1419–31.
65. Suzuki N, Prosser CL, Dahms V. Boundary cells between longitudinal and circular layers: essential for electrical slow waves in cat intestine. Am J Phys. 1986;250(3 Pt 1):G287–94.
66. Ward SM, Sanders KM. Pacemaker activity in septal structures of canine colonic circular muscle. Am J Phys. 1990;259(2 Pt 1):G264–73.
67. Faussone Pellegrini MS. Ultrastructure and topography of Cajal interstitial cells in the circular muscle layer of the ileum and the colon in the rat. Boll Soc Ital Biol Sper. 1982;58(19):1260–5.
68. Rumessen JJ, Thuneberg L. Pacemaker cells in the gastrointestinal tract: interstitial cells of Cajal. Scand J Gastroenterol Suppl. 1996;216:82–94.
69. Rumessen JJ, Vanderwinden JM, Rasmussen H, Hansen A, Horn T. Ultrastructure of interstitial cells of Cajal in myenteric plexus of human colon. Cell Tissue Res. 2009;337(2):197–212.
70. Thuneberg L. Interstitial cells of Cajal: intestinal pacemaker cells? Adv Anat Embryol Cell Biol. 1982;71:1–130.
71. Komuro T, Seki K, Horiguchi K. Ultrastructural characterization of the interstitial cells of Cajal. Arch Histol Cytol. 1999;62(4):295–316.
72. Sanders KM, Stevens R, Burke E, Ward SW. Slow waves actively propagate at submucosal surface of circular layer in canine colon. Am J Phys. 1990;259(2 Pt 1):G258–63.
73. Carlson HC, Code CF, Nelson RA. Motor action of the canine gastroduodenal junction: a cineradiographic, pressure, and electric study. Am J Dig Dis. 1966;11(2):155–72.
74. Sarna SK, Daniel EE. Electrical stimulation of gastric electrical control activity. Am J Phys. 1973;225(1):125–31.
75. Bayguinov O, Hennig GW, Sanders KM. Movement based artifacts may contaminate extracellular electrical recordings from GI muscles. Neurogastroenterol Motil. 2011;23(11):1029–42. e498
76. Sanders KM, Ward SM, Hennig GW. Problems with extracellular recording of electrical activity in gastrointestinal muscle. Nat Rev Gastroenterol Hepatol. 2016;13(12):731–41.
77. Bauer AJ, Publicover NG, Sanders KM. Origin and spread of slow waves in canine gastric antral circular muscle. Am J Phys. 1985;249(6 Pt 1):G800–6.
78. Ward SM, Baker SA, de Faoite A, Sanders KM. Propagation of slow waves requires IP3 receptors and mitochondrial Ca2+ uptake in canine colonic muscles. J Physiol. 2003;549(Pt 1):207–18.
79. Ward SM, Dixon RE, de Faoite A, Sanders KM. Voltage-dependent calcium entry underlies propagation of slow waves in canine gastric antrum. J Physiol. 2004;561(Pt 3):793–810.
80. Bayguinov O, Ward SM, Kenyon JL, Sanders KM. Voltage-gated Ca2+ currents are necessary for slow-wave propagation in the canine gastric antrum. Am J Phys Cell Phys. 2007;293(5):C1645–59.
81. Kelly KA, La Force RC. Pacing the canine stomach with electric stimulation. Am J Phys. 1972;222(3):588–94.
82. Soffer EE. Gastric electrical stimulation for gastroparesis. J Neurogastroenterol Motil. 2012;18(2):131–7.
83. Publicover NG, Sanders KM. Effects of frequency on the wave form of propagated slow waves in canine gastric antral muscle. J Physiol. 1986;371: 179–89.
84. Kito Y, Fukuta H, Yamamoto Y, Suzuki H. Excitation of smooth muscles isolated from the guinea-pig gastric antrum in response to depolarization. J Physiol. 2002;543(Pt 1):155–67.
85. Walsh JV Jr, Singer JJ. Voltage clamp of single freshly dissociated smooth muscle cells: current-voltage relationships for three currents. Pflugers Arch. 1981;390(2):207–10.
86. Yoshino M, Wang SY, Kao CY. Sodium and calcium inward currents in freshly dissociated smooth myocytes of rat uterus. J Gen Physiol. 1997;110(5): 565–77.
87. Mitra R, Morad M. Ca2+ and Ca2+-activated K+ currents in mammalian gastric smooth muscle cells. Science. 1985;229(4710):269–72.
88. Langton PD, Burke EP, Sanders KM. Participation of Ca currents in colonic electrical activity. Am J Phys. 1989;257(3 Pt 1):C451–60.
89. Kuriyama H, Osa T, Toida N. Electrophysiological study of the intestinal smooth muscle of the guinea-pig. J Physiol. 1967;191(2):239–55.
90. Ozaki H, Stevens RJ, Blondfield DP, Publicover NG, Sanders KM. Simultaneous measurement of membrane potential, cytosolic Ca2+, and tension in intact smooth muscles. Am J Phys. 1991;260(5 Pt 1):C917–25.

91. Vogalis F, Publicover NG, Hume JR, Sanders KM. Relationship between calcium current and cytosolic calcium in canine gastric smooth muscle cells. Am J Phys. 1991;260(5 Pt 1):C1012–8.
92. Benham CD, Bolton TB, Denbigh JS, Lang RJ. Inward rectification in freshly isolated single smooth muscle cells of the rabbit jejunum. J Physiol. 1987;383:461–76.
93. Malysz J, Thuneberg L, Mikkelsen HB, Huizinga JD. Action potential generation in the small intestine of W mutant mice that lack interstitial cells of Cajal. Am J Phys. 1996;271(3 Pt 1):G387–99.
94. Ward SM, Burns AJ, Torihashi S, Harney SC, Sanders KM. Impaired development of interstitial cells and intestinal electrical rhythmicity in steel mutants. Am J Phys. 1995;269(6Pt 1):C1577–85.
95. Tashiro N, Tomita T. The effects of papaverine on the electrical and mechanical activity of the guinea-pig taenia coli. Br J Pharmacol. 1970;39(3):608–18.
96. Ward SM, Dalziel HH, Khoyi MA, Westfall AS, Sanders KM, Westfall DP. Hyperpolarization and inhibition of contraction mediated by nitric oxide released from enteric inhibitory neurones in guinea-pig taenia coli. Br J Pharmacol. 1996;118(1):49–56.
97. Duthie HL, Kirk D. Electrical activity of human colonic smooth muscle in vitro. J Physiol. 1978;283:319–30.
98. Vogalis F, Ward SM, Sanders KM. Correlation between electrical and morphological properties of canine pyloric circular muscle. Am J Phys. 1991;260(3 Pt 1):G390–8.
99. Sanders KM. Excitation-contraction coupling without Ca2+ action potentials in small intestine. Am J Phys. 1983;244(5):C356–61.
100. Morgan KG, Szurszewski JH. Mechanisms of phasic and tonic actions of pentagastrin on canine gastric smooth muscle. J Physiol. 1980;301:229–42.
101. Der-Silaphet T, Malysz J, Hagel S, Larry Arsenault A, Huizinga JD. Interstitial cells of cajal direct normal propulsive contractile activity in the mouse small intestine. Gastroenterology. 1998;114(4):724–36.
102. Hennig GW, Spencer NJ, Jokela-Willis S, Bayguinov PO, Lee HT, Ritchie LA, et al. ICC-MY coordinate smooth muscle electrical and mechanical activity in the murine small intestine. Neurogastroenterol Motil. 2010;22(5):e138–51.
103. Yoneda S, Fukui H, Takaki M. Pacemaker activity from submucosal interstitial cells of Cajal drives high-frequency and low-amplitude circular muscle contractions in the mouse proximal colon. Neurogastroenterol Motil. 2004;16(5):621–7.
104. Rae MG, Fleming N, McGregor DB, Sanders KM, Keef KD. Control of motility patterns in the human colonic circular muscle layer by pacemaker activity. J Physiol. 1998;510(Pt 1):309–20.
105. Thuneberg L, Johansen V, Rumessen JJ, Anderson BG. Interstitial cells of Cajal: selective uptake of methylene blue inhibits slow wave activity. In: Roman C, editor. Gastrointestinal motility. Lancaster: Mtp Press Limited; 1984. p. 495–502.
106. Torihashi S, Kobayashi S, Gerthoffer WT, Sanders KM. Interstitial cells in deep muscular plexus of canine small intestine may be specialized smooth muscle cells. Am J Phys. 1993;265(4 Pt 1):G638–45.
107. Maeda H, Yamagata A, Nishikawa S, Yoshinaga K, Kobayashi S, Nishi K, et al. Requirement of c-kit for development of intestinal pacemaker system. Development. 1992;116(2):369–75.
108. Torihashi S, Ward SM, Nishikawa S, Nishi K, Kobayashi S, Sanders KM. c-kit-dependent development of interstitial cells and electrical activity in the murine gastrointestinal tract. Cell Tissue Res. 1995;280(1):97–111.
109. Hirota S, Isozaki K, Moriyama Y, Hashimoto K, Nishida T, Ishiguro S, et al. Gain-of-function mutations of c-kit in human gastrointestinal stromal tumors. Science. 1998;279(5350):577–80.
110. Gomez-Pinilla PJ, Gibbons SJ, Bardsley MR, Lorincz A, Pozo MJ, Pasricha PJ, et al. Ano1 is a selective marker of interstitial cells of Cajal in the human and mouse gastrointestinal tract. Am J Physiol Gastrointest Liver Physiol. 2009;296(6):G1370–81.
111. Hwang SJ, Blair PJ, Britton FC, O'Driscoll KE, Hennig G, Bayguinov YR, et al. Expression of anoctamin 1/TMEM16A by interstitial cells of Cajal is fundamental for slow wave activity in gastrointestinal muscles. J Physiol. 2009;587(Pt 20):4887–904.
112. Wouters M, De Laet A, Donck LV, Delpire E, van Bogaert PP, Timmermans JP, et al. Subtractive hybridization unravels a role for the ion cotransporter NKCC1 in the murine intestinal pacemaker. Am J Physiol Gastrointest Liver Physiol. 2006;290(6):G1219–27.
113. Zhu MH, Sung TS, Kurahashi M, O'Kane LE, O'Driscoll K, Koh SD, et al. Na+-K+-Cl− cotransporter (NKCC) maintains the chloride gradient to sustain pacemaker activity in interstitial cells of Cajal. Am J Physiol Gastrointest Liver Physiol. 2016;311(6):G1037–G46.
114. Ro S, Park C, Jin J, Zheng H, Blair PJ, Redelman D, et al. A model to study the phenotypic changes of interstitial cells of Cajal in gastrointestinal diseases. Gastroenterology. 2010;138(3):1068–78.e1–2.
115. Zhu MH, Kim TW, Ro S, Yan W, Ward SM, Koh SD, et al. A Ca(2+)-activated Cl(−) conductance in interstitial cells of Cajal linked to slow wave currents and pacemaker activity. J Physiol. 2009;587(Pt 20):4905–18.
116. Ordog T, Redelman D, Miller LJ, Horvath VJ, Zhong Q, Almeida-Porada G, et al. Purification of interstitial cells of Cajal by fluorescence-activated cell sorting. Am J Phys Cell Phys. 2004;286(2):C448–56.
117. Lee MY, Ha SE, Park C, Park PJ, Fuchs R, Wei L, et al. Transcriptome of interstitial cells of Cajal reveals unique and selective gene signatures. PLoS One. 2017;12(4):e0176031.
118. Chen H, Ordog T, Chen J, Young DL, Bardsley MR, Redelman D, et al. Differential gene expression in functional classes of interstitial cells of

Cajal in murine small intestine. Physiol Genomics. 2007;31(3):492–509.
119. Koh SD, Sanders KM, Ward SM. Spontaneous electrical rhythmicity in cultured interstitial cells of cajal from the murine small intestine. J Physiol. 1998;513(Pt 1):203–13.
120. Goto K, Matsuoka S, Noma A. Two types of spontaneous depolarizations in the interstitial cells freshly prepared from the murine small intestine. J Physiol. 2004;559(Pt 2):411–22.
121. Caputo A, Caci E, Ferrera L, Pedemonte N, Barsanti C, Sondo E, et al. TMEM16A, a membrane protein associated with calcium-dependent chloride channel activity. Science. 2008;322(5901):590–4.
122. Schroeder BC, Cheng T, Jan YN, Jan LY. Expression cloning of TMEM16A as a calcium-activated chloride channel subunit. Cell. 2008;134(6):1019–29.
123. Yang YD, Cho H, Koo JY, Tak MH, Cho Y, Shim WS, et al. TMEM16A confers receptor-activated calcium-dependent chloride conductance. Nature. 2008;455(7217):1210–5.
124. Kashyap P, Gomez-Pinilla PJ, Pozo MJ, Cima RR, Dozois EJ, Larson DW, et al. Immunoreactivity for Ano1 detects depletion of Kit-positive interstitial cells of Cajal in patients with slow transit constipation. Neurogastroenterol Motil. 2011;23(8):760–5.
125. Huang F, Rock JR, Harfe BD, Cheng T, Huang X, Jan YN, et al. Studies on expression and function of the TMEM16A calcium-activated chloride channel. Proc Natl Acad Sci U S A. 2009;106(50):21413–8.
126. Strege PR, Bernard CE, Mazzone A, Linden DR, Beyder A, Gibbons SJ, et al. A novel exon in the human Ca2+-activated Cl− channel Ano1 imparts greater sensitivity to intracellular Ca2. Am J Physiol Gastrointest Liver Physiol. 2015;309(9):G743–9.
127. Sung TS, O'Driscoll K, Zheng H, Yapp NJ, Leblanc N, Koh SD, et al. Influence of intracellular Ca2+ and alternative splicing on the pharmacological profile of ANO1 channels. Am J Phys Cell Phys. 2016;311(3):C437–51.
128. Mazzone A, Bernard CE, Strege PR, Beyder A, Galietta LJ, Pasricha PJ, et al. Altered expression of Ano1 variants in human diabetic gastroparesis. J Biol Chem. 2011;286(15):13393–403.
129. Hwang SJ, Basma N, Sanders KM, Ward SM. Effects of new-generation inhibitors of the calcium-activated chloride channel anoctamin 1 on slow waves in the gastrointestinal tract. Br J Pharmacol. 2016;173(8):1339–49.
130. Rock JR, Futtner CR, Harfe BD. The transmembrane protein TMEM16A is required for normal development of the murine trachea. Dev Biol. 2008;321(1):141–9.
131. Malysz J, Gibbons SJ, Saravanaperumal SA, Du P, Eisenman ST, Cao C, et al. Conditional genetic deletion of Ano1 in interstitial cells of Cajal impairs Ca2+ transients and slow waves in adult mouse small intestine. Am J Physiol Gastrointest Liver Physiol. 2017;312(3):G228–G45.
132. Heinze C, Seniuk A, Sokolov MV, Huebner AK, Klementowicz AE, Szijarto IA, et al. Disruption of vascular Ca2+-activated chloride currents lowers blood pressure. J Clin Invest. 2014;124(2):675–86.
133. Vooijs M, Jonkers J, Berns A. A highly efficient ligand-regulated Cre recombinase mouse line shows that LoxP recombination is position dependent. EMBO Rep. 2001;2(4):292–7.
134. Huizinga JD, Shin A, Chow E. Electrical coupling and pacemaker activity in colonic smooth muscle. Am J Phys. 1988;255(5 Pt 1):C653–60.
135. van Helden DF, Imtiaz MS. Ca2+ phase waves: a basis for cellular pacemaking and long-range synchronicity in the guinea-pig gastric pylorus. J Physiol. 2003;548(Pt 1):271–96.
136. Gibbons SJ, Strege PR, Lei S, Roeder JL, Mazzone A, Ou Y, et al. The alpha1H Ca2+ channel subunit is expressed in mouse jejunal interstitial cells of Cajal and myocytes. J Cell Mol Med. 2009;13(11–12):4422–31.
137. Zheng H, Park KS, Koh SD, Sanders KM. Expression and function of a T-type Ca2+ conductance in interstitial cells of Cajal of the murine small intestine. Am J Phys Cell Phys. 2014;306(7):C705–13.
138. Catterall WA, Perez-Reyes E, Snutch TP, Striessnig J. International Union of Pharmacology. XLVIII. Nomenclature and structure-function relationships of voltage-gated calcium channels. Pharmacol Rev. 2005;57(4):411–25.
139. Iftinca M, McKay BE, Snutch TP, McRory JE, Turner RW, Zamponi GW. Temperature dependence of T-type calcium channel gating. Neuroscience. 2006;142(4):1031–42.
140. Kito Y, Suzuki H. Effects of temperature on pacemaker potentials in the mouse small intestine. Pflugers Arch. 2007;454(2):263–75.
141. Huang X, Lee SH, Lu H, Sanders KM, Koh SD. Molecular and functional characterization of inwardly rectifying K(+) currents in murine proximal colon. J Physiol. 2018;596(3):379–91.
142. Na JS, Hong C, Kim MW, Park CG, Kang HG, Wu MJ, et al. ATP-sensitive K(+) channels maintain resting membrane potential in interstitial cells of Cajal from the mouse colon. Eur J Pharmacol. 2017;809:98–104.
143. Markadieu N, Delpire E. Physiology and pathophysiology of SLC12A1/2 transporters. Pflugers Arch. 2014;466(1):91–105.
144. Ebihara S, Shirato K, Harata N, Akaike N. Gramicidin-perforated patch recording: GABA response in mammalian neurones with intact intracellular chloride. J Physiol. 1995;484(Pt 1):77–86.
145. Ball ER, Matsuda MM, Dye L, Hoffmann V, Zerfas PM, Szarek E, et al. Ultra-structural identification of interstitial cells of Cajal in the zebrafish Danio rerio. Cell Tissue Res. 2012;349(2):483–91.
146. Rich A, Gordon S, Brown C, Gibbons SJ, Schaefer K, Hennig G, et al. Kit signaling is required for development of coordinated motility patterns in zebrafish gastrointestinal tract. Zebrafish. 2013;10:154–60.

147. Brijs J, Hennig GW, Kellermann AM, Axelsson M, Olsson C. The presence and role of interstitial cells of Cajal in the proximal intestine of shorthorn sculpin (Myoxocephalus scorpius). J Exp Biol. 2017;220(Pt 3):347–57.
148. Singh RD, Gibbons SJ, Saravanaperumal SA, Du P, Hennig GW, Eisenman ST, et al. Ano1, a Ca2+-activated Cl− channel, coordinates contractility in mouse intestine by Ca2+ transient coordination between interstitial cells of Cajal. J Physiol. 2014;592(Pt 18):4051–68.
149. Hennig GW, Hirst GD, Park KJ, Smith CB, Sanders KM, Ward SM, et al. Propagation of pacemaker activity in the guinea-pig antrum. J Physiol. 2004;556(Pt 2):585–99.
150. Lee HT, Hennig GW, Fleming NW, Keef KD, Spencer NJ, Ward SM, et al. The mechanism and spread of pacemaker activity through myenteric interstitial cells of Cajal in human small intestine. Gastroenterology. 2007;132(5):1852–65.
151. Lee HT, Hennig GW, Fleming NW, Keef KD, Spencer NJ, Ward SM, et al. Septal interstitial cells of Cajal conduct pacemaker activity to excite muscle bundles in human jejunum. Gastroenterology. 2007;133(3):907–17.
152. Lee HT, Hennig GW, Park KJ, Bayguinov PO, Ward SM, Sanders KM, et al. Heterogeneities in ICC Ca2+ activity within canine large intestine. Gastroenterology. 2009;136(7):2226–36.
153. Park KJ, Hennig GW, Lee HT, Spencer NJ, Ward SM, Smith TK, et al. Spatial and temporal mapping of pacemaker activity in interstitial cells of Cajal in mouse ileum in situ. Am J Phys Cell Phys. 2006;290(5):C1411–27.
154. Huizinga JD, Chen JH, Zhu YF, Pawelka A, McGinn RJ, Bardakjian BL, et al. The origin of segmentation motor activity in the intestine. Nat Commun. 2014;5:3326.
155. Yamazawa T, Iino M. Simultaneous imaging of Ca2+ signals in interstitial cells of Cajal and longitudinal smooth muscle cells during rhythmic activity in mouse ileum. J Physiol. 2002;538(Pt 3):823–35.
156. Baker SA, Drumm BT, Saur D, Hennig GW, Ward SM, Sanders KM. Spontaneous Ca(2+) transients in interstitial cells of Cajal located within the deep muscular plexus of the murine small intestine. J Physiol. 2016;594(12):3317–38.
157. Drumm BT, Hennig GW, Battersby MJ, Cunningham EK, Sung TS, Ward SM, et al. Clustering of Ca2+ transients in interstitial cells of Cajal defines slow wave duration. J Gen Physiol. 2017;149(7):703–25.
158. Lowie BJ, Wang XY, White EJ, Huizinga JD. On the origin of rhythmic calcium transients in the ICC-MP of the mouse small intestine. Am J Physiol Gastrointest Liver Physiol. 2011;301(5):G835–45.
159. Serio R, Barajas-Lopez C, Daniel EE, Berezin I, Huizinga JD. Slow-wave activity in colon: role of network of submucosal interstitial cells of Cajal. Am J Phys. 1991;260(4 Pt 1):G636–45.
160. Bayguinov PO, Hennig GW, Smith TK. Ca2+ imaging of activity in ICC-MY during local mucosal reflexes and the colonic migrating motor complex in the murine large intestine. J Physiol. 2010;588(Pt 22):4453–74.
161. Huang L, Keyser BM, Tagmose TM, Hansen JB, Taylor JT, Zhuang H, et al. NNC 55-0396 [(1S,2S)-2-(2-(N-[(3-benzimidazol-2-yl)propyl]-N-methylamino)ethyl)-6-fluoro-1,2,3,4-tetrahydro-1-isopropyl-2-naphtyl cyclopropanecarboxylate dihydrochloride]: a new selective inhibitor of T-type calcium channels. J Pharmacol Exp Ther. 2004;309(1):193–9.
162. Kraus RL, Li Y, Gregan Y, Gotter AL, Uebele VN, Fox SV, et al. In vitro characterization of T-type calcium channel antagonist TTA-A2 and in vivo effects on arousal in mice. J Pharmacol Exp Ther. 2010;335(2):409–17.
163. Suzuki H, Takano H, Yamamoto Y, Komuro T, Saito M, Kato K, et al. Properties of gastric smooth muscles obtained from mice which lack inositol trisphosphate receptor. J Physiol. 2000;525(Pt 1):105–11.
164. van Helden DF, Imtiaz MS, Nurgaliyeva K, von der Weid P, Dosen PJ. Role of calcium stores and membrane voltage in the generation of slow wave action potentials in guinea-pig gastric pylorus. J Physiol. 2000;524(Pt 1):245–65.
165. Ganitkevich V, Isenberg G. Membrane potential modulates inositol 1,4,5-trisphosphate-mediated Ca2+ transients in guinea-pig coronary myocytes. J Physiol. 1993;470:35–44.
166. Fukuta H, Kito Y, Suzuki H. Spontaneous electrical activity and associated changes in calcium concentration in guinea-pig gastric smooth muscle. J Physiol. 2002;540(Pt 1):249–60.
167. Malysz J, Donnelly G, Huizinga JD. Regulation of slow wave frequency by IP(3)-sensitive calcium release in the murine small intestine. Am J Physiol Gastrointest Liver Physiol. 2001;280(3):G439–48.
168. Ward SM, Ordog T, Koh SD, Baker SA, Jun JY, Amberg G, et al. Pacemaking in interstitial cells of Cajal depends upon calcium handling by endoplasmic reticulum and mitochondria. J Physiol. 2000;525(Pt 2):355–61.
169. Liu HN, Ohya S, Wang J, Imaizumi Y, Nakayama S. Involvement of ryanodine receptors in pacemaker Ca2+ oscillation in murine gastric ICC. Biochem Biophys Res Commun. 2005;328(2):640–6.
170. Zhu MH, Sung TS, O'Driscoll K, Koh SD, Sanders KM. Intracellular Ca2+ release from endoplasmic reticulum regulates slow wave currents and pacemaker activity of interstitial cells of Cajal. Am J Phys Cell Phys. 2015;308(8):C608–20.
171. Faussone-Pellegrini MS. Cytodifferentiation of the interstitial cells of Cajal related to the myenteric plexus of mouse intestinal muscle coat. An E.M. study from foetal to adult life. Anat Embryol. 1985;171(2):163–9.
172. Rumessen JJ, Thuneberg L. Interstitial cells of Cajal in human small intestine. Ultrastructural identification and organization between the main smooth

muscle layers. Gastroenterology. 1991;100(5 Pt 1):1417–31.
173. Kito Y, Suzuki H. Electrophysiological properties of gastric pacemaker potentials. J Smooth Muscle Res. 2003;39(5):163–73.
174. Kito Y, Fukuta H, Suzuki H. Components of pacemaker potentials recorded from the guinea pig stomach antrum. Pflugers Arch. 2002;445(2):202–17.
175. Faville RA, Pullan AJ, Sanders KM, Koh SD, Lloyd CM, Smith NP. Biophysically based mathematical modeling of interstitial cells of Cajal slow wave activity generated from a discrete unitary potential basis. Biophys J. 2009;96(12):4834–52.
176. Drumm BT, Sung TS, Zheng H, Baker SA, Koh SD, Sanders KM. The effects of mitochondrial inhibitors on Ca2+ signalling and electrical conductances required for pacemaking in interstitial cells of Cajal in the mouse small intestine. Cell Calcium. 2018;72(June):1–17.
177. Kito Y, Suzuki H. Modulation of slow waves by hyperpolarization with potassium channel openers in antral smooth muscle of the guinea-pig stomach. J Physiol. 2003;548(Pt 1):175–89.
178. Lee JY, Ko EJ, Ahn KD, Kim S, Rhee PL. The role of K(+) conductances in regulating membrane excitability in human gastric corpus smooth muscle. Am J Physiol Gastrointest Liver Physiol. 2015;308(7):G625–33.
179. Koh SD, Bradley KK, Rae MG, Keef KD, Horowitz B, Sanders KM. Basal activation of ATP-sensitive potassium channels in murine colonic smooth muscle cell. Biophys J. 1998;75(4):1793–800.
180. Kurahashi M, Mutafova-Yambolieva V, Koh SD, Sanders KM. Platelet-derived growth factor receptor-alpha-positive cells and not smooth muscle cells mediate purinergic hyperpolarization in murine colonic muscles. Am J Phys Cell Phys. 2014;307(6):C561–70.
181. Chow E, Huizinga JD. Myogenic electrical control activity in longitudinal muscle of human and dog colon. J Physiol. 1987;392:21–34.
182. Burns AJ, Lomax AE, Torihashi S, Sanders KM, Ward SM. Interstitial cells of Cajal mediate inhibitory neurotransmission in the stomach. Proc Natl Acad Sci U S A. 1996;93(21):12008–13.
183. Ward SM, Beckett EA, Wang X, Baker F, Khoyi M, Sanders KM. Interstitial cells of Cajal mediate cholinergic neurotransmission from enteric motor neurons. J Neurosci. 2000;20(4):1393–403.
184. Goyal RK. CrossTalk opposing view: interstitial cells are not involved and physiologically important in neuromuscular transmission in the gut. J Physiol. 2016;594(6):1511–3.
185. Goyal RK, Chaudhury A. Mounting evidence against the role of ICC in neurotransmission to smooth muscle in the gut. Am J Physiol Gastrointest Liver Physiol. 2010;298(1):G10–3.
186. Sanders KM, Hwang SJ, Ward SM. Neuroeffector apparatus in gastrointestinal smooth muscle organs. J Physiol. 2010;588(Pt 23):4621–39.
187. Sanders KM, Ward SM, Friebe A. CrossTalk proposal: interstitial cells are involved and physiologically important in neuromuscular transmission in the gut. J Physiol. 2016;594(6):1507–9.
188. Rumessen JJ, Mikkelsen HB, Thuneberg L. Ultrastructure of interstitial cells of Cajal associated with deep muscular plexus of human small intestine. Gastroenterology. 1992;102(1):56–68.
189. Zhou DS, Komuro T. Ultrastructure of the zinc iodide-osmic acid stained cells in guinea pig small intestine. J Anat. 1995;187(Pt 2):481–5.
190. Sternini C, Su D, Gamp PD, Bunnett NW. Cellular sites of expression of the neurokinin-1 receptor in the rat gastrointestinal tract. J Comp Neurol. 1995;358(4):531–40.
191. Vannucchi MG, De Giorgio R, Faussone-Pellegrini MS. NK1 receptor expression in the interstitial cells of Cajal and neurons and tachykinins distribution in rat ileum during development. J Comp Neurol. 1997;383(2):153–62.
192. Iino S, Ward SM, Sanders KM. Interstitial cells of Cajal are functionally innervated by excitatory motor neurones in the murine intestine. J Physiol. 2004;556(Pt 2):521–30.
193. Wang XY, Ward SM, Gerthoffer WT, Sanders KM. PKC-epsilon translocation in enteric neurons and interstitial cells of Cajal in response to muscarinic stimulation. Am J Physiol Gastrointest Liver Physiol. 2003;285(3):G593–601.
194. Baker SA, Drumm BT, Skowronek KE, Rembetski BE, Peri LE, Hennig GW, Perrino BA, Sanders KM. Excitatory neuronal responses of Ca(2+) transients in interstitial cells of Cajal in the small intestine. eNeuro. 2018;5(2). pii: ENEURO.0080-18.2018.
195. Baker SA, Drumm BT, et al. Inhibitory neural regulation of the Ca2+ transients in intramuscular interstitial cells of Cajal in the small intestine. Front Physiol. 2018;9:328.
196. Inoue R, Isenberg G. Effect of membrane potential on acetylcholine-induced inward current in guinea-pig ileum. J Physiol. 1990;424:57–71.
197. Gordienko DV, Zholos AV. Regulation of muscarinic cationic current in myocytes from guinea-pig ileum by intracellular Ca2+ release: a central role of inositol 1,4,5-trisphosphate receptors. Cell Calcium. 2004;36(5):367–86.
198. Tsvilovskyy VV, Zholos AV, Aberle T, Philipp SE, Dietrich A, Zhu MX, et al. Deletion of TRPC4 and TRPC6 in mice impairs smooth muscle contraction and intestinal motility in vivo. Gastroenterology. 2009;137(4):1415–24.
199. Bhetwal BP, Sanders KM, An C, Trappanese DM, Moreland RS, Perrino BA. Ca2+ sensitization pathways accessed by cholinergic neurotransmission in the murine gastric fundus. J Physiol. 2013;591(Pt 12):2971–86.
200. Diamant NE, Bortoff A. Nature of the intestinal slow-wave frequency gradient. Am J Phys. 1969;216(2):301–7.

201. Suzuki N, Prosser CL, DeVos W. Waxing and waning of slow waves in intestinal musculature. Am J Phys. 1986;250(1 Pt 1):G28–34.
202. Zhu MH, Sung IK, Zheng H, Sung TS, Britton FC, O'Driscoll K, et al. Muscarinic activation of Ca2+-activated Cl− current in interstitial cells of Cajal. J Physiol. 2011;589(Pt 18):4565–82.
203. Won KJ, Sanders KM, Ward SM. Interstitial cells of Cajal mediate mechanosensitive responses in the stomach. Proc Natl Acad Sci U S A. 2005;102(41):14913–8.
204. Kaji N, Horiguchi K, Iino S, Nakayama S, Ohwada T, Otani Y, et al. Nitric oxide-induced oxidative stress impairs pacemaker function of murine interstitial cells of Cajal during inflammation. Pharmacol Res. 2016;111:838–48.
205. Joddar B, Tasnim N, Thakur V, Kumar A, McCallum RW, Chattopadhyay M. Delivery of mesenchymal stem cells from gelatin-alginate hydrogels to stomach lumen for treatment of gastroparesis. Bioengineering (Basel). 2018;5(1):E12.
206. Sanders KM, Kito Y, Hwang SJ, Ward SM. Regulation of gastrointestinal smooth muscle function by interstitial cells. Physiology (Bethesda). 2016;31(5):316–26.

Generation of Spontaneous Tone by Gastrointestinal Sphincters

2

Kathleen Keef and Caroline Cobine

Abstract

An important feature of the gastrointestinal (GI) *muscularis externa* is its ability to generate phasic contractile activity. However, in some GI regions, a more sustained contraction, referred to as "tone," also occurs. Sphincters are muscles oriented in an annular manner that raise intraluminal pressure, thereby reducing or blocking the movement of luminal contents from one compartment to another. Spontaneous tone generation is often a feature of these muscles. Four distinct smooth muscle sphincters are present in the GI tract: the lower esophageal sphincter (LES), the pyloric sphincter (PS), the ileocecal sphincter (ICS), and the internal anal sphincter (IAS). This chapter examines how tone generation contributes to the functional behavior of these sphincters. Historically, tone was attributed to contractile activity arising directly from the properties of the smooth muscle cells. However, there is increasing evidence that interstitial cells of Cajal (ICC) play a significant role in tone generation in GI muscles. Indeed, ICC are present in each of the sphincters listed above. In this chapter, we explore various mechanisms that may contribute to tone generation in sphincters including: (1) summation of asynchronous phasic activity, (2) partial tetanus, (3) window current, and (4) myofilament sensitization. Importantly, the first two mechanisms involve tone generation through summation of phasic events. Thus, the historical distinction between "phasic" versus "tonic" smooth muscles in the GI tract requires revision. As described in this chapter, it is clear that the unique functional role of each sphincter in the GI tract is accompanied by a unique combination of contractile mechanisms.

Keywords

Gastrointestinal · Tone · Interstitial cells of Cajal · Myofilament sensitization Electromechanical coupling · Sphincter Slow wave · Membrane potential · Motility ANO1

2.1 Anatomical and Functional Features of Gastrointestinal Sphincters

2.1.1 Lower Esophageal Sphincter

Anatomy and pressure. The lower esophageal sphincter (LES) is a specialized region of smooth muscle located at the junction of the esophagus and stomach (Fig. 2.1a). However, the precise morphological features of the LES are still con-

K. Keef (✉) · C. Cobine
Department of Physiology and Cell Biology, University of Nevada, Reno School of Medicine, Reno, NV, USA
e-mail: kkeef@med.unr.edu

H. Hashitani, R. J. Lang (eds.), *Smooth Muscle Spontaneous Activity*, Advances in Experimental Medicine and Biology 1124, https://doi.org/10.1007/978-981-13-5895-1_2

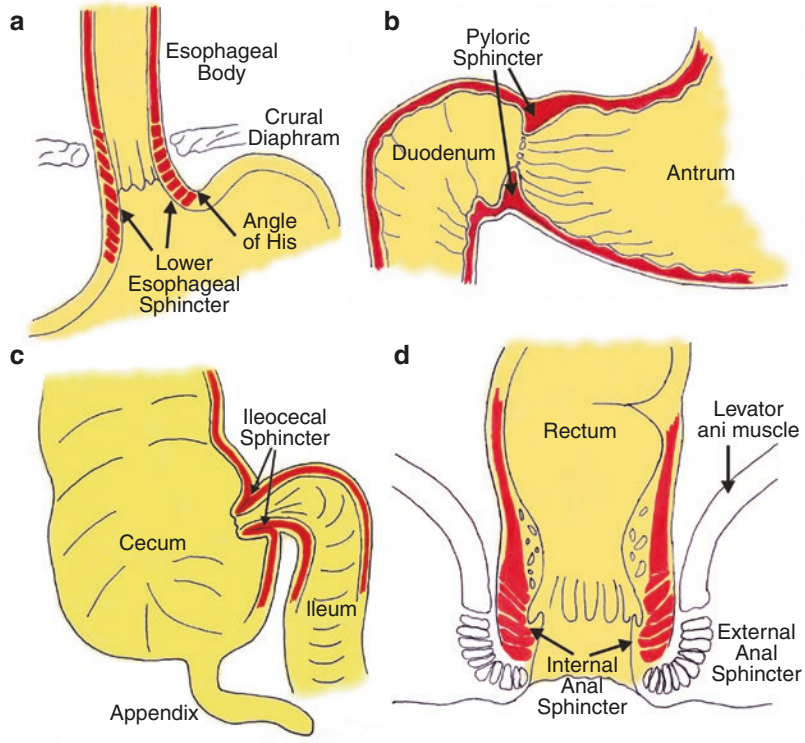

Fig. 2.1 Anatomical location of gastrointestinal sphincters. Highlighted in each diagram is a portion of the circular muscle layer with arrows indicating the location of the sphincter. (**a**) The lower esophageal sphincter (LES) is located at the junction between the esophagus and the stomach. It is comprised of oblique distal esophageal and clasp fibers near the lesser curvature of the stomach (left). These fibers combine with oblique sling fibers at the angle of His (right). The LES in combination with the crural diaphragm constitute the esophagogastric junction (EGJ). (**b**) The pyloric sphincter (PS) is located at the junction of the distal antrum and proximal duodenum. It is a thickening of the circular muscle layer. (**c**) The ileocecal sphincter is located at the junction of the distal ileum and proximal cecum. It is created by a folding over of the circular muscle layer that protrudes into the cecum. (**d**) The internal anal sphincter (IAS) is a thickening of the circular muscle layer at the distal extremity of the gastrointestinal tract. It is surrounded by the external anal sphincter which also extends distal to the IAS

troversial. Historically, the LES was described as consisting of semicircular "clasp" muscle fibers near the lesser curvature of the stomach and obliquely oriented "sling" muscle fibers near the fundus [1–10]. However, it is now recognized that distal circular muscle fibers of the esophagus also contribute to the high-pressure zone [11]. Indeed, there is likely overlap in the literature between muscles described as "clasp" vs. distal esophageal circular muscle fibers. A recent three-dimensional high-resolution pressure profile of the human esophagogastric junction (EGJ) has been undertaken [12, 13]. These studies conclude that the LES is a noose-like structure consisting of oblique distal esophageal circular muscle fibers that cross with sling fibers at the angle of His (i.e., the acute angle at the junction of the esophagus and fundus) producing "purse strings" that raise luminal pressure when contracted.

The LES passes through the crural diaphragm en route to the stomach; thus, the EGJ is considered to include both the LES and the crural diaphragm [14]. Importantly, the high-pressure zone generated by the EGJ is responsible for preventing the reflux of gastric contents into the esophagus. Values for EGJ pressure at end expiration (considered to be exclusively due to the LES) range from 15 to 35 mmHg in humans [13, 15, 16] and similar pressures have been reported for rat [17, 18]. Interestingly, LES pressure is higher

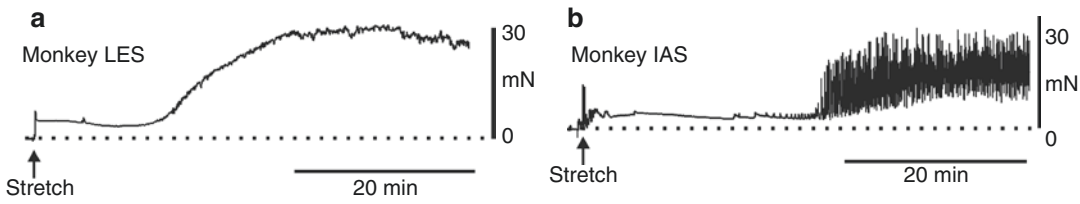

Fig. 2.2 Spontaneous contractile activity generated by strips of the monkey lower esophageal sphincter (LES) and internal anal sphincter (IAS) following dissection in cold (4 °C) Krebs bicarbonate Ringers solution and placement in a warm (37 °C) isolated tissue bath. An initial stretch was applied to both muscles at the arrows. As ionic gradients are reestablished tone and phasic activity develop. Contractile activity in the LES is predominantly tonic (**a**, Keef and Cobine, unpublished observation) while phasic contractions are superimposed upon tone in the IAS (**b** [115])

near the angle of His and encompasses a wider portion of the esophagus near the lesser curvature [2, 13, 19–21].

Neural innervation. Extrinsic neural regulation of the LES is largely mediated by vagal preganglionic cholinergic neurons. These neurons innervate the LES at the level of the myenteric plexus and activate either excitatory or inhibitory motor neurons depending upon the neural pathway involved [22–26]. Stimulation of excitatory motor neurons significantly increases LES pressure [25] while atropine decreases LES pressure [27, 28]. On the other hand, some studies have reported that vagotomy increases LES pressure suggesting a predominance of inhibitory neural pathways [25]. When all neural influences are eliminated there is still elevated pressure at the LES indicating that spontaneous tone generation plays a role in this region [25, 29]. Purines, nitric oxide (NO), and vasoactive intestinal peptide (VIP) each participate in inhibitory neural responses in the LES, with NO being the most important [5, 7, 9, 30, 31]. Sympathetic nerves arising from the celiac ganglia also innervate the LES but their actions appear to be modest since LES pressure is unchanged following sympathectomy [25, 32].

2.1.1.1 In Vitro Contractile and Electrical Activity

Contraction. Muscle strips isolated from the LES spontaneously develop tone in every species examined (e.g., monkey LES, Fig. 2.2a). In vitro studies of human muscles report that tone in clasp muscle is twice that of sling muscle and ten times greater than that of esophageal body muscles [5]. Similar differences are apparent for clasp and sling muscles in cat [8, 33]. The greater tone developed by muscles of the LES than the esophageal body is in agreement with the high-pressure zone noted for the LES in vivo [13, 25]. However, the greater tone developed by clasp muscle compared to sling muscle cannot explain the greater pressure measured in vivo near the sling side of the LES [2, 19–21]. It is possible that clasp muscle receives greater neural inhibition than sling muscle in vivo since inhibitory nerves produce greater inhibition of contraction of clasp than of sling muscles in vitro [5, 9]. Morphological differences in the composition of smooth muscle at the clasp and sling side of the LES have also been proposed to be an important determinant of the circumferential pressure gradient [12, 13].

Electrical activity. The membrane potential of the human and opossum LES is approximately 8–10 mV more depolarized than that of the esophageal body (i.e., ~−40 vs. −50 mV) while clasp and sling muscle membrane potentials are not different [5, 9, 34, 35]. In addition, continuous spike potentials have been observed in the opossum LES but not in the esophageal body [35, 36] (Fig. 2.3). Spikes as well as 70% of tone are abolished by the L-type calcium (Cav_L) channel blocker nifedipine suggesting that electromechanical coupling mechanisms significantly contribute to tone generated in this muscle [35].

2.1.2 Pyloric Sphincter

Anatomy, function, and in vivo pressure. The pyloric sphincter (PS) is located at the

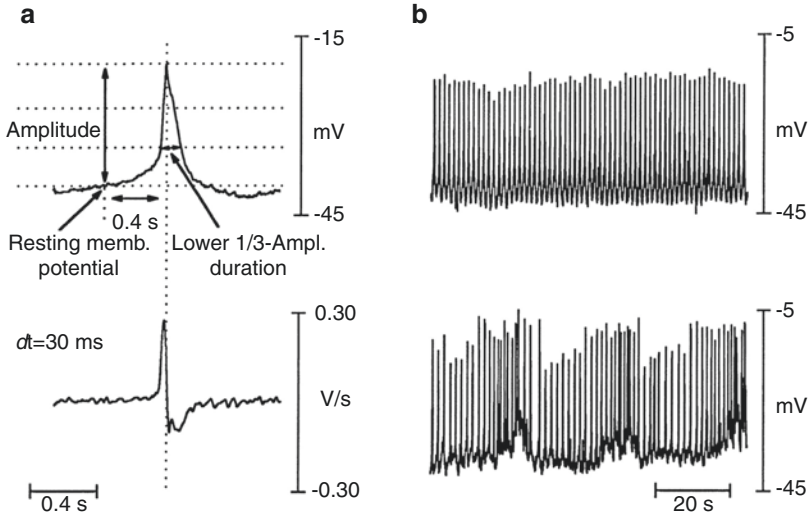

Fig. 2.3 Spontaneous spiking activity recorded from the opossum lower esophageal sphincter [35]. (**a**) Example of a single spike potential. Top: Membrane potential initially undergoes a slow depolarization followed by a rapid upstroke and repolarization. Bottom: Plot of the change in voltage with time (dV/dt) during this recording. The maximum rate of depolarization during the spike was ~0.3 V/s. (**b**) Examples of two patterns of continuous spiking activity shown at a slower sweep speed. Spikes occurred either upon a constant resting membrane potential (upper trace) or on occasion, superimposed upon slow oscillations (3–5/min) of resting membrane potential (lower trace)

gastroduodenal junction (GDJ) and is composed of the thickened circular muscle layer of the pylorus (Fig. 2.1b). The PS plays an important role in regulating the passage of chyme from the stomach to the small intestine. After ingested food has been broken down and the peristaltic contractions of the stomach have lessened, the PS relaxes allowing the passage of small volumes of chyme into the duodenum [37]. A feedback mechanism from the duodenum closes the PS to limit the amount of incoming chyme. The question of whether the PS exists in a state of tonic contracture at rest is controversial [29]. The pressure within the pylorus has been reported to be ≤10 mmHg between meals [38–40] suggesting minimal tone. However an in vivo pressure study of the dog PS described phasic pressure waves (1–5 cpm) superimposed upon elevated basal pressure [41]. The amplitude of phasic events was decreased by addition of atropine and enhanced by tetrodotoxin (TTX) indicating that this activity was modulated by neural input. The discrepancies between Allescher et al. [41] and others may arise from differences in the stage of gastric emptying and the nutrient content of the chyme in the duodenum [42–45]. For example, pyloric pressure is elevated after ingestion of a meal [40].

Neural innervation. Extrinsic neural regulation of the PS is similar to that of the LES, i.e., it is mediated by vagal preganglionic cholinergic neurons. It also receives sympathetic input from the celiac ganglia. Vagal preganglionic cholinergic neurons innervate the PS at the level of the myenteric plexus and give rise to either excitatory or inhibitory motor responses depending upon the neural pathway activated. Excitatory responses are predominantly cholinergic in nature [41, 46–48] whereas inhibitory responses are due to the release of purines, NO, and VIP [46, 47, 49, 50]. Despite innervating the pylorus, sympathetic nerves do not appear to play an important role in excitatory motor responses, rather they appear to modulate cholinergic pathways [51, 52].

2.1.2.1 In Vitro Contractile and Electrical Activity

Contraction. In vitro studies of the PS describe slow frequency (i.e., ~1–3 cycles per minute, cpm) phasic contractions [53–56] (Fig. 2.4). Unlike other sphincters, little tone is observed in the PS

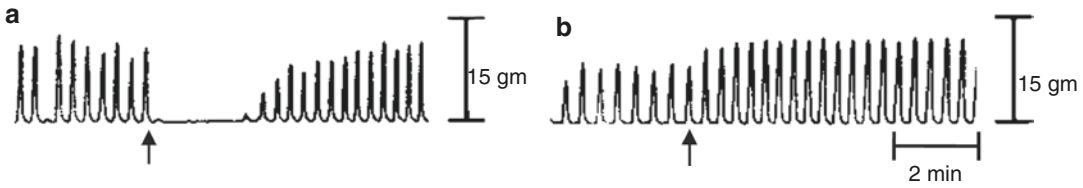

Fig. 2.4 Spontaneous contractile activity observed in isolated strips of the rabbit pyloric sphincter (PS) [53]. (**a**) Low-frequency phasic contractions were observed in the PS without tone. Addition of erythromycin 50 μM (arrow) abolished these contractions. (**b**) In a different muscle strip erythromycin 50 μM (arrow) was applied in the presence of tetrodotoxin (1 μM). In this case, contractile inhibition was abolished. The authors concluded that erythromycin acts predominantly by stimulating motilin receptors on inhibitory motor neurons [53]

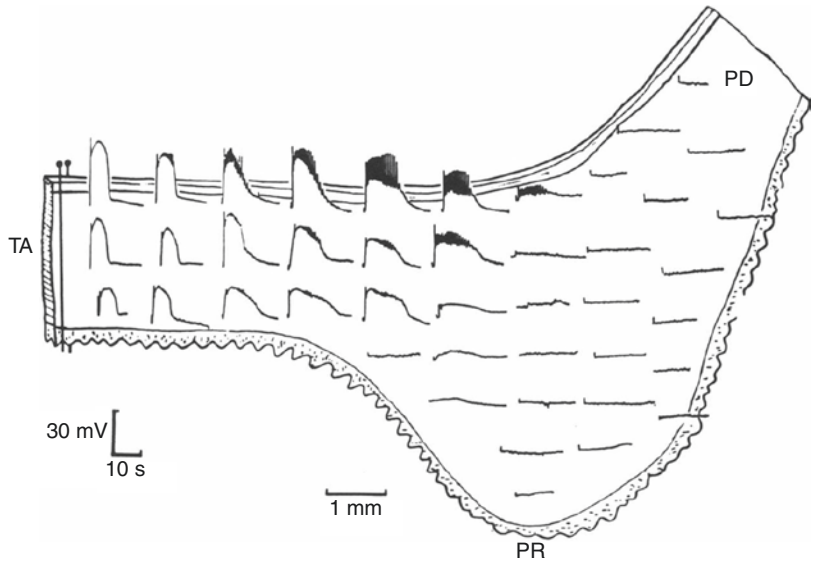

Fig. 2.5 Topography of slow wave activity recorded from cells in the circular muscle layer with microelectrodes across the width of the pyloric canal [59]. Slow waves were repetitively evoked in the antral region and recorded from cells throughout the surface of the preparation. Slow waves spread throughout the circular layer of the terminal antrum (TA) but petered out within the pyloric ring (PR) and proximal duodenum (PD). Much of the circular muscle of the pylorus was electrically quiescent

under "resting" conditions. However, tone is generated in the rat pylorus in response to the NO synthase (NOS)-inhibitor L-NAME suggesting ongoing suppression of tonic activity via nitric oxide (NO) [56]. Cav_L channel antagonists abolish phasic contractions in the PS indicating an important role for these channels in this activity [57].

Electrical activity. A number of intracellular microelectrode measurements from isolated strips of the PS have identified slow waves [54, 58–61]. Studies of the dog PS indicate that slow waves arise at the myenteric edge of the circular muscle layer and conduct toward the lumen, disappearing before reaching the submucosal edge [59]. The average frequency of slow waves recorded from isolated strips of the PS is 0.5–1 cpm [58, 59]. However, when electrical activity is recorded from muscle segments that include the distal antrum, the PS slow wave frequency is entrained by the higher frequency of slow waves in the distal antrum [58, 59]. Figure 2.5 shows how slow waves generated by stimulation of the distal antrum conduct across the distal antrum/PS/proximal duodenum. These topographical recordings indicate that slow waves can conduct to the PS but that much of this region is electrically quiescent under these conditions.

Slow waves in the PS arise from a relatively negative resting level, i.e., −70 mV in the guinea

pig and −63 mV and −61 mV in the myenteric and submucosal regions of the dog PS, respectively [58, 62]. However, there appears to be species-dependent differences in the role of Cav_L channels since slow waves are unaffected by nifedipine in the guinea pig PS [58], whereas both the amplitude and duration of slow waves is substantially reduced in the dog PS [59]. Activity in the pylorus is electrically isolated from that of the duodenum and occurs in the absence of nerves [59].

2.1.3 Ileocecal Sphincter

2.1.3.1 Anatomy, Function, and In Vivo Pressure

The ileocecal sphincter (ICS) is a papillose structure located at the junction between the ileum and cecum (Fig. 2.1c). It has also been referred to as ileocolonic sphincter or valve. The ICS is ~4 cm wide in humans and is composed of two circular muscle layers, an internal one that is continuous with the circular muscle layer of the ileum and an external one that is continuous with the circular muscle layer of the cecum. There is also a single longitudinal muscle layer interposed between the two circular muscle layers [29, 63]. Functionally the ICS plays a role in facilitating the passage of luminal contents from the ileum to the colon. Perhaps more importantly, it plays a role in preventing the reflux of colonic contents, specifically bacteria, into the small intestine [64].

Manometry studies performed on human subjects report a 10–20 mmHg pressure zone over a distance of ~4 cm within the ICS [65, 66]. A similar high-pressure zone is present in dog, i.e., ~26 mmHg over 3 cm [67, 68]. However, there is controversy regarding this pressure zone in vivo since other studies have failed to detect it [69]. In some studies phasic pressure waves (4–8/min) have been observed superimposed upon tone [66]. The differences between these studies may arise from differences in recording techniques, as it is difficult to measure ICS pressure and tone noninvasively. Furthermore, discrepancies may also arise from differences in the fed-state of the subject. Greater tone and phasic activity are noted in the human ICS immediately after a meal versus during the interdigestive phase [66, 70]. Colonic distension results in increased ICS tone and larger amplitude pressure waves in both human and dog [66, 71], a reflex that will limit the reflux of material from the colon back into the ileum.

2.1.3.2 Neural Innervation

The ICS is innervated by sympathetic (via superior and inferior mesenteric ganglia) and parasympathetic (via vagus nerve) neural pathways. Tone in the ICS can occur in the absence of excitatory neural input although stimulation of sympathetic and cholinergic pathways enhance tone [72–76]. Non-adrenergic non-cholinergic (NANC) inhibitory responses are also present in the ICS [76]. A number of studies have identified an important role for NO in inhibitory motor innervation to the ICS [73, 77–80]. However, much less is known about the possible role of purines and VIP. Studies of the dog ICS have reported inhibitory junction potentials consisting of NOS- and apamin-sensitive components [73] while immunohistochemical studies have identified VIP in a subset of neurons in the myenteric ganglia [81]. Thus, VIP and purines likely play some role in the ICS but further studies are required.

2.1.3.3 In Vitro Contractile and Electrical Activity

Contraction. Most in vitro studies of the ICS report tone although not in every muscle strip examined [29, 76, 82, 83]. Spontaneous phasic contractions are also observed but again not in every muscle strip. Phasic activity is typically superimposed upon tone [29, 76, 79, 82–84] (Fig. 2.6). Interestingly, addition of the COX-2 inhibitor indomethacin to mechanically quiescent strips of the guinea pig ICS increases tone generation as well as phasic contractions suggesting that ongoing prostaglandin synthesis suppresses contractile activity [83]. Although the ICS generates tone, this activity represents only 10–20% of maximum contraction [82, 83]. Cav_L channel blockers have limited effects upon tone (i.e., reducing tone by less than half), while phasic contractions are abolished [82, 84].

Electrical activity. Resting membrane potential in the guinea pig ICS is more depolarized than that of the ileum or cecum i.e., ~−43 mV (ICS) vs. −58 mV (ileum) and −62 mV (cecum) [76], whereas in the dog ICS it is more negative

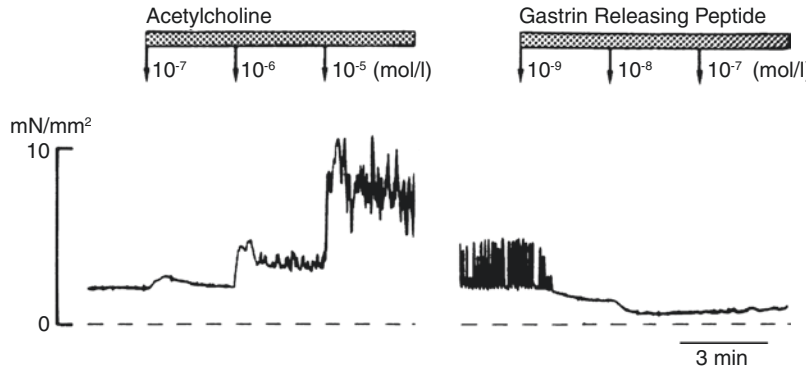

Fig. 2.6 Spontaneous contractile activity observed in isolated strips of the human ileocecal sphincter [82]. Tone was consistently observed in muscles (left and right trace) but in some cases phasic contractions were superimposed upon tone (right). Acetylcholine caused concentration-dependent contraction (left) whereas gastrin releasing peptide abolished phasic activity as well as most tonic contraction

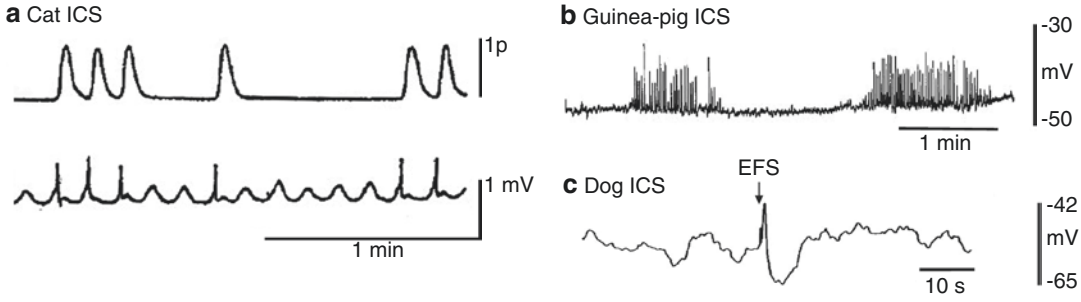

Fig. 2.7 Sample traces of spontaneous electrical activity recorded in the ileocecal sphincter (ICS) of several animal species. (**a**) Simultaneous recording (sucrose gap) of contractile (upper) and electrical (lower) activity in the cat ICS reveals occasional spike discharge associated with phasic contractions [85]. (**b**) Microelectrode recording of periodic bursts of spikes in the guinea pig ICS. Shown is an excerpt taken from the original figure [76]. (**c**) Microelectrode recording of periodic fluctuations in membrane potential in the dog ICS. Electrical field stimulation (EFS; 3 pulses, 20 Hz) gave rise to a fast cholinergic excitatory junction potential followed by a slower inhibitory junction potential due in part to nitric oxide [73]

(i.e., −55 mV) [73]. Differences in resting membrane potential between species may explain why spike-like activity is reported in some species (cat and guinea pig ICS [76, 83, 85]) but not in the dog [73] (Fig. 2.7). However, even in species with spikes, this activity is not observed in all muscle strips. Thus, the variability in contractile behavior (Fig. 2.6) likely reflects the variability in electrical events between muscle strips from the same animal. Indeed, in the only study in which membrane potential and contraction were simultaneously recorded, it was shown that spike potentials were associated with phasic contractile activity [85] (Fig. 2.7a).

2.1.4 Internal Anal Sphincter

Anatomy and in vivo pressure. The internal anal sphincter (IAS) is a thickening of the circular muscle layer at the distal end of the gastrointestinal tract (Fig. 2.1d). Circular and longitudinal muscle layers are separated from one another by a sparsely occupied connective tissue space [86, 87]. Surrounding the IAS is a second sphincter composed of skeletal muscle (i.e., the external anal sphincter). The IAS is responsible for >70% of resting anal pressure [88, 89] and is important for maintaining continence. Anal pressure in humans averages

75–90 mmHg [90–92], making pressure at this sphincter substantially greater than other GI sphincters. In contrast, resting anal pressure in rodents is significantly less than in humans (i.e., 15–21 mmHg) [93–95].

Neural innervation. The IAS receives sympathetic nerve fibers that arise from the inferior mesenteric ganglion and travel in the lumbar colonic nerves (LCN) and hypogastric nerves (HGN) or from the pelvic plexus. High spinal anesthesia or cutting the HGN and/or LCN significantly reduces IAS tone in a number of species suggesting that they exert a tonic excitatory influence on the IAS [96–102]. Varicose sympathetic fibers are located throughout the circular muscle layer of the monkey IAS and their activation doubles tone in vitro [87]. Since anal pressure is maintained in the absence of sympathetic nerves [103], they are not essential for tone generation. However, given the strength of this motor pathway, they likely assist in maintaining continence under some circumstances.

The IAS is also innervated by enteric inhibitory motor neurons that participate in the recto-anal inhibitory reflex and in defecation [87, 95, 104]. In contrast to the LES and ICS, the IAS lacks a myenteric plexus [87, 105]. Nonetheless, the circular muscle layer is richly innervated by NADPH/nNOS positive neurons that arise from cell bodies located within the rectal myenteric plexus and project distally [87, 104]. Nitric oxide plays a prominent role as an inhibitory neurotransmitter in the human and monkey IAS while purinergic transmission is absent [106, 107]. In contrast, both nitrergic and purinergic transmission are present in rodents [108–112]. VIP also significantly contributes to inhibitory neuromuscular transmission in the IAS [113].

2.1.4.1 In Vitro Contractile and Electrical Activity

Contraction. IAS muscle strips develop tone as well as phasic contractile activity in vitro independent of nerves [29, 87, 114–117] (Fig. 2.2b). Tone, and the frequency of phasic contractions, declines in the proximal direction [105, 114, 118]. In all species examined, contractile activity is highly sensitive to Cav_L channel blockers such as nifedipine [111, 115–117]. Indeed, the IC_{50} for nifedipine in the mouse IAS is 0.03 μM [119].

Electrical activity. Resting membrane potential in the IAS (i.e., −43 to −49 mV) is significantly less negative than in the predominantly phasic rectum (5 mV gradient from IAS to distal rectum in mouse [105]; 20 mV gradient from IAS to proximal rectum in dog [118]). Early sucrose gap recordings identified slow waves and associated phasic contractions in the cat IAS [29] while subsequent intracellular microelectrode studies have identified slow waves in dog, monkey, and mouse IAS [105, 110, 114, 118, 120, 121] (Fig. 2.8). The frequency of slow waves in the IAS ranges from ~45–80 cpm in mouse to ~15–30 cpm in dog and monkey IAS. Slow waves in the IAS differ from those of the intestine in that they lack an initial rapid upstroke (i.e., 1–10 V/s maximum dV/dt for intestine [122, 123] versus 10–100 mV/s maximum dV/dt for the IAS [110]). Instead, IAS slow waves reach peak depolarization after 0.38–0.7 s in mouse and after 1–2 s in dog and monkey. Spikes (260–800 mV/s) of variable amplitude are sometimes superimposed

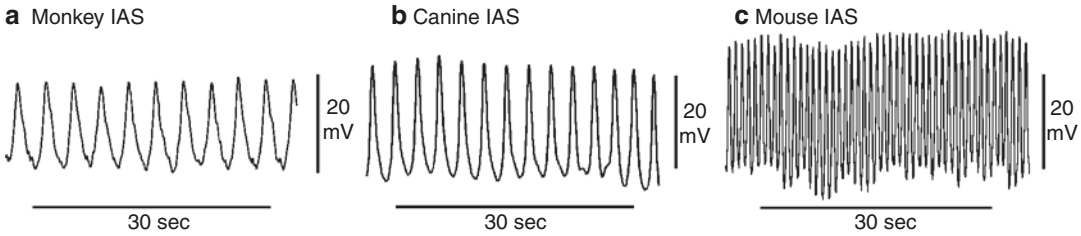

Fig. 2.8 Sample traces of slow wave activity recorded from the internal anal sphincter (IAS) of several animal species (Adapted from [121]). (**a**) Monkey, (**b**) Canine, (**c**) Mouse. Note the significantly higher frequency of slow waves in the mouse IAS

upon slow waves [110]. The amplitude and frequency of slow waves does not vary across the thickness of the IAS circular muscle layer. Indeed, even subsections of this layer exhibit the same electrical activity [118]. Thus, pacemaker potentials appear to be generated throughout the muscle thickness rather than being localized to one specific region (e.g., myenteric or submucosal edge). In contrast, slow wave frequency declines in the proximal direction [105, 114, 118].

2.2 Role of ICC in the Control of Electrical and Contractile Activity in Sphincters

2.2.1 Role of ICC in the Generation of Spontaneous Contractile Activity

Historically, spontaneous contractile activity in the GI tract was believed to arise directly from the properties of smooth muscle cells, hence the name "myogenic." However, since the identification of interstitial cells of Cajal (ICC) in the GI tract and recognition that ICC generate pacemaker potentials [124] it is now widely accepted that spontaneous phasic contractile activity is mediated in large part by slow waves arising from pacemaker-type ICC. Pacemaker ICC are predominantly located at the myenteric (ICC-MY) and submucosal (ICC-SM) surfaces of the circular muscle layer. A second population of ICC has also been identified within the circular and longitudinal muscle layers. These cells are referred to as "intramuscular" ICC (ICC-IM) and they are known to play an important role in excitatory and inhibitory neuromuscular transmission in the GI tract [125]. The morphology of ICC subtypes also differs, with ICC-MY and ICC-SM generally being highly branched stellate cells while ICC-IM are usually spindle-shaped. Pacemaker ICC are electrically coupled to one another and to smooth muscle cells allowing slow waves to conduct into the muscularis in a coordinated fashion [126, 127]. On the other hand, ICC-IM are interspersed within the muscularis, and run parallel to smooth muscle cells. ICC-IM are also electrically coupled to smooth muscle cells forming a syncytium that permits transmission from nerve, through ICC, to adjacent smooth muscle cells [125]. In contrast to this functional difference between ICC subtypes in the intestine, recent studies suggest that some ICC-IM may instead serve as pacemaker cells in the IAS giving rise to tone development (see below).

2.2.2 ICC in Gastrointestinal Sphincters

ICC have been identified in each of the GI sphincters discussed in this chapter (Fig. 2.9). However, there are significant differences in their morphology and distribution. The distribution of ICC in the ICS [128] resembles that of the colon [129] in that ICC-MY, ICC-SM, and ICC-IM are all represented (Fig. 2.9a). However, slow waves like those described in the large and small intestine [130, 131] are absent and phasic contractions are associated with periodic spiking activity (Fig. 2.7). Furthermore, tone in the ICS is relatively insensitive to blockade by dihydropyridines [82, 84]. Thus, the role of ICC in the ICS likely diverges from that of intestine. The distribution of ICC in the remaining three sphincters differs from that of the ICS. Although the antral end of the pylorus contains ICC-MY, ICC-SM, and ICC-IM, the density of ICC-MY and ICC-SM declines distally approaching undetectable levels at the PS while ICC-IM persist (Fig. 2.9b, d) [132]. Since low-frequency slow waves (i.e., 0.5–1/min) occur in isolated strips of the PS [58, 59], some pacemaker-type ICC-MY likely persist in this region. The LES and IAS resemble one another in that ICC-MY and ICC-SM are absent while having a dense population of ICC-IM (LES [129, 133]; IAS [86, 87, 105] Fig. 2.9f). Interestingly, whereas ICC-IM in the monkey LES are spindle shaped (Fig. 2.9c [129]), those of the monkey and dog IAS are highly branched (Fig. 2.9e [86, 87]). Thus, unlike most of the GI tract, the morphology of ICC-IM in the monkey and dog IAS resembles that of pacemaker ICC. ICC in the dog IAS have also been shown to

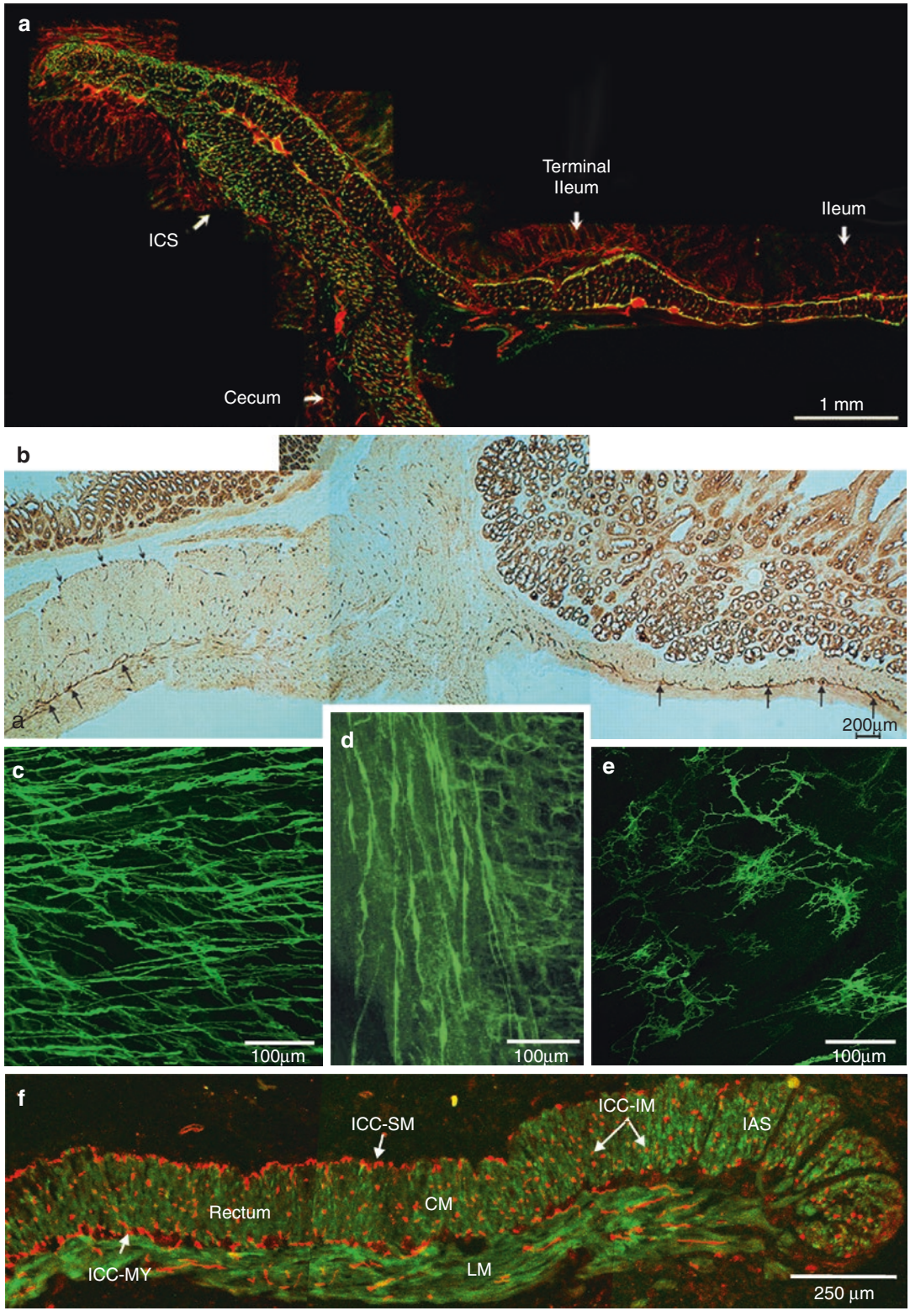
a
Terminal
Ileum
Ileum
ICS
Cecum
1 mm
b
a
200μm
c
100μm
d
100μm
e
100μm
f
ICC-SM
ICC-IM
IAS
Rectum
CM
ICC-MY
LM
250 μm

form gap junctions with one another and with smooth muscle cells [86]. Because the dog and monkey IAS both have slow waves (Fig. 2.8) and "pacemaker like" ICC (Fig. 2.9e), we have proposed that ICC-IM are responsible for the generation of pacemaker potentials in the IAS [87]. Our recent studies with the Kit-GCaMP3$^+$ mouse, a transgenic mouse that expresses the calcium-sensitive fluorophore GCaMP3 in ICC, further support this hypothesis. These studies have revealed that adjacent GCaMP3$^+$ cells generate synchronized whole-cell phasic calcium events at the slow wave frequency [134, 135].

2.2.3 Role of Chloride Channels in the Generation of Slow Waves and the Control of Membrane Potential in Gastrointestinal Sphincters

Intracellular chloride concentration in smooth muscle cells is significantly greater than in skeletal muscle with an estimated chloride reversal potential between −20 and −30 mV [136–138]. Thus, chloride channels have long been proposed as contributors to setting the level of resting membrane potential in smooth muscle. More recently, deep sequencing of smooth muscle cells of the mouse large and small intestine has identified transcript for voltage-gated Cl^- channels, as well as several members of the anoctamin/TMEM16 (ANO1) family of Ca^{2+}-activated Cl^- channels [139]. The resting membrane potential of LES is ~10 mV less negative than the esophageal body [5, 9, 34, 35] and early studies suggested that this was due to a greater chloride conductance in LES cells [140]. Subsequent studies have supported this proposal by showing that chloride channel blockers (i.e., niflumic acid, 9-Anthracene carboxylic acid) hyperpolarize membrane potential, abolished action potentials, and greatly reduced tone in the LES [35, 141].

In the LES studies described above, the cell type responsible for generating chloride currents was not addressed. More recently it has been shown that intestinal ICC also express some voltage-gated Cl^- channels as well as Ca^{2+}-activated Cl^- channels in the ANO channel family [142]. In particular, expression levels of ANO1 in

Fig. 2.9 Immunohistochemical labeling of interstitial cells of Cajal (ICC) in various gastrointestinal sphincters and animals. (**a**) Longitudinal section of the guinea pig ileocecal sphincter (valve) showing ICC (Kit, green) and nerves (PGP, red). ICC are located at the submucosal and myenteric surfaces as well as within the muscle layer. Some ICC are in close association to nerves. The terminal ileum immediately adjacent to the sphincter contains a thickened circular muscle layer [128]. (**b**) A longitudinal section of the rat pyloric sphincter (PS) and adjacent regions immunostained for Kit. In the distal antrum (*left*), ICC are concentrated at the myenteric plexus (arrows) surrounding ganglia. ICC-IM are also scattered in both circular and longitudinal muscle layers. There is also a concentration of ICC at the submucosal border (small arrows). In the pyloric region (*middle*), ICC-MY are markedly decreased in a segment ~4 mm in width while ICC-IM are abundant and diffusively distributed. In the proximal duodenum (*right*), ICC-MY are present (arrows) except for the first 1–2 mm, where ICC are evenly distributed in the whole musculature and not concentrated at the level of the myenteric plexus. From 3–4 mm onward in the duodenum, ICC are present at the deep muscular plexus and submucosa. Background staining of the mucosa is due to endogenous biotin within the mucosal glands only [132]. (**c**) Kit labeling (green) of ICC-IM in a 100 μm cryostat section cut parallel to the circular muscle fibers in the monkey lower esophageal sphincter (LES) [129]. (**d**) Whole mount preparation of the rat pyloric sphincter labeled for Kit (green). ICC-MY are absent from this region. Instead, there are many bipolar-shaped ICC-IM running parallel to circular muscle fibers of the pyloric sphincter (*left*) whereas a loose network of ICC can be seen at the beginning of the proximal duodenum (right) [132]. (**e**) Ten micron optical section taken from a whole mount preparation of the monkey internal anal sphincter cut parallel to circular muscle fibers. Highly branched stellate ICC-IM are seen at this focal plane as well as throughout each muscle bundle within the circular muscle layer [87]. (**f**) Longitudinal section of the *smMHC-Cre-eGFP* mouse anorectum. Kit$^+$ ICC (red) were identified using immunohistochemical techniques while smooth muscle cells were identified through expression of green fluorescent protein (green) [105]. ICC-SM and ICC-MY are apparent along the submucosal and the myenteric edges of the circular muscle layer in rectum respectively but disappear before reaching the distal IAS. In contrast, ICC-IM are present throughout the CM layer of the rectum and IAS. Spindle-shaped ICC-IM can also be seen in the longitudinal muscle layer. Division of the CM layer into bundles (green) can clearly be seen within the IAS. Images are composites of three images taken at 10×. *CM* circular muscle, *ICC* interstitial cells of Cajal, *IAS* internal anal sphincter, *IM* intramuscular, *LM* longitudinal muscle, *MY* myenteric, *SM* submucosa

ICC far exceeds that of smooth muscle cells. There is now substantial evidence that ANO1 in ICC plays a central role in the generation of slow waves as discussed in the other GI chapter in this book. Briefly, in pacemaker ICC, intermittent release of calcium from the endoplasmic reticulum results in activation of ANO1 and spontaneous transient inward currents (STICs). STIC generated membrane depolarization in turn activates voltage-dependent calcium channels giving rise to slow waves that conduct into adjacent smooth muscle cells via gap junctions [143].

Since the IAS exhibits slow waves and phasic contractile activity while only ICC-IM are present, we hypothesized that ICC-IM are responsible for the generation of pacemaker potentials in this muscle. Thus, we investigated whether ANO1 channels in ICC-IM have a similar role to that described for pacemaker ICC in the intestine. These studies revealed that: (1) *Ano1* gene expression is 26× greater in ICC-IM than in smooth muscle cells. (2) Gene expression levels of *Ano1* in whole IAS and rectum are the same. (3) ANO1 protein expression is resolvable in ICC but not in smooth muscle cells. (4) ANO1 channel antagonists abolish slow waves, phasic contractions, and tone as well as causing a small hyperpolarization of resting membrane potential. These data all support the hypothesis that ICC-IM are responsible for the generation of slow waves in the IAS and that ANO1 channels play a central role in this process [119]. Equivalent experiments have not been undertaken in the LES.

2.2.4 Limitations of the *W/W^v* Mouse for Examining the Role of ICC in Sphincters

The *W/W^v* mouse has been used in a number of studies to examine the role of ICC in the generation of pacemaker potentials [144]. Kit-labeling of ICC-IM is not resolvable in the IAS, LES, and PS of the *W/W^v* mouse [145–147] while membrane potential is ~4 mV more polarized [110, 146]. In the IAS tone and slow waves persist in the *W/W^v* mouse [110] while tone is significantly reduced in the LES [146]. These data do not strongly support a role for ICC-IM in the generation of tone and slow waves in the IAS. The *W/W^v* mouse is not a quantitative *Kit* knockout since the W kit allele is null while the *W^V* allele has reduced function [148]. Thus, Kit labeling of ICC throughout the GI tract is "patchy" with Kit resolvable in some regions but not others [149]. Likewise, the degree of functional knockout differs between regions [144]. Indeed, differences in the degree of functional knockout have also been reported for the same region by different groups (e.g., LES [146, 150]). It is possible that functional ICC-IM persist in the *W/W^v* mouse IAS even though Kit protein is no longer resolvable with immunohistochemistry. Alternatively, since the reduced Kit function in the *W/W^v* mouse is constitutive, it is possible that some gain of function occurs during development in other cell types (i.e., smooth muscle cells, PDGFRα$^+$ cells) that compensates for the loss of ICC. Indeed, ICC, PDGFRα$^+$ cells, and smooth muscle cell all have a common precursor, namely, gut mesenchymal cells [151–155]. Because of these issues, the *W/W^v* mouse is not ideal for examining the role of ICC-IM in the generation of slow waves in the IAS. Our observations that Kit-GCaMP3$^+$ cells generate phasic calcium events at the slow wave frequency [134, 135] as well as our studies linking ANO1 to ICC-IM and slow wave generation [119] all provide evidence that ICC-IM generate slow waves in the IAS.

2.3 Specific Mechanisms Proposed for the Generation of Tone in GI Sphincters

In Part I we briefly summarized the anatomy and physiological behavior of the four main sphincters in the GI tract. A general conclusion of this section is that there is stronger evidence supporting a role for spontaneous tone generation in the LES, ICS, and IAS than for the PS. In the following section (Part III) we examine specific mechanisms proposed to underlie tone generation in these GI sphincters.

2.3.1 Mechanism #1: *Tone May Arise from the Summation of Asynchronous Phasic Activity Generated by Adjacent Muscle Bundles that are not Highly Coupled to one Another*

It has long been known that skeletal postural muscles can maintain tone through the asynchronous firing of motor units [156]. Specifically, the asynchronous contractile activity generated by different motor units sum to maintain tone. It is possible that similar events contribute to tone generation in the GI tract. In this case however the "motor unit" corresponds to a small bundle of electrically coupled smooth muscle cells isolated from adjacent muscle bundles. This division of muscle into small bundles differs somewhat from the classic definition of smooth muscle as either "multiunit" (i.e., each cell electrically isolated from its neighbors) or "single unit" (i.e., all cells electrically coupled to neighbors). In fact, most GI muscles fall somewhere between these extremes since they are composed of muscle bundles of various sizes as well as varying degrees of electrical coupling between bundles. In the large and small intestine muscle bundles are generally quite large and cells within them are highly coupled. The activity of the bundles is coordinated by pacemaker ICC located at the myenteric and/or submucosal edge of the muscle layer. In contrast, the IAS is subdivided into numerous smaller "minibundles," each separated by wide connective septa (Fig. 2.10 [86, 87]). ICC-IM and nerves are located within each minibundle. This provides a means for eliciting spontaneous activity within the minibundle (i.e., ICC-IM) and a mechanism (i.e., nerves) to coordinate the activity of all minibundles [87]. To conclude that the electrical activity of minibundles in large animals is asynchronous will require dual microelectrode recordings and/or studies examining the spread of calcium transients across the tissue. However, there is one study that has been undertaken on a smaller, simpler muscle, i.e., the mouse IAS. The mouse IAS is also composed of minibundles but

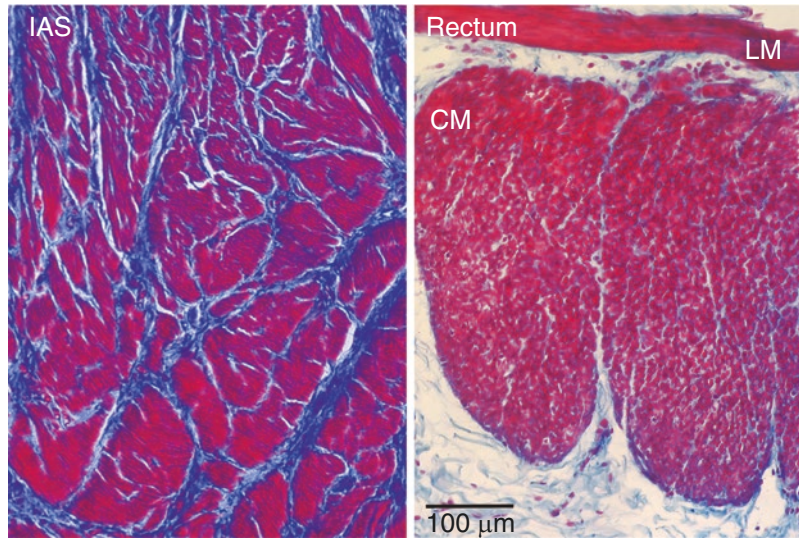

Fig. 2.10 Comparison of the organization of muscle bundles in the monkey IAS (left) and rectum (right) at the same magnification. Thin (3 μm) cross sections of the internal anal sphincter (IAS) and rectum were stained with Masson's trichrome to visualize both smooth muscle (red/purple) and connective tissue (blue). (**a**) Numerous minibundles (red) are present in the IAS separated by connective tissue septa (blue). (**b**) The rectal wall thickness is thinner than the IAS thus at this magnification it is possible to see the entire width of the circular muscle (CM) layer as well as some longitudinal muscle (LM). Muscle bundles are again observed in the rectum but in this case each bundle is larger, spanning the entire CM width and overall, there is less connective tissue within and between muscle bundles [87]

in this case there are only six to ten bundles and each bundle spans the entire width of the circular muscle layer. Dual microelectrode measurements in this tissue have shown that slow waves are only coordinated across a few muscle bundles longitudinally and ~20% of the circumference [105]. Thus, even in the mouse IAS, the circular muscle layer does not behave as a "single unit" but rather as a composite of minibundles that are only loosely coupled to one another supporting mechanism #1.

2.3.2 Mechanism #2: *Tone May Arise from the Accumulation of Intracellular Calcium in the Smooth Muscle Cytoplasm Because Calcium Entry via High-Frequency Slow Waves Outpaces Calcium Efflux/Uptake Mechanisms*

Drawing again from the behavior of skeletal muscle, it is known that the characteristics of contraction in skeletal muscle changes with the frequency of stimulation. Thus, as stimulus frequency increases, contractile amplitude increases until a point is reached at which contraction ceases to return to baseline between stimuli. This condition, referred to as "partial (incomplete) tetanus," occurs because there is insufficient time between stimuli for calcium removal to return intracellular calcium ($[Ca^{2+}]_i$) to subthreshold levels [157]. The pattern of contractile activity in the IAS resembles partial tetanus in that it is composed of phasic contractions superimposed upon tone. Recently, a transgenic mouse has become available that expresses the calcium-sensitive fluorophore GCaMP3 in smooth muscle cells (SM-GCaMP3). This makes the SM-GCaMP3 mouse a valuable tool for evaluating the possible role of mechanism #2 in tone generation. Transient changes in $[Ca^{2+}]_i$ are observed in smooth muscle cells of the SM-GCaMP3 mouse IAS and these occur at the same frequency as slow waves (Fig. 2.11). Stimulation of inhibitory motor neurons (which hyperpolarizes membrane potential and abolishes almost all contractile activity [109, 110]) reveals that $[Ca^{2+}]_i$ between calcium transients is

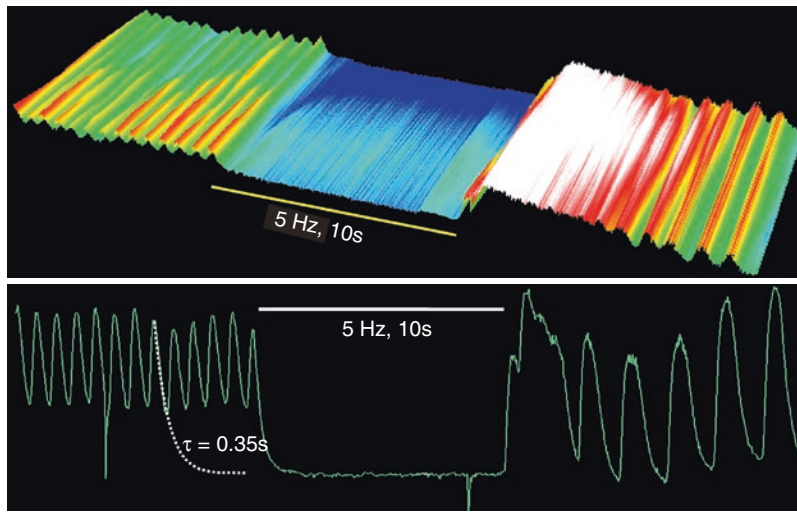

Fig. 2.11 Calcium transients recorded at the distal end of the internal anal sphincter (IAS) of the SM-GCaMP3 mouse. Upper trace: Spatiotemporal map of the spontaneous activity in a 33 s recording taken from a 100 × 200 micron region of interest (ROI) of the distal IAS. A calcium trace taken from this ROI shows the changes in $[Ca^{2+}]_i$ as a function of time. Electrical stimulation of nerves (EFS, 5 Hz, 10 s) was applied in the presence of atropine to eliminate cholinergic transmission. EFS blocked all phasic activity as well as reducing basal calcium levels. The time constant for calcium removal (tau = 0.35 s) was estimated by fitting the decline of individual calcium transients to a simple exponential function from peak to baseline. At the end of the stimulus train a large rebound event was observed before the pattern returned to control levels [134, 135]

significantly elevated. Furthermore, the average time constant for the decline of $[Ca^{2+}]_i$ following each calcium transient is ~0.3–0.5 s. Consequently, there is insufficient time for calcium to reach subthreshold levels before the arrival of the next calcium transient [135] (Fig. 2.11). This observation provides evidence for mechanism #2 in the mouse IAS. Such a mechanism is also likely to contribute to tone generation in the opossum LES where ongoing spike discharge occurs at a high frequency (Fig. 2.3).

In contrast to the above examples, the frequency of slow waves in the IAS of larger animals such as dog and monkey is significantly lower than mouse (see Fig. 2.8). However, the rate of slow wave depolarization and repolarization is also slower in these muscles resulting in the membrane potential remaining above the Cav_L channel threshold for a longer period of time (Fig. 2.12). Thus, the predominant factor keeping $[Ca^{2+}]_i$ above threshold in these muscles is likely the extended period of time that calcium entry continues with each slow wave rather than a partial tetanus type mechanism. To further evaluate the relationship between slow waves and tone generation will require addressing the following questions: (1) Is $[Ca^{2+}]_i$ also tonically elevated in the IAS of animals with low-frequency slow waves? (2) To what extent are there differences in the characteristics of Cav_L channels and/or calcium uptake/efflux mechanisms between species? (3) To what extent are there differences in the cell type and/or ionic conductances that are responsible for slow wave generation between species?

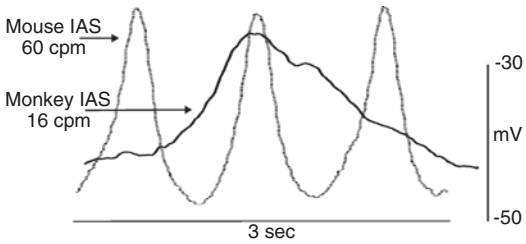

Fig. 2.12 Comparison of slow waves recorded from the mouse and monkey IAS. Slow waves differed in several ways including: (1) Slow wave frequency is significantly less in the monkey IAS than in the mouse IAS. (2) The rate of depolarization and repolarization is significantly slower in the monkey IAS than in the mouse IAS. (3) "Resting" membrane potential is more depolarized in the monkey IAS than in the mouse IAS. Because of these differences, each slow wave in the monkey IAS spends a greater amount of time above the activation threshold for Cav_L channels than a slow wave in the mouse IAS (Adapted from [121])

2.3.3 Mechanism #3: *Tone May Arise from Continuous Calcium Entry into Smooth Muscle Cells via Window Current*

Voltage-dependent calcium channels, in particular Cav_L channels, play an important role in delivering calcium to the cytoplasm for contraction in most GI muscles, including the sphincters covered in this section. Both the activation and inactivation of Cav_L channels are voltage-dependent processes with maximum current occurring around 0 mV and threshold current appearing around −50 to −45 mV [158–160]. At potentials between these two extremes inactivation is incomplete and some sustained calcium current can occur which is referred to as "window current" [160–162]. Window current has long been associated with the sustained contraction that follows exposure of smooth muscles to elevated extracellular potassium solution. In phasic muscles without tone, slow waves arise periodically from a relatively polarized level of membrane potential (e.g., −78 mV for canine colon at the submucosal edge [130]), Cav_L channels open during slow wave depolarization and close as the membrane potential falls below their activation threshold. However, the level of membrane potential between slow waves or spikes in the LES and IAS is less polarized lying within the activation threshold for Cav_L channels. Hence some contribution from window current (mechanism #3) is anticipated.

A further consideration with regard to the relationship between membrane potential and tone relates to the actions of nitrergic nerves. Most GI muscles are under tonic inhibition via the sponta-

neous release of NO from inhibitory motor neurons. NO hyperpolarizes sphincters [73, 163, 164] and blockade of tonic NO release from nerves causes depolarization [73, 111]. Hence, removal of NO (by blocking either NOS or neural activity) results in increased phasic contractions as well as tone [7, 111, 165–168]. Likewise, eliminating guanylate cyclase in ICC and smooth muscle cells (SMC/ICC-GCKO) has been shown to result in a 2.5-fold increase in LES pressure [169].

The monkey IAS is under strong tonic nitrergic inhibition. Thus blockade of NO release from nerves either with TTX or with the NOS inhibitor L-NNA causes increased tone as well as a decrease in phasic contractile activity (Fig. 2.13a). These changes are accompanied by depolarization and a reduction in the amplitude of slow waves (Fig. 2.13b). Under these depolarizing conditions, Ca^{2+} entry associated with Cav_L channel window current will result in more tonic contracture. The effects of NOS blockade can be reversed either by addition of an NO donor such as sodium nitroprusside (Fig. 2.13a, c, d) or by hyperpolarizing the muscle with a potassium channel opener such as pinacidil (Fig. 2.13e) [120]. Thus, tonic release of NO from inhibitory motor neurons appears to play an important role in determining the electromechanical mechanisms underlying contractile activity in the monkey IAS. In the presence of NO, membrane potential is more polarized, and calcium delivery involves more phasic electrical events (i.e., slow waves). On the other hand, when NO is removed and membrane potential is more depolarized, continuous entry of calcium via window current plays a greater role (mechanism #3).

Besides blocking nitrergic inhibition, tone can also be generated by increasing extracellular potassium ($[K]_o$) leading to membrane depolarization. Thus, when $[K]_o$ is raised, the normally phasically active canine gastric antrum generates tone with superimposed phasic contractions [170]. Likewise raising $(K)_o$ in the guinea pig ICS increases tone while lowering $[K]_o$ diminishes tone [76, 83].

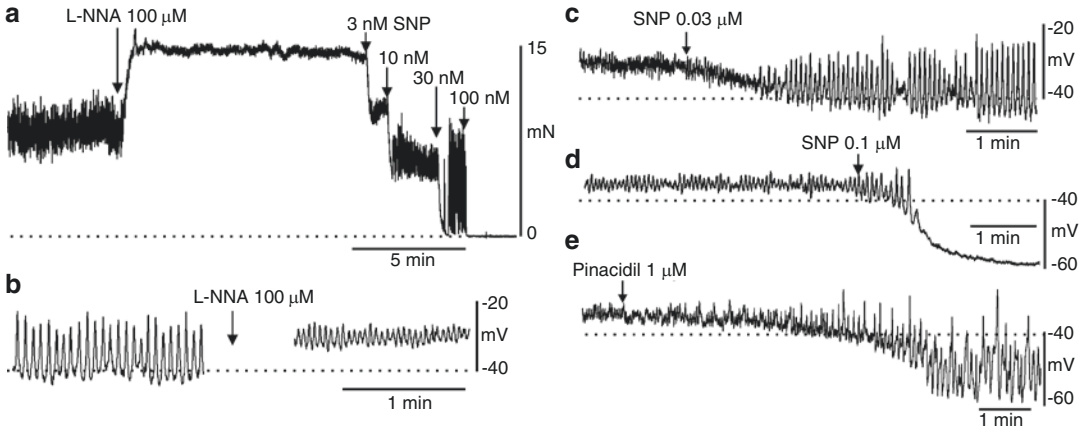

Fig. 2.13 Examples of the electrical and contractile changes that occur in the monkey IAS with blockade of nitric oxide synthase with L-NNA, or following addition of the nitric oxide donor sodium nitroprusside (SNP) or the K_{ATP} activator pinacidil. (**a**) Tone and phasic activity are observed under control conditions in this muscle. Tone is significantly increased with addition of L-NNA while phasic activity is reduced. The effect of L-NNA was reversed by addition of increasing concentrations of SNP while the highest concentration abolished all contractile activity. (**b**) Electrical recording from a different muscle strip showing slow waves occurring in the absence of L-NNA (left). Following L-NNA addition membrane potential depolarized and slow wave amplitude was reduced (right). (**c**) Addition of 0.03 μM SNP in the continued presence of L-NNA restores control slow wave activity and returns membrane potential to the control level. (**d**) Addition of a higher concentration of SNP (0.1 μM) in another muscle strip caused hyperpolarization and a transient period of larger amplitude slow waves followed by further hyperpolarization and blockade of slow waves (L-NNA present throughout). (**e**) Addition of pinacidil to another muscle in the presence of L-NNA also resulted in hyperpolarization and the return of larger amplitude slow waves [120] (**a**–**d** Adapted from [121])

2.3.4 Mechanism #4 *Tone May Arise from Sensitization of the Myofilaments to Calcium*

Spontaneous contractile activity in GI smooth muscles is dependent upon a rise in $[Ca^{2+}]_i$. Furthermore, calcium entry through Cav_L channels plays an important role in this process. The first three mechanisms considered above describe processes linking Cav_L channels to tone generation in sphincters. The fourth mechanism instead addresses how tone in sphincters may result from a greater sensitivity of the myofilaments to calcium.

Smooth muscle myosin is composed of two heavy chains forming head and tail regions and two 20-kD regulatory light chains (MLC_{20}). The phosphorylation of MLC_{20} at S19 by myosin light chain kinase (MLCK) stimulates myosin ATPase activity, cross-bridge cycling, and contraction [171–174]. MLCK is activated by a calcium-calmodulin complex that forms when $[Ca^{2+}]_i$ increases. Contraction is terminated when myosin light chain phosphatase (MLCP) dephosphorylates MLC_{20}. The extent of smooth muscle contraction therefore depends upon a balance between the activities of MLCK and MLCP. MLCP is composed of a catalytic subunit (protein phosphatase 1, or PP1), a regulatory subunit (myosin phosphatase target subunit 1, or MYPT1), and a 20-kD subunit (M20) of unknown function. The regulatory subunit MYPT1 facilitates the ability of PP1 to dephosphorylate MLC20 by serving as a scaffolding protein [175–181].

Several different second messenger pathways have been shown to inhibit MLCP resulting in greater phorphorylation of MLC_{20} at a given $[Ca^{2+}]_i$, i.e., "calcium sensitization" [177–179, 182–184]. One such pathway involves phosphorylation of MYPT1 at threonine 696 (T696) and 853 (T853). Recent studies suggest that T696 phosphorylation is responsible for direct inhibition of MYPT1 whereas T853 phosphorylation causes disassembly of the myosin-MLCP complex [185]. An important regulator of MYPT1 phosphorylation is Ras homolog gene family, member A (RhoA). RhoA is a small, monomeric G-protein that is activated when GDP is exchanged for GTP. Activated RhoA in turn activates Rho-associated protein kinase 2 (ROCK2). In many smooth muscles, the RhoA/ROCK2 pathway is activated by G-protein coupled receptors resulting in phosphorylation of T696 and T853, decreased MLCP activity and calcium sensitization [176, 183, 186, 187]. However, since tone in sphincters arises spontaneously, the more relevant issue is whether constitutive phosphorylation of T696 and T853 also occurs. There is general agreement that constitutive T696 and T853 phosphorylation occurs in both phasic and tone-generating muscles [181, 188] and that constitutive T853 phosphorylation is dependent upon phosphorylation by ROCK2 [176, 183, 186–188]. However, there are reports of ROCK2-independent phosphorylation of T696 [185, 188–190]. Since there are other kinases in smooth muscle cells that can phosphorylate T696 [191], ROCK2-independent T696 phosphorylation likely involves one or more of these other kinases.

Recently a conditional MYPT1 KO mouse ($MYPT1^{SM-/-}$) has become available to further examine the role of MYPT1 and calcium sensitization in the regulation of smooth muscle contraction. Surprisingly, the contractile activity of smooth muscles in the $MYPT1^{SM-/-}$ mouse is only modestly different from that of WT mice [192] including the tone-generating IAS [193]. However, loss of MYPTI in the $MYPT1^{SM-/-}$ mouse has also been shown to result in a reduction in PP1 levels, possibly because the cellular stability of PP1 depends upon MYPT1 [188, 194]. In addition, regulation of MLCP activity by MYPT1 may be shared with the closely related MYPT1 family member myosin binding subunit 85 (MS85) so that loss of one regulator may be compensated for by the other [195]. Given the complexity of molecular pathways that regulate MLCP activity, it appears premature to discount a possible role for calcium sensitization in tone development in the IAS based upon the $MYPT1^{SM-/-}$ mouse [193].

The extent to which myofilament sensitization contributes to tone generation in sphincters likely differs between sphincters as well as between species. The relative ability of Cav_L channel

blockers to abolish tone provide us with some preliminary information regarding the possible mechanisms contributing to tone generation since electromechanical coupling pathways are sensitive to these antagonists while myofilament sensitization pathways are not. The extreme example in this regard is the mouse fundus which is entirely insensitive to dihydropyridines. Biochemical studies have shown that tone in the fundus is generated in large part by the RhoA/ROCK2 pathway [190]. Phasic contractions in the PS are abolished by dihydropyridines [57] while phasic activity and >90% of tone are eliminated in the IAS [115]. These data clearly suggest an important role for electromechanical coupling in the PS and IAS. In contrast, dihydropyridines are less effective at blocking tone in the LES (i.e., 72% inhibition [35]) and least effective in the ICS (i.e., <50% inhibition [82, 84]). From these observations, it is tempting to suggest that the most prominent role for myofilament sensitization is in the ICS followed by the LES and then the IAS. Unfortunately, little attempt has been made to examine myofilament sensitization in the ICS while only limited work has been completed on the LES (see below).

The most comprehensive examination of calcium sensitization pathways in a sphincter are studies of rat and human GI muscles by Rattan and coworkers [196–199]. These studies revealed significantly greater RhoA, ROCK2, and T696 phosphorylation levels in the tone-generating IAS than in rectum, the latter being predominantly a phasic muscle with significantly less tone. ROCK2 antagonists also abolished T696 phosphorylation and were more potent antagonists of contraction in the IAS than in other phasic muscles. From these data, the authors concluded that tone in the IAS is due to greater calcium sensitization via the ROCK2/MYPT1 pathway (i.e., mechanism #4). We reexamined this topic by comparing various proteins in the RhoA/ROCK2 pathway in the monkey IAS and rectum. Our results are in general agreement with those of Rattan et al. in that T696 and T853 phosphorylation and ROCK2 expression levels were all greater in the IAS than in rectum. However, we noted little difference in the potency of ROCK2 inhibitors between muscles [200]. Likewise, little difference has been noted in the potency of ROCK2 inhibitors in the phasically active mouse colon versus the tone-generating fundus [190]. Taken together, these data suggest that some degree of tonic myofilament sensitization is likely to be present in both phasic and tone-generating muscles [191], a concept that is further developed in the summary section.

Another inhibitor of MLCP is C-kinase (PKC) potentiated protein phosphatase-1 Inhibitor protein-17 (CPI-17). Phosphorylation of CPI-17 at threonine 38 (T38) results in a conformational change that permits docking of CPI-17 with PP1 resulting in MLCP inhibition [201]. In smooth muscle, phosphorylation of CPI-17 is predominantly mediated by PKC or ROCK2 [191]. The degree to which PKC-mediated Ca^{2+} sensitization occurs has been correlated with CPI-17 expression levels in the smooth muscle [202, 203]. Constitutive phosphorylation of CPI-17 is generally considered to be low in smooth muscles compared with constitutive MYPT1 phosphorylation [190, 204–211]. In studies of the rat and human IAS and rectum CPI-17 levels and constitutive T38 phosphorylation were reported to be greater in the IAS than in rectum. Nonetheless the authors concluded that calcium sensitization is predominantly mediated by the RhoA/ROCK2/MYPT1 pathway, in part because of the limited ability of PKC blockers to reduce tone. PKC inhibitors also have very limited effects on basal tone in the LES whereas ROCK2 inhibitors produce full relaxation [212, 213], again suggesting a more important role for the RhoA/ROCK2 pathway in calcium sensitization in sphincters than PKC/CPI-17. It should be noted that MYPT1 and CPI-17 phosphorylation were not measured in the LES studies.

NO-mediated desensitization. The discussion thus far has focused on how calcium sensitization might give rise to tone in sphincters. However, as previously described, it is known that contractile activity in sphincters is subject to tonic inhibition due to the release of NO from inhibitory motor neurons [7, 111, 165–168]. NO binds to guanylyl cyclase leading to increased formation of cGMP

and activation of cGMP-dependent protein kinase (PKG). PKG in turn is linked to calcium desensitization in part through phosphorylation of RhoA at serine 188 (S188). This prevents RhoA binding to ROCK2, thereby reducing MYPT1 phosphorylation and restoring MLCP activity [214–219]. Increased cGMP has also been associated with increased phosphorylation of MYPT1 at serine 695 (S695) leading to a reduction in T696 phosphorylation, again restoring MLCP activity [220, 221] although this effect was not observed in cerebral artery [222]. Telokin is another candidate for NO-mediated disinhibition of MLCP. Telokin is a small protein with partial sequence homology to MLCK. Following a rise in cGMP, telokin becomes phosphorylated at serine 13 (S13) leading to stabilization of the unphosphorylated state of MLC20 and relaxation [223]. Studies of a telokin-deficient mouse have reported increased MLCP activity and decreased cGMP-mediated relaxation in ileum [224], further supporting a role for telokin in NO-mediated contractile inhibition.

Most studies examining the role of MLCP phosphorylation and calcium sensitization are undertaken in the presence of NOS inhibitors and/or neural blockers. This approach is likely to underestimate MLCP activity in vivo and consequently overestimates the degree to which calcium sensitization participates in tone generation. Indeed, our contractile and microelectrode measurements in the monkey IAS further emphasize the substantial changes that occur in the pattern of spontaneous electrical and contractile activity following NOS blockade (Fig. 2.13). When tonic neural inhibition is present, there is less tone while phasic electrical and contractile activity are enhanced. In contrast, following NOS blockade, the membrane depolarizes, slow waves and phasic contractile activity are reduced, and tone is increased. Thus, NO can have profound effects upon both electromechanical coupling mechanisms and myofilament sensitization. Tonic neural inhibition may therefore provide a system in which contractile activity in vivo is predominantly controlled by electromechanical mechanisms which are better suited to rapid moment to moment adjustments whereas calcium sensitization represents a means for retaining contracture if neural pathways are compromised.

2.4 Summary

The LES, PS, ICS, and IAS each serve to restrict the movement of luminal contents between adjacent regions of the GI tract. However, the mechanisms by which this function is achieved differ significantly between sphincters. In the first section, we reviewed the basic anatomy and physiology of the various sphincters. A general conclusion of this section is that there is stronger evidence supporting a role for spontaneous tonic contraction in the LES, ICS, and IAS than for the PS. In the second section, we examined the general relationship of contractile and electrical activity in the GI tract to ICC along with the possible role of ICC-IM in the generation of tone in sphincters. In the third section, four different mechanisms were considered that have been proposed to give rise to tone generation in sphincters. Several of these mechanisms are likely to participate in tone generation although the contribution of each will differ between sphincters as well as between species. Both the IAS and LES exhibit ongoing phasic electrical activity while the IAS in particular generates substantial phasic contractile activity as well. Two different mechanisms have been discussed (mechanism #1 and #2) that result in tone generation from phasic electrical events. For this reason, the conventional description of the IAS as a "purely tonic muscle" is mistaken [225]. Instead the IAS is best considered as a phasically active muscle that generates tone. The final figure in this chapter (Fig. 2.14) presents a summary diagram that depicts how electromechanical coupling mechanisms (#1–3) and calcium sensitization (mechanism #4) might interface with one another to generate tone versus phasic contractions in the IAS and rectum, respectively. To further advance this field it is important that future studies consider the entire spectrum of mechanisms that may interact with one another to achieve the final contractile status of each GI sphincter.

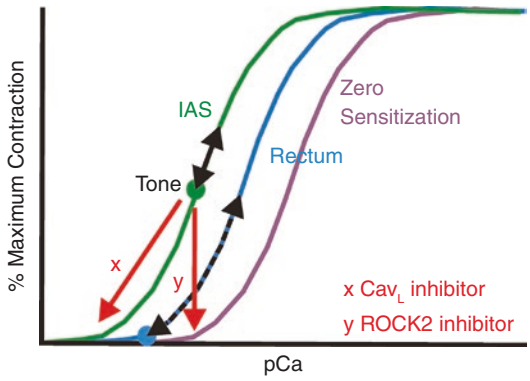

Fig. 2.14 Cartoon depicting the possible interactions occurring between electromechanical coupling, calcium sensitization and contraction in the IAS and rectum (Adapted from [121]). The predicted relationships between contraction and intracellular calcium concentration (pCa) in the IAS (left) and rectum (middle) are shown. The IAS curve is drawn to the left of the rectum because of greater constitutive MYPT1 phosphorylation (i.e., calcium sensitization, mechanism #4). Thus, for a given pCa there will be more contraction in the IAS than in rectum. Tone is observed in the IAS since resting membrane potential is more depolarized and slow wave frequency is greater [105, 118] resulting in a larger, more sustained increase in Cav_L channel activity and pCa (dot, mechanism #2 and #3). Each IAS slow wave causes a further increase in pCa along the pCa/contraction curve (black arrow) resulting in phasic contractions superimposed upon tone. Asynchrony between muscle bundles will dampen the average fluctuation in pCa in whole tissue resulting in smaller amplitude phasic contractions and greater tone (mechanism #1). In contrast to the IAS, resting membrane potential in rectum is more polarized and slow waves occur at a lower frequency. Thus, basal pCa is lower in rectum (dot at the base of the middle curve). Each slow wave causes a large transient increase in pCa (dashed arrow, middle curve) and a phasic contraction followed by return of pCa to low levels. If depolarization in the rectum is sustained in some manner (e.g., by elevating extracellular potassium concentration) then tone will develop (e.g. [170]). Blocking Cav_L channels (x) with nifedipine causes pCa to fall to low levels in both the IAS and rectum abolishing tone and phasic contractions. Blocking ROCK2 (y) with an inhibitor such as Y27632 causes the entire IAS pCa/contraction relationship to shift to the right (zero sensitization curve) eliminating tone with little change in pCa. The pCa/contraction relationship for rectum will also shift to the right with ROCK2 inhibition since these inhibitors also reduce contraction and constitutive MYPT1 phosphorylation in rectum [200]

Clinical Relevance. Changes in the structure and mechanical properties of sphincters can result in a number of different pathological conditions that diminish their ability to carry out normal functions. For example, a reduction in the ability of the lower esophageal/sling/clasp region to contract leads to a return of gastric contents to the esophagus resulting in gastroesophageal reflux disease (i.e., GERD) [11]. Likewise, stenosis of the PS can lead to vomiting, delayed emptying, and gastroparesis [226]. Failure of the ICS to adequately contract can result in an increase in the return of colonic contents to the small intestine giving rise to bacterial overgrowth [64, 227]. Finally, inadequate contraction of the IAS contributes to fecal incontinence [228]. In some cases, sphincter malfunction has been associated with loss of ICC [226, 229–231]. However, since different ICC populations perform different functional roles (e.g., pacemaking versus neuromuscular transmission) additional studies are required before a definitive relationship is established between ICC loss and disease. Clearly, establishing the basic mechanisms that underlie sphincter motility is an important first step in advancing our understanding of the etiology of disease states that compromise sphincter function.

Acknowledgements We are extremely grateful to the NIDDK for their support through Grant No. DK078736.

References

1. Liebermann-Meffert D, Allgower M, Schmid P, Blum AL. Muscular equivalent of the lower esophageal sphincter. Gastroenterology. 1979;76:31–8.
2. Preiksaitis HG, Tremblay L, Diamant NE. Nitric oxide mediates inhibitory nerve effects in human esophagus and lower esophageal sphincter. Dig Dis Sci. 1994;39:770–5.
3. Brookes SJ, Chen BN, Hodgson WM, Costa M. Characterization of excitatory and inhibitory motor neurons to the guinea pig lower esophageal sphincter. Gastroenterology. 1996;111:108–17.
4. Yuan S, Costa M, Brookes SJ. Neuronal pathways and transmission to the lower esophageal sphincter of the guinea pig. Gastroenterology. 1998;115:661–71.
5. Lecea B, Gallego D, Farre R, Opazo A, Auli M, Jimenez M, Clave P. Regional functional specialization and inhibitory nitrergic and nonnitrergic coneurotransmission in the human esophagus. Am J Physiol Gastrointest Liver Physiol. 2011;300:G782–94.
6. Farre R, Auli M, Lecea B, Estrada O, Sunol X, Clave P. Mechanisms controlling function in the clasp and sling regions of porcine lower oesophageal sphincter. Br J Surg. 2007;94:1427–36.

7. Gonzalez AA, Farre R, Clave P. Different responsiveness of excitatory and inhibitory enteric motor neurons in the human esophagus to electrical field stimulation and to nicotine. Am J Physiol Gastrointest Liver Physiol. 2004;287:G299–306.
8. L'Heureux MC, Muinuddin A, Gaisano HY, Diamant NE. Feline lower esophageal sphincter sling and circular muscles have different functional inhibitory neuronal responses. Am J Physiol Gastrointest Liver Physiol. 2006;290:G23–9.
9. Zhang Y, Mashimo H, Paterson WG. Regional differences in nitrergic innervation of the smooth muscle of murine lower oesophageal sphincter. Br J Pharmacol. 2008;153:517–27.
10. Liu JF, Lu HL, Wen SW, Wu RF. Effects of acetylcholine on sling and clasp fibers of the human lower esophageal sphincter. J Gastroenterol Hepatol. 2011;26:1309–17.
11. Miller L, Vegesna A, Ruggieri M, Braverman A. Normal and abnormal physiology, pharmacology, and anatomy of the gastroesophageal junction high-pressure zone. Ann N Y Acad Sci. 2016;1380:48–57.
12. Zifan A, Kumar D, Cheng LK, Mittal RK. Three-dimensional myoarchitecture of the lower esophageal sphincter and esophageal hiatus using optical sectioning microscopy. Sci Rep. 2017;7:13188.
13. Mittal RK, Zifan A, Kumar D, Ledgerwood-Lee M, Ruppert E, Ghahremani G. Functional morphology of the lower esophageal sphincter and crural diaphragm determined by three-dimensional high-resolution esophago-gastric junction pressure profile and CT imaging. Am J Physiol Gastrointest Liver Physiol. 2017;313:G212–9.
14. Mittal RK, Balaban DH. The esophagogastric junction. N Engl J Med. 1997;336:924–32.
15. Cowgill SM, Bloomston M, Al-Saadi S, Villadolid D, Rosemurgy AS. Normal lower esophageal sphincter pressure and length does not impact outcome after laparoscopic Nissen fundoplication. J Gastrointest Surg. 2007;11:701–7.
16. Richter JE, Wu WC, Johns DN, Blackwell JN, Nelson JL III, Castell JA, Castell DO. Esophageal manometry in 95 healthy adult volunteers. Variability of pressures with age and frequency of "abnormal" contractions. Dig Dis Sci. 1987;32:583–92.
17. Jiang Y, Bhargava V, Lal HA, Mittal RK. Variability in the muscle composition of rat esophagus and neural pathway of lower esophageal sphincter relaxation. Am J Physiol Gastrointest Liver Physiol. 2011;301:G1014–9.
18. Vitaic S, Stupnisek M, Drmic D, Bauk L, Kokot A, Klicek R, Vcev A, Luetic K, Seiwerth S, Sikiric P. Nonsteroidal anti-inflammatory drugs-induced failure of lower esophageal and pyloric sphincter and counteraction of sphincters failure with stable gatric pentadecapeptide BPC 157 in rats. J Physiol Pharmacol. 2017;68:265–72.
19. Richardson BJ, Welch RW. Differential effect of atropine on rightward and leftward lower esophageal sphincter pressure. Gastroenterology. 1981;81:85–9.
20. Schulze K, Dodds WJ, Christensen J, Wood JD. Esophageal manometry in the opossum. Am J Phys. 1977;233:E152–9.
21. Vicente Y, Da RC, Yu J, Hernandez-Peredo G, Martinez L, Perez-Mies B, Tovar JA. Architecture and function of the gastroesophageal barrier in the piglet. Dig Dis Sci. 2001;46:1899–908.
22. Rattan S, Goyal RK. Effect of nicotine on the lower esophageal sphincter. Studies on the mechanism of action. Gastroenterology. 1975;69:154–9.
23. Behar J, Kerstein M, Biancani P. Neural control of the lower esophageal sphincter in the cat: studies on the excitatory pathways to the lower esophageal sphincter. Gastroenterology. 1982;82:680–8.
24. Biancani P, Zabinski M, Kerstein M, Behar J. Lower esophageal sphincter mechanics: anatomic and physiologic relationships of the esophagogastric junction of cat. Gastroenterology. 1982;82:468–75.
25. Goyal RK, Chaudhury A. Physiology of normal esophageal motility. J Clin Gastroenterol. 2008;42:610–9.
26. Rossiter CD, Norman WP, Jain M, Hornby PJ, Benjamin S, Gillis RA. Control of lower esophageal sphincter pressure by two sites in dorsal motor nucleus of the vagus. Am J Phys. 1990;259:G899–906.
27. Miller LS, Vegesna AK, Brasseur JG, Braverman AS, Ruggieri MR. The esophagogastric junction. Ann N Y Acad Sci. 2011;1232:323–30.
28. Opie JC, Chaye H, Fraser GC. Fundoplication and pediatric esophageal manometry: actuarial analysis over 7 years. J Pediatr Surg. 1987;22:935–8.
29. Papasova M. Sphincteric function. In: Handbook of physiology: the gastrointestinal system. Washington, DC: American Physiological Society; 1989. p. 987–1024.
30. Imaeda K, Cunnane TC. Electrophysiological properties of inhibitory junction potential in murine lower oesophageal sphincter. J Smooth Muscle Res. 2003;39:119–33.
31. Tottrup A, Svane D, Forman A. Nitric oxide mediating NANC inhibition in opossum lower esophageal sphincter. Am J Phys. 1991;260:G385–9.
32. Kwiatek MA, Kahrilas PJ. Physiology of the LES. Dis Esophagus. 2012;25:286–91.
33. Muinuddin A, Ji J, Sheu L, Kang Y, Gaisano HY, Diamant NE. L-type Ca(2+) channel expression along feline smooth muscle oesophagus. Neurogastroenterol Motil. 2004;16:325–34.
34. Papasova M, Milousheva E, Bonev A, Boev K, Kortezova N. On the changes in the membrane potential and the contractile activity of the smooth muscle of the lower esophageal and ileo-caecal sphincters upon increased K in the nutrient solution. Acta Physiol Pharmacol Bulg. 1980;6:41–9.
35. Zhang Y, Miller DV, Paterson WG. Opposing roles of K(+) and Cl(−) channels in maintenance of opossum lower esophageal sphincter tone. Am J Physiol Gastrointest Liver Physiol. 2000;279:G1226–34.
36. Asoh R, Goyal RK. Electrical activity of the opossum lower esophageal sphincter in vivo. Its role

in the basal sphincter pressure. Gastroenterology. 1978;74:835–40.
37. Camilleri M. Integrated upper gastrointestinal response to food intake. Gastroenterology. 2006;131:640–58.
38. Indireshkumar K, Brasseur JG, Faas H, Hebbard GS, Kunz P, Dent J, Feinle C, Li M, Boesiger P, Fried M, et al. Relative contributions of "pressure pump" and "peristaltic pump" to gastric emptying. Am J Physiol Gastrointest Liver Physiol. 2000;278:G604–16.
39. Friedenberg FK, Palit A, Parkman HP, Hanlon A, Nelson DB. Botulinum toxin A for the treatment of delayed gastric emptying. Am J Gastroenterol. 2008;103:416–23.
40. Desipio J, Friedenberg FK, Korimilli A, Richter JE, Parkman HP, Fisher RS. High-resolution solid-state manometry of the antropyloroduodenal region. Neurogastroenterol Motil. 2007;19:188–95.
41. Allescher HD, Daniel EE, Dent J, Fox JE, Kostolanska F. Extrinsic and intrinsic neural control of pyloric sphincter pressure in the dog. J Physiol. 1988;401:17–38.
42. Keinke O, Ehrlein HJ. Effect of oleic acid on canine gastroduodenal motility, pyloric diameter and gastric emptying. Q J Exp Physiol. 1983;68:675–86.
43. Keinke O, Schemann M, Ehrlein HJ. Mechanical factors regulating gastric emptying of viscous nutrient meals in dogs. Q J Exp Physiol. 1984;69:781–95.
44. Rao SS, Safadi R, Lu C, Schulze-Delrieu K. Manometric responses of human duodenum during infusion of HCl, hyperosmolar saline, bile and oleic acid. Neurogastroenterol Motil. 1996;8:35–43.
45. Deane AM, Besanko LK, Burgstad CM, Chapman MJ, Horowitz M, Fraser RJ. Modulation of individual components of gastric motor response to duodenal glucose. World J Gastroenterol. 2013;19:5863–9.
46. Vogalis F, Sanders KM. Excitatory and inhibitory neural regulation of canine pyloric smooth muscle. Am J Phys. 1990;259:G125–33.
47. Tomita R, Tanjoh K, Fujisaki S, Fukuzawa M. The role of nitric oxide (NO) in the human pyloric sphincter. Hepato-Gastroenterology. 1999;46:2999–3003.
48. Tomita R, Igarashi S, Fijisaki S, Koshinaga T, Tanjoh K. Regulation of enteric nervous system in the proximal and distal parts of the normal human pyloric sphincter—in vitro study. Hepato-Gastroenterology. 2007;54:1289–92.
49. Allescher HD, Tougas G, Vergara P, Lu S, Daniel EE. Nitric oxide as a putative nonadrenergic noncholinergic inhibitory transmitter in the canine pylorus in vivo. Am J Phys. 1992;262:G695–702.
50. Deloof S, Croix D, Tramu G. The role of vasoactive intestinal polypeptide in the inhibition of antral and pyloric electrical activity in rabbits. J Auton Nerv Syst. 1988;22:167–73.
51. Deloof S. Sympathetic control of antral and pyloric electrical activity in the rabbit. J Auton Nerv Syst. 1988;22:1–10.
52. Allescher HD, Ahmad S, Kostolanska F, Kwan CY, Daniel EE. Modulation of pyloric motor activity via adrenergic receptors. J Pharmacol Exp Ther. 1989;249:652–9.
53. Parkman HP, Pagano AP, Ryan JP. Erythromycin inhibits rabbit pyloric smooth muscle through neuronal motilin receptors. Gastroenterology. 1996;111:682–90.
54. Yuan SY, Costa M, Brookes SJ. Neuronal control of the pyloric sphincter of the guinea-pig. Neurogastroenterol Motil. 2001;13:187–98.
55. Mandrek K, Kreis S. Regional differentiation of gastric and of pyloric smooth muscle in the pig: mechanical responses to acetylcholine, histamine, substance P, noradrenaline and adrenaline. J Auton Pharmacol. 1992;12:37–49.
56. Ishiguchi T, Takahashi T, Itoh H, Owyang C. Nitrergic and purinergic regulation of the rat pylorus. Am J Physiol Gastrointest Liver Physiol. 2000;279:G740–7.
57. Milenov K, Golenhofen K. Differentiated contractile responses of gastric smooth muscle to substance P. Pflugers Arch. 1983;397:29–34.
58. Domae K, Hashitani H, Suzuki H. Regional differences in the frequency of slow waves in smooth muscle of the guinea-pig stomach. J Smooth Muscle Res. 2008;44:231–48.
59. Sanders KM, Vogalis F. Organization of electrical activity in the canine pyloric canal. J Physiol. 1989;416:49–66.
60. Van Helden DF, Imtiaz MS. Ca2+ phase waves: a basis for cellular pacemaking and long-range synchronicity in the guinea-pig gastric pylorus. J Physiol. 2003;548:271–96.
61. Van Helden DF, Imtiaz MS, Nurgaliyeva K, von der WP, Dosen PJ. Role of calcium stores and membrane voltage in the generation of slow wave action potentials in guinea-pig gastric pylorus. J Physiol. 2000;524(Pt 1):245–65.
62. Vogalis F, Publicover NG, Hume JR, Sanders KM. Relationship between calcium current and cytosolic calcium in canine gastric smooth muscle cells. Am J Phys. 1991;260:C1012–8.
63. Cserni T, Paran S, Kanyari Z, O'Donnell AM, Kutasy B, Nemeth N, Puri P. New insights into the neuromuscular anatomy of the ileocecal valve. Anat Rec (Hoboken). 2009;292:254–61.
64. Phillips SF, Quigley EM, Kumar D, Kamath PS. Motility of the ileocolonic junction. Gut. 1988;29:390–406.
65. Cohen S, Harris LD, Levitan R. Manometric characteristics of the human ileocecal junctional zone. Gastroenterology. 1968;54:72–5.
66. Dinning PG, Bampton PA, Kennedy ML, Kajimoto T, Lubowski DZ, de Carle DJ, Cook IJ. Basal pressure patterns and reflexive motor responses in the human ileocolonic junction. Am J Phys. 1999;276:G331–40.
67. Quigley EM, Phillips SF, Dent J, Taylor BM. Myoelectric activity and intraluminal pressure of the canine ileocolonic sphincter. Gastroenterology. 1983;85:1054–62.

68. Quigley EM, Dent J, Phillips SF. Manometry of canine ileocolonic sphincter: comparison of sleeve method to point sensors. Am J Phys. 1987;252:G585–91.
69. Nasmyth DG, Williams NS. Pressure characteristics of the human ileocecal region—a key to its function. Gastroenterology. 1985;89:345–51.
70. Quigley EM, Phillips SF, Dent J. Distinctive patterns of interdigestive motility at the canine ileocolonic junction. Gastroenterology. 1984;87:836–44.
71. Quigley EM, Phillips SF, Cranley B, Taylor BM, Dent J. Tone of canine ileocolonic junction: topography and response to phasic contractions. Am J Phys. 1985;249:G350–7.
72. Pelckmans PA, Van Maercke YM, De Maeyer MH, Herman AG, Verbeuren TJ. Cholinergic and adrenergic contractile properties of the canine ileocolonic junction. J Pharmacol Exp Ther. 1990;254:158–64.
73. Ward SM, McKeen ES, Sanders KM. Role of nitric oxide in non-adrenergic, non-cholinergic inhibitory junction potentials in canine ileocolonic sphincter. Br J Pharmacol. 1992;105:776–82.
74. Rubin MR, Fournet J, Snape WJ Jr, Cohen S. Adrenergic regulation of ileocecal sphincter function in the cat. Gastroenterology. 1980;78:15–21.
75. Rubin MR, Cardwell BA, Ouyang A, Snape WJ Jr, Cohen S. Effect of bethanechol or vagal nerve stimulation on ileocecal sphincter pressure in the cat. Gastroenterology. 1981;80:974–9.
76. Kubota M. Electrical and mechanical properties and neuro-effector transmission in the smooth muscle layer of the guinea-pig ileocecal junction. Pflugers Arch. 1982;394:355–61.
77. Boeckxstaens GE, Pelckmans PA, Bult H, De Man JG, Herman AG, Van Maercke YM. Non-adrenergic non-cholinergic relaxation mediated by nitric oxide in the canine ileocolonic junction. Eur J Pharmacol. 1990;190:246.
78. Boeckxstaens GE, De Man JG, Pelckmans PA, Herman AG, Van Maercke YM. Alpha 2-adrenoceptor-mediated modulation of the nitrergic innervation of the canine isolated ileocolonic junction. Br J Pharmacol. 1993;109:1079–84.
79. McKirdy HC, Marshall RW, Taylor BA. Control of the human ileocaecal junction: an in vitro analysis of adrenergic and non-adrenergic non-cholinergic mechanisms. Digestion. 1993;54:200–6.
80. Leelakusolvong S, Sarr MG, Miller SM, Phillips SF, Bharucha AE. Role of extrinsic innervation in modulating nitrergic transmission in the canine ileocolonic region. Am J Physiol Gastrointest Liver Physiol. 2002;283:G230–9.
81. Ward SM, Xue C, Sanders KM. Localization of nitric oxide synthase in canine ileocolonic and pyloric sphincters. Cell Tissue Res. 1994;275:513–27.
82. Vadokas B, Ludtke FE, Lepsien G, Golenhofen K, Mandrek K. Effects of gastrin-releasing peptide (GRP) on the mechanical activity of the human ileocaecal region in vitro. Neurogastroenterol Motil. 1997;9:265–70.
83. Kubota M, Ito Y, Domae M. Actions of prostaglandins and indomethacin on the electrical and mechanical properties of smooth muscle cells of the guinea-pig ileocecal junction. Pflugers Arch. 1982;394:347–54.
84. Papasova M, Boev K, Bonev A, Milusheva E. Relationship between the changes in the membrane potential and the contraction of the smooth muscles of the lower oesophageal sphincter and the ileocaecal sphincter. Agressologie. 1981;22:205–8.
85. Papasova M, Milousheva E, Bonev A, Gachilova S. Specific features in the electrical and contractile activities of the gastro-intestinal sphincters. Acta Physiol Pharmacol Bulg. 1980;6:19–27.
86. Horiguchi K, Keef KD, Ward SM. Distribution of interstitial cells of Cajal in tunica muscularis of the canine rectoanal region. Am J Physiol Gastrointest Liver Physiol. 2003;284:G756–67.
87. Cobine CA, Hennig GW, Bayguinov YR, Hatton WJ, Ward SM, Keef KD. Interstitial cells of Cajal in the cynomolgus monkey rectoanal region and their relationship to sympathetic and nitrergic nerves. Am J Physiol Gastrointest Liver Physiol. 2010;298:G643–56.
88. Rao SS, Meduri K. What is necessary to diagnose constipation? Best Pract Res Clin Gastroenterol. 2011;25:127–40.
89. Bharucha A. Anorectal disorders. In: Spiller R, Grundy D, editors. Pathophysiology of the enteric nervous system: a basis for understanding functional diseases. Oxford: Wiley Blackwell Publishing; 2004. p. 161–75.
90. Lee YY, Erdogan A, Rao SS. High resolution and high definition anorectal manometry and pressure topography: diagnostic advance or a new kid on the block? Curr Gastroenterol Rep. 2013;15:360.
91. Seong MK, Park UC, Jung SI. Determinant of anal resting pressure gradient in association with continence function. J Neurogastroenterol Motil. 2011;17:300–4.
92. Noelting J, Ratuapli SK, Bharucha AE, Harvey DM, Ravi K, Zinsmeister AR. Normal values for high-resolution anorectal manometry in healthy women: effects of age and significance of rectoanal gradient. Am J Gastroenterol. 2012;107:1530–6.
93. de Lorijn F, de Jonge WJ, Wedel T, Vanderwinden JM, Benninga MA, Boeckxstaens GE. Interstitial cells of Cajal are involved in the afferent limb of the rectoanal inhibitory reflex. Gut. 2005;54:1107–13.
94. De Godoy MA, Rattan S. Angiotensin-converting enzyme and angiotensin II receptor subtype 1 inhibitors restitute hypertensive internal anal sphincter in the spontaneously hypertensive rats. J Pharmacol Exp Ther. 2006;318:725–34.
95. Stebbing JF. Nitric oxide synthase neurones and neuromuscular behaviour of the anorectum. Ann R Coll Surg Engl. 1998;80:137–45.
96. Hedlund H, Fasth S, Hulten L. Efferent sympathetic nervous control of rectal motility in the cat. Acta Physiol Scand. 1984;121:317–24.

97. Garrett JR, Howard ER, Jones W. The internal anal sphincter in the cat: a study of nervous mechanisms affecting tone and reflex activity. J Physiol. 1974;243:153–66.
98. Frenckner B, Ihre T. Influence of autonomic nerves on the internal and sphincter in man. Gut. 1976;17:306–12.
99. Carlstedt A, Nordgren S, Fasth S, Appelgren L, Hulten L. Sympathetic nervous influence on the internal anal sphincter and rectum in man. Int J Colorectal Dis. 1988;3:90–5.
100. Carlstedt A, Fasth S, Hulten L, Nordgren S. The sympathetic innervation of the internal anal sphincter and rectum in the cat. Acta Physiol Scand. 1988;133:423–31.
101. Mizutani M, Neya T, Ono K, Yamasato T, Tokunaga A. Histochemical study of the lumbar colonic nerve supply to the internal anal sphincter and its physiological role in dogs. Brain Res. 1992;598:45–50.
102. Brading AF, Ramalingam T. Mechanisms controlling normal defecation and the potential effects of spinal cord injury. Prog Brain Res. 2006;152:345–58.
103. Rattan S. Sympathetic (adrenergic) innervation modulates but does not generate basal tone in the internal anal sphincter smooth muscle. Gastroenterology. 2008;134:2179–81.
104. O'Kelly TJ. Nerves that say NO: a new perspective on the human rectoanal inhibitory reflex. Ann R Coll Surg Engl. 1996;78:31–8.
105. Hall KA, Ward SM, Cobine CA, Keef KD. Spatial organization and coordination of slow waves in the mouse anorectum. J Physiol. 2014;592:3813–29.
106. McKechnie M, Harvey N, Cobine C, Keef K. Comparison of inhibitory motor innervation in the primate and mouse internal anal sphincter. Gastroenterology. 2008;134(4):A686.
107. O'Kelly T, Brading A, Mortensen N. Nerve mediated relaxation of the human internal anal sphincter: the role of nitric oxide. Gut. 1993;34:689–93.
108. McDonnell B, Hamilton R, Fong M, Ward SM, Keef KD. Functional evidence for purinergic inhibitory neuromuscular transmission in the mouse internal anal sphincter. Am J Physiol Gastrointest Liver Physiol. 2008;294:G1041–51.
109. Cobine CA, Sotherton AG, Peri LE, Sanders KM, Ward SM, Keef KD. Nitrergic neuromuscular transmission in the mouse internal anal sphincter is accomplished by multiple pathways and postjunctional effector cells. Am J Physiol Gastrointest Liver Physiol. 2014;307:G1057–72.
110. Duffy AM, Cobine CA, Keef KD. Changes in neuromuscular transmission in the W/W(v) mouse internal anal sphincter. Neurogastroenterol Motil. 2012;24:e41–55.
111. Opazo A, Lecea B, Gil V, Jimenez M, Clave P, Gallego D. Specific and complementary roles for nitric oxide and ATP in the inhibitory motor pathways to rat internal anal sphincter. Neurogastroenterol Motil. 2011;23:e11–25.
112. Rae MG, Muir TC. Neuronal mediators of inhibitory junction potentials and relaxation in the guinea-pig internal anal sphincter. J Physiol Lond. 1996;493:517–27.
113. Keef KD, Saxton SN, McDowall RA, Kaminski RE, Duffy AM, Cobine CA. Functional role of vasoactive intestinal polypeptide in inhibitory motor innervation in the mouse internal anal sphincter. J Physiol. 2013;591:1489–506.
114. Kubota M, Suita S, Szurszewski JH. Membrane properties and the neuro-effector transmission of smooth muscle cells in the canine internal anal sphincter. J Smooth Muscle Res. 1998;34:173–84.
115. Cobine CA, Fong M, Hamilton R, Keef KD. Species dependent differences in the actions of sympathetic nerves and noradrenaline in the internal anal sphincter. Neurogastroenterol Motil. 2007;19:937–45.
116. Cook TA, Brading AF, Mortensen NJ. Effects of nifedipine on anorectal smooth muscle in vitro. Dis Colon Rectum. 1999;42:782–7.
117. Jonas-Obichere M, Scholefield JH, Acheson A, Mundey M, Tyler H, Wilson VG. Comparison of the effects of nitric oxide donors and calcium channel blockers on the intrinsic myogenic tone of sheep isolated internal anal sphincter. Br J Surg. 2005;92:1263–9.
118. Mutafova-Yambolieva VN, O'Driscoll K, Farrelly A, Ward SM, Keef KD. Spatial localization and properties of pacemaker potentials in the canine rectoanal region. Am J Physiol Gastrointest Liver Physiol. 2003;284:G748–55.
119. Cobine CA, Hannah EE, Zhu MH, Lyle HE, Rock JR, Sanders KM, Ward SM, Keef KD. ANO1 in intramuscular interstitial cells of Cajal plays a key role in the generation of slow waves and tone in the internal anal sphincter. J Physiol. 2017;595:2021–41.
120. Harvey N, McDonnell B, McKechnie M, Keef K. Role of L-type calcium channels, membrane potential and nitric oxide in the control of myogenic activity in the primate internal anal sphincter. Gastroenterology. 2008;134(4):A63.
121. Keef KD, Cobine CA. Control of motility in the internal Anal Sphincter. J. Neurogastroenterol Motil. 2019, March 2 [ePub ahead of print] PMID 30827084.
122. Ward SM, Sanders KM. Upstroke component of electrical slow waves in canine colonic smooth muscle due to nifedipine-resistant calcium current. J Physiol Lond. 1992;455:321–37.
123. Kito Y, Mitsui R, Ward SM, Sanders KM. Characterization of slow waves generated by myenteric interstitial cells of Cajal of the rabbit small intestine. Am J Physiol Gastrointest Liver Physiol. 2015;308:G378–88.
124. Sanders KM, Kito Y, Hwang SJ, Ward SM. Regulation of gastrointestinal smooth muscle function by interstitial cells. Physiology (Bethesda). 2016;31:316–26.

125. Ward SM, Sanders KM. Involvement of intramuscular interstitial cells of Cajal in neuroeffector transmission in the gastrointestinal tract. J Physiol. 2006;576:675–82.
126. Komuro T, Seki K, Horiguchi K. Ultrastructural characterization of the interstitial cells of Cajal. Arch Histol Cytol. 1999;62:295–316.
127. Sanders KM, Koh SD, Ro S, Ward SM. Regulation of gastrointestinal motility—insights from smooth muscle biology. Nat Rev Gastroenterol Hepatol. 2012;9:633–45.
128. Miyamoto-Kikuta S, Ezaki T, Komuro T. Distribution and morphological characteristics of the interstitial cells of Cajal in the ileocaecal junction of the guinea-pig. Cell Tissue Res. 2009;338:29–35.
129. Blair PJ, Bayguinov Y, Sanders KM, Ward SM. Interstitial cells in the primate gastrointestinal tract. Cell Tissue Res. 2012;350:199–213.
130. Smith TK, Reed JB, Sanders KM. Origin and propagation of electrical slow waves in circular muscle of canine proximal colon. Am J Phys. 1987;252:C215–24.
131. Ward SM, Harney SC, Bayguinov JR, McLaren GJ, Sanders KM. Development of electrical rhythmicity in the murine gastrointestinal tract is specifically encoded in the tunica muscularis. J Physiol Lond. 1997;505(Pt 1):241–58.
132. Wang XY, Lammers WJ, Bercik P, Huizinga JD. Lack of pyloric interstitial cells of Cajal explains distinct peristaltic motor patterns in stomach and small intestine. Am J Physiol Gastrointest Liver Physiol. 2005;289:G539–49.
133. Farre R, Wang XY, Vidal E, Domenech A, Pumarola M, Clave P, Huizinga JD, Jimenez M. Interstitial cells of Cajal and neuromuscular transmission in the rat lower oesophageal sphincter. Neurogastroenterol Motil. 2007;19:484–96.
134. Cobine C, Foulkes H, Sanders K, Baker S, Keef K. Visualization of pacemaker activity in intramuscular ICC in the internal anal sphincter. Neurogastroenterol Motil. 2016;28(Suppl 1)): 11–2.
135. Keef K, Ward S, Cobine C. Evidence supporting a pivotal role for intramuscular interstitial cells of Cajal in the generation of pacemaker activity, phasic contractions and tone in the internal anal sphincter. Transl Androl Urol. 2016;5(Suppl 2):S346.
136. Aickin CC, Brading AF. Measurement of intracellular chloride in guinea-pig vas deferens by ion analysis, chloride efflux and micro-electrodes. J Physiol. 1982;326:139–54.
137. Kitamura K, Yamazaki J. Chloride channels and their functional roles in smooth muscle tone in the vasculature. Jpn J Pharmacol. 2001;85:351–7.
138. Leblanc N, Ledoux J, Saleh S, Sanguinetti A, Angermann J, O'Driscoll K, Britton F, Perrino BA, Greenwood IA. Regulation of calcium-activated chloride channels in smooth muscle cells: a complex picture is emerging. Can J Physiol Pharmacol. 2005;83:541–56.
139. Lee MY, Park C, Berent RM, Park PJ, Fuchs R, Syn H, Chin A, Townsend J, Benson CC, Redelman D, et al. Smooth muscle cell genome browser: enabling the identification of novel serum response factor target genes. PLoS One. 2015;10:e0133751.
140. Daniel EE, Taylor GS, Holman ME. The myogenic basis of active tension in the lower esophageal sphincter. Gastroenterology. 1976;70:874.
141. Zhang Y, Paterson WG. Role of sarcoplasmic reticulum in control of membrane potential and nitrergic response in opossum lower esophageal sphincter. Br J Pharmacol. 2003;140:1097–107.
142. Lee MY, Ha SE, Park C, Park PJ, Fuchs R, Wei L, Jorgensen BG, Redelman D, Ward SM, Sanders KM, et al. Transcriptome of interstitial cells of Cajal reveals unique and selective gene signatures. PLoS One. 2017;12:e0176031.
143. Sanders KM, Zhu MH, Britton F, Koh SD, Ward SM. Anoctamins and gastrointestinal smooth muscle excitability. Exp Physiol. 2012;97:200–6.
144. Sanders KM, Ward SM. Kit mutants and gastrointestinal physiology. J Physiol. 2007;578:33–42.
145. Ward SM, Sanders KM. Interstitial cells of Cajal: primary targets of enteric motor innervation. Anat Rec. 2001;262:125–35.
146. Zhang Y, Carmichael SA, Wang XY, Huizinga JD, Paterson WG. Neurotransmission in lower esophageal sphincter of W/Wv mutant mice. Am J Physiol Gastrointest Liver Physiol. 2010;298:G14–24.
147. Cobine CA, Hennig GW, Kurahashi M, Sanders KM, Ward SM, Keef KD. Relationship between interstitial cells of Cajal, fibroblast-like cells and inhibitory motor nerves in the internal anal sphincter. Cell Tissue Res. 2011;344:17–30.
148. Nocka K, Tan JC, Chiu E, Chu TY, Ray P, Traktman P, Besmer P. Molecular bases of dominant negative and loss of function mutations at the murine c-kit/white spotting locus: W37, Wv, W41 and W. EMBO J. 1990;9:1805–13.
149. Iino S, Horiguchi S, Horiguchi K, Nojyo Y. Interstitial cells of Cajal in the gastrointestinal musculature of W mutant mice. Arch Histol Cytol. 2007;70:163–73.
150. Ward SM, Morris G, Reese L, Wang XY, Sanders KM. Interstitial cells of Cajal mediate enteric inhibitory neurotransmission in the lower esophageal and pyloric sphincters. Gastroenterology. 1998;115:314–29.
151. Kluppel M, Huizinga JD, Malysz J, Bernstein A. Developmental origin and Kit-dependent development of the interstitial cells of cajal in the mammalian small intestine. Dev Dyn. 1998;211:60–71.
152. Vanderwinden JM, Rumessen JJ, de Kerchove dA Jr, Gillard K, Panthier JJ, De Laet MH, Schiffmann SN. Kit-negative fibroblast-like cells expressing SK3, a Ca2+-activated K+ channel, in the gut musculature in health and disease. Cell Tissue Res. 2002;310:349–58.
153. Carmona R, Cano E, Mattiotti A, Gaztambide J, Munoz-Chapuli R. Cells derived from the coelomic

epithelium contribute to multiple gastrointestinal tissues in mouse embryos. PLoS One. 2013;8:e55890.
154. Bourret A, Chauvet N, de Santa BP, Faure S. Colonic mesenchyme differentiates into smooth muscle before its colonization by vagal enteric neural crest-derived cells in the chick embryo. Cell Tissue Res. 2017;368:503–11.
155. Kurahashi M, Niwa Y, Cheng J, Ohsaki Y, Fujita A, Goto H, Fujimoto T, Torihashi S. Platelet-derived growth factor signals play critical roles in differentiation of longitudinal smooth muscle cells in mouse embryonic gut. Neurogastroenterol Motil. 2008;20:521–31.
156. Martini F. Muscle tissue. In: Anatomy and physiology. San Francisco, CA: Pearson Education, Inc; 2005. p. 209–40.
157. Caputo C, Edman KA, Lou F, Sun YB. Variation in myoplasmic Ca2+ concentration during contraction and relaxation studied by the indicator fluo-3 in frog muscle fibres. J Physiol. 1994;478(Pt 1): 137–48.
158. Lang RJ. The whole-cell Ca2+ channel current in single smooth muscle cells of the guinea-pig ureter. J Physiol. 1990;423:453–73.
159. Sims SM. Calcium and potassium currents in canine gastric smooth muscle cells. Am J Phys. 1992;262:G859–67.
160. Fleischmann BK, Murray RK, Kotlikoff MI. Voltage window for sustained elevation of cytosolic calcium in smooth muscle cells. Proc Natl Acad Sci U S A. 1994;91:11914–8.
161. Langton PD, Standen NB. Calcium currents elicited by voltage steps and steady voltages in myocytes isolated from the rat basilar artery. J Physiol. 1993;469:535–48.
162. Imaizumi Y, Muraki K, Takeda M, Watanabe M. Measurement and simulation of noninactivating Ca current in smooth muscle cells. Am J Phys. 1989;256:C880–5.
163. Bayguinov O, Sanders KM. Role of nitric oxide as an inhibitory neurotransmitter in the canine pyloric sphincter. Am J Phys. 1993;264:G975–83.
164. Farre R, Auli M, Lecea B, Martinez E, Clave P. Pharmacologic characterization of intrinsic mechanisms controlling tone and relaxation of porcine lower esophageal sphincter. J Pharmacol Exp Ther. 2006;316:1238–48.
165. Middleton SJ, Cuthbert AW, Shorthouse M, Hunter JO. Nitric oxide affects mammalian distal colonic smooth muscle by tonic neural inhibition. Br J Pharmacol. 1993;108:974–9.
166. Mule F, D'Angelo S, Amato A, Contino I, Serio R. Modulation by nitric oxide of spontaneous mechanical activity in rat proximal colon. J Auton Pharmacol. 1999;19:1–6.
167. Fox-Threlkeld JE, Woskowska Z, Daniel EE. Sites of nitric oxide (NO) actions in control of circular muscle motility of the perfused isolated canine ileum. Can J Physiol Pharmacol. 1997;75: 1340–9.
168. Yamato S, Spechler SJ, Goyal RK. Role of nitric oxide in esophageal peristalsis in the opossum. Gastroenterology. 1992;103:197–204.
169. Groneberg D, Zizer E, Lies B, Seidler B, Saur D, Wagner M, Friebe A. Dominant role of interstitial cells of Cajal in nitrergic relaxation of murine lower oesophageal sphincter. J Physiol. 2015;593:403–14.
170. Bauer AJ, Sanders KM. Gradient in excitation-contraction coupling in canine gastric antral circular muscle. J Physiol Lond. 1985;369:283–94.
171. Kamm KE, Stull JT. Regulation of smooth muscle contractile elements by second messengers. Annu Rev Physiol. 1989;51:299–313.
172. Nagai R, Kuro-o M, Babij P, Periasamy M. Identification of two types of smooth muscle myosin heavy chain isoforms by cDNA cloning and immunoblot analysis. J Biol Chem. 1989;264:9734–7.
173. Kelley CA, Takahashi M, Yu JH, Adelstein RS. An insert of seven amino acids confers functional differences between smooth muscle myosins from the intestines and vasculature. J Biol Chem. 1993;268:12848–54.
174. White S, Martin AF, Periasamy M. Identification of a novel smooth muscle myosin heavy chain cDNA: isoform diversity in the S1 head region. Am J Phys. 1993;264:C1252–8.
175. Somlyo AP, Somlyo AV. Signal transduction by G-proteins, rho-kinase and protein phosphatase to smooth muscle and non-muscle myosin II. J Physiol (Lond). 2000;522(Pt 2):177–85.
176. Somlyo AP, Somlyo AV. Signal transduction through the RhoA/Rho-kinase pathway in smooth muscle. J Muscle Res Cell Motil. 2004;25:613–5.
177. Matsumura F, Hartshorne DJ. Myosin phosphatase target subunit: many roles in cell function. Biochem Biophys Res Commun. 2008;369:149–56.
178. Hartshorne DJ, Ito M, Erdodi F. Role of protein phosphatase type 1 in contractile functions: myosin phosphatase. J Biol Chem. 2004;279:37211–4.
179. Grassie ME, Moffat LD, Walsh MP, MacDonald JA. The myosin phosphatase targeting protein (MYPT) family: a regulated mechanism for achieving substrate specificity of the catalytic subunit of protein phosphatase type 1delta. Arch Biochem Biophys. 2011;510:147–59.
180. Velasco G, Armstrong C, Morrice N, Frame S, Cohen P. Phosphorylation of the regulatory subunit of smooth muscle protein phosphatase 1M at Thr850 induces its dissociation from myosin. FEBS Lett. 2002;527:101–4.
181. Gao N, Chang AN, He W, Chen CP, Qiao YN, Zhu M, Kamm KE, Stull JT. Physiological signalling to myosin phosphatase targeting subunit-1 phosphorylation in ileal smooth muscle. J Physiol. 2016;594:3209–25.
182. Somlyo AP, Somlyo AV. Ca2+ sensitivity of smooth muscle and nonmuscle myosin II: modulated by G proteins, kinases, and myosin phosphatase. Physiol Rev. 2003;83:1325–58.

183. Dimopoulos GJ, Semba S, Kitazawa K, Eto M, Kitazawa T. Ca2+-dependent rapid Ca2+ sensitization of contraction in arterial smooth muscle. Circ Res. 2007;100:121–9.
184. Kitazawa T. G protein-mediated Ca(2)+-sensitization of CPI-17 phosphorylation in arterial smooth muscle. Biochem Biophys Res Commun. 2010;401:75–8.
185. Khasnis M, Nakatomi A, Gumpper K, Eto M. Reconstituted human myosin light chain phosphatase reveals distinct roles of two inhibitory phosphorylation sites of the regulatory subunit, MYPT1. Biochemistry. 2014;53:2701–9.
186. Wang T, Kendig DM, Smolock EM, Moreland RS. Carbachol-induced rabbit bladder smooth muscle contraction: roles of protein kinase C and Rho kinase. Am J Physiol Renal Physiol. 2009;297:F1534–42.
187. Mori D, Hori M, Murata T, Ohama T, Kishi H, Kobayashi S, Ozaki H. Synchronous phosphorylation of CPI-17 and MYPT1 is essential for inducing Ca(2+) sensitization in intestinal smooth muscle. Neurogastroenterol Motil. 2011;23:1111–22.
188. Tsai MH, Chang AN, Huang J, He W, Sweeney HL, Zhu M, Kamm KE, Stull JT. Constitutive phosphorylation of myosin phosphatase targeting subunit-1 in smooth muscle. J Physiol. 2014;592:3031–51.
189. Woodsome TP, Polzin A, Kitazawa K, Eto M, Kitazawa T. Agonist- and depolarization-induced signals for myosin light chain phosphorylation and force generation of cultured vascular smooth muscle cells. J Cell Sci. 2006;119:1769–80.
190. Bhetwal BP, An CL, Fisher SA, Perrino BA. Regulation of basal LC20 phosphorylation by MYPT1 and CPI-17 in murine gastric antrum, gastric fundus, and proximal colon smooth muscles. Neurogastroenterol Motil. 2011;23:e425–36.
191. Perrino BA. Calcium sensitization mechanisms in gastrointestinal smooth muscles. J Neurogastroenterol Motil. 2016;22:213–25.
192. He WQ, Qiao YN, Peng YJ, Zha JM, Zhang CH, Chen C, Chen CP, Wang P, Yang X, Li CJ, et al. Altered contractile phenotypes of intestinal smooth muscle in mice deficient in myosin phosphatase target subunit 1. Gastroenterology. 2013;144:1456–65–1465.e1–5.
193. Zhang CH, Wang P, Liu DH, Chen CP, Zhao W, Chen X, Chen C, He WQ, Qiao YN, Tao T, et al. The molecular basis of the genesis of basal tone in internal anal sphincter. Nat Commun. 2016;7:11358.
194. Scotto-Lavino E, Garcia-Diaz M, Du G, Frohman MA. Basis for the isoform-specific interaction of myosin phosphatase subunits protein phosphatase 1c beta and myosin phosphatase targeting subunit 1. J Biol Chem. 2010;285:6419–24.
195. Gao N, Tsai MH, Chang AN, He W, Chen CP, Zhu M, Kamm KE, Stull JT. Physiological vs. pharmacological signalling to myosin phosphorylation in airway smooth muscle. J Physiol. 2017;595:6231–47.
196. Patel CA, Rattan S. Cellular regulation of basal tone in internal anal sphincter smooth muscle by RhoA/ROCK. Am J Physiol Gastrointest Liver Physiol. 2007;292:G1747–56.
197. Patel CA, Rattan S. Spontaneously tonic smooth muscle has characteristically higher levels of RhoA/ROK compared with the phasic smooth muscle. Am J Physiol Gastrointest Liver Physiol. 2006;291:G830–7.
198. Rattan S, Patel CA. Selectivity of ROCK inhibitors in the spontaneously tonic smooth muscle. Am J Physiol Gastrointest Liver Physiol. 2008;294:G687–93.
199. Rattan S, Singh J. RhoA/ROCK pathway is the major molecular determinant of basal tone in intact human internal anal sphincter. Am J Physiol Gastrointest Liver Physiol. 2012;302:G664–75.
200. Cobine C, Bhetwal B, Stever J, Keef K, Perrino B. Comparison of proteins involved in the regulation of myosin light chain (MLC(20)) phosphorylation in the monkey IAS and rectum. Neurogastroenterol Motil. 2013;25(Suppl 1)):43.
201. Eto M. Regulation of cellular protein phosphatase-1 (PP1) by phosphorylation of the CPI-17 family, C-kinase-activated PP1 inhibitors. J Biol Chem. 2009;284:35273–7.
202. Hirano K. Current topics in the regulatory mechanism underlying the Ca2+ sensitization of the contractile apparatus in vascular smooth muscle. J Pharmacol Sci. 2007;104:109–15.
203. Woodsome TP, Eto M, Everett A, Brautigan DL, Kitazawa T. Expression of CPI-17 and myosin phosphatase correlates with Ca(2+) sensitivity of protein kinase C-induced contraction in rabbit smooth muscle. J Physiol. 2001;535:553–64.
204. Bhetwal BP, Sanders KM, An C, Trappanese DM, Moreland RS, Perrino BA. Ca2+ sensitization pathways accessed by cholinergic neurotransmission in the murine gastric fundus. J Physiol. 2013;591:2971–86.
205. Bhetwal BP, An C, Baker SA, Lyon KL, Perrino BA. Impaired contractile responses and altered expression and phosphorylation of Ca(2+) sensitization proteins in gastric antrum smooth muscles from ob/ob mice. J Muscle Res Cell Motil. 2013;34:137–49.
206. Huang J, Zhou H, Mahavadi S, Sriwai W, Lyall V, Murthy KS. Signaling pathways mediating gastrointestinal smooth muscle contraction and MLC20 phosphorylation by motilin receptors. Am J Physiol Gastrointest Liver Physiol. 2005;288:G23–31.
207. Ihara E, Moffat L, Ostrander J, Walsh MP, MacDonald JA. Characterization of protein kinase pathways responsible for Ca2+ sensitization in rat ileal longitudinal smooth muscle. Am J Physiol Gastrointest Liver Physiol. 2007;293:G699–710.
208. Hersch E, Huang J, Grider JR, Murthy KS. Gq/G13 signaling by ET-1 in smooth muscle: MYPT1 phosphorylation via ETA and CPI-17 dephosphorylation via ETB. Am J Physiol Cell Physiol. 2004;287:C1209–18.

209. Ohama T, Hori M, Sato K, Ozaki H, Karaki H. Chronic treatment with interleukin-1beta attenuates contractions by decreasing the activities of CPI-17 and MYPT-1 in intestinal smooth muscle. J Biol Chem. 2003;278:48794–804.
210. Ohama T, Hori M, Fujisawa M, Kiyosue M, Hashimoto M, Ikenoue Y, Jinno Y, Miwa H, Matsumoto T, Murata T, et al. Downregulation of CPI-17 contributes to dysfunctional motility in chronic intestinal inflammation model mice and ulcerative colitis patients. J Gastroenterol. 2008;43:858–65.
211. Shimomura A, Ohama T, Hori M, Ozaki H. 17Beta-estradiol induces gastrointestinal motility disorder by decreasing CPI-17 phosphorylation via changes in rho-family G-protein Rnd expression in small intestine. J Vet Med Sci. 2009;71:1591–7.
212. Harnett KM, Cao W, Biancani P. Signal-transduction pathways that regulate smooth muscle function I. Signal transduction in phasic (esophageal) and tonic (gastroesophageal sphincter) smooth muscles. Am J Physiol Gastrointest Liver Physiol. 2005;288:G407–16.
213. Sims SM, Chrones T, Preiksaitis HG. Calcium sensitization in human esophageal muscle: role for RhoA kinase in maintenance of lower esophageal sphincter tone. J Pharmacol Exp Ther. 2008;327:178–86.
214. Himpens B, Matthijs G, Somlyo AP. Desensitization to cytoplasmic Ca2+ and Ca2+ sensitivities of guinea-pig ileum and rabbit pulmonary artery smooth muscle. J Physiol. 1989;413:489–503.
215. Kitazawa T, Somlyo AP. Desensitization and muscarinic re-sensitization of force and myosin light chain phosphorylation to cytoplasmic Ca2+ in smooth muscle. Biochem Biophys Res Commun. 1990;172:1291–7.
216. Lee MR, Li L, Kitazawa T. Cyclic GMP causes Ca2+ desensitization in vascular smooth muscle by activating the myosin light chain phosphatase. J Biol Chem. 1997;272:5063–8.
217. Sausbier M, Schubert R, Voigt V, Hirneiss C, Pfeifer A, Korth M, Kleppisch T, Ruth P, Hofmann F. Mechanisms of NO/cGMP-dependent vasorelaxation. Circ Res. 2000;87:825–30.
218. Etter EF, Eto M, Wardle RL, Brautigan DL, Murphy RA. Activation of myosin light chain phosphatase in intact arterial smooth muscle during nitric oxide-induced relaxation. J Biol Chem. 2001;276:34681–5.
219. Bonnevier J, Arner A. Actions downstream of cyclic GMP/protein kinase G can reverse protein kinase C-mediated phosphorylation of CPI-17 and Ca(2+) sensitization in smooth muscle. J Biol Chem. 2004;279:28998–9003.
220. Wooldridge AA, MacDonald JA, Erdodi F, Ma C, Borman MA, Hartshorne DJ, Haystead TA. Smooth muscle phosphatase is regulated in vivo by exclusion of phosphorylation of threonine 696 of MYPT1 by phosphorylation of Serine 695 in response to cyclic nucleotides. J Biol Chem. 2004;279:34496–504.
221. Nakamura K, Koga Y, Sakai H, Homma K, Ikebe M. cGMP-dependent relaxation of smooth muscle is coupled with the change in the phosphorylation of myosin phosphatase. Circ Res. 2007;101:712–22.
222. Neppl RL, Lubomirov LT, Momotani K, Pfitzer G, Eto M, Somlyo AV. Thromboxane A2-induced bidirectional regulation of cerebral arterial tone. J Biol Chem. 2009;284:6348–60.
223. Shirinsky VP, Vorotnikov AV, Birukov KG, Nanaev AK, Collinge M, Lukas TJ, Sellers JR, Watterson DM. A kinase-related protein stabilizes unphosphorylated smooth muscle myosin minifilaments in the presence of ATP. J Biol Chem. 1993;268:16578–83.
224. Khromov AS, Wang H, Choudhury N, McDuffie M, Herring BP, Nakamoto R, Owens GK, Somlyo AP, Somlyo AV. Smooth muscle of telokin-deficient mice exhibits increased sensitivity to Ca2+ and decreased cGMP-induced relaxation. Proc Natl Acad Sci U S A. 2006;103:2440–5.
225. Rattan S. Ca2+/calmodulin/MLCK pathway initiates, and RhoA/ROCK maintains, the internal anal sphincter smooth muscle tone. Am J Physiol Gastrointest Liver Physiol. 2017;312:G63–6.
226. Bashashati M, Moraveji S, Torabi A, Sarosiek I, Davis BR, Diaz J, McCallum RW. Pathological findings of the antral and pyloric smooth muscle in patients with gastroparesis-like syndrome compared to gastroparesis: similarities and differences. Dig Dis Sci. 2017;62:2828–33.
227. Chander RB, Mullin GE, Passi M, Zheng X, Salem A, Yolken R, Pasricha PJ. A prospective evaluation of ileocecal valve dysfunction and intestinal motility derangements in small intestinal bacterial overgrowth. Dig Dis Sci. 2017;62:3525–35.
228. Bharucha AE. Pelvic floor: anatomy and function. Neurogastroenterol Motil. 2006;18:507–19.
229. Doodnath R, Puri P. Internal anal sphincter achalasia. Semin Pediatr Surg. 2009;18:246–8.
230. Shafik A, Ahmed I, El SO, Shafik AA. Interstitial cells of Cajal in reflux esophagitis: role in the pathogenesis of the disease. Med Sci Monit. 2005;11:BR452–6.
231. Vanderwinden JM, Liu H, De Laet MH, Vanderhaeghen JJ. Study of the interstitial cells of Cajal in infantile hypertrophic pyloric stenosis (published erratum appears in Gastroenterology 1996 Nov;111(5):1403). Gastroenterology. 1996;111:279–88.

Part II

Urinary Tract

3 Pacemaker Mechanisms Driving Pyeloureteric Peristalsis: Modulatory Role of Interstitial Cells

Richard J. Lang and Hikaru Hashitani

Abstract

The peristaltic pressure waves in the renal pelvis that propel urine expressed by the kidney into the ureter towards the bladder have long been considered to be 'myogenic', being little affected by blockers of nerve conduction or autonomic neurotransmission, but sustained by the intrinsic release of prostaglandins and sensory neurotransmitters. In uni-papilla mammals, the funnel-shaped renal pelvis consists of a lumen-forming urothelium and a stromal layer enveloped by a plexus of 'typical' smooth muscle cells (TSMCs), in multi-papillae kidneys a number of minor and major calyces fuse into a large renal pelvis. Electron microscopic, electrophysiological and Ca^{2+} imaging studies have established that the pacemaker cells driving pyeloureteric peristalsis are likely to be morphologically distinct 'atypical' smooth muscle cells (ASMCs) that fire Ca^{2+} transients and spontaneous transient depolarizations (STDs) which trigger propagating nifedipine-sensitive action potentials and Ca^{2+} waves in the TSMC layer. In unicalyceal kidneys, ASMCs predominately locate on the serosal surface of the proximal renal pelvis while in multi-papillae kidneys they locate within the sub-urothelial space. 'Fibroblast-like' interstitial cells (ICs) located in the sub-urothelial space or adventitia are a mixed population of cells, having regional and species-dependent expression of various Cl^-, K^+, Ca^{2+} and cationic channels. ICs display asynchronous Ca^{2+} transients that periodically synchronize into bursts that accelerate ASMC Ca^{2+} transient firing. This review presents current knowledge of the architecture of the proximal renal pelvis, the role Ca^{2+} plays in renal pelvis peristalsis and the mechanisms by which ICs may sustain/accelerate ASMC pacemaking.

Keywords

Pyeloureteric peristalsis · Atypical smooth muscle cells · Interstitial cells · Calcium imaging · Calcium channels · Pacemaking Upper urinary tract

Electronic Supplementary Material The online version of this chapter (https://doi.org/10.1007/978-981-13-5895-1_3) contains supplementary material, which is available to authorized users.

R. J. Lang (✉)
School of Biomedical Sciences, Faculty of Medicine, Nursing and Health Sciences, Monash University, Clayton, VIC, Australia
e-mail: rick.lang@monash.edu

H. Hashitani
Department of Cell Physiology, Graduate School of Medical Sciences, Nagoya City University, Nagoya, Japan
e-mail: hasitani@med.nagoya-cu.ac.jp

H. Hashitani, R. J. Lang (eds.), *Smooth Muscle Spontaneous Activity*, Advances in Experimental Medicine and Biology 1124, https://doi.org/10.1007/978-981-13-5895-1_3

3.1 Introduction

Kidneys are thought to have first evolved in freshwater bony fish. To maintain their body fluids at osmotic concentrations greater than their surrounds, freshwater fish, amphibians and reptiles actively transport salt into their blood via their gills or skin, while their kidneys produce a dilute urine. In contrast, marine fish and reptiles swallow seawater, actively eliminate salt across their gills or via facial salt glands and excrete an isotonic urine by reabsorbing salt and water in their kidneys. Only birds and mammals can excrete waste products in a hypertonic urine. Birds concentrate their urine twice their blood concentration, while human kidneys can concentrate urine about four times greater than blood plasma. The kidneys of desert mammals can excrete urine 10–20-fold more concentrated than their blood plasma. The kidneys of the kangaroo rat are so efficient, it obtains all the its water needs from its food and respiration [1].

The mammalian kidney is a complex organ consisting of up to a million filtrating units called nephrons. Blood pressure forces blood through the glomerulus capillary bed at the top of each nephron. The glomerulus retains the red blood cells, proteins and other large molecules, but allows water, small molecules and waste products to pass into the surrounding Bowman's capsule which empties into the proximal tubule of the nephron. Sugars, amino acids, and ions are recovered by active transport in the proximal tubule, while water and salts are reabsorbed in the lower Loops of Henle which extend deep into the renal medulla. The remaining fluid and metabolic wastes are secreted as urine.

3.2 Ultrastructure of the Upper Urinary Tract

In small mammals, urine produced by the nephron units within a single 'pyramid-shaped' inner-medulla/papilla complex is secreted into a funnel-shaped renal pelvis which has a number of radiating 'finger-like' spokes for attachment to the kidney parenchyma (Fig. 3.1a). Between these spokes the outer margin of the pelvis forms a concave-shaped edge creating secondary pouches between the pelvis and the kidney parenchyma. In sections of kidney, this region between spokes appears as a thick 'bulb' ending of the pelvis wall, while the spokes appear as long gradually thinning tapers [2, 3]. To cope with the filtering of relatively large volumes of blood, some larger mammals have evolved compound (humans, sheep and pigs) or discrete (whales and seals) multi-papillae kidneys, so that urine is expressed by a number of papillae into minor calyces similar in appearance to a single-papilla renal pelvis. These minor calyces fuse into several major calyxes which fuse into a single renal pelvis that extends to the ureter.

In single-papilla kidneys, the renal pelvic wall consists of a lumen-forming squamous urothelium, basal epithelial cells (BECs) and a thin layer of stromal cells enveloped by a plexus of 'typical' smooth muscle cell (TSMC) bundles. The BECs facing the proximal inner medulla are squamous or low cuboidal in shape, contain a large round nucleus, numerous dense bodies, mitochondria and free ribosomes and long interconnecting projections to form a continuous layer of cells [3, 4] (Fig. 3.1c, Supplementary Video 3.1). BECs occupy the same morphological space as cells that are intensely immunoreactive to antibodies raised against the $K_V7.5$ (KCNQ5) channel subunit [3, 5]. TMSCs, intensely immunoreactive to antibodies raised against α-smooth muscle actin (α-SMA), also form a continuous layer of circumferentially orientated bundles of densely packed cells adjacent to the urothelium originating near the base of the papilla and extending into the ureter [6–8]. $K_V7.5^+$ BECs and TSMCs both increase in number and density with distance from the base of the papilla so in regions distal of the fornix the renal pelvis consists of a thick tightly packed transitional epithelial layer enveloped by a thick TSMC coat.

An additional layer of lightly α-SMA^+ obliquely oriented 'atypical' smooth muscle cells (ASMCs) locates on the *serosal* surface of the renal pelvis wall of single-papilla kidneys. These ASMCs are not arranged in bundles, but form a

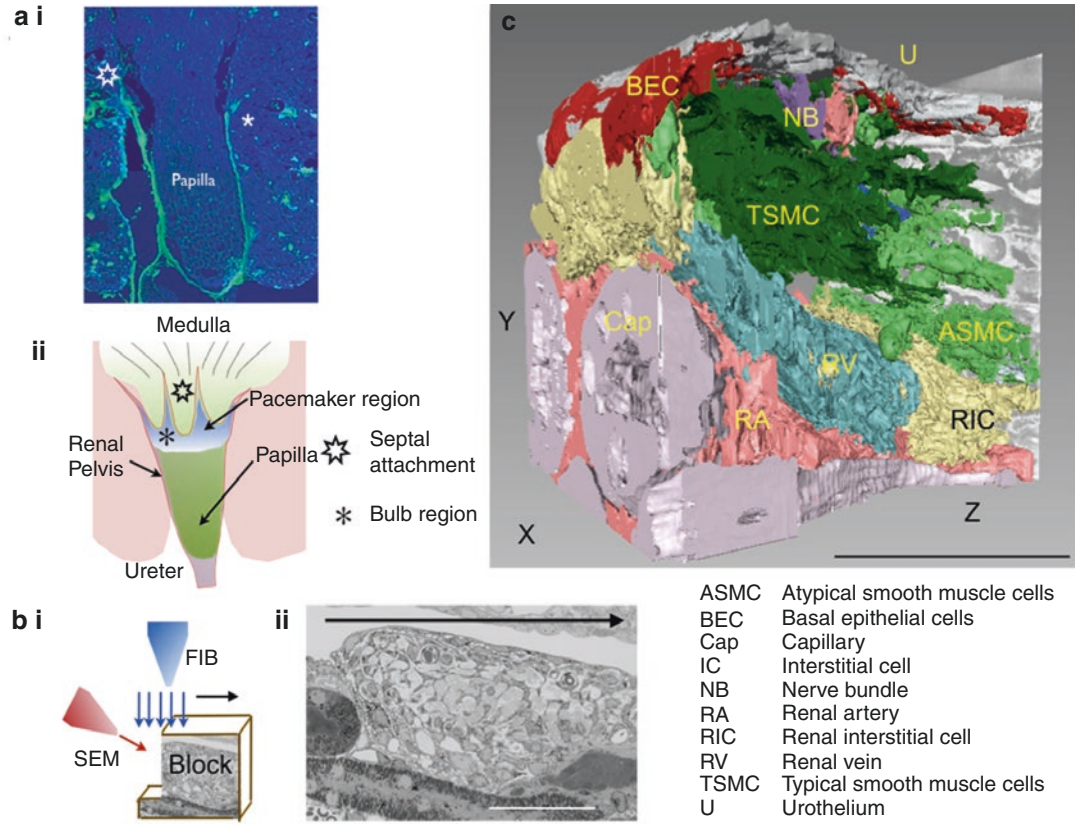

Fig. 3.1 The architecture of the 'bulb' region of mouse proximal renal pelvis examined using FIBSEM tomography. (**ai**) Single caudal section the mouse renal pelvis illustrating that the funnel-shaped muscle wall (**ai** *green*, **aii**) either forms 'spoke-like' attachments (*star*) to the kidney parenchyma or ends abruptly as a 'bulb' (*). (**bi**) Schematic of the focused ion beam scanning electron microscope (FIBSEM) in which the X–Y surface of a block of the bulb region of the renal pelvis is repeatedly milled in the Z direction (**bii** *arrow*) using the FIB, each new X–Y surface is then imaged using the SEM. (**c**) Similar-looking cells and structures within the block of 900 ortho-slice micrographs were identified, volume rendered and colour coded for easy identification. Calibration bars: 50 µm (**bii**), $0.5e^5$ nm (**c**). Figure from Hashitani et al. [3]

thin sheet of loosely arranged groups of cells separated by a network of collagen connective tissue. In multi-papillae kidneys, ASMCs form a thin *inner* layer between the urothelial and TSMC layers of each minor calyx [9, 10]. These ASMCs extend over the renal parenchyma and fuse with the TSMC layer to form a continuous layer between minor calyces. In both single-papilla and multi-papillae kidneys, the ASMC layer does not extend past the pelviureteric junction into the ureter [6, 8–11].

When viewed with a standard electron microscope, TSMCs in single slices display a round darkly stained cytoplasm due to the abundance of numerous longitudinally arranged myofilaments and a large oval-shaped nucleus. In contrast, ASMCs are lightly stained due to their sparsely distributed myofilaments separated by large areas of clear cytoplasm containing small mitochondria, granular endoplasmic reticulum and Golgi cisternae [2, 6, 8, 10]. In single light or electron micrographs, ASMCs appear to have a rounded nuclear region with a number of radiating thin projections and have previously been interpreted as being 'stellate' or 'spindle shaped' (Fig. 3.2ai) [6, 8, 12, 13]. The repeated milling of a block of mouse renal pelvis and imaging of each new surface using focused ion beam scanning electron

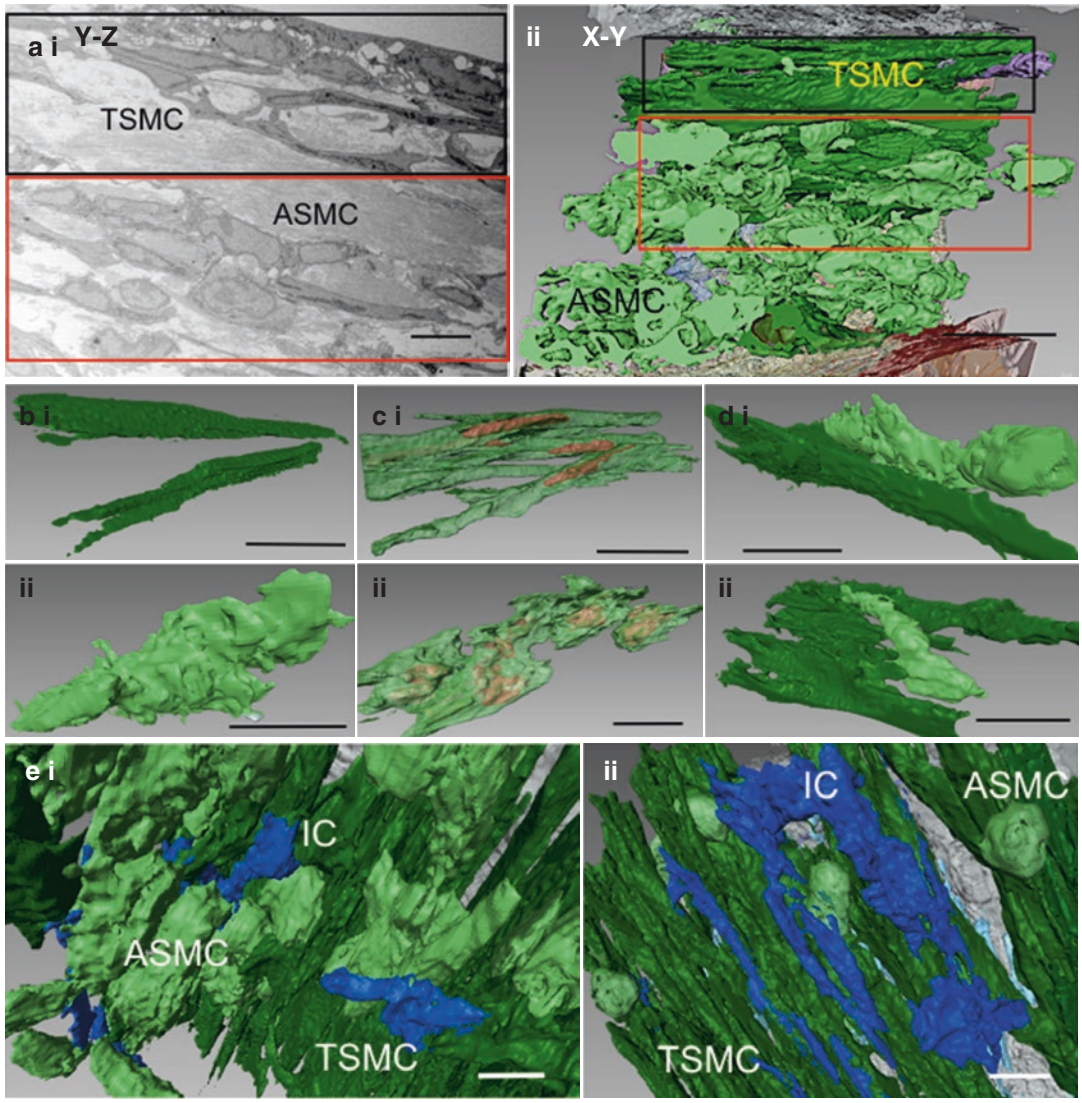

Fig. 3.2 Single cell reconstructions and close appositions of ASMCs, TSMCs and ICs in the mouse renal pelvis. (**ai**) Example of a single X–Y electron micrograph within a stack of ortho-slices illustrating the morphological difference between ASMCs (**ai** *red square*) and TSMCs (**ai** *black square*). (**aii**) Volume rendering all of the cells within the same region reveals the structure and regions occupied by TSMCs (*dark green*) and ASMCs (*light green*) present. Typical examples of single or groups of TSMCs (**bi**, **ci**) and ASMCs (**bii**, **cii**) and their close apposition with like cells, projected as being solid (**bi**, **ii**) or relatively transparent (**ci**, **ii**) to reveal their volume-rendered nuclei. (**di**, **ii**) Examples of close appositions of TSMCs and ASMCs in the proximal renal pelvis. (**e**) Micrographs of volume-rendered TSMCs, ASMCs and serosal ICs (*dark blue cells*), in the bulb (**ei**) and mid region (**eii**) of the renal pelvis to illustrate their architecture and close appositions. Calibration bars: 0.5 μm (**a**), $0.3e^4$ nm (**bi**), $2e^5$ nm (**bii**), $1e^4$ nm (**ci**, **ii**, **di**), $0.2e^4$ nm (**dii**), $2e^{13}$ nm (**e**). Figure adapted from Hashitani et al. [3]

microscope (FIB SEM) tomography (Fig. 3.1) have established that volume-rendered TSMCs are long cigar-shaped 'spindles' (Fig. 3.2bi). In addition, the thin ASMC projections are in fact continuous, resembling the rim of an irregular saucer or a leaf [3] (Fig. 3.2bii) and forming close appositions with neighbouring ASMCs and TSMCs (Fig. 3.2c, d) [3, 6, 8–10, 12, 13]. In the

spoke attachments, ASMCs are loosely arranged in a basket weave arrangement while in the bulb region they are mostly orientated in the longitudinal direction [3] (Supplementary Video 3.1). In contrast, TSMC are mostly absent as the spoke attachments approach the parenchymal tissue [2, 3, 5, 8, 13].

As ASMCs are sparsely endowed with contractile filaments and the relative number of ASMCs, compared to TSMCs, decreases with distance from the inner medulla to the ureteropelvic junction in both single- and multi-papillae kidneys [8, 10], Dixon and Gosling proposed that ASMCs might have a function different from contractile TSMCs, that they may be the pacemaker cells driving the movement of urine towards the bladder [6, 9, 10, 12].

3.3 Pyeloureteric Peristalsis

The upper urinary system has evolved to transport urine from the kidney to the bladder as the absence of an active drainage would lead to the development of back pressure-induced damage and fibrosis within the inner medulla and kidney parenchyma. This movement of urine occurs by the means of spontaneous propagating peristaltic contractions (pyeloureteric peristalsis). From the earliest investigations into pyeloureteric peristalsis [14], it has been recognized that the upper urinary tract exists as a syncytium and that the excitation originates in the proximal renal pelvis and travels distally towards the bladder [15–20]. As the papilla and inner medulla are not contractile, the hydrostatic pressure changes that occur during these peristaltic contractions may also have a 'milking' action to promote the secretion of urine [7, 21]. The myogenic nature of pyeloureteric peristalsis is also demonstrated by the presence of spontaneous contractions in vivo after denervation, or ex vivo after nerve conduction blockade [15, 22–24].

Propagating contractions and associated pressure waves in the renal pelvis and ureter are preceded by an electrical impulse [16, 17, 25–28] that is initiated at the pelvi-papilla border [19, 20, 29]. Early extracellular recordings from the porcine multi-papillae kidney suggested that minor calyces can discharge synchronously or asynchronously [30] and that the calyx firing at the highest frequency drives the pelvic contractions. The excitation frequencies of the major calyces, renal pelvis and ureter are multiples of the discharge frequency within the dominate minor calyx [31–33], thus creating a decreasing frequency gradient down the upper urinary system [27, 34–36]. Recordings in the multi-papillae sheep kidney [37] using multiple-mapping electrodes have demonstrated that excitation originates in only one minor calyx to drive the wave of excitation into the renal pelvis and that this site of initiation moves spontaneously between calyces. If two sites of excitation discharge near simultaneously, one site predominates, sometimes alternatively, blocking the conduction of the wave of excitation from the other site. Complete or partial conduction block of the waves of excitation within the renal pelvis can also occur anywhere, anytime [37].

Rodent uni-papilla kidneys display a similar single origin of the wave of excitation in the most proximal regions of the pelvi-papilla border [38, 39] that will dominate lesser sites of excitation and which can spontaneously shift along the border. Spontaneous contractions can also randomly originate in the mid and distal renal pelvis [22, 40]. In the rat renal pelvis, the peristaltic wave travels from the pelvi-papilla border to the mid renal pelvis and often triggers a number of additional high frequency contractions that can travel in both antegrade and retrograde directions [2, 23, 41]. When the pacemaker drive from the proximal region of uni-papilla or multi-papillae kidneys is prevented upon transection [22, 42, 43] or upon pharmacological blockade of hyperpolarization-activated cation nucleotide gated (HCN) channels [38, 39], the more distal regions readily trigger waves of excitation.

Circumferentially oriented strips cut from the uni-papilla renal pelvis [44–46] or from the minor and major calyces and renal pelvis of multi-papillae kidney [47] contract spontaneously in vitro at the same frequency when they are obtained from the same distance from the inner medulla pelvis border. However, their

contraction frequency decreases as they are cut from regions increasingly more distal of the inner medulla/papilla complex(es) [18, 36, 45–48]. Stretch of strips of renal pelvis and ureter increases contractile force to an optimal maximum muscle length, beyond which muscle force decreases [22, 49]. This stretch-induced increase in muscle tone in human and sheep renal pelvic strips is associated with an increase in contraction frequency [50], but not in strips from the rabbit [51] or guinea pig [15, 22] renal pelvis. However, urine volume or wall stretch appears to increase the likelihood of a one-to-one propagation of excitation from the renal pelvis into the ureter [32, 52].

The *decreasing* frequency of the spontaneous contractions in strips from uni-papilla renal pelvis and the minor and major calyces and renal pelvis of multi-papillae kidneys contraction with distance from the inner medulla/papilla complex(es) [6, 8–10, 12] has been suggested to arise from the *decreasing* number of 'pacemaker' ASMCs [6, 44] and with the *increasing* number of TSMCs expressing 'refractory' K^+ membrane conductances [8, 53]. Alternatively, these data have led to the concept of *'latent' pacemakers* [20], which some suggest arise from the pacemaker activity of intrinsic interstitial cells (ICs).

3.4 Sub-urothelial and Serosal ICs

Light and electron microscopy has established that 'fibroblast-like' ICs in the rodent renal pelvis are sparsely distributed in both the adventitia and sub-urothelial space, separated by regions of dense bundles of collagen [8, 13]; the absence of any fibronexus indicating that they are not myofibroblasts. These ICs display numerous caveolae, an incomplete basal lamina and many other morphological characteristics used previously to distinguish interstitial cells of Cajal (ICC) in the gastrointestinal tract [8]. Volume rendering of ICs imaged in serial sections of mouse renal pelvis using FIBSEM tomography reveals that they are in fact 'ribbon shaped', that they make close appositions with like cells, as well as neighbouring ASMCs and TSMCs (Fig. 3.2e), and that they *increase* in number with distance from the papilla base [3, 8] (see Supplementary Video 3.1).

Immunohistochemical analysis of the mouse renal pelvis has established that ICs represent a mixed population of cells that has yet to be fully characterized. Like ICC, some α-SMA$^-$ ICs are intensely immuno-positive for antibodies against the Ca^{2+}-activated Cl^- channel protein Ano1 and mildly immuno-positive for $K_V7.5$ antibodies [2, 5]. These α-SMA$^-$ Ano1$^+$ $K_V7.5^+$ ICs are likely to be the freshly isolated ICs that display spontaneous niflumic acid-sensitive transient Cl^- currents, as well as voltage-dependent K^+ current sensitive to the $K_V7.x$ channel blocker XE911 when recorded using patch clamp technology [5]. These Ano1$^+$ $K_V7.5^+$ ICs do not appear to have the same distribution as α-SMA$^-$ intensely PDGFRα-eGFP$^+$ ICs in the lamina propria and serosa of the renal pelvis of B6.129S4-Pdgfrα$^{tm11(EGFP)sor}$/J mice [3]. Interestingly, the nuclei of serosal ASMCs displaying spontaneous Ca^{2+} transients also lightly express PDGFRα-eGFP fluorescence (H Hasitani & RJ Lang unpublished observations), suggesting that PDGFRα-eGFP$^+$ cells in the mouse real pelvis are not a homocellular population.

3.4.1 $Ca_V3.x^+$ HCN3$^+$ ICs

In coronal sections of the mouse renal pelvis, ICs immunoreactive to antibodies against T-type voltage-dependent Ca^{2+} channel (TVDCC) $Ca_V3.1$ ($Ca_V3.1^+$) are selectively located in the same proximal regions as ICs that are also immunoreactive to antibodies raised against HCN isoform 3 channel subunits (HCN3$^+$) [3]. Indeed, HCN3 staining has been co-located with $Ca_V3.1$ channel immunoreactivity in the mouse renal pelvis [39] and $Ca_V3.2$ channel immunoreactivity in porcine and human multi-papillae kidneys [54]. There appears to be some confusion as to whether $Ca_V3.1$ or HCN3 staining also co-locates with α-SMA immunoreactivity. HCN3$^+$ cells have been reported to be 'integrated' within the smooth muscle layer of the proximal region of the mouse renal pelvis [38, 39] and the minor calyces of porcine and human kidney [54]. In our hands, $Ca_V3.1^+$ ICs are clearly not α-SMA positive and lay only in the sub-urothelial

space of the proximal renal pelvis [3]. In contrast, Hurtado et al. reported that HCN3$^+$ $Ca_V3.1^+$ cells are also α-SMA$^+$ [38]. In the minor calyces of the porcine kidney, HCN3$^+$ cells display both α-SMA and $Ca_V3.2$ immunoreactivity, while HCN3$^+$ $Ca_V3.2^+$ cells in the human minor calyces don't co-locate with α-SMA immunoreactivity [54]. In spite of pharmacological evidence of the effects of the likely presence and blockade of $Ca_V3.2$ channels on Ca^{2+} signalling and contractility of the mouse renal pelvis [3], we and others [38, 39] have yet to demonstrate the presence of $Ca_V3.2$ channel immunoreactive product. Thus, the results obtained to date using presently available antibodies and methodologies appear to have some selectivity issues that have yet to be resolved.

3.4.2 Kit Staining in the Upper Urinary Tract

A number of researchers have reported the presence of spindle-shaped ICs in *sectioned* material of various regions of the ovine, rat [55], porcine [56], human [57, 58], mouse [59, 60] upper urinary tract that are immunoreactive to antibodies raised against the tyrosine kinase receptor Kit, the selective marker of ICC. In the mouse renal pelvis, this Kit$^+$ staining is found predominately in the serosal adventitia and less often in the muscle, sub-urothelial layers and urothelium [59, 60]. The intensity of this Kit staining also *decreases* slightly with distance from the papilla border [55, 57]. This Kit staining does not co-locate with markers for endothelial and epithelial cells, macrophages, hemopoietic/progenitor stem cells or mast cells [55, 57, 61]. When not tested immunohistologically, Kit$^+$ mast cells are readily identified by their distinctive circular shape [8, 62].

In the guinea pig renal pelvis, fibroblast-like ICs are readily identified using standard electron microscopy, while Kit antibodies only stain mast cells [8]. Recently, we have demonstrated that Kit (CD117 or AK2) staining in *whole mount* or *sectioned* preparations of mouse renal pelvis readily co-locates with the neuronal marker PGP9.5 [2, 5]. Thus, we have suggested that Kit staining of neurons in low-resolution light micrographs of *sectioned* material may well appear as 'spindle-shaped' Kit$^+$ cells. Kit staining of sectioned neural tracts may also explain the appearance of Kit staining during the functional development of the mouse upper urinary tract [60, 63] and its loss with obstruction [62, 64, 65] (see Sect. 3.9). A more rigorous examination of whether Kit and neuronal markers co-localize [55, 56] is required in both normal and pathological samples of the upper urinary tract, as well as animals that display a fluorescent reporter protein in cells that exclusively express Kit (e.g. Kit$^{+/copGFP}$ mice) [66].

3.5 Spontaneous Activity in the Upper Urinary Tract

3.5.1 Typical Smooth Muscle Cells

Early extracellular electrode [16, 17, 25–28], sucrose gap [36, 67–69] and intracellular microelectrode [8, 53, 70–75] recordings established that the upper urinary tract display spontaneous electrical activity and that migrating contractions associate with action potentials consisting of an initial rapidly-rising spike and a long plateau (Fig. 3.3ai, aii) [67, 68, 76–78], which in the guinea pig also triggers a number of additional high frequency spikes [8, 71, 73, 79, 80]. These action potentials that propagate down the renal pelvis (Fig. 3.3ci, cii) into the ureter are associated with a propagating Ca^{2+} wave within long spindle-shaped TSMCs (Fig. 3.4ai) [8] and it's this rise in Ca^{2+} that underlies the propagating contractions [77, 78, 81]. When viewed at higher magnifications, TSMC Ca^{2+} transients occur almost simultaneously along the length of each cell, while the wave propagates between cells in a direction perpendicular to their long axis (Fig. 3.4aii, b) [77], resulting in near simultaneous action potential discharge and contraction in the transverse axis of the renal pelvis and a slow propagation (at a velocity of 1.5–2 mm·s^{-1}) of excitation in the longitudinal axis (Fig. 3.4b) [77, 82, 83].

The action potentials and contractions in the mouse and guinea pig renal pelvis are dose-dependently reduced then abolished by the L-type voltage-dependent Ca^{2+} channel (LVDCC) blocker, nifedipine (1–10 μM) [73, 77, 78, 84] in a manner associated with a

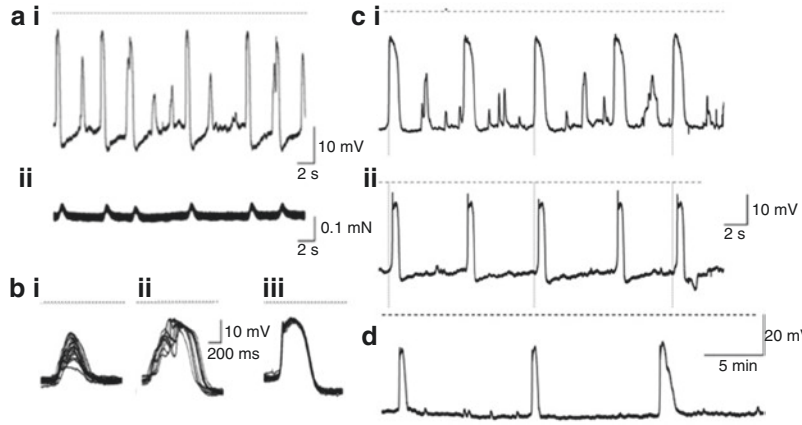

Fig. 3.3 Electrical recordings in the mouse renal pelvis. (**a**) Simultaneous recording of electrical (**ai**) and contractile (**aii**) activity illustrating that only action potentials and not STDS are associated with muscle contraction. (**b**) Recordings of superimposed STDs in the presence (**bi**) and absence (**bii**) of 1 μM nifedipine, illustrating their variable summation (**bi**) and triggering (**bii**) of an action potential. (**biii**) Superimposed action potentials to illustrate their time course. (**ci**, **ii**) Simultaneous recordings from two intracellular microelectrodes 240 μm apart illustrating that only action potentials propagate. (**d**) Recording of IC action potentials in the distal renal pelvis bathed in 1 μM nifedipine containing physiological salt solution, note the large difference in time scale

membrane depolarization of some 5–10 mV [79]. In the mouse renal pelvis, LVDCC blockade (1–3 μM nifedipine) reduces TSMC Ca^{2+} waves (Fig. 3.4ci, cii) and contraction amplitude [3], while blockade of TVDCCs (with Ml218, mibefradil, NNC55-0396 or R(-)efonidipine) reduces contraction frequency [3, 39]. The blockade of $Ca_V3.2$ channels with low concentrations (10 μM) of Ni^{2+} [85] also reduces contraction frequency without affecting their amplitude [3]. Higher concentrations of Ni^{2+} (100–300 μM) evoke a transient acceleration of TSMC Ca^{2+} activity associated with a transient rise in the basal Ca^{2+}, followed by gradual reduction in contraction frequency [3]. Blockade of both LVDCCs and TVDCCs (with 1–3 μM nifedipine and 10–100 μM Ni^{2+}) is necessary to completely arrest contractile activity and its underlying TSMC Ca^{2+} transients in the mouse renal pelvis [3].

3.5.2 Atypical Smooth Muscle Cells

Intracellular microelectrodes impalements of the renal pelvis of the mouse, guinea pig and rat reveal that spontaneous transient depolarizations (STDs) of a simple waveform and varying amplitude [74, 79, 86] are recorded in spindle-shaped ASMCs (Fig. 3.3ai, bi, and ci) [8, 23, 77]. These STDs are recorded most often in the 'spoke-like' attachments and bulb regions of the proximal renal pelvis [3, 8, 87]. Their likelihood of being recorded and their frequency of discharge also decreases with distance from the pelvis papilla border (Fig. 3.3c), they have never been recorded in the ureter [8, 87]. STDs, firing at a high frequency (5–30 min^{-1}) are often (Fig. 3.3ai, ci) but not always present between the spontaneous TSMC action potentials (5–12 min^{-1}), are not associated with muscle contraction (Fig. 3.3ai) and are little affected by the LDVCC- and TDVCC-independent Ca^{2+} entry blockers (Fig. 3.3ai), La^{3+} (or Gd^{3+}) [78] which blocks Ca^{2+} signalling in the rabbit urethra [88].

In the nifedipine (1 μM)-arrested mouse renal pelvis loaded with Ca^{2+} fluorophores fluo-4 or Cal 520, high frequency but slowly propagating intercellular Ca^{2+} waves are recorded in short cells at the same frequency as STDs and in the same adventitial region [77, 78] as ASMCs identified with standard electron microscopy or FIBSEM tomography [3] (see Supplementary

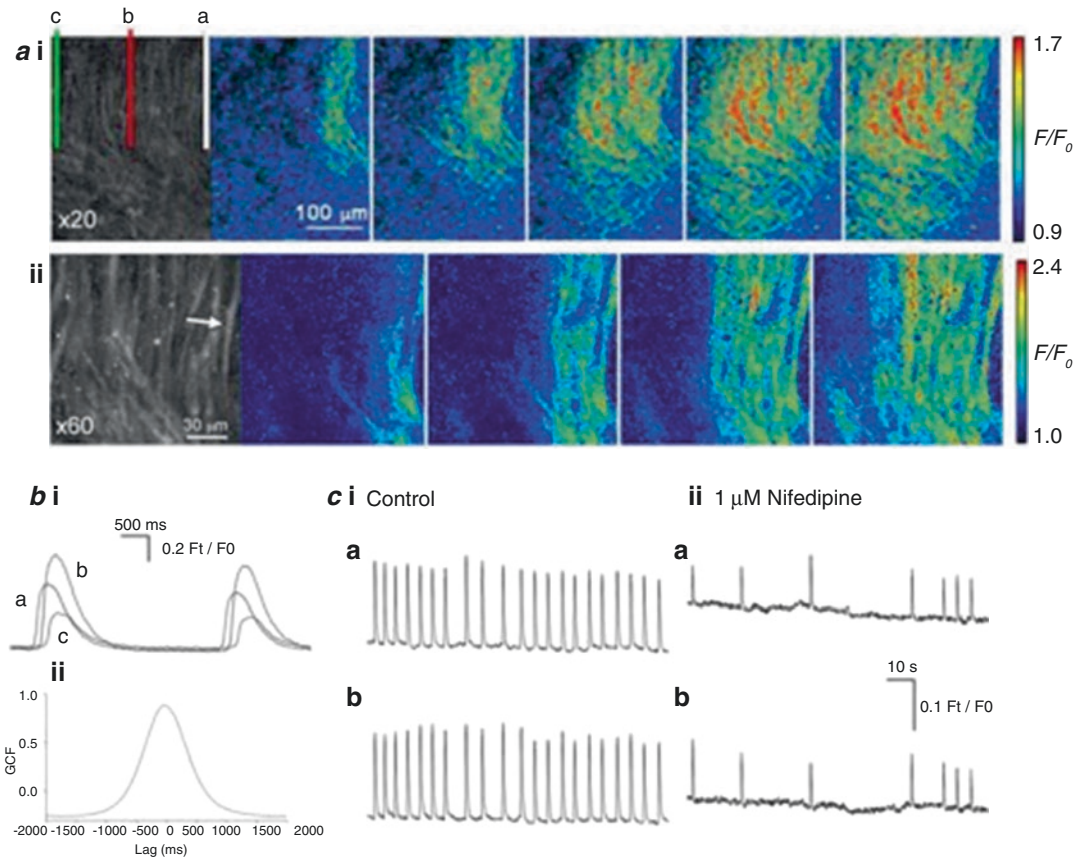

Fig. 3.4 Ca^{2+} waves in typical smooth muscle cells (TSMCs) of the renal pelvis **a** sequential Ca^{2+} fluorescence intensity micrographs of a fluo-4 loaded TSMC layer (time intervals of 66 ms at ×20 (**ai**) or ×60 (**aii**) magnification). The Ca^{2+} wave is clearly seen as a transient increase in Ca^{2+} intensity propagating across the field of view; the arrow indicates a single TSMC. (**bi**) Superimposed fluorescence intensities of the three regions (a–c) in **ai** plotted against time. (**bii**) Correlation of the Ca^{2+} waves recorded at a and c (separation 110 µm) show a high degree of 1:1 synchronicity. (**c**) Ca^{2+} waves recorded at two positions in a field of view (**ci**) were reduced but not completely blocked in 1 µM nifedipine (**cii**). Figure taken from Lang et al. [77]

Video 3.2). These ASMC Ca^{2+} transients sometimes propagate into neighbouring similar-shaped cells if located on their longitudinal axis and are only reduced, not blocked by 3–10 µM nifedipine. When bathed in 1 µM nifedipine and 100 µM Ni^{2+} the parameters (amplitude, frequency ½ width and integral) describing the time course of these ASMC Ca^{2+} transients are fitted by single Gaussian distributions (Fig. 3.5bi–biv) suggesting a single population of cells. ASMC Ca^{2+} transients are mostly asynchronous but appear to burst synchronously every 3–5 min. During these bursts the ASMC basal Ca^{2+} rises, the frequency of these ASMC Ca^{2+} signals doubles, while their other parameters are little affected (Fig. 3.5aiii) [3].

Contraction and action potential discharge in the guinea pig renal pelvis [82] and the firing of STDs and ASMC Ca^{2+} transients in the mouse renal pelvis [78] are dependent on the influx of external Ca^{2+}, sarcoplasmic endoplasmic reticulum Ca^{2+}-ATPase (SERCA)-dependent uptake of Ca^{2+} into internal stores, IP_3-dependent release from these endoplasmic reticulum stores and the cyclic movement of Ca^{2+} through mitochondria [89]. Contraction amplitude and frequency in the guinea pig renal pelvis [82] are little affected by 30 µM ryanodine, the blocker of ryanodine-

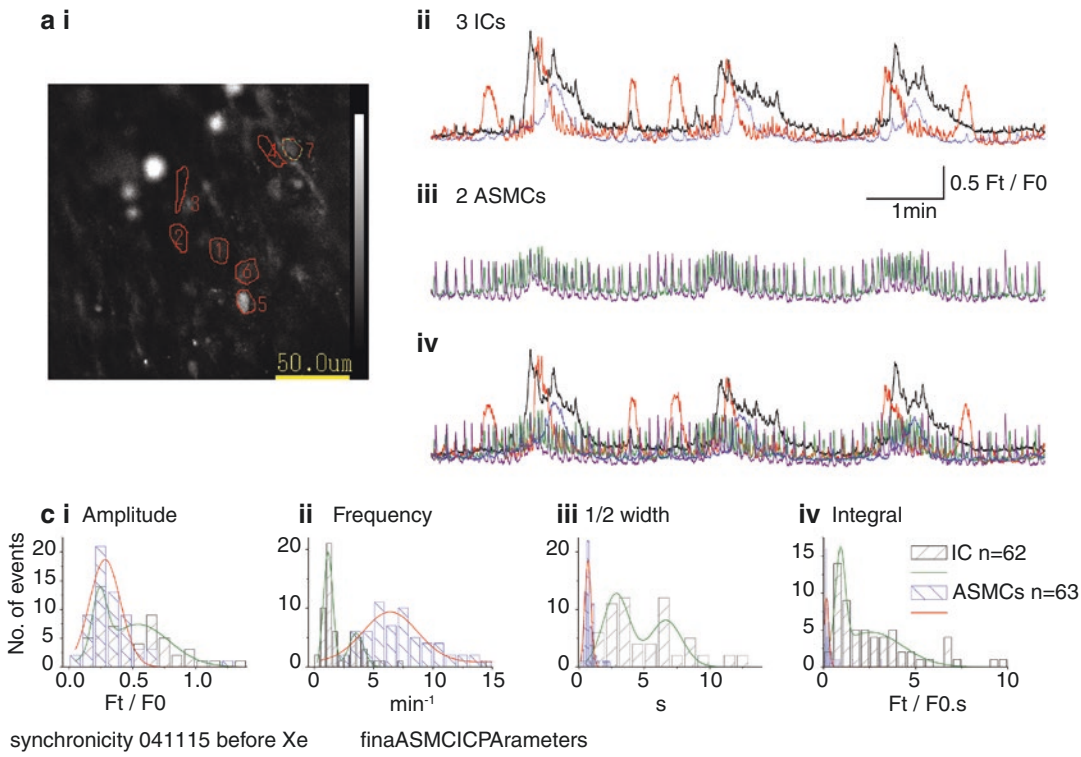

Fig. 3.5 Comparison of spontaneous Ca^{2+} transients in ICs and ASMCs in the mouse renal pelvis. (**ai**) Typical field of view of cells bathed in 1 μM nifedipine: 100 μM Ni^{2+}-containing physiological salt solution. Ca^{2+} transient activity (F_t/F_0) in three ICs (**ai** region of interest (ROIs) 1,2,5, **aii**) and two ASMCs (**ai** ROIs 3,4, **aiii**) plotted against time separately (**aii**, **iii**) and together (**aiv**). (**bi**–**iv**) Frequency distributions of four measured parameters of 63 ICs (*blue columns*) and 62 ASMCs (*black columns*) recorded *between* bursts were fitted (by least squares) with 1 (**b** *red* line ASMC) or 2 (**b** *green line* ICs) Gaussian distributions. ICs display spontaneous low frequency Ca^{2+} transients that synchronize into bursts every 3–5 min. Neighbouring ASMCs displaying higher-frequency spontaneous Ca^{2+} transients, also accelerate their firing in synchrony with the bursting ICs. Figure adapted from Hashitani et al. [3]

sensitive Ca^{2+} release channels. The amplitude, ½ width and synchronization of STDs in the mouse renal pelvis are also reduced by ryanodine (30–100 μM) which reduces their ability to sum into a depolarization sufficiently large to trigger an TSMC action potential [78]. However, ryanodine (100 μM) has little effect on any ASMC Ca^{2+} transient parameters [78]. These minor inhibitory effects of ryanodine have been confirmed using tetracaine which blocks ryanodine-sensitive Ca^{2+} release in the rabbit urethra [88, 90] and corporal tissue of the guinea pig penis [91]. In 17 ASMCs from six preparations of mouse renal pelvis bathed in 1 μM nifedipine and 100 μM Ni^{2+}, tetracaine (100 μM) reduces the amplitude and integral of their Ca^{2+} transients by only 22.2 ± 3.4% and 22.7 ± 3.3%, respectively, while their ½ width and frequency (0.2 ± 1.4 and 33.5 ± 32.8%, respectively) are not significantly altered (Fig. 3.6).

3.5.3 Interstitial Cells

A third pattern of action potential activity has been recorded in both the mouse and guinea pig renal pelvis. These action potentials display particularly long plateaus, occur at a frequency of 0.2–1 min^{-1}, are not associated with TSMC contraction [77] and have been demonstrated to arise

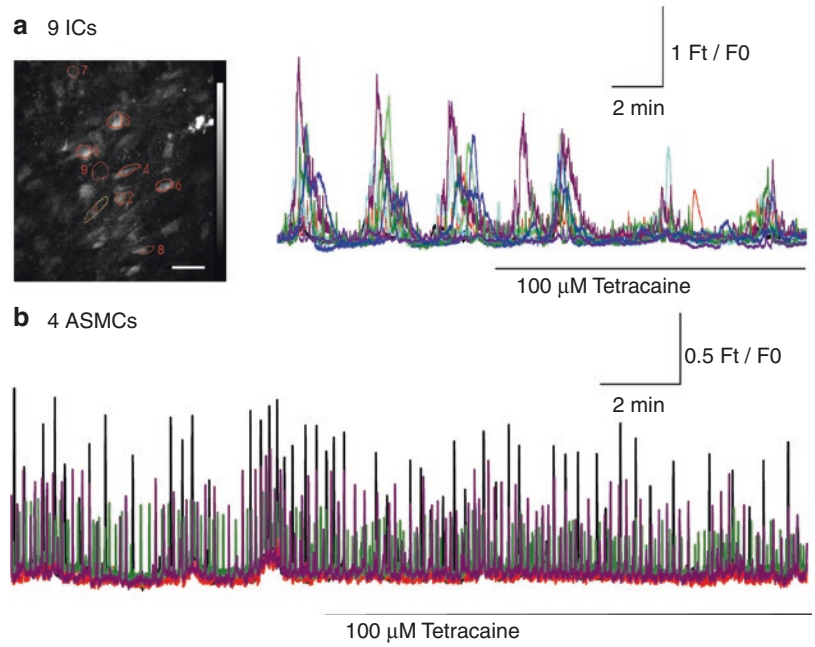

Fig. 3.6 IC Ca^{2+} transient activity and synchronicity (**a**) are more sensitive than ASMC Ca^{2+} transients (**b**) to tetracaine or ryanodine, blockers of CICR from internal stores. Ca^{2+} transient activity (F_t/F_0) in 9 ICs (**a** ROIs 1–9) and 4 ASMCs in a separate experiment (**b**) plotted against time (*t*), preparations bathed in 1 µM nifedipine: 100 µM Ni^{2+}-containing physiological salt solution. Scale bar in **a** left panel represents 50 µm

from irregular-shaped ICs [8, 24]. During intracellular microelectrode impalements, IC action potentials and STDs can be recorded concurrently with TSMC actions potentials. STDs and residual IC depolarizations ('slow waves') (Fig.3.3d) can also readily be recorded after blockade of TSMC discharge with nifedipine [77]. These observations confirm that the cells generating all three electrical events are electrically coupled in a syncytium and that the varying amplitude and time course of STDs and IC action potentials merely reflects the varying distance between the site of their generation in the syncytium and the recording electrode.

Upon blockade of TSMC Ca^{2+} signalling and contraction in the mouse renal pelvis, IC Ca^{2+} transients are mostly recorded in the bulb region and in regions more distal [77, 89]. Previously the use of fluo-4 reveals only a few (1–5) ICs displaying Ca^{2+} transients per field of view (×40–60 magnification) [77]. More recently, the use of Cal 520 with its grater fluorescence, penetration and loading reveals that each field of view contained many more ICs (Fig. 3.4) [3] (see Supplementary Video 3.2). Upon blockade of LDVCCs and TVDCCs with 1 µM nifedipine and 100 µM Ni^{2+}, IC Ca^{2+} transients separated by 20–200 µm fire asynchronously, but display synchronized bursting behaviour every 3–5 min (Figs. 3.5 and 3.6) [3]. The parameters of the time course of IC Ca^{2+} transients *between bursts* are best described by two Gaussian distributions, firing at frequencies of 1.1 and 3.5 min^{-1}, respectively (Fig. 3.5bi–biv), suggesting the presence of two populations of ICs [3]. However, the low frequencies of discharge of these two IC populations during our recording periods (typically 10–20 min) has not allowed any further discrimination based on their sensitivity to test agents.

3.6 Pacemaker Mechanisms in ASMCs and ICs

3.6.1 ASMCs

It seems likely that the initial trigger of the ASMC pacemaker signal involves the spontaneous release of a 'packet' of Ca^{2+} from internal stores that triggers the opening of a small number of Ca^{2+}-activated inward channels, resulting in a small 'unitary' STD and the influx of Ca^{2+}

through a nifedipine-insensitive Ca^{2+} pathway [78]. The 50% decrease in frequency but not blockade of ASMC Ca^{2+} transient firing when 100 μM Ni^{2+} is added to the mouse renal pelvis exposed to only nifedipine [3] suggests that Ca^{2+} entering through TVDCCs enhances a more global release of Ca^{2+} from sarcoplasmic/endoplasmic reticulum stores via Ca^{2+} release channels coupled to both IP_3 receptors and ryanodine receptors using Ca^{2+}-induced Ca^{2+} release (CICR) mechanisms [78, 92]. In the absence of LDVCC blockade, this entrainment would result in more frequent and larger ASMC Ca^{2+} transients and the summation of larger STDs into pacemaker potentials large enough to trigger the opening of TSMC LDVCCs, the firing of regenerative action potentials (Fig. 3.3bii) and the propagation of Ca^{2+} waves and contraction [77, 93].

3.6.2 ICs

Ca^{2+} transients in ICs in the same field of view are equally sensitive as ASMCs to the removal of Ca^{2+} from the bathing solution, blockade of SERCA with cyclopiazonic acid or the blockade of IP_3 receptor signalling with 2-APB [78]. However, in contrast to ASMC's partial sensitive sensitivity to ryanodine, IC Ca^{2+} transient discharge and their bursting behaviour are completely abolished by ryanodine [78] or profoundly reduced in tetracaine (Fig. 3.6a). This suggests that ICs differ fundamentally from ASMCs in their greater dependence on Ca^{2+} influx through TDVCCs and CICR from ryanodine-sensitive Ca^{2+} release channels.

This apparent greater dependence of IC Ca^{2+} signalling on CICR from ryanodine-sensitive stores and nifedipine-insensitive Ca^{2+} entry has been examined using various concentrations of the TVDCC blocker Ni^{2+}. Given the 70-fold difference in the IC_{50} of Ni^{2+} for $Ca_V3.2$ and $Ca_V3.1$ channels (5 and 350 μM, respectively) [85], the near complete blockade of TSMC Ca^{2+} waves and contraction in the presence of 10 μM Ni^{2+} plus nifedipine suggests the presence of active $Ca_V3.2$ channels in the TSMC layer. In addition, 100 μM Ni^{2+} would be expected to completely block $Ca_V3.2$ channels, but only partially block $Ca_V3.1$ channels. IC Ca^{2+} transients in the presence of 100 μM Ni^{2+} plus nifedipine are abolished upon the addition of the HCN channel blocker, ZD7288 [3]. Blockade of HCN channels may well lead to IC hyperpolarization to potentials negative of the opening threshold of any residual $Ca_V3.1$ channels and reduce Ca^{2+} entry. The co-location of immunoreactive product for HCN3 and $Ca_V3.1$ [39] in sub-urothelial ICs in the mouse proximal renal pelvis [3] suggests that voltage-dependent Ca^{2+} entry through $Ca_V3.1$ channels which triggers CICR from ryanodine-sensitive internal Ca^{2+} stores is essential for IC Ca^{2+} signalling [78], and that HCN3 channel-mediated depolarization contributes to the opening of these Ca^{2+} channels [93, 94]. However, single ICs of the mouse renal pelvis have not yet been demonstrated electrophysiologically to display either $Ca_V3.1$ or HCN currents [5], even though TVDCC currents have been recorded in prostatic and urethral myocytes [95] and HCN currents in cultured mouse dorsal root ganglia (RJ Lang unpublished data) under similar conditions.

3.7 IC Modulation of ASMCs

When bathed in 1 μM nifedipine and 100 μM Ni^{2+}, the most distinguishing property of the ICs was their ability to convert their asynchrony activity into synchronous bursts every 3–5 min (Fig. 3.5aii) [3]. This bursting behaviour occurs in cells that have no apparent close appositions, being often separated by 20–200 μm (Figs. 3.5ai and 3.6a). These bursts of IC Ca^{2+} transients also correlate in time with the accelerated activity and change in baseline of ASMCs within the same field of view (see Supplementary Video 3.2). This periodic acceleration of ASMC Ca^{2+} transient firing is blocked when IC Ca^{2+} transients are reduced by teracaine (Fig. 3.6b) or when gap junction cell-to-cell coupling is blocked by carbenoxolone [3]. However, the asynchronous firing of both cell types remains in carbenoxolone, albeit at a reduced level [3, 96]. Thus, it appears that ICs enhance the firing of neighbouring

ASMCs. A small increase in TSMC basal Ca^{2+} is also sometimes observed during these bursts of IC Ca^{2+} transients [3] which presumably also raises the excitability of the smooth muscle layer.

In the presence of both LVDCC and TVDCC blockers, the spread of excitation between ICs and their neighbours is likely to be intercellular and slowly voltage dependent, arising solely from the Ca^{2+}-activated membrane currents triggered by the spontaneous IC Ca^{2+} transients [5]. In the absence of LDVCC blockade, additional Ca^{2+} influx may well result in spontaneous IC Cl^--selective depolarizations that are more frequent and larger, which more effectively accelerate ASMC activity. They may even provide a constant influence on ASMC STD firing. As the number of ASMCs and ICs decrease and increase, respectively, with distance from the papilla pelvis border this IC influence may also increase with distance; even take over in the absence of a proximal pacemaker drive, i.e. act as 'latent pacemakers'.

3.8 Promoters of Pyeloureteric Peristalsis

3.8.1 Prostaglandins

It is well established that the intrinsic release of prostaglandins (PGs) is essential for maintaining spontaneous or evoked contractions in the upper urinary tract [24, 97]. The application of prostanoids has both positive and negative effects on upper urinary tract contractility. Applied $PGF_{2\alpha}$ tends to have an excitatory action on contractility in the upper urinary tract, PGE_1 tends to be inhibitory, while the effects of PGE_2 are more variable [24, 97]. In contrast, inhibition of PG synthesis with indomethacin decreases the spontaneous contractility in the renal pelvis and the spontaneous or evoked contractions in the ureter of various laboratory animals and human [24, 97], as well as reduces the release of cyclooxygenase products such as $PGF_{2\alpha}$, 6-keto $PGF_{1\alpha}$, PGI_2 and thromboxane $B_{2\alpha}$ [98, 99]. This blockade of contractility in the mouse and guinea pig renal pelvis does not arise from a blockade of conduction pathways as originally suggested by Thulelius et al. [28]. Blockers of cell-to cell coupling, 18β-glycyrrhetinic acid and carbenoxolone, rapidly prevent the propagation of action potentials, Ca^{2+} waves and contractions in the TSMC layer [3, 96]. In contrast, TSMC action potential discharge and contraction in the presence of indomethacin can readily be restored by nerve stimulation or the $PGF_{2\alpha}$ analogue, dinoprost [75].

The indomethacin-induced decrease in contractility in the renal pelvis arises from a decrease in the duration and frequency of the spontaneous action potentials due to an increase in the failures of underlying STDs to trigger an action potential [75]. In the mouse renal pelvis, the firing and synchronous bursting of IC Ca^{2+} transients are markedly reduced by indomethacin, which is associated with a 37–46% reduction in the amplitude and frequency of ASMC Ca^{2+} transients (Fig. 3.7b) [3] and a near complete blockade of their IC-evoked bursting behaviour (Fig. 3.7a). This reduction in ASMC Ca^{2+} transients presumably reduces the frequency and amplitude of the Ca^{2+}-activated membrane conductances underlying STD discharge and summation, essential for the triggering of TSMC action potential discharge. This reduction of IC Ca^{2+} transients, ASMC activity and pyeloureteric peristalsis upon cyclooxygenase inhibition suggests that their spontaneous activity is being fuelled by an autocrine/paracrine mechanism (Fig. 3.7c). It seems likely that locally released prostacyclins bind to G protein-coupled receptors on both ICs and ASMCs to contribute to the hydrolysis of phosphatidylinositol 4,5-bisphosphate (PIP_2) and IP_3 formation that drives their Ca^{2+} cycling [100].

A number of non-steroidal anti-inflammatory drugs (NSAIDs) which inhibit cyclooxygenase (COX)-arachidonic acid mediated production of eicosanoids also have various subunit-selective excitatory and inhibitory actions on $K_V7.x$ channels [101]. In the mouse renal pelvis, intense $K_V7.5$ immunoreactivity is present in BECs, while $Ano1^+$ ICs appear moderately $K_V7.5$ immuno-positive; both cells populations form close appositions with neighbouring TSMCs (Fig. 3.9). In single $K_V7.5^+$, $Ano1^+$ ICs from the

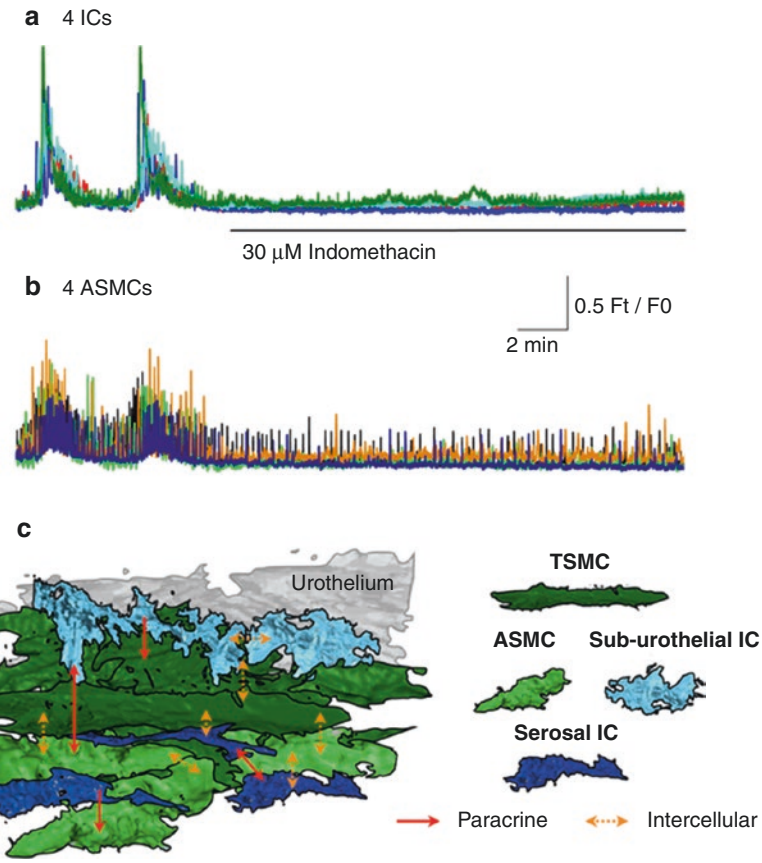

Fig. 3.7 Blockade of prostaglandin synthesis inhibits the firing and synchronous bursting of IC Ca^{2+} transients associated with a similar blockade of ASMC Ca^{2+} transient bursting, but only a 50% reduction in their amplitude and frequency. Ca^{2+} transient activity (F_t/F_0) in three 4 ICs (**a**) and 4 ASMCs (**b**) in the same field of view plotted against time (*t*). Preparation bathed in 1 μM nifedipine: 100 μM Ni^{2+}-containing physiological salt solution. (**c**) Schematic of paracrine (*red arrows*) and intercellular (*orange arrows*) pathways that ICs may modulate their own activity, ASMC pacemaking and TSMC contractility

mouse renal pelvis, the K_V7 channel modulator meclofenamic acid partially decreases an I_K that is abolished by the general K_V7 channel blocker, Xe991 [5]. K_V7 channel blockers Xe991 and linopirdine increase, while flupirtine a K_V7 channel activator decreases the frequency of TSMC contractions in the mouse renal pelvis. However, the excitatory effects of the linopirdine requires the previous blockade of intrinsic primary sensory nerves (PSNs) [2] as linopirdine also directly activates the capsaicin receptor TRPV1 [102]. The selective activation of $K_V7.2$ or $K_V7.4$ subunits with ML-213 (230–510 nM) also significantly decreases the amplitude and frequency of renal pelvis contractions in a manner reversed upon the addition of XE991 (M.J. Nguyen and R.J. Lang unpublished data). These preliminary pharmacological data suggest that native K_V7 ('m-current') channels in the renal pelvis are likely to be hetero-multimeric $K_V7.2$-5 channels constructs which have yet to be fully characterized or examined for their therapeutic potential.

3.8.2 Primary Sensory Nerves

The tonic release of neuropeptides from PSNs is essential for maintaining spontaneous activity in the renal pelvis [24, 97, 100]. Unmyelinated C-fibres and poorly myelinated Aδ-fibres [103] are distributed throughout the upper urinary tract of many mammals, innervating the adventitia, smooth muscle, epithelial layer and blood vessels [2, 104]. The relative proportion of immunoreactivity for tachykinins and calcitonin gene-related peptide (CGRP) neuropeptides are in equal quantities in nerve terminals of the guinea pig [105, 106] and human ureter [106, 107] but present in a ratio of 1:3, respectively, in rat ureter [105]. The rat renal pelvis also contains at least four distinct

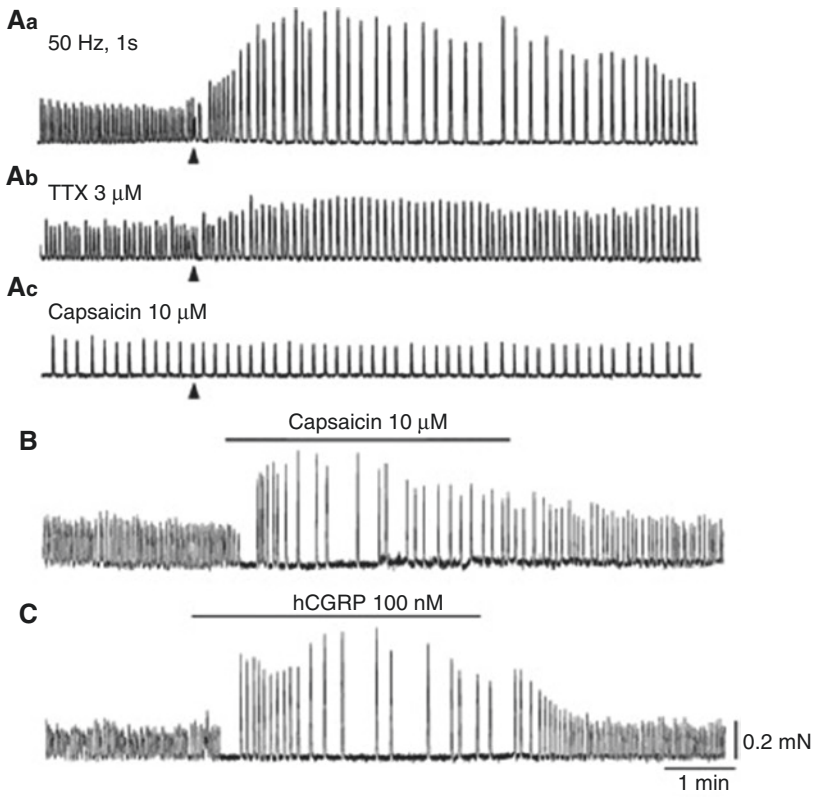

Fig. 3.8 Effects of primary sensory nerve (PSN) stimulation and bath-applied calcitonin gene-related peptide (CGRP) on spontaneous contractions of the mouse renal pelvis. Trains of PSN stimuli (50 Hz, 1 s; triangles) reduce the frequency but increase the amplitude of the spontaneous contractions (**Aa**). Tetrodotoxin (TTX 3 μM), reduces (**Ab**), while capsaicin (10 μM) completely blocks the effects of PSN stimulation (**Ac**). Capsaicin (10 μM) (**B**) and human CGRP (100 nM hCGRP) both have negative chronotropic and positive inotropic effects on the spontaneous contractions (**C**). Scale bars for **c** refer to all traces. Figure taken from Hashitani et al. [89]

populations of PSNs, based on their relative neuropeptide immunoreactivity [108].

Electrical stimulation of PSN terminals in the upper urinary tract [109] in vitro triggers action potentials which propagate into collateral branches, releasing neuropeptides in a manner relatively resistant to the sodium channel blocker tetrodotoxin (TTX) or the 'N-type' Ca^{2+} channel antagonist ω-conotoxin GVIA [110]. PSNs can also directly release and be depleted of their neuropeptides upon capsaicin binding to transient receptor potential vanilloid 1 (TRPV1) channels [89, 111] in a manner dependent on the age and species under investigation, and the method and number of administrations of capsaicin [22, 112–114].

Electrical or capsaicin stimulation of PSNs evokes a predominantly inhibitory effect on urinary tract motility in the rat [115] and guinea pig [116] ureter [110] and distal renal pelvis of the guinea pig [22]. In proximal renal pelvis of the guinea pig [22, 97] and mouse [89], PSN stimulation transiently increases and then inhibits its contraction frequency, this prolonged negative chronotropic effects is associated with an increase in contraction amplitude and duration (Fig. 3.8Aa). In the guinea pig proximal renal pelvis, electrical field stimulation evokes a transient membrane depolarization in ASMCs [84] as well as a prolonged increase in the duration of TSMC action potentials in the distal renal pelvis [84] and ureter [72]. These positive ino-

tropic and chronotropic effects are reduced by the neurokinin A antagonist MEN 10376 suggesting they involve the release of excitatory neuropeptides, Neurokinin A and Substance P [22, 97, 117, 118].

Human CGRP (hCGRP) (Fig. 3.8C) and agents that increase internal cAMP levels [87, 89] mimic the PSN-mediated suppression of motility in the upper urinary tract (Fig. 3.8Aa) [89]. In the guinea pig ureter, the inhibitory effects of hCGRP are reduced in the presence of the blocker of ATP-dependent K^+ channels (K_{ATP}), glibenclamide, the cAMP antagonist, Rp-cAMPS or inhibitors of protein kinase A, H8 and H89 [119, 120]. In the mouse renal pelvis, glibenclamide also blocks the TSMC membrane hyperpolarization evoked by hCGRP or cAMP stimulators, but has little effect on their negative chronotropic and positive inotropic actions [87, 89]. Thus, the membrane potential-independent negative chronotropic effects of hCGRP arise mainly from the suppression of Ca^{2+} cycling in ASMCs via a cAMP-dependent second messenger system [89]. The positive inotropic effects of hCGRP may well be arising from the reduced TSMC action potential frequency which would promote Ca^{2+} store refilling, as well as TSMC hyperpolarization which would increase the availability and driving force of LDVCCs that contribute to the electrical discharge.

3.8.3 Autonomic Nerves

Extensive networks of parasympathetic, nitrergic [121] and sympathetic [122–124] nerves lie within the urothelial, submucosal, TSMC and serosal layers of the upper urinary tract. However, blockers of sympathetic, parasympathetic and nitrergic transmission or antagonists of α-adrenoceptors and muscarinic receptors have little effect on either renal pelvic autorhythmicity or the positive/negative inotropic and chronotropic effects evoked upon electrical or chemical stimulation of intrinsic nerves [15, 22, 86, 97, 117].

Activation of α-adrenoceptors with noradrenaline or adrenaline stimulates spontaneous contractions in the mouse [125], dog [126] and guinea pig [97] renal pelvis and in the pig ureter [36] associated with an increased Ca^{2+} influx during the prolongation of their action potential plateaus. In the guinea pig ureter, norepinephrine increases hydrolysis of PIP_2 and IP_3-dependent Ca^{2+} release from internal stores [127] which activates K^+ conductances that terminate the action potential plateau [97]. β-Adrenoceptor activation, membrane permeable cAMP analogues and inhibition of cAMP degradation [128] all reduce ureteric contractility [97] associated with a shortening of the action potential duration [129]. In the rabbit proximal renal pelvis, β-adrenoceptor activation has also been described to induce a positive inotropic effect [47, 97, 130, 131].

In comparison to other visceral smooth muscles, parasympathetic nerve stimulation or muscarinic receptor agonists have relatively little effect on pyeloureteric peristalsis. Exogenous application of acetylcholine increases contractility in the pig [132] and guinea pig [97] renal pelvis and the pig [133], human [134] and guinea pig [135] ureter, but has little effect on the porcine distal ureter [136]. Carbachol also decreases ureteric pressure and peristalsis in partially or completely obstructed ureters of anaesthetized dogs [137]. High concentrations of muscarinic receptor agonists have a robust negative chronotropic and positive inotropic effect on the spontaneous contractions in the mouse renal pelvis in a manner selectively prevented by either a nicotinic receptor antagonist or PSN depletion with capsaicin [125]. Glibenclamide also blocks this inhibition of pyeloureteric peristalsis, TSMC action potential firing and membrane hyperpolarization suggesting that carbachol activation of PSN nicotinic receptors leads to the release of CGRP that activates TSMC K_{ATP} channels [125].

The glibenclamide-independent inhibition of Ca^{2+} signalling in ASMCs upon PSN nicotinic receptor activation [125] may also arise from a reduction of the release of tachykinins essential

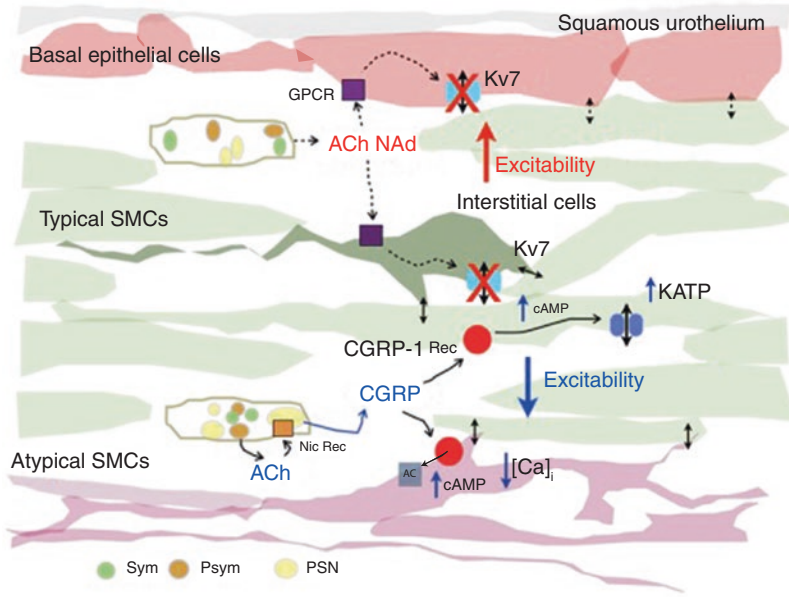

Fig. 3.9 Schematic of possible mechanisms of sympathetic (Sym), parasympathetic (Psym) and PSN modulation of pyeloureteric peristalsis. G protein-coupled receptor (GPCR) activation by acetylcholine (Ach), adrenaline (Ad) or tachykinins can lead to phospholipase C (PLC) metabolism and depletion of PIP2, KV7 channel closure (X) and membrane depolarization in BECs or ICs to increase the excitability of neighbouring electrically coupled ASMCs and TSMCs. Ach released from Psym nerves can also activate nicotinic receptors (Nic Rec) on neighbouring PSNs to release CGRP. This CGRP binds to its receptor (CGRP-1Rec) on both ASMCs and TSMCs to stimulate adenylyl cyclase (AC) and increase intracellular cAMP. In ASMCs, cAMP increases the Ca^{2+} buffering capacity of internal stores which reduces the intracellular cycling of Ca^{2+}, leading to an inhibition of ASMC Ca^{2+} transient discharge. This results in a decreased pacemaker drive and the observed decrease in frequency of contractions, action potentials and Ca^{2+} transients in TSMCs. The rise in cAMP in TSMCs leads to the opening of glibenclamide-sensitive K_{ATP} channels, resulting in membrane hyperpolarization that de-inactivates plasmalemmal Ca^{2+} channels. When a STD in a ASMC triggers an action potential in a neighbouring TSMC, the resulting Ca^{2+} transient and contraction may well be larger and longer than those observed in control

for sustaining pyeloureteric peristalsis. Alternatively, nicotinic receptor evoked release of CGRP may stimulate a cAMP-dependent increase in ASMC Ca^{2+} buffering that results in a reduction in the intracellular cycling of ASMC Ca^{2+} (Fig. 3.9) [100]. Thus, presynaptic PSN nicotinic receptors provide a means by which parasympathetic nerves can modulate the frequency and tone underlying pyeloureteric peristalsis. A combination of the inhibitory effects of PSN-released CGRP, a reduced release of tachykinins and TSMC muscarinic receptor evoked increases in the Ca^{2+} sensitivity of the contractile apparatus via a RhoA/Rho-associated kinase pathway [138] may well explain the often-contradictory effects of cholinergic agonists on the contractility of the upper urinary tract.

The autonomic and sensory innervation may also indirectly modulate the rate of conduction within and between ASMC and TSMC bundles by modulating the activity of neighbouring closely apposed $K_V7.5^+$ BECs or $K_V7.5^+$ ICs (Fig. 3.9) [2]. K_V7 channels require the presence of PIP_2 to remain open. Nerve-released tachykinins and autonomic neurotransmitters could well lead to a depletion of PIP_2 and K_V7 channel closure [139]. The by-products of PIP_2 metabolism, IP_3 and diacylglycerol (DAG) may also stimulate Ca^{2+} release and the activation of protein kinase C (PKC) which both lead to further inhibition of

K_V7.2-5 channels upon binding of Ca^{2+}-calmodulin and a protein kinase C (PKC)/A kinase anchoring protein (AKAP) complex [139]. Thus, closure of K_V7.5 channels in BECS and ICs may well remove a hyperpolarizing influence to increase the pacemaker drive in ASMCs as well as the ability of neighbouring TSMCs to initiate and conduct a wave of excitation (Fig. 3.9). It is interesting to speculate that $K_V7.5^+$ cells in the renal pelvis may control the frequency and size of the bolus at urine which enters the ureter from the renal pelvis in both uni-papilla and multi-papillae kidneys with changes in diuresis [40, 52], they may even control the establishment of the predominant minor calyx pacemaker in multi-papillae kidneys [32, 33, 36].

3.8.4 Renin-Angiotensin System

Angiotensin II acting exclusively on angiotensin receptor 1A (ATr1A) in mice evokes an increase in peristaltic contraction frequency that is associated with a rise in muscle wall tone and an increase in basal Ca^{2+} in both TSMCs and ASMCs [83]. ATr1A receptors are G protein-coupled receptors that leads to the production of G_{q11}-protein, activation of phospholipase C (PLC)–β and metabolism of PIP_2 to IP_3 and DAG [140]. ATr1 activation would therefore be expected to contribute to the intracellular IP_3 drive underlying cycling Ca^{2+} oscillators in both ICs and ASMCs.

3.9 Clinical Implications

Congenital hydronephrosis or ureteropelvic junction obstruction results in a compromised urine flow from the renal pelvis into the ureter that leads to pressure-induced dilatation of the renal collecting system and potential parenchyma injury which, if left untreated, results in renal disease and the development of salt-sensitive hypertension [141]. Renal pelvis dilatation is detected in 1 in 100 prenatal ultrasound screenings, with ureteropelvic junction obstruction being the most frequently diagnosed cause of antenatal hydronephrosis [142]. This hydronephrosis can be caused by a 'physical' stenosis, that usually requires *Anderson-Hynes* pyeloplasty, or by a 'functional' obstruction arising from a subtle developmental defect in the urothelium or muscle wall which usually disappears in 80% of infants within their 1st year [143, 144].

In children presenting with intrinsic ureteropelvic obstruction [62, 145], the site of dysfunction displays a decrease in the number of ASMCs and TSMCs, as well as a loss of their myofilaments and surface caveolae [146, 147]. Also evident is a marked collagen expression [145, 146, 148, 149], hyperplasia of the transitional epithelium [147, 150–152] and a decrease in the number of nerve terminals [145, 148, 149] and neuronal staining [64, 148, 149, 153, 154]. One electron microscopic examination of the structural integrity of ICs within hydronephrotic renal pelvises reports that their numbers are reduced and that their cytoplasm are enlarged with relatively few internal organelles [62]. A change of Kit staining, be it in nerve terminals or ICs, with ureteropelvic obstruction remains controversial; with reports that Kit immunoreactivity is only present in mast cells [155], that Kit staining increases [156], decreases [62, 64, 65] or little altered [157] with obstruction.

Little is known of the effects of hydronephrosis on the initiation or maintenance of pyeloureteric peristalsis. Mice lacking the Atr1A ($ATr1A^{-/-}$) present with a functional ureteropelvic obstruction associated with a hypoplastic papilla and renal cortex, a dilated calyx, proliferating and apoptotic tubulointerstitial cells, macrophage infiltration and fibrosis [158–160]. Mildly-to-moderately hydronephrotic kidneys in $ATr1A^{-/-}$ mice display spontaneous propagating contractions in their pelvic wall similar in frequency, but smaller in amplitude to their control ($ATr1A^{+/+}$, $ATr2^{+/+}$ and $ATr2^{-/-}$) mice [83]. However, the renal pelvis of severely hydronephrotic $ATr1A^{-/-}$ kidneys do not show any pyeloureteric contractile activity due to the complete destruction of the TSMC wall. Thus, the development of a functional obstruction in the

ureteropelvic junction of ATr1A$^{-/-}$ mice does not arise from a lack of development of the pyeloureteric pacemaker and contractile mechanisms [161]. It is more likely that the failure to transmit peristaltic contractions through the obstructed region of the proximal ureter in time leads to the development of back pressure-induced dilatation, apoptosis and fibrosis of the renal pelvis wall and kidney parenchyma [83].

Given the tendency of neonatal renal pelvis dilatation to resolve in the 1st few years after birth, it seems likely that in utero manipulation of the mechanisms that develop, drive or modulate pyeloureteric peristalsis has little therapeutic potential. Post birth, persistent dilatation of the renal pelvis arising from pyeloureteric stenosis can be closely monitored using ultrasound, magnetic resonance imaging or other voiding techniques to establish the necessity of further treatment or the timing of pyeloplasty surgery [162].

On the other hand, the control of pain, stone expulsion and prevention of kidney damage during renal colic already appears to involve many of the mechanism discussed herein. During renal colic, PSN mechanoceptors and chemoceptors in the renal pelvis and upper ureter transmit renal pain via C-fibres and Aδ-fibres to the dorsal horn of the spinal cord, then more centrally to supraspinal structures and the cerebral cortex. Convergence with other somatovisceral signals result in pain radiation to other visceral regions, as well as symptoms such as nausea, tachycardia and reduced gastrointestinal peristalsis [163]. Opiates provide rapid pain relief but also have excitatory contractile effects and appear to be no more effective than NSAIDs. The dependence of renal blood flow, glomerular filtration rate, pyeloureteric peristalsis etc., on prostaglandin, angiotensin and thromboxane A_2 [163] informs the use of NSAIDs for pain relief, but may have detrimental effects in patients with pre-existing renal disease. Interestingly, COX-2 inhibitors reduce ureteric peristalsis without gastric side effects. The short-term pain relief with nifedipine is associated with reduction of ureteric spasm without altering contraction frequency [163], consistent with the effects of LDVCC blockade described above [3]. While anticholinergic agents have proven not to be very useful, the muscle wall relaxation upon inhibition of α1D-adrenoceptors accelerates stone expulsion and reduces the use of analgesics [163]. Thus, there is potential to further refine the therapeutic selectivity of these drug groups upon a greater understanding of their actions in the upper urinary tract. Elucidation of the mechanisms by which ASMCs and ICs control contractility in the upper urinary tract under physiological and pathological conditions may also lead to the development of pharmacological interventions to improve outcomes in hydronephrotic infants and adults. However, future therapies to modulate pyeloureteric peristalsis will need to allow for any central, peripheral and systemic effects, as well as the degree and duration of pelviureteric blockade.

Acknowledgements The authors acknowledge the use of the imaging facilities within the Multi-modal Australian ScienceS Imaging and Visualization Environment (MASSIVE) at the Monash University node of the National Imaging Facility.

References

1. Walsberg GE. Small mammals in hot deserts: some generalizations revisited. Bioscience. 2000;50:109–20.
2. Nguyen MJ, Higashi R, Ohta K, Nakamura KI, Hashitani H, Lang RJ. Autonomic and sensory nerve modulation of peristalsis in the upper urinary tract. Auton Neurosci. 2016;200:1–10.
3. Hashitani H, Nguyen MJ, Noda H, Mitsui R, Higashi R, Ohta K, et al. Interstitial cell modulation of pyeloureteric peristalsis in the mouse renal pelvis examined using FIBSEM tomography and calcium indicators. Pflugers Arch. 2017;469:797–813.
4. Dixon JS, Gosling JA. Electron microscopic observations on the renal caliceal wall in the rat. Zeitschrift Fur Zellforschung Und Mikroskopische Anatomie. 1970;103:328–40.
5. Iqbal J, Tonta MA, Mitsui R, Li Q, Kett M, Li J, et al. Potassium and ANO1/TMEM16A chloride channel profiles distinguish atypical and typical smooth muscle cells from interstitial cells in the mouse renal pelvis. Br J Pharmacol. 2012;165:2389–408.
6. Gosling JA, Dixon JS. Species variation in the location of upper urinary tract pacemaker cells. Investig Urol. 1974;11:418–23.
7. Schmidt-Nielsen B. The renal pelvis. Kidney Int. 1987;31:621–8.

8. Klemm MF, Exintaris B, Lang RJ. Identification of the cells underlying pacemaker activity in the guinea-pig upper urinary tract. J Physiol. 1999;519:867–84.
9. Dixon JS, Gosling JA. The fine structure of pacemaker cells in the pig renal calices. Anat Rec. 1973;175:139–53.
10. Dixon JS, Gosling JA. The musculature of the human renal calices, pelvis and upper ureter. J Anat. 1982;135:129–37.
11. Gosling JA, Dixon JS. Morphologic evidence that the renal calyx and pelvis control ureteric activity in the rabbit. Am J Anat. 1971;130:393–408.
12. Dixon JS, Gosling JA. Fine structural observations on the attachment of the calix to the renal parenchyma in the rat. J Anat. 1970;106:181–2.
13. Lang RJ, Klemm MF. Interstitial cell of Cajal-like cells in the upper urinary tract. J Cell Mol Med. 2005;9:543–56.
14. Englemann TW. Zur Physiologie des Ureter. Pflugers Arch Ges Physiol. 1869;2:243–93.
15. Golenhofen K, Hannappel J. Normal spontaneous activity of the pyeloureteral system in the guinea-pig. Pflugers Arch. 1973;341:257–70.
16. Morita T. The in vitro study of the pacemaker activity of the canine renal pelvis throughout simultaneous recordings of pelvic pressure changes and electromyogram on various regions of the renal pelvis. Nihon Hinyokika Gakkai Zasshi. 1978;69:304–14.
17. Tsuchida S, Morita T, Yamaguchi O. The simultaneous recording of the rhythmic contraction and electrical activity of the renal previs—a new in vitro method. Tohoku J Exp Med. 1978;124:93–4.
18. Longrigg N. Minor calyces as primary pacemaker sites for ureteral activity in man. Lancet. 1975;1:253–4.
19. Weiss R, Wagner ML, Hoffman BF. Localization of the pacemaker for peristalsis in the intact canine ureter. Investig Urol. 1967;5:42–8.
20. Weiss RM, Tamarkin FJ, Wheeler MA. Pacemaker activity in the upper urinary tract. J Smooth Muscle Res. 2006;42:103–15.
21. Dwyer TM, Schmidt-Nielsen B. The renal pelvis: machinery that concentrates urine in the papilla. News Physiol Sci. 2003;18:1–6.
22. Teele ME, Lang RJ. Stretch-evoked inhibition of spontaneous migrating contractions in a whole mount preparation of the Guinea-pig upper urinary tract. Brit J Pharmacol. 1998;123:1143–53.
23. Lang RJ, Takano H, Davidson ME, Suzuki H, Klemm MF. Characterization of the spontaneous electrical and contractile activity of smooth muscle cells in the rat upper urinary tract. J Urol. 2001;166:329–34.
24. Lang RJ, Davidson ME, Exintaris B. Pyeloureteral motility and ureteral peristalsis: essential role of sensory nerves and endogenous prostaglandins. Exp Physiol. 2002;87:129–46.
25. Bozler E. The activity of the pacemaker previous to the discharge of a muscular impulse. Am J Phys. 1942;136:543–52.
26. Hannappel H, Golenhofen K. Comparative studies on normal ureteral peristalsis in dogs, guinea-pigs and rats. Pflugers Arch. 1974;348:65.
27. Djurhuus JC. Dynamics of upper urinary tract. III. The activity of renal pelvis during pressure variations. Investig Urol. 1977;14:475–7.
28. Thulesius O, Ugaily-Thulesius L, Angelo-Khattar M. Generation and transmission of ovine ureteral contractions, with special reference to prostaglandins. Acta Physiol Scand. 1986;127:485–90.
29. Gosling JA, Constantinou CE. The origin and propagation of upper urinary tract contraction waves. A new in vitro methodology. Experientia. 1976;32:266–7.
30. Yamaguchi O, Constantinou CE. Renal calyceal and pelvic contraction rhythms. Am J Phys. 1989;257:R788–95.
31. Constantinou CE. Renal pelvic pacemaker control of ureteral peristaltic rate. Am J Phys. 1974;226:1413–9.
32. Constantinou CE, Silvert MA, Gosling J. Pacemaker system in the control of ureteral peristaltic rate in the multicalyceal kidney of the pig. Investig Urol. 1977;14:440–1.
33. Morita T, Ishizuka G, Tsuchida S. Initiation and propagation of stimulus from the renal pelvic pacemaker in pig kidney. Investig Urol. 1981;19:157–60.
34. Tsuchida S, Morita T, Harada T, Kimura Y. Initiation and propagation of canine renal pelvic peristalsis. Urol Int. 1981;36:307–14.
35. Constantinou CE, Yamaguchi O. Multiple-coupled pacemaker system in renal pelvis of the unicalyceal kidney. Am J Phys. 1981;241:412–8.
36. Hannappel H, Golenhofen K, Hohnsbein J, Lutzeyer W. Pacemaker process of ureteral peristalsis in multicalyceal kidneys. Urol Int. 1982;37:240–6.
37. Lammers WJ, Ahmad HR, Arafat K. Spatial and temporal variations in pacemaking and conduction in the isolated renal pelvis. Am J Phys. 1996;270:F567–74.
38. Hurtado R, Bub G, Herzlinger D. The pelvis-kidney junction contains HCN3, a hyperpolarization-activated cation channel that triggers ureter peristalsis. Kidney Int. 2010;77:500–8.
39. Hurtado R, Bub G, Herzlinger D. A molecular signature of tissues with pacemaker activity in the heart and upper urinary tract involves coexpressed hyperpolarization-activated cation and T-type Ca^{2+} channels. FASEB J. 2014;28:730–9.
40. Constantinou CE, Hrynczuk JR. The incidence of ecotpic peristaltic contractions. Urol Int. 1976;31:476–88.
41. Davidson ME, Lang RJ. Effects of selective inhibitors of cyclo-oxygenase-1 (COX-1) and cyclo- oxygenase-2 (COX-2) on the spontaneous myogenic contractions in the upper urinary tract of the guinea-pig and rat. Br J Pharmacol. 2000;129:661–70.
42. Shiratori T, Kinoshita H. Electromyographic studies on urinary tract. II. Electromyographic study on the genesis of peristaltic movement of the dog's ureter. Tohoku J Exp Med. 1961;73:103–17.

43. Morita T, Kondo S, Suzuki T, Ichikawa S, Tsuchida S. Effect of calyceal resection on pelviureteral peristalsis in isolated pig kidney. J Urol. 1986;135:151–4.
44. Hannappel J, Lutzeyer W. Pacemaker localization in the renal pelvis of the unicalyceal kidney. In vitro study in the rabbit. Eur Urol. 1978;4:192–4.
45. Constantinou CE. Contractility of the pyeloureteral pacemaker system. Urol Int. 1978;33:399–416.
46. Constantinou CE, Neubarth JL, Mensah-Dwumah M. Frequency gradient in the autorhythmicity of the pyeloureteral pacemaker system. Experientia. 1978;34:614–5.
47. Morita T. Characteristics of spontaneous contraction and effects of isoproterenol on contractility in isolated rabbit renal pelvic smooth muscle strips. J Urol. 1986;135:604–7.
48. Longrigg N. In vitro studies on smooth muscle of the human renal pelvis. Eur J Pharmacol. 1975;34:293–8.
49. Weiss RM, Bassett AL, Hoffman BF. Dynamic length-tension curves of cat ureter. Am J Phys. 1972;222:388–93.
50. Thulesius O, Angelo-Khattar M, Sabha M. The effect of ureteral distension on peristalsis. Studies on human and sheep ureters. Urol Res. 1989;17:385–8.
51. Potjer RM, Kimoto Y, Constantinou CE. Topological localization of the frequency and amplitude characteristics of the whole and segmented renal pelvis. Urol Int. 1992;48:278–83.
52. Constantinou CE, Hrynczuk JR. Urodynamics of the upper urinary tract. Investig Urol. 1976;14:233–40.
53. Lang RJ, Zhang Y. The effects of K^+ channel blockers on the spontaneous electrical and contractile activity in the proximal renal pelvis of the guinea pig. J Urol. 1996;155:332–6.
54. Hurtado R, Smith CS. Hyperpolarization-activated cation and T-type calcium ion channel expression in porcine and human renal pacemaker tissues. J Anat. 2016;228:812–25.
55. Metzger R, Schuster T, Till H, Franke FE, Dietz HG. Cajal-like cells in the upper urinary tract: comparative study in various species. Pediatr Surg Int. 2005;21:169–74.
56. Metzger R, Neugebauer A, Rolle U, Bohlig L, Till H. C-Kit receptor (CD117) in the porcine urinary tract. Pediatr Surg Int. 2008;24(1):67–76.
57. Metzger R, Schuster T, Till H, Stehr M, Franke FE, Dietz HG. Cajal-like cells in the human upper urinary tract. J Urol. 2004;172:769–72.
58. van der Aa F, Roskams T, Blyweert W, Ost D, Bogaert G, De Ridder D. Identification of kit positive cells in the human urinary tract. J Urol. 2004;171:2492–6.
59. Pezzone MA, Watkins SC, Alber SM, King WE, de Groat WC, Chancellor MB, et al. Identification of c-kit-positive cells in the mouse ureter: the interstitial cells of Cajal of the urinary tract. Am J Physiol Ren Physiol. 2003;284:F925–9.
60. David SG, Cebrian C, Vaughan ED, Herzlinger D. C-kit and ureteral peristalsis. J Urol. 2005;173:292–5.
61. Arena S, Fazzari C, Arena F, Scuderi MG, Romeo C, Nicotina PA, et al. Altered 'active' antireflux mechanism in primary vesico-ureteric reflux: a morphological and manometric study. BJU Int. 2007;100:407–12.
62. Eken A, Erdogan S, Kuyucu Y, Seydaoglu G, Polat S, Satar N. Immunohistochemical and electron microscopic examination of Cajal cells in ureteropelvic junction obstruction. Can Urol Assoc J. 2013;7:E311–6.
63. Cain JE, Islam E, Haxho F, Blake J, Rosenblum ND. GLI3 repressor controls functional development of the mouse ureter. J Clin Invest. 2011;121:1199–206.
64. Solari V, Piotrowska AP, Puri P. Altered expression of interstitial cells of Cajal in congenital ureteropelvic junction obstruction. J Urol. 2003;170:2420–2.
65. Yang X, Zhang Y, Hu J. The expression of Cajal cells at the obstruction site of congenital pelviureteric junction obstruction and quantitative image analysis. J Pediatr Surg. 2009;44:2339–42.
66. Zhu MH, Kim TW, Ro S, Yan W, Ward SM, Koh SD, et al. A Ca^{2+}-activated Cl^- conductance in interstitial cells of Cajal linked to slow wave currents and pacemaker activity. J Physiol. 2009;587:4905–18.
67. Kobayashi M. Relationship between membrane potential and spike configuration recorded by sucrose gap method in the ureter smooth muscle. Comp Biochem Physiol. 1971;38A:301–8.
68. Zawalinski VC, Constantinou CE, Burnstock G. Ureteral pacemaker potentials recorded with the sucrose gap technique. Experientia. 1975;31:931–3.
69. Santicioli P, Maggi CA. Pharmacological modulation of electromechanical coupling in the proximal and distal regions of the guinea-pig renal pelvis. J Auton Pharmacol. 1997;17:43–52.
70. Irisawa H, Kobayashi M. Effects of repetitive stimuli and temperature on ureter action potentials. Jpn J Physiol. 1963;13:421–30.
71. Kuriyama H, Osa T, Toida N. Membrane properties of the smooth muscle of guinea-pig ureter. J Physiol. 1967;191:225–38.
72. Exintaris B, Lang RJ. Effects of nerve stimulation on spontaneously active preparations of the guinea pig ureter. Urol Res. 1999;27:328–35.
73. Exintaris B, Lang RJ. K(+) channel blocker modulation of the refractory period in spontaneously active guinea-pig ureters. Urol Res. 1999;27:319–27.
74. Tsuchida S, Suzuki T. Pacemaker activity of the pelvicalyceal border recorded by an intracellular glass microelectrode. Urol Int. 1992;48:121–4.
75. Zhang Y, Lang RJ. Effects of intrinsic prostaglandins on the spontaneous contractile and electrical activity of the proximal renal pelvis of the guinea-pig. Br J Pharmacol. 1994;113:431–8.
76. Kobayashi M. Effect of calcium on electrical activity in smooth muscle cells of cat ureter. Am J Phys. 1969;216:1279–85.
77. Lang RJ, Hashitani H, Tonta MA, Parkington HC, Suzuki H. Spontaneous electrical and Ca^{2+} signals in

typical and atypical smooth muscle cells and interstitial cell of Cajal-like cells of mouse renal pelvis. J Physiol. 2007;583:1049–68.
78. Lang RJ, Hashitani H, Tonta MA, Suzuki H, Parkington HC. Role of Ca^{2+} entry and Ca^{2+} stores in atypical smooth muscle cell autorhythmicity in the mouse renal pelvis. Br J Pharmacol. 2007;152:1248–59.
79. Takano H, Nakahira Y, Suzuki H. Properties of spontaneous electrical activity in smooth muscle of the guinea-pig renal pelvis. Jpn J Physiol. 2000;50:597–603.
80. Burdyga T, Wray S. Action potential refractory period in ureter smooth muscle is set by Ca sparks and BK channels. Nature. 2005;436:559–62.
81. Burdyga TV, Wray S. The relationship between the action potential, intracellular calcium and force in intact phasic, guinea-pig uretic smooth muscle. J Physiol. 1999;520:867.
82. Lang RJ, Hashitani H, Keller S, Takano H, Mulholland EL, Fukuta H, et al. Modulators of internal Ca^{2+} stores and the spontaneous electrical and contractile activity of the guinea-pig renal pelvis. Br J Pharmacol. 2002;135:1363–74.
83. Nguyen MJ, Hashitani H, Lang RJ. Angiotensin receptor-1A knockout leads to hydronephrosis not associated with a loss of pyeloureteric peristalsis in the mouse renal pelvis. Clin Exp Pharmacol Physiol. 2016;43:535–42.
84. Lang RJ, Zhang Y, Exintaris B, Vogalis F. Effects of nerve stimulation on the spontaneous action potentials recorded in the proximal renal pelvis of the guinea-pig. Urol Res. 1995;23:343–50.
85. Kang HW, Park JY, Jeong SW, Kim JA, Moon HJ, Perez-Reyes E, et al. A molecular determinant of nickel inhibition in Cav3.2 T-type calcium channels. J Biol Chem. 2006;281:4823–30.
86. Lang RJ, Exintaris B, Teele ME, Harvey J, Klemm MF. Electrical basis of peristalsis in the mammalian upper urinary tract. Clin Exp Pharmacol Physiol. 1998;25:310–21.
87. Lang RJ, Tonta MA, Zoltkowski BZ, Meeker WE, Wendt I, Parkington HC. Pyeloureteric peristalsis: role of atypical smooth muscle cells and interstitial cells of Cajal-like cells as pacemakers. J Physiol. 2006;576:695–705.
88. Johnston L, Sergeant GP, Hollywood MA, Thornbury KD, McHale NG. Calcium oscillations in interstitial cells of the rabbit urethra. J Physiol. 2005;565:449–61.
89. Hashitani H, Lang RJ, Mitsui R, Mabuchi Y, Suzuki H. Distinct effects of CGRP on typical and atypical smooth muscle cells involved in generating spontaneous contractions in the mouse renal pelvis. Br J Pharmacol. 2009;158:2030–45.
90. Hashitani H, Suzuki H. Properties of spontaneous Ca2+ transients recorded from interstitial cells of Cajal-like cells of the rabbit urethra in situ. J Physiol. 2007;583:505–19.
91. Hashitani H, Suzuki H. Identification of interstitial cells of Cajal in corporal tissues of the guinea-pig penis. Br J Pharmacol. 2004;14:199–204.
92. Miyakawa T, Mizushima A, Hirose K, Yamazawa T, Bezprozvanny I, Kurosaki T, et al. Ca^{2+}-sensor region of IP_3 receptor controls intracellular Ca^{2+} signaling. EMBO J. 2001;20:1674–80.
93. Lang RJ, Hashitani H, Tonta MA, Bourke JL, Parkington HC, Suzuki H. Spontaneous electrical and Ca^{2+} signals in the mouse renal pelvis that drive pyeloureteric peristalsis. Clin Exp Pharmacol Physiol. 2010;37:509–15.
94. Biel M, Wahl-Schott C, Michalakis S, Zong X. Hyperpolarization-activated cation channels: from genes to function. Physiol Rev. 2009;89:847–85.
95. Lang RJ, Tonta MA, Takano H, Hashitani H. Voltage-operated Ca^{2+} currents and Ca^{2+}-activated Cl^- currents in single interstitial cells of the guinea pig prostate. BJU Int. 2014;114:436–46.
96. Lang RJ, Zoltkowski BZ, Hammer JM, Meeker WF, Wendt I. Electrical characterization of interstitial cells of Cajal-like cells and smooth muscle cells isolated from the mouse ureteropelvic junction. J Urol. 2007;177:1573–80.
97. Santicioli P, Maggi CA. Myogenic and neurogenic factors in the control of pyeloureteral motility and ureteral peristalsis. Pharmacol Rev. 1998;50:683–722.
98. Thulesius O, Angelo-Khattar M, Ali M. The effect of prostaglandin synthesis inhibition on motility of the sheep ureter. Acta Physiol Scand. 1987;131:51–4.
99. Ali M, Angelo-Khattar M, Thulesius L, Fareed A, Thulesius O. Urothelial synthesis of prostanoids in the ovine ureter. Urol Res. 1998;26:171–4.
100. Lang RJ. Role of hyperpolarization-activated cation channels in pyeloureteric peristalsis. Kidney Int. 2010;77:483–5.
101. Peretz A, Degani-Katzav N, Talmon M, Danieli E, Gopin A, Malka E, et al. A tale of switched functions: from cyclooxygenase inhibition to M-channel modulation in new diphenylamine derivatives. PLoS One. 2007;2:e1332.
102. Neacsu C, Babes A. The M-channel blocker linopirdine is an agonist of the capsaicin receptor TRPV1. J Pharmacol Sci. 2010;114(3):332–40.
103. Ammons WS. Bowditch Lecture. Renal afferent inputs to ascending spinal pathways. Am J Phys. 1992;262:R165–76.
104. Amann R, Skofitsch G, Lembeck F. Species-related differences in the capsaicin-sensitive innervation of the rat and guinea-pig ureter. Naunyn Schmiedeberg's Arch Pharmacol. 1988;338:407–10.
105. Su HC, Wharton J, Polak JM, Mulderry PK, Ghatei MA, Gibson SJ, et al. Calcitonin gene-related peptide immunoreactivity in afferent neurons supplying the urinary tract: combined retrograde tracing and immunohistochemistry. Neuroscience. 1986;18:727–47.

106. Hua XY, Theodorsson-Norheim E, Lundberg JM, Kinn AC, Hokfelt T, Cuello AC. Co-localization of tachykinins and calcitonin gene-related peptide in capsaicin-sensitive afferents in relation to motility effects on the human ureter in vitro. Neuroscience. 1987;23:693–703.
107. Edyvane KA, Smet PJ, Trussell DC, Jonavicius J, Marshall VR. Patterns of neuronal colocalisation of tyrosine hydroxylase, neuropeptide Y, vasoactive intestinal polypeptide, calcitonin gene-related peptide and substance P in human ureter. J Auton Nerv Syst. 1994;48:241–55.
108. Ferguson M, Bell C. Ultrastructural localization and characterization of sensory nerves in the rat kidney. J Comp Neurol. 1988;274:9–16.
109. Maggi CA, Meli A. The sensory-efferent function of capsaicin-sensitive sensory neurons. Gen Pharmacol. 1988;19:1–43.
110. Maggi CA, Giuliani S. The neurotransmitter role of calcitonin gene-related peptide in the rat and guinea-pig ureter: effect of a calcitonin gene- related peptide antagonist and species-related differences in the action of omega conotoxin on calcitonin gene-related peptide release from primary afferents. Neuroscience. 1991;43:261–8.
111. Chung MK, Guler AD, Caterina MJ. TRPV1 shows dynamic ionic selectivity during agonist stimulation. Nat Neurosci. 2008;11:555–64.
112. Hua XY, Lundberg JM. Dual capsaicin effects on ureteric motility: low dose inhibition mediated by calcitonin gene-related peptide and high dose stimulation by tachykinins? Acta Physiol Scand. 1986;128:453–65.
113. Holzer P. Local effector functions of capsaicin-sensitive sensory nerve endings: involvement of tachykinins, calcitonin gene-related peptide and other neuropeptides. Neuroscience. 1988;24:739–68.
114. Maggi CA, Patacchini R, Santicioli P, Giuliani S, Del Bianco E, Geppetti P, et al. The 'efferent' function of capsaicin-sensitive nerves: ruthenium red discriminates between different mechanisms of activation. Eur J Pharmacol. 1989;170:167–77.
115. Maggi CA, Santicioli P, Giuliani S, Abelli L, Meli A. The motor effect of the capsaicin-sensitive inhibitory innervation of the rat ureter. Eur J Pharmacol. 1986;126:333–6.
116. Maggi CA, Giuliani S, Santicioli P. Multiple mechanisms in the smooth muscle relxant action of calcitonin gene-related peptide (CGRP) in the guinea-pig ureter. Naunyn Schmiedeberg's Arch Pharmacol. 1994;350:537–47.
117. Maggi CA, Theodorsson E, Santicioli P, Giuliani S. Tachykinins and calcitonin gene-related peptide as co- transmitters in local motor responses produced by sensory nerve activation in the guinea-pig isolated renal pelvis. Neuroscience. 1992;46:549–59.
118. Maggi CA, Astolfi M, Giuliani S, Goso C, Manzini S, Meini S, et al. MEN 10,627, a novel polycyclic peptide antagonist of tachykinin NK2 receptors. J Pharmacol Exp Ther. 1994;271:1489–500.
119. Maggi CA, Giuliani S, Meini S, Santicioli P. Calcitonin gene related peptide as inhibitory neurotransmitter in the ureter. Can J Physiol Pharmacol. 1995;73:986–90.
120. Maggi CA, Giuliani S, Santicioli P. CGRP inhibition of electromechanical coupling in the Guinea-pig isolated renal pelvis. Naunyn Schmiedeberg's Arch Pharmacol. 1995;352:529–39.
121. Rolle U, Chertin B, Nemeth L, Puri P. Demonstration of nitrergic and cholinergic innervation in whole-mount preparations of rabbit, pig, and human upper urinary tract. Pediatr Surg Int. 2002;18:315–8.
122. Gosling JA, Dixon JS. Catecholamine-containing nerves in the submucosa of the ureter. Experientia. 1971;27:1065–6.
123. Gosling JA, Dixon JS. The effect of 6-hydroxydopamine on nerves in the rat upper urinary tract. J Cell Sci. 1972;10(1):197–209.
124. Warburton AL, Santer RM. Sympathetic and sensory innervation of the urinary tract in young adult and aged rats: a semi-quantitative histochemical and immunohistochemical study. Histochem J. 1994;26:127–33.
125. Nguyen MJ, Angkawaijawa S, Hashitani H, Lang RJ. Nicotinic receptor activation on primary sensory afferents modulates autorhythmicity in the mouse renal pelvis. Br J Pharmacol. 2013;170:1221–32.
126. Morita T, Wada I, Suzuki T, Tsuchida S. Characterization of alpha-adrenoceptor subtypes involved in regulation of ureteral fluid transport. Tohoku Exp Med. 1987;152:111–8.
127. Wheeler MA, Martin TV, Weiss RM. Effect of carbachol and norepinephrine on phosphatidyl-inositol hydrolysis and cyclic-amp levels in guinea-pig urinary-tract. J Urol. 1995;153:2044–9.
128. Weiss RM, Vulliemoz Y, Verosky M, Rosen MR, Triner L. Adenylate cyclase and phosphodiesterase activity in rabbit ureter. Investig Urol. 1977;15:15–8.
129. Kovalev IV, Popov AG, Baskakov MB, Minochenko IL, Kilin AA, Borodin YL, et al. Effect of inhibitors of cyclic nucleotide phosphodiesterases on electrical and contractile activity of smooth muscle cells. Bull Exp Biol Med. 2002;133:38–40.
130. Morita T, Miyagawa I, Wheeler M, Weiss RM. Effect of isoproterenol on contractile force of isolated rabbit renal pelvic smooth muscle. Tohoku J Exp Med. 1985;147:153–5.
131. Kondo S, Morita T, Tsuchida S, Terui M, Tashima Y. Effect of dobutamine on adenylate cyclase activity in rabbit renal pelvis and ureter. Tohoku J Exp Med. 1986;148:113–4.
132. Sorensen SS, Husted SE, Nissen T, Djurhuus JC. Topographic variations in alpha-adrenergic and cholinergic response in the pig renal pelvis. Urol Int. 1983;38:271–4.
133. Hernandez M, Simonsen U, Prieto D, Rivera L, Garcia P, Ordaz E, et al. Different muscarinic

receptor subtypes mediating the phasic activity and basal tone of pig isolated intravesical ureter. Br J Pharmacol. 1993;110:1413–20.
134. Long S, Nergardh A. Autonomic receptor functions of the human ureter: an in vitro study. Scand J Urol Nephrol. 1978;12:23–6.
135. Yoshida S, Kuga T. Effects of field stimulation on cholinergic fibers of the pelvic region in the isolated guinea pig ureter. Jpn J Physiol. 1980;30:415–26.
136. Roshani H, Dabhoiwala NF, Dijkhuis T, Pfaffendorf M, Boon TA, Lamers WH. Pharmacological modulation of ureteral peristalsis in a chronically instrumented conscious pig model. I: effect of cholinergic stimulation and inhibition. J Urol. 2003;170:264–7.
137. Tomiyama Y, Wanajo I, Yamazaki Y, Kojima M, Shibata N. Effects of cholinergic drugs on ureteral function in anesthetized dogs. J Urol. 2004;172:1520–3.
138. Borysova L, Shabir S, Walsh MP, Burdyga T. The importance of Rho-associated kinase-induced Ca^{2+} sensitization as a component of electromechanical and pharmacomechanical coupling in rat ureteric smooth muscle. Cell Calcium. 2011;50:393–405.
139. Delmas P, Brown DA. Pathways modulating neural KCNQ/M (Kv7) potassium channels. Nat Rev Neurosci. 2005;6:850–62.
140. Higuchi S, Ohtsu H, Suzuki H, Shirai H, Frank GD, Eguchi S. Angiotensin II signal transduction through the AT1 receptor: novel insights into mechanisms and pathophysiology. Clin Sci. 2007;112:417–28.
141. Carlstrom M, Brown RD, Edlund J, Sallstrom J, Larsson E, Teerlink T, et al. Role of nitric oxide deficiency in the development of hypertension in hydronephrotic animals. Am J Physiol Ren Physiol. 2008;294:F362–70.
142. Chertin B, Pollack A, Koulikov D, Rabinowitz R, Shen O, Hain D, et al. Does renal function remain stable after puberty in children with prenatal hydronephrosis and improved renal function after pyeloplasty? J Urol. 2009;182:1845–8.
143. Schedl A. Renal abnormalities and their developmental origin. Nat Rev Genet. 2007;8:791–802.
144. Song R, Yosypiv IV. Genetics of congenital anomalies of the kidney and urinary tract. Pediatr Nephrol. 2011;26:353–64.
145. Kaya C, Bogaert G, de Ridder D, Schwentner C, Fritsch H, Oswald J, et al. Extracellular matrix degradation and reduced neural density in children with intrinsic ureteropelvic junction obstruction. Urology. 2010;76:185–9.
146. Gosling JA, Dixon JS. Functional obstruction of the ureter and renal pelvis. A histological and electron microscopic study. Br J Urol. 1978;50:145–52.
147. Faussone-Pellegrini MS, Rizzo M, Grechi G. Ultrastructural modifications of the tunica muscularis in congenital obstruction of the upper urinary tract. Physiopathological interpretations and anatomo-clinical correlations. J Urol (Paris). 1984;90:217–26.
148. Murakumo M, Nonomura K, Yamashita T, Ushiki T, Abe K, Koyanagi T. Structural changes of collagen components and diminution of nerves in congenital ureteropelvic junction obstruction. J Urol. 1997;157:1963–8.
149. Kajbafzadeh AM, Payabvash S, Salmasi AH, Monajemzadeh M, Tavangar SM. Smooth muscle cell apoptosis and defective neural development in congenital ureteropelvic junction obstruction. J Urol. 2006;176:718–23.
150. Baumgart P, Muller KM, Lison AE. Epithelial abnormalities in the renal pelvis in experimental hydronephrosis and pyelonephritis. Pathol Res Pract. 1983;176:185–95.
151. Chiou YY, Shieh CC, Cheng HL, Tang MJ. Intrinsic expression of Th2 cytokines in urothelium of congenital ureteropelvic junction obstruction. Kidney Int. 2005;67:638–46.
152. Stravodimos KG, Koritsiadis G, Lazaris AC, Agrogiannis G, Koutalellis G, Constantinides C, et al. Hydronephrosis promotes expression of hypoxia-inducible factor 1 alpha. Urol Int. 2009;82:38–42.
153. Wang Y, Puri P, Hassan J, Miyakita H, Reen DJ. Abnormal innervation and altered nerve growth factor messenger ribonucleic acid expression in ureteropelvic junction obstruction. J Urol. 1995;154:679–83.
154. Kuvel M, Canguven O, Murtazaoglu M, Albayrak S. Distribution of Cajal like cells and innervation in intrinsic ureteropelvic junction obstruction. Arch Ital Urol Androl. 2011;83:128–32.
155. Ozel SK, Emir H, Dervisoglu S, Akpolat N, Senel B, Kazez A, et al. The roles of extracellular matrix proteins, apoptosis and c-kit positive cells in the pathogenesis of ureteropelvic junction obstruction. J Pediatr Urol. 2010;6:125–9.
156. Koleda P, Apoznanski W, Wozniak Z, Rusiecki L, Szydelko T, Pilecki W, et al. Changes in interstitial cell of Cajal-like cells density in congenital ureteropelvic junction obstruction. Int Urol Nephrol. 2012;44:7–12.
157. Apoznanski W, Koleda P, Wozniak Z, Rusiecki L, Szydelko T, Kalka D, et al. The distribution of interstitial cells of Cajal in congenital ureteropelvic junction obstruction. Int Urol Nephrol. 2013;45:607–12.
158. Oliverio MI, Kim HS, Ito M, Le T, Audoly L, Best CF, et al. Reduced growth, abnormal kidney structure, and type 2 (AT2) angiotensin receptor-mediated blood pressure regulation in mice lacking both AT1A and AT1B receptors for angiotensin II. Proc Natl Acad Sci U S A. 1998;95:15496–501.
159. Burson JM, Aguilera G, Gross KW, Sigmund CD. Differential expression of angiotensin receptor 1A and 1B in mouse. Am J Phys. 1994;267:E260–7.
160. Miyazaki Y, Tsuchida S, Fogo A, Ichikawa I. The renal lesions that develop in neonatal mice during angiotensin inhibition mimic obstructive nephropathy. Kidney Int. 1999;55:1683–95.

161. Miyazaki Y, Tsuchida S, Nishimura H, Pope JC, Harris RC, McKanna JM, et al. Angiotensin induces the urinary peristaltic machinery during the perinatal period. J Clin Invest. 1998;102:1489–97.
162. Ismaili K, Hall M, Piepsz A, Alexander M, Schulman C, Avni FE. Insights into the pathogenesis and natural history of fetuses with renal pelvis dilatation. Eur Urol. 2005;48:207–14.
163. Travaglini F, Bartoletti R, Gacci M, Rizzo M. Pathophysiology of reno-ureteral colic. Urol Int. 2004;72(Suppl 1):20–3.

4 Excitation-Contraction Coupling in Ureteric Smooth Muscle: Mechanisms Driving Ureteric Peristalsis

Theodor Burdyga and Richard J. Lang

Abstract

The ureter acts as a functional syncytium and is controlled by a propagating plateau-type action potential (AP) which gives rise to a wave of contraction (ureteral peristalsis) via a process called excitation-contraction (E-C) coupling. The second messenger Ca^{2+} activates Ca^{2+}/calmodulin-dependent myosin light chain kinase-dependent phosphorylation of 20-kDa regulatory light chains of myosin which leads to ureteric contraction. Ca^{2+} entry from the extracellular space via voltage-gated L-type Ca^{2+} channels (VGCCs) provides the major source of activator Ca^{2+}, responsible for generation of both the AP and a Ca^{2+} transient that appears as an intercellular Ca^{2+} wave. The AP, inward Ca^{2+} current, Ca^{2+} transient and twitch contraction are all fully blocked by the selective L-type Ca^{2+} channel blocker nifedipine. Ca^{2+} entry via VGCCs, coupled to activation of Ca^{2+}-sensitive K^+ (K_{Ca}) or Cl^- (Cl_{Ca}) channels, acts as a negative or positive feedback mechanism, respectively, to control excitability and the amplitude and duration of the plateau component of the AP, Ca^{2+} transient and twitch contraction. The ureter, isolated from the pelvis, is not spontaneously active. However, spontaneous activity can be initiated in the proximal and distal ureter by a variety of biological effectors such as neurotransmitters, paracrine, endocrine and inflammatory factors. Applied agonists depolarise ureteric smooth muscles cells to threshold of AP activation, initiating propagating intercellular AP-mediated Ca^{2+} waves to produce antegrade and/or retrograde ureteric peristalsis. Several mechanisms have been proposed to describe agonist-induced depolarization of ureteric smooth muscle, which include suppression of K^+ channels, stimulation of Cl_{Ca} current and activation of non-selective cation receptor/store operated channels.

Keywords

Ureteric peristalsis · Smooth muscle cells · Contraction · Calcium · Ion channels · Action potentials · Calcium imaging

Electronic Supplementary Material The online version of this chapter (https://doi.org/10.1007/978-981-13-5895-1_4) contains supplementary material, which is available to authorized users.

T. Burdyga (✉)
Department of Cellular and Molecular Physiology, Institute of Translational Medicine, University of Liverpool, Liverpool, UK
e-mail: burdyga@liv.ac.uk

R. J. Lang
School of Biomedical Sciences, Faculty of Medicine, Nursing and Health Sciences, Monash University, Clayton, VIC, Australia
e-mail: rick.lang@monash.edu

H. Hashitani, R. J. Lang (eds.), *Smooth Muscle Spontaneous Activity*, Advances in Experimental Medicine and Biology 1124, https://doi.org/10.1007/978-981-13-5895-1_4

4.1 Introduction

The ureter functions as the mechanical peristaltic pump moving urine from kidney to urinary bladder and serves to remove waste products from the body's tissues. Under normal conditions the contracting ureter fully coapts its wall to generate a positive pressure wave, leading to the propulsion of a bolus of urine from kidney to bladder in front of the propagating mechanical wave. The ability of the ureter to generate mechanical waves requires that the contraction of large group of myocytes of the ureteral wall is synchronized and well coordinated in time and space. Such synchronization and coordination is achieved by fast propagating long-lasting plateau-type action potentials. Based on numerous studies of their structure, electrophysiology, membrane ionic currents, Ca^{2+} signalling and pharmacology it has been established that in ureteric smooth muscle a set of mechanisms collaborates to achieve this task. The Ca^{2+} based AP which originates in the proximal renal pelvis spreads from myocyte to myocyte along the ureter via gap junctions producing an intercellular Ca^{2+} wave accompanied by contraction wave of ureteric peristalsis.

4.2 The Architecture of the Musculature of the Ureter

The morphology of the ureter has been examined in a number of species using light, electron and confocal microscopy [1–7]. These studies revealed that in all species ureteric smooth muscle cells are grouped into muscle bundles of different thickness and orientation (Fig. 4.1). Distinct stratification, such as longitudinal or circular layers, in ureters of all species including humans is absent. In the guinea pig ureter there are segmental differences of muscle bundle orientation. In the upper part, muscle bundles show predominantly circular alignment, while in the lower part longitudinal orientation is evident (Fig. 4.1b) [4]. The bundles are separated from each other by big gaps of irregular width. Thread-like muscle cells extend across forming interbundular connections (Fig. 4.1cii). In addition, ultrastructural studies demonstrate close connections between individual smooth muscle cells within and between the bundles at all levels [3, 6–8]. The close association of the cell membranes and aggregation of intramembranous particles indicate the presence of gap junctions [2, 6, 8]. Gap junctions are noted to be localized within or along the caveolar zones, being elliptical in shape with their long axis parallel to muscle fibres [8]. Microvessels of the ureteric microvascular network are seen in the gaps between the muscle bundles (Fig. 4.1ci) [6, 9].

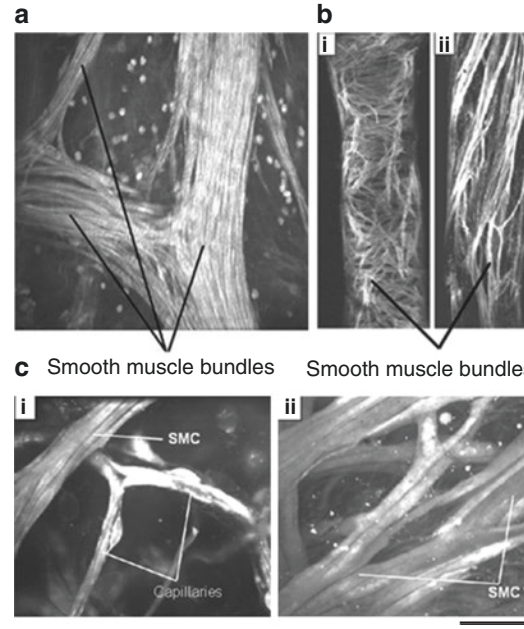

Fig. 4.1 The architecture of the muscle coat of the ureter. (**a**, **b**) The outer aspects of the muscle coat of the upper segment of the human ureter (**a**) and the upper (**bi**) and lower (**bii**) segments of the guinea pig ureter. In the guinea pig ureter, muscle bundles predominantly extend transversely in the upper (**bi**) and longitudinally in the lower segments (**bii**) of ureter. (**c**) Micrographs at higher magnification of the outer aspects of the rat (**ci**) and guinea pig (**cii**) ureter, respectively. SMCs are arranged in interconnected muscle bundles of different thickness and orientation. The calibration bar is 100 μm for **a**, 1 mm for **b** and 40 μm for **c**

4.3 Ureteric Peristalsis

The ureter actively propels tubular fluid from the renal pelvis to the bladder, and this peristalsis, which starts in the foetal period [10, 11], has been a subject of investigation for many years. Temporal aspects of the peristaltic wave have been assessed by measuring the velocity of propagation of internal pressure changes [12, 13], peristaltic waves [14–16] or electrical activity [12, 14, 17–20]. Collectively, these studies reveal that the average conduction velocity of the ureteric AP is 3.4 cm/s in rat [17], 4.5 cm/s in dog [12] and 2.4 cm/s in guinea pig [20]. The velocity of the mechanical wave is 3.4 cm/s in dog [15], 1–2 cm/s in pig [21], 2–3 cm/s in human [21], 1.4–4.5 cm/s in rat [14] and 2.0–2.8 cm/s in the guinea pig ureter (Fig. 4.2a, b) [16]. The

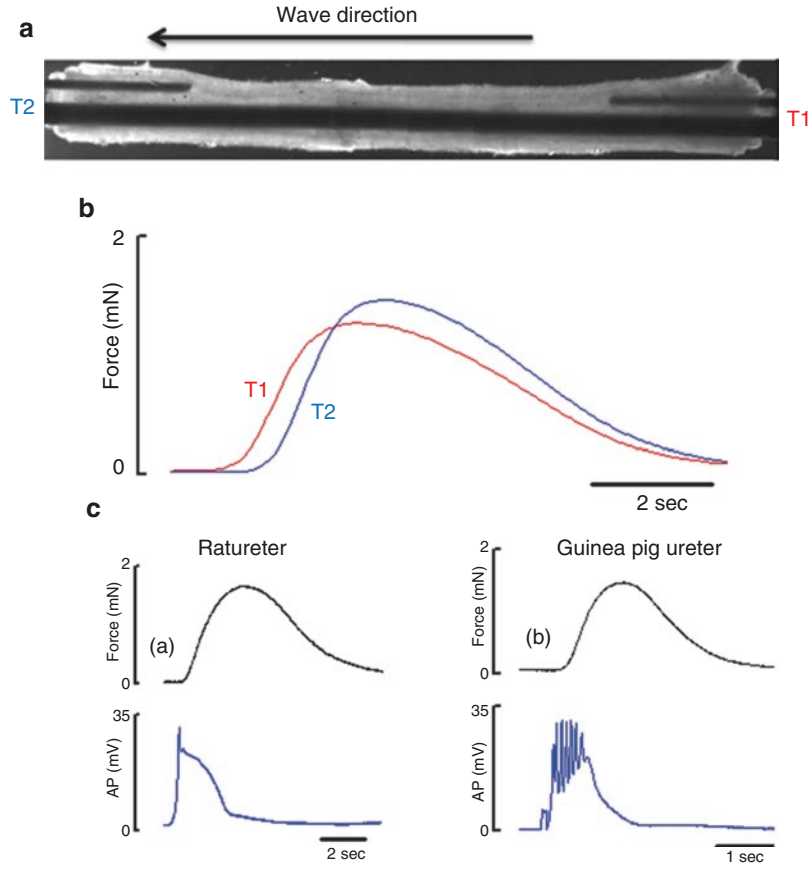

Fig. 4.2 Axial conduction of phasic contraction evoked by local electrical filed stimulation of the guinea pig ureter. (**a**) Image of a guinea pig ureteric segment mounted in the experimental chamber. To measure propagation of contraction along the ureter the force was measured from two ends with two force transducers T1 and T2, respectively. The ureter is mounted on a supporting pin inserted into the lumen and is fixed to the bottom of the experimental chamber. With the help of two 3d manipulators the force transducer extension rods, bent at 90°, are moved into the lumen at each end. (**b**) Superimposed records of a propagating phasic contraction from T1 to T2 in response to a depolarizing pulse of KCl applied at T1. The speed of propagation of force in the guinea pig ureter ranges from 1.2 to 2.2 cm/s. (**c**) Typical records of the evoked AP (bottom trace) and force (top trace) recorded by double sucrose gap method from 1 mm segment of rat (a) and guinea pig (b) ureter in response to an electrical depolarizing pulse

velocity of electrical and mechanical waves is slower in the proximal ureter than in the distal segment [12, 14, 16, 18]. There is a tight coupling between AP and phasic contraction (Fig. 4.2). The delay between electrical activity and the mechanical response is in the order of 0.1–1 s [12, 14].

The earliest recordings of the ureteric electrical activity made with intracellular electrodes established that the conduction of the AP down the length of the ureter could be adequately explained if all ureteric smooth muscle cells are electrically coupled to act as a single electrical cable [22]. Ureteric smooth muscle possesses resistive and capacitative membrane properties similar to those of a cable or core conductor. The transverse resistance of the membrane is higher than the longitudinal resistance of the extracellular or intracellular fluid. This allows current resulting from a stimulus to propagate along the length of the ureteric muscle bundles. The spread of current is referred to as electrotonic spread. The space constant (λ) determines the degree to which the electrotonic potential dissipates with increasing distance from an applied voltage. The space constant of the guinea pig ureter is around 2.5–3 mm [22]. The intercellular resistance of gap junctions is in series with the intracellular resistance of the cytoplasm, and together they represent longitudinal resistance. Both resistances can affect conduction of AP but it is the gap junction channels composed of connexions 43 and 45 that dominates longitudinal resistance [11]. Blockers of gap junctions such as 18β-glycyrrhetinic acid or carbenoxolone prevent the propagation of AP, Ca^{2+} waves and contractions in the ureter [23, 24] and transform normal single-unit into abnormal multi-unit pattern of behaviour in the guinea pig ureter [25]. Recently it was shown that knock-out of the cell adhesion CAR-like membrane protein (CLMP) in mice leads to downregulation of connexion 43 and 45 expression in ureter which prevents normal propagation of peristaltic waves and is associated with functional obstruction in the ureter [11].

4.4 Action Potential

The early recordings of the electrical activity of the ureteric smooth muscle strips made with intracellular microelectrode and extracellular sucrose gap recording techniques [22, 26–29], or in single current-clamped ureteric myocytes [30–32] demonstrated that the ureteric AP is unique in its shape and duration consisting of initial spike followed by a long-lasting plateau phase. In the rat and human ureter, the AP consists of an initial single spike followed by a clear plateau phase (Fig. 4.2c(a)) [33, 34], whereas in the guinea pig ureter the initial spike is normally followed by a group of spikes superimposed on the plateau phase (Fig. 4.2c(b)) [22, 27–29]. The recorded values of resting membrane potentials in ureter of different species are: −45 mV in cat ureter [26], −60 mV in human ureter [35], −55 mV in rat ureter [36], and −68 mV in the guinea pig ureter [22, 37, 38]. The threshold for initiating an AP lies around −40 mV. The AP recorded from single ureteral cells had a remarkable resemblance to that recorded from the intact ureter [30–32], although the spikes recorded from the intact tissue are more regular and regenerative than the potential oscillations seen in isolated cells [31].

The nature of the ionic conductance changes underlying the various phases of the ureteric AP was originally examined using ion replacement protocols, as well as the application of specific ion channel blockers or agonists. Removal of Ca^{2+} from the bathing saline or the application of the Ca^{2+}-entry blockers nifedipine, La^{3+}, Cd^{2+}, Co^{2+} La^{3+} or verapamil, lead to a complete cessation of AP in the guinea pig ureter [39] or ureteric myocytes [30] (Fig. 4.3a bottom panel). In contrast, raising the extracellular Ca^{2+} increases the amplitude of the initial spike(s) and reduces, if not completely abolishes, the plateau phase [27, 35]. In the guinea pig ureter the removal of Na^{+} from the external medium suppresses the plateau phase until only the initial spike is recorded [29, 30, 39, 40]. The effects of Na^{+}-free solution on the plateau phase of the guinea pig ureteric AP were first explained by the opening of voltage-activated, slowly closing inward channels, which

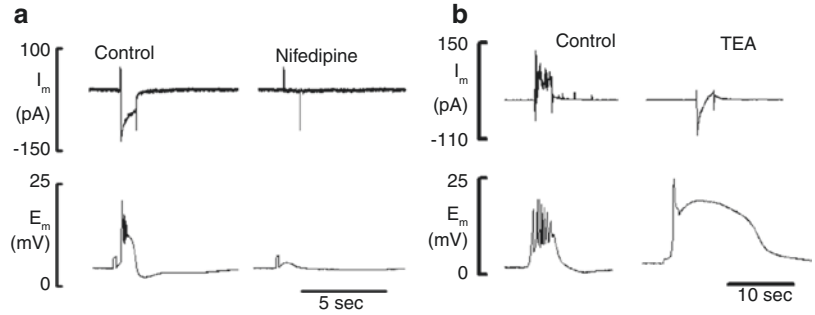

Fig. 4.3 Effects of nifedipine and TEA on membrane ion currents and action potential of the guinea pig ureter. (**a**) Effects of nifedipine (1 μM) on inward Ca^{2+} current recorded from patch clamped guinea pig ureteric myocytes with Cs^+ in the pipette solution (top panel) and AP recorded from guinea pig ureteric segment using double sucrose gap method (bottom panel). Nifedipine fully blocks inward current and AP. (**b**) Effects of TEA (5 mM) on total membrane current recorded from guinea pig ureteric myocytes (top panel) and AP recorded from guinea pig ureteric segment (bottom panel) using double sucrose gap method. TEA fully blocks all oscillatory outward currents to reveal the inward Ca^{2+} current, TEA also blocks the train of spikes and prolongs the plateau phase of the action potential

are permeable for both Na^+ and Ca^{2+} and insensitive to TTX [28]. However the inward current recorded in enzymatically isolated single cells of the guinea pig ureter are selective only for Ca^{2+} and is fully eliminated by the removal of extracellular Ca^{2+}. Thus, it seems that an elevation of $[Ca^{2+}]_i$ is required for establishing the Na^+-dependent contribution to plateau component. This behaviour may involve the activation of an electrogenic Na/Ca exchanger in forward "Ca^{2+} extrusion" mode. Several results indicate that a Na/Ca exchanger exists in the guinea pig ureter and works in reverse "Ca^{2+}-entry" mode in Na^+-loaded preparations [37, 38, 41]. The Ca^{2+} rise and contraction developing under these circumstances are dependent upon the intracellular Na^+ concentration and the presence of extracellular Ca^{2+}, resistant to L-type Ca channel blockers [37, 38, 41]. In single voltage clamped guinea pig ureteric myocytes the Na/Ca exchanger was shown to operate in forward "Ca^{2+}- extrusion" mode over the physiologically relevant range of membrane potential and could generate an inward current contributing to the plateau phase of the AP [42]. The application of low concentrations of nifedipine, papaverine [40] or caffeine [43] suppress the plateau phase until only the initial spike(s) are recorded. In contrast, the duration of the plateau phase of electrically evoked APs in the guinea pig and human ureter can be increased by either replacing extracellular Ca^{2+} with Sr^{2+} or in the presence of the K^+ channel blocker tetraethylammonium [28, 29, 40], the Ca^{2+} channel agonist BayK8644 [44–46] or excitatory agonists [34, 47–49].

4.5 Ionic Currents/Channels in Ureteric Myocytes

4.5.1 Ca^{2+} Current/Ca^{2+} Channels

Membrane ionic currents and channels involved in the generation of the ureteric AP have been characterized by use of voltage clamp techniques in single ureteric smooth muscle cells by several groups [30–32, 50–53]. Several important aspects of inward Ca^{2+} current (I_{Ca}) in ureteric myocytes have been revealed: [1] Ca^{2+}-induced inactivation of I_{Ca} is slow; [2] the inactivation does not increase significantly in response to a train of depolarizing pulses; and [3] a very slowly inactivating or noninactivating "window" current can flow through the Ca^{2+} channels at the plateau potential. This current is increased in amplitude in the presence of Bay K 8644 [32], when the

external Ca^{2+} is replaced with Ba^{2+} [32, 46, 52] and is blocked in the absence of external Ca^{2+} [50] or in the presence of the Ca^{2+} entry blockers, nifedipine, La^{3+}, Cd^{2+}, Co^{2+}, La^{3+} or verapamil (Fig. 4.3a top panel) [30, 31, 50, 51]. Based on these studies it was concluded that the very slow inactivation of I_{Ca} and its poor Ca^{2+}-induced inactivation contribute to the plateau phase of the AP. Simultaneous measurements of Ca^{2+} current through L-type Ca^{2+} channels upon step depolarizations and $[Ca^{2+}]_i$ revealed a close correlation between I_{Ca} and its concomitant increase in $[Ca^{2+}]_i$; both I_{Ca} and the increased $[Ca^{2+}]_i$ exhibit a bell-shaped voltage dependence with a peak at 0 mV and are blocked by nifedipine [42]. Collectively, these studies reveal that voltage-dependent Ca^{2+} channels of the L-type provide the main Ca^{2+} inward current detected in ureteric smooth muscle cells.

4.5.2 K^+ Current/K^+ Channels

Two main outward currents have been identified in the guinea pig ureteric myocytes [30, 31, 50, 51, 53], a TEA- and charybdotoxin-sensitive Ca^{2+}-dependent K^+ current or $I_{K(Ca)}$ and a voltage-dependent Ca^{2+}- and TEA-insensitive transient K^+ current (I_{TO}) which is blocked by 4-aminopyridine (4-AP). The potential oscillations during the initial phase of the AP in the intact ureter correspond in time with the repeating transient outward currents recorded upon membrane depolarization in single ureteric myocytes under voltage clamp. These outward current oscillations in the single ureteric myocytes [31, 53] and membrane potential oscillations in the intact tissue [39, 47] are readily blocked by TEA, while the plateau phase of the AP is significantly increased (Fig. 4.3b bottom panel) [31, 53] and arise from the increased activity of large conductance Ca^{2+}-sensitive K^+ (also known as BK or "maxi-K") channels. These BK channels previously observed in excised ureteric membrane patches have a single channel "slope" conductance of 220 pS in a symmetrical high K^+ (126 mM) gradient [30]. They are readily blocked by TEA and charybdotoxin (Fig. 4.3b top panel) [30, 31, 53] and are activated by both membrane depolarization and rises in $[Ca^{2+}]_i$ [30].

Under voltage clamp conditions, ureteric myocytes display spontaneous transient outward currents (STOCs) arising from the opening of BK channels [30, 43, 54], similar to those described in other types of smooth muscle cells [55]. STOCs are known as the electrophysiological counterpart of Ca^{2+} sparks [55]. Also, $I_{K(Ca)}$ seems to be the major target for the excitatory action of noradrenaline in the guinea pig ureter [48]. By suppressing $I_{K(Ca)}$ more than I_{Ca}, noradrenaline causes a marked prolongation of the AP plateau which may account for its excitatory effect on the guinea pig ureter [48]. The role of I_{TO} is unclear because it would be rapidly inactivated by depolarization and does not seem to be suited for modulating the shape of the AP [30, 31, 53]. I_{TO} may regulate membrane excitability by opposing the Ca^{2+} current activated around the threshold of the AP [30, 31]. Thus, $I_{K(Ca)}$ is the most important current in ureteric smooth muscle controlling both repolarization and AP plateau duration.

4.5.3 Cl^- Currents/Cl^- Channels

There are species differences in the ionic currents involved in the formation of the AP in the ureter, with the Ca^{2+}-activated Cl^- current ($I_{Cl(Ca)}$) being present in the rat but not in the guinea pig ureter [46, 56]. The inward Cl^- current can be activated by Ca^{2+} entering the cell via L-type VGCCs and is seen as a tail current upon stepping back to a holding potential [46, 56] or as a large inward current upon the release of Ca^{2+} from internal store by carbachol [46]. Cl_{Ca} current is inhibited by niflumic acid and by Ba^{2+} [46, 57] and maybe involved in the plateau formation of the AP in the rat ureter [56, 57]. The depolarizing action of $I_{Cl(Ca)}$ can also activate spontaneous activity of the rat ureter in response to agonists (Fig. 4.7) [58]. Cl_{Ca} channels are sensitive to temperature. Cooling has a significant potentiation effect on the $I_{Cl(Ca)}$ and the duration of the AP plateau in rat but not guinea pig ureter [56]. However, a lack of specific pharmacological blockers has hampered

efforts to identify the functional role of Cl^- channels in ureteric smooth muscle.

4.6 Calcium and Excitation-Contraction Coupling in Ureter

The propagating AP gives rise to the wave of contraction of ureteral peristalsis via a process known as excitation-contraction (E-C) coupling. It is generally accepted that the second messenger in this transduction system is Ca^{2+} which acts as the primary regulator of smooth muscle contraction. To activate the contractile apparatus, Ca^{2+} must increase globally throughout the cytoplasm. A global rise in $[Ca^{2+}]_i$ activates Ca^{2+}/calmodulin-dependent myosin light chain kinase (MLCK), which phosphorylates the 20-kDa regulatory light chains of myosin, thereby triggering cross-bridge cycling and contraction in all types of smooth muscle including ureter [46, 58]. Similar to other excitable cells, ureteric myocytes have a sophisticated Ca^{2+} control system that keeps $[Ca^{2+}]_i$ at low levels at rest and ensures, that $[Ca^{2+}]_i$ is rapidly and uniformly elevated within each myocyte in response to the propagating AP.

4.6.1 Action Potential-Mediated Ca^{2+} Transient

The generation, modulation, and termination of the intracellular Ca^{2+} transient is the essence of E-C coupling in ureteric smooth muscle. The Ca^{2+} transient is initiated by the entry of Ca^{2+} into the cell via L-type VGCCs which open during the AP (Fig. 4.3a). The favourable and large electrochemical gradient (low cellular Ca^{2+} concentration, cell interior being electronegative) provides a strong driving force for the influx of Ca^{2+} via VGCCs during the AP. In the guinea pig and rat ureter, the Ca^{2+} transient is closely correlated with the phases of their AP (Fig. 4.4C) [33, 49, 54, 59] and is observed as a spreading intercellular Ca^{2+} wave accompanied by a mechanical wave (Fig. 4.4A, B, Supplementary Video 4.1). The initial spike gives rise to a fast increase in Ca^{2+} (the upstroke of Ca^{2+} transient) followed by gradual rise to the steady state during the AP plateau phase [33, 49, 54, 59]. Approximately 30–40% of the elevation of $[Ca^{2+}]_i$ occurs during the upstroke of the initial spike whereas about 70% of total elevation of $[Ca^{2+}]_i$ is contributed by the plateau phase of the AP [33]. In the guinea pig ureter, the Ca^{2+} wave propagates in a regenerative manner from the point of stimulation via ureteric muscle bundles with a constant amplitude and a speed around 1.5–2 cm/s (Fig. 4.4A, B) and is seen as a Ca^{2+} transient coupled to both components of the AP and associated brief phasic contraction (Fig. 4.4C).

The relation between $[Ca^{2+}]_i$ and contraction force during the rising and the relaxation phases of the AP exhibits hysteresis, i.e. force at a given $[Ca^{2+}]_i$ during the rising phase of contraction is always lower than during the relaxation phase [49, 56]. This indicates that in ureteric smooth muscle there are slow steps linking Ca^{2+} and force development during the time course of the AP-mediated phasic contractions [49, 56]. Ca^{2+} transient and force are fully blocked in the presence of the L-type voltage-dependent Ca^{2+} channel blocker nifedipine or in the absence of extracellular Ca^{2+} [7]. So influx of Ca^{2+} into ureteric smooth muscle cells via L-type VGCCs is causing a quick and uniform rise of $[Ca^{2+}]_i$ throughout the bulk of the cytoplasm. The duration of the Ca^{2+} transient is coupled to the duration of the plateau phase of the AP and plays a key role in controlling the amplitude and duration of the phasic contraction (Fig. 4.6) [49, 59]. The duration of the plateau phase and associated Ca^{2+} transient can be increased by agonists, e.g. noradrenaline, histamine [49], Ca^{2+} channel agonist BayK 8644 [46], the K^+ channels blocker TEA (Fig. 4.6 left panel) [49] and sarco-endoplasmic reticulum Ca^{2+} pump inhibitor cyclopiazonic acid (Fig. 4.6 middle panel) [59]. A decrease in the duration of the plateau and Ca^{2+} transient can be achieved upon removal of external Na^+ [49], or activation of BK channels via stimulation of the Ca^{2+} sparks/STOCs coupling mechanism, e.g. by low concentrations of caffeine (Figs. 4.5 and 4.6 right panel) [43]. The fact that depletion of the sarcoplasmic reticulum

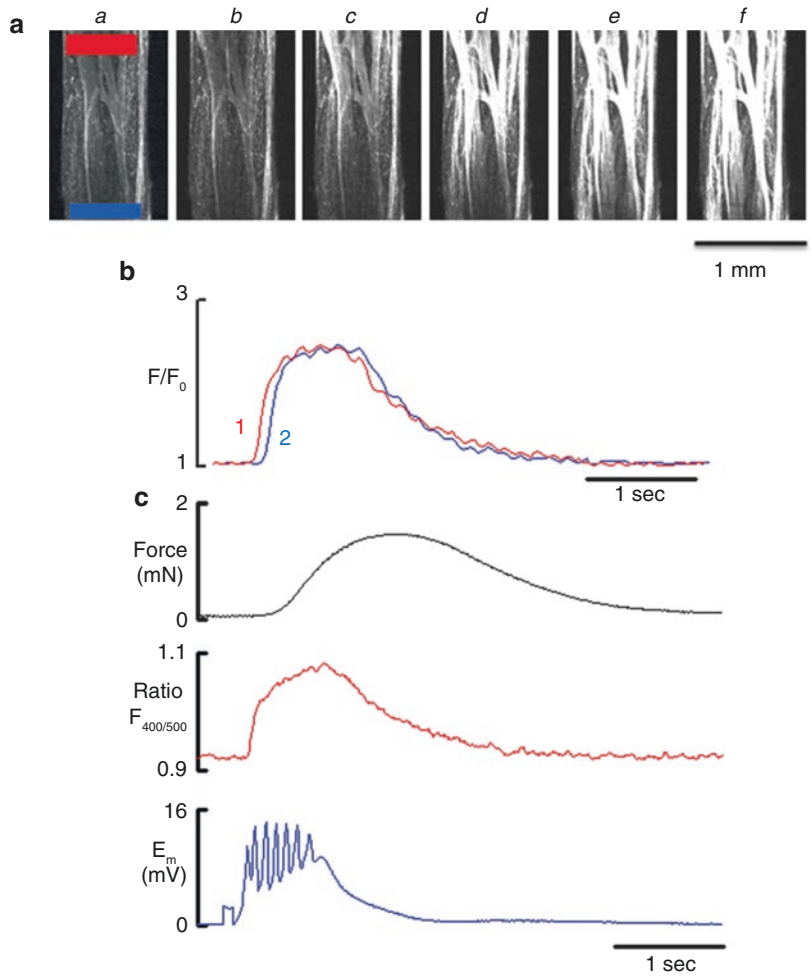

Fig. 4.4 Axial conduction of Ca^{2+} wave evoked by local electrical filed stimulation of the guinea pig ureteric lower segment. (**a**) Sequential images of fluo-4 loaded guinea pig ureteric segment at rest (a) and during propagation (b–f) of the intercellular Ca^{2+} wave evoked by EFS, images captured every 55 ms. (**b**) Superimposed records of propagating Ca^{2+} wave from region 1 (red bar) to region 2 (blue bar) in **A**a. The speed of propagation of the Ca^{2+} wave in the guinea pig ureter ranges between 1.2–2.2 cm/s. (**c**) Typical records of the evoked AP (bottom trace), Ca^{2+} transient (middle trace) and force (top trace) recorded by double sucrose gap method from a 1 mm segment of the guinea pig ureter. The intercellular Ca^{2+} wave appears as a Ca^{2+} transient coupled to the AP. There is a significant delay between rise of Ca^{2+} and force during phasic contraction

(SR) Ca^{2+} stores by cyclopiazonic acid causes a stimulant action in the guinea pig ureter [59, 60] indicates that the SR Ca^{2+} release does not contribute to the global rise in $[Ca^{2+}]_i$ in ureteric smooth muscle. Thus, the major source of activator Ca^{2+} in ureteric smooth muscle during the generation of AP is Ca^{2+} influx through L-type VGCCs alone [7, 40, 44, 45]. In summary, the AP in the ureter plays a pivotal role in control of ureteric smooth muscle contraction through depolarization of the cell membrane coupled to influx of Ca^{2+} through L-type VGCCs. The Ca^{2+} transient associated with the AP appears as a regenerative intercellular Ca^{2+} wave accompanied by wave of contraction, this wave underlies ureteric peristalsis.

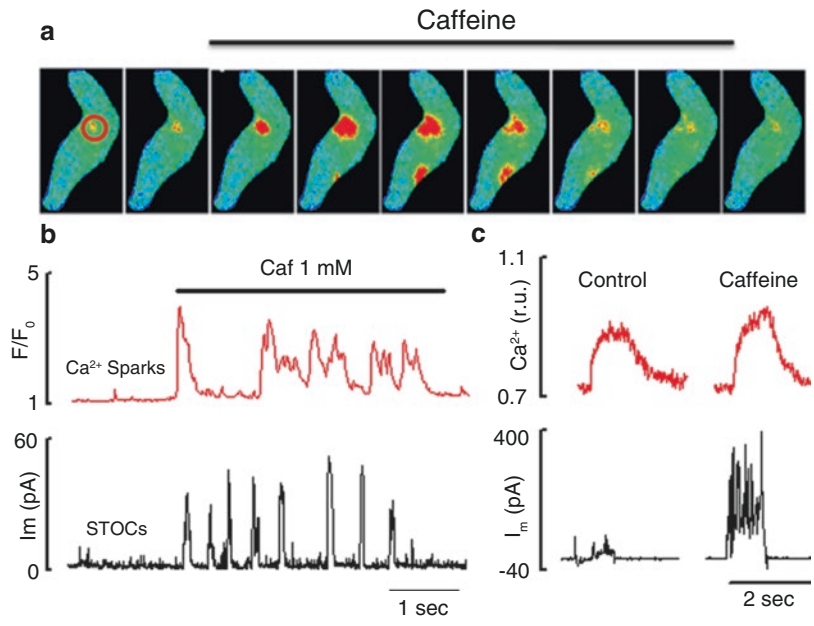

Fig. 4.5 Effects of caffeine on Ca^{2+} sparks and STOCs in the guinea pig ureteric myocytes. (**a**) Sequential images (captured every 30 ms) of a fluo-4 loaded guinea pig ureteric myocyte showing the effects of caffeine on the spatial spread of Ca^{2+} sparks. (**b**) Effects of caffeine (1 mM) on simultaneously recorded Ca^{2+} sparks (top panel) and STOCs (bottom panel). (**c**) Effects of caffeine on the global rise of intracellular Ca^{2+} (top trace) and total ionic currents (bottom trace) evoked by voltage step from −60 to 0 mV in a voltage clamped Fura 2 loaded myocyte

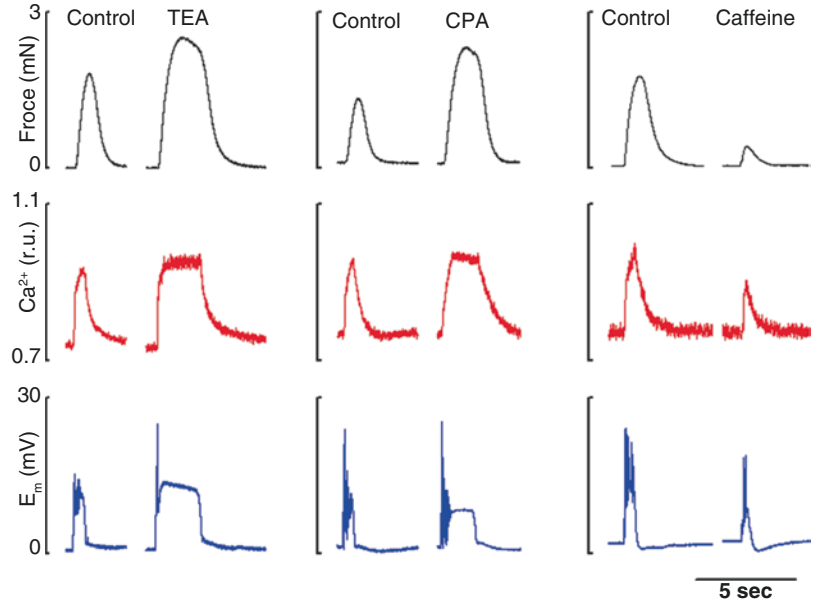

Fig. 4.6 Effects of TEA, cyclopiazonic acid (CPA) and caffeine on temporal relationship between action potential (bottom trace), Ca^{2+} transient (middle trace) and force (top trace) in the guinea pig ureter. Inhibition of K^+ channel blocker by TEA (left panel) or SR function by CPA (middle panel) causes prolongation of the AP plateau associated with an increase in the duration of the Ca^{2+} transient and the amplitude and duration of the phasic contraction. Activation of Ca^{2+} sparks and STOCs by caffeine (right panel) causes inhibition of the plateau component of the AP associated with the decrease in the amplitude and duration of both Ca^{2+} transient and force

4.6.2 Ca^{2+} Signalling Induced by Ca^{2+} Release from the SR

Ca^{2+} release from the SR in smooth muscle cells occurs through activation of two families of Ca^{2+} release channels, the ryanodine receptors (RyRs) and inositol 1,4,5-trisphosphate receptors (IP_3Rs). Both types of receptors occur in three isoforms, RyR1, RyR2, RyR3, and IP3R1, IP3R2, IP3R3, respectively [61]. In ureter, Ca^{2+} release from the SR is species dependent with RyRs being the dominant mechanism for Ca^{2+} release in the guinea pig [62, 63] and IP_3Rs in the rat ureter [63, 64]. In the rat ureter expression of IP_3R is 10–12 times higher than that of RyRs [64]. Both IP_3Rs and RyRs are expressed in the human ureter [7]. Coupling between the SR-mediated Ca^{2+} events and the Ca^{2+}-sensitive ion channels can lead to changes in membrane potential and the parameters of the AP and thus serve as powerful negative or positive feedback mechanisms controlling excitability and contractility of ureteric smooth muscle.

4.6.2.1 Ca^{2+} Sparks

The opening of caffeine- and ryanodine-sensitive Ca^{2+} release channels in smooth muscle produces small local elevations of Ca^{2+} that are termed Ca^{2+} sparks (Fig. 4.5) [65]. In the guinea pig ureter Ca^{2+} sparks are produced by several frequently discharging sites (FDS) located at the edge of the cell membrane and occur spontaneously or in response to low concentration of caffeine (Fig. 4.5a, b) [43, 54]. Caffeine at 1 mM causes an increase in the amplitude, frequency and spatial spread of the these Ca^{2+} sparks as well as an increase in the number of the discharging sites per cell (Fig. 4.5a, b, Supplementary Movie 2) [43]. Ca^{2+} sparks are short lived and show variability in amplitude, time course and spatial spread, suggesting that RyRs channels exist in clusters containing a variable number of channels. In the guinea pig ureter, Ca^{2+} sparks activate BK channels causing STOCs (Fig. 4.5b bottom panel) [54]. Ca^{2+} sparks and STOCs are blocked selectively by ryanodine [43, 54]. Regulating the frequency and amplitude of Ca^{2+} sparks and STOCs is an important factor controlling electrical activity in the ureteric smooth muscle. The amplitude and frequency of Ca^{2+} sparks and STOCs in guinea pig ureter depend on SR Ca^{2+} loading ($SR_{[Ca]}$). The $SR_{[Ca]}$ regulates Ca^{2+} release by stimulating RyRs on the luminal side of the store. The mechanism of this facilitation is still poorly understood. In the guinea pig ureter an increase in the $SR_{[Ca]}$ during the global rise of intracellular Ca^{2+} associated with the AP leads to a transient increase in the amplitude and the frequency of Ca^{2+} sparks and STOCs [54]. As a result, the increase in the summed outward K^+ current hyperpolarizes the cell membrane, decreases the excitability and contributes to the refractory period [54]. The refractory period is important in determining the frequency of ureteral peristalsis [54, 66]. Inhibition of Ca^{2+} sparks, e.g. by ryanodine or cyclopiazonic acid or their target BK channels by TEA or Iberiotoxin results in depolarization, termination of the refractory period and prolongation of the plateau component of the AP, as well as an increase in duration of the Ca^{2+} transient accompanied by an increase in the amplitude and duration of force (Fig. 4.6 left and middle panels) [54]. In contrast, activation of the Ca^{2+} sparks/STOCs coupling mechanism by low concentrations of caffeine results in a decrease in the duration of the plateau component of the AP, Ca^{2+} transient and force without affecting the inward current or global rise of Ca^{2+} induced by depolarising voltage step (Fig. 4.5c right panel), in a manner reversed by ryanodine or BK channels blockers [43]. In summary in the guinea pig ureter Ca^{2+} sparks are produced by several (1–3) FDS and are coupled to activation of BK channels to produce STOCs. The increase in the outward potassium current induced by Ca^{2+} sparks hyperpolarizes the cell membrane, decreases the excitability, increases the refractory period and controls the duration of the plateau phase of the AP.

4.6.2.2 Ca^{2+} Puffs and Waves

Small local elevations of Ca^{2+} produced by the opening of the IP_3 receptor channels are termed Ca^{2+} puffs [67, 68]. The IP_3 receptor-operated store was found to be the main source of Ca^{2+} in rat ureter [63, 64]. Ca^{2+} release by this mecha-

nism is coupled to G protein-regulated receptors [63, 64]. In rat ureteric myocytes Ca^{2+} puffs are observed during photo-release of low concentrations of IP_3 from a caged precursor or in the presence of low concentrations of acetylcholine [64]. They can also occur spontaneously in Ca^{2+}-overloaded myocytes [64]. Spontaneous Ca^{2+} puffs have also been observed in intact rat ureteric preparations [61]. Ca^{2+} puffs showed large variability in amplitude, time course and spatial spread, suggesting that IP_3R—channels in ureteric myocytes also—exist in clusters containing variable numbers of channels and that within these clusters a variable number of channels can be recruited [64]. Immuno-detection of IP_3Rs show that in addition to an homogeneous distribution, IP_3R are also detected in clusters located at several areas within the ureteric myocytes [64]. Ca^{2+} puffs in rat ureteric myocytes are blocked selectively by intracellular applications of heparin or an anti-IP_3R antibody, but are unaffected by ryanodine and intracellular application of an anti-ryanodine receptor antibody [64]. Stimulation with higher concentrations of acetylcholine [64] or carbachol [43] stimulate the generation of propagating intercellular Ca^{2+} waves. Ca^{2+} waves are asynchronous between smooth muscle cells and are initiated frequently at one of the ends and propagate to the other end of the cell. Ca^{2+} waves appear to result from the spatial recruitment of several Ca^{2+}-release sites and propagate at a speed around 30–70 μm/s. To date, the physiological roles of Ca^{2+} puffs in rat ureteric myocytes remain elusive. Ca^{2+} waves are coupled to the activation of both Cl_{Ca} and BK channels (Fig. 4.7a). The coexistence of Cl_{Ca} and BK channels in the cell membrane in rat ureteric myocytes suggests another level of fine control of membrane excitability through Ca^{2+} waves in rat ureter. At negative membrane potentials <-50 mV, the predominant effect of Ca^{2+} waves is to trigger inward current since at these levels of membrane potential the electrochemical driving force for Cl^- is greater than that for K^+. The activation of Cl_{Ca} channels can cause membrane depolarization and thus serve as a positive feedback mechanism to trigger the activation of voltage-gated Ca^{2+} channels and the excitation of the ureteric myocytes (Fig. 4.7b) [43]. In contrast, at more positive potentials the electrochemical driving force for K^+ will make BK channels more active and this will enable large outward current to oppose the effects of any depolarising factors and prevent over-reactivity of ureteric smooth muscles. One can speculate that Ca^{2+} waves in ureteric smooth muscle can control any membrane potential oscillations acting as a pacemaking mechanism. Thus, in rat ureteric myocytes the Ca^{2+} responses to acetylcholine/carbachol depend on the activation of IP_3Rs and appear as Ca^{2+} puffs and waves. Ca^{2+} waves are coupled to activation of both Cl_{Ca} and BK channels presenting a novel mechanism underlying the control of excitability and contractility in at least rat ureter.

4.7 Effects of Biological Effectors

Under normal conditions the ureters, isolated from the renal pelvis, are not spontaneously active. However, spontaneous activity can be initiated by a variety of biological effectors such as mechanical stretch, neurotransmitters, paracrine, endocrine and inflammatory factors [34, 58, 69–78]. Agonist-induced ureteral spontaneous contractions have been shown to play a major role in causing the pain associated with ureteral colic [79]. The effects of agonists depend on species and position on the ureter. In the presence of agonists, ureteric smooth muscles cells depolarise to a threshold of AP activation and begin to act as pacemaker cells producing antegrade and/or retrograde peristalsis of ureter. Majority of the agonists activate the ureter via activation of the G protein-coupled receptor (GPCR) family. Activation of GPCRs leads to the activation of phospholipase C (PLC), which in turn leads to formation of second messengers IP_3 and diacylglycerol (DAG) [68]. IP_3 is involved in the mobilization of Ca^{2+} from the SR [80], whereas DAG increases Ca^{2+} influx across the cell membrane via the activation of protein kinase C [81]. Several mechanisms have been proposed to account for agonist-induced depolarization of ureteric smooth muscles which include suppression of outward

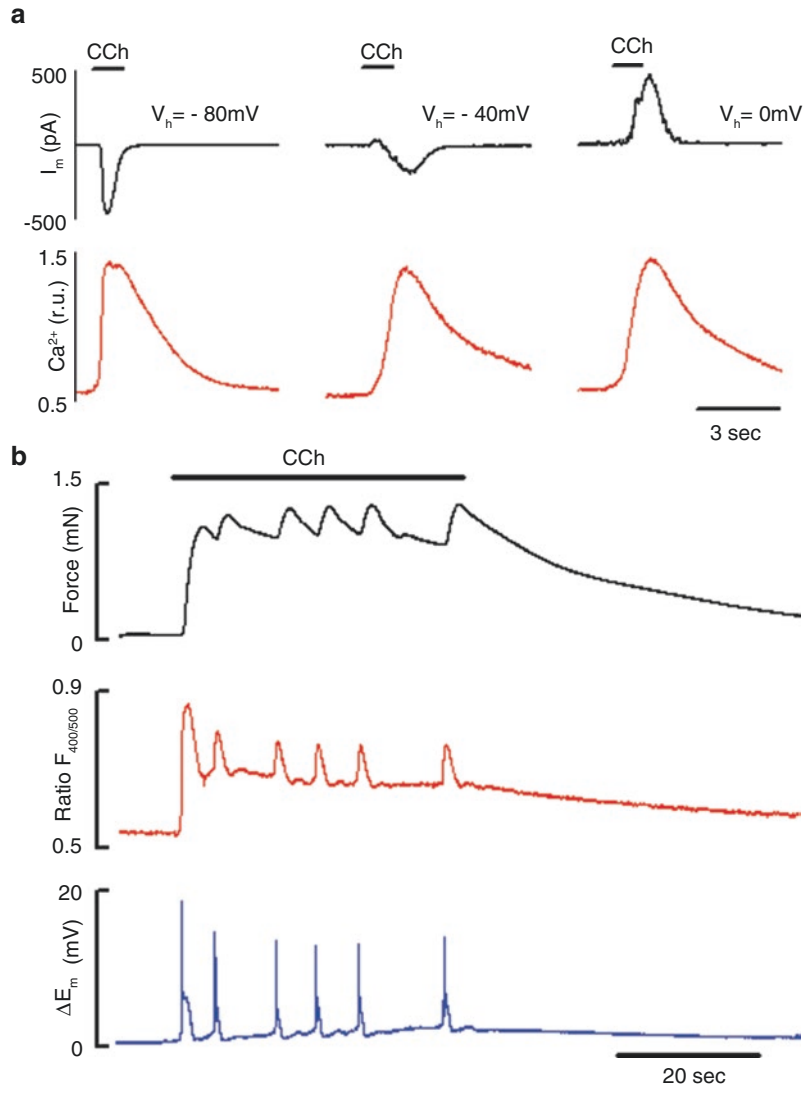

Fig. 4.7 Effects of carbachol (CCh) on the electrical activity, Ca^{2+} signalling and force in the rat ureter. (**a**) Biphasic membrane current (top trace) activated by Ca^{2+} transient (bottom trace) induced by CCh in voltage clamped Indo-1 loaded rat ureteric myocyte at different holding potentials. (**b**) Effects of CCh on electrical activity (bottom trace), Ca^{2+} signalling (middle trace) and force (top trace) of the rat ureter recorded by double sucrose gap method

potassium currents [47, 48], activation of Cl_{Ca} current [46, 58] and activation of non-selective cation receptor/store operated channels [34, 58, 78].

4.7.1 Effects of Neurotransmitters

The ureter is supplied by both sympathetic and parasympathetic systems [82, 83]. The expression and distribution of adrenergic and muscarinic receptors depend on the species and anatomical location on the ureter. The human and canine ureter contains α-adrenergic receptors along their entire length [84–86], with α1 adrenoreceptors predominantly expressed in the distal segment [73]. The presence of five muscarinic receptor subtypes (M1–M5) were immunohistochemically shown in the human ureter [87]. Activation of α-adrenoceptors with noradrenaline or adrenaline stimulates spontaneous contractions in the human [71, 84, 85] and guinea pig [69] ureter. Also in the intact guinea pig ureter [47] or after cell isolation [48] noradrenaline causes a prolongation of the AP plateau. Stimulant action of noradrenaline on the guinea pig ureter is caused by inhibition of K^+ conductance [47] via decreasing the activity of $I_{K(Ca)}$ upon a decrease in the SR Ca^{2+} content [48]. Activation of musca-

rinic receptors stimulates spontaneous contractions in the pig [88], human [89], rat [58] and guinea pig [90] ureter, but has little effect on the porcine distal ureter [90]. In rat ureter, carbachol causes membrane depolarization, superimposed by bursts of action potentials associated with Ca^{2+} transient and phasic contractions (Fig. 4.7b) [58]. The mechanisms of stimulant action of carbachol on rat ureter includes IP_3-mediated Ca^{2+} release from the SR [58, 63, 64] coupled to activation of Cl_{Ca} channels and the opening of nifedipine-resistant Ca^{2+} entry via voltage-independent receptor/store operated and nifedipine-sensitive VGCCs [58].

4.7.2 Effects of Neuropeptides

The ureter contains capsaicin-sensitive sensory nerves [76, 91, 92]. The neuropeptides neurokinin A (NKA) and substance P (SP) may play a significant role in control of the spontaneous activity of the proximal and distal ureter as these areas exhibit a high SP and NKA content and receptors [93]. In the rat ureter, the contractile responses to tachykinins are mediated by NK_2 and NK_3 receptors [74] while in human and guinea pig ureter it is mediated exclusively by NK2 receptors [34]. NKA/SP receptors are proteins belonging to the G protein-coupled receptor family [94]. When applied to the quiescent isolated ureter of the human, rat and guinea pig, NKA and SP produce spontaneous activity characterized by the appearance of rhythmic and long-lasting phasic contractions associated with prolonged APs superimposed on a slow membrane depolarization [34]. In the guinea pig ureter, spontaneous APs and phasic contractions induced by tachykinins are blocked by nifedipine [34] while in the human ureter, the depolarization and tonic contraction are resistant to nifedipine [34]. A nifedipine-resistant depolarization may involve suppression of outward K^+ currents, the activation of $I_{Cl(Ca)}$ and/or activation of non-selective cation channels [34]. It is suggested that NKA-induced prolongation of APs is caused by inhibition of repolarizing K^+ currents [34, 94].

4.7.3 Effect of Bradykinin

Bradykinin is one of pharmacologically active ingredients of kinins present in urine inducing spontaneous activity in ureteric smooth muscle of various species [72, 78]. Bradykinin effects are mediated mostly by the high affinity B_2-subtype receptor a member of the G protein-coupled receptor family and considered as the chief receptor in human and rats [75, 77, 95]. The presence of B_2 receptors in ureter has been established by pharmacological, radio ligand binding studies and receptor cloning and expression analysis [77, 93, 96]. The anatomic distribution of bradykinin receptors in the ureter corresponds to regions of increased spontaneous ureteral contractility, more specifically the proximal and distal ureter [93]. The mechanism of stimulant action of bradykinin on ureteric smooth muscle includes voltage-independent receptor/store operated and L-type VDCCs [78].

4.8 Clinical Implications

From the clinical perspective, pharmacological research on spontaneous ureteric contractility has been prompted by renal colic, vesicoureteric reflux (VUR), and urinary tract infection. There is a great interest in pharmacologic modulation of ureteral contractility during stone passage as the pain associated with acute ureteral colic has been described as one of the most intense experienced by humans. Ureteral stones occupy an important place in daily urological practice, usually causing an acute episode of ureteral colic by obstructing the urinary tract and most of these calculi are usually impacted in the lower portion of the ureter [95, 97]. Ureterovesical junction obstruction causes spontaneous ureteric activity and sensitizes the smooth muscle of distal ureter to cholinergic, adrenergic or serotonergic responses [98]. An increased sensitivity of the distal ureter to humoral agents at least theoretically, can cause urine to flow retrogradely from the bladder to the kidneys. Based on a high expression of α1-adrenoceptors and involvement of adrenergic receptors in control of ureteric

activity in distal ureter, α1-adrenoreceptor antagonists have been introduced for medical expulsion therapy [99, 100]. VUR is a congenital defect of the urinary tract that can also cause urine to flow retrogradely from the bladder to the kidneys which can be associated with ureteric and renal infections [101]. Some clinical observations suggest that bacterial infection can play a significant role in the pathogenesis of ureter and kidney [102–104]. As a result, bacterial infection can cause renal damage and subsequent renal failure [102–104]. Recently it has been shown that strains of uropathogenic *Escherichia coli* isolated from human pyelonephritis patients have an inhibitory effect on Ca^{2+} signalling and contractility of rat and human ureter by inhibiting L-type VGCCs and activation of K_{Ca} channels and this mechanism is dependent on a host-urothelium interaction [105, 106]. As yet, the mechanisms mediating these effects are unknown and clearly warrant further studies. An improvement or even complete recovery of ureteric smooth muscle function normally follows eradication of the bacterial infection [104].

In conclusion, more studies are needed to understand the mechanisms involved in the disruption of normal ureteral function under a variety of pathophysiological conditions.

References

1. Notley RG. The musculature of the human ureter. Br J Urol. 1970;42:124–7.
2. Uehara Y, Burnstock G. Demonstration of gap junctions between smooth muscle cells. J Cell Biol. 1970;44:215–7.
3. Dixon JS, Gosling JA. The musculature of the human renal calices, pelvis and upper ureter. J Anat. 1982;135:129–37.
4. Tachibana S, Takeuchi M, Uehara Y. The architecture of the musculature of the guinea-pig ureter as examined by scanning electron microscopy. J Urol. 1985;134:582–6.
5. Aragona F, Artibani W, de Caro R, Pizzarella M, Passerini G. The morphological basis of ureteral peristalsis. An ultra structural study of the rat ureter. Int Urol Nephrol. 1988;20:239–50.
6. Tahara H. The three-dimensional structure of the musculature and the nerve in the rabbit ureter. J Anat. 1990;170:183–91.
7. Floyd RV, Borisova L, Bakran A, Hart A, Wray S, Burdyga T. Morphology, calcium signalling and mechanical activity in human ureter. J Urol. 2008;180:398–405.
8. Wakahara T, Mori S, Ide C. Ultrastructural study of the ureter smooth muscle of the cat. Nihon Heikatsukin Gakkai Zasshi. 1986;22:63–72.
9. Borysova L, Wray S, Eisner DA Burdyga T. How calcium signals in myocytes and pericytes are integrated across in situ microvascular networks and control microvascular tone. Cell Calcium. 2013;54:163–74.
10. Bush KT, Vaughn DA, Li X, Rosenfield MG, Rose DW, Mendoza SA, Sanjay K, et al. Development and differentiation of the ureteric bud into the ureter in the absence of a kidney collecting system. Dev Biol. 2006;298:571–84.
11. Langhorst H, Jutter R, Groneberg D, Mohtashamdolatshahi A, Pelz L, Purfürst B, et al. The IgCAM CLMP is required for intestinal and ureteral smooth muscle contraction by regulating Connexin 43 and 45 expression in mice. Dis Model Mech. 2018;11:dmm.032128. https://doi.org/10.1242/dmm.032128.
12. Sleator W, Butcher HR. Action potentials and pressure changes in ureteral peristaltic waves. Am J Phys. 1955;180:261–76.
13. Kondo A. The contraction of the ureter. Observations in normal human and dog ureters. Nagoya J Med Sci. 1969;32:387–94.
14. Tindall AR. Preliminary observations on the mechanical and electrical activity of the rat ureter. J Physiol. 1972;223:633–475.
15. Ohhashi T, Miyazawa T, Azuma T. Conduction velocity of peristaltic waves in the in vivo ureter: application of a new diameter guage. Experientia. 1981;37:377–8.
16. Tsuchiya T, Takei N. Pressure responses and conduction of peristaltic wave in guinea-pig ureter. Jpn J Physiol. 1990;40:139–49.
17. Prosser CL, Smith CE, Melton CE. Conduction of action potentials in the ureter of the rat. Am J Phys. 1955;180:651–60.
18. Kobayashi M. Conduction velocity in various regions of the ureter. Tohoku J Exp Med. 1964;83:220–4.
19. Hammad FT, Lammers WJ, Stephen B, Lubbad L. Propagation characteristics of the electrical impulse the normal and obstructed ureter as determined at high electrophysiological resolution. Br J Urol. 2011;108:E36–42.
20. Ishikawa S, Ikeda O. Recovery curve and conduction of action potentials in the ureter of guinea pig. Jpn J Physiol. 1996;10:1–12.
21. Tscholl R, Osypka P, Goetlin J, Zingg E. Measurement of the velocity and rate of ureteral contractions with a video-integrator in a model, in animals, and in humans, peroperatively and with intact body surface. Investig Urol. 1974;12:224–32.

22. Kuriyama H, Osa T, Toida N. Membrane properties of the smooth muscle of guinea-pig ureter. J Physiol. 1967;191:225–38.
23. Lang RJ, Zoltkowski BZ, Hammer JM, Meeker WF, Wendt I. Electrical characterization of interstitial cells of Cajal-like cells and smooth muscle cells isolated from the mouse ureteropelvic junction. J Urol. 2007;177:1573–80.
24. Hashitani H, Nguyen MJ, Noda H, Mitsui R, Higashi R, Ohta K, et al. Interstitial cell modulation of pyeloureteric peristalsis in the mouse renal pelvis examined using FIBSEM tomography and calcium indicators. Pflugers Arch. 2017;469:797–813.
25. Santicioli P, Maggi CA. Effect of 18β-glycyrrhetinic acid on electromechanical coupling in the guinea-pig renal pelvis and ureter. Br J Pharmacol. 2000;129:163–9.
26. Kobayashi M. Relationship between membrane potential and spike configuration recorded by sucrose gap method in the ureter smooth muscle. Comp Biochem Physiol. 1971;38A:301–8.
27. Vereecken RL, Hendrickx H, Casteels R. The influence of calcium on the electrical and mechanical activity of the guinea pig ureter. Urol Res. 1975;3:149–53.
28. Hendrickx H, Vereecken RL, Casteels R. The influence of sodium on the electrical and mechanical activity of the ureter. Urol Res. 1975;3:159–63.
29. Shuba MF. The effect of sodium-free and potassium-free solutions, ionic current inhibitors and ouabain on electrophysiological properties of smooth muscle of guinea-pig ureter. J Physiol. 1977;264:837–85.
30. Imaizumi Y, Muraki K, Watanabe M. Ionic currents in single smooth muscle cells from the ureter of the guinea-pig. J Physiol. 1989;411:131–59.
31. Lang RJ. Identification of the major membrane currents in freshly dispersed single smooth muscle cells of guinea-pig ureter. J Physiol. 1989;412:375–95.
32. Sui JL, Kao CY. Roles of Ca^{2+} and Na^{+} in the inward current and action potential of guinea pig ureteral myocytes. Am J Phys. 1997;41:C535–42.
33. Burdyga T, Wray S. Simultaneous measurements of electrical activity, intracellular [Ca2+] and force in intact smooth muscle. Pflugers Arch. 1997;435:182–4.
34. Patacchini R, Santicioli P, Zagorodnyuk V, Lazzeri M, Turini D, Maggi CA. Excitatory motor and electrical effects produced by tachykinins in the human and guinea-pig isolated ureter and guinea-pig renal pelvis. Br J Pharmacol. 1998;125:987–96.
35. Bennett MR, Burnstock G, Holman ME, Walker JW. The effect of Ca^{2+} on plateau-type action potentials in smooth muscle. J Physiol. 1962;161:47–8.
36. Cole RS, Fry CH, Shuttleworth KE. The action of the prostaglandins on isolated human ureteric smooth muscle. Br J Urol. 1988;61:19–26.
37. Aickin CC, Brading AF, Burdyga TV. Evidence for sodium-calcium exchange in the guinea-pig ureter. J Physiol. 1984;347:411–30.
38. Aickin CC. Investigation of factors affecting the intracellular sodium activity in the smooth muscle of guinea-pig ureter. J Physiol. 1987;385:483–505.
39. Kuriyama H, Tomita T. The action potential in the smooth muscle of the guinea pig taenia coli and ureter studied by the double sucrose-gap method. J Gen Physiol. 1970;55:147–62.
40. Brading AF, Burdyga TV, Scripnyuk ZD. The effects of papaverine on the electrical and mechanical activity of the guinea-pig ureter. J Physiol. 1983;34:79–89.
41. Lamont C, Burdyga T, Wray S. Intracellular Na^{+} measurements in guinea-pig ureteric smooth muscle using SBFI. Pflugers Arch. 1998;435:523–7.
42. Aaronson PI, Benham CD. Alterations in $[Ca^{2+}]i$ mediated by sodium-calcium exchange in smooth muscle cells isolated from the guinea-pig ureter. J Physiol. 1989;416:1–18.
43. Borisova L, Shmygol A, Wray S, Burdyga T. Evidence that Ca^{2+} sparks/STOCs coupling mechanism is responsible for the inhibitory effect of caffeine on the electro-mechanical coupling in guinea pig ureter smooth muscle. Cell Calcium. 2007;42:303–11.
44. Hertle L, Nawrath H. Stimulation of voltage-dependent contractions by calcium channel activator Bay K 8644 in the human upper urinary tract in vitro. J Urol. 1989;41:1014–8.
45. Maggi CA, Giuliani S, Santicioli P. Effect of BayK 8644 and ryanodine on the refractory period, action potential and mechanical response of the guinea-pig ureter to electrical stimulation. Naunyn Schmiedeberg's Arch Pharmacol. 1994;349:510–22.
46. Shabir S, Borisova L, Wray S, Burdyga T. Rho-kinase inhibition and electromechanical coupling in rat and guinea pig ureter smooth muscle: Ca^{2+}-dependent and -independent mechanisms. J Physiol. 2004;560:839–55.
47. Shuba MF. The mechanism of the excitatory action of catecholamines and histamine on the smooth muscle of guinea-pig ureter. J Physiol. 1977;264:853–64.
48. Muraki K, Imaizumi Y, Watanabe M. Effects of noradrenaline on membrane currents and action potential shape in smooth muscle cells from guinea-pig ureter. J Physiol. 1994;481:617–27.
49. Burdyga T, Wray S. The relationship between the action potential, intracellular calcium and force in intact phasic guinea-pig uretic smooth muscle. J Physiol. 1999;520:867–83.
50. Lang RJ. The whole-cell Ca^{2+}channel current in single smooth muscle cells of the guinea-pig ureter. J Physiol. 1990;423:453–73.
51. Imaizumi Y, Muraki K, Watanabe M. Characteristics of transient outward currents in single smooth muscle cells from the ureter of the guinea-pig. J Physiol. 1990;4(27):301–24.
52. Sui JL, Kao CY. Properties of inward calcium current in guinea pig ureteral myocytes. Am J Phys. 1997;41:C543–9.

53. Sui JL, Kao CY. Roles of outward potassium currents in the action potential of guinea pig ureteral myocytes. Am J Phys. 1997;273:C962–72.
54. Burdyga T, Wray S. Action potential refractory period in ureter smooth muscle is set by Ca^{2+} sparks and BK channels. Nature. 2005;28:559–62.
55. Benham CD, Bolton TB. Spontaneous transient outward currents in single visceral and vascular smooth muscle cells of the rabbit. J Physiol. 1986;381:385–406.
56. Burdyga T, Wray S. On the mechanisms whereby temperature affects excitation-contraction coupling in smooth muscle. J Gen Physiol. 2002;19:93–104.
57. Smith RD, Borisova L, Wray S, Burdyga T. Characterisation of the ionic currents in freshly isolated rat ureter smooth muscle cells: evidence for species-dependent currents. Pflugers Arch. 2002;445:444–53.
58. Borysova L, Shabir S, Walsh MP, Burdyga T. The importance of Rho-associated kinase-induced Ca2+ sensitization as a component of electromechanical and pharmacomechanical coupling in rat ureteric smooth muscle. Cell Calcium. 2011;50:393–405.
59. Burdyga T, Wray S. The effect of cyclopiazonic acid on excitation-contraction coupling in guinea-pig ureteric smooth muscle. J Physiol. 1999;517:855–66.
60. Maggi CA, Giuliani S, Santicioli P. Effect of the Ca^{2+}-ATPase inhibitor, cyclopiazonic acid, on electromechanical coupling in the guinea-pig ureter. Br J Pharmacol. 1995;114:127–37.
61. Burdyga T, Wray S. Sarcoplasmic reticulum function and contractile consequences in ureteric smooth muscles. Novartis Found Symp. 2002;246:208–17.
62. Burdyga T, Wray S. Sarcoplasmic reticulum function in smooth muscle. Physiol Rev. 2010;90:113–78.
63. Burdyga T, Taggart MJ, Crichton C, Smith G, Wray S. The mechanism of Ca^{2+} release from the SR of permeabilised guinea pig and rat ureteric smooth muscle. Biochim Biophys Acta. 1998;1402:109–14.
64. Boittin FX, Coussin F, Morel JL, Halet G, Macrez N, Mirroneau J. Ca^{2+} signals mediated by Ins(1,4,5) P(3)-gated channels in rat ureteric myocytes. Biochem J. 2000;349:323–32.
65. Nelson MT, Cheng H, Rubart M, Sanatana LF, Bonev AD, Knot HJ, Ledere WJ. Relaxation of arterial smooth muscle by calcium sparks. Science. 1995;270:633–7.
66. Lang RJ, Zhang Y. The effects of K+ channel blockers on the spontaneous electrical and contractile activity in the proximal renal pelvis of the guinea pig. J Urol. 1996;155:332–6.
67. Berridge MJ, Bootman MD, Roderick HL. Calcium signalling: dynamics, homeostasis and remodelling. Nat Rev Mol Cell Biol. 2003;4:517–29.
68. Berridge MJ. Inositol triphosphate and diacylglycerol as second messengers. Biochem J. 1984;220:345–60.
69. Casteels R, Hendrickx H, Vereecken R, Bulbring E. Effects of catecholamines on the electrical and mechanical activity of the guinea-pig ureter. Br J Pharmacol. 1971;43:429P.
70. Hannappel J, Golenhofen K. The effect of catecholamines on ureteral peristalsis in different species (dog, guinea-pigs and rat). Pflugers Arch. 1974;350:55–68.
71. Hertle L, Nawrath H. Calcium channel blockade in smooth muscle of the human upper urinary tract: II—effects on norepinephrine-induced activation. J Urol. 1984;132:1270–4.
72. Catacutan-Labay P, Boyarski S. Bradykinin: effect on ureteral peristalsis. Science. 1996;151:78–9.
73. Arrighi N, Bodel S, Zani D, Peroni A, Simeone C Mirabella G, et al. Alpha 1adrenoreceptors in human urinary tract: expression, distribution and clinical implications. Urologia. 2007;74:53–60.
74. Maggi CA, Parlani M, Astolfi M, Santicioli P, Rovero P, Abelli V, et al. Neurokinin receptors in the rat lower urinary tract. J Pharmacol Exp Ther. 1988;246:308–15.
75. Maggi CA, Santicioli P, Del Bianco E, Guiliani S. Local motor responses to bradykinin and bacterial chemotactic peptide formyl-methionyl-leucyl-phenylalanine (FMLP) in the guinea-pig isolated renal pelvis and ureter. J Urol. 1992;148:1944–50.
76. Maggi CA, Santicioli P, Guiliani S, Albelli L, Melli A. The motor effect of the capsaicin sensitive inhibitory innervation of the rat ureter. Eur J Pharmacol. 1986;126:333–6.
77. Eggerecks D, Raspe E, Bertrand D, Vassart G, Parmentier M. Molecular cloning, functional expression and pharmacological characterization of human bradykinin B2 receptor gene. Biochem Biophys Res Commun. 1992;187:1306–13.
78. Ribeiro ASF, Fernandes VS, Martiınez MP, Lopez-Oliva ME, Barahona MV, Recio P, et al. Pre- and post-junctional bradykinin B2 receptors regulate smooth muscle tension to the pig intravesical ureter. Neurourol Urodyn. 2016;35:115–21.
79. Laird JM, Roza C, Cervero F. Effects of artificial calculosis on rat ureter motility: peripheral contribution to the pain of ureteric colic. Am J Phys. 1997;272:R1409–16.
80. Streb H, Irvine RF, Berridge MJ, Schulz I. Release of Ca^{2+} from a non- mitochondrial store in pancreatic acinar cell by inositol 1,4,5-triphosphate. Nature. 1983;306:67–9.
81. Nishizuka Y. The role of protein kinase C in cell surface signal transduction and tumor production. Nature. 1984;308:693–8.
82. Weiss RM, Bassett AL, Hoffman BF. Adrenergic innervation of the ureter. Investig Urol. 1978;16:123–7.
83. Del Tacca M. Acetylcholine content of and release from isolated pelviureteral tract. Naunyn Schmiedeberg's Arch Pharmacol. 1978;302:293–7.
84. Malin JM, Deane RF, Boyarsky S. Characterisation of adrenergic receptors in human ureter. Br J Urol. 1979;42:171–4.

85. Sigala S, Dellabella M, Milanese G, Formari S, Faccoli S, Palazzolo F, et al. Evidence for the presence of alpha 1 adrenoreceptorssubtypes in the human ureter. Neurourol Urodyn. 2005;24:142–8.
86. Morita T, Wada I, Suzuki T, Tsuchida S. Characterization of alpha-adrenoceptor subtypes involved in regulation of ureteral fluid transport. Tohoku J Exp Med. 1987;152:111–8.
87. Sakamoto K, Suri D, Rajasekaran M. Characterization of muscarinic receptor subtypes in human ureter. J Endourol. 2006;20:939–42.
88. Hernandez M, Simonsen U, Prieto D, Rivera L, Garcia P, Ordaz E, et al. Different muscarinic receptor subtypes mediating the phasic activity and basal tone of pig isolated intravesical ureter. Br J Pharmacol. 1993;110:141–55.
89. Yoshida S, Kuga T. Effects of field stimulation on cholinergic fibers of the pelvic region in the isolated guinea pig ureter. Jpn J Physiol. 1980;30:415.
90. Roshani H, Dabhoiwala NF, Dijkhuis T, Pfaffendorf M, Boon TA, Lamers WH. Pharmacological modulation of ureteral peristalsis in a chronically instrumented conscious pig model. I: effect of cholinergic stimulation and inhibition. J Urol. 2003;170:264–7.
91. Hua XY, Saria A, Gamse R, Theodorsson-Norheim E, Brodin E, Lunberg JM. Capsaicin-induced release of multiple tachykinins (SP, neurokinin A and eledoisin-like material from guinea-pig spinal cord and ureter). Neuroscience. 1986;19:313–9.
92. Hua XY, Theodorsson-Norheim E, Lundberg JM, Kinn AC, Hokfelt T, Cuello AC. Co-localization of tachykinins and CGRP in capsaicin-sensitive afferents in relation to motility effects in the human ureter in vitro. Neuroscience. 1987;23:693–703.
93. Jerde TJ, Saban R, Bjorling DE, et al. Distribution of neuropeptides, histamine content, and inflammatory cells in the ureter. Urology. 2000;56:173–8.
94. Santicioli P, Maggi CA. Myogenic and neurogenic factors in the control of pyeloureteral motility and ureteral peristalsis. Pharmacol Rev. 1998;50:683–722.
95. Menon M, Resnick MI. Urinary lithiasis: etiology, diagnosis, and medical management. In: Walsh PC, Retik AB, Vaughan ED, et al., editors. Campbell's urology, vol. 4. Philadelphia: Saunders; 2002. p. 3227–92.
96. Golias C, Charalabopoulos A, Stagikas D, Charalabopoulos K, Batistatou A. The kinin system-bradykinin: biological effects and clinical implications. Multiple role of the kinin system–bradykinin. Hippokratia. 2007;11:124–8.
97. Stoller ML, Bolton DM. Urinary stone disease. In: Tanagho EA, McAninch JW, editors. Smith's urology. San Francisco: Lange Medical Book/McGraw-Hill; 2000. p. 291–320.
98. Yalcin S, Ertunc M, Ardicli B, Kabakus IM, Tas TS Sara Y, et al. Ureterovesical junction obstruction causes increment insmooth muscle contractility, and cholinergic and adrenergic activity in distal ureter of rabbits. J Pediatr Surg. 2013;48:1954–61.
99. Canda AE, Turna B, Cinar GM, Nazli O. Physiology and pharmacology of the human ureter: basis for current and future treatments. Urol Int. 2007;78:289–98.
100. Ziemba JB, Matlaga BR. Guideline of guidelines: kidney stones. Br J Urol. 2015;116:184–9.
101. Mak RH, Kuo HJ. Primary ureteral reflux: emerging insights from molecular and genetic studies. Curr Opin Pediatr. 2003;15:181–5.
102. Grana L, Donnellan WL, Swenson O. Effects of gram-negative bacteria on ureteral structure and function. J Urol. 1968;99:539–50.
103. Teague N, Boyarsky S. Further effects of coliform bacteria on on ureteral peristalsis. J Urol. 1968;99:720–4.
104. King WW, Cox CE. Bacterial inhibition of ureteral smooth muscle contractility. I. The effect of common urinary pathogens and endotoxin in an in vitro system. J Urol. 1972;108:700–5.
105. Floyd RV, Winstanley C, Bakran A, Wray S, Burdyga TV. Modulation of ureteric Ca signaling and contractility in humans and rats by uropathogenic *E. coli*. Am J Physiol Ren Physiol. 2010;298:F900–8.
106. Floyd RV, Upton M, Hultgren S, Wray S, Burdyga TV, Winstanley C. *Escherichia coli*-mediated impairment of ureteric contractility is uropathogenic *E. coli* specific. J Infect Dis. 2012;206:1589–96.

5 Spontaneous Activity and the Urinary Bladder

Christopher H. Fry and Karen D. McCloskey

Abstract

The urinary bladder has two functions: to store urine, when it is relaxed and highly compliant; and void its contents, when intravesical pressure rises due to co-ordinated contraction of detrusor smooth muscle in the bladder wall. Superimposed on this description are two observations: (1) the normal, relaxed bladder develops small transient increases of intravesical pressure, mirrored by local bladder wall movements; (2) pathological, larger pressure variations (detrusor overactivity) can occur that may cause involuntary urine loss and/or detrusor overactivity. Characterisation of these spontaneous contractions is important to understand: how normal bladder compliance is maintained during filling; and the pathophysiology of detrusor overactivity. Consideration of how spontaneous contractions originate should include the structural complexity of the bladder wall. Detrusor smooth muscle layer is overlain by a mucosa, itself a complex structure of urothelium and a *lamina propria* containing sensory nerves, micro-vasculature, interstitial cells and diffuse muscular elements.

Several theories, not mutually exclusive, have been advanced for the origin of spontaneous contractions. These include intrinsic rhythmicity of detrusor muscle; modulation by non-muscular pacemaking cells in the bladder wall; motor input to detrusor by autonomic nerves; regulation of detrusor muscle excitability and contractility by the adjacent mucosa and spontaneous contraction of elements of the *lamina propria*. This chapter will consider evidence for each theory in both normal and overactive bladder and how their significance may vary during ageing and development. Further understanding of these mechanisms may also identify novel drug targets to ameliorate the clinical consequences of large contractions associated with detrusor overactivity.

Keywords

Urinary bladder · Overactive bladder · Spontaneous contractions · Detrusor smooth muscle · Mucosa · Trigone

C. H. Fry (✉)
School of Physiology, Pharmacology and Neuroscience, University of Bristol, Bristol, UK
e-mail: chris.fry@bristol.ac.uk

K. D. McCloskey
School of Medicine, Dentistry and Biomedical Sciences, Queen's University Belfast, Belfast, UK

H. Hashitani, R. J. Lang (eds.), *Smooth Muscle Spontaneous Activity*, Advances in Experimental Medicine and Biology 1124, https://doi.org/10.1007/978-981-13-5895-1_5

5.1 Introduction: The Filling and Voiding Cycle of the Bladder

The urinary bladder has two functions: to store urine, normally up to a maximum of about 500 mL; and periodically to completely void this content. Bladder filling is achieved with a small change of intravesical pressure, up to 10–15 cm H_2O, i.e. the bladder is compliant. This is necessary to minimise increases of pressure in the upper urinary tract (ureters and renal pelvis) that would damage renal function. Several times per day urine is completely expelled from the bladder, a process that is under conscious control. This is achieved by active contraction of detrusor smooth muscle, the major tissue component of the bladder wall, to raise intravesical pressure with concomitant reduction of bladder outlet resistance; co-ordinated by central control of sacral and thoraco-lumbar centres [1]. The latter is achieved by relaxation of smooth muscle, comprising an internal sphincter, in the urethra and bladder neck, as well as cessation of contractile activity in skeletal muscle forming the external sphincter (rhabdosphincter). This enables intravesical pressure to be raised to a sufficient level to overcome the fluid resistance offered by the outflow tract.

The periodic rise of intravesical pressure for voiding is achieved by generating co-ordinated contractions of detrusor smooth muscle, principally mediated by activation of post-ganglionic parasympathetic nerve fibres. However, it is not accurate to view the bladder as completely inactive during filling: continuous asynchronous movements of regions of the bladder wall occur that can manifest themselves as small variations of intravesical pressure. This chapter is concerned with the origin of these small movements, what their physiological functions may be and if they change under pathological conditions. These movements are often called spontaneous, in that they are autonomous, with a non-neurogenic origin and so are intrinsic to detrusor smooth muscle itself, modulated or initiated by local factors or nearby tissue. It has been implicitly assumed by some that spontaneous contractions are random and therefore have no role in co-ordinated voiding and filling cycles of bladder function. However, this may not be an accurate description of their role and others consider that spontaneous contractions should be regarded as an integral part of bladder function that may become aberrant during ageing or disease and contribute to pathological activity.

5.2 The Structure of the Bladder Wall

A description of the tissue components of the bladder wall is integral to understand the nature of spontaneous contractions. It is convenient to describe four layers of the bladder wall: an outer serosa; a detrusor (smooth) muscle layer; a *lamina propria* or suburothelium; and uroepithelium (urothelium). The *lamina propria* and urothelium are collectively described as a mucosa as these two layers have an integrated activity in the context of spontaneous activity (Fig. 5.1a).

The serosa protects the underlying tissue and is a reflection of the visceral peritoneum that covers only the superior and upper lateral walls of the bladder. The remainder of the bladder wall is protected by an adventitia that merges with other pelvic floor organs. The detrusor muscle layer comprises most of the bladder wall and consists of detrusor smooth muscle in muscle bundles that can combine in circular and longitudinal directions, although distinct circular and longitudinal muscle layers are not as evident as they would be in the G-I tract or the urethra.

The mucosa is the most complex region of the bladder wall and provides protective and sensory functions, and in regard to spontaneous activity has an intimate relationship with the detrusor muscle layer. The urothelium separates underlying bladder wall tissues from urine and consists of a tight epithelium [2] whose transport characteristics will not be considered further in the context of spontaneous activity. However, it also has the capacity to release bioactive small molecules that are regarded as serving a sensory function in

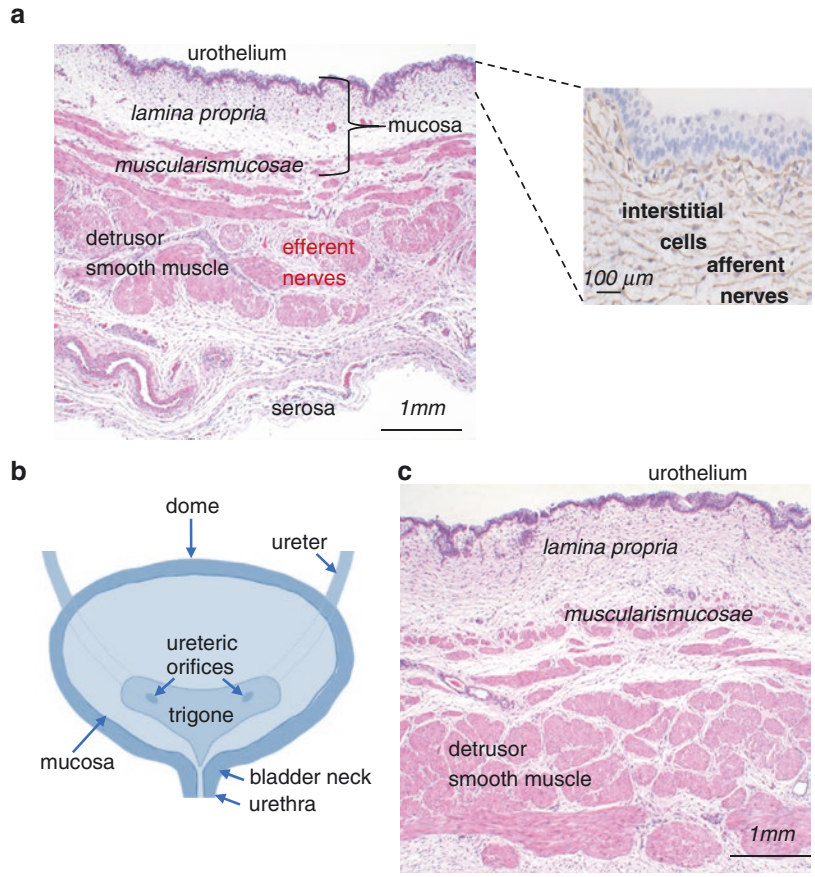

Fig. 5.1 Cross section of the sheep bladder wall; haematoxylin and eosin stain. (**a**) Full thickness section from a normal bladder showing the urothelium, *lamina propria* with *muscularis mucosae*, detrusor layer and serosa. The inset shows the urothelium and *lamina propria* lying immediately below. (**b**) Schematic structure of the lower urinary tract. (**c**) Section from a bladder with outflow obstruction

co-ordination with the *lamina propria*. The *lamina propria* itself consists of numerous interstitial cells (ICs), interspersed with afferent nerve fibres, blood vessels and in some larger species a separate muscle layer—the *muscularis mucosa*.

This basic structure is maintained throughout the bulk of the bladder wall, called the dome. A small triangular region of the bladder, between the ureteric orifices and the bladder neck, is called the trigone. This consists of a superficial layer of trigonal smooth muscle overlaying deeper detrusor contiguous with the dome, and in the guinea pig bladder the two may be separated by blunt dissection. The trigone and bladder neck are regarded by some as part of the outflow tract with characteristic high levels of spontaneous activity that will be described separately. The bladder dome and trigone are conventionally understood to have separate embryological origins, derived, respectively, from the endodermal urinogenital sinus and mesoderm-derived Wolffian (mesonephric) ducts. However, this model has been modified recently with the view that the eventual trigone musculature largely derives from bladder detrusor muscle, with mesodermal tissue confined to the ureteric openings [3].

Pathological conditions such a bladder outflow obstruction, as occurs in men with benign or malignant prostate growth, cause changes to the bladder wall, most evident in an increase of wall thickness (Fig. 5.1c). Not only does the muscle layer undergo cellular hyperplasia and hypertrophy, but the *lamina propria* also thickens with a significant increase of interstitial cell number, an aspect that has consequences for generation of spontaneous activity, as will be discussed in following sections.

5.3 Demonstration of Spontaneous Activity

Overactive bladder syndrome (OAB) is an age-related clinical condition characterised by nocturia, urgency and frequency [4] and occurs in 12–18% of Western populations [5]. A further study showed that about 12% of OAB patients have a condition of detrusor overactivity (DO [6]), i.e. over 1% of the total population. DO is characterised by large, spontaneous contractions of the bladder that are not possible to defer whilst the bladder is being filled. It not only decreases the quality of life for patients, but also can lead to involuntary loss of urine (incontinence) and if persistent a rise of pressure in the ureters that may lead to renal failure, especially if it associated with bladder outflow tract obstruction and detrusor sphincter dyssynergia. Figure 5.2a shows a clinical urodynamic record of a patient with DO. Prior to the voiding contraction associated with flow, there are three greater overactive contractions with no associated voiding, as presumably there is no co-ordinated reduction of outflow tract resistance. One applied objective of fundamental research into the origin of bladder spontaneous activity is to explain the pathophysiology and inform the clinical management of DO.

In vivo, small oscillatory bladder wall movements and intravesical pressure changes have been measured in animals and humans during the filling phase (Fig. 5.2b). Whilst some are associated with respiratory movements [7], others are independent and can coincide with sensations arising from the bladder itself [8, 9]. Bladder wall movements are asynchronous in different parts of the bladder wall, suggestive of localised, independent movements. Because the variations of pressure are lower than those observed in DO, voiding is not generally initiated and so are termed non-voiding contractions. Amalgamation of these localised spontaneous contractions could however generate larger DO contractions, and this raises two questions: what are the origins of spontaneous contractions; and how might they coalesce into larger ones?

Ex vivo, asynchronous, localised micromotions of the bladder wall or pressure transients are also measured (Fig. 5.2c) [10–13], which makes it unlikely they are derived only from external, nervous influences. These are modulated by increased stretch of the bladder wall [14] low concentrations of muscarinic agonists [11, 15] or pathological conditions such as bladder outflow obstruction [10]. Analogous transient electrical events also show limited propagation across the bladder wall [16]. The above observations are mirrored by isometric tension and electrophysiological events from in vitro bladder sheets (Fig. 5.2d), bladder wall strips (Fig. 5.2e) and even isolated detrusor myocytes from several animal and human sources (Fig. 5.2f) [17–22].

Overall, spontaneous contractile and electrical activity is a feature of the intact bladder and associated isolated preparations and is generally enhanced in bladders demonstrating pathological overactive behaviour in vivo. Some of this activity will derive from detrusor myocytes themselves but, as shown below, this activity crucially can be initiated or modulated by external influences.

5.4 Significance of Spontaneous Activity

Spontaneous contractions in the normal bladder wall are generally of small amplitude and occur at multiple sites across the bladder wall. Associated intracellular Ca^{2+} and membrane potential waves do not propagate significant distances in relation to the size of the bladder itself [11, 16, 23]. Such low level, but relatively frequent (2–3 min^{-1}) activity would be suitable to set a background, low level of tension in the bladder wall. When nerve-mediated activation of the detrusor occurs for voiding, the increased muscular contraction would raise wall tension, and hence intravesical pressure, more quickly than if the initial muscle work had to overcome a fully flaccid structure.

Changes to passive and active tension of the bladder wall are proposed as a sensory transduc-

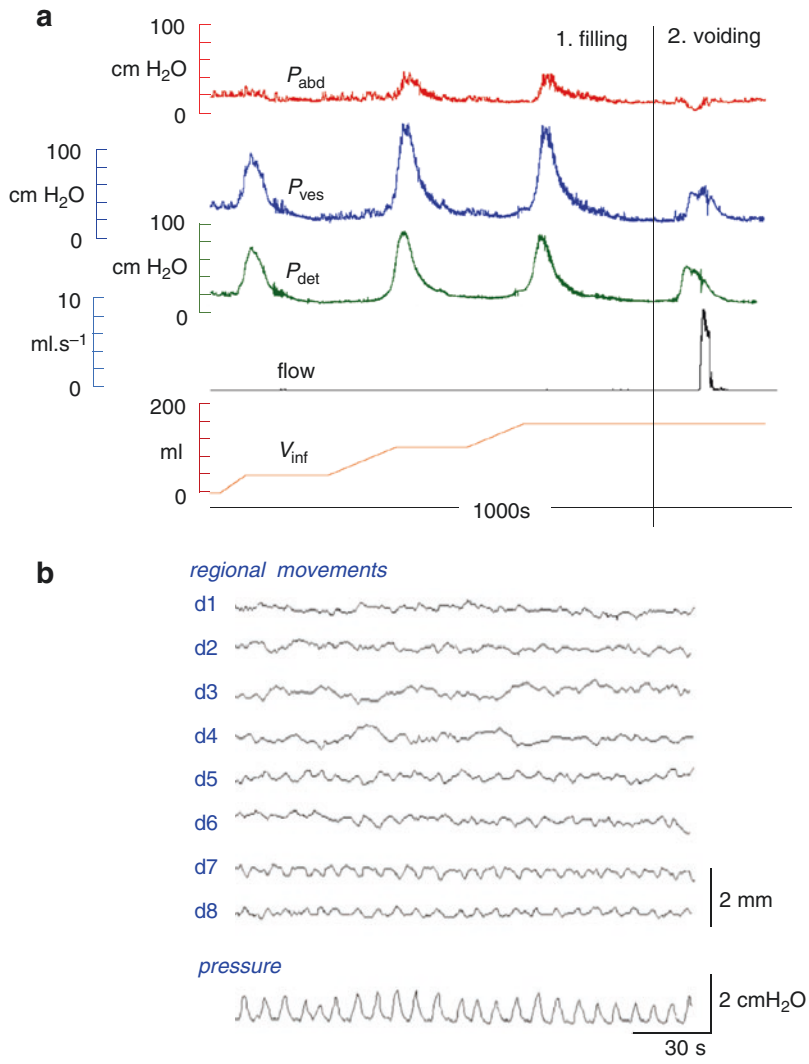

Fig. 5.2 Spontaneous contractions from in vivo, ex vivo and in vitro recordings. (**a**) Urodynamic traces from a patient with detrusor overactivity. Traces, top to bottom, are from catheters in the rectum, to measure abdominal pressure, P_{abd}, and the bladder lumen, to measure vesical pressure, P_{ves}. Detrusor pressure, P_{det}, is obtained from P_{ves}—P_{abd}. The trace below shows urine flow from the bladder. The volume infused, V_{inf}, is shown at the bottom. The vertical line divides the system into filling (left, 1) and voiding (right, 2) periods. The filling period shows three uninhibited P_{det} contractions in the absence of flow, evoked at the end of three periods of infusion. With no further filling a voiding contraction occurs, i.e. a rise of P_{det} accompanied with flow (data courtesy of the Bristol Urological Institute). (**b**) Regional movements of different regions of the bladder wall in vivo (d1–d8) and simultaneous measurement of intravesical pressure [9]. (**c**) Micromotions of an ex vivo perfused pig bladder. Carbon particles are placed on the bladder surface and the scalar distance between pairs were measured from video recordings. Examples of three distances (a, b, c) are shown with time, as well as simultaneous measurement of intravesical pressure [12]. (**d**) Spontaneous isometric contractions from a superfused rat bladder sheet for methods [10]. (**e**) Spontaneous isometric contractions from a superfused guinea pig strip with an intact mucosa [48]. (**f**) Isolated human detrusor myocytes; left, intracellular Ca^{2+} transients, right, spontaneous action potentials for methods [19]

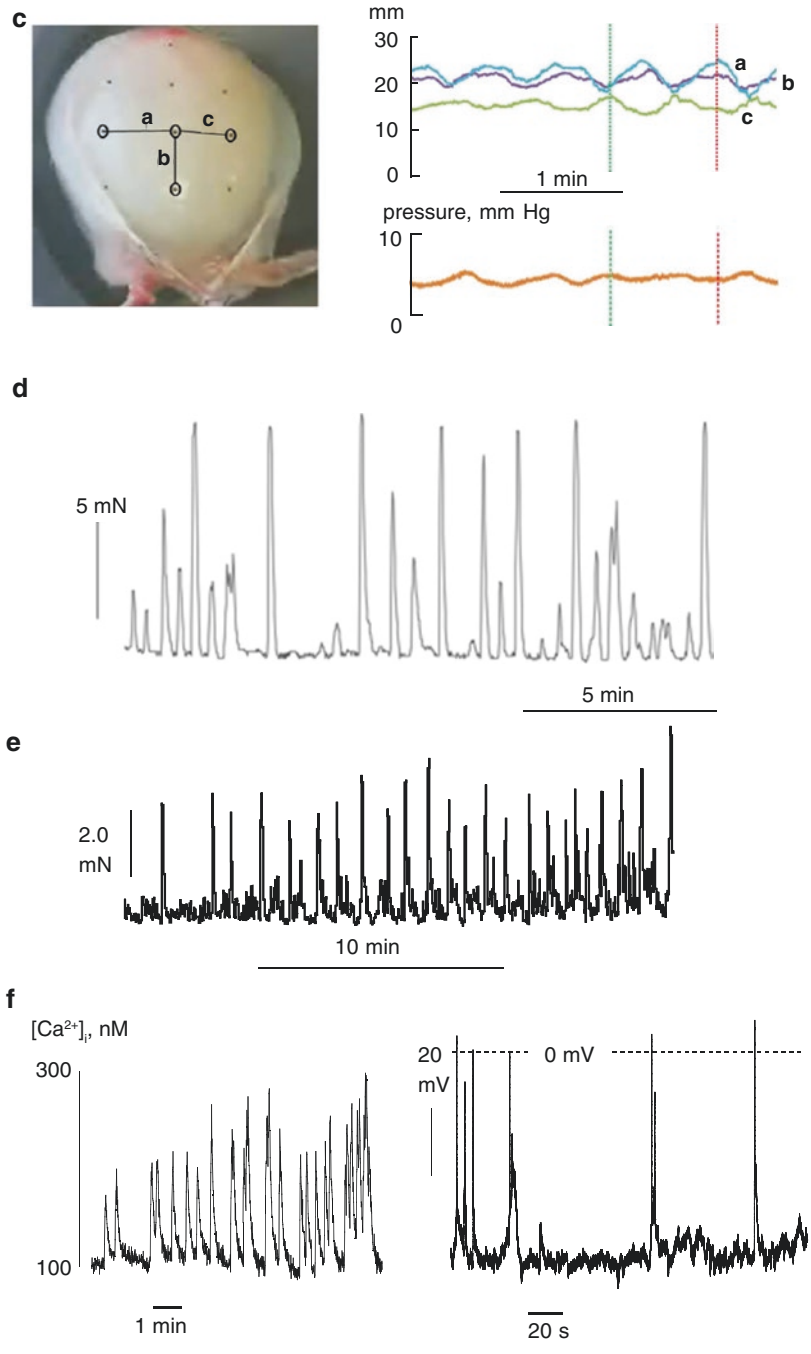

Fig. 5.2 (continued)

tion mechanism to convert bladder filling to sensory signals. An increase of passive wall tension by filling or artificial stretch is associated with augmented afferent nerve activity [24, 25]. Stretch of the bladder wall releases neuromodulators such as ATP and acetylcholine (ACh) that are proposed to activate afferents. It has also been hypothesised that added gain to the system may be provided by spontaneous contractions that will generate additional, transient changes in wall tension. Indeed, increased bladder filling raises the amplitude and frequency of spontaneous contractions [14, 26]. In part, increased spontaneous contraction amplitude on bladder filling will be due to muscle cells adjusting to a new position on their length-tension relationship, but frequency alterations suggest an additional mechanism [26], which might include activation of local nervous reflexes upon neuromodulator release. The important role of spontaneous contractions contributing to afferent activation is gleaned from the fact that afferent firing is dependent not only on static changes to wall tension, but also the rate of change of tension [27]. The mode of transduction of a transient tension/pressure signal to afferent nerve activation is unclear and may involve intermediate cellular responses from *lamina propria* cells (see below). However, the significance of the study is that alteration to spontaneous contractile activity can modulate afferent nerve activity during bladder filling.

5.5 Spontaneous Activity and Detrusor Overactivity

Detrusor overactivity is an involuntary rise of intravesical pressure, interpreted as a contraction of the bladder, measured during the filling phase of a urodynamic investigation [4, 28]. Such contractions are transient, cannot be suppressed by the patient and may be spontaneous or provoked by filling. It is tempting to hypothesise that these transient changes to intravesical pressure are a result of abnormal spontaneous contractile activity of smooth muscle in the bladder wall. However, it must be remembered that spontaneous contractions in isolated preparations are brief and of high frequency whereas overactive bladder contractions are less frequent with very much longer durations. Nevertheless, this hypothesis is consistent with observations made from in vitro preparations from overactive bladders where the amplitude and frequency of spontaneous contractions and action potentials are augmented [22, 23, 29, 30]. Optical imaging experiments show that in rat bladder preparations spontaneous contractions from in vitro bladder sheets, or pressure variations from ex vivo whole bladders, are associated with multiple sites of locally propagating Ca^{2+} and membrane potential transients [11, 23]. With similar preparations from rats that have overactive bladders, there are fewer originating sites, but these propagate more extensively over the bladder wall [11, 23]. Such rises of intravesical pressure can be greater than those achieved during normal voiding and sufficient to overcome the resistance of a still-contracted outflow and so cause urinary leakage. What is unclear is the origin of the overactive bladder contractions. Before pathological mechanisms can be proposed, it is first necessary to consider how bladder contractions arise and whether they are spontaneous or evoked by nervous stimulation of detrusor smooth muscle.

5.6 Generation of Detrusor Contractions

Only a brief description of how detrusor contractions are generated is given, with more detailed descriptions elsewhere [31, 32]. Detrusor contractions are generated by a transient rise of the intracellular Ca^{2+} concentration ($[Ca^{2+}]$), initiated

by intracellular release of Ca^{2+} from stores and/or Ca^{2+} influx via L-type and T-type Ca^{2+} channels. Co-ordinated contraction of the bladder is evoked by parasympathetic post-ganglionic fibres releasing ACh and ATP, and driven by descending fibres, emerging at sacral levels S2-S4. ACh and ATP bind, respectively, to metabotropic M_3 and ionotropic $P2X_1$ receptors. Detrusor muscle is a phasic type and can generate action potentials with a depolarising phase driven by L-type and T-type Ca^{2+} channels and repolarisation driven by K^+ channels, predominantly but not exclusively large conductance Ca^{2+}-activated K^+ (BK) channels [33–35]. It should be noted that with normal human and old-world monkey bladders ACh is the sole functional transmitter, whilst with most other species and also with human detrusor from pathological bladders both ACh and ATP support nerve-mediated contractions [36]. This may be explained by greater extracellular ATP hydrolysis in normal human bladder so that released ATP from motor nerves does not reach the muscle membrane [37].

Between the muscle bundles is a network of detrusor interstitial cells (IC_{det}) that develop Ca^{2+} transients [38, 39]. There is a debate if they contribute a pacemaking mechanism to drive detrusor myocytes, like their counterparts in the G-I tract [40, 41]. However, Ca^{2+} imaging studies show that IC_{det} transients are out of phase with those in detrusor myocytes [39, 42] and it is suggested that they may co-ordinate activity between adjacent muscle bundles. A subset of IC_{det} label for platelet-derived growth factor receptor-α (PDGFRα) [43, 44]. They respond to purines via P2Y receptors, mainly $P2Y_2$ receptors, to generate membrane hyperpolarisation by Ca^{2+}-induced activation of small conductance K^+ (SK) channels. It is proposed that they hyperpolarise adjacent detrusor muscle cells via gap junctions [45], but there is as yet little evidence for direct intracellular coupling between detrusor myocytes and ICs. However, if such coupling is demonstrated this provides a mechanism whereby cyclical variation of ATP release from urothelium and/or *lamina propria* cells would also generate cyclical variation of tension in the detrusor smooth muscle layer, through a direct activating response on detrusor via $P2X_1$ receptors and tempered by the indirect effect via P2Y receptors on PDGFRα-labelled IC_{det}.

5.7 Influence of the Mucosa on Spontaneous Activity

Several groups have reported that the mucosa from pig, guinea pig and rat bladder is capable of developing spontaneous contractile [46–48] or electrical [49] activity independent of detrusor smooth muscle, although others report that contractile activity is absent from rat and mouse isolated mucosa preparations (Hashitani, personal communication). Moreover, when the mucosa and detrusor components are not separated the amplitude of spontaneous contractions is greater than that developed by the two components separately. Figure 5.3 describes the basic phenomenon in guinea pig tissue: Fig. 5.3a (top) shows spontaneous activity in an isolated preparation of the bladder wall with the mucosa dissected away as much as possible (in all species the mucosa may be removed by sharp or blunt dissection), spontaneous activity is present but is relatively low in amplitude. In this example, spontaneous activity is very small but in other publications [50] this may be greater, but still smaller than in intact strips as described below. If the dissected mucosa is similarly attached to an isometric force transducer spontaneous activity is also recorded of equivalent or even greater amplitude (Fig. 5.3a, middle). However, if the mucosa is left intact on the detrusor preparation a proportionately much greater amplitude of spontaneous contractions is measured (Fig. 5.3a bottom), note also the change of vertical calibration bar). Thus, the mucosa itself is capable of spontaneous contractile and electrical activity in many animal species, and in addition there is synergistic enhancement when the two layers of the bladder wall are in contact. The significance of the contribution of the mucosa to bladder spontaneous contractile activity is that the *lamina propria* thickens in many pathological conditions asso-

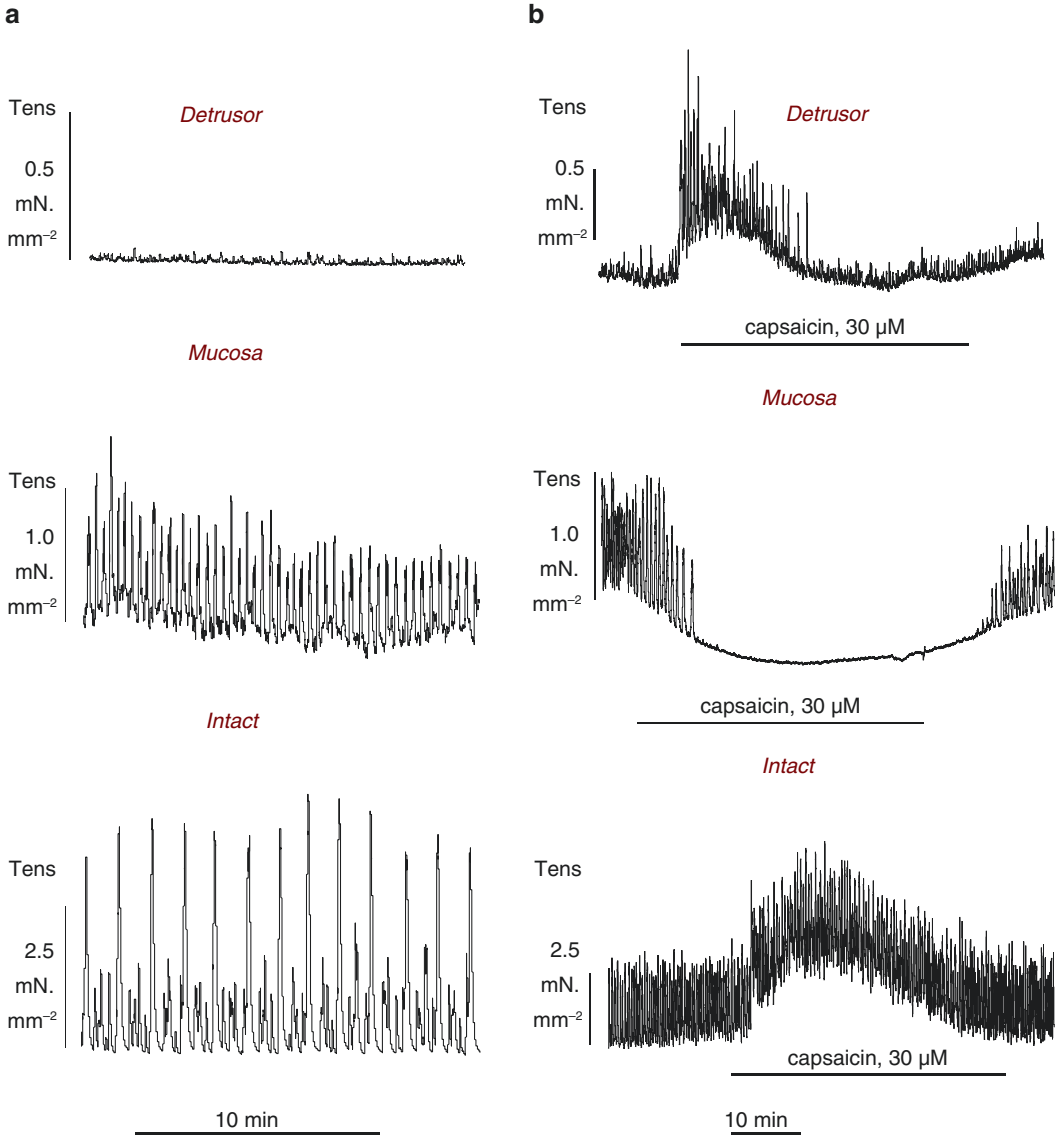

Fig. 5.3 Spontaneous contractions from isolated bladder wall preparations. (**a**) Guinea pig bladder. Baseline spontaneous contractile activity from a detrusor strip with the mucosa removed (upper); a mucosa preparation dissected from detrusor muscle (middle); an intact preparation of detrusor and mucosa (lower). (**b**) Spontaneous contractile activity on addition of 10 μM capsaicin in: a detrusor preparation (upper); a mucosa preparation (middle); an intact preparation (lower). Note the different calibration bars for the three preparations. Adapted from [48]

ciated with neurogenic or idiopathic detrusor overactivity [51, 52]. The particular cells contributing to mucosa spontaneous activity is considered in more detail below (Sect. 5.8) and may be from the *muscularis mucosa*, with contributions also from smooth muscle cells and/or pericytes around blood vessels or even ICs.

5.8 The Origins of Mucosa Spontaneous Activity

The mucosa itself has contractile properties and electrical field stimulation (EFS) can elicit contractions that are abolished by tetrodotoxin, implying they are nerve-mediated. The fre-

quency dependence of EFS detrusor vs. mucosal contractions is different in pig preparations [53], but similar in other species such as guinea pig [49, 54], highlighting the fact that mucosal contractile function can have different properties from detrusor. Moreover, mucosal spontaneous activity demonstrates different pharmacological characteristics whereby: capsaicin augments detrusor activity but inhibits that of the mucosa (Fig 5.3b); extracellular acidosis initially suppresses detrusor activity but has a much smaller effect on isolated mucosa; and the $P2X_1$ agonist α,β methylene ATP, (ABMA) enhances detrusor but attenuates mucosa activity [48]. Moreover, although α- and β-adrenoceptor-dependent modulation of spontaneous activity in the mucosa is evident, the functional receptor subtype populations involved show differences from the detrusor [55]. The actual cell type(s) contributing to mucosa contractions are unknown but may be from several sources, including *muscularis mucosae*, abundant ICs and pericytes around blood vessels. All these cells label for smooth muscle actin [56, 57].

Muscularis mucosae generates bursts of spontaneous action potentials (APs) with a depolarising phase supported by L-type Ca^{2+} channel activity. BK and SK channels, as well as Kv7 K^+ channels which all modulate the bursting characteristics of the AP trains and hence the excitability of the tissue [58]. The current density of K^+ currents in the *muscularis mucosae* is much lower than in detrusor [59] and may contribute to increased electrical excitability. In addition, TRPV4 channels are also present in *muscularis mucosae* and their activation generates a sustained contraction and reduction of spontaneous activity, possibly by Ca^{2+} influx opening BK channels [60]. Overall this might suggest that *muscularis mucosae* can exhibit a phasic contractile response and a background tonus to the bladder wall.

Vascular smooth muscle cells and/or pericytes surround suburothelial blood vessels, generate intracellular Ca^{2+} transients and also generate circular and longitudinal contractions [61, 62]. The physiological properties of these cells will be covered in a separate chapter. Longitudinal contractions would contribute to mucosal force generation, although the proportional effect they have remains to be ascertained.

ICs are the most numerous type of cell in the *lamina propria*; the ratio of ICs to smooth muscle cells in the *muscularis mucosae* in six sheep bladders was 5.1 ± 0.7 (n = 6, Fry, Nyirady, unpublished data). They are especially abundant near the urothelium (see Fig. 5.1a, b) and often appose and even surround the terminals of afferent nerves [63], so that they probably have synapse-like relations. They are electrically excitable, generating transient depolarisations via a Ca^{2+}-activated Cl^- channel, the rise of intracellular Ca^{2+} mediated by release from intracellular stores after membrane receptor activation via, for example, purines acting on P2Y receptors [64]. Moreover, these ICs are coupled by connexin43 (Cx43) gap junctions suggesting they form a functional electrical syncytium [65]. Their excitatory responses to purines are consistent with activation by ATP and its metabolites that may be released from the overlying urothelium in response to stretch. Moreover, some ICs have a myofibroblast-like morphology where they contain myofilaments that form cytoplasmic stress fibres [66]. IC number increases significantly as the *lamina propria* thickens in conditions associated with detrusor overactivity, such as bladder outflow obstruction (Fig. 5.1b), [67] and spinal cord injury [51] when they could augment indirectly mucosal spontaneous activity.

Overall it may be concluded that the mucosa has distinct contractile properties from detrusor with potential contributions from the three major cell types described above. The proportion of mucosal tissue occupied by *muscularis mucosae* is about 4.5% in guinea pig bladder, compared to 73.4% occupied by detrusor in the muscle layer [48] to produce broadly comparable magnitudes of spontaneous contractile activity. Thus, if *muscularis mucosae* solely contributed to spontaneous contractile activity, its unit contractile properties would have to be substantially greater than detrusor.

5.9 Interactions Between Mucosa and Detrusor and the Generation of Spontaneous Activity

Augmentation of spontaneous activity by retaining a mucosa-detrusor structure implies there is interaction between the two layers. This may be though diffusion of chemical modulators or cell-to-cell signalling (Fig. 5.4a, b). One observation to suggest diffusional coupling (Fig. 5.4a) shows that simple placement of mucosa on detrusor muscle rapidly increases the amplitude and frequency of spontaneous contractions. Augmentation of spontaneous activity is not suppressed by atropine implying that ACh is not the diffusible active

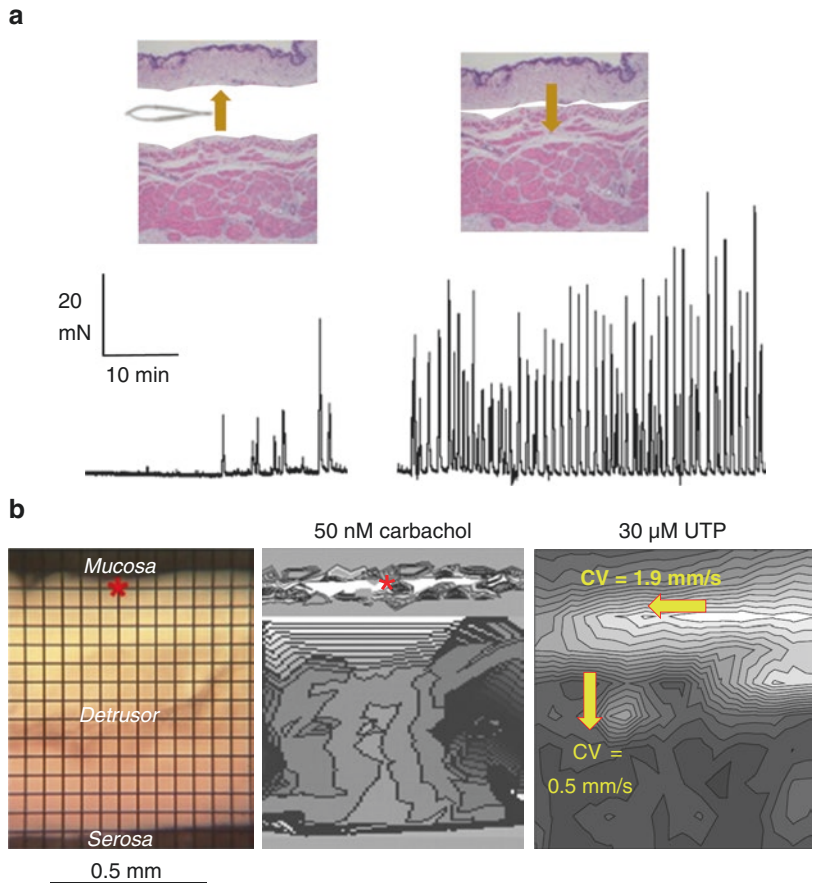

Fig. 5.4 Interaction between mucosa and detrusor in the generation of spontaneous contractions. (**a**) Evidence for non-cell-to-cell contact. Spontaneous activity in a detrusor preparation with the mucosa dissected away as a sheet (left) and when the mucosa was subsequently placed on the detrusor preparation (right): Kitney and Fry, unpublished data. Pig bladder, a schematic of the experiments is shown above the experimental tracings. (**b**) Evidence for cell-to-cell contact. Left, a cross section of a rat bladder used for optical imaging experiments, the superimposed grid delineates separate pixels from which Ca^{2+} waves were recorded to construct conduction maps. Middle, a conduction map constructed from the latencies of Ca^{2+} transients from each pixel on injection of a low carbachol concentration at the *lamina propria* (red star)—increasing delays are designated by areas of greater darkness. Thus, the initiation of a signal propagates transversely in the mucosa before propagating laterally to the detrusor layer. Right: a conduction map again showing rapid transverse propagation and slower invasion of the detrusor after application of UTP, a purine that excites *lamina propria* interstitial cells. Adapted from [11, 23]

agent. However, many other agents are released by mucosal cells that can have local paracrine, contractile effects on detrusor muscle including ATP, prostaglandins and nitric oxide [68]. In particular, it has been shown in guinea pig bladder that spontaneous activity goes through cyclical variations in magnitude that coincides with background release of ATP, after consideration of diffusion times for ATP in the tissue [48]. However, Fig. 5.4b shows evidence also for intercelluar coupling from the mucosa to the detrusor layers. Direct evidence that spontaneous activity can result from localised release of ATP from detrusor or mucosa is shown below (Fig. 5.5b, see Sect. 10.2 below). Although some will be broken down by ecto-ATPases, some ATP undoubtedly persists to generate contractile events. Moreover, ecto-ATPase activity is reduced in bladder wall tissue from overactive bladders that would exacerbate the contractile effects of ATP released from tissue [37].

There are also data to suggest there is cell-to-cell coupling between the mucosa and detrusor. With intact or detrusor-only preparations, gap junction blockers including 18-β glycyrrhetinic acid, carbenoxolone or heptanol attenuate spontaneous activity, especially in animals where activity was increased by spinal cord injury or inflammation [51, 69]. However, it should be cautioned that there is evidence to show some gap junction blockers also block voltage-gated Ca^{2+} channels [70] which would also explain why these agents may reduce spontaneous activity. However, it remains to be shown whether this blockade is occurring solely between detrusor muscle cells or also in the *lamina propria* at the interface between the two layers. There are also optical signalling data that indicate that Ca^{2+} waves and electrical signals can pass within the *lamina propria* and across to the detrusor layer. Ca^{2+} signals, propagating at 60–70 μm.s^{-1} have been measured in isolated *lamina propria* preparations. These were augmented by ATP and TRPV4 agonists and attenuated by the Ca^{2+}-ATPase inhibitor cyclopiazonic acid, implying an intracellular source of Ca^{2+} [71]. Optical imaging of the rat bladder wall, with an absent *muscularis mucosae*, reveals that spontaneous waves of intracellular Ca^{2+} or changes to membrane potential originate not in the detrusor, but in the *lamina propria* where they propagate laterally within this layer before invading the detrusor [10]. Signal propagation velocity is about 0.3 cm s^{-1}, faster than in *muscularis mucosae* [23, 59]. Overall it is possible that the two cellular elements exert different influences over the detrusor layer, with *muscularis mucosae* setting a background tonus and an IC layer providing a more dynamic response to changes of neuromodulator released from the urothelium.

Although the mucosa enhances spontaneous activity in the bladder this has to be set against the observation that it also suppresses contractions evoked by muscarinic receptor agonists, but not when depolarised by raised extracellular [K] [72]. Exhaustive studies by the original authors did not reveal the intermediate diffusible agent, nevertheless the augmentation of spontaneous activity must be offset by this observation.

5.10 Theories for the Origin of Spontaneous Activity in Normal and Pathological Bladders

In principle normal and overactive spontaneous activity may arise from several, not mutually conflicting, mechanisms:

- A myogenic origin
- A neurogenic origin
- A urotheliogenic origin

5.10.1 Myogenic Spontaneous Activity

Isolated detrusor myocytes can develop spontaneous action potentials and intracellular Ca^{2+} transients, the frequencies of which are greater in cells isolated from overactive human bladders (Fig. 5.2f) [22]. The depolarising phase of the action potential is supported by L-type and T-type Ca^{2+} currents; the latter are activated at potentials near to the membrane potential and so in princi-

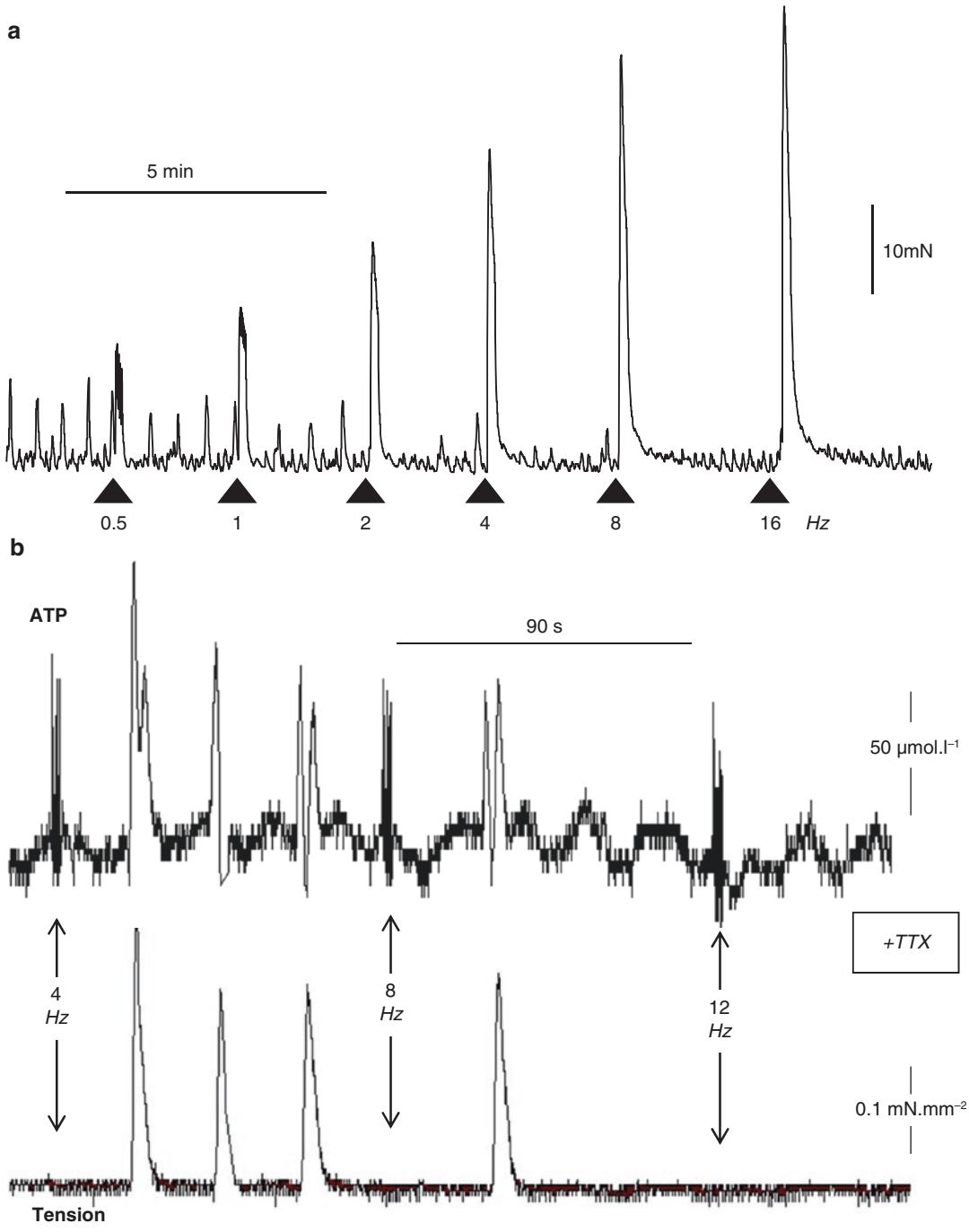

Fig. 5.5 Appearance of spontaneous contractions with absence of nerve-mediated activity. (**a**) Nerve-mediated contractions stimulated by tetanic stimulus with frequencies between 0.5 and 16 Hz. Note the greater spontaneous activity as stimulus frequency decreases. (**b**) Spontaneous contractile activity (lower trace) during abolition of nerve-mediated contractions with 1 µM tetrodotoxin. Upper trace: Extracellular ATP transients accompany spontaneous contractions. Note the stimulus artefacts on the ATP electrode trace co-incident with stimulation at 4, 8 and 12 Hz. Trace in panel **a** adapted from [120]

ple could serve as a pacemaker current. Moreover, the density of T-type Ca^{2+} current is greater in myocytes from overactive human bladders and this could account for the increased frequency of spontaneous action potentials [73]. Detrusor myocytes are connected by connexin45 (Cx45) gap junctions so that electrical activity generated in a cell, or group of cells, could spread to adjacent tissue. However, the expression of Cx45 protein is reduced in human detrusor from overactive bladders, corroborated by an increased electrical resistance between adjacent myocytes. This would limit the speed and extent of spread of electrical signals across the bladder wall [74]. Thus, although localised electrical activity may be generated more in detrusor from overactive bladders, these signals would be confined to a smaller region of the wall bladder. These data do not support the ability of electrical signals to spread across larger regions of the bladder wall that would form the basis of an overactive bladder contraction [23].

It may be hypothesised that during an overactive bladder contraction, detrusor contractility may be greater than that during normal voiding. An estimate of true bladder contractility may be obtained from transformation of the isovolumic phase of detrusor pressure rise during voiding or overactive contractions. However, an overactive contraction does not represent a state of enhanced contractility compared to that for a nerve-mediated voiding contraction, which does not support this hypothesis [75].

Overall, although myogenic activity does occur in detrusor smooth muscle, there is no evidence that the greater frequency and larger amplitude of spontaneous activity in detrusor from overactive bladders is a significant basis of pathological detrusor overactivity.

5.10.2 Neurogenic Detrusor Overactivity (NDO) and Spontaneous Activity

A subset of patients with DO have associated neurological deficits such as spinal cord injury or Parkinson's disease. This subgroup is described as suffering from NDO but whether or not the pathophysiology of the condition is different from that of the majority of DO patients remains unclear at present. However, isolated detrusor preparations from NDO bladders are associated with greater spontaneous contractile activity [76, 77]. Spontaneous contractions from isolated multicellular detrusor preparations obtained from normal or DO bladders are insensitive to application of tetrodotoxin (TTX)—to block nerve action potentials—or atropine—to block the action of Ach that might be released or simply leaks from motor nerves [78]. This implies that intrinsic motor nerves do not generate autonomous activity resulting from release of neurotransmitter. Moreover, nerve-mediated contractions of isolated human detrusor preparations from DO bladders are similar in magnitude or decreased compared to those from normal bladders [36, 78]. This implies that the functional innervation by postganglionic fibres to DO bladders is similar or even reduced compared to normal bladders.

The role of several detrusor K^+ channels in modulating spontaneous activity and their role in the aetiology of NDO in particular has been studied. These channels include small, intermediate and large conductance Ca^{2+}-activated K^+ channels (SK, IK and BK channels, respectively), as well as ATP-dependent K^+ channels. Openers of both BK and SK/IK channels (NS-1619 and SKA-31/NS-309, respectively) reduce spontaneous contractions in rat and human detrusor. These actions are reversed by their respective channel blockers iberiotoxin and apamin [79–82]. IK channels have not been implicated as the IK blocker, TRAM-3K, had no effect [81]. However, with human detrusor samples from NDO patients NS-1619 and iberiotoxin had no effect on spontaneous activity, unlike the situation with detrusor from normal human bladders [76, 77]. This latter result was corroborated by demonstrating a reduced iberiotoxin-sensitive K^+ current and expression of the α-subunit of BK channels, the β1 and β4-subunits were not significantly different [76]. Thus, increased spontaneous activity in isolated detrusor strips from NDO patients may be due, at least in part, to a myogenic response through reduced BK channel density.

An indirect role for motor nerves involvement to generate some spontaneous activity may be inferred from the observation that an increase of nerve stimulation to isolated detrusor samples, with an intact mucosa, leads to a decrease of activity (Fig. 5.5a) [54]. Not only is spontaneous activity resistant to atropine but persists also in the presence of PPADS, an antagonist to most P2X receptors, including $P2X_1$ expressed in detrusor smooth muscle [54]. However, Fig. 5.5b shows an experiment after nerve-mediated contractions had been abolished by addition of TTX where spontaneous activity was also evident and accompanied by transient increases of ATP, as measured by an amperometric ATP-selective sensor placed on the surface of the preparation (McCarthy and Fry, unpublished data). These observations are consistent with the presence of spontaneous transient depolarisations in mouse detrusor that were abolished by the $P2X_1$ receptor antagonist NF449 and increased by latrotoxin [83], a venom that acts on presynaptic nerve terminals and secretory cells to release transmitters [84]. However, the inability of PPADS to diminish spontaneous activity requires explanation.

5.10.3 Mucosal Modulation of Spontaneous Activity and its Significance in Overactive Bladder

The term *Urotheliogenic* derives from the observation that spontaneous contractions are greater when in vitro detrusor preparations retain their covering of mucosa [49]. Although the term implies that it is the urothelium itself that augments detrusor contractions, in fact control may derive from any of the cell types in the mucosa, either singly or in combination. It has been discussed above that diffusional and/or cell-to-cell contacts between mucosa and detrusor layers could generate the augmented spontaneous activity observed when the two layers of the bladder wall are in contact. Moreover, in bladder pathologies thickening of the mucosa occurs, accompanied by an increase in the population of ICs and these are associated with larger amplitude spontaneous contractions that propagate across greater areas of the bladder wall [48]. It is suggested that *lamina propria* IC fall into two subtypes [85], a more abundant population near the urothelium that express α-smooth muscle actin and PDGFRα and not CD34, and a population nearer the detrusor layer that had an inverse expression of these epitopes. It is not clear what are the functional distinctions between these subtypes but any study with isolated ICs is more likely to use the former due to their greater abundance.

With this caveat the pharmacological properties of *lamina propria* ICs can give insight into the interaction between mucosa and detrusor in generating spontaneous activity. Firstly, enzymatically dispersed *lamina propria* ICs do not respond to exogenous cholinergic agonists to generate an intracellular Ca^{2+} transient or electrophysiological responses [64]. However, very low concentrations of carbachol do augment spontaneous activity and Ca^{2+}-wave propagation in isolated bladder sheets with an intact mucosa [11], a potential resolution to this apparent paradox is discussed below. However, ICs respond in a complex way to purines as they generate large inward currents to exogenous ATP, ADP and UTP that suggests that they act via P2Y receptors [64]. This is corroborated by immunohistochemistry that shows an abundance of $P2Y_6$ receptors, with only sparse labelling for $P2X_1$, $P2Y_2$ and $P2Y_4$ receptors on these cells [86]. The inward current is through a Ca^{2+}-activated-Cl^- channel in response to a rise of the intracellular $[Ca^{2+}]$ after purine application. Application of ADP or UTP to bladder sheets with an intact mucosa greatly increases the magnitude of spontaneous contractions, especially in bladders that are already overactive with a thickened mucosa [23]. With these intact bladder sheets, application of P2Y agonists greatly enhances the velocity at which membrane transients or Ca^{2+} waves propagate, as well as increases the area of that bladder wall over which they spread.

The urothelium releases a number of bioactive molecules when subjected to chemical or physical interventions, which include ATP, acetylcholine, prostaglandins and nitric oxide. Most is known about stress-activated ATP release and it is noteworthy that release is augmented from

urothelium obtained from bladders that exhibit overactive pathologies [87–91]. Released ATP is rapidly broken down by ectoATPases to ADP and other metabolites that would have a paracrine effect on the increased numbers of ICs, one result of which would be to upregulate spontaneous activity.

An allied observation is that ACh release from urothelium occurs at much lower levels of physical stress and in much greater quantities compared to ATP release [92]. Moreover, muscarinic receptor agonists augment ATP release from urothelium via M2 receptors [93, 94]. This interaction between muscarinic receptor activation and urothelial ATP release provides a sensory transduction pathway for bladder filling or other stresses to activate suburothelial afferents as well as modulate spontaneous contractions via the above urotheliogenic mechanism. Moreover, the increase of ATP release in pathological bladders provides an understanding of how sensory pathways as well as spontaneous activity is increased in these pathologies.

A final consideration is the range of physical and chemical stressors that can release bioactive molecules. Urothelial cells express purinergic, muscarinic, nicotinic and adrenergic receptors [95–98] among others, which can respond in an autocrine/paracrine mode or to circulating catecholamines. Moreover, a variety of transient receptor potential (TRP) channels [99–101] and piezo-channels [102] have been identified that allow urothelial cells to respond to environmental changes such as low pH, changes to ambient temperature and physical stress or strain changes. This variety of receptor molecules ensures that the urothelium is a sensitive and multimodal sensory structure that provides the link to sensation and outputs such as spontaneous activity and afferent nerve activation.

5.11 The Trigone

Because of its structural connection to the intravesical portion of the ureter, and its potential role as part of the outflow tract, the trigone may play a role in regulating the opening and closure of the ureteric orifices to prevent vesicoureteral reflux. Whilst the main mechanism to prevent reflux is the oblique angle of the insertion of the ureter through the bladder wall, providing a compression valve as the bladder fills, periodic contractions of the trigone may support opening of ureteral orifices to facilitate filling and may also assist compression during voiding contractions of the bladder.

Spontaneous phasic contractions have been recorded in 71% and 89% of trigone strips from pigs and humans, respectively, compared with only 20% in muscle strips from the dome [17]. Moreover, in the trigone spontaneous contractions arise purely from the smooth muscle component, as removal of the mucosa has no effect on their amplitude and frequency [46]. This is in contrast to the situation with tissue from the bulk of the bladder body—the dome—where the presence of the mucosa is crucial to maintain spontaneous activity. The cellular pathways underlying spontaneous contractions have been studied in the superficial trigone of the guinea pig bladder, where the majority of muscle strips also generate spontaneous phasic contractions [103] (Fig. 5.6a). Trigone smooth muscle generates spontaneous bursts of action potentials [104], similar to detrusor from the bladder dome. However, electrical stimulation of this region of the bladder elicits action potentials [105] which do not occur when the dome of the bladder is similarly excited. This demonstrates that the trigone exhibits greater excitability than the bladder dome and that smooth muscle in the two regions are functionally separate. This latter observation is corroborated by the fact that spontaneous electrical activity in the trigone is generated independently from that in the bladder dome [106]. The greater excitability of a functionally independent trigone arises from the fact that its smaller muscle mass, compared to detrusor in the bladder dome, means that the overall electrical resistance of the tissue is greater. Thus, ionic current generated in the tissue will generate larger local potential fields as observed above [105]. The separateness of trigone and detrusor is also indicated by spatiotemporal mapping techniques that show propagating patches of

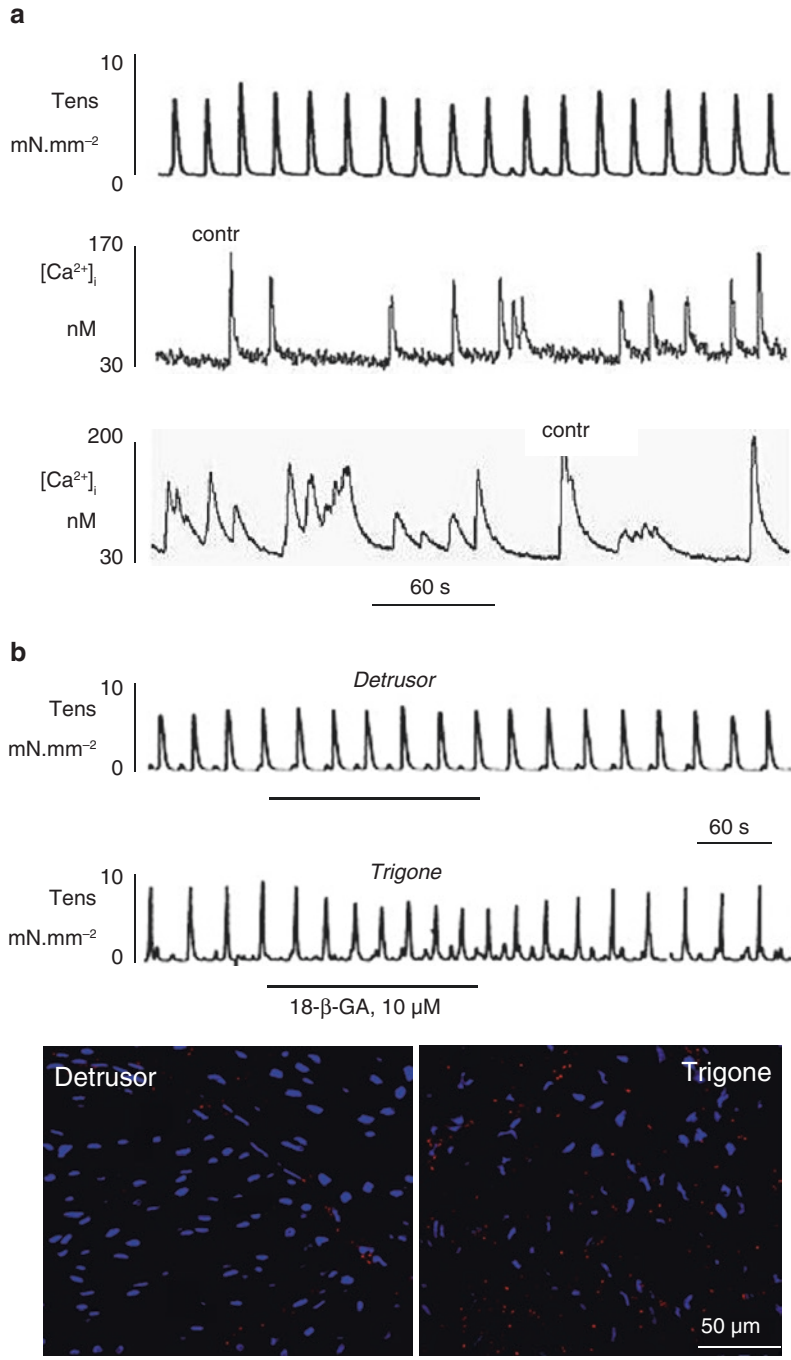

Fig. 5.6 Characteristics of spontaneous activity in trigone. (**a**) Isolated trigone tissue showing regular spontaneous contractions (upper trace). Different patterns of intracellular Ca^{2+} transients in isolated trigone myocytes (middle and lower traces). (**b**) Spontaneous activity and gap junction blockers. Effect of 18-β-glycyrrhetinic acid (GA) on regular spontaneous activity recorded in isolated detrusor (upper trace) or trigone (lower trace) smooth muscle. The two images below are of the muscle layer and are labelled for connexin proteins (red) and nuclei (blue); sections are from detrusor (connexin45, left) and trigone (connexin43, right). (**c**) Effect of a 0-Ca solution (upper panels) on spontaneous contractions (left) and intracellular Ca^{2+} transients (right). Effect of a niflumic acid (100 μM) on spontaneous contractions (middle panel) and intracellular Ca^{2+} transients (lower panel). (**d**) Effect of carbachol (carb, 1 μM) in the absence or presence of 10 μM phenylephrine on tension (upper panel) and intracellular [Ca^{2+}], lower panel. Adapted from [8, 103]

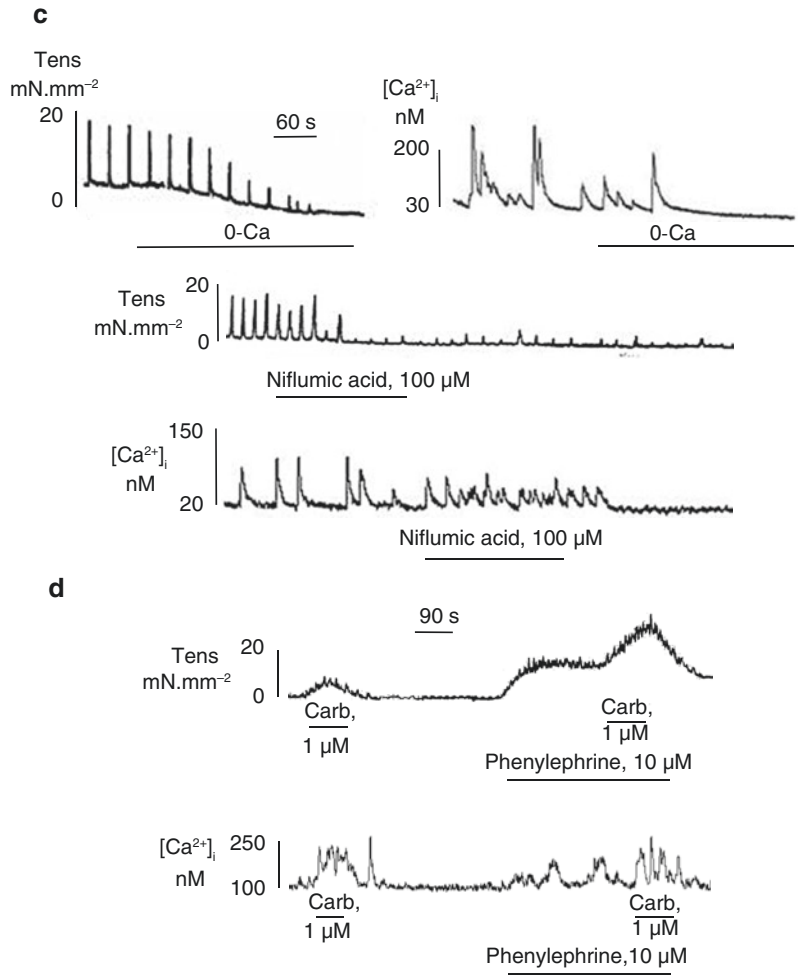

Fig. 5.6 (continued)

contraction in the dome travel mainly along the anterior and lateral surface of the bladder and do not traverse the trigone [107].

The relative ease of electrical transmission in the trigone compared to detrusor is mirrored by a greater abundance of connexin-labelling gap junctions, as determined by immunolabelling [103]. Moreover, the connexin subtype between smooth muscle cells in the trigone is Cx43, rather than Cx45 as in the dome [51], which is of significance as Cx43 gap junctions have a greater unit electrical conductance compared to those formed with Cx45. 18-β glycyrrhetinic acid, a gap junction blocker, reduces the amplitude but increases the frequency of spontaneous contractions in the trigone, whereas under similar conditions it has little effect on detrusor spontaneous activity (Fig. 5.6b). The appearance of less well-coordinated activity in 18-β glycyrrhetinic acid suggests that intercellular communication plays a role in developing such contractions.

The upstroke of the action potential is mainly mediated by Ca^{2+} influx through L-type Ca^{2+} channels as intracellular Ca^{2+} transients are abolished by either an L-type Ca^{2+} channel inhibitor or Ca^{2+} free solution, but not by a T-type Ca^{2+} channel inhibitor. Furthermore, neither thapsigargin, an inhibitor of SR Ca^{2+} uptake, nor FCCP, a mitochondrial uncoupler, are inhibitory, also sug-

gesting the importance of Ca^{2+} influx rather than intracellular Ca^{2+} stores to support contraction [103]. Niflumic acid, a blocker of Ca^{2+}-activated Cl^- channels, also attenuates Ca^{2+} transients and spontaneous contractions of the trigone [103]. At membrane potentials near the resting value such channels would pass inward current which would activate L-type Ca^{2+} channels. Thus L-type Ca^{2+} channel antagonists inhibit both spontaneous contractions and intracellular Ca^{2+} transients (Fig. 5.6c). Carbachol increases intracellular $[Ca^{2+}]$ and thus muscarinic receptor activation would initiate the process of augmenting spontaneous activity.

The trigone is unusual in that both cholinergic and adrenergic agonists augment spontaneous activity, however the rise of intracellular $[Ca^{2+}]$ is greater with carbachol than with the non-selective α-adrenoceptor agonist, phenylephrine. Moreover, phenylephrine increases the cholinergic contractile responses independent of a further rise of intracellular $[Ca^{2+}]$, suggesting that an important action may be to increase the Ca^{2+}-sensitivity of the contractile proteins [108] (Fig. 5.6d). Synergy between cholinergic and adrenergic pathways is also suggested by the fact that a muscarinic receptor antagonist reduces contraction generated by adrenergic agonists [109]. Such synergy between cholinergic and adrenergic pathways allows the autonomic nervous system to regulate spontaneous activity with a high degree of gain and suggests that the trigone exhibits such activity in the filling and voiding phases of bladder activity.

Suppression of spontaneous contractions can be achieved by activation of K^+ channels. However, in contrast to dome detrusor smooth muscle, ATP-dependent K^+ (K_{ATP}) channels appear to have important roles in membrane repolarisation rather than BK and SK channels as is the case in bladder dome detrusor [46].

The greater contractile spontaneity and excitability of the trigone and its functional separation from the bladder dome implies that spontaneous contractions may serve separate purposes. During bladder filling, maintained tonus by the trigone could contribute to the resistance offered by the internal sphincter. Micromotions in the dome of the bladder, which help to keep bladder shape and offer a low tonus, would also not propagate to the trigone as this region of the bladder is fairly rigidly fixed to the bladder base. Thus, the different functions of the two regions of the bladder are reflected in the separate processes that generate and propagate spontaneous activity.

5.12 Changes to Spontaneous Activity in Development and Ageing

Spontaneous contractions develop in the first few post-natal weeks in the neonatal bladder, as exemplified by studies in rats and pigs [11, 110–112]. These are greater in amplitude and less frequent than in the adult bladder, reminiscent of the pattern observed in adult animals with spinal cord injury, an example of pathophysiology recapitulating ontogeny. In the rat, where much work has been done, large bladder contractions may be evoked by mechanical stimulation of the perineum and help to empty the bladder, exemplified by maternal grooming of pups. This indicates the activity of local spinal reflexes when supraspinal pathways are not yet fully developed [113]. Their suppression upon establishment of supraspinal control is supported by the fact that GABA antagonists increase the amplitude of spontaneous contractions in developing animals [114]. Because they have been observed in isolated preparations and intact bladders it is proposed that they result from intrinsic processes in the bladder wall. Such activity is enhanced by low concentrations of muscarinic receptor agonists that initiate excitatory signals that originate in the *lamina propria* and propagate to the detrusor layer [11, 114], potentially mediated by activation of detrusor T-type Ca^{2+} channels [115]. However, the cellular pathways whereby large, infrequent spontaneous contractions in the neonatal bladder change to smaller more frequent ones in the adult bladder remain to be elucidated and have important implications to understand the origin of large contractions in the neurogenic bladder.

An increase of spontaneous activity is also recorded in ageing rats [111, 116] but not mice [117]. However, the pattern is different from that observed in neonatal bladders, consisting of numerous, short-duration events that might imply a different origin. A uniform description of alteration to bladder function with ageing is difficult to describe, as a variety of changes have been observed that may depend on the extent of ageing, as well as the experimental model. However, a number of changes to purinergic and cholinergic signalling systems have been reported in human and animal models. In particular, there is an increased dependence on purinergic signalling during nerve-mediated voiding responses and urothelial transmitter release during filling [117–119]. However, cholinergic signalling changes with age are more variable with a reported decrease [117] or increase [118, 120] of non-neuronal ACh release during filling or supporting nerve-mediated contractions. In view of the association of purinergic signalling with spontaneous activity, or overactive bladder in human detrusor, such a linkage may contribute to increased activity with ageing.

An increase of bladder afferent firing and spontaneous contractions accompanies bladder filling, a phenomenon augmented by administration of P2X receptor agonists or irritants such as cyclophosphamide into the bladder lumen [121]. The induction of spontaneous contractions by raised afferent firing could involve spinal or supraspinal reflexes. A decrease of bladder compliance would therefore be expected to increase bladder afferent firing and hence increase spontaneous activity. Ageing is associated with a spectrum of changes to bladder compliance with reports of it being decreased [122], increased [123] or unchanged [116]. This will reflect various changes that may impact on determining bladder compliance, ranging from altered central or peripheral nervous control that determines detrusor tone during filling [124, 125], or deposition of excess collagen [126] that would reduce bladder compliance. Overall, a number of factors determine how ageing impacts on the biomechanical properties of the bladder during filling, so that there is no single way spontaneous activity may be impacted (see also Sect. 5.14). An additional confounding factor when studying how ageing may impact on any biological function is the range of actual ages that are used for animal models. The life expectancy of a mouse is 2–3 years and for a rat up to 5 years [127], so that many animal models of ageing to date merely reflect middle-aged rather than the aged human for comparison.

5.13 External Influences on the Bladder and Spontaneous Activity

The urinary bladder, due its position immediately above the pelvic floor, is especially prone to external influences that affect its function, particularly in the exacerbation of spontaneous activity and the development of detrusor overactivity. For example, the bladder is prone to irritation by exposure to urinary tract infections or noxious agents, as well as damage from irradiation to treat pelvic organ malignancies which may affect spontaneous activity. Cyclophosphamide or acetic acid are examples of noxious agents often used experimentally to induce bladder pain and inflammation, as well as generate increased spontaneous activity [121, 128]. Cyclophosphamide is a cytotoxic drug with a major side effect of haemorrhagic cystitis mediated importantly through its metabolite acrolein [129]. Acrolein itself has multiple effects including urothelial damage through generation of reactive oxygen species and exposure of the deeper bladder layers to urine [130]. Acetic acid will also reduce urothelial permeability with similar consequences [131]. In consequence, cyclophosphamide or acetic acid infusion into the bladder lumen increases ATP release [132, 133], as well as inducing an overactive bladder as measured by cytometry [132]. Cyclophosphamide-induced detrusor overactivity may be reduced by blocking urothelium receptors to prokineticin 2, a chemokine-like peptide implicated in the development of inflammatory and pain responses in the bladder [128]. The important role of the mucosa has also been implicated in radiation-induced cystitis

and its regulation of bladder contractions [54]. Radiation-treatment increased detrusor contraction after application of contractile agonists such as carbachol; however, this was not observed in mucosal-intact preparations. Radiation cystitis is also associated with increased fibrosis in the bladder wall, a consequent decrease of compliance and development of spontaneous non-voiding contractions with urinary leakage. Resolution of the fibrosis by post-irradiation treatment with the hormone relaxin in rat bladder not only normalised the fibrosis but reversed the decrease of compliance and development of spontaneous non-voiding contractions [134]. Various noxious interventions will impact differently on bladder function, one of the final common pathways being the development of spontaneous contractions, but potentially by different processes. Thus, it is important to characterise the fundamental pathways altered by different interventions to able to ameliorate the consequences to lower urinary tract function by these different processes.

5.14 The Clinical Consequences of Bladder Spontaneous Activity in Health and Disease

Spontaneous contractile activity is a fundamental feature of bladder function and is reflected in recordings from the intact bladder to isolated myocytes. It occurs not just in the smooth muscle layer but also in the *lamina propria*. The physiological functions are postulated to add a resting tone to the bladder wall to enable the bladder itself to efficiently raise detrusor pressure during initiation of voiding and also to affect the gain of signal transduction to afferent nerve activation during bladder filling. Two pathological states may reflect a failure of this basic system: (i) bladder underactivity, when the increase of detrusor pressure is insufficient to completely void the contents of the bladder and (ii) detrusor overactivity when large, uncontrollable contractions during modest bladder filling leads to sensations of urgency and sometimes incontinence. However, whether changes to the processes generating normal spontaneous contractions results in pathological states remains to be answered.

Detrusor underactivity (DU) is a relatively new term to describe poor voiding performance and various publications have attempted to define a clinical picture [135, 136]. However, the clinical criteria used to define DU are currently empirical and do little to identify fundamental causes of the symptom complex. There is no evidence that DU results from contractile failure of detrusor muscle [74], but more likely is due to a replacement of muscle with extracellular matrix. This has relevance to the role of spontaneous activity in symptoms associated with DU. If the extracellular matrix is predominantly of collagen the bladder wall will be stiffer and hence a spontaneous contraction will transmit more energy to afferent transducing mechanisms and so increase a sense of urgency without a powerful contraction [137]. If the extracellular matrix is composed more of a gel-like ground substance of glycosaminoglycans and glycoproteins, then bladder compliance will increase, and transmission of forces depressed [138]. Both states have been reported in failing bladders [139] and the pathways that lead from one state or another have yet to be determined.

Detrusor overactivity has been better described (Fig. 5.2a) and occurs during filling. Again, the precise aetiology is unknown and several theories have been advanced, which need not be mutually exclusive: altered central control of the normal voiding reflex [140]; a myogenic hypothesis of increased detrusor excitability and spontaneous activity [74, 141]; enhanced spinal reflexes; greater urotheliogenic interaction within and between *lamina propria* and detrusor, for example from enhanced stretch-activated ATP release and enhanced spontaneous activity [89].

The uncertainty in characterising, by fundamental research, the extremely common condition of DO, and the recent description of DU, underlies the continuing need to interweave investigative and clinical research to explain how normal spontaneous activity can manifest itself as pathological entities.

References

1. Seth JH, Panicker JN, Fowler CJ. The neurological organization of micturition. Handb Clin Neurol. 2013;117:111–7.
2. Khandelwal P, Abraham SN, Apodaca G. Cell biology and physiology of the uroepithelium. Am J Physiol Ren Physiol. 2009;297:F1477–501.
3. Tanaka ST, Ishii K, DeMarco RT, Pope JC, Brock JW, Hayward SW. Endodermal origin of bladder trigone inferred from mesenchymal-epithelial interactions. J Urol. 2010;183:386–91.
4. Abrams P, Cardozo L, Fall M, Griffiths D, Rosier P, Ulmsten U, van Kerrebroeck P, Victor A, Wein A. The standardisation of terminology of lower urinary tract function. Neurourol Urodyn. 2002;21:167–78.
5. Irwin DE, Milsom I, Hunskaar S, Reilly K, Kopp Z, Herschorn S, Coyne K, Kelleher C, Hampel C, Artibani W, Abrams P. Population-based survey of urinary incontinence, overactive bladder, and other lower urinary tract symptoms in five countries: results of the EPIC study. Eur Urol. 2006;50:1306–14.
6. Diamond P, Hassonah S, Alarab M, Lovatsis D, Drutz HP. The prevalence of detrusor overactivity amongst patients with symptoms of overactive bladder: a retrospective cohort study. Int Urogynecol J. 2012;23:1577–80.
7. Mosso A, Pellacani P. Sur les fonctions de la vessie. Arch Ital Biol 1882; 1: 97–128. Tr. R. Feneley 2011, Burleigh Press, Bristol, UK. ISBN 9780956941305.
8. van Os-Bossagh P, Kosterman LM, Hop WC, Westerhof BE, de Bakker JV, Drogendijk AC, van Duyl WA. Micromotions of bladder wall in chronic pelvic pain (CPP): a pilot study. Int Urogynecol J Pelvic Floor Dysfunct. 2001;12:89–96.
9. Drake MJ, Harvey IJ, Gillespie JI, van Duyl WA. Localized contractions in the normal human bladder and in urinary urgency. BJU Int. 2005;95:1002–5.
10. Drake MJ, Hedlund P, Harvey IJ, Pandita RK, Andersson KE, Gillespie JI. Partial outlet obstruction enhances modular autonomous activity in the isolated rat bladder. J Urol. 2003;170:276–9.
11. Kanai A, Roppolo J, Ikeda Y, Zabbarova I, Tai C, Birder L, Griffiths D, de Groat W, Fry CH. Origin of spontaneous activity in neonatal and adult rat bladders and its enhancement by stretch and muscarinic agonists. Am J Physiol Ren Physiol. 2007;292:F1065–72.
12. Parsons BA, Drake MJ, Gammie A, Fry CH, Vahabi B. The validation of a functional, isolated pig bladder model for physiological experimentation. Front Pharmacol. 2012;3:52.
13. Vahabi B, Drake MJ. Physiological and pathophysiological implications of micromotion activity in urinary bladder function. Acta Physiol. 2015;213:360–70.
14. Lagou M, Drake MJ, Gillespie JI. Volume-induced effects on the isolated bladder: a possible local reflex. BJU Int. 2004;94:1356–65.
15. Drake M, Gillespie J, Hedlund P, Harvey I, Lagou M, Andersson KE. Muscarinic stimulation of the rat isolated whole bladder: pathophysiological models of detrusor overactivity. Auton Autacoid Pharmacol. 2006;26:261–6.
16. Hammad FT, Stephen B, Lubbad L, Morrison JF, Lammers WJ. Macroscopic electrical propagation in the guinea pig urinary bladder. Am J Physiol Ren Physiol. 2014;307:F172–82.
17. Sibley GN. A comparison of spontaneous and nerve-mediated activity in bladder muscle from man, pig and rabbit. J Physiol. 1984;354:431–43.
18. Hashitani H, Brading AF, Suzuki H. Correlation between spontaneous electrical, calcium and mechanical activity in detrusor smooth muscle of the guinea-pig bladder. Br J Pharmacol. 2004;141:183–93.
19. Montgomery BS, Fry CH. The action potential and net membrane currents in isolated human detrusor smooth muscle cells. J Urol. 1992;147:176–84.
20. Nakahira Y, Hashitani H, Fukuta H, Sasaki S, Kohri K, Suzuki H. Effects of isoproterenol on spontaneous excitations in detrusor smooth muscle cells of the guinea pig. J Urol. 2001;166:335–40.
21. Meng E, Young JS, Brading AF. Spontaneous activity of mouse detrusor smooth muscle and the effects of the urothelium. Neurourol Urodyn. 2008;27:79–87.
22. Sui G, Fry CH, Malone-Lee J, Wu C. Aberrant Ca^{2+} oscillations in smooth muscle cells from overactive human bladders. Cell Calcium. 2009;45:456–64.
23. Fry CH, Young JS, Jabr RI, McCarthy C, Ikeda Y, Kanai AJ. Modulation of spontaneous activity in the overactive bladder: the role of P2Y agonists. Am J Physiol Ren Physiol. 2012;302:F1447–54.
24. Vlaskovska M, Kasakov L, Rong W, Bodin P, Bardini M, Cockayne DA, Ford AP, Burnstock G. P2X3 knock-out mice reveal a major sensory role for urothelially released ATP. J Neurosci. 2001;21:5670–7.
25. McCarthy CJ, Zabbarova IV, Brumovsky PR, Roppolo JR, Gebhart GF, Kanai AJ. Spontaneous contractions evoke afferent nerve firing in mouse bladders with detrusor overactivity. J Urol. 2009;181:1459–66.
26. Heppner TJ, Tykocki NR, Hill-Eubanks D, Nelson MT. Transient contractions of urinary bladder smooth muscle are drivers of afferent nerve activity during filling. J Gen Physiol. 2016;147:323–35.
27. Drake MJ, Kanai A, Bijos DA, Ikeda Y, Zabbarova I, Vahabi B, Fry CH. The potential role of unregulated autonomous bladder micromotions in urinary storage and voiding dysfunction; overactive bladder and detrusor underactivity. BJU Int. 2017;119:22–9.
28. Abrams P. Describing bladder storage function: overactive bladder syndrome and detrusor overactivity. Urology. 2003;62:28–37.
29. Kinder RB, Mundy AR. Pathophysiology of idiopathic detrusor instability and detrusor hyper-

reflexia. An in vitro study of human detrusor muscle. Br J Urol. 1987;60:509–15.
30. Kato K, Wein AJ, Radzinski C, Longhurst PA, McGuire EJ, Miller LF, Elbadawi A, Levin RM. Short term functional effects of bladder outlet obstruction in the cat. J Urol. 1990;143:1020–5.
31. Fry CH. Physiological properties of the lower urinary tract. In: Mundy AR, Fitpatrick JM, Neal DE, George NJ, editors. The scientific basis of urology. Colchester: Informa Healthcare; 2010. p. 244–65.
32. Fry CH, Chess-Williams R, Hashitani H, Kanai AJ, McCloskey K, Takeda M, Vahabi B. Cell biology. In: Abrams P, Cardozo L, Wagg A, Wein A, editors. Incontinence. 6th ed. Paris: ICUD ICS; 2016. p. 148–258. ISBN: 978-0-9569607-3-3.
33. Sui GP, Wu C, Fry CH. A description of Ca^{2+} channels in human detrusor smooth muscle. BJU Int. 2003;92:476–82.
34. Anderson UA, Carson C, Johnston L, Joshi S, Gurney AM, McCloskey KD. Functional expression of KCNQ (Kv7) channels in guinea pig bladder smooth muscle and their contribution to spontaneous activity. Br J Pharmacol. 2013;169:1290–304.
35. Petkov GV. Central role of the BK channel in urinary bladder smooth muscle physiology and pathophysiology. Am J Phys Regul Integr Comp Phys. 2014;307:R571–84.
36. Fry CH, Bayliss M, Young JS, Hussain M. Influence of age and bladder dysfunction on the contractile properties of isolated human detrusor smooth muscle. BJU Int. 2011;108:E91–6.
37. Harvey RA, Skennerton DE, Newgreen D, Fry CH. The contractile potency of adenosine triphosphate and ecto-adenosine triphosphatase activity in guinea pig detrusor and detrusor from patients with a stable, unstable or obstructed bladder. J Urol. 2002;168:1235–9.
38. Hashitani H, Yanai Y, Suzuki H. Role of interstitial cells and gap junctions in the transmission of spontaneous Ca^{2+} signals in detrusor smooth muscles of the guinea-pig urinary bladder. J Physiol. 2004;559:567–81.
39. Gray SM, McGeown JG, McMurray G, McCloskey KD. Functional innervation of Guinea-pig bladder interstitial cells of cajal subtypes: neurogenic stimulation evokes in situ calcium transients. PLoS One. 2013;8:e53423.
40. Hirst GD, Edwards FR. Electrical events underlying organized myogenic contractions of the guinea pig stomach. J Physiol. 2006;576:659–65.
41. Sanders KM, Ward SM, Koh SD. Interstitial cells: regulators of smooth muscle function. Physiol Rev. 2014;94:859–907.
42. Hashitani H. Interaction between interstitial cells and smooth muscles in the lower urinary tract and penis. J Physiol. 2006;576:707–14.
43. Koh BH, Roy R, Hollywood MA, Thornbury KD, McHale NG, Sergeant GP, Hatton WJ, Ward SM, Sanders KM, Koh SD. Platelet-derived growth factor receptor-α cells in mouse urinary bladder: a new class of interstitial cells. J Cell Mol Med. 2012;16:691–700.
44. Monaghan KP, Johnston L, McCloskey KD. Identification of PDGFRα positive populations of interstitial cells in human and guinea pig bladders. J Urol. 2012;188:639–47.
45. Lee H, Koh BH, Yamasaki E, George NE, Sanders KM, Koh SD. UTP activates small-conductance Ca^{2+}-activated K^+ channels in murine detrusor PDGFRα+ cells. Am J Physiol Ren Physiol. 2015;309:F569–74.
46. Akino H, Chapple CR, McKay N, Cross RL, Murakami S, Yokoyama O, Chess-Williams R, Sellers DJ. Spontaneous contractions of the pig urinary bladder: the effect of ATP-sensitive potassium channels and the role of the mucosa. BJU Int. 2008;102:1168–74.
47. Moro C, Uchiyama J, Chess-Williams R. Urothelial/lamina propria spontaneous activity and the role of M3 muscarinic receptors in mediating rate responses to stretch and carbachol. Urology. 2011;78:1442.e9–15.
48. Kushida N, Fry CH. On the origin of spontaneous activity in the bladder. BJU Int. 2016;117:982–92.
49. Ikeda Y, Kanai A. Urotheliogenic modulation of intrinsic activity in spinal cord-transected rat bladders: role of mucosal muscarinic receptors. Am J Physiol Ren Physiol. 2008;295:F454–61.
50. Xin W, Li N, Cheng Q, Petkov GV. BK channel-mediated relaxation of urinary bladder smooth muscle: a novel paradigm for phosphodiesterase type 4 regulation of bladder function. J Pharmacol Exp Ther. 2014;349:56–65.
51. Ikeda Y, Fry C, Hayashi F, Stolz D, Griffiths D, Kanai A. Role of gap junctions in spontaneous activity of the rat bladder. Am J Physiol Ren Physiol. 2007;293:F1018–25.
52. Roosen A, Datta SN, Chowdhury RA, Patel PM, Kalsi V, Elneil S, Dasgupta P, Kessler TM, Khan S, Panicker J, Fry CH, Brandner S, Fowler CJ, Apostolidis A. Suburothelial myofibroblasts in the human overactive bladder and the effect of botulinum neurotoxin type A treatment. Eur Urol. 2009;55:1440–8.
53. Moro C, Leeds C, Chess-Williams R. Contractile activity of the bladder urothelium/lamina propria and its regulation by nitric oxide. Eur J Pharmacol. 2012;674:445–9.
54. McDonnell BM, Buchanan PJ, Prise KM, McCloskey KD. Acute radiation impacts contractility of guinea-pig bladder strips affecting mucosal-detrusor interactions. PLoS One. 2018;13:e0193923.
55. Moro C, Tajouri L, Chess-Williams R. Adrenoceptor function and expression in bladder urothelium and lamina propria. Urology. 2013;81:211.e1–7.
56. Sadananda P, Chess-Williams R, Burcher E. Contractile properties of the pig bladder mucosa in response to neurokinin A: a role for myofibroblasts? Br J Pharmacol. 2008;153:1465–73.

57. Hinz B. Masters and servants of the force: the role of matrix adhesions in myofibroblast force perception and transmission. Eur J Cell Biol. 2006;85:175–81.
58. Lee K, Isogai A, Antoh M, Kajioka S, Eto M, Hashitani H. Role of K^+ channels in regulating spontaneous activity in the muscularis mucosae of guinea pig bladder. Eur J Pharmacol. 2018;818:30–7.
59. Heppner TJ, Layne JJ, Pearson JM, Sarkissian H, Nelson MT. Unique properties of muscularis mucosae smooth muscle in guinea pig urinary bladder. Am J Phys Regul Integr Comp Phys. 2011;301:R351–62.
60. Isogai A, Lee K, Mitsui R, Hashitani H. Functional coupling of TRPV4 channels and BK channels in regulating spontaneous contractions of the guinea pig urinary bladder. Pflugers Arch. 2016;468:1573–85.
61. Hashitani H, Mitsui R, Shimizu Y, Higashi R, Nakamura K. Functional and morphological properties of pericytes in suburothelial venules of the mouse bladder. Br J Pharmacol. 2012;167:1723–36.
62. Hashitani H, Lang RJ. Spontaneous activity in the microvasculature of visceral organs: role of pericytes and voltage-dependent Ca^{2+} channels. J Physiol. 2016;594:555–65.
63. Wiseman OJ, Fowler CJ, Landon DN. The role of the human bladder lamina propria myofibroblast. BJU Int. 2003;91:89–93.
64. Wu C, Sui GP, Fry CH. Purinergic regulation of guinea pig suburothelial myofibroblasts. J Physiol. 2004;559:231–43.
65. Sui GP, Rothery S, Dupont E, Fry CH, Severs NJ. Gap junctions and connexin expression in human suburothelial interstitial cells. BJU Int. 2002;90:118–29.
66. Drake MJ, Fry CH, Eyden B. Structural characterization of myofibroblasts in the bladder. BJU Int. 2006;97:29–32.
67. Sharif-Afshar AR, Donohoe JM, Pope JC 4th, Adams MC, Brock JW 3rd, Bhowmick NA. Stromal hyperplasia in male bladders upon loss of transforming growth factor-beta signaling in fibroblasts. J Urol. 2005;174:1704–7.
68. Birder L, Andersson KE. Urothelial signaling. Physiol Rev. 2013;93:653–80.
69. Okinami T, Imamura M, Nishikawa N, Negoro H, Sugino Y, Yoshimura K, Kanematsu A, Hashitani H, Ogawa O. Altered detrusor gap junction communications induce storage symptoms in bladder inflammation: a mouse cyclophosphamide-induced model of cystitis. PLoS One. 2014;9:e104216.
70. Palani D, Ghildyal P, Manchanda R. Effects of heptanol and carbenoxolone on noradrenaline induced contractions in guinea pig vas deferens. Auton Neurosci. 2007;137:56–62.
71. Heppner TJ, Hennig GW, Nelson MT, Vizzard MA. Rhythmic calcium events in the lamina propria network of the urinary bladder of rat pups. Front Syst Neurosci. 2017;11:87.
72. Hawthorn MH, Chapple CR, Cock M, Chess-Williams R. Urothelium-derived inhibitory factor(s) influences on detrusor muscle contractility in vitro. Br J Pharmacol. 2000;129:416–9.
73. Sui GP, Wu C, Severs N, Newgreen D, Fry CH. The association between T-type Ca^{2+} current and outward current in isolated human detrusor cells from stable and overactive bladders. BJU Int. 2007;99:436–41.
74. Sui GP, Coppen SR, Dupont E, Rothery S, Gillespie J, Newgreen D, Severs NJ, Fry CH. Impedance measurements and connexin expression in human detrusor muscle from stable and unstable bladders. BJU Int. 2003;92:297–305.
75. Fry CH, Gammie A, Drake MJ, Abrams P, Kitney DG, Vahabi B. Estimation of bladder contractility from intravesical pressure-volume measurements. Neurourol Urodyn. 2017;36:1009–14.
76. Oger S, Behr-Roussel D, Gorny D, Bernabé J, Comperat E, Chartier-Kastler E, Denys P, Giuliano F. Effects of potassium channel modulators on myogenic spontaneous phasic contractile activity in human detrusor from neurogenic patients. BJU Int. 2011;108:604–11.
77. Hristov KL, Afeli SA, Parajuli SP, Cheng Q, Rovner ES, Petkov GV. Neurogenic detrusor overactivity is associated with decreased expression and function of the large conductance voltage- and Ca^{2+}-activated K^+ channels. PLoS One. 2013;8:e68052.
78. Mills IW, Greenland JE, McMurray G, McCoy R, Ho KM, Noble JG, Brading AF. Studies of the pathophysiology of idiopathic detrusor instability: the physiological properties of the detrusor smooth muscle and its pattern of innervation. J Urol. 2000;163:646–51.
79. Soder RP, Petkov GV. Large conductance Ca^{2+}-activated K^+ channel activation with NS1619 decreases myogenic and neurogenic contractions of rat detrusor smooth muscle. Eur J Pharmacol. 2011;670:252–9.
80. Hristov KL, Parajuli SP, Soder RP, Cheng Q, Rovner ES, Petkov GV. Suppression of human detrusor smooth muscle excitability and contractility via pharmacological activation of large conductance Ca^{2+}-activated K^+ channels. Am J Phys Cell Physiol. 2012;302:C1632–41.
81. Parajuli SP, Hristov KL, Soder RP, Kellett WF, Petkov GV. NS309 decreases rat detrusor smooth muscle membrane potential and phasic contractions by activating SK3 channels. Br J Pharmacol. 2013;168:1611–25.
82. Soder RP, Parajuli SP, Hristov KL, Rovner ES, Petkov GV. SK channel-selective opening by SKA-31 induces hyperpolarization and decreases contractility in human urinary bladder smooth muscle. Am J Phys Regul Integr Comp Phys. 2013;304:R155–63.
83. Young JS, Meng E, Cunnane TC, Brain KL. Spontaneous purinergic neurotransmis-

sion in the mouse urinary bladder. J Physiol. 2008;586:5743–55.
84. Südhof TC. α-Latrotoxin and its receptors: neurexins and CIRL/latrophilins. Annu Rev Neurosci. 2001;24:933–62.
85. Gevaert T, Vanstreels E, Daelemans D, Franken J, van der Aa T, Roskams T, de Ridder D. Identification of different phenotypes of interstitial cells in the upper and deep lamina propria of the human bladder dome. J Urol. 2014;192:1555–63.
86. Sui GP, Wu C, Fry CH. Characterization of the purinergic receptor subtype on guinea-pig suburothelial myofibroblasts. BJU Int. 2006;97: 1327–31.
87. Birder LA, Barrick SR, Roppolo JR, Kanai AJ, de Groat WC, Kiss S, Buffington CA. Feline interstitial cystitis results in mechanical hypersensitivity and altered ATP release from bladder urothelium. Am J Physiol Ren Physiol. 2003;285:F423–9.
88. Sun Y, Chai TC. Augmented extracellular ATP signaling in bladder urothelial cells from patients with interstitial cystitis. Am J Phys Cell Physiol. 2006;290:C27–34.
89. Munoz A, Smith CP, Boone TB, Somogyi GT. Overactive and underactive bladder dysfunction is reflected by alterations in urothelial ATP and NO release. Neurochem Int. 2011;58:295–300.
90. Munoz A, Somogyi GT, Boone TB, Ford AP, Smith CP. Modulation of bladder afferent signals in normal and spinal cord-injured rats by purinergic $P2X_3$ and $P2X_{2/3}$ receptors. BJU Int. 2012;110: E409–14.
91. Shiina K, Hayashida KI, Ishikawa K, Kawatani M. ATP release from bladder urothelium and serosa in a rat model of partial bladder outlet obstruction. Biomed Res. 2016;37:299–304.
92. McLatchie LM, Young JS, Fry CH. Regulation of ACh release from guinea pig bladder urothelial cells: potential role in bladder filling sensations. Br J Pharmacol. 2014;171:3394–403.
93. Kullmann FA, Artim DE, Birder LA, de Groat WC. Activation of muscarinic receptors in rat bladder sensory pathways alters reflex bladder activity. J Neurosci. 2008;28:1977–87.
94. McLatchie LM, Fry CH. ATP release from freshly isolated guinea-pig bladder urothelial cells: a quantification and study of the mechanisms involved. BJU Int. 2015;115:987–93.
95. Birder LA, Ruan H, Chopra B, Xiang Z, Barrick S, Buffington CA, Roppolo JR, Ford AP, de Groat WC, Burnstock G. Alterations in P2X and P2Y purinergic receptor expression in urinary bladder from normal cats and cats with interstitial cystitis. Am J Phys. 2004;287:F1084–91.
96. Beckel JM, Kanai A, Lee SJ, de Groat WC, Birder LA. Expression of functional nicotinic acetylcholine receptors in rat urinary bladder epithelial cells. Am J Phys. 2006;290:F103–10.
97. Chess-Williams R. Muscarinic receptors of the urinary bladder: detrusor, urothelial and prejunctional. Auton Autacoid Pharmacol. 2002;22:1330–145.
98. Birder LA, Nealen M, Kiss S, de Groat WC, Caterina MJ, Wang E, Apodaca G, Kanai AJ. Beta-adrenoceptor agonists stimulate endothelial nitric oxide synthase in rat urinary bladder urothelial cells. J Neurosci. 2002;22:8063–70.
99. Birder LA, Kanai A, de Groat WC, Kiss S, Nealen ML, Burke NE, Dineley KE, Watkins S, Reynolds IJ, Caterina MJ. Vanilloid receptor expression suggests a sensory role for urinary bladder epithelial cells. Proc Natl Acad Sci. 2001;98:13396–401.
100. Stein RJ, Santos S, Nagatomi J, Hayashi Y, Minnery BS, Xavier M, Patel AS, Nelson JB, Futrell WJ, Yoshimura N, Chancellor MB, De Miguel F. Cool ($TRPM_8$) and hot ($TRPV_1$) receptors in the bladder and male genital tract. J Urol. 2004;172: 1175–8.
101. Streng T, Axelsson HE, Hedlund P, Andersson DA, Jordt SE, Bevan S, Andersson KE, Högestätt ED, Zygmunt PM. Distribution and function of the hydrogen sulfide-sensitive $TRPA_1$ ion channel in rat urinary bladder. Eur Urol. 2008;53:391–9.
102. Miyamoto T, Mochizuki T, Nakagomi H, Kira S, Watanabe M, Takayama Y, Suzuki Y, Koizumi S, Takeda M, Tominaga M. Functional role for piezo1 in stretch-evoked Ca^{2+} influx and ATP release in urothelial cell cultures. J Biol Chem. 2014;289:16565–75.
103. Roosen A, Wu C, Sui G, Chowdhury RA, Patel PM, Fry CH. Characteristics of spontaneous activity in the bladder trigone. Eur Urol. 2009;56: 346–53.
104. Callahan SM, Creed KE. Electrical and mechanical activity of the isolated lower urinary tract of the guinea-pig. Br J Pharmacol. 1981;74:353–8.
105. Kelley RS, Vardy MD, Simons GR, Chen H, Ascher-Walsh C, Brodman M. A pilot study of cardiac electrophysiology catheters to map and pace bladder electrical activity. Neurourol Urodyn. 2017;36:1174–7.
106. Shafik A. Role of the trigone in micturition. J Endourol. 1998;12:273–7.
107. Lentle RG, Reynolds GW, Janssen PW, Hulls CM, King QM, Chambers JP. Characterisation of the contractile dynamics of the resting ex vivo urinary bladder of the pig. BJU Int. 2015;116:973–83.
108. Roosen A, Fry CH, Sui G, Wu C. Adreno-muscarinic synergy in the bladder trigone: calcium-dependent and -independent mechanisms. Cell Calcium. 2009;45:11–7.
109. Wuest M, Witte LP, Michel-Reher MB, Propping S, Braeter M, Strugala GJ, Wirth MP, Michel MC, Ravens U. The muscarinic receptor antagonist propiverine exhibits α_1-adreno-ceptor antagonism in human prostate and porcine trigone. World J Urol. 2011;29:149–55.

110. Oh SJ, Lee KH, Kim SJ, Kim KW, Kim KM, Choi H. Active properties of the urinary bladder: in vitro comparative studies between adult and neonatal rats. BJU Int. 2000;85:1126–33.
111. Szigeti GP, Somogyi GT, Csernoch L, Széll EA. Age-dependence of the spontaneous activity of the rat urinary bladder. J Muscle Res Cell Motil. 2005;26:23–9.
112. Vahabi B, Sellers DJ, Bijos DA, Drake MJ. Phasic contractions in urinary bladder from juvenile versus adult pigs. PLoS One. 2013;8(3):e58611.
113. Sugaya K, De Groat WC. Micturition reflexes in the in vitro neonatal rat brain stem-spinal cord-bladder preparation. Am J Phys Regul Integr Comp Phys. 1994;266:R658–67.
114. Ng YK, de Groat WC, Wu HY. Muscarinic regulation of neonatal rat bladder spontaneous contractions. Am J Phys Regul Integr Comp Phys. 2006;291:R1049–59.
115. Ekman M, Andersson KE, Arner A. Receptor-induced phasic activity of newborn mouse bladders is inhibited by protein kinase C and involves T-type Ca^{2+} channels. BJU Int. 2009;104:690–7.
116. Lluel P, Palea S, Barras M, Grandadam F, Heudes D, Bruneval P, Corman B, Martin DJ. Functional and morphological modifications of the urinary bladder in aging female rats. Am J Phys Regul Integr Comp Phys. 2000;278:R964–72.
117. Daly DM, Nocchi L, Liaskos M, McKay NG, Chapple C, Grundy D. Age-related changes in afferent pathways and urothelial function in the male mouse bladder. J Physiol. 2014;592:537–49.
118. Yoshida M, Miyamae K, Iwashita H, Otani M, Inadome A. Management of detrusor dysfunction in the elderly: changes in acetylcholine and adenosine triphosphate release during aging. Urology. 2004;63(3 Suppl):17–23.
119. Sui G, Fry CH, Montgomery B, Roberts M, Wu R, Wu C. Purinergic and muscarinic modulation of ATP release from the urothelium and its paracrine actions. Am J Physiol Ren Physiol. 2014;306:F286–98.
120. Yoshida M, Masunaga K, Satoji Y, Maeda Y, Nagata T, Inadome A. Basic and clinical aspects of non-neuronal acetylcholine: expression of non-neuronal acetylcholine in urothelium and its clinical significance. J Pharmacol Sci. 2008;106:193–8.
121. Yu Y, de Groat WC. Sensitization of pelvic afferent nerves in the in vitro rat urinary bladder-pelvic nerve preparation by purinergic agonists and cyclophosphamide pretreatment. Am J Physiol Ren Physiol. 2008;294:F1146–56.
122. Chun AL, Wallace LJ, Gerald MC, Levin RM, Wein AJ. Effect of age on in vivo urinary bladder function in the rat. J Urol. 1988;139:625–7.
123. Smith PP, DeAngelis A, Kuchel GA. Detrusor expulsive strength is preserved, but responsiveness to bladder filling and urinary sensitivity is diminished in the aging mouse. Am J Phys Regul Integr Comp Phys. 2012;302:R577–86.
124. Hotta H, Morrison JF, Sato A, Uchida S. The effects of aging on the rat bladder and its innervation. Jpn J Physiol. 1995;45:823–36.
125. Smith PP, DeAngelis A, Simon R. Evidence of increased centrally enhanced bladder compliance with ageing in a mouse model. BJU Int. 2015;115(2):322–9.
126. Zhao W, Aboushwareb T, Turner C, Mathis C, Bennett C, Sonntag WE, Andersson KE, Christ G. Impaired bladder function in aging male rats. J Urol. 2010;184:378–85.
127. Gorbunova V, Bozzella MJ, Seluanov A. Rodents for comparative aging studies: from mice to beavers. Age (Dordr). 2008;30:111–9.
128. Chen B, Zhang H, Liu L, Wang J, Ye Z. PK2/PKR1 signaling regulates bladder function and sensation in rats with cyclophosphamide-induced cystitis. Mediat Inflamm. 2015;2015:289519.
129. Brock N, Stekar J, Pohl J, Niemeyer U, Scheffler G. Acrolein, the causative factor of urotoxic side-effects of cyclophosphamide, ifosfamide, trofosfamide and sufosfamide. Arzneimittelforschung. 1979;29:659–61.
130. Haldar S, Dru C, Bhowmick NA. Mechanisms of hemorrhagic cystitis. Am J Clin Exp Urol. 2014;2:199–208.
131. Birder LA, de Groat W, Mills I, Morrison J, Thor K, Drake M. Neural control of the lower urinary tract: peripheral and spinal mechanisms. Neurourol Urodyn. 2010;29:128–39.
132. Sugaya K, Nishijima S, Tasaki S, Kadekawa K, Miyazato M, Ogawa Y. Effects of propiverine and naftopidil on the urinary ATP level and bladder activity after bladder stimulation in rats. Neurosci Lett. 2007;429:142–6.
133. Girard BM, Wolf-Johnston A, Braas KM, Birder LA, May V, Vizzard MA. PACAP-mediated ATP release from rat urothelium and regulation of PACAP/VIP and receptor mRNA in micturition pathways after cyclophosphamide (CYP)-induced cystitis. J Mol Neurosci. 2008;36:310–20.
134. Ikeda Y, Zabbarova IV, Birder LA, Wipf P, Getchell SE, Tyagi P, Fry CH, Drake MJ, Kanai AJ. Relaxin-2 therapy reverses radiation-induced fibrosis and restores bladder function in mice. Neurourol Urodyn. 2018;37:2441–51. https://doi.org/10.1002/nau.23721.
135. Chapple CR, Osman NI, Birder LA, van Koeveringe GA, Oelke M, Nitti VW, Drake MJ, Yamaguchi O, Abrams P, Smith PP. The underactive bladder: a new clinical concept? Eur Urol. 2015;68:351–3.
136. Gammie A, Kaper M, Dorrepaal C, Kos T, Abrams P. Signs and symptoms of detrusor underactivity: an analysis of clinical presentation and urodynamic tests from a large group of patients undergoing pressure flow studies. Eur Urol. 2016;69:361–9.
137. Kanai A, Fry C, Ikeda Y, Kullmann FA, Parsons B, Birder L. Implications for bidirectional signal-

ing between afferent nerves and urothelial cells. Neurourol Urodyn. 2016;35:273–7.
138. Johnston L, Cunningham RM, Young JS, Fry CH, McMurray G, Eccles R, McCloskey KD. Altered distribution of interstitial cells and innervation in the rat urinary bladder following spinal cord injury. J Cell Mol Med. 2012;16:1533–43.
139. Chen J, Drzewiecki BA, Merryman WD, Pope JC. Murine bladder wall biomechanics following partial bladder obstruction. J Biomech. 2013;46:2752–5.
140. Griffiths D, Tadic SD. Bladder control, urgency, and urge incontinence: evidence from functional brain imaging. Neurourol Urodyn. 2008;27:466–74.
141. Bramich NJ, Brading AF. Electrical properties of smooth muscle in the guinea-pig urinary bladder. J Physiol. 1996;492:185–98.

Spontaneous Activity in Urethral Smooth Muscle

6

Gerard P. Sergeant, Mark A. Hollywood, and Keith D. Thornbury

Abstract

The urethra is a muscular tube that extends from the bladder neck and is composed of an inner layer of smooth muscle referred to as the internal urethral sphincter and an outer layer of striated muscle which forms the external urethral sphincter. The smooth muscle layer can be separated into an inner layer of longitudinally orientated smooth muscle and an outer, relatively thinner, layer of circular muscle. Tonic contraction of both the smooth and striated muscle components of the urethra generates a urethral closure pressure which exceeds intravesical pressure in the bladder to maintain urinary continence. It is likely that contraction of urethral smooth muscle is involved in the long-term maintenance of tone, since it can achieve this at relatively low energy cost, whereas the striated muscle contributes more to the rise in urethral tone that accompanies increases in bladder pressure secondary to coughing or other sudden increases in intra-abdominal pressure. The level of urethral smooth muscle tone is regulated by several autonomic neurotransmitters, including noradrenaline, acetylcholine, ATP and nitric oxide. However, it is also clear that urethral smooth muscle is capable of generating significant tone in the absence of neural input. In this chapter we will discuss the mechanisms responsible for contraction of urethral smooth muscle, with specific focus on the role of ion channels and Ca^{2+} handling proteins to this process. The mechanisms underlying spontaneous activity in urethral interstitial cells (UICs), putative pacemaker cells of the urethra, will also be examined along with the modulation of these mechanisms by key excitatory and inhibitory neurotransmitters.

Keywords

Urethra · Smooth muscle · Pacemaker · Interstitial cells of Cajal · Calcium waves · STICs · STDs

6.1 Introduction

Urinary continence is maintained by the concerted actions of the bladder, urethra, pelvic floor muscles, and surrounding connective tissues. The bladder and urethra work as a functional reciprocal unit under normal conditions, such that during the storage phase, the detrusor muscle of the bladder remains relaxed while the urethra is

G. P. Sergeant (✉) · M. A. Hollywood · K. D. Thornbury
Smooth Muscle Research Centre, Dundalk Institute of Technology, Dundalk, Co. Louth, Ireland
e-mail: gerard.sergeant@dkit.ie

H. Hashitani, R. J. Lang (eds.), *Smooth Muscle Spontaneous Activity*, Advances in Experimental Medicine and Biology 1124, https://doi.org/10.1007/978-981-13-5895-1_6

contracted to allow gradual filling of the bladder with urine and prevent leakage. In contrast, during voiding, the urethra relaxes and the detrusor contracts to facilitate emptying of the bladder [1, 2]. Therefore, the primary functions of the urethra are to (1) maintain urinary continence by generating a closure pressure that exceeds intravesical pressure and (2) facilitate voiding of urine at micturition. The urethra is composed of an inner layer of smooth muscle referred to as the internal urethral sphincter and an outer layer of striated muscle which forms the external urethral sphincter. Both muscle layers function together as a sphincter complex, albeit with distinct roles. The striated muscle is thought to be important in resisting rapid increases in abdominal pressure that occur during coughing or laughing. In contrast, contraction of the smooth muscle layer is important for generating and maintaining sufficient urethral closure pressure during bladder filling to prevent leakage [1, 3, 4]. Indeed, Jankowski et al. concluded that 'urethral smooth muscle, in comparison with striated muscle, is capable of imparting a greater influence on the long-term functional responses of the urethra' [5].

Stress urinary incontinence (SUI) arises when intravesical pressure exceeds urethral pressure, in response to sudden increases of intra-abdominal pressure and is common in women after vaginal delivery child birth [6]. Traditionally, this was primarily viewed as being due to loss of urethral support, referred to as urethral hypermobility. However, it has been reported that SUI in women was more likely to be associated with a reduction in urethral resistance, rather than anatomical changes in urethral support [7, 8]. There is also evidence that this may arise through an effect on urethral smooth muscle, as Prantil et al. showed that in a rat model of acute SUI, induced by simulated birth trauma, there was reduced urethral smooth muscle tone, indicating that 'the basal smooth muscle tone acts as a prime coordinator to the continual maintenance of continence' [9]. Urethral closure pressure also declines with age [10, 11], and this is correlated with a decrease in the density of circular smooth muscle in the urethra [12]. Therefore, it is clear that urethral smooth muscle tone makes an important contribution to urinary continence and its dysfunction is associated with urinary incontinence.

The smooth muscle of the urethra can be separated into two layers consisting of an internal longitudinally orientated layer and an outer, relatively thin, circular muscle layer. While it is clear that contraction of circularly orientated smooth muscle could maintain continence by occluding the lumen of the urethra, the precise role of the longitudinal layer is still unclear [1]. Urethral smooth muscle (USM) generates spontaneous tone [13], which can be modulated by several autonomic neurotransmitters including nitric oxide [14, 15], noradrenaline [16, 17], adenosine triphosphate [18–21] and acetylcholine [14, 22–24]. Although there are many unanswered questions regarding the mechanisms that underlie urethral tone, a clearer picture of the cellular mechanisms that contribute to spontaneous activity in USM is beginning to emerge. It is now recognised that several cell types within the smooth muscle layer of the urethra are spontaneously active, including smooth muscle cells and a population of cells, namely urethral interstitial cells (UICs). UICs are also referred to variously as interstitial cells [25], interstitial cells of Cajal (ICC, by analogy with similar cells that have been well described in the gastrointestinal tract [26]), ICC-like cells [27], and Cajal-like interstitial cells [28]. In this chapter we will describe the mechanisms proposed to underlie spontaneous activity in USM and examine how it is modulated by autonomic neurotransmitters.

6.2 Spontaneous Activity in Urethral Smooth Muscle

In comparison with the detrusor and gastrointestinal tract, studies on smooth muscle from the urethra are relatively sparse. The lack of research on this tissue has been attributed to the small size of the urethra in rats, guinea-pigs and mice [29], but it may also reflect an historical underestimation of the functional importance of urethral smooth muscle in maintaining continence. Nevertheless, early intracellular microelectrode recordings by Callahan and Creed on strips of guinea-pig USM, found that it generated spontaneous electrical

activity which consisted of 'bursts of spikes' (once every 1–7 min) separated by quiescent periods [30]. There were 20–30 spikes observed within these bursts, which lasted for 7–10 s. The mean resting membrane potential in the quiescent periods was −42 mV. An interesting observation from this study was that the electrical activity in the USM was poorly coordinated and that there was 'limited spread of activity'. For example, 'if an electrode was withdrawn from one cell and inserted into another, less than 1 mm away, it was frequently found that the patterns of activity were out of phase'. They also reported that, in contrast to observations in the detrusor, it was not possible to record spikes evoked by extracellular current pulses in USM. They suggested that the limited spread of activity 'probably prevents generalised, synchronous contraction'. Later studies by Callahan and Creed [31] on rabbit USM found that spontaneous electrical activity consisted of regular, single or (occasionally) compound spikes occurring at a frequency of 9–30 per min [31]. They also subsequently reported that rabbit USM developed action potentials and spontaneous depolarisations of ~16 mV in amplitude [24].

A seminal study by Hashitani et al. further elucidated the mechanisms underlying spontaneous electrical activity in the urethra [32]. They made intracellular microelectrode recordings from the circular smooth muscle layer of rabbit urethra and found that it produced large, regularly occurring depolarisations, termed slow waves (SWs) as well as smaller, irregularly occurring events, termed spontaneous transient depolarisations (STDs) (Fig. 6.1). Both SWs and STDs were resistant to atropine, phentolamine, guanethidine and tetrodotoxin, indicating that they were not of neural origin. The L-type Ca^{2+} channel antagonist, nifedipine failed to block these events, however, they were inhibited by reducing external [Cl^-] and by application of the Ca^{2+}-activated chloride channel (CACC) blockers niflumic acid and DIDS, suggesting an involvement of CACCs in their generation. Hashitani et al. also found that SWs and STDs were inhibited by the SERCA (sarcoplasmic/endoplasmic reticulum Ca^{2+} ATPase) inhibitor, cyclopiazonic acid (CPA) as well as caffeine, indicating that Ca^{2+} released from intracellular stores was required for the generation of spontaneous electrical activity. These data indicated that the spontaneous electrical activity in USM was mediated by release of Ca^{2+} from intracellular stores which activated CACCs. Similar findings were also reported for guinea-pig USM, whereby STDs and slow waves were also abolished by niflumic acid, low chloride solution, CPA and caffeine [33].

The finding that tonic contraction of USM was associated with phasic electrical activity was not intuitive and was somewhat at odds with the prevailing view that spontaneous myogenic tone depended on continuous entry of calcium through L-type Ca^{2+} channels [13]. However, given the poor coupling of electrical activity observed in the urethra [30], it is possible that asynchronous electrical events and their associated contractions, sum to form an overall tonic contraction. This idea was explored in more detail in imaging studies of intact USM strips [27, 34].

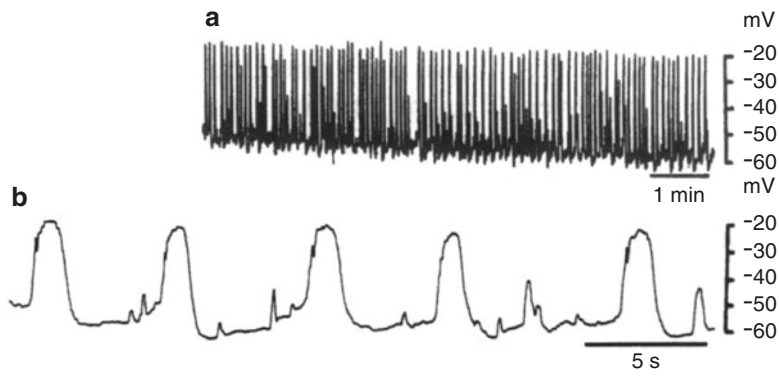

Fig. 6.1 Slow waves (SWs) and spontaneous transient depolarisations (STDs) recorded from the rabbit urethra. (**a**, **b**) Records from the same cell on different time scales. Adapted from [32]

Hashitani and Suzuki examined the properties of spontaneous Ca^{2+} transients recorded from both smooth muscle and interstitial cells of the rabbit urethra in situ [27]. The topic of interstitial cells in USM will be addressed later in this chapter but, for now, we will focus on spontaneous activity that has been recorded in urethral smooth muscle cells (USMCs). They reported that SMC in the rabbit urethra, loaded with fluorescent Ca^{2+} indicator, fluo-4 AM, generated spontaneous Ca^{2+} transients at a frequency of ~11 per min. These events occurred either as 'non-propagated Ca^{2+} transients or intercellular Ca^{2+} waves within a muscle bundle'. However, in contrast to intercellular Ca^{2+} waves observed in detrusor smooth muscle bundles of the guinea-pig bladder [35], the Ca^{2+} waves originating from a single site in USM often failed to spread across muscle bundles. When changes in muscle tension were measured simultaneously with intracellular [Ca^{2+}] it was found that 'there was no correlation between muscle contractions and Ca^{2+} transients in any particular muscle bundle within the preparations, presumably arising from a low synchronicity between bundles' [27].

Drumm et al. investigated this matter further by examining Ca^{2+} transients in USM strips dissected from SmMHC-Cre-GCaMP3 mice, which have a genetically encoded Ca^{2+} sensor, GCaMP3, selectively expressed in SMCs [34]. This study revealed that USMCs within smooth muscle bundles fired spontaneous intracellular Ca^{2+} transients. However, while distinct Ca^{2+} events could be imaged within individual USMC there was no evidence of intercellular propagation of Ca^{2+} events within USM bundles. Indeed, spontaneous Ca^{2+} events that occurred in adjacent SMCs were not synchronised and appeared to be independent of the activity occurring in their neighbouring cell. Furthermore, it was also apparent that the firing of intracellular Ca^{2+} waves in USMCs was associated with small contractions of individual USMC in muscle bundles. These contractions, like the intracellular Ca^{2+} waves, occurred asynchronously and failed to spread cell-to-cell across the muscle bundles.

Therefore, electrical and imaging studies of intact USM strips indicate that USM develops spontaneous depolarisations and Ca^{2+} transients, respectively, but that these events are poorly coupled, resulting in asynchronous contractions across the tissue that sum to give an overall tonic contraction. The cellular mechanisms underlying the spontaneous activity described above are discussed below.

6.3 Spontaneous Activity in Isolated Urethral Smooth Muscle Cells

Ca^{2+} waves recorded from rabbit USM, in situ, appear to rely on a combination of Ca^{2+} release from stores and Ca^{2+} influx via L-type Ca^{2+} channels, since they were inhibited by the SERCA inhibitor, CPA, the ryanodine receptor (RyR) antagonist, ryanodine, the inositol trisphophate receptor (IP_3R) inhibitor, 2-APB and the L-type Ca^{2+} channel antagonist nifedipine [27]. The involvement of L-type Ca^{2+} channels was consistent with other reports showing that nifedipine inhibited spontaneous action potentials and spikes superimposed on slow spontaneous depolarisations in rabbit USM [36, 37] and that application of 60 mM $[K^+]_o$ solution evoked robust Ca^{2+} transients and contractions in isolated rabbit USMCs [38]. Ca^{2+} waves in intact murine USM strips were also inhibited by Ca^{2+} store release modulators, including the SERCA inhibitor, thapsigargin, the RyR antagonist, tetracaine and the IP_3R inhibitor, xestospongin C [34]. Surprisingly however, Ca^{2+} waves in murine USMCs were resistant to the L-type Ca^{2+} channel modulators nifedipine, nicardipine, isradipine and FPL, but were abolished by Ca^{2+}-free bathing media, the store operated Ca^{2+} entry channel (SOCE) blocker SKF 96365 and the Orai channel antagonist, GSK-7975A [34]. Therefore, it appears that, in contrast to rabbit USMCs, Ca^{2+} waves in murine USMCs are not reliant on Ca^{2+} influx via L-type Ca^{2+} channels.

To date, only a few labs have made patch clamp recordings from freshly isolated USMCs. One of the main contributors to this field was Teramoto and colleagues in Alison Brading's Lab in Oxford. They systematically characterised

K^+_{ATP} channels in USM and showed that these channels have an important functional role in regulating membrane potential and relaxation of this tissue [39, 40]. The nature and molecular identity of K^+_{ATP} channels in USM has been comprehensively reviewed elsewhere [29, 41] and therefore will not be recapitulated here.

The intracellular microelectrode recordings by Hashitani et al. indicated that STDs and slow waves recorded from intact rabbit USM strips arose from activation of CACCs [32]. The first study to examine CACC currents (I_{ClCa}) in isolated USMCs was by Cotton et al. [42]. Using the perforated patch configuration of the whole cell voltage clamp technique, they found that freshly isolated SMC from the sheep urethra exhibited robust I_{ClCa}. Furthermore, they found that a proportion of these cells were spontaneously active, developing STDs and action potentials under current clamp that were sensitive to the CACC inhibitor anthracene-9-carboxylic acid (A-9-C, Fig. 6.2). These findings led the authors to propose that CACC in sheep USMCs may function as a pacemaker current. Later investigation of these cells found that ~10% of sheep USMCs developed spontaneous transient inward currents (STICs) when maintained at −60 mV [43]. These events were inhibited by the CACC blockers niflumic acid and A-9-C, and reversed near E_{Cl}, confirming the importance of CACCs to spontaneous activity in USM. STICs in sheep USMCs were also inhibited by ryanodine and caffeine suggesting that Ca^{2+} release from intracellular stores was important for activation of these events. Sancho et al. found that Anoctamin 1 (Ano1), also referred to as TMEM16A, and now recognised as the molecular correlate of CACCs [44–46], was expressed in the smooth muscle layer of the sheep urethra, consistent with idea that Ano1 encoded CACCs in sheep USMCs [47]. This study also reported Ano1 expression in USM of rats and mice, although Huang et al. (2009) failed to detect Ano1 in murine USM [48]. Precise reasons for the divergent findings in these studies is unclear, although differences in antibody specificity and experimental protocols have been suggested [47].

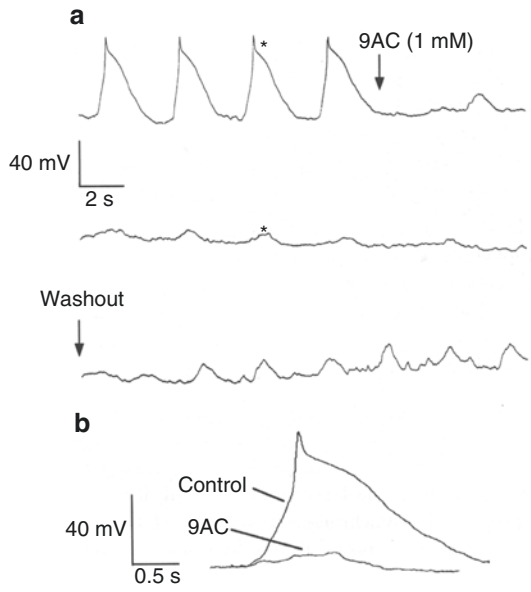

Fig. 6.2 Effect of A-9-C on spontaneous electrical activity in sheep urethral SMC. (**a**) Top panel, shows recordings made in current clamp using a Cs^+-filled pipette before addition of A-9-C (1 mM). The top two traces are a continuous recording. (**b**) events marked by * in **a** are compared on an expanded time scale, showing blockade of the action potential and reduced amplitude of the STD. Adapted from [42]

In order to further explore the cellular basis of the spontaneous activity described by Hashitani et al., in the rabbit urethra, Sergeant et al. undertook a patch clamp investigation to determine the properties of SMC freshly isolated from the rabbit urethra [25, 32]. Surprisingly however, despite having robust L-type Ca^{2+} currents, evidence for I_{ClCa} in these cells was weak. The large slowly developing inward currents and tail currents, typical of I_{ClCa}, that were evident in sheep USMCs, were not readily resolvable in rabbit USMCs. Current-voltage (IV) data averaged from 21 SMCs demonstrated that these cells had only small, sustained, inward currents at −30 mV and which reversed close to E_{Cl}. Furthermore, only ~3% of the rabbit SMC developed spontaneous electrical activity, even though they could respond to depolarising current injection (40 ms) by producing action potentials [25]. A later study by Hollywood et al. examined inward currents in SMCs isolated from the human proximal urethra using the whole cell patch clamp technique, and while L and T-type Ca^{2+} currents were reported,

there was no evidence of I_{ClCa} [49]. However, this subject warrants further investigation, using the perforated patch configuration of the whole cell patch clamp technique to optimise the conditions required to detect I_{ClCa}. Therefore, at the present time, there is still a lack of consensus regarding the contribution of CACCs in USMCs to spontaneous activity in intact USM strips. However, an interesting observation by Sergeant et al. was that although the evidence for I_{ClCa} in rabbit USMCs was weak, there was another cell type, termed 'interstitial cells' (referred to in this review as urethral interstitial cells, UICs) which had a robust I_{ClCa} and were spontaneously active [25].

6.4 Spontaneous Activity in Urethral Interstitial Cells

The first evidence that the urethra may contain a novel population of interstitial cells came from a study by Smet et al., which described a population of interstitial cells in human urethra preparations that were immuno-positive for vimentin and cGMP and bore a striking resemblance to the ICC described in the GI tract [50]. Smet et al. suggested that the UIC could be the targets for neuronally released nitric oxide and, by analogy, act in similar fashion to ICC in the GI tract which are also known to serve as mediators of neurotransmission [51–54]. However, Smet et al. did not propose a role for these cells in the generation of spontaneous electrical activity in USM. Interestingly however, Hashitani et al. did allude to the possibility that ICC could be involved in the development of SWs in USM by noting that interstitial cells of Cajal were mandatory for the development of SWs, in large tissues of the GI tract, but that such cells had not been discovered in USM [32].

Enzymatic dispersal of rabbit USM not only yielded SMCs, as noted above, but also a small population of branched, non-contractile cells that were darker and thinner than the SMCs [25], and were similar in appearance to freshly isolated ICC from the canine proximal colon [55]. These cells were immuno-positive for the intermediate filament vimentin and possessed several ultrastructural characteristics of GI ICC, including an incomplete basal lamina, abundant caveolae, abundant mitochondria, a well-developed smooth endoplasmic reticulum and a sparse rough endoplasmic reticulum. More than 80% of UICs were spontaneously active, generating STDs under current clamp and STICs when voltage clamped at −60 mV. These events reversed close to E_{Cl} and were blocked by the traditional CACC inhibitors, niflumic acid and A-9-C [25, 26]. More recently, Fedigan et al. [56] demonstrated that STICs and STDs in UICs were also sensitive to the TMEM16A channel inhibitors, $T16A_{inh}$-A01 and $CACC_{inh}$-A01, indicating that spontaneous electrical activity in UICs is likely to result from activation of TMEM16A channels (Fig. 6.3). Fedigan et al. also showed that the TMEM16A inhibitors reduced the level of spontaneous tone and the amplitude of nerve-evoked contractions of rabbit USM strips, indicative of an important functional role for these channels in urethral contraction [56].

Spontaneous activity in UIC is also dependent on Ca^{2+} release from intracellular stores as the STICs were abolished by the SERCA inhibitor CPA and were also sensitive to the RyR inhibitor, ryanodine, the phospholipase C (PLC) inhibitor, NCDC and the IP_3R inhibitor, 2-APB [57]. When UIC were held under voltage clamp at ~−30 mV and studied with K^+-rich pipettes, these cells also developed spontaneous transient outward current (STOCs). These STOCs could be categorised into two broad groups, based on their duration; (i) 'slow' STOCs (~1 s duration) that were coupled with STICs and (ii) 'fast' STOCs (<100 ms duration) that occurred independently of slow STOCs and STICs. Interestingly, while all events were abolished when RyRs were inhibited, only the slow STOCs and STICs were sensitive to 2-APB (Fig. 6.4). This observation led the authors to hypothesise that 2-APB-sensitive STICs and 'slow' STOCs arose from global Ca^{2+} events involving IP_3Rs, such as propagating Ca^{2+} waves, whereas the fast STOCs arose from RyR-dependent, localised Ca^{2+} events, such as Ca^{2+} sparks [57]. This idea was largely corroborated by Johnston et al. who, using a Nipkow spinning disc confocal microscope, reported that UIC

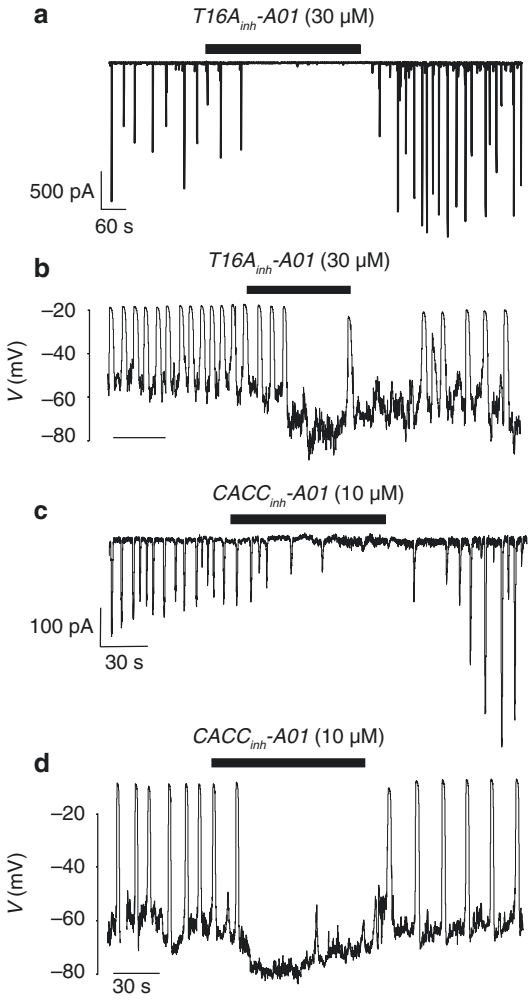

Fig. 6.3 Effect of CACC/TMEM16A inhibitors, *T16A$_{inh}$-A01* and *CACC$_{inh}$-A01*, on STICs (**a**, **c**, respectively) and STDs (**b**, **d**, respectively) recorded from freshly isolated rabbit UICs. Adapted from [56]

loaded with Fluo4-AM, exhibited spontaneous Ca^{2+} waves [58]. Simultaneous voltage clamp and Ca^{2+} imaging experiments revealed that STICs were associated with Ca^{2+} waves (Figs. 6.5 and 6.6). Application of 2-APB abolished STICs, but only reduced the spatial spread of Ca^{2+} waves [58]. In contrast, inhibition of RyRs with tetracaine, or ryanodine, abolished all spontaneous Ca^{2+} events. These findings prompted the idea that propagation of Ca^{2+} waves, and subsequent activation of STICs, required Ca^{2+} release from IP_3Rs, but that the initiation of these events was dependent on Ca^{2+} release via RyRs. In this model, Ca^{2+} release from RyRs was proposed as the 'prime oscillator'.

In addition to Ca^{2+} release from intracellular stores, it is clear that spontaneous activity in UIC is also dependent on Ca^{2+} influx across the plasma membrane [25, 27, 58]. STDs and spontaneous Ca^{2+} waves in UIC were abolished by removal of external Ca^{2+} and the frequency of Ca^{2+} waves was correlated with the external Ca^{2+} concentration ($[Ca^{2+}]_o$) as a reduction in $[Ca^{2+}]_o$ from 1.8 to 0.9 mM decreased Ca^{2+} wave frequency by ~40%, whereas an increase in $[Ca^{2+}]_o$ to 3.6 mM enhanced their frequency [58]. Similar findings were reported for UIC in situ [27]. Figure 6.6 is a representative trace showing the effect of Ca^{2+} removal on STICs and spontaneous Ca^{2+} waves, recorded simultaneously, in an isolated UIC. However, the mechanisms underlying Ca^{2+} influx in UIC and their interaction with Ca^{2+} release mechanisms has only recently been clarified.

Isolated UIC displayed robust L-type Ca^{2+} currents in response to step depolarisation [25];

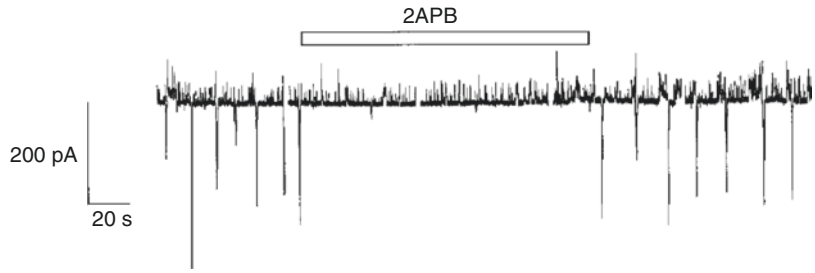

Fig. 6.4 The IP_3R inhibitor 2APB (100 μM) inhibits STICs and 'slow' STOCs, but not 'fast' STOCs in freshly isolated rabbit UIC voltage clamped at −30 mV. Adapted from [57]

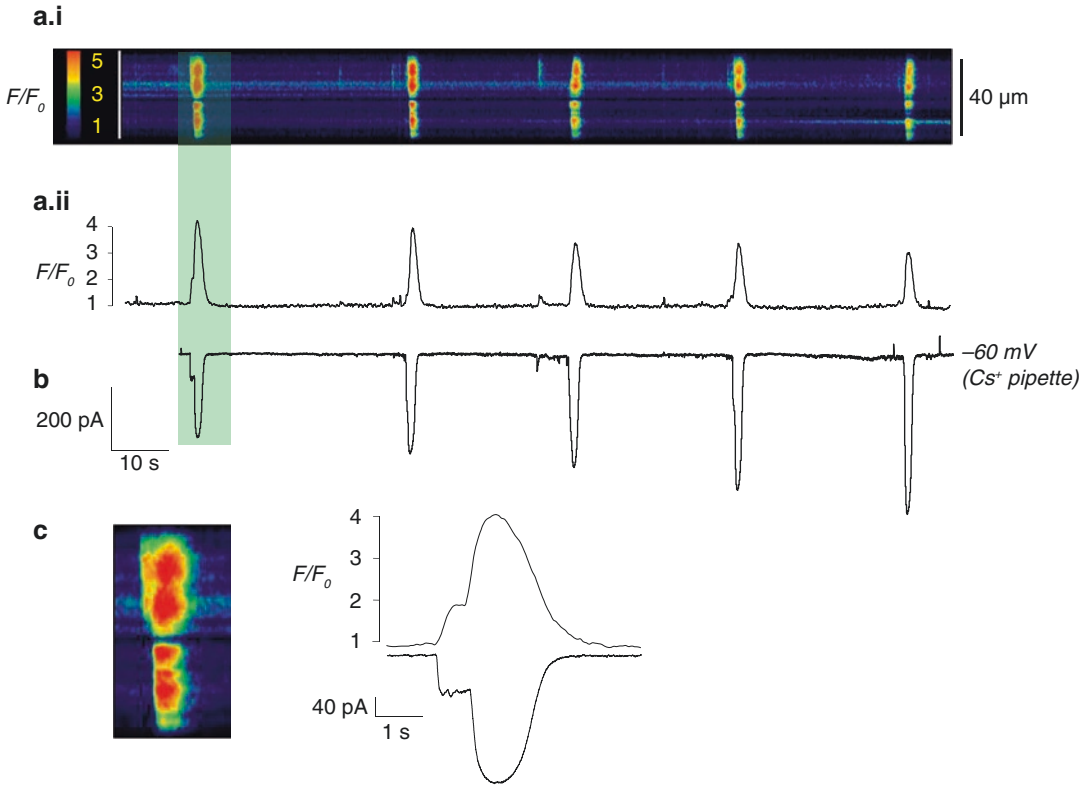

Fig. 6.5 STIC*s* in freshly isolated rabbit UICs are associated with spontaneous Ca^{2+} waves. (**a.i**, **a.ii**) Show a pseudo linescan image and corresponding intensity profile plot, of spontaneous Ca^{2+} waves in a rabbit UIC loaded with fluo4-AM. (**b**), is a simultaneous voltage clamp recording at −60 mV, showing that STICs are associated with the spontaneous Ca^{2+} waves. (**c**) Shows the Ca^{2+} wave and STIC depicted in the highlighted area in **a.i**, **a.ii** and **b** on an expanded time scale

however, STICs recorded at −60 mV in the same cell type were resistant to L-type Ca^{2+} channel blockade with nifedipine [57] or *D-cis* diltiazem [59], demonstrating that spontaneous activity in rabbit UICs is not reliant on Ca^{2+} influx via L-type Ca^{2+} channels. Similarly, spontaneous Ca^{2+} waves in non-voltage-clamped UICs were also unaffected by nifedipine [27, 58], consistent with this idea. Johnston et al. also noted that although spontaneous Ca^{2+} waves were abolished in Ca^{2+}-free media, caffeine-induced Ca^{2+} transients remained intact, suggesting that the abolition of spontaneous activity by removal of external Ca^{2+}, was not a function of Ca^{2+} store depletion. Consistent with this idea were the findings of Bradley et al. who found that although UICs exhibited a robust capacitative Ca^{2+} entry signal upon Ca^{2+} store depletion, blockers of this pathway, including Gd^{3+} (10 µM) and La^{3+} (10 µM), did not abolish spontaneous activity [60].

It now appears that one of the key Ca^{2+} influx pathways that drives spontaneous activity in UICs is via reverse mode-sodium calcium exchange (NCX). The selective reverse NCX inhibitors KB-R7943 and SEA0400 [61–64] significantly reduced both the frequency of Ca^{2+} oscillations and STICs in isolated rabbit UICs, and the level of spontaneous tone in intact USM strips [65]. Furthermore, a reduction in extracellular Na^{+} levels (to promote reverse mode NCX) increased the frequency of Ca^{2+} waves in UICs. Drumm et al. [66] investigated this issue further by examining the effect of the NCX inhibitors, as well as application of Ca^{2+}-free solution, on Ca^{2+} waves recorded using faster acquisition rates (50–97 FPS) than those employed in earlier stud-

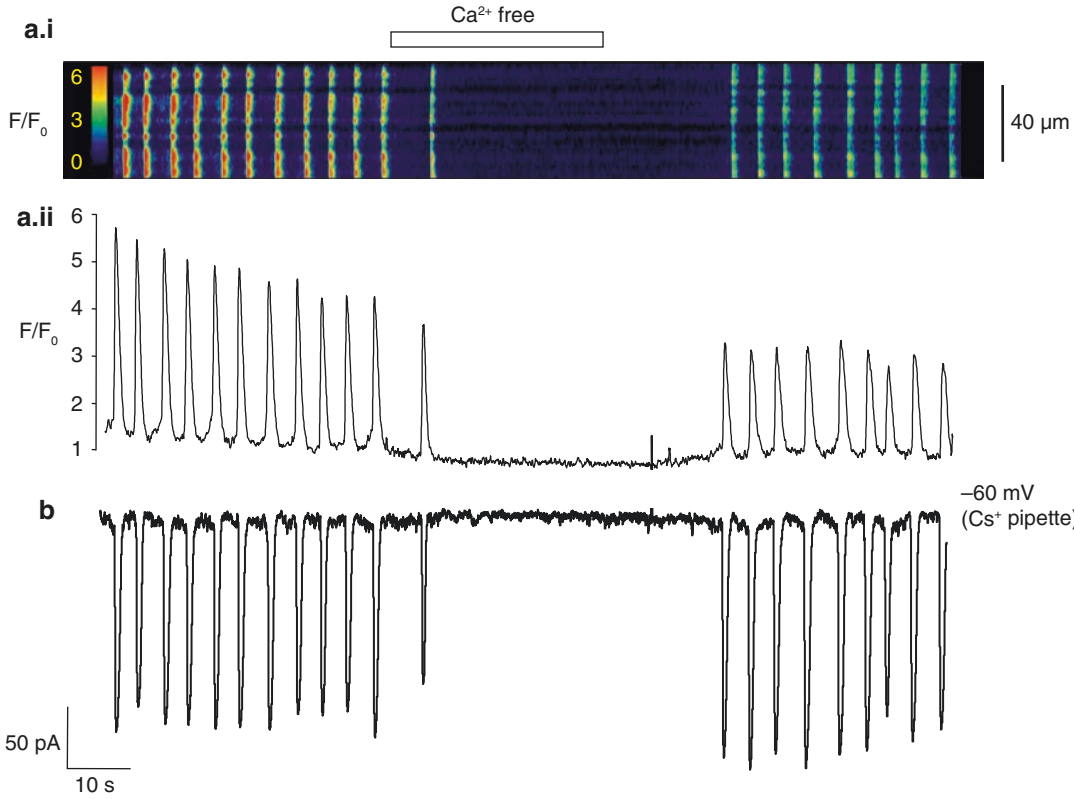

Fig. 6.6 Simultaneous recording showing that STICs and spontaneous Ca^{2+} waves in freshly isolated rabbit UICs are abolished by removal of extracellular Ca^{2+}. (**a.i**, **a.ii**) Show a pseudo linescan image and corresponding intensity profile plot, of spontaneous Ca^{2+} waves in a rabbit UIC loaded with fluo4-AM. (**b**) Simultaneous voltage clamp recording at −60 mV, showing that STICs are abolished by removal of extracellular Ca^{2+}

ies [58, 65]. In contrast to these studies, Drumm et al. [66] found that application of Ca^{2+}-free solution, KB-R7943 and SEA0400 (Fig. 6.7) abolished propagating Ca^{2+} waves, but unmasked brief, localised Ca^{2+} sparks that were not detected in the earlier studies [58, 65]. These effects were very similar to those induced by blockade of IP_3Rs with 2-APB (Fig. 6.7) suggesting that the role of Ca^{2+} influx via reverse NCX was to sensitise IP_3Rs to Ca^{2+}, which allows localised Ca^{2+} release events from RyRs to be converted into propagating Ca^{2+} waves.

Another Ca^{2+} influx pathway that has been proposed to regulate spontaneous activity in UICs is via cyclic nucleotide-gated (CNG) channels [59]. CNG channels are permeable to Na^+ and Ca^{2+} and their activation can induce local changes in cytosolic Ca^{2+} levels in response to a rise in cAMP or cGMP. $CNGA_1$ and $CNGB_1$ subunits, which form functional $CNGA_1$, or rod retinal-like CNG channels, were strongly expressed in a subpopulation of vimentin-positive ICC of the rat urethra, whereas only weak and diffuse CNG1A-immunoreactivity was evident in rat USMCs [67]. Furthermore, inhibition of CNG channels, with *L-cis* diltiazem, reduced the frequency of STICs and Ca^{2+} waves in rabbit UIC [59], however, the precise contribution of CNG channels to spontaneous activity in UIC is still unclear and requires further investigation.

Ward et al. suggested that mitochondrial Ca^{2+} handling may regulate the frequency of pacemaker activity in GI muscles [68]. This was based on the observations that inhibition of the electrochemical gradient across the inner mitochondrial membrane with the mitochondrial uncouplers

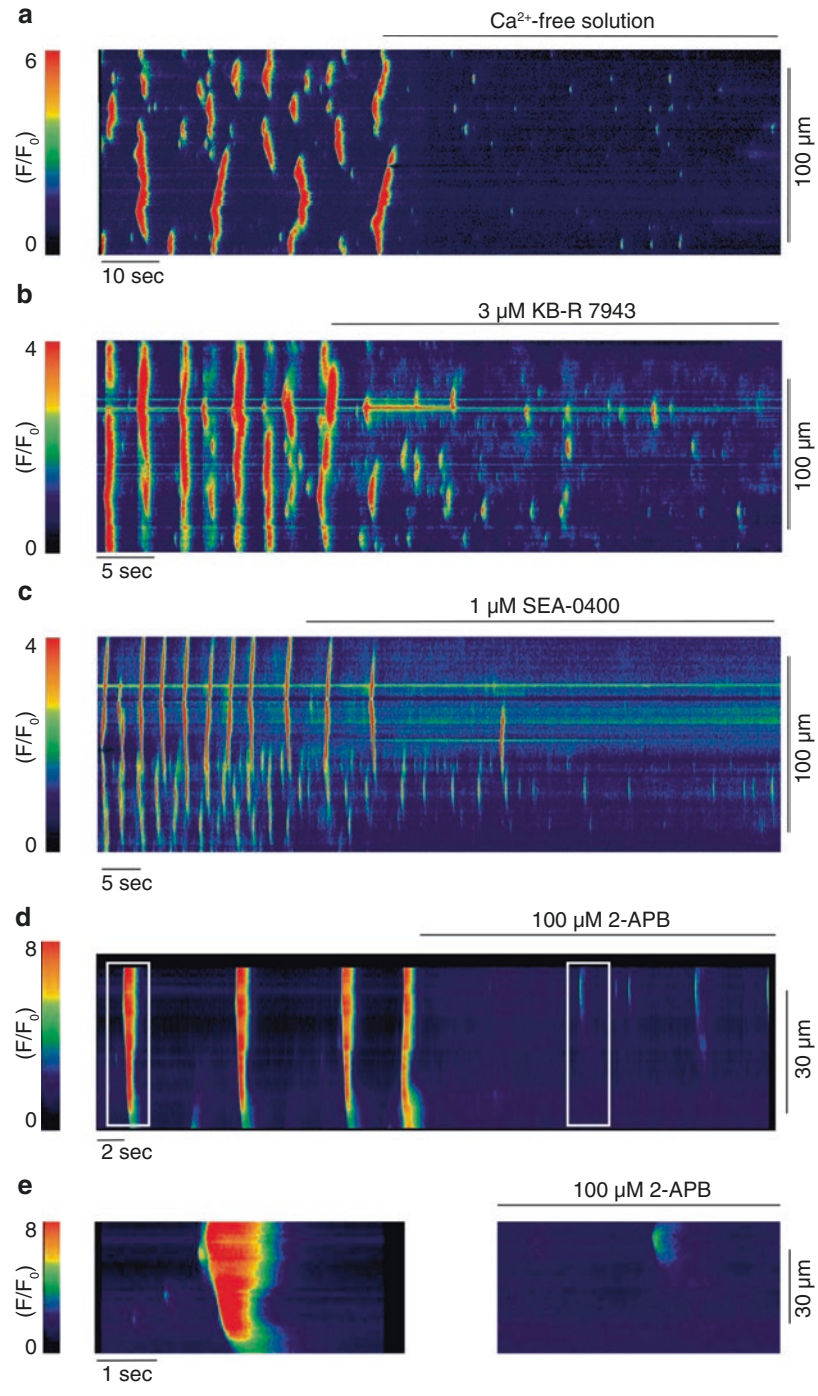

Fig. 6.7 Representative pseudo linescan images showing effects of application of Ca^{2+}-free external solution (**a**), the reverse NCX blockers KB-R 7943 (**b**) and SEA-0400 (**c**) and the IP_3R inhibitor 2-APB (**d**) on Ca^{2+} events, recorded at fast acquisition rates (50–97 FPS), in freshly isolated rabbit UICs. (**e**) Shows the Ca^{2+} events highlighted by the white boxes in **d** (before and during the presence of 2-APB) on an expanded time scale. Adapted from [67]

FCCP and CCCP or the respiratory chain (complex III) inhibitor antimycin, inhibited pacemaker currents in cultured ICC and blocked slow wave activity in intact GI muscles from mouse, dog and guinea-pig. Sergeant et al. reported similar findings on Ca^{2+} waves and STICs recorded from freshly isolated rabbit UICs [69] and Hashitani et al. also reported that CCCP could inhibit spontaneous Ca^{2+} waves in rabbit UICs [70]. These data indicated that spontaneous activity in UICs

may also be dependent on Ca^{2+} handling by mitochondria, as well as on Ca^{2+} release from the sarcoplasmic reticulum and Ca^{2+} influx across the plasma membrane. However, a recent study showed that antimycin blocked TMEM16A currents and that CCCP inhibited $Ca_V3.2$ currents [71]. Therefore, firm conclusions on the role of mitochondrial Ca^{2+} handling, based on use of these agents, should be treated with caution and further investigation is required to determine the contribution of mitochondrial Ca^{2+} handling to spontaneous activity in UIC.

Overall, it is clear that the smooth muscle layer of the rabbit urethra possesses a population of interstitial cells (UICs), which resemble ICC pacemaker cells in the GI tract, and which exhibit a pattern of spontaneous activity that is similar in nature to that recorded from intact strips of rabbit USM [25, 26, 72]. These observations prompted suggestions that UIC may function as pacemaker cells in the urethra. However, this hypothesis still requires further investigation. To date, there has only been one study that has simultaneously measured spontaneous activity in UICs and smooth muscle cells in USM. Hashitani and Suzuki were able to record Ca^{2+} transients in UICs and USMCs in tissue strips loaded with Fluo4-AM [27]. They found that Ca^{2+} transients recorded from rabbit UICs in situ were similar in nature to those recorded in isolated UICs [58]. Thus, they were abolished by application of CPA, ryanodine, caffeine and 2-APB and by removal of extracellular Ca^{2+}, but were resistant to application of nifedipine. On some occasions (21 preparations) spontaneous Ca^{2+} transients in USMCs were observed simultaneously with those of UICs within a field of view. Interestingly, in five of these preparations, UICs and USMCs generated synchronous Ca^{2+} transients with close temporal correlation between the signals in the two cell types, indicative of a degree of synchronicity between these cells (Fig. 6.8). In the remaining 16 preparations, USMCs generated Ca^{2+} transients independently from UICs, albeit at a lower frequency than those in the UICs. In contrast, when pairs of UICs were visualised in the same field of view, synchronous Ca^{2+} transients were observed in 17 out of 22 preparations, indicative a high degree of coupling between UICs. These authors concluded that '*UICs may act as a primary pacemaker in generating spontaneous contractions of USM. However, signal transmission from UICs to USMCs may be much less extensive than that between ICC and smooth muscle cells in the GI tract, and thus electrical pacemaking signals generated by UICs may be less securely transmitted' to smooth muscles*' [27]. Thornbury et al. reached similar conclusions, noting that 'there are multiple pacemakers within the urethra, but unlike the GI tract, these are not well networked' [73]. Therefore, it is apparent that both USMCs and UICs are capable of generating spontaneous activity but, in the rabbit urethra, at least, it appears that spontaneous activity originating from UICs is dominant and forms the basis of pacemaker in the intact tissue. Definitive determination of UIC function in the future will be dependent upon determining the identity of these cells by the presence of selective markers and examining tissue function when these cells are lesioned.

6.5 Modulation of Spontaneous Activity in UIC by Autonomic Neurotransmitters

6.5.1 Nitric Oxide

The principal inhibitory neurotransmitter in the urethra is Nitric Oxide (NO [14, 15]). NO is thought to exert its effects by activating the cGMP/protein kinase G (PKG) pathway, since electrical field stimulation (EFS) of inhibitory nerves or exogenous application of NO can elevate cGMP levels in this tissue [74–76], and neurogenic urethral relaxations are significantly attenuated in mice lacking cGMP-dependent protein kinase G1 [77]. The NO donor, sodium nitroprusside (SNP), reduced the frequency of slow waves in rabbit USM [32] indicating that NO exerts its inhibitory effects in USM by inhibiting spontaneous activity. There is evidence that spontaneous activity in both UICs and USMCs is affected by NO, however, the degree to which these effects account for neurogenic relaxations

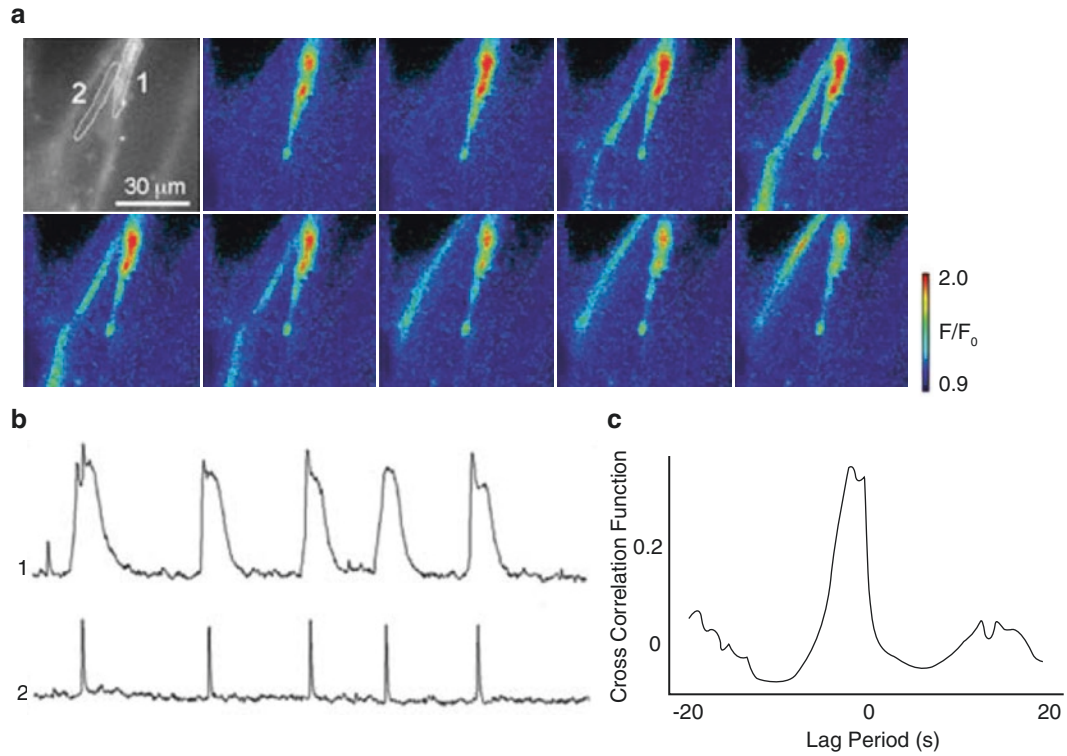

Fig. 6.8 Analysis of the temporal relationship of Ca^{2+} transients between UICs and USMCs. (**a**) A series of frames at intervals of 0.2 s demonstrating USMC Ca^{2+} transients originating from an UIC. (**b**) In the same preparation, synchronous Ca^{2+} transients were generated by an UIC (1) and a USMC (2). (**c**) A cross-correlogram for UICs and USMCs showed a peak near lag period zero. Adapted from [27]

of USM is still under debate. Application of the NO donor, DEA-NONOate, dramatically reduced the frequency of Ca^{2+} transients in USMCs, in situ [34] and relaxations induced by DEA-NONOate were absent in smooth muscle guanylyl cyclase knockout (SM-GCKO) mice USM [78]. These findings prompted the authors to conclude that 'NO-GC found in SMCs of the urethral sphincter mediates NO-induced relaxation'. Unfortunately, this study did not examine nerve-mediated NO responses, as responses to exogenous application of agonists and NO donors can often be quite different to those induced by stimulation of intrinsic nerves. For example, intramuscular ICC (IC-IM) in the murine fundus are known to mediate neural responses to NO, but W/W_v mice, which lack IC-IM can still relax in response to the NO-donor SNP [51]. Lies et al. also showed that DEA-NONOate-induced relaxations were maintained in mice lacking NO-guanylyl cyclase (NO-GC) in c-kit-positive ICC [78]. Therefore, if UICs are involved in mediating NO responses in the murine urethra, they are not c-kit positive.

Several lines of evidence indicate that UICs could be involved in NO signalling in the urethra. Treatment of USM with SNP led to increased levels of cGMP fluorescence in interstitial cells [50, 79] and stimulation of nitrergic nerves in USM, led to increased cGMP production in both UICs and SMCs [80]. Rabbit UICs (identified by c-kit immunoreactivity) had frequent points of contact with neuronal nitric oxide synthase containing nerves, consistent with the idea that they play a role in the inhibitory nitrergic neurotransmission of USM [81]. Sergeant et al. provided direct evidence that spontaneous activity in UICs was modulated by NO, as STDs, recorded under current clamp, and STICs recorded under voltage clamp in freshly isolated rabbit UICs were

inhibited by the NO donor, DEA-NO, the soluble guanylate cyclase activator, YC-1, or the cGMP analogue, 8-Br-cGMP [82]. Finally, spontaneous Ca^{2+} transients recorded in situ from UICs of the rabbit urethra, were inhibited by the NO donor, SIN-1 [27]. It appears that inhibitory effects of NO in UICs are mediated by activation of PKG, and not protein kinase A (PKA), as the PKG activator SP-8-br-cGMP reduced the frequency of STDs and Ca^{2+} waves, whereas application of the adenylate cyclase activator, forskolin or the membrane permeable cyclic AMP analogue, 8-Br-cAMP did not affect spontaneous Ca^{2+} waves in rabbit UIC [83].

6.5.2 Adenosine Triphosphate

Nitric Oxide is not the only inhibitory neurotransmitter in the urethra. Several studies have demonstrated that adenosine triphosphate (ATP) or its derivatives, adenosine and adenosine diphosphate (ADP), may also be potent inhibitory neurotransmitters in USM, since EFS of USM strips induced relaxations that were inhibited by purinergic receptor antagonists and mimicked by exogenous application of ATP [18–21]. However, it has also been noted that ATP, or related compounds, can produce excitatory effects in USM [21, 30, 84–86]. One explanation that could account for these opposite effects is the level of tone on the tissue prior to ATP application. For example, relaxant effects were observed in preparations which had been 'pre-contracted' with agonists such as arginine vasopressin or noradrenaline, whereas contractions were observed if ATP was applied at resting tone. Bradley et al. showed that the contractile effects induced by application of ATP to the rabbit urethra were mimicked by the P2Y receptor agonist, 2-MeSADP and were inhibited by the selective P2Y1 receptor antagonist, MRS2500 suggesting that P2Y receptors were involved in the excitatory effects of ATP in rabbit USM [85]. Involvement of UICs in this response was inferred from experiments which showed that ATP and P2Y receptor agonists increased the frequency of spontaneous Ca^{2+} waves and STICs in freshly isolated UICs (Fig. 6.9). Interestingly however, stimulation of purinergic nerves in strips of rabbit USM yielded contractions that were inhibited by desensitisation of P2X receptors using α,β-methylene ATP but were unaffected by the P2Y receptor antagonist MRS2500 [86]. This suggested that, in USM, neurally released ATP targeted P2X receptors and not P2Y receptors. Further investigation revealed that isolated rabbit USMCs had robust P2X receptor currents that could be inhibited by α,β-methylene ATP. Therefore, it appears that P2Y receptor-dependent responses in UICs are unlikely to be involved in purinergic nerve-mediated responses in rabbit USM.

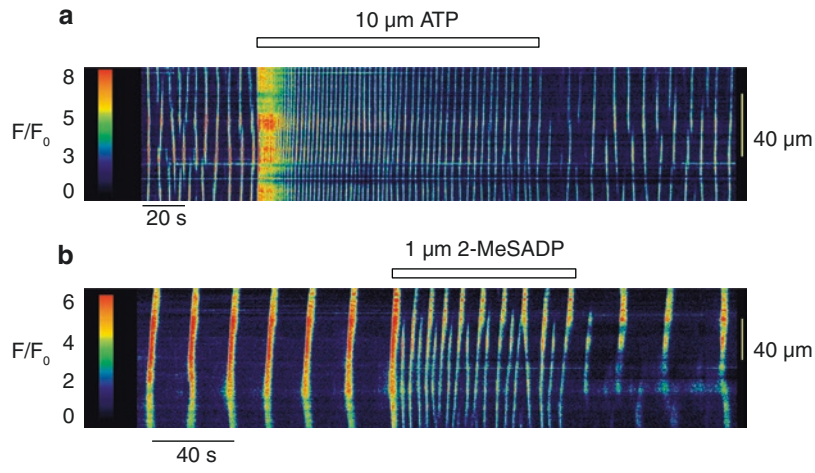

Fig. 6.9 Representative pseudo linescan images showing effects of ATP (**a**) and the P2Y1 receptor agonist 2-MeSADP (**b**) on Ca^{2+} waves in isolated rabbit UICs. Adapted from [85]

6.5.3 Noradrenaline

Noradrenaline (NA) is the principal excitatory neurotransmitter in the urethra [16, 17] and augments the level of urethral tone via activation of post-junctional α_1-adrenoceptors [13, 17]. Hashitani et al. indicated that α_1-adrenoceptor-mediated increases in tone resulted from up-regulation of the endogenous pacemaker mechanism, since exogenous application of NA increased the frequency of slow waves in rabbit USM [32]. Sergeant et al. demonstrated that spontaneous activity in freshly isolated UICs was also enhanced by NA suggesting that these cells could be involved in this response [25, 87]. The effects of NA were attenuated by CPA and 2-APB as well as niflumic acid and A-9-C, suggesting that activation of α_1-adrenoceptors led to release of Ca^{2+} from IP_3-sensitive stores, which in turn stimulated CACC. Similarly, bath application of the α_1-adrenoceptor agonist, phenylephrine increased the frequency of Ca^{2+} transients in UICs in situ and elevated intracellular Ca^{2+} levels [27]. Sergeant et al. [87] and Fedigan et al. [56] demonstrated that EFS-induced contractions of rabbit USM were inhibited by the CACC inhibitors, niflumic acid, A-9-C and $T16A_{inh}$-A01, respectively. Since CACC are more prominent in rabbit urethral UICs, compared to USMCs, it is tempting to speculate on a role for UIC in mediating neural responses in USM, as is the case for IC-IM in the gastric fundus and ICC in the deep muscular plexus (IC-DMP) of the small intestine [88]. However, a comparison of neural responses in USM lacking UICs has yet to be made and therefore this idea remains speculative. Furthermore, Ca^{2+} waves in murine SMC were also accelerated by application of phenylephrine indicating that USMCs can be directly modulated by NA [34]. Kyle et al. also showed that phenylephrine reduced depolarisation-evoked large conductance Ca^{2+}-activated K^+ (BK) currents in rabbit USMCs and suggested that the reduction in this current altered compound action potentials to promote excitability of USM [89].

Walsh et al. [90] demonstrated that contractile responses of rabbit USM in response to EFS and exogenous application of phenylephrine were all potently inhibited by the Rho-associated kinase (ROK) inhibitors, Y27632 and H1152 [90]. Surprisingly, however, ROK inhibition had no effect on the phosphorylation of the known ROK substrates, myosin regulatory light chains (LC20) at S19 or the myosin-targeting subunit of myosin light chain phosphatase (MYPT1), in either the absence or presence of contractile stimuli. Therefore ROK plays an important role in USM contraction induced by NA; however, the mechanisms underlying this response require further investigation.

6.5.4 Acetylcholine

Although the bladder neck and proximal urethra receive a rich cholinergic innervation [84], the functional role of acetylcholine (ACh) in the urethra is still unclear. Studies have indicated that inhibition of muscarinic receptors has little effect on urethral tone in vivo [91] or in vitro [14, 87]. However, stimulation of cholinergic nerves in vitro has been demonstrated to contract the urethra of sheep, pigs, dogs and rabbits [14, 22–24] and these effects appear to be mediated post-junctionally via activation of M_2 and/or M_3 muscarinic receptors [92, 93]. In the isolated sheep urethra, a significant component of the neurogenic contraction is sensitive to atropine [14] consistent with the idea that muscarinic stimulation can augment urethral tone. Similarly, application of cholinergic agonists to porcine urethra in vitro contracts the longitudinal and circular muscle layers equally. However, in the rabbit urethra, although an atropine-sensitive component of excitatory junction potentials has been demonstrated [24, 94], it was small compared to the α_1-adrenoceptor-mediated component, suggesting that muscarinic receptors contributed minimally to the electrical response to nerve stimulation in this preparation. In humans, there is little evidence that muscarinic receptor activation has any significant effect on intraurethral pressure in vivo [95].

In addition to the species variability noted above, a number of observations suggest that the response to muscarinic stimulation varies along the length of the urethra. Thus, Nagahama et al. dem-

onstrated that application of carbachol produced robust contractions in the male proximal urethra but had little effect on the distal urethra [96]. Interestingly, application of carbachol to strips of distal rabbit urethra pre-contracted with noradrenaline, resulted in relaxations of tone. These effects were abolished when NO synthase was inhibited, suggesting that muscarinic stimulation may also induce release of NO from nitrergic nerves.

The role, if any, of interstitial cells in cholinergic innervation of the urethra has not yet been ascertained. However, the cholinergic agonist carbachol evoked a series of oscillatory inward currents when applied to single UIC voltage clamped at −60 mV [26] and these events were inhibited by the CACC inhibitor A-9-C, suggesting a common activation pathway to that described by noradrenaline above. In contrast, Kyle et al. were unable to detect any inward currents elicited by muscarinic agonists in freshly dispersed rabbit USMCs [89]. However, they demonstrated that carbachol altered compound action potential characteristics, elicited by 1 s current injections. Therefore, it is apparent that electrical activity in both UICs and USMCs can be directly modulated by carbachol, but more experiments are required to elucidate the mechanisms involved in cholinergic responses at the whole tissue level.

6.6 Summary

Urethral smooth muscle generates spontaneous tone that makes a contribution to the maintenance of urinary continence by generating a urethral closure pressure that exceeds intravesical bladder pressure. Stress urinary incontinence (SUI) is common in women after vaginal delivery child birth [6] and is typically thought of as being due to reduced urethral support, referred to as urethral hypermobility. However, urethral hypermobility is not predictive of SUI and it is also recognised that it can coexist with a defective closure mechanism, known as 'intrinsic sphincter deficiency' [8, 97]. There are currently no FDA-approved pharmacological treatments for SUI, therefore it is crucial that the mechanisms responsible for the maintenance of urethral tone are elucidated, in order to identify novel therapeutic targets. This chapter provides a summary of the mechanisms responsible for spontaneous activity in urethral smooth muscle.

The urethra is regarded as a 'tonic' smooth muscle but, counterintuitively, there is now consensus that urethral smooth muscle tone is achieved by the averaging effect of numerous small asynchronous 'phasic' contractions in the tissue [27, 34, 73]. The phasic contractions of urethral smooth muscle appear to arise from activation of CACC/Ano1 channels and may originate in specialised cells referred to as urethral interstitial cells. This requires further investigation. Spontaneous activity in both USMCs and UICs involves Ca^{2+} release from intracellular stores and Ca^{2+} influx across the plasma membrane and is regulated by several autonomic neurotransmitters, including noradrenaline, acetylcholine, nitric oxide and adenosine triphosphate. Much of the work described in this chapter is based on animal studies, however it is apparent that there are species differences regarding the role of Ca^{2+} influx via L-type Ca^{2+} channels and on the cellular basis of Ano1 expression and activity. Therefore, it is imperative that future studies should examine the mechanisms responsible for spontaneous activity in human USM samples and examine if this activity, or its modulation by neurotransmitters, is altered in conditions that are associated with USM dysfunction, such as stress urinary incontinence.

Acknowledgments The authors are grateful for grant support from the Wellcome Trust (064212), NIH (RO1 DK68565) and the Health Research Board (PD/2005/4 & RP/2006/127) and for technical support from Ms. Billie McIlveen.

References

1. Brading AF. The physiology of the mammalian urinary outflow tract. Exp Physiol. 1999;84(1):215–21.
2. de Groat WC, Yoshimura N. Anatomy and physiology of the lower urinary tract. Handb Clin Neurol. 2015;130:61–108.
3. Rother P, Löffler S, Dorschner W, Reibiger I, Bengs T. Anatomic basis of micturition and urinary continence. Muscle systems in urinary bladder neck during ageing. Surg Radiol Anat. 1996;18(3):173–7.

4. Greenland JE, Dass N, Brading AF. Intrinsic urethral closure mechanisms in the female pig. Scand J Urol Nephrol Suppl. 1996;179:75–80.
5. Jankowski RJ, Prantil RL, Chancellor MB, de Groat WC, Huard J, Vorp DA. Biomechanical characterization of the urethral musculature. Am J Physiol Ren Physiol. 2006;290(5):F1127–34.
6. Norton P, Brubaker L. Urinary incontinence in women. Lancet. 2006;367:57–67.12.
7. DeLancey JO, Trowbridge ER, Miller JM, Morgan DM, Guire K, Fenner DE, Weadock WJ, Ashton-Miller JA. Stress urinary incontinence: relative importance of urethral support and urethral closure pressure. J Urol. 2008;179:2286–90.13.
8. DeLancey JO. Why do women have stress urinary incontinence? Neurourol Urodyn. 2010;29(Suppl 1):S13–7.
9. Prantil RL, Jankowski RJ, Kaiho Y, de Groat WC, Chancellor MB, Yoshimura N, Vorp DA. Ex vivo biomechanical properties of the female urethra in a rat model of birth trauma. Am J Physiol Ren Physiol. 2007;292(4):F1229–37.
10. Rud T. Urethral pressure profile in continent women from childhood to old age. Acta Obstet Gynecol Scand. 1980;59(4):331–5.
11. Trowbridge ER, Wei JT, Fenner DE, Ashton-Miller JA, DeLancey JO. Effects of aging on lower urinary tract and pelvic floor function in nulliparous women. Obstet Gynecol. 2007;109(3):715–20.
12. Clobes A, DeLancey JO, Morgan DM. Urethral circular smooth muscle in young and old women. Am J Obstet Gynecol. 2008;198(5):587.e1–5.
13. Bridgewater M, MacNeil HF, Brading AF. Regulation of tone in pig urethral smooth muscle. J Urol. 1993;150:223–8.
14. Thornbury KD, Hollywood MA, McHale NG. Mediation by nitric oxide of neurogenic relaxation of the urinary bladder neck muscle in sheep. J Physiol. 1992;451:133–44.
15. Andersson KE, Garcia Pascual A, Persson K, Forman A, Tøttrup A. Electrically-induced, nerve-mediated relaxation of rabbit urethra involves nitric oxide. J Urol. 1992;147(1):253–9.
16. Andersson KE. Pharmacology of lower urinary tract smooth muscles and penile erectile tissues. Pharmacol Rev. 1993;45:253–307.
17. Andersson KE, Wein AJ. Pharmacology of the lower urinary tract: basis for current and future treatments of urinary incontinence. Pharmacol Rev. 2004;56(4):581–631.
18. Ohnishi N, Park YC, Kurita T. Role of ATP and related purine compounds on urethral relaxation in male rabbits. Int J Urol. 1997;4(2):191–7.
19. Pinna C, Puglisi L, Burnstock G. ATP and vasoactive intestinal polypeptide relaxant responses in hamster isolated proximal urethra. Br J Pharmacol. 1998;124(6):1069–74.
20. Pinna C, Glass R, Knight GE. Purine- and pyrimidine-induced responses and P2Y receptor characterization in the hamster proximal urethra. Br J Pharmacol. 2005;144(4):510–8.
21. Hernandez M, Knight GE, Wildman SS, Burnstock G. Role of ATP and related purines in inhibitory neurotransmission to the pig urinary bladder neck. Br J Pharmacol. 2009;157(8):1463–73.
22. Noda K, Takebe M, Oka M, Hirouchi M, Ukai Y, Toda N. Functional role of inhibitory and excitatory nerves in the porcine lower urinary tract. Eur J Pharmacol. 2002;456(1–3):81–90.
23. Van der Werf BA, Creed KE. Mechanical properties and innervation of the smooth muscle layers of the urethra of greyhounds. BJU Int. 2002;90(6):588–95.
24. Creed KE, Oike M, Ito Y. The electrical properties and responses to nerve stimulation of the proximal urethra of the male rabbit. Br J Urol. 1997;79(4):543–53.
25. Sergeant GP, Hollywood MA, McCloskey KD, Thornbury KD, McHale NG. Specialised pacemaking cells in the rabbit urethra. J Physiol. 2000;526(2):359–66.
26. Sergeant GP, Thornbury KD, McHale NG, Hollywood MA. Interstitial cells of Cajal in the urethra. J Cell Mol Med. 2006;10(2):280–91.
27. Hashitani H, Suzuki H. Properties of spontaneous Ca2+ transients recorded from interstitial cells of Cajal-like cells of the rabbit urethra in situ. J Physiol. 2007;583(Pt 2):505–19.
28. Drumm BT, Koh SD, Andersson KE, Ward SM. Calcium signalling in Cajal-like interstitial cells of the lower urinary tract. Nat Rev Urol. 2014;11(10):555–64.
29. Brading AF. Spontaneous activity of lower urinary tract smooth muscles: correlation between ion channels and tissue function. J Physiol. 2006;570(1):13–22.
30. Callahan SM, Creed KE. Electrical and mechanical activity of the isolated lower urinary tract of the guinea-pig. Br J Pharmacol. 1981;74(2):353–8.
31. Callahan SM, Creed KE. The effects of oestrogens on spontaneous activity and responses to phenylephrine of the mammalian urethra. J Physiol. 1985;358:35–46.
32. Hashitani H, Van Helden DF, Suzuki H. Properties of spontaneous depolarizations in circular smooth muscle cells of rabbit urethra. Br J Pharmacol. 1996;118:1627–32.
33. Hashitani H, Edwards FR. Spontaneous and neurally activated depolarizations in smooth muscle cells of the guinea-pig urethra. J Physiol. 1999;514(Pt 2):459–70.
34. Drumm BT, Rembetski BE, Cobine CA, Baker SA, Sergeant GP, Hollywood MA, Thornbury KD, Sanders KM. Ca2+ signalling in mouse urethral smooth muscle in situ: role of Ca2+ stores and Ca2+ influx mechanisms. J Physiol. 2018;596:1433–66.
35. Hashitani H, Fukuta H, Takano H, Klemm MF, Suzuki H. Origin and propagation of spontaneous excitation in smooth muscle of the guinea-pig urinary bladder. J Physiol. 2001;530(Pt 2):273–86.
36. Hashitani H, Yanai Y, Kohri K, Suzuki H. Heterogeneous CPA sensitivity of spontaneous excitation in smooth muscle of the rabbit urethra. Br J Pharmacol. 2006;148(3):340–9.

37. Bradley JE, Anderson UA, Woolsey SM, Thornbury KD, McHale NG, Hollywood MA. Characterization of T-type calcium current and its contribution to electrical activity in rabbit urethra. Am J Phys Cell Physiol. 2004;286(5):C1078–88.
38. Drumm BT, Sergeant GP, Hollywood MA, Thornbury KT, Matsuda TT, Baba A, Harvey BJ, McHale NG. The effect of high [K(+)]o on spontaneous Ca(2+) waves in freshly isolated interstitial cells of Cajal from the rabbit urethra. Phys Rep. 2014;2(1):e00203.
39. Teramoto N, Brading AF. Activation by levcromakalim and metabolic inhibition of glibenclamide-sensitive K channels in smooth muscle cells of pig proximal urethra. Br J Pharmacol. 1996;118(3):635–42.
40. Teramoto N, McMurray G, Brading AF. Effects of levcromakalim and nucleoside diphosphates on glibenclamide-sensitive K+ channels in pig urethral myocytes. Br J Pharmacol. 1997;120(7):1229–40.
41. Kyle BD. Ion channels of the mammalian urethra. Channels (Austin). 2014;8(5):393–401.
42. Cotton KD, Hollywood MA, McHale NG, Thornbury KD. Ca2+ current and Ca(2+)-activated chloride current in isolated smooth muscle cells of the sheep urethra. J Physiol. 1997;505(Pt 1):121–31.
43. Sergeant GP, Hollywood MA, McHale NG, Thornbury KD. Spontaneous Ca2+ activated Cl− currents in isolated urethral smooth muscle cells. J Urol. 2001;166(3):1161–6.
44. Caputo A, Caci E, Ferrera L, Pedemonte N, Barsanti C, Sondo E, Pfeffer U, Ravazzolo R, Zegarra-Moran O, Galietta LJ. TMEM16A, a membrane protein associated with calcium-dependent chloride channel activity. Science. 2008;322(5901):590–4.
45. Schroeder BC, Cheng T, Jan YN, Jan LY. Expression cloning of TMEM16A as a calcium-activated chloride channel subunit. Cell. 2008;134(6):1019–29.
46. Yang YD, Cho H, Koo JY, Tak MH, Cho Y, Shim WS, Park SP, Lee J, Lee B, Kim BM, Raouf R, Shin YK, Oh U. TMEM16A confers receptor-activated calcium-dependent chloride conductance. Nature. 2008;455(7217):1210–5.
47. Sancho M, García-Pascual A, Triguero D. Presence of the Ca2+-activated chloride channel anoctamin 1 in the urethra and its role in excitatory neurotransmission. Am J Physiol Ren Physiol. 2012;302(3):F390–400.
48. Huang F, Rock JR, Harfe BD, Cheng T, Huang X, Jan YN, Jan LY. Studies on expression and function of the TMEM16A calcium-activated chloride channel. Proc Natl Acad Sci U S A. 2009 Dec 15;106(50):21413–8.
49. Hollywood MA, Woolsey S, Walsh IK, Keane PF, McHale NG, Thornbury KD. T- and L- type Ca2+ currents in freshly dispersed smooth muscle cells from the human proximal urethra. J Physiol. 2003;550(Pt 3):753–64.
50. Smet PJ, Jonavicius J, Marshall VR, de Vente J. Distribution of nitric oxide synthase-immunoreactive nerves and identification of the cellular targets of nitric oxide in guinea-pig and human urinary bladder by cGMP immunohistochemistry. Neuroscience. 1996;71(2):337–48.
51. Burns AJ, Lomax AEJ, Torihashi S, Sanders KM, Ward SM. Interstitial cells of Cajal mediate inhibitory neurotransmission in the stomach. Proc Natl Acad Sci U S A. 1996;93:12008–13.
52. Sanders KM. A case for interstitial cells of Cajal as pacemakers and mediators of neurotransmission in the gastrointestinal tract. Gastroenterology. 1996;111:492–515.
53. Ward SM, Morris G, Reese L, Wang XY, Sanders KM. Interstitial cells of Cajal mediate enteric inhibitory neurotransmission in the lower esophageal and pyloric sphincters. Gastroenterology. 1998;115:314–29.
54. Ward SM, Beckett EAH, Wang XY, Baker F, Khoyi M, Sanders KM. Interstitial cells of Cajal mediate cholinergic neurotransmission from enteric motor neurons. J Neurosci. 2000;20(4):1393–403.
55. Langton P, Ward SM, Carl A, Norell MA, Sanders KM. Spontaneous electrical activity of interstitial cells of Cajal isolated from canine proximal colon. Proc Natl Acad Sci U S A. 1989;86:7280–4.
56. Fedigan S, Bradley E, Webb T, Large RJ, Hollywood MA, Thornbury KD, McHale NG, Sergeant GP. Effects of new-generation TMEM16A inhibitors on calcium-activated chloride currents in rabbit urethral interstitial cells of Cajal. Pflugers Arch. 2017;469:1443–55.
57. Sergeant GP, Hollywood MA, McCloskey KD, McHale NG, Thornbury KD. Role of IP(3) in modulation of spontaneous activity in pacemaker cells of rabbit urethra. Am J Phys Cell Physiol. 2001;280(5):C1349–56.
58. Johnston L, Sergeant GP, Hollywood MA, Thornbury KD, McHale NG. Calcium oscillations in interstitial cells of the rabbit urethra. J Physiol. 2005;565(Pt 2):449–61.
59. Sancho M, Bradley E, Garcia-Pascual A, Triguero D, Thornbury KD, Hollywood MA, Sergeant GP. Involvement of cyclic nucleotide-gated channels in spontaneous activity generated in isolated interstitial cells of Cajal from the rabbit urethra. Eur J Pharmacol. 2017;814:216–25.
60. Bradley E, Hollywood MA, McHale NG, Thornbury KD, Sergeant GP. Pacemaker activity in urethral interstitial cells is not dependent on capacitative calcium entry. Am J Phys Cell Physiol. 2005;289(3):C625–32.
61. Iwamoto T, Watano T, Shigekawa M. A novel isothiourea derivative selectively inhibits the reverse mode of Na+/Ca2+ exchange in cells expressing NCX1. J Biol Chem. 1996;271:22391–7.
62. Watano T, Kimura J, Morita T, Nakanishi H. A novel antagonist, KB-R7943, of the Na+/Ca2+ exchange current in guinea-pig cardiac ventricular cells. Br J Pharmacol. 1996;119:555–63.
63. Matsuda T, Arakawa N, Takuma K, Kishida Y, Kawasaki Y, Sakaue M, et al. SEA0400, a novel and selective inhibitor of the Na+-Ca2+ exchanger, attenuates reperfusion injury in the in vitro and in vivo cerebral ischemic models. J Pharmacol Exp Ther. 2001;298:249–56.

64. Lee C, Visen NS, Dhalla NS, Le HD, Isaac M, Choptiany P, et al. Inhibitory profile of SEA0400 [2-[4-[(2,5-difluorophenyl) methoxy]phenoxy]-5-ethoxyaniline] assessed on the cardiac Na+-Ca2+ exchanger, NCX1.1. J Pharmacol Exp Ther. 2004;311:748–57.
65. Bradley E, Hollywood MA, Johnston L, Large RJ, Matsuda T, Baba A, McHale NG, Thornbury KD, Sergeant GP. Contribution of reverse Na+/Ca2+ exchange to spontaneous activity in interstitial cells of Cajal in the rabbit urethra. J Physiol. 2006;574(Pt 3):651–61.
66. Drumm BT, Large RJ, Hollywood MA, Thornbury KD, Baker SA, Harvey BJ, McHale NG, Sergeant GP. The role of Ca(2+) influx in spontaneous Ca(2+) wave propagation in interstitial cells of Cajal from the rabbit urethra. J Physiol. 2015;593(15):3333–50.
67. Triguero D, Sancho M, Garcia-Flores M, Garcia-Pascual A. Presence of cyclic nucleotide-gated channels in the rat urethra and their involvement in nerve-mediated nitrergic relaxation. Am J Physiol Ren Physiol. 2009;297:F1353–60.
68. Ward SM, Ordog T, Koh SD, Baker SA, Jun JY, Amberg G, Monaghan K, Sanders KM. Pacemaking in interstitial cells of Cajal depends upon calcium handling by endoplasmic reticulum and mitochondria. J Physiol. 2000;525(Pt 2):355–61.
69. Sergeant GP, Bradley E, Thornbury KD, McHale NG, Hollywood MA. Role of mitochondria in modulation of spontaneous Ca2+ waves in freshly dispersed interstitial cells of Cajal from the rabbit urethra. J Physiol. 2008;586(19):4631–42.
70. Hashitani H, Lang RJ, Suzuki H. Role of perinuclear mitochondria in the spatiotemporal dynamics of spontaneous Ca2+ waves in interstitial cells of Cajal-like cells of the rabbit urethra. Br J Pharmacol. 2010;161(3):680–94.
71. Drumm BT, Sung TS, Zheng H, Baker SA, Koh SD, Sanders KM. The effects of mitochondrial inhibitors on Ca2+ signalling and electrical conductances required for pacemaking in interstitial cells of Cajal in the mouse small intestine. Cell Calcium. 2018;72:1–17.
72. McHale NG, Hollywood MA, Sergeant GP, Shafei M, Thornbury KT, Ward SM. Organization and function of ICC in the urinary tract. J Physiol. 2006;576(Pt 3):689–94.
73. Thornbury KD, Hollywood MA, McHale NG, Sergeant GP. Cajal beyond the gut: interstitial cells in the urinary system—towards general regulatory mechanisms of smooth muscle contractility? Acta Gastroenterol Belg. 2011;74(4):536–42.
74. Morita T, Tsujii T, Dokita S. Regional difference in functional roles of cAMP and cGMP in lower urinary tract smooth muscle contractility. Urol Int. 1992;49(4):191–5.
75. Dokita S, Smith SD, Nishimoto T, Wheeler MA, Weiss RM. Involvement of nitric oxide and cyclic GMP in rabbit urethral relaxation. Eur J Pharmacol. 1994;266(3):269–75.
76. Persson K, Andersson KE. Non-adrenergic, non-cholinergic relaxation and levels of cyclic nucleotides in rabbit lower urinary tract. Eur J Pharmacol. 1994;268(2):159–67.
77. Persson K, Pandita RK, Aszòdi A, Ahmad M, Pfeifer A, Fässler R, Andersson KE. Functional characteristics of urinary tract smooth muscles in mice lacking cGMP protein kinase type I. Am J Phys Regul Integr Comp Phys. 2000;279(3):R1112–20.
78. Lies B, Groneberg D, Friebe A. Correlation of cellular expression with function of NO-sensitive guanylyl cyclase in the murine lower urinary tract. J Physiol. 2013;591(21):5365–75. https://doi.org/10.1113/jphysiol.2013.262410.
79. Waldeck K, Ny L, Persson K, Andersson KE. Mediators and mechanisms of relaxation in rabbit urethral smooth muscle. Br J Pharmacol. 1998;123(4):617–24.
80. García-Pascual A, Sancho M, Costa G, Triguero D. Interstitial cells of Cajal in the urethra are cGMP-mediated targets of nitrergic neurotransmission. Am J Physiol Ren Physiol. 2008;295(4):F971–83.
81. Lyons AD, Gardiner TA, McCloskey KD. Kit-positive interstitial cells in the rabbit urethra: structural relationships with nerves and smooth muscle. BJU Int. 2007;99(3):687–94.
82. Sergeant GP, Johnston L, McHale NG, Thornbury KD, Hollywood MA. Activation of the cGMP/PKG pathway inhibits electrical activity in rabbit urethral interstitial cells of Cajal by reducing the spatial spread of Ca2+ waves. J Physiol. 2006;574(Pt1):167–81.
83. Drumm BT, Sergeant GP, Hollywood MA, Thornbury KD, McHale NG, Harvey BJ. The role of cAMP dependent protein kinase in modulating spontaneous intracellular Ca2+ waves in interstitial cells of Cajal from the rabbit urethra. Cell Calcium. 2014;56(3):181–7.
84. Deplanne V, Palea S, Angel I. The adrenergic, cholinergic and NANC nerve-mediated contractions of the female rabbit bladder neck and proximal, medial and distal urethra. Br J Pharmacol. 1998;123(8):1517–24.
85. Bradley E, Kadima S, Drumm B, Hollywood MA, Thornbury KD, McHale NG, Sergeant GP. Novel excitatory effects of adenosine triphosphate on contractile and pacemaker activity in rabbit urethral smooth muscle. J Urol. 2010;183(2):801–11.
86. Bradley E, Kadima S, Kyle B, Hollywood MA, Thornbury KD, McHale NG, Sergeant GP. P2X receptor currents in smooth muscle cells contribute to nerve mediated contractions of rabbit urethral smooth muscle. J Urol. 2011;186(2):745–52.
87. Sergeant GP, Thornbury KD, McHale NG, Hollywood MA. Characterization of norepinephrine-evoked inward currents in interstitial cells isolated from the rabbit urethra. Am J Phys Cell Physiol. 2002;283(3):C885–94.
88. Ward SM, Sanders KM. Involvement of intramuscular interstitial cells of Cajal in neuroeffector transmission in the gastrointestinal tract. J Physiol. 2006;576(Pt 3):675–82.

89. Kyle BD, Bradley E, Large R, Sergeant GP, McHale NG, Thornbury KD, Hollywood MA. Mechanisms underlying activation of transient BK current in rabbit urethral smooth muscle cells and its modulation by IP3-generating agonists. Am J Phys Cell Physiol. 2013;305(6):C609–22.
90. Walsh MP, Thornbury K, Cole WC, Sergeant G, Hollywood M, McHale N. Rho-associated kinase plays a role in rabbit urethral smooth muscle contraction, but not via enhanced myosin light chain phosphorylation. Am J Physiol Ren Physiol. 2011;300(1):F73–85.
91. Thind P, Lose G, Colstrup H, Andersson KE. The influence of beta-adrenoceptor and muscarinic receptor agonists and antagonists on the static urethral closure function in healthy females. Scand J Urol Nephrol. 1993;27(1):31–8.
92. Yamanishi T, Chapple CR, Yasuda K, Yoshida K, Chess-Williams R. The role of M2 muscarinic receptor subtypes mediating contraction of the circular and longitudinal smooth muscle of the pig proximal urethra. J Urol. 2002;168(1):308–14.
93. Mutoh S, Latifpour J, Saito M, Weiss RM. Evidence for the presence of regional differences in the subtype specificity of muscarinic receptors in rabbit lower urinary tract. J Urol. 1997;157(2):717–21.
94. Ito Y, Kimoto Y. The neural and non-neural mechanisms involved in urethral activity in rabbits. J Physiol. 1985;367:57–72.
95. Thind P, Lose G, Colstrup H, Andersson KE. The urethral resistance to rapid dilation: an analysis of the effect of autonomic receptor stimulation and blockade and of pudendal nerve blockade in healthy females. Scand J Urol Nephrol. 1995;29(1):83–91.
96. Nagahama K, Tsujii T, Morita T, Azuma H, Oshima H. Differences between proximal and distal portions of the male rabbit posterior urethra in the physiological role of muscarinic cholinergic receptors. Br J Pharmacol. 1998;124(6):1175–80.
97. Fleischmann N, Flisser AJ, Blaivas JG, Panagopoulos G. Sphincteric urinary incontinence: relationship of vesical leak point pressure, urethral mobility and severity of incontinence. J Urol. 2003;169(3):999–1002.

Part III

Reproductive Organs

7 Ion Channels and Intracellular Calcium Signalling in Corpus Cavernosum

Keith D. Thornbury, Mark A. Hollywood, and Gerard P. Sergeant

Abstract

The corpus cavernosum smooth muscle is important for both erection of the penis and for maintaining penile flaccidity. Most of the time, the smooth muscle cells are in a contracted state, which limits filling of the corpus sinuses with blood. Occasionally, however, they relax in a co-ordinated manner, allowing filling to occur. This results in an erection. When contractions of the corpus cavernosum are measured, it can be deduced that the muscle cells work together in a syncytium, for not only do they spontaneously contract in a co-ordinated manner, but they also synchronously relax. It is challenging to understand how they achieve this.

In this review we will attempt to explain the activity of the corpus cavernosum, firstly by summarising current knowledge regarding the role of ion channels and how they influence tone, and secondly by presenting data on the intracellular Ca^{2+} signals that interact with the ion channels. We propose that spontaneous Ca^{2+} waves act as a primary event, driving transient depolarisation by activating Ca^{2+}-activated Cl^- channels. Depolarisation then facilitates Ca^{2+} influx via L-type voltage-dependent Ca^{2+} channels. We propose that the spontaneous Ca^{2+} oscillations depend on Ca^{2+} release from both ryanodine- and inositol trisphosphate (IP_3)-sensitive stores and that modulation by signalling molecules is achieved mainly by interactions with the IP_3-sensitive mechanism. This pacemaker mechanism is inhibited by nitric oxide (acting through cyclic GMP) and enhanced by noradrenaline. By understanding these mechanisms better, it might be possible to design new treatments for erectile dysfunction.

Keywords

Corpus cavernosum · Smooth muscle · Calcium waves · Calcium imaging STICs · STOCS · STDs

7.1 Introduction

Erection of the penis requires the co-ordinated relaxation of the penile arteries and corpus cavernosum smooth muscle, which are contained in two parallel cylindrical structures (the corpora

Electronic Supplementary Material The online version of this chapter (https://doi.org/10.1007/978-981-13-5895-1_7) contains supplementary material, which is available to authorized users.

K. D. Thornbury (✉) · M. A. Hollywood
G. P. Sergeant
Smooth Muscle Research Centre, Regional Development Centre, Dundalk Institute of Technology, Dundalk, Co. Louth, Ireland
e-mail: keith.thornburyt@dkit.ie

H. Hashitani, R. J. Lang (eds.), *Smooth Muscle Spontaneous Activity*, Advances in Experimental Medicine and Biology 1124, https://doi.org/10.1007/978-981-13-5895-1_7

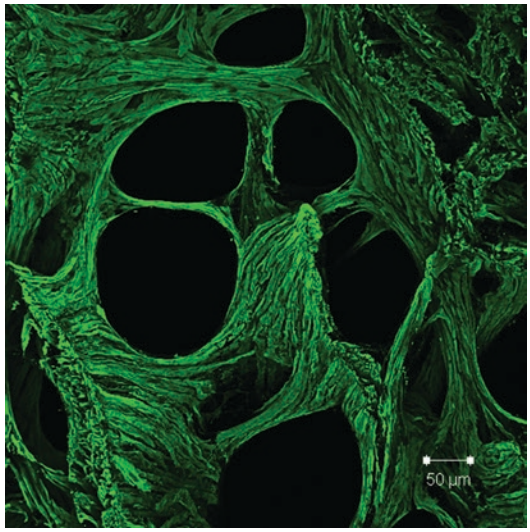

Fig. 7.1 Transverse whole mount section of rabbit corpus cavernosum slice labelled with anti-smooth muscle myosin antibody to show arrangement of the vascular sinuses. Scale bar 50 µm. Adapted from Doyle [1]

cavernosa) running the full length of the shaft of the penis. Each corpus cavernosum is a sponge-like structure composed of multiple vascular sinuses, encased in a fibrous capsule called the tunica albuginea. The walls of the sinuses contain the corpus cavernosum smooth muscle cells (Fig. 7.1) and are lined on the inside with vascular endothelium [1].

Most of the time, these corpus cavernosum smooth muscle cells are in a contracted state, which limits filling of the sinuses with blood. Occasionally, however, they relax in a co-ordinated manner, allowing the sinuses to fill. This results in penile tumescence, and, because further expansion is restricted by the surrounding capsule, intracorporal pressure increases to produce penile rigidity and erection. Erection could not occur if the helicine arteries, which supply the sinuses, did not also dilate; however, the details of the roles played by all of the participants in the erectile process are not the subject of this chapter. For these, the reader is referred to an authoritative review by Andersson and Wagner [2] that describes the anatomical details of the penis, its innervation and central nervous system control and other relevant physiology. The pharmacology of the many mediators that regulate the tone of the corpus cavernosum and the arterial smooth muscle are also comprehensively reviewed elsewhere [3].

Instead, this review will focus only on the corpus cavernosum, unless it is deemed helpful to borrow information from other sources. The remit will be to provide an update on our understanding of how tone is regulated by ion channels and intracellular Ca^{2+} signals, as these are areas that have developed significantly over the last 15–20 years since the previous reviews were written. Also, despite the many mediators that affect the contractility of corpus cavernosum, only excitation by α-adrenergic agonists and inhibition by nitric oxide (NO) will be considered in any detail, as these are of the greatest importance. Reference will be made erectile dysfunction (ED), as it is the desire to find new treatment targets for this disorder that drives research in this field. However, for more detailed and specific information regarding ED, the reader is referred to several recent reviews on this topic [4, 5].

7.2 Mechanical Activity in Corpus Cavernosum

Isolated strips of corpus cavernosum from most species studied develop spontaneous tone and/or phasic contractions that are resistant to blockade with tetrodotoxin or α-adrenoceptor antagonists [2, 6]. One of the best studied species is the rabbit, from which an example of typical activity is presented in Fig. 7.2a. This shows the most frequent type of activity observed, with long bursts of mixed phasic and tonic contraction interspersed with complete relaxations that last for several minutes. The fact that many of the smooth muscle cells in the tissue can not only suddenly contract in a synchronised manner but can also all spontaneously relax is a strong indication that the corpus cavernosum smooth muscle cells work together in a syncytium. There is ample evidence that the cells are coupled by gap junctions consisting of connexion43 that would facilitate electrical coupling and/or cell to cell transfer of second messengers such as IP_3 [6, 8]. Other types of spontaneous activity are also observed in rab-

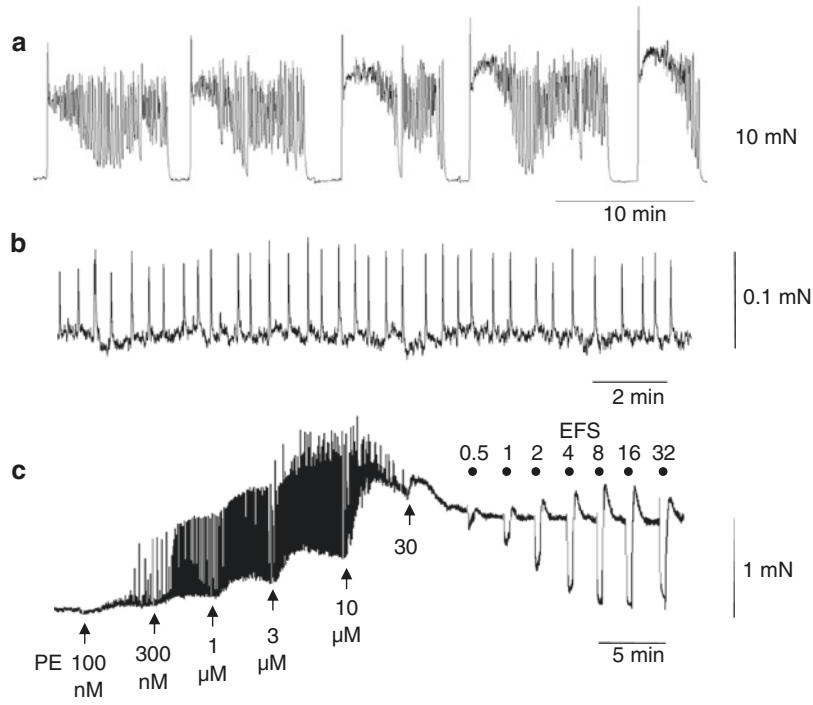

Fig. 7.2 Mechanical activity in corpus cavernosum in vitro. (**a**) Typical spontaneous activity in rabbit corpus cavernosum. (**b**) Spontaneous activity in mouse corpus cavernosum. (**c**) Effect of phenylephrine (PE) and electrical field stimulation (EFS) in mouse corpus cavernosum. EFS parameters (0.3 ms pulses, 30 s trains, frequency in Hz indicated above filled circles). (**a**) Is a previously unpublished record; (**b**) and (**c**) are adapted from Hannigan [7]

bit corpus cavernosum, including more sustained tonic activity [9] or more discrete phasic contractions [10]. In contrast to rabbit, mouse corpus cavernosum has been previously reported to be quiescent [11], except when large conductance Ca^{2+}-activated K^+ channels have been deleted [12]. However, we have found that the majority (10 of 16) of muscle strips isolated from mouse corpus cavernosum developed phasic activity in vitro, as shown in Fig. 7.2b. Phasic activity superimposed on tonic contraction was also evident when mouse corpus cavernosum was stimulated with submaximal concentrations of phenylephrine (PE), though the maximal concentrations produced only tonic contractions (Fig. 7.2c). These could be almost completely relaxed by electrical field stimulation of nerves (Fig. 7.2c) that were susceptible to blockade with L-NOARG, a nitric oxide synthase blocker, or ODQ, a blocker of soluble guanylate cyclase [7, 11].

To try to understand the basis of the spontaneous activity and its regulation by nitric oxide and noradrenaline, it is necessary to first review the ion channels present in corpus cavernosum. Mostly, we have confined the discussion only to channels where there is sound electrophysiological evidence that they are expressed in corpus cavernosum myocytes, except where to draw attention to several promising areas of future research, where less detailed evidence is available.

7.3 Ion Channels in Corpus Cavernosum Myocytes

7.3.1 L-Type Ca^{2+} Current

Circumstantial evidence for a role for L-type Ca^{2+} currents in regulation of tone in corpus cavernosum was compelling long before these currents had actually been directly demonstrated. Thus, L-type Ca^{2+} channel blockers such as nifedipine, diltiazem and verapamil were found to abolish contractures induced by high $[K^+]$ in human corpus cavernosum, while noradrenaline-induced contractions were reduced by around 50% [13]. L-type Ca^{2+} channel blockers also block spontaneous tone, spontaneous depolarisa-

tions and attenuate Ca^{2+} transients in rabbit corpus cavernosum [9, 14, 15].

To date, however, there have only been a few studies where L-type Ca^{2+} current has been measured in corpus cavernosum myocytes. A systematic characterisation of the Ca^{2+} currents in isolated corpus cavernosum myocytes from rabbit was carried out by McCloskey et al. [15]. On the basis of voltage protocols, pharmacology and RT-PCR, both L-type and T-type Ca^{2+} currents (see Sect. 7.3.2) were identified. L-type Ca^{2+} current was blocked by nifedipine with an IC_{50} of 38 nM, but was resistant to mibefradil at 300 nM and to Ni^{2+} at 30 μM. This current activated at around −50 mV, peaked at −5 mV and had an activation $V_{1/2}$ of −27 mV (Fig. 7.3a, b, d). The L-type Ca^{2+} current also voltage-dependently inactivated over a range of −65 to −5 mV, with a

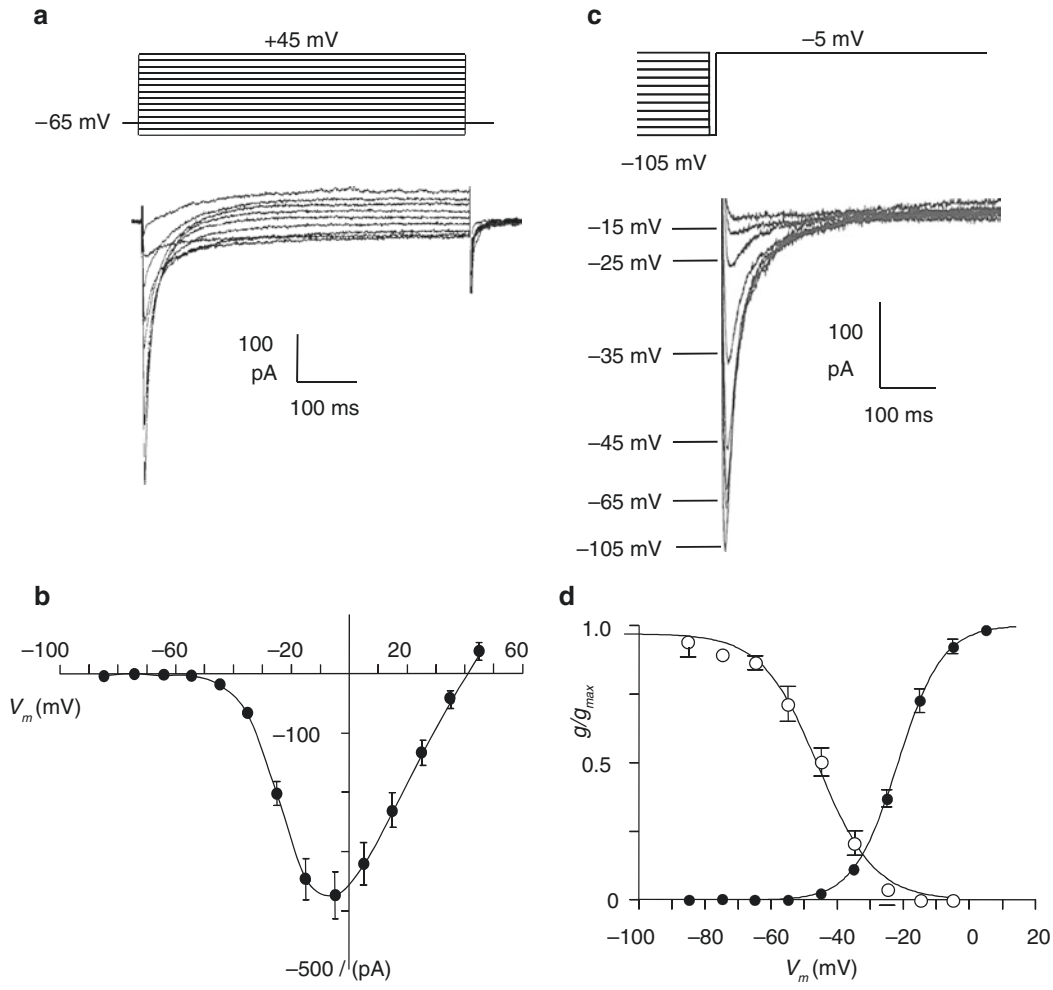

Fig. 7.3 L-type Ca^{2+} currents recorded from myocytes isolated from rabbit corpus cavernosum. Records were obtained in whole-cell mode of the patch clamp technique with Cs^+-rich pipettes. (**a**) Inward Ca^{2+} currents recorded with depolarising steps in 10 mV increments. Insert shows protocol. (**b**) Current-voltage relationship from eight cells (mean ± s.e.m.). (**c**) Inactivation protocol involving steps to conditioning potentials for 2 s before stepping to test potential of −5 mV. Protocol is shown in inset and selected corresponding conditioning potentials are shown in column on left. (**d**) Voltage-dependent activation (n = 8) and inactivation (n = 6) relationships. Solid line show fits of the data with the Boltzmann equation. Adapted from McCloskey et al. [15]

$V_{1/2}$ of −45 mV (Fig. 7.3c, d). Importantly, the steady state activation and inactivation curves intersected at around −30 mV and the area under the intersection extended from −45 to −10 mV (Fig. 7.3d). This area defines the range of voltages over which a small proportion of the L-type Ca^{2+} channels can, in theory, be constantly activated, a phenomenon referred to as the 'window current' [16]. The window current concept explains how continuous Ca^{2+} influx through L-type Ca^{2+} channels can maintain tone in some vascular smooth muscles [17]. Also, it is noteworthy that the maximal window current would occur at −30 mV (the peak where the curves intersect), as this also corresponds to the Nernst equilibrium potential for Cl^- ions in smooth muscle (see Sect. 7.3.8). Therefore, activation of the abundant Ca^{2+}-activated Cl^- current present in corpus cavernosum myocytes would tend to depolarise and clamp the membrane potential at the value where the maximal sustained Ca^{2+} influx via L-type Ca^{2+} channels is possible.

McCloskey and colleagues [15] also showed that nifedipine, at a concentration selective for L-type Ca^{2+} current, reduced phenylephrine (PE)-induced contractions by around 50%, and reduced the frequency of, but did not always abolish, intracellular Ca^{2+} waves in isolated corpus cavernosum myocytes. Given the sensitivity of α-adrenoceptor-induced contractions to L-type Ca^{2+} channel blockers, it was attractive to propose that adrenergic stimulation increased tone by upregulating L-type Ca^{2+} channels [18]. It was suggested that this effect was mediated by the well-known sequence of α_1-adrenoceptor activation of phospholipase C, resultant production of diacylglycerol (DAG), DAG activation of protein kinase C (PKC) and subsequent phosphorylation and activation of L-type Ca^{2+} channels. However, Doyle et al. [19] directly examined the effect of PE on L-type Ca^{2+} current in rabbit corpus cavernosum myocytes and found that it inhibited the current. Instances of depression of Ca^{2+} current in response to α_1-adrenoceptor agonists have usually been attributed to Ca^{2+}-dependent inactivation of the L-type Ca^{2+} channels as a result of IP_3-mediated release of Ca^{2+} from intracellular stores [20]. In agreement with this mechanism, Doyle and colleagues [19] found that 2-aminoethoxy diphenylborate (2-APB), known to inhibit IP_3R-mediated Ca^{2+} release, completely prevented the inhibition of L-type Ca^{2+} current by PE. Also, phorbol 12-myristate 13-acetate (PMA), a PKC activator, failed to enhance the L-type Ca^{2+} current, but chelerythrine, a PKC inhibitor, reduced it. They speculated that PKC was constituently active in isolated rabbit corpus cavernosum myocytes, with the result that the L-type Ca^{2+} channels were already maximally phosphorylated. Whether this would also be true in vivo, of course, is unknown. However, it seems likely to us that the sensitivity of α_1-adrenoceptor-mediated contractures to L-type Ca^{2+} channel blockers depends more on the ability of α_1-agonists to depolarise the corpus cavernosum myocytes [19] towards the threshold of L-type Ca^{2+} channel opening, than the ability to directly stimulate L-type Ca^{2+} channels.

7.3.2 T-Type Ca^{2+} Current

T-type ('transient') Ca^{2+} channels derive their name from that fact that they activate and inactivate more rapidly than L-type Ca^{2+} channels. They also activate and inactivate over more negative voltage-ranges than L-type Ca^{2+} current and have a different pharmacology [21]. Three different subtypes of the pore forming α-subunit have been recognised, namely Cav3.1, Cav3.2 and Cav3.3 (formerly called formerly called α_1G, α_1H, and α_1I) [21]. Zeng and colleagues showed that mRNA transcripts for Cav3.1, but not Cav3.2 or Cav3.3, were present in cultured human corpus cavernosum myocytes, though no electrophysiological characterisation was performed [22]. In experiments where cytosolic Ca^{2+} concentration ($[Ca^{2+}]_i$) was measured using the fura-2 indicator, 30 and 80 mM K^+ caused increases in Ca^{2+} that were only partially sensitive to nifedipine, requiring the addition of NNC 55-0396, a known blocker of T-type Ca^{2+} channels, for complete inhibition. However, these were presented as single experiments that were not replicated. McCloskey and colleagues [15] were also able to distinguish a T-type Ca^{2+} current from the L-type

Ca^{2+} current in freshly isolated rabbit corpus cavernosum myocytes, on the basis of their voltage dependence of inactivation, and its sensitivity to Ni^{2+} or mibefradil, but not nifedipine. These authors also performed RT-PCR on rabbit CSSM tissue and found the presence of mRNA for Cav3.1 and Cav3.2, but not Cav3.3. Their electrophysiological experiments suggested that most, if not all, of the current was mediated by the Cav3.2 subtype, based on sensitivity to micromolar concentrations of Ni^{2+}, a feature thought to apply only to the Cav3.2 subtype. Whether the additional expression of Cav3.2 in freshly isolated rabbit corpus cavernosum myocytes, compared to cultured human cells, represents a true species difference or may be explained by loss of Cav3.2 in cell culture is unknown.

McCloskey and colleagues [15], also examined the effect of Ni^{2+} on intracellular Ca^{2+} waves and PE-induced contractures and found no effect, therefore failing to support a functional role for this T-type Ca^{2+} current, at least under their experimental conditions. Negative findings such as these, however, do not preclude a role for T-type Ca^{2+} current in the corpus cavernosum in vivo. Indeed, T-type Ca^{2+} current is thought to be pro-proliferative in other vascular smooth muscle where the relative expression of T- vs. L-type Ca^{2+} current increases in dedifferentiated cells [23]. The Zeng study [22] showed that a T-type Ca^{2+} channel blocker reduced proliferation of cultured human corpus cavernosum myocytes by 15–25%, suggesting that a proliferative role for T-type Ca^{2+} current in corpus cavernosum is worthy of further investigation.

7.3.3 P2X Receptor-Mediated Cation Current

P2X purinoceptors are a family of cation-permeable ligand-gated ion channels [24]. In the vas deferens, and some blood vessels, ATP behaves as an excitatory cotransmitter with noradrenaline, causing contraction by acting on P2X purinoceptors [25, 26]. P2X receptors can cause depolarisation, thus activating L-type Ca^{2+} channels, or can directly admit Ca^{2+}. There have been relatively few studies on the effect of ATP in corpus cavernosum but, generally, exogenous ATP and its metabolites were found to be inhibitory, causing relaxation by a combination of P2Y receptor-mediated release of NO from the endothelium and a breakdown of ATP to adenosine, which causes relaxation by acting on P1 receptors (reviewed by Phatarpekar et al. [27]). However, ATP also sometimes causes contraction of human corpus cavernosum [28] and of rabbit corpus cavernosum when resting tension is initially low [29].

Doyle et al. [30] provided functional evidence that ATP induces an inward cationic current in isolated corpus cavernosum myocytes from rabbits (Fig. 7.4a). This current was blocked by desensitisation of P2X receptors to α,β-methylene ATP, and by NF449, a powerful selective inhibitor of $P2X_1$ receptors (Fig. 7.4a, b). Ion substitution experiments established that the current was partly carried by Na^+ ions, clearly distinguishing it from the inward Cl^- current, which could be evoked by 2-MeSADP, a specific P2Y receptor agonist. Immunohistochemical studies have confirmed the presence of $P2X_1$ receptors on the membranes of corpus cavernosum smooth muscle cells in rats [31], where they have been implicated in a pathological role in the development of erectile dysfunction in diabetes [32, 33]. $P2X_1$ receptor expression increases as erectile capacity decreases during development of diabetes induced by streptozotocin, while PPADS, a P2X receptor antagonist, improves the otherwise compromised nerve-mediated relaxation responses in diabetic rats, so that they resemble those of control animals [32, 33].

In conclusion, although the functional effects of P2X receptors have been demonstrated in corpus cavernosum, at present it is not clear whether they have a physiological role in contributing to penile flaccidity under normal circumstances. However, they may contribute to the anti-erectile effects of P2X receptors in pathological conditions and thus warrant further study.

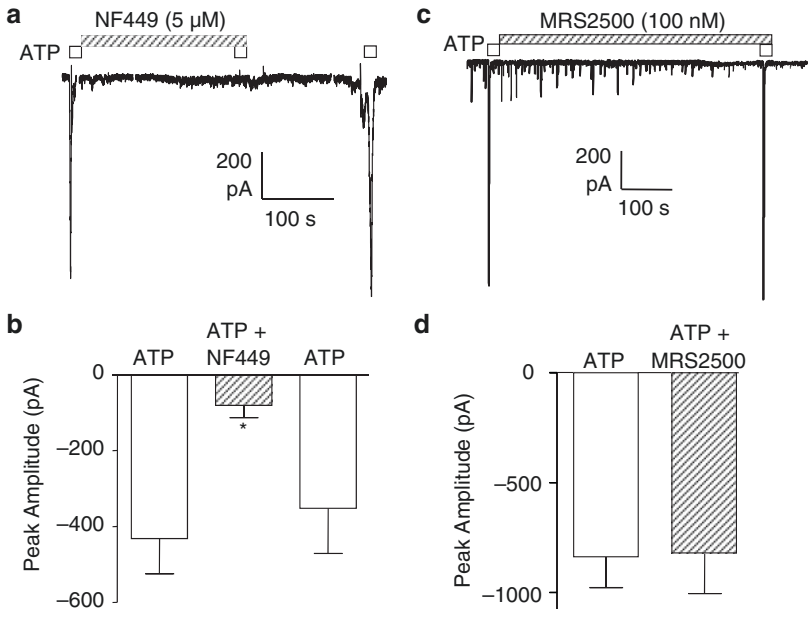

Fig. 7.4 Inward currents evoked by ATP in rabbit corpus cavernosum myocytes studied with the perforated patch technique. (**a**) ATP-evoked currents in the absence and presence of NF449, a $P2X_1$ receptor inhibitor. (**b**) Summary data of experiments as in (**a**), $n = 6$, $^*P < 0.05$. (**c**) ATP-evoked currents in the absence and presence of MRS2500, a P2Y receptor blocker. (**d**) Summary data of experiments as in (**c**), $n = 13$. Adapted from Doyle et al. [30]

7.3.4 TRP Channels

Mammalian transient receptor potential (TRP) channels are a superfamily of Ca^{2+} -permeable nonselective cation channels consisting of six subfamilies, TRPC, TRPV, TRPM, TRPA, TRPP and TRPML, with diverse functions [34]. Members of the TRPC, TRPV, TRPM and TRPP subfamilies are expressed on vascular smooth muscle cells and have been implicated in agonist-induced vasoconstriction, myogenic tone regulation and proliferation [34]. So far, these channels have received very little attention in corpus cavernosum. However, preliminary results indicate that TRPM4 is expressed in mouse corpus cavernosum and phenanthrol, a TRPM4 antagonist, relaxes this tissue [35]. In arteries, TRPM4 is thought to contribute to pressure-induced myogenic tone regulation by causing membrane depolarisation [35]. However, as we shall see, corpus cavernosum myocytes are excitable, and intermittently depolarised by a large Cl^- current (see Sects. 7.3.8 and 7.4), so the role of TRPM4 might be different in this situation.

7.3.5 Large Conductance Ca^{2+} Activated K^+ (BK_{Ca}) Channels

BK_{Ca} channels are widely expressed in vascular smooth muscle and are characterised by their large conductance of several hundred pS, increased open probability in response to both raised cytosolic Ca^{2+} and membrane depolarisation, and susceptibility to blockade with iberiotoxin, charybdotoxin or penitrem A [36, 37]. The channel pore is formed by four identical α-subunits, encoded by the KCNMA1 (alias Slo1) gene. The α-subunits are inherently Ca^{2+}-sensitive and voltage-dependent, but these characteristics, as well as their gating kinetics and pharmacology, are altered by tissue-specific expression of regulatory β_1, β_2, β_3 and β_4 and γ_1, γ_2, γ_3 and γ_4 subunits [38, 39].

In corpus cavernosum, no ion channel has received as much attention as BK_{Ca} in terms of its functional effects, yet, despite this, it has not been very well characterised in this tissue. Thus, to date, there are no published data regarding co-expression of β and γ-subunits in corpus cavernosum and only a handful of single channel recordings have been

made, so their Ca^{2+}-sensitivity and voltage dependence have not been quantified in most species. However, in several studies, single channel recordings in excised inside-out and cell-attached patches, have demonstrated K^+ channels with a single channel conductance of 221–238 pS in rats and humans [40, 41] and 291 pS in rabbits (Fig. 7.5a) [10]. The larger conductance in rabbit corpus cavernosum myocytes might have been because the recordings were made at 37 °C, rather than at room temperature. Lee and Kang [41] demonstrated concentration-dependent increases in channel activity in an excised inside-out patch as $[Ca^{2+}]_i$ was stepped from 10 nM, through to 500 nM, though the effects were not quantified. In rabbit corpus cavernosum, ramp protocols were used to quantify the effects of changing $[Ca^{2+}]_i$ from 100 nM to 1 μM, which shifted the $V_{1/2}$ of activation from 133 mV to 1 mV [7, 10].

Cells that express abundant BK_{Ca} channels often fire spontaneous transient outward currents (STOCs). These are due to activation of BK_{Ca} channels by localised Ca^{2+} sparks, released from the superficial sarcoplasmic reticulum via ryanodine receptors (RyRs) [43]. In arterial smooth muscle, STOCs are believed to cause vasodilation by hyperpolarising the membrane, thus reducing Ca^{2+} influx through L-type Ca^{2+} channels [43]. STOCs have also been demonstrated in corpus cavernosum myocytes from rats, mice and rabbits (Fig. 7.5c) [10, 40, 42, 44]. It is possible, therefore, that Ca^{2+} sparks and BK_{Ca} channels can mechanistically contribute to relaxation and penile erection. However, differences in function need to be considered before adopting the arterial model to corpus cavernosum. Arteries are electrically quiescent, thus allowing BK_{Ca} channels to finely tune the L-type Ca^{2+} current via small adjustments in membrane potential, but as will be discussed in below, corpus cavernosum generate large spontaneous electrical depolarisations due to activation of Cl^- channels. Thus, the corpus cavernosum is bimodal in function, so such fine adjustments are unlikely to occur, or indeed serve any useful purpose.

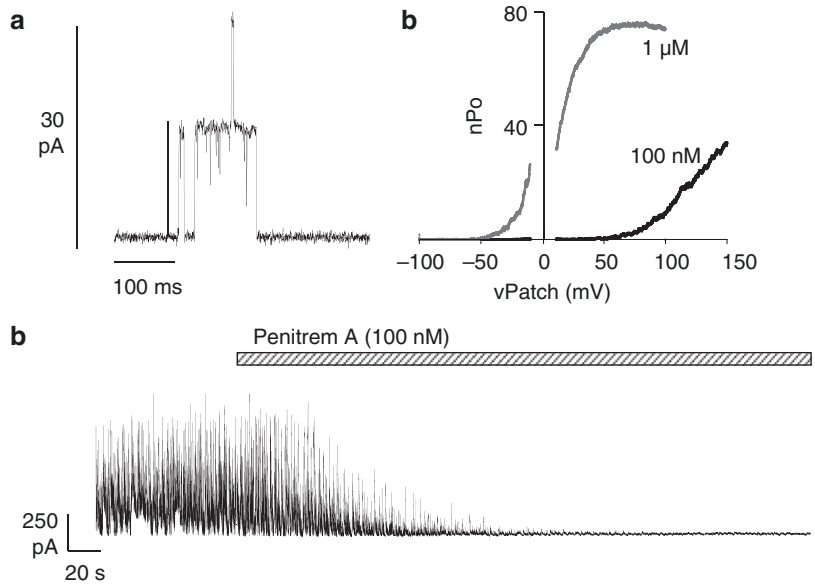

Fig. 7.5 (**a**) Single channel recordings of BK_{Ca} channels in an excised inside-out patch from a rabbit corpus cavernosum myocyte. $[Ca^{2+}]_i$ = 100 nM, V_m = +40 mV. (**b**) Activation curves, derived from ramp protocols, in the presence of 100 nM and 1 μM Ca^{2+} using voltage ramp protocols. (**c**) Example of spontaneous transient outward currents (STOCs) recorded from a rabbit corpus cavernosum myocyte held at 0 mV. (**a**, **b**) Are adapted from Hannigan [7]. (**c**) Is adapted from Craven [42]

7.3.5.1 Effects of NO/cGMP on BK_{Ca} Channels

Although NO has been reported to activate BK_{Ca} channels directly, by *S*-nitrosylation of protein thiol groups [45, 46], in corpus cavernosum NO donors activated BK_{Ca} channels in cell-attached patches, but not in excised inside-out patches, suggesting a requirement for cytosolic mediators, most probably cGMP and cGMP-dependent kinase (PKG, Fig. 7.6a, b) [41, 42]. In rabbit isolated corpus cavernosum myocytes, the NO donor, diethylamine-nitric oxide (DEA-NO) and sildenafil, increased STOCs (Fig. 7.6c, d) [42], as did 8-bromo-cGMP, isoprenaline, forskolin and 8-bromo-cAMP [42, 47]. However, attempts to activate inside-out patches with alpha isoform of cGMP-dependent kinase I (PKG Iα) proved fruitless [42]. This may seem surprising as BK_{Ca} channels have phosphorylation sites for both cGMP-dependent kinase (PKG) and cAMP-dependent kinase (PKA) [48–51]. However, successful activation by PKG and PKA is variable, depending on factors such as cell type and BK_{Ca} α-subunit splice variant [48, 50, 51]. Furthermore, activation of channels by PKG/PKA in excised patches is not always successful in other cells.

In the absence of direct phosphorylation, an indirect way by which PKG and PKA can activate BK_{Ca} channels has been described in arterial smooth muscle. This involves stimulation of the sarcoplasmic reticulum Ca^{2+}/ATPase (SERCA) pump, resulting in increased Ca^{2+} store load and a consequent increase in Ca^{2+} spark frequency [52, 53]. This effect is mediated by disinhibition of the pump by phosphorylation of phospholamban, a SERCA-associated inhibitory protein [54]. In

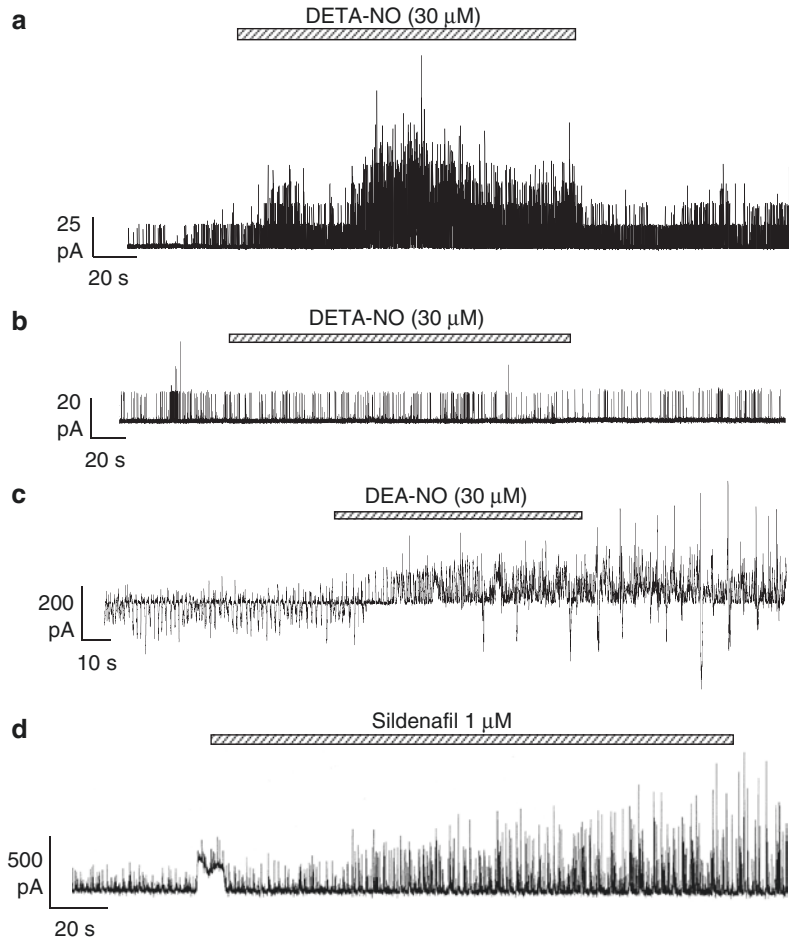

Fig. 7.6 (**a**) DETA-NO activated BK_{Ca} channels in an on-cell patch from a rabbit corpus cavernosum myocyte (holding potential +50 mV). (**b**) DETA-NO did not activate BK_{Ca} channels in an excised, inside-out patch taken from a different cell (Ca^{2+} buffered to 0.5 μM). (**c**) DEA-NO inhibited STICS, but enhanced STOCs in a rabbit corpus cavernosum myocyte, studied with the perforated patch technique (holding potential −30 mV). (**d**) Sildenafil enhanced on STOCs in a rabbit corpus cavernosum myocyte studied with the perforated patch technique (holding potential 0 mV). (**a**–**c**) Are adapted from Craven [42]; (**d**) is adapted from McCloskey [47]

arterial smooth muscle, the stimulatory effect of cAMP on STOCs is completely lost in phospholamban$^{-/-}$ mice [53]. If a similar mechanism was important for mediating the effects of NO in corpus cavernosum, NO-mediated relaxation should be attenuated in phospholamban$^{-/-}$ mice. However, NO is more, rather than less, effective at causing relaxation in these animals [55]. While this does not rule out the possibility that enhanced STOC activity by an increase in Ca^{2+} spark frequency is a factor in NO-mediated relaxation in wild-type mice, it suggests that it is not a requirement.

Another approach to test whether BK_{Ca} channels mediate relaxation in response to NO is to examine responses in mice where the α subunit of the channel has been deleted ($BK_{Ca}^{-/-}$). Several papers where this was done concluded that relaxations in response to both nerve stimulation or sildenafil were impaired [12, 44]. Werner et al. [44] compared the effect of nerve-evoked relaxation in $BK_{Ca}^{-/-}$ mice with their wild-type controls. They concluded that, although the amplitudes of relaxations in response to short (2 s) periods of electrical field stimulation (EFS) were identical in the two animal groups, peak amplitudes in response to 60 s stimulation periods (when the relaxation had longer to develop) were impaired in the $BK_{Ca}^{-/-}$ animals. In a follow up paper [12], it was concluded that sildenafil was less effective at inhibiting phenylephrine-induced contractions in the $BK_{Ca}^{-/-}$ mice. However, it is clear that the effects of sildenafil (10 μM) are, in fact, well preserved in the $BK_{Ca}^{-/-}$ mice, (e.g. Fig. 7.4 of reference [12]), though the authors made the point that greater differences between $BK_{Ca}^{-/-}$ and wild-type mice were seen at lower concentrations of sildenafil. The most obvious difference between the two groups was an increased presence of spontaneous contractions in the $BK_{Ca}^{-/-}$ animals, and these contractions were resistant to the effects of sildenafil. The experience in our own laboratory is that penitrem A, at a concentration ten-fold higher than that required to completely inhibit BK_{Ca} channels, had little or no effect on relaxations evoked by EFS in rabbit corpus cavernosum. Our conclusion, therefore, is that while BK_{Ca} channels are likely to be activated by the NO/cGMP pathway, this mechanism is not essential for the relaxant effect of NO.

7.3.5.2 Targeting BK_{Ca} Channels to Treat Erectile Dysfunction

A number of other studies have also induced relaxation of the corpus cavernosum or penile arteries using BK_{Ca} openers (for detailed discussion see Hannigan et al. 2015) [10]. NS11021, in concentrations of 30 and 100 μM, produced relaxations of 50–90% in human corpus cavernosum strips [56] but, interestingly, lower concentrations (3–30 μM) were effective in human small penile arteries [57]. Other compounds such as 4-aryl-3-(mercapto)quinolin-2-ones and 3-thio-quinolinones were sometimes effective at opening BK_{Ca} channels, but had disappointing relaxant effects on corpus cavernosum, a problem the authors attributed to poor tissue penetration [58, 59]. Recently, we have examined the effects of GoSlo-SR5-130, a novel BK_{Ca} channel opener [60] on BK_{Ca} channels and tension in rabbit corpus cavernosum [10]. This compound activated channels in excised inside-out patches (Fig. 7.7a) and inhibited spontaneous contractions, an effect that was reversed by iberiotoxin (Fig. 7.7b). This study showed that, at least in principle, BK_{Ca} openers could be used as an alternative therapy to PDE5 inhibitors in erectile dysfunction. Of course, many challenges exist before BK_{Ca} channel openers can be used for this purpose, as tissue selectivity is a problem, given that BK_{Ca} channels are widely expressed in vascular and visceral smooth muscle and neurons. Interestingly, in HEK293 cells the efficacy of GoSlo-SR5-130 was greatly enhanced by the presence of β_1 or β_4 regulatory subunits [61], while γ_1 subunits, and to a lesser extent γ_2 and γ_3 subunits, reduced the efficacy of a similar compound, GoSlo-SR-5-44 [39]. However, neither β nor γ subunits affected the efficacy of GoSlo-SR-5-6, another compound in the group [39]. These results raise the hope that tissue expression of accessory subunits will allow selectivity of BK_{Ca} channel openers to be tuned to target specific tissues in future.

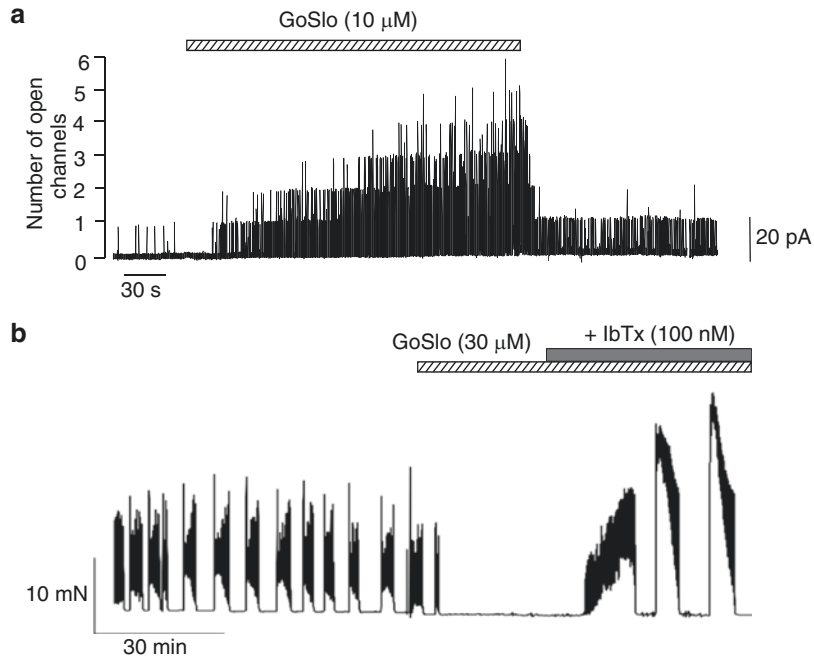

Fig. 7.7 (**a**) Recording from an inside-out patch, taken from a rabbit corpus cavernosum myocyte, showing the effect of GoSlo-SR5-130 (GoSlo) on single BK_{Ca} channel activity. (**b**) Effect of GoSlo-SR5-130 on spontaneous contractions in a rabbit corpus cavernosum strip. The inhibitory effect of GoSlo-SR5-130 was reversed by iberiotoxin (IbTx). Adapted from Hannigan et al. [10]

Gene therapy has also been explored as a future treatment for erectile dysfunction (reviewed in Yoshimura et al. 2010) [62] and the BK_{Ca} channel has been a target in some of these studies [63–67]. The first of these examined the effect of injection of naked hSlo cDNA encoding the pore forming the alpha subunit of the channel in ageing rats, to see if this improved erectile function [63]. The results were quantified with functional measurements which suggested that intracorporal pressures were higher in transfected animals compared to age-marched controls. However, no electrophysiological quantification or comparisons of BK_{Ca} channel activity in the treated and untreated groups were performed. Subsequent studies suggested this technique was effective at restoring erectile function in diabetic rats and atherosclerotic Cynomolgus monkeys [64, 67]. Thus, it has progressed to a Phase I human trial in males suffering from erectile dysfunction [66], where the procedure was deemed safe, but the sample numbers were too small to judge its efficacy. Despite the claimed success of BK_{Ca} gene therapy as a treatment for erectile dysfunction, several issues remain to be addressed for it to gain wide acceptance. There should be a systematic quantification of the expression levels of the transfected BK_{Ca} in the corporal smooth muscle cells in animal models, not only on a molecular level, but also at an electrophysiological level. The expression of β subunits should also be quantified, since these can greatly increase Ca^{2+}-sensitivity. Without this, it seems unlikely that any additionally expressed BK_{Ca} alpha subunits would ever be activated at the physiological membrane potentials and intracellular Ca^{2+} concentrations experienced by smooth muscle cells.

In conclusion, there is still much to be learned regarding regulation of the corpus cavernosum by BK_{Ca} channels in health and disease. While BK_{Ca} channels are highly expressed in corpus cavernosum, the central role ascribed to them in mediating NO-induced relaxation in many previous studies may have overestimated their importance, as it is clear that in laboratory experiments NO/cGMP-mediated relaxations can appear almost normal when they are absent or completely blocked. However, the balance between

erection and flaccidity in vivo is a fine one, and it is likely that BK_{Ca} channels feed into this and contribute to safety factors involved in producing erection. The fact that activating BK_{Ca} channels with drugs can inhibit corpus cavernosum tone demonstrates the principle that upregulation of their function (either pharmacologically, or by gene therapy) could be of potential benefit in treating erectile dysfunction.

7.3.6 K_v2 and Kv7 Channels

When BK_{Ca} channels are blocked or genetically deleted, corpus cavernosum myocytes still display substantial voltage-dependent outward currents [44, 68, 69]. In mice, Werner and colleagues [44] identified two components of a voltage-dependent K^+ current, one which showed little time-dependent inactivation and was TEA sensitive (designated 'delayed rectifier current'), while the other was fast-activating, rapidly inactivating and TEA insensitive (designated 'A-type current'). Individual cells seemed to preferentially express one or other of these two currents, suggesting that at least two phenotypes of smooth muscle cells were present in mouse corpus cavernosum. Malysz et al. [68] also suggested that two phenotypes were present in rabbit corpus cavernosum, but this was based on the presence or absence of a delayed rectifier current that showed very little time- or voltage-dependent inactivation. In a subsequent study Malysz and colleagues [69] amplified mRNA transcripts for Kv2.2 from isolated corpus cavernosum cells and showed that the current was inhibited by 4-aminopyridine and the Kv2-selective blocker Hanatoxin-1, but not the Kv1-selective blocker α-dendrotoxin. Also, cells expressing this current were more hyperpolarised than the other phenotype and, as the current began to activate at −50 mV, it was concluded it contributed to regulation of the resting potential.

Finally, transcripts for Kv7 channels, KCNQ1, KCNQ3, KCNQ4 and KCNQ5, and immunofluorescence for Kv7.4 and Kv7.5 were found in rat corpus cavernosum [70]. Kv7 activators, ML213 and BMS204352, relaxed precontracted corpus cavernosum and a Kv7 channel blocker reduced the effect of sodium nitroprusside (SNP). All of these subunits, except KCNQ1, were also expressed in the penile artery, where the functional effects were greater than in the corpus cavernosum. The expression profile changed in spontaneously hypertensive rats, with downregulation of all but the KCNQ1 subtype (which was upregulated in corpus cavernosum). Both tissues from these animals were also less responsive to sildenafil and SNP. These results suggest that Kv7 channels deserve to be the subject of further study in corpus cavernosum and penile artery.

7.3.7 K_{ATP} Channels

K_{ATP} channels are composed of an inward rectifier, Kir6.1 or Kir6.2, coupled to a sulphonylurea receptor (SUR1, SUR2A or SUR2B), the latter conferring their sensitivity to sulphonylureas, and various channel openers [71]. These channels are expressed in vascular smooth muscle, where they are targets for antihypertensive drugs such as minoxidil, pinacidil, nicorandil and cromakalim, which act as channel openers [72]. The above drugs have also been shown to relax corpus cavernosum in vitro and produced erections when injected in vivo (reviewed in Andersson and Wagner 1995) [2]. Transcripts for Kir6.1, Kir6.2 and SUR2B were found in human corpus cavernosum cultured from explants and single channel studies demonstrated channels with a conductance of 42 pS [73]. These were activated by pinacidil and inhibited by glibenclamide. Whether these channels play a role in corpus cavernosum under normal physiological conditions is unknown. It seems that their expression level is low in cultured human corpus cavernosum cells, as they could only be demonstrated in

10% of excised patches even in the presence of pinacidil [73]. However, the fact that corpus cavernosum myocytes appear to be very well coupled, might still allow K_{ATP} channels to be targeted with channel openers for treatment of erectile dysfunction.

7.3.8 Ca^{2+}-Activated Cl^- Channels

Like many other vascular and non-vascular smooth muscles [74], corpus cavernosum isolated from humans, rats and rabbits express large Ca^{2+}-activated Cl^- currents [19, 40, 75–78]. The physical properties of the channels underlying these currents have not been analysed in corpus cavernosum, but in vascular smooth muscle they have an estimated conductance of <10 pS and are activated by cytosolic Ca^{2+} levels over a range of 180–600 nM [74]. Evidence supporting the presence of these currents in corpus cavernosum was initially based on (i) their susceptibility to block with classical Cl^- channel antagonists such as niflumic acid, anthracene-9-carboxyluc acid (A-9-C), (ii) the fact that they were activated by intracellular Ca^{2+} and (iii) because their reversal potential was affected by the Cl^- gradient in ion substitution experiments [40, 75–77]. In 2008, after many false dawns, the molecular identity of Ca^{2+}-activated Cl^- channels was determined to be TMEM16A, formerly known as ANO1 [79–81]. These channels had a slope conductance of 8.3 pS [81] and showed variable Ca^{2+}-sensitivity depending on their splice variant [82]. Although this identity has not yet been proved in corpus cavernosum, we recently showed that mRNA transcript for TMEM16A was highly expressed in rabbit corpus cavernosum and the current was blocked by TMEM16A inhibitors [78]. However, expression of TMEM16A in corpus cavernosum has yet to be confirmed by Western blotting or immunohistochemistry.

The effect of opening Cl^- channels depends on where E_{Cl} is set, relative to the membrane potential, E_m. Smooth muscle cells accumulate intracellular Cl^- ions by a number of active mechanisms, resulting in a cytosolic Cl^- concentrations ranging between 32 and 44 mM (reviewed by Chipperfield and Harper 2000) [83]. The resultant values for E_{Cl} fall in the range −38 mV to −19 mV and are positive to E_m, so that activating Cl^- channels generates an inward currents due to efflux of Cl^- ions [83]. The resultant depolarisation may excite cells by opening L-type Ca^{2+} channels. Cytosolic concentration of Cl^- has never been measured in corpus cavernosum myocytes and the existence of the Cl^- accumulation mechanisms has not been studied, but there is circumstantial evidence that the Cl^- current is excitatory in these cells.

As in vascular smooth muscle, isolated corpus cavernosum myocytes generate spontaneous transient inward currents (STICs) due to activation of the Cl^- currents by Ca^{2+} spontaneously released from the sarcoplasmic reticulum [40, 75]. In rabbit corpus cavernosum myocytes, the STICS were blocked by the SERCA pump inhibitor, cyclopiazonic acid (CPA), suggesting that this activity depended on Ca^{2+} stored in the sarcoplasmic reticulum (Fig. 7.8a) [75]. STICs were also blocked by 2-APB (Fig. 7.8b) [75], suggesting that the Ca^{2+} release depended on IP_3R, and were reduced by the phospholipase C blocker NCDC [75], suggesting that IP_3 is tonically produced in corpus cavernosum myocytes. When isolated rabbit corpus cavernosum myocytes were held under current clamp, they developed spontaneous transient depolarisations (STDs) that were also inhibited by 2-APB (Fig. 7.8c). We believe that these depolarisations form the basis for generating the electrical activity seen in whole tissue (Sect. 7.4) which, in turn, is responsible for spontaneous tone. Support for this comes from the fact that Cl^- channel blockers reduce both spontaneous and PE-induced tone [78, 84, 85]. The classical blockers, niflumic acid and A-9-C reduced tension in rabbit corpus cavernosum, but only at high concentrations and inhibition was incomplete [84, 85]. This is not surprising, as these agents were rather poor blockers of Cl^- current in rabbit corpus cavernosum myocytes [75]. There are also worries that they are non-specific (see Discussion in Hannigan et al. 2017) [78]. However, a newer more potent drug, $CaCC_{inh}$-A01 (10 μM) was found to block STICs in rabbit corpus

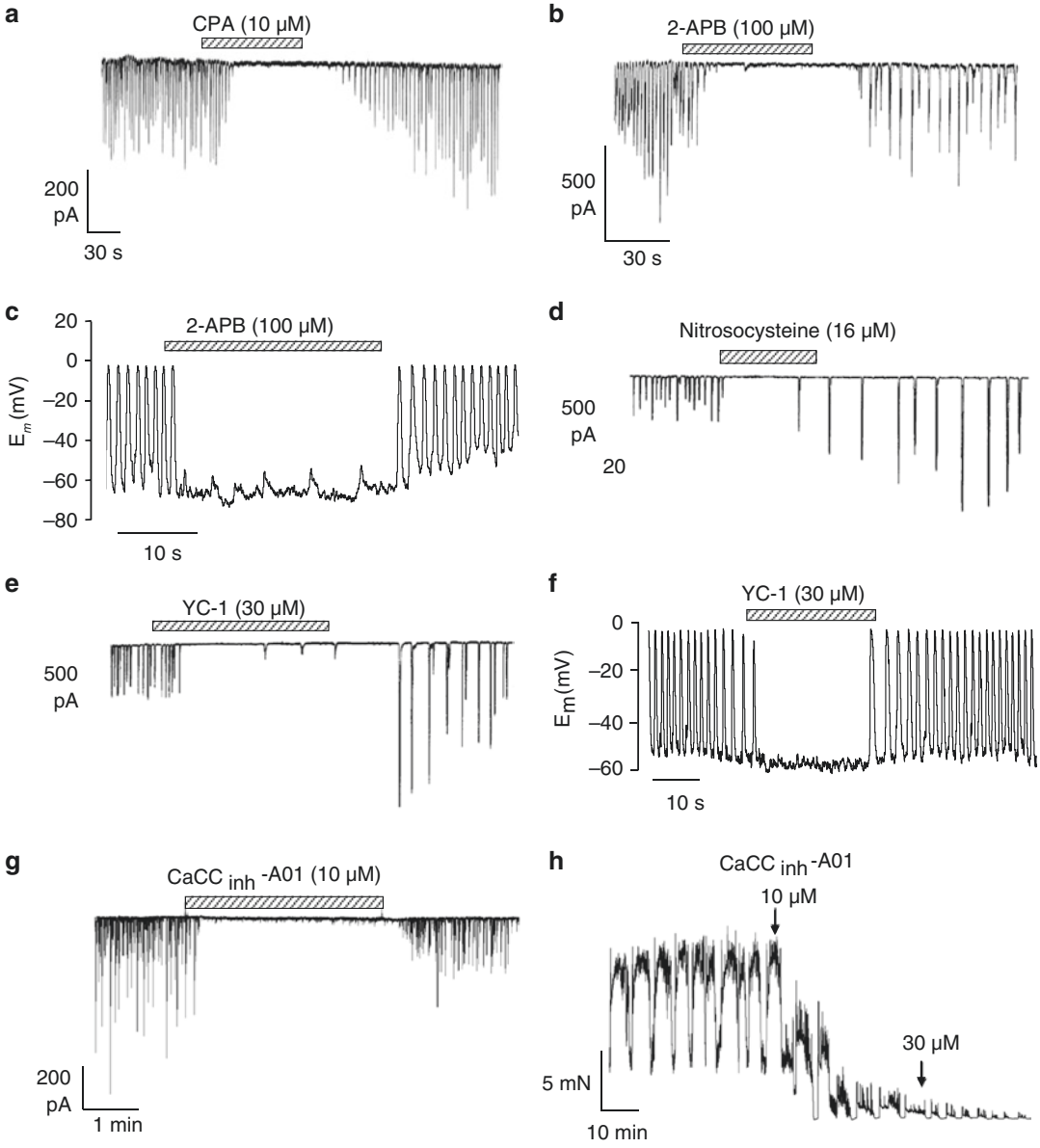

Fig. 7.8 Recordings of spontaneous transient inward currents (STICs) and spontaneous transient depolarisations (STDS) in rabbit corpus cavernosum myocytes. (**a**) The SERCA pump inhibitor, CPA, blocked STICs. (**b**) STICS were also blocked by 2-APB, an inhibitor of IP_3-mediated Ca^{2+} release. (**c**) 2-APB also blocked STDs. (**d**) The NO donor, nitrosocysteine, blocked STICs. (**e**) STICS were also blocked by YC-1, an activator of soluble guanylate cyclase. (**f**) YC-1 also blocked STDs. (**g**) $CaCC_{inh}$-A01, an inhibitor of Ca^{2+}-activated Cl^- channels, blocked STICs. (**h**) $CaCC_{inh}$-A01 also inhibited spontaneous contractions in an isolated rabbit corpus cavernosum strip. (**a**–**e**) Are adapted from Craven et al. [75]; (**c**) is adapted from Doyle et al. [19]; (**f**) is adapted from Doyle [1]; (**g**) and (**h**) are adapted from Hannigan et al. [78]

cavernosum myocytes (Fig. 7.8g), but had no effect on L-type Ca^{2+} current at this concentration [78]. It also concentration-dependently reduces both spontaneous (Fig. 7.8h) and phenylephrine-induced tension [78], at concentrations below the level where it blocks L-type Ca^{2+} current.

STICs in rabbit corpus cavernosum myocytes are inhibited by the NO/cGMP pathway [75] and

also by 8-bromo-cAMP [47]. Craven and colleagues [75] showed that 8-bromo-cGMP, the NO donor nitrosocysteine (Fig. 7.8d) and the soluble guanylate cyclase activator YC-1 (Fig. 7.8e) either abolished STICs or inhibited their frequency. However, on washout of the drugs, or sometimes even before washout, large low frequency STICs develop, which we have assumed to be due to Ca^{2+} overload of the sarcoplasmic reticulum. As expected from its effects on STICs, YC-1 inhibits STDs (Fig. 7.8f), suggesting that the NO/cGMP pathway may inhibit spontaneous corpus cavernosum tone by inhibiting STDs and their underlying STICs.

In contrast to the effect of the NO/cGMP pathway, activation of α_1-adrenoceptors evoked Cl^- currents and increased STIC frequency in rabbit corpus cavernosum myocytes [19]. These effects were blocked by 2-APB, suggesting they involved activation of IP_3 receptors. YC-1 almost completely blocked Cl^- currents evoked by noradrenaline but not when they were induced by caffeine, suggesting that the NO/cGMP pathway potently and specifically inhibits IP_3-mediated Ca^{2+} release [75].

7.4 Electrical Activity and Intracellular Ca^{2+} Signals in Whole Tissue

A few intracellular microelectrode and sucrose-gap recordings have been made from tissues related to corpus cavernosum such as bovine retractor penis muscle, dog corpus spongiosum (see review by Andersson and Wagner 1995) [2] and rat penile bulb [86]. However, we are only aware of one paper where there are published records of intracellular microelectrode recordings from corpus cavernosum, made by Hashitani and colleagues [9]. These were obtained from rabbit corpus cavernosum and examples from the study are presented in Fig. 7.9. Two types of electrical activity were described, namely bursts of spontaneous depolarisations consisting of an initial spike, followed by oscillations (Fig. 7.9a). It is noteworthy that the spontaneous electrical activity in Fig. 7.9a is similar to the spontaneous contractile activity in Fig. 7.2a. More commonly, continuous bursting depolarisations were recorded (Fig. 7.9b). The mean frequency and amplitude of the bursts were 22.6 per minute and 27.0 mV, respectively, with the resting potential (defined as the most negative potential between the bursts) averaging −46 mV. The spontaneous depolarisations were abolished by nifedipine or nicardipine, CPA and niflumic acid, suggesting a role for L-type Ca^{2+} channels, the sarcoplasmic reticulum and Ca^{2+}-activated Cl^- channels. Interestingly, niflumic acid also hyperpolarised the tissue by about 5 mV, but the L-type Ca^{2+} blockers did not. The NO donor, SIN-1 also hyperpolarised the tissue and abolished the spontaneous depolarisations and, significantly, the degree of hyperpolarisation was unaffected by iberiotoxin, suggesting little requirement for BK_{Ca} channels in mediating this effect. The electrical and mechanical events were also blocked by NS-398, a specific COX-2 antagonist, suggesting the prostaglandins had a role in facilitating the development of spontaneous activity.

We also present another previously unpublished intracellular microelectrode recording from rabbit corpus cavernosum, made in our laboratory by Professor Sean Ward (Fig. 7.9c). This shows more discrete depolarisations than described in the Hashitani study [9] and the membrane potential is more negative at −60 mV. Interestingly, they have a similar time course to the phasic contractions shown in Fig. 7.2b. Close inspection of the record in Fig. 7.9c reveals that the depolarisations are sometimes preceded by distinct bumps (marked by arrows). These resemble the spontaneous transient depolarisations seen in portal vein and sheep urethra and were attributed to activation of Cl^- current by release of stored Ca^{2+} [87, 88]. Despite the differences in this recording and those presented by Hashitani et al. [9], the clear similarity is that the corpus cavernosum generates large spontaneous depolarisations capable of activating L-type Ca^{2+} channels, and it is likely that the depolarisations are initiated by Ca^{2+}-release from the sarcoplasmic reticulum which, in turn, activates the Cl^- channels.

Hashitani and colleagues [9] also measured intracellular Ca^{2+} using fura-2 and found spon-

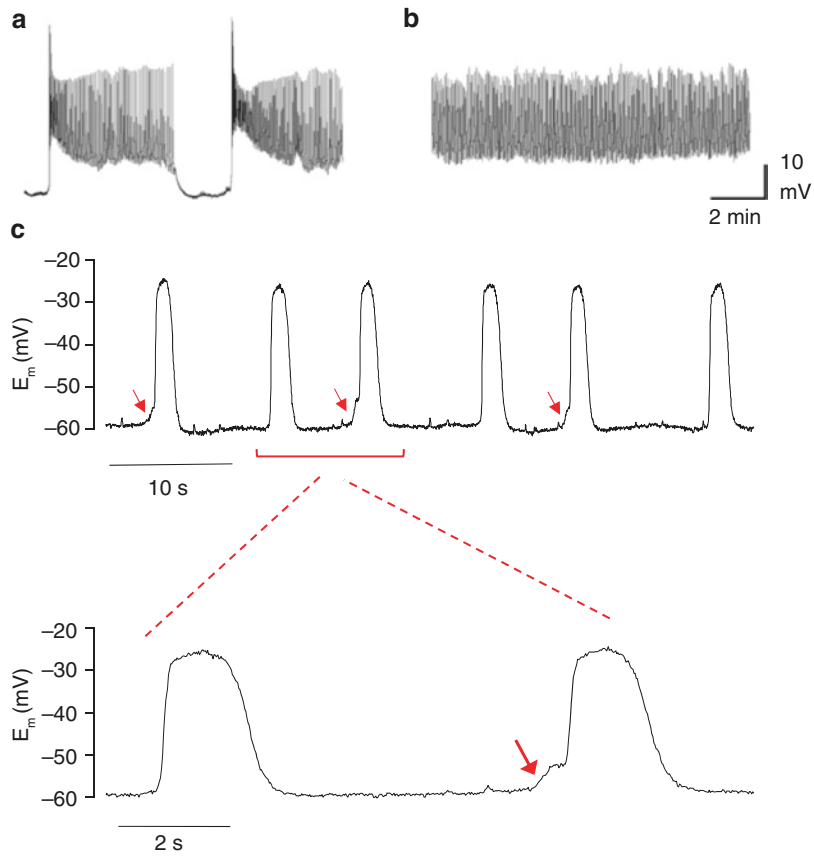

Fig. 7.9 Intracellular microelectrode recordings from rabbit corpus cavernosum. (**a**) Recording showing bursts of oscillations in membrane potential. Each burst is preceded by a rapid spike. (**b**) Recording showing continuous oscillations in membrane potential. (**c**) Previously unpublished recording by Prof. Sean Ward in our laboratory, showing that spontaneous depolarisations were sometimes preceded by discernible 'bump' (arrows). The lower record shows the two events marked in the upper record at a faster time scale. (**a**, **b**) Are adapted from Hashitani et al. [9]

taneous Ca^{2+} transients with patterns very similar to the depolarisations and phasic contractions, i.e. they consisted of a rapid rising phase followed by oscillations. Whole tissue Ca^{2+} measurements were also made by us from tissue slices of rabbit corpus cavernosum loaded with fluo-4AM and studied with a Nipkow spinning disk laser confocal system coupled to an EMCCD camera [77]. This allowed direct visualisation of the Ca^{2+} signals in the tissue. Of eight slices studied, all developed spontaneous phasic Ca^{2+} events associated with phasic contraction of the smooth muscle trabeculae. The spread of the events varied from a few muscle bundles to entire trabeculae, and even across all of the trabeculae within the field of view, to the extent that they were associated with narrowing of the sinuses. The spread was too fast to measure at the image acquisition rate of 5 frames per second; however, it is clear from these observations that the corpus cavernosum smooth muscle cells are indeed very well coupled.

7.5 Intracellular Ca^{2+} Signals in Isolated Corpus Cavernosum Myocytes

Ca^{2+} transients were measured in rat and human freshly dispersed corpus cavernosum myocytes by Sims and colleagues using fura-2 indicator [89]. They showed that NO donors and cGMP analogues, when combined with sildenafil reduced PE-induced Ca^{2+} transients by about 50% but had no effect basal $[Ca^{2+}]$. Surprisingly, neither NO donors nor cGMP analogues had any significant effect on PE transients if used without sildenafil, and the authors suggested that this might be because degradation of

cGMP by PDE5 was accelerated in isolated cells.

Later, the same group imaged rat corpus cavernosum myocytes loaded with fluo-4AM and recorded localised Ca^{2+} sparks [76]. Sparks are generally thought to be due to localised release of Ca^{2+} from the sarcoplasmic reticulum via a coordinated cluster of ryanodine receptors [90]. Larger sparks, involving crosstalk between clusters of RyR and IP_3R have been observed in rabbit portal vein cells and some visceral smooth muscles [91]. The larger sparks in portal vein were reduced by inhibitors of IP_3-induced Ca^{2+} release (2-APB and xestospongin C) or a PLC inhibitor (U-73122), suggesting that they depended on tonic production of IP_3. In the rat corpus cavernosum, the sparks were similar in amplitude and frequency (per release site) to many other smooth muscles [76]. However, most interestingly, their spatial spread and duration were three to five times greater than in arterial smooth muscle (for references see [76]). Also, the number of spark release sites was high compared to many other smooth muscles. The sparks were reduced in amplitude by 2-APB, leading the authors to speculate that they might have involved both IP_3-R and RyR, as in portal vein, but on balance they rejected this idea [76]. In elegant experiments, simultaneous Ca^{2+} imaging and patch clamp recordings revealed that the sparks were able to evoke both STOCs and STICs as well as mixed events involving both currents where the STOC just preceded the STIC (designated 'STOICs'), possibly because the RyRs are located closer to the BK_{Ca} channels than the Ca^{2+}-activated Cl^- channels. As the membrane potential was shifted from −60 mV to −30 mV, the predominance changed from STICs to STOCs, presumably due to the much greater inherent voltage-sensitivity of BK_{Ca} channels compared to Ca^{2+}-activated Cl^- channels. More widespread Ca^{2+} events, such as Ca^{2+} waves, were not observed in rat corpus cavernosum [76].

In contrast, Ca^{2+} waves are a prominent feature of isolated rabbit corpus cavernosum myocytes loaded with fluo-4AM and imaged with a Nipkow spinning disk laser confocal/EMCCD system (see Figs. 7.10, 7.11, and 7.12) [15, 19, 77, 78]. In 57 cells, these propagated without decrement for distances of 20–100 μm at a mean velocity of ~65 μm per second, a mean frequency of ~13 per minute and mean amplitude of 1.77 $\Delta F/F_0$ [77]. In simultaneous patch clamp and Ca^{2+} imaging experiments the Ca^{2+} waves were shown to activate STICs, as might be expected from such widespread Ca^{2+} events (Fig. 7.10) [77]. We have also observed Ca^{2+} waves with very similar characteristics in isolated mouse corpus cavernosum myocytes (Figs. 7.11a, b and 7.12c). In both species, they were abolished by 2-APB, CPA, tetracaine and Ca^{2+}-free external solution, suggesting a role for both Ca^{2+} stores and Ca^{2+} influx in their generation [15, 77]. Nifedipine also either blocked or reduced the frequency of the waves [15]. The effect of 2-APB on Ca^{2+} waves in a mouse corpus cavernosum myocyte is shown in a pseudo-linescan derived from a movie in Fig. 7.11a (see reference [77] for method). 2-APB can be seen to abolish the waves, while leaving more localised events. This is consistent with the idea that the waves depend on IP_3Rs for their propagation, but that their initiation is via another mechanism. We propose that, similar to urethral interstitial cells (see Chap. 6) and rabbit portal vein [91], Ca^{2+} waves are initiated by typical Ca^{2+} sparks arising from RyRs, but require IP_3Rs to propagate.

The initiation of Ca^{2+} waves can be observed in the linescan of a movie acquired at 30 frames per second from a mouse corpus cavernosum in Fig. 7.11bi. In this, it is evident that are some small spark-like events that occur at the same initiation site as most of the waves. The expanded record in Fig. 7.11bii shows this more clearly, where a single localised event is followed 3 s later by a similar event that, this time, propagates as a wave along the cell in both directions. Thus, it appears as if the wave is initiated by a spark. Although we have not yet acquired similar records at fast frame rates whilst also patch clamping the cells, the patch clamp record of STICs and STOCs in Fig. 7.11c, gives some idea of what to expect. This recording was made at −30 mV (with E_{Cl} set to 0 mV and E_K = −85 mV) in order to simultaneously record STICs and STOCs. 2-APB abolished the STICs, while leav-

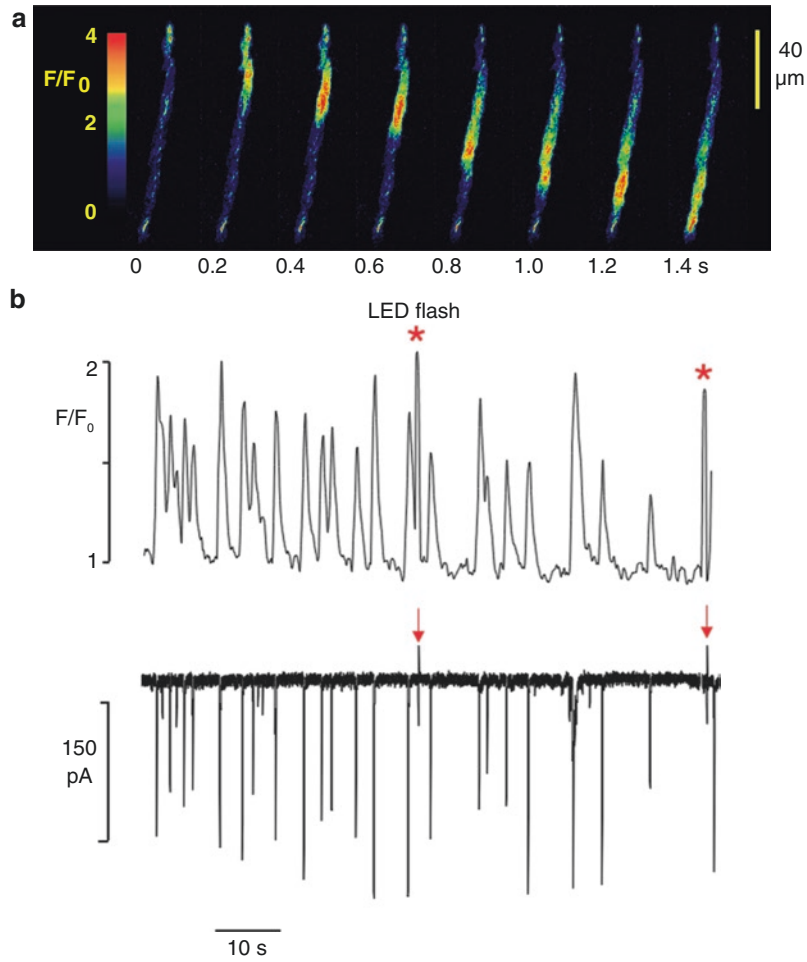

Fig. 7.10 Simultaneous recording of propagating spontaneous Ca^{2+} waves and STICs in an isolated rabbit corpus cavernosum myocyte. (**a**) Montage of a Ca^{2+} wave taken from a movie stack. Successive frames are shown at a recording rate of 5 frames per second. Time at which each frame was acquired is shown in seconds (s). (**b**) Dual patch clamp/confocal recording from a single corpus cavernosum smooth muscle cell showing a plot of the intensity profile of Ca^{2+} waves (upper record) with associated STICs (lower record; cell held at −60 mV). Asterisks mark an LED flash, which allowed alignment of the Ca^{2+} and patch clamp records while arrows show the artefact produced by a corresponding triggering pulse on the patch clamp record. Adapted from Sergeant et al. [77]

ing STOCs intact, suggesting that the smaller events that persist in the presence of 2-APB are sufficient to activate STOCs, but that large STICs (Figs. 7.8 and 7.10), require Ca^{2+} waves. This can be explained by the fact that clusters of RyRs are believed to co-localise with clusters of BK_{Ca} channels [90], so that a spark activates a STOC. However, even if there was similar co-localisation of RyR and Cl^- channels, to get a similar sized current, there would need to be 36-fold more Cl^- channels compared to a BK_{Ca} channel, given the 8:291 ratio of their conductances. (As an aside, the fact that 2-APB does not reduce STOCs to any great extent suggests that it has little effect on sarcoplasmic reticulum filling in these cells. This point is also supported by the fact that caffeine-induced Ca^{2+}-transients were not diminished in 2-APB [19]).

The regulation of the Ca^{2+} waves by NO/cGMP and α-adrenergic stimulation has also been studied [19]. Figure 7.12a, b shows that NO and 8-bromo-cGMP abolish waves and reduce basal Ca^{2+} [77]. Also, sildenafil had a similar effect, suggesting that there is a basal level of production of cGMP in the absence of stimulation [77]. It is evident from the records in Fig. 7.12a, b that the Ca^{2+} waves increase in intensity after washout of the drugs and sometimes, even in the presence of the drug (Fig. 7.12b), albeit at a lower frequency. Interestingly, these 'breakthrough' events are not inhibited by 2-APB but are abolished by tetracaine [47]. Our interpretation of this is that the breakthrough events are due to discharging of an overloaded sarcoplasmic reticulum via RyR, as a result of excessive SERCA pump stimulation and IP_3R inhibition.

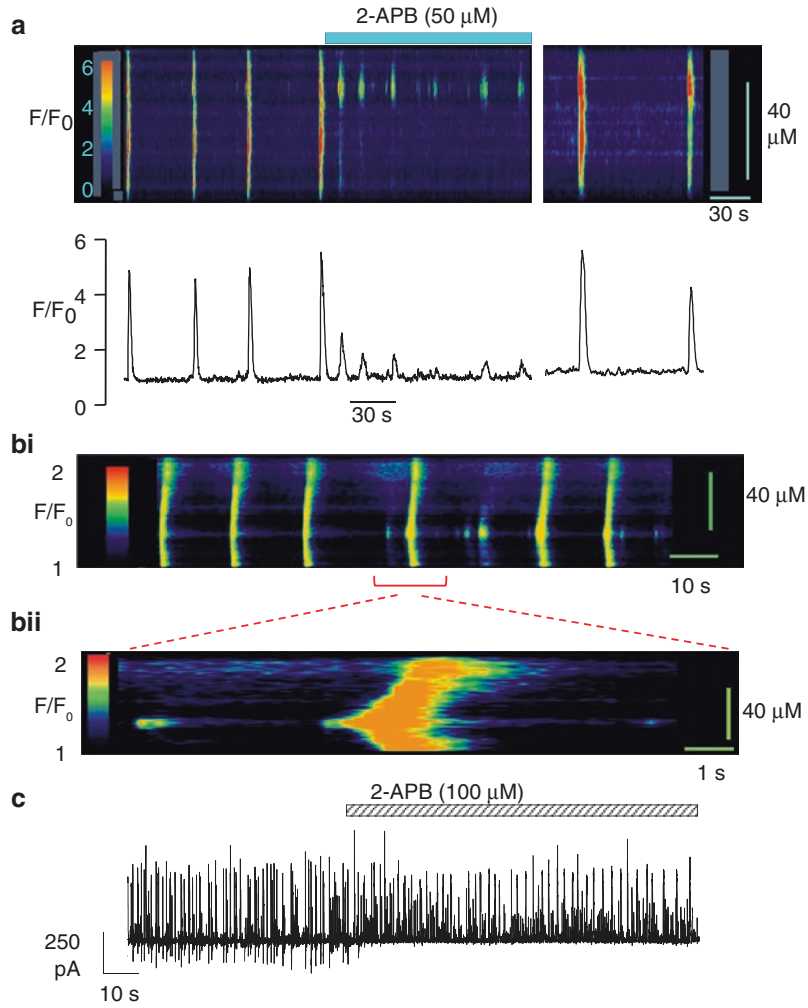

Fig. 7.11 (**a**) Spontaneous Ca^{2+} waves in an isolated mouse corpus cavernosum myocyte. Upper record is a pseudo-linescan derived from a movie stack. Lower record is a profile plot of fluorescence intensity, derived from the pseudo-linescan. 2-APB inhibited the waves but localised Ca^{2+} events persisted. (**bi**) Spontaneous Ca^{2+} waves in an isolated mouse corpus cavernosum myocyte showing that they are initiated by a localised Ca^{2+} event. (**bii**) Expanded record of the events delineated by the red bracket in (**bi**). (**c**) Recordings of STICs and STOCs in a rabbit corpus cavernosum myocyte held at −30 mV. 2-APB blocked the STICs but not the STOCs. (**a**, **b**) Are previously unpublished recordings; (**c**) is adapted from Craven [42]

Predictably, PE has the opposite effect to NO, in that it increases the frequency of Ca^{2+} waves (Fig. 7.12c). Figure 7.12c also shows that this effect is antagonised by NO. The increased frequency in response to PE is also reduced by $CaCC_{inh}$-A01 (Fig. 7.12d), suggesting that the sustained PE response is facilitated by depolarisation and influx via L-type Ca^{2+} channels.

The question is, why have Ca^{2+} waves been observed in rabbit and mouse corpus cavernosum (Figs. 7.10, 7.11, and 7.12), but not in rat [76]? This might be due to species differences, but there were several important differences in the methodology between these studies. Firstly, the rat experiments were conducted at room temperature, while the rabbit and mouse experiments were performed at 35–37 °C. This is likely to have had a significant effect on the kinetics of the IP_3Rs and RyRs and also to slow the accumulation of Ca^{2+} in the SR due to the action of the SERCA pump. Secondly, the rat cells were incubated in 5 μM fluo-4AM for 40 min, while in the rabbit and mouse experiments the sensitivity of the EMCCD camera permitted a much lower loading protocol to be used (0.4 μM fluo-4 AM for 6–8 min). It is possible, therefore, that Ca^{2+} buffering by fluo-4, inhibited the waves in the rat experiments. In support, EGTA-AM (3 μM) uncoupled the Ca^{2+} release sites and abolished waves leaving only sparks, in rabbit urethral interstitial cells [92].

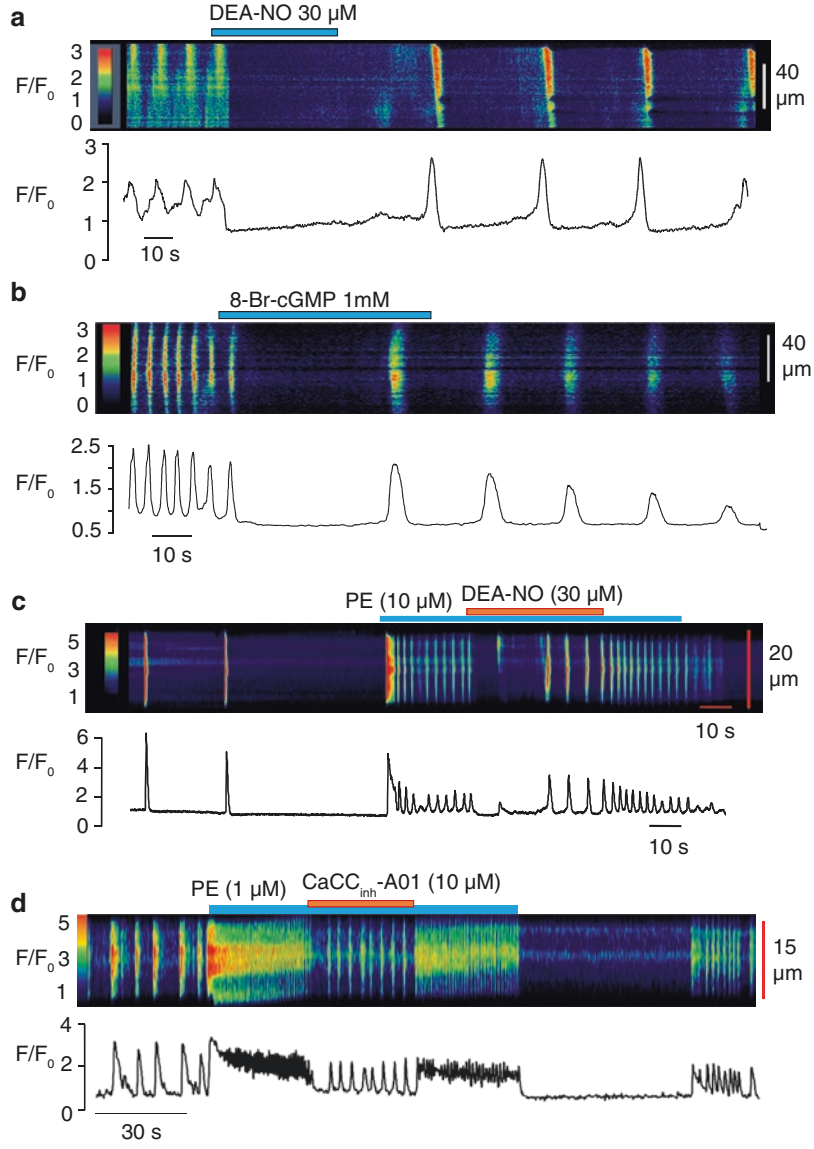

Fig. 7.12 DEA-NO (**a**) and 8-Br-cGMP (**b**) inhibited the Ca^{2+} waves and reduced basal Ca^{2+} in rabbit corpus cavernosum. Note also the large 'breakthrough' event in the presence of 8-Br-cGMP. (**c**) Phenylephrine (PE) increased frequency of Ca^{2+} waves in a mouse corpus cavernosum myocyte. This effect was inhibited by DEA-NO. (**d**) PE also increased Ca^{2+} wave frequency in a rabbit corpus cavernosum myocyte. This effect was reduced by $CaCC_{inh}$-A01. (**a**, **b**) Are adapted from Sergeant et al. [77]; (**c**) is a previously unpublished record; (**d**) is adapted from Hannigan et al. [78]

7.6 Conclusion: Overview of Regulation of Corpus Cavernosum Tone

There are many factors, which are important in regulation of tone that have not been considered in this review. Most notable, is regulation of Ca^{2+}-sensitivity of the contractile proteins by Rho kinase [93]. Another potentially important omission is a putative role for interstitial cells (IC). Hashitani reported cells in rabbit corpus cavernosum, which were Kit, vimentin and COX-2 positive [94]. We have also isolated vimentin positive cells from the rabbit corpus cavernosum that closely resemble those which we have described in the urethra (see Chap. 6). These cells display many of the features described for myocytes described in this review, including Ca^{2+} waves, L-type Ca^{2+} current, Ca^{2+}-activated Cl^- current and BK_{Ca} current (unpublished data). However, in the corpus cavernosum, unlike the rabbit urethra, the myocytes possess the apparatus for the Cl^- current-driven pacemaker to work, so it is not obvious what role corpus cavernosum IC might

play, though they ought to be the subject of further study.

In summary, we propose a basic model in corpus cavernosum myocytes whereby spontaneous tone is generated by Ca^{2+} influx, via L-type Ca^{2+} channels, activated as a result of spontaneous depolarisations. The depolarisations are initiated by Ca^{2+}-activated Cl^- channels (most probably TMEM16A), which are mainly activated by spontaneous Ca^{2+} waves that propagate from an initiating event, most probably a Ca^{2+} spark released via RyRs, but IP_3Rs may also be involved. However, the Ca^{2+} waves need IP_3Rs to propagate. The Ca^{2+} waves not only lead to activation of L-type Ca^{2+} currents and Ca^{2+} influx, but are also facilitated by this mechanism, as suggested by the fact that they are reduced by nifedipine and $CaCC_{inh}$-A01. Both NO and noradrenaline modulate this basic pacemaker mechanism. It is upregulated upon α-adrenoceptor stimulation, via stimulation of PLC and IP_3 generation, and downregulated by NO, mostly by inhibition of IP_3-mediated Ca^{2+} release. This inhibition may be direct, by inhibiting Ca^{2+} release from IP_3Rs [95, 96] or indirect by inhibiting IP_3 synthesis [97]. It is possible that components of this pacemaker mechanism, such as the Ca^{2+}-activated Cl^- channels, may provide new targets for drug therapy to treat cases of erectile dysfunction that are resistant to PDE5 inhibitors. However, the challenge will be to specifically target the corpus cavernosum without producing unwanted effects on other tissues such as the gut, urethra, or blood vessels.

Acknowledgments The authors are grateful for grant support from the Wellcome Trust (064212), NIH (RO1 DK68565), Health Research Board (PD/2005/4 and RP/2006/127), Enterprise Ireland (ARE20080001 and CE20080020) Diabetes UK, Science Foundation Ireland (BIMF377) and IOTI. We wish also to thank Ms Billie McIlveen for technical support.

References

1. Doyle C. Characterisation of interstitial cells of cajal and smooth muscle cells in the corpus cavernosum. PhD thesis, Dundalk Institute of Technology, Dundalk, Co Louth; 2011.
2. Andersson KE, Wagner G. Physiology of penile erection. Physiol Rev. 1995;75:191–236.
3. Andersson KE. Pharmacology of penile erection. Pharmacol Rev. 2001;53:417–50.
4. Shamloul R, Ghanem H. Erectile dysfunction. Lancet. 2013;381:153–65.
5. Hawksworth DJ, Burnett AL. Pharmacotherapeutic management of erectile dysfunction. Clin Pharmacol Ther. 2015;98(6):602–10.
6. Campos de Carvalho AC, Roy C, Moreno AP, Melman A, Hertzberg EL, Christ GJ, Spray DC. Gap junctions formed of connexin43 are found between smooth muscle cells of human corpus cavernosum. J Urol. 1993;149(6):1568–75.
7. Hannigan K. Regulation of corpus cavernosum activity by ion channel modulators. PhD Thesis, Dundalk Institute of Technology, Dundalk, Co Louth; 2016.
8. Moreno AP, Campos de Carvalho AC, Christ G, Melman A, Spray DC. Gap junctions between human corpus cavernosum smooth muscle cells: gating properties and unitary conductance. Am J Phys. 1993;264: C80–92.
9. Hashitani H, Yanai Y, Shirasawa N, Soji T, Tomita A, Kohri K, Suzuki H. Interaction between spontaneous and neurally mediated regulation of smooth muscle tone in the rabbit corpus cavernosum. J Physiol. 2005;569:723–35.
10. Hannigan KI, Large RJ, Bradley E, Hollywood MA, Sergeant GP, McHale NG, Thornbury KD. Effect of a novel BK_{Ca} opener on BK_{Ca} currents and contractility of the rabbit corpus cavernosum. Am J Phys Cell Physiol. 2016;310:C284–92.
11. Mizusawa H, Hedlund P, Håkansson A, Alm P, Andersson KE. Morphological and functional in vitro and in vivo characterization of the mouse corpus cavernosum. Br J Pharmacol. 2001;132:1333–41.
12. Werner ME, Meredith AL, Aldrich RW, Nelson MT. Hypercontractility and impaired sildenafil relaxations in the BK_{Ca} deletion model of erectile dysfunction. Am J Phys Regul Integr Comp Phys. 2008;295:181–8.
13. Fovaeus M, Andersson K-E, Hedlund H. Effects of some calcium channel blockers on isolated human penile erectile tissue. J Urol. 1987;138:1267–72.
14. Hoppner CK, Stief CG, Jonas U, Mandrek K, Noack T, Golenhofen K. Electrical and chemical control of smooth muscle activity of rabbit corpus cavernosum in vitro. Urology. 1996;48(5):12–5 18.
15. McCloskey C, Cagney V, Large R, Hollywood M, Sergeant G, McHale N, Thornbury K. Voltage-dependent Ca^{2+} currents contribute to spontaneous Ca^{2+} waves in rabbit corpus cavernosum myocytes. J Sex Med. 2009;6:3019–31.
16. Imaizumi Y, Muraki K, Takeda M, Watanabe M. Measurement and simulation of noninactivating Ca current in smooth muscle cells. Am J Phys. 1989;256:C880–5.
17. Smirnov SV, Aaronson PI. Ca^{2+} currents in single myocytes from human mesenteric arteries: evidence for a physiological role of L-type channels. J Physiol. 1992;457:455–75.

18. Christ GJ, Hodges S. Molecular mechanisms of detrusor and corporal myocyte contraction: identifying targets for pharmacotherapy of bladder and erectile dysfunction. Br J Pharmacol. 2006;147(Suppl 2):S41–55.
19. Doyle C, Sergeant GP, Hollywood MA, McHale NG, Thornbury KD. Effects of phenylephrine on spontaneous activity and L-type Ca^{2+} current in isolated corpus cavernosum myocytes. J Sex Med. 2012;9:2795–805.
20. Keef KD, Hume JR, Zhong J. Regulation of cardiac and smooth muscle Ca^{2+} channels (CaV1.2a,b) by protein kinases. Am J Phys. 2001;281:C1743–56.
21. Perez-Reyes E. Molecular physiology of low voltage-activated T-type calcium channels. Physiol Rev. 2003;83:117–61.
22. Zeng X, Keyser B, Li M, Sikka SC. T-type (alpha1G) low voltage-activated calcium channel interactions with nitric oxide-cyclic guanosine monophosphate pathway and regulation of calcium homeostasis in human cavernosal cells. J Sex Med. 2005;2:620–30.
23. House SJ, Potier M, Bisaillon J, Singer HA, Trebak M. The non-excitable smooth muscle: calcium signaling and phenotypic switching during vascular disease. Pflugers Arch. 2008;456:769–85.
24. North RA. Molecular physiology of P2X receptors. Physiol Rev. 2002;82:1013–67.
25. Sneddon P, Burnstock G. Inhibition of excitatory junction potentials in guinea-pig vas deferens by alpha, beta-methylene- ATP: further evidence for ATP and noradrenaline as cotransmitters. Eur J Pharmacol. 1984;100:85–90.
26. Sneddon P, Burnstock G. ATP as a co-transmitter in rat tail artery. Eur J Pharmacol. 1984;106:149–52.
27. Phatarpekar PV, Wen J, Xia Y. Role of adenosine signaling in penile erection and erectile disorders. J Sex Med. 2010;7:3553–64.
28. Staerman F, Shalev M, Legrand A, Lobel B, Saïag B. P2Y and P2X purinoceptors are respectively implicated in endothelium-dependent relaxation and endothelium independent contraction in human corpus cavernosum. Adv Exp Med Biol. 2000;486:189–95.
29. Wu HY, Broderick GA, Suh JK, Hypolite JA, Levin RM. Effects of purines on rabbit corpus cavernosum contractile activity. Int J Impot Res. 1993;5:161–7.
30. Doyle C, Sergeant GP, Hollywood MA, McHale NG, Thornbury KD. ATP evokes inward currents in corpus cavernosum myocytes. J Sex Med. 2014;11(1):64–74.
31. Lee HY, Bardini M, Burnstock G. P2X receptor immunoreactivity in the male genital organs of the rat. Cell Tissue Res. 2000;300:321–30.
32. Suadicani SO, Urban-Maldonado M, Tar MT, Melman A, Spray DC. Effects of ageing and streptozotocin-induced diabetes on connexin43 and P2 purinoceptor expression in the rat corpora cavernosa and urinary bladder. BJU Int. 2009;103:1686–93.
33. Gur S, Kadowitz PJ, Abdel-Mageed AB, Kendirci M, Sikka SC, Burnstock G, Hellstrom WJ. Management of erectile function by penile purinergic p2 receptors in the diabetic rat. J Urol. 2009;181:2375–82.
34. Yue Z, Xie J, Yu AS, Stock J, Du J, Yue L. Role of TRP channels in the cardiovascular system. Am J Physiol Heart Circ Physiol. 2015;308:H157–82.
35. Earley S. TRPM4 channels in smooth muscle function. Pflugers Arch. 2013;465:1223–31.
36. Latorre R, Castillo K, Carrasquel-Ursulaez W, Sepulveda RV, Gonzalez-Nilo F, Gonzalez C, Alvarez O. Molecular determinants of BK channel functional diversity and functioning. Physiol Rev. 2017;97:39–87.
37. Knaus HG, McManus OB, Lee SH, Schmalhofer WA, Garcia-Calvo M, Helms LM, Sanchez M, Giangiacomo K, Reuben JP, Smith AB 3rd, et al. Tremorgenic indole alkaloids potently inhibit smooth muscle high-conductance calcium-activated potassium channels. Biochemistry. 1994;3319:5819–28.
38. Yan J, Aldrich RW. LRRC26 auxiliary protein allows BK channel activation at resting voltage without calcium. Nature. 2010;466:513–6.
39. Kshatri AS, Li Q, Yan J, Large RJ, Sergeant GP, McHale NG, Thornbury KD, Hollywood MA. Differential efficacy of GoSlo-SR compounds on BKα and BKαγ(1-4) channels. Channels (Austin). 2017;11:66–78.
40. Karkanis T, DeYoung L, Brock GB, Sims SM. Ca2+-activated Cl− channels in corpus cavernosum smooth muscle: a novel mechanism for control of penile erection. J Appl Physiol. 2003;94(1):301–13.
41. Lee SW, Kang TM. Effects of nitric oxide on the Ca2+-activated potassium channels in smooth muscle cells of the human corpus cavernosum. Urol Res. 2001;29:359–65.
42. Craven M. Regulation of rabbit corpus cavernosum smooth muscle. PhD Thesis, Queen's University of Belfast, Belfast; 2006.
43. Nelson MT, Cheng H, Rubart M, Santana LF, Bonev AD, Knot HJ, Lederer WJ. Relaxation of arterial smooth muscle by calcium sparks. Science. 1995;270:633–7.
44. Werner ME, Zvara P, Meredith AL, Aldrich RW, Nelson MT. Erectile dysfunction in mice lacking the large-conductance calcium-activated potassium (BK) channel. J Physiol. 2005;567:545–56.
45. Bolotina VM, Najibi S, Palacino JJ, Pagano PJ, Cohen RA. Nitric oxide directly activates calcium-dependent potassium channels in vascular smooth muscle. Nature. 1994;368(6474):850–3.
46. Lang RJ, Harvey JR, McPhee GJ, Klemm MF. Nitric oxide and thiol reagent modulation of Ca^{2+}-activated K^+ (BK_{Ca}) channels in myocytes of the guinea-pig taenia caeci. J Physiol. 2000;525:363–76.
47. McCloskey C. Electrical activity in isolated cells of rabbit corpus cavernosum. PhD Thesis, Queen's University of Belfast, Belfast; 2007.
48. Alioua A, Tanaka Y, Wallner M, Hofmann F, Ruth P, Meera P, Toro L. The large conductance, voltage-dependent, and calcium-sensitive K+ channel, Hslo, is a target of cGMP-dependent protein kinase phosphorylation in vivo. J Biol Chem. 1998;273:32950–6.

49. Fukao M, Mason HS, Britton FC, Kenyon JL, Horowitz B, Keef KD. Cyclic GMP-dependent protein kinase activates cloned BKCa channels expressed in mammalian cells by direct phosphorylation at serine 1072. J Biol Chem. 1999;274:10927–35.
50. Zhou X-B, Schlossmann J, Hofmann F, Ruth P, Korth M. Regulation of stably expressed and native BK channels from human myometrium by cGMP- and cAMP-dependent protein kinase. Pflugers Arch. 1998;436:725–34.
51. Zhou XB, Arntz C, Kamm S, Motejlek K, Sausbier U, Wang GX, Ruth P, Korth M. A molecular switch for specific stimulation of the BKCa channel by cGMP and cAMP kinase. J Biol Chem. 2001;276:43239–45.
52. Porter VA, Bonev AD, Knot HJ, Heppner TJ, Stevenson AS, Kleppisch T, Lederer WJ, Nelson MT. Frequency modulation of Ca2 sparks is involved in regulation of arterial diameter by cyclic nucleotides. Am J Phys. 1998;274:C1346–55.
53. Wellman GC, Santana LF, Bonev AD, Nelson MT. Role of phospholamban in the modulation of arterial Ca^{2+}sparks and Ca^{2+} activated K^+ channels by cAMP. Am J Phys. 2001;281:C1029–37.
54. Eggermont JA, Vrolix M, Wuytack F, Raeymaekers L, Casteels R. The Ca^{2+}-Mg^{2+}-ATPases of the plasma membrane and of the endoplasmic reticulum in smooth muscle cells and their regulation. J Cardiovasc Pharmacol. 1988;1(2 Suppl 5):S51–5.
55. Joshi S, Nelson MT, Werner ME. Amplified NO/cGMP-mediated relaxation and ryanodine receptor-to-BK_{Ca} channel signalling in corpus cavernosum smooth muscle from phospholamban knockout mice. Br J Pharmacol. 2012;1652:455–66.
56. Kun A, Matchkov VV, Stankevicius E, Nardi A, Hughes AD, Kirkeby HJ, Demnitz J, Simonsen U. NS11021, a novel opener of large-conductance Ca^{2+}-activated K^+ channels, enhances erectile responses in rats. Br J Pharmacol. 2009;158:1465–76.
57. Király I, Pataricza J, Bajory Z, Simonsen U, Varro A, Papp JG, Pajor L, Kun A. Involvement of large-conductance Ca^{2+}-activated K^+ channels in both nitric oxide and endothelium-derived hyperpolarization-type relaxation in human penile small arteries. Basic Clin Pharmacol Toxicol. 2013;113:19–24.
58. Boy KM, Guernon JM, Sit SY, Xie K, Hewawasam P, Boissard CG, Dworetzky SI, Natale J, Gribkoff VK, Lodge N, Starrett JE Jr. 3-Thio-quinolinone maxi-K openers for the treatment of erectile dysfunction. Bioorg Med Chem Lett. 2004;14:5089–93.
59. Hewawasam P, Fan W, Cook DA, Newberry KS, Boissard CG, Gribkoff VK, Starrett J, Lodge NJ. 4-Aryl-3-(mercapto)quinolin-2-ones: novel maxi-K channel opening relaxants of corporal smooth muscle. Bioorg Med Chem Lett. 2004;14:4479–82.
60. Roy S, Morayo Akande A, Large RJ, Webb TI, Camarasu C, Sergeant GP, McHale NG, Thornbury KD, Hollywood MA. Structure-activity relationships of a novel group of large-conductance Ca^{2+}-activated K^+ (BK) channel modulators: the GoSlo-SRFamily. ChemMedChem. 2012;7(10):1763–9.
61. Large RJ, Kshatri A, Webb TI, Roy S, Akande A, Bradley E, Sergeant GP, Thornbury KD, McHale NG, Hollywood MA. Effects of the novel BK channel opener GoSlo-SR-5-130 are dependent on the presence of BK β subunits. Br J Pharmacol. 2015;172:2544–56.
62. Yoshimura N, Kato R, Chancellor MB, Nelson JB, Glorioso JC. Gene therapy as future treatment of erectile dysfunction. Expert Opin Biol Ther. 2010;10:1305–14.
63. Christ GJ, Rehman J, Day N, Salkoff L, Valcic M, Melman A, Geliebter J. Intracorporal injection of hSlo cDNA in rats produces physiologically relevant alterations in penile function. Am J Phys. 1998;275:H600–8.
64. Christ GJ, Day N, Santizo C, Sato Y, Zhao W, Sclafani T, Bakal R, Salman M, Davies K, Melman A. Intracorporal injection of hSlo cDNA restores erectile capacity in STZ-diabetic F-344 rats in vivo. Am J Phys. 2004;287:H1544–53.
65. Melman A, Zhao W, Davies KP, Bakal R, Christ GJ. The successful long-term treatment of age related erectile dysfunction with hSlo cDNA in rats in vivo. J Urol. 2003;170:285–90.
66. Melman A, Bar-Chama N, McCullough A, Davies K, Christ G. hMaxi-K gene transfer in males with erectile dysfunction: results of the first human trial. Hum Gene Ther. 2006;18:1165–76.
67. Christ GJ, Andersson KE, Williams K, Zhao W, D'Agostino R Jr, Kaplan J, Aboushwareb T, Yoo J, Calenda G, Davies KP, Sellers RS, Melman A. Smooth-muscle-specific gene transfer with the human maxi-k channel improves erectile function and enhances sexual behavior in atherosclerotic cynomolgus monkeys. Eur Urol. 2009;56:1055–66.
68. Malysz J, Gibbons SJ, Miller SM, Gettman M, Nehra A, Szurszewski JH, Farrugia G. Potassium outward currents in freshly dissociated rabbit corpus cavernosum myocytes. J Urol. 2001;166:1167–77.
69. Malysz J, Farrugia G, Ou Y, Szurszewski JH, Nehra A, Gibbons SJ. The Kv2.2 alpha subunit contributes to delayed rectifier K(+) currents in myocytes fromrabbit corpus cavernosum. J Androl. 2002;23:899–910.
70. Jepps TA, Olesen SP, Greenwood IA, Dalsgaard T. Molecular and functional characterization of Kv 7 channels in penile arteries and corpus cavernosum of healthy and metabolic syndrome rats. Br J Pharmacol. 2016;173:1478–90.
71. Ashcroft FM, Gribble FM. Correlating structure and function in ATP-sensitive K+ channels. Trends Neurosci. 1998;21:288–94.
72. Nelson MT. Ca^{2+}-activated potassium channels and ATP-sensitive potassium channels as modulators of vascular tone. Trends Cardiovasc Med. 1993;3:54–60.
73. Insuk SO, Chae MR, Choi JW, DK Yang DK, Sim JH, Lee SW. Molecular basis and characteristics of K_{ATP} channel in human corporal smooth muscle cells. Int J Impot Res. 2003;15:258–66.

74. Large WA, Wang Q. Characteristics and physiological role of the Ca^{2+}-activated Cl^- conductance in smooth muscle. Am J Phys. 1996;271:C435–54.
75. Craven M, Sergeant GP, Hollywood MA, McHale NG, Thornbury KD. Modulation of spontaneous Ca^{2+}-activated Cl^- currents in the rabbit corpus cavernosum by the nitric oxide–cGMP pathway. J Physiol. 2004;566:495–506.
76. Williams BA, Sims SM. Calcium sparks activate calcium-dependent Cl^- current in rat corpus cavernosum smooth muscle cells. Am J Phys. 2007;293:C1239–51.
77. Sergeant GP, Craven M, Hollywood MA, McHale NG, Thornbury KD. Spontaneous Ca^{2+} waves in isolated myocytes from rabbit corpus cavernosum: modulation by the NO/cGMP pathway. J Sex Med. 2009;6:958–66.
78. Hannigan KI, Griffin CS, Large RL, Sergeant GP, Hollywood MA, McHale NG, Thornbury KD. The role of Ca^{2+}-activated Cl^- current in tone generation in the rabbit corpus cavernosum. Am J Phys. 2017;313:C475–86.
79. Caputo A, Caci E, Ferrera L, Pedemonte N, Barsanti C, Sondo E, Pfeffer U, Ravazzolo R, Zegarra-Moran O, Galietta LJ. TMEM16A, a membrane protein associated with calcium-dependent chloride channel activity. Science. 2008;322:590–4.
80. Schroeder BC, Cheng T, Jan YN, Jan LY. Expression cloning of TMEM16A as a calcium-activated chloride channel subunit. Cell. 2008;134:1019–29.
81. Yang YD, Cho H, Koo JY, Tak MH, Cho Y, Shim WS, Park SP, Lee J, Lee B, Kim BM, Raouf R, Shin YK, Oh U. TMEM16A confers receptor-activated calcium-dependent chloride conductance. Nature. 2008;455:1210–5.
82. Ferrera L, Caputo A, Ubby I, Bussani E, Zegarra-Moran O, Ravazzolo R, Pagani F, Galietta LJ. Regulation of TMEM16A chloride channel properties by alternative splicing. J Biol Chem. 2009;284:33360–8.
83. Chipperfield AR, Harper AA. Chloride in smooth muscle. Prog Biophys Mol Biol. 2000;74:175–221.
84. Chu LL, Adaikan PG. Role of chloride channels in the regulation of corpus cavernosum tone: a potential therapeutic target for erectile dysfunction. J Sex Med. 2008;5:813–21.
85. Lau LC, Adaikan PG. Possibility of inhibition of calcium-activated chloride channel rescuing erectile failures in diabetes. Int J Impot Res. 2014;264:151–5.
86. Hashitani H. Neuroeffector transmission to different layers of smooth muscle in the rat penile bulb. J Physiol. 2000;524:549–63.
87. Van Helden DF. Spontaneous and noradrenaline-induced transient depolarizations in the smooth muscle of guinea-pig mesenteric vein. J Physiol. 1991;437:511–41.
88. Cotton KD, Hollywood MA, McHale NG, Thornbury KD. Ca^{2+}-current and Ca^{2+}-activated chloride current in isolated smooth muscle cells of the sheep urethra. J Physiol. 1997;505:121–31.
89. Williams BA, Liu C, DeYoung L, Brock GB, Sims SM. Regulation of intracellular Ca^{2+} release in corpus cavernosum smooth muscle: synergism between nitric oxide and cGMP. Am J Phys. 2005;288:C650–8.
90. Jaggar JH, Porter VA, Lederer WJ, Nelson MT. Calcium sparks in smooth muscle. Am J Phys. 2000;27:C235–56.
91. Gordienko DV, Bolton TB. Crosstalk between ryanodine receptors and IP_3 receptors as a factor shaping spontaneous Ca^{2+}-release events in rabbit portal vein myocytes. J Physiol. 2002;542:743–62.
92. Drumm BT, Large RJ, Hollywood MA, Thornbury KD, Baker SA, Harvey BJ, McHale NG, Sergeant GP. The role of Ca^{2+} influx in spontaneous Ca^{2+}wave propagation in interstitial cells of Cajal from the rabbit urethra. J Physiol. 2015;593:3333–50.
93. Wang H, Eto M, Steers WD, Somlyo AP, Somlyo AV. RhoA-mediated Ca2+ sensitization in erectile function. J Biol Chem. 2002;277:30614–21.
94. Hashitani H. Interaction between interstitial cells and smooth muscles in the lower urinary tract and penis. J Physiol. 2006;576:707–14.
95. Schlossmann J, Ammendola A, Ashman K, Zong X, Huber A, Neubauer G, Wang GX, Allescher HD, Korth M, Wilm M, Hofmann F, Ruth P. Regulation of intracellular calcium by a signalling complex of IRAG, IP_3 receptor and cGMP kinase Ibeta. Nature. 2000;404:197–201.
96. Feil R, Gappa N, Rutz M, Schlossmann J, Rose CR, Konnerth A, Brummer S, Kuhbandner S, Hofmann F. Functional reconstitution of vascular smooth muscle cells with cGMP-dependent protein kinase I isoforms. Circ Res. 2002;90:1080–6.
97. Ruth P, Wang GX, Boekhoff I, May B, Pfeifer A, Penner R, Korth M, Breer H, Hofmann F. Transfected cGMP-dependent protein kinase suppresses calcium transients by inhibition of inositol 1,4,5-trisphosphate production. Proc Natl Acad Sci U S A. 1993;90:2623–7.

8 Generation and Regulation of Spontaneous Contractions in the Prostate

Basu Chakrabarty, Sophie Lee, and Betty Exintaris

Abstract

Spontaneous myogenic contractions have been shown to be significantly upregulated in prostate tissue collected from men with Benign Prostatic Hyperplasia (BPH), an extremely common disorder of the ageing male. Although originally thought likely to be involved in 'housekeeping' functions, mixing prostatic secretions to prevent stagnation, these spontaneous myogenic contractions provide a novel opportunity to understand and treat BPH. This treatment potential differs from previous models, which focused exclusively on attenuating nerve-mediated neurogenic contractions. Previous studies in the rodent prostate have provided an insight into the mechanisms underlying the regulation of myogenic contractions. 'Prostatic Interstitial Cells' (PICs) within the prostate appear to generate pacemaker potentials, which arise from the summation of number of spontaneous transient depolarisations triggered by the spontaneous release of Ca^{2+} from internal stores and the opening of Ca^{2+}-activated Cl^- channels. Pacemaker potentials then conduct into neighbouring smooth muscle cells to generate spontaneous slow waves. These slow waves trigger the firing of 'spike-like' action potentials, Ca^{2+} entry and contraction, which are not attenuated by blockers of neurotransmission. However, these spontaneous prostatic contractions can be modulated by the autonomic nervous system. Here, we discuss the mechanisms underlying rodent and human prostate myogenic contractions and the actions of existing and novel pharmacotherapies for the treatment of BPH. Understanding the generation of human prostatic smooth muscle tone will confirm the mechanism of action of existing drugs, inform the identification and effectiveness of new pharmacotherapies, as well as predict patient outcomes.

Keywords

Prostate · Slow wave activity · Pacemaker activity · Benign prostatic hyperplasia · Spontaneous activity · Prostatic interstitial cells

8.1 Function and Structure of the Prostate

8.1.1 Function

The prostate is the largest male accessory reproductive organ, and produces prostatic secretions that comprise part of the semen. Secretions

B. Chakrabarty · S. Lee · B. Exintaris (✉)
Drug Discovery Biology, Monash Institute of Pharmaceutical Science, Melbourne, VIC, Australia
e-mail: betty.exintaris@monash.edu

H. Hashitani, R. J. Lang (eds.), *Smooth Muscle Spontaneous Activity*, Advances in Experimental Medicine and Biology 1124, https://doi.org/10.1007/978-981-13-5895-1_8

produced by the accessory reproductive organs play a role in optimising conditions for fertilisation by buffering the vaginal acidic environment, enhancing sperm motility and viability, or by improving sperm transport in both the male and female reproductive tracts, thereby playing an important role in reproduction by facilitating fertilisation [1]. The average human ejaculate ranges from 2 to 6 mL, with prostatic secretions contributing approximately 0.5 mL [1]. During ejaculation, the first fraction of human ejaculate is rich in sperm and prostatic secretions, with secretions from the seminal vesicles elevated in the later fraction of ejaculate [2–4]. Components of prostatic secretions include citric acid [5], polyamines, e.g. spermine [6], lipids, cholesterol, and phospholipids [1], zinc [7], prostate secretory proteins, e.g. prostate-specific antigen (PSA) [8], human kallikrein 2 [9], human kallikrein-L1 [10], prostatic acid phosphatase [11], prostatic specific protein 94 [12], Zn_2 glycoprotein [13], leucine aminopeptidase [14], lactic dehydrogenase [15], and immunoglobulins [16].

8.1.2 Anatomy

The anatomy of the prostate differs significantly between species. The human prostate is traversed by the prostatic urethra, and is anatomically defined as having anterior, posterior and lateral surfaces. The prostate has a narrowed apex inferiorly, and a broad base superiorly located posterior to the bladder and is enclosed by a prostatic capsule [1].

Current anatomical and histological knowledge of the human prostate is based on descriptions by McNeal [17–21] and elegantly illustrated in Campbell-Walsh Urology [1]. McNeal describes the prostate as being composed of approximately 70% glandular elements, and 30% fibromuscular stroma extending to the fibromuscular capsule [20]. The glandular elements of the prostate are divided into discrete pathological zones, which are distinguished by the location of their ducts into the urethra. Three distinct zones of the glandular elements of the prostate include the peripheral, central, and transition zones, in addition to the anterior fibromuscular stroma which lacks a glandular component [20]. The vascular supply to the prostate arises from the inferior vesicle artery which branches into two main arteries travelling to different regions. The urethral arteries supply the periurethral and transition zones of the human prostate, while the capsular artery branch pierces the prostate stroma and supplies the glandular tissues [1].

The human prostate has several unique features, including the anatomical zone structure described by McNeal [17–21], and a band of outer condensed fibromuscular stroma encapsulating the prostate [22]. In contrast, the mouse [23] and guinea pig [24] prostates consists of two distinct bilaterally symmetrical lobes, a well-developed dorsal lobe and a smaller ventral lobe, located at specific positions around the urethra, but do not encapsulate it. Nor do they contain an outer fibromuscular stroma.

8.1.3 Cellular Composition

The cellular structure of the prostate can be divided into three components: the epithelium, basement membrane and fibromuscular stroma. The epithelium consists of basal, neuroendocrine and secretory (luminal) cells [25]. The basement membrane consists of extracellular matrix (ECM) secreted by the basal epithelial cells. Underlying these layers is the stroma, which consists of smooth muscle cells, fibroblasts, nerves and blood vessels [26]. There are also a number of immune cells within the stroma.

Epithelial cells arise from a common urogenital epithelial progenitor cell, with the exception of neuroendocrine cells, which are postulated to arise from either the urogenital epithelial or neural crest progenitor cells. Basal progenitors give rise to basal cells, which are essential in the maintenance of ductal integrity and survival of luminal cells. Luminal cells arise from a luminal progenitor, form the lumen of the duct, and are responsible for the generation and secretion of prostatic secretions. The ratio of basal to luminal cells within the human prostate is estimated to be 1:1 [27]. Neuroendocrine cells, while of a

complex developmental origin not completely elucidated, act in a paracrine manner to release endocrine signalling molecules, notably bombesin, neurotensin, parathyroid hormone-related protein (PTHrP), serotonin, and calcitonin [28].

There are four distinct populations of stromal cells within the adult prostate: sub-epithelial interstitial cells, smooth muscle cells, wrapping cells and fibroblasts [27]. Sub-epithelial interstitial cells are located adjacent to the basal membrane and between the smooth muscle cell bundles, which we have called prostatic interstitial cells (PICs) [29]. As interstitial cells of Cajal (ICC) in the gastrointestinal (GI) tract generate electrical activity underlying its spontaneous contractions [30], it was envisaged that PICs are capable of triggering slow waves to drive smooth muscle contractility in the prostate. Smooth muscle cells are the most numerous cell type, and generate muscle contractility within the prostate to facilitate the movement of secretions from the ductal structures to the proximal urethra during ejaculation. Wrapping cells are located with the outer part of the smooth muscle layer, assisting with the formation of the fibromuscular stroma. Fibroblasts and myofibroblast are also located between ducts [27].

There are also notable differences in the cellular structure of the rodent and human prostate. Rodent prostates do not contain a continuous basal cell layer present in the human prostate, leading to a decreased ratio of basal to luminal cells of 1:7 in rodents (compared to 1:1 in humans) [31]. The composition of the stroma also significantly differs, with rodent prostate ducts consisting of a thin smooth muscle layer joined by connective tissue to neighbouring ducts. The human prostate consists of bundles of smooth muscle cells that form a continuous thick mass of fibromuscular stroma. Overall, there is less stromal content in rodent prostates when compared to the human prostate.

8.1.4 Development and Growth of the Prostate

Development of the prostate occurs in four distinct stages following the division of the embryonic cloaca into separate urogenital and anorectal tracts by 8 weeks of development in humans, or 13.5 days post coitum in the mouse. In the first stage of prostate development, androgens produce developmental cues, both directly and indirectly, that lead to prostate development [32]. In the second stage, prostate budding occurs to produce a series of ductal structures. Urogenital sinus epithelium (UGE) directed by Activin, Notch and Hedgehog signalling pathways drive progenitor cells located in the ductal tips into the urogenital sinus mesenchyme (UGM), leading to the initiation of tissue outgrowth [27]. The third stage, branching morphogenesis occurs, leading to ductal outgrowth and the formation of the mature ductal network. This stage is responsible for the development of the different prostate zones (TZ, PZ and CZ) within the unilobular organ of humans. The fourth and final stage consists of the differentiation of the UGE into the ductal lumen and the formation of the glandular epithelium, consisting of basal, luminal, neuroendocrine and intermediate cells. The resultant prostate is approximately two (2) grams in weight.

Growth of the prostate continues over a man's lifetime. During puberty, the prostate undergoes a wave of growth in response to androgens released from the testes. The synthesis and release of testosterone is regulated by the hypothalamus, which releases gonadotropin-releasing hormone to stimulate the pituitary release of luteinising hormone which is then transported to the testes [1]. The prohormone, testosterone is synthesised in the Leydig cells of the testes and is the source of the major androgen in circulation [1]. However, dihydrotestosterone (DHT) converted from testosterone by 5α-reductase in the prostate is more potent, concentrated in the prostate [33–35] and is the major androgen regulating cellular growth, differentiation, and function [36, 37]. There are two isoforms of 5α-reductase (type I and type II), with type I 5α-reductase predominately expressed in prostatic epithelia, and type II 5α-reductase predominately expressed in the fibromuscular stroma [38]. Activation of the androgen receptor by DHT (or testosterone) within the cytoplasm results in various

downstream signalling mechanisms, ultimately resulting in prostatic growth [35].

8.2 Benign Prostatic Hyperplasia

In the fourth decade of a man's life, a pathophysiological wave of growth commences, resulting in Benign Prostatic Hyperplasia (BPH), an extremely common disorder of the ageing male population. BPH has long been regarded as a disease of the prostate stroma, as the ratio of stroma to epithelia increases from 2:1 in the normal prostate to 5:1 in BPH [39]. The encapsulation of an enlarging prostate around the urethra with BPH plays a critical role in the development of Lower Urinary Tract Symptoms (LUTS), be they voiding symptoms or storage symptoms, namely overactive bladder (OAB) associated with bladder outlet obstruction (BOO). However, one consistent clinical observation is that the size of the prostate does not correlate with the severity of LUTS associated with BPH [40]. Therefore, it is proposed that the pathogenesis of BPH can be divided into two distinct components: a static component that is characterised by an increase in the size of the prostate, and a dynamic component, which is thought to involve changes to the contractility and innervation of the smooth muscle [41].

BPH is a hyperplastic process, with the first phase of its development being characterised by an increased number of small glandular and stromal nodules, followed by a second phase associated with a significant increase in large nodules [42]. Early nodules in the periurethral zone are purely stromal in their composition, whereas the earliest nodules in the transition zone represent proliferation of glandular tissue [19, 42]. This proliferative process leads to an increased density of glands within a given area, along with hypertrophy of individual epithelial cells [1]. A significant change in stromal-epithelial ratios in resected tissues suggests that hyperplasia of the stroma predominates, resulting in a greater presence of smooth muscle relative to the glandular epithelium, so that smooth muscle represents a significant volume of the prostate in BPH [43, 44].

Although dogs are the only other species to develop naturally-occurring BPH, LUTS associated with BOO does not develop due to the lack of an encapsulating prostate [45]. An important role of the prostatic capsule in the development of LUTS is highlighted by reports suggesting that a transurethral incision of the prostatic capsule results in a significant improvement of symptoms without affecting the size of the prostate [1, 46]. Similarly, the size of the prostate does not correlate with the severity of symptoms [47], suggesting that there is an additional component involved in the pathophysiology of LUTS. The tone generated by smooth muscle contraction within the prostate plays a major role in the pathophysiology of LUTS related with BPH [43]. An increase in smooth muscle tone results in benign prostatic obstruction (BPO) of the urethra, and subsequent BOO, all of which contribute to LUTS in ageing men [40]. The increase in prostatic urethral obstruction can also result in compensatory changes in bladder function. However, the aetiology of this increase in smooth muscle tone resulting in a dynamic increase in prostatic urethral resistance remains poorly understood. The involvement of stromal-epithelial interactions [48], embryonic awakening [42], prostatic stem cells [49], inflammation [50], and changes in innervation [51–54] in the development of BPH have all been suggested.

8.3 Prostatic Innervation

The prostate is innervated by autonomic postganglionic neurons arising from the pelvic plexus [55]. Two main nerves innervate the pelvic plexus: the pelvic nerve, which carries parasympathetic fibres, and the hypogastric nerve, which carries sympathetic fibres and a small population of sensory neurons. Short noradrenergic nerves ramify from the hypogastric nerve, densely innervating the prostate stroma. Noradrenaline has been postulated as the primary neurotransmitter within the prostate, with early experiments within the human prostate finding that noradrenaline stimulated contraction of the smooth muscle cells within the prostate stroma [56]. The

innervation plays an essential role in prostate function, ramifying to both the stromal and glandular components of the prostate. Stimulation of sympathetic nerves predominately mediates contraction of prostatic smooth muscle, whereas parasympathetic nerves extend to the acini and promote secretion. In addition, non-adrenergic, non-cholinergic mechanisms which play a role in prostatic smooth muscle function have been identified in the human prostate gland.

8.3.1 Sympathetic Innervation

The predominant sympathetic nerve fibres extending to the prostate are adrenergic nerves, with varicosities located 10–20 nm from smooth muscle cells in the human prostate [57]. Immunostaining of adrenergic innervation locates throughout the smooth muscle of the prostatic capsule, predominately around the stroma of individual acini [58], and consistent with a role for sympathetic innervation to cause contraction that promotes expulsion of prostatic secretions during ejaculation [59].

α1-Adrenoceptors are the predominant subtype of adrenoceptors present within the human prostate. Receptor binding experiments indicate that α1-adrenoceptors are localised predominantly to the fibromuscular stroma, with α2-adrenoceptors found only in vascular tissue within the human prostate. The α1-adrenoceptor is not homogenous, and the sub-classifications of the receptor, α_{1A}, α_{1B} and α_{1D}, are present within the human prostate at differing expression levels [60]. The α_{1A}-adrenoceptor is the most prominent sub-classification expressed within the prostate, followed by α_{1D} and α_{1B}-adrenoceptors, respectively [53]. The α1-adrenoceptor is a G-Protein receptor coupled to a G_q alpha subunit, which is responsible for the hydrolysis of phospholipase C (PLC), leading to the activation of diacylglycerol (DAG) and inositol trisphosphate (IP_3). IP_3 acts on IP_3 receptors located on the sarcoplasmic reticulum membrane to release Ca^{2+} from intracellular calcium stores, activating myosin light chain kinase (MLCK). MLCK phosphorylases myosin light chain (MLC), resulting in smooth muscle contraction. DAG activates protein kinase C (PKC), which prevents the dephosphorisation of myosin light chain, preventing smooth muscle relaxation [61].

In addition to α1-adrenoceptors, the prostate contains a population of α2-adrenoceptors localised primarily in the glandular epithelium and vascular tissue [62, 63], which are unlikely to play a role in contraction as α2-adrenoceptor antagonists only slightly reduce contractions induced by noradrenaline [64] and have no effect on electrical field stimulation (EFS)-induced contractions in the human prostate [65]. The application of a β-adrenoceptor agonist inhibits α_1-adrenoceptor-mediated contraction via activation of adenylyl cyclase and accumulation of cyclic adenosine monophosphate (cAMP), resulting in relaxation of prostatic smooth muscle [66–68]. This response is most likely mediated by the β2-adrenoceptor subtype. However, the β1-adrenoceptor subtype and β3-adrenoceptor subtype may also be involved in contractile functions of the human prostate [68–70].

In cell cultures, α1-adrenoceptor antagonists have suppressed stromal and epithelial cell growth, suggesting that the adrenergic innervation and adrenoceptors may have a non-contractile role in normal and diseased prostate tissues [71–74]. In addition, it has been demonstrated that α1-adrenoceptors couple to non-contractile intracellular protein kinases in the human prostate [75–78], suggesting a role for the adrenergic innervation in cellular growth, proliferation, and apoptosis. However, a clinical translation of a reduction in prostate volume in patients clinically prescribed α1-adrenoceptor antagonists has not been observed [79, 80].

Adenosine Triphosphate (ATP) is an adjunct excitatory co-transmitter with noradrenaline in efferent-mediated contraction of the rat and guinea pig prostates [81]. Purinergic P2 receptors have been located in the human prostate, with $P2Y_1$ and P2X1 receptors present within the stroma [82]. Adenosine A_1 and A_{2A} receptors are present in human stromal cells, and have been shown to modulate α1-adrenoceptor-mediated contractions of cultured stromal cells. Functional investigations in the rat prostate indicate that P2 receptor antagonists attenuate nerve-mediated contractility, with ATP modulating the release of noradrenaline from sympathetic nerves via the prejunctional receptors A_1 and P2Y [83].

In the guinea pig prostate, EFS-evoked excitatory junction potentials (EJPs) are abolished by guanethidine (10 μM), α-β-methylene ATP (10 μM) or pyridoxal phosphate-6-azophenyl-2,4-disulphonic acid (PPADS, 10 μM), but not phentolamine (1 μM). Immunostaining of the prostatic smooth muscle reveals the expression of P2X1 receptors. EJPs themselves do not cause contraction, but they readily sum to trigger slow wave generation, spike discharge and contraction (see below) [84].

8.3.2 Parasympathetic Innervation

The predominant parasympathetic nerve fibres innervating the human prostate are cholinergic nerves, which have been identified using markers of acetylcholinesterase or vesicular acetylcholine transferase [58, 85–87]. Electron microscopy has demonstrated that cholinergic nerve varicosities form close associations with the glandular epithelium and the smooth muscle components of the prostate [57].

Muscarinic receptors M2-4, but mainly the M2 receptor, have been located in cultured human prostatic stroma cells, while the M1 receptor subtype was found mostly on epithelium cells [88, 89]. The rabbit prostate produces a small atropine-sensitive contraction to either cholinergic nerve stimulation or applied acetylcholine [88, 89]. Similar cholinergic contractions in the prostate of the rat [90], guinea pig [91] and dog [92] have been attributed to the activation of M2, M1 and M3 muscarinic receptor, respectively. In the mouse prostate, cholinergic contractions were inhibited upon genetic deletion of the M3 receptor [93]. However, the general consensus is that the cholinergic contractions in the prostate are relatively small compared to their adrenergic contractions and that epithelial M1 are likely to be involved in prostatic secretion [88, 89].

8.3.3 Non-adrenergic Non-cholinergic Innervation

Nitric oxide synthase (NOS) is an enzyme responsible for producing nitric oxide (NO) from N_{ω}-nitro-L-Arginine, and has been identified in the endothelium, smooth muscle, blood vessels and nerves supplying the lower urinary tract [86]. NO is commonly co-localised in adrenergic and cholinergic nerves throughout the stromal and glandular epithelium compartments [86, 94–96]. NO is an essential signal transduction component in several physiological processes, notably smooth muscle relaxation and neurotransmission. For example, in agonist-induced in vitro contractions of the human prostate, NO donors results in relaxation [81, 97, 98]. The only established receptor for NO is soluble guanylate cyclase (sGC), with NO binding induces a conformational change in sGC to its active state [99]. It is well established that sGC catalyses the conversion of guanosine 5-triphosphate (GTP) to cyclic guanosine 3,5-monophosphate (cGMP) [100]. cGMP is an important second messenger, as it regulates three classes of proteins: ion channels, phosphodiesterases, and cGMP-dependent protein kinases (cGKs). cGMP and cyclic AMP (cAMP) are degraded by cyclic nucleotide phosphodiesterases (PDEs).

In addition, numerous other non-adrenergic, non-cholinergic mechanisms can elicit or modulate prostatic smooth muscle contraction. These include the sensory innervation releasing calcitonin gene-related peptide [101], tachykinins [102], as well as endothelins [103, 104], the endocannabinoid system [105], prostanoids [106, 107], bradykinins [108, 109] and histamine [110]. However, the physiological role for some of these mechanisms in the human prostate remains uncertain and their contribution to nerve-mediated contractions is considerably less than that of the sympathetic innervation.

8.4 Spontaneous Contractions

Spontaneous contractions in the prostate are likely to be involved in maintaining the momentum of prostatic secretions in the acini and regulating the overall resting smooth muscle tone of the prostate [111, 112]. These spontaneous contractions are observed in isolated strips of the guinea pig, rat and dog prostate [92, 111, 113],

human prostatic tissue [56, 86] and can be maintained in human cultured prostatic smooth muscle cells [114].

The composition of the guinea pig prostate is similar to the human prostate gland as it contains a larger proportion of smooth muscle in comparison to the glandular epithelium, being 40% and 25% of the total prostatic composition, respectively [115, 116]. The guinea pig prostate also undergoes similar age- and androgen-dependent changes as the human prostate [117]. The guinea pig prostate gland grows from 60 mg to 600 mg during puberty, further development with age results in a prostate weight of >1 g [117]. In addition, the smooth muscle component of the guinea pig prostate rises to 75% of the total prostatic composition [117], which is similar to patients exhibiting symptoms of BPH [118]. The innervation of the guinea pig prostate is also similar to the human prostate, arising from the pelvic plexus, which receives sympathetic and parasympathetic inputs from the hypogastric and pelvic nerves, respectively [119, 120]. In addition, immunohistochemical and functional studies have suggested adrenergic, cholinergic and non-adrenergic, non-cholinergic innervation in the guinea pig prostate similar to the human prostate [91, 121–123]. Overall, the findings in the guinea pig prostate have provided extensive insights into the mechanisms involved in the regulation of prostatic smooth muscle tone.

8.4.1 Prostatic Interstitial Cells (PICs)

A number of smooth muscle tissues within the body have been shown to exhibit spontaneous contractions independent of nerve-evoked responses, commonly referred to as myogenic contractions. The most well studied example of spontaneous activity is in the GI tract where ICC generate propagating slow wave activity [30] which triggers the phasic contractions of the GI smooth muscle. Common ultrastructural features of ICC include an electron-dense cytoplasm, caveolae, a basal lamina, well-developed smooth endoplasmic reticulum, relatively sparse rough endoplasmic reticulum, an abundance of mitochondria, free and poly ribosomes, and intermediate and thin filaments with a lack of myosin filaments [124]. Electron microscopic investigations of the guinea pig [111] and gerbil [125] prostates have identified PICs located between the epithelial and stromal compartments with similar morphological features to ICC.

By immunohistochemistry, PICs in the guinea pig prostate are positive for the Kit receptor (CD117) of the receptor tyrosine kinase, which is a well-established marker of ICC within the GI tract. Using Kit as a marker, PICs have been identified between smooth muscle cells and epithelial cells of the guinea pig [111, 126], rat [113], mouse [127] and human [112] prostate. A confounding factor in the identification of PICs is that mast cells, a common prostatic immune infiltrate, also express Kit [128]. Studies characterising PICs in human tissue have used several other markers of GI ICC that co-locate with Kit to exclude the possibility of misidentification of mast cells. Interstitial cells within the human prostate were found to be immunoreactive for Kit, vanilloid receptor 1 (VR1) and connexion43 [112]. Shafik et al. (2005) additionally confirmed the presence of Kit-positive PICs in the human prostate within the sub-epithelial space [29], while Exintaris et al. (2002) described that these Kit-positive PICs formed an interconnecting network in the guinea pig prostate [111]. In contrast, Gevaert et al. failed to detect any Kit immunoreactivity in PICs in the human prostate, attributing all Kit-positive cells as mast cells. However, they characterised a population of sub-epithelial PICs using antibodies against vimentin and CD34 [122], another traditionally used ICC marker [129]. These cells were described as having long cellular processes interconnected by small adheren junctions, similar to the PICs originally described in the guinea pig prostate [103]. Although there is conflicting literature as to whether PICS in the human prostate are indeed immunoreactive to Kit, a population of PICs with similar morphological features has been identified across multiple species.

8.4.2 Spontaneous Electrical Activity

Pacemaker potentials with a distinct biphasic time course of alternating depolarising and repolarising phases have been recorded in young guinea pigs [111, 130]. Pacemaker potentials have been shown to have a similar resting membrane potential and a frequency (5–6 min^{-1}) not significantly different from cells displaying slow waves [131].

Single smooth muscle cells isolated from the guinea pig [132, 133] and human prostate gland [134, 135] are quiescent and have a stable resting membrane potential of approximately −60 mV. They require a depolarisation to evoke their action potentials, presumably in the intact tissue achieved by the slow wave. In isolated strips of the guinea pig prostate, spontaneous slow waves consist of a depolarising transient of 10–20 mV and at least one superimposed action potential of approximately 40 mV in amplitude [111]. Neurobiotin staining has demonstrated that these slow waves arise from spindle-shaped smooth muscle cells which are approximately 80–220 μm in length and 5–10 μm in width [111]. Spontaneous electrical slow waves are likely to underlie the spontaneous contractions recorded in the guinea pig prostate, which are recorded at a similar frequency [111, 131]. Further characterisation of slow wave activity in the guinea pig prostate found that 80% of cells generate slow wave activity, with 13% producing pacemaker potentials [130]. Slow wave activity is myogenic in origin, as it is not modulated by blockers of neural transmission or propagation. However, excitatory agents such as high potassium, phenylephrine and histamine increase the frequency of slow wave activity [111].

In the presence of an 'L-type' voltage-dependent Ca^{2+} channel blocker such as nifedipine the spike potentials superimposed on the slow wave are abolished and the slow wave duration is reduced [111, 131]. The duration of the pacemaker potentials is also reduced considerably in the presence of 1 μM nifedipine [131]. However, the frequency of the depolarising transients they evoke are little affected by 1–10 μM nifedipine [124]. In some recordings, it has been demonstrated that when the depolarising transients are small, 1 μM nifedipine appears to completely block slow wave discharge; which has led to the suggestion that the varying amplitude of the depolarising transients reflexes the passive decay with distance between their site of generation and the recording electrode [118]. Thus, the active propagation of slow waves is dependent on the regenerative activation of voltage-dependent L-type Ca^{2+} channels in the smooth muscle cells [118].

Other spontaneous electrical waveforms recorded in the guinea pig prostate include spontaneous transient depolarisations (STDs) [111] and action potentials [136]. STDs occur irregularly, consisting of a depolarisation followed by a slow repolarisation, and have a smaller amplitude and higher frequency than spontaneous pacemaker potentials or slow waves [130, 136]. STDs fire in clusters, and it is believed that the summation of individual STDs form a large, depolarising transient observed as the pacemaker potential, while the depolarising transient of individual slow waves represents the passively propagated membrane response of a pacemaker potential generated in neighbouring PICs [118, 130]. Spike potentials consist of a rapid depolarisation followed by an after-hyperpolarisation before returning to the resting membrane potential [136, 137]. Spike potentials are more commonly recorded in the prostates of aged guinea pigs and are dependent on the entry of Ca^{2+} via L-type Ca^{2+} channels [136]. It has been suggested that this age-related increase in high frequency action potential discharge reflects a change in the syncytial nature of the prostatic smooth muscle, where multiple electrically isolated smooth muscle bundles fire freely, independent of any PIC influences [118, 138]. Changes in the occurrence of these different spontaneous electrical waveforms recorded from the guinea pig prostate gland are thought likely to underlie the significant increase in smooth muscle tone with age (Figs. 8.1 and 8.2) [136, 139].

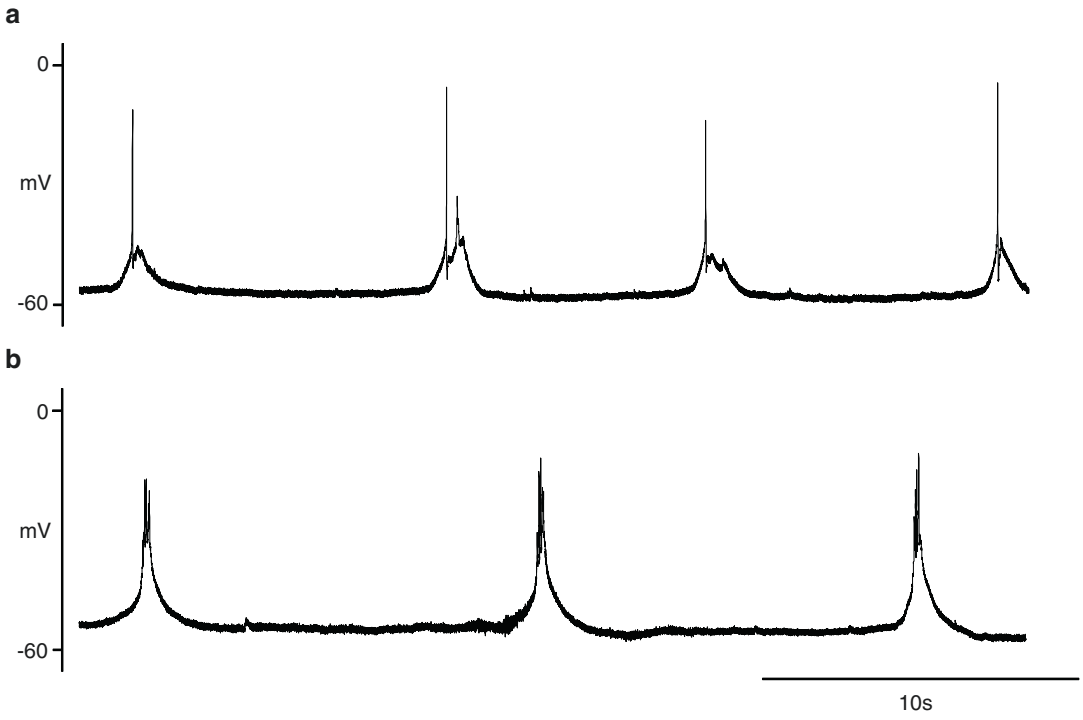

Fig. 8.1 Spontaneous slow wave activity in (**a**) adult and (**b**) ageing guinea pigs. Figure taken from Dey et al. [136]

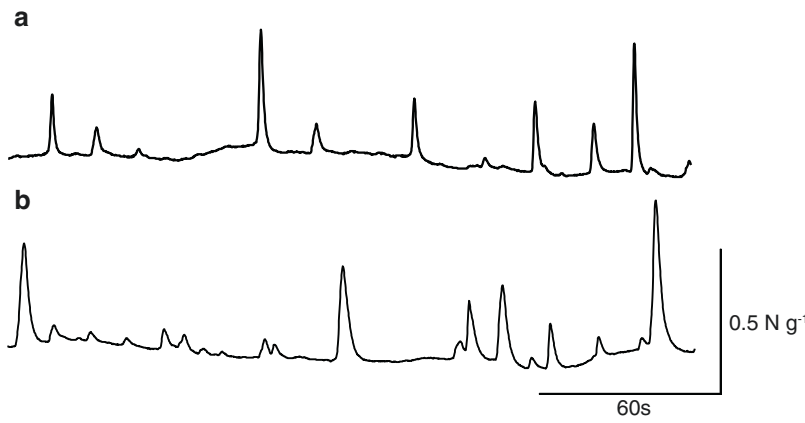

Fig. 8.2 Spontaneous contractile activity in (**a**) adult and (**b**) ageing guinea pigs. Spontaneous contractions occurred at irregular amplitudes in both age groups of animals. Figure taken from Dey et al. [136]

8.5 Mechanisms of Contraction of the Prostate

As with the guinea pig prostate [111, 140], spontaneous contractions in the transition zone of the human prostate are non-neurogenic in nature, being unaffected by blockers of excitation with tetrodotoxin (Fig. 8.3) or neurotransmission with guanethidine, and atropine (Fig. 8.4). The contractile profile of the transition zone is distinct and significantly different from the peripheral zone from matched specimens from the same patient [141]. The transition zone has a significantly greater resting basal tension, and significantly lower amplitude and frequency of spontaneous contractions in comparison to the

peripheral zone (Fig. 8.3). In contrast to the transition zone, tetrodotoxin significantly reduces the resting basal tension of the peripheral zone by approximately 14%, while the amplitude and frequency of its spontaneous contractions were unaffected. However, the lack of documenting the exact zonal location of tissue specimens collected from patients for experimentation limits the value of many previous studies on human prostate contractility. The innervation density of the peripheral zone is significantly greater than the transition zone [142], indicating that there is a neurogenic component in the regulation of spontaneous contractions in the peripheral zone of the human prostate. Furthermore, specific differences in the regulation of spontaneous contractions are likely to correspond to different functions of the anatomically distinct prostatic zones. For example, larger and more frequent contractions of the peripheral zone may play a greater role in the expulsion of prostatic secretion upon ejaculation. Whereas, smaller and less frequent contractions within the transition zone may well to be involved in 'housekeeping' functions such as maintaining the fluidity of prostatic secretions within the acini while at rest.

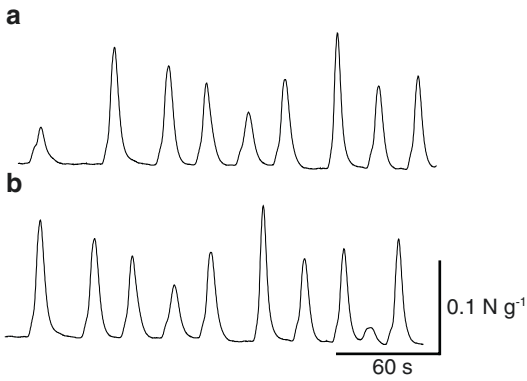

Fig. 8.3 The effects of 1.0 μM tetrodotoxin on spontaneous contractile activity in the transition zone of the human prostate gland. Four minute traces are illustrated for (**a**) control and (**b**) t = 30 min. There were no significant effects on spontaneous contractile activity parameters upon 30 min of incubation of 1.0 μM tetrodotoxin (Student's paired t-test, $p > 0.05$)

8.5.1 Role of Calcium in the Regulation of Spontaneous Activity

Spontaneous contractions in the transition zone of the human prostate were abolished within several minutes after Ca^{2+} removal from the bathing physiological salt solution (PSS). This effect was readily reversed when Ca^{2+} was restored (Fig. 8.5). This suggests that external Ca^{2+} plays an essential role in the generation and maintenance spontaneous contractions in the transition zone of the human prostate gland, presumably by entering through voltage or receptor operated channels.

The role of L-type and T-type voltage-dependent Ca^{2+} channels in the generation of spontaneous contractile activity has been comprehensively described in the guinea pig prostate [111, 124, 131, 137, 143]. Ca^{2+} entry through L-type voltage-dependent Ca^{2+} channels appears responsible for the generation of the plateau of the pacemaker potential and slow wave, while Ca^{2+} entry through T-type voltage-dependent Ca^{2+} channels contributes to the initial depolarisation phase [124]. L-type and T-type Ca^{2+} chan-

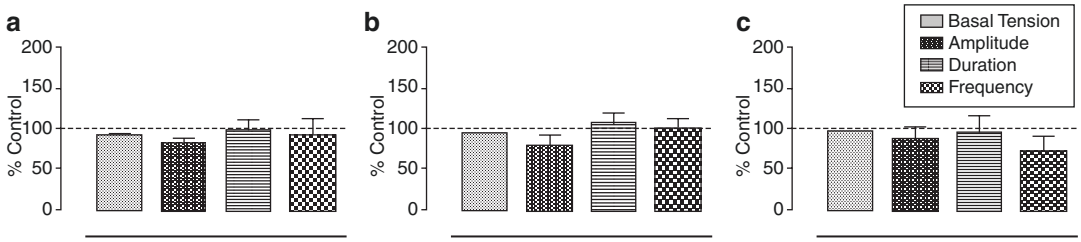

Fig. 8.4 Summary of the effects of (**a**) 1.0 μM tetrodotoxin, (**b**) 1.0 μM guanethidine, and (**c**) 1.0 μM atropine on spontaneous contractile activity in the transition zone of the human prostate gland, expressed as percentage of control data

Fig. 8.5 The effects of removing extracellular Ca^{2+} on spontaneous contractile activity in the transition zone of the human prostate gland. Five minute traces are illustrated for (**a**) control, (**b**) $t = 10$, (**c**) $t = 20$ min, washout of Ca^{2+}-free PSS. There was a time-dependent decrease in frequency of spontaneous contractions, and subsequent abolishment of activity within 20 min of incubation of Ca^{2+}-free PSS, and the effects were readily reversed when Ca^{2+} was restored in the physiological salt solution (**d**)

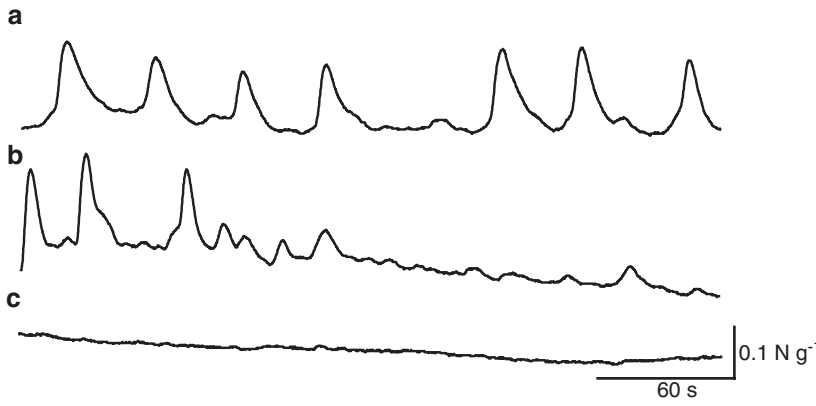

Fig. 8.6 The effects of 1.0 μM nifedipine on spontaneous contractile activity in the transition zone of the human prostate gland. Five minute traces are illustrated for (**a**) control, (**b**) $t = 0$, and (**c**) $t = 15$ min. There was a time-dependent decrease in frequency of spontaneous contractions (Student's paired t-test, $p < 0.05$), and subsequent abolishment of activity within 15 min of incubation of 1.0 μM nifedipine in 67% of preparation

nels have also been identified in isolated smooth muscle cells from the human prostate using patch clamp electrophysiology [135], with the L-type Ca^{2+} channel playing a more important role in the regulation of smooth muscle tone [134]. Spontaneous contractions in the transition zone of the human prostate are significantly reduced and subsequently abolished within 15 min of blocking L-type Ca^{2+} channels with nifedipine (Fig. 8.6). In contrast, both T- and L-type Ca^{2+} channels have been identified in guinea pig PICs; uniquely, T-type but not L-type Ca^{2+} currents in some PICs also selectively activate a Ca^{2+}-activated Cl^- current (CaCC) [138], suggesting a

functional coupling of T-type voltage-dependent Ca^{2+} channels with CaCCs [118].

In addition to extracellular sources, the cycle of release and reuptake of Ca^{2+} from intracellular stores within the sarcoplasmic reticulum can regulate the level of cytosolic Ca^{2+} in smooth muscle [144]. IP_3 and ryanodine receptors localised to the sarcoplasmic reticulum act as Ca^{2+} release channels in smooth muscle [145, 146]. In our preliminary study of human prostate, preventing Ca^{2+} reuptake upon blocking the sarcoplasmic/endoplasmic reticulum Ca^{2+}-ATPase (SERCA) pump with cyclopiazonic acid (CPA) resulted in a 34% reduction in contraction frequency of the transition zone. Inhibiting the buffering of cytosolic Ca^{2+} by using a mitochondrial uncoupler, CCCP, also reduced the amplitude and frequency of spontaneous contractions by 27% and 51%, respectively (Exintaris, unpublished observations).

The important role of intracellular Ca^{2+} cycling and buffering by the sarcoplasmic reticulum and mitochondria has previously been demonstrated in pacemaker potentials recorded from the guinea pig prostate, where the application of CPA (10 μM) and CCCP (1 μM) abolished pacemaker potential discharge [130]. The application of CPA (10 μM) reduced the frequency of spontaneous slow waves, while the addition of CCCP (1 μM) depolarised the membrane potential before abolishing spontaneous slow wave activity [147]. Prostatic contractions and slow waves are similarly reduced when IP_3-dependent Ca^{2+} release is inhibited with 2-aminoethoxydiphenylborate (2-APB), when phospholipase C formation of IP_3 is blocked with U73122 or neomycin, or when IP_3 binding is antagonised with xestospongin C [136]. In contrast, application of ryanodine, which causes the sustained opening of ryanodine receptor channels and depletion of their stores, produces a small transient increase of slow wave frequency [147, 148]. See Lam et al. (2011) [148] and Lang and Hashitani (2017) [124] for a detailed presentation of the Ca^{2+} signalling in guinea pig PICs and smooth muscle cells and their dependence on Ca^{2+} entry and internal stores in whole mount preparations or single cells after enzymatic isolation.

8.5.2 Role of Ca^{2+}-Activated Cl^- (Cl_{Ca}) Channels in the Regulation of Spontaneous Activity

Mechanisms involved in the regulation of cytosolic Ca^{2+} levels by intracellular stores, with the subsequent activation of Cl_{Ca} channels and the generation of spontaneous electrical events have been established in bladder [149] and urethral [150] interstitial cells. In the transition zone of the human prostate, blocking Cl_{Ca} channels with niflumic acid resulted in a reduction in amplitude and frequency of spontaneous contractions by approximately 49% and 68%, respectively. Similarly, application of Cl_{Ca} channel blockers to the guinea pig prostate, results in the blockade of pacemaker potentials [130] and reduction of the spontaneous electrical slow wave activity [151]. It is believed that changes in cytosolic Ca^{2+} levels upon the release of Ca^{2+} from intracellular stores trigger the opening of Cl_{Ca} channels, that results in a pacemaker potential which propagates into neighbouring smooth muscle cells as a slow wave to open L-type Ca^{2+} channels, Ca^{2+} entry and contraction [118]. A new class of Cl_{Ca} channels, the anoctamin 1 (ANO1)/Tmem16a channel, has been identified with a single channel conductance [152, 153] similar to the channel underlying the ICC pacemaker current, which is also sensitive to niflumic acid [154]. In the GI tract, the identical distribution of ANO1/Tmem18a and c-Kit has been revealed using immunohistochemistry and genetic microarray studies [155, 156], indicating that ANO1 is a functional marker for gastrointestinal ICC. ANO1 expression has also been identified in BPH patient specimens from human tissue arrays by immunohistochemical staining [157]. A model of PIC Ca^{2+} signalling and ion channel activation in PIC pacemaking, slow wave generation and spontaneous prostatic contractions has recently been described [124].

8.6 Clinical Relevance of Spontaneous Prostate Contractility

Spontaneous contractions have been hypothesised to be involved in preventing stasis of prostatic fluids in the acini before ejacuation and regulating the overall resting smooth muscle tone of the prostate [111, 112]. During the pathogenesis of BPH, the overall cellular composition of the prostate is significantly altered, leading researchers to hypothesise that spontaneous contractions would be similarly dysregulated by the disease. In the prostate of rats treated with estradiol, a hormone implicated in the development of BPH, the number of PICs identified by c-Kit staining was significantly upregulated [113]. Gevaert et al. observed a semi-quantitative increase in the number of Kit-negative sub-epithelial interstitial cells, in tissues collected from men with BPH compared to benign samples [129]. A recent publication reported an increased frequency of myogenic contractions in human specimens collected from men with clinically diagnosed BPH, when compared to both age- and prostate volume-matched controls [141]. Therefore, targeting myogenic contractility, and its underlying spontaneous electrical activity, is of interest in the treatment of BPH.

8.6.1 Current Pharmaceutical Treatments of Benign Prostatic Hyperplasia

The primary aims of BPH therapy in patients are to alleviate distressing LUTS, improve the quality of life, and prevent further complications such as urinary retention, upper urinary tract dilation or urinary infections. The treatment of LUTS is dependent on the severity of the symptoms, the degree of bother and patient preference. Current management of LUTS associated with BPH can be separated into three categories: conservative treatment for mild symptoms and drug or surgical treatments for moderate to severe symptoms [158–160]. Men with mild, but not significantly bothersome symptoms are managed conservatively by watchful waiting, which includes education, reassurance, lifestyle advice, and periodic monitoring of symptoms [158–160]. Drug treatment is considered for patients who exhibit troublesome symptoms and when there is a preference for drug treatment over surgery, or if surgery is not indicated. Current drug therapies for BPH in Australia include: selective α_{1A}-adrenoceptor antagonists ('α-blockers'), alfuzosin, prazosin, tamsulosin and terazosin; 5-α-reductase inhibitors, dutasteride and finasteride; combination treatments, tamsulosin with dutasteride, and the recently approved PDE5 inhibitor tadalafil [160]. However, there is an overall unpredictable effectiveness associated with current drug therapies, with as many as 30% of patients who receive selective α-blockers and/or 5-α-reductase inhibitors for BPH report less than sufficient improvement in symptoms [161], thus prompting the need for advances and improvement in the treatment of LUTS associated with BPH. Currently, surgical treatment is an appropriate option when symptoms are severe, where drug treatment is ineffective or not tolerated, or when there are complications leading to acute urinary retention [158–160].

8.6.1.1 α-Blockers

The rationale for the use of α-blockers was based on the observation that phenoxybenzamine, an alpha adrenoceptor antagonist, blocked contractions induced by noradrenaline in isolated strips of rat prostate [162]. Application of Tamsulosin (at 0.3 nM concentration), a commonly prescribed α-blocker, also decreases the frequency of slow wave activity in the guinea pig prostate, completely abolishes spontaneous contractions in 5/9 preparations, and reduces significantly the frequency of contractions in the remaining preparations [163]. Further studies using strips of isolated human prostate tissue concluded that the α1A-adrenoceptor subtype-mediated contractile response to noradrenaline [65]. Additionally, it was found that tissue collected from the prostate capsule of men with symptomatic BPH had a four-fold greater maximal contractile response

to phenylephrine, a selective α1-adrenoceptor agonist, than tissue from men with asymptomatic disease [164]. In preparations of transition zone tissue, tamsulosin (0.1 nM) significantly reduced all myogenic contractile parameters, notably amplitude and frequency. However, there was a notable interpatient variability in the percentage decrease in response to tamsulosin [141]. Regression analysis against clinical parameters established a positive correlation between both age and prostate volume with percentage reduction; indicating that tissue from older men, or those with larger prostates, was more significantly attenuated. Along with the increased density of α1-adrenoceptors in the human prostate with age [165], this data provides further rationale for the use of α1-adrenoceptor antagonists specifically in older men (>70 years), or those with larger prostates (>40 cc).

Improvements in symptoms generally take a few weeks to develop, but significant efficacy over placebo has been observed within hours to days [166]. Most common adverse effects include orthostatic hypotension, dizziness, nasal congestion, headache, weakness, fatigue, drowsiness, intraoperative floppy iris syndrome in cataract surgery [167], abnormal ejaculation [168], and particular caution is required when treating patients with cardiovascular comorbidities [169]. Furthermore, there is no reduction in the rate of acute urinary retention or the need for further surgical intervention with the use of selective α-blockers, demonstrating that the risk of disease progression is not reduced [170, 171]. However, selective α-blockers continue to be the first-line drug treatment for symptomatic relief of BPH due to their rapid onset of action, and reasonably good efficacy.

8.6.1.2 PDE5 Inhibitors

PDE5 inhibitors have recently been added to the Australian Medicines Handbook as a treatment option for BPH. However, as PDE5 inhibitors were initially approved for the treatment of erectile dysfunction, there is little proof-of-mechanism data about their role within the prostate [172]. PDE5 is the most commonly expressed PDE within the prostate, although the isoforms PDE4 and PDE9 have also been identified. Slow wave activity was completely abolished by the NO donor, sodium nitroprusside (SNP) in young and old guinea pig prostates. Similarly, another NO donor *S*-nitroso-*N*-acetylpenicillamine (SNAP) reduced slow wave discharge [130]. Addition of L-arginine, the amino acid from which NO is derived, resulted in a decrease in the frequency of spontaneous contractions in both young and old guinea pig prostates [173]. Based on the addition of several agonists and antagonists of the NO/cGMP pathway, Dey et al. concluded that NO/cGMP pathway stimulation attenuated the frequency of spontaneous contractions. The young guinea pig prostate was significantly more affected by agonists of the NO/cGMP pathway, suggesting that age may attenuate tissue responses to NO [173]. In human tissue, application of sildenafil significantly decreased the frequency of spontaneous contractions, with considerable interpatient variability in their response noted [141]. As observed in the guinea pig prostate, regression analysis indicated responsiveness was inversely correlated to age. Therefore, tissue collected from older patients was less responsive to PDE5 inhibitors. This observation is supported by a recent meta-analysis that found older patients experienced limited improvement in International Prostate Symptom Score (IPSS) with PDE5 inhibitors compared to younger men [172], which correlates well with the higher PDE5 expression levels in prostate tissue of younger patients [141].

8.6.2 Future Directions and Implications

The pharmacological treatment for BPH targeting the dynamic component of BPH is currently limited to α-blockers and PDE5 inhibitors. The side effects of these pharmacotherapies, and their limited clinical efficacies in certain men have contradicted their use. Therefore, there is a need to develop further pharmacotherapies. Targeting of myogenic tone is of interest, as the frequency of myogenic contractions is significantly upregulated in men with BPH. There is a strong correlation between the functional response observed in

the guinea pig and human prostate contractions, particularly in response to PDE5 inhibitors where older tissue was less responsive, to clinical outcomes, where PDE5 inhibitors are less clinically effective in older men. Future potential pharmacotherapies for the treatment of BPH should be assessed for their efficacy at attenuating myogenic tone, with individual patient responses stratified to ensure that each patient is prescribed the right pharmacotherapy, at the right time in their life for maximal clinical benefit.

8.7 Concluding Remarks

The prostate is a glandular organ within the male reproductive tract that produces ions and proteins for the semen to help support sperm on its journey through the female reproductive tract. The prostate consists of an epithelial compartment, which produces and secretes prostatic secretions, and an overlying stroma, which facilitates the movement of secretions from the ductal structures to the proximal urethra during ejaculation. The development and growth of the prostate is dependent on androgens, particularly testosterone, and undergoes three periods of growth; the first occurs during embryonic development, the second during puberty, and a third, pathophysiological, period of growth commencing in the fourth decade of life, resulting in BPH. BPH results in both an excess growth of the prostate, and changes to the contractility and innervation of the smooth muscle. Innervation of the smooth muscle is predominantly sympathetic, with noradrenaline the primary neurotransmitter released within the prostate. Cholinergic and non-adrenergic, non-cholinergic innervation are also present, which can modulate smooth muscle tone.

The role of neurogenic contractions in the regulation of smooth muscle tone, and in prostatic urethral resistance has been extensively studied. However, only a few studies have focused on the role of spontaneous contractions in the regulation of smooth muscle tone in the guinea pig and human prostate gland. Spontaneous prostatic contractions are thought to be responsible for generating the smooth muscle tone and play an important role in determining prostatic urethral resistance. Smooth muscle tone is a major component associated in the pathophysiology of LUTS associated with BPH and results in a dynamic increase in prostatic urethral resistance and compensatory changes in bladder function in response to the urethral obstruction. However, the fundamental reason why there is an increase in smooth muscle tone in the transition zone of the human prostate remains poorly understood.

Finally, BPH is the most common benign neoplasm in ageing men, with an increase in prevalence with age. With an ageing population, the incidence of BPH will continue to increase. Patients with BPH exhibit LUTS which severely affect their quality of life and the economic impact is considerable. Current management of LUTS associated with BPH includes using selective α-blockers and 5-α-reductase inhibitors. However, there are many setbacks associated with current standards of care, prompting the need for advances and improvement in the treatment of LUTS associated with BPH. Further elucidation of the mechanisms underlying the spontaneous contractions in the prostate may ultimately identify alternative therapeutic targets to improve the treatment of LUTS associated with BPH.

References

1. Wein AJ, Kavoussi LR, Novick AC, Partin AW, Peters CA. Campbell-Walsh urology. 10th ed. Philadelphia: Saunders; 2011.
2. Amelar RD, Hotchkiss RS. The split ejaculate: its use in the management of male infertility. Fertil Steril. 1965;16:46–60.
3. Tauber PF, Zaneveld LJ, Propping D, Schumacher GF. Components of human split ejaculates. I. Spermatozoa, fructose, immunoglobulins, albumin, lactoferrin, transferrin and other plasma proteins. J Reprod Fertil. 1975;43(2):249–67.
4. Tauber PF, Zaneveld LJ, Propping D, Schumacher GF. Components of human split ejaculates. II. Enzymes and proteinase inhibitors. J Reprod Fertil. 1976;46(1):165–71.
5. Kavanagh JP. Isocitric and citric acid in human prostatic and seminal fluid: implications for prostatic metabolism and secretion. Prostate. 1994;24(3):139–42.
6. van der Graaf M, Schipper RG, Oosterhof GO, Schalken JA, Verhofstad AA, Heerschap A. Proton MR spectroscopy of prostatic tissue focused on

the detection of spermine, a possible biomarker of malignant behavior in prostate cancer. MAGMA. 2000;10(3):153–9.
7. Bedwal RS, Bahuguna A. Zinc, copper and selenium in reproduction. Experientia. 1994;50(7):626–40.
8. Ablin RJ, Soanes WA, Bronson P, Witebsky E. Precipitating antigens of the normal human prostate. J Reprod Fertil. 1970;22(3):573–4.
9. Rittenhouse HG, Finlay JA, Mikolajczyk SD, Partin AW. Human Kallikrein 2 (hK2) and prostate-specific antigen (PSA): two closely related, but distinct, kallikreins in the prostate. Crit Rev Clin Lab Sci. 1998;35(4):275–368.
10. Nelson PS, Gan L, Ferguson C, Moss P, Gelinas R, Hood L, et al. Molecular cloning and characterization of prostase, an androgen-regulated serine protease with prostate-restricted expression. Proc Natl Acad Sci U S A. 1999;96(6):3114–9.
11. Chu TM, Wang MC, Kuciel R, Valenzuela L, Murphy GP. Enzyme markers in human prostatic carcinoma. Cancer Treat Rep. 1977;61(2):193–200.
12. Dube JY, Frenette G, Paquin R, Chapdelaine P, Tremblay J, Tremblay RR, et al. Isolation from human seminal plasma of an abundant 16-kDa protein originating from the prostate, its identification with a 94-residue peptide originally described as beta-inhibin. J Androl. 1987;8(3):182–9.
13. Lin MF, Clinton GM. Human prostatic acid phosphatase has phosphotyrosyl protein phosphatase activity. Biochem J. 1986;235(2):351–7.
14. Niemi M, Harkonen M, Larmi TK. Enzymic histochemistry of human prostate. Localization of oxidative enzymes, esterase, and aminopeptidase in the normal and hyperplastic human prostate. Arch Pathol. 1963;75:528–37.
15. Denis LJ, Prout GR Jr. Lactic dehydrogenase in prostatic cancer. Investig Urol. 1963;1:101–11.
16. Grayhack JT, Wendel EF, Oliver L, Lee C. Analysis of specific proteins in prostatic fluid for detecting prostatic malignancy. J Urol. 1979;121(3):295–9.
17. McNeal JE. Regional morphology and pathology of the prostate. Am J Clin Pathol. 1968;49(3):347–57.
18. McNeal JE. The prostate and prostatic urethra: a morphologic synthesis. J Urol. 1972;107(6):1008–16.
19. McNeal JE. Origin and evolution of benign prostatic enlargement. Investig Urol. 1978;15(4):340–5.
20. McNeal JE. The zonal anatomy of the prostate. Prostate. 1981;2(1):35–49.
21. McNeal JE. Normal histology of the prostate. Am J Surg Pathol. 1988;12(8):619–33.
22. Ayala AG, Ro JY, Babaian R, Troncoso P, Grignon DJ. The prostatic capsule: does it exist? Its importance in the staging and treatment of prostatic carcinoma. Am J Surg Pathol. 1989;13(1):21–7.
23. Oliveira DS, Dzinic S, Bonfil AI, Saliganan AD, Sheng S, Bonfil RD. The mouse prostate: a basic anatomical and histological guideline. Bosn J Basic Med Sci. 2016;16(1):8–13.
24. Neuhaus D, Mondry S. Comparative anatomy of the male guinea-pig and human lower urinary tract: histomorphology and three-dimensional reconstruction. Anat Histol Embryol. 2001;30(3):185–92.
25. Wang Y, Hayward S, Cao M, Thayer K, Cunha G. Cell differentiation lineage in the prostate. Differentiation. 2001;68(4–5):270–9.
26. Cunha GR, Hayward SW, Wang YZ, Ricke WA. Role of the stromal microenvironment in carcinogenesis of the prostate. Int J Cancer. 2003;107(1):1–10.
27. Toivanen R, Shen MM. Prostate organogenesis: tissue induction, hormonal regulation and cell type specification. Development. 2017;144(8):1382–98.
28. Gkonos PJ, Krongrad A, Roos BA. Neuroendocrine peptides in the prostate. Urol Res. 1995;23(2):81–7.
29. Shafik A, Shafik I, el-Sibai O. Identification of c-kit-positive cells in the human prostate: the interstitial cells of Cajal. Arch Androl. 2005;51(5):345–51.
30. Huizinga JD, Liu LW, Blennerhassett MG, Thuneberg L, Molleman A. Intercellular communication in smooth muscle. Experientia. 1992;48(10):932–41.
31. El-Alfy M, Pelletier G, Hermo LS, Labrie F. Unique features of the basal cells of human prostate epithelium. Microsc Res Tech. 2000;51(5):436–46.
32. Kellokumpu-Lehtinen P, Santti R, Pelliniemi LJ. Correlation of early cytodifferentiation of the human fetal prostate and Leydig cells. Anat Rec. 1980;196(3):263–73.
33. Farnsworth WE, Brown JR. Testosterone metabolism in the prostate. Natl Cancer Inst Monogr. 1963;12:323–9.
34. Shimazaki J, Kurihara H, Ito Y, Shida K. Metabolism of testosterone in prostate. 2. Separation of prostatic 17-beta-ol-dehydrogenase and 5-alpha-reductase. Gunma J Med Sci. 1965;14(4):326–33.
35. Wilson JD. The critical role of androgens in prostate development. Endocrinol Metab Clin N Am. 2011;40(3):577–90.. ix
36. Cunha GR, Donjacour AA, Cooke PS, Mee S, Bigsby RM, Higgins SJ, et al. The endocrinology and developmental biology of the prostate. Endocr Rev. 1987;8(3):338–62.
37. Prins GS, Putz O. Molecular signaling pathways that regulate prostate gland development. Differentiation. 2008;76(6):641–59.
38. Silver RI, Wiley EL, Thigpen AE, Guileyardo JM, McConnell JD, Russell DW. Cell type specific expression of steroid 5 alpha-reductase 2. J Urol. 1994;152(2 Pt 1):438–42.
39. Bartsch G, Muller HR, Oberholzer M, Rohr HP. Light microscopic stereological analysis of the normal human prostate and of benign prostatic hyperplasia. J Urol. 1979;122(4):487–91.
40. Roehrborn CG. Pathology of benign prostatic hyperplasia. Int J Impot Res. 2008;20(Suppl 3):S11–8.
41. Adorini L, Penna G, Fibbi B, Maggi M. Vitamin D receptor agonists target static, dynamic, and inflammatory components of benign prostatic hyperplasia. Ann N Y Acad Sci. 2010;1193:146–52.
42. McNeal J. Pathology of benign prostatic hyperplasia. Insight into etiology. Urol Clin North Am. 1990;17(3):477–86.

43. Shapiro E, Hartanto V, Lepor H. Quantifying the smooth muscle content of the prostate using double-immunoenzymatic staining and color assisted image analysis. J Urol. 1992;147(4):1167–70.
44. Shapiro E, Hartanto V, Lepor H. The response to alpha blockade in benign prostatic hyperplasia is related to the percent area density of prostate smooth muscle. Prostate. 1992;21(4):297–307.
45. Berry SJ, Strandberg JD, Saunders WJ, Coffey DS. Development of canine benign prostatic hyperplasia with age. Prostate. 1986;9(4):363–73.
46. Ehrlich Y, Foster RS, Bihrle R, Cheng L, Tong Y, Koch MO. Division of prostatic anterior fibromuscular stroma reduces urethral resistance in an ex vivo human prostate model. Urology. 2010;76(2):511.e10–3.
47. Barry MJ, Cockett AT, Holtgrewe HL, McConnell JD, Sihelnik SA, Winfield HN. Relationship of symptoms of prostatism to commonly used physiological and anatomical measures of the severity of benign prostatic hyperplasia. J Urol. 1993;150(2 Pt 1):351–8.
48. Cunha GR, Chung LW, Shannon JM, Taguchi O, Fujii H. Hormone-induced morphogenesis and growth: role of mesenchymal-epithelial interactions. Recent Prog Horm Res. 1983;39:559–98.
49. Isaacs JT. Prostate stem cells and benign prostatic hyperplasia. Prostate. 2008;68(9):1025–34.
50. Kramer G, Mitteregger D, Marberger M. Is benign prostatic hyperplasia (BPH) an immune inflammatory disease? Eur Urol. 2007;51(5):1202–16.
51. Kondo S, Tashima Y, Morita T. Quantitative analysis of adrenergic alpha-1 and alpha-2 receptors in human prostatic urethral tissue. Br J Urol. 1993;72(1):68–73.
52. Yamada S, Ashizawa N, Ushijima H, Nakayama K, Hayashi E, Honda K. Alpha-1 adrenoceptors in human prostate: characterization and alteration in benign prostatic hypertrophy. J Pharmacol Exp Ther. 1987;242(1):326–30.
53. Nasu K, Moriyama N, Kawabe K, Tsujimoto G, Murai M, Tanaka T, et al. Quantification and distribution of alpha 1-adrenoceptor subtype mRNAs in human prostate: comparison of benign hypertrophied tissue and non-hypertrophied tissue. Br J Pharmacol. 1996;119(5):797–803.
54. Klotz T, Mathers MJ, Bloch W, Nayal W, Engelmann U. Nitric oxide based influence of nitrates on micturition in patients with benign prostatic hyperplasia. Int Urol Nephrol. 1999;31(3):335–41.
55. Chapple CR, Crowe R, Gilpin SA, Gosling J, Burnstock G. The innervation of the human prostate gland--the changes associated with benign enlargement. J Urol. 1991;146(6):1637–44.
56. Caine M, Raz S, Zeigler M. Adrenergic and cholinergic receptors in the human prostate, prostatic capsule and bladder neck. Br J Urol. 1975;47(2):193–202.
57. Vaalasti A, Hervonen A. Nerve endings in the human prostate. Am J Anat. 1980;157(1):41–7.
58. Higgins JR, Gosling JA. Studies on the structure and intrinsic innervation of the normal human prostate. Prostate Suppl. 1989;2:5–16.
59. Ichihara I, Kallio M, Pelliniemi LJ. Light and electron microscopy of the ducts and their subepithelial tissue in the rat ventral prostate. Cell Tissue Res. 1978;192(3):381–90.
60. Pennefather JN, Lau WA, Mitchelson F, Ventura S. The autonomic and sensory innervation of the smooth muscle of the prostate gland: a review of pharmacological and histological studies. J Auton Pharmacol. 2000;20(4):193–206.
61. Christ GJ, Andersson KE. Rho-kinase and effects of Rho-kinase inhibition on the lower urinary tract. Neurourol Urodyn. 2007;26(6 Suppl):948–54.
62. Chapple CR, Aubry ML, James S, Greengrass PM, Burnstock G, Turner-Warwick RT, et al. Characterisation of human prostatic adrenoceptors using pharmacology receptor binding and localisation. Br J Urol. 1989;63(5):487–96.
63. James S, Chapple CR, Phillips MI, Greengrass PM, Davey MJ, Turner-Warwick RT, et al. Autoradiographic analysis of alpha-adrenoceptors and muscarinic cholinergic receptors in the hyperplastic human prostate. J Urol. 1989;142(2 Pt 1):438–44.
64. Hieble JP, Caine M, Zalaznik E. In vitro characterization of the alpha-adrenoceptors in human prostate. Eur J Pharmacol. 1985;107(2):111–7.
65. Hedlund H, Andersson KE, Larsson B. Alpha-adrenoceptors and muscarinic receptors in the isolated human prostate. J Urol. 1985;134(6):1291–8.
66. Tsujii T, Azuma H, Yamaguchi T, Oshima H. A possible role of decreased relaxation mediated by beta-adrenoceptors in bladder outlet obstruction by benign prostatic hyperplasia. Br J Pharmacol. 1992;107(3):803–7.
67. Drescher P, Eckert RE, Madsen PO. Smooth muscle contractility in prostatic hyperplasia: role of cyclic adenosine monophosphate. Prostate. 1994;25(2):76–80.
68. Haynes JM. beta(2) and beta(3)-adrenoceptor inhibition of alpha(1)-adrenoceptor-stimulated Ca(2+) elevation in human cultured prostatic stromal cells. Eur J Pharmacol. 2007;570(1–3):18–26.
69. Goepel M, Wittmann A, Rubben H, Michel MC. Comparison of adrenoceptor subtype expression in porcine and human bladder and prostate. Urol Res. 1997;25(3):199–206.
70. Calmasini FB, Candido TZ, Alexandre EC, D'Ancona CA, Silva D, de Oliveira MA, et al. The beta-3 adrenoceptor agonist, mirabegron relaxes isolated prostate from human and rabbit: new therapeutic indication? Prostate. 2015;75(4):440–7.
71. Kyprianou N, Benning CM. Suppression of human prostate cancer cell growth by alpha1-adrenoceptor antagonists doxazosin and terazosin via induction of apoptosis. Cancer Res. 2000;60(16):4550–5.
72. Garrison JB, Kyprianou N. Doxazosin induces apoptosis of benign and malignant prostate cells via a death receptor-mediated pathway. Cancer Res. 2006;66(1):464–72.
73. Liou SF, Lin HH, Liang JC, Chen IJ, Yeh JL. Inhibition of human prostate cancer cells proliferation by a selective alpha1-adrenoceptor antagonist labedipinedilol-

A involves cell cycle arrest and apoptosis. Toxicology. 2009;256(1–2):13–24.
74. Hori Y, Ishii K, Kanda H, Iwamoto Y, Nishikawa K, Soga N, et al. Naftopidil, a selective {alpha}1-adrenoceptor antagonist, suppresses human prostate tumor growth by altering interactions between tumor cells and stroma. Cancer Prev Res (Phila). 2011;4(1):87–96.
75. Kanagawa K, Sugimura K, Kuratsukuri K, Ikemoto S, Kishimoto T, Nakatani T. Norepinephrine activates P44 and P42 MAPK in human prostate stromal and smooth muscle cells but not in epithelial cells. Prostate. 2003;56(4):313–8.
76. Bauer RM, Strittmatter F, Gratzke C, Gottinger J, Schlenker B, Reich O, et al. Coupling of alpha1-adrenoceptors to ERK1/2 in the human prostate. Urol Int. 2011;86(4):427–33.
77. Strittmatter F, Walther S, Roosen A, Rutz B, Schlenker B, Limmer S, et al. Activation of protein kinase B/Akt by alpha1-adrenoceptors in the human prostate. Life Sci. 2012;90(11–12):446–53.
78. Strittmatter F, Gratzke C, Walther S, Gottinger J, Beckmann C, Roosen A, et al. Alpha1-adrenoceptor signaling in the human prostate involves regulation of p38 mitogen-activated protein kinase. Urology. 2011;78(4):969.e7–13.
79. Roehrborn CG. Three months' treatment with the alpha1-blocker alfuzosin does not affect total or transition zone volume of the prostate. Prostate Cancer Prostatic Dis. 2006;9(2):121–5.
80. Andersson KE, Gratzke C. Pharmacology of alpha1-adrenoceptor antagonists in the lower urinary tract and central nervous system. Nat Clin Pract Urol. 2007;4(7):368–78.
81. Burnstock G. Purinergic signalling in the reproductive system in health and disease. Purinergic Signal. 2014;10(1):157–87.
82. Janssens R, Communi D, Pirotton S, Samson M, Parmentier M, Boeynaems JM. Cloning and tissue distribution of the human P2Y1 receptor. Biochem Biophys Res Commun. 1996;221(3):588–93.
83. Preston A, Frydenberg M, Haynes JM. A1 and A2A adenosine receptor modulation of alpha 1-adrenoceptor-mediated contractility in human cultured prostatic stromal cells. Br J Pharmacol. 2004;141(2):302–10.
84. Lam M, Mitsui R, Hashitani H. Electrical properties of purinergic transmission in smooth muscle of the guinea-pig prostate. Auton Neurosci. 2016;194:8–16.
85. Dunzendorfer U, Jonas D, Weber W. The autonomic innervation of the human prostate. Histochemistry of acetylcholinesterase in the normal and pathologic states. Urol Res. 1976;4(1):29–31.
86. Hedlund P, Ekstrom P, Larsson B, Alm P, Andersson KE. Heme oxygenase and NO-synthase in the human prostate—relation to adrenergic, cholinergic and peptide-containing nerves. J Auton Nerv Syst. 1997;63(3):115–26.
87. Vaalasti A, Hervonen A. Autonomic innervation of the human prostate. Investig Urol. 1980;17(4):293–7.
88. Witte LP, Chapple CR, de la Rosette JJ, Michel MC. Cholinergic innervation and muscarinic receptors in the human prostate. Eur Urol. 2008;54(2):326–34.
89. Seki N, Suzuki H. Electrical and mechanical activity of rabbit prostate smooth muscles in response to nerve stimulation. J Physiol. 1989;419:651–63.
90. Lau WA, Ventura S, Pennefather JN. Pharmacology of neurotransmission to the smooth muscle of the rat and the guinea-pig prostate glands. J Auton Pharmacol. 1998;18(6):349–56.
91. Lau WA, Pennefather JN, Mitchelson FJ. Cholinergic facilitation of neurotransmission to the smooth muscle of the guinea-pig prostate gland. Br J Pharmacol. 2000;130(5):1013–20.
92. Fernandez JL, Rivera L, Lopez PG, Recio P, Vela-Navarrete R, Garcia-Sacristan A. Characterization of the muscarinic receptor mediating contraction of the dog prostate. J Auton Pharmacol. 1998;18(4):205–11.
93. White CW, Short JL, Haynes JM, Matsui M, Ventura S. Contractions of the mouse prostate elicited by acetylcholine are mediated by M(3) muscarinic receptors. J Pharmacol Exp Ther. 2011;339(3):870–7.
94. Bloch W, Klotz T, Loch C, Schmidt G, Engelmann U, Addicks K. Distribution of nitric oxide synthase implies a regulation of circulation, smooth muscle tone, and secretory function in the human prostate by nitric oxide. Prostate. 1997;33(1):1–8.
95. Burnett AL, Maguire MP, Chamness SL, Ricker DD, Takeda M, Lepor H, et al. Characterization and localization of nitric oxide synthase in the human prostate. Urology. 1995;45(3):435–9.
96. Gradini R, Realacci M, Ginepri A, Naso G, Santangelo C, Cela O, et al. Nitric oxide synthases in normal and benign hyperplastic human prostate: immunohistochemistry and molecular biology. J Pathol. 1999;189(2):224–9.
97. Takeda M, Tang R, Shapiro E, Burnett AL, Lepor H. Effects of nitric oxide on human and canine prostates. Urology. 1995;45(3):440–6.
98. Haynes JM, Cook AL. Protein kinase G-induced activation of K(ATP) channels reduces contractility of human prostate tissue. Prostate. 2006;66(4):377–85.
99. Denninger JW, Marletta MA. Guanylate cyclase and the.NO/cGMP signaling pathway. Biochim Biophys Acta. 1999;1411(2–3):334–50.
100. Collins SP, Uhler MD. Cyclic AMP- and cyclic GMP-dependent protein kinases differ in their regulation of cyclic AMP response element-dependent gene transcription. J Biol Chem. 1999;274(13):8391–404.
101. Watts SW, Cohen ML. Effect of bombesin, bradykinin, substance P and CGRP in prostate, bladder body and neck. Peptides. 1991;12(5):1057–62.
102. Palea S, Corsi M, Artibani W, Ostardo E, Pietra C. Pharmacological characterization of tachykinin NK2 receptors on isolated human urinary bladder, prostatic urethra and prostate. J Pharmacol Exp Ther. 1996;277(2):700–5.

103. Langenstroer P, Tang R, Shapiro E, Divish B, Opgenorth T, Lepor H. Endothelin-1 in the human prostate: tissue levels, source of production and isometric tension studies. J Urol. 1993;150(2 Pt 1):495–9.
104. Kedia GT, Uckert S, Kedia M, Kuczyk MA. Effects of phosphodiesterase inhibitors on contraction induced by endothelin-1 of isolated human prostatic tissue. Urology. 2009;73(6):1397–401.
105. Gratzke C, Weinhold P, Reich O, Seitz M, Schlenker B, Stief CG, et al. Transient receptor potential A1 and cannabinoid receptor activity in human normal and hyperplastic prostate: relation to nerves and interstitial cells. Eur Urol. 2010;57(5):902–10.
106. Kitada S, Kumazawa J. Pharmacological characteristics of smooth muscle in benign prostatic hyperplasia and normal prostatic tissue. J Urol. 1987;138(1):158–60.
107. Strittmatter F, Gratzke C, Weinhold P, Steib CJ, Hartmann AC, Schlenker B, et al. Thromboxane A2 induces contraction of human prostate smooth muscle by Rho kinase- and calmodulin-dependent mechanisms. Eur J Pharmacol. 2011;650(2–3):650–5.
108. Walden PD, Lefkowitz GK, Ittmann M, Lepor H, Monaco ME. Mitogenic activation of human prostate-derived fibromuscular stromal cells by bradykinin. Br J Pharmacol. 1999;127(1):220–6.
109. Srinivasan D, Kosaka AH, Daniels DV, Ford AP, Bhattacharya A. Pharmacological and functional characterization of bradykinin B2 receptor in human prostate. Eur J Pharmacol. 2004;504(3):155–67.
110. Kester RR, Mooppan UM, Gousse AE, Alver JE, Gintautas J, Gulmi FA, et al. Pharmacological characterization of isolated human prostate. J Urol. 2003;170(3):1032–8.
111. Exintaris B, Klemm MF, Lang RJ. Spontaneous slow wave and contractile activity of the Guinea pig prostate. J Urol. 2002;168(1):315–22.
112. Van der Aa F, Roskams T, Blyweert W, De Ridder D. Interstitial cells in the human prostate: a new therapeutic target? Prostate. 2003;56(4):250–5.
113. Kusljic S, Exintaris B. The effect of estrogen supplementation on cell proliferation and expression of c-kit positive cells in the rat prostate. Prostate. 2010;70(14):1555–62.
114. Boesch ST, Dobler G, Ramoner R, Corvin S, Thurnher M, Bartsch G, et al. Effects of alpha1-adrenoceptor antagonists on cultured prostatic smooth muscle cells. Prostate Suppl. 2000;9:34–41.
115. Scarano WR, Cordeiro RS, Goes RM, Carvalho HF, Taboga SR. Tissue remodeling in Guinea pig lateral prostate at different ages after estradiol treatment. Cell Biol Int. 2005;29(9):778–84.
116. Cordeiro RS, Scarano WR, Goes RM, Taboga SR. Tissue alterations in the guinea pig lateral prostate following antiandrogen flutamide therapy. Biocell. 2004;28(1):21–30.
117. Horsfall DJ, Mayne K, Ricciardelli C, Rao M, Skinner JM, Henderson DW, et al. Age-related changes in guinea pig prostatic stroma. Lab Investig. 1994;70(5):753–63.
118. Shapiro E, Becich MJ, Hartanto V, Lepor H. The relative proportion of stromal and epithelial hyperplasia is related to the development of symptomatic benign prostate hyperplasia. J Urol. 1992;147(5):1293–7.
119. Crowcroft PJ, Szurszewski JH. A study of the inferior mesenteric and pelvic ganglia of Guinea-pigs with intracellular electrodes. J Physiol. 1971;219(2):421–41.
120. Yokota R, Burnstock G. Decentralisation of neurones in the pelvic ganglion of the guinea-pig: reinnervation by adrenergic nerves. Cell Tissue Res. 1983;232(2):399–411.
121. Ventura S, Lau WA, Buljubasich S, Pennefather JN. Calcitonin gene-related peptide (CGRP) inhibits contractions of the prostatic stroma of the rat but not the guinea-pig. Regul Pept. 2000;91(1–3):63–73.
122. Pennefather JN, Lau WA, Chin C, Story ME, Ventura S. alpha(1L)-adrenoceptors mediate noradrenaline-induced contractions of the guinea-pig prostate stroma. Eur J Pharmacol. 1999;384(1):25–30.
123. Najbar-Kaszkiel AT, Di Iulio JL, Li CG, Rand MJ. Characterisation of excitatory and inhibitory transmitter systems in prostate glands of rats, guinea pigs, rabbits and pigs. Eur J Pharmacol. 1997;337(2–3):251–8.
124. Lang RJ, Hashitani H. Role of prostatic interstitial cells in prostate motility. J Smooth Muscle Res. 2017;53(0):57–72.
125. Corradi LS, Jesus MM, Fochi RA, Vilamaior PS, Justulin LA Jr, Goes RM, et al. Structural and ultrastructural evidence for telocytes in prostate stroma. J Cell Mol Med. 2013;17(3):398–406.
126. Kusljic S, Dey A, Nguyen DTT, Lang RJ, Exintaris B. Prostatic interstitial cells in ageing guinea pig prostates. Curr Urol. 2007;1(3):141–4.
127. Leong KG, Wang BE, Johnson L, Gao WQ. Generation of a prostate from a single adult stem cell. Nature. 2008;456(7223):804–8.
128. Lammie A, Drobnjak M, Gerald W, Saad A, Cote R, Cordon-Cardo C. Expression of c-kit and kit ligand proteins in normal human tissues. J Histochem Cytochem. 1994;42(11):1417–25.
129. Gevaert T, Lerut E, Joniau S, Franken J, Roskams T, De Ridder D. Characterization of subepithelial interstitial cells in normal and pathological human prostate. Histopathology. 2014;65(3):418–28.
130. Lang RJ, Nguyen DT, Matsuyama H, Takewaki T, Exintaris B. Characterization of spontaneous depolarizations in smooth muscle cells of the Guinea pig prostate. J Urol. 2006;175(1):370–80.
131. Shigemasa Y, Lam M, Mitsui R, Hashitani H. Voltage dependence of slow wave frequency in the guinea pig prostate. J Urol. 2014;192(4):1286–92.
132. Oh SJ, Kim KM, Chung YS, Hong EK, Shin SY, Kim SJ. Ion-channel currents of smooth muscle cells isolated from the prostate of guinea-pig. BJU Int. 2003;92(9):1022–30.

133. Lang RJ, Mulholland E, Exintaris B. Characterization of the ion channel currents in single myocytes of the guinea pig prostate. J Urol. 2004;172(3):1179–87.
134. Eckert RE, Schreier U, Drescher P, Madsen PO, Derouet H, Becht E, et al. Regulation of prostatic smooth muscle contractility by intracellular second messengers: implications for the conservative treatment of benign prostatic hyperplasia. Urol Int. 1995;54(1):6–21.
135. Sui GP, Wu C, Fry CH. Ca2+ currents in smooth muscle cells isolated from human prostate. Prostate. 2004;59(3):275–81.
136. Dey A, Nguyen DT, Lang RJ, Exintaris B. Spontaneous electrical waveforms in aging guinea pig prostates. J Urol. 2009;181(6):2797–805.
137. Exintaris B, Nguyen DT, Dey A, Lang RJ. Spontaneous electrical activity in the prostate gland. Auton Neurosci. 2006;126-127:371–9.
138. Lang RJ, Tonta MA, Takano H, Hashitani H. Voltage-operated Ca(2) (+) currents and Ca(2) (+) -activated Cl(−) currents in single interstitial cells of the guinea-pig prostate. BJU Int. 2014;114(3):436–46.
139. Dey A, Kusljic S, Lang RJ, Exintaris B. Role of connexin 43 in the maintenance of spontaneous activity in the guinea pig prostate gland. Br J Pharmacol. 2010;161(8):1692–707.
140. Lam M, Kerr KP, Exintaris B. Involvement of Rho-kinase signaling pathways in nerve evoked and spontaneous contractions of the Guinea pig prostate. J Urol. 2013;189(3):1147–54.
141. Lee SN, Chakrabarty B, Wittmer B, Papargiris M, Ryan A, Frydenberg M, et al. Age related differences in responsiveness to sildenafil and tamsulosin are due to myogenic smooth muscle tone in the human prostate. Sci Rep. 2017;7(1):10150.
142. Powell MS, Li R, Dai H, Sayeeduddin M, Wheeler TM, Ayala GE. Neuroanatomy of the normal prostate. Prostate. 2005;65(1):52–7.
143. Nguyen DT, Dey A, Lang RJ, Ventura S, Exintaris B. Contractility and pacemaker cells in the prostate gland. J Urol. 2011;185(1):347–51.
144. Somlyo AP, Somlyo AV. Signal transduction and regulation in smooth muscle. Nature. 1994;372(6503):231–6.
145. Villa A, Podini P, Panzeri MC, Soling HD, Volpe P, Meldolesi J. The endoplasmic-sarcoplasmic reticulum of smooth muscle: immunocytochemistry of vas deferens fibers reveals specialized subcompartments differently equipped for the control of Ca2+ homeostasis. J Cell Biol. 1993;121(5):1041–51.
146. Herrmann-Frank A, Darling E, Meissner G. Functional characterization of the Ca(2+)-gated Ca2+ release channel of vascular smooth muscle sarcoplasmic reticulum. Pflugers Arch. 1991;418(4):353–9.
147. Exintaris B, Nguyen DT, Lam M, Lang RJ. Inositol trisphosphate-dependent Ca stores and mitochondria modulate slow wave activity arising from the smooth muscle cells of the Guinea pig prostate gland. Br J Pharmacol. 2009;156(7):1098–106.
148. Lam M, Shigemasa Y, Exintaris B, Lang RJ, Hashitani H. Spontaneous Ca2+ signaling of interstitial cells in the guinea pig prostate. J Urol. 2011;186(6):2478–86.
149. Johnston L, Carson C, Lyons AD, Davidson RA, McCloskey KD. Cholinergic-induced Ca2+ signaling in interstitial cells of Cajal from the guinea pig bladder. Am J Physiol Ren Physiol. 2008;294(3):F645–55.
150. Sergeant GP, Hollywood MA, McCloskey KD, McHale NG, Thornbury KD. Role of IP(3) in modulation of spontaneous activity in pacemaker cells of rabbit urethra. Am J Phys Cell Phys. 2001;280(5):C1349–56.
151. Nguyen DT, Lang RJ, Exintaris B. alpha(1)-adrenoceptor modulation of spontaneous electrical waveforms in the guinea-pig prostate. Eur J Pharmacol. 2009;608(1–3):62–70.
152. Caputo A, Caci E, Ferrera L, Pedemonte N, Barsanti C, Sondo E, et al. TMEM16A, a membrane protein associated with calcium-dependent chloride channel activity. Science. 2008;322(5901):590–4.
153. Yang YD, Cho H, Koo JY, Tak MH, Cho Y, Shim WS, et al. TMEM16A confers receptor-activated calcium-dependent chloride conductance. Nature. 2008;455(7217):1210–5.
154. Zhu MH, Kim TW, Ro S, Yan W, Ward SM, Koh SD, et al. A Ca(2+)-activated Cl(−) conductance in interstitial cells of Cajal linked to slow wave currents and pacemaker activity. J Physiol. 2009;587(Pt 20):4905–18.
155. Gomez-Pinilla PJ, Gibbons SJ, Bardsley MR, Lorincz A, Pozo MJ, Pasricha PJ, et al. Ano1 is a selective marker of interstitial cells of Cajal in the human and mouse gastrointestinal tract. Am J Physiol Gastrointest Liver Physiol. 2009;296(6):G1370–81.
156. Hwang SJ, Blair PJ, Britton FC, O'Driscoll KE, Hennig G, Bayguinov YR, et al. Expression of anoctamin 1/TMEM16A by interstitial cells of Cajal is fundamental for slow wave activity in gastrointestinal muscles. J Physiol. 2009;587(Pt 20):4887–904.
157. Liu W, Lu M, Liu B, Huang Y, Wang K. Inhibition of Ca(2+)-activated Cl(−) channel ANO1/TMEM16A expression suppresses tumor growth and invasiveness in human prostate carcinoma. Cancer Lett. 2012;326(1):41–51.
158. Oelke M, Bachmann A, Descazeaud A, Emberton M, Gravas S, Michel MC, et al. EAU guidelines on the treatment and follow-up of non-neurogenic male lower urinary tract symptoms including benign prostatic obstruction. Eur Urol. 2013;64(1):118–40.
159. McVary KT, Roehrborn CG, Avins AL, Barry MJ, Bruskewitz RC, Donnell RF, et al. Update on AUA guideline on the management of benign prostatic hyperplasia. J Urol. 2011;185(5):1793–803.
160. Rossi S, editor. Australian medicines handbook 2014. Adelaide: Australian Medicines Handbook Pty Ltd; 2014.

161. Roehrborn CG. Male lower urinary tract symptoms (LUTS) and benign prostatic hyperplasia (BPH). Med Clin North Am. 2011;95(1):87–100.
162. Raz S, Zeigler M, Caine M. Pharmacological receptors in the prostate. Br J Urol. 1973;45(6):663–7.
163. Chakrabarty B, Dey A, Lam M, Ventura S, Exintaris B. Tamsulosin modulates, but does not abolish the spontaneous activity in the guinea pig prostate gland. Neurourol Urodyn. 2015;34(5):482–8.
164. Lepor H, Gup DI, Baumann M, Shapiro E. Comparison of alpha 1 adrenoceptors in the prostate capsule of men with symptomatic and asymptomatic benign prostatic hyperplasia. Br J Urol. 1991;67(5):493–8.
165. Kojima Y, Sasaki S, Shinoura H, Hayashi Y, Tsujimoto G, Kohri K. Quantification of alpha1-adrenoceptor subtypes by real-time RT-PCR and correlation with age and prostate volume in benign prostatic hyperplasia patients. Prostate. 2006;66(7):761–7.
166. Oelke M, Giuliano F, Mirone V, Xu L, Cox D, Viktrup L. Monotherapy with tadalafil or tamsulosin similarly improved lower urinary tract symptoms suggestive of benign prostatic hyperplasia in an international, randomised, parallel, placebo-controlled clinical trial. Eur Urol. 2012;61(5):917–25.
167. Chang DF, Campbell JR. Intraoperative floppy iris syndrome associated with tamsulosin. J Cataract Refract Surg. 2005;31(4):664–73.
168. van Dijk MM, de la Rosette JJ, Michel MC. Effects of alpha(1)-adrenoceptor antagonists on male sexual function. Drugs. 2006;66(3):287–301.
169. Barendrecht MM, Koopmans RP, de la Rosette JJ, Michel MC. Treatment of lower urinary tract symptoms suggestive of benign prostatic hyperplasia: the cardiovascular system. BJU Int. 2005;95(Suppl 4):19–28.
170. McConnell JD, Roehrborn CG, Bautista OM, Andriole GL Jr, Dixon CM, Kusek JW, et al. The long-term effect of doxazosin, finasteride, and combination therapy on the clinical progression of benign prostatic hyperplasia. N Engl J Med. 2003;349(25):2387–98.
171. Roehrborn CG, Siami P, Barkin J, Damiao R, Major-Walker K, Nandy I, et al. The effects of combination therapy with dutasteride and tamsulosin on clinical outcomes in men with symptomatic benign prostatic hyperplasia: 4-year results from the CombAT study. Eur Urol. 2010;57(1):123–31.
172. Gacci M, Corona G, Salvi M, Vignozzi L, McVary KT, Kaplan SA, et al. A systematic review and meta-analysis on the use of phosphodiesterase 5 inhibitors alone or in combination with alpha-blockers for lower urinary tract symptoms due to benign prostatic hyperplasia. Eur Urol. 2012;61(5):994–1003.
173. Dey A, Lang RJ, Exintaris B. Nitric oxide signaling pathways involved in the inhibition of spontaneous activity in the guinea pig prostate. J Urol. 2012;187(6):2254–60.

9 Mucosa-Dependent, Stretch-Sensitive Spontaneous Activity in Seminal Vesicle

Mitsue Takeya, Tokumasa Hayashi, Hikaru Hashitani, and Makoto Takano

Abstract

Seminal vesicles (SVs), a pair of male accessory glands, contract upon sympathetic nerve excitation during ejaculation while developing spontaneous phasic constrictions in the inter-ejaculatory storage phase. Recently, the fundamental role of the mucosa in generating spontaneous activity in SV of the guinea pig has been revealed. Stretching the mucosa-intact but not mucosa-denuded SV smooth muscle evokes spontaneous phasic contractions arising from action potential firing triggered by electrical slow waves and associated Ca^{2+} flashes. These spontaneous events primarily depend on sarco-endoplasmic reticulum (SR/ER) Ca^{2+} handling linked with the opening of Ca^{2+}-activated chloride channels (CaCCs) resulting in the generation of slow waves. Slow waves in mucosa-intact SV smooth muscle are abolished upon blockade of gap junctions, suggesting that seminal smooth muscle cells are driven by cells distributed in the mucosa. In the SV mucosal preparations dissected free from the smooth muscle layer, a population of cells located just beneath the epithelium develop spontaneous Ca^{2+} transients relying on SR/ER Ca^{2+} handling. In the lamina propria of the SV mucosa, vimentin-immunoreactive interstitial cells including platelet-derived growth factor receptor α (PDGFRα)-immunoreactive cells are distributed, while known pacemaker cells in other smooth muscle tissues, e.g. c-Kit-positive interstitial cells or α-smooth muscle actin-positive atypical smooth muscle cells, are absent. The spontaneously-active subepithelial cells appear to drive spontaneous activity in SV smooth muscle either by sending depolarizing signals or by releasing humoral substances. Interstitial cells in the lamina propria may act as intermediaries of signal transmission from the subepithelial cells to the smooth muscle cells.

Electronic Supplementary Material The online version of this chapter (https://doi.org/10.1007/978-981-13-5895-1_9) contains supplementary material, which is available to authorized users.

M. Takeya (✉) · M. Takano
Division of Integrated Autonomic Function, Department of Physiology, Kurume University School of Medicine, Kurume, Japan
e-mail: takeya@med.kurume-u.ac.jp; takanom@med.kurume-u.ac.jp

T. Hayashi
Department of Urology, Kurume University School of Medicine, Kurume, Japan
e-mail: hayashi_tokumasa@kurume-u.ac.jp

H. Hashitani
Department of Cell Physiology, Graduate School of Medical Sciences, Nagoya City University, Nagoya, Japan
e-mail: hasitani@med.nagoya-cu.ac.jp

H. Hashitani, R. J. Lang (eds.), *Smooth Muscle Spontaneous Activity*, Advances in Experimental Medicine and Biology 1124, https://doi.org/10.1007/978-981-13-5895-1_9

Keywords
Seminal vesicle · Spontaneous contraction · Mucosa · Slow wave · Intracellular calcium release · Calcium-activated chloride channel · Stretch · Male reproductive glands · Seminal fluid · Male fertility

9.1 Introduction

Seminal vesicles (SVs), male accessory reproductive glands, produce the major components of the seminal fluid that is required for male fertility. Both sympathetic and parasympathetic nerves innervate the SVs and regulate their contractions and secretion [1, 2]. During emission, i.e., the early phase of ejaculation, SVs contract and expel their secretion into the urethra when noradrenaline is released from sympathetic nerve excitation and activates α_1-adrenoceptors (α_1-ARs) in SV smooth muscle [3]. Accordingly, silodosin, a selective α_{1A}-AR antagonist, used for the treatment for benign prostate hyperplasia (BPH), has a commonly seen adverse effect, namely ejaculation disorders [4] resulting from the impaired propulsion of the seminal fluid from the SVs [5, 6].

During the inter-ejaculatory storage phase, SVs do not remain quiescent; rather they generate spontaneous phasic contractions that do not rely on autonomic nervous activity. The spontaneous contractions of SVs may contribute to the maintenance of the quality of seminal fluid vital for male fertility. Despite the fact that the SV spontaneous contractions were first reported over a hundred years ago [7], the mechanisms underlying their generation are little understood. Recently, a critical role of the SV mucosa in generating spontaneous phasic contractions in SV smooth muscle of the guinea pig has been demonstrated [8]. In this chapter, properties of SV spontaneous contractions in several mammals are briefly summarized to update our knowledge of the mechanisms underlying SV spontaneous activity based on these recent findings.

9.2 Spontaneous Contractions Recorded from Rodent and Human SVs

9.2.1 Anatomy

9.2.1.1 Gross Anatomy

Human SVs form a paired saclike structure that joins the ampulla of the vas deferens to form the beginning of the ejaculatory ducts that pass through the prostate and terminate within the prostatic urethra [9]. Some rodents including guinea pig, rat, hamster, and mouse have a well-developed pair of SVs, while the domestic rabbit has a large unpaired SV [10, 11].

9.2.1.2 Microanatomy

The SV wall consists of the luminal epithelial layer, thin lamina propria, muscularis and an abluminal serosal layer [9, 12]. The muscularis of the guinea pig SVs is composed of an inner circular smooth muscle layer and an outer longitudinal layer confined to its urethral end. In the distal portion of SVs, only a layer of circularly orientated smooth muscle cells is present [2]. Electron microscopic studies of guinea pig SV revealed spindle-shaped fibroblasts that are distributed in the lamina propria just beneath the basement membrane of the epithelial cells [12, 13].

9.2.2 Spontaneous Contractions of SVs In Vivo

During inter-ejaculatory phases, SVs secrete and store their fluid contents. Spontaneous contractions during the storage phase in vivo have been reported by recording intraluminal pressure of the SVs in anesthetized rodents. In SVs of the adult rabbit, small irregular contractions are continuously generated without nerve stimulation [11]. The SVs of adult rat, which produce vigorous contractions in response to electrical nerve stimulation, also continually exhibit spontaneous phasic contractions during their inter-ejaculatory phases

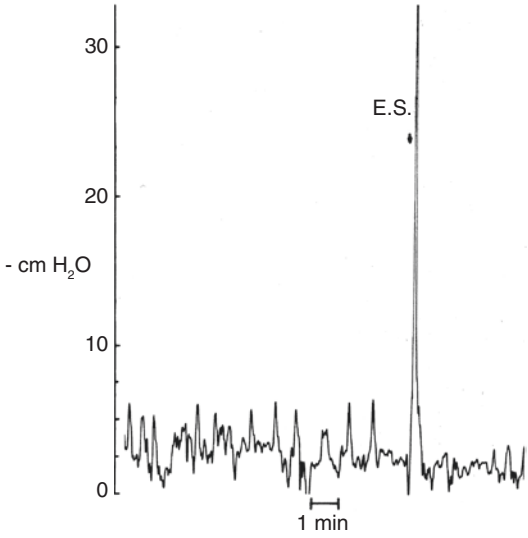

Fig. 9.1 In vivo recording of contractile activity of rat SV. Electrical nerve stimulation (E.S. *arrow*)-induced vigorous contraction and spontaneous irregular contractions (reproduced from Hib et al. [14] with permission of John Wiley & Sons). In further experiments by Hib et al. [15], the E.S.-induced contractions were confirmed to be prevented by phentolamine but not atropine

(Fig. 9.1 [14]). These spontaneous contractions are not affected by the administration of either phentolamine, a nonselective α-AR antagonist, or atropine, a muscarinic antagonist; however, these antagonists successfully prevent the facilitative effects of phenylephrine or acetylcholine (ACh), respectively, on SV contractions [15].

In 2-month-old adult rats, measurement of the luminal pressure during continuous infusion of SVs with normal saline demonstrates that the SV spontaneous contractions are more frequently seen at the nearly maximum infusion rate associated with organ distension [16].

9.2.3 Spontaneous Contractions in Excised Whole SVs

A recent study reported the contractile behavior of the excised guinea pig whole SVs during perfusion with physiological salt solution (PSS) by measuring their intraluminal pressure [6]. These "isolated" whole SVs develop irregular spontaneous phasic contractions independently of neuronal activity, as they are not affected by tetrodotoxin (TTX) that blocks nerve-evoked contractions (Video 9.1). The motility patterns of the spontaneous contractions in the whole SV preparations vary with time, and thus both retrograde and antegrade peristaltic contractions are randomly generated, indicating that any region of SVs can drive the contractions. Both frequency and amplitude of the spontaneous contractions are enhanced by increasing the internal hydrostatic pressure as the SVs are distended (Fig. 9.2). Nifedipine, a blocker of L-type voltage-dependent Ca^{2+} channels (LVDCCs), abolishes the spontaneous contractions [6], suggesting that the contractions primarily rely on the Ca^{2+} influx through LVDCCs.

9.2.4 Spontaneous Contractions of SVs In Vitro

"Spontaneous" rhythmic contractions in excised rat and guinea pig SV tissues were first recorded by Waddell in 1916 [7]. Later, spontaneous TTX-resistant, twitch-like contractions were recorded from the circular smooth muscle in the guinea pig SV [8, 17, 18]. Isometric tension recordings of human SV strips also demonstrate spontaneous contractions [19, 20].

The smooth muscle cells in circumferential muscle SV strips also develop TTX-insensitive spontaneous pacemaker-like depolarizations which trigger action potentials that are associated with the phasic contractions [21]. The generation of the spontaneous contractions is not inhibited upon blockade of α-ARs [18], nicotinic or muscarinic ACh receptors [17]. The periodical spontaneous contractions were generated in ring segments (4 mm width) obtained from either the proximal or distal guinea-pig SVs with a total length of 6–8 cm (M. Takeya and M. Takano, unpublished data). Thus, the site of origin of the SV periodical spontaneous contractions appears not to be localized but distributed along the whole organ.

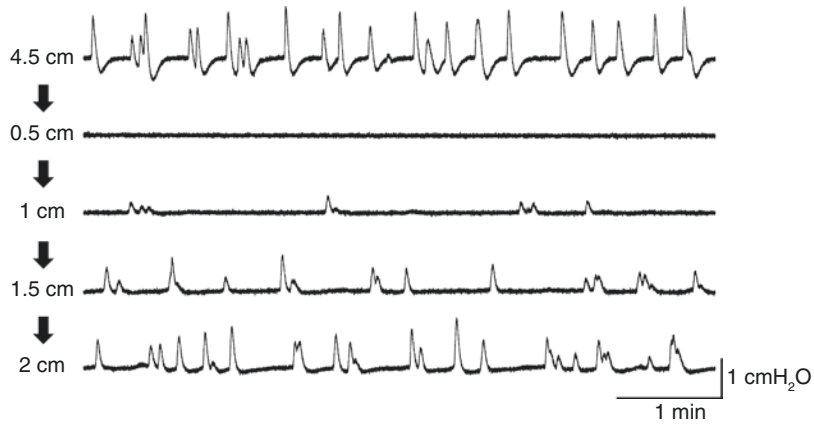

Fig. 9.2 TTX-insensitive phasic contractions in an "isolated" whole-guinea pig SV when the height of the liquid surface of the irrigator was set at 0.5–4.5 cm higher than the preparation. Application of the higher internal hydrostatic pressure by elevating the irrigator results in increasing the frequency of the SV contractions. Modified from Hayashi et al. [6]

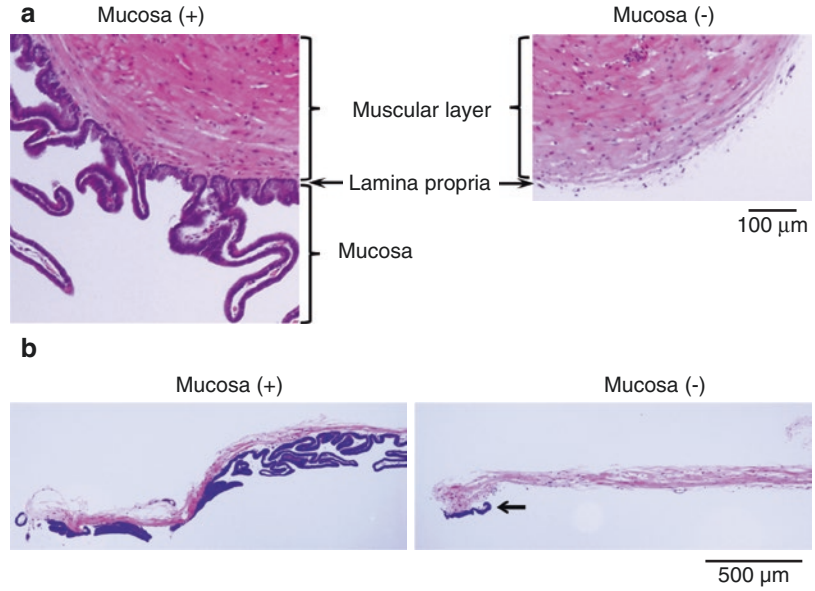

Fig. 9.3 Hematoxylin and eosin-stained coronal sections of mucosa-intact [*Mucosa* (+)] and -denuded [*Mucosa* (−)] guinea pig SV smooth muscle preparations. Reversed ring preparations which contained the whole muscular layer (**a**) were used for tension recordings. Membrane potentials or intracellular Ca^{2+} dynamics were recorded from inner smooth muscle preparations in which the bulk of muscular layers have been removed (**b**). In the right photograph in **b**, some mucosa was left attached to indicate the mucosal side (*arrow*). Adapted from Takeya et al. [8]

9.3 Role of Mucosa in Generating Spontaneous Activity of SV

Recently, the mechanisms underlying the spontaneous activity in adult guinea pig SV circular smooth muscle were investigated using mucosa-intact and mucosa-denuded smooth muscle preparations to explore the role of the mucosa [8].

9.3.1 Mucosa-Dependent Periodical Spontaneous Activity in SV Smooth Muscle

In mucosa-intact SV ring preparations containing the whole muscular layer (Fig. 9.3a), stretch of the wall induces periodical spontaneous contractions (at 36 °C) at a frequency ranging between 3 and 7 min^{-1} (Fig. 9.4a, Mucosa (+)). Mucosa-

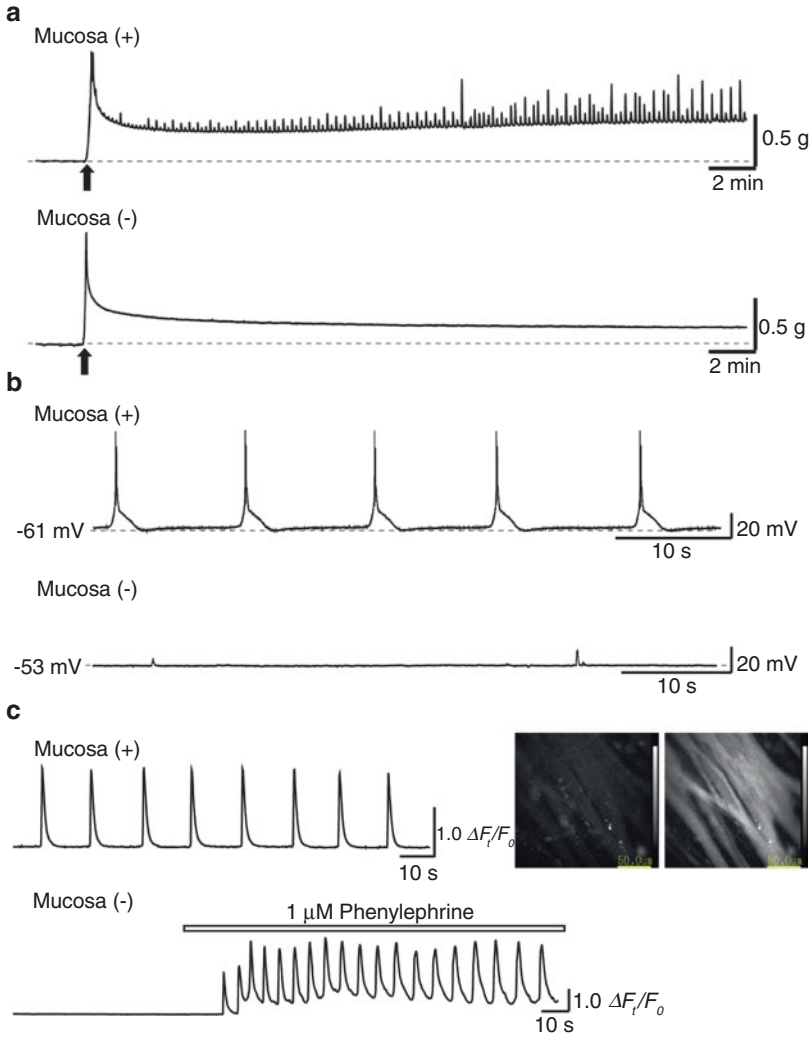

Fig. 9.4 Mucosa dependence of contractile, electrical, and Ca^{2+} activity in guinea pig SV smooth muscle. In mucosa-intact preparations [*Mucosa* (+)], stretched SV smooth muscle develops spontaneous phasic contractions (**a**), slow waves with superimposed action potentials (**b**), and synchronous Ca^{2+} flashes (**c**). *Arrows* indicate the timing of initial stretching to 1 g. Photographs in (**c**) are sequential Cal-520 fluorescence images (frame interval; 548 ms) of the mucosa-intact SV smooth muscle in normal PSS, showing that the spontaneous Ca^{2+} flashes were generated almost synchronously across SV smooth muscle cells. In contrast, mucosa-denuded SV smooth muscle [*Mucosa* (−)] fails to generate periodical spontaneous activity (**a**–**c**). Phenylephrine (1 μM) evoked oscillatory Ca^{2+} transients associated with phasic contractions in the quiescent mucosa-denuded SV smooth muscle (**c**). Adapted from Takeya et al. [8]

intact "trimmed" inner smooth muscle strips in which the bulk of muscular layers had been removed (Fig. 9.3b) also generate spontaneous contractions at a similar frequency. These spontaneous contractions appear to result from action potentials triggered by slow waves and associated Ca^{2+} flashes (Fig. 9.4b, c, Mucosa (+)). In contrast, mucosa-denuded SV smooth muscle preparations, in either a ring or strip configuration, invariably fail to generate spontaneous phasic contractions and periodical electrical or Ca^{2+} activity (Fig. 9.4a–c, Mucosa (−)). Despite the absence of spontaneous activity, the quiescent mucosa-denuded SV smooth muscle cells are

capable of generating action potentials in response to depolarizing current injection [8], as well as developing oscillatory Ca^{2+} transients and contractions upon α_1-AR stimulation (Fig. 9.4c). In addition, nerve-evoked contractions in the mucosa-denuded SV smooth muscle preparations are also well preserved, indicating that the lack of spontaneous activity is not due to impaired excitability or contractility of the SV upon removal of the mucosa. These observations are consistent with a previous report in which mucosa-denuded circular muscle strips of the guinea pig SVs do not exhibit spontaneous electrical activity and associated contractions, whereas electrical and Ca^{2+} activities are evoked by nerve excitation or α_1-AR stimulation [22].

9.3.2 Role of L-Type Voltage-Dependent Ca^{2+} Channels (LVDCCs) in Generating Spontaneous Activity in SV Smooth Muscle

Blockade of LVDCCs by 3 μM nifedipine abolishes the spontaneous phasic contractions in the mucosa-intact guinea pig SV smooth muscle (Fig. 9.5a). At a lower concentration of 1 μM,

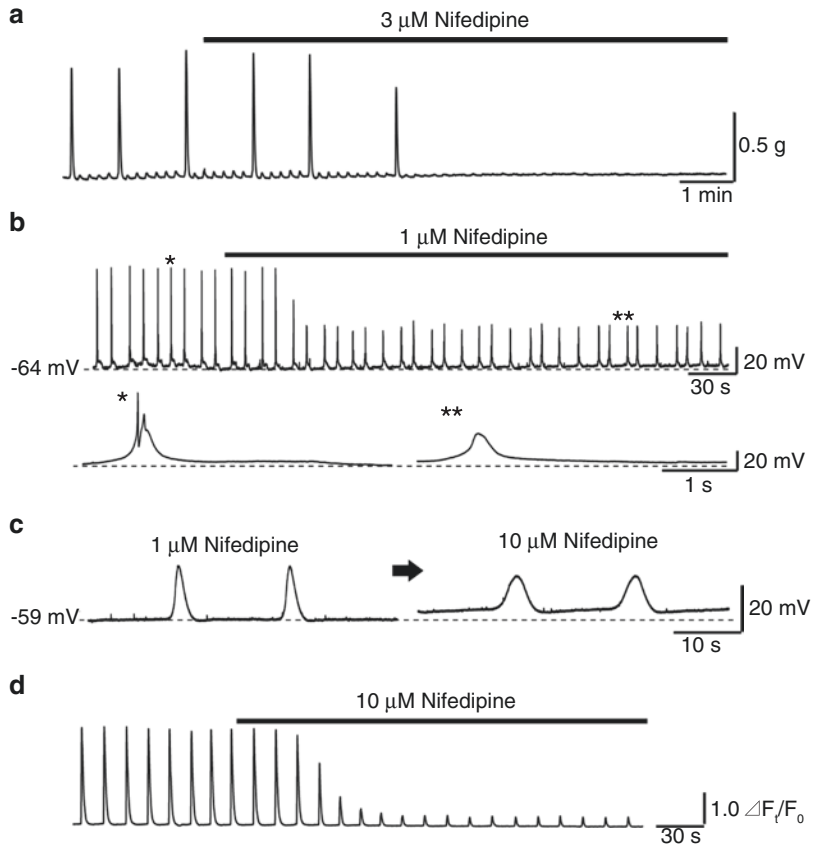

Fig. 9.5 Effects of nifedipine on spontaneous activity in mucosa-intact guinea pig SV smooth muscle. (**a**) Nifedipine (3 μM) abolished spontaneous phasic contractions in the mucosa-intact SV preparation. (**b**) Nifedipine (1 μM) abolished superimposed action potentials leaving slow waves. Lower traces show slow waves in control (*) and nifedipine (**) with an expanded time scale. Traces * and ** were obtained at the timings indicated by the corresponding marks in the upper trace. (**c**) In another mucosa-intact SV smooth muscle preparation, 10 μM nifedipine reduced the slow-wave amplitude, prolonged the slow-wave duration, and depolarized the membrane in the SV smooth muscle of control (in 1 μM nifedipine). (**d**) Spontaneous oscillatory Ca^{2+} flashes were strongly suppressed by 10 μM nifedipine. Adapted from Takeya et al. [8]

nifedipine greatly suppresses the spontaneous contractions and abolishes the superimposed action potentials without preventing the generation of slow waves (Fig. 9.5b). 10 μM Nifedipine largely suppresses spontaneous Ca^{2+} flashes (Fig. 9.5d). These results indicate that the spontaneous phasic contractions largely depend on Ca^{2+} influx via LVDCCs during action potential firing. Since the SV ring preparations consisting of the whole muscular layer develop both large and small phasic contractions (Figs. 9.4a and 9.5a), the electrical activity initiated presumably at the most inner layer of SV muscle facing to the mucosa may not consistently propagate across to the outer circular muscular layer. Similarly, the irregular spontaneous constrictions in the guinea pig-excised whole SVs [6] may result from inconsistent spread of electrical activity in both the transverse and axial directions within the SV wall. Thus, only the occasionally occurring, coordinated contractions of whole SV are strong enough to increase the intraluminal pressure, which may add further mechanical stimuli to the wall in other regions of the SV.

A higher concentration of 10 μM nifedipine reduces the slow-wave amplitude of the SV smooth muscle (Fig. 9.5c), suggesting that activation of LVDCCs partially contributes to the configuration of the slow wave. Thus, the contribution of LVDCCs to slow-wave configuration in the SV smooth muscle differs from that in the smooth muscle of guinea pig prostate [23], urethra of rabbit [24], or guinea pig [25], where LVDCC activation is involved in the plateau phase of the slow wave but not their initial upstroke.

10 μM Nifedipine depolarizes the membrane and also prolongs the slow-wave duration (Fig. 9.5c). Since TEA-sensitive, Ca^{2+}-dependent K^+ currents are recorded in the isolated smooth muscle cells of the guinea pig SV [26], it is likely that large-conductance Ca^{2+}-activated K^+ (BK) channels are activated upon Ca^{2+} entry through LVDCCs during the slow-wave generation. Thus, the blockade of LVDCCs by nifedipine may reduce the activation of BK channels in the SV smooth muscle, which causes membrane depolarization as well as prolongation of the slow-wave duration.

The frequency of the residual slow waves and spontaneous Ca^{2+} transients of SV smooth muscle are not largely affected by 10 μM nifedipine (Fig. 9.5c, d), suggesting that the intrinsic periodicity of spontaneous activity in SV smooth muscle does not depend on the activation of LVDCCs. Thus, the mucosa of guinea pig SV is fundamental in generating LVDCC-independent electrical activity in SV smooth muscle associated with Ca^{2+} transients. Mucosa-dependent slow waves trigger the activation of LVDCCs to amplify themselves resulting in action potential firing that appears to play a major role in generating contractions in SV smooth muscle. Synchrony of the periodical spontaneous Ca^{2+} transients in the SV smooth muscle cells is preserved during the blockade of LVDCCs by 10 μM nifedipine (Fig. 9.6b). This is in marked contrast to the spontaneous Ca^{2+} transients in atypical smooth muscle cells of the renal pelvis [27] or suburothelial venular smooth muscle cells [28, 29] in which LVDCCs play a critical role in maintaining the synchrony amongst spontaneously active cells.

9.3.3 Role of Intracellular Ca^{2+} Stores in Spontaneous Activity of SV Smooth Muscle

Blockade of SR/ER Ca^{2+}-ATPase (SERCA) by 10 μM cyclopiazonic acid (CPA) abolishes the slow waves and synchronous spontaneous Ca^{2+} transients in the 10 μM nifedipine-pretreated mucosa-intact SVs (Fig. 9.6), suggesting that both events depend on Ca^{2+} handling by the SR/ER. Thus, in common with most visceral smooth muscle organs, spontaneous phasic contractions in SV circular smooth muscle appear to be primarily driven by the cycle of Ca^{2+} uptake and release by the SR/ER. Since mucosa-denuded smooth muscle of guinea pig SVs develops LVDCC-independent, CPA-sensitive increases in intracellular Ca^{2+} concentration upon the activation of α_1-ARs that are known to couple with Gq proteins [22], inositol 1,4,5-trisphosphate (IP_3) receptors may well be involved in Ca^{2+} release

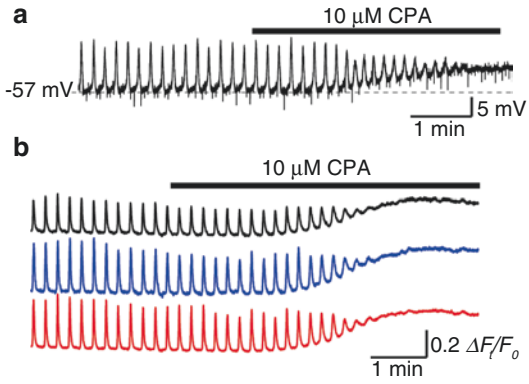

Fig. 9.6 Blockade of SERCA abolished nifedipine-resistant slow waves and spontaneous Ca^{2+} transients in mucosa-intact guinea pig SV smooth muscle. (**a**) In a 10 μM nifedipine-pretreated SV smooth muscle preparation, CPA depolarized the membrane by about 5 mV and prevented the generation of the slow waves. (**b**) Intracellular Ca^{2+} dynamics recorded from three regions of interest in another 10 μM nifedipine-pretreated SV smooth muscle preparation. Note that the synchrony of the spontaneous Ca^{2+} transients amongst smooth muscle cells was maintained in the presence of 10 μM nifedipine. CPA increased the basal Ca^{2+} level and abolished synchronous spontaneous Ca^{2+} transients. Reproduced from Takeya et al. [8]

from SR in SV smooth muscle. However, the relative contribution of IP_3- and ryanodine-receptor Ca^{2+} release channels to the generation of mucosa-dependent activity in SVs has not yet been established.

9.3.4 Role of Ca^{2+}-Activated Cl^- Channel in Spontaneous Activity of SV Smooth Muscle

The LVDCC-independent slow waves in the mucosa-intact guinea pig SV smooth muscle are abolished by lowering extracellular Cl^- concentration from 130 to 13 mM [8]. Nonselective Ca^{2+}-activated Cl^- channel (CaCC) blockers such as DIDS (300 μM) and niflumic acid (100 μM) also abolish or greatly reduce the generation of slow waves in 10 μM nifedipine-pretreated SV smooth muscle preparations [8]. Thus, generation of the slow waves in SV smooth muscle may depend on Cl^- efflux via CaCCs triggered by spontaneous Ca^{2+} release from the SR/ER. Similar mechanisms underlying the slow-wave generation have been confirmed in interstitial cells of Cajal (ICCs) in gastrointestinal (GI) tract [30] and urethra [31].

Anoctamin1 (ANO1) has been established to function as CaCCs that underlie slow waves in ICCs of the GI tract [30]. In guinea pig SV smooth muscle, 3 μM $T16A_{inh}$-A01, a selective ANO1 inhibitor, does not affect the SV slow-wave generation, suggesting the contribution of CaCCs other than ANO1 channels [8]. Since ANO1 immunoreactivity in the guinea pig SVs is restricted to the apical surface of the secretory columnar epithelium (Fig. 9.7), ANO1 channels appear to be involved in Cl^- secretion into seminal fluid [32–34] but not the generation of the SV slow waves.

9.4 How Does the Mucosa Drive Spontaneous Activity in SV Smooth Muscle?

9.4.1 Spontaneously Active Cells in SV Mucosa

Since an intact mucosa is required for generating synchronous spontaneous Ca^{2+} transients and corresponding CaCC-dependent slow waves in guinea pig SV smooth muscle, both events may be driven by spontaneously active cells within the mucosa.

In the basal surface of the mucosal preparations dissected from the muscular layer of guinea pig SV (Fig. 9.8a), a population of cells distributed just beneath the columnar epithelial cells develop asynchronous, irregularly occurred Ca^{2+} transients lasting for more than several seconds in 10 μM nifedipine (Fig. 9.8b, c). The spontaneous Ca^{2+} transients in the subepithelial cells are abolished by 10 μM CPA (Fig. 9.8c), suggesting that these cells generate spontaneous Ca^{2+} activity relying on Ca^{2+} handling by the SR/ER.

Application of 100 μM ATP evokes almost synchronous, robust Ca^{2+} transients in the spontaneously active subepithelial cells (Fig. 9.8b, Video 9.2). The morphology of the subepithelial cells, having irregular-shaped cell bodies with

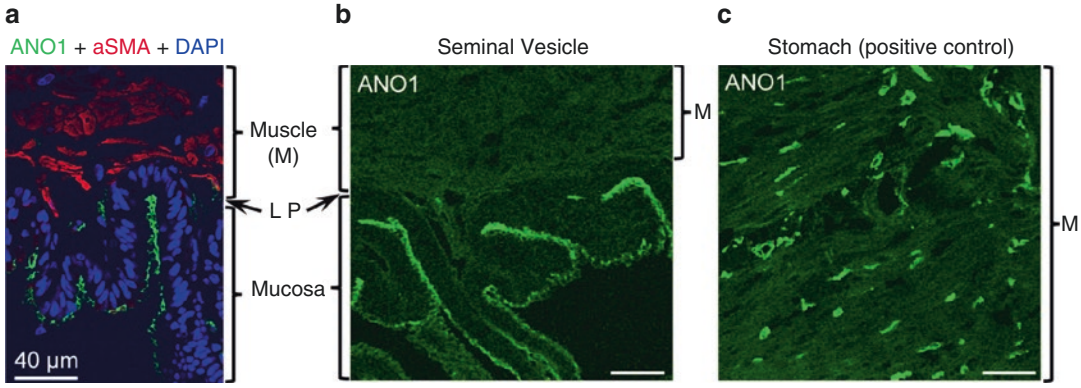

Fig. 9.7 Distribution of ANO1 in guinea pig SV and stomach. (**a**) In the coronal section of guinea pig SV, the apical side of the mucosa, but not lamina propria (*LP*) or muscular layer (*M*), was immunopositive for ANO1. The sections of another guinea pig SV (**b**) and gastric antrum (**c**) were immunolabelled with anti-ANO1 antibody using the same protocol. In the SV, ANO1 immunoreactivity localized in the apical side of the mucosa (**b**), while ANO1-immunoreactive cells were detected in the muscular layer of the stomach. αSMA, α-smooth muscle actin. All scale bar = 40 μm. Modified from Takeya et al. [8]

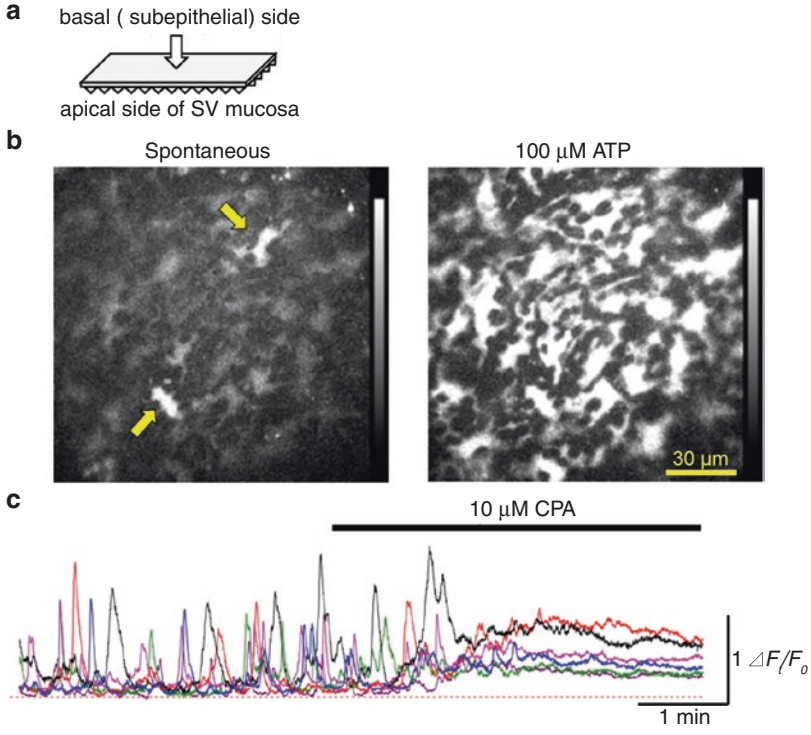

Fig. 9.8 Spontaneous and ATP-induced Ca^{2+} transients in SV "isolated" mucosal preparations. (**a**) An illustration of dissected SV mucosa from the muscular layer used for the Cal-520 fluorescence imaging and for the whole-mount preparation in immunohistochemistry. Functional and morphological properties were examined from basal (subepithelial) side of the preparations. (**b**) In a mucosal preparation that had been pretreated with 10 μM nifedipine, a population of cells located just beneath the columnar epithelium generated the spontaneous Ca^{2+} transients (left image, *arrows*). Subsequent 100 μM ATP evoked a massive increase in the intracellular Ca^{2+} in the spontaneously active subepithelial cells (right image). (**c**) Asynchronous spontaneous Ca^{2+} transients recorded from six subepithelial cells in another 10 μM nifedipine-pretreated preparation. Individual subepithelial cells generated "irregularly occurring" Ca^{2+} transients independently of each other. CPA (10 μM) increased the basal Ca^{2+} level and abolished the Ca^{2+} transients. Adapted from Takeya et al. [8]

several short processes, could clearly be visualized during the ATP-induced Ca^{2+} transients. The density of the ATP-sensitive subepithelial cells is about 30–40 cells per (100 μm)^2 and their cell bodies have a length of 15–20 μm and a width of 6–10 μm [8].

9.4.2 Cellular Composition of SV Mucosa

In the guinea pig SV mucosal preparations (Fig. 9.8a), vimentin-immunoreactive (IR) interstitial cells in lamina propria are situated beneath the pancytokeratin-IR epithelial cells (Fig. 9.9a). In the lamina propria, platelet-derived growth factor receptor α (PDGFRα)-positive interstitial cells are a subpopulation of the vimentin-IR interstitial cells, as evident by the intermediate filaments of these PDGFRα-positive interstitial cells being also stained by a vimentin antibody (Fig. 9.9b, c). In contrast, other vimentin-IR interstitial cells do not express PDGFRα.

The distribution of c-Kit-IR interstitial cells has not been demonstrated in the guinea pig SV mucosa or muscular layer [8]. Furthermore, α-smooth muscle actin (αSMA)-IR cells are observed only in vascular smooth muscle cells in guinea pig SV mucosa [8]. Thus, the origin of spontaneous activity in guinea pig SV mucosa appears to be different from well-known pacemakers such as c-Kit-positive ICCs in GI tract or atypical smooth muscle cells expressing αSMA in renal pelvis.

The morphological characteristics of the subepithelial cells firing spontaneous Ca^{2+} transients (Fig. 9.8b) appear to be different from PDGFRα-IR interstitial cells with their slenderer cell shape (>20 μm in cell length) (Fig. 9.9) in terms of their cell shape or size. PDGFRα-IR and/or vimentin-IR interstitial cells in the lamina propria that ***have*** a longer cell length than the spontaneously active subepithelial cells are also distributed in the mucosal surface of mucosa-denuded SV smooth muscle preparations (Fig. 9.10a, T. Hayashi and M. Takeya, unpublished observation). These morphological examinations reveal that interstitial cells are located between the subepithelial cells firing spontaneous Ca^{2+} transients and the smooth muscle cells (Fig. 9.10b). Since the spontaneous periodical activity is not generated in mucosa-denuded SV

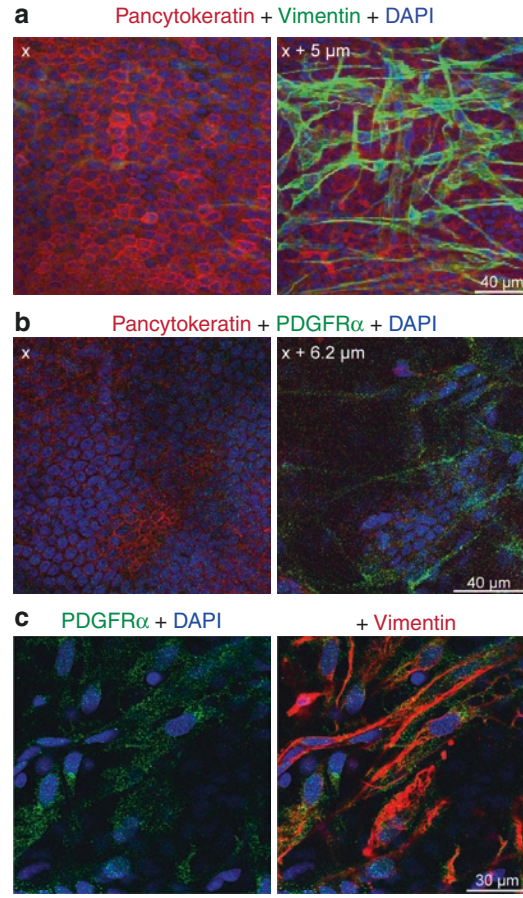

Fig. 9.9 Epithelium and interstitial cells in the lamina propria distributing on the basal surface of the "isolated" SV mucosal preparations. Whole-mount preparations of dissected guinea pig SV mucosa from the muscular layer (Fig. 9.8a) were observed using confocal microscopy. (**a**) Serial images were obtained from the basal (subepithelial) side of the mucosa preparations immunolabelled with anti-pancytokeratin (red: a marker of epithelial cell) and vimentin (green: a marker of interstitial cell). "*x + 5 μm*" in the right image indicates that the image was obtained 5 μm from the basal side of "*x*." Vimentin-immunoreactive (IR) cells located beneath the epithelial layer. (**b**) Serial images of another SV mucosal preparations. PDGFRα-IR (green) cells are found beneath the epithelial layer (*x + 6.2 μm*). (**c**) In other SV mucosal preparation, PDGFRα (green)-IR-positive cells in the lamina propria were immunoreactive for vimentin (red). Adapted from Takeya et al. [8]

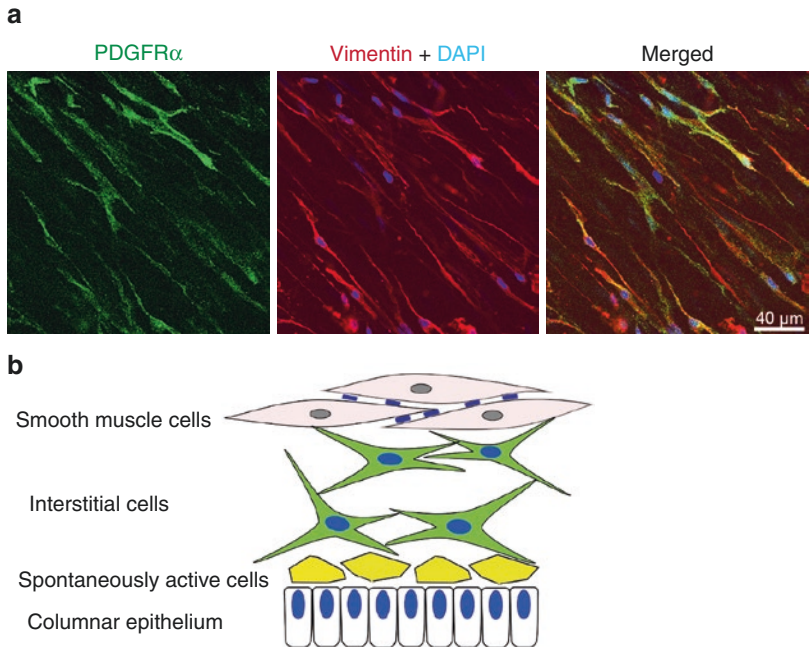

Fig. 9.10 Interstitial cells in the lamina propria also exist on the mucosal surface of SV smooth muscle preparation after removing the mucosa. (**a**) PDGFRα (green)-IR and/or vimentin-positive (red) interstitial cells distributing on the mucosal surface of the mucosa-denuded guinea pig SV smooth muscle. (**b**) A schematic drawing of the guinea pig SV wall based on distribution of vimentin-IR interstitial cells in the striped surface of both dissected mucosal and muscular preparations. There may be interstitial cells between the subepithelial cells firing asynchronous spontaneous Ca^{2+} transients and the smooth muscle cells

smooth muscle, the interstitial cells attached to mucosa-denuded smooth muscle are not capable of driving the auto-rhythmicity in smooth muscle cells.

9.4.3 Communication Between Mucosal and Muscular Cells

Synchronous spontaneous electrical and Ca^{2+} activity generated in SV smooth muscle cells could be driven by either depolarizing signals or humoral substances originated from unidentified mucosal "pacemaker" cells, presumably the subepithelial cells.

9.4.3.1 Role of Humoral Substances Released from Mucosal Cells

Spontaneous Ca^{2+} transients in the subepithelial cells may well trigger the Ca^{2+}-dependent synthesis and/or release of humoral substances. The mucosa-derived factors, if any, may enhance subthreshold "auto-rhythmicity" in the syncytium of SV smooth muscle cells by stimulating IP_3 production to facilitate "cytosolic Ca^{2+} oscillators," i.e., the cycle of Ca^{2+} uptake by SERCA and Ca^{2+} release [35]. This notion is supported by the finding that the "quiescent" mucosa-denuded guinea pig SV smooth muscle invariably develops oscillatory contractions, depolarizations, and Ca^{2+} transients upon the activation of α_1-ARs that couple with Gq signaling pathways (Fig. 9.4c) [22]. However, these mucosa-derived factors triggering SV spontaneous contractions are neither noradrenaline nor ACh, as inhibition of α-ARs or muscarinic receptors does not prevent these spontaneous phasic contractions of the guinea pig SV strips [17, 18].

Since application of ATP evokes robust Ca^{2+} transients in the spontaneously active subepithelial cells (Fig. 9.8), endogenous ATP could be involved in the generation and/or amplification of the spontaneous Ca^{2+} transients in the SV subepithelial cells. In guinea pig and human bladder mucosal preparations, UTP, a P2Y agonist, evokes ATP

release, suggesting that ATP autocrine/paracrine signaling may enhance further ATP release from the urothelium via activation of P2Y receptors [36]. Stretch-induced ATP release from guinea pig bladder mucosa has also been demonstrated [36]. Since SV smooth muscle develops mucosa-dependent periodical activity when stretched, mechanosensitive ATP release from epithelium or the spontaneously active subepithelial cells may be involved in the SV spontaneous contractions.

Prostaglandins (PGs), whose contribution to mucosa-dependent contractions in SV remains to be determined, are well known to be produced as constituents of seminal fluid by SV epithelium [1, 37]. Endogenous PGs play a fundamental role in generating pyeloureteric contraction of several species [38]. In the rabbit corpus cavernosum, cyclooxygenase-2 (COX-2)-dependent PGs may be released by intramuscular interstitial cells to develop the spontaneous phasic activity [39]. In murine gastric antral muscle, production of COX-2-dependent PGs in intramuscular ICC (ICC-IM) is involved in stretch-mediated chronotropic activity [30, 40].

9.4.3.2 Role of Gap Junction in Generating the Mucosa-Dependent Activity in SV Smooth Muscle

In mucosa-intact SV smooth muscle, the CaCC-dependent slow waves are abolished by 100 μM carbenoxolone, a gap junction blocker (Fig. 9.11). The simplest interpretation is that CaCC-dependent slow waves originate in the mucosal "pacemaker" cells and spread into SV musculature via gap junctions. In this case, a functional syncytium appears to be formed by at least three cell populations: spontaneously active subepithelial cells that act as pacemaker cells, interstitial cells in lamina propria that may act as an electrical conducting pathway, and "driven" smooth muscle cells. Since spontaneous Ca^{2+} transients in the SV subepithelial cells are generated independently of each other (Fig. 9.8), the individual subepithelial cells may irregularly generate spontaneous transient depolarizations (STDs) due to opening of CaCCs. Such irregular, asynchronous spontaneous depolarizing signals from the subepithelial cells may act as "point sources" of excitation, and the periodicity of slow waves and Ca^{2+} transients in SV smooth muscle may be determined by the refractory period of the interstitial cells in the lamina propria and/or smooth muscle cells, e.g., reduction in SR/ER Ca^{2+} contents or inactivation/deactivation of ion channels.

Even in cases where mucosa-derived humoral factors diffuse into the smooth muscle layer to activate their subthreshold "auto-rhythmicity," gap junction-mediated coupling may play a fundamental role in the subepithelial cells or intestinal cells in lamina propria. Gap junction coupling amongst the subepithelial "pacemaker" cells allows the cells to trigger a synchronous "surge" release of the humoral factors. Alternatively, mucosa-derived humoral substances released

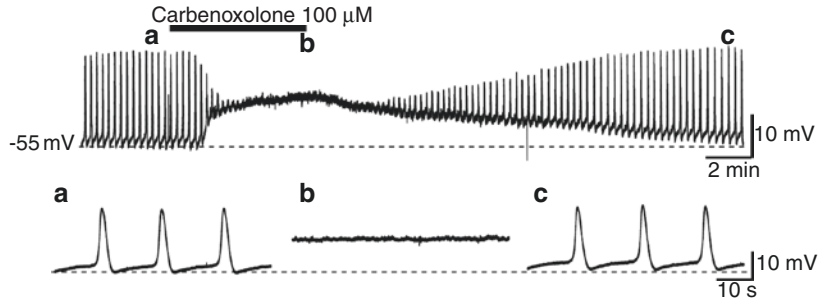

Fig. 9.11 Blockade of gap junctions abolishes CaCC-dependent slow waves in mucosa-intact SV smooth muscle. In a 10 μM nifedipine-pretreated preparation, 100 μM carbenoxolone depolarized the membrane and prevented the generation of slow waves. Lower traces were displayed in control (**a**), carbenoxolone (**b**), and after recovery (**c**) with an expanded time scale. Traces **a**–**c** were obtained at the timings indicated by the corresponding characters in the upper trace. Reproduced from Takeya et al. [8]

from the subepithelial cells may activate interstitial cells in the lamina propria that function as a "mediator" to induce the auto-rhythmicity in SV smooth muscles via gap junctions. In our preliminary observation, placing dissected mucosal preparations close to the quiescent mucosa-denuded SV smooth muscle preparations failed to restore the spontaneous phasic contractions (M. Takeya and M. Takano, unpublished data). These results could be explained by a disruption of gap junction connections between the interstitial cells in the lamina propria and muscular layers. Of course, the results could simply result from insufficient diffusion of the humoral substances from the subepithelial cells to smooth muscle layer due to their degradation.

Since dissecting the mucosa away from the SV smooth muscle layer mechanically breaks their intercellular communications, fundamental mechanisms in generating the mucosal spontaneous activity and/or transmitting the mucosal signals to the muscular layer may have been lost in these "isolated" mucosal preparations. In particular, interstitial cells in the lamina propria that may function as intermediaries or integrators of mucosal signaling will be divided into the mucosal and muscular sides (Figs. 9.9 and 9.10a). The spontaneously active subepithelial cells that generate asynchronous spontaneous electrical and Ca^{2+} activity may well develop "synchronous" oscillatory activity by coupling with the underlying SV smooth muscle syncytium via interstitial cells in lamina propria.

9.5 Perspective: Role of SV Spontaneous Contractions in Male Fertility

SVs secrete the major components of seminal fluid including fructose, prostaglandins, antioxidant agents, as well as a variety of other bioactive proteins such as cytokines [1, 37]. Although seminal fluid is often regarded simply as a vehicle to transport sperm to fertilize the oocyte, novel roles of seminal fluid in reproductive medicine are becoming evident in recent years. In most animals, even though viable pregnancies can be initiated using epididymal or washed ejaculated sperm during in vitro fertilization followed by embryo transfer, their success rate, i.e., normal pregnancy and live birth, is low. It has been demonstrated that the addition of seminal plasma to assisted reproductive procedures can significantly improve pregnancy success in several animals as well as humans [41–43]. Growing evidence indicates that signaling agents in seminal fluid drive multifactorial changes within the maternal uterus to establish an environment conducive to optimal embryo implantation and pregnancy outcome [42, 44]. It is envisaged that spontaneous constrictions of SVs during inter-ejaculatory phase have a "mixing function" to improve the fluidity of the viscous contents and quality of the bioactive substances that are vital for male fertility.

9.6 Conclusions

SVs develop spontaneous phasic contractions during the inter-ejaculatory phase. These events may be produced or enhanced upon muscle wall stretch. Besides the secretion of seminal fluid that are required for male fertility, the mucosa of guinea pig SV plays a crucial role in generating spontaneous contractions. Mucosal signals may well be transmitted to SV smooth muscle via gap junction coupling to drive CaCC-dependent SWs triggering the opening of LVDCCs to contract the SV muscularis. A candidate for the SV pacemaker, is the subepithelial cell that exists just beneath the columnar epithelium and fires spontaneous Ca^{2+} transients which relyies on SR/ER Ca^{2+} cycling; although the identification of the pacemaker cell remains to be determined. There are interstitial cells in lamina propria that may act as an intermediator between the spontaneously active subepithelial cells and the SV smooth muscle cells. It should also be explored whether mucosa-derived humoral substances drive the spontaneous activity in SV smooth muscle. Thus, the pathway of signal transmission from the SV mucosa to muscularis remains to be of great interest.

References

1. Aumüller G, Riva A. Morphology and functions of the human seminal vesicle. Andrologia. 1992;24:183–96. https://doi.org/10.1111/j.1439-0272.1992.tb02636.x.
2. Al-Zuhair A, Gosling JA, Dixon JS. Observation on the structure and autonomic innervation of the guinea-pig seminal vesicle and ductus deferens. J Anat. 1975;120:81–93.
3. Clement P, Giuliano F. Physiology and pharmacology of ejaculation. Basic Clin Pharmacol Toxicol. 2016;119:18–25. https://doi.org/10.1111/bcpt.12546.
4. Capogrosso P, Serino A, Ventimiglia E, Boeri L, Dehò F, Damiano R, et al. Effects of silodosin on sexual function—realistic picture from the everyday clinical practice. Andrology. 2015;3:1076–81. https://doi.org/10.1111/andr.12095.
5. Hisasue S, Furuya R, Itoh N, Kobayashi K, Furuya S, Tsukamoto T. Ejaculatory disorder caused by alpha-1 adrenoceptor antagonists is not retrograde ejaculation but a loss of seminal emission. Int J Urol. 2006;13:1311–6. https://doi.org/10.1111/j.1442-2042.2006.01535.x.
6. Hayashi T, Takeya M, Nakamura K, Matsuoka K. Effects of silodosin and tamsulosin on the seminal vesicle contractile response. LUTS. 2016;8:55–61. https://doi.org/10.1111/luts.12072.
7. Waddell JA. The pharmacology of the seminal vesicles. J Pharmacol Exp Ther. 1916;9:113–20.
8. Takeya M, Hashitani H, Hayashi T, Higashi R, Nakamura KI, Takano M. Role of mucosa in generating spontaneous activity in the guinea pig seminal vesicle. J Physiol. 2017;595:4803–21. https://doi.org/10.1113/JP273872.
9. Gonzales GF. Functional structure and ultrastructure of seminal vesicles. Arch Androl. 1989;22:1–13.
10. Price D, William-Ashman HG. The accessory reproductive glands of mammals. In: Young WC, editor. Sex and internal secretions, vol. 1. 3rd ed. Baltimore, MD: The Williams and Wilkins Co.; 1961. p. 366–448.
11. Melin P. In vivo recording of contractile activity of male accessory genital organs in rabbits. Acta Physiol Scand. 1970;79:109–13. https://doi.org/10.1111/j.1748-1716.1970.tb04706.x.
12. Veneziale CM, Brown AL, Prendergast FG. Histology and fine structure of guinea pig seminal vesicle. Mayo Clin Proc. 1974;49:309–13.
13. Tse MKW, Wong YC. Structural study of the involution of the seminal vesicles of the guinea pig following orchiectomy. Acta Anat. 1980;108:68–78. https://doi.org/10.1159/000145283.
14. Hib J, Ponzio R, Vilar O. In vivo recording of contractile activity of pelvic urethra and seminal vesicle in rats. Effects of electrical stimulations and neurohypophysial hormones. Andrologia. 1983;15:480–5. https://doi.org/10.1111/j.1439-0272.1983.tb00173.x.
15. Hib J, Ponzio R, Vilar O. Effects of autonomic drugs on contractions of rat seminal vesicles *in vivo*. J Reprod Fertil. 1984;70:197–202. https://doi.org/10.1530/jrf.0.0700197.
16. Turek PJ, Aslam K, Younes AK, Nguyen HT. Observation of seminal vesicle dynamics in an in vivo rat model. J Urol. 1998;159:1731–4. https://doi.org/10.1097/00005392-199805000-00102.
17. Ohkawa H. Further evidences for the cholinergic and adrenergic mechanisms in the isolated hypogastric nerve-seminal vesicle preparation of the guinea-pig. Bull Yamaguchi Med Sch. 1973;20:73–84.
18. Ohkawa H. Evidence for adrenergic transmission in the circular smooth muscle of the guinea-pig seminal vesicle. Tohoku J Exp Med. 1981;134:141–58. https://doi.org/10.1620/tjem.134.141.
19. Birowo P, Ückert S, Kedia GT, Sonnenberg JE, Thon WF, Rahardjo D, et al. Characterization of the effects of various drugs likely to affect smooth muscle tension on isolated human seminal vesicle tissue. Urology. 2010;75:974–8. https://doi.org/10.1016/j.urology.2009.09.034.
20. Narita H. The study of sperm transport through the human genital tract—pharmacological responses in vitro of the human genital tract. Jpn J Urol. 1983;74:1734–48. https://doi.org/10.5980/jpnjurol1928.74.10_1734.
21. Ohkawa H. Excitatory junction potentials recorded from the circular smooth muscles of the guinea-pig seminal vesicle. Tohoku J Exp Med. 1982;136:89–102. https://doi.org/10.1620/tjem.136.89.
22. Kubota Y, Hashitani H, Fukuta H, Sasaki S, Kohri K, Suzuki H. Mechanisms of excitatory transmission in circular smooth muscles of the guinea pig seminal vesicle. J Urol. 2003;169:390–5. https://doi.org/10.1016/S0022-5347(05)64134-1.
23. Shigemasa Y, Lam M, Mitsui R, Hashitani H. Voltage dependence of slow wave frequency in the guinea pig prostate. J Urol. 2014;192:1286–92. https://doi.org/10.1016/j.juro.2014.03.034.
24. Hashitani H, van Helden DF, Suzuki H. Properties of spontaneous depolarizations in circular smooth muscle cells of rabbit urethra. Br J Pharmacol. 1996;118:1627–32. https://doi.org/10.1111/j.1476-5381.1996.tb15584.x.
25. Hashitani H, Edwards FR. Spontaneous and neurally activated depolarizations in smooth muscle cells of the guinea-pig urethra. J Physiol. 1999;514:459–70. https://doi.org/10.1111/j.1469-7793.1999.459ae.x.
26. Sadraei H, Beech DJ. Ionic currents and inhibitory effects of glibenclamide in seminal vesicle smooth muscle cells. Br J Pharmacol. 1995;115:1447–54. https://doi.org/10.1111/j.1476-5381.1995.tb16636.x.
27. Lang RJ, Hashitani H, Tonta MA, Parkington HC, Suzuki H. Spontaneous electrical and Ca^{2+} signals in typical and atypical smooth muscle cells and interstitial cell of Cajal-like cells of mouse renal pelvis. J Physiol. 2007;583:1049–68. https://doi.org/10.1113/jphysiol.2007.137034.
28. Hashitani H, Takano H, Fujita K, Mitsui R, Suzuki H. Functional properties of suburothelial microvessels in the rat bladder. J Urol. 2011;185:2382–91. https://doi.org/10.1016/j.juro.2011.02.046.
29. Hashitani H, Mitsui R, Shimizu Y, Higashi R, Nakamura K. Functional and morphological properties of pericytes in suburothelial venules of the mouse

bladder. Br J Pharmacol. 2012;167:1723–36. https://doi.org/10.1111/j.1476-5381.2012.02125.x.
30. Sanders KM, Ward SM, Koh SD. Interstitial cells: regulators of smooth muscle function. Physiol Rev. 2014;94:859–907. https://doi.org/10.1152/physrev.00037.2013.
31. Sergeant GP, Hollywood MA, McCloskey KD, Thornbury KD, McHale NG. Specialised pacemaking cells in the rabbit urethra. J Physiol. 2000;526:359–66. https://doi.org/10.1111/j.1469-7793.2000.t01-2-00359.x.
32. Levine N, Rinaldo JE, Schultz SG. Active chloride secretion by *in vitro* guinea-pig seminal vesicle and its possible relation to vesicular function *in vivo*. J Physiol. 1975;246:197–211. https://doi.org/10.1113/jphysiol.1975.sp010886.
33. Liao SB, Cheung KH, O WS, Tang F. Adrenomedullin increases the short-circuit current in the mouse seminal vesicle: actions on chloride secretion. Biol Reprod. 2014;91:31, 1–6. https://doi.org/10.1095/biolreprod.113.116848.
34. Jang Y, Oh U. Anoctamin 1 in secretory epithelia. Cell Calcium. 2014;55:355–61. https://doi.org/10.1016/j.ceca.2014.02.006.
35. van Helden DF, Imtiaz MS. Ca^{2+} phase waves: a basis for cellular pacemaking and long-range synchronicity in the guinea-pig gastric pylorus. J Physiol. 2003;548:271–96. https://doi.org/10.1111/j.1469-7793.2003.00271.x.
36. Sui G, Fry CH, Montgomery B, Roberts M, Wu R, Wu C. Purinergic and muscarinic modulation of ATP release from the urothelium and its paracrine actions. Am J Physiol Ren Physiol. 2014;306:F286–98. https://doi.org/10.1152/ajprenal.00291.2013.
37. Gonzales GF. Function of seminal vesicles and their role on male fertility. Asian J Androl. 2001;3:251–8.
38. Lang RJ, Davidson ME, Exintaris B. Pyeloureteral motility and ureteral peristalsis: essential role of sensory nerves and endogenous prostaglandins. Exp Physiol. 2002;87:129–46. https://doi.org/10.1113/eph8702290.
39. Hashitani H, Yanai Y, Shirasawa N, Soji T, Tomita A, Kohri K, Suzuki H. Interaction between spontaneous and neutrally mediated regulation of smooth muscle tone in the rabbit corpus cavernosum. J Physiol. 2005;569:723–35. https://doi.org/10.1113/jphysiol.2005.099309.
40. Won KJ, Sanders KM, Ward SM. Interstitial cells of Cajal mediate mechanosensitive responses in the stomach. Proc Natl Acad Sci U S A. 2005;102:14913–8. https://doi.org/10.1073/pnas.0503628102.
41. Robertson SA. Seminal plasma and male factor signalling in the female reproductive tract. Cell Tissue Res. 2005;322:43–52. https://doi.org/10.1007/s00441-005-1127-3.
42. Bromfield JJ. Seminal fluid and reproduction: much more than previously thought. J Assist Reprod Genet. 2014;31:627–36. https://doi.org/10.1007/s10815-014-0243-y.
43. Crawford G, Ray A, Gudi A, Shah A, Homburg R. The role of seminal plasma for improved outcomes during *in vitro* fertilization treatment: review of the literature and meta-analysis. Hum Reprod Update. 2015;21:275–84. https://doi.org/10.1093/humupd/dmu052.
44. Robertson SA, Sharkey DJ. Seminal fluid and fertility in women. Fertil Steril. 2016;106:511–9. https://doi.org/10.1016/j.fertnstert.2016.07.1101.

The Myometrium: From Excitation to Contractions and Labour

10

Susan Wray and Clodagh Prendergast

Abstract

We start by describing the functions of the uterus, its structure, both gross and fine, innervation and blood supply. It is interesting to note the diversity of the female's reproductive tract between species and to remember it when working with different animal models. Myocytes are the overwhelming cell type of the uterus (>95%) and our focus. Their function is to contract, and they have an intrinsic pacemaker and rhythmicity, which is modified by hormones, stretch, paracrine factors and the extracellular environment. We discuss evidence or not for pacemaker cells in the uterus. We also describe the sarcoplasmic reticulum (SR) in some detail, as it is relevant to calcium signalling and excitability. Ion channels, including store-operated ones, their contributions to excitability and action potentials, are covered. The main pathway to excitation is from depolarisation opening voltage-gated Ca^{2+} channels. Much of what happens downstream of excitability is common to other smooth muscles, with force depending upon the balance of myosin light kinase and phosphatase. Mechanisms of maintaining Ca^{2+} balance within the myocytes are discussed. Metabolism, and how it is intertwined with activity, blood flow and pH, is covered. Growth of the myometrium and changes in contractile proteins with pregnancy and parturition are also detailed. We finish with a description of uterine activity and why it is important, covering progression to labour as well as preterm and dysfunctional labours. We conclude by highlighting progress made and where further efforts are required.

Keywords

Uterus · Electrophysiology · Pace-making · Calcium signalling · Sarcoplasmic reticulum · Parturition

10.1 Functions and Structure of the Uterus

10.1.1 Roles of Uterine Contractions

The uterus is a myogenic organ, mostly known for nurturing and protecting a foetus and then delivering it after a lengthy period of contractile activity. The smooth muscle within the uterus, the myometrium, is responsible for generating the electrical activity and thence contractions. The intrinsic, phasic pattern of activity is modulated by hormonal,

S. Wray (✉) · C. Prendergast
Department of Cellular and Molecular Physiology, Harris-Wellbeing Preterm Birth Centre, Institute of Translational Medicine, University of Liverpool, Liverpool, UK
e-mail: s.wray@liv.ac.uk

H. Hashitani, R. J. Lang (eds.), *Smooth Muscle Spontaneous Activity*, Advances in Experimental Medicine and Biology 1124, https://doi.org/10.1007/978-981-13-5895-1_10

metabolic and mechanical factors. Although most apparent during parturition, a low level of this intrinsic contractile activity is present in females throughout their life. This intrinsic activity can be recorded using surface electrodes on the abdomen to pick up electrical signals from the uterus [1], while contractions can be recorded in vitro in myometrial biopsies from women well beyond the age of menopause [2]. By analogy to skeletal muscle, such activity may help stop the tissue atrophying. In addition to childbirth, there are also two other occasions when uterine contractions are important to a woman's reproductive life, menses and fertilisation.

10.1.1.1 Menses

Menses, periods or menstruation, is the sloughing of part of the uterine lining (endometrium) each month between puberty and menopause in non-pregnant women. The shedding of this menstrual debris is aided by uterine contractions. The muscular strength and activity of the non-pregnant myometrium change throughout the menstrual cycle [3]. Waves of contractions produce a rippling effect on the endometrial surface. The frequency and strength of these contractions depend upon the hormonal milieu. Measurements of muscle strength have confirmed that contractile strength values approaching those found at labour (50–200 mmHg) can occur in non-pregnant myometrium during menstruation. Not surprisingly, this muscular effort produces menstrual pain in most women. Uterine activity helps to both slough off dead tissue from the endometrium into the uterine cavity and propel it towards the cervix and beyond.

10.1.1.2 Endometriosis

Endometriosis is a puzzling and painful condition. Often associated with infertility, it occurs in 5–10% of otherwise healthy women and there is no cure. Endometriosis arises because cells from the sloughing uterine lining are deposited at sites in the body, starting with the pelvis. The cells can adhere and cause inflammatory reactions and other problems. The endometrial debris in the pelvis is thought to have been propelled there from the uterus by aberrant, misdirected contractions—so-called retrograde menstruation [4]. It is unknown why some women are susceptible to this and the condition can be hard to diagnose and treat.

10.1.1.3 Fertilisation

Uterine activity is also helpful in moving sperm up from the cervix and towards the fallopian tubes. Sperm are motile using flagella to propel themselves from the vagina to the uterine cavity. The additional directed flow to the fallopian tubes from uterine contractions is considered necessary for them to reach their destination. The tubes are the usual site for fertilisation if a healthy egg has been released by the ovaries and transported down the fallopian tubes. Post-fertilisation, the egg moves down into the uterus, where it will implant, if hormonal conditions have prepared the endometrium appropriately.

It is also believed that a lack of uterine contractile activity is best for implantation of the fertilised egg into the endometrium, although the evidence is not extensive [5]. Using modern imaging techniques, rippling can be seen on the endometrial surface, arising from myometrial activity. This has led to the use of anti-contraction medication in women undergoing IVF egg transfers, e.g. blockers of oxytocin receptors [6] to help increase success rates.

10.1.2 Uterine Anatomy

The anatomical appearance of the uterus is species dependent. While in women there is one pear-shaped cavity, with the cervix at the bottom and fallopian tubes (oviducts) at the top, this is not the structure seen in other mammals. Rodents, which are a frequently used animal model, have a bicornuate uterus—they have two uterine "horns" in which the ten or so embryos implant. Rabbits and marsupials have two horns as well as two cervical canals, and in the case of the latter, two vaginas. These differences occur during embryonic development, as for example the paramesonephric ducts fuse to a greater (e.g. human) or lesser (e.g. rodent) extent.

Although the structure of the uterus varies considerably between species, its basic cellular con-

tent and tissue components are rather similar. There will be an outer serosal coat made of connective tissue, which is continuous with the broad ligament. The next tissue, which itself can be in several layers, and is by far the greatest component of the uterine structure, is the myometrium. It can usually be separated into circularly and longitudinally orientated muscle layers. In women, in contrast to rodents, these two layers are highly interwoven and separating the circular and longitudinal smooth muscle layers is not so easily accomplished due to the presence of interconnections between the two layers. For a detailed analysis of the structure of human myometrium, see [7]. Running along and between these muscle bundles and layers are the uterine blood vessels and nerves.

10.1.2.1 Endometrium

The inner lining of the uterus is the endometrium which contains glands, as well as blood vessels. The endometrium is bounded on the luminal side of the uterus by a single layer of epithelial cells, which may or may not have cilia (depending on the stage of the menstruation cycle) and its basal lamina. Looping in from the epithelium are the uterine glands, and their extent and development also change with the menstrual cycle. The bulk of the tissue is a specialised, cell-rich connective tissue (stroma) containing a rich supply of blood vessels. The cells and glands of the endometrial lining will either grow or die depending on the cyclic changes in the female hormones, oestrogen and progesterone. Thus, it is the structures and cells of the endometrium, including the epithelium, that are lost each month during the menstrual cycle, or built up if pregnancy occurs. The endometrium also accommodates and provides the environment, i.e. constituents and support cells to develop the embryo. The basalis is the name given to the portion of the endometrium that is not shed each month, and from which the endometrium will be rebuilt during the next menstrual cycle. Menstruation only occurs in women, and some primates; in other species there are cyclical changes, referred to as oestrus. As with menstruation the appearance of the uterus can change considerably with the stage of oestrus, and there are accompanying moderate changes in excitability and contractility [8].

10.1.2.2 Cervix

The cervix is contiguous with the uterus and displays a decreasing muscle content and increasing connective tissue, especially collagen. During pregnancy, the cervix serves as a barrier, protecting the foetus from infection and retaining the foetus in utero. The non-pregnant cervix (~3 cm in length) is principally composed of dense fibrous extracellular matrix (predominantly collagen, but also elastin), although 10–15% consists of smooth muscle cells and vascular, immune and glandular cells [9]. In a normal pregnancy, the cervix remains closed until gestation reaches term. The process of labour and birth requires significant cervical remodelling. The prepartum phases of remodelling include (1) softening of the cervix, which starts in the first trimester of pregnancy and is characterised by decreased collagen crosslinking; (2) ripening of the cervix, where the collagen structure further degrades (increased spacing between fibres and a switch from straight to wavy fibres), associated with an increase in hyaluronic acid production and immune cell infiltration; and (3) cervical dilation, which occurs during active labour. The cervix must efface and dilate to a diameter of 10 cm to allow the delivery of the foetus. In the final post-partum repair phase of the remodelling, the cervix recovers its integrity (see [10–12] for detailed reviews of the remodelling process).

10.1.3 Innervation and Nerves in the Uterus

It is important to state at the start that, although the uterus receives both parasympathetic and sympathetic innervation, neither branch of the autonomic nervous system is required for uterine contraction. There is no motor innervation to the uterus. The uterus is a myogenic organ, meaning it can contract without nervous (or hormonal) stimulation. Thus, there are no synapses in the myometrium and no direct associations between axonal endings and myocytes. However,

neurotransmitters, i.e. noradrenaline from the sympathetic fibres and acetylcholine (ACh) from parasympathetic fibres, are released into the spaces between muscle bundles. In their recent review of autonomic innervation of the uterus, Tica et al. [13] conclude that "it is unclear the precise role of the nervous supply on myometrial activity". Furthermore, it has long been known, although not always appreciated, that there is a functional degeneration and hence denervation in myometrium from term-pregnant animals and women [14–17].

10.1.3.1 Innervation of the Cervix

The cervix, unlike the uterus, is well innervated and nerve density is sustained or increased at term [18, 19]. In the rat, if the sensory neuropeptidergic nerves that project to the cervix (and are involved in inflammation and local vasodilation) are transected, the ripening of the cervix and therefore birth are delayed and there is a reduction in immune cell infiltration [20]. Infection and subsequent premature cervical remodelling are recognised to be significant risk factors for preterm birth and are associated with 25–40% of all preterm births. The birefringence from collagen fibrils and impedance changes in the cervix can be used to detect cervical ripening, and therefore provide the basis for testing the risk of preterm labour [21].

10.1.3.2 Innervation of Uterine Blood Vessels

The blood vessels of the uterus are also innervated with sympathetic, parasympathetic and sensory neurons [22]. Parasympathetic stimulation produces vasodilators mainly via activation of muscarinic cholinergic receptors, and the sympathetic innervation produces vasoconstrictors via activation of α-adrenergic receptors [23]. Like the sympathetic denervation seen in the myometrium during pregnancy, fluorescence histochemistry of uterine adrenergic nerves shows abundant perivascular innervation in non-pregnant and early pregnant rats, and degeneration commences by day 15, so that perivascular nerves are practically absent by term [24, 25]. In the guinea pig uterine artery, while the number of noradrenaline-positive nerve fibres is significantly reduced in term pregnancy, the number of neuropeptide Y (NPY)-containing fibres is increased [26].

10.1.3.3 Neuromodulators

The myometrium and its blood vessels are innervated by sensory nerves identified as containing a range of neuromodulators, such as calcitonin gene-related peptide (CGRP), substance P (SP), vasoactive intestinal polypeptide (VIP), neuropeptide Y (NPY) and neurokinins.

Gnanamanickam and Llewellyn-Smith [22] describe in detail the distribution of nerves immunoreactive for CGRP, SP and NPY in non-pregnant rat uterus. Pregnancy affects this innervation. For example, nerve fibres containing CGRP are abundant in non-pregnant rat uterus but rare in term pregnant rat myometrium [27]. CGRP has a relaxant effect on non-pregnant uterus but no effect on the term pregnant rat myometrium. Circulating CGRP levels increase during pregnancy (human and rodent) but then decline sharply at term [28]. CGRP is also a potent vasodilator and sensitivity to CGRP increases during pregnancy [29]. CGRP may therefore have a significant role to play in uterine quiescence during pregnancy as well as the vascular remodelling that occurs in normal pregnancy (described below). CGRP is also implicated in the ripening of the cervix that must occur before cervical effacement and dilation to allow a successful birth [19, 30].

Substance P (SP)-positive nerve fibres are present in the non-pregnant rat myometrium, but there are contradictory reports of either an increase in SP-immunoreactivity in pregnancy [31] or a progressive decrease during pregnancy and absence at term [32]. The vasodilator action of SP on myometrial arteries does not seem to change with pregnancy [33]. While SP can induce contraction of uterine smooth muscle, it appears to have a more significant role in cervical ripening, promoting the inflammatory responses and tissue rearrangements required for cervical remodelling [30].

VIP-immunoreactive fibres are found throughout the uterus, cervix and uterine vasculature [34,

35]. VIP has vasodilatory properties, in addition to its ability to decrease myometrial contractility. However, its main role may involve its anti-inflammatory actions. Inflammation and activation of immune cells are an integral part of normal pregnancy and VIP appears to be involved in the modulation of the inflammatory and immune state throughout pregnancy [36].

10.1.4 Vasculature of the Uterus

Using tyrosine hydroxylase labelling of sympathetic nerves in whole-mount preparations of rat uterus, Gnanamanickam and Llewellyn-Smith were able to map the arterioles supplying blood to the uterus because the vessels are so densely innervated [22]. They showed that the vessels are not organised as a vascular tree, in which arteriole diameters get smaller and smaller until they become capillaries. Rather, the uterine arterioles are organised in an anastomosing network; that is, they are extensively interconnected across the whole circumference of the uterus. Such interconnected systems are associated with organs in which an assured supply of oxygenated blood is essential. In rats, blood is supplied to the uterus by the uterine arteries, which can receive blood from either their ovarian or cervical ends [37]. This potentially bidirectional supply and the anastomosing network ensure considerable redundancy and help maintain uterine perfusion. The human uterus has a similar bidirectional delivery of blood via the uterine arteries and uterine branches of the ovarian arteries. The uterine arteries have branches called arcuate arteries which are within the myometrium but near the surface of the uterus. Radial arteries branch out and traverse the myometrium radially towards the endometrium. At the myometrium/endometrium boundary, the radial arteries branch to form basal arteries and spiral arteries. Basal arteries remain unaltered by the menstrual cycle or pregnancy. Spiral arteries, on the other hand, are highly sensitive to oestrogen and progesterone. While sparsely distributed during the proliferative phase of the menstrual cycle, they undergo a rapid growth phase that outstrips the growth of the surrounding tissue, resulting in a tortuous, highly coiled path through the endometrium. During the secretory phase of the menstrual cycle, there is a constriction of the radial and/or spiral arteries, resulting in ischaemia and necrosis of the functional endometrium leading to its shedding during menstruation. The basal arteries then give rise to new spiral arteries and the cycle begins again.

During pregnancy, major adaptations occur to the uterine vasculature. Firstly, the spiral arteries undergo remodelling from tortuous, contractile vessels to wide conduits that do not respond to vasocontractile stimuli in the maternal system. This is vital to ensure adequate blood flow to the placenta and growing foetus. The remodelling extends up to a third of the way into the myometrium (into the radial arteries). The remodelling process has been reviewed in detail [38]. Briefly, immune cells (macrophages and uterine natural killer cells) initiate the breakdown of the arterial basal lamina and the dedifferentiation and disorganisation of the arterial smooth muscle cells. Interstitial trophoblasts invade and colonise the vessel walls, inducing apoptosis in the endothelial cells, so that ultimately the entire endothelium is removed and replaced with trophoblasts. This remodelling appears to be vital for a successful pregnancy, since a lack of spiral artery remodelling is associated with intrauterine growth restriction and pre-eclampsia [39].

The second major adaptation that occurs is that the larger arteries (uterine, arcuate, radial arteries) dilate to allow a greater blood flow to the uterus, accommodating an increase from ~45 mL/min in the non-pregnant uterus to ~750 mL/min at term. Maternal blood pressure remains the same or decreases in normal pregnancy; therefore this increase in flow is achieved by an increase in vessel size (outward remodelling) and a reduced reactivity to vasoconstrictive agents.

10.1.5 Myometrial Cells

The smooth muscle cells of the uterus have much in common with those in other smooth muscle tissues—spindle shape and central nucleus, mitochondria, sarcoplasmic reticulum (SR) and of course myoproteins (see Fig. 10.1a). What distin-

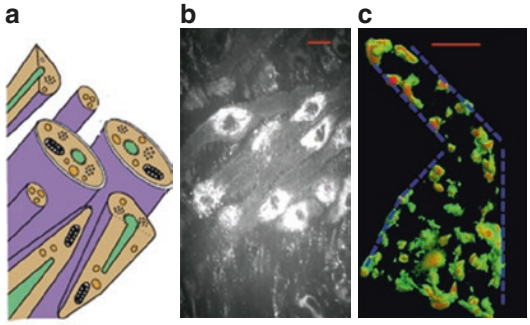

Fig. 10.1 Uterine myocytes. (**a**) Schematic representation of smooth muscle myocytes. (**b**) Uterine myocytes in bundle of longitudinal myometrium from pregnant rat. Bright central nuclei are clearly visible in the spindle-shaped cells. Red bar indicates 5 μm. (**c**) Part of a single-uterine cell, with sarcoplasmic reticulum calcium store revealed by intraluminal fluorescent, Ca-sensitive indicator Mag-Fluo3. Red bar indicates 10 μm. The dotted blue lines indicate the plasma membrane to show how close the SR approaches it

guishes the uterine myocytes is their relatively large size, up to 0.5 mm long (see Fig. 10.1b), large Ca^{2+} currents and powerful contractions.

The plasma membrane bounds the myometrial myocyte and houses the ion channels, pumps and exchangers necessary for uterine function and health. As with other smooth muscles, there are invaginations of the surface membrane, known as caveolae. The invaginations arise because of the insertion of the protein caveolin. We now appreciate that the caveolae are rich in cholesterol and sphingomyelin and constitute a form of lipid rafts, and are involved in cell signalling pathways [40].

10.1.5.1 Gap Junctions

The myocytes in the myometrium are connected by gap junctions. These connections contain mostly connexin 43 and allow for electrical coupling between the cells. The increase in myometrial gap junctions, and with it electrical synchronisation, is thought to play a significant role in the gradual development of uterine contractility during labour. Much of what we know about their role and regulation comes from the work of Garfield's group, which showed that endocrine conditions govern gap junction numbers, as well as conductance [41–43].

10.1.5.2 Sarcoplasmic Reticulum (SR)

The internal calcium store, the sarcoplasmic reticulum (SR), is a feature of all muscle types. Between smooth muscles, its size and role vary, and within the same smooth muscle its function may change with development, disease and physiological state [44]. The myometrium probably has one of the largest SRs, as judged by electron microscopy and X-ray microanalysis [45]. Confocal imaging has also helped show the extent and three-dimensional distribution of the SR in uterine smooth muscle (Fig. 10.1c), as well as identify Ca^{2+} release and uptake sites. Following from the development of Ca^{2+}-sensitive fluorescent indicators to monitor changes in the cytoplasmic concentration of Ca^{2+} ($[Ca^{2+}]$), low-affinity Ca^{2+} indicators were developed to measure SR Ca^{2+}. Mag-Fluo4 has worked particularly well in myometrium. These methodologies revealed that myometrial SR is not just a central store close to the myofilaments, but it also runs very close to the plasma membrane, as can be appreciated from Fig. 10.1c. This enables microdomains of higher than bulk cytosolic $[Ca^{2+}]$ to occur, as SR Ca^{2+} is released into a diffusion-limited space [46]. This is important as it helps to explain how Ca^{2+}-activated ion channels on the surface membrane are exposed to a high enough $[Ca^{2+}]$ to activate them. This link between the SR and excitability, via ion channels, is key to the now accepted view that the role of the SR is not simply a Ca^{2+} store, but also affects excitability in smooth muscle.

The SR can release Ca^{2+} via inositol trisphosphate (IP_3)- or Ca^{2+}-gated channels on its membrane; the latter release channels are also known as ryanodine receptors (RyR). Western blotting has shown that the myometrial SR contains both IP_3 receptors and RyR. The presence of RyR led to the assumption that Ca^{2+}-induced Ca^{2+} release (CICR) would be a feature of myometrial physiology. Thus Ca^{2+} entry upon excitation and depolarisation should elicit a large release of Ca^{2+} from the SR store, via RyR, as occurs in cardiac muscle. Despite thorough and intensive investigations, such a CICR process has not been demonstrated in the myometrium [47]. Furthermore,

caffeine, an agonist at RyR, does not elicit a release of Ca^{2+}; instead it relaxes myometrial tissue, due to its inhibition of phosphodiesterase and subsequent increase in cAMP. In addition, Ca^{2+} sparks, representing small, localised, transient releases of Ca^{2+} via RyR, could not be demonstrated in myometrium, using protocols and techniques that had revealed their presence and role in ureteric smooth muscle [48]. The answer to this puzzle came with more sophisticated molecular biology revealing that RyR expressed in the myometrium were non-functional splice variants [47]. This lack of Ca^{2+} sparks also means that they cannot stimulate Ca^{2+}-activated K^+ or Cl^- channels in myometrium. Calcium release through IP_3 receptors is stimulated by agonists binding to the plasma membrane G-coupled receptors and eliciting IP_3 production from phosphatidylinositol 4,5-bisphosphate (PIP_2) hydrolysis. This released Ca^{2+} augments cytosolic [Ca^{2+}] and helps strengthen uterine contractions. Such augmentation is considered to contribute to the actions of oxytocin, vasopressin and prostaglandins on the myometrium.

Sarco-Endoplasmic Reticulum Calcium ATPase *(SERCA)*

Active transport is required to drive the movement of Ca^{2+} into the SR in smooth muscle cells. The ATPase that catalyses this movement is sarco-endoplasmic reticulum calcium ATPase (SERCA) which is a P-type ATPase and the major protein associated with the SR. As described by Wray and Burdyga [44] in their review of the SR in smooth muscle, calcium-binding proteins enable large amounts of Ca^{2+} to be stored in the SR. In cardiac muscle, the auxiliary protein phospholamban is an important regulator of SERCA, with its inhibition being lifted when it is phosphorylated. In myometrium however, no role for phospholamban has been reported. Perhaps of more importance in the myometrium is regulation of SERCA activity by intracellular pH and metabolites. Using Western blotting, Tribe et al. [49] reported that isoforms 2a and 2b of SERCA are expressed in the myometrium. The expression of both isoforms was also increased in women in labour compared with those not in labour.

Contribution of the SR to Myometrial Contractions

Our group has extensively investigated the role of the SR in the myometrium [48, 50–52]. We have found that the SR Ca^{2+} load has a profound effect on intracellular Ca^{2+} signals. Using single uterine myocytes, we found that an increased SR Ca^{2+} load, produced by maintained depolarisation, inhibited spontaneous Ca^{2+} signals. In contrast, a decreased SR luminal Ca^{2+} load, obtained by inhibiting SERCA, activated intracellular Ca^{2+} spikes. Similar results were found in intact tissues where there was a potentiation of Ca^{2+} transients and contractions when SERCA was inhibited by cyclopiazonic acid (CPA). In pregnant rat uterus, CPA stopped the phasic contractions and transformed activity to be tonic-like, associated with a large increase in the baseline Ca^{2+}. Thus, during spontaneous uterine contractions there is no involvement of the SR, as Ca^{2+} entry and efflux across the plasma membrane account for these phasic contractions [53]. As mentioned above there is also no role for CICR in myometrium, and caffeine relaxes contractions. The lack of Ca^{2+} sparks means that there is no Ca^{2+} spark-STOC mechanism, where the Ca^{2+} released during a spark activates Ca^{2+}-sensitive K^+ channels and produces a spontaneous transient outward current, known as a STOC. The resulting hyperpolarisation leads to relaxation in vascular smooth muscle [54], and curtailment of the action potential in ureteric smooth muscle [55]. We have recently been able to show, using electrophysiology, force and intracellular Ca^{2+} measurements, that depletion of the SR in the myometrium produces depolarisation and Ca^{2+} entry through store-operated channels [56] which can increase contractility upon agonist stimulation.

10.1.5.3 Mitochondria

Uterine myocytes contain round or ovoid mitochondria. In human and rat, light and electron microscopies show these mitochondria to be distributed like "pearls on a string" close to the nuclei and rough endoplasmic reticulum or subsarcolemmally adjacent to caveolae [57]. In all cells, there is an electrical potential difference across the mitochondrial membrane, with their

inside being significantly more negative, (values range in 180–220 mV) than the cytoplasm [58]. As well as their obvious importance to oxidative phosphorylation, evidence has grown that mitochondria are important to Ca^{2+} signalling in smooth muscle [59]. Mitochondria interact with and may link with the SR [60, 61]. They also store significant amounts of Ca^{2+}. Early work conducted by Batra [62] showed rapid and substantial uptake of Ca^{2+} into uterine mitochondria in microsomal preparations. More recently, Gravina et al. [63] have shown that they may be important in modulating spontaneous activity in rat uterus. Work from the same group indicated that oxytocin causes depolarisation of the mitochondrial membrane potential, ψ_m [64]. This was suggested to be likely due to oxytocin inducing an increase in cytosolic [Ca^{2+}], "causing enhanced mitochondrial uptake of Ca^{2+} and resultant dissipation of the mitochondrial electrochemical gradient". The mitochondrial ATP synthase is also stimulated, which further contributes to a decrease in ψ_m. In a study comparing mitochondria from guinea pig uterus and heart, the uterine mitochondria were shown to have higher amounts of hexokinase and adenylate kinase, and to use them with mitochondrial creatine kinase, to enhance local [ADP], which will help the mitochondrial responses to energetic demands [65]. Investigators have looked for changes in mitochondrial appearance or activity in various pregnancy-related disorders, including pre-eclampsia, where small changes were noted [66], and obesity and diabetes, where no changes were found [57, 67]. Myometrial mitochondrial copy number was reduced in older mice, although there were no age-induced changes to the enzymatic activities of the mitochondrial electron transport chain complexes [68].

10.1.5.4 Other Cell Types: Are There Pacemaker Cells?

Neither removing the tissue from the body nor dissection down to the smallest of myometrial strips prevents it from rhythmically contracting. Even freshly dissociated single myocytes can be seen to contract. Despite many hunts for an anatomical pacemaker in the uterus, none has ever been found. This has led to the suggestion that some myocytes, perhaps a third of them based on data from Ca^{2+}-activated Cl^- channels (see later), or groups of cells have inherent pacemaking activity. This can be attributed to them possessing a different cassette of ion channels, leading to unstable membrane potentials. This in turn causes action potentials to fire and membrane depolarisation which spreads quickly through to adjacent myocytes via their gap junctions.

When electrical activity has been mapped in the myometrial strips, using techniques pioneered by Lammers, that involve arrays of multiple electrodes, an erratic, whirling spread of excitation can be seen [69]. Areas initiating excitation appear to be fluid and the pattern of spread of the ensuing depolarisation is also malleable. Similar findings have been described when calcium is used as a surrogate for depolarisation, i.e. mapping the rises of Ca^{2+} throughout myometrial cells and bundles, to illustrate where excitation due to electrical activity is occurring. This can be done using Ca^{2+}-sensitive fluorescent indicators and confocal microscopy. The descriptions of the changes in [Ca^{2+}] closely mirror those for electrical activity. Thus, all these data are consistent with there being no anatomical or histological pacemaking structure in the uterus. A recent review concluded "… previous studies unanimously reveal a unique complexity as compared to other organs in the pattern of uterine electrical activity propagation" [70]. There is consensus that in rodents it is easier to get spontaneous contractions from cells closer to the oviducts than cervix and along the mesometrial border [71]. As far as we are aware, there is no mechanistic explanation for these findings.

Taking a lead from the gastrointestinal system, where a discrete network of cells, interstitial cells of Cajal (ICC), produces pacemaking, researchers have looked for similar-appearing cells around myometrial bundles. Such interstitial cells, called telocytes by some authors [72], and ICC-like cells by others [73, 74], have been identified in the uterus by a variety of techniques from confocal and electron microscopy to immunohistochemistry and molecular biology. Some have suggested that such cells are stem cells or transitional cells, or form some sort of support network, while others have suggested that they are pacemakers. In our

opinion, to make the claim that these interstitial cells are pacemakers they must be capable of depolarisation and spreading excitation. Claiming pacemakers based on histological similarities with ICC or using drugs such as imatinib to inhibit c-KIT signalling is not sufficiently rigorous. Our study in myometrium, where we reported ICC-like cells, passed from excitement to disappointment as we found that they did not depolarise when stimulated [73]. Indeed, it was easier to propose, given their ability to hyperpolarise, that they could form a network to keep the myometrium quiescent ahead of parturition. Similarly telocytes do not show any excitable properties but did display hyperpolarising currents [75]. A recent review of telocytes concluded that they are not pacemakers but perhaps participate in cell renewal and signalling [76]. More recently, another type of interstitial cell, platelet-derived growth factor receptor alpha-positive (PDGFR alpha$^+$), has been reported in the female reproductive tract, including myometrium [77]. These cells however are unlikely to be pacemakers, as they are not reported to express any of the necessary genes. They were able to form connections with myocytes through gap junctions. In bladder and GI tract, these cells may mediate inhibitory neurotransmission [78, 79]. Finally, Young [80] has postulated that long-distance signalling mechanism based on mechano-transduction aids the action potentials spreading in the pregnant myometrium. He refers to these as "mechanically sensitive electrogenic pacemakers, distributed throughout the (uterine) wall".

10.2 Excitation in Myometrial Cells

To understand how electrical activity arises in myometrial cells requires knowledge of the ion channels, pumps and currents in the myometrium, their densities, conductance, activation and inactivation, coupling to neighbouring cells, modulation and how they relate to the resting membrane potential and action potential. Figure 10.2 summarises the uterine myocyte plasma membrane and its ion channels, pumps, receptors and exchangers.

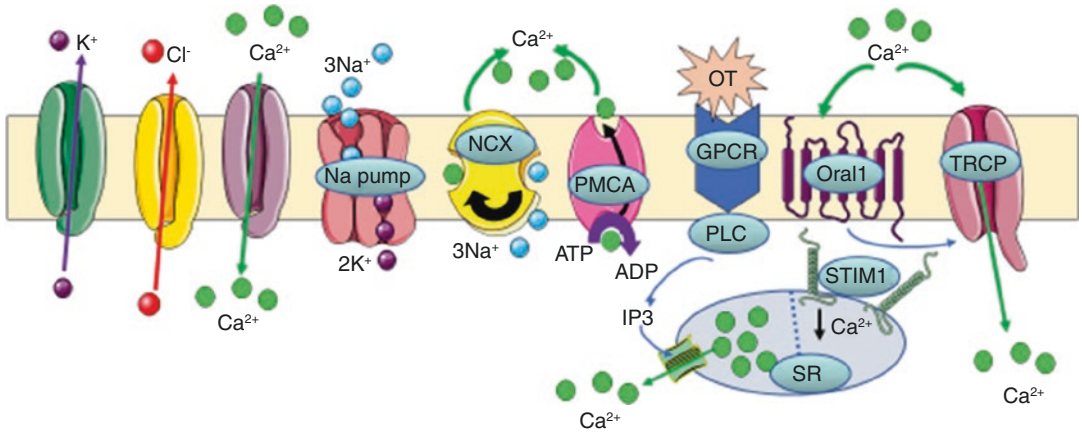

Fig. 10.2 Myometrial channels, pumps and exchangers. Calcium entry is controlled by L-type Ca^{2+} channels, and is essential for contraction. Cells express a wide variety of K^+ channels, gated by voltage, Ca^{2+}, ATP and stretch. Chloride channel opening leads to Cl^- efflux. Plasmalemmal calcium fluxes are balanced by two efflux pathways: PMCA (plasma membrane Ca-ATPase) and NCX (Na,Ca exchanger). The Na pump (Na,K ATPase) removes $3Na^+$ linked to the entry of $2K^+$. The SR (sarcoplasmic reticulum) takes up Ca^{2+} via SERCA (sarco-endoplasmic reticulum Ca-ATPase), and only releases Ca^{2+} via IP_3-gated channels. When SR Ca^{2+} is decreased STIM1 and Orai1 interact, forming a Ca^{2+}-selective pore, and stimulating the opening of non-specific cationic TRCP channels. By this store-operated mechanism producing an inward current, the SR can modulate plasma membrane excitability. Agonists, e.g. oxytocin (OT), bind to G-protein-coupled receptors (GPCR) and via phospholipase C (PLC) generate IP_3 as well as contribute to depolarisation and stimulate Ca^{2+} entry and enhance contractility

10.2.1 Ion Channels Present in Myometrium

10.2.1.1 Calcium Channels

A ubiquitous feature of contraction in muscle cells is the requirement for a rise in intracellular [Ca^{2+}]. This can be understood in smooth muscles by the need of myosin light-chain kinase (MLCK) to be activated by binding of Ca^{2+}-calmodulin. If Ca^{2+} is omitted from a physiological solution bathing a piece of contracting myometrium, contractions will rapidly fail, demonstrating the absolute necessity of external Ca^{2+} entry for the rhythmic contractile activity in the myometrium. Application of blockers of voltage-dependent L-type Ca^{2+} channels (also known as dihydropyridine receptors) abolishes myometrial contractions, even when Ca^{2+} is present in the external bathing solution [50].

L-type Ca^{2+} channels consist of a transmembrane pore-forming α_1-subunit and several auxiliary proteins (β and $\alpha_2\delta$) [81]. The $\alpha_2\delta$ subunit promotes the surface expression of the channel [82], while binding of the β-subunit prevents the ubiquitination and proteasomal degradation of the channel protein and promotes trafficking of the channel to the membrane [83]. In pregnant rat myometrial smooth muscle cells, depolarisation causes a nifedipine-sensitive inward Ca^{2+} current, down its electrochemical gradient [50]. The voltage threshold for activation of this Ca^{2+} current (I_{Ca}) is −50 to −40 mV. The mean maximal I_{Ca} density is calculated to be ~6.3 pA/pF when depolarisation is applied from a holding potential of −80 mV [84, 85]. These channels close when the membrane hyperpolarises. There is also a fast Ca^{2+}-sensitive inactivation which is a negative feedback mechanism preventing Ca^{2+} overload of the cells. Inactivation of the L-type Ca^{2+} channels leads to relaxation of the myometrial contraction.

Expression of L-type Ca^{2+} channel subunits varies during gestation in the rat. A fourfold increase in the number of dihydropyridine-binding sites, measured by saturation binding, was found by day 14 of gestation and maintained through parturition [86]. A gradual increase in α_1-subunit expression was also observed throughout gestation, though it decreased during labour [87] and was accompanied by a rapid increase in the β-subunit. Similar increases in α_1-subunit expression and L-type Ca^{2+} channel function are seen in guinea pig [88] and human [89] myometrium.

Another form of Ca^{2+} channel is the T-type. There is evidence for their expression (mRNA, protein) in myometrium [90, 91] and electrophysiology experiments have identified a nickel-sensitive T-type Ca^{2+} current [89]. However, there is debate concerning their physiological relevance and function in myometrium, as it is questioned whether the uterus will ever be hyperpolarised long enough to significantly activate T-type Ca^{2+} channels.

10.2.1.2 Potassium Channels

Myometrial smooth muscle cells express a wide range of potassium channels, including voltage-dependent channels (K_V), large-conductance voltage and calcium-dependent (BK) channels, small-conductance calcium-dependent (SK) channels and ATP-sensitive (K_{ATP}) channels. Under resting conditions, K^+ conductance is the main determinant of the resting membrane potential. As well as contributing to resting membrane potential, activation/inactivation of K^+ channels will influence the time course of the action potential and repolarisation. For these reasons, K^+ channel activity is usually associated with uterine quiescence and changes in channel expression linked to the onset of labour.

BK channels are expressed in all smooth muscles [92]. In blood vessels, they form part of an important negative feedback loop, where an increase in intracellular Ca^{2+} stimulates contraction, but also activates BK channels (via Ca^{2+} sparks) leading to hyperpolarisation and vasorelaxation. In uterine smooth muscle, BK channels are present with relatively high density and with their large conductance (~200 pS) might be expected to play a significant role. However, blockade of BK channels has little effect on either uterine contractility or calcium signalling [93, 94]. This may be because uterine smooth muscle cells do not produce Ca^{2+} sparks [48], meaning the BK channels are perhaps only minimally activated under physiological conditions. SK channels are also expressed in the myometrium throughout gestation. SK channel blockers

inhibited outward current and caused membrane depolarisation in myometrial cells and increased contractility in myometrial strips throughout gestation [94]. Therefore, the functional effect of SK channel inhibition is greater than BK channel inhibition. In a transgenic mouse model, overexpression of the SK3 channel delays labour [95].

K_{ATP} channels, the predominant isoform consisting of an inward rectifier K^+ channel (Kir6) and a sulfonylurea subunit (SUR2B), which provides the ATP sensitivity, also play an important role in regulation of myometrial quiescence in pregnancy and are downregulated ahead of labour [96]. K_{ATP} channels are inhibited by intracellular ATP and stimulated by MgADP and thus are involved in coupling metabolic state to cellular excitability. These myometrial channels may also be regulated by the endogenously produced gasotransmitter H_2S, leading to sulfhydration and myometrial relaxation [97], as demonstrated upon blockade of K_{ATP} channels with glibenclamide which attenuates the ability of H_2S to relax the myometrium.

Myometrial cells also express stretch-activated K^+ channels [98, 99] which are coded for by the two-pore family of K^+ channels (KCNK). Several groups have identified TREK-1 channels as being expressed in the myometrium and regulated during pregnancy and labour [99, 100]. In both mouse and human myometrial cells, TREK-1 channels were shown to be activated and produce an increased outward current in response to stretch [101]. TREK-1 gene expression is regulated during pregnancy, increasing towards term and falling at the time of labour [100]. In this way perhaps, myometrial quiescence is maintained as the foetus grows and the uterus distends.

Voltage-dependent potassium channels (K_V) are widely expressed in uterine smooth muscle. Depolarisation of the plasma membrane activates these channels and an efflux of K^+ ions from the cell leads to repolarisation to the resting membrane potential. Inhibition of these channels with a non-specific channel blocker, such as tetraethylammonium (TEA), increases uterine contractions clearly demonstrating a role in contractility. Different voltage-dependent K^+ channels have been identified as having a role in maintaining the membrane potential and therefore quiescence or controlling the transition from quiescence to labour. Two novel K_V channels, K_V7 and K_V11, encoded by the KCNQ and KCNH (ERG) gene families, respectively, appear to be important regulators of uterine contractility [102]. Parkington et al. [103] reported that ERG activity (K_V11) leads to inhibition of myometrial contraction, but during labour there is an increase in the expression of ERG's inhibitory β-subunit that causes a decrease in ERG activity and thus a stimulation of contraction. Similar findings were reported for $K_V10.1$ [104]. Interestingly, Parkington et al. also showed that the inhibitory β-subunit is expressed at a lower level in obese women, which results in elevated ERG activity and increased K^+ conductance and presumably poorer myometrial contractility. Indeed, we have shown in electrophysiological studies that cholesterol, which is often elevated in obese women, increases an outward K^+ current. The finding of an enhanced outward K^+ conductance in obese women may be a significant factor in the finding that obese women are more likely to require delivery by caesarean section.

KIR7.1 expression (KCNJ gene family), an inward rectifier channel, was identified in both mouse and human uterus to peak at mid-gestation and decline at term [105]. KIR7.1 current hyperpolarises uterine myocytes and knockdown of the channel leads to an increase in contractile force and duration. Another member of the K_V family that may have a role in uterine quiescence and transition to labour is $K_V4.3$ channels, whose expression is significantly reduced at term in mouse myometrium [106]. It is hoped that specific agonists of these channels may provide a new generation of more effective relaxants of uterine contractions, drugs referred to as tocolytics.

10.2.1.3 Chloride Channels

Work conducted in the 1980s revealed an unusual feature of smooth muscle cells; the intracellular Cl^- concentration is higher than in most cells [107]. Values reported of ~50 mM mean that there must be active mechanisms maintaining intracellular [Cl^-] above a passive distribution, that its membrane permeability is low and that the Cl^-

equilibrium potential is ~−20 mV [107]. The net effect is that if Cl^- channels are activated in the myometrium, their opening will lead to Cl^- leaving the myocytes. In electrical terms, this is equivalent to positive ions entering the cell, and hence depolarisation ensues. Thus, knowledge concerning the types of Cl^- channels in myometrium is important in understanding its excitability.

Ca^{2+}-Activated Cl^- Channels

In addition to Ca^{2+}-activated K^+ channels, the myometrium expresses Ca^{2+}-activated Cl^- channels (CACCs), which are sensitive to both voltage and Ca^{2+}. There has been much speculation over the molecular identity of these channels, with several candidates being proposed, but only two families of proteins (the bestrophin and the anoctamin (Ano1 or TMEM16) families) are able to replicate the classical properties of endogenous CaCC [108–110]. CaCC-mediated responses are stimulated upon activation of G protein-coupled receptors (GPCR) by agonists such as noradrenaline, endothelin-1, acetylcholine, ATP and angiotensin II. These agonists cause release of Ca^{2+} from the internal store via IP_3 receptors and it is this released Ca^{2+}, rather than external Ca^{2+}, that activates CaCCs in many tissues [111]. However, there are examples such as in portal vein and tracheal smooth muscle, where Ca^{2+} entry via L-type Ca^{2+} channels can activate a Cl^- current. Spontaneous release of Ca^{2+} from the internal store, Ca^{2+} sparks, can also activate CaCCs, resulting in spontaneous transient inward currents (STICS), in a similar way to BK channel activation by Ca^{2+} sparks producing STOCs.

CaCC expression has been identified in myometrium of human and rodent species [112–116]. In a study of myometrial isolated cells and muscle strips [117] we investigated the role of CaCCs in myometrium. A CaCC current was evident in 30% of freshly isolated rat myocytes. Blockade of the channels with niflumic acid significantly decreased the frequency of contraction in oxytocin-stimulated and spontaneously contracting strips of myometrium. Later studies have further demonstrated a role for CaCCs in myometrial contractility [115]. In addition, the demonstration that CaCCs are upregulated at term [114] suggests that they may play a role in increasing contractility of the myometrium at parturition.

10.2.1.4 Sodium Channels

Once calcium ions entering via L-type Ca^{2+} channels had been shown to be the dominant carrier of inward current in uterine myocytes, a role for Na^+ channels was understandably neglected. An early comprehensive electrophysiological investigation of membrane currents [118] reported fast sodium channels in rat myometrium. Increased Na^+ current expression in mid- and late pregnancy was reported in human myometrium [119]. Inoue and Sperelakis [85] suggested from their studies on rat that fast Na^+ channels play a role in spreading myometrial excitation and that this becomes more important as term approaches. A more recent study using expression and molecular biology approaches [120] found that veratridine, which increases Na^+ influx through voltage-gated Na^+ channels (VGSC), causes the rapid appearance of phasic contractions accompanied by changes in intracellular [Ca^{2+}]. Using RT-PCR, in the same study the authors detected the VGSC α-subunits Scn2a1, Scn3a, Scn5a and Scn8a in the cDNA from longitudinal myometrium. The mRNAs of the auxiliary β-subunits Scbn1b, Scbn2b and Scbn4b, and traces of Scn3b, were also present. The same group also showed that amiloride-sensitive Na^+ channels were expressed in the rat uterus and that "mRNA expression levels of the alpha, beta and gamma subunits are selectively and differentially regulated during pregnancy" [121].

It is tempting to speculate that fast Na^+ current channels, producing inward current, may be expressed in those myocytes acting as pacemakers within myometrial fibres.

10.2.1.5 Store-Operated Channels

As described earlier, elucidating the role of the sarcoplasmic reticulum in myometrium was not straightforward. Measurements of SR luminal Ca^{2+} showed a fall of Ca^{2+} as it was released into the cytoplasm when IP_3-producing agonists were applied to uterine myocytes [122]. SERCA was shown to bring about a slow refilling of luminal Ca^{2+}. The question then arises as to whether the

uterine myocytes possess a mechanism to refill the store with Ca^{2+} when SR luminal levels fall—in other words, is capacitative- or store-operated calcium entry (SOCE) functional in the uterus? Were there SOCE channels in the plasma membrane, or the more selective calcium release-activated channels (CRAC), or both?

The existence of a pathway between the internal Ca^{2+} store and plasma membrane, that replenishes the Ca^{2+} store, was first demonstrated in non-excitable cells. The store in these cells is referred to as the endoplasmic reticulum (ER). The existence of such a mechanism was postulated as a way of balancing ER Ca^{2+} release and plasma membrane Ca^{2+} entry, and thereby regulating Ca^{2+} signals in cells. Given the important and diverse cellular processes regulated by Ca^{2+}, such control is seen as essential in preventing aberrant signalling and pathologies [123]. The SOCE was eventually demonstrated by showing a steady-state rise in cytoplasmic Ca^{2+} or a small inwardly rectifying current, designated I_{CRAC} [124], upon lowering of ER Ca^{2+}. Both measurements were experimentally hard to obtain due to their small size and the molecular mechanisms involved proved elusive. This situation changed when, in 2005, STIM1 was identified as an ER transmembrane protein that could sense luminal Ca^{2+} [125, 126]. Interestingly, STIM had been identified about 10 years earlier and stands for stromal interacting molecule and is linked to cancer.

As luminal Ca^{2+} falls, Ca^{2+} dissociates from STIM and it undergoes conformational changes. The next step in unravelling the SOCE mechanism followed rapidly, with the plasma membrane channel subunit Orai1 being identified [127–129]. When low ER Ca^{2+} evokes the conformational change in STIM1, it interacts with Orai1 and a functional and selective Ca^{2+}-entry channel is activated. Overexpression of these components of SOCE greatly increased I_{CRAC}. Of note for smooth muscles, Ca^{2+} entry via Orai1 channels can also recruit members of the transient receptor potential channels (TRPCs) [130]. These non-specific cation channels in smooth muscle plasma membrane interact with STIM1 and open to produce cation entry, including Ca^{2+}. Cheng et al. showed that TRPC1 and ORAI1 are components of distinctly different channels, both of which are regulated by STIM1. It is the Orai-1-mediated Ca^{2+} entry that triggers trafficking and insertion of TRPC1 proteins into the plasma membrane where they are gated by STIM1. It is suggested that CRAC channels, which are highly selective for calcium, are restricted to non-excitable cells. The less selective and less well-characterised SOCE channels, and their still controversial relation to TRPCs, are more likely to occur in the uterus [131]. For a current account of STIM and Orai, see the review by Putney [123].

An interesting study in Orai1 knockout mice should be mentioned. The female mice are fertile and give birth to live pups, but they are not able to let down milk from their mammary glands. The explanation for this could be found in examination of their Ca^{2+} signals; Ca^{2+} oscillations induced by oxytocin in myoepithelial cells are substantially reduced, due to lack of Ca^{2+} entry and contraction failure [132]. Interestingly, these findings are similar to those obtained in oxytocin receptor knockout mice; parturition surprisingly occurs normally but milk let-down and contraction of the myoepithelial cells fail [133].

The evidence for a role and the importance of SOCE in smooth muscle has recently been reviewed by Feldman et al., and many key references can be found there [134]. It appears to us fair to conclude that its importance to contractility, as opposed to say proliferation and remodelling, is still debatable. Studies performed on cultured smooth muscle cells and lines have to be treated with extreme caution, due to their phenotypic change to a non-excitable state.

STIM and Orai isoforms have been identified in myometrial biopsies from women undergoing C-section operations [135]. The authors proposed that SOCE may play a role in Ca^{2+} signalling during pregnancy. These findings of STIM1 expression in human myometrium have been confirmed by Feldman et al., and extended to mouse myometrium [134]. In the same reference, an account is given of preliminary work showing a thinning of the myometrium in STIM1 null mice, along with a contractile impairment.

When it comes to directly identifying a role for SOCE in myometrial function, the only study to

date remains that of our group [56]. To understand the protocols necessary to demonstrate SOCE in myometrium, it has to be emphasised that in this excitable tissue, the major source of Ca^{2+} for contractions is entry through the L-type Ca^{2+} channels. This Ca^{2+} influx is necessary and sufficient for contraction. The Ca^{2+} that enters must later be removed by efflux mechanisms across the plasma membrane, as described in Sects. 10.3.4.1 and 10.3.4.2. Thus, a role for SOCE can only be to support agonist-induced contractions. In the study of Noble et al., mentioned above [54], depletion of the SR Ca^{2+} produced a prolongation of the bursts of action potentials and corresponding series of Ca^{2+} spikes, which increased contraction amplitude and duration. The rise of baseline Ca^{2+} and membrane depolarisation continued until all electrical and Ca^{2+} spikes and phasic contractions ceased, revealing a maintained, tonic force and a raised basal Ca^{2+}. We also showed that lanthanum, a blocker of SOCE, but not the L-type Ca^{2+} channel blocker nifedipine, abolished the maintained force and Ca^{2+}. The physiological relevance was emphasised by using an agonist, carbachol, which produces similar effects to depleting the SR upon SERCA blockade, depolarisation and elevation of force and basal Ca^{2+}. A brief, high concentration of carbachol, to cause SR Ca^{2+}depletion without eliciting receptor-operated channel opening, also produces these results. We therefore consider that in pregnant rat myometrium SR Ca^{2+} release is coupled to a marked Ca^{2+} entry via SOCE.

10.2.1.6 Sodium Pump: Na,K ATPase

The Na,K ATPase has long been known to maintain intracellular concentrations of Na^+ ($[Na^+]$) low as it moves $3Na^+$ out of the cell coupled to the entry of $2K^+$. For a review of its enzymatic activity and structure focussed on smooth muscle, see [136]. The resulting Na^+ pump current makes a small contribution to the negative membrane potential found in uterine and other cells [137]. The sodium gradient created can also be linked to the transport of other ions, notably H^+, Cl^- and Ca^{2+}, all of which are important to the excitability and function of the myometrium [138]. In smooth muscle, the Na,K ATPase and Na–Ca exchanger (NCX) colocalise [139]. Golovina et al. [140] showed that intracellular $[Na^+]$ in the sub-plasmalemmal spaces influences the activity of the NCX and the SR Ca^{2+} content. As discussed already, in the myometrium the SR has many close appositions to caveolae and the plasma membrane [141] and thus the presence of Na,K ATPase within these microdomains could affect contraction in the uterus.

The sodium pump is a P-type ATPase, composed of two α-subunits, two β-subunits and usually a third, FXYD, subunit, each of which has several isoforms [142, 143]. Developmental and tissue-specific differences in the expression of these isoforms allow the Na,K ATPase function to be tightly regulated. This is because the isoforms govern kinetics, membrane localisation, sensitivity to ions, and endogenous pump inhibitors. Not surprisingly therefore, it has been suggested that the Na,K ATPase may contribute not just to excitability in myometrium, but also to gestational changes in uterine activity [144]. It has also been reported that inhibitory prostaglandins work, in part, by stimulating the Na,K ATPase and thereby producing a hyperpolarisation [145].

Our group has studied the isoforms present in myometrium from human and animal tissues [144, 146–148] with respect to the expression of mRNA transcripts encoding Na,K ATPase and FXYD isoforms, their protein expression and tissue distribution, as well as their functional effects throughout gestation. In rats, we found that all three isoforms of the α- and β-subunits were expressed, along with FXYD1. Interestingly three of these isoforms, α2, α3 and β2, change their expression during pregnancy, suggesting that they are functionally regulated. In addition, sensitivity to the pump inhibitor, ouabain, changed during gestation; its effect of increasing frequency of contractions and the accompanying Ca^{2+} transients became larger as pregnancy advanced. In human myometrium we also found differences in α-isoform expression between non-pregnant and pregnant tissues. These findings extend and strengthen preliminary studies reporting isoform switching during pregnancy in rat and human myometrium [149, 150]. Furthermore, decreased α3 isoform expression correlates with reduced contractility in oestradiol-treated rats [151] sug-

gesting that changes in expression can have functional consequences in uterine smooth muscle.

In summary we are learning more about how subtleties in both isoform expression and distribution of Na^+ pumps can contribute to uterine function. They have been implicated in some complications of pregnancy, such as pre-eclampsia, a condition characterised by hypertension. Both defects in their activity and derangements mediated by circulating inhibitors can lead to an increase in $[Na^+]$ and therefore contribute to the disease [152].

10.2.2 Membrane Potentials and Action Potentials

The resting membrane potential of a cell is the voltage difference between the inside and outside of a cell, with typical values ranging from −40 to −80 mV. It is the balance of activity of the aforementioned ion channels that determines the resting membrane potential in a cell. The uterine smooth muscle contracts spontaneously. Contractions occur as a direct result of the generation of action potentials within the myometrial smooth muscle cells. The time course of action potentials measured in uterine smooth muscle varies greatly depending on the species, the part of the uterus examined and gestational status. Simple monotonic action potentials have been recorded in longitudinally oriented myometrium from rats and rabbits and circular muscle of sheep and guinea pig myometrium. However more complex action potentials with a sustained plateau of depolarisation have been observed in the circular myometrium of pregnant rats and mice and longitudinal myometrium of pregnant guinea pigs (for review see [153]).

When the membrane potential of uterine smooth muscle cells becomes sufficiently depolarised (threshold potential), voltage-dependent channels are activated, and the upstroke of the action potential resulting from the opening of voltage-dependent L-type Ca^{2+} channels and an inward Ca^{2+} current ensues. The threshold potential for these Ca^{2+} channels is around −40 mV and the inward Ca^{2+} current peaks within about 10 ms and then slowly reduces. Repolarisation is due to a variety of processes, such as the opening of voltage-dependent K^+ channels which generate a hyperpolarising outward K^+ current, and the voltage and Ca^{2+}-dependent inactivation of the L-type Ca^{2+} channels. In the more complex action potentials, an initial spike or series of spikes are followed by a sustained depolarisation (around −30 mV in rat myometrium). The duration of this plateau determines the duration of the resulting contraction.

As pregnancy progresses towards term it is thought that the resting membrane potential of the myometrial cells becomes more depolarised. While this certainly makes physiological sense, the evidence base is limited. This can be explained by the difficulty of making sharp electrode impalements into myometrial cells that are strongly contractile. Probably the best study to date was made in the third trimester of human pregnancy [154]. In this study, the membrane potential went from an average value of −70 mV at 29 weeks to −55 mV at parturition and was accompanied by a progressive increase in the frequency of myometrial contractions. This decrease in the level of negativity of the resting membrane potential would facilitate Ca^{2+} influx through voltage-operated Ca^{2+} channels. Reductions of potassium channels in the myocyte membranes in late pregnancy would also prolong myocyte action potentials and enhance contractility.

10.3 From Excitation to Contraction

10.3.1 Calcium Signalling

In myometrial smooth muscle cells, contraction is critically dependent on Ca^{2+} and removal of extracellular Ca^{2+} [50], abolishes contractions. The uterus exhibits a variety of Ca^{2+} signals; single transients, multiple transients on a raised basal Ca^{2+}, as shown in Fig. 10.3, as well as spikes and waves propagating through cells and bundles. These signals are dependent upon the frequency and duration of action potentials. As for the spread of electrical activity, the origins and rises of $[Ca^{2+}]$ within muscle bundles appear

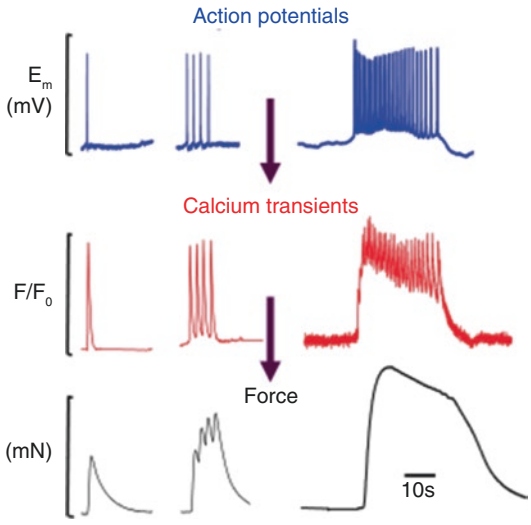

Fig. 10.3 Excitation-contraction coupling in myometrium. Electrical activity in the form of action potentials shapes the intracellular calcium signals and thereby modifies force in the uterus. Altering electrical activity is key to changing [Ca^{2+}] and hence force. E_M: potential measured with sucrose gap technique. Calcium was measured using the fluorescent indicator, Fluo4. Adapted from Burdyga et al. [155]

chaotic. Activity may originate in one area and then switch to another. Calcium waves might propagate to the end of the myocytes or terminate ahead of the cell border. We found that the amplitude of force generated by a single Ca^{2+} spike was around a third of the maximal and was dependent on the number of bundles recruited within the strip. If Ca^{2+} spikes appeared in bursts, they generated longer lasting fused contractions, the amplitudes of which were dependent on the number and the frequency of the spikes [155].

10.3.2 Pathway to Contraction

Figure 10.4 illustrates a schematic representing a uterine myocyte and the pathways leading to contraction, and how they might be inhibited, for example to prevent preterm birth.

Once in the cell, Ca^{2+} binds calmodulin ($4Ca^{2+}$ for every calmodulin molecule) and activates MLCK. MLCK phosphorylates serine 19 on the regulatory light chains of myosin, which in turn triggers interaction of phosphorylated myosin with actin myofilaments. The resulting cross-bridge cycling generates contraction and is an active process that requires ATP hydrolysis. Inhibition of MLCK with wortmannin also abolishes contractions. Relaxation occurs when Ca^{2+} channels are inactivated, and K^+ currents cause the membrane potential to return towards resting levels so that Ca^{2+} concentrations fall and myosin light-chain phosphatase (MLCP) dephosphorylates the myosin light chains. The process of excitation-contraction coupling in the uterus has been comprehensively reviewed [138, 156].

10.3.3 Effects of Agonists and Sensitisation

Binding of hormones such as oxytocin to its receptor in the cell membrane will lead to an increase in intracellular [Ca^{2+}]. The oxytocin receptor is a GPCR, which couples to phospholipase C via $G\alpha_{q/11}$. This in turn controls the hydrolysis of phosphoinositide-bis-phosphate (PIP2) into IP_3 and diacylglycerol (DAG). IP_3 releases Ca^{2+} from the internal store (SR) and triggers the aforementioned activation of MLCK and generation of contraction (see Fig. 10.4 and recent review [157]).

Agonists can also initiate other intracellular pathways and these signals may influence force generation in other ways, such as changing enzyme and channel activity. The phenomenon of Ca^{2+} sensitisation is observed in other smooth muscles, whereby the activity of MLCK and MLCP can be regulated in such a way that the contractions generated are altered without any change in [Ca^{2+}] [158]. However, there is little direct evidence for Ca^{2+} sensitisation occurring in myometrium [159]. Crichton et al. [160] described Ca^{2+} sensitisation in chemically skinned myometrial preparations, but the relevance to in vivo situations is unclear. Certainly, inhibiting the major sensitisation pathways (Rho-Rho kinase) in the uterus has little effect on [Ca^{2+}] or force [161]. It is our considered opinion, in the light of little to no direct evidence of sensitisation in the myometrium, and direct evidence against it, that it is not a feature of the normal physiologi-

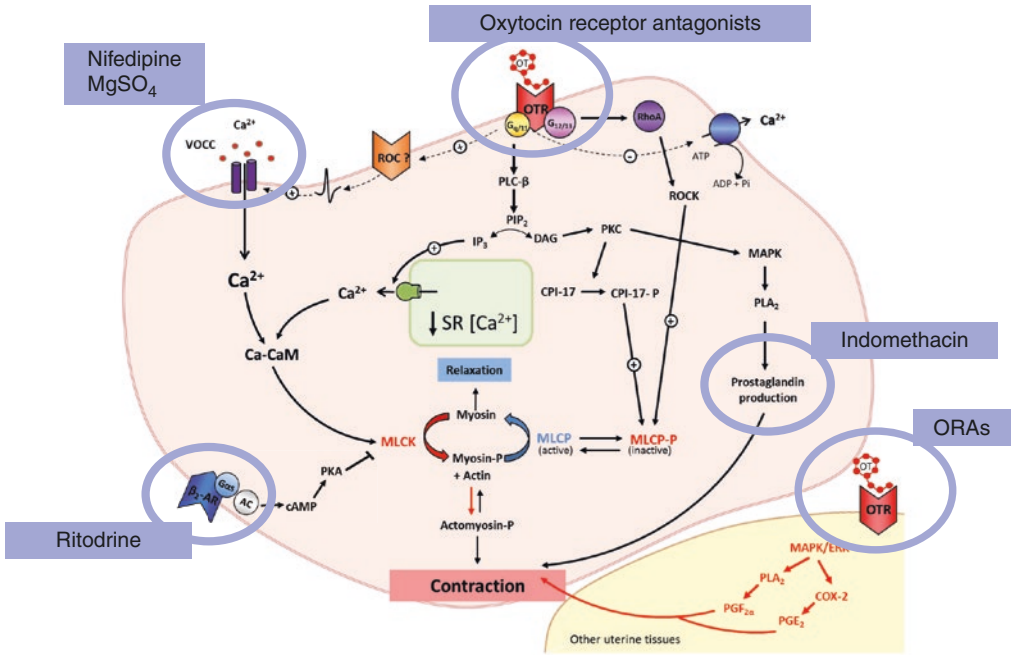

Fig. 10.4 Schematic of uterine force production pathways, and mechanisms of decreasing force used to help prevent preterm delivery, tocolysis. *VOCC* voltage-operated Ca^{2+} channel, *PLC-β* phospholipase C-β, PIP_2 phosphatidylinositol 4,5-bisphosphate, IP_3 inositol 1,4,5-trisphosphate, *DAG* diacylglycerol, *PKC* protein kinases type C, *Ca-CAM* Ca-calmodulin complex, *MLCK* myosin light-chain kinase, *MLCP* myosin light-chain phosphatase, *MAPK* mitogen-activated protein kinase, PLA_2 phospholipase A_2, *ROCK* RhoA-associated protein kinase. Adapted from Arrowsmith and Wray [157]

cal activity of the myometrium. As always, future work may lead to tempering of this view.

10.3.4 Calcium Balance and Efflux Mechanisms

Figure 10.3 demonstrates the close relationship between the intracellular Ca^{2+} transient and force. However, for labour it is important that contractions do not become tonic, as this produces hypoxia in the myometrium and can cause foetal asphyxia (see Sect. 10.4.5.1 and Fig. 10.5). It therefore follows that the mechanisms that terminate both action potentials and associated Ca^{2+} rises are as important as those that initiate them. The Ca^{2+} that entered the uterine myocyte must be removed to ensure flux balance. There are two mechanism that remove Ca^{2+} from myocytes, a plasma membrane Ca-ATPase (PMCA) and a Na/Ca exchanger (NCX). Both of these have been reviewed elsewhere [162, 163], and so we only present a brief overview.

10.3.4.1 Plasma Membrane Ca-ATPase (PMCA)

There is considerable similarity between PMCA and SERCA; both are P-type Ca-ATPases, and both play a crucial role in maintaining Ca^{2+} homeostasis and signalling. By analogy to SERCA uptake of SR-released Ca^{2+} after agonist stimulation, PMCA expels Ca^{2+} that enters the cell during excitation. Furthermore, there is structural homology between the two transporters; they both have transmembrane-spanning regions, have similar ATP-phosphorylated intermediaries, counter transport H^+ and are regulated by second messengers. They both also exist in several splice variant isoforms, which impart some tissue specificity. PMCA is regulated by calmodulin. Four isoforms of PMCA [1–4] have been identified with 80–90% amino acid sequence

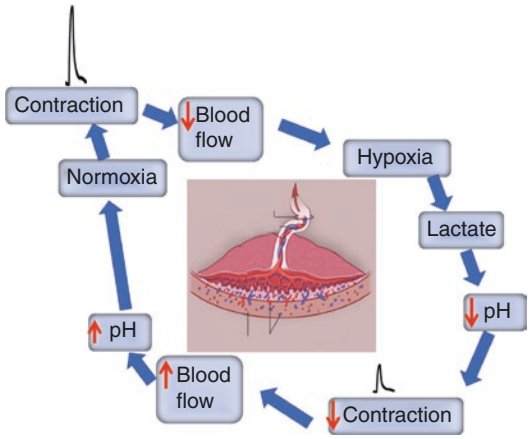

Fig. 10.5 The relation between contractions and blood flow in the uterus. Myometrial contractions are powerful, especially in labour. This leads to compressions of the uterine blood vessels (see central insert showing uterus and placenta and their closeness). The resultant hypoxia increases lactate which acidifies the myocytes. The fall in pH decreases calcium entry and force falls. This relieves the compression on vessels and the uterine environment is restored, and another effective contraction occurs. The feedback cycle will be protective as it prevents hypoxic damage to foetus (and myometrium)

homology and ten membrane-spanning regions. PMCA 1, 2b and 4 have been reported in myometrium [164]. In isolated uterine myocytes, 70% of Ca^{2+} efflux occurs via PMCA during the decay of a calcium transient, with the remaining 30% removed by NCX [165]. Inhibition of both mechanisms prevents all Ca^{2+}calcium efflux. In a study of intact rat uterus, 35% of SR-released Ca^{2+} was extruded by the NCX, and 65% by the PMCA [166]. Therefore, in the uterus, we can conclude that whatever the source of Ca^{2+} influx, PMCA plays the predominant role in Ca^{2+} efflux. We also found that the coupling between SR Ca^{2+} release and the NCX changes with gestation, altering its relative contribution to Ca^{2+} efflux.

10.3.4.2 Na/Ca Exchanger (NCX)

In the myometrium, the Na/Ca exchanger is a membrane-spanning antiporter. It has 938 amino acids and 9 transmembrane domains and utilises the Na^+ gradient provided by the sodium pump to extrude Ca^{2+}. During each cycle, one Ca^{2+} ion is exchanged for $3Na^+$ ions and thus it is electrogenic. The exchanger reaction may occur in either direction, as determined by the relative [Na^+] inside and outside of the uterine myocyte. Under most physiological conditions, the exchanger runs in its Ca^{2+} efflux mode. However, with the presence of plasma membrane microdomains in which NCX lies adjacent to SR, and couples to isoforms of the Na,K ATPase, it is possible that the NCX can bring Ca^{2+} into myocytes [167]. Even though PMCA extrudes more Ca^{2+} than NCX in uterine myocytes, both efflux mechanisms may well function in a compartmentalised fashion. It is suggested that the PMCA regulates the low-resting [Ca^{2+}] in the bulk cytosol while the NCX regulates the small microdomains between the plasma membrane and the SR [167].

10.4 Metabolism in Uterine Smooth Muscle

During labour the myometrium performs a series of sustained and powerful contractions to expel the young. These events are underpinned by growth, biochemical and metabolic changes. Throughout pregnancy there is enormous uterine growth, largely as a result of hypertrophy of the myometrium. Pronounced biochemical changes also occur during this period. These include increases in contractile proteins to support parturition but also changes in glycolytic and oxidative enzymes [168]. Metabolically, the uterus lays down reserves of glycogen and free fatty acid droplets in preparation for the hypoxic conditions it will experience in labour. After parturition these changes are rapidly reversed in a process known as involution. In women the uterus is back to near its pre-pregnancy size in about 6 weeks, a process that occurs due to changes in endocrine levels and removal of mechanical stretch [169]. We will briefly overview growth of the uterus in pregnancy, describe the uterine metabolites involved in contraction and then discuss metabolism and relation between contractions and blood flow. This latter part will include recent data examining the effects of hypoxia and pH in the myometrium.

10.4.1 Uterine Growth in Pregnancy

The human uterus is traditionally described as being a pear-shaped organ situated within the pelvis, ballooning up to the size of a large water melon with pregnancy. By week 20 it reaches the umbilicus and by week 30 it reaches the epigastric region.

In the early days and weeks of pregnancy the uterus does not need to grow. It needs to change to accept the foetus and help make the placenta, as it can easily accommodate the tiny embryo. The uterus contains a volume of about 10–25 mL, and this is ample for the embryo which is only about 5 mm long at 6 weeks. By weeks 12–14, the uterine wall has started to thicken from around 10 to 15 cm. By week 22, the baby will weigh 15 ounces, be the size of a dinner plate and contained in a uterus that is around three times thicker than it was at the start of pregnancy and extending 22 cm from the top of the pubic bone. Over the next 10 weeks the uterus increases its capacity to match the foetus and becomes so stretched it starts to thin. The uterus is so stretched at the end of term that it is thinner (about 5 mm) than at the start of pregnancy. From start to finish of pregnancy, the length of the uterus has increased from around 7 to 20 cm, its weight has increased more than ten times, going from about 70 g to more than 1000 g and its capacity from about 25 to 5000 mL. This adaptive growth of the uterus starts with some hyperplasia of myocytes in early pregnancy, stimulated by the endocrine changes of pregnancy and growth factors. From mid-pregnancy onwards, the myometrial hypertrophic growth is stimulated by wall stretch, with the endocrine environment being necessary in a permissive manner. Experiments of distending one of the two horns of a rodent uterus in a non-pregnant animal reveal that significant growth will occur. Likewise, there is little growth in a uterine horn of a pregnant rodent if there are no foetuses present; the side with foetuses grows normally. The uterine myocytes can increase fivefold in size, mainly due to an increased length but also thickness [170]. Progesterone supports this growth and also helps in dampening the contractile power of the myometrium. There are also changes in the extracellular matrix, with increased integrin expression bridging between the matrix and the hypertrophying myocytes. As with other smooth muscle cells, the uterine myocytes can synthesise some matrix elements, e.g. collagen. It is during the third trimester that the well-recognised contractile phenotype of the uterine myocyte comes to the fore, being packed with contractile proteins. A good account of these changes and the relation between endocrine and mechanical stimuli on the myocytes is provided in the review by Shynlova et al. [171]. Other investigators have pointed to the concurrent increase or appearance of contraction-associated proteins. A cassette of genes is assumed to be switched on at this time leading to increased gap junctions and Na^+ channels, as well as oxytocin and prostaglandin F receptors. In this way contractions can be coordinated and strengthened for labour.

10.4.2 Contractile Proteins and Kinetics

It has been noted that there is a change in the actin isoform close to term in rats, with a switch from α- to γ-actin [172]. As shown by Word et al. [173], the content of myosin and actin per milligram of protein or per tissue cross-sectional area is similar between myometrium of non-pregnant and pregnant women. In other words, despite the significant increase in myocyte size with pregnancy in women, the amount of contractile proteins per cellular cross-sectional area is similar to that found in myometrium obtained from non-pregnant women. In addition, myosin light-chain kinase and phosphatase activities are similar in the two tissues. The content of two thin filament-associated proteins was also examined in this study; caldesmon content was significantly increased in myometrium of pregnant women, whereas calponin was not different. In an earlier study, Sparrow et al. [174] examined the kinetic properties of the myocytes and myosin composition in rats. They concluded that the length-force relationship was of similar shape in the non-gravid and gravid skinned tissues. The energetic

tension cost (ATP turnover/active stress) in skinned fibres was also similar. The mechanical and metabolic characteristics of the gravid and non-gravid rat uterus do not suggest an obvious difference in the intrinsic properties of the myosin, although significant functional alterations in the tissue appear during pregnancy. This corresponds to the lack of a difference in the pattern of the heavy chains. Taken together, at least to a first approximation, the above data surprisingly suggest that there is little other than scale, to differentiate the intrinsic contractile proteins and contractions between non-pregnant and pregnant myometrium.

10.4.3 Metabolites and Contraction

As with other muscle types, the myometrium uses ATP during contraction. ATP is required both for cross-bridge cycling and phosphorylation of myosin light chains. The uterine myocytes also contain a store of phosphocreatine (PCr) which buffers the supply of ATP. In common with other smooth muscles, the store of PCr is low (~5 mM) compared to striated muscles (~30–50 mM). In the myometrium, these values were determined in intact muscle strips using ^{31}P NMR spectroscopy [175]. Some changes occur with pregnancy; PCr concentration ([PCr]) was one- to fourfold greater in late-pregnant than in non-pregnant rat uterus and recovered over several days during involution of the uterus.

When considering the low reserves of high-energy phosphates in the myometrium (and all smooth muscles) it is worth remembering that smooth muscles contract economically; contraction and relaxation are slow compared with striated muscles. This is partly because smooth muscle relies on Ca^{2+}-regulated phosphorylation of myosin rather than the Ca^{2+} troponin system, and partly due to the slower release of inorganic phosphate. This slow-release step means that there is a slow rate of cross-bridge cycling and longer lasting cross-bridge attachment periods and force production per ATP hydrolysed in smooth muscles. The oxygen consumption of smooth muscle is low compared to other muscle types. Consequently, metabolism can keep up with contraction during normal smooth muscle activity and no large increases in oxygen consumption occur. As with all muscles, good control of Ca^{2+} and pH is important for uterine smooth muscle function, and both regulation mechanisms make energetic demands requiring ATP. Further details and references can be found in [176].

10.4.4 Metabolism

There are some major differences in metabolism in smooth muscle compared to other cell types. One of the most striking is the degree of metabolic compartmentalisation. Oxidative phosphorylation directly supports contractile activity, while ionic regulation, especially Na,K ATPase, is supported by the ATP generated from anaerobic metabolism [177, 178]. There is direct interaction between the glycolytic enzymes and subunits of the Na,K ATPase and H-ATPase. The compartmentalisation of metabolism in smooth muscle was further supported by the demonstration that the enzymes for glycolysis are membrane bound, anchored by F-actin [179].

The myometrium produces lactate even with sufficient oxygen supplies for oxidative phosphorylation, i.e. oxygen is not limiting metabolism [180]. Lactic acid is produced by glycolysis and dissociates into lactate and protons at physiological pH. Lactate is produced during normoxic conditions in myometrium and transported out of the myocyte by a family of proton-linked monocarboxylate transporters [181]. Lactate efflux also increases severalfold under hypoxic conditions [180]. In a recent study on rat myometrium the effects of lactate on contractions, intracellular Ca^{2+} and pH were investigated [182]. We found that lactate in the physiological range decreases myometrial contractility because of its inhibition of Ca^{2+} transients. This inhibition in turn was a consequence of lactate acidifying the myometrial cytoplasm. The accumulation of extracellular lactate by reducing myometrial contractions is suggested to play a role in poor labours, discussed further in Sect. 10.5.

10.4.5 Blood Flow, pH and Myometrial Contractions

The myometrium contracts strongly in labour. Repetitive and intense contractions of labour are required to dilate the cervix, so that the foetal head and then body can pass through the birth canal. It is a feature of labour that the contractions increase in amplitude and frequency as they progress. Not always appreciated is that these powerful uterine contractions will compress and occlude the vessels coursing within the myometrium. In all species studied, clear dips in blood flow can be monitored during these contractions, as they compress the myometrial blood vessels [183]. From this it follows that hypoxia and ischemia are a normal occurrence in labour. If, however, the uterus contracts hypertonically and becomes more tonic than phasic, then the clamp on the uterine vessels will produce asphyxia in the foetus and ultimately in utero death. This relation is shown in Fig. 10.5.

10.4.5.1 Protective Feedback Mechanism

Phasic uterine contractions lead to cyclic changes in high-energy phosphates and lactate and pH. During uterine contractions, ATP concentration ([ATP]) would be expected to fall during the periods of hypoxia and ischemia and recover during the reperfusion that occurs between contractions [183]. In addition, because of the increased lactate and hypoxic conditions during force production, intracellular pH falls and is restored to normal values during the intervals between contractions [183]. The fall in [ATP] during normal labour may not be sufficient to limit contractions but the fall of pH will be. In single-uterine myocytes, intracellular acidification significantly decreased Ca^{2+} inward currents [184]. When examined in myometrial strips we found that intracellular acidification caused membrane hyperpolarisation [185], which was associated with failure of action potential firing and cessation of contraction. Thus, at the peak of uterine contractions the myocytes become progressively more acid and the contractions will start to reduce in strength. This, along with the changes in excitability and inactivation of the L-type Ca^{2+} current, results in the phasic contraction returning to baseline (see Fig. 10.5). The ensuing rest period, equivalent to diastole in the heart, should ensure that the metabolic changes produced by hypoxia and ischaemia are reversed, and [ATP], [PCr] and pH are restored. The environmental conditions, including normoxia, are then conducive to firing of action potential and myocytes responding with strong inward Ca^{2+} current and producing coordinated activity and the next, strong uterine contractions.

Thus, there is a negative feedback mechanism intrinsic to uterine myocytes. By acting to limit contraction strength and duration, this metabolic feedback loop will help prevent ischaemic damage to the myometrial muscle bundles. This is because the ischaemic period is curtailed, and blood flow and metabolites can be restored during the intercontraction intervals. There is also a huge importance of this feedback loop to the foetus. Because of the direct link between uterus and foetus via the placenta, myometrial hypoxia and ischaemia will be transmitted to the foetus, as indicated by insert in Fig. 10.5. During normal labour the peak of the uterine contractions can be detected by changes in foetal heart rate that accompany it; the hypoxia detected by the foetal cardiovascular system increases its heart rate. In other words, the cycle of hypoxia and its stimulation of foetal heart rate are a normal part of human labour. The intrinsic mechanism that limits contractile activity, and uterine damage, also protects the foetus. It copes with transient hypoxia by increasing its heart rate but does less well if the hypoxia and ischaemia become prolonged. The foetal heart rate pattern changes and large decelerations are a warning sign of foetal distress. It is for this reason that foetal heart rate is recorded in many labours so that warning signs can be detected and acted on, e.g. by recommending an emergency C-section. It is hard in such in vivo situations to dissect if the root cause of the problem is with the uterine vessels or myometrial cells.

10.4.5.2 Hypoxia-Induced Force Increase (HIFI) in Myometrium

Finally, we would like to draw attention to the possibility of hypoxic conditioning in the uterus, and describe another potential benefit to transient ischaemia and hypoxia in the uterus [176]. Hypoxic preconditioning is a protective effect arising from brief, intermittent hypoxic or ischemic episodes, on subsequent more severe hypoxic episodes. First discovered in cardiac muscle, the effect has now been documented in other organs. We found a novel response in uterus of hypoxic-induced force increase (HIFI), which we suggested helps maintain contractions during labour [186].

We know, as discussed above, that many changes occur towards the transition to labour. A conundrum however of labour is that contractions become progressively stronger as the myometrium experiences the repetitive metabolic stress of hypoxia, i.e. transient decreases of oxygenation, pH and ATP, all of which if sustained can decrease contractile activity. Oxytocin is often cited as driving contractions in labour, but oxytocin receptor knockout mice deliver normally. This led us to search for other, possibly intrinsic or metabolic, drivers of contraction.

Many genes concerned with metabolism and contraction are regulated by hypoxia, and changes in genes have been identified in a transcriptomic study of poorly labouring women [187]. There was, however, no evidence showing how such changes could be important to successful labours, and no mechanism linking hypoxia to an increase in contractions. Given a literature on hypoxic preconditioning and that decreases in oxygenation are part of normal labour, we wanted to consider if the effects of brief, repetitive periods of hypoxia could differ from the chronic changes used in most experimental protocols. We found a novel mechanism whereby brief but repetitive hypoxic episodes stimulated the contractile activity, HIFI. In other words, cycles of brief hypoxia initiate and maintain the progressive augmentation of contractility needed for labour. The underlying mechanism involves adenosine and prostaglandin and a rise in intracellular Ca^{2+} [186]. Of note was that HIFI is present in animal and human uterus, but only close to parturition. We speculate that aberrations in this powerful mechanism could underlie contractions being triggered too early (preterm labour) or, if HIFI is deficient, weak contractions, and thus poor and unsuccessful (dysfunctional) labours.

10.5 Uterine Activity and Parturition

Although this is a scientific chapter, it would be wrong to not, albeit briefly, address uterine contractility with respect to childbirth, and mention some of the problems that can arise due to aberrant uterine contractility. Examples would be contractions starting too early in gestation leading to preterm delivery; dysfunctional labours where contractions are too weak or uncoordinated to deliver the neonate or prevent postpartum haemorrhage, or contractions that are too strong and tonic-like that they lead to foetal hypoxia and stillbirths. Here we describe the progression to labour, followed by an overview of preterm birth and dysfunctional labour.

10.5.1 Progression to Labour

Labour is viewed as the culmination of changes that have been progressing over many months—it is no longer considered that there is one key event that flips a switch to labour. These ongoing changes include the changes in ion channels which in turn will affect the shape and frequency of action potentials. The increase in both gap junctions and their conduction helps ensure that changes in Ca^{2+} and excitability are rapidly transmitted to the muscle bundles and contractions can be coordinated. There is a change in endocrine environment, notably increased oxytocin release and receptors, increased prostaglandin production and reduced efficacy of progesterone due to isoform switching [188]. Coupling between other mediators of contraction, both intra- and extracellular, also increases [189]. As noted earlier there are also increases in myocyte size, myofilament content and iso-

forms, changes in actin polymerisation close to term, and along with increased agonist drive, all contribute to the strong contractions necessary for parturition.

During labour, the resultant coordinated contractions of the myocytes raise intrauterine pressure to dilate the cervix. As noted by Smith et al., "the emergent behaviour of the uterus has parallels in the behaviour of crowds at soccer matches that sing together without a conductor. This contrasts with the behaviour of the heart where sequential contractions are regulated by a pacemaker in a similar way to the actions of a conductor and an orchestra" [190].

10.5.2 Preterm Labour

Preterm labour is classified clinically as one that commences before 37 weeks of gestation. Post-term labours are those that go beyond 42 weeks. It is, however, the preterm births that give rise to the most concern. Preterm births remain the biggest cause of neonatal deaths and handicap. Preterm birth syndrome remains the most important clinical and research challenge facing pregnant women, their families and health professionals. The global burden of preterm birth is 15 million babies, and rates are rising [191, 192].

From a scientific perspective, the key challenges related to preterm birth research lie in its multiple aetiologies, long preclinical stage and complex gene-environment interactions.

The aetiology of premature labour is largely unknown. Risk factors are infection, a short/"incompetent" cervix as well as carrying more than one foetus. Almost half of all women pregnant with twins will deliver prematurely [193]. It is still not clear whether this increased risk comes from mechanical factors, such as uterine distension and pressure on the cervix or altered hormonal levels, as both oestrogens and progesterone are increased and maternal corticotrophin-releasing hormone (CRH) may be elevated [194]. Unfortunately, progress in better understanding of underlying pathologies, phenotyping and more targeted preventative therapies remains slow [195].

10.5.3 Dysfunctional Labour

While most term labours proceed successfully to a normal vaginal delivery and delivery of a healthy baby, unfortunately around 10% will not, due to weak uterine contractions arising from the failure of increasing strength and frequency of contractions that are the hallmark of labour. Contractions that start out well become weak and uncoordinated. This halts the dilation of the cervix and the labour slows or arrests. These labours are termed dysfunctional or dystocic. The condition is particularly a feature of women labouring for the first time. There is little evidence for a genetic cause [138].

The first insight into the physiological cause of dysfunctional labour came from our group [196]. This work involved obtaining a sample of myometrial capillary blood at the time of the first incision into the myometrium at C-section. This blood was immediately analysed for pH, lactate and other standard haematic variables. The data obtained was then matched to the blinded clinical classification of the reason for the C-section, provided by two consultant obstetricians. The results were compelling: women who had a C-section for reasons other than a diagnosis of dystocia had a similar range of myometrial capillary blood pH (around 7.3), but those labouring dysfunctionally had a significantly lower pH near 7.1. Furthermore, these women also had about double the lactate in their myometrial capillary blood. These findings can be understood in terms of a breakdown in the feedback cycle depicted in Fig. 10.5. If uterine blood flow is not restored adequately between contractions, so that lactate and pH are not restored to normal values, then contractions will become progressively impaired—i.e. the labour becomes dysfunctional. We have recently reported the outcome of a small randomised con-

trol trial using oral bicarbonate ingestion to help neutralise the low pH found in dysfunctional labours [197]. The results were extremely encouraging, with a significant reduction in the number of operative deliveries required in women who had had a diagnosis of dysfunctional labour. These results, if replicated in larger studies, could have a major impact in helping women worldwide suffering difficult births.

10.6 Conclusions

In this chapter we have summarised knowledge focussed on how the uterus contracts. We have journeyed from molecules to intracellular organelles, through in vitro and in vivo experiments and to women in labour. We have attempted to show areas where understanding has progressed. We have overviewed the discussion in a balanced manner, but undoubtedly our personal opinions emerge at times. Real progress has been made in understanding the role of the SR in this organ, and more details of K^+ channels and their nuanced roles are emerging. There have been some novel mechanisms uncovered, such as hypoxia-induced force increase (HIFI). There has also been a small clinical trial that has successfully bridged the gap from our basic science understanding around blood flow, contractions and acidity, to using bicarbonate to improve labour outcomes in women destined to have an emergency C-section because of dysfunctional labours. Despite this, true insights into key questions, such as what channels or myocytes determine pacemaking in the myometrium, remain beyond our grasp. We still must tell our students that one of the fundamental questions about this myogenic smooth muscle, which initiates excitation, remains unanswered. Our treatments to prevent preterm delivery are failing as the science has not translated to the clinic. We have now access to fantastic methods, from imaging to genomic, proteomic and metabolomic, as well as better computational techniques to handle and share large data. As a community we need to come together more to test our questions and ideas, so that the best protocols, techniques and collaborations can be made. Real progress will be measured by how quickly some of the missing data and questions arising from this chapter can be provided and the next chapter written.

References

1. Garfield RE, Chwalisz K, Shi L, Olson G, Saade GR. Instrumentation for the diagnosis of term and preterm labour. J Perinat Med. 1998;26(6):413–36.
2. Arrowsmith S, Robinson H, Noble K, Wray S. What do we know about what happens to myometrial function as women age? J Muscle Res Cell Motil. 2012;33(3–4):209–17.
3. Aguilar HN, Mitchell BF. Physiological pathways and molecular mechanisms regulating uterine contractility. Hum Reprod Update. 2010;16(6):725–44.
4. D'Hooghe TM, Debrock S. Endometriosis, retrograde menstruation and peritoneal inflammation in women and in baboons. Hum Reprod Update. 2002;8(1):84–8.
5. Kuijsters NPM, Methorst WG, Kortenhorst MSQ, Rabotti C, Mischi M, Schoot BC. Uterine peristalsis and fertility: current knowledge and future perspectives: a review and meta-analysis. Reprod BioMed Online. 2017;35(1):50–71.
6. Lan VT, Khang VN, Nhu GH, Tuong HM. Atosiban improves implantation and pregnancy rates in patients with repeated implantation failure. Reprod BioMed Online. 2012;25(3):254–60.
7. Young RC, Hession RO. Three-dimensional structure of the smooth muscle in the term-pregnant human uterus. Obstet Gynecol. 1999;93(1):94–9.
8. Wray S, Noble K. Sex hormones and excitation-contraction coupling in the uterus: the effects of oestrous and hormones. J Neuroendocrinol. 2008;20(4):451–61.
9. Danforth DN. The morphology of the human cervix. Clin Obstet Gynecol. 1983;26(1):7–13.
10. Timmons B, Akins M, Mahendroo M. Cervical remodeling during pregnancy and parturition. Trends Endocrinol Metab. 2010;21(6):353–61.
11. Vink J, Feltovich H. Cervical etiology of spontaneous preterm birth. Semin Fetal Neonatal Med. 2016;21(2):106–12.
12. Yellon SM. Contributions to the dynamics of cervix remodeling prior to term and preterm birth. Biol Reprod. 2017;96(1):13–23.
13. Tica AA, Dun EC, Tica OS, Gao X, Arterburn JB, Brailoiu GC, et al. G protein-coupled estrogen receptor 1-mediated effects in the rat myometrium. Am J Phys Cell Phys. 2011;301(5):C1262–9.
14. Elmer M, Alm P, Thorbert G. Electrical field stimulation of myometrial strips from non-pregnant and pregnant guinea-pigs. Acta Physiol Scand. 1980;108(3):209–13.
15. Wikland M, Lindblom B, Dahlstrom A, Haglid KG. Structural and functional evidence for the dener-

vation of human myometrium during pregnancy. Obstet Gynecol. 1984;64(4):503–9.
16. Hervonen A, Kanerva L, Lietzen R, Partanen S. Ultrastructural changes induced by estrogen in the adrenergic nerves of the rabbit myometrium. Acta Physiol Scand. 1972;85(2):283–5.
17. Zupko I, Csonka D, Falkay G. A rat model for functional characterization of pregnancy-induced denervation and postpartum reinnervation in the myometrium and cervix: a superfusion study. Reproduction. 2005;130(5):743–9.
18. Bryman I, Norstrom A, Dahlstrom A, Lindblom B. Immunohistochemical evidence for preserved innervation of the human cervix during pregnancy. Gynecol Obstet Investig. 1987;24(2):73–9.
19. Kirby LS, Kirby MA, Warren JW, Tran LT, Yellon SM. Increased innervation and ripening of the prepartum murine cervix. J Soc Gynecol Investig. 2005;12(8):578–85.
20. Clyde LA, Lechuga TJ, Ebner CA, Burns AE, Kirby MA, Yellon SM. Transection of the pelvic or vagus nerve forestalls ripening of the cervix and delays birth in rats. Biol Reprod. 2011;84(3):587–94.
21. Gandhi SV, Walker D, Milnes P, Mukherjee S, Brown BH, Anumba DO. Electrical impedance spectroscopy of the cervix in non-pregnant and pregnant women. Eur J Obstet Gynecol Reprod Biol. 2006;129(2):145–9.
22. Gnanamanickam GJ, Llewellyn-Smith IJ. Innervation of the rat uterus at estrus: a study in full-thickness, immunoperoxidase-stained whole-mount preparations. J Comp Neurol. 2011;519(4):621–43.
23. Sato Y, Hotta H, Nakayama H, Suzuki H. Sympathetic and parasympathetic regulation of the uterine blood flow and contraction in the rat. J Auton Nerv Syst. 1996;59(3):151–8.
24. Klukovits A, Gaspar R, Santha P, Jancso G, Falkay G. Functional and histochemical characterization of a uterine adrenergic denervation process in pregnant rats. Biol Reprod. 2002;67(3):1013–7.
25. Monica Brauer M, Smith PG. Estrogen and female reproductive tract innervation: cellular and molecular mechanisms of autonomic neuroplasticity. Auton Neurosci. 2015;187:1–17.
26. Mione MC, Cavanagh JF, Lincoln J, Milner P, Burnstock G. Pregnancy reduces noradrenaline but not neuropeptide levels in the uterine artery of the guinea-pig. Cell Tissue Res. 1990;259(3):503–9.
27. Anouar A, Schirar A, Germain G. Relaxant effect of the calcitonin gene-related peptide (CGRP) on the nonpregnant and pregnant rat uterus. Comparison with vascular tissue. Naunyn Schmiedeberg's Arch Pharmacol. 1998;357(4):446–53.
28. Yallampalli C, Chauhan M, Thota CS, Kondapaka S, Wimalawansa SJ. Calcitonin gene-related peptide in pregnancy and its emerging receptor heterogeneity. Trends Endocrinol Metab. 2002;13(6):263–9.
29. Gangula PR, Thota C, Wimalawansa SJ, Bukoski RD, Yallampalli C. Mechanisms involved in calcitonin gene-related peptide-induced relaxation in pregnant rat uterine artery. Biol Reprod. 2003;69(5):1635–41.
30. Mowa CN, Papka RE. The role of sensory neurons in cervical ripening: effects of estrogen and neuropeptides. J Histochem Cytochem. 2004;52(10):1249–58.
31. Amira S, Morrison JF, Rayfield KM. The effects of pregnancy and parturition on the substance P content of the rat uterus: uterine growth is accompanied by hypertrophy of its afferent innervation. Exp Physiol. 1995;80(4):645–50.
32. Schmidt C, Lobos E, Spanel-Borowski K. Pregnancy-induced changes in substance P and neurokinin 1 receptor (NK1-R) expression in the rat uterus. Reproduction. 2003;126(4):451–8.
33. Wimalasundera RC, Thom SA, Regan L, Hughes AD. Effects of vasoactive agents on intracellular calcium and force in myometrial and subcutaneous resistance arteries isolated from preeclamptic, pregnant, and nonpregnant woman. Am J Obstet Gynecol. 2005;192(2):625–32.
34. Stjernquist M, Alm P, Ekman R, Owman C, Sjoberg NO, Sundler F. Levels of neural vasoactive intestinal polypeptide in rat uterus are markedly changed in association with pregnancy as shown by immunocytochemistry and radioimmunoassay. Biol Reprod. 1985;33(1):157–63.
35. Mione MC, Cavallotti C, Burnstock G, Amenta F. The peptidergic innervation of the guinea pig uterine artery in pregnancy. Basic Appl Histochem. 1988;32(1):153–9.
36. Ramhorst R, Calo G, Paparini D, Vota D, Hauk V, Gallino L, et al. Control of the inflammatory response during pregnancy: potential role of VIP as a regulatory peptide. Ann N Y Acad Sci. 2018; https://doi.org/10.1111/nyas.13632.
37. Osol G, Mandala M. Maternal uterine vascular remodeling during pregnancy. Physiology (Bethesda). 2009;24:58–71.
38. Pijnenborg R, Vercruysse L, Hanssens M. The uterine spiral arteries in human pregnancy: facts and controversies. Placenta. 2006;27(9–10):939–58.
39. Chaiworapongsa T, Chaemsaithong P, Yeo L, Romero R. Pre-eclampsia part 1: current understanding of its pathophysiology. Nat Rev Nephrol. 2014;10(8):466–80.
40. Noble K, Zhang J, Wray S. Lipid rafts, the sarcoplasmic reticulum and uterine calcium signalling: an integrated approach. J Physiol. 2006;570(Pt 1):29–35.
41. Miyoshi H, Boyle MB, MacKay LB, Garfield RE. Voltage-clamp studies of gap junctions between uterine muscle cells during term and preterm labor. Biophys J. 1996;71(3):1324–34.
42. Ramondt J, Verhoeff A, Garfield RE, Wallenburg HC. Effects of estrogen treatment and inhibition of prostanoid synthesis on myometrial activity and gap junction formation in the oophorectomized ewe. Eur J Obstet Gynecol Reprod Biol. 1994;54(1):63–9.
43. Sheldon RE, Mashayamombe C, Shi SQ, Garfield RE, Shmygol A, Blanks AM, et al. Alterations in

gap junction connexin43/connexin45 ratio mediate a transition from quiescence to excitation in a mathematical model of the myometrium. J R Soc Interface. 2014;11(101):20140726.
44. Wray S, Burdyga T. Sarcoplasmic reticulum function in smooth muscle. Physiol Rev. 2010;90(1):113–78.
45. Ross R, Klebanoff SJ. Fine structural changes in uterine smooth muscle and fibroblasts in response to estrogen. J Cell Biol. 1967;32(1):155–67.
46. McCarron JG, Chalmers S, Bradley KN, MacMillan D, Muir TC. Ca2+ microdomains in smooth muscle. Cell Calcium. 2006;40(5–6):461–93.
47. Matsuki K, Takemoto M, Suzuki Y, Yamamura H, Ohya S, Takeshima H, et al. Ryanodine receptor type 3 does not contribute to contractions in the mouse myometrium regardless of pregnancy. Pflugers Arch. 2017;469(2):313–26.
48. Burdyga T, Wray S, Noble K. In situ calcium signaling: no calcium sparks detected in rat myometrium. Ann N Y Acad Sci. 2007;1101:85–96.
49. Tribe RM, Moriarty P, Poston L. Calcium homeostatic pathways change with gestation in human myometrium. Biol Reprod. 2000;63(3):748–55.
50. Shmigol AV, Eisner DA, Wray S. Properties of voltage-activated [Ca2+]i transients in single smooth muscle cells isolated from pregnant rat uterus. J Physiol. 1998;511(Pt 3):803–11.
51. Shmygol A, Wray S. Modulation of agonist-induced Ca2+ release by SR Ca2+ load: direct SR and cytosolic Ca2+ measurements in rat uterine myocytes. Cell Calcium. 2005;37(3):215–23.
52. Taggart MJ, Wray S. Contribution of sarcoplasmic reticular calcium to smooth muscle contractile activation: gestational dependence in isolated rat uterus. J Physiol. 1998;511(Pt 1):133–44.
53. Noble K, Matthew A, Burdyga T, Wray S. A review of recent insights into the role of the sarcoplasmic reticulum and Ca entry in uterine smooth muscle.Eur J Obstet Gynecol Reprod Biol. 2009; 144(Suppl 1):S11–9.
54. Nelson MT, Bonev AD. The beta1 subunit of the Ca2+−sensitive K+ channel protects against hypertension. J Clin Invest. 2004;113(7):955–7.
55. Burdyga T, Wray S. Action potential refractory period in ureter smooth muscle is set by Ca sparks and BK channels. Nature. 2005;436(7050):559–62.
56. Noble D, Borysova L, Wray S, Burdyga T. Store-operated Ca(2)(+) entry and depolarization explain the anomalous behaviour of myometrial SR: effects of SERCA inhibition on electrical activity, Ca(2)(+) and force. Cell Calcium. 2014;56(3):188–94.
57. Gam C, Larsen LH, Mortensen OH, Engelbrechtsen L, Poulsen SS, Qvortrup K, et al. Unchanged mitochondrial phenotype, but accumulation of lipids in the myometrium in obese pregnant women. J Physiol. 2017;595(23):7109–22.
58. Danylovych YV, Karakhim SA, Danylovych HV, Kolomiets OV, Kosterin SO. Electrochemical potential of the inner mitochondrial membrane and Ca2+ homeostasis of myometrium cells. Ukr Biochem J. 2015;87(5):61–71.
59. McCarron JG, Muir TC. Mitochondrial regulation of the cytosolic Ca2+ concentration and the InsP3-sensitive Ca2+ store in guinea-pig colonic smooth muscle. J Physiol. 1999;516(Pt 1):149–61.
60. Rizzuto R, Pinton P, Carrington W, Fay FS, Fogarty KE, Lifshitz LM, et al. Close contacts with the endoplasmic reticulum as determinants of mitochondrial Ca2+ responses. Science. 1998;280(5370):1763–6.
61. Csordas G, Renken C, Varnai P, Walter L, Weaver D, Buttle KF, et al. Structural and functional features and significance of the physical linkage between ER and mitochondria. J Cell Biol. 2006;174(7):915–21.
62. Batra S. The role of mitochondrial calcium uptake in contraction and relaxation of the human myometrium. Biochim Biophys Acta. 1973;305(2):428–32.
63. Gravina FS, Parkington HC, Kerr KP, de Oliveira RB, Jobling P, Coleman HA, et al. Role of mitochondria in contraction and pacemaking in the mouse uterus. Br J Pharmacol. 2010;161(6):1375–90.
64. Gravina FS, Jobling P, Kerr KP, de Oliveira RB, Parkington HC, van Helden DF. Oxytocin depolarizes mitochondria in isolated myometrial cells. Exp Physiol. 2011;96(9):949–56.
65. Clark JF, Kuznetsov AV, Radda GK. ADP-regenerating enzyme systems in mitochondria of guinea pig myometrium and heart. Am J Phys. 1997;272(2 Pt 1):C399–404.
66. Shanklin DR, Sibai BM. Ultrastructural aspects of preeclampsia. II. Mitochondrial changes. Am J Obstet Gynecol. 1990;163(3):943–53.
67. McMurtrie EM, Ginsberg GG, Frederick GT, Kirkland JL, Stancel GM, Gardner RM. Effect of a diabetic state on myometrial ultrastructure and isolated uterine contractions in the rat. Proc Soc Exp Biol Med. 1985;180(3):497–504.
68. Patel R, Moffatt JD, Mourmoura E, Demaison L, Seed PT, Poston L, et al. Effect of reproductive ageing on pregnant mouse uterus and cervix. J Physiol. 2017;595(6):2065–84.
69. Lammers WJ. The electrical activities of the uterus during pregnancy. Reprod Sci. 2013;20(2):182–9.
70. Rabotti C, Mischi M. Propagation of electrical activity in uterine muscle during pregnancy: a review. Acta Physiol (Oxford). 2015;213(2):406–16.
71. Lammers WJ, Stephen B, Al-Sultan MA, Subramanya SB, Blanks AM. The location of pacemakers in the uteri of pregnant guinea pigs and rats. Am J Phys Regul Integr Comp Phys. 2015;309(11):R1439–46.
72. Cretoiu SM, Cretoiu D, Popescu LM. Human myometrium—the ultrastructural 3D network of telocytes. J Cell Mol Med. 2012;16(11):2844–9.
73. Duquette RA, Shmygol A, Vaillant C, Mobasheri A, Pope M, Burdyga T, et al. Vimentin-positive, c-kit-negative interstitial cells in human and rat uterus: a role in pacemaking? Biol Reprod. 2005;72(2):276–83.
74. Allix S, Reyes-Gomez E, Aubin-Houzelstein G, Noel D, Tiret L, Panthier JJ, et al. Uterine contrac-

tions depend on KIT-positive interstitial cells in the mouse: genetic and pharmacological evidence. Biol Reprod. 2008;79(3):510–7.
75. Cretoiu SM, Cretoiu D, Marin A, Radu BM, Popescu LM. Telocytes: ultrastructural, immunohistochemical and electrophysiological characteristics in human myometrium. Reproduction. 2013;145(4):357–70.
76. Banciu DD, Banciu A, Radu BM. Electrophysiological features of telocytes. Adv Exp Med Biol. 2016;913:287–302.
77. Peri LE, Koh BH, Ward GK, Bayguinov Y, Hwang SJ, Gould TW, et al. A novel class of interstitial cells in the mouse and monkey female reproductive tracts. Biol Reprod. 2015;92(4):102.
78. Lee H, Koh BH, Peri LE, Sanders KM, Koh SD. Functional expression of SK channels in murine detrusor PDGFR+ cells. J Physiol. 2013;591(2):503–13.
79. Monaghan KP, Johnston L, McCloskey KD. Identification of PDGFRalpha positive populations of interstitial cells in human and guinea pig bladders. J Urol. 2012;188(2):639–47.
80. Young RC. Mechanotransduction mechanisms for coordinating uterine contractions in human labor. Reproduction. 2016;152(2):R51–61.
81. Catterall WA. Voltage-gated calcium channels. Cold Spring Harb Perspect Biol. 2011;3(8):a003947.
82. Bannister JP, Adebiyi A, Zhao G, Narayanan D, Thomas CM, Feng JY, et al. Smooth muscle cell alpha2delta-1 subunits are essential for vasoregulation by CaV1.2 channels. Circ Res. 2009;105(10):948–55.
83. Altier C, Garcia-Caballero A, Simms B, You H, Chen L, Walcher J, et al. The Cavbeta subunit prevents RFP2-mediated ubiquitination and proteasomal degradation of L-type channels. Nat Neurosci. 2011;14(2):173–80.
84. Miyoshi H, Urabe T, Fujiwara A. Electrophysiological properties of membrane currents in single myometrial cells isolated from pregnant rats. Pflugers Arch. 1991;419(3–4):386–93.
85. Inoue Y, Sperelakis N. Gestational change in Na+ and Ca2+ channel current densities in rat myometrial smooth muscle cells. Am J Phys. 1991;260(3 Pt 1):C658–63.
86. Mershon JL, Mikala G, Schwartz A. Changes in the expression of the L-type voltage-dependent calcium channel during pregnancy and parturition in the rat. Biol Reprod. 1994;51(5):993–9.
87. Tezuka N, Ali M, Chwalisz K, Garfield RE. Changes in transcripts encoding calcium channel subunits of rat myometrium during pregnancy. Am J Phys. 1995;269(4 Pt 1):C1008–17.
88. Collins PL, Moore JJ, Lundgren DW, Choobineh E, Chang SM, Chang AS. Gestational changes in uterine L-type calcium channel function and expression in guinea pig. Biol Reprod. 2000;63(5):1262–70.
89. Longo M, Jain V, Vedernikov YP, Hankins GD, Garfield RE, Saade GR. Effects of L-type Ca(2+)-channel blockade, K(+)(ATP)-channel opening and nitric oxide on human uterine contractility in relation to gestational age and labour. Mol Hum Reprod. 2003;9(3):159–64.
90. Ohkubo T, Kawarabayashi T, Inoue Y, Kitamura K. Differential expression of L- and T-type calcium channels between longitudinal and circular muscles of the rat myometrium during pregnancy. Gynecol Obstet Investig. 2005;59(2):80–5.
91. Blanks AM, Zhao ZH, Shmygol A, Bru-Mercier G, Astle S, Thornton S. Characterization of the molecular and electrophysiological properties of the T-type calcium channel in human myometrium. J Physiol. 2007;581(Pt 3):915–26.
92. Berkefeld H, Fakler B, Schulte U. Ca2+-activated K+ channels: from protein complexes to function. Physiol Rev. 2010;90(4):1437–59.
93. Aaronson PI, Sarwar U, Gin S, Rockenbauch U, Connolly M, Tillet A, et al. A role for voltage-gated, but not Ca2+-activated, K+ channels in regulating spontaneous contractile activity in myometrium from virgin and pregnant rats. Br J Pharmacol. 2006;147(7):815–24.
94. Noble K, Floyd R, Shmygol A, Shmygol A, Mobasheri A, Wray S. Distribution, expression and functional effects of small conductance Ca-activated potassium (SK) channels in rat myometrium. Cell Calcium. 2010;47(1):47–54.
95. Pierce SL, Kresowik JDK, Lamping KG, England SK. Overexpression of SK3 channels dampens uterine contractility to prevent preterm labor in mice. Biol Reprod. 2008;78(6):1058–63.
96. Brainard AM, Korovkina VP, England SK. Potassium channels and uterine function. Semin Cell Dev Biol. 2007;18(3):332–9.
97. Robinson H, Wray S. A new slow releasing, H(2)S generating compound, GYY4137 relaxes spontaneous and oxytocin-stimulated contractions of human and rat pregnant myometrium. PLoS One. 2012;7(9):e46278.
98. Bai X, Bugg GJ, Greenwood SL, Glazier JD, Sibley CP, Baker PN, et al. Expression of TASK and TREK, two-pore domain K+ channels, in human myometrium. Reproduction. 2005;129(4):525–30.
99. Buxton IL, Singer CA, Tichenor JN. Expression of stretch-activated two-pore potassium channels in human myometrium in pregnancy and labor. PLoS One. 2010;5(8):e12372.
100. Monaghan K, Baker SA, Dwyer L, Hatton WC, Sik Park K, Sanders KM, et al. The stretch-dependent potassium channel TREK-1 and its function in murine myometrium. J Physiol. 2011;589(Pt 5):1221–33.
101. Heyman NS, Cowles CL, Barnett SD, Wu YY, Cullison C, Singer CA, et al. TREK-1 currents in smooth muscle cells from pregnant human myometrium. Am J Phys Cell Phys. 2013;305(6):C632–42.
102. Greenwood IA, Tribe RM. Kv7 and Kv11 channels in myometrial regulation. Exp Physiol. 2014;99(3):503–9.
103. Parkington HC, Stevenson J, Tonta MA, Paul J, Butler T, Maiti K, et al. Diminished hERG K+ channel activity facilitates strong human labour con-

tractions but is dysregulated in obese women. Nat Commun. 2014;5:4108.
104. Greenwood IA, Yeung SY, Tribe RM, Ohya S. Loss of functional K+ channels encoded by ether-a-go-go-related genes in mouse myometrium prior to labour onset. J Physiol. 2009;587(Pt 10):2313–26.
105. McCloskey C, Rada C, Bailey E, McCavera S, van den Berg HA, Atia J, et al. The inwardly rectifying K+ channel KIR7.1 controls uterine excitability throughout pregnancy. EMBO Mol Med. 2014;6(9):1161–74.
106. Smith RC, McClure MC, Smith MA, Abel PW, Bradley ME. The role of voltage-gated potassium channels in the regulation of mouse uterine contractility. Reprod Biol Endocrinol. 2007;5:41.
107. Aickin CC, Vermue NA. Microelectrode measurement of intracellular chloride activity in smooth muscle cells of guinea-pig ureter. Pflugers Arch. 1983;397(1):25–8.
108. Qu Z, Wei RW, Mann W, Hartzell HC. Two bestrophins cloned from Xenopus laevis oocytes express Ca(2+)-activated Cl(−) currents. J Biol Chem. 2003;278(49):49563–72.
109. Yang YD, Cho H, Koo JY, Tak MH, Cho Y, Shim WS, et al. TMEM16A confers receptor-activated calcium-dependent chloride conductance. Nature. 2008;455(7217):1210–5.
110. Liu Y, Zhang H, Huang D, Qi J, Xu J, Gao H, et al. Characterization of the effects of Cl(−) channel modulators on TMEM16A and bestrophin-1 Ca(2)(+) activated Cl(−) channels. Pflugers Arch. 2015;467(7):1417–30.
111. Large WA, Wang Q. Characteristics and physiological role of the Ca(2+)-activated Cl- conductance in smooth muscle. Am J Phys. 1996;271(2 Pt 1):C435–54.
112. Elble RC, Ji G, Nehrke K, DeBiasio J, Kingsley PD, Kotlikoff MI, et al. Molecular and functional characterization of a murine calcium-activated chloride channel expressed in smooth muscle. J Biol Chem. 2002;277(21):18586–91.
113. Jeong JW, Lee KY, Lydon JP, DeMayo FJ. Steroid hormone regulation of Clca3 expression in the murine uterus. J Endocrinol. 2006;189(3):473–84.
114. Song J, Zhang X, Qi Z, Sun G, Chi S, Zhu Z, et al. Cloning and characterization of a calcium-activated chloride channel in rat uterus. Biol Reprod. 2009;80(4):788–94.
115. Bernstein K, Vink JY, Fu XW, Wakita H, Danielsson J, Wapner R, et al. Calcium-activated chloride channels anoctamin 1 and 2 promote murine uterine smooth muscle contractility. Am J Obstet Gynecol. 2014;211(6):688.e1–10.
116. Danielsson J, Vink J, Hyuga S, Fu XW, Funayama H, Wapner R, et al. Anoctamin channels in human myometrium: a novel target for tocolysis. Reprod Sci. 2018;25:1589–600. https://doi.org/10.1177/1933719118757683.
117. Jones K, Shmygol A, Kupittayanant S, Wray S. Electrophysiological characterization and functional importance of calcium-activated chloride channel in rat uterine myocytes. Pflugers Arch. 2004;448(1):36–43.
118. Yoshino M, Wang SY, Kao CY. Sodium and calcium inward currents in freshly dissociated smooth myocytes of rat uterus. J Gen Physiol. 1997;110(5):565–77.
119. Boyle MB, Heslip LA. Voltage-dependent Na+ channel mRNA expression in pregnant myometrium. Recept Channels. 1994;2(3):249–53.
120. Seda M, Pinto FM, Wray S, Cintado CG, Noheda P, Buschmann H, et al. Functional and molecular characterization of voltage-gated sodium channels in uteri from nonpregnant rats. Biol Reprod. 2007;77(5):855–63.
121. Pinto FM, Cintado CG, Merida A, Hidalgo A, Candenas ML. Differential expression of amiloride-sensitive Na+ channel subunits messenger RNA in the rat uterus. Life Sci. 2000;66(22):Pl313–7.
122. Shmigol AV, Eisner DA, Wray S. Simultaneous measurements of changes in sarcoplasmic reticulum and cytosolic. J Physiol. 2001;531(Pt 3):707–13.
123. Putney JW. Forms and functions of store-operated calcium entry mediators, STIM and Orai. Adv Biol Regul. 2018;68:88–96.
124. Hoth M, Penner R. Depletion of intracellular calcium stores activates a calcium current in mast cells. Nature. 1992;355(6358):353–6.
125. Liou J, Kim ML, Heo WD, Jones JT, Myers JW, Ferrell JE Jr, et al. STIM is a Ca2+ sensor essential for Ca2+-store-depletion-triggered Ca2+ influx. Curr Biol. 2005;15(13):1235–41.
126. Roos J, DiGregorio PJ, Yeromin AV, Ohlsen K, Lioudyno M, Zhang S, et al. STIM1, an essential and conserved component of store-operated Ca2+ channel function. J Cell Biol. 2005;169(3):435–45.
127. Feske S, Gwack Y, Prakriya M, Srikanth S, Puppel SH, Tanasa B, et al. A mutation in Orai1 causes immune deficiency by abrogating CRAC channel function. Nature. 2006;441(7090):179–85.
128. Vig M, Peinelt C, Beck A, Koomoa DL, Rabah D, Koblan-Huberson M, et al. CRACM1 is a plasma membrane protein essential for store-operated Ca2+ entry. Science. 2006;312(5777):1220–3.
129. Zhang SL, Yeromin AV, Zhang XH, Yu Y, Safrina O, Penna A, et al. Genome-wide RNAi screen of Ca(2+) influx identifies genes that regulate Ca(2+) release-activated Ca(2+) channel activity. Proc Natl Acad Sci U S A. 2006;103(24):9357–62.
130. Cheng KT, Liu X, Ong HL, Swaim W, Ambudkar IS. Local Ca(2)+ entry via Orai1 regulates plasma membrane recruitment of TRPC1 and controls cytosolic Ca(2)+ signals required for specific cell functions. PLoS Biol. 2011;9(3):e1001025.
131. Dalrymple A, Slater DM, Beech D, Poston L, Tribe RM. Molecular identification and localization of Trp homologues, putative calcium channels, in pregnant human uterus. Mol Hum Reprod. 2002;8(10):946–51.
132. Davis FM, Janoshazi A, Janardhan KS, Steinckwich N, D'Agostin DM, Petranka JG, et al. Essential role

of Orai1 store-operated calcium channels in lactation. Proc Natl Acad Sci U S A. 2015;112(18):5827–32.
133. Nishimori K, Young LJ, Guo Q, Wang Z, Insel TR, Matzuk MM. Oxytocin is required for nursing but is not essential for parturition or reproductive behavior. Proc Natl Acad Sci U S A. 1996;93(21):11699–704.
134. Feldman CH, Grotegut CA, Rosenberg PB. The role of STIM1 and SOCE in smooth muscle contractility. Cell Calcium. 2017;63:60–5.
135. Chin-Smith EC, Slater DM, Johnson MR, Tribe RM. STIM and Orai isoform expression in pregnant human myometrium: a potential role in calcium signaling during pregnancy. Front Physiol. 2014;5:169.
136. Blaustein MP, Chen L, Hamlyn JM, Leenen FH, Lingrel JB, Wier WG, et al. Pivotal role of alpha2 Na(+) pumps and their high affinity ouabain binding site in cardiovascular health and disease. J Physiol. 2016;594(21):6079–103.
137. Nakamura Y, Ohya Y, Abe I, Fujishima M. Sodium-potassium pump current in smooth muscle cells from mesenteric resistance arteries of the guinea-pig. J Physiol. 1999;519(Pt 1):203–12.
138. Wray S. Insights from physiology into myometrial function and dysfunction. Exp Physiol. 2015; 100(12):1468–76.
139. Moore ED, Etter EF, Philipson KD, Carrington WA, Fogarty KE, Lifshitz LM, et al. Coupling of the Na+/Ca2+ exchanger, Na+/K+ pump and sarcoplasmic reticulum in smooth muscle. Nature. 1993;365(6447):657–60.
140. Golovina V, Song H, James P, Lingrel J, Blaustein M. Regulation of Ca2+ signaling by Na+ pump alpha-2 subunit expression. Ann N Y Acad Sci. 2003;986:509–13.
141. Wray S, Shmygol A. Role of the calcium store in uterine contractility. Semin Cell Dev Biol. 2007;18(3):315–20.
142. Shull GE, Lingrel JB. Isolation and characterization of a cDNA for the catalytic subunit of the (Na+ + K+)-ATPase. Soc Gen Physiol Ser. 1987;41:301–21.
143. Martin-Vasallo P, Dackowski W, Emanuel JR, Levenson R. Identification of a putative isoform of the Na,K-ATPase beta subunit. Primary structure and tissue-specific expression. J Biol Chem. 1989;264(8):4613–8.
144. Floyd R, Mobasheri A, Martin-Vasallo P, Wray S. Na,K-ATPase isoforms in pregnant and nonpregnant rat uterus. Ann N Y Acad Sci. 2003;986:614–6.
145. Parkington HC, Tonta MA, Davies NK, Brennecke SP, Coleman HA. Hyperpolarization and slowing of the rate of contraction in human uterus in pregnancy by prostaglandins E2 and f2alpha: involvement of the Na+ pump. J Physiol. 1999;514(Pt 1):229–43.
146. Floyd RV, Wray S, Quenby S, Martin-Vasallo P, Mobasheri A. Expression and distribution of Na, K-ATPase isoforms in the human uterus. Reprod Sci. 2010;17(4):366–76.
147. Floyd RV, Wray S, Martin-Vasallo P, Mobasheri A. Differential cellular expression of FXYD1 (phospholemman) and FXYD2 (gamma subunit of Na, K-ATPase) in normal human tissues: a study using high density human tissue microarrays. Ann Anat. 2010;192(1):7–16.
148. Floyd RV, Mobasheri A, Wray S. Gestation changes sodium pump isoform expression, leading to changes in ouabain sensitivity, contractility, and intracellular calcium in rat uterus. Phys Rep. 2017;5(23):e13527.
149. Maxwell CV, Tao QF, Seely EW, Repke JT, Graves SW. Regulation of the sodium pump in pregnancy-related tissues in preeclampsia. Am J Obstet Gynecol. 1998;179(1):28–34.
150. Esplin MS, Fausett MB, Faux DS, Graves SW. Changes in the isoforms of the sodium pump in the placenta and myometrium of women in labor. Am J Obstet Gynecol. 2003;188(3):759–64.
151. Tsai ML, Lee CL, Tang MJ, Liu MY. Preferential reduction of Na+/K+ ATPase alpha3 by 17beta-estradiol influences contraction frequency in rat uteri. Chin J Phys. 2000;43(1):1–8.
152. Graves SW. Sodium regulation, sodium pump function and sodium pump inhibitors in uncomplicated pregnancy and preeclampsia. Front Biosci. 2007;12:2438–46.
153. Parkington HC, Coleman HA. Ionic mechanisms underlying action potentials in myometrium. Clin Exp Pharmacol Physiol. 1988;15(9):657–65.
154. Parkington HC, Tonta MA, Brennecke SP, Coleman HA. Contractile activity, membrane potential, and cytoplasmic calcium in human uterine smooth muscle in the third trimester of pregnancy and during labor. Am J Obstet Gynecol. 1999;181(6):1445–51.
155. Burdyga T, Borisova L, Burdyga AT, Wray S. Temporal and spatial variations in spontaneous Ca events and mechanical activity in pregnant rat myometrium. Eur J Obstet Gynecol Reprod Biol. 2009; 144(Suppl 1):S25–32.
156. Wray S, Arrowsmith S. Uterine smooth muscle. In: Hill JA, Olson EN, editors. Muscle: fundamental biology and mechanisms of disease. Boston, MA: Academic Press; 2012. p. 1207–16.
157. Arrowsmith S, Wray S. Oxytocin: its mechanism of action and receptor signalling in the myometrium. J Neuroendocrinol. 2014;26(6):356–69.
158. Somlyo AP, Somlyo AV. Signal transduction by G-proteins, rho-kinase and protein phosphatase to smooth muscle and non-muscle myosin II. J Physiol. 2000;522(Pt 2):177–85.
159. Woodcock NA, Taylor CW, Thornton S. Prostaglandin F2alpha increases the sensitivity of the contractile proteins to Ca2+ in human myometrium. Am J Obstet Gynecol. 2006;195(5):1404–6.
160. Crichton CA, Taggart MJ, Wray S, Smith GL. Effects of pH and inorganic phosphate on force production in alpha-toxin-permeabilized isolated rat uterine smooth muscle. J Physiol. 1993;465:629–45.
161. Kupittayanant S, Burdyga T, Wray S. The effects of inhibiting Rho-associated kinase with Y-27632 on force and intracellular calcium in human myometrium. Pflugers Arch. 2001;443(1):112–4.
162. Floyd R, Wray S. Calcium transporters and signalling in smooth muscles. Cell Calcium. 2007;42(4–5):467–76.

163. Wray S, Burdyga T, Noble K. Calcium signalling in smooth muscle. Cell Calcium. 2005;38(3–4):397–407.
164. Penniston JT, Enyedi A. Modulation of the plasma membrane Ca2+ pump. J Membr Biol. 1998;165(2):101–9.
165. Shmigol AV, Eisner DA, Wray S. The role of the sarcoplasmic reticulum as a Ca2+ sink in rat uterine smooth muscle cells. J Physiol. 1999;520(Pt 1):153–63.
166. Taggart MJ, Wray S. Agonist mobilization of sarcoplasmic reticular calcium in smooth muscle: functional coupling to the plasmalemmal Na+/Ca2+ exchanger? Cell Calcium. 1997;22(5):333–41.
167. Juhaszova M, Blaustein MP. Distinct distribution of different Na+ pump alpha subunit isoforms in plasmalemma. Physiological implications. Ann N Y Acad Sci. 1997;834:524–36.
168. Wynn RM. Cellular biology of the uterus. New York: Appleton-Century-Crofts; 1967. p. xi, 524 p.
169. Wray S. The role of mechanical and hormonal stimuli on uterine involution in the rat. J Physiol. 1982;328:1–9.
170. Shynlova O, Kwong R, Lye SJ. Mechanical stretch regulates hypertrophic phenotype of the myometrium during pregnancy. Reproduction. 2010; 139(1):247–53.
171. Shynlova O, Tsui P, Jaffer S, Lye SJ. Integration of endocrine and mechanical signals in the regulation of myometrial functions during pregnancy and labour. Eur J Obstet Gynecol Reprod Biol. 2009;144(Suppl 1): S2–10.
172. Shynlova O, Tsui P, Dorogin A, Chow M, Lye SJ. Expression and localization of alpha-smooth muscle and gamma-actins in the pregnant rat myometrium. Biol Reprod. 2005;73(4):773–80.
173. Word RA, Stull JT, Casey ML, Kamm KE. Contractile elements and myosin light chain phosphorylation in myometrial tissue from nonpregnant and pregnant women. J Clin Invest. 1993;92(1):29–37.
174. Sparrow MP, Mohammad MA, Arner A, Hellstrand P, Ruegg JC. Myosin composition and functional properties of smooth muscle from the uterus of pregnant and non-pregnant rats. Pflugers Arch. 1988;412(6):624–33.
175. Dawson MJ, Wray S. The effects of pregnancy and parturition on phosphorus metabolites in rat uterus studied by 31P nuclear magnetic resonance. J Physiol. 1985;368:19–31.
176. Almohanna A, Wray S. Hypoxic conditioning in blood vessels and smooth muscle tissues: effects on function, mechanisms, and unknowns. Am J Physiol Heart Circ Physiol. 2018;315:H756–70.
177. Lynch RM, Paul RJ. Compartmentation of carbohydrate metabolism in vascular smooth muscle. Am J Phys. 1987;252(3 Pt 1):C328–34.
178. Paul RJ, Krisanda JM, Lynch RM. Vascular smooth muscle energetics. J Cardiovasc Pharmacol. 1984;6 (Suppl 2):S320–7.
179. Dhar-Chowdhury P, Malester B, Rajacic P, Coetzee WA. The regulation of ion channels and transporters by glycolytically derived ATP. Cell Mol Life Sci. 2007;64(23):3069–83.
180. Wray S. The effects of metabolic inhibition on uterine metabolism and intracellular pH in the rat. J Physiol. 1990;423:411–23.
181. Kirk P, Wilson MC, Heddle C, Brown MH, Barclay AN, Halestrap AP. CD147 is tightly associated with lactate transporters MCT1 and MCT4 and facilitates their cell surface expression. EMBO J. 2000;19(15):3896–904.
182. Hanley JA, Weeks A, Wray S. Physiological increases in lactate inhibit intracellular calcium transients, acidify myocytes and decrease force in term pregnant rat myometrium. J Physiol. 2015;593(20):4603–14.
183. Larcombe-McDouall J, Buttell N, Harrison N, Wray S. In vivo pH and metabolite changes during a single contraction in rat uterine smooth muscle. J Physiol. 1999;518(Pt 3):783–90.
184. Shmigol AV, Smith RD, Taggart MJ, Wray S, Eisner DA. Changes of pH affect calcium currents but not outward potassium currents in rat myometrial cells. Pflugers Arch. 1995;431(1):135–7.
185. Taggart MJ, Burdyga T, Heaton R, Wray S. Stimulus-dependent modulation of smooth muscle intracellular calcium and force by altered intracellular pH. Pflugers Arch. 1996;432(5):803–11.
186. Alotaibi M, Arrowsmith S, Wray S. Hypoxia-induced force increase (HIFI) is a novel mechanism underlying the strengthening of labor contractions, produced by hypoxic stresses. Proc Natl Acad Sci U S A. 2015;112(31):9763–8.
187. Mittal P, Romero R, Tarca AL, Draghici S, Nhan-Chang C-L, Chaiworapongsa T, et al. A molecular signature of an arrest of descent in human parturition. Am J Obstet Gynecol. 2011;204(2):177.e15–33.
188. Brubaker D, Barbaro A, Chance MR, Mesiano S. A dynamical systems model of progesterone receptor interactions with inflammation in human parturition. BMC Syst Biol. 2016;10(1):79.
189. Arkinstall SJ, Jones CT. Pregnancy suppresses G protein coupling to phosphoinositide hydrolysis in guinea pig myometrium. Am J Phys. 1990;259(1 Pt 1): E57–65.
190. Smith R, Imtiaz M, Banney D, Paul JW, Young RC. Why the heart is like an orchestra and the uterus is like a soccer crowd. Am J Obstet Gynecol. 2015; 213(2):181–5.
191. Frey HA, Klebanoff MA. The epidemiology, etiology, and costs of preterm birth. Semin Fetal Neonatal Med. 2016;21(2):68–73.
192. Ryan JG, Dogbey E. Preterm births: a global health problem. MCN Am J Matern Child Nurs. 2015; 40(5):278–83.
193. Turton P, Neilson JP, Quenby S, Burdyga T, Wray S. A short review of twin pregnancy and how oxytocin receptor expression may differ in multiple pregnancy. Eur J Obstet Gynecol Reprod Biol. 2009; 144(Suppl 1):S40–4.
194. Power ML, Bowman ME, Smith R, Ziegler TE, Layne DG, Schulkin J, et al. Pattern of maternal serum corticotropin-releasing hormone concentration dur-

ing pregnancy in the common marmoset (Callithrix jacchus). Am J Primatol. 2006;68(2):181–8.
195. Rubens CE, Sadovsky Y, Muglia L, Gravett MG, Lackritz E, Gravett C. Prevention of preterm birth: harnessing science to address the global epidemic. Sci Transl Med. 2014;6(262):262sr5.
196. Quenby S, Pierce SJ, Brigham S, Wray S. Dysfunctional labor and myometrial lactic acidosis. Obstet Gynecol. 2004;103(4):718–23.
197. Wiberg-Itzel E, Wray S, Akerud H. A randomized controlled trial of a new treatment for labor dystocia. J Matern Fetal Neonatal Med. 2018;31(17):2237–44.

11 Myosalpinx Contractions Are Essential for Egg Transport Along the Oviduct and Are Disrupted in Reproductive Tract Diseases

Rose E. Dixon, Sung Jin Hwang, Bo Hyun Kim, Kenton M. Sanders, and Sean M. Ward

Abstract

Oviducts (also called fallopian tubes) are smooth muscle-lined tubular organs that at one end extend in a trumpet bell-like fashion to surround the ovary, and at the other connect to the uterus. Contractions of the oviduct smooth muscle (myosalpinx) and the wafting motion of the ciliated epithelium that lines these tubes facilitate bidirectional transport of gametes so that newly released ovum(s) are transported in one direction (pro-uterus) while spermatozoa are transported in the opposite direction (pro-ovary). These transport processes must be temporally coordinated so that the ovum and spermatozoa meet in the ampulla, the site of fertilization. Once fertilized, the early embryo begins another precisely timed journey towards the uterus for implantation. Myosalpinx contractions facilitate this journey too, while luminal secretions from secretory epithelial cells aid early embryo maturation.

The previous paradigm was that oviduct transport processes were primarily controlled by fluid currents generated by the incessant beat of the ciliated epithelium towards the uterus. More recently, video imaging and spatiotemporal mapping have suggested a novel paradigm in which ovum/embryo transport is highly dependent upon phasic and propulsive contractions of the myosalpinx. A specialized population of pacemaker cells, termed oviduct interstitial cells of Cajal (ICC-OVI), generate the electrical activity that drives these contractions. The ionic mechanisms underlying this pacemaker activity are dependent upon the calcium-activated chloride conductance, Ano1.

This chapter discusses the basis of oviduct pacemaker activity, its hormonal regulation, and the underlying mechanisms and repercussions when this activity becomes disrupted during inflammatory responses to bacterial infections, such as *Chlamydia*.

R. E. Dixon
Department of Physiology and Membrane Biology, School of Medicine, Tupper Hall, University of California, Davis, Davis, CA, USA

S. J. Hwang · B. H. Kim · K. M. Sanders
S. M. Ward (✉)
Department of Physiology and Cell Biology, University of Nevada, Reno School of Medicine, Reno, NV, USA
e-mail: smward@med.unr.edu

Keywords

Oviduct · Myosalpinx · Ovum transport · Fertilization · Interstitial cells of Cajal · Ano1 · *Chlamydia*

H. Hashitani, R. J. Lang (eds.), *Smooth Muscle Spontaneous Activity*, Advances in Experimental Medicine and Biology 1124, https://doi.org/10.1007/978-981-13-5895-1_11

11.1 Gross Anatomy and Histology of the Oviduct

The mammalian female reproductive tract (FRT) consists of a pair of ovaries, a pair of oviducts, a uterus, one or two cervices, vagina, clitoris, and clitoral glands [1]. The oviducts are open-ended, tubular organs which connect the periovarian space to the uterus or uterine horns. The gross structure of oviducts varies depending upon the species. Adult mouse oviducts are ~15 mm in length and are highly coiled having approximately ten loops. In comparison, human fallopian tubes are approximately 11–12 cm long, display a single slight bend [2, 3], and are held in place by a portion of the broad ligament called the mesosalpinx [4–6].

Along the length of an oviduct, four segments can be distinguished; these are beginning at the segment closest to the ovary: (1) the infundibulum, (2) the ampulla, (3) the isthmus, and (4) the interstitium or intramural segment [3, 5–9]; see Fig. 11.1. These segments are structurally and functionally distinct from one another [6]. Oviducts open into a trumpet-bell[1]-like protraction at the infundibulum side. This entrance point through which the newly released ovum(s) accesses the oviduct is termed the ostium. The ampulla and isthmus meet at the ampullary-isthmic junction (AIJ). The cavity of the uterine horn and the intramural segment meet at the utero-tubal junction (UTJ).

Smooth muscle, known as the myosalpinx, lines the entire length of the oviduct but the thickness and complexity of the muscle vary within each of the segments described above. The muscle in the ampulla is thin whereas multiple, thicker layers of muscle are found in the isthmus [6, 10]. Anatomical sphincters have been described at the AIJ and the UTJ of several species, although in mice an anatomical sphincter consisting of a ring of circular muscle has been described only at the UTJ [10]. However, recent calcium imaging experiments on oviducts isolated from transgenic mice expressing a smooth muscle localized genetically encoded calcium indicator (GCaMP6f) have suggested that a specialized interface may exist in the mouse myosalpinx at an area close to the AIJ (unpublished observations).

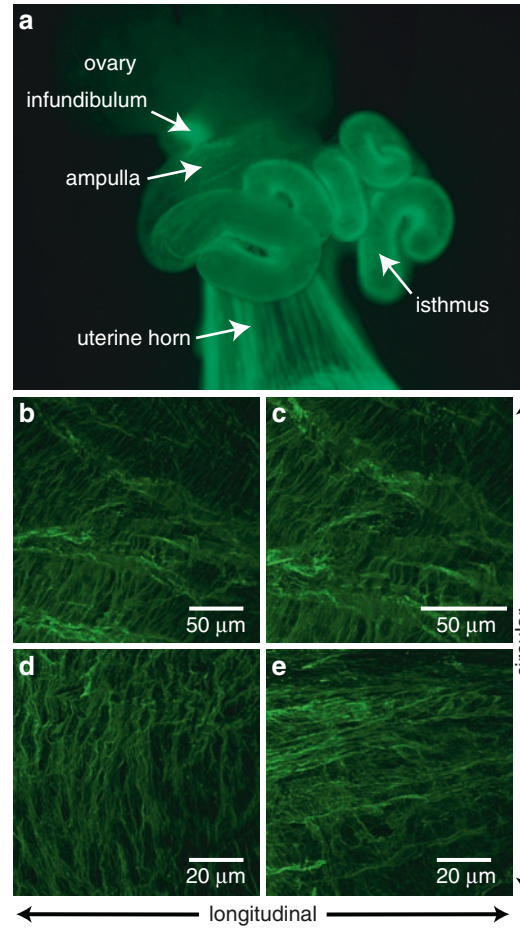

Fig. 11.1 Smooth muscle myosin heavy chain expression in the mouse oviduct. Panel (**a**) shows the expression of eGFP driven by a smooth muscle myosin heavy-chain (SMMHC) Cre recombinase along the entire length of an intact oviduct. Note also the presence of eGFP in the infundibulum region of the duct. Panels (**b**) and (**c**) show the orientation of smooth muscle heavy-chain-positive muscle fibers in the ampulla segment of the oviduct. Panels (**d**) and (**e**) show the same in the isthmus segment. Both the ampulla and isthmus had circularly and longitudinally orientated smooth muscle fibers. Images taken from a transgenic mouse with an eGFP inserted under the promoter for SMMHC 11 (*Myh11*) so that eGFP is selectively expressed in smooth muscle cells [200]. These mice were kindly provided by Mike Kotlikoff (Cornell University, Ithaca, NY)

[1]As an aside point, the term "salpinx" which is often used to refer to the oviducts is derived from the name of a Greek trumpetlike instrument with a shape strongly resembling that of a human oviduct.

The infundibulum has been reported to lack a developed muscle coat. Light and electron microscopy studies have revealed that the infundibulum displays thin, elongated cells, interconnected by slender cytoplasmic processes meshed together in a network with large voids filled by connective tissue. However, these thin, elongated cells were determined to be irregularly shaped smooth muscle cells based on ultrastructural characteristics including the presence of small bundles of myofilaments, smooth endoplasmic reticulum located beneath the plasma membrane, and a discontinuous basal lamina. Using a *B6.Cg-Tg*$^{(Myh11\text{-}cre,e\mathrm{GFP})}$ mouse in which smooth muscle cells express an eGFP reporter, we observed fluorescence in the infundibulum region of the oviduct (Fig. 11.1), supporting the previous observations that there are also some smooth muscle cells in this section of the duct. In contrast to the infundibulum, the ampulla has been reported to show a distinct smooth muscle coat which becomes gradually thicker upon progression from the upper to the lower ampulla. Irregularly shaped smooth muscle cells were also seen to display progressively more myofilament bundles as they approached the AIJ. In the lower ampulla, the irregularly shaped smooth muscle cells were found to be arranged into two interlacing layers with cells in the inner layer being mainly circularly orientated and cells in the outer layer mainly longitudinally orientated. The isthmus region of the oviduct, similar to the lower ampullary segment, has also been shown to possess two definite muscle layers, an inner circular and an outer longitudinal layer. The isthmus myosalpinx is thicker than that of the upper oviduct segments and was composed of more regular, "typical" smooth muscle cells. Finally, at the UTJ, the longitudinal muscle of the oviduct has been reported to become continuous with that of the myometrium. However, at the tip of the intramural segment, the circular muscle was seen to form a ring around the opening of the oviduct to the uterine horn cavity, anatomically similar to a sphincter.

The inner aspect of the mammalian oviduct is lined by a simple cuboidal or columnar epithelial mucosa (also called the endosalpinx) [11, 12]. The mucosa of the ampulla is arranged into extensively branched longitudinal folds giving it a large surface area and the largest luminal diameter of all the oviduct segments [11, 12]. The isthmus mucosa is less folded and has a narrower lumen, while the UTJ has the narrowest lumen of the entire oviduct [11]. The oviduct epithelium is composed of two main cell types, namely ciliated cells (~25%) and non-ciliated secretory cells (~60%); a third, minor cell population called intercalated or peg cells constitute around 10% of the cells but these cells are still poorly characterized; indeed even their existence is not universally accepted [9, 13, 14]. A progressive decrease in the number of ciliated cells occurs along the length of both mouse [15] (Fig. 11.2) and human oviducts [12–14, 16]. In the case of human oviducts, this decrease has been quantified, from over 50% ciliated cells in the fimbria of the infundibulum to less than 35% in the isthmus [12–14, 16]. As the proportion of ciliated epithelial cells decreases, the proportion of secretory cells increases so that the isthmus contains the highest proportion of secretory cells [11]. These non-ciliated secretory cells synthesize and secrete various substances and along with transudates from blood form the tubal fluid that fills the oviduct lumen [11, 17, 18]. Displacement of the tubal fluid caused by contractions of the myosalpinx serves to move eggs in the isthmus [6, 17]. Ovarian hormones can influence the structure of the oviduct epithelium [12]. Estrogen has been reported to produce hypertrophy of the epithelium and increase secretions and ciliogenesis while progesterone promotes atrophy and deciliation [12]. Both progesterone [19, 20] and estrogen [21] have also been suggested to affect ciliary beat frequency.

11.2 Physiological Functions of the Oviduct

The oviducts are not just passive conduits between the ovary and the uterus through which gametes and embryos must pass. Rather, they perform several physiological functions which are critical to fertility. These functions include roles for the oviduct in (1) egg pickup, (2) egg transport, (3) sperm transport and maintenance, (4) fertilization, and (5) embryo transport.

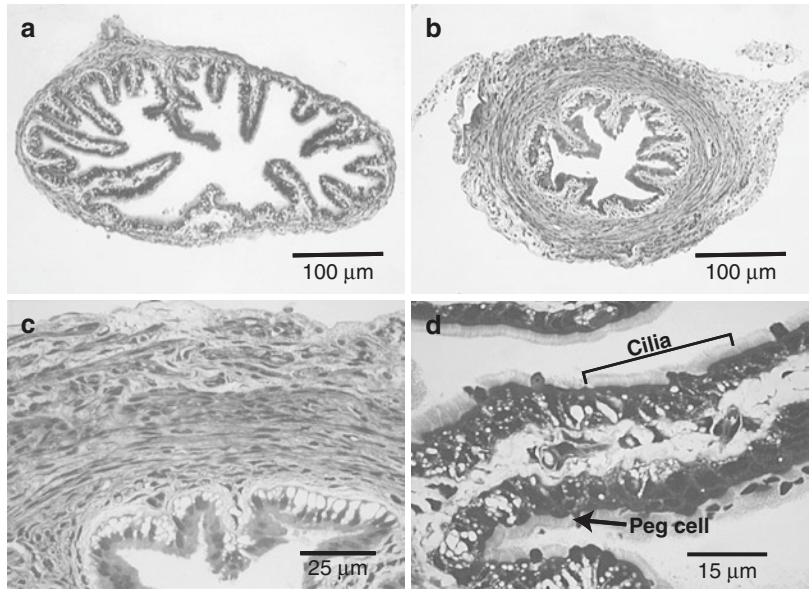

Fig. 11.2 Light micrographs through the murine oviduct and uterus at different levels. Panels (**a**–**d**) show cross sections at the level of the (**a**) ampulla and (**b**) isthmus. Note the increasing thickness of the myosalpinx from ampulla to isthmus and a decrease in the cilia density on the epithelium. (**c**) Shows high power of myosalpinx and goblet cells in the isthmus, but little or no cilia whereas (**d**) shows dense cilia and peg cells in the epithelia of the ampulla region

11.2.1 Egg Pickup

In mammals, a cumulus oocyte mass (COM) is ovulated [22, 23]. The COM is composed of the oocyte, or multiple oocytes, thousands of cumulus cells held together by gap junctions, and an extensive hyaluronan-rich extracellular matrix [23]. COMs rupture through the ovarian follicle wall after the preovulatory surge in luteinizing hormone (LH) and are deposited into the peritoneal or bursal cavity surrounding the ovary [22, 23]. In mice, the fingerlike projections of the infundibulum, termed fimbria, protrude into the ovarian bursa (a membranous sac that surrounds the ovary) where the COM is deposited, ensuring that contact will occur between the COM and the fimbria [17]. However, in humans, the COM is deposited into the large peritoneal cavity and contact between the fimbria and the COM is not guaranteed. Chances of contact in humans are improved by the active movement of the end of the oviduct, accomplished by contractions of the smooth muscle in the mesosalpinx and tubo-ovarian ligaments, permitting the sweeping of the fimbria across the surface of the ovary [17, 24]. The epithelium of the fimbria is highly populated by ciliated cells which beat in the direction of the ostium [22]. Pickup of the COM into the oviduct is achieved by a transient adhesive interaction between the COM and the cilia of the fimbria which then pulls the COM in towards the ostium and into the lumen of the ampulla [22, 25].

11.2.2 Egg Transport

Once the COM enters the ampulla, it passes rapidly to the site of fertilization at the AIJ [4, 6]. The duration of the oviductal phase of egg transport varies between species, lasting 55 h in rabbits, 72 h in mice, and 80 h in humans [6]. Many investigators have reported the rapid to-and-fro, pendular movements of the COM as it progresses through the ampulla of rats [26], rabbits [27], and mice [28]. The relative roles of the myosalpinx contractions and cilia beating in this initial phase of egg transport remain controversial.

Ciliated epithelial cells have been reported to play a role in egg transport along rat and rabbit ampullae [26, 27]. These studies utilized surrogate cumulus egg masses consisting of 15 µm diameter microspheres to imitate eggs and albumen to imitate the cumulus [26]. The transport of these surrogates along the ampullae of rats and rabbits was then observed in the presence of the β-adrenoceptor agonist isoproterenol to inhibit contractions of the myosalpinx [26, 27]. These investigators reported that the motion of surro-

gate egg masses changed from the characteristic pendular, to-and-fro movements, to a slow forward movement towards the AIJ and that the surrogates made it to the AIJ within normal time limits. This led to the conclusion that the role of cilia in egg transport was more important than that of smooth muscle. However, a number of points have been overlooked in these studies; firstly native eggs within naturally ovulated COMs have a diameter of 70–90 μm [29, 30], not 15 μm as used in the surrogate masses in the aforementioned studies. Previously, Talbot et al. [22] and Norwood et al. [25] have reported that "although cilia create currents capable of moving small particles such as *Lycopodium* spores (which have diameters of ~40 μm), ciliary currents alone cannot move larger objects such as COMs." Secondly, isoproterenol was used to inhibit contractions of the oviduct musculature; however, it is also known to increase oviduct ciliary activity [17, 31], perhaps contributing to the unchanged transport rate of the surrogates towards the AIJ.

In another study, microsurgical techniques were used to reverse 1 cm segments of rabbit ampulla [32]. As stated earlier, oviduct cilia beat in the direction of the uterus; however, the cilia in the reversed segments were seen to beat towards the ovary. These animals were rendered infertile by the reversal procedure whereas control animals in which a 1 cm segment of ampulla was transected but not reversed had normal fertility. The authors of this study concluded that cilia beating must be important for egg transport in the rabbit ampulla. However, a major caveat of this study is that the direction of the muscle was also reversed. This altered orientation of the muscle could also explain the observed infertility.

Egg transport ceases in the continued presence of unaltered ciliary beating when myosalpinx contractions are inhibited using the dihydropyridine L-type Ca^{2+} channel blocker nicardipine (1 μM) [28] and others have reported that women suffering from primary ciliary dyskinesia (PCD) or immotile cilia syndrome (also called Kartagener's syndrome) are capable of conceiving and carrying to term natural intrauterine pregnancies [17, 33]. A more recent study that examined the motor protein composition of human fallopian tube cilia reported that the motor protein composition of the human fallopian tube cilia was identical to that of respiratory cilia. Nine patients with PCD that suffered severe dysfunction of respiratory cilia gave birth to children after spontaneous conception [34]. The results of these studies contradict those described above and suggest that myosalpinx contractions are important and likely play a more significant role than cilia beating for oviduct egg transport.

11.2.3 Sperm Transport and Maintenance

The AIJ is the site of fertilization in most mammals and so the segments of the oviducts that are involved in sperm transport are the UTJ, the intramural segment, and the isthmus [3, 6]. In several mammalian species, it has been reported that sperm have been recovered from the oviduct ampulla minutes after mating or insemination [35, 36]. This initial wave is called the rapid phase of sperm transport and is considered to be much too fast to be explained by intrinsic motility of the sperm. In rabbits, it has been determined that these are not the fertilizing spermatozoa as most of the recovered sperm from this phase were found to be immotile and damaged [35]. The authors of this study speculated that the damage may have been caused by muscular contractions stimulated by insemination. The speed with which the sperm arrive at the ampulla certainly suggests some form of active transport along the isthmus segment of the oviduct [3, 35]. The fertilizing spermatozoa have been determined to come from a slower, more sustained phase of sperm transport involving the formation of an isthmic storage reservoir [6]. This phase is described in detail below.

The UTJ of the oviduct represents a physical barrier to sperm and is a means by which the female regulates sperm transport [37]. Although the structure of the UTJ varies across different mammalian species, the passageway is typically narrow. In mice, the UTJ is open shortly after coitus, but closes about an hour later [36–38] which significantly reduces the numbers of spermatozoa that pass through the UTJ before they

continue their journey in the oviduct to the ampulla. Although it has been suggested that spermatozoa swim up through the UTJ by self-propulsion, the use of specific knockout animals does not fully support this hypothesis. Spermatozoa of at least 13 discrete knockout lines are known to fail to enter the UTJ without any detectible abnormalities in their motility or morphology [39]. Once sperm enter the oviduct, it was reported that they moved back and forth in the isthmus region and that their movements were coordinated with the peristaltic contractions of the oviduct myosalpinx [40]. Myosalpinx contractions have also been suggested to play a role in pro-ampullary sperm transport in pigs and hamsters during the periovulatory period [41, 42]. However, oviductal contractions do not appear to be absolutely required for forming the sperm reservoir in the lower isthmus or for enabling sperm to reach the ampulla and COCs [43].

Once sperm make it through the UTJ, they form a reservoir in the pockets of the mucosal folds of the isthmus [36–38]. This reservoir was first described in hamsters in 1963 [44] but has subsequently been identified in mice [38], rabbits [45], pigs, and sheep [36]. Binding of sperm to the oviduct epithelium seems to preserve sperm during the period of storage before ovulation occurs [37]. It has yet to be established whether an isthmus reservoir of sperm exists in human fallopian tubes but since pregnancy can result from intercourse up to 5 days prior to ovulation [46] sperm must be stored at some point within the female reproductive tract. The oviducts are good candidates for this since human sperm co-cultured in vitro with oviduct epithelial cells can remain viable for longer than those cultured alone [47].

To be capable of fertilization, sperm must undergo capacitation. This is a complex physiological process that involves shedding of proteins and cholesterol from the plasma membrane, rendering it more permeable, especially in the apical acrosome region of the sperm head [48]. This prepares sperm for the acrosome reaction which occurs when sperm come into contact with the zona pellucida of the egg. The acrosome reaction involves enzyme release from the acrosomal region of the sperm head which allows the sperm to penetrate through the zona pellucida and layers of cumulus cells that surround the egg and ultimately allows them to fuse with the cell membrane of the egg and achieve fertilization [36, 48]. During capacitation of sperm, they become hyperactivated and display increased flagellar bend amplitudes which generate more power. Mouse oviducts have the advantage of being quite translucent when transilluminated, making them a good model in which to study oviduct sperm or egg transport. In oviducts from mated female mice, transillumination reveals that only hyperactivated sperm detach from the oviduct epithelium in the isthmic reservoir [49]. In that study, hyperactivated sperm were observed to "yank themselves free" of the oviduct epithelium.

Once hyperactivated, capacitated sperm are able to progress on towards the AIJ where they may fertilize an egg. It remains to be established whether this final stage of transport is facilitated by peristaltic contractions of the isthmus myosalpinx directed towards the AIJ, or whether hyperactivation of the sperm provides sufficient propulsion to transport the sperm to the AIJ without additional assistance. One study has found that co-culture of human sperm with human oviduct epithelial cells increased ciliary beat frequency (CBF) on the ciliated epithelial cells [50]. Since oviduct cilia beat in the direction of the uterus, this increase in CBF may represent an additional barrier to sperm transport towards the AIJ.

In summary, the myosalpinx of the UTJ contracts and relaxes to regulate the number of sperm that can enter the oviduct [37]. Peristaltic contractions of the myosalpinx of the isthmus play a role in the rapid phase of sperm transport. Adhesion of sperm to the endosalpinx of the isthmus permits the formation of a storage reservoir and helps to prolong the fertile life of sperm and finally sperm can increase the CBF of the ciliated cells of the endosalpinx, possibly providing a barrier to sperm transport.

11.2.4 Fertilization

When the COM reaches the AIJ, it becomes arrested for several hours or days depending on the

species [6]. In rabbits, humans, and mice there is no structural evidence for a sphincter at the AIJ which could explain this temporary suspension of transport [10, 51]. However, recent studies using oviducts from mice that have a genetically encoded calcium indicator (GCaMP6f) in smooth muscle display a specialized region which may represent the AIJ. At this site, calcium waves travelling along the ducts cease momentarily at this site. Anterograde waves travelling to the uterine horns and retrograde waves, travelling towards the ovaries, can also collide and annihilate each other in this region (unpublished observations). During the time at the AIJ, fertilization may occur if mating has been successful and dispersion of the cumulus follows [6]. The secretory cells of the ampulla mucosa secrete oviduct-specific, estrogen-dependent glycoproteins called "oviductins" which have been found to improve the efficiency of fertilization and first divisions of the zygote [6, 52].

11.2.5 Embryo Transport

Upon progression of the zygote through the AIJ, the final isthmic phase of oviduct transport begins. The isthmic segment contains a well-developed myosalpinx and relatively few ciliated epithelial cells compared to the ampulla. It has been shown that cilia are inefficient at moving denuded eggs (i.e., those that no longer are surrounded by the cumulus) and since the cumulus is rapidly dissolved at the AIJ in most mammals it is therefore thought that cilia play very little, if any, role in the isthmic phase of egg transport [4, 31]. Rhythmic contractions and relaxations of the isthmic myosalpinx create gradients in intraluminal pressure which move eggs within the tubal fluid at high speed back and forth, with an ultimate bias towards the uterus [6]. In humans, the transport of the embryo through the isthmus takes only ~8 h, equating to around 10% of the total time for oviduct egg transport [6]. In mice, isthmic embryo transport takes ~54 h, equating to around 75% of the total time for oviduct egg transport [6]. The reasons behind the differences in the time of egg transport along oviducts are currently unknown.

11.3 Spontaneous Electrical Activity of the Oviduct

Electrical activity has been recorded from the oviducts of several mammals, including rabbits [53–56], guinea pigs [57, 58], mice [28, 57, 59–61], baboons [57, 62], and humans [63–65]. Typically extracellular electrodes [53, 65], double-sucrose gap method [58], or suction electrodes [54–57, 62] were utilized. Other groups recorded oviduct electrical activity using intracellular microelectrodes, including reports from mice [28, 59–61], guinea pigs [57, 66], and humans [63, 64]. Intracellular microelectrode recordings were first applied to smooth muscle tissues over 60 years ago [67]. This technique permits quantitative analysis of resting membrane potential (RMP) and changes that occur in transmembrane potentials. The main difficulty using intracellular recordings is that intracellular impalements can be easily dislodged by the associated contractions of the smooth muscle tissue. This can be overcome by limiting tissue movement with tungsten or stainless steel pins, or by adding an L-type Ca^{2+} channel antagonist to the extracellular solution. In the mouse oviduct, L-type Ca^{2+} channel antagonists could not be utilized for this purpose due to the sensitivity of the electrical activity to these agents [28, 59]. For further explanation and discussion, see Sect. 11.4.3 below.

11.3.1 Myosalpinx Slow Waves

The term slow wave refers to the spontaneous, rhythmic oscillations of smooth muscle membrane potential. Myosalpinx slow waves were first described in the guinea pig oviduct by Tomita and Watanabe in 1973 [58]. These events were recorded using the double-sucrose gap technique and were seen to occur at 10–12 cycles/min with amplitudes of ~30 mV, often with a single spike superimposed onto their apex. Application of depolarizing and hyperpolarizing currents was found to have only weak effects on slow wave

frequency, but their amplitude was reduced upon depolarization and increased by hyperpolarization.

Later, the presence of myosalpinx slow waves was reported in mice, guinea pigs, and immature baboons [68]. Intracellular microelectrode recordings were performed on the isthmus segment of guinea pig oviducts and slow waves were observed to occur at a rate of around 15 cycles/min with an amplitude of 40–50 mV, a duration of 1.5 s, and a rate of rise of approximately 200 mV/s. Slow waves recorded with suction electrodes coincided with an increase in longitudinal tension, implying that slow waves may regulate contractions. However, in this early report, published in a time when extracellular recordings were more commonplace than they are today, no mention is made of whether control experiments were performed to rule out movement artifacts. In recent years, extracellular recording techniques have garnered criticism after it was reported that propagating biopotentials recorded from the well-characterized mouse stomach were completely abolished after inhibition of isotonic contractions of the muscle with nifedipine (2 μM) or the myosin light-chain inhibitor, wortmannin (10 μM; [69]). Since each of these is known to block gastric smooth muscle contractions but leave electrical activity intact [70–73], these results suggest that extracellular recordings primarily report mechanical activity rather than electrical slow waves. This is still a controversial topic in the smooth muscle electrophysiology field as the utility of extracellular recordings remains in question [74–77].

With that caveat in mind, suction electrode recordings from the ampulla revealed lower frequency activity than that observed in the isthmus, suggesting the presence of a frequency gradient along the guinea pig oviduct. This frequency gradient was also observed when suction recordings were made from the mouse ampulla and isthmus. Suction electrodes positioned at three locations along the length of the mouse and baboon oviducts revealed that slow waves originated from a site in the vicinity of the AIJ [57].

In 1981, Kishikawa and Kuriyama performed simultaneous intracellular and mechanical recordings from the circular muscle of the ampulla of human fallopian tubes [64]. Slow waves were reported to occur from a membrane potential of about −50 mV. Cell-to-cell variation of slow wave amplitude and frequency was observed but generally lay in the range of 15–41 mV and 12–60 cycles/min, respectively. Electrical activity was well synchronized with mechanical activity around the time of ovulation and during the estrogen-dominated proliferative period. However, during the progesterone-dominated secretory period, slow waves and contractions became uncoupled such that erratic and irregular contractions were observed to occur in a manner that was not synchronized with the regularly occurring albeit relatively low-frequency (compared to the estrogen-dominated phase) electrical activity [64]. This was speculated to reflect a cellular desynchronization that may occur due to looser cell-to-cell connections during this phase. This may reflect a menstrual cycle-dependent change in the myosalpinx architecture, similar to the estrous cycle-dependent changes reported in the muscle coat of the mouse oviduct [10], where muscle hypertrophy and increased contact between adjacent smooth muscle cells were observed during the estrogen-dominated phases of the cycle (pro-estrus and estrus). These changes subside during the progesterone-dominated phases (metestrus and diestrus). However, it should be noted that the human menstrual cycle is 28 days long whereas the mouse estrous cycle is only 4–5 days; therefore more pronounced changes may occur during the human menstrual cycle.

Slow waves in the circular muscle of the guinea pig oviduct have prolonged plateau potentials and are associated with myosalpinx contractions. Slow waves occurred at 8–19 cycles/min from membrane potentials of −50 to −60 mV, with amplitudes of 30–40 mV in agreement with the previous studies of guinea pig myosalpinx electrical activity [57, 58]. Estrous cycle-dependent changes in the slow wave frequency gradient were observed along the length of the oviduct. These changes involved an increase in slow wave frequency in the ampulla 2 days after ovulation, when the guinea pig eggs would typically be leaving the ampulla and entering the

isthmus region. It has previously been suggested that eggs may be propelled along the rabbit oviduct from regions of high to low contraction frequencies [78]. Similar observations were also made in the guinea pig oviduct as an increase in ampulla slow wave frequency (shown to be coupled to contractions) was observed around the time when the egg leaves the ampulla. An increase in isthmus slow wave frequency was also observed just before ovulation which may be related to transport of the spermatozoa through this region of the oviduct [66].

The most recent studies of slow waves in the oviduct myosalpinx were performed on mouse [28, 59–61]. RMPs were approximately −60 mV and slow waves occurred at a frequency between 7.5 and 10.5 cycles/min. Slow wave amplitudes averaged around 40 mV and ½ maximal durations of 2.5–3 s. The stage of the estrous cycle of the mice was not determined in these studies but in all preparations studied slow waves were found to be coupled on a 1:1 basis with contractions such that the contraction always lagged the upstroke phase of the slow wave by 0.3–0.5 s (Fig. 11.3). Spontaneous electrical and mechanical activities of the oviduct were not dependent on action potential-dependent neuronal activity, since slow waves persisted in the presence of the fast Na^+ channel blocker tetrodotoxin (TTX) [28]. These results provide solid evidence that slow waves are the underlying basis for myosalpinx contractions, but do not rule out the possibility that neuronal inputs can modulate spontaneous myosalpinx activity.

11.3.2 Ciliary Beating Versus Myosalpinx Contractions for Egg Movements

In order to determine whether ciliary beating versus myosalpinx contractions are responsible for egg movements video analysis combined with spatiotemporal mapping (STMaps) has been performed. Individual egg movements within the cumulus-oocyte mass and luminal particle movements were recorded in mouse oviducts [28]. STMaps generated from video recordings revealed that myosalpinx contractions propelled eggs in a pendular manner along the oviduct with an ultimate bias driving the eggs towards the uterus. STMaps revealed that egg movements ceased when myosalpinx contractions were inhibited with the L-type calcium channel blocker, nicardipine (1 μM). Nicardipine did not affect ciliary beating or the movements of small (<25 μm) luminal particles. Data from this study demonstrated that beating of just oviduct cilia was insufficient to propel oocytes within the lumen of the oviduct. Eggs are approximately 80 μm in diameter within a COM, whereas previous studies suggested that ciliary beating was sufficient to propel surrogate egg mass particles of approximately 15 μm in diameter [26].

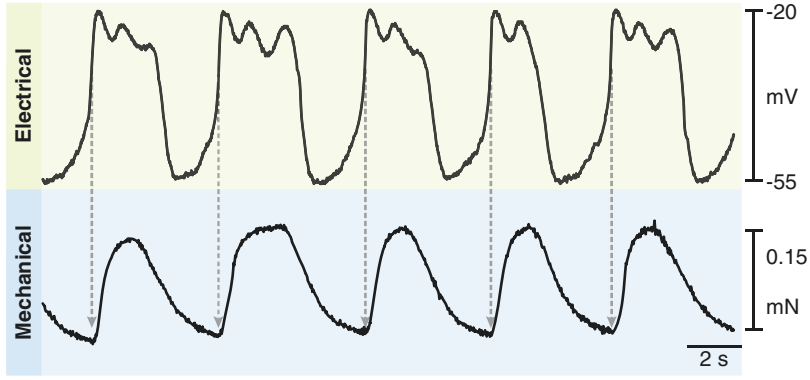

Fig. 11.3 Spontaneous electrical slow waves are coupled to phasic contractions of the myosalpinx. Simultaneous recordings of slow waves (*top*) and oviduct contractions (*bottom*). Note that each electrical slow wave precedes a contraction of the myosalpinx (dashed arrows indicate coupling). Adapted and reprinted with permission from [28]

11.3.3 Cellular Identification of Pacemaker Cells in the Oviduct: ICC-OVI

ICC-OVI were first described in human fallopian tubes in 2005 [79, 80] and subsequently in mouse oviducts in 2009 [28]. Popescu et al. [79] conducted a thorough histochemical characterization of ICC-OVI (referred to as tubal ICC or t-ICC in these studies) by staining tissues and primary cell cultures obtained from ampullary segments of human fallopian tubes. ICC-OVI were visualized using a variety of techniques including methylene blue, crystal violet, Janus-Green B, Mito-Tracker-Green FM, Giemsa, trichrome stainings, Gomori silver impregnation, and transmission electron microscopy. The identity of ICC-OVI was confirmed in some instances using antibodies against c-Kit protein. A network-like distribution of ICC-OVI was reported in the lamina propria and smooth muscle. The morphology of individual ICC-OVI was described as being "octopus-like" in some instances, with long processes that had dilated portions (resembling "beads on a string") containing mitochondria. ICC-OVI were said to represent ~7% of cells in the myosalpinx of the ampulla [69]; this value is comparable to the 5–6% reported for the *tunica muscularis* of the proximal colon [81]. The ultrastructural characteristics of ICC in the gastrointestinal (GI) tract have previously been used as a means by which to identify them. These characteristics have been grouped together into a set of criteria called the "gold standard" [82, 83]. Popescu reported that ICC-OVI satisfied all criteria of the "gold standard." The cells were also noted to form gap junctions with each other and with adjacent smooth muscle cells. This would presumably permit communication within the ICC-OVI network and with neighboring smooth muscle cells. ICC-OVI were also found to be positive for vimentin, CD34, NK-1, and caveolins and negative for the neuronal marker PGP9.5. Popescu comments "Why should not t-ICC be responsible for the human fallopian tube peristalsis?" pointing towards a pacemaker function for these cells.

Not long after this initial report, another group performed immunohistochemistry on cryosections of human fallopian tubes using a c-Kit antibody [80]. In this study, c-Kit-positive ICC-OVI were found in all segments of the fallopian tubes (i.e., infundibulum, ampulla, isthmus, and intramural segment). The ICC-OVI were described as being elongated cells with dendritic processes and large, oval nuclei and their location was said to be within the circular muscular layer of the ampulla and isthmus and also at the interface between the longitudinal and circular muscle layers. Mast cells also stained positive for c-Kit but could be distinguished from ICC-OVI based on their rounded, unbranched morphology and their positive staining with fluorescein-avidin DCS. The authors of this immunohistochemical study speculated that ICC-OVI may be the pacemakers of the fallopian tubes.

The simple presence of c-Kit$^+$ ICC-OVI does not provide any information as to the functional role(s) of these cells in the female reproductive tract. The first de facto evidence of the physiological role of c-Kit$^+$ ICC-OVI appeared in Dixon et al. in 2009 [28] (Fig. 11.4). In this study, the authors exploited knowledge obtained from studies on the functional roles of ICC in the GI tract [84]. Shortly before and immediately following birth the c-Kit receptors expressed in ICC networks in the GI tract are readily amenable to neutralization using the rat anti-mouse monoclonal antibody, ACK2 [85–87], or to the c-kit and platelet-derived growth factor receptor antagonist Gleevec® (imatinib mesylate) [86]. Intracellular recordings performed on oviducts isolated from newborn mice on postnatal day 0 revealed that spontaneous slow waves occurred in oviducts even at this early stage of life suggesting that a functional pacemaker network was already in place. An abundance of c-Kit$^+$ ICC-OVI were visualized by immunohistochemistry using the same antibody. After 5 days in organotypic culture, spontaneous slow wave activity was still recorded in oviducts and became more robust over this time period. Oviducts placed in organotypic culture for 5 days abundantly expressed c-Kit$^+$ ICC-OVI. However, after 5 days in organ-

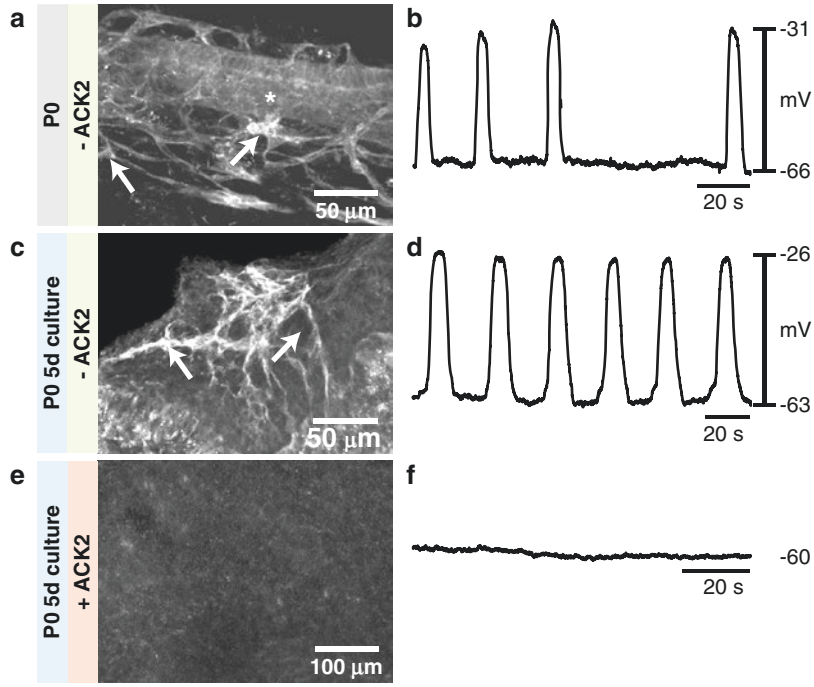

Fig. 11.4 Loss of ICC-OVI within the mouse oviduct myosalpinx leads to abolition of spontaneous electrical activity. Panels (**a**), (**c**), and (**e**) are confocal micrographs of immunolabeled ICC-OVI from oviducts isolated and fixed at P0 (**a**), or after 5 days in culture without (**c**) or with (**e**) c-Kit-neutralizing antibody. Treatment with the ACK2 c-Kit-neutralizing antibody led to loss of ICC-OVI (**e**). White arrows in **a** and **c** indicate the cell bodies of the ICC-OVI and the asterisk in panel **a** indicates the oviduct lumen. Robust, spontaneous electrical slow wave activity was recorded in freshly isolated (**b**) and 5-day-cultured oviducts (**d**) but was absent in ACK2-treated oviducts (**f**). Adapted and reprinted with permission from [28]

otypic culture in the presence of ACK2, spontaneous electrical activity was abolished and expression of c-Kit$^+$ ICC-OVI was significantly reduced or absent. These experiments provided the first tangible evidence that c-Kit$^+$ ICC-OVI perform a pacemaker function in the oviduct, being the cells responsible for the generation of spontaneous slow waves that underlie the phasic contractions of the myosalpinx, essential for egg transport along the oviduct. A possible criticism of this work is that organotypic culture could alter the excitability of the myosalpinx leading to electrical quiescence. Arguing against this, the authors performed experiments which demonstrated that although neonatal oviducts did not display spontaneous slow waves when cultured with c-Kit-neutralizing antibody, they were still electrically excitable and electrical field stimulation generated large depolarizing membrane potentials that were similar in waveform to the observed spontaneous activity [28].

11.4 Ionic Conductances Underlying Oviduct Pacemaker Activity

11.4.1 Expression of Voltage-Dependent Calcium Channel (VDCC) and Calcium-Activated Chloride Channel (CaCC) Transcripts in Oviduct Myosalpinx

Calcium (Ca^{2+}) influx into smooth muscle tissues from the extracellular fluid occurs mostly via dihydropyridine-sensitive L-type ($Ca_V1.2$) and dihydropyridine-resistant T-type (Ca_V3 subfamily)

voltage-dependent Ca^{2+} channels [88]. Another depolarizing conductance which has been identified in a variety of smooth muscle tissues is the Ca^{2+}-activated Cl^- channel (CaCC) ANO1. These channels are important for pacemaker activity in smooth muscles [60, 89–94]. The most convincing demonstration of this assertion has been the work performed on *Ano1*$^{-/-}$ mice, in which electrical slow wave activity fails to develop in GI smooth muscle [95]. Further credence is given to this model by the finding that pharmacological inhibition of ANO1 channels in wild-type mice greatly attenuates or abolishes slow waves in the stomach and small intestine [96–98]. RT-PCR experiments have revealed the presence of the transcripts for L- and T-type Ca^{2+} channels [59], and CaCCs (*Ano1* formerly known as *Tmem16a*) in oviduct myosalpinx [60]. Transcript expression of L-type Ca^{2+} channels $Ca_V1.2$ (*Cacna1c*), 1.3 (*Cacna1d*), and 1.4 (*Cacna1f*) was confirmed in the ampulla and isthmic segments of the mouse oviduct [59]. All three members (*Cacna1g*, *Cacna1h*, and *Cacna1i*) of the T-type (Ca_V3) subfamily of Ca^{2+} channels were expressed in all segments of the oviduct [59]. *Ano1* channel transcripts were also expressed in all segments of epithelium-denuded mouse oviducts [60].

11.4.2 Role of Extracellular Calcium on Oviduct Electrical and Contractile Activity

Reduction in extracellular Ca^{2+} ($[Ca^{2+}]_o$) concentration has been shown to abolish slow wave activity in a variety of visceral smooth muscles [90, 99–103]. Dixon et al. previously examined the dependence of oviduct slow wave activity and smooth muscle contractions on $[Ca^{2+}]_o$ by the sequential reduction of $[Ca^{2+}]_o$ [59]. In experiments [59] in which simultaneous electrical and mechanical activity was recorded, myosalpinx slow waves were coupled on a 1:1 basis with mechanical contractions and it was observed that slow wave depolarization always preceded the accompanying contraction. Amplitude and frequencies of slow waves and contractions decreased as $[Ca^{2+}]_o$ was reduced until spontaneous activity ceased at a $[Ca^{2+}]_o$ concentration of 0.25 mM or lower [59]. Reduction of $[Ca^{2+}]_o$ tended to cause slight depolarization in RMP but did not become statistically significant. The maximum rate of rise (*dV/dt* max) of the upstroke phase of slow waves also decreased with reduction in $[Ca^{2+}]_o$ prior to cessation of slow waves [59]. These data suggest that $[Ca^{2+}]_o$ is critical, either directly or indirectly, for oviduct pacemaker activity.

11.4.3 Effects of L-Type Ca^{2+} Channel Blockade on Slow Waves

The L-type Ca^{2+} channel inhibitor nifedipine (1 μM) has been reported to abolish oviduct slow waves but, unexpectedly, blockade of this depolarizing, inward current was associated with a significant *depolarization* in RMP (−60 ± 2 to −47 ± 2 mV, mean ± s.e.m., $P = 0.002$) [59]. This result suggests that loss of L-type Ca^{2+} influx also affects an outward conductance that influences the setting of the RMP of the cells (perhaps a Ca^{2+}-activated K^+ channel; *see K^+ channel section below*). Depolarization can itself affect slow wave generation and frequency. Indeed a pronounced sensitivity to membrane potential displacement was previously reported in human fallopian tubes when brief pulses of depolarizing or hyperpolarizing current injections were applied and an effect on slow wave frequency and amplitude was observed [64]. Brief hyperpolarizing current injections generating an ~3–5 mV change in the RMP resulted in increased amplitude slow waves and a marked reduction in slow wave frequency. A similar magnitude depolarization in the RMP had the opposite effect, resulting in a decrease in amplitude and increase in frequency of slow waves. Therefore, to parse out whether L-type Ca^{2+} channels themselves play an essential role in slow wave generation or whether the effect on RMP was the determining factor in slow wave abrogation, the membrane potential was repolarized with low extracellular K^+ (0.1 mM)-containing external solution, or the K_{ATP} channel

opener pinacidil (1 nM) in the continued presence of nifedipine. Under these conditions, slow waves returned at membrane potentials close to control levels indicating that L-type Ca^{2+} channels are not essential for generation of slow waves in the oviduct [59].

11.4.4 Effects of T-Type Ca^{2+} Channel Blockade on Slow Waves

T-type Ca^{2+} channels have been found to be important for the generation and propagation of slow waves in a variety of smooth muscle tissues [102–108]. Since L-type Ca^{2+} channels per se are not essential for slow wave generation, yet $[Ca^{2+}]_o$ is critical, it was logical to examine other pathways for Ca^{2+} entry across the plasma membrane of ICC-OVI or smooth muscle cells. T-type Ca^{2+} channel transcript expression had already been confirmed in mouse oviducts [59], so the effect of pharmacological blockade of these channels was investigated next. This was accomplished using the divalent cation nickel (Ni^{2+}; 30–500 μM). Similar to the effect of nifedipine described above, Ni^{2+} caused a graded, concentration-dependent depolarization of the RMP, and significantly reduced the rate of rise of slow wave upstrokes. However, even at the highest concentration tested (500 μM), Ni^{2+} failed to block slow waves in the oviduct, likely ruling out a role of T-type Ca^{2+} channels in murine oviduct pacemaker activity [59]. Currently, it is not clear what the critical pathway is for Ca^{2+} entry across the plasma membrane of these cells. Possible candidates include other voltage-dependent Ca^{2+} channels, a nonselective cation channel such as TRPV4, or store-operated Ca^{2+} entry via Orai. Future investigations should examine these possibilities.

11.4.5 Involvement of Intracellular Ca^{2+} Stores in Oviduct Slow Wave Generation

As described above, it would appear that extracellular Ca^{2+} is important for the maintenance of oviduct RMP and slow wave generation. However, $[Ca^{2+}]_o$ may not be the only Ca^{2+} source critical for oviduct slow waves. Excitability of smooth muscle cells can depend upon the release of Ca^{2+} from intracellular stores [88, 109], and $[Ca^{2+}]_o$ may contribute to the filling intracellular stores through store-operated Ca^{2+} entry [110–112]. To investigate the involvement of intracellular Ca^{2+} stores in the generation of oviduct slow waves, Dixon et al. tested the effects of ryanodine receptor, inositol 1,4,5-trisphosphate (IP_3) receptor, and SERCA pump inhibitors, on these events as described in the next two sections [59].

11.4.6 Role of Ryanodine Receptors (RyRs) and IP_3-Sensitive Intracellular Ca^{2+} Stores in Slow Wave Activity

Application of the ryanodine receptor (RyR) agonist, caffeine (1 mM) [91, 113], to mouse oviducts has been reported to block slow wave generation and significantly hyperpolarize RMP [59, 114]. It was noted that occasionally, as caffeine inhibited slow waves, underlying unitary potentials were revealed but these were also eventually abolished with continued application of caffeine. The caffeine effects were reversible and after washout unitary potentials returned and increased in frequency and amplitude before they developed into slow waves [104]. These results support the hypothesis that ryanodine-sensitive intracellular Ca^{2+} stores are involved in the generation of oviduct slow waves. To further examine the role of ryanodine-sensitive Ca^{2+} stores in oviduct slow wave generation, Dixon et al. examined the effects of the RyR antagonists, ryanodine and tetracaine [59]. Ryanodine (50 μM) caused depolarization in oviduct RMP and slow wave amplitude significantly decreased. During the application of ryanodine, slow wave frequency initially increased markedly. However, in the continued presence of ryanodine, slow wave frequency became irregular and often occurred in clusters. Similar results were obtained using the local anesthetic tetracaine (500 μM) which has also been shown to inhibit RyRs [115]. Further exper-

iments were performed where oviducts were exposed to a combination of caffeine (1 mM) and ryanodine (10 μm) initially and then to ryanodine (10 μM) alone. Co-application of caffeine and ryanodine inhibited slow wave generation, but upon washout of caffeine in the continued presence of ryanodine the membrane potential depolarized and slow wave generation resumed [104]. More recently it has been shown that higher concentrations of ryanodine are required to produce effects in GI muscles [108]; therefore a role of RyRs cannot be ruled out. The effects of caffeine inhibition on oviduct slow waves may involve a mechanism that does not involve RyRs. Further discussion of the complex effects of caffeine on oviduct pacemaker activity appears in a dedicated section below.

Evaluation of the other SR-localized Ca^{2+} release channels in oviduct slow wave activity was performed using the membrane-permeable IP_3R blocker 2-aminoethoxydiphenyl borate (2-APB). 2-APB (30 μM) caused a significant depolarization in RMP and decreased slow wave amplitude [59], reminiscent of the response to ryanodine or tetracaine.

The involvement of intracellular Ca^{2+} stores was further examined using the sarco/endoplasmic reticulum Ca^{2+}-ATPase (SERCA) pump inhibitor cyclopiazonic acid (CPA). CPA significantly depolarized RMP and reduced slow wave frequency at lower concentrations (10 μM) and inhibited them at higher concentrations (50 μM) [59]. To determine if the reduction in slow wave frequency was due to the membrane depolarization, as seen with L-type Ca^{2+} channels, low $[K^+]$ extracellular solution (0.1 mM) was used to repolarize the membrane potential in the continued presence of CPA. This treatment successfully induced membrane hyperpolarization that included a period when membrane potential returned to control levels; importantly, during this period, slow wave activity did not resume. These results suggest that intact intracellular Ca^{2+} stores are necessary for slow wave generation in the oviduct and that SERCA pump activity is necessary for refilling these stores.

11.4.7 Involvement of CaCCs in Oviduct Slow Wave Activity

The results accumulated from studies examining the dependence of oviduct slow wave activity on extracellular and intracellular Ca^{2+} sources suggest the involvement of Ca^{2+}-dependent ion channels. As discussed above, several studies have suggested that the CaCC, Ano1, is important for pacemaker activity in smooth muscles [60, 89–94]. In considering the putative role of these channels in oviduct pacemaker activity, it is noteworthy that the peak depolarization reached during the upstroke phase of oviduct slow waves (−23 ± 1 mV) is close to the equilibrium potential predicted for Cl^- in vas deferens smooth muscle tissues (−24 mV; [116]). On this basis, Dixon et al. investigated whether these channels could be the molecular correlate of the depolarizing conductance responsible for oviduct slow waves [60]. The effects of two chemically distinct pharmacological Cl^- channel blockers, anthracene-9-carboxylic acid (9-AC) and niflumic acid (NFA; [117]), were examined. Recently, more specific Ano1 channel blockers have been developed but these new compounds have not yet been evaluated on oviduct preparations [96].

9-AC (1 mM) hyperpolarized the RMP and often revealed a “hump” on the slow wave upstroke. Such an inflection was previously described as the “primary component” of slow waves in GI smooth muscles [118]. 9-AC also produced a significant reduction in slow wave frequency and inhibited slow wave activity in several of the oviduct preparations examined. Similarly, NFA also caused hyperpolarization. This effect was dose dependent and ultimately led to inhibition of slow waves at higher concentrations (50 μM). To investigate whether abolition of slow waves caused by NFA was due to hyperpolarization, high $[K^+]$ (10 mM) was used to depolarize cells in the continued presence of NFA. Depolarization under these conditions did not restore slow wave activity.

Even more compelling evidence for the essential role of CaCCs in oviduct pacemaker activity was obtained by intracellular recording made

from oviducts of mice that were *Ano1*$^{-/-}$. Previous reports have found that 90% of *Ano1* null mice die within the first 9 days of postnatal life [119]. Several pups die soon after birth on postnatal day zero (P0), so experiments were performed on oviducts from litters humanely sacrificed on P0. Since oviduct slow waves are already established at birth [28], slow waves were compared in oviducts of WT and *Ano1*$^{-/-}$ mice. RMPs were similar in oviducts from wild-type and *Ano1*$^{-/-}$ mutants. Slow waves were absent in *Ano1*$^{-/-}$ oviducts, as opposed to the robust activity observed in oviducts from age-matched WT mice. Collectively, these results suggest that inward currents through Ano1 CaCCs exert a depolarizing influence on RMP of oviduct smooth muscle cells, and are essential for slow wave generation. Studies examining the cellular expression of Ano1 in the oviduct have shown that it is expressed in smooth muscle cells ([120]; Ward SM unpublished observations) but do not exclude its expression in ICC-OVI. Indeed close inspection of the double-labeled (Ano1 and smooth muscle actin, *abbrev.* SMA) immunohistochemical images shown in Huang et al. reveals that Ano1 expression is not limited to cells expressing SMA. In contrast, Ano1 expression in the GI tract is limited to ICC in these visceral organs [121]. The finding that *Ano1*$^{-/-}$ mouse oviducts lack slow wave activity points to a role for these channels in pacemaker activity and given the previous finding that pacemaker activity in the oviduct is mediated by KIT-positive ICC-OVI it is a logical prediction that Ano1 should also be expressed in ICC-OVI, as it is in other smooth muscle ICC populations. So what is the utility of having Ano1 on smooth muscle cells? One hypothesis is that Ano1 expression could enhance the sensitivity of the myosalpinx. In this model, depolarization of the myosalpinx, produced by ICC-OVI-generated slow waves, would activate L-type Ca^{2+} channels on the myocytes, which in turn would activate Ano1 channels (synergistically activated by voltage and calcium) [122]. This would favor a more pronounced depolarization of the smooth muscle cells, leading to enhanced open probability of L-type Ca^{2+} channels and thus more calcium entry to trigger more forceful contractions.

11.4.8 The Role of Potassium Channels (K^+) in Oviduct Myosalpinx

We have also examined expression of K^+ channel transcripts in mouse oviduct myosalpinx. Several types of K^+ channel transcripts were identified in the ampulla, isthmus, and intramural segments, including the two-pore K^+ channel, Trek1; delayed rectifier K^+ channels K_V1.2, 1.5, and 2.2; A-type K^+ channels K_V4.1, 4.2, and 4.3; ether-a-go-go K^+ channel K_V11.1; inward rectifier K^+ channels K_{ir}2.1, 3.1, and 3.2; K_{ATP} channels K_{ir}6.1, 6.2, and their sulfonylurea receptor (SUR) subunits SUR2A and 2B; and Ca^{2+}-activated K^+ channels (K_{Ca}), BK (α-subunit), and SK1–3 (unpublished results).

The K_{ATP} antagonist glibenclamide causes depolarization and increases the frequency and decreases the amplitude of slow waves in mouse oviducts [114]. These observations suggest that K_{ATP} channels are active under basal conditions and contribute to the RMP in oviduct smooth muscle cells. In parallel with this work, we found that pinacidil hyperpolarizes oviduct smooth muscle which would be predicted to promote myosalpinx relaxation [114]. K_{ATP} channels therefore appear to contribute to the setting of myosalpinx membrane potential and regulate slow wave frequency. As stated above, a plethora of K^+ channel transcripts can be detected in mouse oviducts. It remains to be determined what role(s) these remaining K^+ channel populations play in oviduct contractility and function. Future studies should examine this.

11.4.9 Existence of a Slow Wave Gradient Along the Oviduct

Oocytes may be propelled along the rabbit oviduct from regions of high to low contraction frequencies [68]. In the stomach it is well established that there is a gradient in pacemaker activity from the corpus

where there is a higher frequency to the gastric antrum [123]. A similar gradient also exists in small intestine where slow waves are generated at a higher frequency in the jejunum than in the ileum that is thought to aid in the propulsion of luminal contents along the gastrointestinal tract in an oral to aboral direction [124–126]. To determine if such a frequency gradient exists in the oviduct, intracellular recordings at five separate locations in the oviducts of adult mice revealed the presence of gradients in RMP, slow wave frequency, and duration along the oviduct length (unpublished observations). The locations along the oviduct that were examined included the ovarian pole (the infundibulum), 25% along (the ampulla), 50% along (the proximal isthmus), 75% along (the distal isthmus), and the uterine pole (the intramural segment). RMP depolarized from the ovarian pole (−70 ± 3 mV; mean ± s.e.m.) to the 75% location (−52 ± 5 mV) and then became more hyperpolarized again at the uterine pole (−60 ± 4 mV). Associated with the membrane depolarization there was a gradual increase in slow wave frequency from the ovarian pole (1.0 ± 0.4 cycles/min) to the 75% location (14.6 ± 2.0 cycles/min) which then declined again at the uterine pole (8.4 ± 2.3 cycles/min). Slow wave amplitudes varied along the length of the oviducts but no distinct pattern or gradient could be distinguished. A gradient in slow wave duration was observed, such that slow waves were shortest at the ovarian pole (0.8 ± 0.3 s) and longest in duration at the uterine pole (4.6 ± 1.1 s) where prominent plateau phases were observed. The increase in the duration of the plateau phase towards the uterine pole would likely result in greater contractile force in the myosalpinx since membrane potential remains for longer periods in the activation window of voltage-dependent Ca^{2+} channels.

A previous investigation into the electrical activity of the guinea pig oviduct has reported that estrous cycle-dependent changes in slow wave frequency gradients occur in this species [66]. To rule out the possibility that sex hormones could influence the slow wave frequency gradient, intracellular microelectrode recordings were performed at five locations (as above) along the length of oviducts from sexually immature mice (1–3 weeks old). A similar correlation between RMP and slow wave frequency, as seen in adult oviducts, was also observed in the immature oviducts. Cells that were more depolarized tended to generate slow waves with a higher frequency than those with more polarized cells. A less pronounced frequency gradient was observed in the sexually immature mice compared to that observed in the adult oviducts; however the same basic pattern existed. Slow wave frequency was low at the ovarian pole (4.9 ± 0.6 cycles/min) and increased to the highest rate at 50% along the oviduct (5.8 ± 0.7 cycles/min) before decreasing again at 75% (4.2 ± 0.6 cycles/min) and uterine pole (2.2 ± 0.5 cycles/min) locations. Amplitude of slow waves was similar at all impalement locations. Slow waves recorded from the uterine pole location had the longest durations (3.2 ± 0.6 s).

When oviducts were cut into three separate segments, each segment generated slow wave activity. This is evidence that the cells responsible for pacemaker activity (ICC-OVI) are spread along the length of the organ. Cut oviducts also continued to display a slow wave frequency gradient similar to that observed in intact oviducts, again suggesting that each oviduct segment expresses different populations of pacemaker units coupled to ion channels which can influence the electrical activity in that region of the oviduct myosalpinx.

These data demonstrate that a slow wave frequency gradient exists along the length of oviducts and this gradient is established prior to sexual maturity. The observed frequency gradient would appear to favor transport away from the high-frequency isthmus towards the lower frequency ampulla and infundibulum or intramural segments. A correlation between RMP and frequency suggests that ion channel expression may differ along the oviduct, and could potentially explain the variation in slow wave frequency. Future studies should clarify this point and determine whether ion channel expression varies in ICC-OVI and smooth muscle cells. These ion channels may be coupled to pacemaker units which pace individual segments at different intrinsic frequencies. Slow wave durations were observed to be longest at the uterine pole side of oviducts. This too may be explained by different

populations of ion channels in this location that may serve to prolong the plateau phase of slow waves. An alternative explanation is that there could be differences in the Ca^{2+} release mechanisms and Ca^{2+} handling by pacemaker units in different regions of the oviduct.

11.5 Modulation of Motor Activity of the Oviduct

11.5.1 Innervation of the Oviduct

Autonomic motor and sensory fibers innervate the oviducts [3, 127]. In oviducts of rats, most afferent fibers originate from T_{13}-L_1 and L_2 dorsal root ganglia (DRG) and follow the superior ovarian nerves (branches of the celiac plexus) and the ovarian plexus nerves (originating in the intermesenteric plexus) [127–129]. Efferent fibers containing noradrenaline (NA) have been reported to follow the ovarian sympathetic nerves to the oviduct, whereas efferent nerves containing vasoactive intestinal protein (VIP) have their origin in the paracervical ganglia (PG) [129].

Neurotransmitters released by nerves in the oviduct include noradrenaline (NA) that has opposing actions depending upon the muscle layer. NA causes contraction of the longitudinal muscle and relaxation of the circular muscle via activation of α- and β-adrenergic receptors (α-ARs and β-ARs), respectively. Acetylcholine (ACh) and substance P (SP) are contractile; neuropeptide Y has no direct effect on oviduct muscle but will relax NA and ACh-induced contractions; VIP relaxes oviduct muscularis and SP-evoked contractions; and calcitonin gene-related peptide (CGRP) is a relaxant [127, 129–132]. Nitric oxide donors nitroglycerin and spermine NONOate reduce the frequency of spontaneous contractions in human fallopian tubes; however, neuronal nitric oxide synthase (nNOS) protein and transcript expression have been reported in the oviduct of several species. Even though endothelial and inducible isoforms of NOS have been reported in endothelial cells and smooth muscle cells of human oviduct [133–135], there are no evidence of nNOS-positive neurons in the mammalian oviduct or mouse ovary [133–135]. Although the neurotransmitters listed above have been identified and studied for their effects on myosalpinx contractility, a gap in the literature exists when one considers the role of these substances in egg transport along the oviduct.

11.5.2 Hormonal Influences on Oviduct Motor Function

It has been reported that estrous cycle-dependent changes in slow wave frequency gradients occur in guinea pig oviducts [66]. These data strongly support hormonal influences on oviduct motor function. Further evidence supporting a role for ovarian hormones in mediating changes in oviduct contractility includes a 1979 study performed on unmated rats, where the time taken for egg transit through the oviduct to the uterus was significantly accelerated from the normal ~72–96 h to <20 h after a single injection of the estrogen steroid hormone estradiol (E2) [136]. This accelerated transport was associated with an increased frequency of pendular movements in the isthmic segment of the oviduct. These effects of E2 were antagonized by progesterone. The effect of E2 on oviduct transport in unmated rats is thought to occur through a nongenomic pathway involving conversion of E2 to 2-methoxyestradiol and subsequent activation of cAMP/PKA and PLC/IP_3 pathways. In contrast, the accelerative effect of E2 on embryo or microsphere transport through the oviducts of mated rats appears to involve a genomic pathway and can be abrogated by Connexin 43 uncouplers [137]. The dependence of the E2-accelerative effect on transport implies that gap junctions play a critical role in synchronizing the myosalpinx. As mentioned above, during the estrogen-dominated proliferative period in human fallopian tubes, Kishikara and Kuriyama reported that electrical activity was more tightly coupled to mechanical activity than it was during the progesterone-dominated secretory period [64]. Tighter cell-to-cell communication facilitated by gap junctions could explain this effect.

11.6 Pathophysiological Conditions Associated with Oviduct Dysfunction

Evidence supports the hypothesis that coordinated contractions of the oviduct myosalpinx ciliary beating and epithelial secretions are thought to provide the propulsive force and lubrication essential for the transportation of oocytes from the ovary to the site for successful fertilization to occur [6]. These spontaneous contractions also play a critical role in the terminal regions of the oviduct for delivery of the embryo to the uterus for implantation. Under normal conditions the contractions of the myosalpinx along with ciliary beating, providing lubrication of the oviduct, occur in an optimal synchronized manner for successful fertilization and subsequent pregnancy to occur. However, there are a variety of pathophysiological conditions that can influence the proper functions of the oviduct. Disorders including ectopic pregnancy (EP), tubal factor infertility (TFI), pelvic inflammatory disease (PID), and chronic pelvic pain (CPP) are associated with significant morbidity and mortality. For example, ectopic pregnancy, which complicates up to 2% of pregnancies, is associated with significant morbidity and remains the most common cause of maternal death in the first trimester of pregnancy [138, 139]. More than 98% of ectopic pregnancies occur in the fallopian tube, with at least 80% of these occurring in the ampulla [140, 141].

Several common lifestyle habits have been implicated in decreased fertility. Some of these habits are more obviously harmful than others; for example, it is unsurprising that cigarette smoking is detrimental to female fertility [142], and that it increases the risk of EP [143]. Accordingly, nicotine has been reported to impair the oviduct transport of rat embryos [144]. Perhaps less obvious is the idea that daily coffee consumption could impair fertility; yet, a statistically significant progressive decrease in fertility has been reported with increasing caffeine consumption in women, suggesting a negative dose-dependent effect of caffeine on conception [145]. Another commonly consumed substance which has recently been legalized for recreational use in several US states (although not federally) is cannabis. Global consumption of marijuana has remained relatively stable over the past 20 years despite legalization in certain regions [146]. In the United States, medicinal and recreational marijuana usage has been on the rise since the late 1990s and has become the most popular illicit drug used by pregnant women or those planning to become pregnant [147, 148]. For example, a Kaiser Permanente-approved study in Northern California reported a 3% increase in marijuana usage among pregnant females during the time period from 2009 to 2016 [148]. That does not sound like a big rise, but the numbers were already alarmingly high as can be appreciated when one considers that almost a quarter (22%) of young pregnant girls (<18 years old) and a fifth (19%) of pregnant women aged 18–24 tested positive for marijuana use in 2016 when they were screened at ~8 weeks gestation. So does marijuana usage have any known consequences for female fertility and pregnancy, and can any of those effects be attributed to effects on oviduct smooth muscle? Links between marijuana usage and suppression of ovulation [149], higher risk of infertility [150], and lower pregnancy rates compared to nonusers [151] have been reported. More recently, aberrant endocannabinoid signaling has been linked to ectopic pregnancy in human fallopian tubes [152], and disrupted oviductal embryo transport in mice leading to pregnancy failures [153]. High levels of anandamide have also been associated with miscarriages in humans [154].

The physiological mechanism of action of marijuana is predominantly mediated through two G protein-coupled receptors, cannabinoid receptor 1 (CB1) and cannabinoid receptor 2 (CB2), encoded by the genes *Cnr1* and *Cnr2*, respectively [155, 156]. The two endogenous ligands (termed endocannabinoids) for these receptors are anandamide (*N*-arachidonoylethanolamine) and 2-arachidonoyl glycerol [157–159]. Endocannabinoid signaling occurs in many central and peripheral systems including the oviduct [160–162]. Cannabinoid

receptors have been documented in the female reproductive system of mice, where CB1 receptors have been found in preimplantation embryos [163] and anandamide presence has been detected in the oviduct and uterus [164, 165]. The presence of this endocannabinoid in the oviduct implies that endocannabinoid signaling is engaged prior to and during the very early stages of pregnancy. Accordingly, anandamide has been found to exert a concentration-dependent biphasic effect on embryo development and implantation [166], such that low concentrations of it accelerate and facilitate implantation but high concentrations inhibit implantation and are associated with tubal arrest of embryos in mice. It is conceivable then that high anandamide levels could produce a similar effect in women. In a 2004 study examining the effect of endocannabinoid signaling on oviductal embryo transport and implantation in mice, utilizing *Cnr1* knockout mice (*Cnr1*$^{-/-}$), reduced fertility in these animals was attributed to oviductal retention of embryos [153]. *Cnr1*$^{-/-}$ mice did not yield embryos when their uterine lumens were flushed on day 4 of pregnancy while WT and *Cnr2*$^{-/-}$ mice always did [153]. Embryos at the morula and blastocyst stages were instead recovered from the oviducts of *Cnr1*$^{-/-}$ mutants. It was suggested that many embryos become trapped in the oviduct, often for extended periods of time, resulting in pregnancy failure leading to reduced fertility in *Cnr1*$^{-/-}$ mice. This hypothesis was also supported by similar results obtained in WT mice treated with the selective CB1 receptor antagonist, SR141716. These data suggest that the failure of embryos to enter the uterine lumen is related to the absence of *Cnr1* [164]. In mice, this does not result in EP as ectopic implantations in the oviduct are thought to be an exclusively human phenomena. Rather, the consequence is spontaneous pregnancy failure.

The authors of this study sought an answer to why CB1 receptor inhibition or KO should lead to oviductal retention of embryos and based on their observation that CB1 receptors colocalized with β_2-adrenergic receptors (β_2ARs) they speculated that noradrenaline (NA) could play a role in this process. Treatment of *Cnr1*$^{-/-}$ mice with the nonselective β-agonist isoproterenol was found to restore normal embryo transit and implantation, while treatment of WT mice with phenylephrine (an α_1AR agonist) with or without butoxamine (a β_2AR antagonist) recapitulated the mutant phenotype and resulted in oviduct embryo retention. These results suggest that inhibition of CB1 receptors either genetically (with the *Cnr1*$^{-/-}$) or pharmacologically leads to enhanced NA release, which impedes oviduct transport in a mechanism that alters the balance of activation between α-ARs and β-ARs. It was thus hypothesized that CB1 serves as a presynaptic receptor and maintains an endogenous myosalpinx tone, regulating NA release that coordinates oviductal muscle contraction and relaxation to facilitate embryo transport. It is currently unknown if CB1 or CB2 can regulate the release of any other neurotransmitters in the oviduct. It should be noted that in the mouse oviduct mRNA for *Cnr2* has been reported to not be detected [153].

11.6.1 Caffeine Inhibits Myosalpinx Slow Waves and Associated Contractions

Caffeine ingestion in its various forms including tea, coffee, soda, and energy drinks, as well as several over-the-counter medications, has become an integral part of the daily dietary routine of millions of people around the globe. Unsurprisingly then, caffeine is thought to be "the most frequently ingested pharmacologically active substance in the world" [167]. In spite of our casual consumption of this substance, it is not clear that it is without risk, especially when it comes to fertility and conception. Several epidemiological studies have reported a negative impact of caffeine on fecundability [168–170]. Bolumar et al. reported the findings of a European multicenter study on women aged 25–44 years in which an 11% increase in waiting time while trying to conceive was experienced by those who consumed ≥501 mg of caffeine daily [169]. Another US-based study reported that women who drank >300 mg of caffeine a day had a 27% lower chance of conceiving for each cycle com-

pared with women who did not consume caffeine [171]. To put this into context, a large (20 fl oz) caffe Americano contains 300 mg of caffeine.

Caffeine causes dramatic hyperpolarization of mouse oviduct membrane potential and inhibition of spontaneous slow wave activity and associated phasic contractions [59, 114]. Caffeine is commonly used to dump intracellular ER/SR Ca^{2+} stores due to its ability to open ryanodine receptors [113]. This drug has also been reported to inhibit IP_3 receptors [172] and phosphodiesterases (PDEs) [173, 174]. Our group found that the effects of caffeine on the mouse oviduct were not affected by co-application of ryanodine and could not be replicated by the IP_3 receptor blocker 2-APB. We therefore hypothesized that the mechanism of action for caffeine's effects on the oviduct myosalpinx was via PDE inhibition.

To test this hypothesis, experiments were performed using the noncompetitive phosphodiesterase inhibitor 3-isobutyl-1-methylxanthine (IBMX) and the activator of adenylate cyclase, forskolin. Both compounds raise intracellular cyclic adenosine monophosphate (cAMP) levels, which leads to PKA activation. PKA can phosphorylate a number of target proteins within cells; we considered several of these proteins and their possible role in mediating the caffeine-induced effects on oviduct membrane potential and contractility. One PKA target is the ER/SR-associated regulatory protein, phospholamban (PLN). PLN is well known as a regulator of cardiac SERCA activity but several studies have pointed to a role for this protein in smooth muscle also. In particular, PLN knockout mice have revealed altered Ca^{2+} dynamics and contractility in GI [175, 176], and bladder [177] smooth muscle. In its native, unphosphorylated state, PLN inhibits the SERCA pump to limit store refilling but once phosphorylated this inhibition is relieved [178]. The resultant enhanced store refilling leads to increased frequency of calcium-release events which can stimulate K_{Ca} channels and promote membrane hyperpolarization and smooth muscle relaxation [175], which could potentially explain the effects of caffeine. PKA has also been reported to directly stimulate K_{Ca} channels [179, 180] and is known to also phosphorylate myosin light-chain kinase (MLCK), decreasing its affinity for the calcium-calmodulin complex and inhibiting smooth muscle contraction [181]. Finally, in vascular smooth muscle tissues, PKA has been reported to phosphorylate and activate K_{ATP} channels [182–186]. Relevant to this last point, we found that the effects of caffeine on the oviduct were similar to the effects seen with application of the K_{ATP} channel opener pinacidil and could be reversed by the K_{ATP} inhibitor glibenclamide [114]. In addition, we found that application of IBMX or forskolin which mimicked the effects of caffeine was also reversed by glibenclamide. These data strongly suggest that caffeine's effects on the oviduct are mediated, at least in part, through cAMP.

It still remains to be determined whether cAMP stimulates K_{ATP} channels directly or activates them via PKA-mediated phosphorylation. The hyperpolarization induced by K_{ATP} channel activation likely shifts membrane potential out of the activation range for voltage-dependent Ca^{2+} channels and promotes oviduct smooth muscle relaxation. Since phasic contractions of the myosalpinx are essential for egg transport along the oviduct [28] this may provide an explanation why women that consume moderate amounts of caffeine take longer to conceive than women who do not consume caffeinated drinks. One important caveat of these experiments is that the concentration of caffeine utilized in these experiments (1 mM) is likely to be supraphysiological [187]. A recent study reported that human subjects who consumed 160 mg caffeine in a beverage in one sitting had a peak plasma concentration of 3.74 μg/mL [188]. Assuming a formula weight of caffeine of 194.19 g/mol, this mass equates to a concentration of ~19 μM. As stated above, a 20 oz. Americano contains ~300 mg which is ~1.8-fold the amount consumed in the aforementioned study; scaling accordingly we would predict a plasma concentration of around 36 μM after ingestion of this higher amount. Plasma caffeine concentrations could therefore conceivably reach upwards of 100 μM with high consumption of caffeinated beverages and/or other caffeine-containing substances. Previously, we have reported that concentrations in the 100–300 μM range induce hyperpolarization of mouse

oviduct RMP and reduce slow wave frequency [114] so while 1 mM caffeine may be excessive in this context it is likely that lesser concentrations can also affect oviduct electrical and phasic mechanical activity.

11.6.2 *Chlamydia* Infection Causes Loss of Pacemaker Cells Within the Oviduct Resulting in Inhibition of Oocyte Transport

One of the most common causes of the pregnancy disorders EP, TFI, PID, and CPP is the sexually transmitted bacterial infection, *Chlamydia trachomatis* (*C. trachomatis*). The prevalence of this infection is staggering, with the World Health Organization estimating that up to 100 million new cases of *Chlamydia* occur globally every year [189]. Recent estimates suggest that 1 in 20 sexually active young women (14–24 years of age) in the United States has *Chlamydia*. The total financial cost of treating *Chlamydia* infections and associated pathologies is predicted to amount to ~$2 billion per year [190].

One of the core issues with *Chlamydia* is that the infections are commonly asymptomatic, and thus often go undiagnosed and untreated [191]. Without treatment, the infections can become chronic or persistent. Another common complication is reoccurrence or reinfection after the initial clearance of *Chlamydia* that often results in the development of significant tissue damage as a consequence of the host inflammatory immune response [192]. Women are at high risk of developing significant health complications, including urethritis, cervicitis, and CPP [193]. If untreated, more serious complications including PID, EP, and TFI can develop. According to a a World Health Organization report, 10–40% of women will develop PID if *Chlamydia* is untreated. Postinfection damage of fallopian tubes as a consequence of *Chlamydia* is estimated to be responsible for 30–40% of female infertility. In the forthcoming section, we discuss the consequences of this pathophysiological condition on oviduct motility.

Currently, the underlying, mechanistic etiology of ectopic pregnancies and TFI is poorly understood. As covered in early sections of this chapter, contractions of the smooth muscle (myosalpinx) that lines oviducts/fallopian tubes, incessant beating of cilia, and epithelial secretions are thought to provide the propulsive forces and lubrication necessary to transport oocytes from the ovary to the uterus [6]. *Chlamydia* infection can lead to stasis of the oviduct and eventual hydrosalpinx (serous fluid-filled oviduct) or pyosalpinx (pus-filled oviduct) and subsequent epithelial scarring that can eventually occlude the lumen of the oviduct. We hypothesized that infections like *Chlamydia*, and the ensuing host inflammatory response, could damage ICC-OVI networks, resulting in a cessation of oviduct motility and producing pseudo-obstruction of luminal contents and functional inhibition of oocyte transport and retention of luminal secretions. To test this hypothesis, we examined the response of mouse oviducts to *Chlamydia muridarum* (*C. muridarum*), a murine model of *Chlamydia* infection [194–196]. We focused our attentions on the effect of this infection on ICC-OVI populations and myosalpinx electrical and mechanical activity. In humans, chronic persistent or recurrent infections of *C. trachomatis* can cause infertility. A similar sequelae can occur in rodent animal models (mice) with induced infections of *C. muridarum*. The genetic profile of *C. muridarum* is comparable to human *C. trachomatis* and acute *C. muridarum* infection in mice provides a suitable approximation of the acute phase of infection seen in females [195]. Sharp electrode electrophysiological recordings and immunohistochemistry were performed on control and *C. muridarum*-infected oviducts. Results from these studies suggest that *C. muridarum* infection disrupts pacemaker activity in mouse oviducts and causes loss of ICC-OVI populations along the organ (Fig. 11.5).

A variety of pro-inflammatory mediators are released by the host upon infection with *Chlamydia* and the pathways through which *Chlamydia* affects oviduct pathogenesis are extensive. In particular, two pro-inflammatory mediators that have been reported to be upregulated during the response to

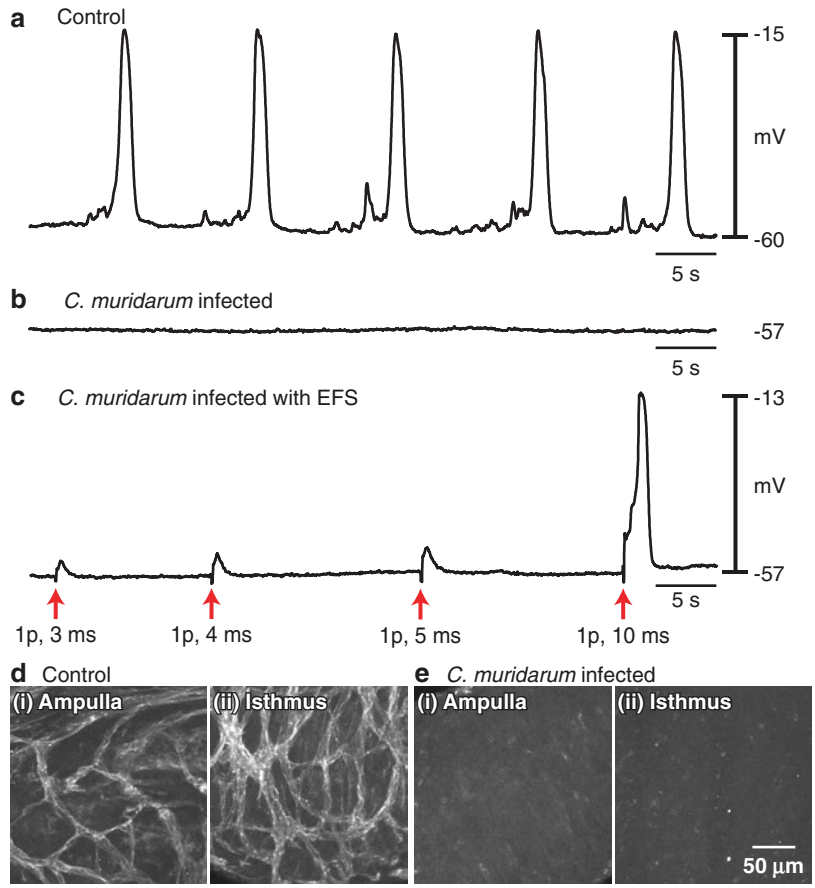

Fig. 11.5 *Chlamydia muridarum* infection abolishes spontaneous rhythmicity in the oviduct. Spontaneous electrical activity in uninfected adult control oviducts (**a**) is absent in *C. muridarum*-infected oviducts (**b**). Electrical field stimulation (*red arrows*) was used to elicit slow waves from the quiescent infected oviducts to confirm tissue viability and ability to generate excitable events (**c**). Confocal micrographs show that c-Kit-labeled ICC-OVI populations in the ampulla (**di**) and isthmus (**dii**) regions of a control oviduct are absent in the ampulla and isthmus of infected oviducts (**ei** and **eii**, respectively). Adapted and reprinted with permission from [28]

Chlamydia caught our attention since they have previously been implicated as players in the host-dependent damage to ICC produced during inflammation of the GI tract [197–199]. The expression of these two mediators, PTGS2 (A.K.A. COXII) and NOS2 (A.K.A. iNOS), was thus examined in *C. muridarum*-infected oviducts to determine whether a similar sequel of events occurred in these tubular smooth muscle-lined organs [28]. Immunohistochemical and western blot results confirmed that the pro-inflammatory mediators PTGS2 and NOS2 were significantly upregulated in *C. muridarum*-infected oviducts. NOS2 expression was localized to leukocytes and macrophages within the wall of the oviduct including the myosalpinx. Thus, part of the host immune response to *Chlamydia* infection and disruption of ICC networks could likely be due to PTGS2 and NOS2.

The significance of NOS2 upregulation was tested in week-long organotypic cultures in which oviducts were constantly exposed to lipopolysaccharide (LPS), a derivative of bacterial cell walls. Subsequent sharp microelectrode recordings performed on the oviducts after this culture period revealed that, similar to *Chlamydia* infection, LPS treatment inhibited ICC-OVI-mediated pacemaker activity. NOS2 was implicated in this damaging host-response as application of the NOS2 inhibitor 1400 W preserved oviduct pacemaker activity. Loss of oviduct pacemaker activity and associated contractions causes stasis of the oviduct and the ensuing pseudo-obstruction may lead to blockage and scarring, because secretions and oocytes cannot be cleared. This occlusion may ultimately result in TFI.

11.6.3 Concluding Thoughts

In summary, the oviducts or fallopian tubes are not simply a passive conduit through which gametes and embryos pass on their way to the uterus. On the contrary, they are complex organs with intrinsic pacemaker cells, ICC-OVI, that generate the electrical activity underlying the phasic mechanical contractions of the smooth muscle within their walls to precisely coordinate elaborate processes such as fertilization, early embryo development, and timely transport of the embryo to the uterus for implantation. This activity can be influenced by an extensive innervation and a cyclic hormonal milieu that choreographs contractions of the myosalpinx at various stages of the estrus/menstrual cycle, and during very early pregnancy. Aberrant oviduct smooth muscle function stimulated by consumption of active substances such as marijuana, nicotine, or even the seemingly innocuous caffeine can have detrimental and sometimes devastating effects on female fertility. Loss of ICC-OVI during bacterial infections such as *Chlamydia* can lead to loss of electrical and contractile activity, ultimately producing stasis in the oviduct which could conceivably lead to ectopic pregnancy or tubal factor infertility. These relatively understudied organs are critically important for female reproductive capacity and are deserving of rigorous investigation.

References

1. Cook MJ. The anatomy of the laboratory mouse, vol. 143. London: Academic Press; 1965.
2. Nilsson O, Reinius S. Light and electron microscopic structure of the oviduct. In: Hafez ESE, Blandau RJ, Washington State University, editors. The mammalian oviduct comparative biology and methodology. Chicago, IL: University of Chicago Press; 1969. p. 57–83.
3. Eddy CA, Pauerstein CJ. Anatomy and physiology of the fallopian tube. Clin Obstet Gynecol. 1980; 23(4):1177–93.
4. Blandau RJ. Gamete transport—comparative aspects. In: Hafez ESE, Blandau RJ, Washington State University, editors. The mammalian oviduct comparative biology and methodology. Chicago, IL: University of Chicago Press; 1969. p. 129–62.
5. Paton DM, Widdicombe JH, Rheaume DE, Johns A. The role of the adrenergic innervation of the oviduct in the regulation of mammalian ovum transport. Pharmacol Rev. 1977;29(2):67–102.
6. Croxatto HB. Physiology of gamete and embryo transport through the fallopian tube. Reprod Biomed Online. 2002;4(2):160–9.
7. Hafez ESE, Black DL. The mammalian uterotubal junction. In: Hafez ESE, Blandau RJ, Washington State University, editors. The mammalian oviduct comparative biology and methodology. Chicago, IL: University of Chicago Press; 1969. p. 105–6.
8. Foster HL, Small JD, Fox JG. The mouse in biomedical research, American College of Laboratory Animal Medicine series, vol. 4. New York: Academic Press; 1981.
9. Ezzati M, Djahanbakhch O, Arian S, Carr BR. Tubal transport of gametes and embryos: a review of physiology and pathophysiology. J Assist Reprod Genet. 2014;31(10):1337–47. https://doi.org/10.1007/s10815-014-0309-x.
10. Faussone-Pellegrini MS, Bani G. The muscle coat morphology of the mouse oviduct during the estrous cycle. Arch Histol Cytol. 1990;53(2):167–78.
11. Abe H. The mammalian oviductal epithelium: regional variations in cytological and functional aspects of the oviductal secretory cells. Histol Histopathol. 1996;11(3):743–68.
12. Lyons RA, Saridogan E, Djahanbakhch O. The reproductive significance of human Fallopian tube cilia. Hum Reprod Update. 2006;12(4):363–72.
13. Amso NN, Crow J, Lewin J, Shaw RW. A comparative morphological and ultrastructural study of endometrial gland and fallopian tube epithelia at different stages of the menstrual cycle and the menopause. Hum Reprod. 1994;9(12):2234–41.
14. Crow J, Amso NN, Lewin J, Shaw RW. Morphology and ultrastructure of fallopian tube epithelium at different stages of the menstrual cycle and menopause. Hum Reprod. 1994;9(12):2224–33.
15. Dirksen ER, Satir P. Ciliary activity in the mouse oviduct as studied by transmission and scanning electron microscopy. Tissue Cell. 1972;4(3):389–403.
16. Patek E. The epithelium of the human Fallopian tube. A surface ultrastructural and cytochemical study. Acta Obstet Gynecol Scand Suppl. 1974;31:1–28.
17. Croxatto HB, Villalon M. Oocyte transport. In: Grudzinskas JG, Yovich J, editors. Gametes the oocyte. Cambridge reviews in human reproduction. Cambridge: Cambridge University Press; 1995. p. 253–76.
18. Leese HJ, Tay JI, Reischl J, Downing SJ. Formation of Fallopian tubal fluid: role of a neglected epithelium. Reproduction. 2001;121(3):339–46.
19. Paltieli Y, Eibschitz I, Ziskind G, Ohel G, Silbermann M, Weichselbaum A. High progesterone levels and ciliary dysfunction—a possible

cause of ectopic pregnancy. J Assist Reprod Genet. 2000;17(2):103–6.
20. Mahmood T, Saridogan E, Smutna S, Habib AM, Djahanbakhch O. The effect of ovarian steroids on epithelial ciliary beat frequency in the human Fallopian tube. Hum Reprod. 1998;13(11):2991–4.
21. Nishimura A, Sakuma K, Shimamoto C, Ito S, Nakano T, Daikoku E, Ohmichi M, Ushiroyama T, Ueki M, Kuwabara H, Mori H, Nakahari T. Ciliary beat frequency controlled by oestradiol and progesterone during ovarian cycle in guinea-pig Fallopian tube. Exp Physiol. 2010;95(7):819–28. https://doi.org/10.1113/expphysiol.2010.052555.
22. Talbot P, Geiske C, Knoll M. Oocyte pickup by the mammalian oviduct. Mol Biol Cell. 1999;10(1):5–8.
23. Zhuo L, Kimata K. Cumulus oophorus extracellular matrix: its construction and regulation. Cell Struct Funct. 2001;26(4):189–96.
24. Pauerstein CJ, Eddy CA. The role of the oviduct in reproduction; our knowledge and our ignorance. J Reprod Fertil. 1979;55(1):223–9.
25. Norwood JT, Hein CE, Halbert SA, Anderson RG. Polycationic macromolecules inhibit cilia-mediated ovum transport in the rabbit oviduct. Proc Natl Acad Sci USA. 1978;75(9):4413–6.
26. Halbert SA, Becker DR, Szal SE. Ovum transport in the rat oviductal ampulla in the absence of muscle contractility. Biol Reprod. 1989;40(6):1131–6.
27. Halbert SA, Tam PY, Blandau RJ. Egg transport in the rabbit oviduct: the roles of cilia and muscle. Science. 1976;191(4231):1052–3.
28. Dixon RE, Hwang SJ, Hennig GW, Ramsey KH, Schripsema JH, Sanders KM, Ward SM. Chlamydia infection causes loss of pacemaker cells and inhibits oocyte transport in the mouse oviduct. Biol Reprod. 2009;80(4):665–73. https://doi.org/10.1095/biolreprod.108.073833.
29. Griffin J, Emery BR, Huang I, Peterson CM, Carrell DT. Comparative analysis of follicle morphology and oocyte diameter in four mammalian species (mouse, hamster, pig, and human). J Exp Clin Assist Reprod. 2006;3:2.
30. Fitzharris G, Baltz JM. Granulosa cells regulate intracellular pH of the murine growing oocyte via gap junctions: development of independent homeostasis during oocyte growth. Development. 2006;133(4):591–9.
31. Hodgson BJ, Talo A, Pauerstein CJ. Oviductal ovum surrogate movement: interrelation with muscular activity. Biol Reprod. 1977;16(3):394–6.
32. Eddy CA, Flores JJ, Archer DR, Pauerstein CJ. The role of cilia in fertility: an evaluation by selective microsurgical modification of the rabbit oviduct. Am J Obstet Gynecol. 1978;132(7):814–21.
33. Afzelius BA, Camner P, Mossberg B. On the function of cilia in the female reproductive tract. Fertil Steril. 1978;29(1):72–4.
34. Raidt J, Werner C, Menchen T, Dougherty GW, Olbrich H, Loges NT, Schmitz R, Pennekamp P, Omran H. Ciliary function and motor protein composition of human fallopian tubes. Hum Reprod. 2015;30(12):2871–80. https://doi.org/10.1093/humrep/dev227.
35. Overstreet JW, Cooper GW. Sperm transport in the reproductive tract of the female rabbit: I. The rapid transit phase of transport. Biol Reprod. 1978;19(1):101–14.
36. Suarez SS, Pacey AA. Sperm transport in the female reproductive tract. Hum Reprod Update. 2006;12(1):23–37.
37. Suarez SS. Regulation of sperm storage and movement in the mammalian oviduct. Int J Dev Biol. 2008;52(5–6):455–62.
38. Suarez SS. Sperm transport and motility in the mouse oviduct: observations in situ. Biol Reprod. 1987;36(1):203–10.
39. Okabe M. Mechanisms of fertilization elucidated by gene-manipulated animals. Asian J Androl. 2015;17(4):646–52. https://doi.org/10.4103/1008-682X.153299.
40. Muro Y, Hasuwa H, Isotani A, Miyata H, Yamagata K, Ikawa M, Yanagimachi R, Okabe M. Behavior of mouse spermatozoa in the female reproductive tract from soon after mating to the beginning of fertilization. Biol Reprod. 2016;94(4):80. https://doi.org/10.1095/biolreprod.115.135368.
41. Blandau RJ, Gaddum-Rosse P. Mechanism of sperm transport in pig oviducts. Fertil Steril. 1974;25(1):61–7.
42. Battalia DE, Yanagimachi R. Enhanced and coordinated movement of the hamster oviduct during the periovulatory period. J Reprod Fertil. 1979;56(2):515–20.
43. Chang H, Suarez SS. Unexpected flagellar movement patterns and epithelial binding behavior of mouse sperm in the oviduct. Biol Reprod. 2012;86(5):140, 141–8. https://doi.org/10.1095/biolreprod.111.096578.
44. Yanagimachi R, Chang MC. Sperm ascent through the oviduct of the hamster and rabbit in relation to the time of ovulation. J Reprod Fertil. 1963;6:413–20.
45. Overstreet JW, Cooper GW. Sperm transport in the reproductive tract of the female rabbit: II. The sustained phase of transport. Biol Reprod. 1978;19(1):115–32.
46. Wilcox AJ, Weinberg CR, Baird DD. Timing of sexual intercourse in relation to ovulation. Effects on the probability of conception, survival of the pregnancy, and sex of the baby. N Engl J Med. 1995;333(23):1517–21.
47. Kervancioglu ME, Djahanbakhch O, Aitken RJ. Epithelial cell coculture and the induction of sperm capacitation. Fertil Steril. 1994;61(6):1103–8.
48. Rodriguez-Martinez H. Role of the oviduct in sperm capacitation. Theriogenology. 2007;68(Suppl 1):S138–46.
49. Demott RP, Suarez SS. Hyperactivated sperm progress in the mouse oviduct. Biol Reprod. 1992;46(5):779–85.
50. Morales P, Palma V, Salgado AM, Villalon M. Sperm interaction with human oviductal cells in vitro. Hum Reprod. 1996;11(7):1504–9.

51. Pauerstein CJ. Pathophysiology of the Fallopian tube. Clin Obstet Gynecol. 1974;17(2):89–119.
52. Killian GJ. Evidence for the role of oviduct secretions in sperm function, fertilization and embryo development. Anim Reprod Sci. 2004;82-83:141–53.
53. Nishimura T, Nakajima A, Hayashi T. The basic pattern of electrical activities in the rabbit fallopian tube. Acta Obstet Gynaecol Jpn. 1969;16(2):97–103.
54. Brundin J, Talo A. The effects of estrogen and progesterone on the electric activity and intraluminal pressure of the castrated rabbit oviduct. Biol Reprod. 1972;7(3):417–24.
55. Talo A. Electric and mechanical activity of the rabbit oviduct in vitro before and after ovulation. Biol Reprod. 1974;11(3):335–45.
56. Talo A, Brundin J. Muscular activity in the rabbit oviduct: a combination of electric and mechanic recordings. Biol Reprod. 1971;5(1):67–77.
57. Talo A, Hodgson BJ. Spike bursts in rabbit oviduct. I. Effect of ovulation. Am J Physiol. 1978;234(4):E430–8.
58. Tomita T, Watanabe H. Factors controlling myogenic activity in smooth muscle. Philos Trans R Soc Lond B Biol Sci. 1973;265(867):73–85.
59. Dixon RE, Britton FC, Baker SA, Hennig GW, Rollings CM, Sanders KM, Ward SM. Electrical slow waves in the mouse oviduct are dependent on extracellular and intracellular calcium sources. Am J Physiol Cell Physiol. 2011;301(6):C1458–69. https://doi.org/10.1152/ajpcell.00293.2011.
60. Dixon RE, Hennig GW, Baker SA, Britton FC, Harfe BD, Rock JR, Sanders KM, Ward SM. Electrical slow waves in the mouse oviduct are dependent upon a calcium activated chloride conductance encoded by Tmem16a. Biol Reprod. 2012;86(1):1–7. https://doi.org/10.1095/biolreprod.111.095554.
61. Dixon RE, Ramsey KH, Schripsema JH, Sanders KM, Ward SM. Time-dependent disruption of oviduct pacemaker cells by Chlamydia infection in mice. Biol Reprod. 2010;83(2):244–53. https://doi.org/10.1095/biolreprod.110.083808.
62. Johns A, Coons LW. Physiological and pharmacological characteristics of the baboon (Papio anubis) oviduct. Biol Reprod. 1981;25(1):120–7.
63. Zasztowt O. [Studies on the bioelectrical phenomena of the cell membrane of the muscle of oviducts]. Ginekol Pol. 1969;40(4):371–6.
64. Kishikawa T, Kuriyama H. Electrical and mechanical activities recorded from smooth muscle cells of the human fallopian tube. Jpn J Physiol. 1981;31(3):417–22.
65. Lindblom B, Wikland M. Simultaneous recording of electrical and mechanical activity in isolated smooth muscle of the human oviduct. Biol Reprod. 1982;27(2):393–8.
66. Parkington HC. Intracellularly recorded electrical activity of smooth muscle of guinea pig oviduct. Am J Physiol. 1983;245(5 Pt 1):C357–64.
67. Holman ME. Membrane potentials recorded with high-resistance micro-electrodes; and the effects of changes in ionic environment on the electrical and mechanical activity of the smooth muscle of the taenia coli of the guinea pig. J Physiol. 1958;141(3):464–88.
68. Talo A, Hodgson BJ. Electrical slow waves in oviductal smooth muscle of the guinea-pig, mouse and the immature baboon. Experientia. 1978;34(2):198–200.
69. Bayguinov O, Hennig GW, Sanders KM. Movement based artifacts may contaminate extracellular electrical recordings from GI muscles. Neurogastroenterol Motil. 2011;23(11):1029–42, e1498. https://doi.org/10.1111/j.1365-2982.2011.01784.x.
70. Ozaki H, Stevens RJ, Blondfield DP, Publicover NG, Sanders KM. Simultaneous measurement of membrane potential, cytosolic Ca2+, and tension in intact smooth muscles. Am J Physiol. 1991;260(5 Pt 1):C917–25.
71. Forrest AS, Ordog T, Sanders KM. Neural regulation of slow-wave frequency in the murine gastric antrum. Am J Physiol Gastrointest Liver Physiol. 2006;290(3):G486–95. https://doi.org/10.1152/ajpgi.00349.2005.
72. Hirst GD, Bramich NJ, Teramoto N, Suzuki H, Edwards FR. Regenerative component of slow waves in the guinea-pig gastric antrum involves a delayed increase in [Ca(2+)](i) and Cl(−) channels. J Physiol. 2002;540(Pt 3):907–19.
73. Burke EP, Gerthoffer WT, Sanders KM, Publicover NG. Wortmannin inhibits contraction without altering electrical activity in canine gastric smooth muscle. Am J Phys. 1996;270(5 Pt 1):C1405–12. https://doi.org/10.1152/ajpcell.1996.270.5.C1405.
74. Sanders KM, Ward SM, Hennig GW. Problems with extracellular recording of electrical activity in gastrointestinal muscle. Nat Rev Gastroenterol Hepatol. 2016;13(12):731–41. https://doi.org/10.1038/nrgastro.2016.161.
75. Du P, Calder S, Angeli TR, Sathar S, Paskaranandavadivel N, O'Grady G, Cheng LK. Progress in mathematical modeling of gastrointestinal slow wave abnormalities. Front Physiol. 2017;8:1136. https://doi.org/10.3389/fphys.2017.01136.
76. O'Grady G, Paskaranandavadivel N, Du P, Angeli T, Erickson JC, Cheng LK. Correct techniques for extracellular recordings of electrical activity in gastrointestinal muscle. Nat Rev Gastroenterol Hepatol. 2017;14(6):372. https://doi.org/10.1038/nrgastro.2017.15.
77. Sanders KM, Ward SM, Hennig GW. Extracellular gastrointestinal electrical recordings: movement not electrophysiology. Nat Rev Gastroenterol Hepatol. 2017;14(6):372. https://doi.org/10.1038/nrgastro.2017.39.
78. Hodgson BJ, Talo A. Spike bursts in rabbit oviduct. II. Effects of estrogen and progesterone. Am J Physiol. 1978;234(4):E439–43.
79. Popescu LM, Ciontea SM, Cretoiu D, Hinescu ME, Radu E, Ionescu N, Ceausu M, Gherghiceanu M, Braga RI, Vasilescu F, Zagrean L, Ardeleanu

C. Novel type of interstitial cell (Cajal-like) in human fallopian tube. J Cell Mol Med. 2005;9(2):479–523.
80. Shafik A, Shafik AA, El Sibai O, Shafik IA. Specialized pacemaking cells in the human Fallopian tube. Mol Hum Reprod. 2005;11(7):503–5.
81. Ordog T, Redelman D, Horvath VJ, Miller LJ, Horowitz B, Sanders KM. Quantitative analysis by flow cytometry of interstitial cells of Cajal, pacemakers, and mediators of neurotransmission in the gastrointestinal tract. Cytometry A. 2004;62(2):139–49.
82. Christensen J. A commentary on the morphological identification of interstitial cells of Cajal in the gut. J Auton Nerv Syst. 1992;37(2):75–88.
83. Huizinga JD, Thuneberg L, Vanderwinden JM, Rumessen JJ. Interstitial cells of Cajal as targets for pharmacological intervention in gastrointestinal motor disorders. Trends Pharmacol Sci. 1997;18(10):393–403.
84. Sanders KM. A case for interstitial cells of Cajal as pacemakers and mediators of neurotransmission in the gastrointestinal tract. Gastroenterology. 1996;111(2):492–515.
85. Torihashi S, Ward SM, Nishikawa S, Nishi K, Kobayashi S, Sanders KM. c-Kit-dependent development of interstitial cells and electrical activity in the murine gastrointestinal tract. Cell Tissue Res. 1995;280(1):97–111.
86. Beckett EA, Ro S, Bayguinov Y, Sanders KM, Ward SM. Kit signaling is essential for development and maintenance of interstitial cells of Cajal and electrical rhythmicity in the embryonic gastrointestinal tract. Dev Dyn. 2007;236(1):60–72.
87. Maeda H, Yamagata A, Nishikawa S, Yoshinaga K, Kobayashi S, Nishi K, Nishikawa S. Requirement of c-kit for development of intestinal pacemaker system. Development. 1992;116(2):369–75.
88. Sanders KM. Regulation of smooth muscle excitation and contraction. Neurogastroenterol Motil. 2008;20(Suppl 1):39–53.
89. Hashitani H, van Helden DF, Suzuki H. Properties of spontaneous depolarizations in circular smooth muscle cells of rabbit urethra. Br J Pharmacol. 1996;118(7):1627–32.
90. Kito Y, Fukuta H, Suzuki H. Components of pacemaker potentials recorded from the guinea pig stomach antrum. Pflugers Arch. 2002;445(2):202–17.
91. von der Weid PY, Rahman M, Imtiaz MS, van Helden DF. Spontaneous transient depolarizations in lymphatic vessels of the guinea pig mesentery: pharmacology and implication for spontaneous contractility. Am J Physiol Heart Circ Physiol. 2008;295(5):H1989–2000.
92. Cobine CA, Hannah EE, Zhu MH, Lyle HE, Rock JR, Sanders KM, Ward SM, Keef KD. ANO1 in intramuscular interstitial cells of Cajal plays a key role in the generation of slow waves and tone in the internal anal sphincter. J Physiol. 2017;595(6):2021–41. https://doi.org/10.1113/JP273618.
93. Zhu MH, Kim TW, Ro S, Yan W, Ward SM, Koh SD, Sanders KM. A Ca(2+)-activated Cl(−) conductance in interstitial cells of Cajal linked to slow wave currents and pacemaker activity. J Physiol. 2009;587(Pt 20):4905–18. https://doi.org/10.1113/jphysiol.2009.176206.
94. Huang F, Zhang H, Wu M, Yang H, Kudo M, Peters CJ, Woodruff PG, Solberg OD, Donne ML, Huang X, Sheppard D, Fahy JV, Wolters PJ, Hogan BL, Finkbeiner WE, Li M, Jan YN, Jan LY, Rock JR. Calcium-activated chloride channel TMEM16A modulates mucin secretion and airway smooth muscle contraction. Proc Natl Acad Sci U S A. 2012;109(40):16354–9. https://doi.org/10.1073/pnas.1214596109.
95. Hwang SJ, Blair PJ, Britton FC, O'Driscoll KE, Hennig G, Bayguinov YR, Rock JR, Harfe BD, Sanders KM, Ward SM. Expression of anoctamin 1/TMEM16A by interstitial cells of Cajal is fundamental for slow wave activity in gastrointestinal muscles. J Physiol. 2009;587(Pt 20):4887–904. https://doi.org/10.1113/jphysiol.2009.176198.
96. Hwang SJ, Basma N, Sanders KM, Ward SM. Effects of new-generation inhibitors of the calcium-activated chloride channel anoctamin 1 on slow waves in the gastrointestinal tract. Br J Pharmacol. 2016;173(8):1339–49. https://doi.org/10.1111/bph.13431.
97. Sanders KM, Zhu MH, Britton F, Koh SD, Ward SM. Anoctamins and gastrointestinal smooth muscle excitability. Exp Physiol. 2012;97(2):200–6. https://doi.org/10.1113/expphysiol.2011.058248.
98. Singh RD, Gibbons SJ, Saravanaperumal SA, Du P, Hennig GW, Eisenman ST, Mazzone A, Hayashi Y, Cao C, Stoltz GJ, Ordog T, Rock JR, Harfe BD, Szurszewski JH, Farrugia G. Ano1, a Ca2+-activated Cl− channel, coordinates contractility in mouse intestine by Ca2+ transient coordination between interstitial cells of Cajal. J Physiol. 2014;592(18):4051–68. https://doi.org/10.1113/jphysiol.2014.277152.
99. El-Sharkawy TY, Daniel EE. Ionic mechanisms of intestinal electrical control activity. Am J Physiol. 1975;229(5):1287–98.
100. El-Sharkawy TY, Szurszewski JH. Modulation of canine antral circular smooth muscle by acetylcholine, noradrenaline and pentagastrin. J Physiol. 1978;279:309–20.
101. Dahms V, Prosser CL, Suzuki N. Two types of 'slow waves' in intestinal smooth muscle of cat. J Physiol. 1987;392:51–69.
102. Huizinga JD, Farraway L, Den Hertog A. Generation of slow-wave-type action potentials in canine colon smooth muscle involves a non-L-type Ca2+ conductance. J Physiol. 1991;442:15–29.
103. Ward SM, Sanders KM. Dependence of electrical slow waves of canine colonic smooth muscle on calcium gradient. J Physiol. 1992;455:307–19.
104. Ward SM, Sanders KM. Upstroke component of electrical slow waves in canine colonic smooth muscle due to nifedipine-resistant calcium current. J Physiol. 1992;455:321–37.
105. Kito Y, Suzuki H. Properties of pacemaker potentials recorded from myenteric interstitial cells of Cajal

distributed in the mouse small intestine. J Physiol. 2003;553(Pt 3):803–18.
106. Ward SM, Dixon RE, de Faoite A, Sanders KM. Voltage-dependent calcium entry underlies propagation of slow waves in canine gastric antrum. J Physiol. 2004;561(Pt 3):793–810.
107. Bayguinov O, Ward SM, Kenyon JL, Sanders KM. Voltage-gated Ca2+ currents are necessary for slow-wave propagation in the canine gastric antrum. Am J Physiol Cell Physiol. 2007;293(5):C1645–59.
108. Drumm BT, Hennig GW, Battersby MJ, Cunningham EK, Sung TS, Ward SM, Sanders KM, Baker SA. Clustering of Ca(2+) transients in interstitial cells of Cajal defines slow wave duration. J Gen Physiol. 2017;149(7):703–25. https://doi.org/10.1085/jgp.201711771.
109. Berridge MJ. Smooth muscle cell calcium activation mechanisms. J Physiol. 2008;586(Pt 21):5047–61.
110. Feske S, Gwack Y, Prakriya M, Srikanth S, Puppel SH, Tanasa B, Hogan PG, Lewis RS, Daly M, Rao A. A mutation in Orai1 causes immune deficiency by abrogating CRAC channel function. Nature. 2006;441(7090):179–85. https://doi.org/10.1038/nature04702.
111. Prakriya M, Lewis RS. Store-operated calcium channels. Physiol Rev. 2015;95(4):1383–436. https://doi.org/10.1152/physrev.00020.2014.
112. Putney JWJ. Capacitative calcium entry revisited. Cell Calcium. 1990;11(10):611–24.
113. Berridge MJ. Inositol trisphosphate and calcium signalling. Nature. 1993;361(6410):315–25.
114. Dixon R, Hwang S, Britton F, Sanders K, Ward S. Inhibitory effect of caffeine on pacemaker activity in the oviduct is mediated by cAMP-regulated conductances. Br J Pharmacol. 2011;163(4):745–54. https://doi.org/10.1111/j.1476-5381.2011.01266.x.
115. Johnston L, Sergeant GP, Hollywood MA, Thornbury KD, McHale NG. Calcium oscillations in interstitial cells of the rabbit urethra. J Physiol. 2005;565(Pt 2):449–61.
116. Aickin CC, Brading AF. Measurement of intracellular chloride in guinea-pig vas deferens by ion analysis, 36chloride efflux and micro-electrodes. J Physiol. 1982;326:139–54.
117. Greenwood IA, Leblanc N. Overlapping pharmacology of Ca2+-activated Cl− and K+ channels. Trends Pharmacol Sci. 2007;28(1):1–5.
118. Ohba M, Sakamoto Y, Tomita T. The slow wave in the circular muscle of the guinea-pig stomach. J Physiol. 1975;253(2):505–16.
119. Rock JR, Harfe BD. Expression of TMEM16 paralogs during murine embryogenesis. Dev Dyn. 2008;237(9):2566–74.
120. Huang F, Rock JR, Harfe BD, Cheng T, Huang X, Jan YN, Jan LY. Studies on expression and function of the TMEM16A calcium-activated chloride channel. Proc Natl Acad Sci U S A. 2009;106(50):21413–8. https://doi.org/10.1073/pnas.0911935106.
121. Gomez-Pinilla PJ, Gibbons SJ, Bardsley MR, Lorincz A, Pozo MJ, Pasricha PJ, de Rijn MV, West RB, Sarr MG, Kendrick ML, Cima RR, Dozois EJ, Larson DW, Ordog T, Farrugia G. Ano1 is a selective marker of interstitial cells of Cajal in the human and mouse gastrointestinal tract. Am J Physiol Gastrointest Liver Physiol. 2009;296(6):G1370–81.
122. Xiao Q, Yu K, Perez-Cornejo P, Cui Y, Arreola J, Hartzell HC. Voltage- and calcium-dependent gating of TMEM16A/Ano1 chloride channels are physically coupled by the first intracellular loop. Proc Natl Acad Sci U S A. 2011;108(21):8891–6. https://doi.org/10.1073/pnas.1102147108.
123. Szurszewski JH. Electrical basis for gastrointestinal motility. In: Johnson LR, editor. Physiology of the gastrointestinal tract. 2nd ed. New York: Raven Press; 1987. p. 1435.
124. Diamant NE, Bortoff A. Nature of the intestinal slow-wave frequency gradient. Am J Physiol. 1969;216(2):301–7.
125. Szurszewski JH, Elveback LR, Code CF. Configuration and frequency gradient of electric slow wave over canine small bowel. Am J Phys. 1970;218(5):1468–73. https://doi.org/10.1152/ajplegacy.1970.218.5.1468.
126. Siegle ML, Buhner S, Schemann M, Schmid HR, Ehrlein HJ. Propagation velocities and frequencies of contractions along canine small intestine. Am J Physiol. 1990;258(5 Pt 1):G738–44.
127. Traurig HH, Papka RE. Autonomic efferent and visceral sensory innervation of the female reproductive system: special reference to the functional roles of nerves in reproductive organs. In: Maggi CA, editor. Nervous control of the urogenital system, The autonomic nervous system, vol. 3. Chur: Harwood Academic Publishers; 1993. p. 103–41.
128. Nance DM, Burns J, Klein CM, Burden HW. Afferent fibers in the reproductive system and pelvic viscera of female rats: anterograde tracing and immunocytochemical studies. Brain Res Bull. 1988;21(4):701–9.
129. Papka RE, Traurig HH. Autonomic efferent and visceral sensory innervation of the female reproductive tract: special reference to neurochemical markers in nerves and ganglionic connections. In: Maggi CA, editor. Nervous control of the urogenital system, The autonomic nervous system, vol. 3. Chur: Harwood Academic Publishers; 1993. p. 423–66.
130. Jankovic SM, Protic BA, Jankovic SV. Contractile effect of acetylcholine on isolated isthmic segment of fallopian tubes. Methods Find Exp Clin Pharmacol. 2004;26(2):87–91.
131. Jankovic SM, Protic BA, Jankovic SV. Contractile effect of acetylcholine on isolated ampullar segment of Fallopian tubes. Pharmacol Res. 2004;49(1):31–5.
132. Helm GH, Hakanson R, Leander S, Owman C, Sjoberg NO, Sporrong B. Neurogenic relaxation mediated by vasoactive intestinal polypeptide (VIP) in the isthmus of the human fallopian tube. Regul Pept. 1982;3(2):145–53.
133. Grozdanovic Z, Mayer B, Baumgarten HG, Bruning G. Nitric oxide synthase-containing nerve fibers and

neurons in the genital tract of the female mouse. Cell Tissue Res. 1994;275(2):355–60.
134. Ekerhovd E, Brannstrom M, Weijdegard B, Norstrom A. Localization of nitric oxide synthase and effects of nitric oxide donors on the human Fallopian tube. Mol Hum Reprod. 1999;5(11):1040–7.
135. Lapointe J, Roy M, St-Pierre I, Kimmins S, Gauvreau D, MacLaren LA, Bilodeau JF. Hormonal and spatial regulation of nitric oxide synthases (NOS) (neuronal NOS, inducible NOS, and endothelial NOS) in the oviducts. Endocrinology. 2006;147(12):5600–10.
136. Ortiz ME, Villalon M, Croxatto HB. Ovum transport and fertility following postovulatory treatment with estradiol in rats. Biol Reprod. 1979;21(5):1163–7.
137. Rios M, Hermoso M, Sanchez TM, Croxatto HB, Villalon MJ. Effect of oestradiol and progesterone on the instant and directional velocity of microsphere movements in the rat oviduct: gap junctions mediate the kinetic effect of oestradiol. Reprod Fertil Dev. 2007;19(5):634–40.
138. Norwitz ER, Schust DJ, Fisher SJ. Implantation and the survival of early pregnancy. N Engl J Med. 2001;345(19):1400–8. https://doi.org/10.1056/NEJMra000763.
139. Wilcox AJ, Weinberg CR, O'Connor JF, Baird DD, Schlatterer JP, Canfield RE, Armstrong EG, Nisula BC. Incidence of early loss of pregnancy. N Engl J Med. 1988;319(4):189–94. https://doi.org/10.1056/NEJM198807283190401.
140. Pisarska MD, Carson SA. Incidence and risk factors for ectopic pregnancy. Clin Obstet Gynecol. 1999;42(1):2–8; quiz 55–56
141. From the Centers for Disease Control and Prevention. Ectopic pregnancy—United States, 1990–1992. JAMA. 1995;273(7):533.
142. Talbot P, Riveles K. Smoking and reproduction: the oviduct as a target of cigarette smoke. Reprod Biol Endocrinol. 2005;3:52. https://doi.org/10.1186/1477-7827-3-52.
143. Saraiya M, Berg CJ, Kendrick JS, Strauss LT, Atrash HK, Ahn YW. Cigarette smoking as a risk factor for ectopic pregnancy. Am J Obstet Gynecol. 1998;178(3):493–8.
144. Yoshinaga K, Rice C, Krenn J, Pilot RL. Effects of nicotine on early pregnancy in the rat. Biol Reprod. 1979;20(2):294–303.
145. Jensen TK, Henriksen TB, Hjollund NH, Scheike T, Kolstad H, Giwercman A, Ernst E, Bonde JP, Skakkebaek NE, Olsen J. Caffeine intake and fecundability: a follow-up study among 430 Danish couples planning their first pregnancy. Reprod Toxicol. 1998;12(3):289–95.
146. United Nations Office on Drugs and Crime. World drug report.
147. Feng T. Substance abuse in pregnancy. Curr Opin Obstet Gynecol. 1993;5(1):16–23.
148. Young-Wolff KC, Tucker LY, Alexeeff S, Armstrong MA, Conway A, Weisner C, Goler N. Trends in self-reported and biochemically tested Marijuana use among pregnant females in California from 2009–2016. JAMA. 2017;318(24):2490–1. https://doi.org/10.1001/jama.2017.17225.
149. Maykut MO. Health consequences of acute and chronic marihuana use. Prog Neuropsychopharmacol Biol Psychiatry. 1985;9(3):209–38.
150. Mueller BA, Daling JR, Weiss NS, Moore DE. Recreational drug use and the risk of primary infertility. Epidemiology. 1990;1(3):195–200.
151. Klonoff-Cohen HS, Natarajan L, Chen RV. A prospective study of the effects of female and male marijuana use on in vitro fertilization (IVF) and gamete intrafallopian transfer (GIFT) outcomes. Am J Obstet Gynecol. 2006;194(2):369–76. https://doi.org/10.1016/j.ajog.2005.08.020.
152. Horne AW, Phillips JA 3rd, Kane N, Lourenco PC, McDonald SE, Williams AR, Simon C, Dey SK, Critchley HO. CB1 expression is attenuated in Fallopian tube and decidua of women with ectopic pregnancy. PLoS One. 2008;3(12):e3969. https://doi.org/10.1371/journal.pone.0003969.
153. Wang H, Guo Y, Wang D, Kingsley PJ, Marnett LJ, Das SK, DuBois RN, Dey SK. Aberrant cannabinoid signaling impairs oviductal transport of embryos. Nat Med. 2004;10(10):1074–80. https://doi.org/10.1038/nm1104.
154. Maccarrone M, Valensise H, Bari M, Lazzarin N, Romanini C, Finazzi-Agro A. Relation between decreased anandamide hydrolase concentrations in human lymphocytes and miscarriage. Lancet. 2000;355(9212):1326–9. https://doi.org/10.1016/S0140-6736(00)02115-2.
155. Matsuda LA, Lolait SJ, Brownstein MJ, Young AC, Bonner TI. Structure of a cannabinoid receptor and functional expression of the cloned cDNA. Nature. 1990;346(6284):561–4. https://doi.org/10.1038/346561a0.
156. Munro S, Thomas KL, Abu-Shaar M. Molecular characterization of a peripheral receptor for cannabinoids. Nature. 1993;365(6441):61–5. https://doi.org/10.1038/365061a0.
157. Sugiura T, Kodaka T, Nakane S, Miyashita T, Kondo S, Suhara Y, Takayama H, Waku K, Seki C, Baba N, Ishima Y. Evidence that the cannabinoid CB1 receptor is a 2-arachidonoylglycerol receptor. Structure-activity relationship of 2-arachidonoylglycerol, ether-linked analogues, and related compounds. J Biol Chem. 1999;274(5):2794–801.
158. Sugiura T, Kondo S, Sukagawa A, Nakane S, Shinoda A, Itoh K, Yamashita A, Waku K. 2-Arachidonoylglycerol: a possible endogenous cannabinoid receptor ligand in brain. Biochem Biophys Res Commun. 1995;215(1):89–97.
159. Mechoulam R, Ben-Shabat S, Hanus L, Ligumsky M, Kaminski NE, Schatz AR, Gopher A, Almog S, Martin BR, Compton DR, et al. Identification of an endogenous 2-monoglyceride, present in canine gut, that binds to cannabinoid receptors. Biochem Pharmacol. 1995;50(1):83–90.

160. Maccarrone M, Finazzi-Agro A. Endocannabinoids and their actions. Vitam Horm. 2002;65:225–55.
161. Piomelli D. The molecular logic of endocannabinoid signalling. Nat Rev Neurosci. 2003;4(11):873–84. https://doi.org/10.1038/nrn1247.
162. De Petrocellis L, Cascio MG, Di Marzo V. The endocannabinoid system: a general view and latest additions. Br J Pharmacol. 2004;141(5):765–74. https://doi.org/10.1038/sj.bjp.0705666.
163. Paria BC, Das SK, Dey SK. The preimplantation mouse embryo is a target for cannabinoid ligand-receptor signaling. Proc Natl Acad Sci U S A. 1995;92(21):9460–4.
164. Paria BC, Song H, Wang X, Schmid PC, Krebsbach RJ, Schmid HH, Bonner TI, Zimmer A, Dey SK. Dysregulated cannabinoid signaling disrupts uterine receptivity for embryo implantation. J Biol Chem. 2001;276(23):20523–8. https://doi.org/10.1074/jbc.M100679200.
165. Schmid PC, Paria BC, Krebsbach RJ, Schmid HH, Dey SK. Changes in anandamide levels in mouse uterus are associated with uterine receptivity for embryo implantation. Proc Natl Acad Sci U S A. 1997;94(8):4188–92.
166. Wang H, Matsumoto H, Guo Y, Paria BC, Roberts RL, Dey SK. Differential G protein-coupled cannabinoid receptor signaling by anandamide directs blastocyst activation for implantation. Proc Natl Acad Sci U S A. 2003;100(25):14914–9. https://doi.org/10.1073/pnas.2436379100.
167. Nawrot P, Jordan S, Eastwood J, Rotstein J, Hugenholtz A, Feeley M. Effects of caffeine on human health. Food Addit Contam. 2003;20(1):1–30. https://doi.org/10.1080/0265203021000007840.
168. Stanton CK, Gray RH. Effects of caffeine consumption on delayed conception. Am J Epidemiol. 1995;142(12):1322–9.
169. Bolumar F, Olsen J, Rebagliato M, Bisanti L. Caffeine intake and delayed conception: a European multicenter study on infertility and subfecundity. European Study Group on Infertility Subfecundity. Am J Epidemiol. 1997;145(4):324–34.
170. Florack EI, Zielhuis GA, Rolland R. Cigarette smoking, alcohol consumption, and caffeine intake and fecundability. Prev Med. 1994;23(2):175–80. https://doi.org/10.1006/pmed.1994.1024.
171. Hatch EE, Bracken MB. Association of delayed conception with caffeine consumption. Am J Epidemiol. 1993;138(12):1082–92.
172. Parker I, Ivorra I. Caffeine inhibits inositol trisphosphate-mediated liberation of intracellular calcium in Xenopus oocytes. J Physiol. 1991;433:229–40.
173. Butcher RW, Sutherland EW. Adenosine 3′,5′-phosphate in biological materials. I. Purification and properties of cyclic 3′,5′-nucleotide phosphodiesterase and use of this enzyme to characterize adenosine 3′,5′-phosphate in human urine. J Biol Chem. 1962;237:1244–50.
174. Beavo JA. Cyclic nucleotide phosphodiesterases: functional implications of multiple isoforms. Physiol Rev. 1995;75(4):725–48.
175. Kim M, Cho SY, Han IS, Koh SD, Perrino BA. CaM kinase II and phospholamban contribute to caffeine-induced relaxation of murine gastric fundus smooth muscle. Am J Physiol Cell Physiol. 2005;288(6):C1202–10.
176. Kim M, Hennig GW, Smith TK, Perrino BA. Phospholamban knockout increases CaM kinase II activity and intracellular Ca2+ wave activity and alters contractile responses of murine gastric antrum. Am J Physiol Cell Physiol. 2008;294(2):C432–41. https://doi.org/10.1152/ajpcell.00418.2007.
177. Nobe K, Sutliff RL, Kranias EG, Paul RJ. Phospholamban regulation of bladder contractility: evidence from gene-altered mouse models. J Physiol. 2001;535(Pt 3):867–78.
178. Eggermont JA, Vrolix M, Wuytack F, Raeymaekers L, Casteels R. The (Ca2+-Mg2+)-ATPases of the plasma membrane and of the endoplasmic reticulum in smooth muscle cells and their regulation. J Cardiovasc Pharmacol. 1988;12(Suppl 5):S51–5.
179. Meera P, Anwer K, Monga M, Oberti C, Stefani E, Toro L, Sanborn BM. Relaxin stimulates myometrial calcium-activated potassium channel activity via protein kinase A. Am J Physiol. 1995;269(2 Pt 1):C312–7.
180. Sanborn BM, Yue C, Wang W, Dodge KL. G protein signalling pathways in myometrium: affecting the balance between contraction and relaxation. Rev Reprod. 1998;3(3):196–205.
181. Price SA, Bernal AL. Uterine quiescence: the role of cyclic AMP. Exp Physiol. 2001;86(2):265–72.
182. Quayle JM, Bonev AD, Brayden JE, Nelson MT. Calcitonin gene-related peptide activated ATP-sensitive K+ currents in rabbit arterial smooth muscle via protein kinase A. J Physiol. 1994;475(1):9–13.
183. Wellman GC, Quayle JM, Standen NB. ATP-sensitive K+ channel activation by calcitonin gene-related peptide and protein kinase A in pig coronary arterial smooth muscle. J Physiol. 1998;507(Pt 1):117–29.
184. Quinn KV, Giblin JP, Tinker A. Multisite phosphorylation mechanism for protein kinase A activation of the smooth muscle ATP-sensitive K+ channel. Circ Res. 2004;94(10):1359–66.
185. Shi Y, Wu Z, Cui N, Shi W, Yang Y, Zhang X, Rojas A, Ha BT, Jiang C. PKA phosphorylation of SUR2B subunit underscores vascular KATP channel activation by beta-adrenergic receptors. Am J Physiol Regul Integr Comp Physiol. 2007;293(3):R1205–14.
186. Shi Y, Chen X, Wu Z, Shi W, Yang Y, Cui N, Jiang C, Harrison RW. cAMP-dependent protein kinase phosphorylation produces interdomain movement in SUR2B leading to activation of the vascular KATP channel. J Biol Chem. 2008;283(12):7523–30.
187. Burg AW. Physiological disposition of caffeine. Drug Metab Rev. 1975;4(2):199–228. https://doi.org/10.3109/03602537508993756.

188. White JR Jr, Padowski JM, Zhong Y, Chen G, Luo S, Lazarus P, Layton ME, McPherson S. Pharmacokinetic analysis and comparison of caffeine administered rapidly or slowly in coffee chilled or hot versus chilled energy drink in healthy young adults. Clin Toxicol (Phila). 2016;54(4):308–12. https://doi.org/10.3109/15563650.2016.1146740.
189. Adderley-Kelly B, Stephens EM. Chlamydia: a major health threat to adolescents and young adults. ABNF J. 2005;16(3):52–5.
190. Stamm WE. Chlamydia screening: expanding the scope. Ann Intern Med. 2004;141(7):570–2.
191. World Health Organization. Global prevalence and incidence of selected curable sexually transmitted infections overview and estimates. Geneva: WHO; 2001.
192. Entrican G, Wattegedera S, Rocchi M, Fleming DC, Kelly RW, Wathne G, Magdalenic V, Howie SE. Induction of inflammatory host immune responses by organisms belonging to the genera Chlamydia/Chlamydophila. Vet Immunol Immunopathol. 2004;100(3–4):179–86.
193. World Health Organization. Global strategy for the prevention and control of sexually transmitted infections: 2006–2015: breaking the chain of transmission. Geneva: WHO; 2007.
194. Read TD, Brunham RC, Shen C, Gill SR, Heidelberg JF, White O, Hickey EK, Peterson J, Utterback T, Berry K, Bass S, Linher K, Weidman J, Khouri H, Craven B, Bowman C, Dodson R, Gwinn M, Nelson W, DeBoy R, Kolonay J, McClarty G, Salzberg SL, Eisen J, Fraser CM. Genome sequences of Chlamydia trachomatis MoPn and Chlamydia pneumoniae AR39. Nucleic Acids Res. 2000;28(6):1397–406.
195. Brunham RC, Rey-Ladino J. Immunology of Chlamydia infection: implications for a Chlamydia trachomatis vaccine. Nat Rev Immunol. 2005;5(2):149–61.
196. Shah AA, Schripsema JH, Imtiaz MT, Sigar IM, Kasimos J, Matos PG, Inouye S, Ramsey KH. Histopathologic changes related to fibrotic oviduct occlusion after genital tract infection of mice with Chlamydia muridarum. Sex Transm Dis. 2005;32(1):49–56.
197. Eskandari MK, Kalff JC, Billiar TR, Lee KK, Bauer AJ. LPS-induced muscularis macrophage nitric oxide suppresses rat jejunal circular muscle activity. Am J Physiol. 1999;277(2 Pt 1):G478–86.
198. Kalff JC, Schraut WH, Billiar TR, Simmons RL, Bauer AJ. Role of inducible nitric oxide synthase in postoperative intestinal smooth muscle dysfunction in rodents. Gastroenterology. 2000;118(2):316–27.
199. Yanagida H, Sanders KM, Ward SM. Inactivation of inducible nitric oxide synthase protects intestinal pacemaker cells from postoperative damage. J Physiol. 2007;582(Pt 2):755–65.
200. Xin HB, Deng KY, Rishniw M, Ji G, Kotlikoff MI. Smooth muscle expression of Cre recombinase and eGFP in transgenic mice. Physiol Genomics. 2002;10(3):211–5.

Part IV

Blood Vessels

Cellular and Ionic Mechanisms of Arterial Vasomotion

12

William C. Cole, Grant R. Gordon, and Andrew P. Braun

Abstract

Rhythmical contractility of blood vessels was first observed in bat wing veins by Jones (Philos Trans R Soc Lond 1852:142, 131–136), and subsequently described in arteries and arterioles of multiple vascular beds in several species. Despite an abundance of descriptive literature regarding the presence of vasomotion, to date we do not have an accurate picture of the cellular and ionic basis of these oscillations in tone, or the physiological relevance of the changes in pulsatile blood flow arising from vasomotion. This chapter reviews our current understanding of the cellular and ionic mechanisms underlying vasomotion in resistance arteries and arterioles. Focus is directed to the ion channels, changes in cytosolic Ca^{2+} concentration, and involvement of intercellular gap junctions in the development and synchronization of rhythmic changes in membrane potential and cytosolic Ca^{2+} concentration within the vessel wall that contribute to vasomotion. The physiological consequences of vasomotion are discussed with a focus on the cerebral vasculature, as recent advances show that rhythmic oscillations in cerebral arteriolar diameter appear to be entrained by cortical neural activity to increase the local supply of blood flow to active regions of the brain.

Keywords

Vasomotion · Artery · Arteriole · Vascular smooth muscle · Endothelium · Sympathetic nerve · Neurovascular coupling

12.1 Introduction

Rhythmic oscillations in the diameter of blood vessels have been observed for more than 150 years beginning with the initial description by Jones [1]. In his analysis of veins in the bat wing, Jones [1] stated that there was "something peculiar in the flow of blood in the veins; that they contracted and dilated rhythmically," with an average of 7–13 contractions per minute. Similar spontaneous and evoked oscillations in diameter, now generally referred to as *vasomotion*, are accepted to be a common feature of arteries and veins ranging in size from conduit vessels (e.g., carotid arteries) to microvasculature of animals and humans studied *in vitro* and *in*

W. C. Cole (✉) · G. R. Gordon · A. P. Braun
Department of Physiology and Pharmacology, Libin Cardiovascular Institute, Cumming School of Medicine, University of Calgary, Calgary, AB, Canada
e-mail: wcole@ucalgary.ca

H. Hashitani, R. J. Lang (eds.), *Smooth Muscle Spontaneous Activity*, Advances in Experimental Medicine and Biology 1124, https://doi.org/10.1007/978-981-13-5895-1_12

vivo under various experimental and physiological conditions (reviewed in [2–7]). Vasomotion is dependent on mechanisms within the vascular wall, as it is observed in isolated segments of arterioles maintained *in vitro* in the absence of neural activity and blood flow, but it can be modulated by neurohumoral factors in a vessel- and species-specific manner [4, 5, 7]. An example of spontaneous vasomotion in a segment of rat middle cerebral artery studied *in vitro* by pressure myography is presented in Fig. 12.1. Varied patterns of modulation and different sensitivities to pharmacological manipulation and endothelium removal have been described for vessels of different vascular beds and varied caliber, suggesting that multiple mechanisms may contribute to the appearance and maintenance of vasomotion in a vessel-specific manner [4–8]. Despite these complexities, considerable progress has been made in understanding the factors and mechanisms responsible for vasomotion. This chapter presents a current understanding of vasomotion in arteries and arterioles. Emphasis has been placed on the cellular and ionic mechanisms that have been postulated to contribute to the rhythmic oscillations in membrane potential, cytosolic Ca^{2+} concentration, and cross-bridge cycling in vascular smooth muscle cells during vasomotion. Furthermore, we explore recent advancements in our understanding of the influence of neural activity in the brain on vasomotion in the cerebral vasculature, and the link between the presence of vasomotion and metabolic demand associated with information processing in the brain cortex.

12.2 Vasomotion is a Common Feature of the Macrovasculature

Vasomotion has been observed in segments of conduit arteries, as well as small-resistance arteries and arterioles studied *in vitro* by wire (isometric) and pressure (isobaric) myography (Fig. 12.1), and in vessels *in vivo* through the application of multiple techniques that assess blood flow (e.g., laser Doppler flow, blood cell velocity, capillary pressure). For a more comprehensive presentation and

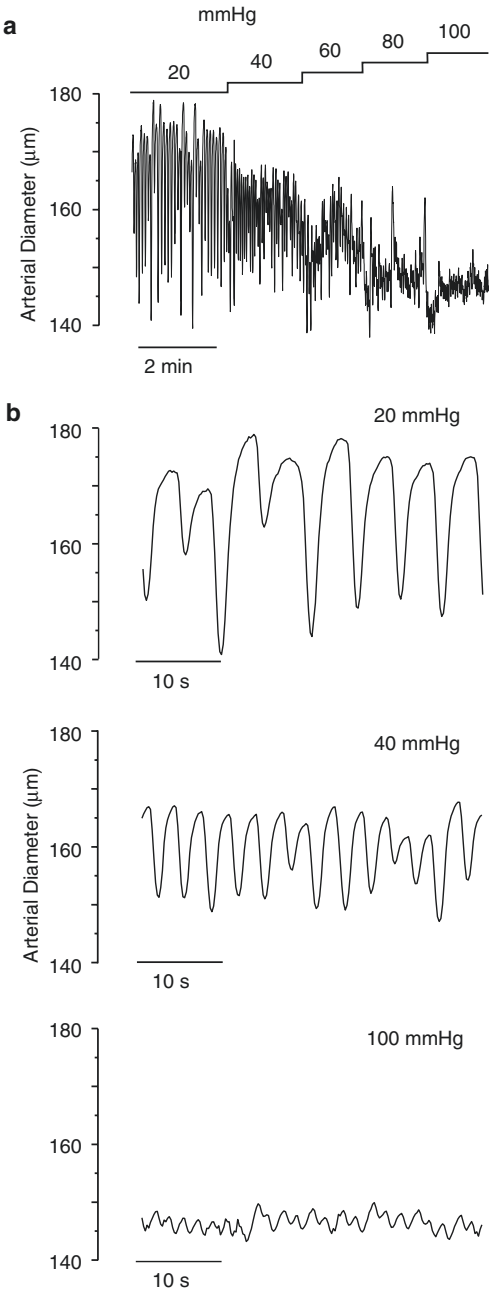

Fig. 12.1 Vasomotion in pressurized middle cerebral arteries *in vitro*. Panel **a**: Continuous recording of arterial diameter over a range of intraluminal pressures from 20 to 100 mmHg. The "noisy" appearance of the recording results from oscillations in diameter of decreasing amplitude with increased intraluminal pressure. Panel **b**: Representative expanded segments of the trace in panel **a** at 20, 40, and 100 mmHg illustrating the change in amplitude and frequency of vasomotion associated with increased intraluminal pressure

historical perspective the interested reader should consult the following review articles [2–4, 6, 8]. In the case of blood flow measurements, the rhythmic oscillations in arterial diameter during vasomotion evoke corresponding variations in flow velocity, or "flowmotion" [9, 10]. Blood flow measurements include variations in flow due to multiple causes; these include a "myogenic" component of temporal variability resulting from vasomotion, as well as fluctuations in flow due to cardiac and respiratory activity, and rhythmic endothelium-dependent and neurogenic mechanisms [11, 12].

Rhythmic, synchronous contraction over several millimeters of individual vessel segments is a ubiquitous feature of the arterial vasculature [4, 8]; examples include cerebral [13, 14], mesenteric [15–18], irideal [19], skeletal muscle [20], and cutaneous arteries and arterioles [21, 22]. In some instances, vasomotion can exhibit a more irregular character owing to the superimposition of multiple rhythms (Fig. 12.1), generated by multiple intrinsic oscillators at different frequencies [23, 24], or superimposed activity originating from multiple initiating sites along the vessel wall. Reported variations in the amplitude and frequency (0.01–0.3 Hz) of spontaneous vasomotion, or vasomotion observed in the presence of intraluminal pressure, stretch, vasoconstrictors, or vasodilators, arise from varied physiological or experimental conditions, species and vascular bed, and vessel caliber (Fig. 12.1). Different stable patterns of vasomotion at varied frequencies can also emerge in the presence of various ion channel and transport-blocking drugs, consistent with the presence of multiple oscillatory mechanisms in the vessel wall [7, 8]. In general, branch vessels of similar size behave independently and differences in frequency are detected at the branch points, with smaller downstream vessels oscillating at a higher frequency [5–7, 21, 25, 26]. Vasomotion is generally observed at intermediate levels of tone development, and may be reduced in amplitude or not detected towards extremes of full dilation or constriction [27]. The characteristics of noradrenaline- and arginine vasopressin-evoked vasomotion in rat mesenteric arteries assessed *in vitro* and *in vivo* were similar [16, 17, 28]. However, differences in amplitude and frequency of the oscillations were detected *in vivo* depending on the combination of anesthetic and vasoconstrictor employed [28]. Effects of anesthesia on vasomotion were previously reported in several studies, i.e., including an inhibition or a stimulation of rhythmic contractions [7, 9, 21, 29–32]. For this reason, analysis of vasomotion in vessels *in vivo* is best performed in the awake, unanesthetized condition [14, 22, 31, 32].

12.3 Cellular Mechanisms of Arterial Vasomotion

No clear pattern of pharmacological sensitivity, endothelium removal, or neuronal dependence has emerged for arterial vasomotion, prompting the view that multiple mechanisms may be involved in a vessel- and species-dependent manner [4, 6–8]. This section provides a summary of the major mechanisms postulated to underlie vasomotion that are largely based on an analysis of vasomotion in rat mesenteric arteries. Also presented are recent advances that (1) identify a role for bestrophin- and/or ANO1/TMEM16A-containing Ca^{2+}-sensitive chloride channels as a cause of rhythmic depolarizations in vasomotion [33–35] and (2) present contrasting views concerning the role of asynchronous Ca^{2+} waves in the initiation of vasomotion *in vitro* and *in vivo* [7, 16, 22, 32, 36].

Vasomotion is dependent on simultaneous, rhythmic contraction and relaxation of smooth muscle cells over the length of individual vessel segments that may span several millimeters. By necessity this contractile behavior requires two key elements, a mechanism that synchronizes electrical and contractile activity in individual myocytes along the vessel wall, and an oscillatory mechanism that provides temporal control over Ca^{2+}-dependent activation of cross-bridge cycling. Synchronized contractile behavior in individual vascular smooth muscle cells is not attributed to innervation, as neurotransmitters are released "*en passant*" from intermittent varicosities within a loose network of perivascular (mostly sympathetic) nerves in the outer adventitial connective tissue layer surrounding vessels [37]. Rather, there

is general agreement that synchronization is dependent on the presence of gap junctions that permit intercellular electrical communication between individual smooth muscle cells (homocellular junctions), and between smooth muscle and endothelial cells (heterocellular junctions) at myoendothelial projections (i.e., myoendothelial gap junctions; Fig. 12.2) [5, 7, 8, 38–40]. Gap junctions are formed by the alignment of two connexon hemichannels in opposing cell membranes, with each connexon composed of six transmembrane connexin proteins (i.e., connexins 37, 40,

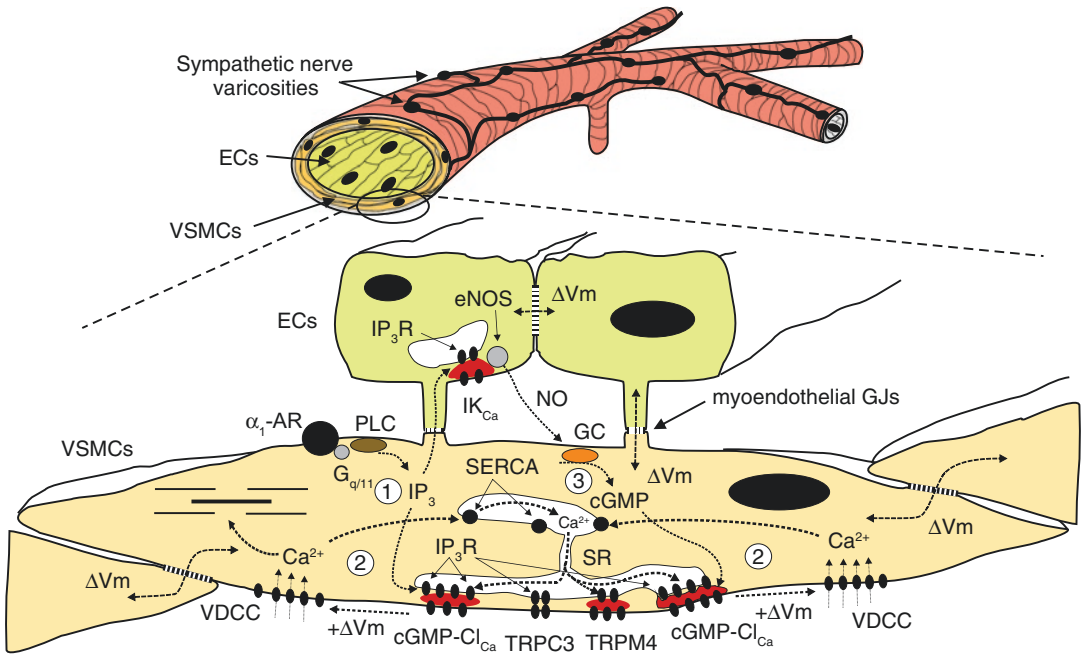

Fig. 12.2 Cartoon representation of the key elements postulated to contribute to arterial vasomotion. The upper cartoon depicts a branching resistance arteriole showing the key structural elements, endothelial cells (ECs) lining the vessel lumen and arranged parallel to the direction of blood flow, surrounded by vascular smooth muscle cells (VSMCs) oriented in a perpendicular manner around the vessel wall, and the loose meshwork of sympathetic nerves and intermittent varicosities within the adventitial layer of connective tissue around the vessel. The lower cartoon is an expanded version showing that the ECs are electrically coupled to the surrounding VSMCs by heterocellular gap junctions (GJs) within myoendothelial projections that extend between the cell types. The postulated mechanisms of vasomotion within ECs and VSMCs include (1) $G_{q/11}$ G protein-coupled receptors, such as the α_1-adrenoceptor (α_1-AR), that evoke synthesis of inositol 1,4,5-trisphosphate (IP_3) via phospholipase C (PLC) activation and PIP_2 hydrolysis that is required to elicit the release of internal Ca^{2+} stores in the sarcoplasmic reticulum (SR) via IP_3 receptors (IP_3Rs) near the plasma membrane in VSMCs and within myoendothelial projections of ECs. The localized release of Ca^{2+} at these sites is denoted by the red shading in the cytosol between the IP_3Rs and plasma membrane. (2) A cytosolic oscillator mechanism that involves cycles of Ca^{2+} release by IP_3Rs to evoke depolarization by activating cGMP-dependent Ca^{2+}-activated chloride channels (cGMP-Cl_{Ca}), or nonselective cation channels consisting of TRPC3 (activation by a direct protein-protein interaction with IP3Rs is postulated for this conductance) or TRPM4 proteins, in the plasma membrane. The depolarization ($+\Delta V_m$) activates nearby voltage-gated Ca^{2+} channels resulting in Ca^{2+} influx and a global change in cytosolic Ca^{2+} concentration that evokes cross-bridge cycling in the myofilaments, and propagates electrotonically into adjacent VSMCs via homocellular GJs (ΔV_m). Cytosolic Ca^{2+} concentration is subsequently reduced by transport into the SR via sarco/endoplasmic reticulum Ca^{2+}-ATPase (SERCA) for subsequent release during the next cycle of vasomotion as well as extrusion out of the cell (not shown). (3) IP_3 from VSMCs may transit myoendothelial GJs to evoke Ca^{2+} release and activation of endothelial nitric oxide synthase (eNOS) and intermediate-conductance, Ca^{2+}-activated K^+ channels (IK_{Ca}) localized within and in close proximity to the myoendothelial projection (slightly displaced out of the projection for clarity in this cartoon), with the resultant synthesis and release of nitric oxide (NO) activating soluble and particulate guanylyl cyclase (GC) to produce the second messenger, cGMP, that is required for cGMP-Cl_{Ca} activity

43, and/or 45) that surround an aqueous cell-to-cell pathway that permits electrical coupling, as well as the movement of ions and small molecules (<~1 kDa) between the cytosol of connected cells (reviewed in [39, 40]). Evidence that functional gap junctions are essential for vasomotion in rabbit mesenteric arteries was provided through the use of inhibitor peptides that disrupt the interaction between gap junction hemichannels [41]. Vasomotion was suppressed by these peptides without an effect on basal tone suggesting that a specific block of gap junction communication was achieved [41]. Vasomotion was also assessed following genetic knockout of connexin 40 in mice, and only irregular contractile activity was observed in cremaster arterioles [42]. Finally, inhibition of gap junctions with heptanol or glycyrrhetinic acid derivatives was also reported to suppress vasomotion, with the caveat that these agents are known to have off-target effects [41, 43, 44].

There is also consensus that the signal that promotes synchronization along the vessel wall must be electrical in nature, i.e., a change in membrane potential (ΔV_m) [5–8]. Only an electrical signal appears sufficient to account for synchronization over millimeter lengths of arteriolar segments that are considerably greater than the width of individual myocytes (~3–5 μm) positioned perpendicularly around the vessel wall [5, 16]. In this scenario, independent oscillations in membrane potential within individual myocytes are thought to be entrained by rapid cell-to-cell spread of electrotonic current via gap junctions. This results in synchronized phases of depolarization, voltage-dependent Ca^{2+} channel activation, and Ca^{2+} influx that evoke a simultaneous, global rise in cytosolic Ca^{2+} concentration and cross-bridge cycling in all myocytes along the vessel wall (i.e., a coupled oscillator model [5, 16, 45]).

Three generalized mechanisms are thought to be responsible for rhythmic contractile behavior of smooth muscle (reviewed in [46]), and examples of each mechanism are presented in this book. The postulated mechanisms involve (1) oscillations in membrane potential in individual smooth muscle cells that are evoked by specialized pacemaker cells, such as interstitial cells of Cajal associated with gastrointestinal smooth muscle cells, and atypical smooth muscle cells within urogenital smooth muscle tissues; (2) a membrane oscillator mechanism within the plasma membrane that periodically depolarizes and hyperpolarizes membrane potential, leading to intermittent voltage-dependent Ca^{2+} entry and rhythmic activation of cross-bridge cycling; and (3) a cytosolic oscillator involving intermittent release of Ca^{2+} from internal Ca^{2+} stores via inositol trisphosphate receptors (IP_3R) and/or ryanodine receptors (RyR) in the sarcoplasmic reticulum [46]. It is this third scenario involving oscillatory Ca^{2+} release and refilling of internal Ca^{2+} stores that is postulated to be involved in arterial vasomotion (Fig. 12.2) [5, 7, 16]. However, Ca^{2+} released from the internal stores does not activate contraction directly, as global elevations in cytosolic Ca^{2+} concentration are only achieved with depolarization and voltage-dependent Ca^{2+} channel activity in vascular smooth muscle cells [47]. Rather, localized Ca^{2+} release from IP_3Rs in close proximity to the plasma membrane is postulated to cause the activation of a Ca^{2+}-sensitive depolarizing current, and subsequent Ca^{2+} influx through voltage-dependent Ca^{2+} channels leading to contraction (Fig. 12.2) [7, 16]. Uptake of Ca^{2+} from the cytosol into the sarcoplasmic reticulum via sarco/endoplasmic reticulum Ca^{2+}-ATPase (SERCA) activity refills the internal Ca^{2+} store in preparation for the next release event. The delay required for store refilling is postulated to provide the necessary time lag needed for rhythmicity; that is, in this model, IP_3R-dependent store release and refilling is the primary cytosolic oscillator [7, 8, 16], with release from the store dependent on the combination of IP_3 concentration and luminal Ca^{2+} concentration [48]. Factors that influence the refilling process, including changes in the level of Ca^{2+} influx across the plasma membrane, cytosolic concentration of IP_3, and level of luminal Ca^{2+} in the store, may alter the frequency of vasomotion by affecting this cytosolic oscillator mechanism.

The current view that arterial vasomotion is dependent on a cytosolic oscillator involving the periodic release of internal Ca^{2+} stores via IP_3Rs, coupled to rhythmic oscillations in membrane depolarization and elevations of global cytosol Ca^{2+} concentration due to the activation of a Ca^{2+}-

sensitive inward current, is supported by several observations:

1. Oscillations in membrane potential are detected in a variety of vessels exhibiting vasomotion, with depolarization observed to precede the onset of constriction [5, 16, 17, 27, 49–53], with the apparent exception of irideal arterioles [19, 54]. That oscillations in membrane potential are required for vasomotion is indicated by experiments showing an inhibition of vasomotion in the presence of ATP-sensitive K^+ channel-activator drugs that cause sustained smooth muscle hyperpolarization [16, 55].
2. Rhythmic, synchronized oscillations in global cytosolic Ca^{2+} concentration in smooth muscle cells are detected during vasomotion in arterioles studied *in vitro* [15, 16] and *in vivo* [22, 32, 36], with cytosolic Ca^{2+} rapidly increasing prior to the onset of contraction in both experimental conditions. An ~0.3 s delay was detected between the peak elevation in cytosolic Ca^{2+} and maximal rate of constriction in murine ear arterioles *in vivo* [22], and a delay of ~0.9 s was detected in basilar arterial segments *in vitro* [53]. These values are consistent with the time lag between the rise in global Ca^{2+} concentration, and subsequent phosphorylation of myosin regulatory light chain (i.e., LC_{20}) by Ca^{2+}-calmodulin-dependent myosin light-chain kinase and contraction during depolarization-evoked contraction of urinary bladder smooth muscle following neural activation [56, 57].
3. The oscillations in cytosolic Ca^{2+} concentration associated with vasomotion are suppressed by inhibiting L-type, voltage-gated Ca^{2+} channels, or removal of extracellular Ca^{2+} [16, 17, 56, 58, 59], whereas vasomotion is enhanced by treatment with the Ca^{2+} channel activator BayK8644 [59]. Ca^{2+} influx via voltage-dependent Ca^{2+} channels is required for cross-bridge cycling, and to refill the internal Ca^{2+} stores following Ca^{2+} release by IP_3Rs (Fig. 12.2) [5, 7]. Global elevations in cytosolic Ca^{2+} in smooth muscle cells are widely recognized to be dependent on membrane electrical activity, in which depolarization evokes the activation of voltage-gated Ca^{2+} channels, and oscillations in Ca^{2+} entry lead to rhythmic variations in membrane potential and vasomotion through intermittent filling and release of internal Ca^{2+} stores [47].
4. Inhibition of the release of internal Ca^{2+} stores in vascular myocytes by blocking phospholipase C-dependent inositol 1,4,5-trisphosphate (IP_3) synthesis from phosphoinositide 4,5-bisphosphate (PIP_2) with U73122, or IP_3Rs with the nonselective inhibitor 2-aminoethyl diphenylborinate (2-APB), was shown to prevent rhythmic oscillations in cytosolic Ca^{2+} concentration and vasomotion, as does blocking Ca^{2+} uptake into the sarcoplasmic reticulum with cyclopiazonic acid (CPA) or thapsigargin [16, 24, 27, 56, 58–61]. The key role played by IP_3R is also indicated by the stimulation of vasomotion by different vasoconstrictor agonists, noradrenaline, serotonin, and vasopressin, that all act on $G_{q/11}$-coupled receptors to evoke phospholipase C-mediated generation of IP_3 (Fig. 12.2) [7].

Treating arteries and arterioles with ryanodine to alter RyR-mediated release of internal Ca^{2+} stores has varied effects on vasomotion, including a block of cytosolic Ca^{2+} oscillations and rhythmic contraction [16, 56, 59], alteration in the frequency and amplitude of Ca^{2+} oscillations and vasomotion (as was also noted for CPA in rabbit mesenteric arteries), and a change in endothelium dependency of vasomotion from necessary to not required [60, 62]. These contrasting observations may reflect a varied contribution of RyR to the cytosolic oscillator in different vessels and experimental conditions, and/or that depleting internal Ca^{2+} stores with ryanodine or CPA may reveal the presence of additional oscillator mechanisms in the vascular wall that may or may not involve endothelium-dependent mechanisms [7]. Based on our current understanding, there is general agreement that periodic release of Ca^{2+} from the sarcoplasmic reticulum via IP_3Rs in vascular myocytes represents the key component of the cytosolic oscillator necessary for vasomotion, but RyRs may be involved in vessel-specific manner,

a view consistent with the evidence of a differential expression and functional contribution of RyRs, but not IP_3Rs, to the regulation of cytosolic Ca^{2+} in smooth muscle cells within arteries and arterioles of varied size and location [63, 64].

Identification of the ionic conductance responsible for rhythmic depolarization of membrane potential during vasomotion has been hampered by a lack of selective pharmacological tools to inhibit or activate the suspected channel candidates, but the recent application of molecular approaches has provided novel insight. Several lines of evidence suggest that cGMP-dependent, Ca^{2+}-activated chloride channels are stimulated by IP_3R-dependent release of Ca^{2+} from the sarcoplasmic reticulum to evoke membrane potential depolarization during vasomotion in rat mesenteric arteries (i.e., E_{Cl} is ~−25 mV, so activation of the channels elicits outward Cl^- flux and depolarization; Fig. 12.2) (reviewed in [7, 8]). Ca^{2+} released from the sarcoplasmic reticulum via IP_3R may be localized within microdomains between the sarcoplasmic reticulum and plasma membrane such that chloride channel gating is stimulated without activation of cross-bridge cycling (Fig. 12.2). This mechanism parallels the regulation of membrane potential by localized Ca^{2+} sparks created by the focal release of Ca^{2+} from RyRs that stimulate juxtaposed large-conductance Ca^{2+}-activated potassium channels in the plasma membrane to evoke hyperpolarization and relaxation [47].

The rhythmic depolarizations, oscillations in cytosolic Ca^{2+} concentration, and vasomotion of rat mesenteric arteries evoked by α_1-adrenoceptor activation with phenylephrine were shown to be dependent on the presence of cytosolic cGMP [16]. Moreover, a cGMP-dependent, Ca^{2+}-activated chloride current was observed in myocytes from these arteries [65]. This current was found to possess biophysical and pharmacological properties distinct from those of "classical" Ca^{2+}-activated chloride channels in vascular smooth muscle [65] that are thought to be due to expression of ANO1/TMEM16A chloride channel proteins [66, 67]. Expression of another putative Ca^{2+}-activated Cl^- channel protein, bestrophin, was demonstrated to be essential for the cGMP dependence of the chloride current [33], and the amplitude of vasomotion in rat mesenteric arteries was reduced following siRNA knockdown of bestrophin-3 [34]. Although ANO1/TMEM16A silencing produced a similar suppression of vasomotion as bestrophin-3 knockdown, this strategy also reduced bestrophin expression, so it remains unclear if the two proteins form distinct channels, or that bestrophin confers cGMP sensitivity and unique properties to ANO1/TMEM16A channels by acting as an auxiliary subunit [35].

Alternatively, it is possible that rhythmic activation of a depolarizing, nonselective cation conductance is responsible for the IP_3R-dependent depolarization of membrane potential in vasomotion (Fig. 12.2). Recent electrophysiological analysis has identified two mechanisms by which IP_3Rs could potentially evoke rhythmic depolarization by activating nonselective cation channels in vascular smooth muscle cells. Specifically, a direct interaction of IP_3Rs with transient receptor potential cation channels composed of TRPC3 proteins was identified [68]. In this case, the conformational change associated with IP_3R activation is coupled to the gating of TRPC3 channels via a direct, protein-protein interaction [68]. Alternatively, localized Ca^{2+} release by IP_3R near the plasma membrane could evoke the activation of cation channels containing Ca^{2+}-sensitive TRPM4 subunits [69, 70]. Consistent with a role for nonselective cation channels, an increased level of vasomotion was observed in mesenteric arteries of spontaneously hypertensive rats (SHR) compared to normotensive controls (WKY), and found to be associated with a greater expression of TRPC1, TRPC3, and TRPC5 cation channel proteins [71]. The extent of vasomotion was reduced by exposing the arteries to putative nonselective cation channel inhibitors, gadolinium, SKF-96365, and 2-APB, or antibodies against TRPC1 and TRPC3 proteins [71]. Furthermore, chronic treatment of the SHRs with angiotensin AT_1 receptor antagonist, but not the L-type Ca^{2+} channel blocker amlodipine, was demonstrated to suppress TRPC protein expression and vasomotion in the mesenteric vessels [71].

An intact, functional endothelium is essential for vasomotion in many, but not all, arteries [7]. For example, endothelial removal blocks vasomotion in rat mesenteric arteries [16, 59, 72–74], but it is potentiated by endothelial denudation or inhibition of NO synthesis in other vessels [23, 75, 76]. The endothelium appears to be required for nitric oxide synthesis and release (Fig. 12.2). Nitric oxide is thought to be necessary because it evokes cGMP synthesis by guanylyl cyclase in the myocytes, and cGMP is required to facilitate cGMP-dependent Ca^{2+}-activated Cl^- channel activity and depolarization during vasomotion in rat mesenteric arteries (Fig. 12.2) [7, 8]. Consistent with this view, inhibition of nitric oxide synthesis (e.g., with L-N^G-nitroarginine (L-NNA)) also blocked vasomotion in these vessels, and it was partially restored with sodium nitroprusside or membrane-permeant analogs of cGMP [16, 59, 74, 77].

Alternatively, the endothelium may be required to facilitate electrical conduction and/or synchronization along the vessel wall. The longitudinal orientation of electrically coupled endothelial cells and presence of myoendothelial gap junctions would be expected to permit synchronization over greater distances along vessels than what is possible with electrotonic current spread within the smooth muscle layer alone [78, 79]. It is also possible that vasomotion is affected by endothelium-dependent hyperpolarization [73]. In this case, IP_3 generated in smooth muscle cells by α_1-adrenoceptor activation may diffuse into endothelial cells via myoendothelial gap junctions to cause the release of Ca^{2+} stores within the myoendothelial projections. Subsequent activation of intermediate-conductance Ca^{2+}-activated potassium (IK_{Ca}) channels in the endothelial cells may evoke hyperpolarization that spreads back through the junctions to regulate smooth muscle membrane potential and contractility [80, 81]. This mechanism involving IP_3- and endothelial IK_{Ca} channel-dependent feedback dilation is thought to account for endothelium-mediated inhibition of constriction evoked by α_1-adrenoceptors (see [81]), but it may also modulate vasomotion [73] (Fig. 12.2).

The cellular mechanism by which vasomotion is initiated is controversial; recent studies (e.g., [22, 32]) using *in vivo* experimental approaches have cast doubt on the established model involving asynchronous Ca^{2+} waves arising from analyses of vasoconstrictor-evoked vasomotion in rat mesenteric arterioles under isometric recording conditions *in vitro* [7, 8, 16]. An abundant literature on Ca^{2+} signaling in arteries *in vitro* indicates that activation of $G_{q/11}$-coupled receptors by vasoconstrictor agonists is associated with the presence of asynchronous, IP_3R-dependent (and/or RyR-dependent) oscillations in cytosolic Ca^{2+} concentration within individual vascular myocytes [47, 82]. These oscillations in cytosolic Ca^{2+} occur as waves of Ca^{2+} elevation that spread through the cytosol due to regenerative Ca^{2+}-induced Ca^{2+} release from nearby IP_3Rs [47, 82]. Significantly, asynchronous Ca^{2+} waves are consistently detected in individual myocytes within the vessel wall prior to the appearance of synchronous, global elevations in cytosolic Ca^{2+} concentration and the onset of vasomotion in arteries studied *in vitro* [7, 8, 15, 16]. Peng et al. [16] postulated that the initiation of vasomotion occurs when these asynchronous Ca^{2+} wave events in individual cells are entrained to produce synchronized, global Ca^{2+} elevations in myocytes along the length of the vessel wall. Entrainment was postulated to involve Ca^{2+}-dependent activation of depolarizing cGMP-dependent, Ca^{2+}-activated chloride current and cell-to-cell electrical communication via gap junctions [16]. In this case, the oscillations in membrane potential in individual myocytes influence the electrical behavior of adjacent cells via electrotonic current flow, leading to simultaneous depolarization, global Ca^{2+} elevation, and contraction of increasingly greater numbers of myocytes along the vessel in the absence of a defined pacemaker. This mechanism of self-organizing behavior is comparable to that of crowds at sports events, such as soccer matches, in which songs initiated by small groups of supporters spread through the crowd, and unison is achieved in the absence of a conductor [83].

The Peng et al. [16] model for the initiation of vasomotion is compelling, but it remains to be

established that this mechanism is applicable to arteries and arterioles *in vivo*. Indeed, although synchronous elevations in global cytosolic Ca^{2+} concentration and vasomotion are readily observed in small arteries and arterioles *in vivo* (or surgically exposed vessels *in situ*), asynchronous propagating Ca^{2+} waves were only rarely detected in cremaster skeletal muscle arterioles [36, 84], femoral arteries [85, 86], and intact ear arterioles [22, 32]. The genetically encoded GCaMP2 and exMLCK fluorescent probes used to monitor cytosolic Ca^{2+} concentration by confocal microscopy in these studies were shown to be appropriate for detecting asynchronous Ca^{2+} waves in arterial segments exposed to α_1-adrenoceptor agonist *in vitro* [36]. These observations suggest that technical limitations are likely not involved. Alternatively, Mauban et al. [36] indicated that a Ca^{2+}-dependent desensitization of IP_3Rs may underlie the absence of asynchronous Ca^{2+} waves *in vivo*. An increased cytosolic Ca^{2+} concentration is expected in arterial myocytes *in vivo* due to myogenic constriction evoked by intraluminal pressure, and the influence of neurohumoral vasoconstrictors that are not present under *in vitro* isometric recording conditions [36]. This elevated cytosolic Ca^{2+} may cause desensitization of the IP_3Rs and preclude propagating Ca^{2+} waves, but have a limited impact on Ca^{2+} release due to receptor- and phospholipase C-dependent IP_3 synthesis [36]. This hypothesis needs to be tested experimentally. Alternatively, it is possible that there are multiple routes to vasomotion initiated by different mechanisms under varied physiological conditions [7, 8]. Further study is required to resolve this key issue.

12.4 Cerebral Arterial Vasomotion and Neural Activity in the Brain

A long-held, but widely debated, view holds that the physiological function of vasomotion is to increase blood flow to supply the metabolic needs of downstream parenchyma [2, 21, 87–94]. However, whether vasomotion is a physiological or pathophysiological characteristic of the vasculature remains unresolved [7, 8]. Historically, attention has focused on the peripheral vasculature due to ease of access for experimentation. Multiple studies have shown that flowmotion in cutaneous microcirculation is associated with increased tissue perfusion, greater O_2 content, and increased O_2 extraction, consistent with a physiological role [5, 7, 8, 94]. Recent analysis of the cerebral vasculature reinforces this view, indicating that vasomotion is associated with increased oxygen delivery to active regions and a direct consequence of neural activity in the brain [14]. These new findings coupled with evidence that the regulation of the cerebral vasculature and vasomotion may be impaired in situations of cognitive dysfunction such as Alzheimer's disease [95, 96] highlight the importance of understanding the physiological role(s) and regulation of vasomotion, and the differences between the peripheral and cerebral vasculature.

The high metabolic cost of neural electrical activity and lack of substantive energy reserves in the brain require that a mechanism known as neurovascular coupling mediates dynamic regulation of blood flow in response to changes in neural activity. This regulation permits precise, spatiotemporal matching of neuronal metabolic demand with the supply of O_2 and glucose, and removal of metabolic by-products [97–99]. Blood oxygen level-dependent (BOLD) functional magnetic resonance imaging (BOLD fMRI) [100, 101] and intrinsic optical signal (IOS) imaging techniques have been widely employed as a proxy for neural activity related to sensory stimulation, movement, and decision-making. A local positive BOLD signal (i.e., decreased deoxyhemoglobin) is indicative of augmented blood flow in response to an increase in neural activity. For example, sensory stimulation evokes a rapid increase in penetrating and pial arterial diameter and blood flow that is accompanied by a local increase in BOLD signal within the cortical region responsible for processing the sensory signal [31, 102].

Growing attention has recently focused on localized, spontaneous fluctuations in BOLD signals that are detected in the absence of sensory stimulation, but synchronized in functionally

related yet distant regions of the brain that are connected by long range and commissural neural pathways, for example in symmetric regions across the brain midline [103–106]. Significantly, these so-called resting-state BOLD signals occur at frequencies focused around ~0.1 Hz, matching the frequency of the oscillations in arterial diameter associated with cerebral vasomotion and flowmotion [9, 14, 31, 107, 108].

The precise neural correlate of resting-state BOLD signal fluctuations has been widely debated [104, 109–113], and the interested reader is directed to a 2016 themed issue in *Philosophical Transactions of the Royal Society B* entitled "Interpreting BOLD: a dialogue between cognitive and cellular neuroscience" [114]. However, consensus has developed around the idea that they are the result of rhythmic fluctuations in the activity of intracortical neural networks which can be detected via extracellular electrophysiological recordings of local field potentials [111, 112, 115–118]. Specifically, the resting-state BOLD signal correlates with γ-band (30–80 Hz) rhythms in the local field potential that are generated by tightly synchronized electrical activity within local networks of fast-spiking cortical interneurons [111, 112, 115–118]. For example, such γ-band activity is observed in response to increased sensory drive in the somatosensory cortex [119], and increased neural activity associated with working memory and learning [120, 121].

Direct evidence that cerebral vasomotion is entrained by oscillations in γ-band power and is responsible for resting-state BOLD signal was recently provided by Mateo and co-workers [14]. In their study, Mateo et al. [14] assessed the local field potentials generated by superficial layers of neurons within the vibrissa area of the parietal cortex in head-restrained, conscious mice fitted with a transcranial window to permit two-photon fluorescence microscopy of vasomotion in pial arterioles. Vasomotion in the arterioles was found to be phase-locked to γ-band oscillations produced by cortical neuronal activity with a lag of ~2 s, and accompanied by a positive BOLD IOS signal due to increased blood flow that followed the arteriolar dilation by ~0.7 s [14]. Significantly, the vasomotion was transhemispheric in nature, with arterioles in mirrored regions across the midline showing identical behavior that was markedly reduced in mice lacking callosal connections [14]. An optogenetic approach was further used to establish causality between the γ-band oscillations and vasomotion. Specifically, transgenic mice expressing the channelrhodopsin protein in layer 5b pyramidal neurons were stimulated with a 40 Hz γ-like train of laser light pulses with a sinusoidal variation in intensity around 0.1 Hz [14] (i.e., 0.05–0.3 Hz consistent with the frequency range of vasomotion in the preparation; [31]). Driving the cortical circuitry in this manner caused phase-locked vasomotion in pial arterioles identical to that observed during spontaneous activity [14]. Identical illumination in wild-type mice did not elicit a vasomotor response, ruling out a direct effect of the light stimulation protocol on blood flow. In contrast, mice with smooth muscle-specific expression of the light-sensitive chloride pump protein, halorhodopsin, exhibited light-driven vasomotion consisting of ~20% changes in resting arterial diameter, but with no coherent neural activity [14]. This data set demonstrates that the functional interaction is unidirectional, with the neural activity entraining vasomotion in the arterioles, but not the reverse. Significantly, the amplitude of vasodilations observed during spontaneous vasomotion and functional hyperemia in response to whisker stimulation were of similar magnitude and both were attenuated by urethane anesthesia [31], reminiscent of the sensitivity of vasomotion in other vascular beds to anesthetics [7].

To appreciate how cerebral vasomotion may be phase-locked to γ-band neural activity, it is appropriate to consider the mechanisms of neurovascular coupling, as they may foster vasomotion. Our understanding of neurovascular coupling is still evolving, but the contemporary view presented by Iadecola [99] indicates that vasomotor responses are caused by stimulus- and brain region-dependent release of vasoactive mediators, such as nitric oxide, prostaglandins, vasoactive peptides, ATP, adenosine, and/or potassium ions (K^+) from neurons and/or astrocytes, that affect membrane potential within capillary endothelial cells [122], pericytes [123], and/or nearby

smooth muscle cells in the cerebral microvasculature to evoke dilation or constriction (a decline in local O_2 or glucose content may also be involved; see [99]).

For example, evidence consistent with the potential involvement of capillary endothelial cells in sensing modest elevations in extracellular K^+ concentration due to neural activity, and communicating this vasodilatory signal to upstream arterioles was recently provided by Longden et al. [122]. The cortical capillary endothelium of mice was demonstrated to possess the Ba^{2+}-sensitive Kir2.1 subtype of inward-rectifier K^+ channel that conducts hyperpolarizing K^+ current of increased magnitude in the presence of elevated extracellular K^+ concentration (from ~4 to 8–10 mM) [122], as previously shown for endothelial cells in other vascular beds [124]. Exposing cerebral capillary endothelial cells to 10 mM external K^+ resulted in a rapid (~2 mm/s) propagating hyperpolarization and dilation in upstream arterioles in an *ex vivo* parenchymal arteriolar-capillary preparation, and increased red blood cell flux in the cortical vasculature of mice *in vivo*, that were similarly suppressed by either Ba^{2+} treatment or endothelium-specific knockout of Kir2.1 channels [122].

Hyperpolarization and vasodilation in the cerebral microvasculature in response to extracellular K^+ accumulation, prostaglandin, or nitric oxide release during neurovascular coupling [99] evoke vasodilation in upstream penetrating and pial arterioles by a mechanism of ascending, retrograde vasodilation, identical to that described for the peripheral vasculature [81, 122, 125–127]. The functional hyperemic response in the cerebral vasculature consists of: (1) a propagating electrical signal of membrane potential hyperpolarization that rapidly spreads (~2–2.5 mm/s) into upstream pial and penetrating arterioles to evoke immediate vasodilation and (2) a second, slower mechanism of ascending vasodilation involving cytosolic Ca^{2+}-dependent release of nitric oxide and prostacyclin from the endothelium in response to increased flow and shear stress due to dilation of distal terminal arterioles [102, 122, 125, 126]. Retrograde propagation of the hyperpolarization involves cell-to-cell electrical communication through the endothelium and then into smooth muscle cells via myoendothelial gap junctions to evoke vasodilation, being inhibited by focal disruption of the endothelium or suppression of endothelial Kir2.1 expression [102, 122, 126].

Retrograde, ascending propagation of hyperpolarization evoked by neurovascular coupling thus represents a likely mechanism to account for the entrainment of vasomotion by neural activity in the cerebral vasculature. Rhythmic ascending waves of hyperpolarization evoked by neurovascular coupling may serve to entrain the oscillations in membrane potential responsible for vasomotion at the level of the penetrating and pial arterioles. Periodic hyperpolarization may additionally reinforce the subsequent depolarization phase of each oscillation by favoring recovery from inactivation and increased availability of voltage-gated Ca^{2+} channels. Additionally, release of nitric oxide owing to increased shear stress could facilitate cGMP-dependent Ca^{2+}-activated chloride current and oscillatory depolarization. A role for perivascular nerves in the modulation of vasomotion may also be postulated. Further research is required to delineate the precise mechanism(s) contributing to the entrainment of vasomotion by neural activity in the brain.

As a final point, vasomotion in the peripheral vasculature is similarly affected by nerve activity, and oscillations in separate vessel segments can be entrained by bursts of sympathetic nerve activity [128, 129]. This is achieved through a prolongation of cycle length when nerve activity occurs after peak relaxation until a critical point after which cycle length is reduced [129]. However, in contrast to the role of neurovascular coupling in entrainment in the cerebral vasculature, entrainment and vasomotion in peripheral vessels are facilitated by the release of noradrenaline from adventitial sympathetic nerve varicosities. Oscillations in forearm skin blood flow at 0.1 Hz were suppressed by sympathetic blockade following anesthesia by brachial plexus infiltration in humans [128]. Suppression of sympathetic nerve activity following application of the ganglionic blocker hexamethonium was shown to inhibit synchronous oscillations in cytosolic Ca^{2+} concentration and vasomotion in rabbit ear arteri-

oles *in vivo* [22, 36]. Finally, 0.1 Hz fluctuations in cutaneous microcirculatory blood flow disappear in conditions of sympathetic dysfunction such as in diabetes [130, 131]. The contribution of rhythmic ascending vasodilation to vasomotion in peripheral vasculature is not known at present. The presence of these different mechanisms for entrainment of vasomotion in cerebral and peripheral vasculature illustrates the challenge in developing a comprehensive understanding of vasomotion and its regulation in varied vascular beds.

12.5 Summary

Despite more than 150 years of research, there are many questions concerning vasomotion that remain to be adequately addressed. Key issues for future study should include (1) identification of the inward current activated by the IP_3R-dependent release of Ca^{2+} stores: Specifically, is the contribution of cGMP-dependent, Ca^{2+}-activated Cl^- channels ubiquitous or restricted to mesenteric arteries, and what is the role of nonselective cation channels? (2) Why does the contribution of the endothelium to vasomotion vary in a vessel-specific manner? (3) What is the mechanism by which vasomotion in cerebral pial and penetrating arterioles is entrained to cortical neural activity: specifically, is this process dependent on rhythmic hyperpolarization associated with ascending vasodilation and Kir2.1 channels in the cerebrovascular endothelium and capillaries? (4) If asynchronous Ca^{2+} waves are not involved in synchronization of contractile activity in individual myocytes *in vivo*, what is the mechanism responsible for the self-organizing behavior? (5) Does entrainment of vasomotion in peripheral and cerebral vasculature involve a differential contribution of neural- versus endothelium-dependent mechanisms of modulation, respectively? Novel understanding in these areas will undoubtedly be facilitated by technological advancements permitting *in vivo* imaging of arterial diameter and cytosolic Ca^{2+} concentration, as well as cell type-specific expression of functional and genetically compromised proteins to selectively augment and disrupt cellular processes postulated to contribute to vasomotion and its regulation in health and disease.

Acknowledgements The authors thank Drs. HL Zhu and XZ Zhong for the original recordings of vasomotion presented in Fig. 12.1. The work is supported by a research operating grant from the Canadian Institutes of Health Research (PJT-155963).

References

1. Jones TW. Discovery that veins of the bat's wing (which are furnished with valves) are endowed with rhythmical contractility and that the onward flow of blood is accelerated by each contraction. Philos Trans R Soc Lond. 1852;142:131–6.
2. Funk W, Intaglietta M. Spontaneous arteriolar vasomotion. Prog Appl Microcirc. 1983;3:66–82.
3. Shimamura K, Sekiguchi F, Sunano S. Tension oscillation in arteries and its abnormality in hypertensive animals. Clin Exp Pharmacol Physiol. 1999;26:275–84.
4. Nilsson H, Aalkjaer C. Vasomotion: mechanisms and physiological importance. Mol Interv. 2003;3:79–89.
5. Aalkjaer C, Nilsson H. Vasomotion: cellular background for the oscillator and for the synchronization of smooth muscle cells. Br J Pharmacol. 2005;144:605–16.
6. Haddock RE, Hill CE. Rhythmicity in arterial smooth muscle. J Physiol. 2005;566:645–56.
7. Aalkjaer C, Boedtkjer D, Matchkov V. Vasomotion—what is currently thought? Acta Physiol (Oxford). 2011;202:253–69.
8. Matchkov VV. Mechanisms of cellular synchronization in the vascular wall. Mechanisms of vasomotion. Dan Med Bull. 2010;57:B4191.
9. Intaglietta M. Vasomotion and flowmotion: physiological mechanisms and clinical evidence. Vasc Med Rev. 1990;1:101–12.
10. Schmidt JA. Periodic hemodynamics in health and disease. Georgetown, TX: R.G. Landes Company; 1996.
11. Kvandal P, Landsverk SA, Bernjak A, Stefanovska A, Kvernmo HD, Kirkebøen KA. Low-frequency oscillations of the laser Doppler perfusion signal in human skin. Microvasc Res. 2006;72:120–7.
12. Stefanovska A. Coupled oscillators. Complex but not complicated cardiovascular and brain interactions. IEEE Eng Med Biol Mag. 2007;26:25–9.
13. Gokina NI, Bevan RD, Walters CL, Bevan JA. Electrical activity underlying rhythmic contraction in human pial arteries. Circ Res. 1996;78:148–53.
14. Mateo C, Knutsen PM, Tsai PS, Shih AY, Kleinfeld D. Entrainment of arteriole vasomotor fluctuations

by neural activity is a basis of blood-oxygenation-level-dependent "resting-state" connectivity. Neuron. 2017;96:936–48.
15. Mauban JR, Lamont C, Balke CW, Wier WG. Adrenergic stimulation of rat resistance arteries affects Ca^{2+} sparks, Ca^{2+} waves, and Ca^{2+} oscillations. Am J Physiol Heart Circ Physiol. 2001;280:H2399–405.
16. Peng H, Matchkov V, Ivarsen A, Aalkjaer C, Nilsson H. Hypothesis for the initiation of vasomotion. Circ Res. 2001;88:810–5.
17. Oishi H, Schuster A, Lamboley M, Stergiopulos N, Meister JJ, Bény JL. Role of membrane potential in vasomotion of isolated pressurized rat arteries. Life Sci. 2002;71:2239–48.
18. Zacharia J, Zhang J, Wier WG. Ca^{2+} signaling in mouse mesenteric small arteries: myogenic tone and adrenergic vasoconstriction. Am J Physiol Heart Circ Physiol. 2007;292(3):H1523–32.
19. Haddock RE, Hirst GD, Hill CE. Voltage independence of vasomotion in isolated irideal arterioles of the rat. J Physiol. 2002;540:219–29.
20. Bakker EN, Sorop O, Spaan JA, VanBavel E. Remodeling of resistance arteries in organoid culture is modulated by pressure and pressure pulsation and depends on vasomotion. Am J Physiol Heart Circ Physiol. 2004;286:H2052–6.
21. Colantuoni A, Bertuglia S, Intaglietta M. Quantitation of rhythmic diameter changes in arterial microcirculation. Am J Phys. 1984;246:H508–17.
22. Fairfax ST, Mauban JR, Hao S, Rizzo MA, Zhang J, Wier WG. Ca^{2+} signaling in arterioles and small arteries of conscious, restrained, optical biosensor mice. Front Physiol. 2014;5:387.
23. Griffith TM, Edwards DH. Mechanisms underlying chaotic vasomotion in isolated resistance arteries: roles of calcium and EDRF. Biorheology. 1993;30:333–47.
24. Griffith TM, Edwards DH. Ca^{2+} sequestration as a determinant of chaos and mixed-mode dynamics in agonist-induced vasomotion. Am J Phys. 1997;272:H1696–709.
25. Colantuoni A, Bertuglia S, Intaglietta M. Variations of rhythmic diameter changes at the arterial micro-vascular bifurcations. Pflugers Arch. 1985;403:289–95.
26. Oude Vrielink HHE, Slaaf DW, Tangelder GJ, Weijmer-Van Velzen S, Reneman RR. Analysis of vasomotion waveform changes during pressure reduction and adenosine application. Am J Phys. 1990;258:H29–37.
27. Gustafsson H. Vasomotion and underlying mechanisms in small arteries. An *in vitro* study of rat blood vessels. Acta Physiol Scand. 1993;149(Suppl. 614):1–44.
28. Nyvad J, Mazur A, Postnov DD, Straarup MS, Soendergaard AM, Staehr C, Brøndum E, Aalkjaer C, Matchkov VV. Intravital investigation of rat mesenteric small artery tone and blood flow. J Physiol. 2017;595:5037–53.
29. Burrows ME, Johnson PC. Diameter, wall tension, and flow in mesenteric arterioles during autoregulation. Am J Phys. 1981;241:H829–37.
30. Hundley WG, Renaldo GJ, Levasseur JE, Kontos HA. Vasomotion in cerebral microcirculation of awake rabbits. Am J Phys. 1988;254:H67–71.
31. Drew PJ, Shih AY, Kleinfeld D. Fluctuating and sensory-induced vasodynamics in rodent cortex extend arteriole capacity. Proc Natl Acad Sci U S A. 2011;108:8473–8.
32. Mauban JR, Fairfax ST, Rizzo MA, Zhang J, Wier WG. A method for noninvasive longitudinal measurements of $[Ca^{2+}]$ in arterioles of hypertensive optical biosensor mice. Am J Physiol Heart Circ Physiol. 2014;307:H173–81.
33. Matchkov VV, Larsen P, Bouzinova EV, Rojek A, Boedtkjer DM, Golubinskaya V, Pedersen FS, Aalkjaer C, Nilsson H. Bestrophin-3 (vitelliform macular dystrophy 2-like 3 protein) is essential for the cGMP-dependent calcium-activated chloride conductance in vascular smooth muscle cells. Circ Res. 2008;103:864–72.
34. Broegger T, Jacobsen JC, Secher Dam V, Boedtkjer DM, Kold-Petersen H, Pedersen FS, Aalkjaer C, Matchkov VV. Bestrophin is important for the rhythmic but not the tonic contraction in rat mesenteric small arteries. Cardiovasc Res. 2011;91:685–93.
35. Dam VS, Boedtkjer DM, Nyvad J, Aalkjaer C, Matchkov V. TMEM16A knockdown abrogates two different Ca^{2+}-activated Cl^- currents and contractility of smooth muscle in rat mesenteric small arteries. Pflugers Arch. 2014;466:1391–409.
36. Mauban JR, Zacharia J, Zhang J, Wier WG. Vascular tone and Ca^{2+} signaling in murine cremaster muscle arterioles *in vivo*. Microcirculation. 2013;220: 269–77.
37. Westcott EB, Segal SS. Perivascular innervation: a multiplicity of roles in vasomotor control and myoendothelial signaling. Microcirculation. 2013;20:217–38.
38. Haddock RE, Grayson TH, Brackenbury TD, Meaney KR, Neylon CB, Sandow SL, Hill CE. Endothelial coordination of cerebral vasomotion via myoendothelial gap junctions containing connexins 37 and 40. Am J Physiol Heart Circ Physiol. 2006;291:H2047–56.
39. Sandow SL, Senadheera S, Bertrand PP, Murphy TV, Tare M. Myoendothelial contacts, gap junctions, and microdomains: anatomical links to function? Microcirculation. 2012;19:403–15.
40. de Wit C, Griffith TM. Connexins and gap junctions in the EDHF phenomenon and conducted vasomotor responses. Pflugers Arch. 2010;459:897–914.
41. Chaytor AT, Evans WH, Griffith TM. Peptides homologous to extracellular loop motifs of connexin 43 reversibly abolish rhythmic contractile activity in rabbit arteries. J Physiol. 1997;503:99–110.
42. de Wit C, Roos F, Bolz SS, Pohl U. Lack of vascular connexin 40 is associated with hypertension and irregular arteriolar vasomotion. Physiol Genomics. 2003;13:169–77.

43. Tsai ML, Watts SW, Loch-Caruso R, Webb RC. The role of gap junctional communication in contractile oscillations in arteries from normotensive and hypertensive rats. J Hypertens. 1995;13:1123–33.
44. Matchkov VV, Rahman A, Peng H, Nilsson H, Aalkjaer C. Junctional and nonjunctional effects of heptanol and glycyrrhetinic acid derivates in rat mesenteric small arteries. Br J Pharmacol. 2004;142:961–72.
45. Imtiaz MS, von der Weid PY, van Helden DF. Synchronization of Ca^{2+} oscillations: a coupled oscillator-based mechanism in smooth muscle. FEBS J. 2010;277:278–85.
46. Berridge MJ. Smooth muscle cell calcium activation mechanisms. J Physiol. 2008;586:5047–61.
47. Hill-Eubanks DC, Werner ME, Heppner TJ, Nelson MT. Calcium signaling in smooth muscle. Cold Spring Harb Perspect Biol. 2011;3:a004549.
48. Missiaen L, Taylor CW, Berridge MJ. Luminal Ca^{2+} promoting spontaneous Ca^{2+} release from inositol trisphosphate-sensitive stores in rat hepatocytes. J Physiol. 1992;455:623–40.
49. Mulvany MJ, Nilsson H, Flatman JA. Role of membrane potential in the response of rat small mesenteric arteries to exogenous noradrenaline stimulation. J Physiol. 1982;332:363–73.
50. Segal SS, Beny JL. Intracellular recording and dye transfer in arterioles during blood flow control. Am J Phys. 1992;263:H1–7.
51. von der Weid PY, Bény JL. Simultaneous oscillations in the membrane potential of pig coronary artery endothelial and smooth muscle cells. J Physiol. 1993;471:13–24.
52. Bartlett IS, Crane GJ, Neild TO, Segal SS. Electrophysiological basis of arteriolar vasomotion *in vivo*. J Vasc Res. 2000;37:568–75.
53. Haddock RE, Hill CE. Differential activation of ion channels by inositol 1,4,5-trisphosphate IP_3- and ryanodine-sensitive calcium stores in rat basilar artery vasomotion. J Physiol. 2002;545:615–27.
54. Hill CE, Eade J, Sandow SL. Mechanisms underlying spontaneous rhythmical contractions in irideal arterioles of the rat. J Physiol. 1999;521:507–16.
55. Bouskela E, Grampp W. Spontaneous vasomotion in hamster cheek pouch arterioles in varying experimental conditions. Am J Phys. 1992;262:H478–85.
56. Isotani E, Zhi G, Lau KS, Huang J, Mizuno Y, Persechini A, Geguchadze R, Kamm KE, Stull JT. Real-time evaluation of myosin light chain kinase activation in smooth muscle tissues from a transgenic calmodulin-biosensor mouse. Proc Natl Acad Sci U S A. 2004;101:6279–84.
57. Ding HL, Ryder JW, Stull JT, Kamm KE. Signaling processes for initiating smooth muscle contraction upon neural stimulation. J Biol Chem. 2009;284:15541–8.
58. Gustafsson H, Nilsson H. 1993. Rhythmic contractions of isolated small arteries from rat: role of calcium. Acta Physiol Scand. 1993;149:283–91.
59. Gustafsson H, Mulvany MJ, Nilsson H. Rhythmic contractions of isolated small arteries from rat: influence of the endothelium. Acta Physiol Scand. 1993;143:153–63.
60. Lamont C, Wier WG. Different roles of ryanodine receptors and inositol (1,4,5)-trisphosphate receptors in adrenergically stimulated contractions of small arteries. Am J Physiol Heart Circ Physiol. 2004;287:H617–25.
61. Rahman A, Hughes A, Matchkov V, Nilsson H, Aalkjaer C. Antiphase oscillations of endothelium and smooth muscle $[Ca^{2+}]i$ in vasomotion of rat mesenteric small arteries. Cell Calcium. 2007;42: 536–47.
62. Omote M, Mizusawa H. The role of sarcoplasmic reticulum in endothelium-dependent and endothelium-independent rhythmic contractions in the rabbit mesenteric artery. Acta Physiol Scand. 1993;149:15–21.
63. Westcott EB, Jackson WF. Heterogeneous function of ryanodine receptors, but not IP3 receptors, in hamster cremaster muscle feed arteries and arterioles. Am J Physiol Heart Circ Physiol. 2011;300:H1616–30.
64. Westcott EB, Goodwin EL, Segal SS, Jackson WF. Function and expression of ryanodine receptors and inositol 1,4,5-trisphosphate receptors in smooth muscle cells of murine feed arteries and arterioles. J Physiol. 2012;590:1849–69.
65. Matchkov VV, Aalkjaer C, Nilsson H. A cyclic GMP-dependent calcium-activated chloride current in smooth-muscle cells from rat mesenteric resistance arteries. J Gen Physiol. 2004;123:121–34.
66. Manoury B, Tamuleviciute A, Tammaro P. TMEM16A/anoctamin 1 protein mediates calcium-activated chloride currents in pulmonary arterial smooth muscle cells. J Physiol. 2010;588:2305–14.
67. Thomas-Gatewood C, Neeb ZP, Bulley S, Adebiyi A, Bannister JP, Leo MD, Jaggar JH. TMEM16A channels generate Ca^{2+}-activated Cl^- currents in cerebral artery smooth muscle cells. Am J Phys. 2011;301:H1819–27.
68. Adebiyi A, Zhao G, Narayanan D, Thomas-Gatewood CM, Bannister JP, Jaggar JH. Isoform-selective physical coupling of TRPC3 channels to IP3 receptors in smooth muscle cells regulates arterial contractility. Circ Res. 2010;106:1603–12.
69. Gonzales AL, Amberg GC, Earley S. Ca^{2+} release from the sarcoplasmic reticulum is required for sustained TRPM4 activity in cerebral artery smooth muscle cells. Am J Phys Cell Phys. 2010;299:C279–88.
70. Gonzales AL, Yang Y, Sullivan MN, Sanders L, Dabertrand F, Hill-Eubanks DC, Nelson MT, Earley S. A PLCγ1-dependent, force-sensitive signaling network in the myogenic constriction of cerebral arteries. Sci Signal. 2014;7:ra49.
71. Chen X, Yang D, Ma S, He H, Luo Z, Feng X, Cao T, Ma L, Yan Z, Liu D, Tepel M, Zhu Z. Increased rhythmicity in hypertensive arterial smooth muscle is linked to transient receptor potential canonical channels. J Cell Mol Med. 2010;14:2483–94.
72. Jackson WF. Oscillations in active tension in hamster aortas: role of the endothelium. Blood Vessels. 1988;25:144–56.

73. Mauban JR, Wier WG. Essential role of EDHF in the initiation and maintenance of adrenergic vasomotion in rat mesenteric arteries. Am J Physiol Heart Circ Physiol. 2004;287:H608–16.
74. Rahman A, Matchkov V, Nilsson H, Aalkjaer C. Effects of cGMP on coordination of vascular smooth muscle cells of rat mesenteric small arteries. J Vasc Res. 2005;42:301–11.
75. Dirnagl U, Lindauer U, Villringer A. Nitric oxide synthase blockade enhances vasomotion in the cerebral microcirculation of anesthetized rats. Microvasc Res. 1993;45:318–23.
76. Bertuglia S, Colantuoni A, Intaglietta M. Capillary reperfusion after L-arginine, L-NMMA, and L-NNA treatment in cheek pouch microvasculature. Microvasc Res. 1995;50:162–74.
77. Jackson WF, Mulsch A, Busse R. Rhythmic smooth muscle activity in hamster aortas is mediated by continuous release of NO from the endothelium. Am J Phys. 1991;260:H248–53.
78. Yamamoto Y, Klemm MF, Edwards FR, Suzuki H. Intercellular electrical communication among smooth muscle and endothelial cells in guinea-pig mesenteric arterioles. J Physiol. 2001;535:181–95.
79. Jacobsen JC, Aalkjaer C, Matchkov VV, Nilsson H, Freiberg JJ, Holstein-Rathlou NH. Heterogeneity and weak coupling may explain the synchronization characteristics of cells in the arterial wall. Philos Trans A Math Phys Eng Sci. 2008;366:3483–502.
80. Ledoux J, Taylor MS, Bonev AD, Hannah RM, Solodushko V, Shui B, Tallini Y, Kotlikoff MI, Nelson MT. Functional architecture of inositol 1,4,5-trisphosphate signaling in restricted spaces of myoendothelial projections. Proc Natl Acad Sci U S A. 2008;105:9627–32.
81. Segal SS. Integration and modulation of intercellular signaling underlying blood flow control. J Vasc Res. 2015;52:136–57.
82. Zang WJ, Balke CW, Wier WG. Graded α1-adrenoceptor activation of arteries involves recruitment of smooth muscle cells to produce 'all or none' Ca^{2+} signals. Cell Calcium. 2001;29:327–34.
83. Smith R, Imtiaz M, Banney D, Paul JW, Young RC. Why the heart is like an orchestra and the uterus is like a soccer crowd. Am J Obstet Gynecol. 2015;213:181–5.
84. Zhang J, Chen L, Raina H, Blaustein MP, Wier WG. *In vivo* assessment of artery smooth muscle $[Ca^{2+}]$ i and MLCK activation in FRET-based biosensor mice. Am J Physiol Heart Circ Physiol. 2010;299:H946–56.
85. Wang Y, Chen L, Wier WG, Zhang J. Intravital Förster resonance energy transfer imaging reveals elevated $[Ca^{2+}]$i and enhanced sympathetic tone in femoral arteries of angiotensin II-infused hypertensive biosensor mice. J Physiol. 2013;591:5321–36.
86. Zacharia J, Mauban JR, Raina H, Fisher SA, Wier WG. High vascular tone of mouse femoral arteries *in vivo* is determined by sympathetic nerve activity via alpha1A- and alpha1D-adrenoceptor subtypes. PLoS One. 2013;8:e65969.
87. Funk W, Endrich B, Messmer K, Intaglietta M. Spontaneous arteriolar vasomotion as a determinant of peripheral vascular resistance. Int J Microcirc Clin Exp. 1983;2:11–25.
88. Bertuglia S, Colantuoni A, Coppini G, Intaglietta M. Hypoxia- or hyperoxia-induced changes in arteriolar vasomotion in skeletal muscle microcirculation. Am J Phys. 1991;260:H362–72.
89. Tsai AG, Intaglietta M. Evidence of flowmotion induced changes in local tissue oxygenation. Int J Microcirc Clin Exp. 1993;12:75–88.
90. Parthimos D, Edwards DH, Griffith TM. Comparison of chaotic and sinusoidal vasomotion in the regulation of microvascular flow. Cardiovasc Res. 1996;31:388–99.
91. Gratton RJ, Gandley RE, McCarthy JF, Michaluk WK, Slinker BK, McLaughlin MK. Contribution of vasomotion to vascular resistance: a comparison of arteries from virgin and pregnant rats. J Appl Physiol. 1998;85:2255–60.
92. Rücker M, Strobel O, Vollmar B, Roesken F, Menger MD. Vasomotion in critically perfused muscle protects adjacent tissues from capillary perfusion failure. J Physiol Heart Circ Physiol. 2000;279:H550–8.
93. Meyer C, de Vries G, Davidge ST, Mayes DC. Reassessing the mathematical modeling of the contribution of vasomotion to vascular resistance. J Appl Physiol. 2002;92:888–9.
94. Thorn CE, Kyte H, Slaff DW, Shore AC. An association between vasomotion and oxygen extraction. Am J Physiol Heart Circ Physiol. 2011;301:H442–9.
95. Di Marco LY, Farkas E, Martin C, Venneri A, Frangi AF. Is vasomotion in cerebral arteries impaired in Alzheimer's disease? J Alzheimers Dis. 2015;46:35–53.
96. Tarantini S, Tran CHT, Gordon GR, Ungvari Z, Csiszar A. Impaired neurovascular coupling in aging and Alzheimer's disease: contribution of astrocyte dysfunction and endothelial impairment to cognitive decline. Exp Gerontol. 2017;94:52–8.
97. Iadecola C, Nedergaard M. Glial regulation of the cerebral microvasculature. Nat Neurosci. 2007;10:1369–76.
98. Lecrux C, Hamel E. The neurovascular unit in brain function and disease. Acta Physiol (Oxford). 2011;203:47–59.
99. Iadecola C. The neurovascular unit coming of age: a journey through neurovascular coupling in health and disease. Neuron. 2017;96:17–42.
100. Ogawa S, Lee TM, Nayak AS, Glynn P. Oxygenation-sensitive contrast in magnetic resonance image of rodent brain at high magnetic fields. Magn Reson Med. 1990;14:68–78.
101. Ogawa S, Lee TM, Kay AR, Tank DW. Brain magnetic resonance imaging with contrast dependent on blood oxygenation. Proc Natl Acad Sci U S A. 1990;87:9868–72.
102. Chen BR, Bouchard MB, McCaslin AF, Burgess SA, Hillman EM. High-speed vascular dynamics of the hemodynamic response. NeuroImage. 2011;54:1021–30.

103. Nir Y, Hasson U, Levy I, Yeshurun Y, Malach R. Widespread functional connectivity and fMRI fluctuations in human visual cortex in the absence of visual stimulation. NeuroImage. 2006;30:1313–24.
104. Fox MD, Raichle ME. Spontaneous fluctuations in brain activity observed with functional magnetic resonance imaging. Nat Rev Neurosci. 2007;8:700–11.
105. Bruyns-Haylett M, Harris S, Boorman L, Zheng Y, Berwick J, Jones M. The resting-state neurovascular coupling relationship: rapid changes in spontaneous neural activity in the somatosensory cortex are associated with haemodynamic fluctuations that resemble stimulus-evoked haemodynamics. Eur J Neurosci. 2013;38:2902–16.
106. Liu TT. Neurovascular factors in resting-state functional MRI. NeuroImage. 2013;80:339–48.
107. Mayhew JEW, Askew S, Zheng Y, Porrill J, Westby GWM, Redgrave P, Rector DM, Harper RM. Cerebral vasomotion: a 0.1-Hz oscillation in reflected light imaging of neural activity. NeuroImage. 1996;4:183–93.
108. Obrig H, Neufang M, Wenzel R, Kohl M, Steinbrink J, Einhäupl K, Villringer A. Spontaneous low frequency oscillations of cerebral hemodynamics and metabolism in human adults. NeuroImage. 2000;12:623–39.
109. Logothetis NK. The neural basis of the blood-oxygen-level-dependent functional magnetic resonance imaging signal. Philos Trans R Soc Lond B. 2002;357:1003–37.
110. Logothetis NK. The underpinnings of the BOLD functional magnetic resonance imaging signal. J Neurosci. 2003;23:3963–71.
111. Logothetis NK. What we can do and what we cannot do with fMRI. Nature. 2008;453:869–78.
112. Lauritzen M. Reading vascular changes in brain imaging: is dendritic calcium the key? Nat Rev Neurosci. 2005;6:77–85.
113. Devor A, Sakadžić S, Srinivasan VJ, Yaseen MA, Nizar K, Saisan PA, Tian P, Dale AM, Vinogradov SA, Franceschini MA, Boas DA. Frontiers in optical imaging of cerebral blood flow and metabolism. J Cereb Blood Flow Metab. 2012;32:1259–76.
114. Mishra A, Kurth-Nelson Z, Hall C, Howarth C. Interpreting BOLD: a dialogue between cognitive and cellular neuroscience. Theo Murphy Meeting Themed Issue. Philos Trans R Soc B. 2016;371(1705):20150348–61.
115. Logothetis NK, Pauls J, Augath M, Trinath T, Oeltermann A. Neurophysiological investigation of the basis of the fMRI signal. Nature. 2001;412:150–7.
116. Niessing J, Ebisch B, Schmidt KE, Niessing M, Singer W, Galuske RA. Hemodynamic signals correlate tightly with synchronized gamma oscillations. Science. 2005;309:948–51.
117. Nir Y, Mukamel R, Dinstein I, Privman E, Harel M, Fisch L, Gelbard-Sagiv H, Kipervasser S, Andelman F, Neufeld MY, Kramer U, Arieli A, Fried I, Malach R. Interhemispheric correlations of slow spontaneous neuronal fluctuations revealed in human sensory cortex. Nat Neurosci. 2008;11:1100–8.
118. He BJ, Raichle ME. The fMRI signal, slow cortical potential and consciousness. Trends Cogn Sci. 2009;13:302–9.
119. Henrie JA, Shapley R. LFP power spectra in V1 cortex: the graded effect of stimulus contrast. J Neurophysiol. 2005;94:479–90.
120. Pesaran B, Pezaris JS, Sahani M, Mitra PP, Andersen RA. Temporal structure in neuronal activity during working memory in macaque parietal cortex. Nat Neurosci. 2002;5:805–11.
121. Bauer EP, Paz R, Paré D. Gamma oscillations coordinate amygdalo-rhinal interactions during learning. J Neurosci. 2007;27:9369–79.
122. Longden T, Dabertrand F, Koide M, Gonzales AL, Tykocki NR, Brayden JE, Hill-Eubanks D, Nelson MT. Capillary K+-sensing initiates retrograde hyperpolarization to increase local cerebral blood flow. Nat Neurosci. 2017;20:717–26.
123. Hall CN, Reynell C, Gesslein B, Hamilton NB, Mishra A, Sutherland BA, O'Farrell FM, Buchan AM, Lauritzen M, Attwell D. Capillary pericytes regulate cerebral blood flow in health and disease. Nature. 2014;508:55–60.
124. Jackson WF. Boosting the signal: Endothelial inward rectifier K^+ channels. Microcirculation. 2017;24:e12319.
125. Tallini YN, Brekke JF, Shui B, Doran R, Hwang SM, Nakai J, Salama G, Segal SS, Kotlikoff MI. Propagated endothelial Ca^{2+} waves and arteriolar dilation *in vivo*: measurements in Cx40BAC–GCaMP2 transgenic mice. Circ Res. 2007;101:1300–9.
126. Chen BR, Kozberg MG, Bouchard MB, Shaik MA, Hillman EMC. A critical role of the vascular endothelium in functional neurovascular coupling in the brain. J Am Heart Assoc. 2014;3:e000787.
127. Sinkler SY, Segal SS. Rapid versus slow ascending vasodilatation: intercellular conduction versus flow-mediated signalling with tetanic versus rhythmic muscle contractions. J Physiol. 2017;595:7149–65.
128. Bernardi L, Rossi M, Fratino P, Finardi G, Mevio E, Orlandi C. Relationship between phasic changes in human skin blood flow and autonomic tone. Microvasc Res. 1989;37:16–27.
129. Borovik A, Golubinskaya V, Tarasova O, Aalkjaer C, Nilsson H. Phase resetting of arterial vasomotion by burst stimulation of perivascular nerves. J Vasc Res. 2005;42:165–73.
130. Bernardi L, Rossi M, Leuzzi S, Mevio E, Fornasari G, Calciati A, Orlandi C, Fratino P. Reduction of 0.1 Hz microcirculatory fluctuations as evidence of sympathetic dysfunction in insulin-dependent diabetes. Cardiovasc Res. 1997;34:185–91.
131. Meyer MF, Rose CJ, Hülsmann JO, Schatz H, Pfohl M. Impaired 0.1-Hz vasomotion assessed by laser Doppler anemometry as an early index of peripheral sympathetic neuropathy in diabetes. Microvasc Res. 2003;65:88–95.

Venous Vasomotion

13

Dirk F. van Helden and Mohammad S. Imtiaz

Abstract

Veins exhibit spontaneous contractile activity, a phenomenon generally termed *vasomotion*. This is mediated by spontaneous rhythmical contractions of mural cells (i.e. smooth muscle cells (SMCs) or pericytes) in the wall of the vessel. Vasomotion occurs through interconnected oscillators within and between mural cells, entraining their cycles. Pharmacological studies indicate that a key oscillator underlying vasomotion is the rhythmical calcium ion (Ca^{2+}) release-refill cycle of Ca^{2+} stores. This occurs through opening of inositol 1,4,5-trisphosphate receptor (IP_3R)- and/or ryanodine receptor (RyR)-operated Ca^{2+} release channels in the sarcoplasmic/endoplasmic (SR/ER) reticulum and refilling by the SR/ER reticulum Ca^{2+}ATPase (SERCA). Released Ca^{2+} from stores near the plasma membrane diffuse through the cytosol to open Ca^{2+}-activated chloride (Cl^-) channels, this generating inward current through an efflux of Cl^-. The resultant depolarisation leads to the opening of voltage-dependent Ca^{2+} channels and possibly increased production of IP_3, which through Ca^{2+}-induced Ca^{2+} release (CICR) of IP_3Rs and/or RyRs and IP_3R-mediated Ca^{2+} release provide a means by which store oscillators entrain their activity. Intercellular entrainment normally involves current flow through gap junctions that interconnect mural cells and in many cases this is aided by additional connectivity through the endothelium. Once entrainment has occurred the substantial Ca^{2+} entry that results from the near-synchronous depolarisations leads to rhythmical contractions of the mural cells, this often leading to vessel constriction. The basis for venous/venular vasomotion has yet to be fully delineated but could improve both venous drainage and capillary/venular absorption of blood plasma-associated fluids.

Keywords

Veins · Smooth muscle · Vasomotion · Cellular rhythms · Coupled oscillator-based entrainment · Ca^{2+} stores · Inositol 1,4,5-trisphosphate receptors · Ryanodine receptors · Cardiac muscle · Pericytes

D. F. van Helden (✉)
Faculty of Health and Medicine,
School of Biomedical Sciences and Pharmacy,
University of Newcastle, Newcastle, NSW, Australia
e-mail: dirk.vanhelden@newcastle.edu.au

M. S. Imtiaz
Department of Electrical and Computer Engineering,
Bradley University, Peoria, IL, USA
e-mail: mimtiaz@fsmail.bradley.edu

H. Hashitani, R. J. Lang (eds.), *Smooth Muscle Spontaneous Activity*, Advances in Experimental Medicine and Biology 1124, https://doi.org/10.1007/978-981-13-5895-1_13

13.1 Introduction

Veins, arteries and arterioles unlike most venules and all capillaries have an inner, middle and outer layer termed the *tunica intima*, *tunica media* and *tunica adventitia*, respectively [1]. The *tunica intima* is primarily composed of endothelial cells (ECs). The *tunica media* is comprised of smooth muscle cells (SMCs), which controls vessel diameter, and elastic fibres though there are fewer elastic fibres in veins. The *tunica adventitia* is primarily composed of connective tissue and in veins and venules provides the majority of the wall thickness [1]. Nerves while generally sparse also course through this layer to innervate the SMCs. ECs and SMCs form separate syncytia through EC-EC and SMC-SMC gap junctions. These intercellular channels are comprised of proteins termed connexins (Cxs) of which there are three primary types in blood vessels: Cx37, Cx40 and Cx43, though the distribution of these is variable within the EC and SM layers of vessels and between species [2–5]. In some vessels there are myoendothelial gap junctions that bridge between the endothelium and smooth muscle (SM) [6]. With the exception of peripheral capillaries, blood and lymphatic vessels can constrict, arising from the contraction of SMCs in the vessel walls. Exceptions to this include small vessels (e.g. precapillary arterioles and venules) where constriction can be mediated by pericytes [7] and vessels entering the heart, where constriction can be mediated by cardiomyocytes that line the vessel walls [8, 9].

The phenomenon referred to as vasomotion, namely spontaneous rhythmical constrictions of blood and lymphatic vessels, has long been recognised, first being reported for lymphatic vessels by W. Hewson in 1764 (see [10, 11]). Vasomotion was subsequently reported for cardiac muscle-associated contractions of veins that enter the heart (J.J. Allison, 1839—see [8]), this being followed by rhythmical SMC-mediated constrictions of bat wing veins [12]. Jones described the phenomenon as follows: "*I had not observed the circulation under the microscope long, before I was struck by something peculiar in the flow of blood in the veins; I therefore directed my attention to them, and discovered that they contracted and dilated rhythmically Following the veins for some extent in their course, I further discovered them to be provided with valves, some of which completely opposed regurgitation of blood, others only partially …. I was able to make out exactly its mode of operation. The act of contraction of the vein is manifested by progressive constriction of its calibre and increasing thickness of its wall; the relaxation of the vessel, by a return to the former width of calibre and thickness of wall … the average number of contractions in a minute, I have found to be ten … The supervening dilatations take place rather more quickly than the contractions … I have sometimes estimated [relative constriction] at nearly a third, sometimes at not more than a sixth*" (reproduced with permission [11]).

The physiological role for vasomotion may serve very different purposes depending on the vessel. The most obvious is in lymphatics where vasomotion compresses single or multiple lymphatic chambers, each formed by regularly occurring unidirectional valves providing a means for the intrinsic propulsion of lymph (Fig. 13.1) [13–15]. As many veins also have

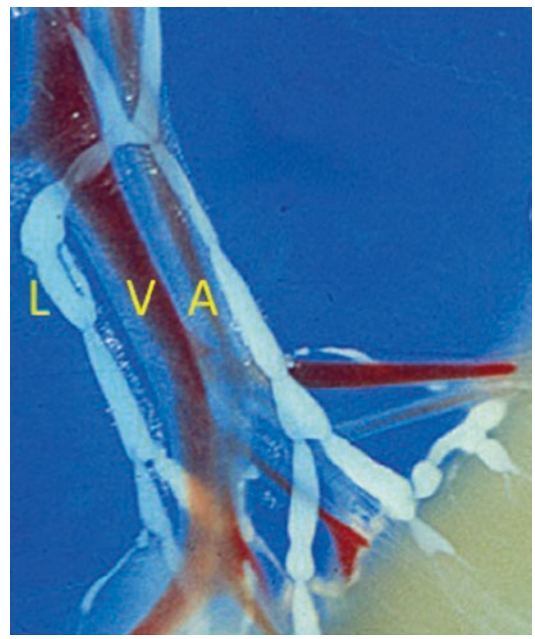

Fig. 13.1 Vein (V), artery (A) and lymphatic (L) vessels in the guinea pig mesentery. Diameter of the vein near label is ~350 μm

valves [16] including those of bat wings [11], venous vasomotion will improve venous return. However, independent of the presence of valves, vasomotion should also reduce the possibility of blood stasis and resultant coagulation.

13.2 Pacemaking

The existence of vasomotion in a large array of vessels depends on a pacemaker mechanism that times and triggers contractions by rhythmically depolarising the effector cells to cause transmembrane entry of Ca^{2+} through the opening of voltage-dependent Ca^{2+} channels and contraction. This process has and continues to provide a fertile area of research, as mechanisms and the effector cells involved differ. Thus, while venous vasomotion in the bat wing [12] and many other veins including the portal and mesenteric vein of various species [8, 17–20] exhibit vasomotion caused by contraction of SMCs, veins near the region of attachment to the heart have cardiac muscle in their walls and can constrict at heart rate (see [21]). In contrast venules generally exhibit vasomotion through contraction of pericytes [7, 22–24].

It has long been known that vasomotion is not neurally generated, as the constrictions persist in the presence of nerve blockade and hence are considered to be myogenic [20, 25]. While not generated by nerve activity, the strength and frequency of contractions in the portal vein are enhanced by stimulation of sympathetic nerves or by exogenous activation of alpha-adrenoceptors [20]. Stretch can also increase the frequency of vasomotion [20]. Studies on isolated guinea pig mesenteric veins, where SMC membrane potential rather than contraction force was measured demonstrated that sympathetic nerve stimulation (20 stimuli at 20 Hz) had the initial effect of generating a biphasic depolarising response [26]. However, in freshly dissected tissues ($\lesssim$2 h post-isolation), such stimulation could at times initiate rhythmical depolarisations that gradually increase in frequency and size and last up to 20 min. This activity was myogenic as it persisted after nerve blockade with tetrodotoxin or upon blockade of alpha-adrenoceptors by phentolamine. Application of noradrenaline caused a maintained depolarisation with superimposed rhythmic depolarisations the author termed "slow waves".

Electrically short segments of guinea pig mesenteric vein, where the SM syncytium is effectively isopotential and hence can be voltage clamped, allow the investigation of spontaneous activity in this muscle. Events termed spontaneous transient depolarisations (STDs) and underlying spontaneous transient inward currents (STICs) were recorded. These were proposed to occur through the regenerative opening of Ca^{2+} release channels in intracellular sarcoplasmic/endoplasmic reticulum (SR/ER) Ca^{2+} stores [27]. The events share parallels with previously reported spontaneous transient outward currents (STOCs [28]) both being activated by spontaneous Ca^{2+} release from intracellular stores, but differing in that the Ca^{2+} release that generates STICs acts on excitatory channels (i.e. that cause depolarisation) rather than inhibitory channels (i.e. K^+ channels that cause hyperpolarisation). The frequency of these events is markedly enhanced by stimulation of alpha-adrenoceptors [27]. This increases production of IP_3 through phospholipase C (PLC) cleaving phosphatidylinositol 4,5-bisphosphate (PIP_2) into the second messengers IP_3 and sn-1,2-diacylglycerol (DAG), leading to IP_3-induced Ca^{2+} release (IICR) from intracellular Ca^{2+} stores [29, 30]. The events are regenerative because released Ca^{2+} causes further activation of IP_3 receptors (IP_3Rs) and ryanodine receptor (RyR)-operated Ca^{2+} release channels by Ca^{2+}-induced Ca^{2+} release (CICR). Dependent on the level of stimulation (i.e. IP_3 or Ca^{2+} levels), multiple stores will be activated. Thus, noradrenaline or other agents that increase production of IP_3 and/or intracellular Ca^{2+} concentration ($[Ca^{2+}]_i$) increase the frequency of store Ca^{2+} release events and resultant STICs/STDs. Stretch also has an effect on STD activity causing a marked increase in STD amplitude [31].

The primary ionic nature of the current underlying STICs/STDs in venous SM has been found to be primarily due to an efflux of Cl^-. Studies

with rapidly applied noradrenaline or brief high-frequency nerve stimulation that produces large irregularly shaped transient depolarisations in the SM of guinea pig mesenteric veins indicate this, as ionic substitution experiments, where sodium chloride in the buffer solution was fully substituted with Na isethionate, demonstrated the activity resulted through opening of Cl^- channels [32, 33]. Studies on STICs/STDs in guinea pig mesenteric vein segments indicated the involvement of both Ca^{2+}-activated Cl^- with isethionate substitution (see above) and cation-selective conductances with Tris chloride substituted for all the sodium chloride [27]. Studies on isolated rabbit portal vein myocytes provided evidence that STICs were dominantly generated by a Ca^{2+}-activated Cl^- conductance [34]. Figure 13.2 presents a schematic displaying the generally accepted mechanism underlying the generation of STICs/STDs. The Ca^{2+} release channels are IP_3Rs, which are opened by agonists such as noradrenaline to enhance the production of IP_3 and Ca^{2+} release through CICR, and RyRs, where present which are opened by CICR. Findings from Ca^{2+} imaging studies on rat and rabbit portal vein myocytes indicate that both IP_3R and RyR Ca^{2+} release channels are present on SR/ER stores [35, 36]. These authors found that large-amplitude slow Ca^{2+} release events were selectively abolished by agents known to inhibit IP_3R-mediated Ca^{2+} release channels and that all Ca^{2+} release events were abolished by a relatively low concentration of ryanodine (50–100 μM), which is thought to lock open the RyR channels in a substate causing depletion of Ca^{2+} from the SR/ER [37]. Inhibition of the SR/ER reticulum Ca^{2+}ATPase (SERCA), the Ca^{2+} pump that refills the SR/ER Ca^{2+} stores, also abolished STICs/STDs. There is considerable variability within SMs as to the presence and location of RyRs but their presence should boost IP_3R-mediated store Ca^{2+} release, which in turn may enhance the likelihood that nearby stores are activated, thereby increasing the generation of Ca^{2+} waves [36]. STICs/STDs exhibit large variability in their amplitude [27, 34] which may relate to factors

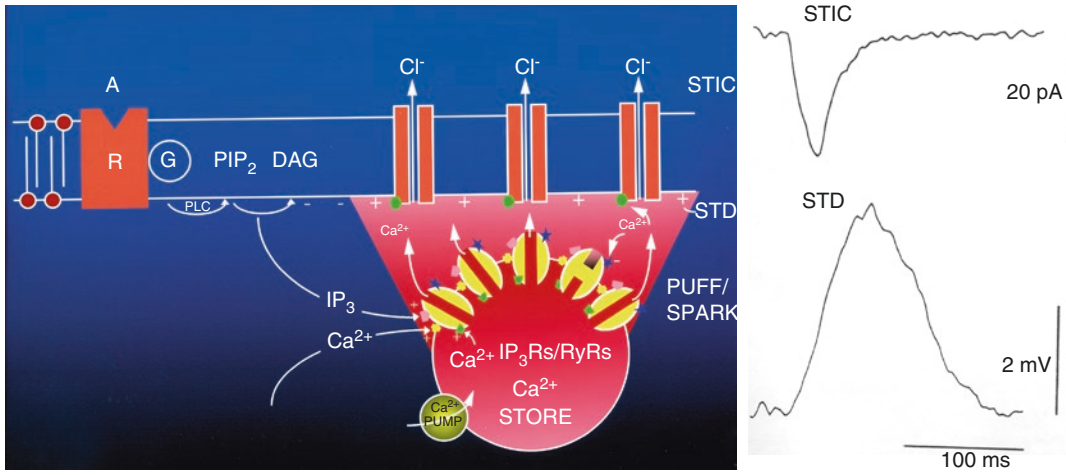

Fig. 13.2 Schematic of a Ca^{2+} release event proposed to underlie generation of a spontaneous transient inward current (STIC) and resultant spontaneous transient depolarisation (STD). Endogenous IP_3, agonist-induced IP_3 and/or cytosolic Ca^{2+} activate IP_3Rs and/or RyRs, the associated Ca^{2+} release triggering regenerative release of Ca^{2+} from the sub-plasmalemmal SR/ER store through CICR. This generates a local event, which if visualised with a Ca^{2+}-sensing fluorophore is termed a Ca^{2+} puff/spark (though for release from stores very close to the cell plasmalemma puffs/sparks may not be readily visualised due to their small volume). Then, according to key factors such as the degree of store emptying and cytosolic [Ca^{2+}], Ca^{2+} release channels close and release ceases, the SERCA Ca^{2+} pump then refilling the store. The example STIC and STD were recorded from the SM of a small vein. Their large size indicates recruitment of multiple stores. STICs/STDs in veins and lymphatics tend to be generated by opening of Ca^{2+}-activated Cl^- channels though there may also be a contribution of a cationic current [27] (reproduced with permission from [146])

such as the total number of Ca^{2+} release channels per store, the ratio of IP_3Rs to RyRs given their different kinetics and conductances, the number of stores activated near synchronously and the distance of the store release site from the plasmalemmal Ca^{2+} activated channels.

Supportive evidence that STICs/STDs are elemental in the generation of vasomotion came from parallel studies made on guinea pig mesenteric lymphatics [38, 39]. Here STDs in lymphatic SM have similar characteristics to STICs/STDs in veins, being generated by spontaneous Ca^{2+} release from intracellular Ca^{2+} stores, the localised transient increase in $[Ca^{2+}]_i$ activating Ca^{2+}-activated Cl^- channels which generates an inward current and resultant STD. Significantly, these studies demonstrated that summations of STDs could reach threshold for generation of an action potential (AP) through regenerative opening of L-type voltage-dependent Ca^{2+} channels, the resultant Ca^{2+} entry causing contraction. These events were proposed to be the pacemaker for vasomotion in *non-perfused* lymphatic SM. The venous SM recordings demonstrating rhythmic pacemaker-like depolarisations [26] combined with the evidence that summation of STDs generates APs and resultant vessel constriction [27] also fit this model. Thus STDs, events that are independent of voltage-dependent Ca^{2+} channels, can rhythmically summate and when of sufficient amplitude pace contractions in SM and induce vasomotion. Vasomotion induced by stimulation of α-adrenoceptors in rat portal vein also occurs through the cyclical release of Ca^{2+} from SR/ER stores and opening of Ca^{2+}-activated Cl^- channels [40]. However, an exception to this has been reported for spontaneous vasomotion in the mouse portal vein, as this vasomotion persists despite blockade of Ca^{2+} stores [41] and hence is likely to be driven by pacemaker currents in the plasma membrane. Thus, vasomotion can be generated by at least two pacemaker mechanisms, one driven by an intracellular pacemaker termed the "Ca^{2+} clock" and the other by a plasma membrane pacemaker termed the "membrane clock". This fits with the concept that there are two pacemakers as first introduced by Griffith in describing arterial chaos/vasomotion [42, 43]. These concepts were later taken up to describe heart pacemaking which involves both the classical membrane clock through pacemaker currents such as I_{funny} [44] and the Ca^{2+} clock which in the heart is driven by cardiac RyRs, with Ca^{2+} release generating an inward current by activating a sodium/calcium exchange [45–47].

13.2.1 Coupled Oscillators

The finding that store Ca^{2+} release when coupled to generation of an excitatory current rhythmically summates is both intriguing and fundamental to generation of vasomotion. It is fundamental, as individually store Ca^{2+} release events that, if observed with a fluorescent Ca^{2+} indicator and referred to as Ca^{2+} puffs for IP_3Rs [48, 49] or Ca^{2+} sparks for RyRs [50], are very small with their resultant STDs causing little depolarisation in syncytial SM. Therefore, it is essential that there is rhythmical summation of these elementary events as otherwise there would be a massive impedance mismatch and pacemaking could not occur. Moreover, independent of the underlying pacemaker mechanism, groups of pacemaker cells that drive a large cell syncytium need to entrain their cycling to be effective as a pacemaker. The mechanisms by which this occurs can be explained by the theory of coupled oscillators, a physical process that widely applies, particularly to natural phenomena (e.g. cicadas chirping, firefly displays, entrainment of menstrual cycling). The process was first described in the sixteenth century by a Dutch physicist, Christian Huygens, inventor of the pendulum clock, who noted the pendulums of two clocks hung side by side on the same wall swung in synchrony. The clocks maintained synchrony for the several hours of observation and resynchronised after deliberate desynchronisation. Synchrony was lost when the clocks were positioned on different walls. Huygens concluded that synchrony must be maintained by "tiny air movements or imperceptible vibrations in their common support". This "fortuitous observation initiated an

entire sub-branch of mathematics: *the theory of coupled oscillators*" (see [51]).

Many cellular systems entrain their oscillatory activity, the heart pacemaker being a good example. Indeed, the heart was the first application of coupled oscillator entrainment to explain its multicellular rhythmicity [52]. Consequently, application of this theory to describe heartbeats was generally discarded given that cardiac muscle is not self-oscillatory but is driven by a centralised pacemaker. This was a significant overreaction given that the pacemaker itself depends on coupled oscillator-based synchronisation, as noted in 1975 by Charles S. Peskin of New York University (see [51]). Cardiac pacemaker cells are self-oscillating and being coupled electrically by gap junctions will synchronise. Indeed, without this physical process the heart would not function, as individual pacemaker cells would not produce sufficient pacemaker current to drive the atrial cardiac muscle. Even if they did there would be no coordination between pacemaker cells, so the heart could not rhythmically contract.

13.2.2 Rhythmicity Through Coupled Oscillator-Based Entrainment of the Release/Refill Cycle of Intracellular Calcium Stores

Modelling of vasomotion by coupled oscillator-based entrainment of the activity of Ca^{2+} stores has arisen from several observations. ***First***, store Ca^{2+} release/refill is an oscillatory process. Release arises through the rapid opening of Ca^{2+} release channels in the SR/ER membrane of intracellular Ca^{2+} stores. Triggering of store Ca^{2+} release depends on factors such as the store lumen [Ca^{2+}], as determined by much slower SERCA-mediated refill (Fig. 13.2). The oscillatory nature of store release was initially investigated in non-excitable cells where stimulation of receptors such as the α_1-adrenoceptor caused rhythmical store Ca^{2+} release with the frequency of this activity increasing with higher agonist stimulation [53–56]. This behaviour also applies to store Ca^{2+} release/refill underlying STICs/STDs [27]. The fact that there is a rapid release followed by slow refill which rhythmically repeats means that these fall into the category of *relaxation oscillators*, which can entrain their cycles when the frequency of oscillator activity and coupling between oscillators is sufficiently strong [52]. ***Second***, studies on arterial vasomotion determined that the process fitted the mathematical description of being "chaotic" [42]. This conclusion arose from studies of *perfused* isolated rabbit ear arteries pharmacologically activated/modulated with the agonist histamine and measuring variables such as perfusion pressure.

In a subsequent publication by this group [43], the authors concluded that there were two oscillatory mechanisms that they termed the "membrane oscillator" (i.e. membrane clock) in which membrane Ca^{2+} and K^+ fluxes had a role, and an "intracellular oscillator" mediated by store Ca^{2+} release/refill (i.e. Ca^{2+} clock). The oscillators interacted as weakly coupled oscillators entraining through phase to produce a "global" pacemaker with a single frequency producing vasomotion. In their analysis they determined that entrainment derived from the membrane clock rather than the Ca^{2+} clock. In contrast, in the relatively simplified circumstance of *non-perfused* vessels, the store oscillator is likely to be dominant, as stretch-activated channels in the cell membrane which could make the membrane clock the dominant pacemaker mechanism would not be functional. This is the case for vasomotion in *non-perfused* mesenteric lymphatic vessels with pacemaking dominantly driven by the Ca^{2+} clock with pacemaking being mediated by oscillatory Ca^{2+} release from intracellular Ca^{2+} stores and resultant STDs [39]. It also applies to *non-perfused* mesenteric veins, where summation of STDs is associated with the triggering of recurring action potentials, as evident upon noradrenaline application [27]. In contrast, the finding that spontaneous vasomotion in mouse portal vein occurs independently of SR/ER Ca^{2+} stores [41] suggests that the dominant oscillator in this tissue is likely to be the membrane clock though this has yet to be fully resolved.

Coupled oscillator theory has long been proposed to explain slow wave-mediated gastrointestinal tract (GIT) motility [57–62]. While such interpretation reasonably fits the observations of GIT motility, there has been opposition [63, 64]. This was based on arguments such as there being no direct evidence of the underlying oscillator and insufficient account taken of other properties of the system. These authors instead propose a physical model with intercellular coupling through which action potentials propagate (see also [60, 65]). The physical model satisfies some of the criteria but does not readily explain aspects such as the frequency gradient of slow wave-driven motility down the stomach whereas the coupled oscillator model does [62, 66–68]. There is now also evidence of an underlying oscillator, this again being the Ca^{2+} clock. This, as for vasomotion, is mediated by SR/ER Ca^{2+} store release/refill cycle, store Ca^{2+} release activating Ca^{2+}-activated Cl^- channels to generate STDs (also termed unitary potentials) with slow waves dependent on rhythmical entrainment of these underlying events [69–73].

Entrainment of cycling Ca^{2+} stores, which is fundamental to the establishment of the Ca^{2+} clock pacemaker, involves specific mechanisms. For example, while local diffusion of Ca^{2+} and IP_3 provides a potential of coupling, this is too weak for intercellular entrainment of oscillatory release from Ca^{2+} stores [74]. However, the existence of voltage coupling whereby Ca^{2+} from intracellular stores and resultant STDs feed back to cause more store Ca^{2+} release provides a much greater coupling, facilitating intercellular entrainment of the Ca^{2+} release/refill cycle of multiple stores. Voltage coupling is effective because intercellular current flow has three orders of magnitude more intercellular range than coupling by diffusion of IP_3 and Ca^{2+} [74–76].

Pacemaker entrainment underlying vasomotion is also fundamentally dependent on voltage feedback. This is mediated by opening of T-type and L-type voltage-activated Ca^{2+} channels, the resultant rise in $[Ca^{2+}]_i$ increasing recruitment and frequency of store Ca^{2+} release through CICR. In addition, as shown in arteries [77] and as occurs in GIT pacemaking [70, 72, 78], there is likely to be a depolarisation-induced increase in the production of IP_3, which will also recruit and increase the frequency of store Ca^{2+} release (Fig. 13.3). These mechanisms underpin the onset and maintenance of vasomotion in various blood and lymphatic vessels [74, 79]. Agonist-induced vasomotion in mesenteric and portal veins indicates that such vasomotion is also mediated by the Ca^{2+} clock [27, 40]. In contrast, if membrane clock pacemaking indeed underlies vasomotion in mouse portal vein [41], then this will occur through entrainment of membrane pacemaker/AP firing in the cells with pacemaker function within the cellular syncytium.

The physical process whereby cycling intracellular Ca^{2+} stores interact as coupled oscillators to pace vasomotion in various veins, arteries and lymphatics is also applicable to other cellular syn-

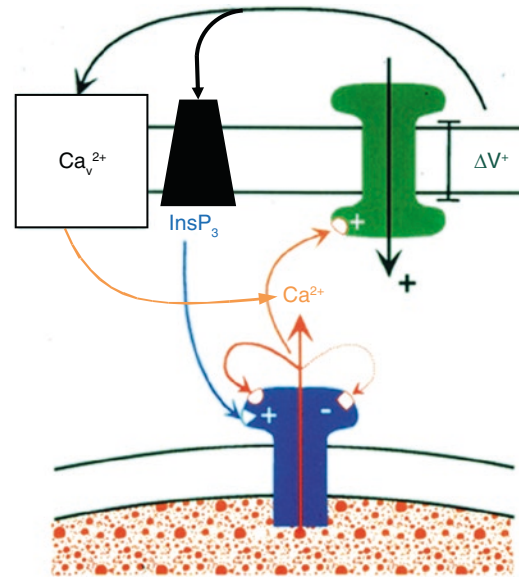

Fig. 13.3 Feedback interactions between the cell membrane potential and SR/ER store Ca^{2+} release. Depolarisation (ΔV^+) across the cell membrane causes Ca^{2+} entry through activation of voltage-dependent Ca^{2+} channels and/or acts at unknown functional site(s) such as agonist receptors, G proteins or PLC to activate PLC and initiate synthesis of IP_3. In turn Ca^{2+} and/or IP_3 activate IP_3R- and/or RyR-operated Ca^{2+} release channels in the SR/ER, with the Ca^{2+} activating a Ca^{2+}-activated inward current causing further depolarisation (see also Fig. 13.2; reproduced with permission in modified form from [72])

cytia. These include pericyte cells that pace and mediate vasomotion in venules and precapillary arterioles; rhythmic contractions in various other SMs; and cellular syncytia such as ICC cells that pace GIT motility. In case of the latter, it transpires that the pacemaker mechanism underlying GIT motility involves both a membrane clock pacemaker involving T-type Ca^{2+} channels [65, 80–86] and a Ca^{2+} clock pacemaker (considered above). IP_3 receptor-operated Ca^{2+} channels have a key role in the GIT slow-wave Ca^{2+} clock pacemaker though RyR Ca^{2+} release channels are also involved [72, 87]. As for vasomotion, coupled oscillator-based entrainment of cycling Ca^{2+} stores provides an explanation for the observation of rhythmical summation of STDs pacing generation of slow waves in strips of gastric smooth muscle [72, 76]. Thus, the Ca^{2+} clock and the membrane clock provide physical oscillators underlying the long-held proposal that slow wave-related GIT motility arises through intercellular coupled oscillator-based entrainment, a model that fits observations of a frequency gradient along the intestine [62, 67, 88]. In the case of the Ca^{2+} clock, voltage coupling again provides feedback to recruit or increase oscillatory Ca^{2+} release from Ca^{2+} stores, due presumably to STDs increasing depolarisation-induced production of IP_3 [70, 72, 78] and/or entry of Ca^{2+} through T-type Ca channels [65]. This strengthens coupling allowing intercellular entrainment of store Ca^{2+} release, the store release/refill cycle in ICCs now entrained to cycle at the same frequency, the resultant depolarisation transmitting through gap junctions to pace slow waves and resultant contractions in the SM [72, 76].

In an overview, vasomotion may arise from the Ca^{2+} clock or membrane clock or through pacemaking involving both clocks. Regardless, effective pacemaking at the multicellular level depends on coupled oscillator-based entrainment. In the case of the Ca^{2+}clock this involves entrainment of cycling Ca^{2+} stores, whereas for the membrane clock it involves entrainment of membrane pacemaker-driven APs in pacemaker cells. In the case where both pacemaker mechanisms are functional, studies on heart pacemaking indicate a symbiotic interaction [89, 90].

13.3 Do Specific Pacemaker Cells Underlie Venous Vasomotion?

The finding that pacemaking in the GIT is mediated by a separate network of cells termed interstitial cells of Cajal (ICCs) [63, 91–95] opens up the possibility that this may be more general phenomena. Indeed, this was found to be the case in other SMs including SM in the urethra and prostate where interstitial cells (ICs) are present and have been implicated as pacemakers [96, 97]. As for the GIT, ICs drive contractions in urethral and prostatic SM by inducing depolarisation through store Ca^{2+} release activating Ca^{2+}-activated Cl^- channels and resultant STDs [98, 99]. Entrainment of the underlying activity together with enhancement through resultant increased Ca^{2+} entry and CICR generates pacemaker current that flows through gap junctions into the SM opening voltage-dependent Ca^{2+} channels and resultant contraction. A defining characteristic of GIT, urethral and prostatic interstitial cells is that most are revealed by staining procedures using an antibody against tyrosine-protein kinase KIT (CD117). However, in organs such as the guinea pig prostate there are also ICs that are Kit negative but vimentin positive [100]. At present, it is not known whether Kit-positive, Kit-negative or both types of prostatic ICs are the pacemaker cells [97].

The case that ICs pace vasomotion in veins and more generally in other blood vessels and lymphatics has yet to be substantiated. In very small vessels such as venules, pericytes both generate and mediate vasoconstriction [7]. Vasomotion in veins that enter the heart near the point of entry is driven by atrial-like cardiomyocytes which appear to self-pace to generate vasomotion. Thus, at present there is no evidence implicating ICs as pacemaker cells in both of these instances of vasomotion. The existence of ICs in the walls of blood and lymphatic vessels is known [101–103] but whether they subserve a pacemaker role to drive SM-based vasomotion is still inconclusive [104]. This said, there is considerable heterogeneity between the strength of pacemaker potentials in different lymphatic

chambers so in this tissue there is at least some form of specialisation in relation to generation of pacemaking [39]. While guinea pig mesenteric arteries have ICs, there is no evidence for these having a pacemaker role [105]. In contrast, as considered further below, it remains possible that ICs present in the walls of the rabbit portal vein and the frog postcaval vein have a pacemaker role [104, 106]. However, a study on mouse portal vein found no evidence for IC-driven pacemaking [41]. ICs are also present in human pulmonary veins but their role has yet to be investigated [107].

The morphology of rabbit portal veins is atypical, while having a normal endothelium and surrounding circular SM there is also an outer layer of longitudinal SM. An ultrastructural study noted that proposed "SM" cells in the inner media were irregular in shape and made membrane contacts with neighbouring cells through a network of cytoplasmic processes [108]. The role of ICs in other veins has yet to be explored, though proof of the presence of ICs in rabbit portal vein has arisen through immunohistochemical labelling and enzymatic cell isolation of two populations of non-contractile Kit-positive ICs were found in the media. One of the IC populations presented as small round cells in the sub-endothelial layer and the other were long spindle cells in the intramuscular layer, located about 30 μm and 70 μm, respectively, from the endothelium [109]. Electrophysiological recording and Ca^{2+} imaging indicated that ICs and SM cells (SMCs) exhibited STDs, Ca^{2+} sparks and waves. Proof that ICs were pacemaker cells was inconclusive as SMCs were at times also observed to be spontaneously active, triggered by their own STDs. A factor presented in support of ICs having a pacemaker role relates to the density of rabbit portal vein ICs which is variable [104], a finding that could be consistent with observations of multiple pacemaker sites as reported in the rat portal vein [110]. Studies on groups of ICs indicate rapid signal transmission between rabbit portal vein ICs, the rise in $[Ca^{2+}]_i$ occurring within ~0.2 s. However, communication between ICs and SMCs occurs with a markedly slower delay with the rise in $[Ca^{2+}]_i$ occurring up to 4 s following IC depolarisation. This suggests that SMCs are not tightly coupled via gap junctions to ICs and hence are not electrically interconnected, thus communication most likely occurring through IC-based release of a paracrine agent [111]. Whether ICs could pace vasomotion in this circumstance would depend on factors such as spatial release and spread of the paracrine agent, which would need to activate sufficient SMCs to drive them to threshold for voltage-dependent Ca^{2+} entry and resultant SM contraction/vasomotion. Thus, while it remains possible that ICs pace vasomotion in this atypical rabbit portal vein further proof is required. The functional role of ICs in veins has only been reported in one other study, the frog postcaval vein [106]. A 5-min exposure to laser light aimed at inactivating ICs identified by methylene blue slowed pacemaking in methylene blue-treated veins but not in the absence of methylene blue. This study suggests that ICs in the frog postcaval vein may have either a pacemaker or a modulatory role. The role of ICs in other veins has yet to be explored.

13.4 Modulation of Vasomotion

So far, discussion of modulatory factors has been confined to agents that modulate vasomotion by interacting with store Ca^{2+} release. Noradrenaline is a key example which by increasing production of IP_3 enhances store Ca^{2+} release and hence vasomotion. However, there are various other mechanisms by which vasomotion is modulated, the endothelium being a major modulator.

13.4.1 The Endothelium

Endothelial cells (ECs) exhibit different morphologies and functions dependent on the vessel, be they veins or arteries. Venous ECs tend to be shorter and wider than arterial ECs [1]. Additionally, some veins, like lymphatics, have valves which inhibit the backflow of blood.

In smaller arteries and arterioles, ECs connect to the SM by myoendothelial gap junctions but this is not so common for larger arteries and veins, with the exception of pulmonary veins [112]. In lymphatic vessels there is also no evidence for myoendothelial gap junction-based connectivity between the endothelium and SM [113, 114]. Thus veins, as for lymphatics [115–117], will modulate vasomotion largely through release of modulating factors including vessel-relaxing factors such as endothelium-derived nitric oxide (EDNO) which relaxes SM through increasing soluble guanylate cyclase and hence increasing cGMP [114, 118–121]. The vascular endothelium also releases prostaglandins such as PGE_2, which causes relaxation through increasing cAMP [120, 122]. One mechanism by which cAMP causes relaxation involves activation of protein kinase A (PKA) which is proposed to both reduce $[Ca^{2+}]_i$ and inhibit myosin light-chain (MLC-20) phosphorylation and hence contraction [123]. However, studies on lymphatic SM indicate that the cAMP/PKA pathway also causes hyperpolarisation by activation of K_{ATP} channels, the net effect being a decrease in lymphatic vasomotion and decrease in the STDs arising from store Ca^{2+} release events [124–126]. EDNO increases cGMP to cause relaxation [118] and hence will inhibit venous vasomotion [120]. PGE_2 can cause either relaxation or contraction depending on the receptor subtypes activated; in veins PGE_2 causes relaxation by acting on the EP_4 receptor which increases cAMP [127, 128] and therefore inhibits venous vasomotion.

13.5 Voltage-Dependent Ca^{2+} Entry

Vasomotion depends on Ca^{2+} entry into the SM to trigger contraction. This involves activation of voltage-dependent Ca^{2+} channels which once regenerative result in an AP. The AP in veins is primarily carried by L-type voltage-dependent Ca^{2+} channels with little if any evidence for a substantial role of voltage-dependent Na^+ channels, though they are present in some venous SM (e.g. rat portal vein [129]). SM contraction occurs through the increased $[Ca^{2+}]_i$ resulting from the Ca^{2+} that enters the cell during the AP combined with amplification by CICR from Ca^{2+} stores. Following from the initial evidence that action potentials in portal venous SM were dependent on extracellular $[Ca^{2+}]$ [130], two types of Ca^{2+} channels were demonstrated. One is an L-type Ca^{2+} channel and the other has characteristics similar to low-threshold T-type Ca^{2+} channels [131–134]. These channels are fundamental to vasomotion as they provide a positive-feedback pathway between the depolarisation caused by store Ca^{2+} release and more global store Ca^{2+} release, thus allowing store oscillators to entrain. In this regard, it has been found that rabbit portal vein ICs also have L-type Ca^{2+} channels though the presence of T-type Ca^{2+} channels was not reported [109].

13.6 K^+ Channels

The hyperpolarisation induced by K^+ channel activation is inhibitory, slowing or stopping vasomotion, with the pacemaker taking longer to reach threshold or failing to do so. Studies on blood vessels indicate that there are four classes of K^+ channels: ATP-sensitive (K_{ATP}); Ca^{2+}-activated K^+ channels including large-conductance (BK_{Ca}), intermediate-conductance (IK_{Ca}) and small-conductance (SK_{Ca}) channels; voltage-gated K^+ (K_V); and inward rectifier (K_{IR}) channels [135]. The relative contribution of these varies with vessel. For example, BK_{Ca} has a dominant role in pulmonary and saphenous veins but K_{ATP} channels are also functional [120, 136].

K_{ATP} channels provide a means for fine regulation of vascular tone and hence blood pressure; in the case of veins, K_{ATP} channels may regulate vascular volume. K_{ATP} channels also have the potential to modulate vasomotion. Indeed, just as Ca^{2+}-activated Cl^- channels or the sodium/calcium exchanger (NCX) couple store Ca^{2+} release to the membrane potential (V_m), K_{ATP} channels couple intracellular metabolic events (e.g. ATP/ADP ratio, pH) to V_m activity [137]. K_{ATP} channel activity and hence venous tone are also modulated by endogenous vasodilators (VIP, adenosine,

CGRP) as well as vasoconstrictors (e.g. angiotensin II, noradrenaline, histamine) [137]. The family of K_{ATP} channels comprises four inwardly rectifying K^+ channel subunits and four regulatory sulphonylurea receptors. The properties of K_{ATP} channels in venous SM have dominantly been studied in the rabbit portal vein [138–141]. More recently, studies on mouse portal vein SM have determined the molecular nature of the K_{ATP} channel subunits present, demonstrating the presence of KIR6.1, an inwardly rectifying K^+ channel that is associated with the sulphonylurea receptor subunit SUR2B [142].

13.7 Conclusions

Vasomotion in veins while less well studied than that in arteries/arterioles or lymphatics is functional in many vessels. In arteries/arterioles vasomotion has been shown to improve vascular perfusion and is proposed to improve delivery of oxygen to tissues surrounding their capillary beds [143, 144]. Many veins have unidirectional valves so vasomotion may also improve venous return from these vessels. Movement induced by vasomotion would also reduce stasis and hence the potential for blood clotting. Vasomotion may also be a mechanism that increases the reactivity of a blood vessel, hence avoiding maintained force generation [145], and in pulmonary veins vasomotion has been shown to modulate fluid filtration pressures by regulating recruitment and distension of upstream alveolar wall capillaries "and thus ventilation-perfusion matching in the lung" [120].

The mechanism of vasomotion is well described by a coupled oscillator model. In most cases this occurs through entrainment of the store release/refill cycle of SR/ER Ca^{2+} stores (i.e. the Ca^{2+} clock) which causes membrane depolarisation by influx of inward current across the cell membrane. This normally occurs in veins through the activation of Ca^{2+}-activated Cl^- channels but in other tissues can be activated by different channels and/or by sodium/calcium exchange. Pacemaking may also occur by pacemaker-generated APs in the cell membrane (i.e. membrane clock). In both cases, entrainment of the oscillators requires intercellular coupling, which in most tissues including veins is mediated by electrical pathways. This occurs through gap junctions between the SMCs but in cases where there are myoendothelial gap junctions is enhanced by current flow through the ECs, which provide a lower resistance pathway. Another fundamental requirement for establishment of vasomotion is long-range interaction between cell membrane depolarisation and oscillatory activity [74, 79]. In the case of the Ca^{2+} clock pacemaker, this functions through the depolarisation-associated current caused by local Ca^{2+} release causing depolarisation over wider regions. This in turn leads to voltage-dependent Ca^{2+} entry and presumably also through enhanced synthesis of IP_3, both initiating or enhancing oscillatory Ca^{2+} release from other stores facilitating global entrainment of the store Ca^{2+} release/refill cycle. Voltage coupling has a 500–1000-fold longer range than achieved by intercellular diffusion of Ca^{2+} or IP_3 [76]. The process for the membrane clock pacemaker also depends on long-range voltage coupling the intercellular current flow between oscillatory activity in individual cells facilitating global entrainment. Vasomotion is readily modulated being enhanced by agents that increase $[Ca^{2+}]_i$ and/or synthesis of IP_3 (e.g. noradrenaline) and inhibited by agents that increase cGMP or cAMP (e.g. EDNO or PGE2, respectively). Ca^{2+} clock-based vasomotion in veins shares close parallels with vasomotion in arteries and lymphatics and more generally with rhythmic contractions/constrictions in other smooth muscles such as the GIT [74, 76, 79].

Rhythmic multicellular activity is a building block of life being fundamental to the function of many organs including the heart and brain, the latter exhibiting an enormous array of rhythms. The concept that pacemaking can be generated by one or more clocks is nicely demonstrated in the heart with pacemaking mediated by a symbiosis between the Ca^{2+} and membrane clock pacemakers [89]. While most studies on vein vasomotion indicate a Ca^{2+} clock pacemaker, the finding that mouse portal vein does not operate this way [41] and is likely to

operate by a membrane clock pacemaker opens up the concept that both mechanisms are functional in veins depending on species and conditions. As is evident from heart pacemaker studies, the combined presence of the Ca^{2+} and membrane clock pacemaker mechanisms allows exquisite neural and hormonal modulation of pacemaking while maintaining stability [90]. The same may well apply to vein vasomotion with neurotransmitters/hormones acting through the Ca^{2+} clock pathway to have a "starter motor" function to initiate vasomotion and/or to modulate the frequency and/or strength of ongoing vasomotion.

References

1. dela Paz NG, D'Amore PA. Arterial versus venous endothelial cells. Cell Tissue Res. 2009;335(1):5–16.
2. Reed KE, Westphale EM, Larson DM, Wang HZ, Veenstra RD, Beyer EC. Molecular cloning and functional expression of human connexin37, an endothelial cell gap junction protein. J Clin Invest. 1993;91(3):997–1004.
3. Bruzzone R, Haefliger JA, Gimlich RL, Paul DL. Connexin40, a component of gap junctions in vascular endothelium, is restricted in its ability to interact with other connexins. Mol Biol Cell. 1993;4(1):7–20.
4. Pepper MS, Montesano R, el Aoumari A, Gros D, Orci L, Meda P. Coupling and connexin 43 expression in microvascular and large vessel endothelial cells. Am J Phys. 1992;262(5 Pt 1):C1246–57.
5. Hill CE, Rummery N, Hickey H, Sandow SL. Heterogeneity in the distribution of vascular gap junctions and connexins: implications for function. Clin Exp Pharmacol Physiol. 2002;29(7):620–5.
6. Haddock RE, Hill CE. Rhythmicity in arterial smooth muscle. J Physiol. 2005;566(Pt 3):645–56.
7. Hashitani H, Mitsui R, Shimizu Y, Higashi R, Nakamura K. Functional and morphological properties of pericytes in suburothelial venules of the mouse bladder. Br J Pharmacol. 2012;167(8):1723–36.
8. Franklin KT. The physiology and pharmacology of veins. Physiol Rev. 1928;8:346–66.
9. Liu R, Feng H-Z, Jin J-P. Physiological contractility of cardiomyocytes in the wall of mouse and rat azygos vein. Am J Physiol Cell Physiol. 2014;306(7):C697–704.
10. Yoffey JM, Coutice C. Lymphatics, lymph and the lymphomyeloid complex. New York: Academic Press; 1970.
11. Barrowman JA. Physiology of the gastro-intestinal lymphatic system. Cambridge: Cambridge University Press; 1978.
12. Jones TW. Discovery that the veins of the bat's wing (which are furnished with valves) are endowed with rhythmical contractility, and that the onward flow of blood is accelerated by each contraction. Phil Trans R Soc Lond. 1852;142:131–46. https://doi.org/10.1098/rstl.1852.0011.
13. Florey HW. Observations on the contractility of lacteals. Part I. J Physiol (Lond). 1927;62:267–72.
14. Mislin H. Active contractility of the lymphangion and coordination of lymphangion chains. Experientia. 1976;32(7):820–2.
15. Crowe MJ, von der Weid PY, Brock JA, van Helden DF. Co-ordination of contractile activity in guinea-pig mesenteric lymphatics. J Physiol (Lond). 1997;500(Pt 1):235–44.
16. Caggiati A, Phillips M, Lametschwandtner A, Allegra C. Valves in small veins and venules. Eur J Vasc Endovasc Surg. 2006;32(4):447–52.
17. Funaki S, Bohr DF. Electrical and mechanical activity of isolated vascular smooth muscle of the rat. Nature. 1964;203:192–4.
18. Cuthbert AW, Sutter MC. Electrical activity of a mammalian vein. Nature. 1964;202:95.
19. Axelsson J, Wahlstrom B, Johansson B, Jonsson O. Influence of the ionic environment on spontaneous electrical and mechanical activity of the rat portal vein. Circ Res. 1967;21(5):609–18.
20. Holman ME, Kasby CB, Suthers MB, Wilson JA. Some properties of the smooth muscle of rabbit portal vein. J Physiol. 1968;196(1):111–32.
21. Gunn JA, Chavasse FB. The action of adrenin on veins. Proc R Soc B. 1913;86(586):192–7.
22. Mitsui R, Miyamoto S, Takano H, Hashitani H. Properties of submucosal venules in the rat distal colon. Br J Pharmacol. 2013;170(5):968–77.
23. Mitsui R, Hashitani H. Functional properties of submucosal venules in the rat stomach. Pflugers Arch. 2015;467(6):1327–42.
24. Mitsui R, Hashitani H. Mechanisms underlying spontaneous constrictions of postcapillary venules in the rat stomach. Pflugers Arch. 2016;468(2):279–91.
25. Ito Y, Kuriyama H. Membrane properties of the smooth-muscle fibres of the guinea-pig portal vein. J Physiol. 1971;214(3):427–41.
26. Suzuki H. Effects of endogenous and exogenous noradrenaline on the smooth muscle of guinea-pig mesenteric vein. J Physiol. 1981;321:495–512.
27. Van Helden DF. Spontaneous and noradrenaline-induced transient depolarizations in the smooth muscle of guinea-pig mesenteric vein. J Physiol. 1991;437:511–41.
28. Benham CD, Bolton TB. Spontaneous transient outward currents in single visceral and vascular smooth muscle cells of the rabbit. J Physiol. 1986;381:385–406.
29. Berridge MJ. Inositol trisphosphate and diacylglycerol as second messengers. Biochem J. 1984;220(2):345–60.
30. Berridge MJ, Irvine RF. Inositol trisphosphate, a novel second messenger in cellular signal transduction. Nature. 1984;312(5992):315–21.

31. Van Helden DF, von der Weid P-Y, Crowe MJ. Electrophysiology of lymphatic smooth muscle. In: Reed RK, McHale NG, Bert JL, Winlove CP, Laine GA, editors. Interstitium, connective tissue and lymphatics. London: Portland Press; 1995. p. 221–36.
32. Van Helden DF. Electrophysiology of neuromuscular transmission in guinea-pig mesenteric veins. J Physiol (Lond). 1988;401:469–88.
33. Van Helden DF. An alpha-adrenoceptor-mediated chloride conductance in mesenteric veins of the guinea-pig. J Physiol (Lond). 1988;401:489–501.
34. Wang Q, Hogg RC, Large WA. Properties of spontaneous inward currents recorded in smooth muscle cells isolated from the rabbit portal vein. J Physiol. 1992;451:525–37.
35. Pacaud P, Loirand G. Release of Ca2+ by noradrenaline and ATP from the same Ca2+ store sensitive to both InsP3 and Ca2+ in rat portal vein myocytes. J Physiol. 1995;484(Pt 3):549–55.
36. Gordienko DV, Bolton TB. Crosstalk between ryanodine receptors and IP(3) receptors as a factor shaping spontaneous Ca(2+)-release events in rabbit portal vein myocytes. J Physiol. 2002;542(Pt 3):743–62.
37. Nagasaki K, Fleischer S. Ryanodine sensitivity of the calcium release channel of sarcoplasmic reticulum. Cell Calcium. 1988;9(1):1–7.
38. Van Helden DF. Spontaneous activity in the smooth muscle of lymphatic vessels of the guinea-pig mesentery. Proc Int Union Physiol Sci. 1989;XVII:4386.
39. Van Helden DF. Pacemaker potentials in lymphatic smooth muscle of the guinea-pig mesentery. J Physiol. 1993;471:465–79.
40. Burt RP. Phasic contractions of the rat portal vein depend on intracellular Ca2+ release stimulated by depolarization. Am J Physiol Heart Circ Physiol. 2003;284(5):H1808–17.
41. Spencer NJ, Greenwood IA. Characterization of properties underlying rhythmicity in mouse portal vein. Auton Neurosci. 2003;104(2):73–82.
42. Griffith TM, Edwards DH. Fractal analysis of role of smooth muscle Ca2+ fluxes in genesis of chaotic arterial pressure oscillations. Am J Phys. 1994;266(5 Pt 2):H1801–11.
43. Edwards DH, Griffith TM. Entrained ion transport systems generate the membrane component of chaotic agonist-induced vasomotion. Am J Phys. 1997;273(2 Pt 2):H909–20.
44. Noble D. The surprising heart: a review of recent progress in cardiac electrophysiology. J Physiol. 1984;353:1–50.
45. Bogdanov KY, Vinogradova TM, Lakatta EG. Sinoatrial nodal cell ryanodine receptor and Na(+)-Ca(2+) exchanger: molecular partners in pacemaker regulation. Circ Res. 2001;88(12):1254–8.
46. Vinogradova TM, Zhou YY, Maltsev V, Lyashkov A, Stern M, Lakatta EG. Rhythmic ryanodine receptor Ca2+ releases during diastolic depolarization of sinoatrial pacemaker cells do not require membrane depolarization. Circ Res. 2004;94(6):802–9.
47. Lakatta EG, Maltsev VA, Vinogradova TM. A coupled SYSTEM of intracellular Ca2+ clocks and surface membrane voltage clocks controls the timekeeping mechanism of the heart's pacemaker. Circ Res. 2010;106(4):659–73.
48. Parker I, Yao Y. Regenerative release of calcium from functionally discrete subcellular stores by inositol trisphosphate. Proc Biol Sci. 1991;246(1317):269–74.
49. Parker I, Choi J, Yao Y. Elementary events of InsP3-induced Ca2+ liberation in Xenopus oocytes: hot spots, puffs and blips. Cell Calcium. 1996;20(2):105–21.
50. Cheng H, Lederer WJ, Cannell MB. Calcium sparks: elementary events underlying excitation-contraction coupling in heart muscle. Science. 1993;262(5134):740–4.
51. Strogatz SH, Stewart I. Coupled oscillators and biological synchronization. Sci Am. 1993;269(6):102–9.
52. van der Pol B, van der Mark J. The heartbeat considered as a relaxation oscillation, and an electrical model of the heart. Phil Magn. 1926;6(Suppl):763–75.
53. Woods NM, Cuthbertson KS, Cobbold PH. Repetitive transient rises in cytoplasmic free calcium in hormone-stimulated hepatocytes. Nature. 1986;319(6054):600–2.
54. Jacob R, Merritt JE, Hallam TJ, Rink TJ. Repetitive spikes in cytoplasmic calcium evoked by histamine in human endothelial cells. Nature. 1988;335(6185):40–5.
55. Wakui M, Potter BV, Petersen OH. Pulsatile intracellular calcium release does not depend on fluctuations in inositol trisphosphate concentration. Nature. 1989;339(6222):317–20.
56. Berridge MJ. Inositol trisphosphate and calcium signalling. Nature. 1993;361(6410):315–25.
57. Nelsen TS, Becker JC. Simulation of the electrical and mechanical gradient of the small intestine. Am J Phys. 1968;214(4):749–57.
58. Diamant NE, Rose PK, Davison EJ. Computer simulation of intestinal slow-wave frequency gradient. Am J Phys. 1970;219(6):1684–90.
59. Sarna SK, Daniel EE. Electrical stimulation of small intestinal electrical control activity. Gastroenterology. 1975;69(3):660–7.
60. Bortoff A. Myogenic control of intestinal motility. Physiol Rev. 1976;56(2):418–34.
61. Daniel EE, Sarna S. The generation and conduction of activity in smooth muscle. Annu Rev Pharmacol Toxicol. 1978;18:145–66.
62. Daniel EE, Bardakjian BL, Huizinga JD, Diamant NE. Relaxation oscillator and core conductor models are needed for understanding of GI electrical activities. Am J Physiol. 1994;266(3 Pt 1):G339–49.
63. Sanders KM. A case for Interstitial cells of Cajal as pacemakers and mediators of neurotransmission in the gastrointestinal tract. Gastroenterology. 1996;111:492–515.
64. Publicover NG. Generation and propagation of rhythmicity in gastrointestinal smooth muscle. In: Huizinga JD, editor. Pacemaker activity and intercel-

lular communication. Ann Arbor, MI: CRC; 1995. p. 175–90.
65. Bayguinov O, Ward SM, Kenyon JL, Sanders KM. Voltage-gated Ca2+ currents are necessary for slow-wave propagation in the canine gastric antrum. Am J Physiol Cell Physiol. 2007;293(5):C1645–59.
66. Lammers WJ, Stephen B. Origin and propagation of individual slow waves along the intact feline small intestine. Exp Physiol. 2008;93(3):334–46.
67. Huizinga JD, Chen JH, Zhu YF, Pawelka A, McGinn RJ, Bardakjian BL, et al. The origin of segmentation motor activity in the intestine. Nat Commun. 2014;5:3326.
68. Parsons SP, Huizinga JD. Effects of gap junction inhibition on contraction waves in the murine small intestine in relation to coupled oscillator theory. Am J Physiol Gastrointest Liver Physiol. 2015;308(4):G287–97.
69. Liu LW, Thuneberg L, Huizinga JD. Cyclopiazonic acid, inhibiting the endoplasmic reticulum calcium pump, reduces the canine colonic pacemaker frequency. J Pharmacol Exp Therap. 1995;275(2):1058–68.
70. Suzuki H, Hirst GD. Regenerative potentials evoked in circular smooth muscle of the antral region of guinea-pig stomach. J Physiol (Lond). 1999;517(Pt 2):563–73.
71. Edwards FR, Hirst GD, Suzuki H. Unitary nature of regenerative potentials recorded from circular smooth muscle of guinea-pig antrum. J Physiol (Lond). 1999;519(Pt 1):235–50.
72. Van Helden DF, Imtiaz MS, Nurgaliyeva K, von der Weid P, Dosen PJ. Role of calcium stores and membrane voltage in the generation of slow wave action potentials in guinea-pig gastric pylorus. J Physiol. 2000;524(Pt 1):245–65.
73. Zhu MH, Kim TW, Ro S, Yan W, Ward SM, Koh SD, et al. A Ca(2+)-activated Cl(−) conductance in interstitial cells of Cajal linked to slow wave currents and pacemaker activity. J Physiol. 2009;587(Pt 20):4905–18.
74. Van Helden DF, Zhao J. Lymphatic vasomotion. Clin Exp Physiol Pharmacol. 2000;27:1014–8.
75. Allbritton NL, Meyer T, Stryer L. Range of messenger action of calcium ion and inositol 1,4,5-trisphosphate. Science. 1992;258(5089):1812–5.
76. van Helden DF, Imtiaz MS. Ca2+ phase waves: a basis for cellular pacemaking and long-range synchronicity in the guinea-pig gastric pylorus. J Physiol. 2003;548(1):271–96.
77. Itoh T, Seki N, Suzuki S, Ito S, Kajikuri J, Kuriyama H. Membrane hyperpolarization inhibits agonist-induced synthesis of inositol 1,4,5-trisphosphate in rabbit mesenteric artery. J Physiol. 1992;451:307–28.
78. Hirst GD, Bramich NJ, Teramoto N, Suzuki H, Edwards FR. Regenerative component of slow waves in the guinea-pig gastric antrum involves a delayed increase in [Ca(2+)](i) and Cl(−) channels. J Physiol. 2002;540(Pt 3):907–19.
79. Peng H, Matchkov V, Ivarsen A, Aalkjaer C, Nilsson H. Hypothesis for the initiation of vasomotion. Circ Res. 2001;88(8):810–5.
80. Lee HK, Sanders KM. Comparison of ionic currents from interstitial cells and smooth muscle cells of canine colon. J Physiol. 1993;460:135–52.
81. Kim YC, Koh SD, Sanders KM. Voltage-dependent inward currents of interstitial cells of Cajal from murine colon and small intestine. J Physiol. 2002;541(Pt 3):797–810.
82. Kito Y, Fukuta H, Suzuki H. Components of pacemaker potentials recorded from the guinea pig stomach antrum. Pflugers Arch. 2002;445(2):202–17.
83. Kito Y, Suzuki H. Properties of pacemaker potentials recorded from myenteric interstitial cells of Cajal distributed in the mouse small intestine. J Physiol. 2003;553(Pt 3):803–18.
84. Kito Y, Ward SM, Sanders KM. Pacemaker potentials generated by interstitial cells of Cajal in the murine intestine. Am J Physiol Cell Physiol. 2005;288(3):C710–20.
85. Edwards FR, Hirst GD. An electrical description of the generation of slow waves in the antrum of the guinea-pig. J Physiol. 2005;564(Pt 1):213–32.
86. Zheng H, Park KS, Koh SD, Sanders KM. Expression and function of a T-type Ca2+ conductance in interstitial cells of Cajal of the murine small intestine. Am J Physiol Cell Physiol. 2014;306(7):C705–13.
87. Zhu MH, Sung TS, O'Driscoll K, Koh SD, Sanders KM. Intracellular Ca(2+) release from endoplasmic reticulum regulates slow wave currents and pacemaker activity of interstitial cells of Cajal. Am J Physiol Cell Physiol. 2015;308(8):C608–20.
88. Wei R, Parsons SP, Huizinga JD. Network properties of interstitial cells of Cajal affect intestinal pacemaker activity and motor patterns, according to a mathematical model of weakly coupled oscillators. Exp Physiol. 2017;102(3):329–46.
89. Lakatta EG, Vinogradova T, Lyashkov A, Sirenko S, Zhu W, Ruknudin A, et al. The integration of spontaneous intracellular Ca2+ cycling and surface membrane ion channel activation entrains normal automaticity in cells of the heart's pacemaker. Ann N Y Acad Sci. 2006;1080:178–206.
90. Maltsev VA, Lakatta EG. Synergism of coupled subsarcolemmal Ca2+ clocks and sarcolemmal voltage clocks confers robust and flexible pacemaker function in a novel pacemaker cell model. Am J Physiol Heart Circ Physiol. 2009;296(3):H594–615.
91. Faussone Pellegrini MS, Cortesini C, Romagnoli P. [Ultrastructure of the tunica muscularis of the cardial portion of the human esophagus and stomach, with special reference to the so-called Cajal's interstitial cells]. Arch Ital Anat Embriol. 1977;82(2):157–77.
92. Thuneberg L. Interstitial cells of Cajal: intestinal pacemaker cells? Adv Anat Embryol Cell Biol. 1982;71:1–130.
93. Ward SM, Burns AJ, Torihashi S, Sanders KM. Mutation of the proto-oncogene c-kit blocks

development of interstitial cells and electrical rhythmicity in murine intestine. J Physiol. 1994;480(Pt 1):91–7.
94. Huizinga JD, Thuneberg L, Kluppel M, Malysz J, Mikkelsen HB, Bernstein A. W/kit gene required for interstitial cells of Cajal and for intestinal pacemaker activity. Nature. 1995;373(6512):347–9.
95. Komuro T, Seki K, Horiguchi K. Ultrastructural characterization of the interstitial cells of Cajal. Arch Histol Cytol. 1999;62(4):295–316.
96. Sergeant GP, Hollywood MA, McCloskey KD, Thornbury KD, McHale NG. Specialised pacemaking cells in the rabbit urethra. J Physiol. 2000;526(Pt 2):359–66.
97. Lang RJ, Hashitani H. Role of prostatic interstitial cells in prostate motility. J Smooth Muscle Res. 2017;53(0):57–72.
98. Hashitani H, Van Helden DF, Suzuki H. Properties of spontaneous depolarizations in circular smooth muscle cells of rabbit urethra. Br J Pharmacol. 1996;118(7):1627–32.
99. Hashitani H, Edwards FR. Spontaneous and neurally activated depolarizations in smooth muscle cells of the guinea-pig urethra. J Physiol. 1999;514(Pt 2):459–70.
100. Shigemasa Y, Lam M, Mitsui R, Hashitani H. Voltage dependence of slow wave frequency in the guinea pig prostate. J Urol. 2014;192(4):1286–92.
101. Meyling HA. Structure and significance of the peripheral extension of the autonomic nervous system. J Comp Neurol. 1953;99(3):495–543.
102. Dahl E, Nelson E. Electron microscopic observations on human intracranial arteries. II. Innervation. Arch Neurol. 1964;10:158–64.
103. McCloskey KD, Hollywood MA, Thornbury KD, Ward SM, McHale NG. Kit-like immunopositive cells in sheep mesenteric lymphatic vessels. Cell Tissue Res. 2002;310(1):77–84.
104. Bolton TB, Gordienko DV, Povstyan OV, Harhun MI, Pucovsky V. Smooth muscle cells and interstitial cells of blood vessels. Cell Calcium. 2004;35(6):643–57.
105. Pucovsky V, Moss RF, Bolton TB. Non-contractile cells with thin processes resembling interstitial cells of Cajal found in the wall of guinea-pig mesenteric arteries. J Physiol. 2003;552(Pt 1):119–33.
106. Ghose D, Jose L, Manjunatha S, Rao MS, Rao JP. Inherent rhythmicity and interstitial cells of Cajal in a frog vein. J Biosci. 2008;33(5):755–9.
107. Morel E, Meyronet D, Thivolet-Bejuy F, Chevalier P. Identification and distribution of interstitial Cajal cells in human pulmonary veins. Heart Rhythm. 2008;5(7):1063–7.
108. Komuro T, Burnstock G. The fine structure of smooth muscle cells and their relationship to connective tissue in the rabbit portal vein. Cell Tissue Res. 1980;210(2):257–67.
109. Povstyan OV, Gordienko DV, Harhun MI, Bolton TB. Identification of interstitial cells of Cajal in the rabbit portal vein. Cell Calcium. 2003;33(4):223–39.
110. Hermsmeyer K. Multiple pacemaker sites in spontaneously active vascular muscle. Circ Res. 1973;33(2):244–51.
111. Harhun MI, Gordienko DV, Povstyan OV, Moss RF, Bolton TB. Function of interstitial cells of Cajal in the rabbit portal vein. Circ Res. 2004;95(6):619–26.
112. Heberlein KR, Straub AC, Isakson BE. The myo-endothelial junction: breaking through the matrix? Microcirculation. 2009;16(4):307–22.
113. von der Weid PY, Van Helden DF. Functional electrical properties of the endothelium in lymphatic vessels of the guinea-pig mesentery. J Physiol. 1997;504(Pt 2):439–51.
114. Roizes S, von der Weid P-Y. Oubain blocks EDNO-mediated relaxation in mesenteric veins and EDHF-mediated relaxation in mesenteric arteries of the guinea pig. In: Vanhoutte PM, editor. EDHF 2002. Boca Raton, FL: CRC Press; 2005. p. 297–306.
115. Yokoyama S, Ohhashi T. Effects of acetylcholine on spontaneous contractions in isolated bovine mesenteric lymphatics. Am J Phys. 1993;264(5 Pt 2):H1460–4.
116. Reeder LB, Yang LH, Ferguson MK. Modulation of lymphatic spontaneous contractions by EDRF. J Surg Res. 1994;56(6):620–5.
117. von der Weid PY, Crowe MJ, Van Helden DF. Endothelium-dependent modulation of pacemaking in lymphatic vessels of the guinea-pig mesentery. J Physiol. 1996;493(Pt 2):563–75.
118. Ignarro LJ, Gold ME, Buga GM, Byrns RE, Wood KS, Chaudhuri G, et al. Basic polyamino acids rich in arginine, lysine, or ornithine cause both enhancement of and refractoriness to formation of endothelium-derived nitric oxide in pulmonary artery and vein. Circ Res. 1989;64(2):315–29.
119. Gao Y, Zhou H, Raj JU. Endothelium-derived nitric oxide plays a larger role in pulmonary veins than in arteries of newborn lambs. Circ Res. 1995;76(4):559–65.
120. Gao Y, Raj JU. Role of veins in regulation of pulmonary circulation. Am J Physiol Lung Cell Mol Physiol. 2005;288(2):L213–26.
121. Shimokawa H. 2014 Williams Harvey Lecture: importance of coronary vasomotion abnormalities-from bench to bedside. Eur Heart J. 2014;35(45):3180–93.
122. Dunham EW, Haddox MK, Goldberg ND. Alteration of vein cyclic 3′:5′ nucleotide concentrations during changes in contractility. Proc Natl Acad Sci U S A. 1974;71(3):815–9.
123. Morgan SJ, Deshpande DA, Tiegs BC, Misior AM, Yan H, Hershfeld AV, et al. β-Agonist-mediated relaxation of airway smooth muscle is protein kinase A-dependent. J Biol Chem. 2014;289(33):23065–74.
124. von der Weid PY, Van Helden DF. Beta-adrenoceptor-mediated hyperpolarization in lymphatic smooth muscle of guinea pig mesentery. Am J Phys. 1996;270(5 Pt 2):H1687–95.
125. Chan AK, von der Weid PY. 5-HT decreases contractile and electrical activities in lymphatic vessels of

the guinea-pig mesentery: role of 5-HT 7-receptors. Br J Pharmacol. 2003;139(2):243–54.
126. Hosaka K, Rayner SE, von der Weid PY, Zhao J, Imtiaz MS, van Helden DF. Calcitonin gene-related peptide activates different signaling pathways in mesenteric lymphatics of guinea pigs. Am J Physiol Heart Circ Physiol. 2006;290(2):H813–22.
127. Norel X. Prostanoid receptors in the human vascular wall. ScientificWorldJournal. 2007;7:1359–74.
128. Foudi N, Kotelevets L, Louedec L, Leseche G, Henin D, Chastre E, et al. Vasorelaxation induced by prostaglandin E2 in human pulmonary vein: role of the EP4 receptor subtype. Br J Pharmacol. 2008;154(8):1631–9.
129. Mironneau J, Martin C, Arnaudeau S, Jmari K, Rakotoarisoa L, Sayet I, et al. High-affinity binding sites for [3H]saxitoxin are associated with voltage-dependent sodium channels in portal vein smooth muscle. Eur J Pharmacol. 1990;184(2–3):315–9.
130. Cuthbert AW, Sutter MC. The effects of drugs on the relation between the action potential discharge and tension in a mammalian vein. Br J Pharmacol Chemother. 1965;25(3):592–601.
131. Yatani A, Seidel CL, Allen J, Brown AM. Whole-cell and single-channel calcium currents of isolated smooth muscle cells from saphenous vein. Circ Res. 1987;60(4):523–33.
132. Loirand G, Mironneau C, Mironneau J, Pacaud P. Two types of calcium currents in single smooth muscle cells from rat portal vein. J Physiol. 1989;412:333–49.
133. Arnaudeau S, Boittin FX, Macrez N, Lavie JL, Mironneau C, Mironneau J. L-type and Ca2+ release channel-dependent hierarchical Ca2+ signalling in rat portal vein myocytes. Cell Calcium. 1997;22(5):399–411.
134. Saleh SN, Greenwood IA. Activation of chloride currents in murine portal vein smooth muscle cells by membrane depolarization involves intracellular calcium release. Am J Physiol Cell Physiol. 2005;288(1):C122–31.
135. Wareing M, Bai X, Seghier F, Turner CM, Greenwood SL, Baker PN, et al. Expression and function of potassium channels in the human placental vasculature. Am J Physiol Regul Integr Comp Physiol. 2006;291(2):R437–46.
136. Mauricio MD, Serna E, Cortina B, Novella S, Segarra G, Aldasoro M, et al. Role of Ca2+-activated K+ channels on adrenergic responses of human saphenous vein. Am J Hypertens. 2007;20(1):78–82.
137. Brayden JE. Functional roles of KATP channels in vascular smooth muscle. Clin Exp Pharmacol Physiol. 2002;29(4):312–6.
138. Kajioka S, Kitamura K, Kuriyama H. Guanosine diphosphate activates an adenosine 5′-triphosphate-sensitive K+ channel in the rabbit portal vein. J Physiol. 1991;444:397–418.
139. Noack T, Edwards G, Deitmer P, Weston AH. Potassium channel modulation in rat portal vein by ATP depletion: a comparison with the effects of levcromakalim (BRL 38227). Br J Pharmacol. 1992;107(4):945–55.
140. Kamouchi M, Kitamura K. Regulation of ATP-sensitive K+ channels by ATP and nucleotide diphosphate in rabbit portal vein. Am J Phys. 1994;266(5 Pt 2):H1687–98.
141. Zhang HL, Bolton TB. Two types of ATP-sensitive potassium channels in rat portal vein smooth muscle cells. Br J Pharmacol. 1996;118(1):105–14.
142. Yamamoto T, Takahara K, Inai T, Node K, Teramoto N. Molecular analysis of ATP-sensitive K(+) channel subunits expressed in mouse portal vein. Vasc Pharmacol. 2015;75:29–39.
143. Sakurai T, Terui N. Effects of sympathetically induced vasomotion on tissue-capillary fluid exchange. Am J Physiol Heart Circ Physiol. 2006;291(4):H1761–7.
144. Nilsson H, Aalkjaer C. Vasomotion: mechanisms and physiological importance. Mol Interv. 2003;3(2):79–89, 51.
145. Koenigsberger M, Sauser R, Seppey D, Beny JL, Meister JJ. Calcium dynamics and vasomotion in arteries subject to isometric, isobaric, and isotonic conditions. Biophys J. 2008;95(6):2728–38.
146. van Helden DF, Imtiaz MS. Ca2+ phase waves emerge. Physiol News. 2003;52:7–11.

14 Role of Pericytes in the Initiation and Propagation of Spontaneous Activity in the Microvasculature

Hikaru Hashitani and Retsu Mitsui

Abstract

The microvasculature is composed of arterioles, capillaries and venules. Spontaneous arteriolar constrictions reduce effective vascular resistance to enhance tissue perfusion, while spontaneous venular constrictions facilitate the drainage of tissue metabolites by pumping blood. In the venules of visceral organs, mural cells, i.e. smooth muscle cells (SMCs) or pericytes, periodically generate spontaneous phasic constrictions, Ca^{2+} transients and transient depolarisations. These events arise from spontaneous Ca^{2+} release from the sarco-endoplasmic reticulum (SR/ER) and the subsequent opening of Ca^{2+}-activated chloride channels (CaCCs). CaCC-dependent depolarisation further activates L-type voltage-dependent Ca^{2+} channels (LVDCCs) that play a critical role in maintaining the synchrony amongst mural cells. Mural cells in arterioles or capillaries are also capable of developing spontaneous activity. Non-contractile capillary pericytes generate spontaneous Ca^{2+} transients primarily relying on SR/ER Ca^{2+} release. Synchrony amongst capillary pericytes depends on gap junction-mediated spread of depolarisations resulting from the opening of either CaCCs or T-type VDCCs (TVDCCs) in a microvascular bed-dependent manner. The propagation of capillary Ca^{2+} transients into arterioles requires the opening of either L- or TVDCCs again depending on the microvascular bed. Since the blockade of gap junctions or CaCCs prevents spontaneous Ca^{2+} transients in arterioles and venules but not capillaries, capillary pericytes appear to play a primary role in generating spontaneous activity of the microvasculature unit. Pericytes in capillaries where the interchange of substances between tissues and the circulation takes place may provide the fundamental drive for upstream arterioles and downstream venules so that the microvasculature network functions as an integrated unit.

Keywords

Microvasculature · Pericyte · Sarco-endoplasmic reticulum Ca^{2+} release · Ca^{2+}-activated chloride channel · Voltage-dependent Ca^{2+} channel · Intercellular coupling

Electronic Supplementary Material The online version of this chapter (https://doi.org/10.1007/978-981-13-5895-1_14) contains supplementary material, which is available to authorized users.

H. Hashitani (✉) · R. Mitsui
Department of Cell Physiology, Graduate School of Medical Sciences, Nagoya City University, Nagoya, Japan
e-mail: hasitani@med.nagoya-cu.ac.jp

H. Hashitani, R. J. Lang (eds.), *Smooth Muscle Spontaneous Activity*, Advances in Experimental Medicine and Biology 1124, https://doi.org/10.1007/978-981-13-5895-1_14

14.1 Introduction

The function of circulation is to serve the tissue demands to maintain an appropriate environment for cellular activity. The rate of blood flow in individual tissues can be substantially varied, and is precisely regulated corresponding to the activity of cells within each tissue. The microvasculature of each tissue, consisting of arterioles, capillaries and venules, functions as an integrated unit to maintain microcirculation. The microcirculation serves to regulate regional blood flow and capillary perfusion, thereby ensuring the delivery of oxygen and nutrients to meet the spatiotemporal dynamics in local metabolic demands as well as the removal of cellular metabolites.

Arterioles are considered to play a predominant role in controlling the vascular resistance and hence the distribution and rate of blood flow into individual tissues, while substance exchange between blood and tissues primarily occurs across the wall of capillaries. Thus, there must be intrinsic mechanisms for transmitting the metabolic state of the tissue to the upstream arteriolar contractility, which determines arteriolar diameter. In arterioles, locally evoked vasomotor responses, i.e. both vasoconstriction and vasodilatation, conduct bidirectionally over distances by the spread of electrical signals via gap junctions, indicating that arteriolar networks function as a coordinated syncytium [1, 2]. Physiologically, the conducted vasomotor responses originate from capillaries, where metabolic demands occur and are promptly sensed, and spread to their upstream arterioles to adjust blood flow of the arterioles to meet the tissue demands [3, 4]. Furthermore, capillary perfusion in different regions within each tissue is precisely regulated to meet the energetic demands of neighbouring metabolically active cells, and thus there is a considerable heterogeneity of capillary perfusions even within the same tissue [5–7].

There is growing evidence indicating that capillaries play a more active role in regulating regional blood flow than previously thought. Thus, capillary pericytes in several vascular beds of the central nervous system (CNS) are contractile and play an active role in regulating capillary diameter and their blood flow [8–11]. In addition, the dilatory signals generated in capillary pericytes spread to upstream arterioles to facilitate capillary perfusion [9, 12]. Thus, capillary pericytes may well sense neighbouring neuronal activity or metabolic conditions and regulate the contractility of capillaries as well as the upstream arterioles resulting in functional hyperaemia. Similarly, the propagated vasodilatation originating from capillaries is the mechanism underlying active hyperaemia matching blood supply to meet metabolic demands of skeletal muscle during exercise [3, 4, 13].

In the microvasculature of visceral organs, the mechanisms in regulating vascular contractility have been investigated mostly in the arterioles, particularly focusing on their neuronal or endothelial regulation [14–16], while those in capillaries or venules are less understood. Since capillary filtration and reabsorption are functions of hydrostatic pressure that is determined by the gradient of arteriolar and venular pressures, the determinant of the capillary exchange is changes in the contractile properties of not only arterioles but also venules [17–19]. As the microcirculation in visceral organs is substantially affected by extravascular factors, e.g. rises in the intraluminal pressure of the organs, compression by luminal contents or organ wall distension, it may have intrinsic contractile properties to resist such extravascular influences. Indeed, in visceral organs that undergo considerable wall distensions or rises in the luminal pressure upon filling, e.g. urinary bladder [20–23], stomach [24–26], colon [27] or rectum [28], the microvasculature displays spontaneous, periodic Ca^{2+} transients, transient depolarisations and corresponding phasic constrictions. Thus, it is envisaged that spontaneous activity of the microvasculature network in visceral organs plays a fundamental role in maintaining the microcirculation.

14.2 Spontaneous Vasomotion

In many vascular beds, periodical oscillations in vascular diameter and/or tone, known as spontaneous vasomotion, arise from cycles of

spontaneous phasic contraction and relaxation in vascular smooth muscles both in vivo and in vitro [29–32]. Since the early study of Jones [33], properties of spontaneous vasomotion in veins or venules of the bat wing in vivo have been extensively studied [34, 35]. Spontaneous vasomotion in vivo has also been investigated in a variety of other arteriolar or arterial vascular beds, including arterioles in hamster skin fold window preparations [36], arterioles in rabbit skeletal muscle [37], cerebral arterioles of rabbit [38], rat basilar arteries [39] and hamster cheek pouch arterioles [40]. More recently, oscillatory vasomotion and associated Ca^{2+} signals in SMCs of ear arterioles are simultaneously recorded using transgenic mice which express the fluorescence resonance energy transfer (FRET)-based Ca^{2+}/myosin light-chain kinase (MLCK) biosensor [41].

In both intact and isolated vessels of the bat wing, similar patterns of rhythmic venous vasomotion are observed [34], indicating that vasomotion is generated within the vascular wall as an intrinsic property. In the cerebral microvasculature of rabbit, variations in vessel diameter occur simultaneously in adjacent arterioles and venules [38], suggesting that vasomotion in different microvascular segments is driven by local factors that may include a common pacemaker site. In this microvasculature unit, smaller vessels are much more resistant to the effects of anaesthesia that abolishes spontaneous vasomotion in larger vessels (>50 μm). In rabbit skeletal muscle, after the release of an occlusion, vasomotion reappears much earlier in the first-order side branches than in their feeding transverse arterioles [37]. Thus, spontaneous vasomotion may originate from peripheral microvascular segments and then spread to central segments.

Isolated arterial or arteriolar segments are also capable of developing spontaneous phasic contractions, supporting the notion that spontaneous vasomotion seen in vivo is generated within the vascular wall. Spontaneous phasic contractions are preferentially demonstrated in arterioles or smaller arteries such as rat ideal arterioles [42, 43], several arterioles of hamster [44] and rat basilar arteries [45]. A unique study using a rabbit head-mounted preparation in which the neural control of ocular blood flow is eliminated, perfused choroidal arterioles in situ develop spontaneous vasomotion [46]. Oscillatory phasic contractions can be induced in arteries from various vascular beds by vasoconstrictor agonists, such as rat mesenteric arteries (noradrenaline [47], phenylephrine [48]), rabbit mesenteric arteries (phenylephrine) [49] or rabbit ear resistance arteries (histamine) [50], suggesting that even quiescent arterial segments have the potential to develop oscillatory activity but require an external stimulus.

When changes in the membrane potential or intracellular Ca^{2+} concentrations are recorded simultaneously with vascular contractions, spontaneous phasic contractions are associated or preceded by oscillatory electrical or Ca^{2+} activity [42, 45, 51–54]. Nifedipine-sensitive spontaneous slow waves or action potentials are generated in vivo in hamster cheek pouch arterioles [51]. In the same preparation, cycling of intracellular Ca^{2+} concentration precedes their corresponding diameter reductions [55]. In isolated rat basilar arteries, nifedipine abolishes spontaneous rhythmical depolarisations and contractions [45]. In contrast, spontaneous slow waves, Ca^{2+} transients and corresponding contractions in rat iridial arterioles are not inhibited by nifedipine [42]. Vasomotion and intracellular Ca^{2+} oscillations in these arterioles are voltage independent and appear to result from the cyclical release of Ca^{2+} from inositol 1,4,5-trisphosphate ($InsP_3$)-sensitive stores. Thus, the Ca^{2+} source and membrane ion channels underlying spontaneous vasomotion vary considerably amongst different vascular beds.

There appears to be a gradation in the occurrence of spontaneous vasomotion in different microvascular segments, in which spontaneous vasomotion is more prevalent in smaller vascular segments. In human pial arteries, 75% of the vessels with a diameter of less than 200 μm generate spontaneous electrical activity, while only 35% of the vessels with a diameter >200 μm are spontaneously active [52]. Thus, spontaneous depolarisations and associated Ca^{2+} transients are also more prevalent in smaller vascular segments.

Taken together, the propagation of spontaneous transient depolarisations from the peripheral to central vascular segments appears to be the mechanism underlying spontaneous vasomotion [1, 2, 54]. Of particular interest is whether capillaries that have a close communication with neighbouring metabolically active cells may drive the spontaneous activity in other microvascular segments.

14.2.1 Spontaneous Activity in Different Microvascular Segments

The microvasculature network can be divided into five segments, i.e. arterioles, precapillary arterioles (PCA), capillaries, postcapillary venules (PCV) and venules, and there are heterogeneity and transition in mural cells of different microvascular segments [56, 57]. Arterioles are surrounded by densely packed, circumferentially arranged vascular SMCs, while venules are covered by stellate-shaped pericytes or spindle-shaped SMCs. PCAs, capillaries and PCVs are covered by morphologically distinct pericytes that have a typical 'bump-on-a-log' appearance with processes extending from their soma. These morphological characteristics of the mural cells in different microvascular units are ubiquitously demonstrated in ureteric microvascular networks [58] or the CNS [59, 60] by the fluorescence labelling of specific marker proteins of the mural cells or genetically engineering mural cell-specific expression of fluorescent marker proteins. Widely used markers for pericytes include platelet-derived growth factor receptor β (PDGFRβ), a transmembrane protein; neuron-glial antigen 2 (NG2), also known as chondroitin sulphate proteoglycan 4 (CSPG4); desmin, an intracellular intermediate filament; or α-smooth muscle actin (α-SMA) [56]. Morphological properties of mural cells in different microvascular segments, including pericytes, have also been revealed by scanning electron microscopy in several vascular beds [61–63]. Thus, different segments of the microvasculature network can be identified by the morphology of the mural cells present.

NG2-DsRed mice express a red fluorescent protein variant (DsRed.T1) under the control of NG2 chondroitin sulphate proteoglycan 4 (Cspg4) promoter [64]. In the bladder suburothelium of NG2-DsRed mice, the NG2-DsRed fluorescence localises in mural cells of arterioles and branched capillaries forming an extensive tree-like network [20]. Staining of endothelium with endothelial markers, e.g. CD31, endothelial nitric oxide synthase (eNOS) or von Willebrand factor (vWF), allows the visualization of the whole microvasculature network including NG2 (−) segments. The extensive network of NG2 (+) pericyte-wrapped capillaries is located just beneath the urothelium, while the arteriole-capillary tree covered by NG2 (+) pericytes or SMCs is distributed in the lamina propria facing the detrusor smooth muscle layer. Circumferentially arranged arteriolar SMCs express strong NG2-DsRed fluorescence, while no NG2-DsRed fluorescence is detected in the pericytes of venules running in parallel. NG2 (+) pericytes in PCAs have a typical 'bump-on-a-log' appearance with an oval-shaped soma extending circumferentially arranged processes. In capillaries, NG2 (+) pericytes also have a bump-on-a-log appearance with an oval-shaped soma but extend bipolar longitudinal processes running along the capillaries. Inter-pericyte distance is larger in capillaries than PCAs, and thus the density of pericytes in capillaries is less compared with PCAs as in the case of the rat retina [65]. Pericytes in PCVs have a short oval-shaped soma with extending processes and expressing a faint NG2-DsRed fluorescence. Similar NG2 expression patterns in different microvascular segments have been demonstrated by immunohistochemical studies of fixed bladder suburothelium using NG2 antibodies where arteriolar SMCs and capillary pericytes but not venular pericytes express NG2 [21, 66]. Desmin staining reveals the morphology of not only NG2 (+) mural cells, but also stellate-shaped NG2 (−) pericytes in venules (Fig. 14.1).

NG2 (+) pericytes in PCAs develop highly synchronous spontaneous Ca^{2+} transients, while NG2 (+) pericytes in capillaries that have a larger soma length exhibit nearly synchronous or propagated spontaneous Ca^{2+} transients at a simi-

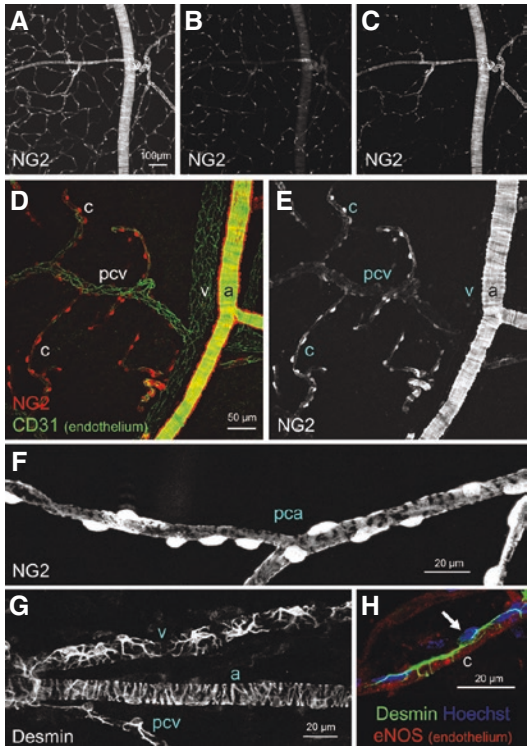

Fig. 14.1 Morphology of mural cells in different microvascular segments. (**A**) NG2 (+) mural cells in the microvascular network of NG2-DsRed mouse bladder mucosa. Extracted single-plane images of the same area show an extensive network of pericyte-covered capillaries distributed just beneath the urothelium (**B**), while arteriolar tree branching capillaries located in the outermost part of the suburothelium (**C**). (**D**, **E**) In a suburothelial microvascular network, endothelium is visualised by endothelium marker CD31 (green). Arteriolar SMCs express a strong NG2-DsRed signal (red, a), while no fluorescence is detected in venular pericytes (v). Capillary pericytes (c) also express a strong NG2-DsRed signal, while pericytes in PCV (pcv) show a faint NG2-DsRed signal. (**F**) NG2 (+) pericytes in a PCA (pca) have an oval cell body with extending circumferentially arranged processes. (**G**) Stellate-shaped pericytes in a venule (v) and a PCV (pcv) are revealed by desmin immunohistochemistry, while an arteriole (a) is covered by circumferentially arranged SMCs. A pericyte is visualised by its immunoreactivity for desmin (green) on a capillary where endothelium is stained by nitric oxide synthase immunoreactivity (eNOS, red). Nuclear staining with Hoechst (blue) indicates the pericyte cell body (arrow) with extending longitudinally oriented bipolar long processes. The scale bar in (**A**) also refers to (**B**, **C**), and the scale bar in (**D**) also refers to (**E**)

lar frequency [20]. Within a capillary network, spontaneous Ca^{2+} transients in NG2 (+) capillary pericytes propagate from one to another over an inter-pericyte distance of up to 50 µm. In a PCA tree containing several capillaries, Ca^{2+} transients in the capillary pericytes spread into the 'trunk' PCA triggering Ca^{2+} transients in PCA pericytes as well as pericytes in other capillary branches. Despite the generation of temporally correlated spontaneous Ca^{2+} transients in pericytes of the connected capillaries and PCAs, SMCs in connected arterioles remain quiescent. Both NG2 (+) pericytes in PCVs and NG2 (−) pericytes in venules also exhibit propagated spontaneous Ca^{2+} transients at a similar frequency. At the junction of PCVs and venules, Ca^{2+} transients in PCV pericytes spread into venules to trigger Ca^{2+} transients in venular pericytes and vice versa, and thus pericytes in connected PCVs and venules generate temporally correlated Ca^{2+} transients (Fig. 14.2).

In several vascular beds where capillary pericytes are not spontaneously active, oscillatory Ca^{2+} transients and/or membrane depolarisations in pericytes can be evoked upon stimulation with neurotransmitters or humoral substances, e.g. acetylcholine (ACh) [67], angiotensin II [68] or arginine vasopressin [58], suggesting that even quiescent capillary pericytes have a potential oscillator that could be activated by physiological factors, e.g. neurohumoral substances, metabolic conditions or mechanical stimuli.

In the regions of the gastrointestinal (GI) tract that undergo wall stretch and/or compression during accommodation of their luminal content, mural cells in different microvascular segments develop spontaneous activity. In the submucosa of rat stomach, circumferentially arranged SMCs in venules [25] and pericytes in PCVs [26] generate spontaneous nearly synchronous Ca^{2+} transients, while arteriolar SMCs remain quiescent. In the myenteric layer of the guinea pig stomach, pericytes in capillaries and/or PCAs develop spontaneous nearly synchronous Ca^{2+} transients that spread into their connected arterioles to trigger synchronous Ca^{2+} transients in arteriolar SMCs [24]. In the submucosa of the rat rectum, both pericytes in PCAs and SMCs in the venules exhibit spontaneous Ca^{2+} transients [28]. Thus, the identification of the mural cells developing spontaneous Ca^{2+} transients in different microvascular segments varies amongst different microvascular beds.

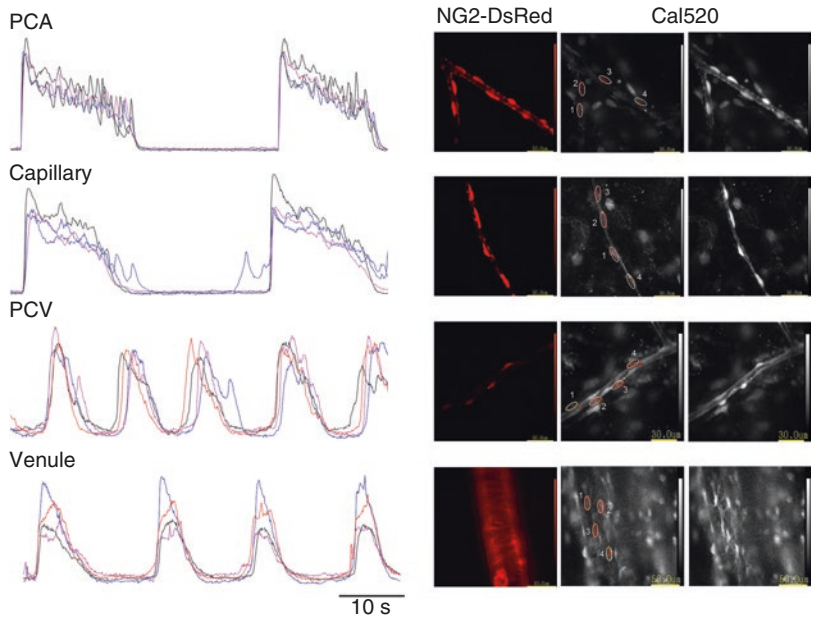

Fig. 14.2 Spontaneous Ca^{2+} transients in different microvascular segments. NG2 (+) pericytes in PCAs of the NG2-DsRed mouse bladder develop synchronous spontaneous Ca^{2+} transients lasting about 20 s. NG2 (+) pericytes in capillaries develop nearly synchronous spontaneous Ca^{2+} transients. PCV pericytes expressing a faint DsRed fluorescence generate propagated spontaneous Ca^{2+} transients lasting about 10 s. NG2 (−) venular pericytes generate propagated spontaneous Ca^{2+} transients. The timescale bar refers to all traces. Images of NG2 DsRed fluorescence (left row) and Cal520 florescence (middle row, resting; right row, Ca^{2+} transients) in pericytes of PCA, capillary, PCV and venule. Note that NG2 (−) venular pericytes but not NG2 (+) arteriolar SMCs generate spontaneous Ca^{2+} transients. In each trace, spontaneous Ca^{2+} transients shown in different colours were recorded from four pericytes shown in the corresponding Cal 520 image

14.2.2 Contractility of Different Microvascular Segments

Arterioles or venules are surrounded by contractile SMCs, while PCAs, capillaries and PCVs are covered by morphologically distinct pericytes. Pericytes in PCAs and PCVs express α-SMA and are contractile, while capillary pericytes are often not stained by α-SMA immunohistochemistry or actin staining using fluorescently labelled phalloidin [58, 59, 69, 70], thus displaying a hierarchy of α-SMA expression in mural cells of microvascular trees [71]. Nevertheless, capillary pericytes in several vascular beds of the CNS, e.g. brain and retina [8, 9, 11] or heart [72], are contractile and play an active role in regulating capillary diameter and their blood flow. A recent study employing a technique to prevent filamentous actin depolymerisation demonstrated α-SMA expression in capillary pericytes of the retina [73]. Thus, actin polymerisation and depolymerisation in capillary pericytes may be dynamic, and a lack of α-SMA detection in fixed preparations does not necessarily mean non-contractile cells.

In different microvascular segments of bladder suburothelium of NG2-DsRed mice, α-SMA is strongly expressed in NG2 (+) arteriolar SMCs and pericytes in PCAs, as well as NG2 (−) venular pericytes where spontaneous Ca^{2+} transients are associated with vasoconstrictions [20]. The morphological characteristics of venular pericytes are consistent with those of other vascular beds, having a stellate-shaped appearance due to their extensive processes [58, 74] and a NG2 (−), α-SMA (+) phenotype [69]. In contrast, no α-SMA expression is evident in NG2 (+) pericytes in capillaries that are not con-

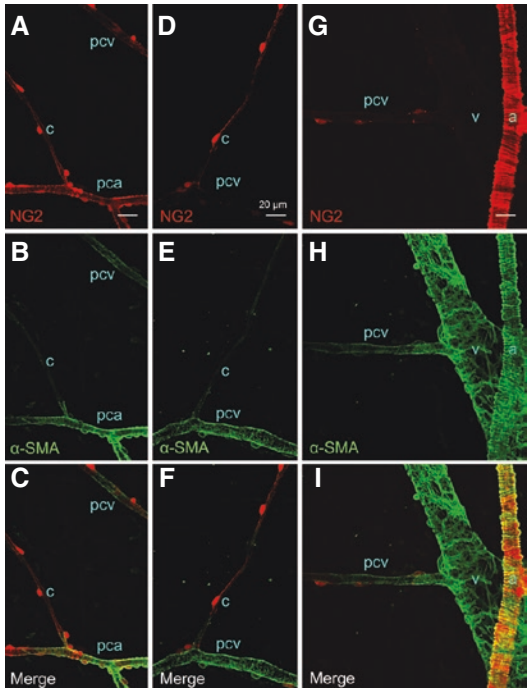

Fig. 14.3 α-SMA expression in mural cells of different microvascular segments. (**A**–**C**) NG2 (+) pericytes (red) in a PCA (pca) of the NG2-DsRed mouse bladder express α-smooth muscle actin (α-SMA) immunoreactivity (green), while NG2 (+) pericytes in a capillary (c) branching from the PCA are α-SMA (−). NG2 (+) pericytes in a PCV (pcv) express faint α-SMA immunoreactivity. (**D**–**F**) NG2 (+) pericytes in a PCV (pcv) but not those in a connecting capillary (c) exhibit α-SMA immunoreactivity. (**G**–**I**) NG2 (−) pericytes in a venule (v) show strong α-SMA-immunoreactivity, while NG2 (+) pericytes in a connecting PCV (pcv) exhibit weaker α-SMA-immunoreactivity. NG2 (+) SMCs in an arteriole (a) show strong α-SMA immunoreactivity. The scale bar in (**A**) = 20 µm also refers to (**B**–**I**)

tractile. NG2 (+) contractile pericytes in distal PCVs express α-SMA, but their α-SMA expression and contractility gradually diminish in PCVs as their diameters decrease. Similar heterogeneity in the α-SMA expression and contractility is reported in the microvascular units of the CNS [59, 70]. Thus, 'non-contractile' capillary pericytes in the bladder suburothelium may function as a driver of other contractile segments to regulate capillary blood flow rather than having their own contractile machinery to alter capillary diameter (Fig. 14.3).

In the rat bladder suburothelium, spontaneous venular constrictions predominately arise through synchronous Ca^{2+} transients and associated contractions of spindle-shaped SMCs, while stellate-shaped pericytes also exhibit spontaneous Ca^{2+} transients resulting in constrictions. In the venular segments where these SMCs and pericytes are co-localised, they display synchronous Ca^{2+} transients suggesting that they are coupled with each other. Pericytes have been considered to be multipotent precursors for several different cell types, including SMCs [56, 75], and thus there seems to be a transition from pericyte-enveloped to SMC-enveloped venules, presumably to meet functional demands.

Submucosal venules of rat proximal stomach [25], distal colon [27] and rectum [28] develop spontaneous phasic constrictions. Unlike the suburothelial venules of the mouse bladder [20, 21], the contractile mural cells in the submucosal venules of these microvascular beds are circumferentially arranged SMCs, not stellate-shaped pericytes. Stellate-shaped pericytes in PCVs of the proximal stomach exhibit spontaneous Ca^{2+} transients that are associated with spontaneous vasomotion [26], while PCAs in the rectum exhibit spontaneous Ca^{2+} transients that are seldom associated with vasoconstrictions [28]. In the myenteric layer of the guinea pig stomach, spontaneous synchronous Ca^{2+} transients in pericytes of capillaries and/or PCAs are not associated with constrictions, while synchronous Ca^{2+} transients in arteriolar SMCs result in spontaneous constrictions upon the blockade of endogenous NO production [24]. Thus, there seems to be heterogeneity of mural cells that develop spontaneous Ca^{2+} transients with or without contractility in different microvascular beds of visceral organs.

14.2.3 Origin of Spontaneous Activity

In the bladder suburothelium of NG2-DsRed mice, NG2 (+) pericytes in the connected PCA and capillaries generate synchronous spontaneous Ca^{2+} transients at the same frequency [20].

Since the blockade of gap junctions prevents Ca^{2+} transients in the PCA but not capillaries, pericytes in capillaries appear to drive PCA pericytes to generate their Ca^{2+} transients. However, in a PCA tree with several branching capillaries, the 'driver' capillary switches randomly from one capillary to another with time, suggesting that active capillaries that initiate spontaneous Ca^{2+} transients do not generally maintain their dominance in vitro. In vivo, it is envisaged that the dominance of a particular 'driver' capillary is determined by its local metabolic activity, adjusting the capillary blood flow to meet energetic demands in the area it supplies. In the myenteric microvasculature network of the guinea pig stomach, synchronous spontaneous Ca^{2+} transients are also initiated in the pericyte-covered capillaries and spread into connected SMC-wrapped arterioles [24]. Imaging the cerebral microvasculature in vivo shows that capillary dilatation in response to the excitation of vasodilatory neurons precedes arteriolar dilatation, suggesting that hyperpolarising signals initiated in capillary pericytes may spread to arteriolar SMCs to facilitate capillary perfusion [9]. This notion is supported by electrophysiological experiments in the retina demonstrating the upstream spread of K_{ATP} current generated in capillaries [12]. Depolarisations induced by current injection into capillary pericytes in the retina are also effectively transmitted to not only pericytes within the capillary network but also arterioles via gap junctions [76]. Capillary pericytes in visceral organs may well sense local metabolic conditions to generate spontaneous Ca^{2+} transients and associated depolarisations that are transmitted to PCA pericytes and arteriolar SMCs in which the activation of LVDCCs results in oscillatory constrictions of the mural cells.

Spontaneous Ca^{2+} transients in capillary pericytes do not consistently spread into connected PCA pericytes, suggesting that there may be gating functions at the junctions between capillaries and PCAs [20]. Studies on the retinal microvasculature indicate that the axial electrotonic voltage transmission is highly efficient, particularly in capillaries, but significant voltage dissipation occurs at branching points [76]. Although specialised units of SMCs located at arterial bifurcations may serve as originators of rhythmic vasomotion in the microvasculature of kidney and skin [77, 78], this is not the case in the capillary-arteriolar network of the mouse bladder suburothelium [20] or the guinea pig stomach myenteric layer [24]. Thus, capillary pericytes appear to act as driver cells generating spontaneous Ca^{2+} transients and associated depolarising signals that entrain PCA pericytes as well as arteriolar SMCs to develop nearly synchronous Ca^{2+} transients in mural cells of these microvasculature units. Since pericytes in capillaries are often non-contractile, measurements of vascular diameter changes without their Ca^{2+} or electrical signals may conclude that spontaneous vasomotion originates from bifurcations where mural cells switch from non-contractile pericytes to contractile pericytes or SMCs. Interestingly, a higher density of LVDCCs is expressed in the bifurcations compared with non-branching segments [78], and thus the bifurcations may function as converters of driving electrical signals originating from capillary pericytes into contractile signals in PCAs and arterioles.

The termination of spontaneous Ca^{2+} transients at the PCA-arteriolar junction of the bladder suburothelium is likely to be due to the more hyperpolarised membrane potential of arteriolar SMCs (around −70 mV) [20], and thus there may be a relatively abrupt drop in the membrane potentials at the junction between the PCA and the arterioles. Blockade of inward rectifier K^+ channels (Kir) with Ba^{2+} depolarises the membrane by about 30 mV, suggesting that inward rectifier K^+ channels play a fundamental role in stabilising SMC excitability. In the pericyte-containing retinal microvasculature, hyperpolarisations generated by the opening of weakly rectifying Kir channels in pericytes located in the proximal segments spread to distal segments [65]. A recent study in mouse bladder feed arterioles demonstrated that the arteriolar SMC membrane potential remains about −70 mV irrespective of intraluminal pressure [79]. In the feed arterioles, blockade of these Kir channels restores pressure-induced constriction and membrane depolarisation. Voltage dissipation at the

branch point between a capillary and its tertiary arteriole is also evident in the retinal microvasculature [76]. In the myenteric microvasculature network of the guinea pig stomach, low-threshold TVDCCs appear to be functionally expressed [24]. Either Ca^{2+} entry or depolarisations upon the opening of TVDCCs would amplify spontaneous Ca^{2+} transients and in turn Ca^{2+}-dependent depolarisation, and thus permit the spread of Ca^{2+} transients in PCA pericytes into arteriolar SMCs.

Spontaneous Ca^{2+} transients in the microvasculature of visceral organs are not affected by tetrodotoxin, guanethidine or phentolamine, indicating that they occur independently of nerves, more specifically sympathetic nerve activity [21, 22, 24, 25, 27, 28]. In the myenteric microvasculature, comparison of spontaneous Ca^{2+} transients in myenteric interstitial cells of Cajal (ICC-MY) with those in neighbouring microvessels indicates that there are no temporal correlation [24]. Thus, Ca^{2+} transients in capillary pericytes or arteriolar SMCs occur independently of ICC, well-established pacemaker cells electrically driving SMCs in the GI tract [80]. Furthermore, pericytes or SMCs of the myenteric microvasculature and perivascular interstitial cells are not immunoreactive for Kit receptor, the universal marker for ICC [80]. Therefore, neither ICC nor Kit-positive interstitial cells found in other visceral organs act as pacemakers driving the spontaneous Ca^{2+} transients in the visceral microvasculature. Perivascular Ca^{2+}-activated K^+ channel SK3 (+) fibroblast-like cells [80] also fire asynchronous spontaneous Ca^{2+} transients but have no temporal correlation with microvascular Ca^{2+} transients. Therefore, spontaneous activity in microvasculature originates within the mural cells themselves, more specifically capillary pericytes.

14.3 Cytosolic Calcium Oscillators

Cytosolic Ca^{2+} oscillators arising from the cyclic release and uptake of Ca^{2+} by the sarcoendoplasmic reticulum (SR/ER) function as a ubiquitous mechanism underlying smooth muscle pacemaking. While the uptake of Ca^{2+} into SR/ER is exclusively mediated by sarcoendoplasmic reticulum Ca^{2+}-ATPase (SERCA), two distinct Ca^{2+} release channels, i.e. $InsP_3$ receptors and ryanodine receptors (RYRs), are involved in the Ca^{2+} release from SR/ER. Thus, $InsP_3$ receptors, Ca^{2+} release channels in SR/ER membranes, play a predominant role in the spontaneous Ca^{2+} release in ICC of the GI tract [80–82] and lymphatic SMCs [83, 84]. In comparison, interstitial cells of the urethra, atypical SMCs in renal pelvis and some arteriolar SMCs have Ca^{2+} stores that function to a varying extent through both ryanodine and $InsP_3$ receptors to develop spontaneous activity [31, 85, 86].

Spontaneous Ca^{2+} transients in pericytes or SMCs in the microvascular of visceral organ segments are abolished by cyclopiazonic acid (CPA), an inhibitor for SERCA, indicating that Ca^{2+} handling by SR/ER plays a primary role in the initiation of the spontaneous Ca^{2+} transients [87]. Thus, uptake and release from SR/ER Ca^{2+} stores are well established as a ubiquitous mechanism underlying spontaneous vasomotion in arterioles or arteries [29, 31].

In the suburothelial venules of rat and mouse bladders, spontaneous Ca^{2+} transients in both pericytes and SMCs are abolished by caffeine [88] or 2-aminoethoxydiphenylborane (2-APB) that is known to block $InsP_3$-induced Ca^{2+} release, or U73122, a phospholipase C (PLC) inhibitor, but not ryanodine, suggesting that $InsP_3$ receptors rather than RYRs play a predominant role in generating the spontaneous Ca^{2+} release from SR/ER [21, 22]. 2-APB but not tetracaine, a blocker for Ca^{2+}-induced Ca^{2+} release (CICR) via RYRs [89], prevents spontaneous Ca^{2+} transients and associated constrictions in submucosal venules of the rat stomach [25], indicating that mechanisms underlying spontaneous activity of the intestinal venules are basically similar to those of suburothelial venules of the bladder (Fig. 14.4).

In contrast, both caffeine and tetracaine inhibit spontaneous Ca^{2+} transients in PCAs and capillaries of the bladder suburothelium [20] and the myenteric microvasculature of stomach [24], suggesting that not only $InsP_3$-induced Ca^{2+} release but also CICR via RYRs are involved in the spontaneous Ca^{2+} release from SR/ER. In

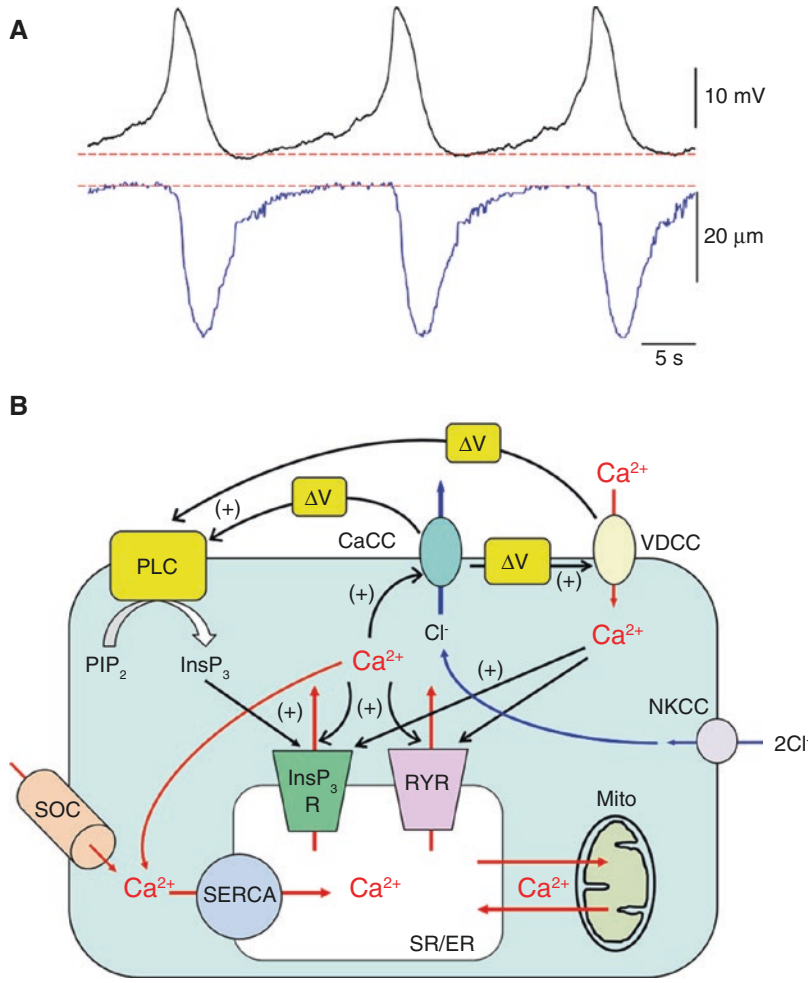

Fig. 14.4 Cytosolic Ca^{2+} oscillator in mural cells. (**A**) Simultaneous recording of spontaneous action potentials and vasoconstrictions (shown as reductions in vascular diameter) in venules of the rat bladder suburothelium. The temporal relationship between electrical and mechanical activities indicates that cytosolic Ca^{2+} oscillator generates rhythms but requires LVDCC activation to contract mural cells. (**B**) Mural cells, i.e. pericytes or SMCs, operate a 'cytosolic Ca^{2+} oscillator' primarily arising from Ca^{2+} release from SR/ER via inositol trisphosphate receptors ($InsP_3Rs$). Ryanodine receptor (RYRs) may also contribute to Ca^{2+}-induced Ca^{2+} release (CICR) from SR/ER. Increased cytosolic Ca^{2+} causes openings of Ca^{2+}-activated Cl^- channels (CaCCs) resulting in Cl^- efflux to depolarise the membrane (ΔV). Na^+–K^+–$2Cl^-$ co-transporter (NKCC) may contribute to the maintenance of relatively high cytosolic Cl^- concentration. The depolarisation (ΔV) triggers the opening of voltage-dependent Ca^{2+} channels (VDCCs) to induce Ca^{2+} influx that would be amplified by CICR via $InsP_3Rs$ and RYRs. The depolarisation (ΔV) may also stimulate $InsP_3$ production to facilitate 'cytosolic Ca^{2+} oscillator'. Reduction in sarco-endoplasmic reticulum (SR/ER) Ca^{2+} content triggers Ca^{2+} influx via store-operated Ca^{2+} channels (SOCs) that will be taken up via SR/ER Ca^{2+}-ATPase (SERCA) to refill SR/ER. Ca^{2+} shuttling between SR/ER and mitochondria (Mito) may also be involved in maintaining 'cytosolic Ca^{2+} oscillator'. Arrows in red indicate flows of Ca^{2+}. Arrows in blue indicate flows of Cl^-. Arrows in black indicate stimulating action. Note that this schema is a montage of various mural cells, and thus does not mean ubiquitous mechanisms amongst spontaneously active mural cells

submucosal PCAs of the rat rectum, caffeine at 20 mM but not 1 mM abolishes spontaneous Ca^{2+} transients [28]. In guinea pig urethra, caffeine 1 mM abolishes slow waves but not spontaneous transient depolarisations (STDs), while caffeine 10 mM blocks both slow waves and STDs, suggesting that 10 mM caffeine is required to deplete ryanodine-sensitive stores [90]. Besides

caffeine and 2-APB that are known to exert multiple cellular targets in Ca^{2+} signalling pathway, tetracaine also inhibits $InsP_3$-mediated Ca^{2+} release that does not activate subsequent CICR via RYRs in isolated colonic myocytes [91]. Therefore, caution must be paid to discriminate between $InsP_3$-induced and RYR-mediated Ca^{2+} release using these pharmacological blockers.

Besides the periodical cycle of SR/ER Ca^{2+} handling, Ca^{2+} influx via SKF96365-sensitive presumably store-operated Ca^{2+} entry channels (SOCs) but not sodium calcium exchangers (NCX) is required in maintaining spontaneous activity of the suburothelial venules of the bladder [21] and submucosal venules of the colon [27]. In pericytes of the rat descending vasa recta, angiotensin II induces oscillatory depolarisations and associated Ca^{2+} transients that appear to be maintained by Ca^{2+} release from ryanodine-sensitive stores and SKF96365-sensitive SR/ER refilling, i.e. SOCs [92]. Extracellular Ca^{2+} influx via a pathway other than LVDCCs and TVDCCs is also required to maintain the cytosolic Ca^{2+} oscillator in pericytes distributed in the myenteric layer of the stomach, as both synchronous and asynchronous Ca^{2+} transients are abolished by nominally Ca^{2+}-free solution [24]. This is in contrast to the pacemaking mechanism of interstitial cells of the urethra that relies on Ca^{2+} influx via NCX and not SOCs [93, 94]. In addition, Ca^{2+} handling by mitochondria may also be involved in the operation of cytosolic Ca^{2+} oscillators underlying spontaneous venular constrictions in the mouse bladder suburothelium [21] as has been demonstrated in ICC in the GI tract [95], interstitial cells in the urethra [96] or atypical SMCs in the renal pelvis [97].

14.4 Synchrony Amongst Mural Cells

A common mechanism underlying pericyte synchronisation is coupled oscillators arising from the reciprocal interaction between Ca^{2+} release from SR/ER and membrane depolarisations. Ca^{2+} released from SR/ER triggers the opening of Ca^{2+}-activated chloride (CaCCs) or cation channels to generate depolarisations. The depolarisations facilitate voltage-dependent $InsP_3$ production that induces regenerative Ca^{2+} release resulting in larger depolarisations. The Ca^{2+}-activated depolarisations also activate VDCCs to cause larger depolarisations as well as Ca^{2+} influx that trigger CICR. This has been proposed in lymphatics [83], arteries and arterioles [31, 98] and gastric antrum [99].

Coupled oscillator mechanisms require membrane depolarisation linked with SR/ER Ca^{2+} release. In pericytes of suburothelial venules of the bladder [21, 22] or venular SMCs in the stomach submucosa [26], this appears to be mediated by depolarisation associated with the opening of LVDCCs that cause Ca^{2+} influx to activate SR/ER Ca^{2+} release through CICR. Spontaneous SR/ER Ca^{2+} release opens CaCCs, the resultant depolarisation triggering the opening of LVDCCs and associated Ca^{2+} influx to cause venular constrictions. Such a primary role of CaCCs in electromechanical coupling in pericytes has been demonstrated in other vascular beds [67, 100].

In contrast, TVDCCs undertake a similar role in maintaining the synchrony amongst myenteric capillary pericytes or their spread into arteriolar SMCs [24]. Functional coupling between TVDCCs and SR/ER Ca^{2+} release to drive pacemaker mechanisms has been reported in ICC of the GI tract [101, 102]. Interestingly, in interstitial cells of the guinea pig prostate, Ca^{2+} influx through TVDCCs but not LVDCCs stimulates CaCCs, suggesting a tight coupling of TVDCCs with SR/ER Ca^{2+} release [103].

In microvascular units of the bladder suburothelium, capillary pericytes and a population of PCV pericytes appear to function as 'driver cells' that are capable of operating spontaneous cytosolic Ca^{2+} oscillator linked with membrane CaCCs. Pericytes in the descending vasa recta and retina have CaCCs associated with cyclic oscillations in $[Ca^{2+}]_i$ [68, 100]. In contrast, 'driven' pericytes in PCAs and venules also have their own cytosolic Ca^{2+} oscillator but require the input of depolarisation from 'driver cells'. This notion is supported by the fact that SMCs or pericytes in a variety of vascular beds are not spontaneously active, but are capable of generating oscillatory activity upon agonist stimulation or LVDCC activation [29, 31, 58].

14.4.1 Role of L-Type Voltage-Dependent Ca^{2+} Channels (LVDCCs)

Blockers of LVDCCs largely suppress spontaneous Ca^{2+} transients in venular mural cells and also disrupt their synchrony amongst the mural cells of the bladder suburothelium, indicating that LVDCCs play a critical role in maintaining intercellular coupling [21, 22]. Because of the regenerative nature of LVDCC activation, spontaneous action potentials generated in any mural cells within their network readily spread to 'electrically coupled' mural cells irrespective of their length constant (Fig. 14.5).

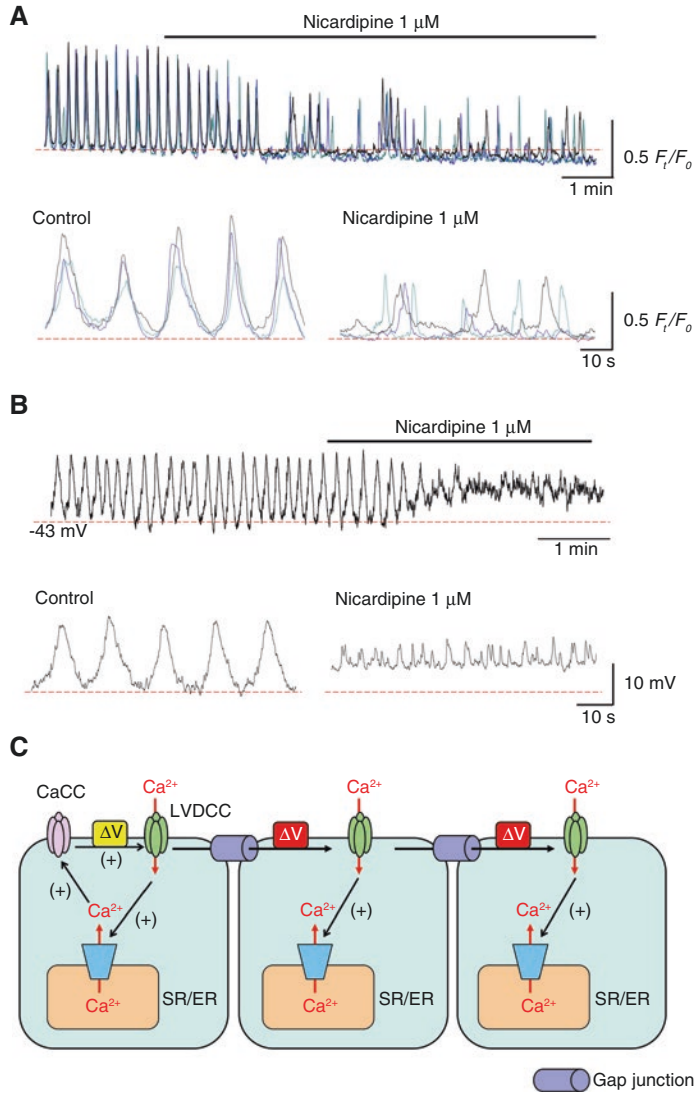

Fig. 14.5 LVDCC-dependent coupled oscillators. (**A**) In suburothelial venules of mouse bladder where synchronous spontaneous Ca^{2+} transients are periodically generated (control), nicardipine (1 μM), an LVDCC blocker, suppresses spontaneous Ca^{2+} transients and disrupts their synchrony. (**B**) In suburothelial venules where pericytes periodically generate slow waves (control), nicardipine (1 μM) depolarises the membrane and prevents the slow-wave generation leaving spontaneous transient depolarisations (STDs). (**C**) Spontaneous SR/ER Ca^{2+} release in a mural cell triggers the opening of CaCCs resulting in membrane depolarisation (ΔV in yellow). This depolarisation triggers the opening of LVDCCs to cause the firing of 'regenerative' action potentials (ΔV in red) spreading into adjacent mural cells via gap junctions. The Ca^{2+} influx via LVDCCs triggers nearly synchronous Ca^{2+}-induced Ca^{2+} release in electrically coupled mural cells to synchronise cytosolic Ca^{2+} oscillators amongst mural cells

Spontaneous action potentials are recorded from mural cells of the rat bladder suburothelial venules and invariably precede their associated phasic constrictions [22]. Blockers for LVDCCs largely suppress the action potentials leaving small fluctuations of the membrane potential, and prevent the associated constrictions. The Ca^{2+} influx during action potentials would be amplified by CICR to trigger the constrictions, and thus electromechanical coupling upon the opening of LVDCCs plays a fundamental role in spontaneous venular constriction. In the venules of mouse bladder suburothelium, slow waves are recorded from venular pericytes [20]. LVDCC blockade prevents periodical slow-wave generation revealing the presence of STDs (Fig. 14.5).

Blockade of LVDCCs suppresses spontaneous Ca^{2+} transients and also disrupts synchrony amongst the venular SMCs [25] or PCV pericytes [26] of the rat stomach submucosa, indicating that LVDCCs play a critical role in promoting intercellular coupling of mural cells. In PCA or PCV pericytes of the mouse bladder suburothelium, LVDCC blockade disrupts the synchrony of spontaneous Ca^{2+} transients in a manner reversed by Bay K8644, an LVDCC activator, confirming the fundamental role of LVDCCs in maintaining the synchrony amongst mural cells [20].

In the rat retinal microvasculature, LVDCC currents are recorded from capillary pericytes that express α1C subunit of LVDCCs, although their current density is much smaller compared with that of arteriolar SMCs [104]. Consistently, capillary pericytes are capable of developing nifedipine-sensitive Ca^{2+} transients in response to an increase in extracellular K^+ concentration. In pericytes of descending vasa recta, diltiazem, an LVDCC blocker, suppresses the plateau phase of angiotensin II-induced Ca^{2+} transients, while Bay K8644 itself constricts the microvessels [105].

In marked contrast to spontaneous Ca^{2+} transients in contractile mural cells of the venules in the bladder suburothelium [20–22] or the submucosa of stomach [25, 26], blockade of LVDCCs does not disrupt either the generation or the synchrony of Ca^{2+} transients in capillary pericytes in myenteric layer of the guinea pig stomach [24]. LVDCC blockade also fails to disrupt the synchrony amongst PCA pericytes in the rat rectum [28] and capillary pericytes in the mouse bladder suburothelium [20]. In the retinal microvasculature, arteriolar SMCs but not capillary pericytes relax during hyperpolarisations, suggesting that LVDCCs play a minimal role in establishing the basal Ca^{2+} concentration of capillary pericytes [12]. Thus, the relative contribution of LVDCCs to Ca^{2+} transients in the microvasculature appears to vary amongst vascular beds and also exhibit regional differences even within a microvascular network [69].

14.4.2 Role of T-Type Voltage-Dependent Ca^{2+} Channels (TVDCCs)

In the myenteric microvasculature of the guinea pig stomach, blockers of TVDCCs abolish synchronous spontaneous Ca^{2+} transients in arteriolar SMCs, and also disrupt the synchrony amongst pericytes in capillaries/PCAs [24]. Thus, TVDCCs appear to play a fundamental role in maintaining the intercellular coupling between pericytes as well as the spread of pericyte Ca^{2+} transients into arteriolar SMCs.

TVDCCs are low-threshold channels that open at membrane potentials as negative as −70 mV [106]. The window current for TVDCCs usually occurs over membrane potentials, which are more hyperpolarised than those for LVDCCs (e.g. TVDCCs, −65 to −45 mV c.f. LVDCCs, −30 to 0 mV) [107]. Since the reported values of the resting membrane potential of retinal or renal pericytes range between −60 and −50 mV [68, 100], window currents for TVDCCs in pericytes may well contribute to these cells establishing voltage-dependent coupling. Pericytes in myenteric capillaries are capable of generating spontaneous, asynchronous Ca^{2+} transients that do not rely on either LVDCCs or TVDCCs, and thus the asynchronous Ca^{2+} transients arising from spontaneous SR/ER Ca^{2+} release appear to be primary events. Nevertheless, resultant STDs by the opening Ca^{2+}-activated chloride or cation channels may not be large enough to electrically couple the pericytes with each other, and thus require the subsequent activation of TVDCCs. In the PCA pericytes of the rat rectum, TVDCC blockade slows spontaneous Ca^{2+} transients without disrupting their synchrony

[28], while TVDCC blockade has no obvious effect on spontaneous Ca^{2+} transients in capillary pericytes of the mouse bladder suburothelium [20]. In both microvasculature, the synchrony of spontaneous Ca^{2+} transients appears to exclusively rely on the spread of CaCC-dependent depolarisations. Thus, differences in the contribution of TVDCCs to spontaneous activity are evident in various vascular beds or different vascular segments within a microvasculature tree.

TVDCCs are functionally expressed in arterial and arteriolar SMCs and their relative contribution, cf. LVDCCs, to the whole-cell Ca^{2+} current and/or vascular contractility appears to increase as the vessel size decreases [108]. In rat cerebral arteries, nifedipine-resistant, mibefradil-sensitive currents comprise about 20% of Ca^{2+} current in SMCs of main arteries and some 45% of the Ca^{2+} current in SMCs of their branches [109]. Consistently, nifedipine-resistant, mibefradil-sensitive components of pressure-induced vascular tone increase with decreasing vessel size [109]. In rat mesentery, conducted vasoconstriction of the arterioles (luminal diameter <40 μm) in vivo relies exclusively on TVDCCs in accordance with the expression of TVDCC α_{1G} and α_{1H}, but not LVDCC α_{1C} subunits [110]. Depolarisation-induced Ca^{2+} transients in isolated mesenteric arterioles (luminal diameter 10–25 μm) also predominantly depend on TVDCCs [111]. The relative presence of TVDCC channels (cf. LVDCCs) in freshly isolated vascular SMCs increases dramatically along the lower branches of the guinea pig mesenteric artery, rising to almost 100% in submucosal arterioles [112]. To date, functional expression of TVDCCs in pericytes has not been observed, although expression of $Ca_V3.1$ (α_{1G}) or $Ca_V3.2$ (α_{1H}) subunits in pericyte-covered rat outer medullary vasa recta has been reported [113].

14.4.3 Role of Ca^{2+}-Activated Chloride Channels (CaCCs)

In capillaries of the mouse bladder suburothelium, the synchrony of LVDCC/TVDCC-resistant Ca^{2+} transients is disrupted by DIDS, a known blocker of CaCCs, suggesting that CaCCs play a critical role in maintaining their synchrony [20]. A similar role of CaCCs has been reported in PCA pericytes of the rat rectal submucosa, where the synchrony of LVDCC/TVDCC-resistant Ca^{2+} transients is disrupted by lowering extracellular chloride ion concentration [28]. In pericytes of the rat descending vasa recta, AT II induces oscillatory depolarisations resulting from the opening of CaCCs [68, 92]. In the rat retina, spontaneous transient inward currents resulting from the opening of CaCCs are recorded from about 70% of freshly isolated pericytes [100]. The fundamental role of CaCCs but not LVDCCs is also proposed in the irideal arterioles [43] where voltage-independent coupled oscillators may be operating to generate vasomotion [31].

In other microvascular beds where LVDCCs play a predominant role in maintaining synchrony amongst mural cells, blockers for CaCCs suppress phasic constrictions associated with a dilatation, suggesting that depolarisations resulting from the opening of CaCCs trigger the subsequent opening of LVDCCs [21, 25–28]. Consistently, in suburothelial venules of the rat bladders, LVDCC-dependent spontaneous action potentials are blocked by CaCC blockers [22]. In the venules of mouse bladder suburothelium, blockade of CaCCs with niflumic acid, another blocker of CaCCs, largely suppresses STDs associated with a membrane hyperpolarisation, suggesting that CaCCs contribute to not only the generation of STDs but also the relatively depolarised membrane potentials [20]. Since levcromakalim, a K_{ATP} channel opener, hyperpolarises the venular membrane and also prevents the generation of slow waves without leaving STDs, the relatively depolarised membrane due to the opening of CaCCs appears to be fundamental in generating spontaneous Ca^{2+} transients presumably by constitutive, voltage-dependent $InsP_3$ production [83, 98].

Interestingly, the blockade of either CaCCs or gap junctions invariably prevents the generation of spontaneous Ca^{2+} transients in PCAs or venules, but not capillaries or PCVs of the mouse bladder suburothelium [20]. Thus, the capillary pericytes appear to be located upstream of PCA pericytes in terms of the generation of spontaneous Ca^{2+} transients, while PCV pericytes may also be capable of driving downstream venular pericytes (Fig. 14.6).

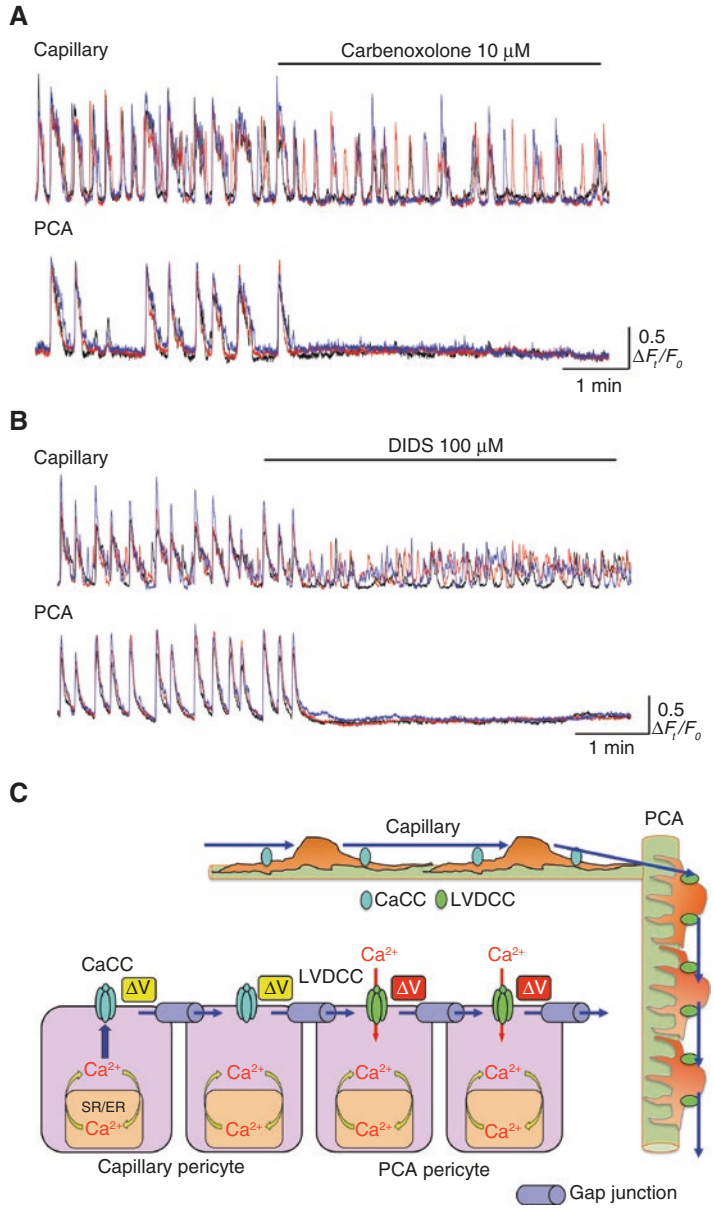

Fig. 14.6 Role of CaCC and gap junction in the synchrony of mural cells. (**A**) In a capillary-PCA network of the mouse bladder suburothelium, simultaneous recording demonstrates nearly synchronous spontaneous Ca^{2+} transients in pericytes of capillaries and connected PCA. Note that some Ca^{2+} transients generated in capillary fail to trigger PCA Ca^{2+} transients. Carbenoxolone (10 μM), a gap junction blocker, prevents the generation of PCA Ca^{2+} transients while disrupting the synchrony of capillary Ca^{2+} transients. (**B**) Similarly, DIDS (100 μM), a CaCC blocker, also prevents spontaneous Ca^{2+} transients in PCA while disrupting the synchrony of Ca^{2+} transients amongst capillary pericytes. (**C**) Capillary pericytes acting as 'driver cells' operate 'cytosolic Ca^{2+} oscillator' relying on spontaneous SR/ER Ca^{2+} handling to generate CaCC-dependent depolarisations (ΔV in yellow) that are sufficiently effective to electrically couple capillary pericytes with each other. PCA pericytes are driven by a spread of the depolarisation (ΔV in yellow) originated from capillary pericytes via gap junctions that activate (LVDCCs). The spread of 'regenerative' depolarisations (ΔV in red) is required for electrical coupling of PCA pericytes with each other

ICC in the GI tract expresses transmembrane member 16A (TMEM16A)/anoctamin-1 (Ano1) CaCCs [114, 115]. In the myenteric microvasculature of the stomach, TMEM16A/Ano1 immunofluorescence is detected in ICC-MY but not in the mural cells of microvasculature [24]. In the mouse small intestine, pericytes associated with the microvasculature near the myenteric plexus express cation-permeable, maxi-anion channels and are not immunoreactive for Ano1 [116]. Thus, the Ca^{2+}-activated inward currents that trigger the opening of TVDCCs in myenteric pericytes remain to be established. Interestingly, in the rat stomach submucosa, T16Ainh-A01 that blocks TMEM16A channels expressed in HEK293 cells prevents spontaneous phasic constrictions in the venules or PCVs, despite the lack of TMEM16A expression in the mural cells [25]. Thus, CaCCs expressed in venular or PCV mural cells may be TMEM16B, not TMEM16A. In rat mesenteric small arteries both in vivo and in vitro, siRNA-induced TMEM16A knockdown preferentially suppresses the amplitude but not frequency of noradrenaline-induced vasomotion [117].

Cl^- accumulation in mural cells of gastric PCV is fundamental for the Cl^- efflux upon CaCC opening resulting in membrane depolarisations. In the rabbit small intestine where ICC-MY expresses Na^+–K^+–$2Cl^-$ co-transporter (NKCC), bumetanide or furosemide, NKCC inhibitors, shortens and supresses the plateau phase of pacemaker potentials attributed to the opening of CaCCs [118]. In the PCV of rat stomach submucosa, bumetanide or furosemide reduces the amplitude of pericyte Ca^{2+} transients without affecting their synchrony or frequency [26]. Thus, other Cl^- accumulation mechanisms such as anion exchangers may also maintain a relatively high intracellular Cl^- concentration in the microcirculation.

14.4.4 Coupling Pathways

In capillaries of the mouse bladder suburothelium, gap junction blockade disrupts or diminishes the synchrony of Ca^{2+} transients in capillary pericytes, indicating that capillary pericytes communicate with each other via gap junctions [20]. Blockade of gap junctions also effectively disrupts the synchrony of Ca^{2+} transients in pericytes of PCVs in the rat stomach [26] or PCAs in the rat rectum [28]. In venules of the mouse bladder suburothelium, electron microscopy demonstrates that pericytes and endothelial cells are frequently in close proximity, although no specialised gap junctions or other junctional structures are evident [21]. Nevertheless, close appositions of pericyte and endothelium membranes are abundant, especially in their processes. Pericyte-endothelial gap junctions have been demonstrated by electron microscopy in human cerebral capillaries [119].

The fundamental role of the endothelium in maintaining intercellular coupling amongst pericytes has been reported in the microvasculature of rat retina [76]. The measured voltage decays between distant mural cells cannot be predicted by a 'homocellular' model in which electrical signals generated in a mural cell spread axially via mural cell-to-mural cell transmissions. Instead a 'heterocellular' model is required. Thus, electrical signals generated in a mural cell spread into the adjacent endothelium via mural cell-to-endothelium transmission and then axially to distant mural cells via endothelium-to-endothelium transmissions. In descending vasa recta of the rat, the endothelial layer also acts as an efficient pathway for an axial transmission between pericytes [120], despite the high-resistance pericyte-endothelial coupling [121]. Lucifer yellow injected into an endothelial cell spreads along the endothelial layer, while the same dye injected into pericytes is restricted to these cells [120]. In vasa recta where pericytes are closely packed along the microvasculature, pericytes themselves are also electrically coupled with each other and capable of maintaining highly coordinated membrane potentials without the endothelium [122]. Nevertheless, in capillaries where the pericytes are more sparsely located, the tip of the elongated process of two adjacent pericytes comes within close proximity, but does not contact or overlap [123]. Thus, electrical coupling between capillary pericytes is predominantly mediated via the

underlying endothelium as each pericyte process contacts and communicates with multiple endothelial cells.

Endothelial cells in the microvasculature appear to be well coupled to each other and act as a low-resistance pathway of electrical transmission as in the case of SMC-covered arterioles [124]. Thus, spontaneous depolarisation generated in capillary pericytes may be effectively transmitted to electrically remote pericytes via the endothelium, resulting in nearly synchronous or propagated spontaneous activity within the microvascular unit.

14.5 Neurohumoral Modulation

14.5.1 Sympathetic Nerves

In the suburothelium of rat bladder, noradrenaline released from sympathetic nerves activates α-adrenoceptors on venular mural cells to accelerate spontaneous phasic constrictions of the suburothelial venules [23]. After the blockade of α-adrenoceptors, sympathetic nerve stimulation abolishes spontaneous constrictions or reduces their frequency upon the activation of β-adrenoceptors. This inhibition of spontaneous constrictions is largely diminished upon blockade of nitric oxide (NO) production, suggesting that β-adrenoceptors presumably located on the endothelium stimulate NO production. Fluorescence Ca^{2+} imaging reveals that suburothelial venules are covered by a meshwork of spindle-shaped SMCs or stellate-shaped pericytes [22]. In the suburothelium of mouse bladder, scanning electron microscopy reveals that the venules are covered by interconnecting stellate-shaped pericytes [21], while transmission electron microscopy demonstrates that the venular wall consists of a layer of endothelium and adjacent monolayer of pericytes. Thus, neurally released noradrenaline may readily have access to endothelial receptors through inter-process spaces of the pericyte meshwork. α-Adrenoceptors are coupled to Gq/11 proteins which activate PLC to produce $InsP_3$, while cGMP, a second messenger of NO, is known to inhibit $InsP_3R$-induced Ca^{2+} release [125]. Therefore, the sympathetic nerve-mediated changes in the frequency of spontaneous venular constrictions may result from the modulation of $InsP_3R$-induced Ca^{2+} release in venular pericytes. In pericytes of several vascular beds, the binding of neurohumoral substances to G protein-coupled receptors, including α-adrenoceptors, is reported to induce $InsP_3$-induced Ca^{2+} release from the SR/ER [58, 67] (Fig. 14.7).

In the suburothelium of mouse bladder, sympathetic nerve fibres immunoreactive for tyrosine hydroxylase (TH) containing many varicosities, the sites of neurotransmission, are distributed around the arterioles, while their distribution around the venules is less extensive [20, 66]. Sympathetic never excitation evokes rapid Ca^{2+} transients in the arterioles, while slow-onset, long-lasting Ca^{2+} transients are induced in the venules [20]. In nifedipine-treated venules where the synchrony of spontaneous Ca^{2+} transients has been disrupted, sympathetic nerve stimulation evokes synchronous Ca^{2+} transients, suggesting that venular pericytes receive an effective innervation (unpublished observation). Unlike these larger microvascular segments that constrict upon sympathetic nerve excitation, suburothelial PCA-capillary-PCV that are covered by NG2-positive pericytes do not respond to nerve stimulation [20]. Their lack of TH-immunoreactive perivascular sympathetic nerves is consistent with their lack of nerve-evoked Ca^{2+} transients or contractions. Similar innervation patterns in different microvascular segments are reported in the microvascular network of the bat wing that develops spontaneous vasomotion in vivo [126]. An in vivo study in the mesenteric vasculature also demonstrates that arteries, terminal arterioles or veins, but not PCAs, capillaries or venules less than 30 μm in internal diameter, respond to perivascular nerve stimulation [127].

In the myenteric microvasculature of guinea pig stomach, spontaneous Ca^{2+} transients in the SMC-covered arterioles are not affected by nerve stimulation [24]. Consistently, PGP9.5 immunohistochemistry revealed that perivascular nerve fibres are not found along the myenteric microvasculature, whereas perivascular nerve fibres

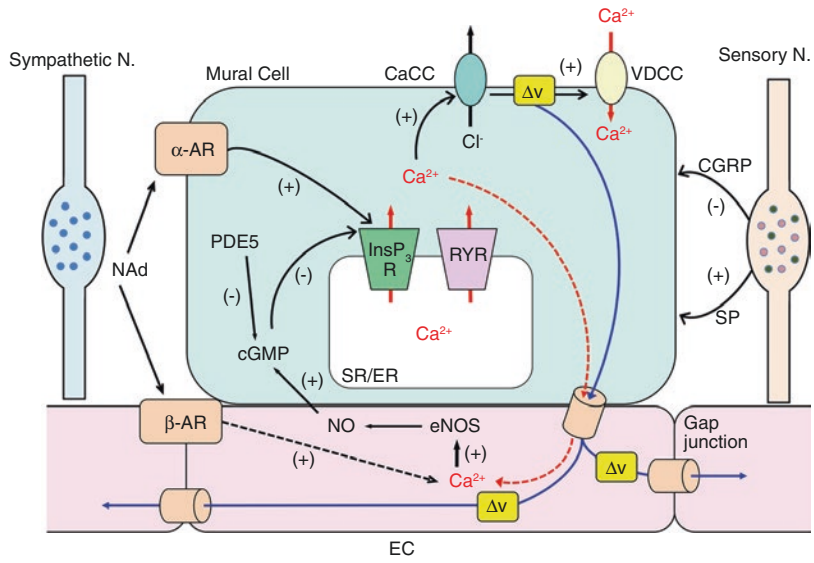

Fig. 14.7 Modulation of mural cell activity. Noradrenaline (NAd) released from sympathetic nerves acting on α-adrenoceptors (αARs) stimulates the production of $InsP_3$ to facilitate SR/ER Ca^{2+} release via $InsP_3R$. Increased cytosolic Ca^{2+} concentration causes CaCC-dependent depolarisation (ΔV) triggering the activation of VDCCs. NAd binding to β-adrenoceptors (βARs) on endothelial cells (ECs) stimulates the production of nitric oxide (NO), presumably by increasing endothelial cytosolic Ca^{2+} concentration. NO increases cGMP in mural cells to inhibit SR/ER Ca^{2+} release via $InsP_3R$. Phosphodiesterase type5 (PDE5) in mural cells breaks down cGMP. CGRP released from sensory nerves has inhibitory actions on mural cells, while substance P exerts excitatory actions. Membrane depolarisations (ΔV) in mural cells readily spread into EC via gap junctions and travel to adjacent ECs. In contrast, increased Ca^{2+} in the cytosol of mural cells may not spread into EC. Arrows and dashed arrows in red indicate flows of Ca^{2+}. Arrows in blue indicate flows of ΔV. Dashed arrows indicate proposed or unidentified signalling pathways. *eNOS* endothelial NO synthase; Note that this schema is a montage of various mural cells, and thus does not mean ubiquitous mechanisms amongst mural cells

containing many varicosities are adjacent to the intramuscular microvasculature. This is in contrast to the microvasculature in the submucosal layer of the stomach and colon where both arterioles and venules are functionally innervated by sympathetic nerves [25, 27]. A 3-D imaging of the 'transparent' mouse small intestine combined with a technique termed 'vessel painting' revealed that TH-positive sympathetic nerve fibres encircle the submucosal arterioles, while TH-positive fibres are intraganglionic, not perivascular in the myenteric layer [128].

Dense bundles of TH-positive sympathetic fibres run along the arterioles, while single varicose sympathetic nerve fibres project to the venules in the submucosal microvasculature of the rat stomach [25] or colon [27]. In the submucosal venules of rat stomach, noradrenaline released from sympathetic nerves induces slow-onset, long-lasting vasoconstriction that is exclusively mediated upon the activation of α-adrenoceptors [25]. Unlike nerve-evoked constrictions of the submucosal arterioles, purinergic transmission is not involved in nerve-mediated venular constrictions [25]. Consistent with this, immunoreactivity of P2X1 purinoceptors is detected in the arterioles, but not in venules running in parallel. In the suburothelial venules of rat bladder, bath-applied ATP or ADP inhibits spontaneous phasic constrictions by stimulating NO release, while α,β-methylene ATP causes vasoconstrictions [23]. Thus, the activation of P2Y receptors, presumably located on the endothelium, appears to result in NO release, while venular mural cells functionally express P2X receptors.

14.5.2 Cholinergic Nerves

In the mouse bladder suburothelium, cholinergic nerve varicosities expressing choline acetyltransferase (ChAT) immunoreactivity run along the arterioles [66]. ChAT-positive fibres are also associated with the suburothelial venules, although the fibre density is sparse compared with the arterioles. Nevertheless, single ChAT-positive varicose nerve fibres are in close proximity with α-SMA-positive mural cells in the venules. In the guinea pig small intestine, ChAT-immunoreactive cholinergic neurons innervating submucosal microvasculature have their cell bodies in the submucosal ganglia [129], and the activation of these neurons evokes dilation of submucosal arterioles [130]. Such cholinergic vasodilatations in the microvasculature of the bladder suburothelium are not evident. Interestingly, in the rat bladder suburothelium, exogenous ACh increases spontaneous phasic constrictions associated with a reduction in venular diameter, but causes NO-dependent dilatation of pre-constricted arterioles [23]. Thus, ACh may not be able to stimulate endothelial NO production in this particular venule.

14.5.3 Sensory Nerves

In submucosal venules of the rat colon that have been pretreated with phentolamine, electrical nerve stimulation induces a suppression of spontaneous venular constrictions associated with a sustained dilatation [27]. Capsaicin also induces similar inhibitory responses, suggesting that transmitter(s) released from primary afferent nerves attenuate the contractility of venular SMCs. Since a calcitonin gene-related peptide (CGRP) receptor antagonist prevents the afferent nerve-induced inhibitory responses, and unmasks capsaicin-induced constrictions, the inhibitory responses are predominantly mediated by CGRP. CGRP-immunoreactive varicose afferent nerves run along the submucosal venules as well as arterioles. CGRP and substance P (SP) are co-localised in varicose nerve fibres projecting to the venules. In the submucosal venules of the rat stomach, capsaicin also induces a suppression of spontaneous phasic constrictions and a dilatation that is blocked by a CGRP antagonist [25] (Fig. 14.7).

In the rat bladder suburothelium, immunohistochemical studies demonstrated that SP- and CGRP-positive nerves ran along the suburothelial arterioles and venules [23]. Despite the lack of afferent nerve-induced modulation of spontaneous venular constrictions, SP predominantly causes venular constriction, while CGRP induces a NO-independent sustained venular relaxation, presumably by stimulating adenylate cyclase in mural cells. SP and CGRP could be released from afferent nerves during inflammation or tissue acidification. In the suburothelium of the mouse bladder, dense SP-immunoreactive nerve fibres run along the mucosal arterioles. At higher magnification, SP-positive nerve varicosities are observed close to arteriolar and venular α-SMA-positive mural cells [66].

14.5.4 Endothelium

In submucosal venules of rat stomach, whose endothelium is nitric oxide synthase (NOS) immunoreactive, spontaneous venular constrictions are accelerated upon blockade of NO production, while ACh suppresses constrictions in a NO-dependent manner [25]. Thus, endothelium-derived NO may increase cGMP in venular SMCs to inhibit $InsP_3$-induced Ca^{2+} release and in turn cytosolic Ca^{2+} oscillations. In submucosal PCVs that also express endothelial NOS immunoreactivity, tadalafil, a phosphodiesterase type 5 (PDE5) inhibitor, supresses spontaneous Ca^{2+} transients in pericytes and disrupts their synchrony, suggesting that endogenous PDE5 activity plays an important role in maintaining spontaneous venular constrictions by counteracting the NO-cGMP pathway [26]. Consistently, tadalafil induces a cessation of spontaneous venular constrictions associated with a dilatation in a manner partially blocked by NOS inhibitors. Pericytes in other vascular beds express soluble guanylate cyclase (sGC) and

protein kinase G (PKG), and NO donor-induced dilatation is prevented upon sGC inhibition [131].

Blockade of NO production increases the frequency of spontaneous phasic constrictions in suburothelial venules of the rat and mouse bladders [21, 22], suggesting that endogenous NO tonically reduces spontaneous constrictions of venular pericytes. Since electron microscopy reveals numerous close appositions of pericyte and endothelial membranes, especially in their processes [21], spontaneous Ca^{2+} transients in pericytes may well spread to the endothelium to increase $[Ca^{2+}]_i$ resulting in the production and release of NO. Indeed, the increased Ca^{2+} and/or $InsP_3$ in arteriolar SMCs may even diffuse into the endothelium to stimulate Ca^{2+}-dependent NO production or the opening of Ca^{2+}-activated K^+ channels resulting in the endothelium-mediated feedback vasodilation [132–134]. In the descending vasa recta of the rat, AT II induces similar depolarisations in pericytes and the endothelium, suggesting electrical coupling via myoendothelial gap junctions [121]. However, AT II increases $[Ca^{2+}]_i$ in pericytes but reduces endothelial $[Ca^{2+}]_i$ [92] suggesting that the increased Ca^{2+} and/or $InsP_3$ in pericytes does not spread into endothelium at least during AT II receptor stimulation. Thus, the Ca^{2+}-mediated interaction between pericytes and endothelium in the microvasculature may not function as a self-limiting mechanism to prevent excessive vasoconstrictions. Nevertheless, it may be possible that spontaneous depolarisation in pericytes transmits to the endothelium to activate TVDCCs to cause Ca^{2+}-dependent NO production as suggested in other vascular preparations [108, 134, 135]. In the myenteric layer of the guinea pig stomach, spontaneous Ca^{2+} transients in arteriolar SMCs are not associated with vasoconstrictions [24]. After blockade of NO production, the spontaneous Ca^{2+} transients result in arteriolar constrictions, suggesting that NO may diminish contractility of arteriolar SMCs via Ca^{2+}-independent mechanisms.

Capillary endothelial cells of the cerebral vasculature express Kir channels [136] while not expressing small- and intermediate-conductance Ca^{2+}-activated K^+ channels that play a predominant role in endothelium-dependent vasodilatation in small arteries or arterioles in other vascular beds [137]. Such unique properties of capillary endothelial cells may well explain the lack of inhibition of spontaneous Ca^{2+} transients in pericytes upon a robust increase in endothelial Ca^{2+} with bath-applied SP in PCVs of mouse bladder suburothelium (unpublished observation). The opening of the endothelial Kir channels upon a rise in local $[K^+]_o$ results in membrane hyperpolarisations that retrogradely spread to cause upstream arteriolar dilatation [136]. Similarly, electrical coupling between pericytes and endothelial cells in visceral microvasculature may allow the spread of the endothelial hyperpolarisations to the adjacent pericytes to suppress spontaneous vasomotion.

14.6 Relevance in Health and Disease

14.6.1 Physiological Aspects

Arteriolar vasomotion is considered to reduce effective vascular resistance and thus enhances tissue perfusion, resulting in the facilitation of capillary-tissue exchanges [19]. Active venular vasomotion produces an increase in the blood flow and exhibits temporal vessel diameter-blood velocity and pressure relationships characteristic of a peristaltic pump [17]. Since capillary filtration and reabsorption are functions of hydrostatic pressure that is determined by the ratio of post- to precapillary resistance, regulation of contractility of ‘upstream’ arterioles and ‘downstream’ venules by capillary pericytes seems to be an ideal mechanism to adjust microcirculation to meet tissue demands.

The urinary bladder is capable of accommodating large volumes of urine with remarkably little increase in intravesical pressure. Since intravesical pressure during bladder filling does not exceed capillary pressure, normal bladders maintain their circulation, so that the blood supply only transiently drops during voiding [138]. Blood vessels in the bladder wall are characterised by their winding arrangement, which pre-

vents them from being stretched in their longitudinal direction during the filling phase [139]. Thus, they are capable of maintaining their diameter so that the resistance against blood flow is not increased. Besides such structural characteristics, the suburothelial microvasculature in the bladder of rat [22, 23] and mouse [20, 21] develops spontaneous phasic constrictions suggesting that it actively contributes to the regulation of the suburothelial microcirculation. Since the bladder suburothelial layer is rich in microvasculature as well as sensory nerves that convey bladder sensation, and is directly exposed to urothelium-derived bioactive substances [140], maintenance of the suburothelial microcirculation is fundamental to ensure normal bladder functions.

In the GI tract, the distribution of blood flow within the GI tract layers is not uniform, and appears to correspond to the metabolic demands of the individual layers [141]. Thus, the mucosal layer receives 70–80% of total blood flow providing nutrients and oxygen to the metabolically active cells, particularly epithelial cells, that maintain the barrier function, absorption as well as secretion. Contractility of large arteries and arterioles (>50 μm in diameter) is primarily under the influence of neural regulation predominantly from sympathetic nerves, while metabolic and paracrine mediators contribute proportionally more to the smaller microvessels [141]. During postprandial hyperaemia, blood flow is substantially shifted to the mucosal layer by capillary recruitment where existing but closed capillaries open. Therefore, contractility of capillary pericytes, if any, and their ability to drive spontaneous vasomotion of the submucosal microvessels may be involved in regulating the mucosal microcirculation.

In the bladder suburothelium, capillary pericytes express NG2 but not α-SMA, and their spontaneous Ca^{2+} transients are not associated with a reduction in capillary diameter, suggesting that 'non-contractile' capillary pericytes drive spontaneous rhythmic vasoconstrictions in 'upstream' arterioles and 'downstream' venules [20]. Capillary pericytes in myenteric microcirculation of the guinea pig stomach also appear to act as 'non-contractile' pacemaker cells to drive 'upstream' arterioles [24]. This is in contrast to pericytes in retinal and cerebral capillaries, which contract upon electrical stimulation or application of excitatory neurotransmitters [8, 9, 11]. Moreover, capillary pericytes in the CNS appear to play a predominant role in vasodilatation to increase capillary perfusion to meet local metabolic demands of active neurons. Such differences in the role of pericytes may reflect fundamental characteristics of different microcirculatory beds. Since both the retinal and cerebral microvasculature are located within organs which are relatively inflexible in terms of their architecture and limited volumes, fine regulation and/or distribution of blood supply may be required. In contrast, in visceral organs that undergo progressive wall distension or wall compression by their luminal contents, simple vasodilatation as seen in the retina and cerebral microcirculation would result in compression or collapse of the microvasculature, particularly in venules where the intraluminal pressure is the lowest. Thus, periodical vasomotions may be more required to maintain microcirculation blood flow. Distension of visceral organs may facilitate pericyte-driven vasomotion by opening transient receptor potential (TRP) channels that could stimulate a cytosolic Ca^{2+} oscillator by Ca^{2+} influx or membrane depolarisation [137], although their roles have not yet been proven in visceral microvasculature. Therefore, pericytes may play different roles in different microcirculatory beds to meet the characteristics of individual organs.

14.6.2 Clinical Implications

Lower urinary tract symptom (LUTS), including a storage symptom, overactive bladder syndrome (OAB), has been recognised as a consequence of ischaemic and reperfusion damage to the cells in the bladder wall, although the precise pathological mechanisms underlying LUTS/OAB remain to be elucidated [142–144]. Since the prevalence of LUTS/OAB increases with ageing or comorbidity on metabolic syndrome that is inevitably

associated with vascular dysfunction, these symptoms are likely to be a manifest of systemic vascular disease as predicted by animal experiments [145, 146]. The beneficial effects of α-adrenoceptor antagonists, β3-adrenoceptor agonists or PDE5 inhibitors on bladder storage symptoms may be attributed to an improvement of the bladder circulation [142, 143]. In fact, these pharmacological agents improve bladder storage function without improving the narrowed luminal diameters of the feeding arteries [142], suggesting that the microcirculation within the bladder wall is the site of initiation of LUTS/OAB. Thus, it is envisaged that the suburothelial microvascular unit maintaining metabolic demands of the urothelium-suburothelium complex plays a critical role in developing LUTS/OAB and provides a potential therapeutic target.

Despite the fact that complaints of dysphagia, dyspepsia, anorexia, constipation or faecal incontinence increase with ageing, the age-related changes in the GI neuromuscular function are relatively mild, and thus the disorder in GI tract motility is not clinically significant in the elderly person unless suffering from comorbidity [147, 148]. Since the mucosal layer of the GI tract receives 70–80% of total blood that preferentially supplies metabolically active epithelial cells, the mucosal functions may more readily manifest the ageing-related vascular dysfunction. In mesenteric arteries of mice in vivo, ageing is associated with a reduction in the basal vascular diameter and a loss of sensory nerve-mediated limitation of sympathetic constrictions, while α1-adrenocetor-mediated constrictions are diminished, demonstrating an ageing-related visceral vascular dysfunction [148]. It remains to be elucidated if the functions of capillary pericytes, particularly their ability to drive spontaneous vasomotion, may also be changed with ageing.

In the normal bladder, intravesical pressure rises during the storage phase are minimal [138], so that it is likely that blood flow in highly pressured segments of the microcirculation, i.e. arteries or arterioles, is well maintained. However, even small rises in the intravesical pressure may readily attenuate low-pressure segments of the microcirculation, i.e. capillaries or venules, resulting in the disturbance of capillary perfusion and venular drainage. Diminished spontaneous phasic constrictions in contractile segments of the microvascular units would also decrease capillary-tissue exchange.

Spontaneous phasic constrictions in arterioles are considered to reduce the blood flow resistance [149]. In retinal arterioles in patients with diabetic retinopathy, diminished vasomotion is associated with the impaired retinal microcirculation [150]. In a mouse model of diabetic retinopathy, diminished connexion43-containing gap junction-mediated pericyte-to-pericyte interactions as well as reduced pericyte coverage resulting in impaired propagated vasomotor responses are reported [151]. A recent study using loss-of-function pericyte-deficient platelet-derived growth factor receptor-β (Pdgfrβ+/−) mice demonstrated that pericyte degeneration diminishes cerebral capillary blood flow responses to nerve stimulation resulting in neurovascular uncoupling, limiting oxygen supply to brain and metabolic stress [152].

Spontaneous venular constrictions are considered to facilitate venular drainage [17]. In skeletal muscle of rats with metabolic syndrome, an increased tone in PCVs and venules is suggested to contribute to the alterations in upstream capillary pressure profiles and in turn the transcapillary exchange [153]. Thus, dysfunction of 'driving' mechanisms of capillary pericytes and/or transmission of 'driving' depolarisations would be a common cause of insufficient tissue oxygenation and/or stagnation of tissue excreta.

In addition, the multipotency of pericytes [56] may contribute to the remodelling of the bladder suburothelium that is commonly seen in an overactive bladder. Increased pericyte coverage associated with their smooth muscle phenotype transformation may contribute to pulmonary vascular remodelling in patients of pulmonary arterial hypertension and a murine retinal angiogenesis model [154]. Thus, increased pericyte number and their phenotype changes may reduce substance exchange across capillary wall by altering contractility of microvasculature and/or reducing capillary endothelial surface area.

There is growing evidence that capillaries or capillary pericytes play a critical role not only in regulating physiological microcirculation but also in the pathology of brain ischemia [9, 152, 155], diabetic retinopathy [151, 156, 157] or cardiac ischemia [72]. No-flow phenomenon after catheterisation treatments of various cerebral or cardiac ischemic diseases appears to be attributable to the rigor mortis in dead capillary pericytes [9, 72, 155]. In the retina, the hyperpolarisations resulting from the opening of ATP-sensitive K^+ (K_{ATP}) channels that are predominantly expressed in capillary pericytes [12] appear to transmit to the upstream arterioles. The hyperpolarisations suppress the activity of LVDCCs that are predominantly expressed in arterioles to increase regional blood flow [104], and thus K_{ATP} channels have a protective role against hypoxic conditions. However, this opening of K_{ATP} channels increases the driving force for Ca^{2+} influx into the pericytes through non-selective cation channels which eventually causes their death in rigor [156]. In the bladder microvasculature, the rigor mortis in dead capillary pericytes may also result in capillary constrictions, although normal pericytes in the capillary appear to be intrinsically non-contractile. Since capillary pericytes express CaCCs, their Ca^{2+} overload would cause sustained depolarisations resulting in constrictions of the electrically connected PCAs or arterioles by activating LVDCCs.

Acknowledgments The authors are grateful for grant support from the Japan Society for Promotion of the Science (JSPS) (Nos. 21659377, 23659763, 26860521, 16K19361).

References

1. Segal SS, Damon DN, Duling BR. Propagation of vasomotor responses coordinates arteriolar resistances. Am J Phys. 1989;256:H832–7.
2. Segal SS, Duling BR. Conduction of vasomotor responses in arterioles: a role for cell-to-cell coupling? Am J Phys. 1989;256:H838–45.
3. Dietrich HH, Tyml K. Capillary as a communicating medium in the microvasculature. Microvasc Res. 1992;43:87–99.
4. Song H, Tyml K. Evidence for sensing and integration of biological signals by the capillary network. Am J Physiol Heart Circ Physiol. 1993;265:H1235–42.
5. Ellis CG, Wrigley SM, Groom AC. Heterogeneity of red blood cell perfusion in capillary networks supplied by a single arteriole in resting skeletal muscle. Circ Res. 1994;75:357–68.
6. Tyml K, Ellis CG, Safranyos RG, Fraser S, Groom AC. Temporal and spatial distributions of red cell velocity in capillaries of resting skeletal muscle, including estimates of red cell transit times. Microvasc Res. 1981;22:14–31.
7. Villringer A, Them A, Lindauer U, Einhäupl K, Dirnagl U. Capillary perfusion of the rat brain cortex. An in vivo confocal microscopy study. Circ Res. 1994;75:55–62.
8. Fernández-Klett F, Offenhauser N, Dirnagl U, Priller J, Lindauer U. Pericytes in capillaries are contractile in vivo, but arterioles mediate functional hyperemia in the mouse brain. Proc Natl Acad Sci U S A. 2010;107:22290–5.
9. Hall CN, Reynell C, Gesslein B, Hamilton NB, Mishra A, Sutherland BA, O'Farrell FM, Buchan AM, Lauritzen M, Attwell D. Capillary pericytes regulate cerebral blood flow in health and disease. Nature. 2014;508:55–60.
10. Mishra A, Reynolds JP, Chen Y, Gourine AV, Rusakov DA, Attwell D. Astrocytes mediate neurovascular signaling to capillary pericytes but not to arterioles. Nat Neurosci. 2016;19:1619–27.
11. Peppiatt CM, Howarth C, Mobbs P, Attwell D. Bidirectional control of CNS capillary diameter by pericytes. Nature. 2006;443:700–4.
12. Ishizaki E, Fukumoto M, Puro DG. Functional K_{ATP} channels in the rat retinal microvasculature: topographical distribution, redox regulation, spermine modulation and diabetic alteration. J Physiol. 2009;587:2233–53.
13. Lamb IR, Novielli NM, Murrant CL. Capillary response to skeletal muscle contraction: evidence that redundancy between vasodilators is physiologically relevant during active hyperaemia. J Physiol. 2018;596:1357–72.
14. Hirst GDS. Neuromuscular transmission in arterioles of guinea-pig submucosa. J Physiol. 1977;273:263–75.
15. Kotecha N, Neild TO. Actions of vasodilator nerves on arteriolar smooth muscle and neurotransmitter release from sympathetic nerves in the guinea-pig small intestine. J Physiol. 1995;489:849–55.
16. Hashitani H, Suzuki H. K^+ channels which contribute to the acetylcholine-induced hyperpolarization in smooth muscle of the guinea-pig submucosal arteriole. J Physiol. 1997;501:319–29.
17. Dongaonkar RM, Quick CM, Vo JC, Meisner JK, Laine GA, Davis MJ, Stewart RH. Blood flow augmentation by intrinsic venular contraction in vivo. Am J Phys Regul Integr Comp Phys. 2012;302:R1436–42.

18. Levick JR. Capillary filtration-absorption balance reconsidered in light of dynamic extravascular factors. Exp Physiol. 1991;76:825–57.
19. Sakurai T, Terui N. Effects of sympathetically induced vasomotion on tissue-capillary fluid exchange. Am J Physiol Heart Circ Physiol. 2006;291:H1761–7.
20. Hashitani H, Mitsui R, Miwa-Nishimura K, Lam M. Role of capillary pericytes in the integration of spontaneous Ca^{2+} transients in the suburothelial microvasculature of the mouse bladder. J Physiol. 2018; 596:3531–52
21. Hashitani H, Mitsui R, Shimizu Y, Higashi R, Nakamura K. Functional and morphological properties of pericytes in suburothelial venules of the mouse bladder. Br J Pharmacol. 2012;167:1723–36.
22. Hashitani H, Takano H, Fujita K, Mitsui R, Suzuki H. Functional properties of suburothelial microvessels in the rat bladder. J Urol. 2011;185:2382–91.
23. Shimizu Y, Mochizuki S, Mitsui R, Hashitani H. Neurohumoral regulation of spontaneous constrictions in suburothelial venules of the rat urinary bladder. Vasc Pharmacol. 2014;60:84–94.
24. Hashitani H, Mitsui R, Masaki S, Van Helden DF. Pacemaker role of pericytes in generating synchronized spontaneous Ca^{2+} transients in the myenteric microvasculature of the guinea-pig gastric antrum. Cell Calcium. 2015;58:442–56.
25. Mitsui R, Hashitani H. Functional properties of submucosal venules in the rat stomach. Pflugers Arch. 2015;467:1327–42.
26. Mitsui R, Hashitani H. Mechanisms underlying spontaneous constrictions of postcapillary venules in the rat stomach. Pflugers Arch. 2016;468:279–91.
27. Mitsui R, Miyamoto S, Takano H, Hashitani H. Properties of submucosal venules in the rat distal colon. Br J Pharmacol. 2013;170:968–77.
28. Mitsui R, Hashitani H. Properties of synchronous spontaneous Ca^{2+} transients in the mural cells of rat rectal arterioles. Pflugers Arch. 2017;469: 1189–202.
29. Aalkjaer C, Nilsson H. Vasomotion: cellular background for the oscillator and for the synchronization of smooth muscle cells. Br J Pharmacol. 2005;144:605–16.
30. Aalkjær C, Boedtkjer D, Matchkov V. Vasomotion—what is currently thought? Acta Physiol (Oxford). 2011;202:253–69.
31. Haddock RE, Hill CE. Rhythmicity in arterial smooth muscle. J Physiol. 2005;566:645–56.
32. Nilsson H, Aalkjaer C. Vasomotion: mechanisms and physiological importance. Mol Interv. 2003;3:79–89.
33. Jones TW. Discovery that the veins of the bat's wing (which are furnished with valves) are endowed with rhythmical contractility, and that the onward flow of blood is accelerated by each contraction. Phil Trans R Soc London. 1852;142:131–6.
34. D'Agrosa LS. Patterns of venous vasomotion in the bat wing. Am J Phys. 1970;218:530–5.
35. Davis MJ, Shi X, Sikes PJ. Modulation of bat wing venule contraction by transmural pressure changes. Am J Phys. 1992;262:H625–34.
36. Colantuoni A, Bertuglia S, Intaglietta M. The effects of alpha- or beta-adrenergic receptor agonists and antagonists and calcium entry blockers on the spontaneous vasomotion. Microvasc Res. 1984;28:143–58.
37. Slaaf DW, Tangelder GJ, Teirlinck HC, Reneman RS. Arteriolar vasomotion and arterial pressure reduction in rabbit tenuissimus muscle. Microvasc Res. 1987;33:71–80.
38. Hundley WG, Renaldo GJ, Levasseur JE, Kontos HA. Vasomotion in cerebral microcirculation of awake rabbits. Am J Phys. 1988;254:H67–71.
39. Fujii K, Heistad DD, Faraci FM. Vasomotion of basilar arteries in vivo. Am J Phys. 1990;258:H1829–34.
40. Bouskela E, Grampp W. Spontaneous vasomotion in hamster cheek pouch arterioles in varying experimental conditions. Am J Phys. 1992;262:H478–85.
41. Fairfax ST, Mauban JR, Hao S, Rizzo MA, Zhang J, Wier WG. Ca^{2+} signaling in arterioles and small arteries of conscious, restrained, optical biosensor mice. Front Physiol. 2014;5:387.
42. Haddock RE, Hirst GD, Hill CE. Voltage independence of vasomotion in isolated irideal arterioles of the rat. J Physiol. 2002;540:219–29.
43. Hill CE, Eade J, Sandow SL. Mechanisms underlying spontaneous rhythmical contractions in irideal arterioles of the rat. J Physiol. 1999;521:507–16.
44. Duling BR, Gore RW, Dacey RGJ, Damon DN. Methods for isolation, cannulation, and in vitro study of single microvessels. Am J Phys. 1981;241:H108–16.
45. Haddock RE, Hill CE. Differential activation of ion channels by inositol 1,4,5-trisphosphate (IP_3)- and ryanodine-sensitive calcium stores in rat basilar artery vasomotion. J Physiol. 2002;545:615–27.
46. Delgado E, Marques-Neves C, Rocha I, Sales-Luís J, Silva-Carvalho L. Endothelin-1 effects on spontaneous oscillations in choroidal arterioles. Acta Ophthalmol. 2010;88:742–7.
47. Gustafsson H, Bülow A, Nilsson H. Rhythmic contractions of isolated, pressurized small arteries from rat. Acta Physiol Scand. 1994;152:145–52.
48. Lamboley M, Schuster A, Bény JL, Meister JJ. Recruitment of smooth muscle cells and arterial vasomotion. Am J Physiol Heart Circ Physiol. 2003;285:H562–9.
49. Omote M, Kajimoto N, Mizusawa H. The role of endothelium in the phenylephrine-induced oscillatory responses of rabbit mesenteric arteries. Jpn J Pharmacol. 1992;59:37–41.
50. Griffith TM, Edwards DH. Fractal analysis of role of smooth muscle Ca^{2+} fluxes in genesis of chaotic arterial pressure oscillations. Am J Phys. 1994;266:H1801–11.
51. Bartlett IS, Crane GJ, Neild TO, Segal SS. Electrophysiological basis of arteriolar vasomotion in vivo. J Vasc Res. 2000;37:568–75.

52. Gokina NI, Bevan RD, Walters CL, Bevan JA. Electrical activity underlying rhythmic contraction in human pial arteries. Circ Res. 1996;78:148–53.
53. Morgan KG. Comparison of membrane electrical activity of cat gastric submucosal arterioles and venules. J Physiol. 1983;345:135–47.
54. Segal SS, Bény JL. Intracellular recording and dye transfer in arterioles during blood flow control. Am J Phys. 1992;263:H1–7.
55. Brekke JF, Jackson WF, Segal SS. Arteriolar smooth muscle Ca^{2+} dynamics during blood flow control in hamster cheek pouch. J Appl Physiol. 2006;101:307–15.
56. Armulik A, Genové G, Betsholtz C. Pericytes: developmental, physiological, and pathological perspectives, problems, and promises. Dev Cell. 2011;21:193–215.
57. Attwell D, Mishra A, Hall CN, O'Farrell FM, Dalkara T. What is a pericyte? J Cereb Blood Flow Metab. 2016;36:451–5.
58. Borysova L, Wray S, Eisner DA, Burdyga T. How calcium signals in myocytes and pericytes are integrated across in situ microvascular networks and control microvascular tone. Cell Calcium. 2013;54:163–74.
59. Hill RA, Tong L, Yuan P, Murikinati S, Gupta S, Grutzendler J. Regional blood flow in the normal and ischemic brain is controlled by arteriolar smooth muscle cell contractility and not by capillary pericytes. Neuron. 2015;87:95–110.
60. Hughes S, Chan-Ling T. Characterization of smooth muscle cell and pericyte differentiation in the rat retina in vivo. Invest Ophthalmol Vis Sci. 2004;45:2795–806.
61. Fujiwara T, Uehara Y. The cytoarchitecture of the wall and the innervation pattern of the microvessels in the rat mammary gland: a scanning electron microscopic observation. Am J Anat. 1984;170:39–54.
62. Shimada T, Kitamura H, Nakamura M. Three-dimensional architecture of pericytes with special reference to their topographical relationship to microvascular beds. Arch Histol Cytol. 1992;55(Suppl):77–85.
63. Zhang JQ, Nagata K, Iijima T. Scanning electron microscopy and immunohistochemical observations of the vascular nerve plexuses in the dental pulp of rat incisor. Anat Rec. 1998;251:214–20.
64. Zhu X, Bergles DE, Nishiyama A. NG2 cells generate both oligodendrocytes and gray matter astrocytes. Development. 2008;135:145–57.
65. Matsushita K, Puro DG. Topographical heterogeneity of K_{IR} currents in pericyte-containing microvessels of the rat retina: effect of diabetes. J Physiol. 2006;573:483–95.
66. Mitsui R, Hashitani H. Immunohistochemical characteristics of suburothelial microvasculature in the mouse bladder. Histochem Cell Biol. 2013;140:189–200.
67. Wu DM, Kawamura H, Sakagami K, Kobayashi M, Puro DG. Cholinergic regulation of pericyte-containing retinal microvessels. Am J Physiol Heart Circ Physiol. 2003;284:H2083–90.
68. Pallone TL, Huang JM. Control of descending vasa recta pericyte membrane potential by angiotensin II. Am J Physiol Ren Physiol. 2002;282:F1064–74.
69. Burdyga T, Borysova L. Calcium signalling in pericytes. J Vasc Res. 2014;51:190–9.
70. Nehls V, Drenckhahn D. Heterogeneity of microvascular pericytes for smooth muscle type alpha-actin. J Cell Biol. 1991;113:147–54.
71. Grant RI, Hartmann DA, Underly RG, Berthiaume AA, Bhat NR, Shih AY. Organizational hierarchy and structural diversity of microvascular pericytes in adult mouse cortex. J Cereb Blood Flow Metab. 2017. https://doi.org/10.1177/0271678X17732229.
72. O'Farrell FM, Mastitskaya S, Hammond-Haley M, Freitas F, Wah WR, Attwell D. Capillary pericytes mediate coronary no-reflow after myocardial ischaemia. elife. 2017;6:e29280.
73. Alarcon-Martinez L, Yilmaz-Ozcan S, Yemisci M, Schallek J, Kılıç K, Can A, Di Polo A, Dalkara T. Capillary pericytes express α-smooth muscle actin, which requires prevention of filamentous-actin depolymerization for detection. elife. 2018;7:e34861.
74. Higuchi K, Hashizume H, Aizawa Y, Ushiki T. Scanning electron microscopic studies of the vascular smooth muscle cells and pericytes in the rat heart. Arch Histol Cytol. 2000;63:115–26.
75. Hirschi KK, D'Amore PA. Pericytes in the microvasculature. Cardiovasc Res. 1996;32:687–98.
76. Zhang T, Wu DM, Xu GZ, Puro DG. The electrotonic architecture of the retinal microvasculature: modulation by angiotensin II. J Physiol. 2011;589:2383–99.
77. Colantuoni A, Bertuglia S, Intaglietta M. Variations of rhythmic diameter changes at the arterial microvascular bifurcations. Pflugers Arch. 1985;403:289–95.
78. Goligorsky MS, Colflesh D, Gordienko D, Moore LC. Branching points of renal resistance arteries are enriched in L-type calcium channels and initiate vasoconstriction. Am J Phys. 1995;268:F251–7.
79. Tykocki NR, Bonev AD, Longden TA, Heppner TJ, Nelson MT. Inhibition of vascular smooth muscle inward-rectifier K^+ channels restores myogenic tone in mouse urinary bladder arterioles. Am J Physiol Ren Physiol. 2017;312:F836–47.
80. Sanders KM, Ward SM, Koh SD. Interstitial cells: regulators of smooth muscle function. Physiol Rev. 2014;94:859–907.
81. Suzuki H, Takano H, Yamamoto Y, Komuro T, Saito M, Kato K, Mikoshiba K. Properties of gastric smooth muscles obtained from mice which lack inositol trisphosphate receptor. J Physiol. 2000;525:105–11.
82. Van Helden DF, Imtiaz MS, Nurgaliyeva K, von der Weid P-Y, Dosen PJ. Role of calcium stores and membrane voltage in the generation of slow wave

action potentials in guinea-pig gastric pylorus. J Physiol. 2000;524:245–65.
83. Imtiaz MS, Zhao J, Hosaka K, von der Weid PY, Crowe M, van Helden DF. Pacemaking through Ca^{2+} stores interacting as coupled oscillators via membrane depolarization. Biophys J. 2007;92:3843–61.
84. Van Helden DF. Pacemaker potentials in lymphatic smooth muscle of the guinea-pig mesentery. J Physiol. 1993;471:465–79.
85. Lang RJ, Hashitani H, Tonta MA, Suzuki H, Parkington HC. Role of Ca^{2+} entry and Ca^{2+} stores in atypical smooth muscle cell autorhythmicity in the mouse renal pelvis. Br J Pharmacol. 2007;152:1248–59.
86. Sergeant GP, Hollywood MA, McCloskey KD, McHale NG, Thornbury KD. Role of IP_3 in modulation of spontaneous activity in pacemaker cells of rabbit urethra. Am J Phys Cell Physiol. 2001;280:C1349–56.
87. Hashitani H, Lang RJ. Spontaneous activity in the microvasculature of visceral organs: role of pericytes and voltage-dependent Ca^{2+} channels. J Physiol. 2016;594:555–65.
88. Parker I, Ivorra I. Caffeine inhibits inositol trisphosphate-mediated liberation of intracellular calcium in Xenopus oocytes. J Physiol. 1991;433:229–40.
89. Thomas NL, Williams AJ. Pharmacology of ryanodine receptors and Ca^{2+}-induced Ca^{2+} release. WIREs Membr Transp Signal. 2012;1:383–97.
90. Hashitani H, Edwards FR. Spontaneous and neurally activated depolarizations in smooth muscle cells of the guinea-pig urethra. J Physiol. 1999;514:459–70.
91. MacMillan D, Chalmers S, Muir TC, McCarron JG. IP_3-mediated Ca^{2+} increases do not involve the ryanodine receptor, but ryanodine receptor antagonists reduce IP_3-mediated Ca^{2+} increases in guinea-pig colonic smooth muscle cells. J Physiol. 2005;569:533–44.
92. Zhang Q, Cao C, Zhang Z, Wier WG, Edwards A, Pallone TL. Membrane current oscillations in descending vasa recta pericytes. Am J Physiol Ren Physiol. 2008;294:F656–66.
93. Bradley E, Hollywood MA, Johnston L, Large RJ, Matsuda T, Baba A, McHale NG, Thornbury KD, Sergeant GP. Contribution of reverse Na^{+}-Ca^{2+} exchange to spontaneous activity in interstitial cells of Cajal in the rabbit urethra. J Physiol. 2006;574:651–61.
94. Bradley E, Hollywood MA, McHale NG, Thornbury KD, Sergeant GP. Pacemaker activity in urethral interstitial cells is not dependent on capacitative calcium entry. Am J Phys Cell Physiol. 2005;289:C625–32.
95. Ward SM, Ordog T, Koh SD, Baker SA, Jun JY, Amberg G, Monaghan K, Sanders KM. Pacemaking in interstitial cells of Cajal depends upon calcium handling by endoplasmic reticulum and mitochondria. J Physiol. 2000;525:355–61.
96. Sergeant GP, Bradley E, Thornbury KD, McHale NG, Hollywood MA. Role of mitochondria in modulation of spontaneous Ca^{2+} waves in freshly dispersed interstitial cells of Cajal from the rabbit urethra. J Physiol. 2008;586:4631–42.
97. Hashitani H, Lang RJ, Mitsui R, Mabuchi Y, Suzuki H. Distinct effects of CGRP on typical and atypical smooth muscle cells involved in generating spontaneous contractions in the mouse renal pelvis. Br J Pharmacol. 2009;158:2030–45.
98. Peng H, Matchkov V, Ivarsen A, Aalkjaer C, Nilsson H. Hypothesis for the initiation of vasomotion. Circ Res. 2001;88:810–5.
99. Van Helden DF, Imtiaz MS. Ca^{2+} phase waves: a basis for cellular pacemaking and long-range synchronicity in the guinea-pig gastric pylorus. J Physiol. 2003;548:271–96.
100. Sakagami K, Wu DM, Puro DG. Physiology of rat retinal pericytes: modulation of ion channel activity by serum-derived molecules. J Physiol. 1999;521:637–50.
101. Kito Y, Suzuki H. Properties of pacemaker potentials recorded from myenteric interstitial cells of Cajal distributed in the mouse small intestine. J Physiol. 2003;553:803–18.
102. Zheng H, Park KS, Koh SD, Sanders KM. Expression and function of a T-type Ca^{2+} conductance in interstitial cells of Cajal of the murine small intestine. Am J Phys Cell Physiol. 2014;306:C705–13.
103. Lang RJ, Tonta MA, Takano H, Hashitani H. Voltage-operated Ca^{2+} currents and Ca^{2+}-activated Cl^{-} currents in single interstitial cells of the guinea-pig prostate. BJU Int. 2014;114:436–46.
104. Matsushita K, Fukumoto M, Kobayashi T, Kobayashi M, Ishizaki E, Minami M, Katsumura K, Liao SD, Wu DM, Zhang T, Puro DG. Diabetes-induced inhibition of voltage-dependent calcium channels in the retinal microvasculature: role of spermine. Invest Ophthalmol Vis Sci. 2010;51:5979–90.
105. Zhang Z, Rhinehart K, Pallone TL. Membrane potential controls calcium entry into descending vasa recta pericytes. Am J Phys Regul Integr Comp Phys. 2002;283:R949–57.
106. Perez-Reyes E. Molecular physiology of low-voltage-activated T-type calcium channels. Physiol Rev. 2003;83:117–61.
107. Hirano Y, Fozzard HA, January CT. Characteristics of L- and T-type Ca^{2+} currents in canine cardiac Purkinje cells. Am J Phys. 1989;256:H1478–92.
108. Kuo IY, Wölfle SE, Hill CE. T-type calcium channels and vascular function: the new kid on the block? J Physiol. 2011;589:783–95.
109. Kuo IY, Ellis A, Seymour VA, Sandow SL, Hill CE. Dihydropyridine-insensitive calcium currents contribute to function of small cerebral arteries. J Cereb Blood Flow Metab. 2010;30:1226–39.
110. Gustafsson F, Andreasen D, Salomonsson M, Jensen BL, Holstein-Rathlou N. Conducted vasoconstriction in rat mesenteric arterioles: role for dihydropyridine-

insensitive Ca^{2+} channels. Am J Physiol Heart Circ Physiol. 2001;280:H582–90.
111. Jensen LJ, Salomonsson M, Jensen BL, Holstein-Rathlou NH. Depolarization-induced calcium influx in rat mesenteric small arterioles is mediated exclusively via mibefradil-sensitive calcium channels. Br J Pharmacol. 2004;142:709–18.
112. Morita H, Cousins H, Onoue H, Ito Y, Inoue R. Predominant distribution of nifedipine-insensitive, high voltage-activated Ca^{2+} channels in the terminal mesenteric artery of guinea pig. Circ Res. 1999;85:596–605.
113. Hansen PB, Jensen BL, Andreasen D, Skøtt O. Differential expression of T- and L-type voltage-dependent calcium channels in renal resistance vessels. Circ Res. 2001;89:630–8.
114. Gomez-Pinilla PJ, Gibbons SJ, Bardsley MR, Lorincz A, Pozo MJ, Pasricha PJ, Van de Rijn M, West RB, Sarr MG, Kendrick ML, Cima RR, Dozois EJ, Larson DW, Ordog T, Farrugia G. Ano1 is a selective marker of interstitial cells of Cajal in the human and mouse gastrointestinal tract. Am J Physiol Gastrointest Liver Physiol. 2009;296:G1370–81.
115. Hwang SJ, Blair PJ, Britton FC, O'Driscoll KE, Hennig G, Bayguinov YR, Rock JR, Harfe BD, Sanders KM, Ward SM. Expression of anoctamin 1/TMEM16A by interstitial cells of Cajal is fundamental for slow wave activity in gastrointestinal muscles. J Physiol. 2009;587:4887–904.
116. Parsons SP, Kunze WA, Huizinga JD. Maxi-channels recorded in situ from ICC and pericytes associated with the mouse myenteric plexus. Am J Phys Cell Physiol. 2012;302:C1055–69.
117. Dam VS, Boedtkjer DM, Nyvad J, Aalkjaer C, Matchkov V. TMEM16A knockdown abrogates two different Ca^{2+}-activated Cl^- currents and contractility. Pflugers Arch. 2014;466:1391–409.
118. Kito Y, Mitsui R, Ward SM, Sanders KM. Characterization of slow waves generated by myenteric interstitial cells of Cajal of the rabbit small intestine. Am J Physiol Gastrointest Liver Physiol. 2015;308:G378–88.
119. Cuevas P, Gutierrez-Diaz JA, Reimers D, Dujovny M, Diaz FG, Ausman JI. Pericyte endothelial gap junctions in human cerebral capillaries. Anat Embryol (Berl). 1984;170:155–9.
120. Zhang Z, Lin H, Cao C, Payne K, Pallone TL. Descending vasa recta endothelial cells and pericytes form mural syncytia. Am J Physiol Ren Physiol. 2014;306:F751–63.
121. Zhang Z, Payne K, Pallone TL. Syncytial communication in descending vasa recta includes myo-endothelial coupling. Am J Physiol Ren Physiol. 2014;307:F41–52.
122. Zhang Z, Payne K, Pallone TL. Descending vasa recta endothelial membrane potential response requires pericyte communication. PLoS One. 2016;11:e0154948.
123. Berthiaume AA, Grant RI, McDowell KP, Underly RG, Hartmann DA, Levy M, Bhat NR, Shih AY. Dynamic remodeling of pericytes in vivo maintains capillary coverage in the adult mouse brain. Cell Rep. 2018;22:8–16.
124. Yamamoto Y, Klemm MF, Edwards FR, Suzuki H. Intercellular electrical communication among smooth muscle and endothelial cells in guinea-pig mesenteric arterioles. J Physiol. 2001;535:181–95.
125. Kannan MS, Prakash YS, Johnson DE, Sieck GC. Nitric oxide inhibits calcium release from sarcoplasmic reticulum of porcine tracheal smooth muscle cells. Am J Phys. 1997;272:L1–7.
126. Fleming BP, McKinney ME. Adrenergic innervation in the microcirculation of the bat wing. Microvasc Res. 1985;29:387–400.
127. Furness JB, Marshall JM. Correlation of the directly observed responses of mesenteric vessels of the rat to nerve stimulation and noradrenaline with the distribution of adrenergic nerves. J Physiol. 1974;239:75–88.
128. Fu YY, Peng SJ, Lin HY, Pasricha PJ, Tang SC. 3-D imaging and illustration of mouse intestinal neurovascular complex. Am J Physiol Gastrointest Liver Physiol. 2013;304:G1–11.
129. Brookes SJ, Steele PA, Costa M. Calretinin immunoreactivity in cholinergic motor neurones, interneurons and vasomotor neurones in the guinea-pig small intestine. Cell Tissue Res. 1991;263:471–81.
130. Neild TO, Shen KZ, Surprenant A. Vasodilatation of arterioles by acetylcholine released from single neurones in the guinea-pig submucosal plexus. J Physiol. 1990;420:247–65.
131. Hamilton NB, Attwell D, Hall CN. Pericyte-mediated regulation of capillary diameter: a component of neurovascular coupling in health and disease. Front Neuroenerg. 2010;2:1–14.
132. Dora KA, Doyle MP, Duling BR. Elevation of intracellular calcium in smooth muscle causes endothelial cell generation of NO in arterioles. Proc Natl Acad Sci U S A. 1997;94:6529–34.
133. Garland CJ, Bagher P, Powell C, Ye X, Lemmey HAL, Borysova L, Dora KA. Voltage-dependent Ca^{2+} entry into smooth muscle during contraction promotes endothelium-mediated feedback vasodilation in arterioles. Sci Signal. 2018;10(486):eaal3806.
134. Tran CH, Taylor MS, Plane F, Nagaraja S, Tsoukias NM, Solodushko V, Vigmond EJ, Furstenhaupt T, Brigdan M, Welsh D. Endothelial Ca^{2+} wavelets and the induction of myoendothelial feedback. Am J Phys Cell Physiol. 2012;302:C1226–42.
135. Svenningsen P, Andersen K, Thuesen AD, Shin HS, Vanhoutte PM, Skøtt O, Jensen BL, Hill C, Hansen PB. T-type Ca^{2+} channels facilitate NO-formation, vasodilatation and NO-mediated modulation of blood pressure. Pflugers Arch. 2014;466:2205–14.
136. Longden TA, Dabertrand F, Koide M, Gonzales AL, Tykocki NR, Brayden JE, Hill-Eubanks D, Nelson MT. Capillary K^+-sensing initiates retrograde hyperpolarization to increase local cerebral blood flow. Nat Neurosci. 2017;20:717–26.

137. Longden TA, Hill-Eubanks DC, Nelson MT. Ion channel networks in the control of cerebral blood flow. J Cereb Blood Flow Metab. 2016;36:492–512.
138. Greenland JE, Brading AF. Urinary bladder blood flow changes during the micturition cycle in a conscious pig. J Urol. 1996;156:1858–61.
139. Sarma KP. Microangiography of the bladder in health. Br J Urol. 1981;53:237–40.
140. Birder L, Andersson KE. Urothelial signaling. Physiol Rev. 2013;93:653–80.
141. Matheson PJ, Wilson MA, Garrison RN. Regulation of intestinal blood flow. J Surg Res. 2000;93:182–96.
142. Andersson KE, Boedtkjer DB, Forman A. The link between vascular dysfunction, bladder ischemia, and aging bladder dysfunction. Ther Adv Urol. 2017;9:11–27.
143. Andersson KE, Nomiya M, Sawada N, Yamaguchi O. Pharmacological treatment of chronic pelvic ischemia. Ther Adv Urol. 2014;6:105–14.
144. Thurmond P, Yang JH, Azadzoi KM. LUTS in pelvic ischemia: a new concept in voiding dysfunction. Am J Physiol Ren Physiol. 2016;310:F738–43.
145. Azadzoi KM, Tarcan T, Siroky MB, Krane RJ. Atherosclerosis-induced chronic ischemia causes bladder fibrosis and non-compliance in the rabbit. J Urol. 1999;161:1626–35.
146. Yoshida M, Masunaga K, Nagata T, Satoji Y, Shiomi M. The effects of chronic hyperlipidemia on bladder function in myocardial infarction-prone Watanabe heritable hyperlipidemic (WHHLMI) rabbits. Neurourol Urodyn. 2010;29:1350–4.
147. Britton E, McLaughlin J. Ageing and the gut. Proc Nutr Soc. 2013;72:173–7.
148. Westcott EB, Segal SS. Ageing alters perivascular nerve function of mouse mesenteric arteries in vivo. J Physiol. 2013;591:1251–63.
149. Meyer C, de Vries G, Davidge ST, Mayes DC. Reassessing the mathematical modeling of the contribution of vasomotion to vascular resistance. J Appl Physiol. 2002;92:888–9.
150. Bek T, Jeppesen P, Kanters JK. Spontaneous high frequency diameter oscillations of larger retinal arterioles are reduced in type 2 diabetes mellitus. Invest Ophthalmol Vis Sci. 2013;54:636–40.
151. Ivanova E, Kovacs-Oller T, Sagdullaev BT. Vascular pericyte impairment and connexin43 gap junction deficit contribute to vasomotor decline in diabetic retinopathy. J Neurosci. 2017;37:7580–94.
152. Kisler K, Nelson AR, Rege SV, Ramanathan A, Wang Y, Ahuja A, Lazic D, Tsai PS, Zhao Z, Zhou Y, Boas DA, Sakadžić S, Zlokovic BV. Pericyte degeneration leads to neurovascular uncoupling and limits oxygen supply to brain. Nat Neurosci. 2017;20:406–16.
153. Lemaster KA, Farid Z, Brock RW, Shrader CD, Goldman D, Jackson DN, Frisbee JC. Altered postcapillary and collecting venular reactivity in skeletal muscle with metabolic syndrome. J Physiol. 2017;595:5159–74.
154. Ricard N, Tu L, Le Hiress M, Huertas A, Phan C, Thuillet R, Sattler C, Fadel E, Seferian A, Montani D, Dorfmüller P, Humbert M, Guignabert C. Increased pericyte coverage mediated by endothelial-derived fibroblast growth factor-2 and interleukin-6 is a source of smooth muscle-like cells in pulmonary hypertension. Circulation. 2014;129:1586–97.
155. Yemisci M, Gursoy-Ozdemir Y, Vural A, Can A, Topalkara K, Dalkara T. Pericyte contraction induced by oxidative-nitrative stress impairs capillary reflow despite successful opening of an occluded cerebral artery. Nat Med. 2009;15:1031–7.
156. Nakaizumi A, Puro DG. Vulnerability of the retinal microvasculature to hypoxia: role of polyamine-regulated K_{ATP} channels. Invest Ophthalmol Vis Sci. 2011;52:9345–52.
157. Nakaizumi A, Zhang T, Puro DG. The electrotonic architecture of the retinal microvasculature: diabetes-induced alteration. Neurochem Int. 2012;61:948–53.

Lymphatic Vessel Pumping

15

Pierre-Yves von der Weid

Abstract

The lymphatic system extends its network of vessels throughout most of the body. Lymphatic vessels carry a fluid rich in proteins, immune cells, and long-chain fatty acids known as lymph. It results from an excess of interstitial tissue fluid collected from the periphery and transported centrally against hydrostatic pressure and protein concentration gradients. Thus, this one-way transport system is a key component in the maintenance of normal interstitial tissue fluid volume, protein concentration and fat metabolism, as well as the mounting of adequate immune responses as lymph passes through lymph nodes. In most cases, lymph is actively propelled via rhythmical phasic contractions through a succession of valve-bordered chambers constituting the lymphatic vessels. This contraction/relaxation cycle, or lymphatic pumping, is initiated in the smooth muscle cells present in the vessel wall by a pacemaker mechanism generating voltage-gated Ca^{2+} channel-induced action potentials. The action potentials provide the depolarization and Ca^{2+} influx essential for the engagement of the contractile machinery leading to the phasic constrictions of the lymphatic chambers and forward movement of lymph. The spontaneous lymphatic constrictions can be observed in isolated vessels in the absence of any external stimulation, while they are critically regulated by physical means, such as lymph-induced transmural pressure and flow rate, as well as diffusible molecules released from the lymphatic endothelium, perivascular nerve varicosities, blood and surrounding tissues/cells. In this chapter, we describe the latest findings which are improving our understanding of the mechanisms underlying spontaneous lymphatic pumping and discuss current theories about their physiological initiation.

Keywords

Lymphatic system · Lymphatic vessel · Lymphatic pumping · Lymphatic muscle cell · Lymphatic pacemaker · Spontaneous transient depolarization · Ca^{2+}-activated Cl^- channel · Intracellular Ca^{2+} store

P.-Y. von der Weid (✉)
Department of Physiology and Pharmacology, Inflammation Research Network and Smooth Muscle Research Group, Snyder Institute for Chronic Diseases, Cumming School of Medicine, University of Calgary, Calgary, AB, Canada
e-mail: vonderwe@ucalgary.ca

15.1 Introduction

The network of lymphatic vessels, or lymphatics, is widely distributed throughout the body and connects interstitial tissue space to lymphoid

H. Hashitani, R. J. Lang (eds.), *Smooth Muscle Spontaneous Activity*, Advances in Experimental Medicine and Biology 1124, https://doi.org/10.1007/978-981-13-5895-1_15

organs and to the blood circulation. It is through these vessels that the pool of fluid and proteins, which physiologically accumulates in the interstitium, is drained away in order to maintain tissue fluid balance. Once it enters the lymphatic vessels, the interstitial fluid is known as *lymph.* Unlike the cardiovascular system, which is a close circuit relying on a central pump to move blood, lymphatic vessels form a one-way system that collects lymph from the periphery and propels it, most of the time against hydrostatic pressure and protein concentration gradients [1], via the pumping action of successive individual lymphatic vessel chambers back into the venous circulation. In the process, lymph passes through several lymph nodes where particulate matter, antigens and immune cells interact with lymphocytes and participate in the immune surveillance.

This chapter first reviews the anatomy and functions of the lymphatic vessels, and then discusses our current knowledge of the specific aspects of lymphatic pumping and the mechanisms regulating the initiation of this spontaneous electrical and contractile activity.

15.2 Structural and Functional Organization of the Lymphatic Vessels

15.2.1 Initial Lymphatics

Interstitial fluid, along with various cellular components and proteins, enters the vessels through blind-ended structures known as *initial lymphatics*. The initial lymphatic vessels, also called *terminal* or *peripheral lymphatics*, or *lymphatic capillaries*, have walls devoid of muscle cells or pericytes. They are composed of a single layer of flattened, non-fenestrated endothelial cells laid on an incomplete basement membrane [2, 3], which overlap in an oak leaf-shaped manner.

Neighbouring endothelial cells are connected by button-like junctions made of vascular endothelial (VE)-cadherin and tight-junction proteins such as occluding, claudin-5, zonula occludens (ZO)-1, endothelial cell-selective adhesion molecule (ESAM) and junctional adhesion molecule-A (JAM-A). These junctions tightly join adjacent cells only at discrete locations [4]. The non-connected flaps of the endothelial cells form a primitive primary valve system, which when open creates 2–3 μm diameter pores allowing interstitial fluid to enter into the vessel lumen, and preventing leakage of lymph in the opposite direction [5–8]. Performance of these small valves is supported by *anchoring filaments*, collagenous fibrils linking the surface of the endothelial flaps to elastin fibers in the surrounding interstitial matrix [9]. These filaments prevent the thin-walled vessels from collapsing under high interstitial pressure, keeping them expanded to favor the entry of fluid, particulate matter, immune cells, proteins, chylomicrons [10, 11], as well as infectious pathogens such as bacteria and virus particles.

15.2.2 Collecting Lymphatics

Initial lymphatics empty their contents into collecting lymphatics, which connect with lymph nodes along their path and coalesce to form larger and larger vessels. Ultimately, lymph is returned to the venous circulation via the thoracic and the right lymphatic ducts which are connected to the left and right subclavian veins at the root of the neck.

The collecting vessels contain an intimal monolayer of endothelial cells, which unlike the initial vessels are tightly connected by zipper-like junctions that contain VE-cadherin, occluding, claudin-5, ZO-1, ESAM, and more evenly distributed JAM-A when compared with the initials [4]. The endothelial cells are surrounded by a basement membrane. Collecting lymphatics are distinguished from initials by the presence of a media comprised of one to three layers of smooth muscle cells intermixed with collagen and elastic fibers and an adventitia containing fibroblasts, connective tissue elements, and axons that innervate the vessel [12]. Tissue and species differences exist and, in smaller vessels, the three layers may not be easily distinguishable. However, as vessels progress centrally, the

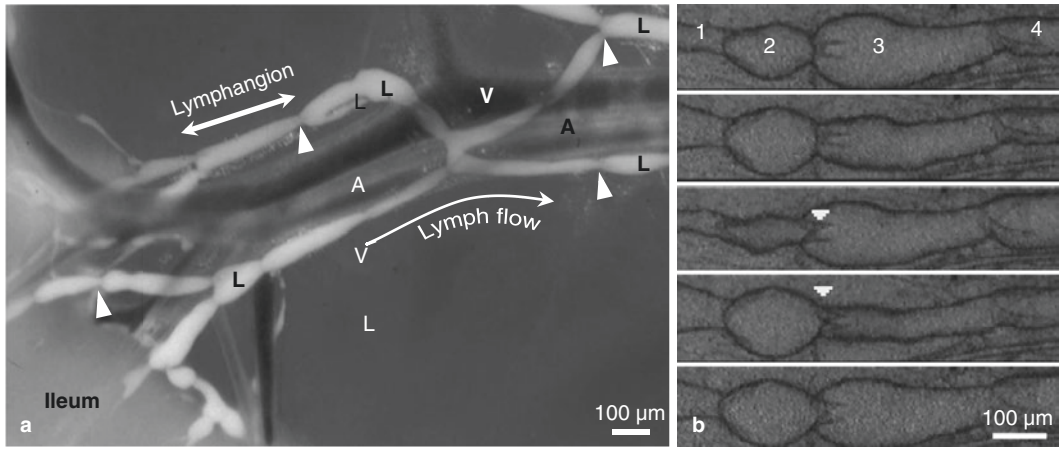

Fig. 15.1 Collecting lymphatic vessels in the guinea pig mesentery. (**a**) Mesentery containing ileum, artery (A), vein (V), and collecting lymphatic vessels (L), which are comprised of a succession of lymphangions, delineated by unidirectional valves (arrowheads). (**b**) Successive images of a lymphatic vessel under luminal perfusion. Four chambers (#1–4) are displayed, which underwent sequential contractions. A unidirectional valve (arrowhead) is visible between chambers #2 and 3

amount of smooth muscle increases, with fibers lying in a more circular orientation [13]. Another critical functional structure of the collecting lymphatics is the presence of unidirectional valves distributed along the length of the vessel. These valves consist of a matrix core sandwiched between endothelial cells and defined functional units termed lymphatic chambers or *lymphangions* [14] (see Fig. 15.1a).

Although extrinsic compression caused by skeletal muscle contraction, respiratory activity, and bodily movement also contributes, the main mechanism of lymphatic contraction is provided by the intrinsic contractile activity of the lymphatic smooth muscle which transiently and independently constricts each lymphangion. This phasic cycle of contractions and relaxations allows the lymph to be propelled into the next chamber through the downstream valve, while the generated fluid pressure closes the upstream valve limiting lymph backflow (see Fig. 15.1b). The ability of the lymphatic vessels to exhibit such rhythmic phasic constrictions is known as *lymphatic pumping* and is the mechanism whereby this vessel system performs its essential functions.

15.3 Roles and Functions of the Lymphatic Vasculature

15.3.1 Tissue Fluid Balance

In spite of daily variations in water and salt content, extracellular fluid volume is maintained remarkably constant. This consistency relies heavily on the control of transport of salts and fluid across the capillary wall, and the return of fluid to the plasma. About 90% of the fluid that leaks out of the blood circulation is reabsorbed into the venous system, and the remaining 10%, or about 5–6 L/day, enters the initial lymphatics and circulates as lymph through the human lymphatic vessels [15]. Lymphatics are also responsible for the daily clearance of about 60% of vascular proteins, as well as lipids and liposoluble vitamins incorporated into chylomicrons [10].

The largest determinants of fluid flux are the Starling forces across the capillary wall, namely *hydrostatic* and *colloid osmotic pressures*. Plasma and interstitial colloid osmotic pressure is determined by the concentration of solute molecules in these fluids. A higher plasma colloid osmotic pressure will favor osmotic absorption of fluid

into the capillary, because water will tend to move into an area of higher solute concentration. On the other hand, a high interstitial colloid osmotic pressure will favor an outward fluid flux in order to balance colloid concentrations across the wall. In most tissues, net colloid osmotic pressure drives fluid into the capillary, and the overall hydrostatic pressure forces fluid out into the tissue. The resulting net balance of forces tends to direct fluid out of capillaries and into the interstitium. Since lymphatic loading is directly proportional to interstitial fluid volume, the amount of lymph that is propelled in the vessels is also determined by the plasma volume filtrated into the interstitium; the greater this volume, the larger the amount of fluid that is transported via the lymphatics back into the bloodstream.

Protein transport out of capillaries must also be balanced with the same amount of proteins leaving the interstitium via the lymphatics. An inability to transport filtered proteins out of the interstitium results in edema. Proteins move across the capillary membrane by means of both diffusion and convection. There are several determinants of transvascular protein transfer, some which relate to characteristics of the capillary membrane itself, and others which relate to the relative concentrations of protein across the membrane. The flux of proteins across the capillary wall is regulated by a complex set of physiological mechanisms. This is important because fluid flux depends largely on osmotic pressure, and protein concentration can have a large impact on fluid volumes. As in fluid loading in lymphatics, the amount of protein loaded into the initial lymphatics is determined by interstitial protein concentrations. Lymph formation must match the net transcapillary flux of fluid and solutes in order to prevent excessive tissue swelling and edema [15].

15.3.2 Lymph Formation and Transport

Fluid, electrolytes, proteins, and cellular elements, such as immune cells, do not just passively drift into the lumen. The current theory proposes that the phasic expansion/relaxation phases generated by the lymphatic pump in the initial or downstream collecting lymphatics (see below) allow the transient development of hydrostatic pressure differences between the interstitium and the lumen of the initials that favor fluid entry [16–21]. The efficiency of lymph entry into the initial vessels and its central movement strongly rely on the competency of the initial and collecting valve systems [5, 22, 23]. Fluid movement through the tissue towards the lymphatic vessel lumen is vital to maintain vessel filling, and can only be preserved if the downstream lymphatic vessels continue to drain fluid away.

15.3.3 Lymphatic Vessels and Immunity

The lymphatic system is strongly implicated in the adaptive immune response. As part of this system, lymphatic vessels are responsible for transporting antigens to lymphoid tissues, where they are sequestered to bring about immune responses during disease and in response to infection. Antigens present in fluid entering the lymph node can effectively elicit an immune response upon activation of resident naïve T- and B-cells, which enter lymph nodes from tissues via afferent lymphatic vessels or from the cardiovascular network via high endothelial venules. Immune cells exit the lymphatic system and eventually return to the bloodstream to be transported throughout the body looking out for foreign antigens.

The lymphatic system provides an exclusive environment in which immune cells can respond to foreign antigens, as well as proliferate and circulate lymphocytes and return them to the bloodstream. Importantly, lymphatic vessels also serve as preferred routes for the spreading of metastatic cancer cells from the primary to different organs. Indeed, lymph nodes are regarded as a favorable environment for metastatic tumor development [24].

The lymphatic system also functions as a one-way communication system for molecular messages, such as cytokines and chemokines, which

can be transmitted to cellular constituents in lymph nodes. These messengers are also potential candidates for controlling lymph flow by modulating lymphatic pumping [25–27]. A major role for the lymphatic vessels has also been demonstrated in the transport of venom after snakebite, due to the usually large size of the toxic molecules [28, 29].

15.3.4 Digestive Functions

Following initial observations by Asselli of the key role lymphatics of the mesentery played in digestion and absorption (reviewed in [30]), it is now well recognized that intestinal lymphatics are crucial to the absorption of dietary lipids [31–34]. Fat absorption involves emulsification of bile salts, hydrolysis of long-chain triglyceride species by lipase, passive and/or transporter-mediated diffusion into enterocytes, and resynthesis and repackaging of large triacylglycerol-rich lipoproteins into chylomicrons. Chylomicrons are exocytosed by the enterocytes and enter the lymphatic system through lacteals, initial lymphatics in the villi of the small intestine, which empty into submucosal lymphatics and then into mesenteric collecting lymphatics. It is well accepted that intestinal lymph flow is enhanced following fat feeding [35, 36], but the precise mechanisms by which this occurs and the impact of lipid metabolism on lymphatic function still require further investigation.

15.4 Lymphatic Pumping and Spontaneous Contractions

Lymphatic pumping is the main driving force for lymph transport against adverse pressure gradients [37]. This active propulsive process is generated by the robust constriction/relaxation cycle of the lymphangions in the collectors, each lymphangion behaving like little ventricles in series. The centripetal and upstream movement of lymph is also facilitated by the system of one-way valves within the lymphatic network, which minimizes backflow [38].

15.4.1 Lymphatic Muscle Contraction

The lymphatic muscle cells invested in the walls of collectors generate and control the movement of lymph along the lymphatic network. As they bear similarities with vascular smooth muscle cells, lymphatic muscle cells are usually classified as smooth muscle cells. However, they display important differences in both their contractile function and contractile machinery that make them unique. Lymphatic contraction is mainly regulated by the rate of myosin light-chain phosphorylation/dephosphorylation, controlled by the balanced activity of myosin light-chain kinase (MLCK) and myosin light-chain phosphatase (MLCP), a mechanism well studied in blood vessels (reviewed in [39]). As intracellular Ca^{2+} ($[Ca^{2+}]_i$) increases, it binds to calmodulin, and the Ca^{2+}-calmodulin complex activates MLCK. MLCK phosphorylates the regulatory myosin light chain 20 (MLC_{20}) [40], causing activation of the myosin ATPase by actin and thus contraction. When $[Ca^{2+}]_i$ decreases, MLCK is deactivated leading to the dephosphorylation of MLC_{20} by MLCP, the myosin ATPase is deactivated, and the muscle relaxes. MLCK and MLCP activities and contractile status can also be regulated by mechanisms independent of $[Ca^{2+}]_i$ [40, 41]. Although these mechanisms explain well how tonic contraction is regulated, studies by Muthuchamy et al. [42] characterizing the contractile proteins expressed by lymphatic muscle cells shed some light on the mechanisms that could explain the ventricular-like pumping function of the lymphangions. They demonstrated that rat mesenteric and thoracic lymphatic muscle cells contain striated contractile elements and share biochemical and functional characteristics with cardiac muscle cells [42]. Specifically, lymphatic muscle cells express the SMB-MHC isoforms, as well as fetal cardiac/skeletal slow-twitch β-MHC, a faster non-smooth muscle MHC isoform, conferring them relatively

fast contractile properties. Furthermore, lymphatic tissues express messages and proteins for both vascular smooth muscle actin and sarcomeric actin (reviewed in [43]). Whether the striated muscle and smooth muscle isoforms are expressed in the same lymphatic muscle cells has not been determined yet.

15.5 Electrophysiological Properties of the Lymphatic Muscle

As mentioned earlier, rhythmical constrictions can be observed in isolated collectors maintained in physiological conditions in the absence of innervation or a functional endothelial layer [44, 45]. They are driven by action potentials generated by the cells constituting the muscular part of the vessel [46–48]. The regularity of these events suggests a pacemaking mechanism. While several molecular and electrical entities have been proposed to underlie the lymphatic pacemaker, the precise/complete characterization of its mechanisms is still under study. We discuss in the following sections studies that have forged our current understanding of the pacemaker activity driving lymphatic pumping.

15.5.1 Historical Perspective

Lymphatic muscle membrane potential and action potentials have been investigated with recording methods of increased complexity over the years. The first successful attempts were obtained by Mislin [49, 50] using extracellular electrodes. He was able to record a series of peaks of short duration followed by a slower "after-potential" that he referred to as electrolymphangiograms (ELG) and that he interpreted as action potentials preceding the lymphangion constriction. Measurements of lymphatic intracellular voltage changes were initially made with the sucrose gap technique. Although providing an approximate and dynamic description of intracellular voltage changes rather than absolute membrane potentials, this technique originally used by Orlov et al. [51] in bovine mesenteric lymphatics allowed the recording of the action potential time course as a single spike followed by a gradually declining plateau, further confirming the correlation between action potential and constrictions [46–48]. Sharp intracellular microelectrodes have subsequently been used, providing a more reliable measurement of the action potential and the first accurate measurement of the lymphatic muscle membrane potential.

15.5.2 Lymphatic Muscle Membrane Potential

Using intracellular microelectrodes, mean resting membrane potential values ranging from −66 to −48 mV were obtained from mesenteric lymphatic vessel preparations of the guinea pig [52–54], rat [55, 56], and bovine [57–59]. The small variation between values could be due to species or methodological differences or more plausibly relate to the consistently more active (and more depolarized) bovine and rat vessels compared to the generally more quiescent (and hyperpolarized) guinea pig lymphatics. The polarized values of these recorded membrane potentials probably reflect the fact that these measurements were obtained in mesenteric vessels in the absence of applied transmural pressure. More recent recordings have been successfully obtained from pressurized or stretched lymphatic vessels. Because of the higher action potential frequency induced by the vessel pressure/stretch, the measured membrane potential is more correctly defined as mean diastolic membrane potential, with reported values being more depolarized. Indeed, isolated rat mesenteric lymphatics mounted on a wire myograph displayed a mean diastolic membrane potential of −39 mV that did not significantly change with increase in vessel stretch [55]. Using the same wire myograph technique, Telinius et al. reported membrane potentials of ~−45 mV in human thoracic ducts [60]. A limitation of the wire myograph procedure is that, due to the small size of the vessels, the lym-

phatic endothelial layer may well be damaged by the wires inserted through the vessel lumen, compromising the release of nitric oxide (NO) and prostaglandins known to hyperpolarize the muscle. Furthermore, the horizontal and lateral stretch stimulus applied by the myograph might lead to different electrical response than the radial pressure normally experienced by the vessel. Thus, whether stretch truly depolarizes the lymphatic muscle cannot be unequivocally confirmed with this method. More recently, Davis et al. successfully obtained membrane potential recordings from pressurized mouse, rats, and human lymphatic vessels, where sharp, intracellular microelectrode impalements could be maintained when contractions were blunted with low millimolar concentration of the MLCK inhibitor wortmannin [61]. With this technique, the authors reported diastolic membrane potentials of −40 mV for rat mesenteric vessels, and −35 and −40 mV for mouse inguinal and mesenteric collectors pressurized to 3 cm H_2O [61, 62]. In addition to these values being more depolarized compared to unstretched vessels and not noticeably different from those obtained with a wire myograph, they were little altered (~3 mV) with increases in pressure (M.J. Davis, personal communication).

Based on pharmacological experiments performed on sheep and guinea pig mesenteric lymphatics, large-conductance Ca^{2+}-activated K^+ channels, inward-rectified K^+ channels, delayed rectifier K^+ channels, ATP-sensitive K^+ channels, and Ca^{2+}-activated Cl^- channels (Cl_{Ca}) have been suggested to be expressed and involved in the establishment of the lymphatic muscle membrane potential [63–67]. The functional contribution of all these classes of K^+ channels was also more recently demonstrated in human thoracic ducts and their expression confirmed at the mRNA level [68]. The difficulty to acutely isolate lymphatic muscle cells has limited the use of the patch clamp technique to characterize the currents involved in lymphatic muscle membrane potential, so that only a very few studies using this technique have been published. Thus far, a large-conductance Ca^{2+}-activated K^+ current (blocked by penitrem A) and several components of voltage-dependent K^+ currents are characterized by their partial blockade by TEA or 4-AP, thereby resembling "delayed rectifier" currents identified in acutely dissociated sheep mesenteric lymphatic muscle cells [64]. Furthermore, a nifedipine- and Bay K8644-sensitive L-type Ca^{2+} current and a 9-anthracene carboxylic acid (9-AC)-sensitive Cl_{Ca} current activated by Ca^{2+} release from intracellular stores were recorded from a significant number (~70%) of the same isolated sheep mesenteric lymphatic muscle cells [66].

Several electrogenic ion pumps and exchangers have also been suggested to be involved in the establishment of the lymphatic muscle resting membrane potential. Inhibition of the sodium-potassium-ATPase with ouabain causes a 6–10 mV depolarization in bovine and guinea pig mesenteric lymphatics [57] (von der Weid, unpublished data). Similarly, a hyperpolarization of ~6 mV is observed in rat mesenteric lymphatics during inhibition of the Na^+–K^+–$2Cl^-$ co-transporter with bumetanide [56], which correlates with a significant decrease in contraction frequency (Fig. 15.2). Together with the reported sensitivity of the resting membrane potential to ion substitution and ion channel inhibition [56, 69], these data demonstrated the strong lymphatic muscle membrane potential dependency to K^+ and Cl^- conductances.

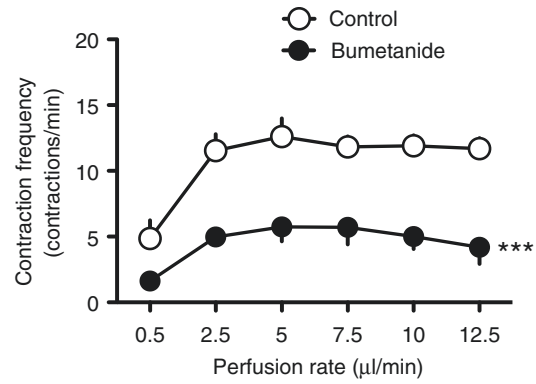

Fig. 15.2 Effect of the Na^+–K^+–$2Cl^-$ co-transporter (NKCC) blocker bumetanide (10 µM) on the perfusion-induced increase in contraction frequency of guinea pig mesenteric lymphatic vessels ($n = 7$; ***$p < 0.001$, two-way ANOVA with Bonferroni posttest)

15.5.3 Action Potential

Due to their frequent occurrence and their importance in lymphatic contractions, characterization of the electrophysiological mechanisms involved in the action potential and the initiation of this event has been the subject of much attention. In bovine mesenteric vessel, intracellular microelectrode recordings showed a diastolic slow depolarization and followed by a spike complex superimposed to a plateau phase [70]. Similar spike complexes were reported in sheep and human mesenteric collectors [71, 72]. While action potentials in guinea pig mesenteric lymphatics displayed the initial transient depolarization and plateau phases, a slow depolarization and superimposed burst of spikes were not evident in this species [73]. Spontaneous action potentials were more recently recorded from mouse main collectors [61]. In this study, the authors reported differences in action potential properties between lymphatic vessels in the leg and vessels from the visceral cavity. While inguinal/axillary action potential was characterized by a diastolic depolarization, spike, plateau, and repolarization phases without a noticeable after-hyperpolarization, mesenteric action potentials lacked spike and plateau phases. This difference, partially explained by L-type Ca^{2+} channel activity, is likely correlated with the notorious lack of contractile activity of mouse mesenteric collectors [61].

Like most smooth muscles, action potentials and constrictions in lymphatics depend heavily on extracellular Ca^{2+} ions and are inhibited by L-type Ca^{2+} channel blockers [47, 74, 75]. Electrophysiological evidence for L-type Ca^{2+} current was confirmed in freshly isolated sheep mesenteric smooth muscle cells with the whole-cell patch clamp method [66, 76]. Involvement of L-type Ca^{2+} channels in rat, mouse and human mesenteric vessel action potentials was assessed pharmacologically [60, 61, 77] and expression of the main L-type Ca^{2+} channel isoform, Cav1.2, confirmed by PCR and immunofluorescence [60, 61, 77], although expression of Cav1.1 and Cav1.3 was also revealed.

A fast voltage-activated Na^+ current, inhibited by TTX and which contributes to the rising phase of the action potential, was also identified in the sheep mesenteric smooth muscle cells [78]. TTX also significantly depressed spontaneous contractions of isolated sheep mesenteric lymphatic vessel rings suggesting the involvement of Na^+ channels in spontaneous constrictions [78]. However, TTX did not affect action potentials in bovine mesenteric lymphatics [47] or constrictions induced by luminal perfusion in guinea pig mesenteric lymphatics [52]. Telinius and colleagues, using pharmacological characterization and mRNA expression profiling, reported expression of multiple voltage-activated Na^+ channels (Nav1 family) in samples of human thoracic duct and mesenteric lymphatic muscle with Nav1.3, the most prevalent, facilitating the action potential generation [72].

15.5.4 Lymphatic Pacemaker

The strict voltage dependence of L-type Ca^{2+} channels and the regularity of the action potentials during lymphatic pumping suggest the involvement of an electrical event that transiently depolarizes the muscle membrane potential (pacemaker potential). Two main mechanisms have been proposed for the generation of pacemaker activity in lymphatic vessels.

Studies on large lymphatic vessels (bovine mesenteric lymphatics) have demonstrated that the pacemaker mechanisms underlying lymphatic constrictions relate to a slow depolarization leading to the generation of regularly occurring action potentials [48, 70]. Such activity bears time- and voltage-dependent similarities with that observed in the heart. Indeed, investigations in sheep mesenteric lymphatics have demonstrated the existence of a hyperpolarization-activated inward current with properties similar to hyperpolarization-activated cyclic nucleotide-gated (HCN or "funny" current I_f) current in the sinoatrial node [79]. This current could however be only recorded in a low number of cells. HCN blockers, cesium and ZD7288, partially inhibited the frequency of spontaneous constrictions of isolated lymphatic segments. A more profound effect of the selective HCN

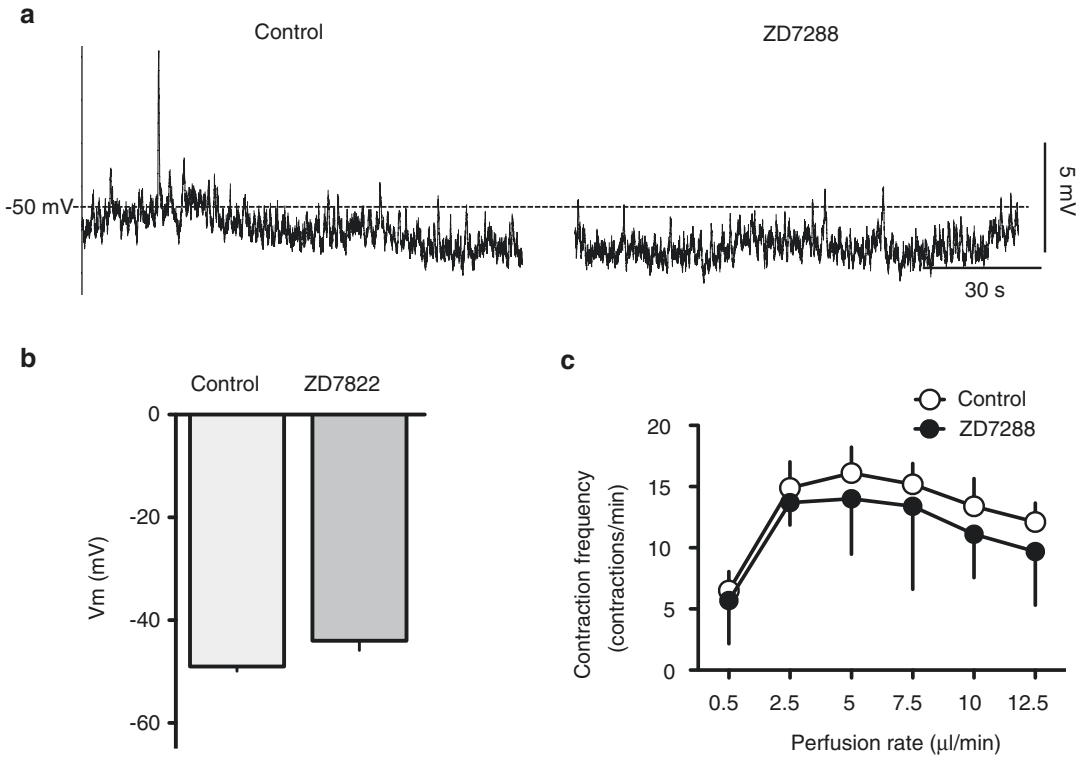

Fig. 15.3 Lack of effects of the HCN channel blocker ZD7288 on membrane potential and contractile activity of guinea pig mesenteric lymphatic vessels. Original intracellular microelectrode recording of membrane potential in control condition and 10 min after the start of a 1 µM ZD7288 superfusion (**a**: note small and large upward deflections denoting STDs), and summary graph data (**b**: $n = 4$). (**c**) Contractile responses of guinea pig mesenteric lymphatic vessels luminally perfused at increasing flow rates in control condition and in the presence of 1 µM ZD7288 ($n = 2$)

blocker ivabradine, as well as to a lesser extent cesium and ZD7288 (at rather high concentrations), to inhibit lymphatic pumping was more recently reported in rat diaphragmatic lymphatics, which express all four HCN channel isoforms [80]. However, ZD7288 exhibited no significant effects on the membrane potential of guinea pig mesenteric lymphatic muscle, nor did it alter the frequency of action potentials and constrictions in rat and guinea pig mesenteric vessels (Fig. 15.3 and von der Weid, unpublished data), or the activity of spontaneous transient depolarizations (STDs) [69], the events proposed to mediate pacemaking in these vessels (see below). Altogether, these findings suggest that while a HCN conductance may be important for lymphatic pacemaking in several vessels or species, it plays a lesser role in others, where additional conductances predominate.

An issue associated with pacemaker potentials that has hampered their characterization is the electrical characteristics of the muscle syncytium present within the lymphatic chamber. In large vessels, pacemaker activity is difficult to study because of uncertainties in the electrical distance of the pacemaker cells from the site at which recordings are made in the smooth muscle. Thus, the pacemaker potential that generates each action potential cannot readily be distinguished from the potential change, underlying the propagated action potential. By studying smaller, more segmented vessels in the guinea pig mesentery, van Helden circumvented this problem and proposed a second model for lymphatic pacemaking. In these small, presumably isopotential short vessel segments, lymphatic muscle membrane potentials recorded with a intracellular microelectrode consistently displayed small STDs that

were proposed to be the lymphatic pacemaker, because either individually or through summation they underlie the action potentials and muscle contractions [53]. This hypothesis is supported by a number of observations reported in this original paper and subsequent studies [69, 81–84]. First, the initial phase of the spontaneously generated action potentials has the same time course as the rising phase of STDs. Second, agonists, such as noradrenaline, histamine, endothelin-1, or thromboxane A_2 mimetic U46619, which all increase lymphatic pumping rate, enhance STD activity. Third, STDs occur independently of both the innervation and the endothelium, making them likely to be generated by the lymphatic muscle cells. STDs reflect the opening of Ca^{2+}-activated inward current carried by Cl^- ions upon the "packeted" release of Ca^{2+} from IP_3-sensitive stores within the muscle cells [69]. In support of these findings, Toland et al. identified a Cl_{Ca} current in isolated sheep mesenteric lymphatic smooth muscle cells, using the perforated patch technique [66]. The authors demonstrated that while in current clamp mode inhibition of this current with 9-AC reduced STDs and action potentials, the same treatment also caused abolition of pumping in a pressurized vessel. This hypothesis that Cl_{Ca} channels underlie STDs and participate in the lymphatic pacemaking is also in agreement with the growing body of evidence showing that Cl_{Ca} channels are involved in agonist-induced rat vascular smooth muscle contraction [85, 86].

Elusive for a long time, the identity of the gene underlying these Cl_{Ca} channels has now been determined as anoctamin-1 (*Ano1*), also known as TMEM16a. ANO1 channels have been recently shown to be expressed in human, mouse, and rat lymphatics [87] (S.D. Zawieja and M.J. Davis, personal communication; von der Weid, unpublished data) and Cl_{Ca} currents have been recorded from lymphatic muscle cells acutely dissociated from mouse inguinal-axillary collectors (S.D. Zawieja and M.J. Davis, personal communication). The important role of ANO1 channels in lymphatic pumping was further demonstrated by the strong reduction of lymphatic contraction frequency and a lack of response to increase in transmural pressure after selective deletion of the *Ano1* gene in mouse lymphatic muscle cells (S.D. Zawieja and M.J. Davis, personal communication). In these transgenic mice, the lymphatic muscle cells were hyperpolarized, lacked the characteristic diastolic depolarization, and had a blunted action potential plateau, a time course similar to that reported in sheep lymphatic muscle cells treated with 9-AC [66]. Despite the strong evidences that STDs underlie lymphatic pacemaking and that STD inhibition correlates strictly with abolition of action potentials, several observations challenge the STD hypothesis for lymphatic pacemaker. Although it is likely that other conductances such as HCN currents also contribute, it is troubling that while Cl_{Ca} channel blockers, niflumic acid or 9-AC, are very potent at inhibiting STDs [66, 69], they only slightly decrease the frequency of contractions [55] (see Fig. 15.4). The argument that the notoriously nonspecific actions of these Cl_{Ca} channel blockers may also target other channels, such as L-type Ca^{2+} channels, is refuted by the fact that if the contraction frequency is not affected, neither should the action poten-

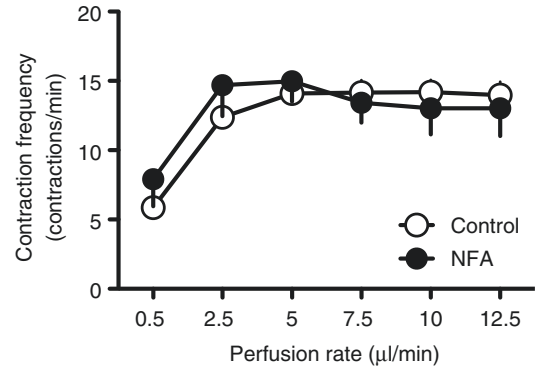

Fig. 15.4 Lack of effect of the Ca^{2+}-activated Cl^- channel blocker niflumic acid (NFA; 50 µM) on the perfusion-induced increase in contraction frequency of guinea pig mesenteric lymphatic vessels ($n = 7$)

tials. Moreover, although lymphatic pumping is markedly impaired in the pressurized ANO1$^{-/-}$ transgenic vessels, it is not totally abolished, thus aligning well with the finding that niflumic acid did not alter action potential frequency in wire myograph-mounted rat mesenteric lymphatics [55]. A careful examination of the possible reasons for the differences in the effects of the Cl_{Ca} channel blockers points to the different experimental conditions used for the different studies. In order to allow electrical recordings with sharp microelectrodes, inhibition of STDs was mostly assessed in quiescent, unstimulated vessel segments, displaying what we can consider to be true "spontaneous contractile activity." On the other hand, assessment of the effects of these blockers on lymphatic pumping was typically performed on isolated vessels under pressure/stretch conditions. It is legitimate to suggest that the strong mechanical stimulation activates another rhythmical mechanism, and to hypothesize that pressure-induced pacemaking requires activation of a set of ion channels different than those underlying spontaneous pacemaking.

It is well known that the degree of distension or stretch of the lymphatic vessel wall is an important factor in determining the intrinsic contractile ability of these vessels and hence the propulsion of lymph. Raising transmural pressure in doubly cannulated mesenteric lymphatic vessels causes an increase in both constriction frequency and amplitude and thus an increase in the amount of fluid propelled [88]. Benoit et al. [89] reported an increase in volume and constriction frequency of intact mesenteric lymphatics of the rat during edemagenic stress created by plasma dilution and concluded that a stretch-dependent mechanism was involved. Although STD frequency was shown to increase with stretch in rat mesenteric lymphatics mounted on a wire myograph [55] and with intraluminal flow [82, 90] other ion channels may underlie the response to stretch or pressure.

15.5.5 Roles of Intracellular Calcium in the Lymphatic Pacemaker

In addition to being the ion permeating through L-type channels to generate action potential and excitation-contraction (E–C) coupling [91], Ca^{2+} released from intracellular store is also involved with lymphatic pacemaking [65, 66, 82, 92–94].

Atchison et al. [93] first reported that intracellular Ca^{2+} store modulators, caffeine, ryanodine, and cyclopiazonic acid (CPA), all inhibited lymphatic pumping in actively-contracting isolated bovine mesenteric lymphatic vessels, implicating intracellular Ca^{2+} stores (including a ryanodine sensitive store) in the phasic contractile activity. When transmural pressure was increased the inhibition evoked by caffeine and CPA was greater than that produced by ryanodine. This observation led to their suggestion that stores other than the ryanodine-sensitive stores were also involved. This work is concordant with studies on guinea pig mesenteric vessels, which shows that STDs are not blocked in Ca^{2+}-free solution, but inhibited by either BAPTA-AM to chelate $[Ca^{2+}]_i$ and or CPA to inhibit Ca^{2+} reuptake by the sacro-endoplasmic Ca^{2+} ATPase (SERCA). In this preparation, STDs were untouched by treatment with ryanodine or tetracaine [69], pointing to the specific contribution of IP_3-sensitive stores in their generation [53, 92]. This conclusion is further confirmed by the observations that IP_3 receptor (IP_3R) blockers, 2-aminoethoxydiphenyl borate (2-APB) and xestospongin C, reduced STD amplitude. Thimerosal, known to sensitize IP_3R for IP_3, and Bt3(1,3,5)IP_3/AM, a membrane-permeant analog of IP_3, increase STD amplitudes, further confirming the specific involvement of IP_3-sensitive Ca^{2+} stores [69]. Importantly, 2-APB has no significant effect on contraction and action potential frequency of myograph-mounted rat mesenteric lymphatics (Fig. 15.5), again suggesting that different/additional molecular elements might be involved in pacemaking when vessels are activated by wall stretch.

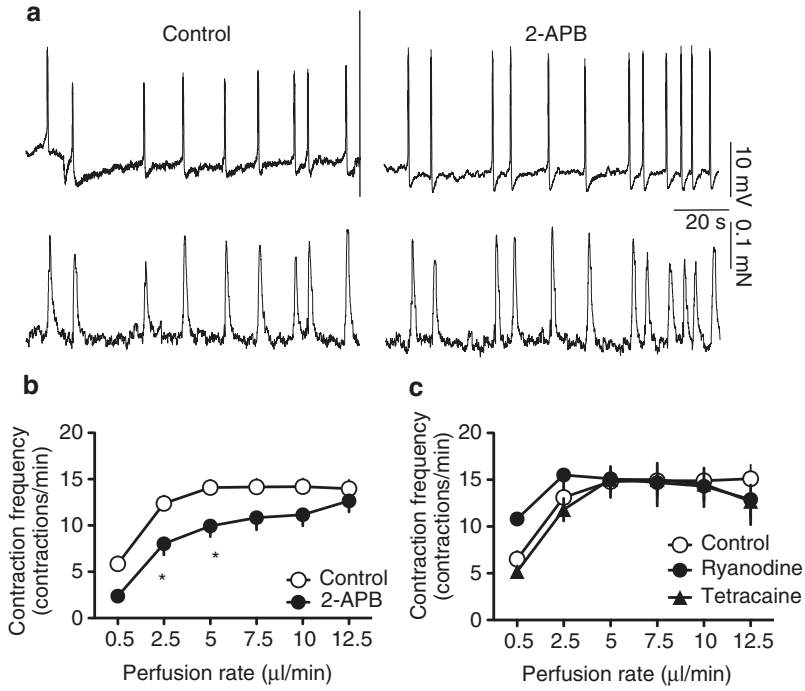

Fig. 15.5 Minimal involvement of intracellular Ca^{2+} stores in pacemaking of stretched lymphatics. (**a**) Original simultaneous recordings of membrane potential (top traces) and force (bottom traces) under control conditions (left) and 10 min after addition of 50 µM 2-APB to the solution bathing rat mesenteric lymphatic vessels mounted on a wire myograph under a preload of 0.3 mN. Traces are representative of five experiments. (**b**, **c**) Contractile responses of guinea pig mesenteric lymphatic vessels luminally perfused at increasing flow rates in control condition and in the presence of 50 µM 2-APB ($n = 13$; **b**) and 30 µM ryanodine ($n = 5$) or 50 µM tetracaine ($n = 5$; **c**)

15.5.6 Spontaneous and Stretch-Induced Pacemaker

A model for lymphatic pacemaking proposed by Imtiaz and colleagues can be used as a starting point to reconcile differences in pacemaker characteristics observed in unstretched and stretched vessels. In their model, the authors propose that the interactions of two coupled oscillators account for the rhythmic lymphatic pacemaker [84, 94]. The first oscillator is composed of the interaction of IP_3 with IP_3R and the subsequent sensitization of IP_3R by Ca^{2+} that is released internally. The second oscillator is represented by the electrical membrane potential changes leading to action potential firing in one cell that spreads and triggers depolarization and action potentials in adjacent cells coupled through gap junctions. Nonselective gap junction inhibitors have established a critical role for gap junctions in maintaining coordinated intra- and inter-lymphangion contractions in pressurized lymphatic vessel studies [95–97], but the identity of the various connexins mediating coupling between lymphatic smooth muscle cells is unknown at this time.

The limited ability of 2-APB, as well as ryanodine, to disrupt the contractile rhythmicity of lymphatic vessels under stretch [93] (see Fig. 15.5) suggests that the contribution of Ca^{2+} released from intracellular Ca^{2+} stores to pacemaking lessens as pressure/stretch of the vessel wall increases. However, as contractility strongly increases with pressure, the second, membrane-based, oscillator becomes more important. The ability of the cell membrane to sense and respond to increases in intraluminal pressure is critical and certainly involves the activation of a mecha-

nosensor. While the molecular identity of this structure is still unknown, it presumably involves the opening of ion channels to provide the depolarization and/or Ca^{2+} entry necessary for the direct or indirect initiation of action potentials and contraction. We thus hypothesize that under stretch, activation of the mechanosensor and the ensuing depolarization and/or Ca^{2+} entry take over the mechanism of initiation of spontaneous action potential/contraction, exemplified by STDs, to increase lymphatic pumping.

A study by Lee et al. investigating the role of voltage-dependent Ca^{2+} channels in stretch-induced lymphatic pumping showed a critical contribution of T-type voltage-dependent Ca^{2+} channels in pacing contractions generated by stretch [77]. Specifically, the authors revealed a significant inhibition of the increase in frequency of action potentials and contractions generated by stretch or transmural pressure in rat mesenteric lymphatics when vessels were treated with T-type voltage-dependent Ca^{2+} channel blockers, Ni^{2+} or mibefradil. These findings strongly contrasted with the effects of L-type voltage-dependent Ca^{2+} channel blockers, nifedipine and diltiazem, which significantly decreased only the force of contractions [77]. In addition to demonstrating the important role of T-type Ca^{2+} channels in lymphatic pacemaking, the study also revealed that Ni^{2+} and mibefradil differentially modulated lymphatic muscle membrane potential in wire myograph-mounted lymphatic vessels and unstretched vessels. Administration of the T-type Ca^{2+} channel blockers on unstretched vessels where lymphatic muscle membrane potentials ranged from −55 to −65 mV revealed a significant hyperpolarization, suggesting a contribution of these T-type Ca^{2+} channels to the resting membrane potential. Indeed, these channels are classified as low-voltage activation channels, which open at polarized membrane potentials [98]. On the other hand, when applied to lymphatic segments mounted on the wire myograph where muscle cells are more depolarized (−35 to −45 mV) [55], these blockers caused no significant changes in membrane potential, while inducing a decrease in contraction frequency. The involvement of T-type Ca^{2+} channels in the regulation of membrane potential in unstretched vessels and in the frequency of lymphatic contractions strongly suggests their participation in the pacemaking mechanism of lymphatic pumping [69, 71]. Indeed, T-type Ca^{2+} channels have also been reported to modulate electrical activity in other smooth muscles, such as rabbit urethra and guinea pig detrusor muscle of the urinary bladder, where their inhibition leads to a decrease in action potential frequency [99, 100]. Moreover, a role for T-type Ca^{2+} channels in the pacemaking mechanism of the heart has been demonstrated, as blocking T-type Ca^{2+} channels in the sinoatrial node slows the cardiac diastolic depolarization, also referred to as the "pacemaker potential" [101, 102]. Indeed it has been observed that increases in action potential/contraction frequency evoked by step increases in stretch in rat mesenteric collectors can occur without changes in membrane potential [55]. Thus, it is likely that stretch activates a collection of depolarizing ion conductances, including a T-type Ca^{2+} conductance, that modulate the frequency of action potentials/contractions in lymphatic muscle. Inhibition of one of these conductances, such as T-type Ca^{2+} channels, would lead to slower frequencies, but not necessarily affect the membrane potential. Further investigations are required to determine the specific role of T-type Ca^{2+}channels in the generation of APs leading to lymphatic contractions.

Other ion channels, which could, individually or in combination, play a role in the mechanosensor mechanism are members of the transient receptor potential family (TRP), such as TRPC6, TRPM4, and TRPM7 [103–107]. They have been shown to participate in cardiac automaticity [108] or pacemaking in intestinal interstitial cells of Cajal (ICC), sometimes in concert with ANO1 Cl_{Ca} channels [106, 107]. Importantly, like Cl_{Ca} channels, many TRP channels are permeable to Ca^{2+} and/or have their activity modulated by this ion [105, 109–111]. Although most are expressed in lymphatic vessels [112] (von der Weid, unpublished data), TRP channels have not been investigated in the context of lymphatic pacemaking.

15.6 Pathologies of the Lymphatic Vessels

15.6.1 Lymphedema

The importance of the lymphatic vessels in fluid and macromolecule balance is obvious in a case of lymphatic failure. One of the most common clinical consequences of inadequate lymphatic functioning is *lymphedema*. This affliction is a swelling of the tissues caused by an accumulation of fluid and proteins [113], usually consequent to abnormalities in the regional lymphatic drainage of the extremities, although visceral lymphatic abnormalities can also occur [114]. In contrast to venous edema in which enhanced capillary pressure indirectly stimulates lymph production, lymphedema is caused by a reduction in lymphatic transport. Lymphedema is typically categorized as *primary* (congenital) if the abnormality preventing lymph flow exists in the lymph vessels or lymph nodes, or as *secondary* (acquired) if the disease obstructing or obliterating the lymph conducting pathways began elsewhere [115].

The development of lymphedema can be the result of anatomic problems, including lymphatic hypoplasia and functional insufficiency or absence of lymphatic valves [116, 117]. Indeed, if lymphatic endothelial dysfunction is present, lymphatic muscle dysfunction is likely to follow. Impaired lymphatic drainage fosters the accumulation of protein and cellular metabolites, followed by an increase in tissue colloid osmotic pressure, which leads to water accumulation and increased interstitial hydraulic pressure. Once a chronic state is reached, an increase in the number of fibroblasts, adipocytes, and keratinocytes in the edematous tissues is observed. Macrophages often denote the chronic inflammatory response [118]. Increased collagen deposition, with adipose and connective tissue overgrowth in and around the edematous tissue (usually skin), also occurs, leading to progressive fibrosis [114].

Recent advance in the genetic investigation of primary lymphedemas has permitted the identification of forkhead transcription factor FOXC2 as a candidate gene for lymphedema-distichiasis [119]. FOXC2 is involved in abnormal interactions between lymphatic endothelial cells and pericytes as well as valve defects, which are characteristic of the pathology of lymphedema-distichiasis [120]. Hereditary primary lymphedema (also referred to as Milroy's disease) is attributed to a mutation that inactivates VEGFR-3 tyrosine kinase signaling important mainly in lymphatic vessels [121, 122].

Secondary lymphedema is much more common than the primary form. It develops after disruption or obstruction of lymphatic pathways by surgical, traumatic, inflammatory, and neoplastic disease processes. Edema of the arm after excision of axillary lymph nodes and subsequent irradiation, classical procedures to alleviate breast cancer, is probably the most common cause of lymphedema in developed countries [123]. Although multiple contributing mechanisms can be suggested, lymphoscintigraphy experiments have demonstrated that lymphatic pump failure participates in the lymphatic dysfunction observed in these patients [124].

However, the most common cause of secondary lymphedema is lymphatic filariasis, a major public health problem throughout many regions of the tropics, which affects an estimated 120 million persons worldwide [125]. The disease is caused by several species of filarial nematode, the most common being *Wuchereria bancrofti*. Parasites are transmitted by mosquitos and infective larvae develop into adult worms in afferent lymphatic vessels, causing severe distortion of the lymphatic system. In their life span of several years, adult *Wuchereria* can release millions of larvae into the blood, which often lodge in the lymphatics of the spermatic cord, causing scrotal damage and swelling.

Elephantiasis—a painful, disfiguring swelling of the limbs—is a classic sign of late-stage disease. In addition to these chronic pathologies, infected people experience several episodes of acute inflammatory disease each year, associated with the death of adult worms and infection with opportunistic organisms invading damaged and dysfunctional lymphatics and surrounding tissues. Until recently, understanding of filarial disease was considered to be due to complex interactions

between the parasite, host immune responses, and opportunistic infections. Studies aiming at characterizing the molecular nature of the inflammatory stimuli derived from filarial nematodes have revealed the critical role played by the worms' symbiont *Wolbachia* [126, 127]. Indeed, lipopolysaccharide (LPS)-like molecules released from these intracellular bacteria are responsible for potent pro-inflammatory responses by macrophages in animal models of filarial disease [128]. *Wolbachia* has also been associated with severe inflammatory reactions to filarial chemotherapy, being released into the blood following death of the parasites. Recent studies in animal models even implicate *Wolbachia* in the onset of lymphedema. Taken together, these studies imply a major role for *Wolbachia* in the pathogenesis of filarial disease. It may be possible, through the use of antibiotic therapy, to clear worms of their symbiotic bacteria, with the intent that this approach will prevent the development of filarial pathology [129].

While the precise pathological mechanisms that produce lymphedema during filariasis are not completely understood, symptoms including lymphangitis, dilated lymphatics, and decreased lymphatic contractile function both *in situ* and *ex vivo* point to an inhibition of lymphatic muscle function leading to a loss of lymphatic contractile activity and ultimately the development of lymphedema [130, 131].

15.6.2 Inflammation-Induced Lymphatic Contractile Dysfunction

As eluded above, the low-grade inflammation underlying the lymphedema condition might be a contributing factor in the lymphatic dysfunction. Indeed, collecting lymphatic vessels usually change their contractile behavior upon inflammatory stimulation. These inflammation-induced alterations are characterized first by dilation of the vessel and decrease in contraction frequency. Many studies have been performed to dissect out the role of individual components of the inflammatory soup in lymphatic pumping modulation. Classical inflammatory mediators, such as prostanoids, histamine, or NO, have all been shown to modulate lymphatic pumping and lymph drainage (see reviews [43, 132]). In addition, neuromediators important in immune and inflammatory responses, such as substance P, calcitonin gene-related peptide (CGRP), neuropeptide Y, or vasoactive intestinal polypeptide (VIP), have also been reported to strongly modulate lymphatic vessel contractility [133–136].

In a physiological and homeostatic context, it has been widely demonstrated that endothelium-derived mediators such as NO, prostacyclin, or prostaglandin E_2 inhibit lymphatic contractility [54, 137–145], while on the other hand thromboxane A_2 increases it [140, 143–146]. As these molecules are strongly associated with and upregulated during the inflammatory process, they are very credible candidates to influence lymphatic pumping during inflammation. Indeed, studies demonstrated that the inhibition of mesenteric lymphatic pumping during 2,4,6-trinitrobenzenesulfonic acid (TNBS)-induced ileitis was due to an increase in the production of both NO and prostaglandins [147, 148]. NO was also heavily involved in dilation and suppression of contractions in popliteal lymphatic vessels of mice after oxazolone-induced acute skin inflammation that decreased the lymphatic transport capacity. In this situation, NO was produced by infiltrated $CD11b^{+}Gr\text{-}1^{+}$ cells expressing inducible NO synthase (iNOS) [149]. However, dilation and slow pumping of the vessel may be caused by high lymph pressure driven by the upstream edema. In some circumstances, this would favor faster material transport, as demonstrated in isolated vessels from control/healthy animals where increased intraluminal pressure causes dilation and reduced pumping to allow material to quickly travel through the vessel network [150]. The role of pro-inflammatory cytokines has also been experimentally addressed. A study by Hanley et al. [151] reported that in isolated pressurized bovine mesenteric lymphatics interleukin (IL)-1α and 1β caused a significant inhibition of the pressure-dependent increase in lymphatic pumping. Interestingly, this effect occurred within minutes of IL-1 application, precluding a transcription-mediated action. Another study using noninva-

sive near-infrared fluorescence imaging described cessation of murine lymphatic propulsion as early as 4 h following intradermal administration of LPS, IL-1β, TNFα, or IL-6 [26]. Importantly, these effects were noted to be systemic and driven by NO production. In our own hands, we were not able to observe such rapid effects but did observe significant inhibition of pumping in isolated vessels or tonic contraction in cultured lymphatic muscle cells incubated for 24 h with the cytokines IL-1β or TNFα (unpublished observations; [25, 27]). The TNFα-induced decrease in lymphatic pumping requires activation of the NF-κB signaling pathway, upregulation of NOS, and production of NO, which drives lymphatic muscle hyperpolarization via the opening of ATP-sensitive K^+ channels [27].

Metabolic syndrome, which is characterized by chronic subclinical inflammation, also displays impaired intrinsic lymphatic contractility. Prenodal mesenteric collectors in a rat model of metabolic syndrome were significantly smaller in diameter than their control counterparts and had markedly reduced contraction frequency, effectively reducing the intrinsic flow-generating capacity of these vessels by almost 50%. These vessels also exhibited a twofold reduction in their total force production and their myofilaments were significantly less sensitive to Ca^{2+} compared with control myofilament [152].

Collectively, these studies directly indicate that inflammatory changes in the surrounding microenvironment significantly affect the lymphatic contractile behavior and subsequent flow of lymph and highlight the pivotal contribution of the collecting lymphatic vessels in the perpetuation of inflammatory and immune responses.

15.7 Conclusion

Lymphatic pumping is the main driving force behind lymph drainage, which when inappropriate contributes to the development of conditions such as lymphedema and chronic inflammatory diseases. It is initiated in the lymphatic muscle cells comprising the wall of lymphatic collectors by a pacemaker mechanism yet to be fully elucidated. Over the last decades, studies have implicated several different membrane ion channels and a strong dependence on intracellular Ca^{2+} transients in this intrinsic contractile activity. The precise interaction between these elements appears to vary between lymphatic beds and/or animal species. It is likely that given the ability of the lymphatic vessels to respond to changes in lymph pressure, the varying conclusions reached to date are due to differences in experimental design and whether or not stretch was applied to the vessel. Taking these methodological differences into consideration, most of the findings can be reconciled under the premise that several mechanisms are involved in lymphatic pacemaking and that their individual contribution changes depending on the strength or the origin of the mechanical stimulation. Based on current literature, we can suggest that spontaneous contractions occurring in unstimulated vessels heavily rely on the random release of Ca^{2+} from IP_3-sensitive intracellular stores activating ANO1 Cl_{Ca} channels and the generation of STDs, which if large enough allows the triggering of action potentials upon the opening of L-type Ca^{2+} channels. While the involvement of other channels, such as T-type Ca^{2+} channels, in this process can be suggested, there is good consensus as to a primary role for IP_3-sensitive Ca^{2+} stores and Cl_{Ca} channels. When a lymphatic collector is pressurized, the importance of these elements decreases as the increase in wall tension activates a different set of molecular entities that constitute the stretch-induced pacemaker. The molecular elements involved in this stretch-induced activity then provide the depolarization (directly or via intracellular Ca^{2+} changes) necessary for the action potential-induced contraction. Current investigations, testing the role of mechanosensitive TRP channels, should shed some light on this fascinating research area and may lead to the development of therapeutic tools useful to correct lymphatic contractile dysfunction and regulate edema and inflammation as it occurs in lymphedema and chronic inflammatory diseases.

References

1. Schmid-Schonbein GW. Microlymphatics and lymph flow. Physiol Rev. 1990;70(4):987–1028.
2. Azzali G, Arcari ML. Ultrastructural and three-dimensional aspects of the lymphatic vessels of the absorbing peripheral lymphatic apparatus in Peyer's patches of the rabbit. Anat Rec. 2000;258(1):71–9.
3. Casley-Smith JR. The role of the endothelial intercellular junctions in the functioning of the initial lymphatics. Angiologica. 1972;9(2):106–31.
4. Baluk P, Fuxe J, Hashizume H, Romano T, Lashnits E, Butz S, et al. Functionally specialized junctions between endothelial cells of lymphatic vessels. J Exp Med. 2007;204(10):2349–62.
5. Mendoza E, Schmid-Schonbein GW. A model for mechanics of primary lymphatic valves. J Biomech Eng. 2003;125(3):407–14.
6. Ryan TJ. Structure and function of lymphatics. J Invest Dermatol. 1989;93(2 Suppl):18S–24S.
7. Schmid-Schonbein GW. The second valve system in lymphatics. Lymphat Res Biol. 2003;1(1):25–9; discussion 9–31
8. Schulte-Merker S, Sabine A, Petrova TV. Lymphatic vascular morphogenesis in development, physiology, and disease. J Cell Biol. 2011;193(4):607–18.
9. Leak L, Burke J. Ultrastructural studies on the lymphatic anchoring filaments. J Cell Biol. 1968;36:129–49.
10. Barrowman JA, Tso P, Kvietys PR, Granger DN. Gastrointestinal lymph and lymphatics. In: Johnston M, editor. Experimental biology of the lymphatic circulation. Amsterdam: Elsevier Science Publishers; 1985.
11. Casley-Smith JR. Electron microscopical observations on the dilated lymphatics in oedematous regions and their collapse following hyaluronidase administration. Br J Exp Pathol. 1967;48:680–6.
12. Yoffey JM, Courtice FC. Lymphatics, lymph and the lymphomyeloid complex. London: Academic Press; 1970.
13. Horstmann E. Uber die funktionelle Struktur der mesenterialen Lymphgefasse. Morphol Jahrb. 1952;91:483–510.
14. Florey HW. Observations on the contractility of lacteals. Part I. J Physiol. 1927;62:267–72.
15. Aukland K, Reed RK. Interstitial-lymphatic mechanisms in the control of extracellular fluid volume. Physiol Rev. 1993;73(1):1–78.
16. Grimaldi A, Moriondo A, Sciacca L, Guidali ML, Tettamanti G, Negrini D. Functional arrangement of rat diaphragmatic initial lymphatic network. Am J Physiol Heart Circ Physiol. 2006;291(2):H876–85.
17. Moriondo A, Mukenge S, Negrini D. Transmural pressure in rat initial subpleural lymphatics during spontaneous or mechanical ventilation. Am J Physiol Heart Circ Physiol. 2005;289(1):H263–9.
18. Negrini D, Ballard ST, Benoit JN. Contribution of lymphatic myogenic activity and respiratory movements to pleural lymph flow. J Appl Physiol (1985). 1994;76(6):2267–74.
19. Negrini D, Del Fabbro M. Subatmospheric pressure in the rabbit pleural lymphatic network. J Physiol. 1999;520(Pt 3):761–9.
20. Negrini D, Moriondo A, Mukenge S. Transmural pressure during cardiogenic oscillations in rodent diaphragmatic lymphatic vessels. Lymphat Res Biol. 2004;2(2):69–81.
21. Nicoll PA, Hogan RD. Pressures associated with lymphatic capillary contraction. Microvasc Res. 1978;15(2):257–8.
22. Higuchi M, Fokin A, Masters TN, Robicsek F, Schmid-Schonbein GW. Transport of colloidal particles in lymphatics and vasculature after subcutaneous injection. J Appl Physiol (1985). 1999;86(4):1381–7.
23. Trzewik J, Mallipattu SK, Artmann GM, Delano FA, Schmid-Schonbein GW. Evidence for a second valve system in lymphatics: endothelial microvalves. FASEB J. 2001;15(10):1711–7.
24. Farnsworth RH, Achen MG, Stacker SA. The evolving role of lymphatics in cancer metastasis. Curr Opin Immunol. 2018;53:64–73.
25. Al-Kofahi M, Becker F, Gavins FN, Woolard MD, Tsunoda I, Wang Y, et al. IL-1beta reduces tonic contraction of mesenteric lymphatic muscle cells, with the involvement of cycloxygenase-2 and prostaglandin E2. Br J Pharmacol. 2015;172(16):4038–51.
26. Aldrich MB, Sevick-Muraca EM. Cytokines are systemic effectors of lymphatic function in acute inflammation. Cytokine. 2013;64(1):362–9.
27. Chen Y, Rehal S, Roizes S, Zhu HL, Cole WC, von der Weid PY. The pro-inflammatory cytokine TNF-alpha inhibits lymphatic pumping via activation of the NF-kappaB-iNOS signaling pathway. Microcirculation. 2017;24(3):e12364.
28. Paniagua D, Jimenez L, Romero C, Vergara I, Calderon A, Benard M, et al. Lymphatic route of transport and pharmacokinetics of Micrurus fulvius (coral snake) venom in sheep. Lymphology. 2012;45(4):144–53.
29. McLennan DN, Porter CJ, Edwards GA, Heatherington AC, Martin SW, Charman SA. The absorption of darbepoetin alfa occurs predominantly via the lymphatics following subcutaneous administration to sheep. Pharm Res. 2006;23(9):2060–6.
30. Chikly B. Who discovered the lymphatic system. Lymphology. 1997;30(4):186–93.
31. Tso P, Balint JA. Formation and transport of chylomicrons by enterocytes to the lymphatics. Am J Phys. 1986;250(6 Pt 1):G715–26.
32. Phan CT, Tso P. Intestinal lipid absorption and transport. Front Biosci. 2001;6:D299–319.
33. Nordskog BK, Phan CT, Nutting DF, Tso P. An examination of the factors affecting intestinal lymphatic transport of dietary lipids. Adv Drug Deliv Rev. 2001;50(1–2):21–44.

34. Tso P, Nauli A, Lo CM. Enterocyte fatty acid uptake and intestinal fatty acid-binding protein. Biochem Soc Trans. 2004;32(Pt 1):75–8.
35. Borgstrom B, Laurell CB. Studies of lymph and lymph-proteins during absorption of fat and saline by rats. Acta Physiol Scand. 1953;29(2–3):264–80.
36. Simmonds WJ. The effect of fluid, electrolyte and food intake on thoracic duct lymph flow in unanaesthetized rats. Aust J Exp Biol Med Sci. 1954;32(3):285–99.
37. Zweifach BW, Prather JW. Micromanipulation of pressure in terminal lymphatics in the mesentery. Am J Phys. 1975;228(5):1326–35.
38. Davis MJ, Rahbar E, Gashev AA, Zawieja DC, Moore JE Jr. Determinants of valve gating in collecting lymphatic vessels from rat mesentery. Am J Physiol Heart Circ Physiol. 2011;301(1):H48–60.
39. Chakraborty S, Davis MJ, Muthuchamy M. Emerging trends in the pathophysiology of lymphatic contractile function. Semin Cell Dev Biol. 2015;38:55–66.
40. Somlyo AP, Somlyo AV. Signal transduction and regulation in smooth muscle. Nature. 1994;372(6503):231–6.
41. Pfitzer G. Invited review: regulation of myosin phosphorylation in smooth muscle. J Appl Physiol. 2001;91(1):497–503.
42. Muthuchamy M, Gashev A, Boswell N, Dawson N, Zawieja D. Molecular and functional analyses of the contractile apparatus in lymphatic muscle. FASEB J. 2003;17(8):920–2.
43. von der Weid PY, Muthuchamy M. Regulatory mechanisms in lymphatic vessel contraction under normal and inflammatory conditions. Pathophysiology. 2010;17(4):263–76.
44. McHale NG, Roddie IC, Thornbury KD. Nervous modulation of spontaneous contractions in bovine mesenteric lymphatics. J Physiol Lond. 1980;309(461):461–72.
45. Hanley CA, Elias RM, Johnston MG. Is endothelium necessary for transmural pressure-induced contractions of bovine truncal lymphatics? Microvasc Res. 1992;43(2):134–46.
46. Allen JM, McHale NG, Rooney BM. Effect of norepinephrine on contractility of isolated mesenteric lymphatics. Am J Phys. 1983;244(4):H479–86.
47. Azuma T, Ohhashi T, Sakaguchi M. Electrical activity of lymphatic smooth muscles. Proc Soc Exp Biol Med. 1977;155(2):270–3.
48. Kirkpatrick CT, McHale NG. Electrical and mechanical activity of isolated lymphatic vessels [proceedings]. J Physiol. 1977;272(1):33P–4P.
49. Mislin H. Die motorik Lymphgefässe und der Regulation der Lymphherzen. Handbuch der Algemeinen Pathologie. 3/6. Berlin: Springer-Verlag; 1973. p. 219–38.
50. Mislin H. The lymphangion. In: Foldi M, Casley-Smith R, editors. Lymphangiology. Stuttgart: Schattauer-Verlag; 1983. p. 165–75.
51. Orlov RS, Borigora RP, Mundriko ES. Investigation of contractile and electrical activity of smooth muscle of lymphatic vessels. In: Bulbring EaS MF, editor. Physiology of smooth muscle. New York: Ranon; 1976. p. 147–52.
52. Chan AK, Vergnolle N, Hollenberg MD, von der Weid P-Y. Proteinase-activated receptor 2 modulates guinea-pig mesenteric lymphatic vessel pacemaker potential and contractile activity. J Physiol. 2004;560:563–76.
53. van Helden DF. Pacemaker potentials in lymphatic smooth muscle of the guinea-pig mesentery. J Physiol. 1993;471:465–79.
54. von der Weid PY, van Helden DF. Beta-adrenoceptor-mediated hyperpolarization in lymphatic smooth muscle of guinea pig mesentery. Am J Phys. 1996;270(5 Pt 2):H1687–95.
55. von der Weid PY, Lee S, Imtiaz MS, Zawieja DC, Davis MJ. Electrophysiological properties of rat mesenteric lymphatic vessels and their regulation by stretch. Lymphat Res Biol. 2014;12(2):66–75.
56. Hugues GA, Harper AA. The effect of Na+-K+-2Cl− cotransport inhibition and chloride channel blockers on membrane potential and contractility in rat lymphatic smooth muscle in vitro. J Physiol. 1999;518P:127P.
57. Ohhashi T, Azuma T. Effect of potassium on membrane potential and tension development in bovine mesenteric lymphatics. Microvasc Res. 1982;23(1):93–8.
58. Ohhashi T, Azuma T, Sakaguchi M. Transmembrane potentials in bovine lymphatic smooth muscle. Proc Soc Exp Biol Med. 1978;159:350–2.
59. Ward SM, McHale NG, Sanders KM. A method for recording transmembrane potentials in bovine mesenteric lymphatics. Ir J Med Sci. 1989;158:129 (abstract).
60. Telinius N, Mohanakumar S, Majgaard J, Kim S, Pilegaard H, Pahle E, et al. Human lymphatic vessel contractile activity is inhibited in vitro but not in vivo by the calcium channel blocker nifedipine. J Physiol. 2014;592(21):4697–714.
61. Zawieja SD, Castorena-Gonzalez JA, Scallan J, Davis MJ. Differences in L-type calcium channel activity partially underlie the regional dichotomy in pumping behavior by murine peripheral and visceral lymphatic vessels. Am J Physiol Heart Circ Physiol. 2018;314:H991–H1010.
62. Scallan JP, Zawieja SD, Castorena-Gonzalez JA, Davis MJ. Lymphatic pumping: mechanics, mechanisms and malfunction. J Physiol. 2016;594:5749–68.
63. Allen JM, McHale NG. The effect of known K+-channel blockers on the electrical activity of bovine lymphatic smooth muscle. Pflugers Arch. 1988;411(2):167–72.
64. Cotton KD, Hollywood MA, McHale NG, Thornbury KD. Outward currents in smooth muscle cells isolated from sheep mesenteric lymphatics. J Physiol Lond. 1997;503:1–11.

65. Cotton KD, Hollywood MA, McHale NG, Thornbury KD. Ca2+ current and Ca(2+)-activated chloride current in isolated smooth muscle cells of the sheep urethra. J Physiol Lond. 1997;505:121–31.
66. Toland HM, McCloskey KD, Thornbury KD, McHale NG, Hollywood MA. Ca(2+)-activated Cl(−) current in sheep lymphatic smooth muscle. Am J Phys Cell Physiol. 2000;279(5):C1327–35.
67. von der Weid P-Y. ATP-sensitive K+ channels in smooth muscle cells of guinea-pig mesenteric lymphatics: role in nitric oxide and beta-adrenoceptor agonist-induced hyperpolarizations. Br J Pharmacol. 1998;125(1):17–22.
68. Telinius N, Kim S, Pilegaard H, Pahle E, Nielsen J, Hjortdal V, et al. The contribution of K(+) channels to human thoracic duct contractility. Am J Physiol Heart Circ Physiol. 2014;307(1):H33–43.
69. von der Weid P-Y, Rahman M, Imtiaz MS, van Helden DF. Spontaneous transient depolarizations in lymphatic vessels of the guinea pig mesentery: pharmacology and implication for spontaneous contractility. Am J Physiol Heart Circ Physiol. 2008;295(5):H1989–2000.
70. Ward SM, Sanders KM, Thornbury KD, McHale NG. Spontaneous electrical activity in isolated bovine lymphatics recorded by intracellular microelectrodes. J Physiol. 1991;438:168P.
71. Beckett EA, Hollywood MA, Thornbury KD, McHale NG. Spontaneous electrical activity in sheep mesenteric lymphatics. Lymphat Res Biol. 2007;5(1):29–43.
72. Telinius N, Majgaard J, Kim S, Katballe N, Pahle E, Nielsen J, et al. Voltage-gated sodium channels contribute to action potentials and spontaneous contractility in isolated human lymphatic vessels. J Physiol. 2015;593(14):3109–22.
73. van Helden DF, von der Weid P-Y, Crowe MJ. Electrophysiology of lymphatic smooth muscle. In: Bert J, Laine GA, McHale NG, Reed R, Winlove P, editors. Interstitium, connective tissue, and lymphatics. London: Portland Press; 1995. p. 221–36.
74. Atchison DJ, Johnston MG. Role of extra- and intracellular Ca2+ in the lymphatic myogenic response. Am J Phys. 1997;272:R326–R33.
75. McHale NG, Allen JM, Iggulden HL. Mechanism of alpha-adrenergic excitation in bovine lymphatic smooth muscle. Am J Phys. 1987;252(5 Pt 2):H873–8.
76. Hollywood MA, Cotton KD, Thorbury KD, McHale NG. Isolated sheep mesenteric lymphatic smooth muscle possess both T- and L-type calcium currents. J Physiol. 1997;501P:P109–10.
77. Lee S, Roizes S, von der Weid PY. Distinct roles of L- and T-type voltage-dependent Ca2+ channels in regulation of lymphatic vessel contractile activity. J Physiol. 2014;592(Pt 24):5409–27.
78. Hollywood MA, Cotton KD, Thorbury KD, McHale NG. Tetrodotoxin-sensitive sodium current in sheep lymphatic smooth muscle. J Physiol. 1997;503:13–20.
79. McCloskey KD, Toland HM, Hollywood MA, Thorbury KD, McHale NG. Hyperpolarization-activated inward current in isolated sheep mesenteric lymphatic smooth muscle. J Physiol. 1999;521:201–11.
80. Negrini D, Marcozzi C, Solari E, Bossi E, Cinquetti R, Reguzzoni M, et al. Hyperpolarization-activated cyclic nucleotide-gated channels in peripheral diaphragmatic lymphatics. Am J Physiol Heart Circ Physiol. 2016;311(4):H892–903.
81. Fox JL, von der Weid PY. Effects of histamine on the contractile and electrical activity in isolated lymphatic vessels of the guinea-pig mesentery. Br J Pharmacol. 2002;136(8):1210–8.
82. van Helden DF, von der Weid P-Y, Crowe MJ. Intracellular Ca2+ release: a basis for electrical pacemaking in lymphatic smooth muscle. In: Tomita T, Bolton TB, editors. Smooth muscle excitation. London: Academic Press; 1996. p. 355–73.
83. von der Weid P-Y, Zhao J, van Helden DF. Nitric oxide decreases pacemaker activity in lymphatic vessels of guinea pig mesentery. Am J Phys. 2001;280(6):H2707–16.
84. Imtiaz MS, Zhao J, Hosaka K, von der Weid PY, Crowe M, van Helden DF. Pacemaking through Ca2+ stores interacting as coupled oscillators via membrane depolarization. Biophys J. 2007;92(11):3843–61.
85. Lamb FS, Barna TJ. Chloride ion currents contribute functionally to norepinephrine-induced vascular contraction. Am J Phys. 1998;275:H151–60.
86. Yuan XJ. Role of calcium-activated chloride current in regulating pulmonary vasomotor tone. Am J Phys. 1997;272:L959–68.
87. Gui P, Zawieja SD, Li M, Bulley S, Jaggar JH, Rock JR, et al. The Ca2+-activated Cl- Channel TMEM16A(ANO1) modulates, but is not required for, pacemaking in mouse lymphatic vessels. FASEB J. 2016;30:726.3.
88. McHale NG, Roddie IC. The effect of transmural pressure on pumping activity in isolated bovine lymphatic vessels. J Physiol Lond. 1976;261(2):255–69.
89. Benoit JN, Zawieja DC, Goodman AH, Granger HJ. Characterization of intact mesenteric lymphatic pump and its responsiveness to acute edemagenic stress. Am J Phys. 1989;257:H2059–69.
90. van Helden DF. Spontaneous and noradrenaline-induced transient depolarizations in the smooth muscle of guinea-pig mesenteric vein. J Physiol. 1991;437(511):511–41.
91. Munn LL. Mechanobiology of lymphatic contractions. Semin Cell Dev Biol. 2015;38:67–74.
92. Ferrusi I, Zhao J, van Helden DF, von der Weid P-Y. Cyclopiazonic acid decreases spontaneous transient depolarizations in guinea pig mesenteric lymphatic vessels in endothelium-dependent and -independent manners. Am J Phys. 2004;286(6):H2287–95.
93. Atchison DJ, Rodela H, Johnston MG. Intracellular calcium stores modulation in lymph vessels

depends on wall stretch. Can J Physiol Pharmacol. 1998;76(4):367–72.
94. Imtiaz MS, von der Weid PY, van Helden DF. Synchronization of Ca^{2+} oscillations: a coupled oscillator-based mechanism in smooth muscle. FEBS J. 2010;277(2):278–85.
95. Crowe MJ, von der Weid PY, Brock JA, Van Helden DF. Co-ordination of contractile activity in guinea-pig mesenteric lymphatics. J Physiol. 1997;500(Pt 1):235–44.
96. Zawieja DC, Davis KL, Schuster R, Hinds WM, Granger HJ. Distribution, propagation, and coordination of contractile activity in lymphatics. Am J Physiol Heart Circ Physiol. 1993;264(4 Pt 2):H1283–H91.
97. McHale NG, Meharg MK. Co-ordination of pumping in isolated bovine lymphatic vessels. J Physiol. 1992;450:503–12.
98. Hirano Y, Fozzard HA, January CT. Characteristics of L- and T-type Ca^{2+} currents in canine cardiac Purkinje cells. Am J Phys. 1989;256(5 Pt 2):H1478–92.
99. Bradley JE, Anderson UA, Woolsey SM, Thornbury KD, McHale NG, Hollywood MA. Characterization of T-type calcium current and its contribution to electrical activity in rabbit urethra. Am J Phys Cell Physiol. 2004;286(5):C1078–88.
100. Yanai Y, Hashitani H, Kubota Y, Sasaki S, Kohri K, Suzuki H. The role of Ni(2+)-sensitive T-type Ca(2+) channels in the regulation of spontaneous excitation in detrusor smooth muscles of the guinea-pig bladder. BJU Int. 2006;97(1):182–9.
101. Huser J, Blatter LA, Lipsius SL. Intracellular Ca2+ release contributes to automaticity in cat atrial pacemaker cells. J Physiol. 2000;524(Pt 2):415–22.
102. Zhou Z, Lipsius SL. T-type calcium current in latent pacemaker cells isolated from cat right atrium. J Mol Cell Cardiol. 1994;26(9):1211–9.
103. Fleig A, Penner R. The TRPM ion channel subfamily: molecular, biophysical and functional features. Trends Pharmacol Sci. 2004;25(12):633–9.
104. Harteneck C. Function and pharmacology of TRPM cation channels. Naunyn Schmiedeberg's Arch Pharmacol. 2005;371(4):307–14.
105. Nilius B, Mahieu F, Prenen J, Janssens A, Owsianik G, Vennekens R, et al. The Ca2+-activated cation channel TRPM4 is regulated by phosphatidylinositol 4,5-biphosphate. EMBO J. 2006;25(3):467–78.
106. Kim BJ, Lim HH, Yang DK, Jun JY, Chang IY, Park CS, et al. Melastatin-type transient receptor potential channel 7 is required for intestinal pacemaking activity. Gastroenterology. 2005;129(5):1504–17.
107. Kim BJ, So I, Kim KW. The relationship of TRP channels to the pacemaker activity of interstitial cells of Cajal in the gastrointestinal tract. J Smooth Muscle Res. 2006;42(1):1–7.
108. Sah R, Mesirca P, Van den Boogert M, Rosen J, Mably J, Mangoni ME, et al. Ion channel-kinase TRPM7 is required for maintaining cardiac automaticity. Proc Natl Acad Sci U S A. 2013;110(32):E3037–46.
109. Shi J, Mori E, Mori Y, Mori M, Li J, Ito Y, et al. Multiple regulation by calcium of murine homologues of transient receptor potential proteins TRPC6 and TRPC7 expressed in HEK293 cells. J Physiol. 2004;561(Pt 2):415–32.
110. Welsh DG, Morielli AD, Nelson MT, Brayden JE. Transient receptor potential channels regulate myogenic tone of resistance arteries. Circ Res. 2002;90(3):248–50.
111. Launay P, Fleig A, Perraud AL, Scharenberg AM, Penner R, Kinet JP. TRPM4 is a Ca2+-activated nonselective cation channel mediating cell membrane depolarization. Cell. 2002;109(3):397–407.
112. Bridenbaugh EA, Wang W, von der Weid P-Y, Zawieja DC. Detection of TRPV channel expression in rat lymphatic vessels. In: Andrade M, editor. Progress in lymphology XX. Salvador: Icone; 2005. p. 234–5.
113. Harwood CA, Mortimer PS. Causes and clinical manifestations of lymphatic failure. Clin Dermatol. 1995;13(5):459–71.
114. Rockson SG. Lymphedema. Am J Med. 2001;110(4):288–95.
115. Szuba A, Rockson SG. Lymphedema: classification, diagnosis and therapy. Vasc Med. 1998;3(2):145–56.
116. Browse NL, Stewart G. Lymphoedema: pathophysiology and classification. J Cardiovasc Surg. 1985;26(2):91–106.
117. Olszewski WL. Continuing discovery of the lymphatic system in the twenty-first century: a brief overview of the past. Lymphology. 2002;35(3):99–104.
118. Piller NB. Lymphoedema, macrophages and benzopyrones. Lymphology. 1980;13(3):109–19.
119. Kriederman BM, Myloyde TL, Witte MH, Dagenais SL, Witte CL, Rennels M, et al. FOXC2 haploinsufficient mice are a model for human autosomal dominant lymphedema-distichiasis syndrome. Hum Mol Genet. 2003;12(10):1179–85.
120. Petrova TV, Karpanen T, Norrmen C, Mellor R, Tamakoshi T, Finegold D, et al. Defective valves and abnormal mural cell recruitment underlie lymphatic vascular failure in lymphedema distichiasis. Nat Med. 2004;10(9):974–81.
121. Ferrell RE, Levinson KL, Esman JH, Kimak MA, Lawrence EC, Barmada MM, et al. Hereditary lymphedema: evidence for linkage and genetic heterogeneity. Hum Mol Genet. 1998;7(13):2073–8.
122. Irrthum A, Karkkainen MJ, Devriendt K, Alitalo K, Vikkula M. Congenital hereditary lymphedema caused by a mutation that inactivates VEGFR3 tyrosine kinase. Am J Hum Genet. 2000;67(2):295–301.
123. Segerstrom K, Bjerle P, Graffman S, Nystrom A. Factors that influence the incidence of brachial oedema after treatment of breast cancer. Scand J Plast Reconstr Surg Hand Surg. 1992;26(2):223–7.
124. Modi S, Stanton AW, Svensson WE, Peters AM, Mortimer PS, Levick JR. Human lymphatic pumping measured in healthy and lymphoedematous arms by lymphatic congestion lymphoscintigraphy. J Physiol. 2007;583(Pt 1):271–85.

125. Taylor MJ. A new insight into the pathogenesis of filarial disease. Curr Mol Med. 2002;2(3):299–302.
126. Taylor MJ, Hoerauf A. Wolbachia bacteria of filarial nematodes. Parasitol Today. 1999;15(11):437–42.
127. Taylor MJ, Hoerauf A. A new approach to the treatment of filariasis. Curr Opin Infect Dis. 2001;14(6):727–31.
128. Taylor MJ, Cross HF, Bilo K. Inflammatory responses induced by the filarial nematode Brugia malayi are mediated by lipopolysaccharide-like activity from endosymbiotic Wolbachia bacteria. J Exp Med. 2000;191(8):1429–36.
129. Pfarr KM, Debrah AY, Specht S, Hoerauf A. Filariasis and lymphoedema. Parasite Immunol. 2009;31(11):664–72.
130. Kaiser L, Mupanomunda M, Williams JF. Brugia pahangi-induced contractility of bovine mesenteric lymphatics studied in vitro: a role for filarial factors in the development of lymphedema? Am J Trop Med Hyg. 1996;54(4):386–90.
131. Chakraborty S, Gurusamy M, Zawieja DC, Muthuchamy M. Lymphatic filariasis: perspectives on lymphatic remodeling and contractile dysfunction in filarial disease pathogenesis. Microcirculation. 2013;20(5):349–64.
132. von der Weid PY. Review article: lymphatic vessel pumping and inflammation—the role of spontaneous constrictions and underlying electrical pacemaker potentials. Aliment Pharmacol Ther. 2001;15(8):1115–29.
133. Davis MJ, Lane MM, Davis AM, Durtschi D, Zawieja DC, Muthuchamy M, et al. Modulation of lymphatic muscle contractility by the neuropeptide substance P. Am J Physiol Heart Circ Physiol. 2008;295(2):H587–97.
134. Hosaka K, Rayner SE, von der Weid PY, Zhao J, Imtiaz MS, van Helden DF. Calcitonin gene-related peptide activates different signaling pathways in mesenteric lymphatics of guinea pigs. Am J Physiol Heart Circ Physiol. 2006;290(2):H813–22.
135. Rayner SE, van Helden DF. Evidence that the substance P-induced enhancement of pacemaking in lymphatics of the guinea-pig mesentery occurs through endothelial release of thromboxane A_2. Br J Pharmacol. 1997;121(8):1589–96.
136. von der Weid PY, Rehal S, Dyrda P, Lee S, Mathias R, Rahman M, et al. Mechanisms of VIP-induced inhibition of the lymphatic vessel pump. J Physiol. 2012;590(Pt 11):2677–91.
137. Ferguson MK, DeFilippi VJ, Reeder LB. Characterization of contractile properties of porcine mesenteric and tracheobronchial lymphatic smooth muscle. Lymphology. 1994;27(2):71–81.
138. Gashev AA, Davis MJ, Zawieja DC. Inhibition of the active lymph pump by flow in rat mesenteric lymphatics and thoracic duct. J Physiol. 2002;540(Pt 3):1023–37.
139. Gasheva OY, Zawieja DC, Gashev AA. Contraction-initiated NO-dependent lymphatic relaxation: a self-regulatory mechanism in rat thoracic duct. J Physiol. 2006;575(Pt 3):821–32.
140. Mizuno R, Koller A, Kaley G. Regulation of the vasomotor activity of lymph microvessels by nitric oxide and prostaglandins. Am J Phys. 1998;274(3 Pt 2):R790–6.
141. Rehal S, Blanckaert P, Roizes S, von der Weid PY. Characterization of biosynthesis and modes of action of prostaglandin E2 and prostacyclin in guinea pig mesenteric lymphatic vessels. Br J Pharmacol. 2009;158(8):1961–70.
142. Elias RM, Johnston MG. Modulation of fluid pumping in isolated bovine mesenteric lymphatics by a thromboxane/endoperoxide analogue. Prostaglandins. 1988;36(1):97–106.
143. Johnston MG, Kanalec A, Gordon JL. Effects of arachidonic acid and its cyclo-oxygenase and lipoxygenase products on lymphatic vessel contractility in vitro. Prostaglandins. 1983;25(1):85–98.
144. Johnston MG, Gordon JL. Regulation of lymphatic contractility by arachidonate metabolites. Nature. 1981;293(5830):294–7.
145. Johnston MG, Feuer C. Suppression of lymphatic vessel contractility with inhibitors of arachidonic acid metabolism. J Pharmacol Exp Ther. 1983;226(2):603–7.
146. Plaku KJ, von der Weid PY. Mast cell degranulation alters lymphatic contractile activity through action of histamine. Microcirculation. 2006;13(3):219–27.
147. Mathias R, von der Weid PY. Involvement of the NO-cGMP-KATP channel pathway in the mesenteric lymphatic pump dysfunction observed in the guinea pig model of TNBS-induced ileitis. Am J Physiol Gastrointest Liver Physiol. 2013;304:G623–34.
148. Wu TF, Carati CJ, Macnaughton WK, von der Weid PY. Contractile activity of lymphatic vessels is altered in the TNBS model of guinea pig ileitis. Am J Physiol Gastrointest Liver Physiol. 2006;291(4):G566–74.
149. Liao S, Cheng G, Conner DA, Huang Y, Kucherlapati RS, Munn LL, et al. Impaired lymphatic contraction associated with immunosuppression. Proc Natl Acad Sci U S A. 2011;108(46):18784–9.
150. Gashev AA. Physiologic aspects of lymphatic contractile function: current perspectives. Ann N Y Acad Sci. 2002;979:178–87; discussion 88–96.
151. Hanley CA, Elias RM, Movat HZ, Johnston MG. Suppression of fluid pumping in isolated bovine mesenteric lymphatics by interleukin-1: interaction with prostaglandin E2. Microvasc Res. 1989;37(2):218–29.
152. Zawieja SD, Wang W, Wu X, Nepiyushchikh ZV, Zawieja DC, Muthuchamy M. Impairments in the intrinsic contractility of mesenteric collecting lymphatics in a rat model of metabolic syndrome. Am J Physiol Heart Circ Physiol. 2012;302(3):H643–53.

Part V

Airways

Regulation of Airway Smooth Muscle Contraction in Health and Disease

16

Maggie Lam, Emma Lamanna, and Jane E. Bourke

Abstract

Airway smooth muscle (ASM) extends from the trachea throughout the bronchial tree to the terminal bronchioles. *In utero*, spontaneous phasic contraction of fetal ASM is critical for normal lung development by regulating intraluminal fluid movement, ASM differentiation, and release of key growth factors. In contrast, phasic contraction appears to be absent in the adult lung, and regulation of tonic contraction and airflow is under neuronal and humoral control. Accumulating evidence suggests that changes in ASM responsiveness contribute to the pathophysiology of lung diseases with lifelong health impacts.

Functional assessments of fetal and adult ASM and airways have defined pharmacological responses and signaling pathways that drive airway contraction and relaxation. Studies using precision-cut lung slices, in which contraction of intrapulmonary airways and ASM calcium signaling can be assessed simultaneously *in situ*, have been particularly informative. These combined approaches have defined the relative importance of calcium entry into ASM and calcium release from intracellular stores as drivers of spontaneous phasic contraction *in utero* and excitation-contraction coupling.

Increased contractility of ASM in asthma contributes to airway hyperresponsiveness. Studies using animal models and human ASM and airways have characterized inflammatory and other mechanisms underlying increased reactivity to contractile agonists and reduced bronchodilator efficacy of β_2-adrenoceptor agonists in severe diseases. Novel bronchodilators and the application of bronchial thermoplasty to ablate increased ASM within asthmatic airways have the potential to overcome limitations of current therapies. These approaches may directly limit excessive airway contraction to improve outcomes for difficult-to-control asthma and other chronic lung diseases.

M. Lam · E. Lamanna · J. E. Bourke (✉)
Department of Pharmacology, Biomedicine Discovery Institute, Monash University, Clayton, VIC, Australia
e-mail: jane.bourke@monash.edu

Keywords

Airway smooth muscle · Phasic · Tonic · Contraction · Calcium · Bronchodilator · Asthma

H. Hashitani, R. J. Lang (eds.), *Smooth Muscle Spontaneous Activity*, Advances in Experimental Medicine and Biology 1124, https://doi.org/10.1007/978-981-13-5895-1_16

16.1 Introduction/Background

Airway smooth muscle (ASM) plays major functional and structural roles within the lung throughout life. ASM is present as muscle bands in the posterior portion of large cartilaginous central airways and arranged circumferentially around the smaller peripheral airways located in the distal lung. Spontaneous phasic contractions of ASM are evident *in utero* only, and are implicated in airway development. Tonic contractions of ASM and responses to physiological and pathophysiological stimuli throughout life determine airway caliber, regulating airflow to optimize ventilation, and may be required for protective reflexes such as cough. In both large and small airways, ASM has intrinsic tone, and further contraction can be induced in response to acetylcholine (ACh) released from parasympathetic nerves or to mediators released from other cells, such as mast cells and basophils. Airway relaxation is predominantly mediated by circulating adrenaline, although epithelial-derived factors may also play a role. Both phasic and tonic airway contractions are controlled and regulated by Ca^{2+} signaling, with differential contributions from Ca^{2+} influx, mobilization from intracellular stores, and sensitivity of the ASM contractile apparatus to Ca^{2+}.

Chronic lung diseases such as asthma are associated with dysregulation of ASM function and may be initiated in early life or have later onset. Increased reactivity of ASM to contractile agonists, termed airway hyperresponsiveness (AHR), leads to exaggerated airway contraction and obstruction. Evidence that the recurrence of spontaneous phasic contraction may also contribute is limited. In addition to its contractile function, ASM may also be a source of inflammatory mediators and cytokines and matrix proteins, and the increased proliferation of ASM in disease is thought to contribute to airway inflammation, remodeling, and associated AHR in asthma. These changes in ASM contractile and synthetic function are drivers of acute and chronic narrowing of the airways in asthma. While bronchodilators and anti-inflammatory agents can oppose some of these changes in ASM function, their efficacy is limited in severe disease and they do not provide a cure.

This chapter describes the development of ASM and its role *in utero*, before outlining its broader contractile and synthetic functions. The major focus is on the regulation of ASM function in health and disease, and the assessment of ASM contraction and relaxation and associated cellular signaling *ex vivo* at both the cellular level and in large and small airways. These mechanistic and functional studies in human samples and disease-relevant animal models have characterized signaling pathways that differentiate ASM from other types of smooth muscle, and have implicated numerous factors underlying airway dysfunction. This in turn has led to increased understanding of the mechanisms of action of existing therapies and the identification of novel therapeutic approaches targeting ASM that offer promise for asthma and other chronic lung diseases.

16.2 Airway Development

16.2.1 Lung Development

Human lung development begins during early embryogenesis and extends into childhood, with most postnatal growth occurring within the first 2 years of life. The process is arbitrarily divided into embryonic, pseudo-glandular, canalicular, saccular, alveolar, and vascular maturation stages.

During the embryonic stage, the lung begins to form as a diverticulum from the primitive foregut as early as 4 weeks gestation, and divides into two buds that will become the left and right lungs [1]. Further division of the airway buds occurs during the subsequent pseudoglandular stage of fetal development from 5 to 17 weeks, with cells within the airway wall undergoing differentiation to ASM, epithelial cells, and cartilage. By 17 weeks gestation when the pseudoglandular stage is ending, both the pre-acinar pulmonary vasculature and airways are formed [1]. Division continues up to 27 weeks gestation during the canalicular stage of fetal development, with subsequent dichotomous branching leading to the

Table 16.1 Stages of lung development (in gestation days) in different species [2]

Species	Glandular	Canalicular	Saccular	Alveolar
Mouse	14–16	16.5–17.4	17.4	PD 5
Rat	13–18	19–20	21–PD	PD 7–21
Rabbit	19–24	24–27	27	
Sheep	95	95–120	120	
Human	42–112	112–196	196–252	252–childhood

ASM has been identified as early as 6 weeks gestation in human airways [3]. *PD* postnatal day

formation of almost all the airways that will be present at birth [1]. Alveolar development in the final stage until term is evidenced by the appearance of dents in the saccule wall from 27 to 29 weeks gestation, progressing to cup-shaped structure by 34 weeks gestation. Alveoli continue to divide distally until 2–3 years of age, distal to the final total of 23 generations of airways present within the left and right lobes of the postnatal human lung.

Comparisons between species have shown that the timing of each developmental stage and the degree of lung development at birth vary considerably (Table 16.1).

16.2.2 Branching Structure and Functional Zones Within the Lungs

In the mature human lung, the airways form a branching structure, segmentally dividing in an irregular dichotomous manner from the trachea (generation 1) into two daughter branches at each subsequent generation through to the estimated 480 million alveoli (generation 23, [4]). This pattern varies between species, with the small airways of sheep also showing dichotomous branching, while mouse lungs have only 13 airway generations and exhibit a monopodial branching pattern.

The conducting zone of the lungs (human airway generations 1–16) is responsible for the transport of inhaled air. Subsequent generations act as a transition zone until the terminal bronchioles lead to the respiratory acinar zone where gas exchange occurs (generations 17–23). In considering the contribution of airways of different sizes to resistance to airflow, most resistance is determined by changes in the caliber of the relatively few large bronchioles (generations 1–7). The numerous smaller airways (defined as <2 mm in diameter, generations 8–23) contribute <10% to total airway resistance in healthy lungs [5], but have been implicated in the pathogenesis of chronic lung diseases such as asthma and chronic obstructive pulmonary disease (COPD) [6]. As such, it is important to define the functional responses of large and small airways, in both health and disease.

16.2.3 Differentiation of Airway Smooth Muscle

The formation of new airspaces during branching morphogenesis early in gestation is closely followed by the differentiation of mesenchymal cells into ASM cells. Evidenced by cellular expression of the contractile protein alpha-smooth muscle actin (αSMA) as an early differentiation marker [3], ASM progenitor cells have been identified in both the proximal and distal lung mesenchyme [7, 8]. This differentiation of ASM is characterized by the simultaneous production of smooth muscle myosin heavy-chain (MHC) filaments in fetal human lungs [9]. ASM development occurs in response to stretch and autocrine and epithelial derived paracrine factors including RhoA, serum response factor and transforming growth factor-β (TGF-β). This leads to the expression of additional smooth muscle markers such as calponin, smooth muscle protein 22α (sm22α, also known as transgelin), and desmin in fetal ASM [10].

ASM has been identified by 6 weeks gestation in human fetal trachea and primary and

lobar bronchi [3], and similarly between the end of the embryonic and the beginning of the pseudoglandular stage of fetal development across multiple species [11]. By 8 weeks gestation, ASM completely surrounds the trachea and is present on the branching epithelial tubules that will later become the bronchial tree [12]. Although there are few studies directly addressing the phenomenon of ASM cell migration *in vivo* during lung development, it is likely that the addition of ASM cells to the developing airway wall is a result of both proliferation and cell migration, occurring under the influence of many of the same stimuli.

ASM eventually runs continuously from the trachea, where it forms a closely packed and multilayered band attached to the anterior airway cartilage rings, to the distal lung where the muscle layer is only one to two cells deep. In contrast to other visceral organs where circular and longitudinal bands of muscle develop to propel internal contents, ASM cells form characteristic criss-crossed bundles in the postnatal airways [12]. This structure is consistent with the functions of adult ASM in maintaining airway patency as well as regulating diameter during both quiet breathing and in response to endogenous mediators including neurotransmitters, hormones, and autacoids.

16.2.4 Development of Airway Innervation

As ASM differentiation becomes evident within the lung, neural crest-derived cells and axons begin to migrate into the elongating lung buds from the foregut. It has been proposed that glial derived neurotrophic factor (GDNF) produced by the ASM acts as a chemoattractant for growing nerve endings. Neural development follows the newly differentiated ASM as it is laid down at the ends of the tubules [12].

By the end of the embryonic period (53 days gestation), the branching epithelial tubules in the primordial lung are covered with ASM to the base of the terminal sacs. Around this ASM layer, an extensive plexus of nerve bundles, ganglia, and Schwann cells develops as a sheath. By the canalicular stage, maturation of the innervation is advanced with two major nerve trunks running the length of the bronchial tree, giving rise to varicose fibers lying on the ASM, gradually becoming more compact and larger in diameter. Furthermore, increased numbers of larger and more spherical ganglia are present in the segmental and subsegmental airways. At this time point, a network of small fibers lies on the ASM layer. In adults, there are few ganglia present, mostly accompanying extrapulmonary airways with a scarce number of small ganglia present at junctions of intrapulmonary bronchi [12, 13].

Enzymes responsible for the synthesis of specific neurotransmitters and the transmitters themselves are expressed during maturation of airway innervation [12, 13]. Choline acetyltransferase and neuronal nitric oxide synthase (n-NOS), required for synthesis of acetylcholine and NO, respectively, and the neuropeptide vasoactive intestinal peptide (VIP) are co-localized in cholinergic, parasympathetic nerves in human and pig fetal airways by the early canalicular stage. Tyrosine hydroxylase required for noradrenaline synthesis and neuropeptide tyrosine (NPY) are co-localized in sympathetic nerve fibers by the saccular stage. Additionally, the neuropeptides substance P (SP) and calcitonin gene-related peptide (CGRP) can be detected in fetal airways, providing evidence of sensory nerves *in utero*.

16.3 Functions of Airway Smooth Muscle

Differentiated ASM has the potential to be mechanically active from the early stages of lung development. Spontaneous phasic contractions of fetal airways are evident and contribute to *in utero* development, but do not persist in postnatal life. Both developing and mature ASM expresses multiple receptors, and the downstream signaling pathways and contractile elements to respond to neurotransmitters and other mediators, while ASM also possesses additional proliferative and

secretory functions that have potential autocrine effects on airway structure and function.

16.3.1 Spontaneous Phasic Contractions of ASM *In Utero*

Spontaneous narrowing of airways in the fetal lung was first observed in chicken embryo lung explants in culture [14]. The first studies in first-trimester human lung showed that this phenomenon was myogenic in nature [15]. This property of fetal ASM has been established in multiple species including mouse at gestation day 11 [16], rabbit in third trimester [11], and pig in the early second trimester [11]. The development of these phasic airway contractions is temporally related to ASM development and generation of regular waves of spontaneous action potentials [17].

The origin of the peristaltic waves of fetal airway contraction has been explored. In cultures of separate lobes of mouse lungs, contractions originate proximally at the lobar bronchus and travel to the periphery, whereas narrowing starts at the trachea in complete lungs [11]. In rat lungs, airway peristalsis commences during embryonic lung development along with the earliest detection of αSMA [18]. By early stages of development, discrete pacemaker sites are evident within the trachea and proximal airways, dominated by the right lung. This pacemaker hierarchy appears to change during development, as phasic contractions originating in the trachea subside as morphogenesis progresses [18].

16.3.1.1 Functions of Spontaneous Phasic Contractions

Spontaneous phasic airway contractions *in utero* have been implicated in key functions associated with normal lung development, leading to the suggestion that fetal ASM plays a key role as an "architect of the lung" [18]. The movement of intraluminal fluid through epithelial tubules as a consequence of the peristaltic activity of fetal ASM maintains positive pressure in the lumen area to keep the tubules in a distended state [19]. Experiments in fetal sheep have demonstrated a direct link between reduced distension due to fluid loss and lung hypoplasia. Conversely, tracheal obstruction *in utero*, leading to fluid accumulation, results in more rapid lung maturation [20]. These differences in pressure between the airway lumen and surrounding tissue are essential for normal airway development, with tension and mechanical stretch playing additional roles in cellular differentiation and airway growth [21].

The force generated by contraction of fetal ASM may also stimulate lung growth by mechanically inducing the expression of growth factors [11]. Fibroblast growth factor-10 (FGF10) has been identified as a mitogen produced by ASM precursor cells in the distal lung, driving their own growth and entry into the smooth muscle cell lineage. This growth factor elicits dose-dependent proliferation of progenitor cells in early lung development, while in knockout mice lacking the Fgf10 gene the airways fail to extend beyond the carina [7]. In separate studies in rat lungs, phasic contractions occur at a frequency of 0.5–1 min^{-1}; both serum and FGF10 promoted lung growth associated with an increase in peristalsis frequency [22].

Studies performed using undifferentiated mouse and human lung mesenchymal cells have shown that upregulation of contractile proteins specific to smooth muscle can be induced by stretch or prevented by reducing airway intraluminal pressure [10, 12]. In both the intact bronchial tree and in culture, airway contraction pushes the lung liquid in the airway lumen towards the periphery [11]. Interestingly, lung growth is concentrated at the end buds of the lung where the periodic distensions and relaxations occur [10]. These combined findings support the coupling of spontaneous phasic contractions of fetal airways with normal lung development.

16.3.1.2 Mechanisms of Spontaneous Phasic Contractions

The ionic mechanisms underlying the spontaneous phasic activity of fetal airways have been studied in freshly isolated ASM cells and intact airways [15, 23]. The first study of membrane ion currents in fetal single ASM cells demonstrated a small voltage-independent cationic current and a large

variation in an outward current that was sensitive to tetraethylammonium (TEA) and the scorpion venom toxins charybdotoxin (ChTX) and iberiotoxin (IbTX), but resistant to 4-aminopyridine (4-AP), consistent with the activation of large-conductance Ca^{2+}-activated K^+ (BK) channels. In current clamp mode, ChTX, but not 4-AP, caused a substantial depolarization of human fetal ASM cells, suggesting that BK channels are the major determinant of the membrane potential in this tissue [23]. Depending on the size of the BK current, the mean resting membrane potential of these fetal ASM cells (−48 mV) [23] is more depolarized than that reported for adult ASM (between −65 and −45 mV) [15, 24, 25] and falls within the voltage range required to activate L-type voltage-dependent Ca^{2+} channels (VDCCs) [15, 24]. This is consistent with intact prenatal airways being more electrically excitable and therefore more prone to spontaneous phasic activity than postnatal airways.

Mechanical studies of fetal human airway preparations have shown that spontaneous contractility of fresh ASM-covered epithelial tubules is maintained in the presence of the muscarinic antagonist atropine, providing evidence that cholinergic nerve activation is not fundamental [26]. Furthermore, this spontaneous activity is unaffected by the sodium channel blocker, tetrodotoxin (TTX), suggesting that contractions are an intrinsic property of the ASM itself or closely associated sodium channel-independent pacemaker cells that do not require a neuronal input [22, 26]. These spontaneous contractions are prevented upon L-type Ca^{2+} channel blockade with nifedipine, demonstrating a fundamental role of Ca^{2+} influx upon the opening of L-type VDCCs [16, 26]. Simultaneous measurements of isometric force and membrane potential in human trachea isolated between 12 and 16 weeks of gestational development similarly show spontaneous electrical activity that is completely suppressed by Ca^{2+} channel blocker verapamil or removal of extracellular Ca^{2+} [15].

The first study to demonstrate prenatal ASM Ca^{2+} oscillations used embryonic rat lungs loaded with the fluorescent indicator Fluo-4 and showed travelling waves of intracellular Ca^{2+} [27]. In these preparations, the gap junction uncoupler 18-β glycyrrhetinic acid (40 μM) abolishes both Ca^{2+} waves and coordinated peristalsis. The spontaneous contractions are prevented by nifedipine or removal of extracellular Ca^{2+}, and increased in amplitude and frequency by TEA (10 mM). These combined findings suggest that the spontaneous contractions result from the spread of L-type Ca^{2+} channel-dependent depolarizations via gap junctions, while K^+ channels (voltage-gated or BK channels or both) appear to suppress ASM excitability.

Calcium release from sarcoplasmic reticulum (SR) stores via activation of inositol trisphosphate receptors (IP_3Rs) and ryanodine receptors (RyRs) also regulates Ca^{2+} waves and phasic contractility in fetal ASM [27]. In rat embryonic lungs, phasic contraction is inhibited by 2-aminoethoxydiphenyl borate (2-APB) that is known to block the IP_3R-mediated Ca^{2+} release. Activating RyRs with caffeine or blocking these channels with ryanodine increases or reduces phasic contractions, respectively [27]. Thus, spontaneous contractions of the fetal airways are produced by Ca^{2+} oscillations and are dependent not only on extracellular Ca^{2+} influx but also on intracellular release from the SR.

The rhythmic and spontaneous contractions of the fetal airways increase in frequency through gestation [11, 12]. Although Ca^{2+} oscillations have been demonstrated in human cultured ASM cells, organ cultures of whole embryonic rat lungs [28, 29], and ASM cells from both healthy and asthmatic patients [30], there is little evidence that spontaneous rhythmic contractions of the airways persist in postnatal life. However, it may well be that the summation of these Ca^{2+} signals is responsible for the generation of tone in mature ASM, presumably via mechanisms discussed in gastrointestinal sphincters (Chap. 2) and urethra (Chap. 6).

16.3.2 *In Utero* and Postnatal Tonic Contractions of ASM

16.3.2.1 Functions of Tonic Contractions

There is considerable debate about the physiological function of ASM beyond its regulation of

fetal airway fluid homeostasis and lung development via spontaneous phasic contractions *in utero*. The levels of smooth muscle contractile proteins and calcium regulatory proteins expressed in fetal ASM are retained at qualitatively comparable levels in adult human ASM [31], so ASM is clearly capable of contracting the mature airways. After birth, tonic contraction occurs in response to neurotransmitters and circulating stimuli, reducing airway lumen area and increasing resistance to airflow. While this establishes the contribution of ASM to airway disease, its role in healthy airways is less clear. Indeed, there are several proponents of the idea that contractility of ASM contributes little to airway regulation after birth. They have described the ASM layer as "the appendix of the lung" [32] and ASM as a "frustrated cell" [33].

Suggested functions of ASM include stabilizing airway structure to prevent maximal narrowing and airway closure. However, the airway basement membrane alone is likely to provide a relatively nondistensible natural limit to oppose airway collapse [34]. ASM contraction is not required for exhalation, and clearance of mucus and respirable irritants is achieved by the actions of beating cilia lining the airways rather than requiring ASM peristalsis [35]. Even an active role for ASM contraction in enhancing the effectiveness of cough remains uncertain [33]. Airway narrowing increases airflow velocity, and could therefore lead to increased mucus clearance. However, there is no localized reflex that could initiate bronchoconstriction through flow-limiting segments, suggesting that ASM contraction has limited potential to oppose mucus obstruction in the airways [36].

While the physiological function of ASM remains elusive, it is clear that excessive ASM contraction has adverse consequences in the context of disease. It therefore remains important to define the numerous factors that regulate airway and ASM responsiveness. ASM plays a major role in the pathogenesis of asthma and other airway diseases when it contracts "too easily and too much" [37]. This AHR has been attributed to the increased reactivity of ASM to contractile stimuli and the increased ASM mass within the inflamed, remodeled airways.

16.3.2.2 *In Vitro* Assessment of Airway and ASM Contraction

The majority of *in vitro* studies examining responses of isolated airways to electrical field stimulation (EFS) or contractile agonists have used readily accessible airway muscle strips and intact tracheal or bronchial rings under isometric conditions (reviewed by [38]). The relative inaccessibility of small intrapulmonary airways that previously limited their *in vitro* assessment has been overcome by the development of the precision-cut lung slice (PCLS) technique, in which responsiveness to EFS or added agonists can be visualized as changes in the area of small airways (and adjacent arterioles) (Fig. 16.1) [39].

To prepare PCLS, intact lungs, lobes, or wedge preparations are inflated with liquid agarose, which is then forced through the airways into alveoli by subsequent inflation with a small volume of air. After cooling, the lungs stiffen for slicing on a tissue slicer or vibratome. In PCLS, contraction is measured under auxotonic conditions, whereby ASM shortens against an increasing load imposed by airway attachments to the surrounding lung parenchyma including its extracellular matrix (ECM). This provides an innovative approach for *in situ* assessment of pharmacological responses of small airways to added agonists such as serotonin, as well as reactivity of adjacent pulmonary arterioles (Fig. 16.1). Additionally, responses to EFS can also be assessed using PCLS [40], and confocal imaging of PCLS loaded with Ca^{2+}-sensing dyes allows simultaneous examination of ASM signaling pathways related to contraction [39].

Other *in vitro* approaches can assess contractile responses of individual ASM cells, as their contractile phenotype is maintained at early passage (reviewed by [38]). Using optical magnetic twisting cytometry (OMTC), contraction of single ASM cells is assessed using measurements of cell stiffness. The ASM cytoskeleton is coupled via integrins to Arg-Gly-Asp-coated ferromagnetic microbeads. The beads are magnetized hor-

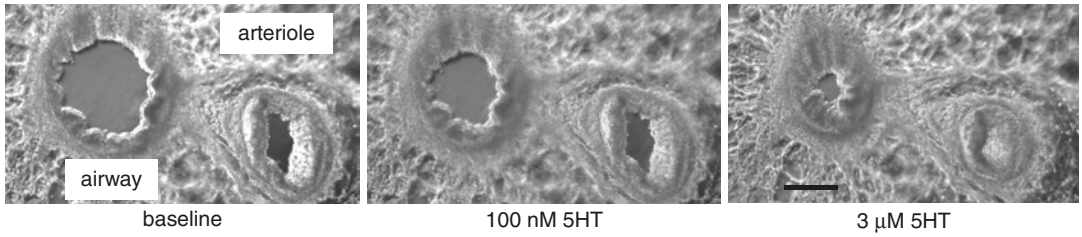

Fig. 16.1 Rat precision-cut lung slice (PCLS) showing intrapulmonary airway (left) and arteriole (right) and differential contraction in response to perfusion with increasing concentrations of serotonin (5HT). PCLS is an innovative way to measure *in vitro* responses of the relatively inaccessible small airways and arteries in health and disease [39]. In PCLS prepared from agarose-inflated lungs, airways and adjacent arterioles remain attached to the surrounding alveolar tissue. Contraction can be visualized under phase-contrast microscopy as progressive decreases in lumen area in the presence of increasing 5HT. In this PCLS, the airway but not the arteriole contracted to 100 nM 5HT, while the arteriole but not the airway was completely occluded at 3 μM 5HT, demonstrating differences in potency and efficacy (scale bar, 200 μm)

izontally and sinusoidally varying torque is then applied by a vertically aligned magnetic field. In the presence of contractile agonists, changes in bead displacement are consistent with mechanical responses observed in intact airways [41]. For traction force microscopy (TFM), ASM is grown on elastic polyacrylamide substrates coated with ECM proteins and embedded with fluorescent particles. Displacement of the particles in response to ASM traction forces generated by the cell can be tracked microscopically, and compared with initial particle locations determined after cells are removed [41].

16.3.3 Noncontractile Functions of ASM

ASM has potential additional roles beyond its contractile function in both health and disease. These noncontractile functions have been identified and characterized in studies of ASM in culture, where ASM proliferation occurs in response to serum and a range of specific mitogenic stimuli (reviewed by [42]). This process is critical to airway development but also contributes to airway remodeling in asthma with the potential to increase airway contraction purely by its increased mass in the airway wall.

ASM also secretes biologically active mediators that can act in an autocrine fashion to regulate its own contractile, proliferative, and synthetic responses [43]. Prostanoids and other metabolites of arachidonic acid (AA) are produced by ASM, as well as by other structural and inflammatory cells. These mediators can contribute to airway contraction and relaxation, as well as regulate the local production of inflammatory cytokines [44, 45]. In addition, ASM itself is a source of cytokines and chemokines implicated in changes in its responsiveness in chronic lung diseases [43].

ASM also produces multiple ECM proteins and ECM-degrading enzymes, identifying it as a putative cellular source and regulator of ECM composition in the airways [46]. Bidirectional interactions between ASM and its surrounding ECM have been shown to influence multiple ASM functions, both synthetic and contractile [47].

16.4 Endogenous Mediators of Tonic ASM Responses

Tonic responses of ASM to neural input and other endogenous stimuli are evident in both fetal and mature airways, and can be measured *in vitro* in both isolated airways and cultured ASM. This section outlines the major neurotransmitters and other endogenous stimuli that regulate ASM contractile function along with their associated ASM receptor targets (Table 16.2). The list is not exhaustive, and the relative importance of each of

Table 16.2 Major endogenous mediators of airway contraction and relaxation (modified from [45, 102–104])

Agonist		Cellular origin	Mechanism	
			Contraction (G_q)	Relaxation (G_s)
Acetylcholine		Parasympathetic cholinergic nerves	M_3	M_2 (pre-junctional G_i)
Adenosine			A_1	A_{2b}
Adrenaline		Adrenal chromaffin cells		β_2
Bradykinin		Mast cells	BK_1	
Ca^{2+}, polycations		Extracellular	CaSR	
Endothelin-1		Epithelium, endothelium, inflammatory cells	ET_A, ET_B	ET_B (epithelium) via PGE_2/NO
GABA			$GABA_B$ (G_i)	$GABA_A$
H^+		Extracellular pH	OGR1	
Histamine		Mast cells, basophils	H_1	H_2
LTB_4, cys-leukotrienes (LTC_4, D_4, E_4)		Mast cells, leukocytes, epithelium, platelets	BLT_1/BLT_2, $CysLT_1$	
Neuropeptides CGRP, neurokinin A, substance P		Sensory nerves	NK_1 (direct); NK_1/NK_2 via prostanoid	
Nitric oxide		Parasympathetic cholinergic nerves, epithelium		GC via cGMP
Platelet-activating factor		Platelets, leukocytes		
Prostanoids	PGD_2	Mast cells, leukocytes, epithelium, ASM	TP	DP_1
	PGE_2		EP_1, EP_3	EP_2, EP_4
	$PGF_{2\alpha}$		TP, EP_1, FP	
	PGI_2			IP_1
	TXA_2		TP	
Serotonin		Mast cells (rodent > human)	$5HT_2$	
Thrombin, trypsin		Mast cells	PAR_1	$PAR_{2/4}$ via PGE_2
Vasoactive intestinal peptide		Parasympathetic cholinergic nerves		$VPAC_2$

Additional indirect contractile mechanisms are mediated by increased release of ACh from parasympathetic nerves by adenosine, bradykinin, endothelin, and prostanoids

these mediators is dependent on the expression of its particular receptor target, which can vary with the stage of maturation of the airways or its distribution throughout the bronchial tree. A particular mediator may play a major role in the homeostatic regulation of ASM function or only become a significant contributor if its levels are sufficiently elevated in disease context. Changes in ASM responses to these mediators can occur if expression of a specific receptor is altered, or more broadly as a consequence of changes to common downstream signaling pathways.

As outlined below, endogenous mediators of airway contraction and relaxation may originate from nerve terminals, from structural cells within the airways, or from circulating or resident inflammatory cells. Development of airway innervation occurs relatively early in gestation, and anatomically follows the formation of the airways. As detailed later, this ultimately results in functional parasympathetic cholinergic and sensory innervation that drives airway contraction. ASM contraction and relaxation also occur in response to circulating and locally produced stimuli such as histamine, cysteinyl-leukotrienes (cys-LTs), and some prostaglandins (PGs). Irrespective of their origin, the majority of these stimuli act on G protein-coupled receptors (GPCRs) expressed on ASM. GPCRs for contractile agonists are typically G_q-coupled and drive increases in intracellular Ca^{2+} via multiple mechanisms.

While mature airways are sympathetically innervated, circulating adrenaline is more impor-

tant in mediating relaxation of human airways than noradrenaline released from sympathetic nerves. Dilator stimuli can be directly G_s-coupled to adenylate cyclase (AC) to increase cyclic adenosine monophosphate (cAMP) synthesis from adenosine triphosphate (ATP), or increase the release of mediators that act via this pathway, to oppose pro-contractile signaling irrespective of the stimulus. An alternative dilator pathway involves nitric oxide (NO) and activation of guanylate cyclase (GC) to increase cGMP.

Further details of the intracellular signaling mechanisms regulating ASM contraction and relaxation and their changes in the context of asthma are provided later.

16.4.1 Parasympathetic and Sensory Innervation Leading to Contraction

The parasympathetic innervation carried by the vagus to the airways is present in all species, providing the dominant neuronal pathway in the control of ASM tone. Nerve fibers containing the specific cholinergic marker choline acetyltransferase are present *in utero* [12] and in the mature lung at high densities in ASM layers from the trachea down to the peripheral bronchi [48]. There is some evidence that density of this excitatory cholinergic innervation is higher in human upper airways than in the distal lung [49].

Parasympathetic innervation of human airways is probably most similar to that of guinea pigs and cats but is well conserved across species [48]. Contractile responses to ACh released from postganglionic nerves are mediated by postjunctional M3 receptors, prevented by atropine, and terminated by breakdown of the neurotransmitter by acetylcholinesterase. As described later in detail, binding of M3 G_q-coupled receptors by ACh activates multiple pathways that drive increases in intracellular Ca^{2+}, MLC phosphorylation and the subsequent formation of actin-myosin cross-bridges during contraction. M2 autoinhibitory receptors on postganglionic nerve terminals in both central airways and bronchi can inhibit ACh release to oppose contraction [50](Fig. 16.2).

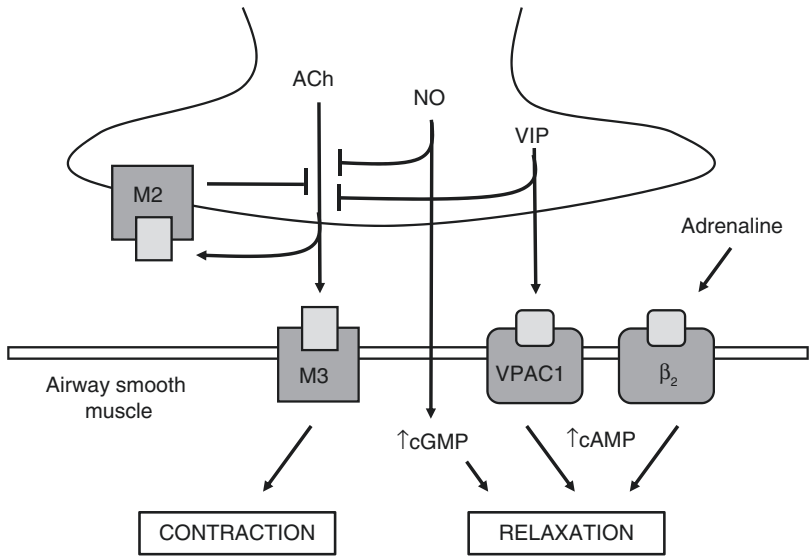

Fig. 16.2 Functional antagonism in the airways. Acetylcholine (ACh) release from parasympathetic cholinergic nerves activates M3 receptors on airway smooth muscle (ASM) to cause contraction. Autoinhibitory M2 receptors, and the co-localized NANC transmitters nitric oxide (NO) and vasoactive intestinal peptide (VIP), inhibit ACh release to oppose contraction. In human airways, VIP and NO mediate airway relaxation via VPAC1/cAMP and cGMP, respectively. Circulating adrenaline also increases cAMP via ASM β_2-adrenoceptors leading to relaxation

Electrophysiological recordings from both pre- and postganglionic parasympathetic nerves show a persistent outflow of nerve activity to the airways [51, 52]. EFS leads to contraction of small airways in rat, guinea pig, marmoset, and human PCLS, but not mouse PCLS, with guinea pig airways showing the most similar frequency-response relationship to humans [53]. The lack of response to mouse PCLS is presumably due to the absence of significant innervation of airways in the distal lung in this species [53]. Various interventions that interrupt parasympathetic neurotransmission, such as vagotomy or muscarinic receptor blockade, lead to bronchodilation [51, 52]. These findings support the role of the parasympathetic cholinergic system in maintaining the airways in a partially contracted state with the potential to drive increased bronchoconstriction. Selective inhibition of this vagal signaling with muscarinic antagonists provides a therapeutic option in chronic lung diseases, including asthma and COPD.

Exogenous muscarinic receptor agonists such as methacholine (MCh) or carbachol are resistant to breakdown by acetylcholinesterase, and can be used to induce stable contractions for pharmacological studies. These agonists increase the spontaneous phasic contraction of developing tubules in human explants in first trimester, leading to tetanic contraction [26], and similar expression of M3 receptors has been shown in human fetal and adult ASM [31]. Contraction of isolated airways from newborn sheep to both EFS and to MCh provides further evidence that this pathway is fully developed *in utero* [54]. A general pattern of relatively higher contraction in neonatal airways than fetal airways has been reported in several species, as well as a subsequent age-related decrease in contractility [55].

The degree of contraction to muscarinic agonists and other contractile mediators varies with airway size. In studies measuring isometric force in isolated airways from humans [56], and changes in lumen area in mouse PCLS [57], small airways were markedly more sensitive to contractile agonists than large airways. Similar heterogeneity was evident in pig airways using an optical imaging technique called anatomical optical coherence tomography, such that narrowing to carbachol increased from proximal to distal airways [58]. An elegant study comparing contractility to MCh in different generations of the same airway in mouse PCLS [59] revealed that airway contraction in response to the same agonist concentration was greater in the middle generation than either the distal or the proximal airway. Given the intermediate thickness of the ASM layer in the middle generation, it is clear that additional factors such as receptor density and/or expression of downstream signaling factors are also likely to vary with airway size to regulate airway contraction.

An additional sensory system located in a subpopulation of nonmyelinated sensory C fibers innervates the airways and may mediate airway contraction seen in response to EFS in the presence of muscarinic blockade. Capsaicin directly activates transient receptor potential (TRP) V1 channels expressed in these afferent fibers, leading to the release of the neuropeptides SP, neurokinin A (NKA), and CGRP, which bind to specific airway receptors to exert their contractile effects (the so-called local axon reflex) [13]. SP can directly elicit contraction in first-trimester human fetal airways, increasing tone above that produced by spontaneous phasic contractions [60]. In mature airways, contractile responses to SP vary between species. Studies using tracheal preparations or small intrapulmonary airways in PCLS show that contraction is greater in guinea pig airways than human airways, and absent in airways from rats or sheep [40, 61].

NKA mediates airway contraction via activation of G_q-coupled NK1 and NK2 receptors. NKA is more potent than SP, and its contractile effects in most species including human appear to be indirect via NK2-mediated release of histamine [61, 62]. However, NK1 receptors are fully responsible for contraction in pig airways [61] and also contribute to contraction in both guinea pig and human airways [63]. Furthermore, the mechanism of NK1-mediated contraction differs with airway size, being dependent on prostanoid production in small airways but attributed to direct effects on ASM in moderate-sized human bronchi [62, 63].

CGRP also regulates ASM tone [64, 65]. CGRP is expressed at higher levels in cartilaginous airways than smaller airways [64], and its receptor CGRP-1 is expressed on both ASM and epithelial cells [65]. Bath-applied CGRP elicits contraction of bronchial preparations with higher potency than carbachol. This contraction is maintained in the presence of muscarinic and histamine receptor antagonists and TTX, suggesting a direct effect of CGRP on ASM [64]. However, more recent evidence suggests that CGRP only elicits contraction in epithelial-denuded airway preparations, so it may also mediate relaxation via the release of epithelial-derived relaxing factors to oppose its direct effects on ASM [65].

16.4.2 Sympathetic and NANC Responses Leading to Relaxation

Neural input to ASM from sympathetic nerves and NANC transmitters has the potential to oppose responses to cholinergic activation or other circulating constrictor stimuli. However, there are considerable species differences in the distribution and functional role of these nerves and transmitters in the airways.

Sympathetic adrenergic nerves containing noradrenaline and NPY have been shown to innervate the airways *in utero* [66]. Sympathetic innervation derived from both the cervical and the thoracic stellate sympathetic ganglia is present in the mature airways of multiple species including guinea pigs [67] and pigs [68]. Although present in mature human airways, sympathetic adrenergic nerves are relatively sparse in comparison to cholinergic nerves and do not specifically innervate ASM [69].

Sympathetic nerve-mediated relaxation has an established functional role in some species, but does not play a major role in human airways, where relaxation via β-adrenoceptors (βARs) is predominantly mediated by circulating adrenaline released from the adrenal medulla acting on ASM (Fig. 16.2). In airways from guinea pigs, but not rodents or humans, nerve stimulation causes airway relaxation to oppose contractile responses to concurrent stimulation of cholinergic nerves [40, 51]. In rodents, stimulation of sympathetic nerves following additional blockade of βARs evokes contractions of ASM through the effects of noradrenaline acting on αARs [48]. Human fetal airways are responsive to the action of noradrenaline mediated via βARs, leading to dilation of the contractile regions of the epithelial tubules and cessation of the spontaneous contractions [26]. In addition, dilator responses in guinea pig airways to noradrenaline can be opposed by modest contractile responses to NPY [70], while epithelial-derived NPY has recently been shown to potentiate contraction of human airways [71].

Numerous studies have assessed βAR expression in ASM, and the relative potency and efficacy of selective and nonselective agonists for these receptors in mediating relaxation in isolated airways. It has been shown that the β_1AR subtype is more important in rodents, while β_2ARs predominate in guinea pig airways, and are almost solely responsible for relaxation of human airways [72–74]. βAR-mediated airway relaxation occurs via signaling pathways common to diverse G_s-coupled receptors, namely activation of AC and increased ASM cAMP. The ability of cAMP to oppose multiple aspects of contractile signaling, irrespective of the stimulus, and the regulation of this pathway in asthma are described in detail later in this chapter.

In the absence of a functional sympathetic innervation, the release of the NANC transmitters VIP and NO co-localized with ACh in parasympathetic cholinergic nerves may play a major role in human airways as the only neural bronchodilator pathway [12, 13]. *In utero*, dilator responsiveness to exogenous VIP is present by third-trimester gestation in fetal pigs, along with contraction to the muscarinic agonist carbachol [68]. The frequency of spontaneous contractions of human fetal lung tissue in explant culture is decreased by NO donors such as sodium nitroprusside, demonstrating that the downstream pathways for NO signaling are also established early in development [9].

VIP and NO also elicit relaxation postnatally, including in human airways [75, 76]. VIP has been shown to elicit cAMP-mediated airway relaxation via activation of G_s-coupled VPAC1

receptors expressed on ASM [77], while NO can activate soluble GC in ASM to increase cGMP, while both also inhibit ACh release (Fig. 16.2). In guinea pig trachea, an additional dilator pathway for VIP dependent on cyclo-oxygenase (COX) and the generation of prostaglandin E_2 (PGE_2) have been proposed since the COX inhibitor indomethacin reduces the relaxant effect of VIP [78]. Of note, VIP is 100–1000 times more potent than either the nonselective βAR agonist isoprenaline or NO in mediating dilatation in human bronchi, making VIP the most potent endogenous bronchodilator so far described [75].

A functional role for these inhibitory NANC transmitters is evidenced by the pronounced bronchodilation of precontracted bronchi in response to stimulation of efferent vagus nerves under conditions of ASM cholinergic and adrenergic receptor blockade [40, 76]. Since the response to EFS is sensitive to TTX and inhibited by the NOS inhibitor, N^{ω}-nitro-L-arginine (L-NOARG), this NANC-mediated relaxation can be attributed to NO release rather than VIP [76]. However, this interpretation may reflect a lack of expression of VIP receptors in the airway size under investigation, since exogenous VIP relaxes central airways but not peripheral airways, while a NO donor is equipotent [76].

16.4.3 Circulating and Local Mediators

Responsiveness of ASM to stimuli other than neurotransmitters is also evident at early stages of airway development, with numerous other biologic amines and peptides shown to elicit contraction and relaxation. The endogenous source of these mediators may be resident or circulating cells such as mast cells and basophils, from epithelial cells lining the airways, or ASM itself (Table 16.2).

16.4.3.1 Mast Cell-Derived Mediators

Autacoids released from mast cells such as *histamine* and *5HT* have the potential to contribute to airway contraction as well as inflammation during an allergic response, via activation of G_q-coupled H_1 and $5HT_2$ receptors present on ASM. Human fetal airways are responsive to histamine by the first trimester [26], despite relatively lower expression of H_1 receptors at the canalicular stage in human fetal than adult ASM [31]. Postnatally, histamine-induced contraction of guinea pig airways is greater at 1 week than 4 months of age [79], while the converse is seen for 5HT in airways of newborn versus adult sheep [54]. Contraction to histamine is observed in mature small and large airways from guinea pigs and human subjects, while contraction to 5HT is minimal or absent [79, 80]. In contrast, rodent and sheep airways react to 5HT but not histamine [54, 81], although histamine-mediated contraction in sheep PCLS is revealed when opposing H_2-mediated relaxation was blocked with cimetidine [54].

Mast cell-derived *thrombin* and *trypsin* also exert direct and indirect effects on ASM to regulate airway contraction *in vitro* and *in vivo* via protease-activated receptors (PARs) 1–4. They are also broadly pro-inflammatory and induce proliferation of ASM *in vitro* although these actions may by receptor independent [82]. PARs are a family of GPCRs with an unusual irreversible mechanism of activation. Extracellular proteolytic activation results in cleavage of specific sites in the extracellular domain, leading to formation of a new N-terminus which functions as a tethered ligand. Binding of this ligand to an exposed site in the second transmembrane loop of the receptor triggers G protein binding and intracellular signaling. PAR agonists have been shown to mediate relaxation via endogenous PGE_2 production in mouse, rat, guinea pigs, and human airways, a mechanism that is at least partly dependent on the presence of a functional epithelium [83, 84]. Activation of PAR-2 can induce contractions of human airways when endogenous PGE_2 production is inhibited by indomethacin, and can also potentiate contractions to histamine [83].

16.4.3.2 Arachidonic Acid Metabolites

A diverse range of metabolites of AA-modulating airway contraction and relaxation as well as inflammation are also synthesized by mast cells,

as well as by the airway epithelium and ASM itself (reviewed by [45]). Phospholipase A2 (PLA2) initiates this pathway, releasing AA from membrane phospholipids. Subsequent degradation via COX produces the prostanoids, encompassing the prostaglandins PGD_2, PGE_2, $PGF_{2\alpha}$, and PGI_2 (prostacyclin) and thromboxane A_2 (TXA_2). The alternative lipoxygenase (LOX) pathway gives rise to the cys-LTs [45].

Of the lipid mediators, the *cys-LTs LTC4*, *LTD4*, and *LTE4* are the most potent contractile agonists via their activation of $CysLT_1$ receptors. Initially recognized as the active components of slow-reacting substance of anaphylaxis (SRS-A), they are at least 200 times more potent than histamine in human airways [85] and are markedly more potent in small (<2 mm) than large human airways [86]. Strong contraction to LTB4 is also evident in guinea pig airways mediated via stimulation of BLT1/BLT2 receptors [45], but rodents generally respond weakly or not at all to leukotrienes [53]. Consistent with the general observation of greater responses to contractile agonists in early life, LTD4 is more potent in airways from newborn than adult sheep [54].

Prostanoids can mediate contraction or relaxation of ASM, or both. PGE_2 and PGI_2 are generally considered to be bronchodilators, while PGD_2, $PGF_{2\alpha}$, and TXA_2 induce varying degrees of bronchoconstriction [45]. The response to PGE_2 is mediated via its four EP (EP1–4) receptor subtypes. EP4 receptors mediate potent relaxation to PGE_2 in human airways, via activation of AC and increased synthesis of cAMP [87]. PGE_2 maintains the tone of the guinea pig trachea through a balance between activation of contractile EP1 receptors and relaxant EP2 receptors [88]. EP2 receptors have been implicated in PGE_2-mediated relaxation of mouse airways, where the EP1/2 antagonist AH6809, but not the EP4 antagonist L-161982, reduces the dilator potency of PGE_2 [45, 89]. In addition, PGE_2 acts via EP3 receptors to decrease the release of contractile neurotransmitters from parasympathetic neurons in guinea pig airways [44]. In canine bronchial segments, a stable analogue of PGI_2 causes direct relaxation and at higher concentrations also inhibits ACh release in response to EFS to reduce cholinergic contraction [45].

PGD_2, $PGF_{2\alpha}$, and TXA_2 mediate airway contraction via nonselective thromboxane receptors (TPs). The stable TXA_2 mimetic elicits direct contraction of human and guinea pig airways [90], but its actions in mouse airways are indirectly mediated by increasing M3-mediated bronchoconstriction [91]. TP-dependent contraction to PGD_2 in guinea pig airways and human bronchial rings is opposed by its actions at prostaglandin D1 receptors (DP1), which mediate relaxation [45]. Human and rat airways are markedly more sensitive to the contractile effects of $PGF_{2\alpha}$ via TPs than guinea pig airways [45].

16.4.3.3 Endothelin-1 (ET-1) and NO

Endothelin-1 (ET-1) and *NO* are other endogenous mediators produced by the airway endothelium with opposing effects on airway tone. ET-1 is a 21-amino-acid peptide that mediates potent contraction in many species. These actions are mediated via actions at ET_A and ET_B receptors expressed on ASM as well as by potentiating cholinergic responses [92, 93]. Contraction to ET-1 is opposed by its dilator responses mediated via activation of ET_B receptors on the airway epithelium that cause the release of NO [94]. Age-dependent changes in reactivity to ET-1 have been reported, with more effective contraction in newborn rabbits, and relatively increased relaxation in adult due to ET-1 mediated PGE_2 release [95]. As described earlier, NO also plays a role as a NANC neurotransmitter mediating airway relaxation.

16.4.3.4 Gamma-Aminobutyric Acid (GABA)

Gamma-aminobutyric acid (GABA) has been implicated in the regulation of ASM function, and is also produced locally by the airway epithelium [96]. $GABA_A$ and $GABA_B$ are expressed on both the ASM and epithelium [97, 98]. The selective $GABA_A$ agonist muscimol relaxes guinea pig and mouse airways *in vitro* and *in vivo*, and potentiates β_2AR-mediated bronchodilation [96, 98, 99]. Conversely, activation of $GABA_B$ mediates contraction directly via G_i rather than G_q

coupling, as well as augmenting pro-contractile signaling pathways downstream of G_q [98].

16.4.3.5 Extracellular H^+ and Ca^{2+}

Extracellular H^+ and Ca^{2+} are other mediators of airway tone which influence airway contraction via their actions at two different GPCRs, namely the G_q/G_s-coupled ovarian cancer G protein-coupled receptor 1 (OGR1, previously known as GPR168) and the G_q-coupled calcium-sensing receptor (CasR). OGR1 is a proton-sensing receptor expressed in ASM that responds to decreased pH by mediating ASM contraction, as measured by OMTC [100]. However, the physiological and potential clinical relevance of OGR1-mediated contraction is yet to be defined in intact tissues.

CaSR has previously been described as a master regulator of Ca^{2+} homeostasis and parathyroid hormone release. It is also expressed in human airways, immunolocalized within the SM22a-positive ASM layer, as well as in the bronchial epithelium [101]. A single study has demonstrated that the CaSR is activated by polycations eosinophil cationic protein (ECP), major basic protein (MBP), and spermine, as well as by the elevation of extracellular Ca^{2+}. This increases contractile signaling pathways in human ASM and enhances contractile responses to MCh in isolated mouse airways [101]. Further investigations are required to elucidate the role of CaSR as a novel regulator of ASM function.

16.5 Mechanisms of Airway Contraction

16.5.1 ASM Membrane Potential and Calcium Homeostasis

The resting membrane potential in adult ASM ranges between −65 and −45 mV, more negative than reported values for fetal ASM [15, 23–25]. This relatively lower electrical excitability tends to make the intact adult tissue less prone to spontaneous phasic activity, with only tonic contractions observed [11, 105]. KCl elicits airway contraction accompanied by ASM membrane depolarization resulting in the activation of VDCCs. However, at concentrations that induce contraction, agonists such as ACh do not generate action potentials or depolarize ASM sufficiently to fully activate VDCCs (for electrophysiology of ASM, see review by [24]).

The mechanisms that regulate intracellular Ca^{2+} levels within the cytosol and SR stores in ASM are tightly controlled under basal conditions. Using Ca^{2+} fluorescent dyes, basal cytosolic levels of Ca^{2+} in ASM have been measured at 100–200 nM, increasing twofold in the presence of effective concentrations of contractile agonists [106]. In addition, Ca^{2+} is extruded from the cytoplasm by plasma membrane Ca^{2+} ATPase (PMCA) and sodium/calcium exchanger (Na^+/Ca^{2+} exchanger, NCX). The pivotal importance of Ca^{2+} sequestration into the ASM SR via sarcoplasmic/endoplasmic reticulum Ca^{2+}-ATPase (SERCA) is evidenced by the rise in intracellular Ca^{2+} and subsequent contraction when SERCA is inhibited by cyclopiazonic acid (CPA) or thapsigargin (TG). These combined mechanisms play a key regulatory role in setting baseline tone as well as regulating the response to mediators of ASM contraction and relaxation.

16.5.2 ASM Signaling Leading to Contraction

ASM contraction in response to the release of contractile neurotransmitters or direct exposure to other contractile agonists is mediated via activation of their specific G_q protein-coupled receptors (GPCRs) and their common associated downstream mechanisms (Table 16.1, Fig. 16.3). Contractions are predominantly initiated by Ca^{2+} release from intracellular stores in response to activation of SR-localized IP_3Rs and also by calcium-induced calcium release (CICR) via RyRs. An influx of Ca^{2+} via L-type VDCCs may only be required to initiate contraction at low concentrations of contractile agonists [24, 107]. However, this influx may also amplify the increase in intracellular Ca^{2+} mediated by IP_3Rs and RyRs, and play a role in replenishing SR stores to sustain contraction.

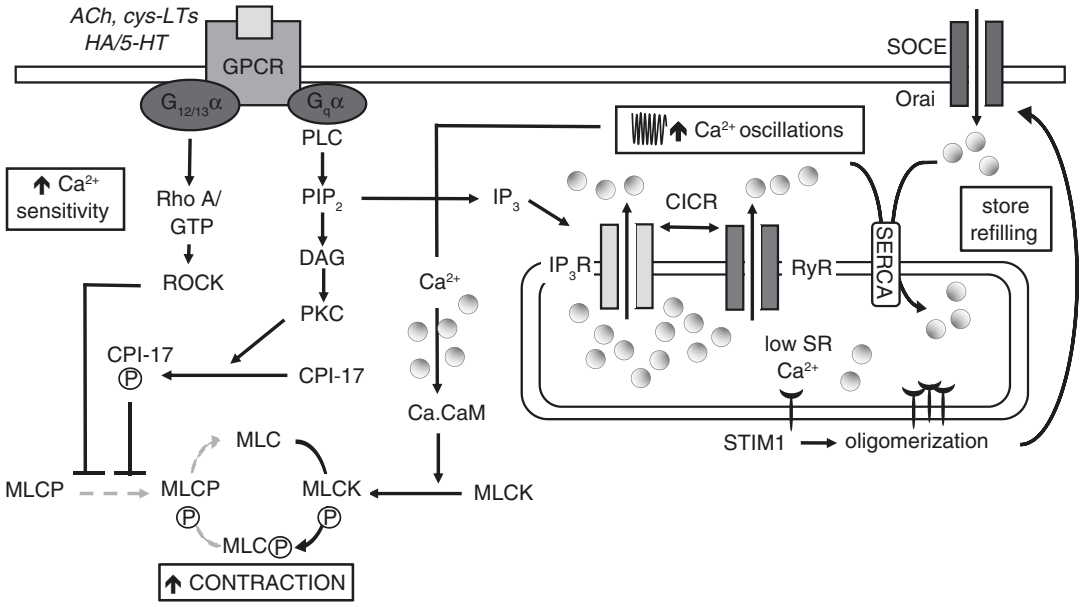

Fig. 16.3 Contractile mechanisms in airway smooth muscle. Receptor binding by a contractile agonist such as acetylcholine (ACh) , histamine (HA, in human airways), serotonin (5HT, in rodent airways), or cysteinyl-leukotrienes (cys-LTs) initiates a signaling cascade that leads to airway contraction via the parallel pathways of calcium (Ca^{2+}) oscillations and sensitivity. Through coupling to G_q, inositol-1,4,5-trisphosphate (IP_3) is generated from the hydrolysis of phosphatidylinositol 4,5-bisphosphate (PIP_2) by phospholipase C (PLC). IP_3 initiates Ca^{2+} oscillations by activating IP_3 receptors on the sarcoplasmic reticulum (SR) to release Ca^{2+}. SR-localized ryanodine receptors are activated by calcium-induced calcium release (CICR) and by cADP ribose (cADPR, not shown). Ca^{2+} oscillations occur as the Ca^{2+} released by IP_3R and RyR is taken up into SR stores via sarcoplasmic/endoplasmic reticulum Ca^{2+}-ATPase (SERCA). Increased Ca^{2+} binds to calmodulin (CaM) to activate myosin light-chain kinase (MLCK). This phosphorylates myosin (MLC), leading to the formation of actin-myosin cross-bridges and contraction. The parallel Ca^{2+} sensitivity pathway inhibits the activity of MLC phosphatase (MLCP) to maintain contraction. Agonist binding activates the guanine-exchange protein RhoGEF (not shown) to convert GDP-RhoA (inactive) to GTP-RhoA (active). This activates Rho-kinase (ROCK) to phosphorylate MYPT1, the regulatory subunit of MLCP, to inhibit its enzymatic activity. Additionally, DAG-induced activation of protein kinase C (PKC) phosphorylates the PKC-potentiated protein phosphatase 1 inhibitor protein of 17 kDa (CPI-17) to inhibit MLCP. Sustained phosphorylation of MLC provides the main driver of the latter phase of a prolonged airway contraction. ASM Ca^{2+} stores are replenished via SERCA and by the oligomerization of the SR-localized STIM1, which then associates with Orai in the plasma membrane causing it to form channels, which mediate store-operated Ca^{2+} entry (SOCE)

Early studies in isolated ASM showed that G_q-coupled receptor agonists induced a simple biphasic Ca^{2+} signal, seen as a whole-cell Ca^{2+} transient followed by a lower, sustained plateau [24]. However, with higher resolution microscopy, it is apparent that Ca^{2+} oscillations in freshly isolated ASM are present under basal conditions, at least in a proportion of cells, in the absence of phasic contractions [28, 29]. These Ca^{2+} oscillations are increased in frequency by contractile agonists ACh and LTD_4 [28, 108].

The relationship between ASM Ca^{2+} oscillations and airway contraction was originally measured separately as changes in intracellular Ca^{2+} in myocytes and changes in force in tracheal preparations [109]. However, visualization of Ca^{2+} signaling inside individual ASM cells within intact airways has been achieved using confocal microscopy of PCLS loaded with Ca^{2+} indicator [81]. Ca^{2+} oscillations in mouse PCLS are increased by ACh, ATP, and 5HT [81, 110] and in human PCLS by ACh and histamine [111]. The frequency of

these Ca^{2+} oscillations, ranging from 20 to 60 min^{-1}, is proportional to the agonist concentration and extent of contraction [81, 111, 112]. All agonists induce an initial phase of low-amplitude and high-frequency Ca^{2+} oscillations superimposed on an elevated intracellular Ca^{2+}. A second phase of oscillations occurs with a stable frequency and similar amplitude and is superimposed on decreasing baseline Ca^{2+} levels. Each Ca^{2+} oscillation occurs in the form of a Ca^{2+} wave, propagating along the length of the individual ASM but not to adjacent cells, resulting in asynchronous Ca^{2+} oscillations throughout the airway.

16.5.2.1 SR-Dependent Calcium Release and Reuptake

The initial phase of airway contraction in response to G_q-coupled contractile agonists is due to the coordinated activation of SR-localized IP_3Rs, RyRs, and SERCA (Fig. 16.3). IP_3Rs and RyRs are homotetramers comprised of subunits of 300 and 2200 kDa, respectively. In human ASM, three different isoforms of each receptor are expressed on the SR, while the predominant isoform of SERCA is SERCA2B [113–115].

In ASM cells, either in culture or in intact airways, the binding of contractile agonists stimulates phospholipase C-β1 (PLC-β1) to catalyze the conversion of membrane-bound phosphatidylinositol 4,5-bisphosphate (PIP_2) into IP_3 and diacylglycerol (DAG). These second messengers activate the key parallel signaling pathways that initiate and sustain airway contraction.

Agonist-induced IP_3 production activates IP_3Rs and Ca^{2+} release from the SR. This can also occur in response to flash photolysis of caged IP_3, which increases free intracellular IP_3 [116]. Ca^{2+} oscillations leading to contraction in response to agonists or IP_3 itself are abolished by the PLC inhibitor U-73122, or IP_3R inhibitors, xestospongin or 2-APB [116, 117]. One mechanism implicated in widely reported age-related decreases in ASM contraction is the decreased accumulation of IP_3 due to increased activities of enzymes responsible for its degradation, such as IP_3-5 phosphatase [95].

Neighboring RyRs on the SR can be activated in response to the IP_3R-dependent rise in intracellular Ca^{2+} via CICR [118]. ASM RyRs are also activated via cyclic adenosine diphosphate ribose (cADPR), synthesized in response to agonist-induced activation of the ADP-ribosyl cyclase, CD38 [119]. Current evidence suggests that cADPR increases RyR activity by causing the dissociation of the 12.6 kDa tacrolimus (FK506)-binding protein (FKBP12.6) that usually inhibits RyR activation [119].

The synchronized opening of IP_3R and RyR channels gives rise to so-called Ca^{2+} puffs and sparks, respectively, leading to Ca^{2+} waves and oscillations. Release of SR Ca^{2+} via these SR-localized mechanisms is critical to initiate airway contraction. Many studies have shown that contraction is maintained when Ca^{2+} influx via VDCC is prevented by nifedipine, and during voltage clamp at <−40 mV at potentials only a few Ca^{2+} channels would be open [24, 120]. However, an established agonist-induced contraction is reversed by acute removal of external Ca^{2+} [110] and repeated contractions decline over time in its absence [107].

SERCA pumps are responsible for the uptake of Ca^{2+} back into the SR to contribute to oscillations. SERCA activity in most cells is generally regulated by the inhibitory protein phospholamban (PLB). PLB can be phosphorylated by cyclic nucleotides, by Ca^{2+}/calmodulin (CaM)-dependent protein kinase (CaMKII), or by protein kinase C (PKC). This reduces inhibition of SERCA, and has been shown to accelerate SR Ca^{2+} reuptake into the SR in porcine ASM. However, there is evidence that PLB is only expressed at low levels in human ASM, with the activity of SERCA directly regulated by CaMKII [121]. Uptake of Ca^{2+} via SERCA during repeated contractions is not sufficient to completely replenish SR stores; thus additional mechanisms are required for sustained contraction.

The SR Ca^{2+} response varies both with airway size and between species. Comparisons of different generations of airways within PCLS from the same mouse show greater oscillation frequency in response to the same agonist in the smaller airways in the distal lung compared with higher order airways [59]. The same frequency of Ca^{2+}

oscillations induces greater contraction in rat than in mouse airways irrespective of the airway generation [112]. Finally, the frequency of the Ca^{2+} oscillations in the presence of the same concentration of agonist varies from 5 to 20 peaks/min in mouse, rat, and human PCLS, with MCh inducing Ca^{2+} oscillations of 8–9 peaks/min while decreasing airway area by 50% in human PCLS [111, 112].

The fast and transient elevation of cytosolic Ca^{2+} concentration associated with agonist-induced oscillations leads to the sequential occupancy of the four Ca^{2+}-binding sites of CaM. The complex then binds and activates the serine–threonine kinase, myosin light-chain kinase (MLCK). The 20 kDa regulatory light chain of myosin (MLC) is then phosphorylated by MLCK. This allows the rapid formation of actin-myosin cross-bridges, and the cyclical movement of myosin heads along actin filaments that leads to contraction. The formation of slowly cycling cross-bridges, known as latch-bridges, is thought to contribute to sustained contraction, even when intracellular Ca^{2+} concentrations and associated MLCK activity are no longer elevated.

16.5.2.2 Calcium Influx Mechanisms

The initiation of contraction in response to raised extracellular KCl, but not to EFS or added G_q-coupled contractile agonists, is dependent on Ca^{2+} entry via nifedipine-sensitive L-type VDCCs. In mouse and human PCLS, KCl-induced membrane depolarization leads to Ca^{2+} oscillations that are lower in frequency and longer in duration, and result in only small transient contractions compared to the sustained responses seen with G_q-coupled contractile agonists [81, 111]. Each KCl-induced Ca^{2+} oscillation consists of a large Ca^{2+} wave preceded by multiple localized Ca^{2+} transients. These oscillations are inhibited by ryanodine, suggesting that Ca^{2+} influx stimulates the periodic opening of RyRs via CICR to generate Ca^{2+} waves leading to transient contraction [81, 111].

16.5.2.3 Calcium Sensitivity

Airway contraction can still be maintained even when free intracellular Ca^{2+} is reduced by its reuptake into SR Ca^{2+} stores via SERCA or other mechanisms. A parallel pathway, termed Ca^{2+} sensitivity, contributes to sustained ASM contraction by regulating the amount of force produced for a given level of free intracellular Ca^{2+} (Fig. 16.3) [111, 112, 122]. Ca^{2+} sensitivity is associated with decreased activity of type-1 protein phosphatase, MLC phosphatase (MLCP), mediated by RhoA/Rho and DAG/PKC/CPI-17 signaling pathways detailed below. MLCP normally dephosphorylates MLC to provide constraint on MLCK-induced contraction. Inhibition of MLCP leads to sustained phosphorylation of MLC and associated cross-bridge activity to provide the main driver of the latter phase of a prolonged airway contraction [118].

RhoA is a member of the Rho family of small GTPases. It is highly expressed in ASM, present in the cell membrane as an active form bound to GTP (GTP-RhoA) and an inactive cytoplasmic form bound to GDP (GDP-RhoA). Agonist binding to receptors coupled to heterotrimeric GTP-binding proteins, G_q and $G_{12/13}$, activates the guanine-exchange protein RhoGEF. This converts GDP-RhoA to GTP-RhoA to activate Rho-kinase (ROCK). The active enzyme then phosphorylates the regulatory subunit (MYPT1) of MLCP to inhibit its enzymatic activity. As a consequence, MLC remains in its phosphorylated form and contraction is sustained.

DAG-induced activation of PKC provides an additional mechanism that regulates MLCP activity. PKC phosphorylates the PKC-potentiated protein phosphatase 1 inhibitor protein of 17 kDa (CPI-17). Phosphorylated CPI-17 has higher affinity for the catalytic subunit of MLCP (PP1c), inhibiting its activity and thereby reducing the dephosphorylation of MLC.

A recent study has compared pharmacological responses to carbachol and KCl with physiological responses to EFS in bovine trachea to compare the signaling leading to sustained MLC phosphorylation and airway contraction [123]. Carbachol treatment increases phosphorylation of the MLCP regulatory subunit MYPT1 (via ROCK) and the phosphorylation of CPI-17 (via PKC), while KCl does not induce CPI-17 phosphorylation. In contrast to carbachol, atropine-

sensitive EFS does not lead to MYPT1 phosphorylation, except in the presence of the cholinesterase inhibitor neostigmine. The authors suggest that a single stimulus provides sufficient ACh to induce rapid CPI-17 phosphorylation, but that ACh-induced $G_{q12/13}$ signaling leading to ROCK and MYPT1 occurs more slowly, and is thus only activated when the rapid degradation of ACh released by EFS is inhibited [123].

The mechanisms underlying Ca^{2+} sensitivity in response to contractile agonists have been explored further by clamping the ASM intracellular Ca^{2+} to a fixed concentration so that contraction occurs in the absence to SR-localized Ca^{2+} oscillations. Two experimental approaches have been used to achieve this. So-called skinned airways can be prepared by permeabilizing ASM cell membranes with pore-forming α-toxin or nonionic detergents such as saponin, β-escin, or Triton X-100 [118, 122, 124]. An alternative pharmacological approach employing caffeine and ryanodine applied to PCLS avoids the potential loss of cell constituents with these chemical treatments [110]. Caffeine activates and opens RyRs by increasing their sensitivity to Ca^{2+}. The addition of ryanodine then maintains the RyR receptor in a partially open state. The emptying of Ca^{2+} from the SR results in the activation of store-operated Ca^{2+} entry (SOCE), leading to sustained Ca^{2+} influx. It is likely that extrusion of Ca^{2+} via PMCA and NCX is still active under these conditions to limit SOCE. Consequently, the intracellular and extracellular Ca^{2+} levels are stabilized when the Ca^{2+} movements across the ASM membrane reach a new equilibrium. This protocol allows assessment of responses to graded concentrations of extracellular Ca^{2+}, as well as contribution of ROCK and PKC signaling to contractile responses.

Y-27632, a specific ROCK inhibitor, reverses contraction to MCh in α-toxin-permeabilized rabbit and human airway preparations [124]. In caffeine/ryanodine-treated mouse PCLS, a sustained MCh-induced contraction is reversed by Y27632 or by GF-109203X, a highly selective PKC inhibitor, without changes in intracellular Ca^{2+} [110]. The effects of direct activation of PKC have also been assessed in mouse PCLS exposed to the caffeine/ryanodine treatment [125]. Phorbol esters elicit strong airway contraction, associated with phosphorylation of CPI-17 and MLC, suggesting that PKC mediates sensitization of the contractile response to Ca^{2+} via MLCP inhibition [125].

ASM Ca^{2+} sensitivity varies with age and between species. In chemically skinned tracheal fibers from fetal and suckling pig airways, sensitivity to Ca^{2+} is three- to fourfold higher than airways from older animals [126]. The Ca^{2+} sensitivity of mouse ASM is Ca^{2+} dependent, whereas the Ca^{2+} sensitivity of rat or human ASM is not [111, 112]. In caffeine/ryanodine-treated human PCLS, intracellular Ca^{2+} can be progressively increased by increasing extracellular Ca^{2+}, leading to stepwise increases in sustained contraction of small airways. Airway contraction in these permeabilized human PCLS is increased further by histamine, even though intracellular Ca^{2+} levels are clamped [111, 112].

16.5.2.4 Refilling of Calcium Stores

Following Ca^{2+} depletion from the SR, SOCE mediated via membrane TRP channels is the major pathway for Ca^{2+} influx in ASM to replenish SR stores (Fig. 16.3) [127, 128]. Stromal-interacting molecule-1 (STIM1) and Orai family members are the molecular components of SOCE. In ASM, decreased Ca^{2+} levels in the SR cause the oligomerization of the SR-localized STIM1, which then associates with Orai in the plasma membrane causing it to form channels that mediate SOCE [129]. MCh-induced Ca^{2+} oscillations and airway contraction in mouse PCLS are fully reversed by SOCE inhibitors GSK7975A and GSK5498A, in a manner similar to that observed with the removal of extracellular Ca^{2+}. However, the inhibitors do not reduce contraction in response to photolysis of caged IP_3, mediated by direct IP_3R activation and intracellular Ca^{2+} release [128].

Studies in ASM and permeabilized airways also implicate L-type VDCCs in the refilling of SR stores that is required for sustained contraction [110, 120]. However, in mouse PCLS containing intact airways, addition of nifedipine to precontracted airways only partially reverses contraction

and associated increases in Ca^{2+} oscillation frequency, while inhibitors of SOCE abolish these responses [128]. Based on these findings, mathematical modeling predicts that Ca^{2+} entry through L-type VDCCs may only contribute to contraction when the cell is depolarized (e.g., by a raised external K^+ concentration) and that L-type VDCCs are less important than store-operated channels in the control of ASM tone and store refilling [127].

16.6 Mechanisms of Relaxation

Airway relaxation can be achieved by activating pathways to oppose Ca^{2+} signaling and sensitivity that drive ASM contraction (Table 16.1, Fig. 16.4). This may be mediated by AC-induced cAMP production or GC-induced cGMP production in ASM [130]. Short- and long-acting β_2AR agonists (SABA, LABA) increase cAMP and are commonly used in the treatment of asthma and COPD. PDE inhibitors decrease cyclic nucleotide breakdown and can enhance responsiveness to β_2AR agonists [130]. A clear benefit of these agents is their potential to simultaneously provide functional antagonism to the actions of the numerous pro-contractile agonists, but as outlined later their efficacy may be limited in severe asthma. Characterization of the signaling mechanisms that promote airway relaxation has focused on salbutamol but other agents that increase cAMP and cGMP also share some common

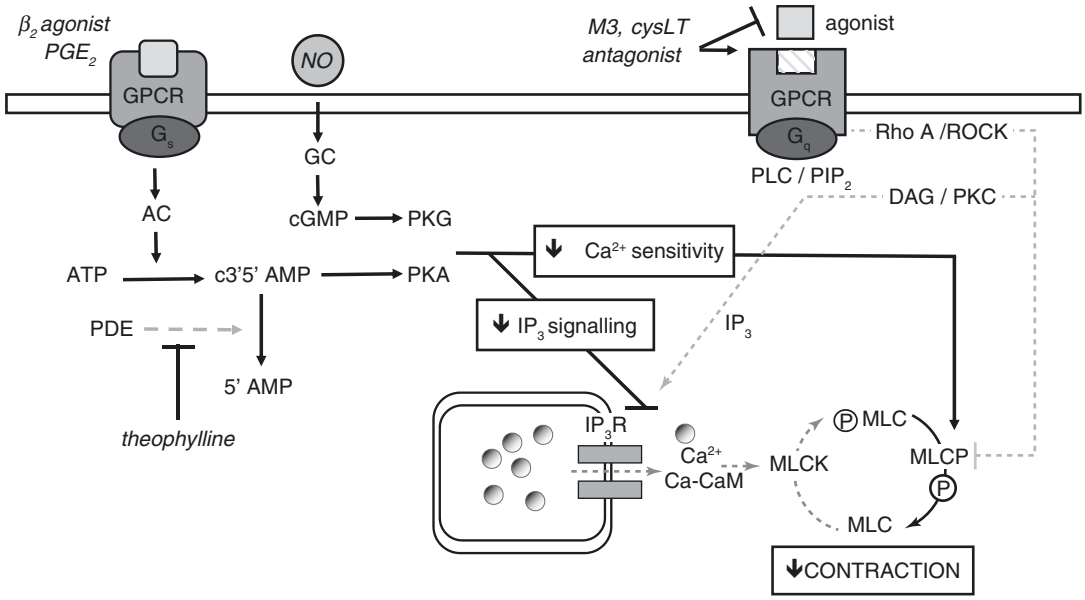

Fig. 16.4 Dilator mechanisms in airway smooth muscle. Airway relaxation can be elicited when bronchodilators bind to G_s-coupled receptors on ASM. Agonists include β_2-adrenoceptor agonists (adrenaline, short- and long-acting β_2-adrenoceptor agonists (SABA, LABA)) and prostaglandin E_2 (PGE_2). Activation of adenylate cyclase (AC) generates 3′5′cAMP from intracellular ATP. This can activate Epac signaling (not shown) and the cAMP-dependent protein kinase (protein kinase A, PKA). PKA phosphorylates multiple targets that regulate airway contraction, leading to decreased sensitivity of IP_3R to IP_3 and reduced Ca^{2+} oscillations. Ca^{2+} sensitivity is decreased through increased activity of myosin light-chain phosphatase (MLCP). Dephosphorylation of myosin light chain (MLC) reduces formation of actin-myosin cross-bridges and opposes contraction. The breakdown of c3′5′AMP to 5′AMP by phosphodiesterase (PDE) can be inhibited by theophylline to elicit slowly developing airway relaxation and to enhance the actions of β_2-adrenoceptor agonists. An alternative dilator pathway via guanylate cyclase (GC) and cGMP in response to nitric oxide (NO) results in similar downstream signaling to the AC/cAMP pathway. Antagonists of muscarinic receptors for acetylcholine (ACh) or cysteinyl-leukotrienes (cys-LTs) selectively oppose the signaling cascades that lead to airway contraction via the parallel pathways of Ca^{2+} oscillations and sensitivity, but unlike β_2-adrenoceptor agonists do not actively oppose the actions of other mediators of bronchoconstriction

mechanisms, and target multiple pathways that contribute to airway contraction (Fig. 16.4).

While pharmacological antagonists of muscarinic receptors and leukotriene receptors are also used clinically, the selectivity of their actions only provides bronchoprotection against airway contraction to ACh or cys-LTs, respectively. Of note, histamine receptor antagonists are not effective, even in allergic asthma, as they do not oppose the contribution of other mediators to the allergic response leading to airway contraction. However, muscarinic receptor antagonists and leukotriene receptor antagonists are of benefit when vagal tone and cholinergic signaling are increased as in COPD, or if levels of the potent bronchoconstrictor cys-LTs are elevated as proposed in aspirin-sensitive asthma. These drugs inhibit all the downstream signaling activated by ACh and CysLT as previously outlined in detail (Fig. 16.3) to limit contraction (Fig. 16.4) and as such are not described in further detail.

16.6.1 Contribution of Cyclic Nucleotides to Relaxation

Airway relaxation can occur in response to activation of ASM β_2ARs by endogenous adrenaline or synthetic selective SABA and LABA, EP_2/EP_4 receptors by prostaglandin E_2, IP receptors by prostacyclin, or A2b receptors by adenosine [130]. Agonist binding leads to downstream signaling via receptor-coupled G_α subunits of the G_s subfamily of heterotrimeric G proteins. Stimulation of AC activity increases synthesis of cAMP and results in bronchoprotection (preventing the development of contraction) or bronchodilation (reversal of established contraction). Substances that release NO directly activate intracellular GC to increase cGMP and cause airway relaxation. Dilator responses can also be induced by pharmacological agents that either directly stimulate cAMP and cGMP synthesis or inhibit their breakdown by phosphodiesterases, although agents that elevate cGMP are less efficacious than those that increase cAMP.

16.6.2 PKA and ePAC as Effectors of Airway Relaxation

Although PKA has long been implicated as the downstream mediator of ASM relaxation following activation by cAMP, it is only recently that this has been established experimentally. Direct inhibition of PKA in human ASM cells by stable expression of the PKA-inhibiting peptide PKI-GFP, or the mutant regulatory subunit RevAB-GFP (which does not bind cAMP), reduces the inhibitory effects of isoprenaline on histamine-induced increases in ASM Ca^{2+} oscillations, MLC phosphorylation, and cytoskeletal stiffness measured using OMTC. In mouse tracheal rings infected with lentivirus encoding PKI-GFP, isoprenaline-induced relaxation is also reduced [131].

However, another effector is implicated in βAR-mediated relaxation, based on the observation that relaxation to isoprenaline in guinea pig trachea is not inhibited by selective inhibitors of PKA [132]. An exchange protein directly activated by cAMP (Epac), a GTP exchange factor for the small GTPase Rap1, is thought to mediate this additional PKA-independent relaxation [132, 133]. An Epac-selective cAMP analogue decreases MCh-induced contraction in guinea pig trachea and human airway muscle strips by reducing MLC phosphorylation and RhoA [132], while cAMP-mediated relaxation in mouse bronchi is mediated through activation of both Epac and PKA leading to RhoA inhibition [133].

16.6.3 Inhibition of Ca^{2+} Signaling and Sensitivity

The inhibitory effects of βAR agonists on ACh-induced Ca^{2+} oscillations were first described in isolated ASM [134]. Inhibition was also evident in response to other cAMP-elevating agents, namely the stable cell-permeant analogue of cAMP (8-bromo-cAMP), the AC activator forskolin (FSK), and the nonselective PDE inhibitor 3-isobutyl-1-methylxanthine (IBMX) [130, 134].

Recent evidence is consistent with inhibitory effects of cAMP on Ca^{2+} release from the SR, the

major mechanism initiating airway contraction. In mouse and human PCLS, βAR agonists (isoprenaline, nonselective, and salbutamol and formoterol, both β_2-selective), as well as FSK and 8-bromo-cAMP, simultaneously reduce the amplitude and frequency of Ca^{2+} oscillations within ASM and relax intrapulmonary airways precontracted with MCh or histamine [110, 111, 135]. In addition, IP_3-induced Ca^{2+} oscillations are reduced by the elevation in intracellular cAMP induced by FSK [110].

NOC-5, an NO donor, also decreases 5HT-induced Ca^{2+} oscillations and airway contraction, and inhibits the increase of intracellular Ca^{2+} and contraction in response to photolytic release of IP_3 [136]. The effects of NOC-5 are mimicked by the stable cGMP analogue, blocked by the GC inhibitor ODQ, and increased in the presence of zaprinast or vardenafil, two selective inhibitors of cGMP-specific PDE5 [136]. These combined findings imply that elevated levels of cAMP and cGMP reduce the sensitivity of the IP_3Rs to IP_3, resulting in reduced Ca^{2+} release from SR stores and airway relaxation [110, 136].

Agents that increase cAMP can also cause airway relaxation by decreasing Ca^{2+} sensitivity [130]. In intact (i.e., not chemically permeabilized) guinea pig trachea, isoprenaline and FSK reduce MCh-induced contraction to a greater extent than Ca^{2+} mobilization, implicating inhibition of an additional Ca^{2+}-independent mechanism [137]. More direct measures show that βAR agonists reverse carbachol-induced phosphorylation of Rho and ROCK, measured by Western blot in bovine trachea [138] and that isoprenaline also increases MLCP activity, assayed directly using ^{32}P-labeled myosin [24].

In PCLS following caffeine/ryanodine treatment, increased Ca^{2+} oscillations in response to contractile agonists are abolished, and contraction is due to Ca^{2+} sensitivity alone. Under these conditions, relaxation to salbutamol, FSK, and IBMX at fixed Ca^{2+} concentrations is maintained [135]. Of note, lower concentrations of formoterol are required to relax human airways when contraction is due to ASM Ca^{2+} sensitivity alone than when Ca^{2+} oscillations are also occurring [111, 135], while neither NOC-5 nor a stable cGMP analogue induced relaxation in agonist-contracted airways after caffeine/ryanodine treatment [136]. These differences may contribute to the longer duration of action of formoterol, and may contribute to the relatively lower dilator responses to agents that increase cGMP compared to cAMP.

cAMP-dependent hyperpolarization and consequent reduction of Ca^{2+} influx via activation of BK channels has been reported in ASM [139]. However, airway relaxation to βAR agonists and NO donors in many species including humans is either unaffected or only partially inhibited in the presence of K^+ channel blockers [130]. This suggests that it is the inhibition of Ca^{2+} oscillations and sensitivity, rather than opening of BK channels, that mediates relaxation in the response to these agents.

16.6.4 β-Adrenoceptor Phosphorylation and cAMP Metabolism

Two major feedback mechanisms terminate dilator responses to βAR agonists. GPCR kinases (GRKs) phosphorylate and uncouple the receptor from its G_s protein. This promotes the association of intracellular β-arrestin, which provides steric hindrance to further association between the agonist-occupied receptor and G_s, thereby "arresting" signaling. Other kinases, including PKA and PKC, can also phosphorylate βARs to promote uncoupling, even in the absence of agonist [130].

Alternatively, PDEs hydrolyze cAMP, the intracellular second messenger of βAR agonists, as well as cGMP. Of the five PDE classes found in human ASM cells, PDE3 and PDE4 are the two major cAMP-hydrolyzing enzymes [140] and the PDE4D subfamily, particularly the PDE4D5 isoform, appears to play a pivotal role in controlling cAMP degradation in human ASM cells [141].

16.7 Dysregulation of Airway Contraction in Lung Disease

Increased airway contraction is a feature of many chronic lung diseases, with airway narrowing leading to symptoms of breathlessness. While this may occur as a direct consequence of increased levels of neurally derived or circulating contractile mediators, it is clear that *in utero* and postnatal exposures can exert complex influences on both the amount of ASM within the airway wall and the responsiveness of ASM to stimuli that induce contraction.

Asthma is a heterogeneous disease most commonly associated with allergic sensitization, although multiple subtypes of asthma have been defined, based on differing causal pathways, natural histories, and responses to treatment [142]. In all forms of asthma, the airways show an increased sensitivity and maximal response to an inhaled constrictor agonist, defined as AHR [37]. This hallmark feature is associated with airway inflammation due to cellular infiltration and elevated cytokine levels, and airway remodeling as evidenced by increased ASM, fibrosis, goblet cell hyperplasia, higher levels of resident mast cells, and increased vascularity. COPD is characterized by chronic bronchitis and emphysema and is most commonly caused by cigarette smoking, although it may be caused or exacerbated by genetic deficiency of α1-antitrypsin resulting in loss of protection from tissue destruction by neutrophil elastase [143]. The degree of AHR in COPD is related to the level of fixed airway obstruction and the contribution of airway remodeling, including increased ASM.

In the disease setting, the presence of increased ASM, higher levels of a specific mediator or its receptor target, dysregulation of common downstream signaling pathways, or changes in the contractile apparatus itself can have broad implications for the control of airway contraction (Fig. 16.5). The contribution of these multiple factors may vary between asthma and COPD, as well as between asthma phenotypes, as different inflammatory profiles and mediators are implicated in allergic versus nonallergic asthma.

Numerous studies have been performed *in vitro* using ASM or airways or *in vivo* animal models to assess the effects of inflammatory stimuli, allergen challenge, or disease on ASM contractility. Determining whether AHR is associated with changes in the contractile properties of isolated ASM is of critical importance. *In vitro* studies of ASM signaling and reactivity in isolated airways have provided further insights into the mechanisms underlying increased contraction. Animal models of allergic airways disease, most commonly in mice, employ sensitization and challenge protocols to allergens such as ovalbumin (OVA) and house dust mite (HDM) to mimic key features of human asthma, while chronic cigarette smoke exposure can be used to model COPD. These models allow the integrated assessment of lung inflammation and airway remodeling to implicate drivers of increased *in vivo* airway reactivity to bronchoconstrictors.

16.7.1 Increased Contractile Mediators

ACh is a key mediator of airway contraction, via its release from parasympathetic nerves and activation of postjunctional muscarinic M3 receptors on ASM. Although increased expression of M3 receptors is not a feature of AHR, elevation of vagal tone has been reported in chronic lung diseases, including both asthma and COPD [144]. This could be due to dysfunction of the autoinhibitory prejunctional muscarinic M2 receptor that normally limits ACh release [145]. This mechanism has been demonstrated in models of airways disease following allergen exposure and in some but not all asthmatics [144].

Increased levels of other contractile agonists may also exert direct effects on ASM or indirect effects by increasing neuronal ACh release. The synthesis and release of mediators from activated mast cells in the early and late phases of the allergic response in asthma are important in this regard. Histamine mediates

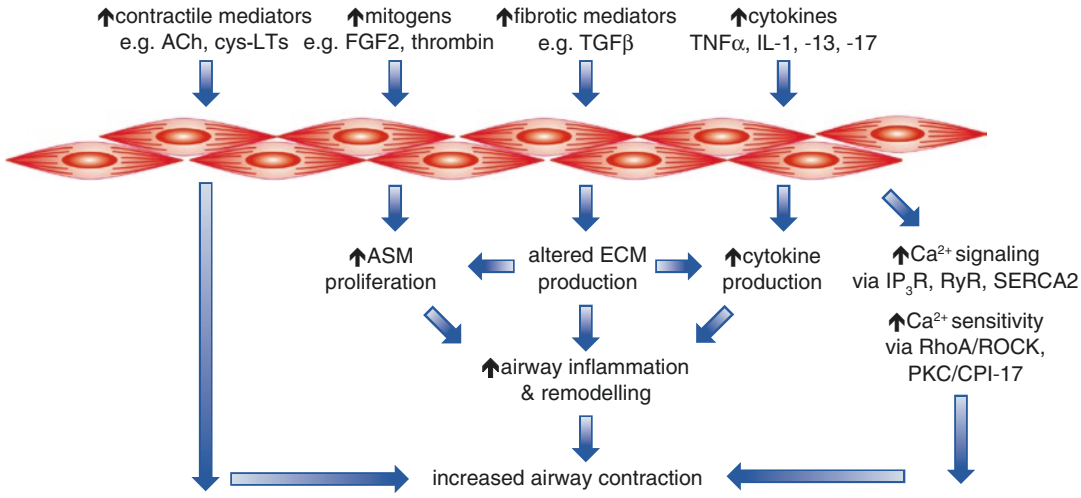

Fig. 16.5 Mechanisms of increased airway contraction. Airway narrowing in chronic lung diseases may be increased as a consequence of multiple influences on ASM. These include elevated levels of contractile agonists acting on increased bulk of ASM in the remodeled airway. ASM can both produce and respond to inflammatory cytokines that increase the expression of receptors and dysregulate major pathways of SR-dependent Ca^{2+} signaling and Ca^{2+} sensitivity leading to contraction. Profibrotic mediators alter the extracellular matrix (ECM) in the airways and promote further ASM proliferation and inflammation

many allergic symptoms, but is not a major driver of increased contraction in asthma, as evidenced by the lack of efficacy of antihistamines in opposing bronchoconstriction. However, *de novo* synthesis of cys-LTs via lipoxygenase and prostanoids via COX can contribute to AHR. The soluble form of PLA2 that initiates synthesis of these eicosanoids is increased in airways of asthmatics [146]. Increased cys-LTs are present in bronchoalveolar lavage (BAL) fluid collected from atopic human subjects after endobronchial challenge with allergen [147]. Increases in BAL PGD_2 and the enzyme responsible for its synthesis in airway epithelium are both associated with exacerbations in severe asthma [148]. This combined evidence supports the contribution of mast cell degranulation and local release of mediators of bronchoconstriction to increased airway contraction.

ET-1 is strongly implicated in the pathophysiology of pulmonary hypertension but may also play a role in other lung diseases due to its potent bronchoconstrictor properties [92, 149]. ET-1 is increased in the epithelium in airway biopsies from asthmatics, and in BAL from patients with allergic asthma, and in plasma of hypoxemic patients with COPD [150, 151]. Importantly, ET-1 levels measured in BAL during acute asthma attacks are sufficiently elevated to contribute directly to bronchoconstriction or induce ACh release [149].

Inflammatory mediators such as tumor necrosis factor α (TNF-α) and various interleukins are implicated in the pathophysiology of chronic lung diseases, with Th2 cytokines playing a key role in allergic asthma. As detailed later, there is considerable evidence that these mediators regulate multiple mechanisms that promote airway contraction and oppose relaxation.

16.7.2 Airway Remodeling

Increased ASM is a key feature of airway remodeling in many chronic lung diseases, and has been implicated as the most important factor contributing to AHR [152]. This remodeling may occur as a consequence of early-life influences, as seen in bronchopulmonary dysplasia (BPD). This perinatal disease of prematurity is characterized by ASM hyperplasia and alveolar

dysmorphogenesis, increasing the risk of developing asthma and COPD [153]. Based on biopsies from subjects with fatal or severe asthma, the thickness of the ASM layer is related to disease severity rather than duration [154, 155]. Although less significant, increased ASM is also evident in COPD, potentially contributing to the development of greater tension and thus more airway contraction [152].

Mitogenic stimuli known to be elevated in asthmatic airways include growth factors such as FGF-2, inflammatory cell-derived mediators such as thrombin, and contractile agonists such as ET-1, SP, TXA_2, and LTD_4. Despite convincing evidence of increased ASM in asthma, it has been difficult to establish that ongoing proliferation occurs *in situ*, as airway biopsies from asthmatic subjects with established remodeling show limited staining for proliferative markers in ASM [155]. However, the proliferative response of primary cultured human ASM from those with asthma is increased compared to ASM from those without asthma [42]. This increased proliferation may be specific to ASM, since airway myofibroblasts from asthmatic subjects do not show a similar increase [156].

Mechanisms implicated in the increased proliferation of asthmatic ASM *in vitro* are inadequate expression of the transcription and differentiation factor CCAAT/enhancer-binding protein-α (C/EBP-α), and Ca^{2+}-dependent increases in mitochondrial biogenesis and activity [157, 158]. Increased proliferation of ASM from COPD patients has also been described [159], with analysis of metabolic reprogramming showing increased glycolysis and glutamine catabolism to support the biosynthetic and redox balance required for cellular growth [160].

Another mechanism that may contribute to the increase in ASM in remodeled airways is migration [161]. *In vitro* studies show that many mediators implicated in asthma increase ASM migration. These include growth factors such as platelet-derived growth factor (PDGF), lipid metabolites such as cys-LTs and PGD_2, and inflammatory Th2 cytokines such as interleukin-5 (IL-5), IL-4, and IL-13 [161]. An isolated report has demonstrated increased migration in ASM from asthmatics compared to non-asthmatics [162].

ASM can both produce and respond to the pleiotropic cytokine TGF-β to produce ECM proteins (reviewed in [47]). Both TGF-β and connective tissue growth factor (CTGF), which are implicated in mediating the effects of TGF-β, are increased in asthma [43, 163, 164]. The profile of ECM produced by ASM from asthmatics differs from ASM from healthy subjects, namely increases in collagen I, III, and V and fibronectin and decreases in collagen IV and elastin [46]. This altered ECM promotes the production of inflammatory cytokines such as eotaxin [165], as well as ASM proliferation, as demonstrated by the increased proliferation of ASM from non-asthmatics grown on an ECM bed produced by asthmatic ASM [166]. Additional *in vitro* studies have shown that migration of ASM cells grown on membranes coated with collagens III and V and fibronectin is increased compared to cells grown on collagen I, elastin, and laminin [167]. Thus, altered ECM production by ASM can act in an autocrine fashion to promote the contribution of ASM to inflammation and airway remodeling, and in turn to altered airway contraction. These multiple influences of ECM on ASM functions in asthma are less studied in COPD. However, the broader consequence of increased ECM production is airway fibrosis, leading to the significant fixed airway obstruction that characterizes this disease [143].

Irrespective of the mechanisms increasing ASM proliferation, migration, and survival, the increased bulk of ASM in the airway wall has the potential to exacerbate the influence of multiple factors to further increase ASM contraction. Airway remodeling is not targeted by current pharmacological treatments with either anti-inflammatory drugs used as preventer medication or bronchodilators used as relievers to oppose airway contraction. As outlined later, this provides a rationale for the recent introduction of bronchial thermoplasty, a novel approach to ablate the increase in ASM to limit excessive uncontrolled contraction in severe asthma.

16.7.3 Inflammatory Cytokines

The role of inflammation in promoting increased airway contraction in chronic lung diseases is well established, and forms the basis for the use of anti-inflammatory treatment with glucocorticoids to reduce the frequency and severity of asthma attacks. Indeed, AHR is evident in short-term animal models of allergic airway disease when airway inflammation, characterized by elevated eosinophils and Th2 cytokines, is present, even when airway wall remodeling is absent.

The cellular sources of inflammatory mediators in the airways vary with different chronic lung diseases. Eosinophils, mast cells, and Th2 cells are key players in allergic asthma, while neutrophils are implicated in more severe asthma. Both neutrophils and macrophages produce cytokines that contribute to the pathophysiology of COPD, while eosinophils are implicated in COPD exacerbations. These circulating inflammatory cells and the resident airway epithelium are a rich source of mediators contributing to inflammation. TNF-α, IL-1, IL-8, IL-17, and Th2 cytokines (IL-4, IL-5, IL-13) are major drivers of airway inflammation in asthma and/or COPD [142, 143].

ASM itself can respond to these stimuli by producing inflammatory chemokines and cytokines such as eotaxin, IL-1, and IL-8. This may attract inflammatory cells into the airways and amplify the signals they generate (reviewed in [43]). The release of eotaxin from asthmatic ASM in culture is higher than from non-asthmatic ASM, both under basal conditions and in response to asthma-relevant cytokines [165]. This observation has been confirmed by increased immunostaining of eotaxin in the ASM layer of asthmatic airways [168], consistent with a hypersecretory phenotype of ASM both *in vitro* and *in vivo* in human asthma. The numerous synthetic products of ASM and their autocrine and paracrine effects have the potential to promote inflammation-associated increases in contraction [43].

Key cytokines elevated in the airways in asthma and COPD can directly increase ASM responsiveness of isolated airway preparations. For example, treatment with TNF-α exaggerates contraction of human airways to muscarinic agonists, bradykinin, and 5HT [169–171], with increased expression of contractile agonist receptors providing a possible mechanism [172]. IL-13 also significantly increases maximal force generation in mouse trachea [173] and small airway contraction in mouse and human PCLS [171, 174]. $CysLT_1$ expression on ASM is also increased by the Th2 cytokine IL-13 [28]. More recently, the Th17 subset of T cells has been shown to contribute to the development of more severe asthma phenotypes, particularly associated with neutrophilia [175]. The Th17 cytokine IL-17A enhances contractile force generation of mouse tracheal rings and human bronchi [176].

These *in vitro* findings have been validated in animal models of allergic airway disease. Administration of IL-13 causes rapid induction of AHR in mice *in vivo*, independently of allergen challenge [174]. Conversely, the development of *in vivo* AHR due to allergen sensitization is prevented by targeting specific cytokines using monoclonal antibodies or receptor antagonists or by gene deletion. For example, the inhibitory effects of IL-13 antibodies [177], deficiency of IL-17 [176], or a soluble TNF-α antagonist [178] have been demonstrated. Notably, TNF-α inhalation increases AHR to MCh challenge in human subjects with mild asthma [179].

16.7.4 Altered Calcium Handling

Changes in Ca^{2+} homeostasis and abnormal Ca^{2+} handling by ASM in response to contractile agonists have been identified as key mechanisms underlying increased ASM contraction. It is clear that elevated cytokines can influence the responsiveness of the increased bulk of ASM in the remodeled airway wall, and may regulate multiple aspects of Ca^{2+} signaling to drive increased airway contraction in chronic lung diseases. Studies in ASM and intact airways have assessed the direct effects of inflammatory stimuli as well as disease status. Changes in SR-dependent Ca^{2+}

oscillations and Ca^{2+} sensitivity, as well as in the dynamic properties of ASM, are evident, consistent with the increased airway contraction observed *in vivo*.

Recurrent Ca^{2+} oscillations in mature ASM become aberrant in severe asthma, with increases in frequency related to disease severity [29]. Furthermore, the Th2-derived cytokine IL-13 increases basal oscillations in human ASM [28]. Given the contribution of Ca^{2+} to both contractile and synthetic functions of ASM, these changes provide indirect evidence of altered Ca^{2+} signaling as a driver of changes in structure and function of inflamed airways in asthma and COPD.

Calcium responses to contractile agonists are increased in isolated ASM treated with inflammatory cytokines such as TNF-α and IL-13 [180, 181]. The exaggerated response in IL-13-treated ASM was attributed to enhanced Ca^{2+} release since levels of calponin, smooth muscle α-actin, vinculin, and myosin were unchanged [181]. ASM from asthmatics also shows exaggerated Ca^{2+} responses relative to ASM from non-asthmatics [182, 183].

There are multiple sites in the Ca^{2+} mobilization pathways for dysregulation under inflammatory conditions and in disease. To date, there is no evidence that expression of IP_3Rs is increased in human ASM from asthmatics [115, 184] despite its upregulation in response to IL-13 [185]. Levels of bradykinin-induced IP_3 and Ca^{2+} responsiveness to photolysis of caged IP_3 are also similar in ASM from non-asthmatic and asthmatic subjects [184]. However, both IP_3 levels and IP_3R-mediated Ca^{2+} release are increased in ASM cells from a rat asthma model [186]. This is associated with lower expression/activity of IP_3–5 phosphatase, providing a mechanism promoting AHR through increased availability of IP_3, rather than increased IP_3R expression.

RyR activity may be increased in asthma by changes in the receptor itself or in response to increased cADPR via CD38. IL-13 upregulates RyR expression in human ASM [185]. FKBP12.6 normally stabilizes RyRs in a closed (inactive) state, but this regulatory protein is dissociated in rat ASM treated with asthmatic serum or with the cytokines IL-5, IL-13, or TNF-α, and also in isolated airways from a guinea pig model of OVA-induced AHR [187]. Expression of CD38 in human ASM is increased by TNF-α [180], and elevated in the airways of sensitized and challenged mice and in ASM from asthmatic compared to non-asthmatic donors [182, 188]. The TNF-α-induced increase in contractile responses of tracheal rings from non-sensitized mice is abrogated in mice deficient in CD38 [188]. Thus, increased RyR expression, reduced inhibition of its activity, or increased activation via CD38 could induce higher ASM Ca^{2+} for the same level of agonist to increase contraction, as recently modeled [189].

Increased SR-dependent Ca^{2+} signaling, via effects on both IP_3Rs and RyRs, is implicated in the pro-contractile effects of IL-13 [185]. Treatment of human ASM with IL-13 also further enhances the frequency of LTD4-induced Ca^{2+} oscillations, and the proportion of oscillating ASM cells [28]. The increases in Ca^{2+} oscillations are suppressed to a similar degree by inhibitors of IP_3Rs or RyRs [28]. These changes are associated with increased mRNA for CD38 as well as the LTD4 receptor $CysLT_1$ [28]. These findings support the integrated contribution of increases in receptor expression and signaling to promote contraction.

Reduced SERCA2-mediated Ca^{2+} reuptake into the ASM SR could also increase airway contraction. IL-13 decreases the expression of SERCA2 in human ASM, associated with increased cytokine release [185]. Expression of SERCA2 is lower in both native and cultured ASM from endobronchial biopsies of patients with mild and moderate/severe asthma compared to healthy subjects, and associated with increased ASM proliferation and cytokine release [115]. However, the finding of decreased SERCA2 in asthmatic ASM is not universal [184] and its contribution to increased airway contraction has yet to be assessed. Further studies are required to fully define the contribution of SR-dependent Ca^{2+} signaling to AHR.

Increased Ca^{2+} sensitivity of ASM via RhoA/ROCK and CPI-17 leading to increased contraction has also been demonstrated under inflammatory conditions and in allergen models (reviewed

by [190]). Both TNF-α and IL-13 induce RhoA transcription in human ASM, via STAT6 and NFkB signaling, and increased phosphorylation of the regulatory subunit of MLCP [191]. In α-toxin-permeabilized guinea pig airways, the TNF-α-induced increases in the proportion of active GTP-bound RhoA and increased MLC phosphorylation are inhibited by preincubation with the ROCK inhibitor Y27632 [191]. IL-17A enhances contraction of mouse tracheal rings and human bronchi through an epithelial-independent effect that is not mediated via TNF-α, but is prevented by Y27632 [176]. Repeated allergen challenge also appears to increase Ca^{2+} sensitization via ROCK or CPI-17 associated with AHR [190]. These findings remain to be confirmed in ASM and airways from asthmatic subjects.

A recent study suggests that expression of G_q protein-coupled calcium-sensing receptors (CaSRs) is increased in the ASM layer of bronchial biopsies from asthmatic subjects and in the airways of allergen-challenged mice [101]. These receptors are known to control Ca^{2+} homeostasis by regulating the release of parathyroid hormone from the parathyroid gland via PLC-dependent pathways, but their role in the lungs has not previously been characterized. In addition to elevated levels in asthmatic ASM, CaSR expression is increased in ASM from non-asthmatic subjects by treatment with asthma-relevant cytokines TNF-α and IL-13. Activation of CaSRs with polycations elevates intracellular Ca^{2+} in human ASM and increases the contractile response of mouse trachea and airways in PCLS to ACh [101]. This novel pathway may not only contribute to increased ASM responsiveness but also increase Ca^{2+} sensitivity.

16.7.5 Altered Intrinsic ASM Properties

Compelling evidence implicates inflammation as a major influence on ASM that increases airway contraction. However, it remains unclear whether ASM itself has intrinsic and persistent hypercontractility that contributes to AHR. *In vitro*, the contraction of human airways from subjects with asthma is reported to be increased, decreased, or not different compared to airways from control subjects (reviewed in [38]). Airway preparations from animal models of allergic airways disease with established *in vivo* AHR also yield conflicting results. For example, MCh-induced contraction of mouse tracheal rings, measured as increased isometric force, is increased following chronic OVA challenge but contraction of small airways in PCLS, measured as reductions in airway area, is reduced in the same model [192]. These inconsistent findings may reflect differential contributions of inflammatory and structural influences on contraction. While increased ASM and inflammation may synergize to promote contraction in tracheal rings, interactions of ASM with noncontractile airway wall elements such as fibrosis in the smaller airways within PCLS may limit contraction.

Differences in the physical properties of individual ASM cells in the disease setting have the potential to influence contraction, and have recently been characterized using novel approaches such as TFM and OMTC [41]. Higher cell traction forces at baseline and enhanced stiffening (contraction) in response to MCh and histamine demonstrate that ASM may have an inflammation-independent contraction mechanophenotype in asthma [41].

The shortening velocity of ASM *in vitro* is an additional measure of intrinsic ASM contractility. At the single-cell level, the maximum capacity and velocity of shortening of zero-loaded single-ASM cells can be recorded. The response to EFS is significantly increased in ASM from subjects with asthma relative to controls [193]. Furthermore, using collagen gel contraction assays, gels containing ASM cells from asthmatic donors have greater reductions in area in response to histamine and bradykinin [194, 195]. In explants from agarose-inflated lungs, the rate of airway contraction is also greater in the hyperresponsive Fischer rat than Lewis rats [196], while greater velocity and maximum ASM shortening are observed in human bronchi passively sensitized with serum containing high IgE [197]. This intrinsic ASM hypercontractility may also correlate with *in vivo* measurements of airway responsiveness.

Several mechanisms underlying these intrinsic differences in ASM contraction have been described. MLCK is expressed at higher levels in biopsies from patients with asthma of increasing severity and COPD [155], and increased in ASM from asthmatics associated with increased shortening velocity [193]. However, elevated MLCK was not detected in asthmatic ASM in collagen gels where greater contraction to histamine was detected [194]. Fast MHC isoform and transgelin are also increased in human asthma and in hyperresponsive Fischer rats [198]. Of note, assessment of the rate of actin filament propulsion in purified tracheal myosin from Fischer rats is increased compared to normoresponsive Lewis rats, demonstrating the potential functional significance of increased fast MHC overexpression. Conversely, transgelin did not alter the rate of actin filament propulsion [198]. Further studies to define the molecular mechanics of ASM are required to provide further insights into the contribution of intrinsic dynamics of ASM to AHR and asthma.

16.8 Limitations of β-Adrenoceptor Agonists as Dilator Therapy

The SABA salbutamol is the most commonly used inhaler medication to provide relief of acute asthma symptoms, while LABAs, such as formoterol, are only used in combination with glucocorticoids as preventer medication in more severe disease. Consistent with the contribution of increased vagal input to the pathophysiology of COPD, chronic breathlessness is treated with long-acting muscarinic antagonists (LAMA) and/or LABA, while glucocorticoids provide benefit in exacerbations. β_2AR agonists remain the gold standard for asthma treatment, as glucocorticoids do not fully prevent asthma attacks and some patients are resistant to steroid therapy. However, the efficacy of SABA and LABA as bronchodilators may be limited in inflamed hyperresponsive airways and it is estimated that more than half of asthmatic patients do not receive adequate control with current available treatments [199].

16.8.1 Functional Antagonism

Mechanistically, the extent of airway relaxation versus contraction is a balance between the actions of bronchodilators versus bronchoconstrictors, known as functional or physiological antagonism. Thus, a highly potent β_2AR agonist that is maximally effective in a partially contracted airway becomes a less potent partial agonist in a maximally contracted airway. This is demonstrated *in vitro* in guinea pig trachea when both the potency and efficacy of salbutamol are reduced at increasing levels of carbachol-induced contraction [200]. The reduced tracheal smooth muscle relaxation correlates with a reduced ability of the drug to stimulate β_2AR-coupled AC, resulting in lower levels of cAMP to oppose contraction. β_2AR agonist-induced cAMP levels are also reduced in ASM from asthmatics; however the underlying mechanism is enhanced degradation rather than decreased synthesis, due to increased expression of PDE4D and hydrolysis of cAMP [201].

In the clinical context, more severe disease leads to greater AHR, increased airway contraction, and potential lack of symptom control with standard doses of SABA. While this may be managed by the introduction of anti-inflammatory glucocorticoids to reduce the severity of symptoms, this is not always effective. The more frequent use of higher doses of β_2AR agonists promotes harmful effects in both the short and long terms. Acute high doses of inhaled SABA can cause adverse effects if significant systemic absorption occurs. Loss of selectivity as a bronchodilator acting only in the airways occurs in terms of both location and site of action, exemplified by β_1AR-mediated tachycardia and β_2-mediated skeletal muscle tremor [102].

16.8.2 Homologous Receptor Desensitization and Downregulation

SABA and LABA treatment can cause homologous desensitization and potentially downregulation of ASM β_2ARs [130]. As previously stated, agonist occupation of β_2ARs leads to the binding

of β-arrestin, which if prolonged leads to receptor internalization. Internalized receptors can then be trafficked to lysosomes for degradation, resulting in a reduction in total ASM β_2-AR protein. Of note, siRNA targeting of β-arrestin in human ASM increases signaling downstream of β_2AR activation, while genetic ablation of β-arrestin increases both signaling and relaxation of contracted mouse airways *ex vivo* and *in vivo* [202, 203]. Although GRK and β-arrestin are expressed at similar levels in ASM from non-asthmatic and asthmatic subjects, a recent study has shown a defect in the dephosphorylation of endosomal β_2ARs which normally promotes their recycling back to the plasma membrane as resensitized receptors ready for agonist binding [204]. Thus, GRK/arrestin-dependent mechanisms leading to desensitization of ASM β_2ARs and reduced resensitization are both likely to contribute to the loss of dilator efficacy with chronic use of β_2AR agonists in asthma.

16.8.3 Heterologous Receptor Desensitization Due to Inflammation

A significant complication of chronic β_2AR activation was revealed when a prospective trial to introduce LABA in addition to usual therapy, the Salmeterol Multicenter Asthma Research Trial (SMART), was terminated early due to an increase in mortality in the treated group [205]. Subsequent meta-analysis suggested that symptomatic relief provided by LABA was masking the underlying effect of uncontrolled airway inflammation, leading to increased severe and life-threatening asthma exacerbations, as well as asthma-related deaths [206]. As such, LABA are not used as sole therapy in the treatment of asthma, but only in combination with anti-inflammatory glucocorticoids.

The importance of controlling inflammation in asthma is therefore paramount. While inflammatory cytokines and lipid mediators can indirectly and directly increase airway contraction, they can also reduce airway sensitivity to bronchodilators. *In vitro*, both IL-4 and IL-13 impair isoprenaline-induced decreases in ASM cell stiffness [207]. Moreover, chronic treatment of mouse tracheal rings with IL-1β or TNF-α attenuates the relaxant effect of β_2AR agonists [208], and these cytokines synergize to reduce ASM responsiveness [209]. The loss of sensitivity to β_2AR agonists after IL-1β or TNF-α is mediated via induction of COX2 [209]. Subsequent increased PGE_2 production and activation of PKA lead to receptor phosphorylation and heterologous desensitization of β_2AR signaling [130, 208].

16.9 New Targets to Limit Airway Contraction

Multiple factors contribute to increased airway contraction and impaired relaxation in chronic lung diseases. The introduction of biologics to limit the contribution of key drivers of inflammation to AHR is showing promise in the clinic. New bronchodilator agents acting via both known and novel pathways and receptor targets to cause airway relaxation have also been identified, with several of these drugs having other beneficial effects in chronic lung diseases (Table 16.3). Experimental evidence supports their potential to overcome some of the limitations of current therapy with β_2AR agonists in severe disease, although their clinical efficacy has yet to be fully established.

16.9.1 Biologics Targeting Inflammation

Given the influence of inflammation on airway contraction and relaxation, it is important to optimize anti-inflammatory therapy, especially when glucocorticoids are ineffective. Clinical translation of experimental findings implicating specific mediators of inflammation in chronic lung diseases has proved challenging, due to the potential redundancy of the multiple inflammatory cells and cytokines impacting the airway reactivity. To date, the use of selec-

Table 16.3 Selected bronchodilators in current use and under investigation in asthma and/or COPD

Target	Drug	Action	Asthma	COPD
M3 mAChR	Ipratropium, tiotropium, glycopyrronium, aclidinium	Antagonist	✓	✓
CysLT1R	Montelukast, zafirlukast, pranlukast	Antagonist	✓	
β_2AR	Albuterol, formoterol, salmeterol, indacaterol, olodaterol	Agonist	✓	✓
PDE	Theophylline, roflumilast, RPL554	Inhibitor	✓	✓
TAS2R	Chloroquine, quinine, saccharin, flufenamic acid	Agonist	✓	
EP2/4	ONO-AE1259, ONO-AE1-329	Agonist	✓	
RXFP1	Relaxin	Agonist	✓	
CaSR	Calcilytics, e.g., NPS89636	Antagonist	✓	
Transgelin-2	TSG12	Agonist	✓	
G_q	FR900359	Inhibitor	✓	

Modified from [102]

tive biologics targeting elevated IgE, eosinophilic inflammation by IL-5, and Th2 cytokines including IL-13 has been shown to be of benefit in selected patients with asthma and COPD exacerbations [210, 211], while targeting neutrophils and other pro-inflammatory cytokines implicated in the pathogenesis of COPD has been relatively disappointing [211]. It is clear that careful phenotyping of patients is required to identify the major inflammatory cells and mediators driving their symptoms, so that effective personalized treatment can be achieved to oppose inflammation and reduce AHR [212].

16.9.2 Improved PDE Inhibitors with Anti-inflammatory Properties

PDE inhibitors prevent the hydrolysis of cAMP and cGMP to their inactive forms, so mediate their effects in ASM via the gradual accumulation of second messengers rather than driving their rapid synthesis. The most commonly used PDE inhibitor theophylline is nonspecific and has limited bronchodilator potency and efficacy compared to β_2AR agonists, although its additional beneficial anti-inflammatory actions have been described [102]. The recent identification of PDE inhibitors with selectivity for airway PDE3 and PDE4 isoforms is of particular interest, but combined treatment with selective PDE3 inhibitor SKF94120 and PDE4 inhibitor rolipram is required to effectively inhibit contraction of human bronchi [213]. In human airways that have been passively sensitized by treatment with allergic serum, PDE inhibitors reduce allergen-induced contractions. This suggests that their bronchodilator actions are mediated in part through inhibition of mediator release rather than through direct airway relaxation [213]. The current focus in testing PDE subtype inhibitors is on the use of such drugs as adjunct therapy, in combination with glucocorticoids or direct bronchodilators. For COPD, the selective PDE4 inhibitor roflumilast is showing considerable benefit based on its inhibitory effects in inflammatory cells rather than ASM [214], while the PDE3/4 inhibitor RPL554 is progressing in clinical development, also for COPD.

16.9.3 Targeting Novel Receptors and Signaling Pathways

A number of novel bronchodilators have been identified in experimental studies using rodent and human airways (Table 16.3), but have yet to be evaluated clinically.

Agonists for G_q-coupled type 2 bitter-taste receptors (TAS2Rs) increase ASM Ca^{2+} in isolated human ASM so they would be expected to cause contraction, but instead cause paradoxical relaxation of ASM and dilation of mouse and human airways [215]. It is proposed that the relaxation to TAS2R agonists such as saccharin and chloroquine is mediated by elemental Ca^{2+}

events that activate BK leading to membrane hyperpolarization [216]. However, other investigators have queried this mechanism, and show that TAS2R agonists inhibit Ca^{2+} oscillations and sensitivity [217]. While IL-13 treatment impairs relaxation of carbachol-contracted human airways to the LABA formoterol, TAS2R-mediated relaxation is maintained [218]. Although TAS2R themselves are susceptible to receptor internalization via GRK/β-arrestin-mediated processes, the dilator efficacy of TAS2R agonists is preserved under conditions of β_2AR desensitization [219], suggesting that TAS2R are resistant to heterologous desensitization. Of note, TAS2R expression and function are similar in ASM cells derived from patients with or without asthma so they may provide a novel tractable target for therapy [218].

Relaxin is a relaxin family peptide receptor 1 (RXFP1) agonist originally identified as a hormone of pregnancy. Relaxin has unique combined effects as a bronchodilator and anti-fibrotic agent that clearly differentiates it from existing asthma therapies [220]. Chronic relaxin treatment in animal models of COPD and asthma inhibits AHR as well as reduces ASM thickening and established fibrosis [221]. Acute relaxin treatment also reduces the release of mast cell-derived bronchoconstrictors in guinea pigs [222] and directly elicits dilation of both large and small airways [223]. Relaxin-mediated relaxation is partially inhibited by airway epithelial removal and inhibitors of NOS, COX, AC, and GC. This is consistent with both epithelial-dependent and -independent dilator mechanisms, likely via RXFP1 activation and generation of NO, dilator prostanoids, and cAMP/cGMP [223]. Relaxin also enhances dilator responsiveness to salbutamol, suggesting its potential as an alternative or add-on therapy for severe asthma [223]. Relaxin has already undergone clinical trials for the treatment of acute heart failure, establishing its safe clinical profile [224]. Translation of the promising preclinical findings to human airways is critical in the development of relaxin as a novel alternative or adjunct therapeutic opposing multiple aspects of airway pathology in lung diseases.

Novel Ca^{2+} signaling pathways, common G_q signaling pathways, and ASM contractile proteins are also being explored as potential therapeutic strategies to oppose excessive airway contraction (Table 16.3). While not yet clearly established, the ASM CaSR is implicated in increased airway contraction and CaSR antagonists, termed calcilytics, can oppose its activation [101]. In allergen-sensitized mice, polycation CaSR agonists further increased bronchial hyperreactivity in tracheal and PCLS preparations. Both AHR and polycation-induced contraction were prevented by calcilytics and absent in mice with CaSR ablation from ASM. Given evidence of functional upregulation of CaSR in ASM from asthmatic patients, it remains to be determined whether calcilytics may represent a new class of novel asthma therapeutics [101].

Multiple GPCR agonists activate G_q to drive excessive contraction in asthma. As such, inhibition of G_q itself may be of benefit in treating airway obstruction, with potential off-target effects minimized by local administration into the lung. FR900359 is a membrane-permeable inhibitor of G_q that can be loaded into cells of interest, effectively silencing the gene for functional studies [225]. Treatment with FR900359 prevents bronchoconstriction and produces sustained airway relaxation in mouse, pig, and human airways *ex vivo*. Acute inhalation of FR90039 in healthy naïve mice prevents airway contraction to MCh without acute cardiovascular effects, while chronic administration also protects against the development of AHR in mouse models using OVA and HDM as allergens [225].

Transgelin-2 is currently under investigation as a novel bronchodilator target [226]. Transgelin-2 is a member of the calponin family that regulates actin cross-linking. An agonist that binds to transgelin-2, called TG12, inactivates the RhoA-ROCK-MYPT1-MLC pathway, and reduces human ASM cell stiffness, and the contraction of ASM-containing collagen gels, isolated arteries, and PCLS. Of note, TG2 offers potential clinical advantages relative to salbutamol since it causes potent airway relaxation *in vivo* without causing desensitization [226].

16.9.4 Targeting ASM with Bronchial Thermoplasty

A novel nonpharmacological approach has been introduced to reduce the amount of ASM and its contribution to dysregulated contraction in severe asthma. Bronchial thermoplasty (BT) entails the delivery of local, radiofrequency energy to the larger airways via bronchoscopy [227, 228]. This minimally invasive technique can be used to ablate ASM within multiple segments of asthmatic airways. Early studies in dogs showed that the reduction in ASM mass at the site where BT was applied is correlated with diminished contraction to MCh *in vivo* [228]. Although this decrease in AHR is not evident in clinical trials to date, the application of BT to patients with severe unresponsive asthma is shown to improve quality of life and reduce exacerbations [229]. It is likely that a combination of different mechanisms beyond relatively local ASM reduction will be responsible for the benefits of BT. Indeed, both submucosal and ASM associated nerve fibers are also significantly reduced in airway biopsies collected 3 months post-BT [230] which could impact the responses in smaller airways beyond the site of ablation. The long-term impact of BT is yet to be determined, while further assessment of outcomes to date may better define the pathways targeted by BT and the distinct phenotypes of asthma that benefit the most from BT [228].

16.10 Summary

ASM plays key roles in the development of the lung through spontaneous phasic contractions *in utero*. Only tonic ASM contractions to neurotransmitters and other mediators persist after birth. These are initiated by the coordinated activation of SR-localized IP_3Rs, RyRs, and SERCA to cause Ca^{2+} oscillations and sustained by mechanisms involving Ca^{2+} sensitization and influx. In asthma, the increased sensitivity and response to bronchoconstrictors are due to the inflammation-induced dysregulation of these tonic contractions, as well as the increased bulk of ASM in the remodeled airways. ASM relaxation may be impaired in severe asthma due to the loss of functional β_2ARs and/or signaling. This may be a consequence of homologous desensitization of β_2AR due to frequent use of high doses of bronchodilator therapy or heterologous desensitization due to the influence of uncontrolled inflammation.

It is estimated the asthma symptoms of more than half of patients are not adequately controlled with available treatments. Further understanding of the regulation of ASM contraction and relaxation in health and disease will continue to inform the development of new pharmacological approaches and novel interventions (such as bronchial thermoplasty) to overcome the limitations of current therapy, and improve outcomes for difficult-to-treat lung diseases.

References

1. Hislop AA. Airway and blood vessel interaction during lung development. J Anat. 2002;201(4):325–34.
2. Zoetis T, Hurtt ME. Species comparison of lung development. Birth Defects Res B Dev Reprod Toxicol. 2003;68(2):121–4.
3. Leslie KO, Mitchell JJ, Woodcock-Mitchell JL, Low RB. Alpha smooth muscle actin expression in developing and adult human lung. Differentiation. 1990;44(2):143–9.
4. Ochs M, Nyengaard JR, Jung A, Knudsen L, Voigt M, Wahlers T, et al. The number of alveoli in the human lung. Am J Respir Crit Care Med. 2004;169(1):120–4.
5. Macklem PT, Mead J. Resistance of central and peripheral airways measured by a retrograde catheter. J Appl Physiol. 1967;22(3):395–401.
6. Braido F, Scichilone N, Lavorini F, Usmani OS, Dubuske L, Boulet LP, et al. Manifesto on small airway involvement and management in asthma and chronic obstructive pulmonary disease: an Interasma (Global Asthma Association—GAA) and World Allergy Organization (WAO) document endorsed by Allergic Rhinitis and its Impact on Asthma (ARIA) and Global Allergy and Asthma European Network (GA(2)LEN). World Allergy Organ J. 2016;9(1):37.
7. Mailleux AA, Kelly R, Veltmaat JM, De Langhe SP, Zaffran S, Thiery JP, et al. Fgf10 expression identifies parabronchial smooth muscle cell progenitors and is required for their entry into the smooth muscle cell lineage. Development. 2005;132(9):2157–66.
8. Shan L, Subramaniam M, Emanuel R, Degan S, Johnston P, Tefft D, et al. Centrifugal migration of

mesenchymal cells in embryonic lung. Dev Dyn. 2008;237(3):750–7.
9. Pandya HC, Innes J, Hodge R, Bustani P, Silverman M, Kotecha S. Spontaneous contraction of pseudoglandular-stage human airspaces is associated with the presence of smooth muscle-alpha-actin and smooth muscle-specific myosin heavy chain in recently differentiated fetal human airway smooth muscle. Biol Neonate. 2006;89(4):211–9.
10. Yang Y, Beqaj S, Kemp P, Ariel I, Schuger L. Stretch-induced alternative splicing of serum response factor promotes bronchial myogenesis and is defective in lung hypoplasia. J Clin Invest. 2000;106(11):1321–30.
11. Schittny JC, Miserocchi G, Sparrow MP. Spontaneous peristaltic airway contractions propel lung liquid through the bronchial tree of intact and fetal lung explants. Am J Respir Cell Mol Biol. 2000;23(1):11–8.
12. Sparrow MP, Lamb JP. Ontogeny of airway smooth muscle: structure, innervation, myogenesis and function in the fetal lung. Respir Physiol Neurobiol. 2003;137(2–3):361–72.
13. van der Velden VH, Hulsmann AR. Autonomic innervation of human airways: structure, function, and pathophysiology in asthma. Neuroimmunomodulation. 1999;6(3):145–59.
14. Lewis M. Spontaneous rhythmical contractions of the muscle of the bronchial tubes and air sacs of the chick embryo. Am J Physiol. 1924;68:385–8.
15. Richards IS, Kulkarni A, Brooks SM. Human fetal tracheal smooth muscle produces spontaneous electromechanical oscillations that are Ca2+ dependent and cholinergically potentiated. Dev Pharmacol Ther. 1991;16(1):22–8.
16. Roman J. Effects of calcium channel blockade on mammalian lung branching morphogenesis. Exp Lung Res. 1995;21(4):489–502.
17. Yang Y, Palmer KC, Relan N, Diglio C, Schuger L. Role of laminin polymerization at the epithelial mesenchymal interface in bronchial myogenesis. Development. 1998;125(14):2621–9.
18. Jesudason EC. Airway smooth muscle: an architect of the lung? Thorax. 2009;64(6):541–5.
19. Hooper SB, Harding R. Fetal lung liquid: a major determinant of the growth and functional development of the fetal lung. Clin Exp Pharmacol Physiol. 1995;22(4):235–47.
20. Nardo L, Hooper SB, Harding R. Stimulation of lung growth by tracheal obstruction in fetal sheep: relation to luminal pressure and lung liquid volume. Pediatr Res. 1998;43(2):184–90.
21. Badri KR, Zhou Y, Schuger L. Embryological origin of airway smooth muscle. Proc Am Thorac Soc. 2008;5(1):4–10.
22. Jesudason EC, Smith NP, Connell MG, Spiller DG, White MR, Fernig DG, et al. Developing rat lung has a sided pacemaker region for morphogenesis-related airway peristalsis. Am J Respir Cell Mol Biol. 2005;32(2):118–27.
23. Snetkov VA, Pandya H, Hirst SJ, Ward JP. Potassium channels in human fetal airway smooth muscle cells. Pediatr Res. 1998;43(4 Pt 1):548–54.
24. Janssen LJ. Ionic mechanisms and Ca^{2+} regulation in airway smooth muscle contraction: do the data contradict dogma? Am J Physiol. 2002;282:L1161–78.
25. Ito Y, Suzuki H, Aizawa H, Hakoda H, Hirose T. The spontaneous electrical and mechanical activity of human bronchial smooth muscle: its modulation by drugs. Br J Pharmacol. 1989;98(4):1249–60.
26. McCray PB. Spontaneous Contractility of Human Fetal Airway Smooth Muscle. Am J Respir Cell Mol Biol. 1993;8(5):573–80.
27. Featherstone NC, Jesudason EC, Connell MG, Fernig DG, Wray S, Losty PD, et al. Spontaneous propagating calcium waves underpin airway peristalsis in embryonic rat lung. Am J Respir Cell Mol Biol. 2005;33(2):153–60.
28. Matsumoto H, Hirata Y, Otsuka K, Iwata T, Inazumi A, Niimi A, et al. Interleukin-13 enhanced Ca2+ oscillations in airway smooth muscle cells. Cytokine. 2012;57(1):19–24.
29. Sweeney D, Hollins F, Gomez E, Saunders R, Challiss RA, Brightling CE. [Ca2+]i oscillations in ASM: relationship with persistent airflow obstruction in asthma. Respirology. 2014;19(5):763–6.
30. Linden A, Lofdahl CG, Ullman A, Skoogh BE. *In vitro* characteristics of spontaneous airway tone in the guinea-pig. Acta Physiol Scand. 1991;142(3):351–7.
31. Hartman WR, Smelter DF, Sathish V, Karass M, Kim S, Aravamudan B, et al. Oxygen dose responsiveness of human fetal airway smooth muscle cells. Am J Physiol Lung Cell Mol Physiol. 2012;303(8):L711–9.
32. Mitzner W. Airway smooth muscle: the appendix of the lung. Am J Respir Crit Care Med. 2004;169(7):787–90.
33. Seow CY, Fredberg JJ. Historical perspective on airway smooth muscle: the saga of a frustrated cell. J Appl Physiol (1985). 2001;91(2):938–52.
34. James AL, Hogg JC, Dunn LA, Pare PD. The use of the internal perimeter to compare airway size and to calculate smooth muscle shortening. Am Rev Respir Dis. 1988;138(1):136–9.
35. Widdicombe JG. Regulation of tracheobronchial smooth muscle. Physiol Rev. 1963;43:1–37.
36. Nadel JA, Widdicombe JG. Reflex control of airway size. Ann N Y Acad Sci. 1963;109:712–23.
37. Woolcock AJ, Salome CM, Yan K. The shape of the dose-response curve to histamine in asthmatic and normal subjects. Am Rev Respir Dis. 1984;130(1):71–5.
38. Wright D, Sharma P, Ryu MH, Risse PA, Ngo M, Maarsingh H, et al. Models to study airway smooth muscle contraction *in vivo*, *ex vivo* and *in vitro*: implications in understanding asthma. Pulm Pharmacol Ther. 2013;26(1):24–36.
39. Sanderson MJ. Exploring lung physiology in health and disease with lung slices. Pulm Pharmacol Ther. 2011;24(5):452–65.

40. Schlepütz M, Rieg AD, Seehase S, Spillner J, Perez-Bouza A, Braunschweig T, et al. Neurally mediated airway constriction in human and other species: a comparative study using precision-cut lung slices (PCLS). PLoS One. 2012;7(10):e47344.
41. An SS, Mitzner W, Tang WY, Ahn K, Yoon AR, Huang J, et al. An inflammation-independent contraction mechanophenotype of airway smooth muscle in asthma. J Allergy Clin Immunol. 2016;138(1):294–7.e4.
42. Hirst SJ, Martin JG, Bonacci JV, Chan V, Fixman ED, Hamid QA, et al. Proliferative aspects of airway smooth muscle. J Allergy Clin Immunol. 2004;114(2 Suppl):S2–17.
43. Howarth PH, Knox AJ, Amrani Y, Tliba O, Panettieri RA Jr, Johnson M. Synthetic responses in airway smooth muscle. J Allergy Clin Immunol. 2004;114(2 Suppl):S32–50.
44. Spicuzza L, Giembycz MA, Barnes PJ, Belvisi MG. Prostaglandin E2 suppression of acetylcholine release from parasympathetic nerves innervating guinea-pig trachea by interacting with prostanoid receptors of the EP3-subtype. Br J Pharmacol. 1998;123(6):1246–52.
45. Clarke DL, Dakshinamurti S, Larsson AK, Ward JE, Yamasaki A. Lipid metabolites as regulators of airway smooth muscle function. Pulm Pharmacol Ther. 2009;22(5):426–35.
46. Johnson PR. Role of human airway smooth muscle in altered extracellular matrix production in asthma. Clin Exp Pharmacol Physiol. 2001;28(3):233–6.
47. Ward JE, Hirst SJ. Airway smooth muscle bidirectional interactions with extracellular matrix. In: Chung KF, editor. Airway smooth muscle biology and pharmacology in airways disease. Chichester: Wiley; 2007. p. 105–26.
48. Canning BJ. Reflex regulation of airway smooth muscle tone. J Appl Physiol (1985). 2006;101(3):971–85.
49. Barnes PJ, Basbaum CB, Nadel JA. Autoradiographic localization of autonomic receptors in airway smooth muscle. Marked differences between large and small airways. Am Rev Respir Dis. 1983;127(6):758–62.
50. Zaagsma J, Roffel AF, Meurs H. Muscarinic control of airway function. Life Sci. 1997;60(13–14):1061–8.
51. Taylor SM, Pare PD, Schellenberg RR. Cholinergic and nonadrenergic mechanisms in human and guinea pig airways. J Appl Physiol Respir Environ Exerc Physiol. 1984;56(4):958–65.
52. Mitchell RA, Herbert DA, Baker DG, Basbaum CB. *In vivo* activity of tracheal parasympathetic ganglion cells innervating tracheal smooth muscle. Brain Res. 1987;437(1):157–60.
53. Seehase S, Schleputz M, Switalla S, Matz-Rensing K, Kaup FJ, Zoller M, et al. Bronchoconstriction in nonhuman primates: a species comparison. J Appl Physiol (1985). 2011;111(3):791–8.
54. Lambermont VA, Schleputz M, Dassow C, Konig P, Zimmermann LJ, Uhlig S, et al. Comparison of airway responses in sheep of different age in precision-cut lung slices (PCLS). PLoS One. 2014;9(9):e97610.
55. Chitano P, Murphy TM. Maturational changes in airway smooth muscle shortening and relaxation. Implications for asthma. Respir Physiol Neurobiol. 2003;137(2–3):347–59.
56. Finney MJ, Karlsson JA, Persson CG. Effects of bronchoconstrictors and bronchodilators on a novel human small airway preparation. Br J Pharmacol. 1985;85(1):29–36.
57. Martin C, Uhlig S, Ullrich V. Videomicroscopy of methacholine-induced contraction of individual airways in precision-cut lung slices. Eur Respir J. 1996;9(12):2479–87.
58. Noble PB, McLaughlin RA, West AR, Becker S, Armstrong JJ, McFawn PK, et al. Distribution of airway narrowing responses across generations and at branching points, assessed *in vitro* by anatomical optical coherence tomography. Respir Res. 2010;11:9.
59. Bai Y, Zhang M, Sanderson MJ. Contractility and Ca2+ signaling of smooth muscle cells in different generations of mouse airways. Am J Respir Cell Mol Biol. 2007;36(1):122–30.
60. Sparrow MP, Weichselbaum M. Structure and function of the adventitial and mucosal nerve plexuses of the bronchial tree in the developing lung. Clin Exp Pharmacol Physiol. 1997;24(3–4):261–8.
61. Sheldrick RL, Ball DI, Coleman RA. Characterisation of the neurokinin receptors mediating contraction of isolated tracheal preparations from a variety of species. Agents Actions Suppl. 1990;31:205–9.
62. Advenier C, Naline E, Toty L, Bakdach H, Emonds-Alt X, Vilain P, et al. Effects on the isolated human bronchus of SR 48968, a potent and selective non-peptide antagonist of the neurokinin A (NK2) receptors. Am Rev Respir Dis. 1992;146(5 Pt 1):1177–81.
63. Amadesi S, Moreau J, Tognetto M, Springer J, Trevisani M, Naline E, et al. NK1 receptor stimulation causes contraction and inositol phosphate increase in medium-size human isolated bronchi. Am J Respir Crit Care Med. 2001;163(5):1206–11.
64. Palmer JB, Cuss FM, Mulderry PK, Ghatei MA, Springall DR, Cadieux A, et al. Calcitonin gene-related peptide is localised to human airway nerves and potently constricts human airway smooth muscle. Br J Pharmacol. 1987;91(1):95–101.
65. Springer J, Amadesi S, Trevisani M, Harrison S, Dinh QT, McGregor GP, et al. Effects of alpha calcitonin gene-related peptide in human bronchial smooth muscle and pulmonary artery. Regul Pept. 2004;118(3):127–34.
66. Sheppard MN, Marangos PJ, Bloom SR, Polak JM. Neuron specific enolase: a marker for the early development of nerves and endocrine cells in the human lung. Life Sci. 1984;34(3):265–71.
67. O'Donnell SR, Saar N. Histochemical localization of adrenergic nerves in the guinea-pig trachea. Br J Pharmacol. 1973;47(4):707–10.

68. Mitchell HW, Sparrow MP, Tagliaferri RP. Inhibitory and excitatory responses to field stimulation in fetal and adult pig airway. Pediatr Res. 1990;28(1):69–74.
69. Doidge JM, Satchell DG. Adrenergic and non-adrenergic inhibitory nerves in mammalian airways. J Auton Nerv Syst. 1982;5(2):83–99.
70. Cadieux A, Benchekroun MT, St-Pierre S, Fournier A. Bronchoconstrictor action of neuropeptide Y (NPY) in isolated guinea pig airways. Neuropeptides. 1989;13(4):215–9.
71. Li S, Koziol-White C, Jude J, Jiang M, Zhao H, Cao G, et al. Epithelium-generated neuropeptide Y induces smooth muscle contraction to promote airway hyperresponsiveness. J Clin Invest. 2016;126(5):1978–82.
72. Henry PJ, Goldie RG. Beta 1-adrenoceptors mediate smooth muscle relaxation in mouse isolated trachea. Br J Pharmacol. 1990;99(1):131–5.
73. Carstairs JR, Nimmo AJ, Barnes PJ. Autoradiographic visualization of beta-adrenoceptor subtypes in human lung. Am Rev Respir Dis. 1985;132(3):541–7.
74. Carswell H, Nahorski SR. Beta-adrenoceptor heterogeneity in guinea-pig airways: comparison of functional and receptor labelling studies. Br J Pharmacol. 1983;79(4):965–71.
75. Palmer JB, Cuss FM, Barnes PJ. VIP and PHM and their role in nonadrenergic inhibitory responses in isolated human airways. J Appl Physiol (1985). 1986;61(4):1322–8.
76. Ellis JL, Undem BJ. Inhibition by L-NG-nitro-L-arginine of nonadrenergic-noncholinergic-mediated relaxations of human isolated central and peripheral airway. Am Rev Respir Dis. 1992;146(6):1543–7.
77. Mathioudakis A, Chatzimavridou-Grigoriadou V, Evangelopoulou E, Mathioudakis G. Vasoactive intestinal Peptide inhaled agonists: potential role in respiratory therapeutics. Hippokratia. 2013;17(1):12–6.
78. Regal JF, Johnson DE. Indomethacin alters the effects of substance-P and VIP on isolated airway smooth muscle. Peptides. 1983;4(4):581–4.
79. Douglas JS, Duncan PG, Mukhopadhyay A. The antagonism of histamine-induced tracheal and bronchial muscle contraction by diphenhydramine: effect of maturation. Br J Pharmacol. 1984;83(3):697–705.
80. Persson GA, Ekman M. Contractile effects of histamine in large and small respiratory airways. Agents Actions. 1976;6(4):389–93.
81. Perez JF, Sanderson MJ. The frequency of calcium oscillations induced by 5-HT, ACH, and KCl determine the contraction of smooth muscle cells of intrapulmonary bronchioles. J Gen Physiol. 2005;125(6):535–53.
82. Tran T, Stewart AG. Protease-activated receptor (PAR)-independent growth and pro-inflammatory actions of thrombin on human cultured airway smooth muscle. Br J Pharmacol. 2003;138(5):865–75.
83. Chambers LS, Black JL, Poronnik P, Johnson PR. Functional effects of protease-activated receptor-2 stimulation on human airway smooth muscle. Am J Physiol Lung Cell Mol Physiol. 2001;281(6):L1369–78.
84. Cocks TM, Fong B, Chow JM, Anderson GP, Frauman AG, Goldie RG, et al. A protective role for protease-activated receptors in the airways. Nature. 1999;398(6723):156–60.
85. Capra V, Thompson MD, Sala A, Cole DE, Folco G, Rovati GE. Cysteinyl-leukotrienes and their receptors in asthma and other inflammatory diseases: critical update and emerging trends. Med Res Rev. 2007;27(4):469–527.
86. Mechiche H, Naline E, Candenas L, Pinto FM, Birembault P, Advenier C, et al. Effects of cysteinyl leukotrienes in small human bronchus and antagonist activity of montelukast and its metabolites. Clin Exp Allergy. 2003;33(7):887–94.
87. Benyahia C, Gomez I, Kanyinda L, Boukais K, Danel C, Leseche G, et al. PGE(2) receptor (EP(4)) agonists: potent dilators of human bronchi and future asthma therapy? Pulm Pharmacol Ther. 2012;25(1):115–8.
88. Safholm J, Dahlen SE, Delin I, Maxey K, Stark K, Cardell LO, et al. PGE2 maintains the tone of the guinea pig trachea through a balance between activation of contractile EP1 receptors and relaxant EP2 receptors. Br J Pharmacol. 2013;168(4):794–806.
89. FitzPatrick M, Donovan C, Bourke JE. Prostaglandin E2 elicits greater bronchodilation than salbutamol in mouse intrapulmonary airways in lung slices. Pulm Pharmacol Ther. 2014;28(1):68–76.
90. Ressmeyer AR, Larsson AK, Vollmer E, Dahlen SE, Uhlig S, Martin C. Characterisation of guinea pig precision-cut lung slices: comparison with human tissues. Eur Respir J. 2006;28(3):603–11.
91. Allen IC, Hartney JM, Coffman TM, Penn RB, Wess J, Koller BH. Thromboxane A2 induces airway constriction through an M3 muscarinic acetylcholine receptor-dependent mechanism. Am J Physiol Lung Cell Mol Physiol. 2006;290(3):L526–33.
92. Goldie RG, Henry PJ, Knott PG, Self GJ, Luttmann MA, Hay DW. Endothelin-1 receptor density, distribution, and function in human isolated asthmatic airways. Am J Respir Crit Care Med. 1995;152(5 Pt 1):1653–8.
93. Knott PG, Fernandes LB, Henry PJ, Goldie RG. Influence of endothelin-1 on cholinergic nerve-mediated contractions and acetylcholine release in rat isolated tracheal smooth muscle. J Pharmacol Exp Ther. 1996;279(3):1142–7.
94. Hay DW. Putative mediator role of endothelin-1 in asthma and other lung diseases. Clin Exp Pharmacol Physiol. 1999;26(2):168–71.
95. Grunstein MM, Rosenberg SM, Schramm CM, Pawlowski NA. Mechanisms of action of endothelin 1 in maturing rabbit airway smooth muscle. Am J Phys. 1991;260(6 Pt 1):L434–43.
96. Gallos G, Townsend E, Yim P, Virag L, Zhang Y, Xu D, et al. Airway epithelium is a predominant

source of endogenous airway GABA and contributes to relaxation of airway smooth muscle tone. Am J Physiol Lung Cell Mol Physiol. 2013;304(3): L191–7.
97. Osawa Y, Xu D, Sternberg D, Sonett JR, D'Armiento J, Panettieri RA, et al. Functional expression of the GABAB receptor in human airway smooth muscle. Am J Physiol Lung Cell Mol Physiol. 2006;291(5):L923–31.
98. Mizuta K, Xu D, Pan Y, Comas G, Sonett JR, Zhang Y, et al. GABAA receptors are expressed and facilitate relaxation in airway smooth muscle. Am J Physiol Lung Cell Mol Physiol. 2008;294(6): L1206–16.
99. Gleason NR, Gallos G, Zhang Y, Emala CW. The GABAA agonist muscimol attenuates induced airway constriction in guinea pigs *in vivo*. J Appl Physiol (1985). 2009;106(4):1257–63.
100. Saxena H, Deshpande DA, Tiegs BC, Yan H, Battafarano RJ, Burrows WM, et al. The GPCR OGR1 (GPR68) mediates diverse signalling and contraction of airway smooth muscle in response to small reductions in extracellular pH. Br J Pharmacol. 2012;166(3):981–90.
101. Yarova PL, Stewart AL, Sathish V, Britt RD Jr, Thompson MA, Lowe APP, et al. Calcium-sensing receptor antagonists abrogate airway hyperresponsiveness and inflammation in allergic asthma. Sci Transl Med. 2015;7(284):284ra60.
102. Pera T, Penn RB. Bronchoprotection and bronchorelaxation in asthma: new targets, and new ways to target the old ones. Pharmacol Ther. 2016;164:82–96.
103. Thirstrup S. Control of airway smooth muscle tone: II—pharmacology of relaxation. Respir Med. 2000;94(6):519–28.
104. Thirstrup S. Control of airway smooth muscle tone. I—electrophysiology and contractile mediators. Respir Med. 2000;94(4):328–36.
105. Kirkpatrick CT. Excitation and contraction in bovine tracheal smooth muscle. J Physiol. 1975;244(2):263–81.
106. Murray RK, Kotlikoff MI. Receptor-activated calcium influx in human airway smooth muscle cells. J Physiol. 1991;435:123–44.
107. Farley JM, Miles PR. The sources of calcium for acetylcholine-induced contractions of dog tracheal smooth muscle. J Pharmacol Exp Ther. 1978;207(2):340–6.
108. Liu X, Farley JM. Depletion and refilling of acetylcholine- and caffeine-sensitive Ca++ stores in tracheal myocytes. J Pharmacol Exp Ther. 1996;277(2):789–95.
109. Roux E, Guibert C, Savineau JP, Marthan R. [Ca2+] i oscillations induced by muscarinic stimulation in airway smooth muscle cells: receptor subtypes and correlation with the mechanical activity. Br J Pharmacol. 1997;120(7):1294–301.
110. Sanderson MJ, Delmotte P, Bai Y, Perez-Zogbhi JF. Regulation of airway smooth muscle cell contractility by Ca2+ signaling and sensitivity. Proc Am Thorac Soc. 2008;5(1):23–31.
111. Ressmeyer AR, Bai Y, Delmotte P, Uy KF, Thistlethwaite P, Fraire A, et al. Human airway contraction and formoterol-induced relaxation is determined by Ca2+ oscillations and Ca2+ sensitivity. Am J Respir Cell Mol Biol. 2010;43(2): 179–91.
112. Bai Y, Sanderson MJ. The contribution of Ca2+ signaling and Ca2+ sensitivity to the regulation of airway smooth muscle contraction is different in rats and mice. Am J Physiol Lung Cell Mol Physiol. 2009;296(6):L947–58.
113. Wang YX, Zheng YM, Mei QB, Wang QS, Collier ML, Fleischer S, et al. FKBP12.6 and cADPR regulation of Ca2+ release in smooth muscle cells. Am J Physiol Cell Physiol. 2004;286(3):C538–46.
114. Du W, Stiber JA, Rosenberg PB, Meissner G, Eu JP. Ryanodine receptors in muscarinic receptor-mediated bronchoconstriction. J Biol Chem. 2005;280(28):26287–94.
115. Mahn K, Hirst SJ, Ying S, Holt MR, Lavender P, Ojo OO, et al. Diminished sarco/endoplasmic reticulum Ca2+ ATPase (SERCA) expression contributes to airway remodelling in bronchial asthma. Proc Natl Acad Sci U S A. 2009;106(26):10775–80.
116. Bai Y, Edelmann M, Sanderson MJ. The contribution of inositol 1,4,5-trisphosphate and ryanodine receptors to agonist-induced Ca2+ signaling of airway smooth muscle cells. Am J Physiol Lung Cell Mol Physiol. 2009;297(2):L347–L61.
117. Bergner A, Sanderson MJ. Acetylcholine-induced calcium signaling and contraction of airway smooth muscle cells in lung slices. J Gen Physiol. 2002;119(2):187–98.
118. Pelaia G, Renda T, Gallelli L, Vatrella A, Busceti MT, Agati S, et al. Molecular mechanisms underlying airway smooth muscle contraction and proliferation: implications for asthma. Respir Med. 2008;102(8):1173–81.
119. Deshpande DA, White TA, Dogan S, Walseth TF, Panettieri RA, Kannan MS. CD38/cyclic ADP-ribose signaling: role in the regulation of calcium homeostasis in airway smooth muscle. Am J Physiol Lung Cell Mol Physiol. 2005;288(5):L773–88.
120. Janssen LJ, Sims SM. Emptying and refilling of Ca2+ store in tracheal myocytes as indicated by ACh-evoked currents and contraction. Am J Phys. 1993;265(4 Pt 1):C877–86.
121. Sathish V, Thompson MA, Bailey JP, Pabelick CM, Prakash YS, Sieck GC. Effect of proinflammatory cytokines on regulation of sarcoplasmic reticulum Ca2+ reuptake in human airway smooth muscle. Am J Physiol Lung Cell Mol Physiol. 2009;297(1):L26–34.
122. Somlyo AP, Somlyo AV. Ca2+ sensitivity of smooth muscle and nonmuscle myosin II: modulated by G proteins, kinases, and myosin phosphatase. Physiol Rev. 2003;83(4):1325–58.

123. Gao N, Tsai MH, Chang AN, He W, Chen CP, Zhu M, et al. Physiological vs. pharmacological signalling to myosin phosphorylation in airway smooth muscle. J Physiol. 2017;595(19):6231–47.
124. Yoshii A, Iizuka K, Dobashi K, Horie T, Harada T, Nakazawa T, et al. Relaxation of contracted rabbit tracheal and human bronchial smooth muscle by Y-27632 through inhibition of Ca2+ sensitization. Am J Respir Cell Mol Biol. 1999;20(6):1190–200.
125. Mukherjee S, Trice J, Shinde P, Willis RE, Pressley TA, Perez-Zoghbi JF. Ca2+ oscillations, Ca2+ sensitization, and contraction activated by protein kinase C in small airway smooth muscle. J Gen Physiol. 2013;141(2):165–78.
126. Sparrow MP, Mitchell HW. Contraction of smooth muscle of pig airway tissues from before birth to maturity. J Appl Physiol (1985). 1990;68(2): 468–77.
127. Boie S, Chen J, Sanderson MJ, Sneyd J. The relative contributions of store-operated and voltage-gated Ca(2+) channels to the control of Ca(2+) oscillations in airway smooth muscle. J Physiol. 2017;595(10):3129–41.
128. Chen J, Sanderson MJ. Store-operated calcium entry is required for sustained contraction and Ca(2+) oscillations of airway smooth muscle. J Physiol. 2017;595(10):3203–18.
129. Peel SE, Liu B, Hall IP. ORAI and store-operated calcium influx in human airway smooth muscle cells. Am J Respir Cell Mol Biol. 2008;38(6):744–9.
130. Billington CK, Ojo OO, Penn RB, Ito S. cAMP regulation of airway smooth muscle function. Pulm Pharmacol Ther. 2013;26(1):112–20.
131. Morgan SJ, Deshpande DA, Tiegs BC, Misior AM, Yan H, Hershfeld AV, et al. beta-Agonist-mediated relaxation of airway smooth muscle is protein kinase A-dependent. J Biol Chem. 2014;289(33):23065–74.
132. Roscioni SS, Maarsingh H, Elzinga CR, Schuur J, Menzen M, Halayko AJ, et al. Epac as a novel effector of airway smooth muscle relaxation. J Cell Mol Med. 2011;15(7):1551–63.
133. Zieba BJ, Artamonov MV, Jin L, Momotani K, Ho R, Franke AS, et al. The cAMP-responsive Rap1 guanine nucleotide exchange factor, Epac, induces smooth muscle relaxation by down-regulation of RhoA activity. J Biol Chem. 2011;286(19):16681–92.
134. Nuttle LC, Farley JM. Frequency modulation of acetylcholine-induced oscillations in Ca++ and Ca(++)-activated Cl- current by cAMP in tracheal smooth muscle. J Pharmacol Exp Ther. 1996;277(2):753–60.
135. Delmotte P, Ressmeyer AR, Bai Y, Sanderson MJ. Mechanisms of airway smooth muscle relaxation induced by beta2-adrenergic agonists. Front Biosci (Landmark Ed). 2010;15:750–64.
136. Perez-Zoghbi JF, Bai Y, Sanderson MJ. Nitric oxide induces airway smooth muscle cell relaxation by decreasing the frequency of agonist-induced Ca2+ oscillations. J Gen Physiol. 2010;135(3): 247–59.
137. Oguma T, Kume H, Ito S, Takeda N, Honjo H, Kodama I, et al. Involvement of reduced sensitivity to Ca in beta-adrenergic action on airway smooth muscle. Clin Exp Allergy. 2006;36(2):183–91.
138. Liu C, Zuo J, Janssen LJ. Regulation of airway smooth muscle RhoA/ROCK activities by cholinergic and bronchodilator stimuli. Eur Respir J. 2006;28(4):703–11.
139. Kotlikoff MI, Kamm KE. Molecular mechanisms of beta-adrenergic relaxation of airway smooth muscle. Annu Rev Physiol. 1996;58:115–41.
140. Torphy TJ, Undem BJ, Cieslinski LB, Luttmann MA, Reeves ML, Hay DW. Identification, characterization and functional role of phosphodiesterase isozymes in human airway smooth muscle. J Pharmacol Exp Ther. 1993;265(3):1213–23.
141. Billington CK, Le Jeune IR, Young KW, Hall IP. A major functional role for phosphodiesterase 4D5 in human airway smooth muscle cells. Am J Respir Cell Mol Biol. 2008;38(1):1–7.
142. Holgate ST, Wenzel S, Postma DS, Weiss ST, Renz H, Sly PD. Asthma. Nat Rev Dis Primers. 2015;1:15025.
143. Barnes PJ, Burney PG, Silverman EK, Celli BR, Vestbo J, Wedzicha JA, et al. Chronic obstructive pulmonary disease. Nat Rev Dis Primers. 2015;1:15076.
144. Gosens R, Zaagsma J, Meurs H, Halayko AJ. Muscarinic receptor signaling in the pathophysiology of asthma and COPD. Respir Res. 2006;7:73.
145. ten Berge RE, Zaagsma J, Roffel AF. Muscarinic inhibitory autoreceptors in different generations of human airways. Am J Respir Crit Care Med. 1996;154(1):43–9.
146. Hallstrand TS, Lai Y, Henderson WR Jr, Altemeier WA, Gelb MH. Epithelial regulation of eicosanoid production in asthma. Pulm Pharmacol Ther. 2012;25(6):432–7.
147. Wenzel SE, Larsen GL, Johnston K, Voelkel NF, Westcott JY. Elevated levels of leukotriene C4 in bronchoalveolar lavage fluid from atopic asthmatics after endobronchial allergen challenge. Am Rev Respir Dis. 1990;142(1):112–9.
148. Fajt ML, Gelhaus SL, Freeman B, Uvalle CE, Trudeau JB, Holguin F, et al. Prostaglandin D(2) pathway upregulation: relation to asthma severity, control, and TH2 inflammation. J Allergy Clin Immunol. 2013;131(6):1504–12.
149. Fagan KA, McMurtry IF, Rodman DM. Role of endothelin-1 in lung disease. Respir Res. 2001;2(2):90–101.
150. Ackerman V, Carpi S, Bellini A, Vassalli G, Marini M, Mattoli S. Constitutive expression of endothelin in bronchial epithelial cells of patients with symptomatic and asymptomatic asthma and modulation by histamine and interleukin-1. J Allergy Clin Immunol. 1995;96(5 Pt 1):618–27.
151. Celik G, Karabiyikoglu G. Local and peripheral plasma endothelin-1 in pulmonary hypertension

secondary to chronic obstructive pulmonary disease. Respiration. 1998;65(4):289–94.
152. Lambert RK, Wiggs BR, Kuwano K, Hogg JC, Pare PD. Functional significance of increased airway smooth muscle in asthma and COPD. J Appl Physiol (1985). 1993;74(6):2771–81.
153. O'Reilly M, Sozo F, Harding R. Impact of preterm birth and bronchopulmonary dysplasia on the developing lung: long-term consequences for respiratory health. Clin Exp Pharmacol Physiol. 2013;40(11):765–73.
154. James AL, Bai TR, Mauad T, Abramson MJ, Dolhnikoff M, McKay KO, et al. Airway smooth muscle thickness in asthma is related to severity but not duration of asthma. Eur Respir J. 2009;34(5):1040–5.
155. Benayoun L, Druilhe A, Dombret MC, Aubier M, Pretolani M. Airway structural alterations selectively associated with severe asthma. Am J Respir Crit Care Med. 2003;167(10):1360–8.
156. Ward JE, Harris T, Bamford T, Mast A, Pain MC, Robertson C, et al. Proliferation is not increased in airway myofibroblasts isolated from asthmatics. Eur Respir J. 2008;32(2):362–71.
157. Trian T, Benard G, Begueret H, Rossignol R, Girodet PO, Ghosh D, et al. Bronchial smooth muscle remodeling involves calcium-dependent enhanced mitochondrial biogenesis in asthma. J Exp Med. 2007;204(13):3173–81.
158. Roth M, Black JL. An imbalance in C/EBPs and increased mitochondrial activity in asthmatic airway smooth muscle cells: novel targets in asthma therapy? Br J Pharmacol. 2009;157(3):334–41.
159. Perry M, Baker J, Chung KF. Airway smooth muscle cells from patients with COPD exhibit a higher degree of cellular proliferation and steroid insensitivity than that from healthy patients. Eur Respir J. 2011;38(Suppl 55):748.
160. Michaeloudes C, Kuo CH, Haji G, Finch DK, Halayko AJ, Kirkham P, et al. Metabolic repatterning in COPD airway smooth muscle cells. Eur Respir J. 2017;50(5):1700202.
161. Salter B, Pray C, Radford K, Martin JG, Nair P. Regulation of human airway smooth muscle cell migration and relevance to asthma. Respir Res. 2017;18(1):156.
162. Kanabar V, Simcock DE, Mahn K, O'Connor BJ, Hirst SJ. Airway smooth muscle migration is increased in asthmatics. Proc Am Thorac Soc. 2006;3:A280.
163. Johnson PR, Burgess JK, Ge Q, Poniris M, Boustany S, Twigg SM, et al. Connective tissue growth factor induces extracellular matrix in asthmatic airway smooth muscle. Am J Respir Crit Care Med. 2006;173(1):32–41.
164. Al-Alawi M, Hassan T, Chotirmall SH. Transforming growth factor beta and severe asthma: a perfect storm. Respir Med. 2014;108(10):1409–23.
165. Chan V, Burgess JK, Ratoff JC, O'Connor BJ, Greenough A, Lee TH, et al. Extracellular matrix regulates enhanced eotaxin expression in asthmatic airway smooth muscle cells. Am J Respir Crit Care Med. 2006;174(4):379–85.
166. Johnson PR, Burgess JK, Underwood PA, Au W, Poniris MH, Tamm M, et al. Extracellular matrix proteins modulate asthmatic airway smooth muscle cell proliferation via an autocrine mechanism. J Allergy Clin Immunol. 2004;113(4):690–6.
167. Parameswaran K, Radford K, Zuo J, Janssen LJ, O'Byrne PM, Cox PG. Extracellular matrix regulates human airway smooth muscle cell migration. Eur Respir J. 2004;24(4):545–51.
168. Ghaffar O, Hamid Q, Renzi PM, Allakhverdi Z, Molet S, Hogg JC, et al. Constitutive and cytokine-stimulated expression of eotaxin by human airway smooth muscle cells. Am J Respir Crit Care Med. 1999;159(6):1933–42.
169. Chen H, Tliba O, Van Besien CR, Panettieri RA Jr, Amrani Y. TNF-[alpha] modulates murine tracheal rings responsiveness to G-protein-coupled receptor agonists and KCl. J Appl Physiol (1985). 2003;95(2):864–72; discussion 3.
170. Sukkar MB, Hughes JM, Armour CL, Johnson PR. Tumour necrosis factor-alpha potentiates contraction of human bronchus *in vitro*. Respirology. 2001;6(3):199–203.
171. Cooper PR, Lamb R, Day ND, Branigan PJ, Kajekar R, San Mateo L, et al. TLR3 activation stimulates cytokine secretion without altering agonist-induced human small airway contraction or relaxation. Am J Physiol Lung Cell Mol Physiol. 2009;297(3):L530–7.
172. Zhang Y, Adner M, Cardell LO. Up-regulation of bradykinin receptors in a murine *in-vitro* model of chronic airway inflammation. Eur J Pharmacol. 2004;489(1–2):117–26.
173. Tliba O, Deshpande D, Chen H, Van Besien C, Kannan M, Panettieri RA Jr, et al. IL-13 enhances agonist-evoked calcium signals and contractile responses in airway smooth muscle. Br J Pharmacol. 2003;140(7):1159–62.
174. Jiang H, Xie Y, Abel PW, Toews ML, Townley RG, Casale TB, et al. Targeting phosphoinositide 3-kinase gamma in airway smooth muscle cells to suppress interleukin-13-induced mouse airway hyperresponsiveness. J Pharmacol Exp Ther. 2012;342(2):305–11.
175. Hirose K, Iwata A, Tamachi T, Nakajima H. Allergic airway inflammation: key players beyond the Th2 cell pathway. Immunol Rev. 2017;278(1):145–61.
176. Kudo M, Melton AC, Chen C, Engler MB, Huang KE, Ren X, et al. IL-17A produced by alphabeta T cells drives airway hyper-responsiveness in mice and enhances mouse and human airway smooth muscle contraction. Nat Med. 2012;18(4):547–54.
177. Wills-Karp M, Luyimbazi J, Xu X, Schofield B, Neben TY, Karp CL, et al. Interleukin-13: central mediator of allergic asthma. Science. 1998;282(5397):2258–61.

178. Renzetti LM, Paciorek PM, Tannu SA, Rinaldi NC, Tocker JE, Wasserman MA, et al. Pharmacological evidence for tumor necrosis factor as a mediator of allergic inflammation in the airways. J Pharmacol Exp Ther. 1996;278(2):847–53.
179. Thomas PS, Heywood G. Effects of inhaled tumour necrosis factor alpha in subjects with mild asthma. Thorax. 2002;57(9):774–8.
180. Amrani Y. TNF-alpha and calcium signaling in airway smooth muscle cells: a never-ending story with promising therapeutic relevance. Am J Respir Cell Mol Biol. 2007;36(3):387–8.
181. Risse PA, Jo T, Suarez F, Hirota N, Tolloczko B, Ferraro P, et al. Interleukin-13 inhibits proliferation and enhances contractility of human airway smooth muscle cells without change in contractile phenotype. Am J Physiol Lung Cell Mol Physiol. 2011;300(6):L958–66.
182. Jude JA, Solway J, Panettieri RA Jr, Walseth TF, Kannan MS. Differential induction of CD38 expression by TNF-{alpha} in asthmatic airway smooth muscle cells. Am J Physiol Lung Cell Mol Physiol. 2010;299(6):L879–90.
183. Mahn K, Ojo OO, Chadwick G, Aaronson PI, Ward JP, Lee TH. Ca(2+) homeostasis and structural and functional remodelling of airway smooth muscle in asthma. Thorax. 2010;65(6):547–52.
184. Sweeney D, Hollins F, Gomez E, Mistry R, Saunders R, Challiss RA, et al. No evidence for altered intracellular calcium-handling in airway smooth muscle cells from human subjects with asthma. BMC Pulm Med. 2015;15:12.
185. Kellner J, Tantzscher J, Oelmez H, Edelmann M, Fischer R, Huber RM, et al. Mechanisms altering airway smooth muscle cell Ca+ homeostasis in two asthma models. Respiration. 2008;76(2):205–15.
186. Tao FC, Tolloczko B, Mitchell CA, Powell WS, Martin JG. Inositol (1,4,5)trisphosphate metabolism and enhanced calcium mobilization in airway smooth muscle of hyperresponsive rats. Am J Respir Cell Mol Biol. 2000;23(4):514–20.
187. Du Y, Zhao J, Li X, Jin S, Ma WL, Mu Q, et al. Dissociation of FK506-binding protein 12.6 kD from ryanodine receptor in bronchial smooth muscle cells in airway hyperresponsiveness in asthma. Am J Respir Cell Mol Biol. 2014;50(2):398–408.
188. Jain D, Keslacy S, Tliba O, Cao Y, Kierstein S, Amin K, et al. Essential role of IFNbeta and CD38 in TNFalpha-induced airway smooth muscle hyper-responsiveness. Immunobiology. 2008;213(6):499–509.
189. Croisier H, Tan X, Chen J, Sneyd J, Sanderson MJ, Brook BS. Ryanodine receptor sensitization results in abnormal calcium signaling in airway smooth muscle cells. Am J Respir Cell Mol Biol. 2015;53(5):703–11.
190. Sakai H, Suto W, Kai Y, Chiba Y. Mechanisms underlying the pathogenesis of hyper-contractility of bronchial smooth muscle in allergic asthma. J Smooth Muscle Res. 2017;53(0):37–47.
191. Hunter I, Cobban HJ, Vandenabeele P, MacEwan DJ, Nixon GF. Tumor necrosis factor-alpha-induced activation of RhoA in airway smooth muscle cells: role in the Ca2+ sensitization of myosin light chain20 phosphorylation. Mol Pharmacol. 2003;63(3):714–21.
192. Donovan C, Royce SG, Esposito J, Tran J, Ibrahim ZA, Tang ML, et al. Differential effects of allergen challenge on large and small airway reactivity in mice. PLoS One. 2013;8(9):e74101.
193. Ma X, Cheng Z, Kong H, Wang Y, Unruh H, Stephens NL, et al. Changes in biophysical and biochemical properties of single bronchial smooth muscle cells from asthmatic subjects. Am J Physiol Lung Cell Mol Physiol. 2002;283(6):L1181–9.
194. Matsumoto H, Moir LM, Oliver BG, Burgess JK, Roth M, Black JL, et al. Comparison of gel contraction mediated by airway smooth muscle cells from patients with and without asthma. Thorax. 2007;62(10):848–54.
195. Sutcliffe A, Hollins F, Gomez E, Saunders R, Doe C, Cooke M, et al. Increased nicotinamide adenine dinucleotide phosphate oxidase 4 expression mediates intrinsic airway smooth muscle hypercontractility in asthma. Am J Respir Crit Care Med. 2012;185(3):267–74.
196. Wang CG, Almirall JJ, Dolman CS, Dandurand RJ, Eidelman DH. *In vitro* bronchial responsiveness in two highly inbred rat strains. J Appl Physiol (1985). 1997;82(5):1445–52.
197. Mitchell RW, Ruhlmann E, Magnussen H, Leff AR, Rabe KF. Passive sensitization of human bronchi augments smooth muscle shortening velocity and capacity. Am J Phys. 1994;267(2 Pt 1):L218–22.
198. Leguillette R, Laviolette M, Bergeron C, Zitouni N, Kogut P, Solway J, et al. Myosin, transgelin, and myosin light chain kinase: expression and function in asthma. Am J Respir Crit Care Med. 2009;179(3):194–204.
199. Peters SP, Jones CA, Haselkorn T, Mink DR, Valacer DJ, Weiss ST. Real-world Evaluation of Asthma Control and Treatment (REACT): findings from a national Web-based survey. J Allergy Clin Immunol. 2007;119(6):1454–61.
200. Lemoine H, Overlack C. Highly potent beta-2 sympathomimetics convert to less potent partial agonists as relaxants of guinea pig tracheae maximally contracted by carbachol. Comparison of relaxation with receptor binding and adenylate cyclase stimulation. J Pharmacol Exp Ther. 1992;261(1):258–70.
201. Trian T, Burgess JK, Niimi K, Moir LM, Ge Q, Berger P, et al. beta2-Agonist induced cAMP is

decreased in asthmatic airway smooth muscle due to increased PDE4D. PLoS One. 2011;6(5):e20000.
202. Deshpande DA, Theriot BS, Penn RB, Walker JK. Beta-arrestins specifically constrain beta2-adrenergic receptor signaling and function in airway smooth muscle. FASEB J. 2008;22(7):2134–41.
203. Pera T, Hegde A, Deshpande DA, Morgan SJ, Tiegs BC, Theriot BS, et al. Specificity of arrestin subtypes in regulating airway smooth muscle G protein-coupled receptor signaling and function. FASEB J. 2015;29(10):4227–35.
204. Gupta MK, Asosingh K, Aronica M, Comhair S, Cao G, Erzurum S, et al. Defective resensitization in human airway smooth muscle cells evokes beta-adrenergic receptor dysfunction in severe asthma. PLoS One. 2015;10(5):e0125803.
205. Nelson HS, Weiss ST, Bleecker ER, Yancey SW, Dorinsky PM, Group SS. The Salmeterol Multicenter Asthma Research Trial: a comparison of usual pharmacotherapy for asthma or usual pharmacotherapy plus salmeterol. Chest. 2006;129(1):15–26.
206. Salpeter SR, Buckley NS, Ormiston TM, Salpeter EE. Meta-analysis: effect of long-acting beta-agonists on severe asthma exacerbations and asthma-related deaths. Ann Intern Med. 2006;144(12):904–12.
207. Laporte JC, Moore PE, Baraldo S, Jouvin MH, Church TL, Schwartzman IN, et al. Direct effects of interleukin-13 on signaling pathways for physiological responses in cultured human airway smooth muscle cells. Am J Respir Crit Care Med. 2001;164(1):141–8.
208. Guo M, Pascual RM, Wang S, Fontana MF, Valancius CA, Panettieri RA Jr, et al. Cytokines regulate beta-2-adrenergic receptor responsiveness in airway smooth muscle via multiple PKA- and EP2 receptor-dependent mechanisms. Biochemistry. 2005;44(42):13771–82.
209. Shore SA, Laporte J, Hall IP, Hardy E, Panettieri RAJ. Effect of IL-1 beta on responses of cultured human airway smooth muscle cells to bronchodilator agonists. Am J Respir Cell Mol Biol. 1997;16(6):702–12.
210. Darveaux J, Busse WW. Biologics in asthma—the next step toward personalized treatment. J Allergy Clin Immunol Pract. 2015;3(2):152–60; quiz 61
211. Yousuf A, Brightling CE. Biologic drugs: a new target therapy in COPD? COPD. 2018;15(2):99–107.
212. Ntontsi P, Papathanassiou E, Loukides S, Bakakos P, Hillas G. Targeted anti-IL-13 therapies in asthma: current data and future perspectives. Expert Opin Investig Drugs. 2018;27(2):179–86.
213. Schmidt DT, Watson N, Dent G, Ruhlmann E, Branscheid D, Magnussen H, et al. The effect of selective and non-selective phosphodiesterase inhibitors on allergen- and leukotriene C(4)-induced contractions in passively sensitized human airways. Br J Pharmacol. 2000;131(8):1607–18.
214. Wedzicha JA, Calverley PM, Rabe KF. Roflumilast: a review of its use in the treatment of COPD. Int J Chron Obstruct Pulmon Dis. 2016;11:81–90.
215. Deshpande DA, Robinett KS, Wang WC, Sham JS, An SS, Liggett SB. Bronchodilator activity of bitter tastants in human tissue. Nat Med. 2011;17(7):776–8.
216. Deshpande DA, Wang WC, McIlmoyle EL, Robinett KS, Schillinger RM, An SS, et al. Bitter taste receptors on airway smooth muscle bronchodilate by localized calcium signaling and reverse obstruction. Nat Med. 2010;16(11):1299–304.
217. Tan X, Sanderson MJ. Bitter tasting compounds dilate airways by inhibiting airway smooth muscle calcium oscillations and calcium sensitivity. Br J Pharmacol. 2014;171(3):646–62.
218. Robinett KS, Koziol-White CJ, Akoluk A, An SS, Panettieri RA Jr, Liggett SB. Bitter taste receptor function in asthmatic and nonasthmatic human airway smooth muscle cells. Am J Respir Cell Mol Biol. 2014;50(4):678–83.
219. An SS, Wang WC, Koziol-White CJ, Ahn K, Lee DY, Kurten RC, et al. TAS2R activation promotes airway smooth muscle relaxation despite beta(2)-adrenergic receptor tachyphylaxis. Am J Physiol Lung Cell Mol Physiol. 2012;303(4):L304–11.
220. Lam M, Royce SG, Samuel CS, Bourke JE. Serelaxin as a novel therapeutic opposing fibrosis and contraction in lung diseases. Pharmacol Ther. 2018;187:61–70.
221. Pini A, Boccalini G, Lucarini L, Catarinicchia S, Guasti D, Masini E, et al. Protection from cigarette smoke-induced lung dysfunction and damage by H2 relaxin (Serelaxin). J Pharmacol Exp Ther. 2016;357(3):451–8.
222. Bani D, Ballati L, Masini E, Bigazzi M, Sacchi TB. Relaxin counteracts asthma-like reaction induced by inhaled antigen in sensitized guinea pigs. Endocrinology. 1997;138(5):1909–15.
223. Lam M, Royce SG, Donovan C, Jelinic M, Parry LJ, Samuel CS, et al. Serelaxin elicits bronchodilation and enhances beta-adrenoceptor-mediated airway relaxation. Front Pharmacol. 2016;7:406.
224. Diez J. Serelaxin: a novel therapy for acute heart failure with a range of hemodynamic and non-hemodynamic actions. Am J Cardiovasc Drugs. 2014;14(4):275–85.
225. Matthey M, Roberts R, Seidinger A, Simon A, Schroder R, Kuschak M, et al. Targeted inhibition of Gq signaling induces airway relaxation in mouse models of asthma. Sci Transl Med. 2017;9(407):eaag2288.
226. Yin LM, Xu YD, Peng LL, Duan TT, Liu JY, Xu Z, et al. Transgelin-2 as a therapeutic target for asthmatic pulmonary resistance. Sci Transl Med. 2018;10(427):eaam8604.

227. Cox PG, Miller J, Mitzner W, Leff AR. Radiofrequency ablation of airway smooth muscle for sustained treatment of asthma: preliminary investigations. Eur Respir J. 2004;24(4):659–63.
228. d'Hooghe JNS, Ten Hacken NHT, Weersink EJM, Sterk PJ, Annema JT, Bonta PI. Emerging understanding of the mechanism of action of bronchial thermoplasty in asthma. Pharmacol Ther. 2018;181:101–7.
229. Thomson NC, Chanez P. How effective is bronchial thermoplasty for severe asthma in clinical practice? Eur Respir J. 2017;50(2):1701140.
230. Pretolani M, Bergqvist A, Thabut G, Dombret MC, Knapp D, Hamidi F, et al. Effectiveness of bronchial thermoplasty in patients with severe refractory asthma: clinical and histopathologic correlations. J Allergy Clin Immunol. 2017;139(4):1176–85.

Index

H. Hashitani, R. J. Lang (eds.), *Smooth Muscle Spontaneous Activity*, Advances in Experimental Medicine and Biology 1124, https://doi.org/10.1007/978-981-13-5895-1